MUNI
FACULTY
OF SCIENCE

Habilitation Thesis

Functions of Plant Proteins associated with Telomeric Repeats and Telomerase

Mgr. Petra Procházková Schrumpfová, Ph.D.

Brno, 2023

Acknowledgement

I would like to express my deep gratitude to the head of the group, Prof. Jiří Fajkus, who has not only continuously supported my research, but also motivated me and provided fruitful scientific comments and advice. Additionally, he has been the person I turned to during challenging moments of my life.

I would also like to acknowledge both current and former colleagues who contributed to the friendly, tolerant, and supportive atmosphere.

Thanks also go to many of my students for their enthusiasm, patience, and contribution to the successful work on my scientific project. Their efforts exceeded my expectations, especially when considering the context of my maternity leave, which made our work more demanding.

The greatest thanks belong to my family, especially my husband Pavel, who has supported me in all aspects of my life and decisions, and my lovely two children, Verunka and Martínek.

Contents

Commentary

This Habilitation Thesis is a compilation of selected scientific publications in which I have contributed as a primary author or co-author. The primary goal of my research was to contribute to a fundamental understanding of the nature and characteristics of proteins and enzymes associated with long or short telomeric repeats.

At the very beginning of my scientific career, I initially focused on characterizing previously unknown plant putative homologues of proteins linked to telomeric sequences *in vitro*, known as TRBs. Interestingly, this protein family turned out to be a fruitful discovery in my scientific journey. Over the course of nearly two decades, we have uncovered that these proteins not only interact with the physical ends of chromosomes but also serve as the first described plant interactors of telomerase, the enzyme responsible for elongating telomeres. Furthermore, I found out that TRB proteins are associated with short telomeric sequences in the promoters of various genes, which resulted in very fruitful collaborations with laboratories investigating the epigenetic regulation of gene transcription. Moreover, my exploration of telomeric sequences and associated proteins has led me to the characterization of other diverse proteins linked to telomeric sequences or telomerase, such as RUVBLs, HMGBs, POTs, the PRC2 complex, and many others. These investigations have also touched subjects like plant gametogenesis, alternative lengthening of telomeres, and even the development of novel software for detecting short regulatory motifs within gene promoters.

To investigate and characterize the proteins associated with telomeric repeats and telomerase, we employed a range of general biochemical and molecular biological techniques. These included cloning, protein expression and purification, Electrophoretic mobility shift assay (EMSA), yeast two hydrid assay (Y2H), Co-Immunoprecipitation (Co-IP), Bimolecular Fluorescence Complementation (BiFC), Tandem Affinity Purification (TAP-tag), Chromatin Immunoprecipitation (ChIP) followed by Next-gen sequencing or hybridization and many others. Additionally, I utilized specialized techniques focused on telomeres or telomerase, such as Telomere Restriction Fragment (TRF) analysis and the Telomerase Repeated Amplification protocol (TRAP). In order to characterize plant material, I also employed techniques necessary for the analysis of T-DNA insertion mutant plants or plant cell cultures. Furthermore, as a supervisor for several bachelor's, master's, and doctoral theses, as well as a principal investigator of grants or a member of the grant-investigating team, I took on the responsibility of establishing and conducting research on various topics. This included the characterization of protein localization using microscopic techniques, the investigation of plant gametogenesis, and even the bioinformatic analysis.

Our findings have already been published in total of 20 publications on WoS, including articles and reviews. Among these, there is 1 correction to a research article (Schrumpfová and Majerská et al., Protoplasma, 2017), where Schrumpfová P.P. was recognized as the first co-author. Additionally, apart from these 20 publications, there is 1 book chapter published in Methods in Molecular Biology, The Nucleus, Book Series, Springer protocols (Schořová et al., 2020) and 1 Meeting abstract (Schrumpfová et al., 2005, FEBS Journal) listed in WoS.

Among these 20 publications, I have served as the primary author in 9 of them and as the corresponding author in 7.

The habitation theses comprise a compilation of 18 of these publications relevant to the thesis title:

*Corresponding Author

[1] Teano G., Concia L., Wolff L., Carron L., Biocanin I., Adamusová K., Fojtová M., Bourge M., Kramdi A., Colot V., Grossniklaus U., Bowler Ch., Baroux C., Carbone A., Probst A.V., **Schrumpfová P.P.**, Fajkus J., Amiard S., Grob S., Bourbousse C., and Barneche F. 2023. Histone H1 protects telomeric repeats from H3K27me3 invasion in Arabidopsis. Cell Reports, 42(8):112894. (IF 8.8, Q1)

Experimental work (%)	Supervision (%)	Manuscript (%)	Research direction (%)
0%	5%	5%	10%

[2] Kusová A., Steinbachová L., Přerovská T., Drábková Z.L., Paleček J, Khan A., Rigóová G., Gadiou Z., Jourdain C., Stricker T., Schubert D., Honys D., and **Schrumpfová P.P.***. Completing the TRB family: newly characterized members show ancient evolutionary origins and distinct localization, yet similar interactions. PLANT MOLECULAR BIOLOGY 112:61–83 2023 (IF 4.076, Q1)

Experimental work (%)	Supervision (%)	Manuscript (%)	Research direction (%)
5%	50%	90%	90%

[3] Tomaštíková E.D., Yang F., Mlynárová K., Hafidh S., Schořová Š., Kusová A., Pernisová M., Přerovská T., Klodová B., Honys D., Fajkus J., Pecinka A., **Schrumpfová P.P.***. RUVBL proteins are involved in plant gametophyte development. THE PLANT JOURNAL, Volume: 114, Issue: 2 Pages: 325–337, 2023 (IF 7.091, Q1)

Experimental work (%)	Supervision (%)	Manuscript (%)	Research direction (%)
5%	90%	90%	80%

[4] Pecinka A., **Schrumpfova P.P.**, Fisher L., Tomastikova E., Mozgova I. The Czech Plant Nucleus Workshop. Biologia Plantarum, Volume: 66, Pages: 39-45, 2021 (IF 1.122, Q4)

Experimental work (%)	Supervision (%)	Manuscript (%)	Research direction (%)
-	-	25%	-

[5] Schrumpfová P.P.* and Fajkus J. Composition and Function of Telomerase—A Polymerase Associated with the Origin of Eukaryotes. Biomolecules, 10(10), 2020 (IF 4.879, Q2)

Experimental work (%)	Supervision (%)	Manuscript (%)	Research direction (%)
-	-	80%	-

[6] Schořová Š., Fajkus J., Drábkova L., Honys D., **Schrumpfová P.P.*** The plant Pontin and Reptin homologues, RuvBL1 and RuvBL2a, colocalize with TERT and TRB proteins in vivo, and participate in telomerase biogenesis. THE PLANT JOURNAL, 98(2):195-212, 2019 (IF 5.775, Q1)

Experimental work (%)	Supervision (%)	Manuscript (%)	Research direction (%)
-	80%	90%	90%

[7] Schrumpfová P.P., Fojtova M., Fajkus J. Telomeres in Plants and Humans: Not So Different, Not So Similar. CELLS Volume: 8 Issue: 1 Article Number: 58 Published: 2019 (IF 4.366, Q2)

Experimental work (%)	Supervision (%)	Manuscript (%)	Research direction (%)
-	-	40%	-

[8] Schrumpfová P.P., Majerská J., Dokládal L., Schořová Š., Stejskal K., Obořil M., Honys D., Kozáková, L., Polanská P.S., Sýkorová E. Tandem affinity purification of AtTERT reveals putative interaction partners of plant telomerase in vivo. PROTOPLASMA Volume: 254 Issue: 4 Pages: 1547-1562, 2017 (IF 2.457, Q2)

Experimental work (%)	Supervision (%)	Manuscript (%)	Research direction (%)
20%	70%	5%	10%

[9] Schrumpfová P.P.*, Schořová Š., Fajkus J. Telomere- and telomerase-associated proteins and their functions in the plant cell. FRONTIERS IN PLANT SCIENCE Volume: 7 Article Number: 851, 2016 (IF 4.291, Q1)

Experimental work (%)	Supervision (%)	Manuscript (%)	Research direction (%)
-	-	80%	-

[10] Schrumpfová P.P., Vychodilová I., Hapala J., Schořová Š., Dvořáček V., Fajkus J. Telomere binding protein TRB1 is associated with promoters of translation machinery genes in vivo. PLANT MOLECULAR BIOLOGY Volume: 90 Issue: 1-2 Pages: 189-206, 2016 (IF 3.359, Q1)

Experimental work (%)	Supervision (%)	Manuscript (%)	Research direction (%)
70%	50%	90%	90%

[11] Schrumpfová P.P.*, Vychodilová I., Dvořáčková M., Majerská J., Dokládal L., Schořová S., Fajkus J. Telomere repeat binding proteins are functional components of Arabidopsis telomeres and interact with telomerase. PLANT JOURNAL Volume: 77 Issue: 5 Pages: 770-781, 2014 (IF 6.815, Q1)

Experimental work (%)	Supervision (%)	Manuscript (%)	Research direction (%)
80%	30%	70%	50%

[12] Schrumpfová P.P.*, Fojtová M., Mokroš P., Grasser K.D., Fajkus J. Role of HMGB proteins in chromatin dynamics and telomere maintenance in Arabidopsis thaliana. CURRENT PROTEIN & PEPTIDE SCIENCE Volume: 12 Issue: 2 Pages: 105-111, 2011 (IF 3,790, Q2)

Experimental work (%)	Supervision (%)	Manuscript (%)	Research direction (%)
80%	-	30%	10%

[13] Peška V., **Schrumpfová P.P.**, Fajkus J. Using the telobox to search for plant telomere binding proteins. CURRENT PROTEIN & PEPTIDE SCIENCE Volume: 12 Issue: 2 Pages: 75-83, 2011 (IF 3,790, Q2)

Experimental work (%)	Supervision (%)	Manuscript (%)	Research direction (%)
-	-	20%	-

[14] Hofr C., Šultesová P., Zimmermann M., Mozgová I., **Schrumpfová P.P.**, Wimmerová M., Fajkus J. Single-Myb-histone proteins from Arabidopsis thaliana: a quantitative study of telomere-binding specificity and kinetics. BIOCHEMICAL JOURNAL Volume: 419 Pages: 221-228, 2009 (IF 3.857, Q1)

Experimental work (%)	Supervision (%)	Manuscript (%)	Research direction (%)
10%	-	-	-

[15] Mozgová I., **Schrumpfová P.P.**, Hofr C., Fajkus J. Functional characterization of domains in AtTRB1, a putative telomere-binding protein in Arabidopsis thaliana. PHYTOCHEMISTRY Volume: 69 Issue: 9 Pages: 1814-1819, 2008 (IF 3.186, Q1)

Experimental work (%)	Supervision (%)	Manuscript (%)	Research direction (%)
5%	50%	10%	30%

[16] Schrumpfová P.P., Kuchař M., Paleček J., Fajkus J. Mapping of interaction domains of putative telomere-binding proteins AtTRB1 and AtPOT1b from Arabidopsis thaliana. FEBS LETTERS Volume: 582 Issue: 10 Pages: 1400-1406, 2008 (IF 3.264, Q2)

Experimental work (%)	Supervision (%)	Manuscript (%)	Research direction (%)
70%	-	10%	-

[17] Růčková E., Friml J., **Schrumpfová P.P.,** Fajkus J. Role of alternative telomere lengthening unmasked in telomerase knock-out mutant plants. PLANT MOLECULAR BIOLOGY Volume: 66 Issue: 6 Pages: 637-646, 2008 (IF 3.543, Q1)

Experimental work (%)	Supervision (%)	Manuscript (%)	Research direction (%)
20%	40%	10%	-

[18] Schrumpfová P., Kuchař M., Miková G., Skřišovská L., Kubičárová T., Fajkus J. Characterization of two Arabidopsis thaliana myb-like proteins showing affinity to telomeric DNA sequence. GENOME Volume: 47 Issue: 2 Pages: 316-324, 2004 (IF 2.100, Q2)

Experimental work (%)	Supervision (%)	Manuscript (%)	Research direction (%)
80%	-	20%	10%

Telomeric repeats and their interactome

Repetitive G-rich nucleotide sequences have been detected at the ends of the chromosomes of most living organisms, and hence named telomeric DNA repeats – from the ancient Greek télos 'end' and méros 'part' (Blackburn & Gall, 1978; reviewed in Jenner et al., 2022). Subsequently, it has become clear that telomeric motifs are also present within chromosomes. These internally localized telomeric repeats can be distinguished into two groups: short telomeric DNA repeats called *telo*-boxes and long telomeric DNA tracts, called interstitial telomeric sequences (ITSs) (Tremousaygue et al., 1999; Uchida et al., 2002). However, the defining of these two groups is not entirely precise, it is assumed that *telo*-boxes are composed of one to two telomeric DNA units and ITSs contain from several units to hundreds or thousands of telomeric DNA repeats. Moreover, ITSs are not composed of absolutely pure tracts of telomeric DNA repeats, but they are generally composed of telomeric repeats interspaced with degenerate repeats. The telomeric repeats, either located at the ends of or within the chromosomes, act as binding targets for large number of proteins. Some of these proteins recognize telomeric repeats specifically, while some of the telomeric-sequence associated proteins show higher sequence variability. Despite the initial assumptions that telomere-binding proteins are exclusively localized at the terminal telomeric tracts (Palm & de Lange, 2008), nowadays it is clearer that functions of telomeric-sequence associated proteins, including enzyme elongating telomeres - telomerase, is more complex and these proteins possess a broad spectrum of activities.

1 Telomeric repeats at the physical ends of linear chromosomes - telomeres

Telomeres are nucleoprotein structures forming and protecting the ends of linear chromosomes. They serve at least three functions which are essential for cell viability. First, they protect chromosome physical ends from fusion, endogenous nucleases and erroneous recognition as unrepaired chromosomal breaks. Secondly, telomeres facilitate the complete replication of the physical ends of the DNA. Finally, telomeres are implicated in intranuclear chromosome localization and meiotic chromosome pairing (reviewed in Blackburn et al., 2015; **Procházková Schrumpfová et al., 2019**; **see Suppl. M;** Shay & Wright, 2019; Schmidt & Cech, 2015; **Schrumpfová & Fajkus, 2020; see Suppl. O**).

For its potential significance to aging, cancer and cell viability serve telomeres, telomerase and telomere-associated proteins as a subject of intensive research. Barbara McClintock was the first to recognized that induced chromosome ends were distinctly different from natural ends and Hermann Müller, based in part on some of the findings of McClintock, called the ends of linear chromosomes "telomeres" (Müller, 1938; McClintock, 1942). However, the intensive research on the telomeres was started only three decades ago with a description of telomere DNA component (Blackburn & Gall, 1978), detection of telomerase

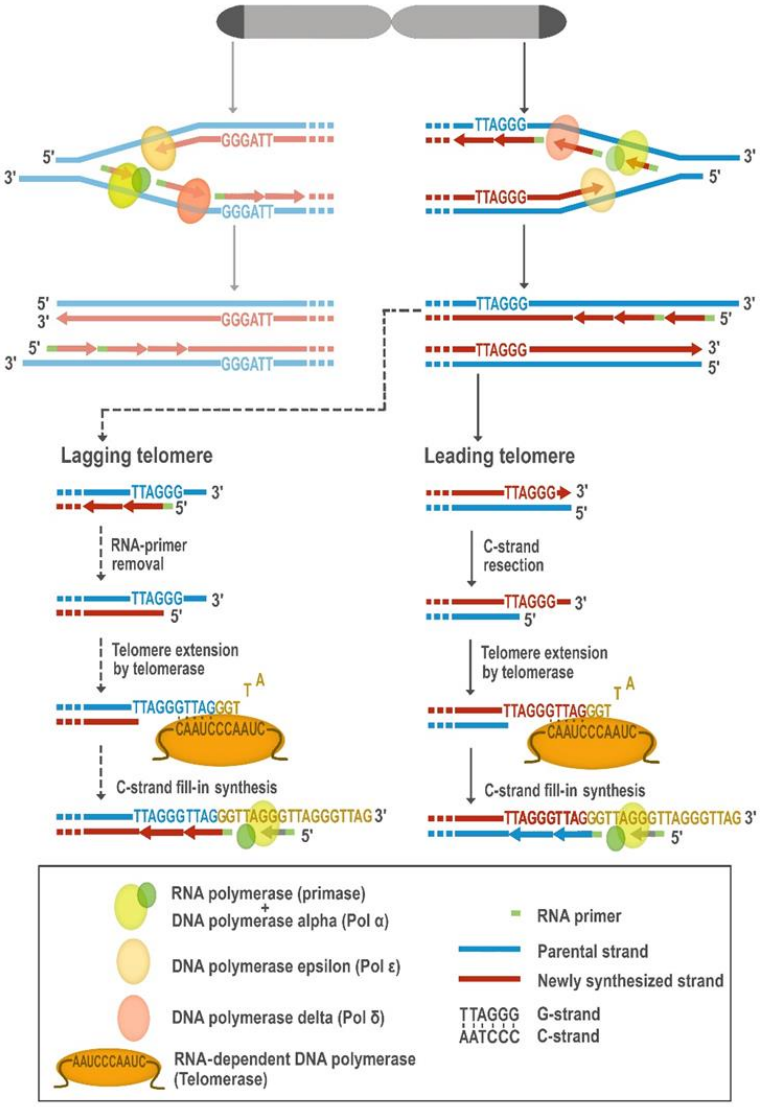

Figure 1. The replicating DNA in eukaryotes: DNA polymerases involved in replication (adopted from **Schrumpfova et al., 2020; see Suppl. O**).

During semiconservative DNA replication, each strand serves as a template for DNA polymerases to synthesize a new complementary strand. A specialized RNA polymerase (primase), that is a part of DNA Pol α, synthesizes the RNA primer. A single RNA primer aids DNA replication on the leading strand and multiple primers initiate Okazaki fragment synthesis on the lagging strand. Further DNA synthesis is carried out by DNA Pol ε and DNA Pol δ. The newly replicated telomere resulting from the lagging strand synthesis (Lagging telomere) retains the terminal RNA primer, which is subsequently removed. Attachment of the last RNA primer more proximally on the DNA strand, together with RNA-primer removal, creates an overhang on the G-rich strand. The initial product of the leading strand DNA synthesis (Leading telomere) is a blunt terminus whose C-strand is then resected by an exonuclease to create the mature G-rich overhang. In cells with an active RNA-dependent DNA polymerase (Telomerase), the G-rich overhangs originating from Lagging or Leading telomeres, can undergo elongation. Telomerase carries its own RNA molecule, which is used as a template, and can anneal through the first few nucleotides of its template region to the distal-most nucleotides of the G-rich overhang of the telomere DNA, add a new telomere repeat (GGTTAG) sequence, translocate and then repeat the process. The complementary C-strand is then in-filled by DNA Pol α-primase.

(ribonucleoprotein with a reverse transcriptase function) (Greider & Blackburn, 1985, 1989) and uncovering telomere binding proteins (Bianchi et al., 1997; Broccoli et al., 1997).

Telomeres cannot be fully replicated by enzymes that duplicate DNA. Conventional DNA polymerases cannot fully replicate telomeres all the way to the end of a chromosome. The synthesis of Okazaki fragments on the lagging strand requires RNA primers attaching ahead, resulting in shortening of the chromosome's end with each duplication (Olovnikov, 1973). Moreover, the product of the leading strand DNA synthesis is a blunt terminus whose C-strand is then resected by an exonuclease to create the mature G-rich overhang (**see Figure 1**).

Telomeric DNA in most organisms consists of tandem arrays of a short repetitive sequence. Two strands are recognized: one strand of the telomeric repeat tract running towards the 3′ end that is rich in guanines, called G-strand, whereas the complementary strand rich in cytosines is called C-strand (Makarov et al., 1997). The telomere in most of the species terminates in a 3′ single-stranded G-rich DNA overhang. In human telomeres a G-overhang is prevalent whose length varies from several tens to 280 base pairs (bp) (Cimino-Reale et al., 2001; Makarov et al., 1997; Wright et al., 1997). Telomeric sequence is highly conserved in Unikonta, where telomere motif is composed from $(TTAGGG)_n$ (Moyzis et al., 1988). This motif is the predominant terminal repeat sequence for fungi, animals, and Amoebozoa (Fulnecková et al., 2013) and sometimes is referred to as the vertebrate telomeric sequence. However even among Unikonts, the DNA sequence at chromosome ends is not completely uniform, e.g. there was detected presence of $(TTAGGC)_n$ in Nematoda, $(TGTGGG)_n$ in Rotifera or $(TTAGG)_n$ in insect Coleoptera (Frydrychová & Marec, 2002; Mason et al., 2016; Müller et al., 1991). While most filamentous fungi use $(TTAGGG)_n$ at their chromosome ends, yeasts telomeric sequence is not regular and can be described as T(G1–3) (reviewed in Kupiec, 2014; Peska et al., 2020; Tomáška et al., 2018). Moreover in addition to 3′ G-overhangs, *Caenorhabditis elegans* possess telomeric 5′ C-overhangs (Oganesian & Karlseder, 2011; Raices et al., 2008). Recently, in *Hymenoptera* (Insecta) various sequences (e.g. TTAGGTTGGG, TTAGG, TTTAGGTTAGG) were identified in terminal regions of assembled genomes (Fajkus et al., 2023).

In land plants, the telomere is mostly composed of *Arabidopsis*-type $(TTTAGGG)_n$ repeats (Richards & Ausubel, 1988; reviewed in **Schrumpfová et al., 2016a**; **see Supp. J; Schrumpfova et al., 2020; see Suppl. O**) (**see Figure 2**). Several groups of flowering plants are known in which a replacement of the plant telomere sequence has occurred. Known exceptions are species in the order *Asparagales*, starting from divergence of the *Iridaceae* family. *Iridaceae* family shares the human-type telomeric repeat $(TTAGGG)_n$, probably caused by a mutation that altered the telomerase RNA subunit of telomerase ~80 Mya (Adams et al., 2001; Sýkorová et al., 2003). The human-type telomere is also shared by species of the *Allioideae* subfamily (Sýkorová et al., 2006), except for the *Allium* genus where unusual telomeric sequence $(CTCGGTTATGGG)_n$ was detected (Fajkus et al., 2016). An unusual telomeric motif $(TTTTTTAGGG)_n$ was also found in the closely related genera *Cestrum elegans* (family Solanaceae) (Peška et al., 2015). Moreover, outside of land plants in red and green algae and glaucophytes (Koonin, 2010), telomere types also vary.

For example, in algae, not only the *Arabidopsis*-type of telomeric repeat, but also human-type $(TTAGGG)_n$, the Chlamydomonas-type $(TTTTAGGG)_n$ and a $(TTTTAGG)_n$ repeat were described (Fulnecková et al., 2013). Even within one plant carnivorous genus *Genlisea*, the telomeric sequence can vary from the *Arabidopsis*-type telomere repeat present in *G. nigrocaulis* to two variant sequences $(TTCAGG)_n$ and $(TTTCAGG)_n$ in *G. hispidula* and its close relative *G. subglabra* (Tran et al., 2015) (reviewed in **Schrumpfová et al., 2016a; see Supp. J**; **Schrumpfova et al., 2020; see Suppl. O**).

In plants, as well as in most of other species, replication of chromosomal ends results in G-overhangs after degradation of the last RNA primer at the 5′ terminus of a nascent strand. In *A. thaliana* or *Silene latifolia*, relatively short (20–30 nucleotides (nt)) G-overhangs were detected. Moreover, half of the *Arabidopsis* and *Silene* telomeres showed no overhangs or overhangs less than 12 nt in length (Kazda et al., 2012; Riha et al., 2000). A substantial portion of telomeres in *Arabidopsis* does not apparently undergo nucleolytic resection. Říha et al. showed that *A. thaliana* contain blunt-ended and short (1- to 3-nucleotide) G-overhang-containing telomeres (Riha et al., 2000).

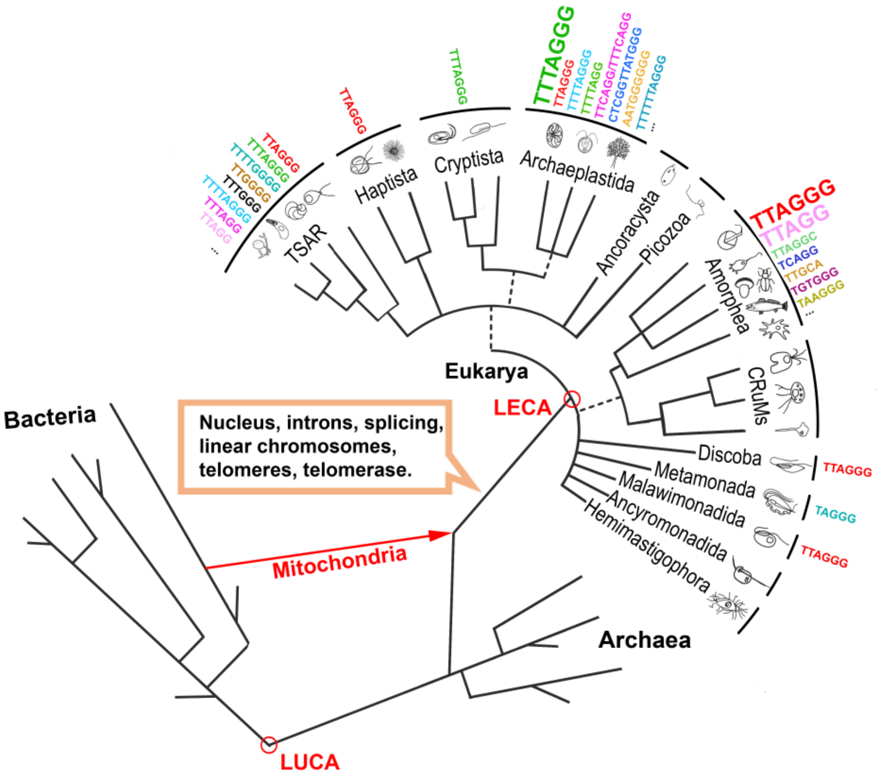

Figure 2. Telomeres in the evolutionary tree (adopted from **Schrumpfova et al., 2020; see Suppl. O).**
A simplified phylogenetic tree is shown, where telomeres and telomerase evolved upon linearization of chromosomes by the insertion of Group II self-splicing introns. In the Eukaryote branch, the groupings correspond to the current 'supergroups' according to the recent eukaryotic Tree of Life (eToL). Unresolved branching orders among lineages are shown as multifurcations. Broken lines reflect lesser uncertainties about the monophyly of certain groups. Examples of known telomeric repeat variants are listed next to respective supergroups. The major known telomeric repeat variants in the supergroups are marked with a larger font. Last eukaryote common ancestor (LECA); last universal common ancestor (LUCA).

Human telomere length at birth is highly heterogeneous, ranging from roughly 5-15 kilobase pairs (kb) (Sanders & Newman, 2013). The length of the germline human telomeres varies from 15–20 kb and laboratory mice have 25–150 kb telomeres (Sanders & Newman, 2013; Shay & Wright, 2000). It is obvious that length of the telomeres can vary not only between the species but also in between one genus (Gomes et al., 2011). Estimates of telomeric bp loss vary between 30–200 bp per division (Lansdorp et al., 1996).

The length of plant telomeric DNA at a single chromosomal arm can be as small as 500 bp in *Physcomitrella patens* (Fojtová et al., 2015; Shakirov et al., 2010) as long as 160 kb in *Nicotiana tabacum* (Fajkus et al., 1995) or 200 kb in *N. sylvestris* (Kovařik et al., 1996). Besides the remarkable variation in telomere length among diverse plant genera or orders, telomere lengths can also vary at the level of the species or ecotypes, e.g. *Arabidopsis* telomeres range from 1.5 to 9 kb, depending on the ecotype (Maillet et al., 2006; Shakirov & Shippen, 2004); telomeres from inbred lines of maize range from 1.8 to 40 kb (Burr et al., 1992). Additionally, in the long-living organism *Betula pendula*, telomeres in different genotypes varied from a minimum length of 5.9 - 9.6 kb to a maximum length of 15.3 - 22.8 kb (Aronen & Ryynänen, 2014) reviewed in **Schrumpfová et al., 2016a; see Supp. J**).

1.1 Proteins associated with telomeres in mammals

Telomere-associated proteins can regulate the length of the telomere tract by modulating access of telomerase or affecting conventional DNA replication machinery. In mammals, telomeric DNA is maintained primarily by six-protein complex called Shelterin: Telomere Repeat Binding Factors 1 and 2 (TRF1, TRF2), Protection of telomeres 1 (POT1), TRF1- and TRF2-Interacting Nuclear Protein 2 (hTIN2), telomere protection protein 1 (TPP1) and Repressor/activator protein 1 (RAP1). Moreover, the physical ends of the chromosomes are associated with a nucleoprotein complex named CST (Cdc13/CTC1, STN1, TEN1). The specific telomeric dsDNA binding of Shelterin complex is mediated by TRF1 and TRF2 proteins (Broccoli et al., 1997) through their Myb-like domain, with an LKDKWRT amino acid motif. The Myb-like domain is conserved in telomeric sequence binding proteins not only in mammals but also in plants or yeasts (Bilaud et al., 1996; Feldbrügge et al., 1997). Myb-like domains of the TRF1 and TRF2 proteins are located at their C-terminus. Another Shelterin subunit - POT1 protein - is linked to the Shelterin complex by TPP1 protein, which in turn binds to TIN2 and RAP1 proteins and interacts with TRF2 protein (reviewed in Schmidt & Cech, 2015) (**see Figure 3A**).

TRF2 protein has a central protective role in shelterin complex because it specifically inhibits Ataxia Telangiectasia Mutated (ATM) kinase-dependent DNA damage signalling and the classical Ku70/80- and Ligase IV-mediated non-homologous enjoining pathway (NHEJ) at telomeres. The POT1 proteins (POT1a and POT1b in the mouse) associate with single-stranded (ss) telomeric DNA and POT1 protein safeguards

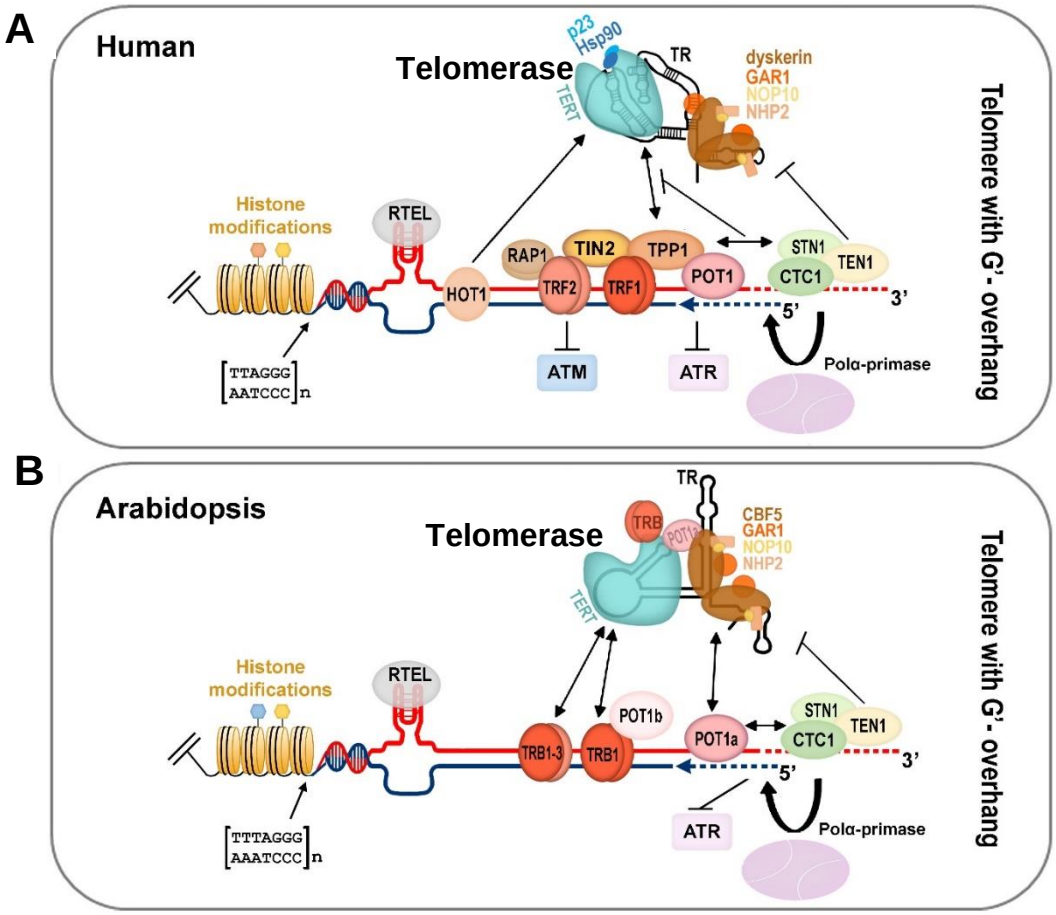

Figure 3. An integrative schematic view of the human and plant terminal telomeric complex (adopted from Schrumpfová et al. 2019; see Suppl. M).

A) Human active telomerase is associated with chaperones as well as with TR associated conserved scaffold box H/ACA of small nucleolar RNAs proteins. Mammalian shelterin proteins (TRF1/2, RAP1, TIN2, TPP1 and POT1) modulate access to the telomerase complex and the ATR/ATM-dependent DNA damage response pathway. The CST complex (CTC1-STN1-TEN1) affects telomerase and DNA polymerase α recruitment to the chromosomal termini and, thus, coordinates G-overhang extension by telomerase with fill-in synthesis of the complementary C-strand (blue dashed line). G-quadruplexes, D-loops and T-loops during telomere replication are resolved by RTEL helicase. HOT1 directly binds double strand telomere repeats and associates with the active telomerase. Telomere nucleosomes show a shorter periodicity than that in the other parts of chromosomes.

B) *Arabidopsis* telomerase is associated with TRB proteins as well as with POT1a that interacts with the dyskerin orthologue CBF5. Plants possess all orthologue proteins of conserved scaffold box H/ACA of small nucleolar RNAs (CBF5, GAR1, NOP10, NHP2). Moreover, TRB proteins interact with the telomeric sequence due to the same Myb-like binding domain as that in mammalian TRF1/2. TRB proteins interact with TERT and POT1b and, when localized at chromosomal ends, they are eligible to function as components of the plant shelterin complex. An evolutionarily conserved CST complex is suggested to coordinate the unique requirements for efficient replication of telomeric DNA in plants as well as in other organisms. In addition, plant RTEL contributes to telomere homeostasis. For the sake of clarity, only the situation in telomere with 3' overhang is depicted. For further information and for human and plant telomere histone modifications **see Schrumpfová et al. (2019; see Suppl. M).**

telomeres against Ataxia Telangiectasia and Rad3 related (ATR) kinase pathway (Denchi & de Lange, 2007; Smogorzewska et al., 2002). A bridge between proteins directly associated with DNA-TRF1, TRF2 and POT1 is mediated by TIN2 and the oligosaccharide/oligonucleotide binding (OB)-fold domain of TPP1 protein (reviewed in (Schmidt & Cech, 2015). Moreover protein RAP1, interacts with TRF2 (Arat & Griffith, 2012) and modulates its recruitment to telomeric DNA (Janoušková et al., 2015; Nečasová et al., 2017). The most of the Shelterin complexes can be purified without dissociation, indicating they form stable complexes at least *in vitro*. It was published that TRF2 interacts with TIN2 with an 2:1 stoichiometry in the context of Shelterin ($RAP1_2$:$TRF2_2$:$TIN2_1$:$TPP1_1$:$POT1_1$) (Lim et al., 2017).

The maintenance of telomere repeats in most eukaryotic organisms requires enzyme telomerase. Telomerase consists of a telomerase reverse transcriptase (TERT) and telomerase RNA subunits (TR) that dictates the synthesis of the G-rich strand of telomere terminal repeats and elongates telomeric tracts at the chromosomal terminus (Blackburn & Gall, 1978; Greider & Blackburn, 1985, 1989). Most enzymes encounter their substrates by simple diffusion but both telomerase and its chromosome end substrate have very low abundance and the telomerase enzyme is recruited to telomeres rather than simply encountering them by diffusion (Schmidt & Cech, 2015; Xi & Cech, 2014). The Shelterin component TPP1 is the key telomeric component necessary for telomerase recruitment to telomeres (Xin et al., 2007). In addition, TPP1 in complex with POT1 stimulates telomerase to synthesize additional telomeric repeats *in vitro* and has therefore been proposed to be a processivity factor for telomerase action at telomeres (Wang et al., 2007). Protein TPP1 is composed of an N-terminal OB-fold domain required for telomerase recruitment, a central domain that directly binds to POT1 and a C-terminal domain necessary for its association with TIN2. Loss of any of the members of Shelterin protein complex can result in inappropriate DNA damage response (DDR), can lead to chromosome fusion, telomere loss or activate replicative senescence or apoptosis (Sfeir, 2012).

Kappei et al. identified by the proteomics of isolated chromatin segments (PICh) approach a telomeric DNA binding protein named homeobox telomere-binding protein 1 (HOT1). HOT1 directly binds ds telomere repeats and associates with the active telomerase and is required for telomerase chromatin binding. HOT1 is the telomere-binding protein that acts as a positive regulator of telomere length (Déjardin & Kingston, 2009; Kappei et al., 2013).

1.2 Proteins associated with telomeres in plants

1.2.1 Telomeric dsDNA associated proteins in plants

In plants, telomeric dsDNA sequence binding proteins with a Myb-like domain can be classified into three main groups: (i) with a Myb-like domain at the N-terminus (Smh/TRB family) (ii) with a Myb-like domain at the C-terminus (TRFL family) (iii) with a Myb-like domain at the C-terminus (AID family) (reviewed in Du et al., 2013; **Peška et al., 2011; Schrumpfová et al., 2016a; see Supp. F and J**).

The first group of proteins, with a Myb-like domain at the N-terminus, contain a central histone-like domain (H1/5 domain) with homology to the H1 globular domain found in the linker histones H1/H5 and is therefore called the Smh (Single myb histone) family (Marian et al., 2003; Marian & Bass, 2005; **Schrumpfová et al., 2004; see Supp. A**). Members belonging to Smh family are frequently named Telomere Repeat Binding (TRB) proteins so we call this family also Smh/TRB family (**see Figure 3B and Figure 5**).

Within the second family of the proteins with a Myb-like domain - TRFL family - there were also identified several plant orthologues. In *A. thaliana* there were characterised six proteins with the C-terminal Myb-like domain (AtTBP1, AtTRP1 and AtTRFL1, 2, 4, 9) belonging to the subfamily of proteins named TRFL I with characteristic features. Proteins from TRFL I family can homo- and heterodimerize and they can efficiently bind to telomeric DNA *in vitro* (Karamysheva et al., 2004). A key feature of this subfamily is a ~30 amino acid extension of the Myb-like domain that is likely responsible for specific binding to plant telomeric DNA. Moreover, the TRFL family includes six proteins, that are unable to bind telomeric DNA *in vitro* and are also unable to form homo- and heterodimers, despite possessing the C-terminal Myb-like domain. These proteins are members of subfamily named TRFL II (AtTRFL3, 5, 6, 7, 8, 10) (Karamysheva et al., 2004).

The proteins from the third family contain a single Myb-like domain at the C-terminus and contains only a few described members.

All three Myb-like protein subfamilies were already detected in the moss *P. patens* and separation of Smh/TRB and TRFL and is apparent already in unicellular algae. These data suggest ancient origin of the three protein subfamilies and their diversification early in evolution of the plant lineage (Fulcher & Riha, 2016).

Especially the first (Smh/TRB) family and the second (TRFL) family contain increased number of family members. However, this observation is not surprising as whole genome duplication events (WGDs) have occurred in many plant families (Freeling, 2009; Qiao et al., 2022). These WGDs result in a multitude of genomic changes, such as deletions of large fragments of chromosomes, silencing of duplicate genes and recombining of homologous chromosomal segments, as was shown, e.g. in crucifer species (Freeling, 2009; Mandáková & Lysak, 2008). Increased numbers of genes of the same family may lead to gene sub-

functionalization, neo-functionalization and partial or full redundancy, and complicates assignment of an actual and specific function for individual proteins *in vivo*.

Overall, the conserved domain composition of the plant proteins with respect to their mammalian counterparts does not guarantee conservation of their function. It seems that some proteins are involved in a similar biochemical pathways, but their interaction partners, and consequently potential regulatory factors, might slightly differ (reviewed in **Schrumpfová et al., 2019; see Supp. M**).

Smh/TRB family

Screening of *Z. mays* cDNA led to identification of gene coding ZmSmh1 protein (Marian et al., 2003). The Smh1 gene is expressed in leaf tissue and the ZmSmh1 protein binds ds oligonucleotide probes with at least two internal tandem copies of the maize telomere repeat, TTTAGGG.

Simultaneously as Smh protein from *Zea* was characterized, we searched *A. thaliana* databases in our laboratory for putative genes coding for proteins with the Myb-like domain. This search resulted in two candidate protein sequences at that time, AtTRB2 and AtTRB3, formerly named AtTBP3 and AtTBP2, respectively (Kuchař & Fajkus, 2004; **Schrumpfová et al., 2004; see Supp. A**). We characterised these two candidates and we found out that AtTRB2 and AtTRB3 proteins able to bind the G-rich strand and dsDNA of plant telomeric sequence with an affinity proportional to a number of telomeric repeats. The binding of AtTRB proteins to telomeric ds telomeric oligonucleotides is highly specific, because even a 100-fold abundance of non-telomeric sequence cannot displace their binding to tetramers of the telomeric sequence (**Schrumpfová et al., 2004; see Supp. A**). Binding affinity to ds- and ss-oligonucleotides of the plant telomeric sequence is roughly proportional to the number of telomeric repeat.

Additionally, the later identified member of Smh/TRB family - AtTRB1 protein - is able to bind related telomeric DNA sequences (plant (TTTAGGG) or human (TTAGGG)) with a certain flexibility, as well as AtTRB2 or AtTRB3 proteins. We analysed DNA-protein interaction of the full-length and truncated variants of AtTRB1. We showed that preferential interaction of AtTRB1 with ds telomeric DNA is mediated by the Myb-like domain while the H1/5 domain interacts non-specifically with any DNA without preference for either telomeric or non-telomeric sequence (Ellen & van Holde, 2004; **Mozgová et al., 2008; see Supp. D**). The partial non-selective binding of the Myb-like domain to either plant (TTTAGGG) or human (TTAGGG) telomeric sequence appears to be a general feature of the *A. thaliana* Smh/TRB family proteins (**Mozgová et al., 2008; Schrumpfová et al., 2004; see Supp. D and A**).

Recently, we have completed characterization of the TRB family as we described two novel members of the TRB family from *Arabidopsis* (AtTRB4 and AtTRB5) (**see Figure 4)**. The results clearly showed that AtTRB4 and AtTRB5 do preferentially bind long arrays of telomeric sequences. However, the AtTRB minimal

recognition motif was newly defined as one *telo*-box positioned within a non-telomeric DNA sequence **(Kusova et al., 2023; see Suppl. R).**

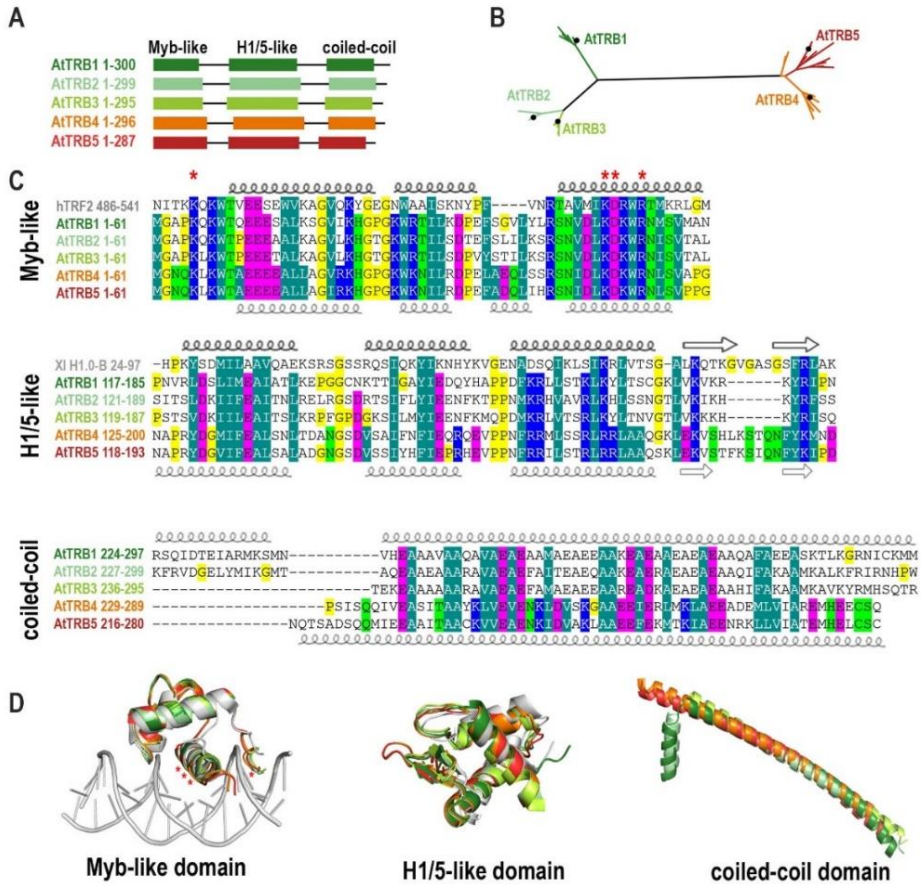

Figure 4. Sequence and structural alignments of TRB family proteins (Kusová et al., 2023; see Supp. R).

A) Schematic representation of the conserved domains of TRBs from *A. thaliana*. *Myb-like*, Myb-like domain; *H1/5-like*, histone-like domain; *coiled-coil*, C-terminal domain.

B) Unrooted Maximum likelihood (ML) phylogenetic tree of *Brassicaceae* TRB proteins. The length of the branches are proportional, and the black dots indicate the position of TRB1-5 from *A. thaliana*.

C) Multiple alignments of the Myb-like, H1/5-like and coiled-coil domains. The positions of α-helices or β-sheets of the uppermost or the lowermost sequence in each alignment are highlighted: *bold*, experimentally determined structures (cryo-EM or X-ray crystallography); *thin*, AlphaFold prediction. Human Telomeric repeat-binding factor 2 (hTRF2) and *Xenopus laevis* histone H1.0 (Xl H1.0-B) were used to show the most conserved amino acid (aa) residues. Amino acid shading indicates the following conserved amino acids: *dark green*, hydrophobic and aromatic; *light green*, polar; *blue*, basic; *magenta*, acidic; *yellow*, without side chain (glycine and proline). The aa of hTRF2 that mediate intermolecular contacts between telomeric DNA and hTRF2 are marked with an asterisk.

D) A certain flexibility in binding related telomeric DNA sequences was observed from the *A. thaliana* telomeric DNA: *A. thaliana* (TTTAGGG), *Chlamydomonas reinhardtii* (TTTTAGGG), human (TTAGGG), *Bombyx mori* $[TTAGG]_5TTAG$ and *Ascaris lumbricoides* (TTAGGC) (Niedermaier and Moritz, 2000; Okazaki et al., 1993; Petracek and Berman, 1992), however, the ability to bind variant telomere sequences decreased with sequence divergence. In addition to being able to bind ds telomeric sequences, AtTRB proteins can also bind to the G-rich ss telomeric DNA although with lower affinity compared to ds telomeric sequences. The C-rich telomeric strand is not preferentially bound (**Schrumpfová et al., 2004; see Supp. A**). Our observation are consistent with the findings that also other members of Smh/TRB family proteins in land plants show telomeric dsDNA binding capability, e.g. *Z. mays* ZmSMHs or *O. sativa* OsTRBFs (Byun et al., 2018; Marian et al., 2003).

We performed comprehensive phylogenetic analysis and found out that TRB proteins first evolved in Streptophyta in *Klebsormidiophyceae*. In *Klebsormidium nites* only one TRB homolog was identified. Following the evolutionary tree, an increasing number of TRB homologues were found in Bryophyta and Tracheophyta. In seed plants, which have undergone more rounds of WGDs than Bryophyta and Lycophyta (Clark & Donoghue, 2018), predominantly three TRB proteins were recognized. Within *Brassicaceae*, which has undergone an additional recent round of WGD (Walden et al., 2020), five TRB homologs were revealed **(Kusová et al., 2023; see Supp. R).**

The ability of AtTRB proteins to bind typical plant and human telomeric motifs with a similar affinity could be important for an easier adaptation to a change in telomere sequence from a plant to divergent telomeric motifs, which has occurred during the evolution of plants of several species as was described above. It is also consistent with the Kováč et al. that argued that there is an upper limit for the specificity of interaction between binding partners (e.g. enzyme-substrate, ligand-receptor, protein-DNA sequence), since interactions that are too specific would lack flexibility and a perfect recognition would be too rigid and possibly non-functional (Kováč, 1987), e.g. Tay1 (telomere-associated in *Yarrowia lipolytica* 1) protein, the double strand (ds) sequence telomere-binding protein of the yeast *Y. lipolytica,* exhibits lower affinity for its own telomeres (TTAGTCAGGG) than for the mammalian-type telomeric repeats (TTAGGG) (reviewed in Tomáška et al., 2018).

Another typical character of a telomere dsDNA-binding proteins seems to be capability for multimerization. Dimerization has been proved to increase the efficiency of the binding of telomere-associated proteins, TRF1 and TRF2, to telomeric DNA also in mammalian cells. Mammalian TRF1 is a homodimer *in vivo* and its accumulation at telomeres depends on homotypic interactions. Similarly, the TRF homology (TRFH) domain near their N-terminus from TRF2 protein mediates homotypic interactions, but TRF1 and TRF2 do not form heterodimers (Bianchi et al., 1997; Fairall et al., 2001).

In our studies we demonstrated that AtTRBs show strong mutual and self-interactions using yeast two hydrid assay (Y2H) assay (**Schrumpfová et al., 2004; see Supp. A; Kusova et al., 2023; see Suppl. R).** Additionally, we investigated the ability of the AtTRB1 fragments to form self-dimers or multimers using Poly Acrylamide Gel Electrophoresis (PAGE) with a weak detergent, perfluoro-octanoic acid (PFO) (**Mozgová et al., 2008; see Supp. D**). This method can be used for detection and molecular mass determination of protein complexes since (in contrast to SDS-PAGE with sodium dodecyl sulfate), PFO-PAGE preserves high affinity protein–protein interactions (Ramjeesingh et al., 1999). The results confirmed the strong tendency of the H1/5 domain to multimerize and the same holds true for all the fragments of AtTRB1 which contain the H1/5 domain. Myb-like domain of the rice RTBP, TRFL family protein, also interacts with plant telomeric DNA in the form of a homodimer (Yu et al., 2000). In contrast to H1/5 domain, the N-terminal Myb-like

domain itself did not form higher molecular weight complexes. According to these results we proposed model of binding of AtTRB proteins to plant telomeric DNA where the Myb-like domain primarily ensures direct sequence-specific binding of AtTRB1 to telomeric DNA, while the H1/5 domain may enhance this binding by protein dimerization and sequence-non-specific binding to DNA (**Mozgová et al., 2008; see Supp. D**).

The study of stoichiometry and kinetics of AtTRB1 and AtTRB3 proteins binding to the telomeric DNA revealed that the affinity of AtTRB1 to telomeric substrate with four telomeric repeats is 4-fold higher than that of AtTRB3, although AtTRB1 and AtTRB3 are relatively similar in their primary sequences **(Hofr et al., 2009; see Supp. E**). Similarly to our results, human hTRF1 binds telomeric DNA with a 4-fold higher affinity than that of hTRF2 when interacting with human telomeric DNA (Hanaoka et al., 2005). In **Mozgova et al. (2008; see Supp. D)** we assumed that the non-specific interaction of H1/5 domain with any DNA without preference for either telomeric or non-telomeric sequence (Ellen & van Holde, 2004), together with the high pI of the AtTRB1 fragments, suggests that electrostatic interactions take part in the interaction of the fragments of AtTRB1 with telomeric dsDNA (**Mozgová et al., 2008; see Supp. D**). Interestingly, our model showing model of Myb-like domain revealed that the solution accessible surface of AtTRB4 and AtTRB5 differ to the solution accessible surface of AtTRB2/AtTRB3 and to AtTRB1 (**Kusova et al., 2023; see Suppl. R).**

All five AtTRB members preferentially localize to the nucleus and nucleolus during interphase. Both the central H1/H5-like domain and the Myb-like domain from AtTRB1 can direct a GFP fusion protein to the nucleus and nucleolus (Dvořáčková et al., 2010a; **Kusova et al., 2023; see Suppl. R).** AtTRB1-GFP localization is cell cycle-regulated, as the level of nuclear-associated GFP diminishes during mitotic entry and GFP progressively re-associates with chromatin during anaphase/telophase. Although a possible association of AtTRB1-GFP with the telomere was suggested previously in Dvořáčková et al. (2010a) the small size of *Arabidopsis* chromosomes, in combination with short telomere lengths, precluded the authors to visualize the AtTRB-telomere association. We took advantage of the well-established protocol of *Nicotiana benthamiana* leaf infiltration and the fact that *N. benthamiana* has longer telomeres that are easier to visualize compared to *Arabidopsis*. In our study **Schrumpfová et al. (2014; see Supp. H)** we proved that AtTRB proteins are not only binding to the telomeric DNA sequence *in vitro*, as was described above, but that they also co-localize with telomeres *in situ.*

Later on, localization of AtTRB1 protein at the plant telomeres *in vivo was* verified by independent technique by the teams of Holger Puchta and Andreas Houben. They used imaging technique based on two orthologues of the bacterial clustered regularly interspaced short palindromic repeats (CRISPR)–CRISPR associated protein 9 (Cas9). Dreissig et al. demonstrated not only that CRISPR–dCas9 can be used to

visualize specific DNA sequences in combination with fluorescently tagged proteins interacting with those DNA sequences but they also demonstrated that around 87.6 % of telomeres were simultaneously bound by AtTRB1 protein and CRISPR–dCas9 signals resembling telomeres (Dreissig et al., 2017).

Telomere shortening was observed in *attrb1* mutants in the *A. thaliana* ecotype Columbia, with otherwise-stable telomere lengths (Shakirov & Shippen, 2004; **Schrumpfová et al., 2014; see supp. H)**. In contrast, telomere extension was detected in *attrb2* knockout mutants of the *A. thaliana* ecotype Wassilewskija, which exhibits telomere length polymorphism in wild-type plants (W. K. Lee & Cho, 2016; Maillet et al., 2006; Shakirov & Shippen, 2004). Triple homozygous mutant plants, containing the alleles from *A. thaliana* Columbia (*attrb1* and *attrb3*) and from Wassilewskija (*attrb2*), exhibit telomere shortening (Zhou et al., 2016, 2018).

Our suggestion, that AtTRBs are part of telomere-associated interactome was supported by the group of Simon Amiard and Charles White that used pull-down assays to identify potential telomeric interactors in the *Arabidopsis*. They identified several candidate proteins, including TRB1 and TRB3 proteins. The TRB proteins were enriched in pull-down with telomeric probe even more than the GH1-HMGA1 proteins that are the main objects their study (Charbonnel et al., 2018).

Involvement of AtTRB proteins in telomere interactome was furthermore boosted by our detection of direct interaction between AtTERT and AtTRB proteins (**Kusova et al., 2023; see Suppl. R).** AtTRB proteins interact in Y2H, Co-Immunoprecipitation (Co-IP) or Bimolecular Fluorescence Complementation (BiFC) systems with the N-terminal part of AtTERT that contains telomerase-specific motifs. Moreover, AtTRB1 was, among the others, co-purified with N-terminal constructs of AtTERT from *A. thaliana* suspension cultures **(Schrumpfová and Majerská et al., 2017, 2018; see Supp. K and L**). However, neither of the AtTRB2 and AtTRB3 proteins purified from *Escherichia coli*, nor their mixture, had any effect on telomerase activity *in vitro*, measured by Telomerase Repeat Amplification Protocol (TRAP) (**Schrumpfová et al., 2004; see Supp. A**). Likewise, no changes in telomerase activity or processivity were observed in extracts from *attrb1* mutant plants. Correspondingly, no variations in telomerase activity were detected in transformed plants (TRB1pro:TRB1-GFP) expressing higher levels of protein (**Schrumpfová et al., 2014; see Supp. H**).

Kuchař et al. (2004) detected that AtTRB2 and AtTRB3 proteins interact with AtPOT1b protein, one of two homologues of human telomeric ssDNA binding protein POT1 (Baumann & Cech, 2001; Kuchař & Fajkus, 2004). In our study **Schrumpfová et al., (2008; see Supp. C)** we found out that also other member of Smh/TRB family - AtTRB1 protein - interacts with AtPOT1b. Using combination of Y2H and Co-IP we detected that AtTRB1 protein physically interacts with N-terminus AtPOT1b via its H1/5 domain (**Schrumpfová et al., 2008; see Supp. C**). Recently we detected also interaction between AtTRB4 and AtTRB5 and AtPOT1a (**Kusova et al., 2023; see Suppl. R).**

Moreover, proteins from Smh/TRB family physically interact with AtRUVBLs. RUVBL proteins belong to the evolutionarily highly conserved AAA+-family (ATPase Associated with various cellular Activities) that are involved in ATP binding and hydrolysis (Matias et al., 2006). AtTRBs together with AtTERT and AtRUVBLs form trimeric complex AtTERT-AtTRB-AtRUVBL (see also bellow) **(Schořová et al., 2019; see Supp. N)**. Our results suggested that AtTRB proteins thus play a role of interaction hubs not only in telomere chromatin structure but also in telomerase biogenesis.

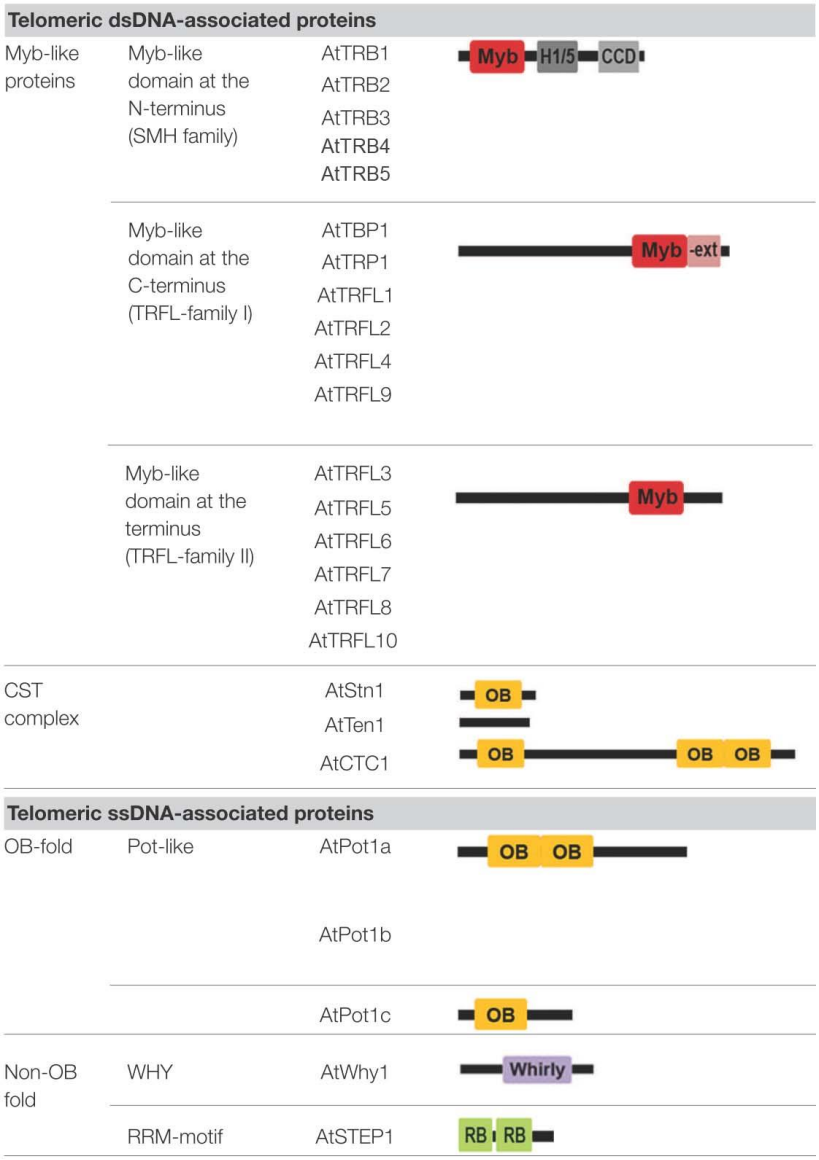

Figure 5. Telomeric and putative telomeric dsDNA- and ssDNA-binding proteins from *A. thaliana* (adopted from Schrumpfová et al., 2016a, see Supp. J).
Myb-like domain (Myb); Myb-extension (-ext); Histone-like domain (H1/5); Coiled Coil Domain (CCD); Oiigonucleotide/Oligosaccharide-Binding Fold domain (OB); Whirly domain (Whirly); RNA-binding domain (RB); A. thaliana (At); Telomere Repeat Binding Protein (AtTRB); TRF-like family (TRFL family); Suppressor of cdc thirteen homolog (AtStn1); Conserved telomere maintenance component 1 (AtCTC1); (CTC1-Stn1-Ten1) complex (CST); RNA recognition motifs (RRM); Protection of telomeres 1a, b, c (AtPot1 a,b,c); Whirly 1 (Why1); Single-stranded telomere-binding protein 1 (STEP1).

In *O. sativa* there were three proteins from Smh/TRB family identified (Byun et al., 2008). Proteins OsTRBF1 and OsTRBF2 are constitutively transcribed in rice plants grown under greenhouse conditions. Gel retardation assays showed that these OsTRBF proteins bind specifically to the plant double-stranded telomeric sequence, TTTAGGG, with markedly different binding affinities. Y2H and Co-IP assays indicated that both OsTRBF1 and OsTRBF2 interact with one another to form homo- and hetero-complexes, while OsTRBF3 appeared to act as a monomer (Byun et al., 2008). In an affinity pull-down technique, 80 proteins from *O. sativa* were identified for their ability to bind to a telomeric repeat (He et al., 2013). Among them, two of three previously reported proteins from the Smh/TRB family - OsTRBF1 and OsTRBF2 were isolated.

TRFL family

The second group of proteins, with a Myb-like domain at the C-terminus, is named TRFL (TRF-like). TRFL family can be divided into two subfamilies named TRFL I (possess extension of the Myb-like domain (Myb-ext) that is likely responsible for specific binding to plant telomeric DNA proteins *in vitro*) and TRFL II (unable to bind telomeric DNA *in vitro*) (Karamysheva et al., 2004; Ko et al., 2008) **(see Figure 5).**

The first identification of a TRFL family protein from *O. sativa* - Telomere-binding protein 1 (OsRTBP1) (Yu et al., 2000) - was soon followed by numerous other TRFL members, e.g. *Nicotiana glutinosa* (NgTRF1) (Yang et al., 2003), *Solanum lycopersicum* (LeTBP1) (Moriguchi et al., 2006), *A. thaliana* (AtTBP1, AtTRP1, AtTRFL2-10) (Hwang et al., 2001; Chen et al., 2001; Karamysheva et al., 2004) or *Cestrum parqui* (CpTBP) (**Peška et al., 2011; see Supp. F**). Even though *O. sativa* or *N. glutinosa* mutants for TRFL members exhibited markedly longer telomeres (Hong et al., 2007; Yang et al., 2004), in *A. thaliana*, a knockout of AtTRP1, member of TRFLI subfamily with a Myb-ext, did not change telomere length significantly (Chen et al., 2005). In *A. thaliana* even multiple knockout plant, deficient for all six proteins from TRFLI subfamily (AtTBP1, AtTRP1, AtTRFL1, AtTRFL2, AtTRFL4 and AtTRF9) did not exhibit changes in telomere length or phenotypes associated with telomere dysfunction (Fulcher & Riha, 2016; reviewed in **Schrumpfová et al., 2016a; see Supp. J**).

A structurally related member to TRFLI subfamily was found in *Cestrum parqui*, CpTBP1, a plant species lacking typical telomeres and telomerase (**Peška et al., 2011; see Supp. F**). The protein shows nuclear localisation and association with chromatin while transiently expressed in *N. benthamiana* after infiltration *Agrobacterium tumefaciens* into young leaves.

Although, no functional evidence exists for the role of AtTRFL proteins at telomeres so far, plausible involvement in telomere maintenance in plants was suggested in Kuchař and Fajkus (Kuchař & Fajkus, 2004). Kuchař and Fajkus observed a specific interaction between AtTRP1 (member of TRFLI subfamily) and AtKu70. The AtTRP1 domain responsible for AtKu70 interaction occurs between amino acid sequence positions 80 and 269. It was hypothesized that AtKu, a DNA repair factor with a high affinity for DNA ends,

sequesters chromosome termini within its DNA loading channel and protects them from nuclease processing (Valuchova et al., 2017).

Another member of the TRFL family - ZmIBP2 (Initiator-binding protein) protein – binds not only telomeric repeats (Moore, 2009), but was originally identified as a promoter binding ligand (Lugert & Werr, 1994).

AID family

The third group with a Myb-like domain at the C-terminus (AID family) contains only a few described members. The AID family is named according to anther indehiscence 1 (AID) protein from *O. sativa* - OsAID1 (Zhu et al., 2004). OsAID1 was initially identified as being involved in anther development, however, OsAID1 also isolated in an affinity pull-down technique within 80 proteins from *O. sativa* showing ability to bind to a telomeric repeat, while no member with a Myb-like domain at the C-terminus of the TRFL family could be found (He et al., 2013). Another member of this family - ZmTacs1 (Terminal acidic SANT) from *Z. mays* - may function in chromatin remodelling within the meristem. *In silico* expression analysis revealed that ZmTacs1 is expressed in meristem-enriched tissues and in contrast, the Myb-like domains of known Myb-like domain such as ZmSMH1, or human TRF1 all have basic isoelectric points (Marian & Bass, 2005; reviewed in **Schrumpfová et al., 2016a; see Supp. J**). Marian and Bass proposed that the acidic patches observed on the surfaces of the plant TACS-type proteins are not compatible with direct DNA binding and may reflect areas for the binding of basic moieties, such as histone tails or basic regions of other proteins (Marian & Bass, 2005).

1.2.2 Telomeric ssDNA associated proteins in plants

Proteins with OB-fold

The majority of telomeric ssDNA binding proteins bind through OB motifs (oligonucleotide/oligosaccharide binding, OB-fold) and are required for both chromosomal end protection and regulation of telomere length, e.g., telomere-binding protein subunit alpha/beta (TEBPαβ) from *Oxytricha nova*; (C. M. Price & Cech, 1987), Cell division cycle 13 (Cdc13p) from *S. cerevisiae* (Garvik et al., 1995) and POT1, are present in diverse organisms including human, mouse, chicken or *S. pombe* (Baumann & Cech, 2001; Lei et al., 2002; Wei & Price, 2004; L. Wu et al., 2006).

In *A. thaliana*, three POT-like proteins were named AtPOT1a (previously named AtPOT1-1, AtPot1), AtPOT1b (previously named AtPOT1-2, AtPot2) and AtPOT1c (Kuchař & Fajkus, 2004; Lei et al., 2002; Rossignol et al., 2007; Shakirov et al., 2005; Tani & Murata, 2005). AtPOT1a and AtPOT1b proteins contain two OB motifs as well as mammalian POT1 proteins, but share only 49 % sequence similarity, while mouse

proteins share 72 % similarity. AtPOT1c protein is short version of AtPOT1a and originates by gene duplication and contain only one OB motif (Rossignol et al., 2007) (**see Figure 3B and Figure 5)**.

However, descriptions of plant POT protein functions and binding properties are not unanimously agreed. While a very weak, but specific affinity of AtPOT1a and AtPOT1b expressed in *E. coli* for plant telomeric ssDNA was originally described (Shakirov et al., 2005), later these authors could not demonstrate AtPOT1a and AtPOT1b binding to telomeric ssDNA *in vitro* (Shakirov, McKnight, et al., 2009; Shakirov, Song, et al., 2009). In our laboratory, AtPOT1a and AtPOT1b proteins were expressed in bacteria or using *in vitro* WG transcription/translation extract. Unfortunately, none of these systems or their modifications resulted in expression of intact AtPOT1 proteins. AtPOT1 proteins were either not expressed or due to their hydrophobicity localized mainly in the bacterial inclusion bodies or they were co-purified with chaperon GroEL (**Schrumpfova, dissertation thesis**). There was no proof that the AtPOT1b, purified from bacterial extract or expressed *in vitro* translation extract, had the ability to bind telomeric ss oligonucleotides (**Schrumpfová, 2008; see Supp. C).** Subsequently it was demonstrated that functional human and mouse POT1 should be isolated from baculovirus-infected insect cells (Palm et al., 2009).

Nevertheless, stable telomeric ssDNA binding was observed for two full-length plant POT1 proteins: OlPOT1 from the green alga *O. lucimarinus* as well as for ZmPOT1b from *Z. mays* (Shakirov, Song, et al., 2009). Although POT1 proteins from plant species as diverse as *Populus trichocarpa* (poplar), *Hordeum vulgare* (barley), *Gossypium hirsutum* (cotton), *Helianthus argophyllus* (sunflower), *S. moellendorffii* (spikemoss), *Pinus taeda* (pine), *Solanum tuberosum* (potato), *Asparagus officinalis* (garden asparagus) and Z*. mays* (maize) (ZmPOT1a) failed to bind telomeric DNA when expressed in a RRL expression system *in vitro* and subjected to an electrophoretic mobility shift assay (EMSA) (Shakirov, Song, et al., 2009), binding of plant POT1 proteins to telomeric DNA under native conditions cannot be excluded.

Plants expressing AtPOT1a truncated by an N-terminal OB-fold, showed progressive loss of telomeric DNA. These findings denote that AtPOT1a plays role in positive regulation of telomere length (Surovtseva et al., 2007). In contrast, expression of only N-terminal part of AtPOT1b leads to severe defects in plant growth and development, telomeres are shortened and there is a high formation of anaphase bridges or defective segregation of chromosome, which means that AtPOT1b plays role in protection of chromosomal ends (Shakirov et al., 2005).

POT1 proteins from *A. thaliana* differ not only in their functions, but also have divergent interaction partners. AtPOT1a binds AtSTN1 and AtCTC1 proteins from CST complex (Renfrew et al., 2014). AtPOT1a, but not AtPOT1b, is associated with an N-terminal part of AtTERT in nucleoplasm *in vitro* (Rossignol et al., 2007). Among other interactors of AtPOT1a belongs CBL-interacting protein kinase (CIPK21). This kinase belongs to the large family in *A. thaliana* of which several members were shown to be involved in Ca^{2+}

signalling and moreover, CIPK21 is presumed to have a function in DDR signalling (Rossignol et al., 2007). These data suggest a potential role of AtPOT1a in DDR pathway as was described to many other telomeric proteins (Gallego & White, 2005). We found AtPOT1a protein among proteins that we co-purified with N-terminal domains of AtTERT using (TAP-MS) (**Schrumpfová and Majerská et al., 2017, 2018; see Supp. K and L**). Using BiFC it was confirmed that AtPOT1a interacts with AtCBF5 protein (Centromere-binding factor 5; a plant homologue of dyskerin) in the cytoplasmic or nucleolus foci (Kannan et al., 2008; Lermontova et al., 2007; **Schořová et al., 2019; see Supp. N**). Interestingly, AtPOT1a forms weak interaction with AtRUVBL1 protein. This fact corelates with our recent observation that AtPOT1a, AtTERT, AtTRB, AtCBF5 and AtRUVBL1 proteins are involved in assembly of the plant telomerase (**Schořová et al., 2019; see Supp. N**). Moreover, both AtPOT proteins directly interacts with AtTRB proteins (Kuchař & Fajkus, 2004; **Kusova et al., 2023; see Suppl. R)**, nevertheless, AtPOT1b does not seem to substantially contribute to telomere maintenance (Cifuentes-Rojas et al., 2012). Using Y2H and BiFC have also recently detected novel interaction between AtTRB4-5 and AtPOT1a (Kuchař & Fajkus, 2004; **Kusova et al., 2023; see Suppl. R)**.

CST is an evolutionarily conserved trimeric protein complex that in budding yeast is composed of the proteins Cdc13, Stn1 and Ten1, whereas in mammals the CST complex consists of the proteins CTC1, STN1 and TEN1. CST complex plays role in DNA replication and telomere maintenance through its ability to interact with ssDNA. Nevertheless, it was found out that CST is neither a nonspecific nor a telomere ssDNA specific binder, and rather CST is a tight binder of ssDNA with a preference for G-rich sequences (Hom & Wuttke, 2017). In yeast, these OB-fold proteins are required for recruitment of telomerase and DNA polymerase α to the chromosomal termini and thus coordinate G-overhang extension by telomerase with the fill-in synthesis of the complementary C-strand (Giraud-Panis et al., 2010; Grossi et al., 2004; Qi & Zakian, 2000; Wellinger & Zakian, 2012). Mammalian CST is ortholog of an archaeal RPA complex and is involved in the rescue of stalled replication forks either at the telomere or elsewhere in the genome and C-strand fill-in. However, CST in mammals is also proposed to limit telomerase action, perhaps by competing for binding to the telomere protein TPP1 (reviewed in Lue, 2018; Rice & Skordalakes, 2016; **Schrumpfova et al., 2019; see Supp. M**) (**see Figure 3A**).

CST in plants is needed for telomere integrity (Leehy et al., 2013; Surovtseva et al., 2007), however, clear evidence that would show any direct physical interaction of any component of the CST complex with plant telomeric DNA is absent. It seems that the CST complex controls access of telomerase, end-joining recombination and the ATR-dependent (ATM and Rad3-related) DNA damage response pathway at the chromosomal ends in wild-type plants (**see Figure 3B**) (Amiard et al., 2011; Boltz et al., 2012; Derboven et al., 2014; Leehy et al., 2013; **reviewed in Schrumpfova et al., 2019; see Supp. M**).

Non-OB-fold proteins

Aside predominantly characterised proteins with OB-fold domain associated with telomeric ssDNA sequence in plants, several proteins lacking the OB-fold domain were also identified, such as Whirly proteins or proteins with RNA recognition (RRM) motifs **(see Figure 5).**

The transcriptional activator protein Whirly 1 (AtWhy1), from a small protein family found mainly in land plants (Desveaux et al., 2000, 2002; Krause et al., 2005), was also identified in a fraction of AtTERT binding proteins in *A. thaliana* **(Schrumpfová and Majerská et al., 2017, 2018; see Supp. K and L)**. Although a T-DNA insertional mutation of AtWHY1 did not result in detectable abnormal phenotypes, *atwhy1* mutant plants contained longer telomeres, whereas AtWHY1 overexpressing plants showed shortened telomeres and decreased telomerase activity (Yoo et al., 2007). While proteins from *A. thaliana* (AtWhy1) and from *Hordeum vulgare* (HvWhy1) (Grabowski et al., 2008) were found to bind plant telomeric repeat sequences *in vitro*, diverse organelle localization of other Why family members from *O. sativa*, *A. thaliana*, *S. tuberosum* (Krause et al., 2005; Schwacke et al., 2007) and proposed binding to ssDNA of melted promoter regions (Desveaux et al., 2002), rather indicate a role in communication between plastid and nuclear genes encoding photosynthetic proteins (Comadira et al., 2015; Foyer et al., 2014). Overall, it seems that Why proteins bind to various DNA sequences, including: telomeres; a distal element upstream of a kinesin gene; the promoter region of the early senescence marker gene AtWRKY53 (in a development-dependent manner) in *Arabidopsis*. It was further proposed that WHY1 proteins bind to both ssDNA and RNA in *Z. mays* chloroplasts, where it plays a role in intron splicing and WHY1 is associated with intron-containing RNA in barley chloroplasts (Guan et al., 2018).

Among other proteins lacking OB-fold from *A. thaliana*, belongs truncated derivative of chloroplast RNA-binding protein (AtCP31) with RRM motif, named AtSTEP1 (single- stranded telomere-binding protein 1) **(see Figure 5)**. AtSTEP protein localizes exclusively to the nucleus, specifically binds single-stranded G-rich plant telomeric DNA sequences and inhibits telomerase-mediated telomere extension (Kwon & Chung, 2004).

A 36-kD protein identified by EMSA that specifically binds the G-strand of telomeric ssDNA from *N. tabacum* (NtGTBP1) also contains a tandem pair of RRM motifs (Hirata et al., 2004). NtGTBP1 is not only associated with telomeric sequences, as well as two additional GTBP paralogs (NtGTBP2 and NtGTBP3), but also inhibits telomeric strand invasion *in vitro* and leaves of knockdown tobacco plants contained longer telomeres with frequent formation of extrachromosomal T-circles (see bellow) (Lee & Kim, 2010). These observations correspond to a previously detected protein from tobacco nuclei that binds G-rich telomeric strands and reduces accessibility to telomerase or terminal transferase (Fulnečková & Fajkus, 2000). Fulnečková and Fajkus detected a 40 kDa polypeptide by SDS-PAGE after cross-linking the complex formed

by extracts from tobacco leaf nuclei. In addition to the above described proteins, various telomeric ssDNA binding proteins have also been reported in nuclear extracts from *Glycine max*, *A. thaliana*, *O. sativa* or *Vigna radiata* (Ho Lee et al., 2000; Kim et al., 1998; Kwon & Chung, 2004; Zentgraf, 1995). However, precise characterization of these proteins, identified by EMSA is mostly missing.

2 Interstitially located telomeric repeats

Telomeric repeats are not exclusively located at the physical ends of chromosomes, known as telomeres. They are also present in multiple internal sites of chromosomes in many species, where they are referred to as interstitial telomeric sequences (ITSs) (also named interstitial telomeric repeats (ITRs) or even very short internally localized telomeric repeats (named *telo*-boxes). ITSs are relatively abundant in subtelomeric, pericentromeric, and centromeric regions of most eukaryotic organisms, but can also be found at various positions throughout chromosomes. Short internally localized telomeric repeats - called *telo*-boxes - are composed of one to two telomeric DNA repeats. However, the defining of these groups is not entirely precise and may vary in various scientific resources (Aksenova & Mirkin, 2019; Tremousaygue et al., 1999; Uchida et al., 2002).

Most interstitial telomeric sequences studied in the human genome are short ITSs with lengths varying from 2–25 copies. They are present in all human chromosomes in subtelomeric regions as well as far from chromosomal ends (Aksenova & Mirkin, 2019; Azzalin et al., 2001; Ruiz-Herrera et al., 2009). Recent studies suggested function of ITSs in the stability of the genome and specifically at the role played by ITSs in interacting with the nuclear envelope and shaping the genome's 3D structure. A model of mammalian chromosomal organization involves interaction of telomeres with ITSs and nuclear Lamins (Lamin A/C) (Vicari et al., 2022; A. M. Wood et al., 2014). Long ITSs represent fragile parts of chromosomes, which are prone to rearrangements and recombination's (reviewed in Aksenova & Mirkin, 2019).

In *A. thaliana*, 8 regions of long ITSs were described on three chromosomes, ranging from 300 bp to 1.2 kb (Uchida et al., 2002). Large blocks of telomeric repeats were found in pericentromeric regions of some chromosomes in representatives of the Solanaceae family (He et al., 2013). Interestingly, the large blocks of imperfect telomeric repeats were found as well in the proximity of centromeres of all *Ballantinia antipoda* (Brassicaceae) chromosomes (Mandáková et al., 2010), however, in *N. tabacum*, no detectable ITS regions were observed (Majerová et al., 2014) while telomere lengths ranged from 20 to 160 kb (Fajkus et al., 1995; Kovařik et al., 1996).

Aside of long telomeric repeats the *Arabidopsis* genome contains very short interspersed segments (*telo*-boxes) of the telomeric sequence both mainly in interstitial positions. These short *telo*-boxes, exhibit a non-random distribution. They were described in the promoters of genes coding for translation elongation

factor EF1a (Liboz et al., 1990), promoters of many ribosomal protein coding genes (Tremousaygue et al., 1999) and promoters of genes involved in the biogenesis of the translation machinery (Gaspin et al., 2010).

We developed our own program, named Gene RegulatOry ELEMents (GOLEM) https://golem.ncbr.muni.cz/ **(Nevosad et al., in preparation)**, to precisely localize the distribution of *telo*-boxes in the vicinity of the Transcription Start Site (TSS) and Translation Start Site (ATG). Using this program, we found that most of the *telo*-boxes in the *Arabidopsis* genome are located in very close proximity to the TSS. Additionally, we discovered that genes with high transcription levels in plant leaves or during certain stages of gametophyte development tend to have *telo*-boxes located predominantly 100 bp downstream of the TSS **(Klodová et al., in preparation)**.

2.1 Proteins associated with long interstitial telomeric repeats (ITSs)

The long extra-telomeric repeats can be recognised by the proteins that were previously characterised as telomere-binding. In yeast several proteins were found to be associated with an artificial interstitial telomeric tract or subtelomeric ITSs, e.g. Rap1, KU or Tbf1 proteins (reviewed in Aksenova & Mirkin, 2019). Also in mammals Shelterin components occupy selective ITSs in the human genome, e.g. long artificial ITSs showed enrichment in hTRF1 and hTRF2 proteins, as well as in the hTRF2-interacting partner, Apollo exonuclease (Simonet et al., 2011; Ye et al., 2010). The region 2q14 on human chromosome, containing stretches of degenerate TTAGGG repeats, binds hTRF1, hTRF2, hRAP1 and hTIN2 proteins (Fan et al., 2002). These extra-telomere located Shelterin components thus participate in additional roles, e.g. gene activation and repression, DNA replication, heterochromatin boundary-element formation, creation of hotspots for meiotic recombination and chromatin opening (reviewed in Aksenova & Mirkin, 2019; **Schrumpfová et al., 2016a; see Supp. J**).

Using Chromatin immunoprecipitation assay combined with Next generation sequencing (ChIP-Seq) we revealed preferential association of AtTRB1 protein with long telomeric repeats, but not centromeric or 18S rDNA sequences **(Schrumpfová et al., 2016b; see Supp. I**).

Recently we contributed to the findings that histone H1 selectively prevents accumulation of trimethylation of lysine 27 of histone H3 (H3K27me3) at telomeres and long-ITSs by restricting DNA accessibility to AtTRB proteins. It was proposed that H1 safeguards telomeres and long-ITSs against excessive H3K27me3 deposition and preserves their topological organization. Despite low protein sequence similarity of H1/H5 domain of AtTRBs and H1 (14%), AtTRBs display a typical H1/H5 domain, that may antagonize chromatin incorporation of the H1/H5 of AtTRB and H1 proteins and might modulate PRC2 recruitment at ITSs (**Teano et al, 2023; see Suppl. S)**.

2.2 Proteins associated with short internally localized telomeric repeats (*telo*-boxes)

In our study Schrumpfová et al., we were the first group to describe the association of AtTRB1 with *telo*-boxes in the plant genome **(Schrumpfová et al., 2016b; see Supp. I)**. Moreover, we found out that AtTRB1 is bound to *telo*-boxes in promoters all over the genome. Almost 28 % of *telo*-box sequences located in the 5' UTR region of the genes coding proteins are covered by AtTRB1. As *telo*-box sequences are preferentially located in the promoters of genes involved in the biogenesis of the translation machinery we proposed role of AtTRB proteins in regulation of several genes, especially genes involved in biogenesis of the translational machinery **(Schrumpfová et al., 2016b; see Supp. I)** (**see Figure 6**).

Our observation that AtTRB proteins are associated with *telo*-box sequences located outside the telomeres was later proven by group of Franziska Turck. Zhou et. al. (2016) showed that AtTRB1 binds to thousands of genomic sites containing *telo*-box or related cis-elements with a significant increase of sites and strength of binding in the mutant plants for Like Heterochromatin Protein 1 (AtLHP1) (Zhou et al., 2016, 2018). AtLHP1 is a plant Polycomb Repressive Complex 1 (PRC1) component that directly binds to H3K27me3 (Turck et al., 2007).

It was further shown that *telo*-boxes are part of the cis-regulatory elements that may relate to recruitment of Polycomb repressive complex 2 (PRC2) which may regulate transcription of target genes through histone

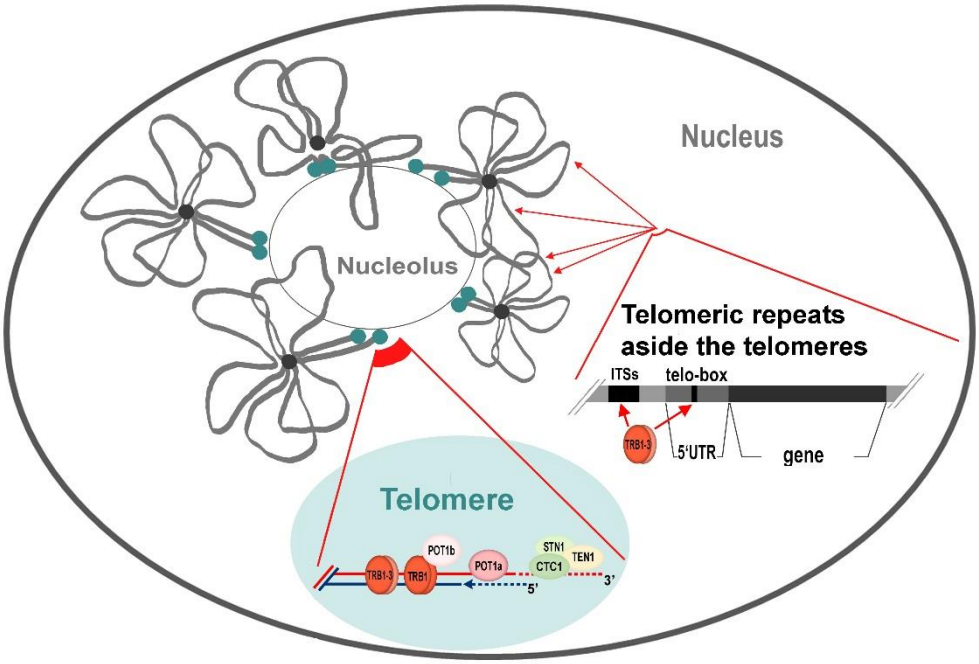

Figure 6. **An overview of telomeric and non-telomeric locations of TRB1 protein within *A. thaliana* nucleus, where the telomeres are clustered in a rosette-like configuration, including nucleolus-associated telomeres.** Modified from **Schrumpfová et al. (2016b, see Supp. I).**

modifications. Zhou et al., 2018 have show direct interaction between AtTRB1,2,3 and CURLY LEAF (AtCLF) and SWINGER (AtSWN) subunits of PRC2 complex. Recently we have described novel interaction between AtTRBs and EMBRYONIC FLOWER 2 (AtEMF2) and VERNALIZATION 2 (AtVRN2) subunits of PRC2 complex (**Kusova et al., 2023; see Suppl. R)**.

There was also proposed role of AtTRB proteins in PEAT complex (PWWPs-EPCRs-ARIDs-TRBs). PEAT complex may mediate histone deacetylation and heterochromatin condensation and thereby facilitate

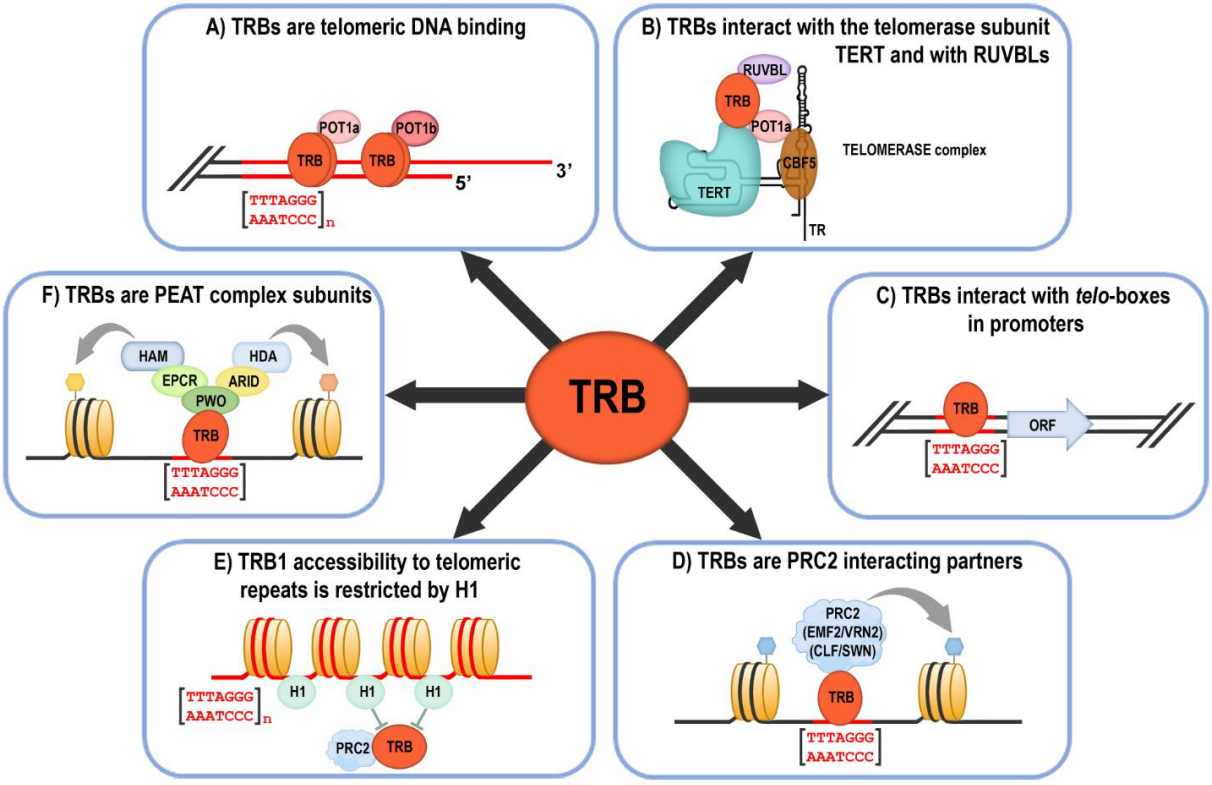

Figure 7. Overview of the main Telomere repeat binding proteins (TRBs) functions (Kusova et al., 2023; see Suppl. R).

A) TRBs are associated with the physical ends of chromosomes (telomeres) via their Myb-like domain **(Schrumpfová et al. 2004; see Suppl. A; Mozgová et al. 2008; see Suppl. D;** Dvořáčková et al. 2010; **Schrumpfová et al. 2014; see Suppl. H;** Dreissig et al. 2017). TRBs interact with Arabidopsis homologs of the G-overhang binding protein Protection of telomere 1a, b (POT1a, b) (**Schrumpfová et al. 2008; see Suppl. D; Kusova et al., 2023; see Suppl. R**).

B) TRBs mediate interactions of Recombination UV B – like (RUVBL) proteins with the catalytic subunit of telomerase (TERT) (Oguchi et al. 1999), and participate in telomerase biogenesis **(Schrumpfová et al. 2014; see Suppl. H; Schořová et al. 2019; see Suppl. N).** TRBs are associated in the nucleus/nucleolus with POT1a **(Schořová et al. 2019; see Suppl. N)**, and also with a plant orthologue of dyskerin, named CBF5 (Lermontova et al. 2007) that binds the RNA subunit of telomerase (TR) (Fajkus et al. 2019; Song et al. 2021).

C) TRBs are associated with short telomeric sequences (telo-boxes) in the promoters of various genes in vivo, mainly with translation machinery genes **(Schrumpfová et al. 2016; see Suppl. I)** . ORF, Open reading frame.

D) Telo-box motifs recruit Polycomb repressive complexes (PRC2) via interactions of PRC2 subunits with TRB (Zhou et al. 2016; Zhou et al. 2018, this study) CLF, CURLY LEAF; SWN, SWINGER; EMF2, EMBRYONIC FLOWER 2; VRN2, VERNALIZATION 2.

E) Histone H1 prevents the invasion of H3K27me3 and TRB1 over telomeres and long interstitial telomeric regions **(Teano et. al, 2023; see Suppl. S).**

F) TRB proteins, as subunits of the PEAT (PWO-EPCR-ARID-TRB) complex, are involved in heterochromatin formation and gene repression, but also have a locus-specific activating role, possibly through the promotion of histone acetylation (Tan et al. 2018; Tsuzuki and Wierzbicki 2018; Mikulski et al. 2019).

heterochromatin silencing. PEAT complex represses in heterochromatin regions the production of small interfering RNAs (siRNAs) and DNA methylation in *A. thaliana* (Tan et al., 2018; Tsuzuki & Wierzbicki, 2018). On the other hand, PEAT complex may possess a locus-specific activating role, possibly through promoting histone acetylation through two MYST-type histone acetyltransferases, AtHAM1 and AtHAM2. The composition of PEAT indicates that it binds to specific regions of chromatin, probably *telo*-boxes via AtTRB protein, and adds or removes acetyl groups from histones (Tan et al., 2018; Tsuzuki & Wierzbicki, 2018).

Additionally, AtTRB2 directly interacts with histone deacetylases, AtHDT4 and AtHDA6, *in vitro* and *in vivo* (Lee & Cho, 2016). Deacetylase activity of AtHDT4 (W. K. Lee & Cho, 2016) and AtHDA6 (To et al., 2011) against acetylation of lysine 27 of histone H3 (H3K27ac), could be important for subsequent methylations of H3K27me3, that is among others target also for AtLHP1.

Recently was identified a PWWP Interactor of Polycombs 1 (PWO1) as a novel plant-specific factor associated with chromatin and PRC (Hohenstatt et al., 2018). PWO1 associates physically with CRWN1, that is one of the Lamin-like genes in *Arabidopsis* forming the plant-specific CROWDED NUCLEI (CRWN) family. The authors speculated that PWO1 links H3K27me3-marked chromatin and the nuclear periphery in plants. Interestingly, AtTRB1 protein was identified as putative interactors of PWO1 in Co-IP experiments coupled with MS using the PWO1:PWO1-GFP *Arabidopsis* transgenic line (Mikulski et al., 2019).

Very recent it was demonstrated AtTRBs also associate and colocalize with JUMONJI14 (JMJ14) and trigger H3K4me3 demethylation at some loci (Wang et al., 2023). JMJ14 is histone H3K4 demethylase regulating flowering time in *Arabidopsis* (Lu et al., 2010). The *attrb1/2/3* triple mutant and the *atjmj14-1* mutant show an increased level of H3K4me3 over AtTRB and JMJ14 binding sites, resulting in up-regulation of their target genes (Wang et al., 2023).

Overall, we can hypothesise that although the TRBs were originally characterized as being associated with long arrays of telomeric repeats (see **Figure 7A, E**), recent observations indicate broad engagement of TRB proteins in various cellular pathways via recruiting various complexes to *telo*-boxes (**see Figure 7C, D, F**).

3 Orchestration of telomere homeostasis

Regulation of the telomere length homeostasis is very complex problem and is achieved via a balance between telomere lengthening and erosion over successive cell divisions. Additionally, the processes of telomere maintenance can be orchestrated by various telomere- and telomerase-associated proteins. Mammalian telomeres are recognized not only with above mentioned proteins (Shelterin complex, POT proteins, CST complex etc.) but telomere maintenance mechanisms appear to be affected by hundreds of proteins, However, activities of these plant telomere, and telomerase-associated proteins, are only partly understood. Some of these proteins were described in several broad studies, e.g. the hTERT associated

proteins (proteins were detected using TAP-MS) (Fu & Collins, 2007), telomeric factors associated with human telomeric chromatin (Déjardin & Kingston, 2009) or protein network surrounding Shelterin subunits - TRF1, TRF2, POT1 and TIN2 (Giannone et al., 2010; Grolimund et al., 2013; Nittis et al., 2010). The putative partners associating with Shelterin proteins fell into functional categories such as DNA damage repair, ubiquitination, chromosome cohesion, chromatin modification/remodelling, DNA replication, cell cycle and transcription regulation, nucleotide metabolism, RNA processing and nuclear transport. These putative protein-protein associations may participate in different biological processes at telomeres or, intriguingly, outside telomeres.

3.1 Telomerase

As was already described above, telomeres cannot be fully replicated by enzymes that duplicate DNA, so the telomere shortening occurs with each round of DNA replication. Critically shortened telomeres are no longer able to protect chromosome ends from DNA repair and degradation activities and these phenomena can lead to replicative senescence and finally cell death (Lundblad & Szostak, 1989).

Telomerase is a ribonucleoprotein that adds a species-dependent telomere repeat sequence to the 3' end of telomeres and elongates the telomeres. In humans, telomerase activity was detected in all early developmental stages. However, just after birth, telomerase activity in somatic cells is downregulated with the exception of highly dividing cells (e.g. proliferating cells, T-lymphocytes, hair follicle bulbs) (reviewed in **Schrumpfová et al., 2019; see Supp. M**).

However, somatic downregulation of telomerase is not conserved mechanism across species, and the presence of telomerase activity has to be individually tested in each individual species, tissue or even in different age-classes (Gomes et al., 2011; Haussmann et al., 2007; Seluanov et al., 2007). For example: most rodent species show high telomerase activity in multiple somatic tissues (*Mus musculus*, *Rattus norvegicus*, *Hetrocephalus glaber* etc.) and only beaver and capybara show nearly complete somatic repression of telomerase activity, similar to humans (Seluanov et al., 2007). There was shown a clear tendency for species smaller than 1 kg to have long telomeres and active telomerase, but species larger than 1 kg have tendency to have short telomeres and repress telomerase (Gomes et al., 2011).

Also plant cells possess telomerase which is used for maintenance of their telomeres (Fajkus et al., 1996; Heller et al., 1996). Active telomerase was detected in organs and tissues containing highly dividing meristem cells such as seedlings, young and middle-age leaves, root tips, floral buds and flowers (Fajkus et al., 1998; Fitzgerald et al., 1996). In terminally differentiated tissues (stems, mature leaves), telomerase activity is suppressed (Jurečková et al., 2017; Ogrocká et al., 2012; Riha et al., 1998; reviewed in **Schrumpfová et al., 2019; see Supp. M**).

As was already mentioned above, the two core subunits of telomerase are telomerase reverse transcriptase (TERT), which possesses catalytic activity, and telomerase RNA subunits (TR), which contain a template region directing the synthesis of DNA repeats at the ends of chromosomes.

3.1.1 Telomerase reverse transcriptase (TERT)

Telomerase protein catalytic subunit (TERT) contains several conserved motifs and domains. The TERT protein contains N-terminally located telomerase-specific motifs important for binding the telomerase RNA subunit (TRBD), centrally located catalytic domains with the RT motifs essential for enzyme activity (RT) and the C-terminal extension (CTE), which is highly conserved among vertebrates as well as among plants (**see Figure 8B**). The motifs localized at the N-terminus are telomerase-specific (T2, CP, QFP and T) and are

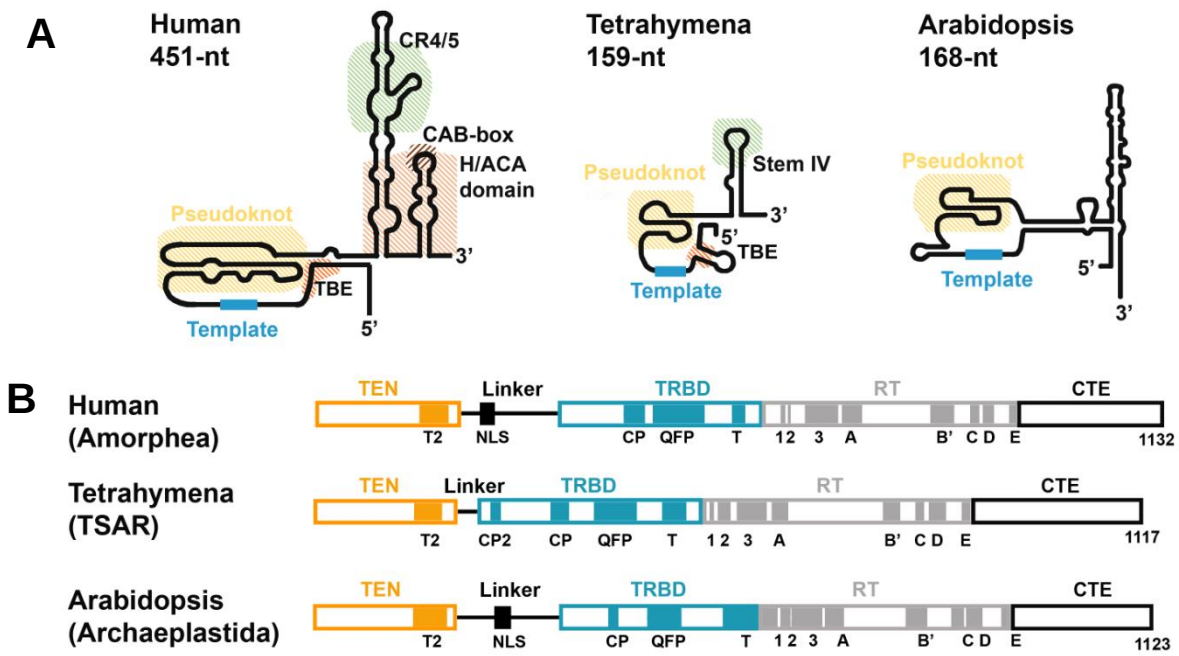

Figure 8. Conservation of functional domains of two core telomerase subunits – TERT and TR (adopted from Schrumpfová et al., 2020; see Supp. O) .

A) Models of secondary structures of human, *Tetrahymena* and *Arabidopsis* TRs suggest conservation of several structural motives including pseudoknot in the vicinity of the template (t/PK domain) and stem-loop region. In humans the stem-loop region contains the conserved 4/5 (CR4/5) region, the H (AnAnnA) and ACA-boxes (H/ACA) domains and the Cajal body box (CAB-box) motif that serve as binding sites for other protein components of the telomerase holoenzyme complex (dyskerin, NOP10, NHP2, and GAR1). In Tetrahymena the stem-loop 4 (SL4) is directly bound by p65 protein. To date, particular interactors and their binding sites have not been demonstrated directly in *Arabidopsis*.

B) Domain arrangement of human (Animals), *Tetrahymena* (Ciliates) and *Arabidopsis* (Plants) TERTs. The supergroup for each species is given. N-terminus: telomerase essential N-terminal (TEN) domain and RNA-binding domain (TRBD domain) are separated by Linker that contains a nucleus localization-like signal (NLS). The central RT domain: catalytical part of the enzyme that contains seven evolutionary-conserved RT motifs (1, 2, A, B', C, D and E motifs) and also telomerase specific 3 motif. C-terminus: C-terminal extension (CTE) domain.

important for binding the telomerase RNA subunit. The centrally located RT motifs (1, 2 and A–E) are essential for enzyme activity (reviewed in Sýkorová & Fajkus, 2009). The human telomerase complex purified from human cell line overexpressing hTERT and hTR forms a dimeric structure (Sauerwald et al., 2013). However, the presence of two catalytically active hTERT subunits has been a topic of controversy, as indicated by other studies. Although, the biological significance of a dimeric telomerase RNP is unclear, it could perhaps facilitate telomerase recruitment to telomeres by providing multiple binding sites, thus increasing the affinity for its telomeric receptor (reviewed in Schmidt & Cech, 2015). We performed Y2H screening of several AtTERT fragments. These fragments of AtTERT were previously designed to variously cover N-terminal, TRBD, RT or CTE domains (Zachová et al., 2013). According our results, dimerization of AtTERT in *A. thaliana* can be mediated by the RNA binding domain (TRBD) that is able to interact separately with the N-terminal fragments and itself **(Schrumpfová and Majerská et al., 2017, 2018; see Supp. K and L).**

In AtTERT, multiple nuclear localization signals (NLS), nuclear export signal (NES) or a mitochondrial targeting signal were reported (Zachová et al., 2013). Due to the presence of these signals, AtTERT protein and its domains localize mainly within the nucleus and the nucleolus of *A. thaliana* (Rossignol et al., 2007; Zachová et al., 2013). Similarly in our study we localised AtTERT domains in the nucleolus. According to our observation that AtTERT domains can be colocalized together with the AtRUVBL, AtTRB and AtCBF5 proteins in the nucleolus, we hypothesised that AtTERT nucleolus localisation may be part of the telomerase assembly pathway **(Schořová et al., 2019; see Supp. N**).

Apart from telomeric functions of telomerase in the nucleus, there was reported the presence of telomerase in other subcellular compartments or telomerase putative involvement in signalling pathways, transcriptional regulation and stress protection (reviewed in Majerská et al., 2011).

It has been proposed that human telomerase is subjected to posttranslational regulation such as phosphorylation (Kang et al., 1999). Putative phosphorylation sites were also detected in the TERT sequences from *O. sativa* or *N. tabacum* BY-2 cells but not in AtTERT from *A. thaliana* (Oguchi et al., 2004; Yang et al., 2002). Moreover, in tobacco cell culture, phytohormones such as auxin or abscisic acid regulate phosphorylation of telomerase protein, which is required for the generation of a functional telomerase complex (Tamura et al., 1999; Yang et al., 2002).

3.1.2 Telomerase RNA (TR)

Compared to the conserved structure of the TERT subunit, TRs show high sequence diversity among more distant organisms, as exemplified by the length differences of TRs in protozoa (159 nt in ciliate *Tetrahymena*, 2200 nt in *Plasmodium*), zebrafish (317 nt), mouse (397 nt), human (451 nt) and budding

yeasts (1160 nt). Even within yeasts, the homology among TRs is rather low and their lengths range from 930 nt to more than 2000 nt (**see Figure 8B)** (reviewed in **Schrumpfová et al., 2019**; **see Supp. M;** Webb & Zakian, 2016; Zhang et al., 2011).

In *A. thaliana*, there were earlier reported two AtTR candidates, named AtTER1 and AtTER2 (Cifuentes-Rojas et al., 2011, 2012). It was shown that AtTER1 is able to provide a templating function in telomerase reconstitution experiments *in vitro* but direct evidence of its *in vivo* function were missing (Fajkus et al., 2019). However, later it was found out that neither AtTER1 nor AtTER2 serve as RNA subunits of active telomerase and the article Cifuentes-Rojas et 2011 was retracted.

It seems that the natural templating subunit of telomerase in *Arabidopsis*, as well in other land plants, are TRs identified by our group (Fajkus et al., 2019). My colleagues used unusually large length of the *Allium* telomere repeat unit (12 nt) and identified the candidate TRs in transcriptomes. Based on the *Allium* TRs, they consequently identified TRs orthologs in the other land plants. AtTR has been characterized earlier as a hypoxic stress-responsive long non-coding RNA (lncRNA) transcribed by RNA polymerase III (Pol III) in *A. thaliana* (AtR8) and related *Brassicaceae* species. All AtTR identified homologs in other plant species possess the conserved Pol III type 3 promotor with specific localization of USE and TATA boxes and poly-U terminator elements (Wu et al., 2012, 2019). It seems that land plant *TR* gene is highly conserved in contrary to the very divergent *TR* genes found in animal, yeast or protozoan models (Fajkus et al., 2019).

Models of secondary structures of human, *Tetrahymena* and *Arabidopsis* TRs suggest conservation of several structural motives. The most prominent are pseudoknot in the vicinity of the template (t/PK domain), stem-loop regions and template boundary element (TBE). In humans the stem-loop region contains the conserved 4/5 (CR4/5) region, the H (AnAnnA) and ACA-boxes (H/ACA) domains and the Cajal body box (CAB-box) motif that serve as binding sites for other protein components of the telomerase holoenzyme complex. The TBE defines the end of the sequence recognized by TERT as a template (reviewed in **Schrumpfová et al., 2020; see Supp. O**).

Evolution of both subunits of telomerase, TERT and TR, were discussed at The Czech Plant Nucleus Workshop 2021. The results, together with other results focused on maintenance of the chromosome ends, were summarized in the Conference report named The Czech Plant Nucleus Workshop 2021 **(Pecinka et al., 2022; see Supp. P).**

3.1.3 Telomerase-associated proteins

Besides these two core subunits, TERT and TR, the telomerase complex comprises several other accessory proteins with diverse roles in telomerase assembly, trafficking, localization, recruitment to telomeres or the processivity of telomere synthesis (Chan et al., 2017; Nguyen et al., 2018) (**see Figure 9 and Figure 10**).

In humans the active telomerase is associated with Hsp90 and p23 chaperones as well as with TR associated with conserved scaffold proteins of box H/ACA small nucleolar RNAs (dyskerin, Non-histone protein 2 (NHP2), Nucleolar protein 10 (NOP10), Glycine arginine rich 1 (GAR1)). The telomerase RNP is probably retained into the nucleoli through the interaction between TERT and nucleolin. Assembly of TR and TERT into catalytically active telomerase is aided by Pontin (RUVBL1) and Reptin (RUVBL2) **(**reviewed in **Schořová et al., 2019; see Supp. N) (see Figure 9A)**.

In plants, a limited number of proteins that directly interact with TERT were described. Using Tandem Affinity Purification coupled to Mass Spectrometry (TAP-MS) we co-purified and identified several putative AtTERT interaction partners **(Schrumpfová and Majerská et al., 2017, 2018; see Supp. K and L**). To confirm putative protein-protein interactions between AtTERT and proteins of interest, we used Y2H, Co-IP and BiFC systems. As some of the proteins of interest showed indirect interaction with AtTERT, to achieve reproducible results we used many modifications, improvements and mutual combination of Y2H, BiFC and Co-IP. Our optimized BiFC protocol in *A. thaliana* protoplasts provided us a robust tool to observe direct or even indirect interactions of (not only) telomere- and telomerase-associated proteins and to distinguish nucleus, nucleolus or cytoplasmic localization of these interactions. Our modification of Co-IP technique (Co-Immunoprecipitation with Three Proteins of Interest) allowed detection not only of two proteins of interest, as is common, but also detection of trimeric complexes, where two proteins of interest interact indirectly via a protein sandwiched in between them and mediating the interaction. Our improvements and modifications of these protein-protein interaction techniques were described in the book chapter named

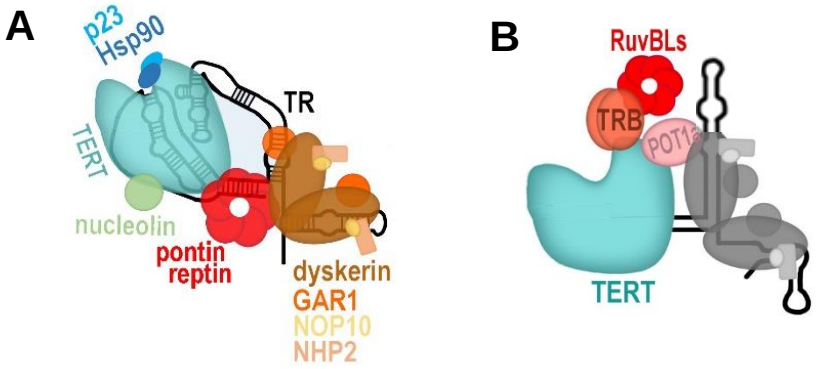

Figure 9. Comparative model of telomerase in human and *Arabidopsis* localised in the nucleolus.

A) Human active telomerase is associated with Hsp90 and p23 chaperones as well as with TR associated with conserved scaffold proteins of box H/ACA small nucleolar RNAs (dyskerin, NHP2, NOP10, GAR1). The telomerase RNP is retained into the nucleoli through the interaction between TERT and nucleolin. Assembly of TR and TERT into catalytically active telomerase is aided by Pontin (RUVBL1) and Reptin (RUVBL2).

B) TERT colocalize with RUVBL proteins, bridged by telomeric TRB proteins, in the nucleolus as well as the interaction of telomeric protein POT1a with *Arabidopsis* CBF5 (dyskerin). CBF5 together with GAR1, NOP10, NHP2, but in contrast with human cells also NAF1, were localized in the plant nucleolus, however entire association with active telomerase holoenzyme has to be elucidated. Modified from **Schořová et al., 2019; see Supp. N**.

'Analysis of direct and indirect protein-protein interactions of telomere-associated proteins' (Methods in Molecular Biology, The Nucleus, Book Series, Springer protocols (**Schořová et al., 2020**).

In our laboratory, we have demonstrated that AtTRB proteins, physically interact with N-terminal domains of AtTERT (**see Figure 3B and 9B).** We also suggested a mediated interaction between Telomeric Repeat Binding Protein 1 (AtTRP1) protein and AtTERT (**Schrumpfová et al., 2014; see Supp. H**). Rossignol et al. observed that the N-terminal part of AtTERT exclusively interacts with AtPOT1a but not AtPOT1b (Rossignol et al., 2007). As well various other proteins from *A. thaliana* were shown to be associated with AtTERT: AtRRM (RNA recognition motif (RRM)), AtARM (armadillo/β-catenin-like repeat-containing protein), AtCHR19 (chromatin remodeling protein), AtMT2A (Metallothionein-like), AtG2p (RNA-binding), AtPURα1 (Pur-alpha 1), AtNUC-L1 (Nucleolin like 1) or Importin4 (ImpA4) (Dokládal et al., 2015, 2018; Fulnečková et al., 2022; Pontvianne et al., 2010, 2016; reviewed in **Schrumpfová et al., 2019; see Supp. M**). Some of these AtTERT partners that we co-purified with N-terminal fragments of AtTERT are possibly involved also in non-telomeric functions of telomerase, e.g. the human homologue of the AtPURα1 protein, named PURα, has been implicated in the control of gene transcription (Safak et al., 1999) and DNA replication (Bergemann & Johnson, 1992).

Among proteins co-purified with AtTERT fragments using TAP-MS we identified also AtRUVBL1 and AtRUVBL2a proteins (plant homologues of human Pontin and Reptin) **(Schrumpfová and Majerská et al., 2017, 2018; see Supp. K and L).** We closely characterised AtRUVBL1-AtTERT and AtRUVBL2a-AtTERT interactions in the plant cell and found out that, against mammalian counterparts, interaction between AtRUVBLs and AtTERT proteins in *A. thaliana* is not direct and is more likely mediated by one of the AtTRB proteins. Our data show that AtRUVBLs, together with AtTRBs protein, colocalize with N-terminal part of AtTERT subunit of plant telomerase in the plant nucleolus. It seems that AtRUVBLs are recruited into the AtTERT complex through an interaction with AtTRBs protein, which mediate interaction with both proteins: AtTERT and also with AtRUVBLs. Our data indicate the presence of AtTERT-AtTRB-AtRUVBL complex in the plant nucleolus (**Schořová et al., 2019; see Supp. N**).

In humans, proper catalysis, accumulation, 3' end processing, and localization of hTR are necessary for the creation of functional mature hTR, which provides the template for the synthesis of telomere DNA repeats. Human TR is associated with dyskerin, NOP10, NHP2 and GAR1, that displaces previously bound Nuclear assembly factor 1 (hNAF1) in the hTR RNP.

In *A. thaliana*, expression of putative AtGAR1, AtNOP10, AtNHP2 genes encoding protein components of the H/ACA box snoRNP complex correlate with that of AtCBF5 - plant homologue of dyskerin (Lermontova et al., 2007). AtCBF5 has been identified as a component of the enzymatically active *A. thaliana* telomerase RNP (Kannan et al., 2008; Lermontova et al., 2007). Scaffold proteins AtCBF5, AtGAR1, AtNOP10, AtNHP2,

but in contrast to human cells also AtNAF1, were localized into the plant nucleolus (Lermontova et al., 2007; Pendle et al., 2005). The association of TRs with dyskerin appears to be conserved between plant and animal kingdoms as telomerase activity was immunoprecipitated with the anti-plant dyskerin antibody from protein extract from *Allium cepa* seedlings (Fajkus et al., 2019). Moreover, despite the absence of a canonical H/ACA binding motif within AtTR, dyskerin binds AtTR with high affinity and specificity *in vitro* via a plant specific three-way junction (Song et al., 2021). However, it has not yet been elucidated whether plant homologues of human GAR1, NOP10, NHP2, or NAF1 are also part of the active holoenzyme of telomerase in plants.

Comparative overview of human and plant homologues of proteins associated either with the telomerase catalytic subunit TERT or with the RNA component of telomerase is reviewed in **Schrumpfová et al., 2019 (see Supp. M**).

3.1.4 Telomerase assembly

Proper assembly of TERT with TR into active and functional complex is stepwise regulated procedure governed also by multiple associated proteins (reviewed in Shepelev et al., 2023; reviewed in **Schrumpfova et al., 2020; see Suppl. O)**. Telomerase and its chromosome end substrate have very low abundance (~250 telomerases/184 telomeres in a human cell in late S phase) thus, it is perhaps not surprising that the telomerase enzyme is recruited to telomeres rather than simply encountering them by diffusion (Xi & Cech, 2014).

Transcription of the human *TERT* gene by RNA polymerase II (RNA Pol II) is regulated by several activators and repressors acting at the promoter level (e.g., c-MYC, Nuclear Factor κB (NF- κB), Signal Transducer and Activator of Transcription 3 (hSTAT3), Specificity Protein 1/3 (SP1/3). Histone modification H3K27me3 often silences *hTERT*, however the mutated *hTERT* allele is marked by the active histone marks H3K4me2, H3K4me3 and H3K9ac. All Pol II transcripts undergo processing events that are essential for their function. The *hTERT* pre-mRNA with a 5' mono-methylguanosine (MMG) cap and poly(A) 3' tail can be spliced into full-length (FL) or multiple alternative isoforms (Alternative splicing) that are catalytically inactive or even inhibit telomerase activity. The binding of heat shock protein 90 (hHsp90) with its co-chaperone (p23) in the cytoplasm enables hTERT phosphorylation (P). hTERT is further imported back to the nucleus by Importin α or β1 (hImp) via nuclear pores (n.p.), while the export of hTERT may be mediated by the chromosome region maintenance 1 protein homolog (hCRM1, also known as exportin-1). The ubiquitin (Ubq)-proteasomal degradation of hTERT is driven by E3 ubiquitin-protein ligase makorin-1 (MKRN1), heat shock protein 70 (Hsp70) and carboxyl-terminus of Hsp70 Interacting Protein (CHIP) (**see Figure 10A,** for references see **Schrumpfova et al., 2020; see Suppl. O).**

Histone modifications H3K4me2/3 or H3K9Ac help to regulate read-through of the human *hTR* gene by RNA Pol II in telomerase-positive cell lines. SHQ1 chaperone and RUVBLs facilitate the assembly of nascent RNA with RNA scaffold proteins (dyskerin, hNOP10, hNHP2, and hNAF1). Mature hTR is capped with a tri-methylguanosine (TMG) cap at the 5' end, polyadenylated at the 3' end and co-transcriptionally associated with scaffold proteins. The hTR variants with shorter or longer 3' ends, or those associated with variant proteins, may lead to the degradation of hTR. hNAF1 is replaced by hGAR1 before the hTR ribonucleoprotein complex reaches the nucleolus (**see Figure 10B).**

RUVBLs (Pontin and Reptin) enable telomerase assembly and allow hTERT recruitment to the nucleolus to form a mature telomerase complex while bound by nucleolin (hNCL). PIN2/TERF1-interacting telomerase inhibitor 1 (hPINX1), together with nucleophosmin (hNPM) and microspherule protein 2 (hMCRS2), regulate hTERT availability in a cell cycle-dependent manner. Telomere Cajal body protein 1 (hTCAB1, also known as hWRAP53) recognizes the Cajal body box (CAB-box) of the hTR in the mature telomerase complex and recruits it to the Cajal bodies (CBs). In CBs, hTR interacts with local proteins such as coilin while survival motor neuron protein (hSMN) binds hTERT (**see Figure 10C and Figure 11A).**

In the S-phase, the CBs colocalize with telomeres and facilitate the recruitment of the mature telomerase complex to the telomeres via interaction with hTPP1 protein, which is one of the subunits of a protein complex localized at telomeres, termed as Shelterin. The presence of Shelterin proteins (hTRF1/2, hPOT1, hTIN2, hRAP1 and TPP1) helps distinguish chromosomal ends (telomeres) from DNA breaks **see Figure 10D).**

Despite the fact that the entire TERT subunit is highly conserved across the phylogenetic tree and shows significant sequence homology between humans and plants (as reviewed in **Schrumpfova et al., 2020; see Suppl. O**), the assembly pathway of plant telomerase holoenzyme is not fully understood. However, our research has helped to partially elucidate the proteins associated with plant telomerase and their possible involvement in telomerase assembly.

In humans, the production of hTERT is highly regulated at the transcriptional levels and also post-transcriptional levels, whereas the *hTR* transcript is constitutively produced (Gladych et al., 2011). However, in plants, the transcription of both telomerase subunits (AtTERT and AtTR) is regulated during the plant development, as both subunits show high transcription in seedlings and young leaves, but diminished transcription in fully maturated leaves (Jurečková et al., 2017; Ogrocká et al., 2012; Riha et al., 1998; Fajkus et al., 2019; reviewed in **Schrumpfova et al., 2020; see Suppl. O**).

Plant *TERT* gene has a weak promoter. Fojtova et al. identified region 271 bp upstream of ATG as an putative 'minimal promoter' able to drive sufficient transcription of the telomerase protein subunit gene, resulting in normal telomerase function (Fojtová et al., 2011). In Crhak et al. it was proposed that unknown factors necessary for tissue-specific expression of telomerase activity and restoration of telomerase function in the

maintenance of telomere are needed (Crhák et al., 2019). Additionally, *AtTERT* gene might be regulated by regulatory element at the 5' end, e.g. within the intron 1, that has function at the level of transcription, while it is not involved in tissue-specific regulation (Fojtová et al., 2011).

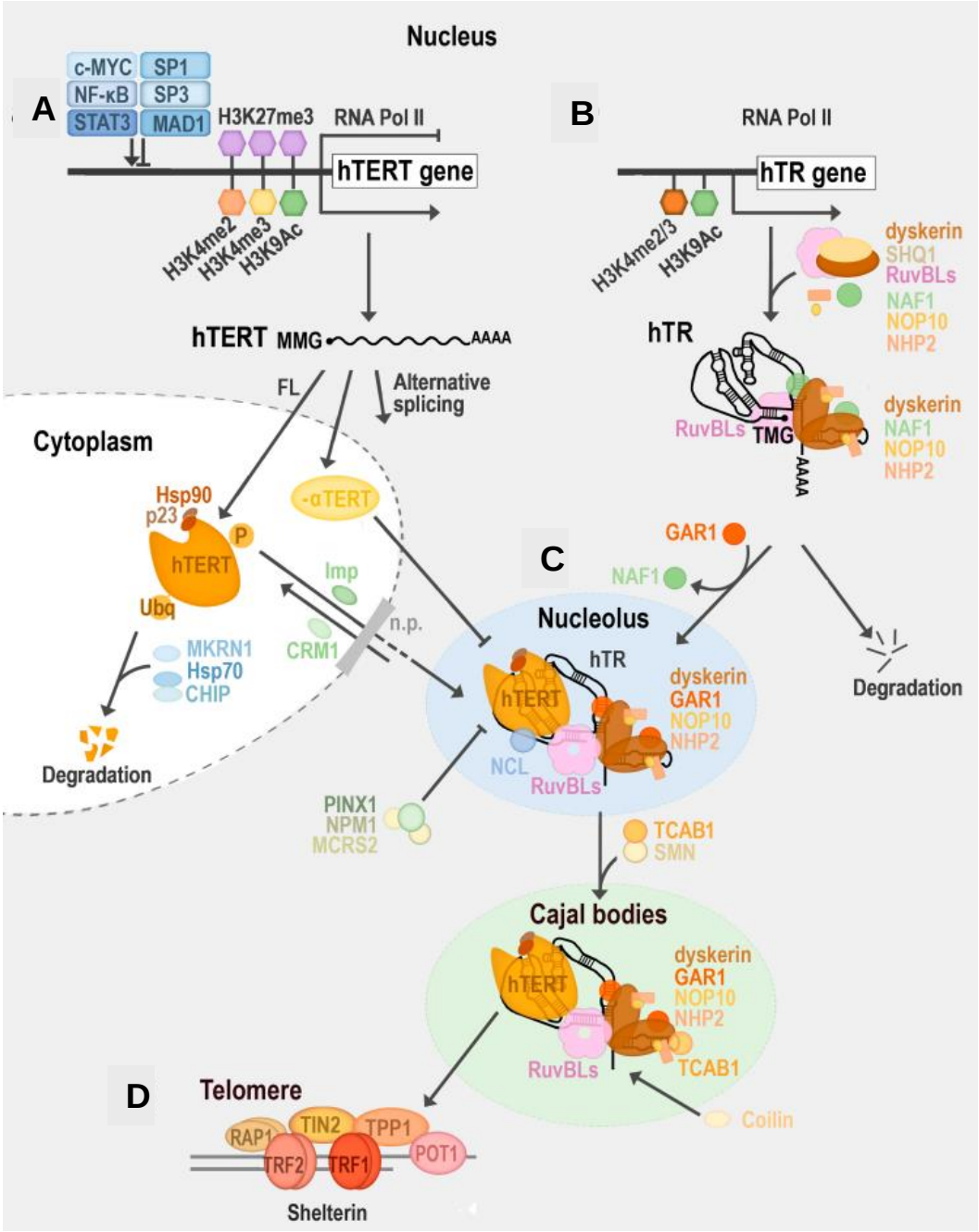

Figure 10. Regulation of human telomerase biogenesis (for description see text) (Schrumpfova et al., 2020; see Suppl. O).

A) Transcription of the hTERT is regulated by several activators and repressors acting at the promoter level.
B) Histone modifications help to regulate read-through of the human telomerase RNA (hTR) gene. Mature hTR is capped and recognised by several associated proteins.
C) RuvBLs (pontin and reptin) enable telomerase assembly and allow hTERT recruitment to the nucleolus to form a mature telomerase complex while bound by several other proteins.
D) In the S-phase, the CBs colocalize with telomeres and facilitate the recruitment of the mature telomerase complex to the telomeres.

In *A. thaliana*, mutation in the *attac1* (Telomerase activator 1) gene led to the induction of telomerase in fully differentiated leaves without stimulating progression through the cell cycle (Ren et al., 2004). However, AtTAC1 protein does not directly bind the *AtTERT* promoter and rather regulates telomerase activity through regulation of the AtBT2 (protein with BTB,TAZ and calmodulin binding domains) gene expression (Ren et al., 2007).

Alternatively spliced variants of *TERT* transcripts were also described in many plant species, e.g. *A. thaliana* (AtTERT), *Zea mays* (ZmTERT), *Oryza sativa* (OsTERT), *Iris tectorum* and tobacco (Rossignol et al., 2007; Sýkorová & Fajkus, 2009).

We have characterised RUVBL homologues in *A. thaliana* and outlined plausible conservation of the telomerase trafficking pathway in the land plants. We showed, that RUVBL1 and RUVBL2 proteins from *A. thaliana* are able to form either homo- or heteromers as well as their homologues in diverse organisms, although they preferably form mutual heteromers (**Schrumpfová and Majerská et al., 2017; Schořová et al., 2019; see Supp. K and N**). Our experiments with plant RUVBL proteins showed that depletion of AtRUVBL1 and especially of AtRUVBL2a protein, reduced telomerase activity in plants with T-DNA insertion in *AtRUVBL1* or *AtRUVBL2a* genes, respectively. We did not observe significant changes in transcripts of *AtTERT* gene in *AtRUVBL1* heterozygous mutant plants and very slight, though significant, increase, in transcripts of *AtTERT* gene in *AtRUVBL2* heterozygous mutant plant lines (**Schořová et al., 2019**; **see Supp. N**). Similarly to our results, both human RUVBL proteins, hRUVBL1 and hRUVBL2, regulate *hTERT* both on the gene and protein levels, only hRUVBL2 depletion inhibits *hTERT* promoter activity through the regulation of c-Myc (Mao & Houry, 2017; Venteicher et al., 2008).

It was already mentioned that our data indicate AtRUVBL1 recruitment into the AtTERT complex through an interaction with AtTRB3 protein (see above). Formation of AtRUVBL1-AtRUVBL2 heteromer is distributed in whole nucleus but the localization of protein complex AtRUVBL1-AtTRB3-AtTERT occurs in nucleolus. We showed, that depletion of AtRUVBL1 and especially of AtRUVBL2 proteins causes reduced telomerase activity and suggests conserved role of AtRUVBL proteins in maturation of functional telomerase complex across the mammals and also plant species **(see Figure 11B)** (**Schořová et al., 2019; see Supp. N**).

Very recently, we have shown that AtRUVBL1 and AtRUVBL2A play roles in reproductive development. We showed that mutant plants produce embryo sacs with abnormal structure or with various numbers of nuclei and pollen grains of heterozygous mutant plants exhibit reduced viability and reduced pollen tube growth in vitro. The activity of the *AtRUVBL1* and *AtRUVBL2A* promoters was observed in the embryo sac, pollen grains, and tapetum cells, and for *AtRUVBL2A* also in developing ovules. It seems that RUVBL proteins are essential for the proper development of both male and particularly female gametophytes in Arabidopsis **(Tomaštíková et al., 2023, see Supp. Q)**.

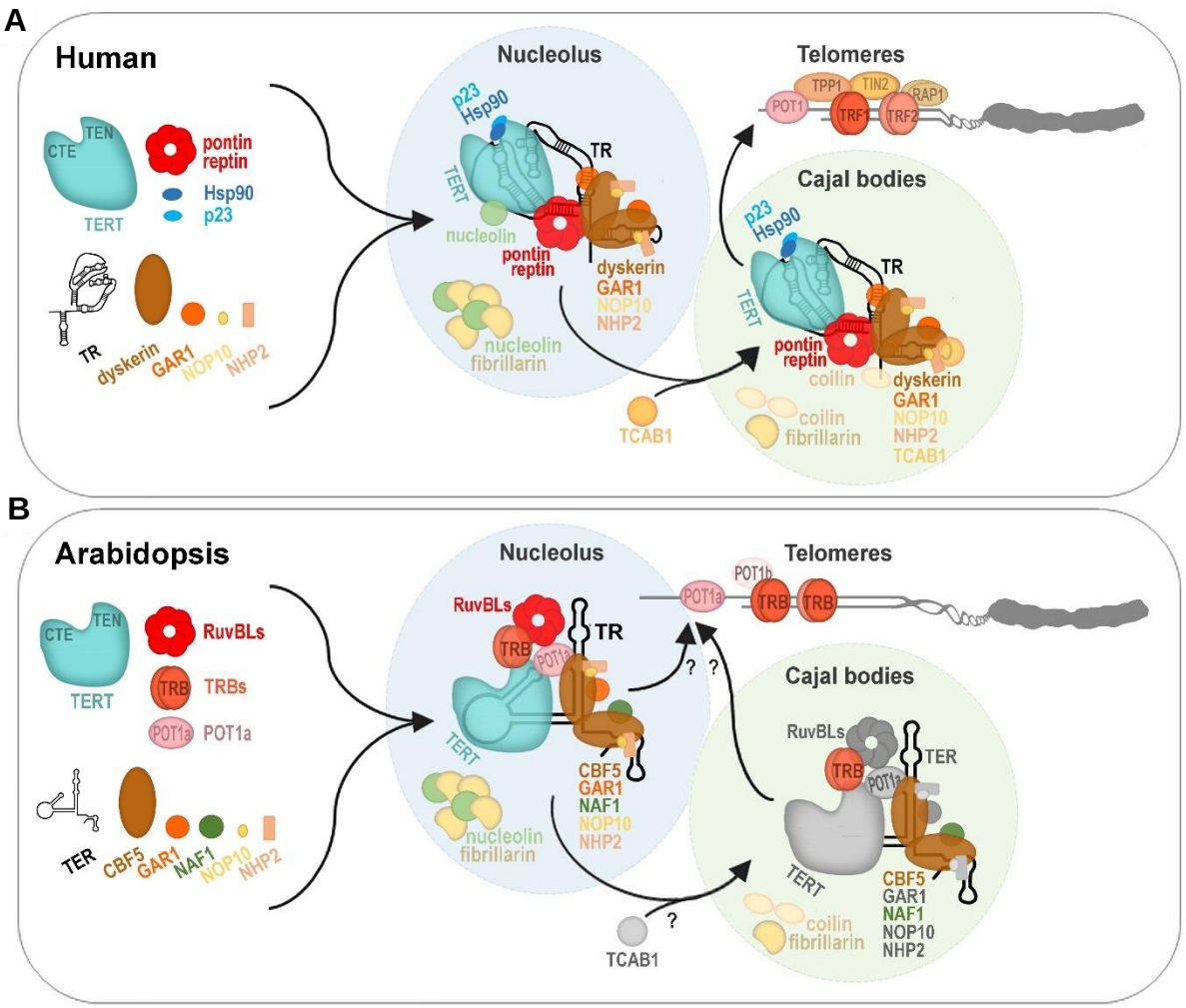

Figure 11. Comparative model of telomerase assembly in human and *Arabidopsis* (adopted from Schořová et al., 2019; see Supp. N)

A) Human TR, located in the nucleolus, is bound by dyskerin, NHP2, NOP10 and GAR1 and human TERT associates with the chaperones Hsp90 and p23. Assembly of TR and TERT into catalytically active telomerase is aided by RUVBL1 (Pontin) and RUVBL2 (Reptin)) AAA^+ ATPases. Telomerase is recruited to Cajal bodies by its interaction with TCAB1. The CBs will colocalize with telomeres and telomerase is recruited to telomeres by the interaction with the shelterin component TPP1.

B) *Arabidopsis* CBF5, GAR1, NOP10, NHP2 and also NAF1, were localized into the plant nucleolus. TERT interaction with RUVBL proteins is bridged by telomeric TRBs. *Arabidopsis* telomeres cluster at the periphery of the nucleolus which is mediated by the presence of nucleolin. Recruitment of the mature telomerase complex to telomeres with or without commitment of Cajal bodies in *Arabidopsis* needs further investigation. Proteins already proven as associated with Cajal bodies are highlighted in Cajal bodies in color. Proteins that have not yet been experimentally proven as Cajal bodies associated are marked with black and white.

Plant homologue of dyskerin, named AtCBF5 (or AtNAP57), is localized within nucleoli and Cajal bodies (Lermontova et al., 2007) and associates with enzymatically active telomerase RNP particles in an RNA-dependent fashion (Kannan et al., 2008). We observed indirect interaction of AtTRBs with AtCBF5 in plant nucleus. Moreover, we detected that the AtCBF5 is interacting with AtPOT1a not only in Y2H and Co-IP as was shown in Kannan et al. (2008) but we also showed nucleolar and partly cytoplasmic localization using BiFC assay. In addition, we observed weak interaction between AtPOT1a-AtRUVBL1 proteins in Y2H and Co-

IP assays (**Schořová et al., 2019; see Supp. N**). Additionally, *Arabidopsis* GAR1, NOP10, NHP2 and also NAF1 homologues, were localized into the plant nucleolus (Lermontova et al., 2007; Pendle et al., 2005).

The telomerase trafficking pathway during the telomerase maturation, which comprises movement of maturating telomerase complex through nucleolus to CBs and finally to the telomeres, may be conserved also in land plants. Dvořáčkova et al. observed that AtTRBs are located not only in the nucleolus but also in nuclear bodies of different size, some of which might be CBs adjacent to the nucleolus (visualized by a marker protein Coilin) (Dvořáčková et al., 2010b). Furthermore, plant dyskerin, AtCBF5, indirectly interacts with AtTRB proteins not only in the plant nucleolus but also in other nuclear bodies that might be CBs (**Schořová et al., 2019; see Supp. N**).

Notably, not all the organisms (e.g., budding yeast and ciliates) rely on the CBs trafficking since telomerase RNAs from these species do not have H/ACA or CAB box motifs, e.g., in *Saccharomyces cerevisiae*, telomerase assembly requires export of the TR out of the nucleus and is regulated in a cell cycle-dependent manner. RNA component of *S. cerevisiae* telomerase, named TLC1, is assembled with Sm proteins in nucleoplasm, 5' TMG cap is added to the TLC1 in nucleoli, TLC1 is assembled in cytoplasm with holoenzyme proteins and consequently telomerase holoenzyme is transported again in the nucleoplasm, where telomerase can be recruited to telomeres (reviewed in Shepelev et al., 2023; R. A. Wu et al., 2017).

As was already mentioned above, we used Y2H, BiFC and Co-IP techniques to detect and characterise protein-protein interactions of the telomere and telomerase associated proteins. The Co-IP technique is based on precipitation a of intact protein complexes formed by proteins usually produced in *in vitro* transcription/translation systems and using an antibody that specifically binds to the particular protein antigen. Interestingly, we chose mammalian Reticulocyte lysate (RRL) instead of plant Wheat germ (WG) system to express plant AtTRB proteins *in vitro* (**Schořová et al., 2019; Schrumpfová et al., 2014; see Supp. N and H**). Wheat germ extract is isolated from embryos of dry wheat seeds while Rabbit reticulocyte lysate is prepared from anaemic rabbits that are stimulated for production of immature red blood cells responsible for the synthesis of haemoglobin that have already lost their nuclei (reticulocytes). When we used for protein expression WG transcription/translation system (TnT Coupled Wheat Germ Extract System, Promega) instead of RRL (TNT T7 Quick Coupled Transcription/Translation System (Promega)), AtTRB proteins were successfully expressed but revealed no interactions, including well established positive controls (**Schořová et al., 2020: Methods in Molecular Biology - The Nucleus, Book Series, Springer).** This observation might relate to the HSP90 chaperone. HSP90 chaperone is present in WGE extract but is a deficient in its function (Antonsson et al., 1995). The addition of purified human or yeast co-chaperone p23 to WGE fully reconstitutes HSP90 chaperone activity (Dittmar et al., 1997; Hutchison et al., 1995). Zhang et al. showed that p23-like proteins are present in plants, they are capable of binding HSP90, but unlike human

p23, the plant p23-like proteins do not reconstitute HSP90 chaperone activity (Zhang et al., 2010). As human chaperone HSP90 and its co-chaperone p23 participate in the folding of a number of cell regulatory proteins, stably associate with hTERT and remain associated also with active telomerase (Forsythe et al., 2001; Holt et al., 1999) it will be interesting to learn whether and how are these chaperones in the plant cells involved in telomere- and telomerase-associated proteins folding and telomerase assembly.

Generally, assembly of functional AtTR RNP, as well as the assembly of mammalian hTR RNP, is certainly a multistep process that may include AtTR, AtCBF5, AtTRBs, AtRUVBLs, AtPOT1a and many other factors, whose presence/participation/mutual interactions will be the subjects of our future research. Dynamics and complexity of mutual interactions can be demonstrated by the fact that we detect the interacting complex of AtCBF5-AtPOT1a in the nucleolus or in the cytoplasmic and nuclear foci, while AtCBF5-AtTRBs interactions are localized entirely to the nucleoli and additional nuclear bodies (**Schořová et al., 2019; see Supp. N**). Our first model of plant telomerase holoenzyme assembly was achieved by editors of The Plant Journal, who wrote a special article named "RESEARCH HIGHLIGHT: The journey to the end of the chromosome: delivering active telomerase to telomeres in plants."(Sweetlove & Gutierrez, 2019; **see Supp. N**).

As we already mentioned - regulation of telomerase assembly, maturation and trafficking is a very complex process, involving a wide range of co-factors. Moreover, these co-factors are not involved exclusively into the telomerase assembly but they also participate in various other biochemical pathways. Although in mammals the telomerase assembly pathway has been partially described, our understanding of telomerase assembly in plants is still far to be perfect and is still ongoing process.

3.2 Telomere maintenance proteins

3.2.1 Mammalian telomere maintenance proteins

The mammalian Shelterin complex is involved in the repression of the primary signal transducers of DNA breakage, two phosphatidylinositol-3-kinase-like (PI3K) protein kinases: ataxia telangiectasia mutated (ATM) and ATM- and RAD3-related (ATR) kinases. Mice TRF2 acts mainly to protect telomeres against ATM activation (Celli & de Lange, 2005) and POT1 is principally involved in repression of the ATR pathway (Denchi & de Lange, 2007; Guo et al., 2007) (**see Figure 3A**). In mammals as well as in other organisms, DSBs activate ATM kinase in a manner dependent on the meiotic recombination 11 (MRE11), DNA repair protein 50 (RAD50) and Nijmegen breakage syndrome 1 (NBS1) named MRN complex. The MRN complex has been found to associate with telomeres and contributes to their maintenance (reviewed in Lamarche et al., 2010). Other proteins involved in DDR machinery are Ku proteins. Human Ku70 protein directly interacts

not only with the Shelterin proteins hTRF1, hTRF2 and hRAP1, but also with telomerase subunits hTERT and hTR (reviewed in Fell & Schild-Poulter, 2015; **Schrumpfová et al., 2019; see Supp. M**).

Aside DNA damage factors, the mammalian telomere proteome comprises additional telomere-associated proteins, e.g. regulator of telomere elongation helicase 1 (RTEL1) **(see Figure 3A)** and many other proteins interactors (reviewed in Ghisays et al., 2021; Lazzerini-Denchi & Sfeir, 2016). RTEL1 helicase connects telomeric loops and circles with DNA recombination and telomere replication. RTEL1 play role in dissolving higher-order structures referred as the telomeric loops (T-loops). These lariat structures are composed of each chromosome terminus being folded back upon itself, which enables the G-rich DNA overhang to invade and base-pair with the complementary strand (Griffith et al., 1999). The 3' G-strand extension that invades the duplex telomeric repeats forms a D-loop (displacement loop, ~150 bp) (Greider, 1999). In addition to its role in T-loop stability, mouse RTEL1 can dissolve G4-DNA structures (quadruplexes), which are predicted to form in the G-rich telomeric regions and might block replication fork progression and the extension of telomeres by telomerase.

3.2.2 Plant telomere maintenance proteins

In *A. thaliana* short telomeres in telomerase-deficient plants activate both the ATM and ATR, whereas absence of members of the plant CST complex initiates only AtATR-dependent, but not AtATM-dependent DNA damage response **(see Figure 3B)** (Amiard et al., 2011; Boltz et al., 2012). In contrast to a massive loss of telomeric DNA that was observed in human cells (Wang et al., 2009), mutations in Ku70 and Ku80 in the dicotyledonous *A. thaliana*, as well as in the monocotyledonous *O. sativa*, resulted in longer telomeres, suggesting their conserved role in the negative regulation of plant telomerase (Bundock et al., 2002; Gallego et al., 2003; Hong et al., 2010; Riha et al., 2002).

A. thaliana RTEL1 homolog suppresses HR and is involved in processing DNA replication intermediates and interstrand and intrastrand DNA cross-links. Deficiency of the AtRTEL1 triggers a SOG1-dependent replication checkpoint in response to DNA crosslinks. AtSOG1 targets numerous genes required for repair by HR, including AtRAD51 (Ogita et al., 2018). Similarly to the situation in mammals, the *Arabidopsis* RTEL1 contributes to telomere homeostasis (Recker et al., 2014).

In contrast with the effects of the loss of function of HR factors, the loss of key factors of NHEJ (MRE11, RAD50, NBS1, KU70 and LIG4) has little or no impact on growth phenotype, overall DSB repair and telomere maintenance in *P. patens*, while a clear telomere phenotype can be seen in the corresponding *A. thaliana* mutants. Therefore, it is not possible to simply generalize the results obtained in only one of these model plants as applying to DNA repair and telomere biology in all plants (Fojtová et al., 2015; Goffová et al., 2019; Holá et al., 2013).

3.2.3 HMG proteins

Proteins classified within the High Mobility Group (HMG) family have been observed to exhibit the capacity to impact the maintenance of telomeres. These HMG proteins constitute a diverse cohort of non-histone proteins that are comparatively small in size, and are relatively abundant within the chromatin of eukaryotic organisms. There are three structurally distinct classes of HMG proteins: the HMG-nucleosome binding subfamily (HMGN), the HMG-AT-hook subfamily (HMGA) and the HMG-box subfamily (HMGB) (reviewed in Reeves, 2015).

In mammals, the HMGA subfamily is composed of two proteins: HMGA1 and HMGA2. Both proteins are expressed in embryonic tissues and embryonic stem cells, are absent in most somatic adult cells and, interestingly, are highly abundant in tumorigenic cells. HMGA proteins are believed to play a role in transcription by promoting the joining of regulatory elements and were shown to have a clear role in development (Ozturk et al., 2014). There was indicated a role for HMGA1 in TERRA (TElomeric Repeat-containing RNA) localization to the telomeres (Scheibe et al., 2013). HMGA2 positively regulates the transcription of the catalytic subunit of the telomerase in human HeLa cells (Li et al., 2011) and increases telomere stability in cancer cells (Natarajan et al., 2016).

In *Arabidopsis*, several uncharacterized HMGA proteins are present, including AtGH1-HMGA1 (reviewed in Kotliński et al., 2017). Chabonnel et al. performed a label-free quantitative proteomics analysis of a telomere pull-down with either the *Arabidopsis* TTTAGGG repeat sequence or a shuffled DNA control. They identified several candidate proteins, including AtTRB1, AtTRB3 and AtGH1-HMGA1 enriched with the telomeric bait. AtGH1-HMGA1 can be present at some DNA extremities but is not associated exclusively with the telomeres. AtGH1-HMGA1 is required for efficient DNA damage repair and telomere integrity in *Arabidopsis*. AtGH1-HMGA1 mutants exhibit developmental and growth defects, accompanied by ploidy defects, increased telomere dysfunction-induced foci, mitotic anaphase bridges and degraded telomeres. It seems that GH1-HMGA1 in *A. thaliana* is involved directly in the repair process by allowing the completion of homologous recombination (Charbonnel et al., 2018). Interestingly, AtTRB proteins, associated with telomeres, possess centrally located H1/H5 domain (**Schrumpfová et al., 2004; see Supp. A**) **(see Figure 5)** that are evolutionary related to the H1/H5 domain located at the N-terminus of the AtGH1-HMGBA proteins in *A. thaliana* (Kotliński et al., 2017).

In mammals, it has been observed that additional members of the HMG family originating from the HMGB subfamily, particularly HMGB1, are capable of regulating the activity of telomerase. However, this effect was not due to changes in expression of either of the telomerase subunits, but rather through the involvement of the HMGB1 in assembly of telomerase nucleoprotein complex. Accordingly, HMGB1

physically interacts with both mouse TERT and TR, as well as with active telomerase complex *in vitro* (Polanská et al., 2012).

In contrast to mammalian HMGB proteins, which contain two HMG-box domains, the typical plant HMGB-type proteins have a single HMG-box domain, which is flanked by a basic N-terminal domain and an acidic C-terminal domain. The HMG-box domains of the various plant HMGB proteins are relatively conserved, but compared to the mammalian homologues the basic and acidic flanking regions vary considerably in length and sequence (Pedersen & Grasser, 2010). According to results of *in vitro* studies, plant HMGB proteins bind linear DNA in non-sequence-specifical manner with moderate affinity. They also recognise specifically certain DNA structures such as minicircles and four-way junctions and they severely bend linear DNA upon binding. In *Arabidopsis* is complicated by the existence of seven proteins that contain HMG-box domain flanked by a basic and acidic domain and thus can be classified as HMGB-type proteins (Lildballe et al., 2008). Most of the AtHMGB proteins were shown to be involved in various stress-response pathways (Roy et al., 2016).

In our study **Schrumpfová et al., 2011**, T-DNA insertion lines with *athmgb1* gene knockout were characterised. AtHMGB1 protein appears as a typical member of the plant HMGB-type proteins in *A. thaliana* and could be regarded as the ortholog of mammalian HMGB1, but not necessarily performing the equivalent functions. Similarly to mammals, general telomere lengths were significantly shortened in mutant *athmgb1* plants compared to wild-type plants. In accordance with these results, in the plant lines overexpressing AtHMGB1, elongated telomeres are not dispersed continuously but they rather migrate on agarose gel as discrete bands, which is typical for telomeres generated by alternative lengthening of telomeres (ALT) (see below). These observations were proven by fluorescence *in situ* hybridisation on metaphase chromosomes where moderate but significant increase of telomeric signal in the AtHMGB1 overexpressing line samples as compared to the wild type (**Schrumpfová et al., 2011; see Supp. G**).

However, the pathway mediating this effect seems to be in different between plant and mammals. While the telomere shortening in mouse cells lacking mHMGB1 can be attributed to the insufficient telomerase activity, no changes in telomerase activity and telomerase processivity could be observed in either *athmgb1* or AtHMGB1 overexpressing plants. From our results we can conclude that AtHMGB1 protein does not exert its effect on telomere length via direct regulation of telomerase, however, AtHMGB1 is involved in the stress- or stimulus-responsive pathways affecting telomere length **(Schrumpfová et al., 2011; see Supp. G).**

3.3 Telomerase-independent telomere maintenance

Besides the telomerase-based mechanism of telomere elongation, various organisms as well as plants, utilize a telomerase-independent telomere maintenance mechanism: alternative lengthening of telomeres (ALT). The exact mechanism behind telomere maintenance in the ALT pathway is unclear, but likely is based

on homologous recombination (HR) and may become active upon the loss of telomerase (Dunham et al., 2000; Min et al., 2017; Zhang et al., 2019).

ALT relies on the formation of terminal T-loops, which parallels the first steps of HR **(see Figure 12)**. The eventual resolution of these T-loops and aberrant HR at telomeres generates not only telomeres of highly heterogeneous lengths but also extrachromosomal T-circles, which are the known hallmarks of ALT. These ALT hallmarks include not only already mentioned heterogenous distribution of the telomere lengths and several classes of extrachromosomal telomeric repeats in the nucleus. ALT-positive cells show also increased telomere sister chromatid exchanges (T-SCE) and presence of promyelocytic leukemia nuclear bodies (APBs) associated with some telomeres. APBs are special variety of PML (promyelocytic leukemia) nuclear bodies found in the normal interphase nucleus. PML bodies are donut-shaped nuclear domains composed of PML and SP100 proteins, which are stabilized by non-covalent interactions of the posttranslational modification SUMO but they do not contain nucleic acids in normal cells (reviewed in Corpet et al., 2020). However, in ALT-positive cells, a subset of PML nuclear bodies, APBs, co-localizes with telomeric DNA. APBs contain PML nuclear bodies components such as PML, SP100 and SUMO and, moreover, telomeric DNA and telomere associated proteins including the Shelterin components TRF1, TRF2, POT1, TIN2, TPP1 and RAP1. Additionally, APBs contain factors that are involved in DNA damage response (DDR) and repair reviewed in Corpet et al., 2020). ALT mechanism is predominantly activated in a

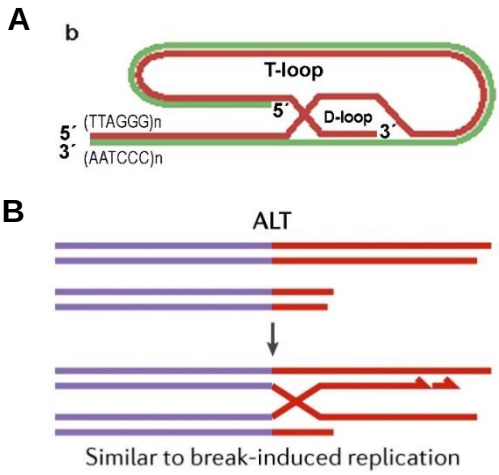

Figure 12. T-loops and Alternative lengthening of telomeres (ALT).

A) Specific telomeric structure T-loop, where the 3' G-strand extension invades the duplex telomeric repeats and forms a D-loop (displacement loop), prevent telomerase access to the telomeres. Figure modified from de Lange, 2004.

B) Telomeres progressively shorten in normal cells with each division in the absence of a telomere maintenance mechanism. In in ~10–15% of tumours, a DNA homologous recombination mechanism, instead of telomerase activation, can be engaged. ALT cells use a telomeric DNA template that is copied to a telomere of a non-homologous chromosome, This telomeric DNA could add telomeric repetitive sequences to another region of the same telomere via loop formation or to the telomere of a sister chromatid (Shay and Wright, 2019).

number of human tumours and in human cells immortalized in culture but also was observed in normal somatic tissues (Neumann et al., 2013). ALT is active in about 10-15 % of cancers (Heaphy et al., 2011).

Telomerase-mediated synthesis of telomeres is also essential for sustained growth and propagation in plants. Inactivation of a gene coding for catalytical subunit of telomerase, AtTERT, leads to a gradual shortening of telomeres by 200-500 nt per generation (Fitzgerald et al., 1999; Riha et al., 2001). After 6-8 generations, some telomeres in *attert* mutants shorten to ~300-400 nt and start fusing with other chromosome ends (Heacock et al., 2007; Riha et al., 2001). Plants with such dysfunctional telomeres exhibit developmental defects and reduced fertility. The severity of these phenotypes worsens with progressive telomere shortening and mutant populations cannot be propagated beyond 8-10 generations (Riha et al., 2001).

However, while yeast and human telomerase-deficient cell lines appear to readily adopt ALT for telomere maintenance, extensive selection of cells derived from *Arabidopsis attert* mutants failed to recover cultures featuring hallmarks of ALT (Watson et al., 2005; Zellinger et al., 2007; reviewed in **Schrumpfová et al., 2019; see Supp. M**).

In our study **Růčková et al. (2008)** we described that the ALT mechanism is activated not only in mutant plants with telomerase dysfunction but possibly also during the earliest stages of normal plant development **(Růčková et al., 2008; see Supp. B**). In this study we hypothesised that extremely low rates of telomere shortening per plant generation (250-500 nt) in telomerase-deficient *A. thaliana* mutants (*attert*) does not correspond to the expected outcome of replicative telomere shortening. The meristem cells in *A. thaliana*, which give rise to all tissues including germ-line cells, undergo many divisions, calculated by Andrew Leitch (Queen Mary, University of London) and Jiří Friml (Institute of Science and Technology Austria, Austria) at approximately 1000 divisions from seed to seed. When considering only 5-10 nt lost per cell division (the average length of RNA primer for synthesis of Okazaki fragments) as the minimum plausible loss of telomeric DNA at each round of replication (under the very improbable scenario that the primer sits exactly at the 3' end of the parental DNA strand), then the number of cell divisions accounting for the observed telomere erosion per generation in *attert* mutants would be only 25-50 cell divisions. Moreover, in mammalian cells the primer does not sit exactly at the 3' end of the parental DNA strand and the loss at telomere is between 50-100 nt per cell division. Then it would be only 5-10 cell divisions per plant generation but not already 1000 division as was stated for *A. thaliana* (Fajkus et al., 2005).

We propagated *attert* mutant plants from seeds coming either from the Lower-most or the Upper-most siliques and we followed the length of their telomeres over several generations. We proved that in the absence of telomerase, the number of cell divisions within one generation influences the control of telomere lengths. Our data showed a fast and efficient activation of a telomerase-independent mechanism

in response to the loss of telomerase activity and imply that ALT is probably involved also in normal plant development (Fajkus et al., 2005; **Růčková et al., 2008; see Supp. B**).

The group of Karel Říha speculated that the meristem cells, however, do not undergo so many cell divisions as was proposed above, as they observed that the number of DNA replications is only slightly increased in plant growing under long-lived conditions in comparison to the plant growing in short-day conditions. They showed that the cell depth of gametes is not linearly proportional to the vegetative growth period and suggested that older plants may not be passing on more mutations to their offspring relative to younger plants (Watson et al., 2016).

The involvement of ALT in the earliest stages of normal plant development is still questionable and needs further investigation.

Conclusion

The ends of the linear chromosomes, called telomeres, are shields that protect the exposed chromosome ends from DNA damage machinery. Due to their significance in cell viability, cancer, and ageing, there has been intensive research on telomeric DNA, telomere-associated proteins, and telomere-related proteins for over four decades. However, the protein interactome associated with plant telomeres and telomerase is not as well-studied as the mammalian telomeric proteome. It is interesting to note that telomeric repeats can also be found dispersed throughout the genome as interstitial telomeric tracts or short *telo*-boxes.

In plants, telomeres are primarily composed of short tandem repeats that are associated with various proteins involved in regulating telomere maintenance and the telomerase holoenzyme complex's access. Telomere Repeat Binding proteins (TRBs) play a crucial role in telomere maintenance, and they are associated not only with terminally located telomeric repeats but also with *telo*-boxes, which are mainly found in gene promoters. These TRBs can recruit and regulate various protein complexes and significantly influence the chromatin's epigenetic status.

In my habilitation thesis, I presented data that expand our understanding of plant telomere biology, telomeric sequence- or telomerase-associated proteins, and their roles in telomere homeostasis maintenance. I discussed the involvement of these proteins in telomerase assembly, recruitment, and activity, as well as their role in regulating and protecting the chromosomes' physical ends' genomic integrity. Additionally, I comment on the involvement of these proteins in non-telomeric functions in epigenetic regulations.

Bibliography

Adams, S. P., Hartman, T. P. V., Lim, K. Y., Chase, M. W., Bennett, M. D., Leitch, I. J., & Leitch, A. R. (2001). Loss and recovery of Arabidopsis–type telomere repeat sequences 5′–(TTTAGGG)n–3′ in the evolution of a major radiation of flowering plants. Proceedings of the Royal Society of London. Series B: Biological Sciences, 268(1476), 1541–1546. https://doi.org/10.1098/rspb.2001.1726

Akimcheva, S., Zellinger, B., & Riha, K. (2009). Genome stability in Arabidopsis cells exhibiting alternative lengthening of telomeres. Cytogenetic and Genome Research, 122(3–4), 388–395. https://doi.org/10.1159/000167827

Aksenova, A. Y., & Mirkin, S. M. (2019). At the Beginning of the End and in the Middle of the Beginning: Structure and Maintenance of Telomeric DNA Repeats and Interstitial Telomeric Sequences. Genes, 10(2), Article 2. https://doi.org/10.3390/genes10020118

Amiard, S., Depeiges, A., Allain, E., White, C. I., & Gallego, M. E. (2011). Arabidopsis ATM and ATR Kinases Prevent Propagation of Genome Damage Caused by Telomere Dysfunction. The Plant Cell, 23(12), 4254–4265. https://doi.org/10.1105/tpc.111.092387

Antonsson, C., Whitelaw, M. L., McGuire, J., Gustafsson, J.-Å., & Poellinger, L. (1995). Distinct Roles of the Molecular Chaperone hsp90 in Modulating Dioxin Receptor Function via the Basic Helix-Loop-Helix and PAS Domains. Molecular and Cellular Biology, 15(2), 756–765. https://doi.org/10.1128/MCB.15.2.756

Arat, N. Ö., & Griffith, J. D. (2012). Human Rap1 Interacts Directly with Telomeric DNA and Regulates TRF2 Localization at the Telomere*. Journal of Biological Chemistry, 287(50), 41583–41594. https://doi.org/10.1074/jbc.M112.415984

Aronen, T., & Ryynänen, L. (2014). Silver birch telomeres shorten in tissue culture. Tree Genetics & Genomes, 10(1), 67–74. https://doi.org/10.1007/s11295-013-0662-4

Arora, A., Beilstein, M. A., & Shippen, D. E. (2016). Evolution of Arabidopsis protection of telomeres 1 alters nucleic acid recognition and telomerase regulation. Nucleic Acids Research, 44(20), 9821–9830. https://doi.org/10.1093/nar/gkw807

Azzalin, C. M., Nergadze, S. G., & Giulotto, E. (2001). Human intrachromosomal telomeric-like repeats: Sequence organization and mechanisms of origin. Chromosoma, 110(2), 75–82. https://doi.org/10.1007/s004120100135

Baumann, P., & Cech, T. R. (2001). Pot1, the Putative Telomere End-Binding Protein in Fission Yeast and Humans. Science, 292(5519), 1171–1175. https://doi.org/10.1126/science.1060036

Bergemann, A. D., & Johnson, E. M. (1992). The HeLa Pur factor binds single-stranded DNA at a specific element conserved in gene flanking regions and origins of DNA replication. Molecular and Cellular Biology, 12(3), 1257–1265. https://doi.org/10.1128/mcb.12.3.1257-1265.1992

Bianchi, A., Smith, S., Chong, L., Elias, P., & de Lange, T. (1997). TRF1 is a dimer and bends telomeric DNA. The EMBO Journal, 16(7), 1785–1794. https://doi.org/10.1093/emboj/16.7.1785

Bilaud, T., Koering, C. E., Binet-Brasselet, E., Ancelin, K., Pollice, A., Gasser, S. M., & Gilson, E. (1996). The Telobox, a Myb-Related Telomeric DNA Binding Motif Found in Proteins from Yeast, Plants and Human. Nucleic Acids Research, 24(7), 1294–1303. https://doi.org/10.1093/nar/24.7.1294

Blackburn, E. H., Epel, E. S., & Lin, J. (2015). Human telomere biology: A contributory and interactive factor in aging, disease risks, and protection. Science, 350(6265), 1193–1198. https://doi.org/10.1126/science.aab3389

Blackburn, E. H., & Gall, J. G. (1978). A tandemly repeated sequence at the termini of the extrachromosomal ribosomal RNA genes in Tetrahymena. Journal of Molecular Biology, 120(1), 33–53. https://doi.org/10.1016/0022-2836(78)90294-2

Boltz, K. A., Leehy, K., Song, X., Nelson, A. D., & Shippen, D. E. (2012). ATR cooperates with CTC1 and STN1 to maintain telomeres and genome integrity in Arabidopsis. Molecular Biology of the Cell, 23(8), 1558–1568. https://doi.org/10.1091/mbc.e11-12-1002

Broccoli, D., Smogorzewska, A., Chong, L., & de Lange, T. (1997). Human telomeres contain two distinct Myb–related proteins, TRF1 and TRF2. Nature Genetics, 17(2), Article 2. https://doi.org/10.1038/ng1097-231

Bundock, P., van Attikum, H., & Hooykaas, P. (2002). Increased telomere length and hypersensitivity to DNA damaging agents in an Arabidopsis KU70 mutant. Nucleic Acids Research, 30(15), 3395–3400. https://doi.org/10.1093/nar/gkf445

Burr, B., Burr, F. A., Matz, E. C., & Romero-Severson, J. (1992). Pinning down loose ends: Mapping telomeres and factors affecting their length. The Plant Cell, 4(8), 953–960. https://doi.org/10.1105/tpc.4.8.953

Byun, M. Y., Hong, J.-P., & Kim, W. T. (2008). Identification and characterization of three telomere repeat-binding factors in rice. Biochemical and Biophysical Research Communications, 372(1), 85–90. https://doi.org/10.1016/j.bbrc.2008.04.181

Celli, G. B., & de Lange, T. (2005). DNA processing is not required for ATM-mediated telomere damage response after TRF2 deletion. Nature Cell Biology, 7(7), Article 7. https://doi.org/10.1038/ncb1275

Cifuentes-Rojas, C., Kannan, K., Tseng, L., & Shippen, D. E. (2011). Two RNA subunits and POT1a are components of Arabidopsis telomerase. Proceedings of the National Academy of Sciences, 108(1), 73–78. https://doi.org/10.1073/pnas.1013021107

Cifuentes-Rojas, C., Nelson, A. D. L., Boltz, K. A., Kannan, K., She, X., & Shippen, D. E. (2012). An alternative telomerase RNA in Arabidopsis modulates enzyme activity in response to DNA damage. Genes & Development, 26(22), 2512–2523. https://doi.org/10.1101/gad.202960.112

Cimino-Reale, G., Pascale, E., Battiloro, E., Starace, G., Verna, R., & D'Ambrosio, E. (2001). The length of telomeric G-rich strand 3'-overhang measured by oligonucleotide ligation assay. Nucleic Acids Research, 29(7), e35.

Clark, J. W., & Donoghue, P. C. J. (2018). Whole-Genome Duplication and Plant Macroevolution. Trends in Plant Science, 23(10), 933–945. https://doi.org/10.1016/j.tplants.2018.07.006

Colgin, L. M., Wilkinso, C., Englezou, A., Kilian, A., Robinson, M. O., & Reddel, R. R. (2000). The hTERTα Splice Variant is a Dominant Negative Inhibitor of Telomerase Activity. Neoplasia, 2(5), 426–432. https://doi.org/10.1038/sj.neo.7900112

Comadira, G., Rasool, B., Kaprinska, B., García, B. M., Morris, J., Verrall, S. R., Bayer, M., Hedley, P. E., Hancock, R. D., & Foyer, C. H. (2015). WHIRLY1 Functions in the Control of Responses to Nitrogen Deficiency But Not Aphid Infestation in Barley. Plant Physiology, 168(3), 1140–1151. https://doi.org/10.1104/pp.15.00580

Corpet, A., Kleijwegt, C., Roubille, S., Juillard, F., Jacquet, K., Texier, P., & Lomonte, P. (2020). PML nuclear bodies and chromatin dynamics: Catch me if you can! Nucleic Acids Research, 48(21), 11890–11912. https://doi.org/10.1093/nar/gkaa828

Crhák, T., Zachová, D., Fojtová, M., & Sýkorová, E. (2019). The region upstream of the telomerase reverse transcriptase gene is essential for in planta telomerase complementation. Plant Science, 281, 41–51. https://doi.org/10.1016/j.plantsci.2019.01.001

Déjardin, J., & Kingston, R. E. (2009). Purification of Proteins Associated with Specific Genomic Loci. Cell, 136(1), 175–186. https://doi.org/10.1016/j.cell.2008.11.045

Denchi, E. L., & de Lange, T. (2007). Protection of telomeres through independent control of ATM and ATR by TRF2 and POT1. Nature, 448(7157), Article 7157. https://doi.org/10.1038/nature06065

Derboven, E., Ekker, H., Kusenda, B., Bulankova, P., & Riha, K. (2014). Role of STN1 and DNA Polymerase α in Telomere Stability and Genome-Wide Replication in Arabidopsis. PLOS Genetics, 10(10), e1004682. https://doi.org/10.1371/journal.pgen.1004682

Desveaux, D., Allard, J., Brisson, N., & Sygusch, J. (2002). A new family of plant transcription factors displays a novel ssDNA-binding surface. Nature Structural Biology, 9(7), Article 7. https://doi.org/10.1038/nsb814

Desveaux, D., Després, C., Joyeux, A., Subramaniam, R., & Brisson, N. (2000). PBF-2 Is a Novel Single-Stranded DNA Binding Factor Implicated in PR-10a Gene Activation in Potato. The Plant Cell, 12(8), 1477–1489. https://doi.org/10.1105/tpc.12.8.1477

Dittmar, K. D., Demady, D. R., Stancato, L. F., Krishna, P., & Pratt, W. B. (1997). Folding of the Glucocorticoid Receptor by the Heat Shock Protein (hsp) 90-based Chaperone Machinery: THE ROLE OF p23 IS TO STABILIZE RECEPTOR·hsp90 HETEROCOMPLEXES FORMED BY hsp90·p60·hsp70*. Journal of Biological Chemistry, 272(34), 21213–21220. https://doi.org/10.1074/jbc.272.34.21213

Dokládal, L., Benková, E., Honys, D., Dupľáková, N., Lee, L.-Y., Gelvin, S. B., & Sýkorová, E. (2018). An armadillo-domain protein participates in a telomerase interaction network. Plant Molecular Biology, 97(4), 407–420. https://doi.org/10.1007/s11103-018-0747-4

Dokládal, L., Honys, D., Rana, R., Lee, L.-Y., Gelvin, S. B., & Sýkorová, E. (2015). CDNA Library Screening Identifies Protein Interactors Potentially Involved in Non-Telomeric Roles of Arabidopsis Telomerase. Frontiers in Plant Science, 6. https://www.frontiersin.org/articles/10.3389/fpls.2015.00985

Dreissig, S., Schiml, S., Schindele, P., Weiss, O., Rutten, T., Schubert, V., Gladilin, E., Mette, M. F., Puchta, H., & Houben, A. (2017). Live-cell CRISPR imaging in plants reveals dynamic telomere movements. The Plant Journal, 91(4), 565–573. https://doi.org/10.1111/tpj.13601

Du, H., Wang, Y.-B., Xie, Y., Liang, Z., Jiang, S.-J., Zhang, S.-S., Huang, Y.-B., & Tang, Y.-X. (2013). Genome-Wide Identification and Evolutionary and Expression Analyses of MYB-Related Genes in Land Plants. DNA Research, 20(5), 437–448. https://doi.org/10.1093/dnares/dst021

Dunham, M. A., Neumann, A. A., Fasching, C. L., & Reddel, R. R. (2000). Telomere maintenance by recombination in human cells. Nature Genetics, 26(4), 447–450. https://doi.org/10.1038/82586

Dvořáčková, M., Rossignol, P., Shaw, P. J., Koroleva, O. A., Doonan, J. H., & Fajkus, J. (2010a). AtTRB1, a telomeric DNA-binding protein from Arabidopsis, is concentrated in the nucleolus and shows highly dynamic association with chromatin. The Plant Journal, 61(4), 637–649. https://doi.org/10.1111/j.1365-313X.2009.04094.x

Dvořáčková, M., Rossignol, P., Shaw, P. J., Koroleva, O. A., Doonan, J. H., & Fajkus, J. (2010b). AtTRB1, a telomeric DNA-binding protein from Arabidopsis, is concentrated in the nucleolus and shows highly dynamic association with chromatin. The Plant Journal, 61(4), 637–649. https://doi.org/10.1111/j.1365-313X.2009.04094.x

Ellen, T. P., & van Holde, K. E. (2004). Linker Histone Interaction Shows Divalent Character with both Supercoiled and Linear DNA. Biochemistry, 43(24), 7867–7872. https://doi.org/10.1021/bi0497704

Fairall, L., Chapman, L., Moss, H., de Lange, T., & Rhodes, D. (2001). Structure of the TRFH Dimerization Domain of the Human Telomeric Proteins TRF1 and TRF2. Molecular Cell, 8(2), 351–361. https://doi.org/10.1016/S1097-2765(01)00321-5

Fajkus, J., Fulnečková, J., Hulánová, M., Berková, K., Říha, K., & Matyášek, R. (1998). Plant cells express telomerase activity upon transfer to callus culture, without extensively changing telomere lengths. Molecular and General Genetics MGG, 260(5), 470–474. https://doi.org/10.1007/s004380050918

Fajkus, J., Kovařík, A., & Královics, R. (1996). Telomerase activity in plant cells. FEBS Letters, 391(3), 307–309. https://doi.org/10.1016/0014-5793(96)00757-0

Fajkus, J., Kovařík, A., mKrálovics, R., & Bezděk, M. (1995). Organization of telomeric and subtelomeric chromatin in the higher plant Nicotiana tabacum. Molecular and General Genetics MGG, 247(5), 633–638. https://doi.org/10.1007/BF00290355

Fajkus, J., Sýkorová, E., & Leitch, A. R. (2005). Telomeres in evolution and evolution of telomeres. Chromosome Research, 13(5), 469–479. https://doi.org/10.1007/s10577-005-0997-2

Fajkus, P., Adámik, M., Nelson, A. D. L., Kilar, A. M., Franek, M., Bubeník, M., Frydrychová, R. Č., Votavová, A., Sýkorová, E., Fajkus, J., & Peška, V. (2023). Telomerase RNA in Hymenoptera (Insecta) switched to plant/ciliate-like biogenesis. Nucleic Acids Research, 51(1), 420–433. https://doi.org/10.1093/nar/gkac1202

Fajkus, P., Peška, V., Sitová, Z., Fulnečková, J., Dvořáčková, M., Gogela, R., Sýkorová, E., Hapala, J., & Fajkus, J. (2016). Allium telomeres unmasked: The unusual telomeric sequence (CTCGGTTATGGG)n is synthesized by telomerase. The Plant Journal, 85(3), 337–347. https://doi.org/10.1111/tpj.13115

Fajkus, P., Peška, V., Závodník, M., Fojtová, M., Fulnečková, J., Dobias, Š., Kilar, A., Dvořáčková, M., Zachová, D., Nečasová, I., Sims, J., Sýkorová, E., & Fajkus, J. (2019). Telomerase RNAs in land plants. Nucleic Acids Research, 47(18), 9842–9856. https://doi.org/10.1093/nar/gkz695

Fan, Y., Linardopoulou, E., Friedman, C., Williams, E., & Trask, B. J. (2002). Genomic Structure and Evolution of the Ancestral Chromosome Fusion Site in 2q13–2q14.1 and Paralogous Regions on Other Human Chromosomes. Genome Research, 12(11), 1651–1662. https://doi.org/10.1101/gr.337602

Feldbrügge, M., Sprenger, M., Hahlbrock, K., & Weisshaar, B. (1997). PcMYB1, a novel plant protein containing a DNA-binding domain with one MYB repeat, interacts in vivo with a light-regulatory promoter unit. The Plant Journal, 11(5), 1079–1093. https://doi.org/10.1046/j.1365-313X.1997.11051079.x

Fell, V. L., & Schild-Poulter, C. (2015). The Ku heterodimer: Function in DNA repair and beyond. Mutation Research/Reviews in Mutation Research, 763, 15–29. https://doi.org/10.1016/j.mrrev.2014.06.002

Fitzgerald, M. S., McKnight, T. D., & Shippen, D. E. (1996). Characterization and developmental patterns of telomerase expression in plants. Proceedings of the National Academy of Sciences, 93(25), 14422–14427. https://doi.org/10.1073/pnas.93.25.14422

Fitzgerald, M. S., Riha, K., Gao, F., Ren, S., McKnight, T. D., & Shippen, D. E. (1999). Disruption of the telomerase catalytic subunit gene from Arabidopsis inactivates telomerase and leads to a slow loss of telomeric DNA. Proceedings of the National Academy of Sciences, 96(26), 14813–14818. https://doi.org/10.1073/pnas.96.26.14813

Fojtová, M., Peška, V., Dobšáková, Z., Mozgová, I., Fajkus, J., & Sýkorová, E. (2011). Molecular analysis of T-DNA insertion mutants identified putative regulatory elements in the AtTERT gene. Journal of Experimental Botany, 62(15), 5531–5545. https://doi.org/10.1093/jxb/err235

Fojtová, M., Sýkorová, E., Najdekrová, L., Polanská, P., Zachová, D., Vagnerová, R., Angelis, K. J., & Fajkus, J. (2015). Telomere dynamics in the lower plant Physcomitrella patens. Plant Molecular Biology, 87(6), 591–601. https://doi.org/10.1007/s11103-015-0299-9

Forsythe, H. L., Jarvis, J. L., Turner, J. W., Elmore, L. W., & Holt, S. E. (2001). Stable Association of hsp90 and p23, but Not hsp70, with Active Human Telomerase*. Journal of Biological Chemistry, 276(19), 15571–15574. https://doi.org/10.1074/jbc.C100055200

Foyer, C. H., Karpinska, B., & Krupinska, K. (2014). The functions of WHIRLY1 and REDOX-RESPONSIVE TRANSCRIPTION FACTOR 1 in cross tolerance responses in plants: A hypothesis. Philosophical Transactions of the Royal Society B: Biological Sciences, 369(1640), 20130226. https://doi.org/10.1098/rstb.2013.0226

Freeling, M. (2009). Bias in Plant Gene Content Following Different Sorts of Duplication: Tandem, Whole-Genome, Segmental, or by Transposition. Annual Review of Plant Biology, 60(1), 433–453. https://doi.org/10.1146/annurev.arplant.043008.092122

Frydrychová, R., & Marec, F. (2002). Repeated Losses of TTAGG Telomere Repeats in Evolution of Beetles (Coleoptera). Genetica, 115(2), 179–187. https://doi.org/10.1023/A:1020175912128

Fu, D., & Collins, K. (2007). Purification of Human Telomerase Complexes Identifies Factors Involved in Telomerase Biogenesis and Telomere Length Regulation. Molecular Cell, 28(5), 773–785. https://doi.org/10.1016/j.molcel.2007.09.023

Fulcher, N., & Riha, K. (2016). Using Centromere Mediated Genome Elimination to Elucidate the Functional Redundancy of Candidate Telomere Binding Proteins in Arabidopsis thaliana. Frontiers in Genetics, 6, 349. https://doi.org/10.3389/fgene.2015.00349

Fulnecková, J., & Fajkus, J. (2000). Inhibition of plant telomerase by telomere-binding proteins from nuclei of telomerase-negative tissues. FEBS Letters, 467(2–3), 305–310. https://doi.org/10.1016/s0014-5793(00)01178-9

Fulnecková, J., Sevcíková, T., Fajkus, J., Lukesová, A., Lukes, M., Vlcek, C., Lang, B. F., Kim, E., Eliás, M., & Sykorová, E. (2013). A broad phylogenetic survey unveils the diversity and evolution of telomeres in eukaryotes. Genome Biology and Evolution, 5(3), 468–483. https://doi.org/10.1093/gbe/evt019

Fulnečková, J., Dokládal, L., Kolářová, K., Nešpor Dadejová, M., Procházková, K., Gomelská, S., Sivčák, M., Adamusová, K., Lyčka, M., Peska, V., Dvořáčková, M., & Sýkorová, E. (2022). Telomerase Interaction Partners–Insight from Plants. International Journal of Molecular Sciences, 23(1), Article 1. https://doi.org/10.3390/ijms23010368

Gallego, M. E., Jalut, N., & White, C. I. (2003). Telomerase Dependence of Telomere Lengthening in ku80 Mutant Arabidopsis. The Plant Cell, 15(3), 782–789. https://doi.org/10.1105/tpc.008623

Gallego, M. E., & White, C. I. (2005). DNA repair and recombination functions in Arabidopsis telomere maintenance. Chromosome Research: An International Journal on the Molecular, Supramolecular and Evolutionary Aspects of Chromosome Biology, 13(5), 481–491. https://doi.org/10.1007/s10577-005-0995-4

Garvik, B., Carson, M., & Hartwell, L. (1995). Single-Stranded DNA Arising at Telomeres in cdc13 Mutants May Constitute a Specific Signal for the RAD9 Checkpoint. Molecular and Cellular Biology, 15(11), 6128–6138. https://doi.org/10.1128/MCB.15.11.6128

Gaspin, C., Rami, J.-F., & Lescure, B. (2010). Distribution of short interstitial telomere motifs in two plant genomes: Putative origin and function. BMC Plant Biology, 10(1), 283. https://doi.org/10.1186/1471-2229-10-283

Ghisays, F., Garzia, A., Wang, H., Canasto-Chibuque, C., Hohl, M., Savage, S. A., Tuschl, T., & Petrini, J. H. J. (2021). RTEL1 influences the abundance and localization of TERRA RNA. Nature Communications, 12(1), Article 1. https://doi.org/10.1038/s41467-021-23299-2

Giannone, R. J., McDonald, H. W., Hurst, G. B., Shen, R.-F., Wang, Y., & Liu, Y. (2010). The Protein Network Surrounding the Human Telomere Repeat Binding Factors TRF1, TRF2, and POT1. PLOS ONE, 5(8), e12407. https://doi.org/10.1371/journal.pone.0012407

Giraud-Panis, M.-J., Teixeira, M. T., Géli, V., & Gilson, E. (2010). CST Meets Shelterin to Keep Telomeres in Check. Molecular Cell, 39(5), 665–676. https://doi.org/10.1016/j.molcel.2010.08.024

Gladych, M., Wojtyla, A., & Rubis, B. (2011). Human telomerase expression regulation. Biochemistry and Cell Biology, 89(4), 359–376. https://doi.org/10.1139/o11-037

Goffová, I., Vágnerová, R., Peška, V., Franek, M., Havlová, K., Holá, M., Zachová, D., Fojtová, M., Cuming, A., Kamisugi, Y., Angelis, K. J., & Fajkus, J. (2019). Roles of RAD51 and RTEL1 in telomere and rDNA stability in Physcomitrella patens. The Plant Journal, 98(6), 1090–1105. https://doi.org/10.1111/tpj.14304

Gomes, N. M. V., Ryder, O. A., Houck, M. L., Charter, S. J., Walker, W., Forsyth, N. R., Austad, S. N., Venditti, C., Pagel, M., Shay, J. W., & Wright, W. E. (2011). Comparative biology of mammalian telomeres: Hypotheses on ancestral states and the roles of telomeres in longevity determination. Aging Cell, 10(5), 761–768. https://doi.org/10.1111/j.1474-9726.2011.00718.x

Grabowski, E., Miao, Y., Mulisch, M., & Krupinska, K. (2008). Single-Stranded DNA-Binding Protein Whirly1 in Barley Leaves Is Located in Plastids and the Nucleus of the Same Cell. Plant Physiology, 147(4), 1800–1804. https://doi.org/10.1104/pp.108.122796

Grandin, N., & Charbonneau, M. (2001). Hsp90 levels affect telomere length in yeast. Molecular Genetics and Genomics: MGG, 265(1), 126–134. https://doi.org/10.1007/s004380000398

Greider, C. W. (1999). Telomeres Do D-Loop–T-Loop. Cell, 97(4), 419–422. https://doi.org/10.1016/S0092-8674(00)80750-3

Greider, C. W., & Blackburn, E. H. (1985). Identification of a specific telomere terminal transferase activity in tetrahymena extracts. Cell, 43(2, Part 1), 405–413. https://doi.org/10.1016/0092-8674(85)90170-9

Greider, C. W., & Blackburn, E. H. (1989). A telomeric sequence in the RNA of Tetrahymena telomerase required for telomere repeat synthesis. Nature, 337(6205), 331–337. https://doi.org/10.1038/337331a0

Griffith, J. D., Comeau, L., Rosenfield, S., Stansel, R. M., Bianchi, A., Moss, H., & de Lange, T. (1999). Mammalian Telomeres End in a Large Duplex Loop. Cell, 97(4), 503–514. https://doi.org/10.1016/S0092-8674(00)80760-6

Grolimund, L., Aeby, E., Hamelin, R., Armand, F., Chiappe, D., Moniatte, M., & Lingner, J. (2013). A quantitative telomeric chromatin isolation protocol identifies different telomeric states. Nature Communications, 4(1), Article 1. https://doi.org/10.1038/ncomms3848

Grossi, S., Puglisi, A., Dmitriev, P. V., Lopes, M., & Shore, D. (2004). Pol12, the B subunit of DNA polymerase α, functions in both telomere capping and length regulation. Genes & Development, 18(9), 992–1006. https://doi.org/10.1101/gad.300004

Guan, Z., Wang, W., Yu, X., Lin, W., & Miao, Y. (2018). Comparative Proteomic Analysis of Coregulation of CIPK14 and WHIRLY1/3 Mediated Pale Yellowing of Leaves in Arabidopsis. International Journal of Molecular Sciences, 19(8), Article 8. https://doi.org/10.3390/ijms19082231

Guo, X., Deng, Y., Lin, Y., Cosme-Blanco, W., Chan, S., He, H., Yuan, G., Brown, E. J., & Chang, S. (2007). Dysfunctional telomeres activate an ATM-ATR-dependent DNA damage response to suppress tumorigenesis. The EMBO Journal, 26(22), 4709–4719. https://doi.org/10.1038/sj.emboj.7601893

Harrington, L., McPhail, T., Mar, V., Zhou, W., Oulton, R., Program, A. E., Bass, M. B., Arruda, I., & Robinson, M. O. (1997). A Mammalian Telomerase-Associated Protein. Science, 275(5302), 973–977. https://doi.org/10.1126/science.275.5302.973

Haussmann, M. F., Winkler, D. W., Huntington, C. E., Nisbet, I. C. T., & Vleck, C. M. (2007). Telomerase activity is maintained throughout the lifespan of long-lived birds. Experimental Gerontology, 42(7), 610–618. https://doi.org/10.1016/j.exger.2007.03.004

He, L., Liu, J., Torres, G. A., Zhang, H., Jiang, J., & Xie, C. (2013). Interstitial telomeric repeats are enriched in the centromeres of chromosomes in Solanum species. Chromosome Research, 21(1), 5–13. https://doi.org/10.1007/s10577-012-9332-x

He, Q., Chen, L., Xu, Y., & Yu, W. (2013). Identification of centromeric and telomeric DNA-binding proteins in rice. Proteomics, 13(5), 826–832. https://doi.org/10.1002/pmic.201100416

Heacock, M. L., Idol, R. A., Friesner, J. D., Britt, A. B., & Shippen, D. E. (2007). Telomere dynamics and fusion of critically shortened telomeres in plants lacking DNA ligase IV. Nucleic Acids Research, 35(19), 6490–6500. https://doi.org/10.1093/nar/gkm472

Heaphy, C. M., Subhawong, A. P., Hong, S.-M., Goggins, M. G., Montgomery, E. A., Gabrielson, E., Netto, G. J., Epstein, J. I., Lotan, T. L., Westra, W. H., Shih, I.-M., Iacobuzio-Donahue, C. A., Maitra, A., Li, Q. K., Eberhart, C. G., Taube, J. M., Rakheja, D., Kurman, R. J., Wu, T. C., … Meeker, A. K. (2011). Prevalence of the Alternative Lengthening of Telomeres Telomere Maintenance Mechanism in Human Cancer Subtypes. The American Journal of Pathology, 179(4), 1608–1615. https://doi.org/10.1016/j.ajpath.2011.06.018

Heller, K., Kilian, A., Piatyszek, M. A., & Kleinhofs, A. (1996). Telomerase activity in plant extracts. Molecular & General Genetics: MGG, 252(3), 342–345. https://doi.org/10.1007/BF02173780

Hirata, Y., Suzuki, C., & Sakai, S. (2004). Characterization and gene cloning of telomere-binding protein from tobacco BY-2 cells. Plant Physiology and Biochemistry, 42(1), 7–14. https://doi.org/10.1016/j.plaphy.2003.10.002

Ho Lee, J., Hyun Kim, J., Taek Kim, W., Kang, B. G., & Kwon Chung, I. (2000). Characterization and developmental expression of single-stranded telomeric DNA-binding proteins from mung bean (Vigna radiata). Plant Molecular Biology, 42(4), 547–557. https://doi.org/10.1023/A:1006373917321

Hofr, C., Šultesová, P., Zimmermann, M., Mozgová, I., Procházková Schrumpfová, P., Wimmerová, M., & Fajkus, J. (2009). Single-Myb-histone proteins from Arabidopsis thaliana: A quantitative study of telomere-binding specificity and kinetics. Biochemical Journal, 419(1), 221–230. https://doi.org/10.1042/BJ20082195

Hohenstatt, M. L., Mikulski, P., Komarynets, O., Klose, C., Kycia, I., Jeltsch, A., Farrona, S., & Schubert, D. (2018). PWWP-DOMAIN INTERACTOR OF POLYCOMBS1 Interacts with Polycomb-Group Proteins and Histones and Regulates Arabidopsis Flowering and Development. The Plant Cell, 30(1), 117–133. https://doi.org/10.1105/tpc.17.00117

Holá, M., Kozák, J., Vágnerová, R., & Angelis, K. J. (2013). Genotoxin Induced Mutagenesis in the Model Plant Physcomitrella patens. BioMed Research International, 2013, e535049. https://doi.org/10.1155/2013/535049

Holt, S. E., Aisner, D. L., Baur, J., Tesmer, V. M., Dy, M., Ouellette, M., Trager, J. B., Morin, G. B., Toft, D. O., Shay, J. W., Wright, W. E., & White, M. A. (1999). Functional requirement of p23 and Hsp90 in telomerase complexes. Genes & Development, 13(7), 817–826.

Hom, R. A., & Wuttke, D. S. (2017). Human CST Prefers G-Rich but Not Necessarily Telomeric Sequences. Biochemistry, 56(32), 4210–4218. https://doi.org/10.1021/acs.biochem.7b00584

Hong, J.-P., Byun, M. Y., An, K., Yang, S.-J., An, G., & Kim, W. T. (2010). OsKu70 Is Associated with Developmental Growth and Genome Stability in Rice. Plant Physiology, 152(1), 374–387. https://doi.org/10.1104/pp.109.150391

Hong, J.-P., Byun, M. Y., Koo, D.-H., An, K., Bang, J.-W., Chung, I. K., An, G., & Kim, W. T. (2007). Suppression of RICE TELOMERE BINDING PROTEIN1 Results in Severe and Gradual Developmental Defects Accompanied by Genome Instability in Rice. The Plant Cell, 19(6), 1770–1781. https://doi.org/10.1105/tpc.107.051953

Hrdličková, R., Nehyba, J., Liss, A. S., & Bose, H. R. (2006). Mechanism of Telomerase Activation by v-Rel and Its Contribution to Transformation. Journal of Virology, 80(1), 281–295. https://doi.org/10.1128/JVI.80.1.281-295.2006

Hutchison, K. A., Stancato, L. F., Owens-Grillo, J. K., Johnson, J. L., Krishna, P., Toft, D. O., & Pratt, W. B. (1995). The 23-kDa Acidic Protein in Reticulocyte Lysate Is the Weakly Bound Component of the hsp Foldosome That Is Required for Assembly of the Glucocorticoid Receptor into a Functional Heterocomplex with hsp90 (∗). Journal of Biological Chemistry, 270(32), 18841–18847. https://doi.org/10.1074/jbc.270.32.18841

Hwang, M. G., Chung, I. K., Kang, B. G., & Cho, M. H. (2001). Sequence-specific binding property of Arabidopsis thaliana telomeric DNA binding protein 1 (AtTBP1). FEBS Letters, 503(1), 35–40. https://doi.org/10.1016/S0014-5793(01)02685-0

Chai, W., Ford, L. P., Lenertz, L., Wright, W. E., & Shay, J. W. (2002). Human Ku70/80 Associates Physically with Telomerase through Interaction with hTERT*. Journal of Biological Chemistry, 277(49), 47242–47247. https://doi.org/10.1074/jbc.M208542200

Chan, H., Wang, Y., & Feigon, J. (2017). Progress in Human and Tetrahymena Telomerase Structure Determination. Annual Review of Biophysics, 46(1), 199–225. https://doi.org/10.1146/annurev-biophys-062215-011140

Charbonnel, C., Rymarenko, O., Da Ines, O., Benyahya, F., White, C. I., Butter, F., & Amiard, S. (2018). The Linker Histone GH1-HMGA1 Is Involved in Telomere Stability and DNA Damage Repair. Plant Physiology, 177(1), 311–327. https://doi.org/10.1104/pp.17.01789

Chen, C. M., Wang, C. T., & Ho, C. H. (2001). A Plant Gene Encoding a Myb-like Protein That Binds Telomeric GGTTTAG Repeats in Vitro *. Journal of Biological Chemistry, 276(19), 16511–16519. https://doi.org/10.1074/jbc.M009659200

Chen, C.-M., Wang, C.-T., Kao, Y.-H., Chang, G.-D., Ho, C.-H., Lee, F., Hseu, M.-J. (2005). Functional redundancy of the duplex telomeric DNA-binding proteins in Arabidopsis.

Janoušková, E., Nečasová, I., Pavloušková, J., Zimmermann, M., Hluchý, M., Marini, V., Nováková, M., & Hofr, C. (2015). Human Rap1 modulates TRF2 attraction to telomeric DNA. Nucleic Acids Research, 43(5), 2691–2700. https://doi.org/10.1093/nar/gkv097

Jenner, L. P., Peska, V., Fulnečková, J., & Sýkorová, E. (2022). Telomeres and Their Neighbors. Genes, 13(9), 1663. https://doi.org/10.3390/genes13091663

Jurečková, J. F., Sýkorová, E., Hafidh, S., Honys, D., Fajkus, J., & Fojtová, M. (2017). Tissue-specific expression of telomerase reverse transcriptase gene variants in Nicotiana tabacum. Planta, 245(3), 549–561. https://doi.org/10.1007/s00425-016-2624-1

Kang, S. S., Kwon, T., Kwon, D. Y., & Do, S. I. (1999). Akt Protein Kinase Enhances Human Telomerase Activity through Phosphorylation of Telomerase Reverse Transcriptase Subunit*. Journal of Biological Chemistry, 274(19), 13085–13090. https://doi.org/10.1074/jbc.274.19.13085

Kannan, K., Nelson, A. D. L., & Shippen, D. E. (2008). Dyskerin Is a Component of the Arabidopsis Telomerase RNP Required for Telomere Maintenance. Molecular and Cellular Biology, 28(7), 2332–2341. https://doi.org/10.1128/MCB.01490-07

Kappei, D., Butter, F., Benda, C., Scheibe, M., Draškovič, I., Stevense, M., Novo, C. L., Basquin, C., Araki, M., Araki, K., Krastev, D. B., Kittler, R., Jessberger, R., Londoño-Vallejo, J. A., Mann, M., & Buchholz, F. (2013). HOT1 is a mammalian direct telomere repeat-binding protein contributing to telomerase recruitment. The EMBO Journal, 32(12), 1681–1701. https://doi.org/10.1038/emboj.2013.105

Karamysheva, Z. N., Surovtseva, Y. V., Vespa, L., Shakirov, E. V., & Shippen, D. E. (2004). A C-terminal Myb extension domain defines a novel family of double-strand telomeric DNA-binding proteins in Arabidopsis. The Journal of Biological Chemistry, 279(46), 47799–47807. https://doi.org/10.1074/jbc.M407938200

Kazda, A., Zellinger, B., Rössler, M., Derboven, E., Kusenda, B., & Riha, K. (2012). Chromosome end protection by blunt-ended telomeres. Genes & Development, 26(15), 1703–1713. https://doi.org/10.1101/gad.194944.112

Kim, J. H., Kim, W. T., & Chung, I. K. (1998). Rice proteins that bind single-stranded G-rich telomere DNA. Plant Molecular Biology, 36(5), 661–672. https://doi.org/10.1023/A:1005994719175

Ko, S., Jun, S.-H., Bae, H., Byun, J.-S., Han, W., Park, H., Yang, S. W., Park, S.-Y., Jeon, Y. H., Cheong, C., Kim, W. T., Lee, W., & Cho, H.-S. (2008). Structure of the DNA-binding domain of NgTRF1 reveals unique features of plant telomere-binding proteins. Nucleic Acids Research, 36(8), 2739–2755. https://doi.org/10.1093/nar/gkn030

Koonin, E. V. (2010). The origin and early evolution of eukaryotes in the light of phylogenomics. Genome Biology, 11(5), 209. https://doi.org/10.1186/gb-2010-11-5-209

Kotliński, M., Knizewski, L., Muszewska, A., Rutowicz, K., Lirski, M., Schmidt, A., Baroux, C., Ginalski, K., & Jerzmanowski, A. (2017). Phylogeny-Based Systematization of Arabidopsis Proteins with Histone H1 Globular Domain. Plant Physiology, 174(1), 27–34. https://doi.org/10.1104/pp.16.00214

Kováč, L.. Overview: bioenergetics between chemistry, genetics and physics (1987) Curr. Top. Bioenerg. 15, 331–372.

Kovařik, A., Fajkus, J., Koukalová, B., & Bezděk, M. (1996). Species-specific evolution of telomeric and rDNA repeats in the tobacco composite genome. Theoretical and Applied Genetics, 92(8), 1108–1111. https://doi.org/10.1007/BF00224057

Krause, K., Kilbienski, I., Mulisch, M., Rödiger, A., Schäfer, A., & Krupinska, K. (2005). DNA-binding proteins of the Whirly family in Arabidopsis thaliana are targeted to the organelles. FEBS Letters, 579(17), 3707–3712. https://doi.org/10.1016/j.febslet.2005.05.059

Kuchař, M., & Fajkus, J. (2004). Interactions of putative telomere-binding proteins in Arabidopsis thaliana: Identification of functional TRF2 homolog in plants. FEBS Letters, 578(3), 311–315. https://doi.org/10.1016/j.febslet.2004.11.021

Kupiec, M. (2014). Biology of telomeres: Lessons from budding yeast. FEMS Microbiology Reviews, 38(2), 144–171. https://doi.org/10.1111/1574-6976.12054

Kusová, A., Steinbachová, L., Přerovská, T., Drábková, L. Z., Paleček, J., Khan, A., Rigóová, G., Gadiou, Z., Jourdain, C., Stricker, T., Schubert, D., Honys, D., & Schrumpfová, P. P. (2023). Completing the TRB family: Newly characterized members show ancient evolutionary origins and distinct localization, yet similar interactions (s. 2022.11.23.517682). Plant Mol Biol

. 2023 May;112(1-2):61-83 DOI: 10.1007/s11103-023-01348-2

Kwon, C., & Chung, I. K. (2004). Interaction of an Arabidopsis RNA-binding Protein with Plant Single-stranded Telomeric DNA Modulates Telomerase Activity*. Journal of Biological Chemistry, 279(13), 12812–12818. https://doi.org/10.1074/jbc.M312011200

Lamarche, B., Orazio, N., & Weitzman, M. (2010). The MRN complex in Double-Strand Break Repair and Telomere Maintenance. FEBS letters, 584, 3682–3695. https://doi.org/10.1016/j.febslet.2010.07.029

Lansdorp, P. M., Verwoerd, N. P., van de Rijke, F. M., Dragowska, V., Little, M.-T., Dirks, R. W., Raap, A. K., & Tanke, H. J. (1996). Heterogeneity in Telomere Length of Human Chromosomes. Human Molecular Genetics, 5(5), 685–691. https://doi.org/10.1093/hmg/5.5.685

Lazzerini-Denchi, E., & Sfeir, A. (2016). Stop pulling my strings—What telomeres taught us about the DNA damage response. Nature Reviews Molecular Cell Biology, 17(6), Article 6. https://doi.org/10.1038/nrm.2016.43

Lee, W. K., & Cho, M. H. (2016). Telomere-binding protein regulates the chromosome ends through the interaction with histone deacetylases in Arabidopsis thaliana. Nucleic Acids Research, 44(10), 4610–4624. https://doi.org/10.1093/nar/gkw067

Lee, Y. W., & Kim, W. T. (2010). Tobacco GTBP1, a Homolog of Human Heterogeneous Nuclear Ribonucleoprotein, Protects Telomeres from Aberrant Homologous Recombination. The Plant Cell, 22(8), 2781–2795. https://doi.org/10.1105/tpc.110.076778

Leehy, K. A., Lee, J. R., Song, X., Renfrew, K. B., & Shippen, D. E. (2013). MERISTEM DISORGANIZATION1 Encodes TEN1, an Essential Telomere Protein That Modulates Telomerase Processivity in Arabidopsis. The Plant Cell, 25(4), 1343–1354. https://doi.org/10.1105/tpc.112.107425

Lei, M., Baumann, P., & Cech, T. R. (2002). Cooperative Binding of Single-Stranded Telomeric DNA by the Pot1 Protein of Schizosaccharomyces pombe. Biochemistry, 41(49), 14560–14568. https://doi.org/10.1021/bi026674z

Lermontova, I., Schubert, V., Börnke, F., Macas, J., & Schubert, I. (2007). Arabidopsis CBF5 interacts with the H/ACA snoRNP assembly factor NAF1. Plant Molecular Biology, 65(5), 615–626. https://doi.org/10.1007/s11103-007-9226-z

Li, A. Y.-J., Lin, H. H., Kuo, C.-Y., Shih, H.-M., Wang, C. C. C., Yen, Y., & Ann, D. K. (2011). High-mobility group A2 protein modulates hTERT transcription to promote tumorigenesis. Molecular and Cellular Biology, 31(13), 2605–2617. https://doi.org/10.1128/MCB.05447-11

Liboz, T., Bardet, C., Le Van Thai, A., Axelos, M., & Lescure, B. (1990). The four members of the gene family encoding the Arabidopsis thaliana translation elongation factor EF-1α are actively transcribed. Plant Molecular Biology, 14(1), 107–110. https://doi.org/10.1007/BF00015660

Lildballe, D. L., Pedersen, D. S., Kalamajka, R., Emmersen, J., Houben, A., & Grasser, K. D. (2008). The Expression Level of the Chromatin-Associated HMGB1 Protein Influences Growth, Stress Tolerance, and Transcriptome in Arabidopsis. Journal of Molecular Biology, 384(1), 9–21. https://doi.org/10.1016/j.jmb.2008.09.014

Lim, C. J., Zaug, A. J., Kim, H. J., & Cech, T. R. (2017). Reconstitution of human shelterin complexes reveals unexpected stoichiometry and dual pathways to enhance telomerase processivity. Nature Communications, 8(1), Article 1. https://doi.org/10.1038/s41467-017-01313-w

Liu, T., Li, S., Xia, C., & Xu, D. (2022). TERT promoter mutations and methylation for telomerase activation in urothelial carcinomas: New mechanistic insights and clinical significance. Frontiers in Immunology, 13, 1071390. https://doi.org/10.3389/fimmu.2022.1071390

Lu, F., Cui, X., Zhang, S., Liu, C., & Cao, X. (2010). JMJ14 is an H3K4 demethylase regulating flowering time in Arabidopsis. Cell Research, 20(3), Article 3. https://doi.org/10.1038/cr.2010.27

Lue, N. F. (2018). Evolving Linear Chromosomes and Telomeres: A C-Strand-Centric View. Trends in Biochemical Sciences, 43(5), 314–326. https://doi.org/10.1016/j.tibs.2018.02.008

Lugert, T., & Werr, W. (1994). A novel DNA-binding domain in theShrunken initiator-binding protein (IBP1). Plant Molecular Biology, 25(3), 493–506. https://doi.org/10.1007/BF00043877

Lundblad, V., & Szostak, J. W. (1989). A mutant with a defect in telomere elongation leads to senescence in yeast. Cell, 57(4), 633–643. https://doi.org/10.1016/0092-8674(89)90132-3

Maillet, G., White, C. I., & Gallego, M. E. (2006). Telomere-length regulation in inter-ecotype crosses of Arabidopsis. Plant Molecular Biology, 62(6), 859–866. https://doi.org/10.1007/s11103-006-9061-7

Majerová, E., Mandáková, T., Vu, G. T. H., Fajkus, J., Lysak, M. A., & Fojtová, M. (2014). Chromatin features of plant telomeric sequences at terminal vs. Internal positions. Frontiers in Plant Science, 5. https://www.frontiersin.org/articles/10.3389/fpls.2014.00593

Majerská, J., Sýkorová, E., & Fajkus, J. (2011). Non-telomeric activities of telomerase. Molecular BioSystems, 7(4), 1013–1023. https://doi.org/10.1039/C0MB00268B

Makarov, V. L., Hirose, Y., & Langmore, J. P. (1997). Long G Tails at Both Ends of Human Chromosomes Suggest a C Strand Degradation Mechanism for Telomere Shortening. Cell, 88(5), 657–666. https://doi.org/10.1016/S0092-8674(00)81908-X

Mandáková, T., Joly, S., Krzywinski, M., Mummenhoff, K., & Lysak, M. A. (2010). Fast Diploidization in Close Mesopolyploid Relatives of Arabidopsis. The Plant Cell, 22(7), 2277–2290. https://doi.org/10.1105/tpc.110.074526

Mandáková, T., & Lysak, M. A. (2008). Chromosomal Phylogeny and Karyotype Evolution in x=7 Crucifer Species (Brassicaceae). The Plant Cell, 20(10), 2559–2570. https://doi.org/10.1105/tpc.108.062166

Mao, Y.-Q., & Houry, W. A. (2017). The Role of Pontin and Reptin in Cellular Physiology and Cancer Etiology. Frontiers in Molecular Biosciences, 4. https://www.frontiersin.org/articles/10.3389/fmolb.2017.00058

Marian, C. O., & Bass, H. W. (2005). The Terminal acidic SANT 1 (Tacs1) gene of maize is expressed in tissues containing meristems and encodes an acidic SANT domain similar to some chromatin-remodeling complex proteins. Biochimica et Biophysica Acta (BBA) - Gene Structure and Expression, 1727(2), 81–86. https://doi.org/10.1016/j.bbaexp.2004.12.010

Marian, C. O., Bordoli, S. J., Goltz, M., Santarella, R. A., Jackson, L. P., Danilevskaya, O., Beckstette, M., Meeley, R., & Bass, H. W. (2003). The maize Single myb histone 1 gene, Smh1, belongs to a novel gene family and encodes a protein that binds telomere DNA repeats in vitro. Plant Physiology, 133(3), 1336–1350. https://doi.org/10.1104/pp.103.026856

Mason, J. M., Randall, T. A., & Capkova Frydrychova, R. (2016). Telomerase lost? Chromosoma, 125(1), 65–73. https://doi.org/10.1007/s00412-015-0528-7

Matias, P. M., Gorynia, S., Donner, P., & Carrondo, M. A. (2006). Crystal Structure of the Human AAA+ Protein RuvBL1*. Journal of Biological Chemistry, 281(50), 38918–38929. https://doi.org/10.1074/jbc.M605625200

McClintock, B. (1942). The Fusion of Broken Ends of Chromosomes Following Nuclear Fusion. Proceedings of the National Academy of Sciences of the United States of America, 28(11), 458–463.

Mikulski, P., Hohenstatt, M. L., Farrona, S., Smaczniak, C., Stahl, Y., Kalyanikrishna, Kaufmann, K., Angenent, G., & Schubert, D. (2019). The Chromatin-Associated Protein PWO1 Interacts with Plant Nuclear Lamin-like Components to Regulate Nuclear Size. The Plant Cell, 31(5), 1141–1154. https://doi.org/10.1105/tpc.18.00663

Min, J., Wright, W. E., & Shay, J. W. (2017). Alternative lengthening of telomeres can be maintained by preferential elongation of lagging strands. Nucleic Acids Research, 45(5), 2615–2628. https://doi.org/10.1093/nar/gkw1295

Moore, J. M. (2009). Investigating the DNA Binding Properties of the Initiator Binding Protein 2 (IBP2) in Maize (Zea Mays). https://diginole.lib.fsu.edu/islandora/object/fsu%3A180521/

Moriguchi, R., Kanahama, K., & Kanayama, Y. (2006). Characterization and expression analysis of the tomato telomere-binding protein LeTBP1. Plant Science, 171(1), 166–174. https://doi.org/10.1016/j.plantsci.2006.03.010

Moyzis, R. K., Buckingham, J. M., Cram, L. S., Dani, M., Deaven, L. L., Jones, M. D., Meyne, J., Ratliff, R. L., & Wu, J. R. (1988). A highly conserved repetitive DNA sequence, (TTAGGG)n, present at the telomeres of human chromosomes. Proceedings of the National Academy of Sciences, 85(18), 6622–6626. https://doi.org/10.1073/pnas.85.18.6622

Mozgová, I., Schrumpfová, P. P., Hofr, C., & Fajkus, J. (2008). Functional characterization of domains in AtTRB1, a putative telomere-binding protein in Arabidopsis thaliana. Phytochemistry, 69(9), 1814–1819. https://doi.org/10.1016/j.phytochem.2008.04.001

Muller, H.J. The remaking of chromosomes. Collect. Net. (1938), 13, 181–195.

Müller, F., Wicky, C., Spicher, A., & Tobler, H. (1991). New telomere formation after developmentally regulated chromosomal breakage during the process of chromatin diminution in ascaris lumbricoides. Cell, 67(4), 815–822. https://doi.org/10.1016/0092-8674(91)90076-B

Natarajan, S., Begum, F., Gim, J., Wark, L., Henderson, D., Davie, J. R., Hombach-Klonisch, S., & Klonisch, T. (2016). High Mobility Group A2 protects cancer cells against telomere dysfunction. Oncotarget, 7(11), 12761–12782. https://doi.org/10.18632/oncotarget.6938

Nečasová, I., Janoušková, E., Klumpler, T., & Hofr, C. (2017). Basic domain of telomere guardian TRF2 reduces D-loop unwinding whereas Rap1 restores it. Nucleic Acids Research, 45(21), 12170–12180. https://doi.org/10.1093/nar/gkx812

Neumann, A. A., Watson, C. M., Noble, J. R., Pickett, H. A., Tam, P. P. L., & Reddel, R. R. (2013). Alternative lengthening of telomeres in normal mammalian somatic cells. Genes & Development, 27(1), 18–23. https://doi.org/10.1101/gad.205062.112

Nguyen, T. H. D. (2021). Structural biology of human telomerase: Progress and prospects. Biochemical Society Transactions, 49(5), 1927–1939. https://doi.org/10.1042/BST20200042

Nguyen, T. H. D., Tam, J., Wu, R. A., Greber, B. J., Toso, D., Nogales, E., & Collins, K. (2018). Cryo-EM structure of substrate-bound human telomerase holoenzyme. Nature, 557(7704), Article 7704. https://doi.org/10.1038/s41586-018-0062-x

Nittis, T., Guittat, L., LeDuc, R. D., Dao, B., Duxin, J. P., Rohrs, H., Townsend, R. R., & Stewart, S. A. (2010). Revealing Novel Telomere Proteins Using in Vivo Cross-linking, Tandem Affinity Purification, and Label-free Quantitative LC-FTICR-MS*. Molecular & Cellular Proteomics, 9(6), 1144–1156. https://doi.org/10.1074/mcp.M900490-MCP200

Oganesian, L., & Karlseder, J. (2011). Mammalian 5′ C-Rich Telomeric Overhangs Are a Mark of Recombination-Dependent Telomere Maintenance. Molecular Cell, 42(2), 224–236. https://doi.org/10.1016/j.molcel.2011.03.015

Ogita, N., Okushima, Y., Tokizawa, M., Yamamoto, Y. Y., Tanaka, M., Seki, M., Makita, Y., Matsui, M., Okamoto-Yoshiyama, K., Sakamoto, T., Kurata, T., Hiruma, K., Saijo, Y., Takahashi, N., & Umeda, M. (2018). Identifying the target genes of SUPPRESSOR OF GAMMA RESPONSE 1, a master transcription factor controlling DNA damage response in Arabidopsis. The Plant Journal, 94(3), 439–453. https://doi.org/10.1111/tpj.13866

Ogrocká, A., Sýkorová, E., Fajkus, J., & Fojtová, M. (2012). Developmental silencing of the AtTERT gene is associated with increased H3K27me3 loading and maintenance of its euchromatic environment. Journal of Experimental Botany, 63(11), 4233–4241. https://doi.org/10.1093/jxb/ers107

Oguchi, K., Tamura, K., & Takahashi, H. (2004). Characterization of Oryza sativa telomerase reverse transcriptase and possible role of its phosphorylation in the control of telomerase activity. Gene, 342(1), 57–66. https://doi.org/10.1016/j.gene.2004.07.011

Olovnikov, A. M. (1973). A theory of marginotomy: The incomplete copying of template margin in enzymic synthesis of polynucleotides and biological significance of the phenomenon. Journal of Theoretical Biology, 41(1), 181–190. https://doi.org/10.1016/0022-5193(73)90198-7

Ozturk, N., Singh, I., Mehta, A., Braun, T., & Barreto, G. (2014). HMGA proteins as modulators of chromatin structure during transcriptional activation. Frontiers in Cell and Developmental Biology, 2. https://www.frontiersin.org/articles/10.3389/fcell.2014.00005

Palm, W., & de Lange, T. (2008). How Shelterin Protects Mammalian Telomeres. Annual Review of Genetics, 42(1), 301–334. https://doi.org/10.1146/annurev.genet.41.110306.130350

Palm, W., Hockemzer, D., Kibe, T., &cde Lange, T.. (2009) Functional Dissection of Human and Mouse POT1 Proteins. Mol Cell Biol. 29(2): 471–482. doi: 10.1128/MCB.01352-08

Pecinka, A., Procházková Schrumpfová, P., Fischer, L., Dvořák Tomaštíková, E., & Mozgová, I. (2022). The Czech Plant Nucleus Workshop 2021. Biologia Plantarum, 66(1), 39–45. https://doi.org/10.32615/bp.2022.003

Pedersen, D. S., & Grasser, K. D. (2010). The role of chromosomal HMGB proteins in plants. Biochimica et Biophysica Acta (BBA) - Gene Regulatory Mechanisms, 1799(1), 171–174. https://doi.org/10.1016/j.bbagrm.2009.11.004

Pendle, A. F., Clark, G. P., Boon, R., Lewandowska, D., Lam, Y. W., Andersen, J., Mann, M., Lamond, A. I., Brown, J. W. S., & Shaw, P. J. (2005). Proteomic Analysis of the Arabidopsis Nucleolus Suggests Novel Nucleolar Functions. Molecular Biology of the Cell, 16(1), 260–269. https://doi.org/10.1091/mbc.e04-09-0791

Peska, V., Mátl, M., Mandáková, T., Vitales, D., Fajkus, P., Fajkus, J., & Garcia, S. (2020). Human-like telomeres in Zostera marina reveal a mode of transition from the plant to the human telomeric sequences. Journal of Experimental Botany, 71(19), 5786–5793. https://doi.org/10.1093/jxb/eraa293

Peška, V., Fajkus, P., Fojtová, M., Dvořáčková, M., Hapala, J., Dvořáček, V., Polanská, P., Leitch, A. R., Sýkorová, E., & Fajkus, J. (2015). Characterisation of an unusual telomere motif (TTTTTTAGGG)n in the plant Cestrum elegans

(Solanaceae), a species with a large genome. The Plant Journal: For Cell and Molecular Biology, 82(4), 644–654. https://doi.org/10.1111/tpj.12839

Peška, V., Schrumpfová, P. P., & Fajkus, J. (2011). Using the telobox to search for plant telomere binding proteins. Current Protein & Peptide Science, 12(2), 75–83. https://doi.org/10.2174/138920311795684968

Peška, V., Sýkorová, E., & Fajkus, J. (2009). Two faces of Solanaceae telomeres: A comparison between Nicotiana and Cestrum telomeres and telomere-binding proteins. Cytogenetic and Genome Research, 122(3–4), 380–387. https://doi.org/10.1159/000167826

Polanská, E., Dobšáková, Z., Dvořáčková, M., Fajkus, J., & Štros, M. (2012). HMGB1 gene knockout in mouse embryonic fibroblasts results in reduced telomerase activity and telomere dysfunction. Chromosoma, 121(4), 419–431. https://doi.org/10.1007/s00412-012-0373-x

Pontvianne, F., Abou-Ellail, M., Douet, J., Comella, P., Matia, I., Chandrasekhara, C., DeBures, A., Blevins, T., Cooke, R., Medina, F. J., Tourmente, S., Pikaard, C. S., & Sáez-Vásquez, J. (2010). Nucleolin Is Required for DNA Methylation State and the Expression of rRNA Gene Variants in Arabidopsis thaliana. PLOS Genetics, 6(11), e1001225. https://doi.org/10.1371/journal.pgen.1001225

Pontvianne, F., Carpentier, M.-C., Durut, N., Pavlištová, V., Jaške, K., Schořová, Š., Parrinello, H., Rohmer, M., Pikaard, C. S., Fojtová, M., Fajkus, J., & Sáez-Vásquez, J. (2016). Identification of Nucleolus-Associated Chromatin Domains Reveals a Role for the Nucleolus in 3D Organization of the A. thaliana Genome. Cell Reports, 16(6), 1574–1587. https://doi.org/10.1016/j.celrep.2016.07.016

Price, C., Boltz, K. A., Chaiken, M. F., Stewart, J. A., Beilstein, M. A., & Shippen, D. E. (2010). Evolution of CST function in telomere maintenance. Cell Cycle, 9(16), 3177–3185. https://doi.org/10.4161/cc.9.16.12547

Price, C. M., & Cech, T. R. (1987). Telomeric DNA-protein interactions of Oxytricha macronuclear DNA. Genes & Development, 1(8), 783–793. https://doi.org/10.1101/gad.1.8.783

Qi, H., & Zakian, V. A. (2000). The Saccharomyces telomere-binding protein Cdc13p interacts with both the catalytic subunit of DNA polymerase alpha and the telomerase-associated est1 protein. Genes & Development, 14(14), 1777–1788.

Qiao, X., Zhang, S., & Paterson, A. H. (2022). Pervasive genome duplications across the plant tree of life and their links to major evolutionary innovations and transitions. Computational and Structural Biotechnology Journal, 20, 3248–3256. https://doi.org/10.1016/j.csbj.2022.06.026

Raices, M., Verdun, R. E., Compton, S. A., Haggblom, C. I., Griffith, J. D., Dillin, A., & Karlseder, J. (2008). C. elegans Telomeres Contain G-Strand and C-Strand Overhangs that Are Bound by Distinct Proteins. Cell, 132(5), 745–757. https://doi.org/10.1016/j.cell.2007.12.039

Ramjeesingh, M., Huan, L. J., Garami, E., & Bear, C. E. (1999). Novel method for evaluation of the oligomeric structure of membrane proteins. Biochemical Journal, 342(Pt 1), 119–123.

Recker, J., Knoll, A., & Puchta, H. (2014). The Arabidopsis thaliana Homolog of the Helicase RTEL1 Plays Multiple Roles in Preserving Genome Stability. The Plant Cell, 26(12), 4889–4902. https://doi.org/10.1105/tpc.114.132472

Reeves, R. (2015). High mobility group (HMG) proteins: Modulators of chromatin structure and DNA repair in mammalian cells. DNA Repair, 36, 122–136. https://doi.org/10.1016/j.dnarep.2015.09.015

Ren, S., Johnston, J. S., Shippen, D. E., & McKnight, T. D. (2004). TELOMERASE ACTIVATOR1 Induces Telomerase Activity and Potentiates Responses to Auxin in Arabidopsis. The Plant Cell, 16(11), 2910–2922. https://doi.org/10.1105/tpc.104.025072

Ren, S., Mandadi, K. K., Boedeker, A. L., Rathore, K. S., & McKnight, T. D. (2007). Regulation of Telomerase in Arabidopsis by BT2, an Apparent Target of TELOMERASE ACTIVATOR1. The Plant Cell, 19(1), 23–31. https://doi.org/10.1105/tpc.106.044321

Rice, C., & Skordalakes, E. (2016). Structure and function of the telomeric CST complex. Computational and Structural Biotechnology Journal, 14, 161–167. https://doi.org/10.1016/j.csbj.2016.04.002

Riha, K., Fajkus, J., Siroky, J., & Vyskot, B. (1998). Developmental Control of Telomere Lengths and Telomerase Activity in Plants. The Plant Cell, 10(10), 1691–1698. https://doi.org/10.1105/tpc.10.10.1691

Riha, K., McKnight, T. D., Fajkus, J., Vyskot, B., & Shippen, D. E. (2000). Analysis of the G-overhang structures on plant telomeres: Evidence for two distinct telomere architectures. The Plant Journal, 23(5), 633–641. https://doi.org/10.1046/j.1365-313x.2000.00831.x

Riha, K., McKnight, T. D., Griffing, L. R., & Shippen, D. E. (2001). Living with Genome Instability: Plant Responses to Telomere Dysfunction. Science, 291(5509), 1797–1800. https://doi.org/10.1126/science.1057110

Riha, K., Watson, J. M., Parkey, J., & Shippen, D. E. (2002). Telomere length deregulation and enhanced sensitivity to genotoxic stress in Arabidopsis mutants deficient in Ku70. The EMBO Journal, 21(11), 2819–2826. https://doi.org/10.1093/emboj/21.11.2819

Richards, E. J., & Ausubel, F. M. (1988). Isolation of a higher eukaryotic telomere from Arabidopsis thaliana. Cell, 53(1), 127–136. https://doi.org/10.1016/0092-8674(88)90494-1

Rossignol, P., Collier, S., Bush, M., Shaw, P., & Doonan, J. H. (2007). Arabidopsis POT1A interacts with TERT-V(I8), an N-terminal splicing variant of telomerase. Journal of Cell Science, 120(20), 3678–3687. https://doi.org/10.1242/jcs.004119

Roy, A., Dutta, A., Roy, D., Ganguly, P., Ghosh, R., Kar, R. K., Bhunia, A., Mukhobadhyay, J., & Chaudhuri, S. (2016). Deciphering the role of the AT-rich interaction domain and the HMG-box domain of ARID-HMG proteins of Arabidopsis thaliana. Plant Molecular Biology, 92(3), 371–388. https://doi.org/10.1007/s11103-016-0519-y

Růcková, E., Friml, J., Procházková Schrumpfová, P., & Fajkus, J. (2008). Role of alternative telomere lengthening unmasked in telomerase knock-out mutant plants. Plant Molecular Biology, 66(6), 637–646. https://doi.org/10.1007/s11103-008-9295-7

Ruiz-Herrera, A., Nergadze, S. G., Santagostino, M., & Giulotto, E. (2009). Telomeric repeats far from the ends: Mechanisms of origin and role in evolution. Cytogenetic and Genome Research, 122(3–4), 219–228. https://doi.org/10.1159/000167807

Safak, M., Gallia, G. L., & Khalili, K. (1999). Reciprocal interaction between two cellular proteins, Puralpha and YB-1, modulates transcriptional activity of JCVCY in glial cells. Molecular and Cellular Biology, 19(4), 2712–2723. https://doi.org/10.1128/MCB.19.4.2712

Sanders, J. L., & Newman, A. B. (2013). Telomere Length in Epidemiology: A Biomarker of Aging, Age-Related Disease, Both, or Neither? Epidemiologic Reviews, 35(1), 112–131. https://doi.org/10.1093/epirev/mxs008

Sauerwald, A., Sandin, S., Cristofari, G., Scheres, S. H. W., Lingner, J., & Rhodes, D. (2013). Structure of active dimeric human telomerase. Nature Structural & Molecular Biology, 20(4), Article 4. https://doi.org/10.1038/nsmb.2530

Seluanov, A., Chen, Z., Hine, C., Sasahara, T. H. C., Ribeiro, A. A. C. M., Catania, K. C., Presgraves, D. C., & Gorbunova, V. (2007). Telomerase activity coevolves with body mass not lifespan. Aging Cell, 6(1), 45–52. https://doi.org/10.1111/j.1474-9726.2006.00262.x

Sfeir, A. (2012). Telomeres at a glance. Journal of Cell Science, 125(18), 4173–4178. https://doi.org/10.1242/jcs.106831

Shakirov, E. V., McKnight, T. D., & Shippen, D. E. (2009). POT1-independent single-strand telomeric DNA binding activities in Brassicaceae. The Plant Journal, 58(6), 1004–1015. https://doi.org/10.1111/j.1365-313X.2009.03837.x

Shakirov, E. V., Perroud, P.-F., Nelson, A. D., Cannell, M. E., Quatrano, R. S., & Shippen, D. E. (2010). Protection of Telomeres 1 Is Required for Telomere Integrity in the Moss Physcomitrella patens. The Plant Cell, 22(6), 1838–1848. https://doi.org/10.1105/tpc.110.075846

Shakirov, E. V., & Shippen, D. E. (2004). Length Regulation and Dynamics of Individual Telomere Tracts in Wild-Type Arabidopsis. The Plant Cell, 16(8), 1959–1967. https://doi.org/10.1105/tpc.104.023093

Shakirov, E. V., Song, X., Joseph, J. A., & Shippen, D. E. (2009). POT1 proteins in green algae and land plants: DNA-binding properties and evidence of co-evolution with telomeric DNA. Nucleic Acids Research, 37(22), 7455–7467. https://doi.org/10.1093/nar/gkp785

Shakirov, E. V., Surovtseva, Y. V., Osbun, N., & Shippen, D. E. (2005). The Arabidopsis Pot1 and Pot2 Proteins Function in Telomere Length Homeostasis and Chromosome End Protection. Molecular and Cellular Biology, 25(17), 7725–7733. https://doi.org/10.1128/MCB.25.17.7725-7733.2005

Shay, J. W., & Wright, W. E. (2000). Hayflick, his limit, and cellular ageing. Nature Reviews Molecular Cell Biology, 1(1), Article 1. https://doi.org/10.1038/35036093

Shay, J. W., & Wright, W. E. (2019). Telomeres and telomerase: Three decades of progress. Nature Reviews Genetics, 20(5), Article 5. https://doi.org/10.1038/s41576-019-0099-1

Shepelev, N., Dontsova, O., & Rubtsova, M. (2023). Post-Transcriptional and Post-Translational Modifications in Telomerase Biogenesis and Recruitment to Telomeres. International Journal of Molecular Sciences, 24(5), Article 5. https://doi.org/10.3390/ijms24055027

Scheibe, M., Arnoult, N., Kappei, D., Buchholz, F., Decottignies, A., Butter, F., & Mann, M. (2013). Quantitative interaction screen of telomeric repeat-containing RNA reveals novel TERRA regulators. Genome Research, 23(12), 2149–2157. https://doi.org/10.1101/gr.151878.112

Schmidt, J. C., & Cech, T. R. (2015). Human telomerase: Biogenesis, trafficking, recruitment, and activation. Genes & Development, 29(11), 1095–1105. https://doi.org/10.1101/gad.263863.115

Schmidt, J. C., Dalby, A. B., & Cech, T. R. (2014). Identification of human TERT elements necessary for telomerase recruitment to telomeres. eLife, 3, e03563. https://doi.org/10.7554/eLife.03563

Schořová, Š., Fajkus, J., & Schrumpfová, P. P. (2020). Optimized Detection of Protein-Protein and Protein-DNA Interactions, with Particular Application to Plant Telomeres. In R. Hancock (Ed.), The Nucleus (s. 139–167). Springer US. https://doi.org/10.1007/978-1-0716-0763-3_11

Schořová, Š., Fajkus, J., Záveská Drábková, L., Honys, D., & Schrumpfová, P. P. (2019). The plant Pontin and Reptin homologues, RuvBL1 and RuvBL2a, colocalize with TERT and TRB proteins in vivo, and participate in telomerase biogenesis. The Plant Journal, 98(2), 195–212. https://doi.org/10.1111/tpj.14306

Schrumpfová, P., Kuchař, M., Miková, G., Skřišovská, L., Kubičárová, T., & Fajkus, J. (2004). Characterization of two Arabidopsis thaliana myb-like proteins showing affinity to telomeric DNA sequence. Genome, 47(2), 316–324. https://doi.org/10.1139/g03-136

Schrumpfová, P. P., Kuchař, M., Paleček, J., & Fajkus, J. (2008). Mapping of interaction domains of putative telomere-binding proteins AtTRB1 and AtPOT1b from Arabidopsis thaliana. FEBS Letters, 582(10), 1400–1406. https://doi.org/10.1016/j.febslet.2008.03.034

Schrumpfová, P. P., Fojtová, M., Mokroš, P., Grasser, K. D., & Fajkus, J. (2011). Role of HMGB proteins in chromatin dynamics and telomere maintenance in Arabidopsis thaliana. Current Protein & Peptide Science, 12(2), 105–111. https://doi.org/10.2174/138920311795684922

Schrumpfová, P., Vychodilová, I., Dvořáčková, M., Majerská, J., Dokládal, L., Schořová, Š., & Fajkus, J. (2014). Telomere repeat binding proteins are functional components of Arabidopsis telomeres and interact with telomerase. The Plant Journal, 77(5), 770–781. https://doi.org/10.1111/tpj.12428

Schrumpfová, P., Schořová, Š., & Fajkus, J. (2016a). Telomere- and Telomerase-Associated Proteins and Their Functions in the Plant Cell. Frontiers in Plant Science, 7. https://www.frontiersin.org/articles/10.3389/fpls.2016.00851

Schrumpfová, P. P., Vychodilová, I., Hapala, J., Schořová, Š., Dvořáček, V., & Fajkus, J. (2016b). Telomere binding protein TRB1 is associated with promoters of translation machinery genes in vivo. Plant Molecular Biology, 90(1), 189–206. https://doi.org/10.1007/s11103-015-0409-8

Schrumpfová, P. P., Majerská, J., Dokládal, L., Schořová, Š., Stejskal, K., Obořil, M., Honys, D., Kozáková, L., Polanská, P. S., & Sýkorová, E. (2017). Tandem affinity purification of AtTERT reveals putative interaction partners of plant telomerase in vivo. Protoplasma, 254(4), 1547–1562. https://doi.org/10.1007/s00709-016-1042-3

Schrumpfová, P. P., Majerská, J., Dokládal, L., Schořová, Š., Stejskal, K., Obořil, M., Honys, D., Kozáková, L., Polanská, P. S., & Sýkorová, E. (2018). Correction to: Tandem affinity purification of AtTERT reveals putative interaction partners of plant telomerase in vivo. Protoplasma, 255(2), 715–715. https://doi.org/10.1007/s00709-018-1224-2

Schrumpfová, P., Fojtová, M., & Fajkus, J. (2019). Telomeres in Plants and Humans: Not So Different, Not So Similar. Cells, 8(1), Article 1. https://doi.org/10.3390/cells8010058

Schrumpfová, P. P., & Fajkus, J. (2020). Composition and Function of Telomerase-A Polymerase Associated with the Origin of Eukaryotes. Biomolecules, 10(10), 1425. https://doi.org/10.3390/biom10101425

Schwacke, R., Fischer, K., Ketelsen, B., Krupinska, K., & Krause, K. (2007). Comparative survey of plastid and mitochondrial targeting properties of transcription factors in Arabidopsis and rice. Molecular Genetics and Genomics, 277(6), 631–646. https://doi.org/10.1007/s00438-007-0214-4

Simonet, T., Zaragosi, L.-E., Philippe, C., Lebrigand, K., Schouteden, C., Augereau, A., Bauwens, S., Ye, J., Santagostino, M., Giulotto, E., Magdinier, F., Horard, B., Barbry, P., Waldmann, R., & Gilson, E. (2011). The human TTAGGG repeat factors 1 and 2 bind to a subset of interstitial telomeric sequences and satellite repeats. Cell Research, 21(7), Article 7. https://doi.org/10.1038/cr.2011.40

Smogorzewska, A., Karlseder, J., Holtgreve-Grez, H., Jauch, A., & de Lange, T. (2002). DNA Ligase IV-Dependent NHEJ of Deprotected Mammalian Telomeres in G1 and G2. Current Biology, 12(19), 1635–1644. https://doi.org/10.1016/S0960-9822(02)01179-X

Song, J., Castillo-González, C., Ma, Z., & Shippen, D. E. (2021). Arabidopsis retains vertebrate-type telomerase accessory proteins via a plant-specific assembly. Nucleic Acids Research, 49(16), 9496–9507. https://doi.org/10.1093/nar/gkab699

Surovtseva, Y. V., Shakirov, E. V., Vespa, L., Osbun, N., Song, X., & Shippen, D. E. (2007). Arabidopsis POT1 associates with the telomerase RNP and is required for telomere maintenance. The EMBO Journal, 26(15), 3653–3661. https://doi.org/10.1038/sj.emboj.7601792

Sweetlove, L., & Gutierrez, C. (2019). The journey to the end of the chromosome: Delivering active telomerase to telomeres in plants. The Plant Journal, 98(2), 193–194. https://doi.org/10.1111/tpj.14328

Sýkorová, E., & Fajkus, J. (2009). Structure—Function relationships in telomerase genes. Biology of the Cell, 101(7), 375–406. https://doi.org/10.1042/BC20080205

Sýkorová, E., Fulnečková, J., Mokroš, P., Fajkus, J., Fojtová, M., & Peška, V. (2012). Three TERT genes in Nicotiana tabacum. Chromosome Research, 20(4), 381–394. https://doi.org/10.1007/s10577-012-9282-3

Sýkorová, E., Leitch, A. R., & Fajkus, J. (2006). Asparagales Telomerases which Synthesize the Human Type of Telomeres. Plant Molecular Biology, 60(5), 633–646. https://doi.org/10.1007/s11103-005-5091-9

Sýkorová, E., Lim, K. Y., Kunická, Z., Chase, M. w., Bennett, M. D., Fajkus, J., & Leitch, A. R. (2003). Telomere variability in the monocotyledonous plant order Asparagales. Proceedings of the Royal Society of London. Series B: Biological Sciences, 270(1527), 1893–1904. https://doi.org/10.1098/rspb.2003.2446

Tamura, K., Liu, H., & Takahashi, H. (1999). Auxin Induction of Cell Cycle Regulated Activity of Tobacco Telomerase*. Journal of Biological Chemistry, 274(30), 20997–21002. https://doi.org/10.1074/jbc.274.30.20997

Tan, L.-M., Zhang, C.-J., Hou, X.-M., Shao, C.-R., Lu, Y.-J., Zhou, J.-X., Li, Y.-Q., Li, L., Chen, S., & He, X.-J. (2018). The PEAT protein complexes are required for histone deacetylation and heterochromatin silencing. The EMBO Journal, 37(19), e98770. https://doi.org/10.15252/embj.201798770

Tani, A., & Murata, M. (2005). Alternative splicing of Pot1 (Protection of telomere)-like genes in Arabidopsis thaliana. Genes & Genetic Systems, 80(1), 41–48. https://doi.org/10.1266/ggs.80.41

Teano G., Concia L., Wolff L., Carron L., Biocanin I., Adamusová K., Fojtová M., Bourge M., Kramdi A., Colot V., Grossniklaus U., Bowler Ch., Baroux C., Carbone A., Probst A.V., Schrumpfová P.P., Fajkus J., Amiard S., Grob S., Bourbousse C., and Barneche F. 2023. Histone H1 protects telomeric repeats from H3K27me3 invasion in Arabidopsis. Cell Reports, 42(8):112894. doi: 10.1016/j.celrep.2023

To, T. K., Kim, J.-M., Matsui, A., Kurihara, Y., Morosawa, T., Ishida, J., Tanaka, M., Endo, T., Kakutani, T., Toyoda, T., Kimura, H., Yokoyama, S., Shinozaki, K., & Seki, M. (2011). Arabidopsis HDA6 Regulates Locus-Directed Heterochromatin Silencing in Cooperation with MET1. PLOS Genetics, 7(4), e1002055. https://doi.org/10.1371/journal.pgen.1002055

Tomaštíková, E., Yang, F., Mlynárová, K., Hafidh, S., Schořová, Š., Kusová, A., Pernisová, M., Přerovská, T., Klodová, B., Honys, D., Fajkus, J., Pecinka, A., & Schrumpfová, P. P. (b.r.). RUVBL proteins are involved in plant gametophyte development. The Plant Journal, n/a(n/a). https://doi.org/10.1111/tpj.16136

Tomáška, Ľ., Nosek, J., Sepšiová, R., Červenák, F., Juríková, K., Procházková, K., Neboháčová, M., Willcox, S., & Griffith, J. D. (2018). Commentary: Single-stranded telomere-binding protein employs a dual rheostat for binding affinity and specificity that drives function. Frontiers in Genetics, 9, 742. https://doi.org/10.3389/fgene.2018.00742

Tran, T. D., Cao, H. X., Jovtchev, G., Neumann, P., Novák, P., Fojtová, M., Vu, G. T. H., Macas, J., Fajkus, J., Schubert, I., & Fuchs, J. (2015). Centromere and telomere sequence alterations reflect the rapid genome evolution within the carnivorous plant genus Genlisea. The Plant Journal, 84(6), 1087–1099. https://doi.org/10.1111/tpj.13058

Tremousaygue, D., Manevski, A., Bardet, C., Lescure, N., & Lescure, B. (1999). Plant interstitial telomere motifs participate in the control of gene expression in root meristems. The Plant Journal, 20(5), 553–561. https://doi.org/10.1046/j.1365-313X.1999.00627.x

Tsuzuki, M., & Wierzbicki, A. T. (2018). Buried in PEAT—discovery of a new silencing complex with opposing activities. The EMBO Journal, 37(19), e100573. https://doi.org/10.15252/embj.2018100573

Turck, F., Roudier, F., Farrona, S., Martin-Magniette, M.-L., Guillaume, E., Buisine, N., Gagnot, S., Martienssen, R. A., Coupland, G., & Colot, V. (2007). Arabidopsis TFL2/LHP1 Specifically Associates with Genes Marked by Trimethylation of Histone H3 Lysine 27. PLoS Genetics, 3(6), e86. https://doi.org/10.1371/journal.pgen.0030086

Uchida, W., Matsunaga, S., Sugiyama, R., & Kawano, S. (2002). Interstitial telomere-like repeats in the Arabidopsis thaliana genome. Genes & Genetic Systems, 77(1), 63–67. https://doi.org/10.1266/ggs.77.63

Valuchova, S., Fulnecek, J., Prokop, Z., Stolt-Bergner, P., Janouskova, E., Hofr, C., & Riha, K. (2017). Protection of Arabidopsis Blunt-Ended Telomeres Is Mediated by a Physical Association with the Ku Heterodimer. The Plant Cell, 29(6), 1533–1545. https://doi.org/10.1105/tpc.17.00064

Vannier, J.-B., Sarek, G., & Boulton, S. J. (2014). RTEL1: Functions of a disease-associated helicase. Trends in Cell Biology, 24(7), 416–425. https://doi.org/10.1016/j.tcb.2014.01.004

Venteicher, A. S., Meng, Z., Mason, P. J., Veenstra, T. D., & Artandi, S. E. (2008). Identification of ATPases Pontin and Reptin as Telomerase Components Essential for Holoenzyme Assembly. Cell, 132(6), 945–957. https://doi.org/10.1016/j.cell.2008.01.019

Vicari, M. R., Bruschi, D. P., Cabral-de-Mello, D. C., & Nogaroto, V. (2022). Telomere organization and the interstitial telomeric sites involvement in insects and vertebrates chromosome evolution. Genetics and Molecular Biology, 45(3 Suppl 1), e20220071. https://doi.org/10.1590/1678-4685-GMB-2022-0071

Walden, N., German, D. A., Wolf, E. M., Kiefer, M., Rigault, P., Huang, X.-C., Kiefer, C., Schmickl, R., Franzke, A., Neuffer, B., Mummenhoff, K., & Koch, M. A. (2020). Nested whole-genome duplications coincide with diversification and high morphological disparity in Brassicaceae. Nature Communications, 11(1), Article 1. https://doi.org/10.1038/s41467-020-17605-7

Wang, F., Podell, E. R., Zaug, A. J., Yang, Y., Baciu, P., Cech, T. R., & Lei, M. (2007). The POT1–TPP1 telomere complex is a telomerase processivity factor. Nature, 445(7127), Article 7127. https://doi.org/10.1038/nature05454

Wang, M., Zhong, Z., Gallego-Bartolomé, J., Feng, S., Shih, Y.-H., Liu, M., Zhou, J., Richey, J. C., Ng, C., Jami-Alahmadi, Y., Wohlschlegel, J., Wu, K., & Jacobsen, S. E. (2023). Arabidopsis TRB proteins function in H3K4me3

demethylation by recruiting JMJ14. Nature Communications, 14(1), Article 1. https://doi.org/10.1038/s41467-023-37263-9

Wang, Y., Ghosh, G., & Hendrickson, E. A. (2009). Ku86 represses lethal telomere deletion events in human somatic cells. Proceedings of the National Academy of Sciences, 106(30), 12430–12435. https://doi.org/10.1073/pnas.0903362106

Watson JM, Bulankova P, Riha K, Shippen DE, Vyskot B: Telomerase-independent cell survival in Arabidopsis thaliana. Plant J 43:662–674 (2005)

Watson, J. M., Platzer, A., Kazda, A., Akimcheva, S., Valuchova, S., Nizhynska, V., Nordborg, M., & Riha, K. (2016). Germline replications and somatic mutation accumulation are independent of vegetative life span in Arabidopsis. Proceedings of the National Academy of Sciences, 113(43), 12226–12231. https://doi.org/10.1073/pnas.1609686113

Webb, C. J., & Zakian, V. A. (2016). Telomerase RNA is more than a DNA template. RNA Biology, 13(8), 683–689. https://doi.org/10.1080/15476286.2016.1191725

Wei, C., & Price, C. M. (2004). Cell Cycle Localization, Dimerization, and Binding Domain Architecture of the Telomere Protein cPot1. Molecular and Cellular Biology, 24(5), 2091–2102. https://doi.org/10.1128/MCB.24.5.2091-2102.2004

Wellinger, R. J., & Zakian, V. A. (2012). Everything You Ever Wanted to Know About Saccharomyces cerevisiae Telomeres: Beginning to End. Genetics, 191(4), 1073–1105. https://doi.org/10.1534/genetics.111.137851

Wong, M. S., Wright, W. E., & Shay, J. W. (2014). Alternative splicing regulation of telomerase: A new paradigm? Trends in Genetics, 30(10), 430–438. https://doi.org/10.1016/j.tig.2014.07.006

Wood, A. M., Danielsen, J. M. R., Lucas, C. A., Rice, E. L., Scalzo, D., Shimi, T., Goldman, R. D., Smith, E. D., Le Beau, M. M., & Kosak, S. T. (2014). TRF2 and lamin A/C interact to facilitate the functional organization of chromosome ends. Nature Communications, 5(1), Article 1. https://doi.org/10.1038/ncomms6467

Wood, M. A., McMahon, S. B., & Cole, M. D. (2000). An ATPase/helicase complex is an essential cofactor for oncogenic transformation by c-Myc. Molecular Cell, 5(2), 321–330. https://doi.org/10.1016/s1097-2765(00)80427-x

Wright, W. E., Tesmer, V. M., Huffman, K. E., Levene, S. D., & Shay, J. W. (1997). Normal human chromosomes have long G-rich telomeric overhangs at one end. Genes & Development, 11(21), 2801–2809. https://doi.org/10.1101/gad.11.21.2801

Wu, J., Liu, C., Liu, Z., Li, S., Li, D., Liu, S., Huang, X., Liu, S., & Yukawa, Y. (2019). Pol III-Dependent Cabbage BoNR8 Long ncRNA Affects Seed Germination and Growth in Arabidopsis. Plant and Cell Physiology, 60(2), 421–435. https://doi.org/10.1093/pcp/pcy220

Wu, J., Okada, T., Fukushima, T., Tsudzuki, T., Sugiura, M., & Yukawa, Y. (2012). A novel hypoxic stress-responsive long non-coding RNA transcribed by RNA polymerase III in Arabidopsis. RNA Biology, 9(3), 302–313. https://doi.org/10.4161/rna.19101

Wu, L., Multani, A. S., He, H., Cosme-Blanco, W., Deng, Y., Deng, J. M., Bachilo, O., Pathak, S., Tahara, H., Bailey, S. M., Deng, Y., Behringer, R. R., & Chang, S. (2006). Pot1 Deficiency Initiates DNA Damage Checkpoint Activation and Aberrant Homologous Recombination at Telomeres. Cell, 126(1), 49–62. https://doi.org/10.1016/j.cell.2006.05.037

Wu, R. A., Upton, H. E., Vogan, J. M., & Collins, K. (2017). Telomerase Mechanism of Telomere Synthesis. Annual Review of Biochemistry, 86(1), 439–460. https://doi.org/10.1146/annurev-biochem-061516-045019

Xi, L., & Cech, T. R. (2014). Inventory of telomerase components in human cells reveals multiple subpopulations of hTR and hTERT. Nucleic Acids Research, 42(13), 8565–8577. https://doi.org/10.1093/nar/gku560

Xin, H., Liu, D., Wan, M., Safari, A., Kim, H., Sun, W., O'Connor, M. S., & Songyang, Z. (2007). TPP1 is a homologue of ciliate TEBP-β and interacts with POT1 to recruit telomerase. Nature, 445(7127), Article 7127. https://doi.org/10.1038/nature05469

Yang, S. W., Jin, E., Chung, I. K., & Kim, W. T. (2002). Cell cycle-dependent regulation of telomerase activity by auxin, abscisic acid and protein phosphorylation in tobacco BY-2 suspension culture cells. The Plant Journal, 29(5), 617–626. https://doi.org/10.1046/j.0960-7412.2001.01244.x

Yang, S. W., Kim, D. H., Lee, J. J., Chun, Y. J., Lee, J.-H., Kim, Y. J., Chung, I. K., & Kim, W. T. (2003). Expression of the Telomeric Repeat Binding Factor Gene NgTRF1 Is Closely Coordinated with the Cell Division Program in Tobacco BY-2 Suspension Culture Cells*. Journal of Biological Chemistry, 278(24), 21395–21407. https://doi.org/10.1074/jbc.M209973200

Yang, S. W., Kim, S. K., & Kim, W. T. (2004). Perturbation of NgTRF1 Expression Induces Apoptosis-Like Cell Death in Tobacco BY-2 Cells and Implicates NgTRF1 in the Control of Telomere Length and Stability. The Plant Cell, 16(12), 3370–3385. https://doi.org/10.1105/tpc.104.026278

Ye, J., Lenain, C., Bauwens, S., Rizzo, A., Saint-Léger, A., Poulet, A., Benarroch, D., Magdinier, F., Morere, J., Amiard, S., Verhoeyen, E., Britton, S., Calsou, P., Salles, B., Bizard, A., Nadal, M., Salvati, E., Sabatier, L., Wu, Y., … Gilson, E.

(2010). TRF2 and Apollo Cooperate with Topoisomerase 2α to Protect Human Telomeres from Replicative Damage. Cell, 142(2), 230–242. https://doi.org/10.1016/j.cell.2010.05.032

Yoo, H. H., Kwon, C., Lee, M. M., & Chung, I. K. (2007). Single-stranded DNA binding factor AtWHY1 modulates telomere length homeostasis in Arabidopsis. The Plant Journal, 49(3), 442–451. https://doi.org/10.1111/j.1365-313X.2006.02974.x

Yu, E. Y., Kim, S. E., Kim, J. H., Ko, J. H., Cho, M. H., & Chung, I. K. (2000). Sequence-specific DNA recognition by the Myb-like domain of plant telomeric protein RTBP1. The Journal of Biological Chemistry, 275(31), 24208–24214. https://doi.org/10.1074/jbc.M003250200

Zachová, D., Fojtová, M., Dvořáčková, M., Mozgová, I., Lermontova, I., Peška, V., Schubert, I., Fajkus, J., & Sýkorová, E. (2013). Structure-function relationships during transgenic telomerase expression in Arabidopsis. Physiologia Plantarum, 149(1), 114–126. https://doi.org/10.1111/ppl.12021

Zellinger, B., Akimcheva, S., Puizina, J., Schirato, M., & Riha, K. (2007). Ku Suppresses Formation of Telomeric Circles and Alternative Telomere Lengthening in Arabidopsis. Molecular Cell, 27(1), 163–169. https://doi.org/10.1016/j.molcel.2007.05.025

Zentgraf, U. (1995). Telomere-binding proteins of Arabidopsis thaliana. Plant Molecular Biology, 27(3), 467–475. https://doi.org/10.1007/BF00019314

Zhang, J.-M., Yadav, T., Ouyang, J., Lan, L., & Zou, L. (2019). Alternative Lengthening of Telomeres through Two Distinct Break-Induced Replication Pathways. Cell Reports, 26(4), 955-968.e3. https://doi.org/10.1016/j.celrep.2018.12.102

Zhang, Q., Kim, N.-K., & Feigon, J. (2011). Architecture of human telomerase RNA. Proceedings of the National Academy of Sciences, 108(51), 20325–20332. https://doi.org/10.1073/pnas.1100279108

Zhang, Z., Sullivan, W., Felts, S. J., Prasad, B. D., Toft, D. O., & Krishna, P. (2010). Characterization of plant p23-like proteins for their co-chaperone activities. Cell Stress and Chaperones, 15(5), 703–715. https://doi.org/10.1007/s12192-010-0182-1

Zhou, Y., Hartwig, B., James, G. V., Schneeberger, K., & Turck, F. (2016). Complementary Activities of TELOMERE REPEAT BINDING Proteins and Polycomb Group Complexes in Transcriptional Regulation of Target Genes. The Plant Cell, 28(1), 87–101. https://doi.org/10.1105/tpc.15.00787

Zhou, Y., Wang, Y., Krause, K., Yang, T., Dongus, J. A., Zhang, Y., & Turck, F. (2018). Telobox motifs recruit CLF/SWN–PRC2 for H3K27me3 deposition via TRB factors in Arabidopsis. Nature Genetics, 50(5), Article 5. https://doi.org/10.1038/s41588-018-0109-9

Zhu, Q.-H., Ramm, K., Shivakkumar, R., Dennis, E. S., & Upadhyaya, N. M. (2004). The ANTHER INDEHISCENCE1 Gene Encoding a Single MYB Domain Protein Is Involved in Anther Development in Rice. Plant Physiology, 135(3), 1514–1525. https://doi.org/10.1104/pp.104.041459

Supplements

Relevant publications of the applicant arranged in chronological order.

All publications referred in Supplements have been included in the thesis (references in bold and marked with letters of alphabet in the text).

*Corresponding Author

Supplement A
Schrumpfová, P., Kuchar, M., Miková, G., Skrísovská, L., Kubicárová, T., Fajkus, J., **2004.** Characterization of two Arabidopsis thaliana myb-like proteins showing affinity to telomeric DNA sequence. Genome 47, 316–324

Supplement B
Růčková, E., Friml, J., **Schrumpfová, P.P.**, Fajkus, J., **2008**. Role of alternative telomere lengthening unmasked in telomerase knock-out mutant plants. Plant Mol. Biol. 66, 637–646

Supplement C
Schrumpfová, P.P., Kuchar, M., Palecek, J., Fajkus, J., **2008**. Mapping of interaction domains of putative telomere-binding proteins AtTRB1 and AtPOT1b from Arabidopsis thaliana. FEBS Lett. 582, 1400–1406.

Supplement D
Mozgová, I., **Schrumpfová, P.P.**, Hofr, C., Fajkus, J., **2008**. Functional characterization of domains in AtTRB1, a putative telomere-binding protein in Arabidopsis thaliana. Phytochemistry 69, 1814–1819

Supplement E
Hofr, C., Sultesová, P., Zimmermann, M., Mozgová, I., **Schrumpfová, P.P.**, Wimmerová, M., Fajkus, J., **2009**. Single-Myb-histone proteins from Arabidopsis thaliana: a quantitative study of telomere-binding specificity and kinetics. Biochem. J. 419, 221–228

Supplement F
Peška, V., **Schrumpfová, P.P.,** Fajkus, J., **2011**. Using the telobox to search for plant telomere binding proteins. Curr. Protein Pept. Sci. 12, 75–83

Supplement G
Schrumpfová, P.P.*, Fojtová, M., Mokroš, P., Grasser, K.D., Fajkus, J., **2011**. Role of HMGB proteins in chromatin dynamics and telomere maintenance in Arabidopsis thaliana. Curr. Protein Pept. Sci. 12, 105–111

Supplement H
Schrumpfová, P.P.*, Vychodilová, I., Dvořáčková, M., Majerská, J., Dokládal, L., Schořová, S., Fajkus, J., **2014.** Telomere repeat binding proteins are functional components of Arabidopsis telomeres and interact with telomerase. Plant J. Cell Mol. Biol. 77, 770–781

Supplement I

Schrumpfová, P.P., Vychodilová, I., Hapala, J., Schořová, Š., Dvořáček, V., Fajkus, J., **2016**. Telomere binding protein TRB1 is associated with promoters of translation machinery genes in vivo. Plant Mol.Biol. 90, 189–206

Supplement J
Schrumpfová, P.P.*, Schořová, Š., Fajkus, J., **2016**. Telomere- and Telomerase-Associated Proteins and Their Functions in the Plant Cell. Front. Plant Sci. 7:851

Supplement K
Schrumpfová, P.P., Majerská, J., Dokládal, L., Schořová, Š., Stejskal, K., Obořil, M., Honys, D., Kozáková, L., Polanská, P.S., Sýkorová, E., **2017**. Tandem affinity purification of AtTERT reveals putative interaction partners of plant telomerase in vivo. Protoplasma 254, 1547–1562

Supplement L
Schrumpfová, P.P., Majerská, J., Dokládal, L., Schořová, Š., Stejskal, K., Obořil, M., Honys, D., Kozáková, L., Polanská, P.S., Sýkorová, E., **2018**. Correction to: Tandem affinity purification of AtTERT reveals putative interaction partners of plant telomerase in vivo. Protoplasma 255, 715

Supplement M
Schrumpfová, P.P., Fojtová, M., Fajkus, J., **2019**. Telomeres in Plants and Humans: Not So Different, Not So Similar. Cells 8

Supplement N
Schořová, Š., Fajkus, J., Drábková, L.Z., Honys, D., **Schrumpfová, P.P.***, **2019**. The plant Pontin and Reptin homologues, RuvBL1 and RuvBL2a, colocalize with TERT and TRB proteins in vivo, and participate in telomerase biogenesis. Plant J. 98, 195–212

Supplement O
Schrumpfová, P.P.* and Fajkus, J. **2020**. Composition and Function of Telomerase - a polymerase associated with the origin of eukaryotes. Review. Biomolecules, 10(10):1425

Supplement P
Pecinka A, **Schrumpfová, P.P.**, Fischer L., Dvořák Tomaštíková E., and Mozgová I., **2022**. The Czech Plant Nucleus Workshop 2021. Biologia Plantarum, 66: 39-45

Supplement Q
Dvořák Tomaštíková E., Yang F., Mlynárová K., Hafid S., Schořová Š., Kusová A., Pernisová M., Přerovská M., Klodová B., Honys D., Fajkus J., Pecinka A., and **Schrumpfova P.P.*, 2023** RUVBL proteins are involved in plant gametophyte development, The Plant Journal 114, 325–337

Supplement R
Kusova A., Steinbachova L., Přerovská T., Záveská Drábková L., Paleček J., Khan A., Rigóová G., Gadoiu Z., Jourdain C., Stricker T., Schubert D., Honys D., and **Schrumpfová P.P**.*, **2023**. Completing the TRB family: newly characterized members show ancient evolutionary origins and distinct localization, yet similar interactions Plant Molecular Biology 112:61–83

Supplement S
Teano G., Concia L., Wolff L., Carron L., Biocanin I., Adamusová K., Fojtová M., Bourge M., Kramdi A., Colot V., Grossniklaus U., Bowler Ch., Baroux C., Carbone A., Probst A.V., Schrumpfová P.P., Fajkus J., Amiard S., Grob S., Bourbousse C., and Barneche F. 2023. Histone H1 protects telomeric repeats from H3K27me3 invasion in Arabidopsis. Cell Reports, 42(8):112894.

Supplement A

Schrumpfová, P., Kuchar, M., Miková, G., Skrísovská, L., Kubicárová, T., Fajkus, J., **2004.** Characterization of two Arabidopsis thaliana myb-like proteins showing affinity to telomeric DNA sequence. Genome 47, 316–324

P.P.S. performed most of the experiments (protein expression, EMSA, telomerase activity detection), evaluated data and participated in the ms writing and editing

This journal did not provide open access, hence the article is not freely available.

Supplement B

Růčková, E., Friml, J., **Schrumpfová, P.P.**, Fajkus, J., **2008**. Role of alternative telomere lengthening unmasked in telomerase knock-out mutant plants. Plant Mol. Biol. 66, 637–646

P.P.S. was involved in the experimental part (plant cultivation and genotyping, telomere length measurement) and participated in the ms writing and editing

Plant Mol Biol
DOI 10.1007/s11103-008-9295-7

Role of alternative telomere lengthening unmasked in telomerase knock-out mutant plants

Eva Růčková · Jiří Friml · Petra Procházková Schrumpfová · Jiří Fajkus

Received: 23 November 2007 / Accepted: 14 January 2008

Abstract Telomeres in many eukaryotes are maintained by telomerase in whose absence telomere shortening occurs. However, telomerase-deficient *Arabidopsis thaliana* mutants (*Attert*$^{-/-}$) show extremely low rates of telomere shortening per plant generation (250–500 bp), which does not correspond to the expected outcome of replicative telomere shortening resulting from ca. 1,000 meristem cell divisions per seed-to-seed generation. To investigate the influence of the number of cell divisions per seed-to-seed generation, *Attert*$^{-/-}$ mutant plants were propagated from seeds coming either from the lower-most or the upper-most siliques (L- and U-plants) and the length of their telomeres were followed over several generations. The rate of telomere shortening was faster in U-plants, than in L-plants, as would be expected from their higher number of cell divisions per generation. However, this trend was observed only in telomeres whose initial length is relatively high and the differences decreased with progressive general telomere shortening over generations. But in generation 4, the L-plants frequently show a net telomere elongation, while the U-plants fail to do so. We propose that this is due to the activation of alternative telomere lengthening (ALT), a process which is activated in early embryonic development in both U- and L-plants, but is overridden in U-plants due to their higher number of cell divisions per generation. These data demonstrate what so far has only been speculated, that in the absence of telomerase, the number of cell divisions within one generation influences the control of telomere lengths. These results also reveal a fast and efficient activation of ALT mechanism(s) in response to the loss of telomerase activity and imply that ALT is probably involved also in normal plant development.

Keywords Alternative telomere lengthening · ALT · Replicative telomere shortening · Telomerase-deficient plants

E. Růčková · J. Friml · P. Procházková Schrumpfová · J. Fajkus (✉)
Department of Functional Genomics and Proteomics, Faculty of Science, Masaryk University, Building A2 – ILBIT, Kamenice 5, 625 00 Brno, Czech Republic
e-mail: fajkus@sci.muni.cz

E. Růčková · J. Fajkus
Institute of Biophysics ASCR, v.v.i., Královopolská 135, 61265 Brno, Czech Republic

J. Friml
VIB Department of Plant Systems Biology, Ghent University, Technologiepark 927, 9052 Gent, Belgium

Introduction

Incomplete replication of chromosome ends results in progressive telomere shortening unless a mechanism to elongate telomeres takes effect. It has been known for more than a decade that the common system of telomere maintenance in plants is provided by telomerase (Fajkus et al. 1996; Heller et al. 1996), although exemptions, in which a different type of telomeres and mechanism of their maintenance are in use have been described since about the same time in *Allium* (Pich et al. 1996; Sykorova et al. 2006) and later on in three Solanaceae genera (Sykorova et al. 2003). We hypothesized recently that alternative telomere lengthening (ALT) mechanisms are probably not restricted to species possessing "unusual" telomeres, but may be a normal part of plant development (Fajkus et al. 2005), an idea explored here. *Arabidopsis thaliana* knockout mutants in Telomerase Reverse Transcriptase (AtTERT) exhibit telomere shortening of 250–500 bp per generation

(Fitzgerald et al. 1999) and survive up to 10 generations with severe cytological and chromosomal abnormalities occurring after about eight generations (Riha et al. 2001; Siroky et al. 2003). The rate of the observed inter-generation shortening of telomeres is surprisingly low, given the high number of cell divisions per seed-to-seed generation. The high number results from the mode of plant development, which does not involve stem cell mobility and cell lines are not sequestrated for later use (as in the germ line of mammals). In plants an apical meristem consists of a small group of stem cells that generate a linear series of cells, which differentiate into an array of cell types that make a shoot and root. Flowers initiate from the shoot apical meristem in mature plants, which is organized in cell layers L1, L2 and L3, and divisions of those are roughly synchronized. L2 cell layer derivatives provide the mesodermal cells and the germ cells of pollen grains and ovules (Fletcher 2002, Grandjean et al. 2004). Consequently, meristem cells, which give rise to all tissues, including germ-line cells, undergo many divisions, calculated in *A. thaliana* to be approximately 1,000 divisions from seed to seed (Fajkus et al. 2005). When considering only 5–10 nucleotides lost per cell division (the average length of RNA primer for synthesis of Okazaki fragments) as the minimum plausible loss of telomeric DNA at each round of replication (under the very improbable scenario that the primer sits exactly at the 3'end of the parental DNA strand), then the number of cell divisions accounting for the observed telomere erosion per generation in *Attert*$^{-/-}$ mutants would be only 25–50 cell divisions (as in mammals). But as already stated for *A. thaliana* the actual number of divisions is closer to 1,000. Thus we proposed that ALT system operates in telomerase-deficient plants and possibly also in normal plant development to partially compensate for replicative shortening of telomeres (Fajkus et al. 2005).

To test this hypothesis, we compared telomere shortening in telomerase knock-out plants differing in the number of cell divisions per generation. We generated *Attert*$^{-/-}$ and *Attert*$^{+/+}$ plants from heterozygous *A. thaliana* (*Attert*$^{+/-}$) line (SALK_061434.56.00.X) bearing T-insertion in *Attert* gene. In the obtained homozygous *Attert*$^{-/-}$ plants, seeds were collected individually from the lowermost or uppermost siliques and seeds propagated. In subsequent generations, plants coming from the lowermost siliques were propagated again through seeds from the lowermost siliques, while plants coming from the uppermost siliques were again propagated through seeds from uppermost siliques. If our hypothesis is correct, the plant propagation scheme (Fig. 1) should result in additional cell divisions occurring in "upper silique" lines (U) compared with lower silique" lines (L). The number of additional cell divisions in U-plants compared with L-plants can be estimated as follows: the cell division rate after floral transition is 1–2 divisions per 24 h. That corresponds to 1–2 flower initiations for the same time, so the difference is 1 cell division between 2 consecutive flower initiations (Grandjean et al. 2004). Since ca. 30 siliques occur between the lowermost and the uppermost silique, we can expect about 30 additional cell divisions. Therefore in *Attert*$^{-/-}$ mutants we might expect about 150–300 bp-shorter telomere lengths in the U-lines compared with L-lines.

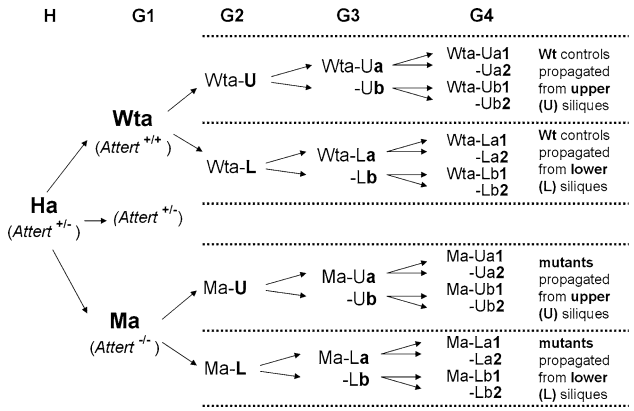

Fig. 1 Schematic diagram of plant propagation system for the generation of plants derived from the heterozygote *Attert*+/− mutant Ha. The same scheme applies to the heterozygous mutants Hb1 and Hb2 and the nomenclature of the derived plants follow accordingly. For further details of the source materials see Materials and methods

We show here that differential telomere shortening does occur between U- and L-lines but that the results are complicated through the activation of ALT. We reveal a differential rate of telomere shortening in different generations of mutants and telomere length oscillations, which, at least in *Attert*$^{-/-}$ mutants, cannot be attributed to telomerase activity.

Material and methods

Plant material

Homozygous mutant *Attert*$^{-/-}$ plants (M) and corresponding *Attert*$^{+/+}$ controls (Wt) were prepared from heterozygous *A. thaliana* line (*Attert*$^{+/-}$, H) bearing T-insertion in *Attert* gene (SALK_061434.56.00.X). Plants were initially cultivated on short day (8 h of light) and after 6 weeks at long day (16 h of light) in a greenhouse. Lines were derived from three heterozygous plant lineages (Ha, Hb1 and Hb2). Mutant (M) and control plants (Wt) were selected from their progeny and designated accordingly (Ma and Wta from Ha; Mb1, Mb2 and Wtb1 and Wtb2 from Hb). First generation plants (G1) were divided into lines propagated either from the lowermost or the uppermost siliques (L- and U-plants, respectively, see the schematic Fig. 1). These lines were cultured until the fourth generation (G4).

Genotyping

DNA was extracted according to Edwards et al. (1991). A set of three primers was used for genotyping. Two primers were complementary to genomic DNA upstream and downstream of the T-insertion (tel+ and tel−, respectively) and produced a 876 bp product in wild-type. In mutants, a 702 bp product was synthesized using primer LBb1 (complementary to T-insertion) and tel−. Primer sequences were: tel+: 5′-CTg CTACTTTCAgCTTCAgC-3′, tel−: 5′-gCAAgAggATgCA TTgAAgTCCgg-3′, LBb1: 5′-gCgTggACCgCTTgCTgCA ACT-3′. The reaction mix (15 µl) contained 1× buffer (DyNAzyme II, Finnzymes), 0.25 mM dNTPs, 0.3 µM forward and 0.3 µM reverse primer, 0.3 U DyNAzyme II DNA polymerase (Finnzymes) and 5 ng of DNA. Initial denaturation (94°C/3 min) was followed by 35 thermal cycles (94°C/30 s, 56.5°C/30 s and 72°C/1 min), and a final extension (72°C/10 min).

Induction of callus cultures

Seeds were sterilized by shaking for 15 min in 50 mg ml^{-1} $Ca(OCl)_2$ solution, then rinsed three times with sterile water with 0.01% Triton X-100 and placed on solid MS medium supplemented with 20 g l^{-1} sucrose. Plants were genotyped and leaves from mutant, wild-type and heterozygous plants were harvested, cut and cultivated on solid MS medium (Duchefa M0231) supplemented with 1 mg/l 2,4-D (2,4-dichlorophenoxyacetic acid), 0.2 mg/l kinetin and 20 g/l sucrose. Calli were maintained on this medium and transferred to fresh medium every 4 weeks.

Detection of telomerase activity

Protein extracts from calli were prepared as described in Fitzgerald et al. (1996). These extracts were then tested for telomerase activity by plant telomere repeat amplification protocol (TRAP) as described by Fajkus et al. (1998).

Determination of telomere length

DNA was extracted from three rosette leaves according to Dellaporta et al. (1983). Primer extension telomere repeat amplification (PETRA) analysis was performed with an equivalent amount of DNA as described in Heacock et al. (2004) and Watson and Shippen (2007). Individual telomeres were designated according to Heacock et al. (2004) with a number identifying a chromosome, and R or L letter indicating a chromosome arm, where R corresponds to South and L to North (Arabidopsis Genome Initiative 2000). To measure telomere length, signals of PETRA products were analyzed by TotalLab using a 1-kb DNA ladder (Fermentas) as standard. The distance of the PETRA primer to the telomere was subtracted from the total length of PETRA product to give the actual length of the telomere tract. The average telomere lengths were visualized using Southern hybridization of terminal restriction fragments (TRF) (Fajkus et al. 1995) produced by digestion with *Mse*I restriction endonuclease. Both PETRA and TRF products were detected using telomeric oligonucleotide (5′-GGTT TAGGGTTTAGGGTTTAGGGTTTAG-3′) end-labelled with [γ-^{32}P]ATP using polynucleotide kinase (NEB).

Results

Arabidopsis tert mutants do not possess residual telomerase activity

To make sure that *A. thaliana* *Attert*$^{-/-}$ mutants do not possess any residual telomerase activity, tissue cultures derived from original *Attert*$^{+/-}$ plants and their mutant (*Attert*$^{-/-}$) and Wt (*Attert*$^{+/+}$) progeny were assayed for telomerase activity by TRAP assay. The results (Fig. 2) show the absence of telomerase activity in extracts obtained from *Attert*$^{-/-}$ mutant, while both *Attert*$^{+/-}$ *and* *Attert*$^{+/+}$ cultures are telomerase-positive.

Telomere lengthening upon transition from *Attert*$^{+/-}$ (H) to *Attert*$^{+/+}$ (Wt) state

To evaluate telomere length changes between mutant plants propagated via upper and lower silique seeds (undergoing a different number of cell divisions per seed-to-seed generation) and to distinguish them from natural variations in telomere lengths in telomerase-positive plants, control Wt plants were generated from the same original heterozygous plants as *Attert*$^{-/-}$ mutants. Wt plants were propagated according to the same schematic protocol as U- and L-lines of *Attert*$^{-/-}$ mutants (Fig. 1) to reveal any potential stochastic changes in telomere lengths. Examples of primary PETRA and TRF results are shown in Fig. 3. The results were repeated in three independent lineages (Ha, Hb1 and Hb2). Measurement of PETRA fragment sizes revealed increases in both 2R and 3L telomeres in most first generation *Attert*$^{+/+}$ plants within a range of 120–380 bp (Figs. 4, 5). The exception is the 3L telomere in Wta plant where telomere lengths show a mild (90 bp) shortening (Fig. 5). Telomere dynamics in the following generations of Wt plants displayed changes in both directions, but overall most plants showed a net increase in telomere lengths in G4 compared to their length in the

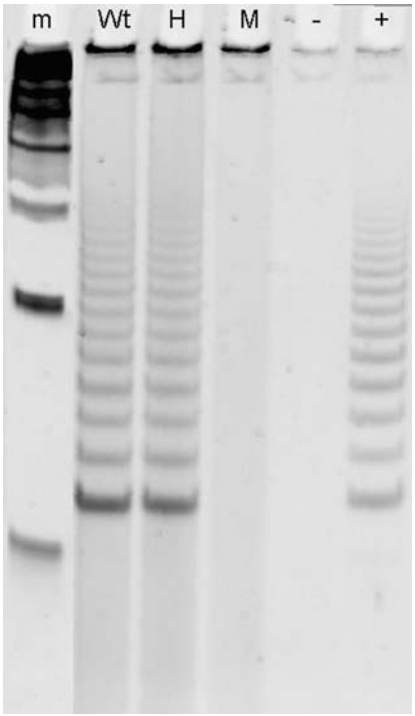

Fig. 2 Results of TRAP assay in calli derived from the original heterozygous *Attert*$^{+/-}$ plant (H), and its progeny—mutant *Attert*$^{-/-}$ (M) and wild type *Attert*$^{+/+}$ (Wt). A 50 bp marker (GeneRuler, Fermentas) is used as a marker (m). Telomerase extract from standard *A. thaliana wt* seedlings was used as positive control (+), and the extraction buffer served as a negative control (−)

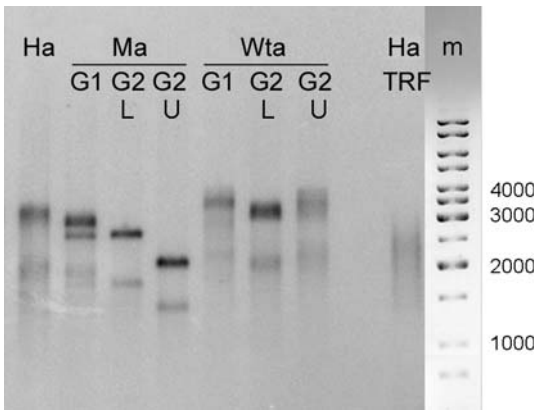

Fig. 3 Example of PETRA and TRF results. One of the *Attert*$^{+/-}$ plants (Ha) and two generations of *Attert*$^{-/-}$ (Ma) and *Attert*$^{+/+}$ (Wta) plants derived from the Ha plant, were propagated as L- and U-lines (as indicated) and assayed by PETRA with a primer specific for the subtelomere 2R. Apart from stronger bands that correspond to main products of PETRA there are also weaker bands of a higher mobility. These weaker bands in a given lane correspond to the stronger bands in both their number and mutual position. The result labelled as TRF shows the hybridization pattern of terminal restriction fragments generated with restriction enzyme *Mse*I in Ha plant. A 1 kb GeneRuler (Fermentas) has been used as marker (m)

original heterozygotes. This observation suggests that the mutation of a single *Attert* allele acts via haploinsufficiency, as in human (Hauguel and Bunz 2003; Zhang et al. 2003) and mouse *tert* genes (Erdmann et al. 2004). No substantial differences in telomere lengths were observed between U- and L-lines of corresponding *Attert*$^{+/+}$ plants, revealing that telomerase in meristem cells maintains telomere stability during plant development (Fajkus et al. 1998; Riha et al. 1998) regardless of number of cell divisions.

Telomere dynamics in *Attert*$^{-/-}$ plants

The key question of this study was to analyze if there is a relationship between telomere shortening per plant generation and the number of meristem cell divisions between generations. To address this question, telomere lengths were measured during propagation of *Attert*$^{-/-}$ mutants as U- and L-lines. Only the first few generations of *Attert*$^{-/-}$ mutants were analyzed (G1–G4) to avoid accumulated cytogenetic abnormalities expected from the 6th generation (Riha et al. 2001). Results of telomere analysis (Figs. 4, 5) revealed:

(i) Telomere length differences between consecutive plant generations can be highly variable ranging from tens of bp to 800 bp. There is some evidence that large changes in telomere length (>500 bp) in one generation is followed by smaller changes in the subsequent generation. For example, in 2R telomeres in mutant Ma-derived U-plant lines, large changes occur between G1 and G2 (Figs. 4, 5) and subsequently are less dramatic. In 3L telomeres of all the Ma-derived U-lines, substantial telomere shortening occurs between G3 and G4, while in earlier generations there are only moderate changes (Fig. 5).

(ii) Telomeres 2R and 3L in the same plants behave relatively independently. Compare e.g., a 150 bp shortening between G1 and G2 generations in the 2R telomere in L-plants derived from the Mb1 mutant with ca. 800 bp shortening of 3L telomeres in the same plants (Figs. 4–6).

(iii) Two patterns were observed in the dynamics of telomere shortening in *Attert*$^{-/-}$ mutants. The first is represented by 2R telomeres of plants derived from Ma and Mb1 mutants. These results reveal, as predicted, a faster rate of telomere shortening per generation in plants propagated through seeds from the upper siliques (U-lines) than in those from the lower siliques (L-lines, Figs. 4, 7A). The second is observed in 3L telomeres of all lines and of 2R telomeres of Mb2-derived lines. Here the rate of

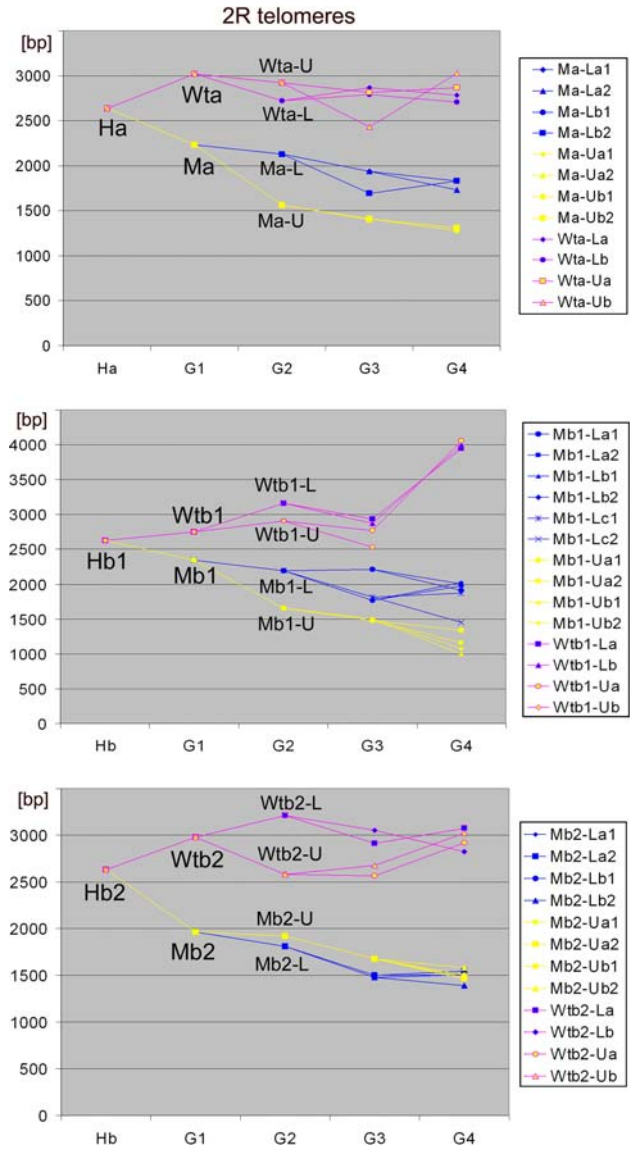

Fig. 4 Telomere lengths in 2R chromosome arms in wild-type (Wta, Wtb1, Wtb2) and mutant (Ma, Mb1, Mb2) plants. Each graph consists of consecutive results from the original heterozygous *Attert*$^{+/-}$ plant (Ha or Hb), and four subsequent generations (G1–G4) of the individual U- or L-lines coming from the given first-generation plant (Wta, Wtb1, Wtb2 and Ma, Mb1, Mb2). Overlapping points cannot be seen separately

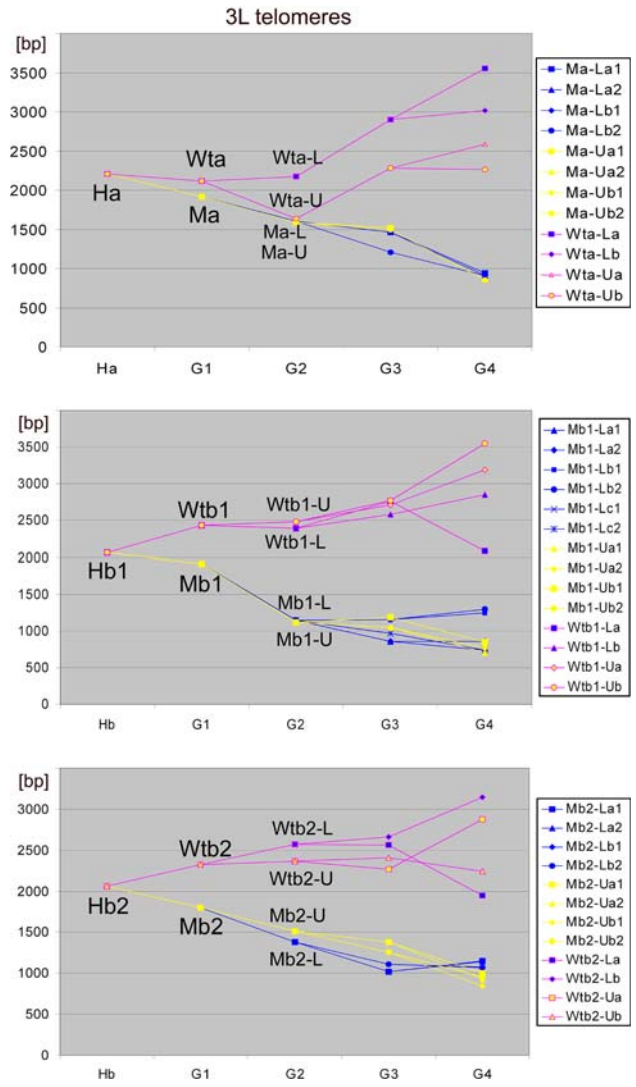

Fig. 5 Telomere lengths in 3L chromosome arms in wild-type (Wta, Wtb1, Wtb2) and mutant (Ma, Mb1, Mb2) plants. Each graph consists of consecutive results from the original heterozygous *Attert*$^{+/-}$ plant (Ha or Hb), and four subsequent generations (G1–G4) of the individual U- or L-lines coming from the given first-generation plant (Wta, Wtb1, Wtb2 and Ma, Mb1, Mb2)

telomere shortening is not substantially different between U- and L-lines (Figs. 4, 5, 7B). If it is assumed that ALT becomes activated in response to telomere shortening, then the mechanism is more active in 3L telomeres in earlier generations compared to 2R telomeres, and acts to override any losses incurred through an increased number of cell divisions between U- and L-plant generations.

(iv) A difference between U- and L-lines is apparent from the evaluation of relative telomere length changes between generations (Fig. 6). While the overall telomere lengthening is occasionally observed between G2 and G3 generations in both U- and L-lines, it is much more frequent between G3 and G4 generations—but only in L-lines, whereas it is entirely absent in any of the U-line plants between the same generations. This remarkable difference suggests that ALT processes may be more frequent in gametogenesis or early developmental stages. In L-plants, such elongation can sometimes be even higher than replicative shortening corresponding to formation of lower-silique seeds, while in U-plants the greater number of cell divisions overrides the efficiency of ALT.

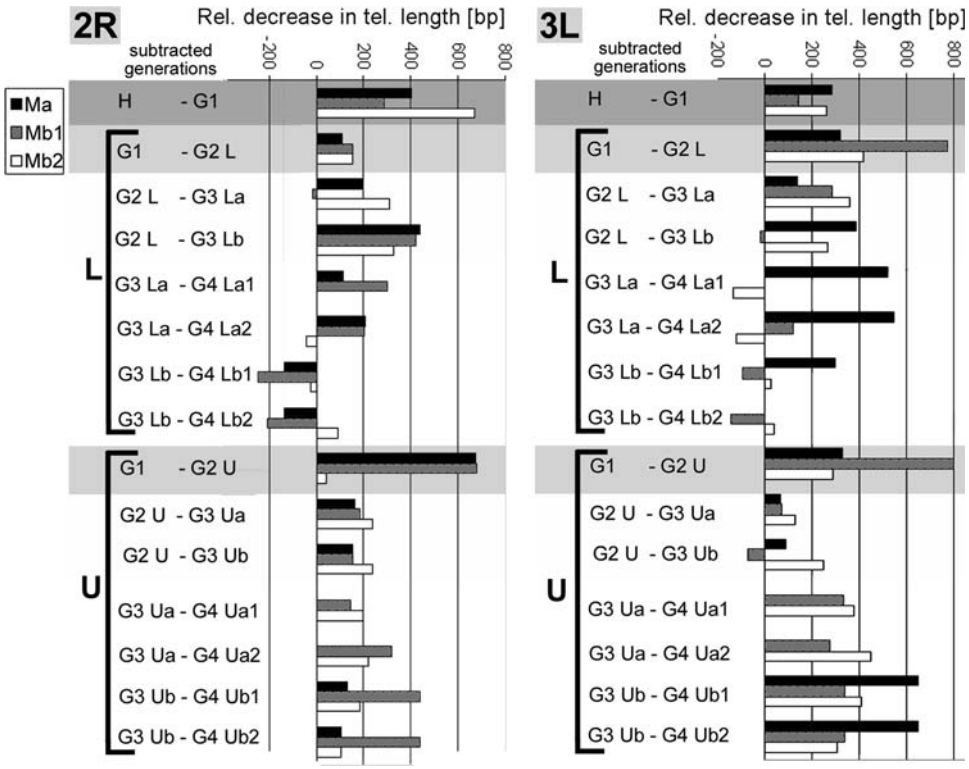

Fig. 6 Summary of relative telomere shortening in each generation of all three mutant lines (Ma, Mb1 and Mb2). Telomere lengths in each generation were subtracted from lengths in the previous generation, therefore values are positive in case of shortening and negative in elongation events

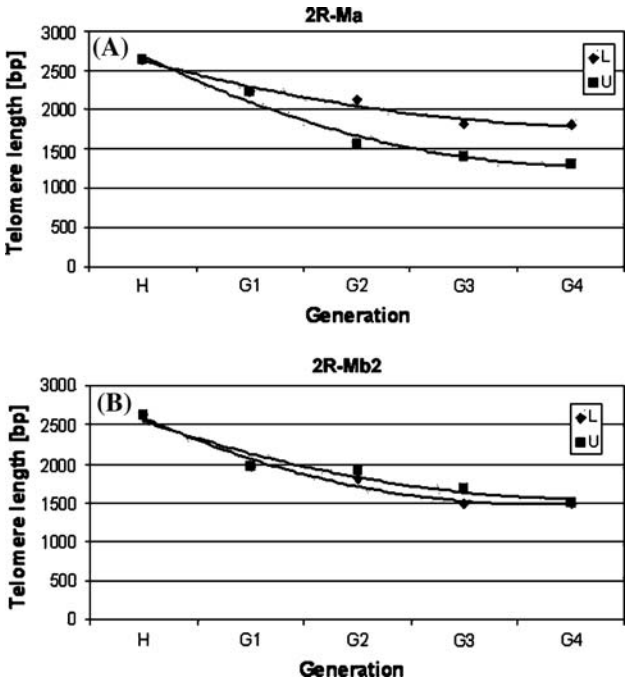

Fig. 7 Graphs showing two different trends observed in rates of telomere shortening between plants from U- and L-lines. Telomere lengths of all plants in either U- or L-line were averaged in a given generation. (**A**) (2R telomeres in Ma lines) shows example of the case in which the rate of telomere shortening is faster in the U-line then in L-line. (**B**) (2R telomeres in Mb2 lines) exemplifies the similar rate of telomere shortening in U- and L-lines. The former course was observed in 2R telomeres in Ma and Mb1 lines, while the latter occurred in 2R telomeres in Mb2 line and 3L telomeres of all lines

Early onset of phenotype changes in *Attert* mutants

The first phenotypic abnormalities appeared in some plants from the U- and L-lines in the 4th generation of *Attert*$^{-/-}$ mutants, primarily from Mb1 and Mb2 plants. Some plants showed mild abnormalities, leaves were asymmetric and lobed. Other plants had more serious abnormalities both in leaf morphology and shoot structure—stems were split and in some cases appeared to have lost the apical dominance; leaves were smaller than wild-type, had an irregular shape, a rough surface and were more plentiful than in wild-type plants (Fig. 8); siliques were smaller with fewer seeds, or were completely sterile. The most severe phenotype arose in a G4 plant from U-line derived from the Mb1 mutant. In that plant there were many abnormalities including leaves with a distinct trichomes, a small stem and sterile siliques (Fig. 8A–C). 2R and 3L telomeres in this G4 plant were 1340 and 770 bp long, respectively, i.e. similar to the other G4 mutant plants included in Figs. 4–7. For other plants, the occurrence of abnormal phenotypes did not differ substantially between mutants of the U- and L-lines. The phenotypic abnormalities observed correspond well to those described by Riha et al. (2001), but in our experiments some plants had severe phenotypes in the 4th generation rather than the 8th generation described in that earlier work.

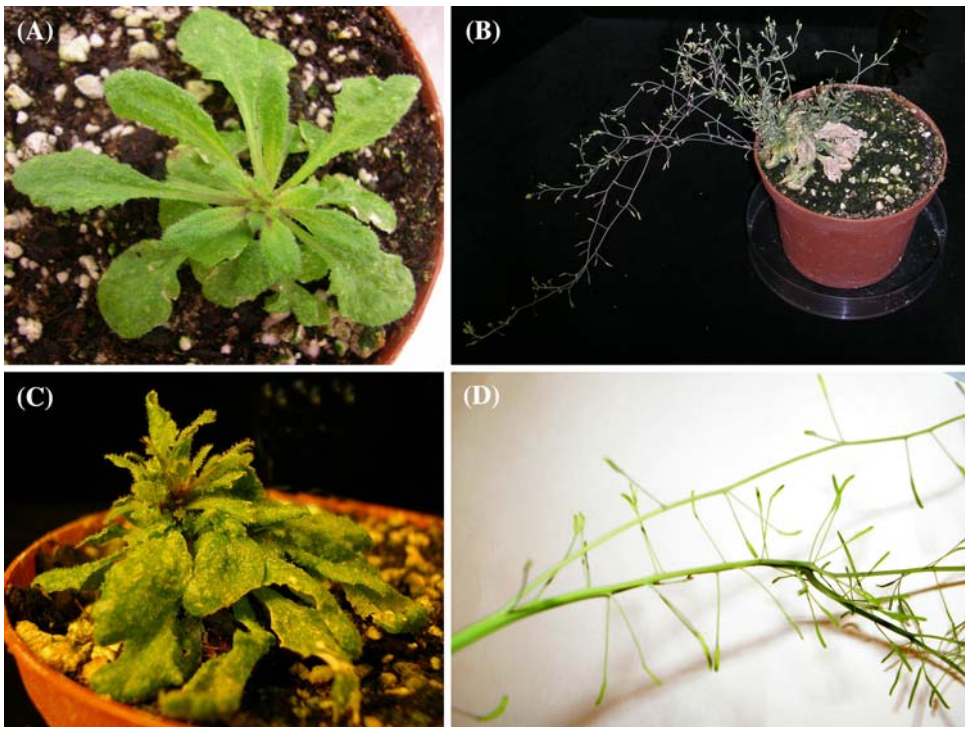

Fig. 8 Examples of mutant phenotypes. Different life stages of the G4 plant from U-line, which had the most serious phenotype defects (**A**–**C**). Leaves were asymmetric and rough, had conspicuous trichomes, stem was short and thin and the plant was sterile. A detailed picture of a split stem is given in panel **D**

Discussion

Involvement of telomerase-independent processes in plant telomere dynamics

Our analysis of telomere dynamics in Arabidopsis *Attert*$^{-/-}$ mutants challenges current perceptions of the relative contributions of telomerase activity, ALT and telomere rapid deletion (TRD) in plant telomere dynamics. Watson and Shippen (2007) showed that elongated telomeres in *A. thaliana Ku70* mutants shorten to the length typical for *wt* plants after three generations when restored with wild-type *Ku70*. This corresponds to an average loss of 2.3 ± 0.8 kb of telomeric DNA per generation, which is interpreted as the result of TRD, as it exceeds the previously reported rate of telomere shortening per generation in *tert* mutants. The rate of telomere shortening per generation observed in this work, as well as in our study was not constant (Fig. 7), but decreased as telomeres approached the length of about 2 kb. In addition to the reported TRD, the opposing process—ALT—was detected in *ku70 tert* double mutants with elongated telomeres (Watson and Shippen 2007). Although it is possible that both TRD and ALT are actively involved in telomere length regulation in *A. thaliana*, according to our previous estimates and calculations (Fajkus et al. 2005), the observed rate of telomere shortening in *Attert*$^{-/-}$ mutants is about ten times less than the expected replicative loss resulting from number of cell divisions that occurs between generations. As telomeres approach a critical length, the frequency of ALT events may increase, which results in more substantial telomere length changes in both directions. This hypothesis might also explain why 3L telomeres respond similarly between U- and L-lines. The initial length of 3L telomeres is about 500 bp shorter than 2R telomeres. Perhaps because the telomeres are shorter, stochastic ALT processes are active in both lines in earlier generations in 3L telomeres. Therefore we conclude that the apparent slower rates of telomere attrition in G3–G4 generations are presumably due to the up-regulation of ALT by shortened telomeres themselves, or by their changed nucleoprotein structure.

Is ALT restricted to a specific developmental stage?

Frequently telomere elongation was observed between G3 and G4 in L-plants, while they are entirely absent in U-plants. This remarkable difference suggests that ALT processes may be more frequent in gametogenesis or early developmental stages. In L-plants, such elongation can sometimes be even greater than subsequent replicative shortening corresponding to formation of lower-silique seeds, while in U-plants the additional 30 divisions counteract length gains produced by ALT at a particular time in development. The activity of ALT in early embryonic

development is supported also by recent observations of Liu et al. (2007) in mammalian oocyte cells. They show that oocytes have shorter telomeres than somatic cells and lack telomerase activity, but their telomeres lengthen remarkably during early cleavage cycles following fertilization through a recombination-based mechanism. From the blastocyst stage onwards, telomerase becomes activated and maintains the telomere length established by this alternative mechanism. The involvement of ALT in normal development thus gains support in such divergent organisms as mammalians and plants, and this conservation suggests its key importance.

The observation of the overall telomere elongation events in L-plants also poses an interesting question: why is the ALT process not able to compensate completely for the lack of telomerase in *Attert*$^{-/-}$ mutants? A possible explanation is provided by ALT itself. Studies on different model systems show that ALT involves homologous recombination (HR) and HR-dependent DNA replication (reviewed in Cesare and Reddel 2008). Experimental evidence supports a "roll and spread" model of ALT, in which a 3′ telomeric overhang invades either the duplex region of its own telomere (forming the t-loop), or an extrachromosomal telomeric circle (a product of t-loop junction resolution), and is extended with DNA polymerase using either of the above templates. The extended telomere can then spread to other chromosome termini via HR. This scenario is supported by the presence of both types of candidate templates (t-loops and t-circles) for the initial phase of ALT in plants (Cesare et al. 2003; Zellinger et al. 2007). Moreover, it was shown recently that Ku protein suppresses formation of t-circles and ALT lengthening in *A. thaliana* (Zellinger et al. 2007). If initial telomere elongation events are limited to the early embryogenesis or gametogenesis, as suggested above, and the "reservoir" of elongated telomere sequence available for the individual plant generation is finite, then the extension potential will depend on the initial length of telomere. In early generations, when the initial telomere length is relatively long, the ALT is able to compensate for the replicative telomere shortening almost completely (compare the expected telomere loss of several kb per generation in *Attert*$^{-/-}$ mutants with the observed average rate of telomere shortening of ca. 250–500 bp per generation (Fitzgerald et al. 1999)). The slow but progressive telomere shortening, nevertheless, gradually decreases the efficiency of ALT, and the observed massive increase in genome instability observed since the 6th generation of *Attert* mutants (Riha et al. 2001) may reflect this. Moreover, the increase of recombination frequency due to the excessive activation of ALT itself can contribute to an increase in genome instability (Jeyapalan et al. 2005).

Immortal strand hypothesis resurrected in animal cells—does it live in plant cells too?

The remarkably low telomere-shortening rate of *Attert*$^{-/-}$ mutants could be also explained without invoking ALT-mechanisms. The "immortal strand hypothesis" proposed decades ago (Cairns 1975) suggests stem cells might limit acquired mutations that give rise to cancer through the directed inheritance of parental DNA strands. Though largely disregarded, this hypothesis of the template DNA strand co-segregation in dividing stem cells and their progeny has implications in telomere biology. Recent results (Conboy et al. 2007) provide experimental support to this hypothesis. These authors used sequential pulses of three different halogenated thymidine analogs and analyzed stem cell progeny during induced regeneration in vivo. They observed extraordinarily high frequencies of segregation of older and younger template strands during a period of proliferative expansion of muscle stem cells. Template strand co-segregation was strongly associated with asymmetric cell divisions yielding daughters with divergent fates. Daughter cells inheriting the older templates retained the more immature phenotype, whereas daughters inheriting the newer templates acquired a more differentiated phenotype (Conboy et al. 2007). It has yet to be shown if this behaviour is also present in plant meristem cells, but the idea is certainly worth considering and testing experimentally. While the mechanism could contribute to the low telomere shortening rate, it does not provide explanation for the overall telomere lengthening observed namely between G3 and G4 generations of L-line plants.

The onset of abnormal phenotype preceeds critical telomere shortening

The onset of abnormal phenotype effects was observed at least two generations earlier in this work than in the previous study (Riha et al. 2001). The severity of phenotype changes, however, did not show any direct relationship to telomere lengths or the occurrence of plants in either U- or L-lines. In particular, the severely affected G4 mutant plant did not show markedly shorter 2R or 3L telomeres than the other mutants of the same generation. Moreover, we also measured other telomeres in this particular plant (1R = 840 bp, 1L = 820 bp, 4R = 1,170 bp, 5R = 850 bp, 5L = 970 bp) and all of these ranged well above the previously published minimum functional telomere length in *Arabidopsis* (300–400 bp), which was based on measurement of telomere fusion sites (Heacock et al. 2004). Potentially therefore the phenotype characteristics may not be due to reduced telomere lengths directly, but perhaps a result of ALT-associated abundant level of telomere recombination, leading to genome instability.

Possible origins of multiple products in PETRA assays

The presence of two or multiple signals coming from a given chromosome arm using the PETRA technique is usually attributed to different telomere lengths at homologous chromosome arms, or to the hypothetical TRD events in a subpopulation of telomeres (Watson and Shippen 2007). Besides these bands of comparable intensity, we observed also some weaker bands of higher mobility, which corresponded to the stronger bands in the same lane in their number and mutual positions (see Fig. 3). Interestingly, the length differences between weaker and stronger products decreased proportionally with the size of the stronger band (see Fig. 9). The weaker band occasionally disappears in association with the shortest telomeres. We propose that these bands arise through secondary annealing sites of the telomeric PETRA primer to the region of the displacement loop (D-loop) at the site of G-overhang invasion into the double-stranded telomere region (see Fig. 10). Since the annealing occurs under native conditions, at least a fraction of t-loops may be preserved at the initial phase of PETRA. Subsequent convergence of the sizes of the two products could then be explained by tightening of the t-loop which is, however critically limited by bendability of the chromatin fibre (Fajkus and Trifonov 2001). Continued telomere shortening below the critical lengths impedes further t-loop formation (Forsyth et al. 2002), thus leading to a single telomere product in PETRA.

In conclusion, our results suggest that telomere dynamics in *Attert*$^{-/-}$ knock-out mutants can be explained solely by involvement of ALT, without a necessity to presume TRD events. The ALT events appear to be time-limited, probably to gametogenesis or early embryonic development. The fast and efficient activation of ALT in response to the loss of telomerase activity, and its probable developmental regulation imply that ALT may be a normal part of plant development.

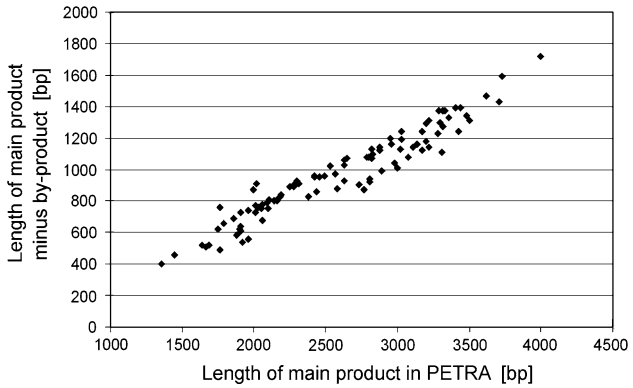

Fig. 9 By-products of PETRA. Besides major products of PETRA, we observed also weaker and faster-migrating bands, which correspond to bands of the major products both in their number and lengths ratio (compare to Fig. 3). The length differences between the main products and by-products in a given lane obtained from all PETRA experiments were plotted against the lengths of main products. These differences are proportional to the lengths of corresponding main products as is displayed in the graph. The graph includes data obtained in both 2R and 3L telomeres in all plants till G3

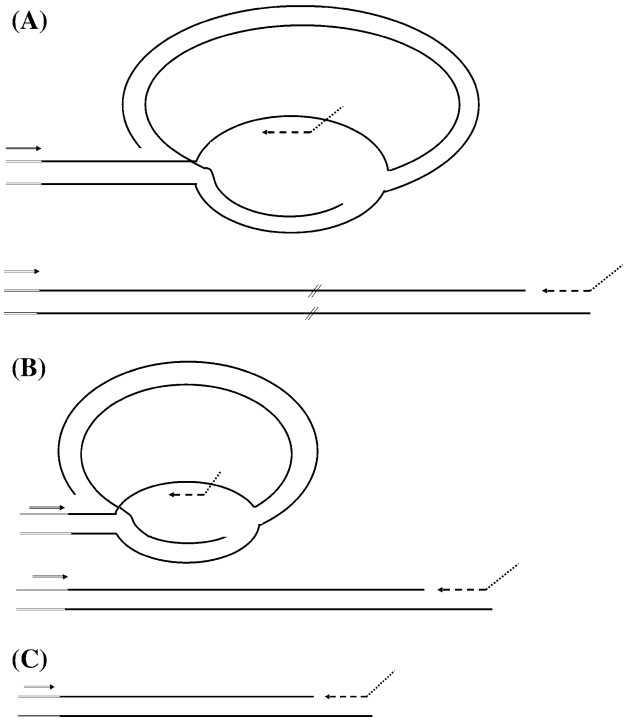

Fig. 10 Schematic picture of a possible origin of the shorter and weaker bands accompanying the main products of PETRA (see also Figs. 3 and 9). These by-products may originate from a secondary annealing of telomeric PETRA primer (dashed arrow) in the displacement loop in a fraction of t-loops surviving DNA isolation (**A**). Telomere shortening results in the corresponding tightening of the t-loop (**B**) which is limited by the bendability of telomeric chromatin fibre. Shortening below the critical limit results in the complete opening of t-loop (**C**) and the loss of the by-products of PETRA

Acknowledgements We thank Professor Andrew R. Leitch for insightful comments and the manuscript revision, Eva Sýkorová and Dagmar Zachová for helpful advice for cultivation of plant tissue cultures. This work was supported by the Czech Ministry of Education (MSM0021622415, LC06004), Czech Academy of Sciences (AVOZ50040507) and grants from GACR (521/05/0055) and GA ASCR (IAA600040505 and IAA601630703).

References

Arabidopsis Genome Initiative (2000) Analysis of the genome sequence of the flowering plant *Arabidopsis thaliana*. Nature 408:796–815

Cairns J (1975) Mutation selection and the natural history of cancer. Nature 255:197–200

Cesare AJ, Reddel RR (2008) Alternative lengthening of telomeres in mammalian cells. In: Nosek J, Tomaska L (eds) Origin and evolution of telomeres. Austin, Landes Bioscience (in press)

Cesare AJ, Quinney N, Willcox S, Subramanian D, Griffith JD (2003) Telomere looping in *P-sativum* (common garden pea). Plant J 36:271–279

Conboy MJ, Karasov AO, Rando TA (2007) High incidence of non-random template strand segregation and asymmetric fate determination in dividing stem cells and their progeny. PLoS Biol 5:e102

Dellaporta SL, Wood J, Hicks JB (1983) A plant DNA minipreparation: version II. Plant Mol Biol Rep 1:19–21

Edwards K, Johnstone C, Thompson C (1991) A simple and rapid method for the preparation of plant genomic DNA for PCR analysis. Nucleic Acids Res 19:1349

Erdmann N, Liu Y, Harrington L (2004) Distinct dosage requirements for the maintenance of long and short telomeres in mTert heterozygous mice. Proc Natl Acad Sci USA 101:6080–6085

Fajkus J, Trifonov EN (2001) Columnar packing of telomeric nucleosomes. Biochem Biophys Res Commun 280:961–963

Fajkus J, Kovarik A, Kralovics R, Bezdek M (1995) Organization of telomeric and subtelomeric chromatin in the higher-plant *Nicotiana-tabacum*. Mol Gen Genet 247:633–638

Fajkus J, Kovarik A, Kralovics R (1996) Telomerase activity in plant cells. FEBS Lett 391:307–309

Fajkus J, Fulneckova J, Hulanova M, Berkova K, Riha K, Matyasek R (1998) Plant cells express telomerase activity upon transfer to callus culture, without extensively changing telomere lengths. Mol Gen Genet 260:470–474

Fajkus J, Sykorova E, Leitch AR (2005) Telomeres in evolution and evolution of telomeres. Chromosome Res 13:469–479

Fitzgerald MS, McKnight TD, Shippen DE (1996) Characterization and developmental patterns of telomerase expression in plants. Proc Natl Acad Sci USA 93:14422–14427

Fitzgerald MS, Riha K, Gao F, Ren S, McKnight TD, Shippen DE (1999) Disruption of the telomerase catalytic subunit gene from Arabidopsis inactivates telomerase and leads to a slow loss of telomeric DNA. Proc Natl Acad Sci USA 96:14813–14818

Fletcher JC (2002) Coordination of cell proliferation and cell fate decisions in the angiosperm shoot apical meristem. Bioessays 24:27–37

Forsyth NR, Wright WE, Shay JW (2002) Telomerase and differentiation in multicellular organisms: turn it off, turn it on, and turn it off again. Differentiation 69:188–197

Grandjean O, Vernoux T, Laufs P, Belcram K, Mizukami Y, Traas J (2004) In vivo analysis of cell division, cell growth, and differentiation at the shoot apical meristem in *Arabidopsis*. Plant Cell 16:74–87

Hauguel T, Bunz F (2003) Haploinsufficiency of hTERT leads to telomere dysfunction and radiosensitivity in human cancer cells. Cancer Biol Ther 2:679–684

Heacock M, Spangler E, Riha K, Puizina J, Shippen DE (2004) Molecular analysis of telomere fusions in Arabidopsis: multiple pathways for chromosome end-joining. Embo J 23:2304–2313

Heller K, Kilian A, Piatyszek MA, Kleinhofs A (1996) Telomerase activity in plant extracts. Mol Gen Genet 252:342–345

Jeyapalan JN, Varley H, Foxon JL, Pollock RE, Jeffreys AJ, Henson JD, Reddel RR, Royle NJ (2005) Activation of the ALT pathway for telomere maintenance can affect other sequences in the human genome. Hum Mol Genet 14:1785–1794

Liu L, Bailey SM, Okuka M, Munoz P, Li C, Zhou L, Wu C, Czerwiec E, Sandler L, Seyfang A et al (2007) Telomere lengthening early in development. Nat Cell Biol 9:1436–1441

Pich U, Fuchs J, Schubert I (1996) How do Alliaceae stabilize their chromosome ends in the absence of TTTAGGG sequences? Chromosome Res 4:207–213

Riha K, Fajkus J, Siroky J, Vyskot B (1998) Developmental control of telomere lengths and telomerase activity in plants. Plant Cell 10:1691–1698

Riha K, McKnight TD, Griffing LR, Shippen DE (2001) Living with genome instability: plant responses to telomere dysfunction. Science 291:1797–1800

Siroky J, Zluvova J, Riha K, Shippen DE, Vyskot B (2003) Rearrangements of ribosomal DNA clusters in late generation telomerase-deficient *Arabidopsis*. Chromosoma 112:116–123

Sykorova E, Lim KY, Chase MW, Knapp S, Leitch IJ, Leitch AR, Fajkus J (2003) The absence of Arabidopsis-type telomeres in *Cestrum* and closely related genera *Vestia* and *Sessea* (Solanaceae): first evidence from eudicots. Plant J 34:283–291

Sykorova E, Fajkus J, Meznikova M, Lim KY, Neplechova K, Blattner FR, Chase MW, Leitch AR (2006) Minisatellite telomeres occur in the family Alliaceae but are lost in Allium. Am J Bot 93:814–823

Watson JM, Shippen DE (2007) Telomere rapid deletion regulates telomere length in *Arabidopsis thaliana*. Mol Cell Biol 27:1706–1715

Zellinger B, Akimcheva S, Puizina J, Schirato M, Riha K (2007) Ku suppresses formation of telomeric circles and alternative telomere lengthening in *Arabidopsis*. Mol Cell 27:163–169

Zhang A, Zheng C, Hou M, Lindvall C, Li KJ, Erlandsson F, Bjorkholm M, Gruber A, Blennow E, Xu D (2003) Deletion of the telomerase reverse transcriptase gene and haploinsufficiency of telomere maintenance in Cri du chat syndrome. Am J Hum Genet 72:940–948

Supplement C

Schrumpfová, P.P., Kuchar, M., Palecek, J., Fajkus, J., **2008**. Mapping of interaction domains of putative telomere-binding proteins AtTRB1 and AtPOT1b from Arabidopsis thaliana. FEBS Lett. 582, 1400–1406

P.P.S. was significantly involved in the experimental part (more then 50 % of experiments) and participated in the ms writing and editing

FEBS Letters 582 (2008) 1400–1406

Mapping of interaction domains of putative telomere-binding proteins AtTRB1 and AtPOT1b from *Arabidopsis thaliana*

Petra Procházková Schrumpfová[a,1], Milan Kuchař[a,1], Jan Paleček[a], Jiří Fajkus[a,b,*]

[a] *Department of Functional Genomics and Proteomics, Institute of Experimental Biology, Faculty of Science, Masaryk University, Kamenice 5, CZ-62500 Brno, Czech Republic*

[b] *Laboratory of DNA-Molecular Complexes, Institute of Biophysics, Czech Academy of Sciences, Královopolská 135, CZ-61265 Brno, Czech Republic*

Received 12 December 2007; revised 19 February 2008; accepted 2 March 2008

Available online 1 April 2008

Edited by Gianni Cesareni

Abstract **We previously searched for interactions between plant telomere-binding proteins and found that AtTRB1, from the single-myb-histone (Smh) family, interacts with the Arabidopsis POT1-like-protein, AtPOT1b, involved in telomere capping. Here we identify domains responsible for that interaction. We also map domains in AtTRB1 responsible for interactions with other Smh-family-members. Our results show that the N-terminal OB-fold-domain of AtPOT1b mediates the interaction with AtTRB1. This domain is characteristic for POT1- proteins and is involved with binding the G-rich-strand of telomeric DNA. AtPOT1b also interacts with AtTRB2 and AtTRB3. The central histone-globular-domain of AtTRB1 is involved with binding to AtTRB2 and 3, as well as to AtPOT1b. AtTRB1-heterodimers with other Smh-family-members are more stable than AtTRB1-homodimers. Our results reveal interaction networks of plant telomeres.**

Structured summary:
MINT-6440051:
AtTRB1 (uniprotkb:Q8VWK4) *physically interacts* (MI:0218) with *AtTRB1* (uniprotkb:Q8VWK4) by *two-hybrid* (MI:0018)
MINT-6440068:
AtTRB2 (uniprotkb:Q8VX38) *physically interacts* (MI:0218) with *AtTRB1* (uniprotkb:Q8VWK4) by *two-hybrid* (MI:0018)
MINT-6440083:
AtTRB3 (uniprotkb:Q9M2X3) *physically interacts* (MI:0218) with *AtTRB1* (uniprotkb:Q8VWK4) by *two-hybrid* (MI:0018)
MINT-6440099:
AtPOT1b (uniprotkb:Q6Q835) *physically interacts* (MI:0218) with *AtTRB1* (uniprotkb:Q8VWK4) by *two-hybrid* (MI:0018)
MINT-6440119:
AtPOT1b (uniprotkb:Q6Q835) *physically interacts* (MI:0218) with *AtTRB2* (uniprotkb:Q8VX38) by *two-hybrid* (MI:0018)
MINT-6440138:
AtPOT1b (uniprotkb:Q6Q835) *physically interacts* (MI:0218) with *AtTRB3* (uniprotkb:Q9M2X3) by *two-hybrid* (MI:0018)
MINT-6440216:
AtPOT1b (uniprotkb:Q6Q835) *physically interacts* (MI:0218) with *AtTRB1* (uniprotkb:Q8VWK4) by *coimmunoprecipitation* (MI:0019)
MINT-6440157:
AtTRB2 (uniprotkb:Q8VX38) *physically interacts* (MI:0218) with *AtTRB1* (uniprotkb:Q8VWK4) by *coimmunoprecipitation* (MI:0019)
MINT-6440177:
AtTRB3 (uniprotkb:Q9M2X3) *physically interacts* (MI:0218) with *AtTRB1* (uniprotkb:Q8VWK4) by *coimmunoprecipitation* (MI:0019)

Keywords: Plant; Telomere; Protein–protein interaction; AtTRB1; AtTRB2; AtTRB3; AtPOT1b

1. Introduction

Telomere proteins play a role in the protection and maintenance of chromosome ends. In human cells, the minimal functional set of proteins participating in telomere protection is collectively called ''shelterin'' [1]. Shelterin consists of three proteins (TRF1, TRF2 and POT1) that directly recognize telomeric DNA and are interconnected by at least three other proteins (TIN2, TPP1 and Rap1), forming a telomere-specific protective cap. Similar complexes are also likely to exist in plants and these are particularly attractive to study due to the telomerase-competent status (i.e., reversible telomerase activity regulation) of plant somatic cells [2,3]. A number of putative plant telomeric proteins have been found by homology searches of DNA and protein sequence databases and tested for their affinity to telomeric DNA sequences in vitro (reviewed in [4]). There is however very little data relevant to their telomeric function. Of the putative ''plant shelterin'' components, functional data relevant to telomere homeostasis is available for two *Arabidopsis thaliana* POT1-like proteins, AtPOT1a and AtPOT1b. These proteins contain the oligonucleotide-binding (OB) fold domain which binds to the G-rich strand of telomeric DNA but their overall sequence similarity is low (49%). The functions of AtPOT1a and AtPOT1b proteins are different: AtPOT1a functions mainly in telomerase regulation, while AtPOT1b contributes to chromosome end-protection and genome stability [5–9].

Recently, another *Arabidopsis* protein, AtTBP1, has been shown to be involved in telomere length regulation [10]. This

*Corresponding author. Address: Department of Functional Genomics and Proteomics, Institute of Experimental Biology, Faculty of Science, Masaryk University, Kamenice 5, CZ-62500 Brno, Czech Republic. Fax: +420 549492654.
E-mail address: fajkus@sci.muni.cz (J. Fajkus).

[1]First two authors contributed equally to this work.

0014-5793/$34.00
doi:10.1016/j.febslet.2008.03.034

protein binds double-stranded telomeric DNA in vitro via a characteristic Myb-like domain, referred to as a telobox, located at its C-terminus [11,12]. To identify other components of "plant shelterin", we analyzed a number of putative *A. thaliana* telomere proteins for their mutual interactions. We previously found that AtTRP1, the *Arabidopsis* myb-like protein bearing a C-terminal telobox, interacts with AtKu70 [5], which itself plays a role in plant telomere homeostasis [13,14]. Furthermore AtTRP1 may be a functional homolog of mammalian TRF2 [5]. In addition, an *Arabidopsis* POT1-like protein, AtPOT1b, interacts with AtTRB1, a protein from the single myb histone (Smh) family [5]. The Smh family is characterised by a unique triple motif structure containing a N-terminal myb-like domain, a central GH1/GH5 histone globular domain and a C-terminal coiled-coil domain [15]. Proteins of this family in *Arabidopsis* show specific binding to telomeric DNA and can form homo- and heteromeric protein–protein complexes [16].

The abundance of candidate telomere proteins in plants, arising from numerous paralogs of telomere-binding protein and plant-specific proteins, coupled with an apparent absence of some constitutive animals and fungi shelterin components, makes imperative analyses of interactions between the candidate plant telomere proteins. Using a combination of the yeast two-hybrid system (Y2H) and co-immunoprecipitation (CoIP), we characterise here the protein domains involved in interactions between AtTRB1 and AtPOT1b, as well as domains engaged in the formation of homomeric and heteromeric complexes of AtTRB proteins.

2. Materials and methods

2.1. Cloning of full length proteins and their deletion variants for two-hybrid assay

An overview of cloned candidate telomeric DNA-binding proteins is given in Table 1. cDNA sequences of AtTRB1, AtTRB2, AtTRB3 and AtPOT1b have been cloned as described previously [16]. To localize the interaction domains the deletion forms of AtTRB1 and AtPOT1b were generated by PCR and cloned into the vector pGBKT7 or pGADT7, respectively. Sequence-specific primers with restriction sites were used for cloning individual cDNAs as shown in Table 2.

To localize the interaction domain(s) in AtTRB1, cDNA fragments were cloned in pGADT7 and denominated according to primers used (for example, the fragment F1R1 was generated using TRB1 F1 as forward and TRB1 R1 as reverse primers – see Figs. 1A and 2B). Similarly, AtPOT1b fragments were generated to localize the region of AtPOT1b responsible for interaction with AtTRB1 (see Fig. 2C).

Prior to two-hybrid screening, cloned constructs were checked for the correct reading frame and absence of mutations by DNA sequencing on an ABI PRISM 310 sequencer (Perkin–Elmer).

2.2. Yeast two-hybrid (Y2H) system

Two strains of *Saccharomyces cerevisiae*, PJ69-4a and PJ69-4α were used [17]. Protein AtPOT1b, its deletion variants and AtTRB2, AtTRB3 were expressed from the yeast vector pGBKT7 in strain PJ69-4α, and AtTRB1 and its fragments from vector pGADT7 in strain PJ69-4a. This division enabled proper combining of the proteins and their deletion variants in interaction assays. Both strains, identical except for the mating type, were mixed on Petri-dishes with YPD medium (1.1% yeast extract, 2.2% bacteriological peptone, 2% glucose and 2% agar) to fuse yeast haploid cells of different strains, and incubated at 30 °C for 8–10 h. The diploid cells were printed by velvet stamp onto control -Leu,-Trp selective plates (0.67% yeast nitrogen base, 2% glucose, 0.12% amino acid mixture without Leu and Trp, 2% agar, pH adjusted by NaOH to 6.8) and then onto -Ade selective plates to test the interaction (0.67% yeast nitrogen base, 2% glucose, 0.12% amino acid mixture without Ade, 2% agar, pH adjusted by NaOH to 6.8) and were incubated at 30 °C for a few days until colonies had grown. Alternatively, PJ69-4a cells were cotransformed with both pGBKT7 and pGADT7 plasmids and grown on -Leu,-Trp plates. Colonies were inoculated into YPD liquid medium and incubated at 30 °C overnight. Ten-times diluted aliquots were dropped onto both -Ade and -His plates. For a semi-quantitative test, 5 μl aliquots were dropped onto selective -His plates containing increasing concentrations of 3-aminotriazol (3-AT). As the 3-AT inhibits His3 activity, the ability of yeast cells to grow on higher concentrations correlates with the higher binding affinity of the hybrid proteins.

To verify our results we also used the yeast strain MaV203, where the His3-reporter gene is under a less tightly controlled promoter (Invitrogen). The drop test was executed in the similar way as with the PJ69 strain.

Table 2
Complete list of primers used for cloning

Primer	Restriction site	Sequence of primer (5′ → 3′)
POT1b F	BamHI	ATGGATCCTAATGGAGGAGGAGAGAAGAG
POT1b F1	BamHI	ATGGATCCTAAAGATTGTGCTGATTAACC
POT1b F2	BamHI	TAGGATCCACTTCTTATCGAATCTGAGAG
POT1b F3	BamHI	TTGGATCCTTAAGTCAGAAAGGCTTC
POT1b R	XhoI	ATTCTCGAGTCATGAAGCATTGATCCAAG
POT1b R1	XhoI	TTACTCGAGCCCTTCATCAGCATATAGAG
POT1b R2	XhoI	TTACTCGAGCCTGTGATTTCAGAATGTG
POT1b R3	XhoI	TTACTCGAGGGTTGAAGACAGTGAATG
POT1b R4	XhoI	TTACTCGAGATCTTCAAACTTGTACGTG
POT1b R5	XhoI	CTTCTCGAGGGTTAATCAGCACAATCTTTA
TRB1 F	BamHI	ATGGATCCGAATGGGTGCTCCTAAGCAG
TRB1 F1	BamHI	CGGGATCCAAGATGCGACCTCTGGACTCC
TRB1 F2	BamHI	GAGGATCCAAGGTCTGGGGGTGTTTGGA
TRB1 F01	BamHI	CGGGATCCTAGTCATGGCAAATGGCTGG
TRB1 R	XhoI	TGGCTCGAGAGGCACGGATCATCATTTTG
TRB1 R1	BamHI	TCGGATCCTCCAAACACCCCCAGACC
TRB1 R2	BamHI	GAGGATCCGGAGTCCAGAGGTCGCATC
TRB1 R12	BamHI	CAGGATCCGCGTTTGAAGTCTGGTGGAG

2.3. In vitro translation and co-immunoprecipitation

Proteins were co-expressed from the same constructs as were used in Y2H system with an hemagglutinin tag (pGADT) or a myc-tag (pGBKT) by use of the TNT Quick Coupled Transcription/Translation System (Promega) in 15–25 μl of each reaction according to the manufacturer's instruction. For Myc pull-down experiments, 15–25 μl of in vitro-expressed proteins in total volume of 100 μl of HEPES buffer (25 mM HEPES, 150 mM KCl, 50 mM NaCl, 3 mM $MgCl_2$, 10% glycerol, 0.1% NP-40, 1 mM DTT, 2 mM PMSF, 2 μg/μl leupeptine, 1 μg/μl pepstatine) were mixed with 1 μg anti-Myc-tag polyclonal antibody (Abcam) and incubated overnight at 4 °C (Input fraction). 10 μl of Protein G magnetic particles (Dynabeads, Invitrogen-Dynal) were then added, and the mixture was incubated for 1 h/4 °C (Un-

Table 1
Overview of cloned proteins

Protein	Protein group	Characteristic domain	GenBank accession number	Reference
AtTRB1	dsDNA binding	N-terminal Myb domain	AAL73123	[16]
AtTRB2	Proteins		AAL73441	[17]
AtTRB3			NP_190554	
AtPOT1b	ssDNA binding proteins	Pot1 domain	NP_196249	[5,9,23]

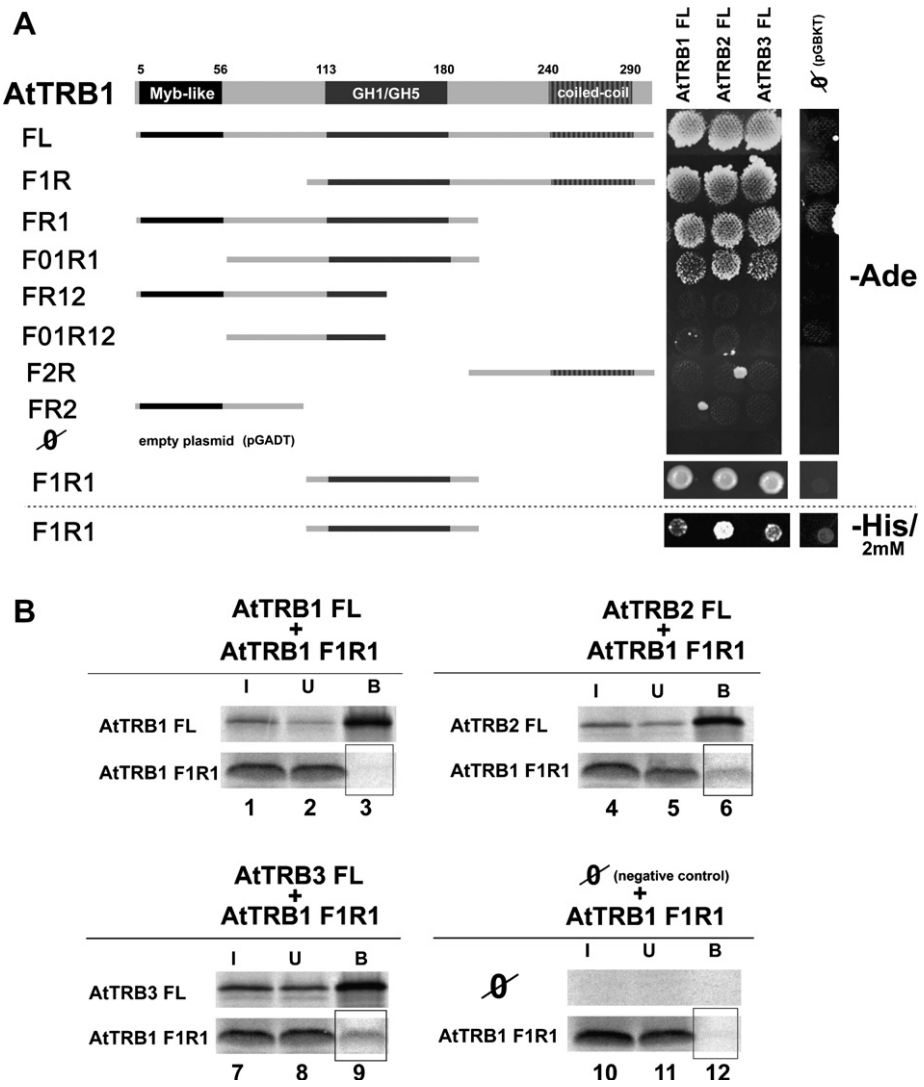

Fig. 1. Histone GH1/GH5 globular domain of AtTRB1 binds to AtTRB1, 2 and 3 protein. (A) The AtTRB1 protein contains a myb-like domain (myb-like), followed by GH1/GH5 histone globular domain and C-terminal coiled-coil domain (coiled-coil). Full-length (FL) AtTRB1, F1R (aa 101–300), FR1 (aa 1–201), F01R1 (aa 58–201), FR12 (aa 1–159), F01R12 (aa 58–159), F2R (aa 196–300), FR2 (1–106), F1R1 (aa 101–201) fragments (in PJ69-4a yeast strain) are combined with AtTRB1 FL, AtTRB2 FL, AtTRB3 FL two-hybrid constructs (in PJ69-4α yeast strain) and the diploid cells are tested on -Ade plates (-Ade) for protein–protein interactions (top and middle panel). Only fragments containing the GH1/GH5 histone globular domain interact with all three AtTRB proteins. The PJ69-4 cells containing the F1R1 construct are also tested on -His plates with 2 mM concentration of 3-AT (-His/2 mM). Only the interactions of F1R1 with AtTRB2 and AtTRB3 are detectable (bottom panel). Empty pGBKT7 (right panel) and pGADT7 vectors are used as negative controls. (B) AtTRB2 and AtTRB3 proteins are able to pull-down F1R1 fragment. The TNT expressed full-length AtTRB1 FL (lanes 1–3), AtTRB2 FL (lanes 4–6) and/or AtTRB3 FL (lanes 7–9) proteins were mixed with AtTRB1 GH1/GH5 fragment (F1R1, lanes 1–12) and incubated with anti-myc antibody overnight. Then protein G magnetic beads were added and proteins were immunoprecipitated for 1 h. In the control experiment, the F1R1 fragment was incubated with antibody and beads in the absence of partner protein (lanes 10–12). Input (I), unbound (U), and bound (B) fractions were collected and run in SDS–12% PAGE gels.

bound fraction). The beads were washed five times with HEPES buffer and then incubated with 10 μl of SDS-loading buffer for 10 min/85 °C to elute bound proteins (Bound fraction). Input, unbound, and bound fractions were separated by 12% SDS–PAGE and analyzed by STORM860 (GE Healthcare).

3. Results

3.1. Interactions between AtTRB proteins

We have shown previously that the telomere-binding proteins AtTRB1, AtTRB2, and AtTRB3 form homodimeric and heterodimeric complexes in Y2H assays [5,16]. These proteins are similar to each other at the level of amino acid sequence and belong to the same family of Smh proteins [15]. In contrast to other myb-like telomere-binding proteins, in Smh proteins the myb-like domain is N-terminal. The myb-like domain is followed by GH1/GH5 histone globular domain and a C-terminal coiled-coil domain (Fig. 1A). Interactions of AtTRB proteins were expected to be mediated by the C-terminal coiled-coil domain because this domain supports protein oligomerization [18]. Therefore, we designed two deletion mutants AtTRB1 F1R (aa position 101–300) and AtTRB1 F2R (196–300) that comprised the C-terminus. Each construct was transformed into PJ69-4a two-hybrid strain and crossed with PJ69-4α containing full-length (FL) AtTRB constructs. Only AtTRB1 F1R construct containing both coiled-coil and

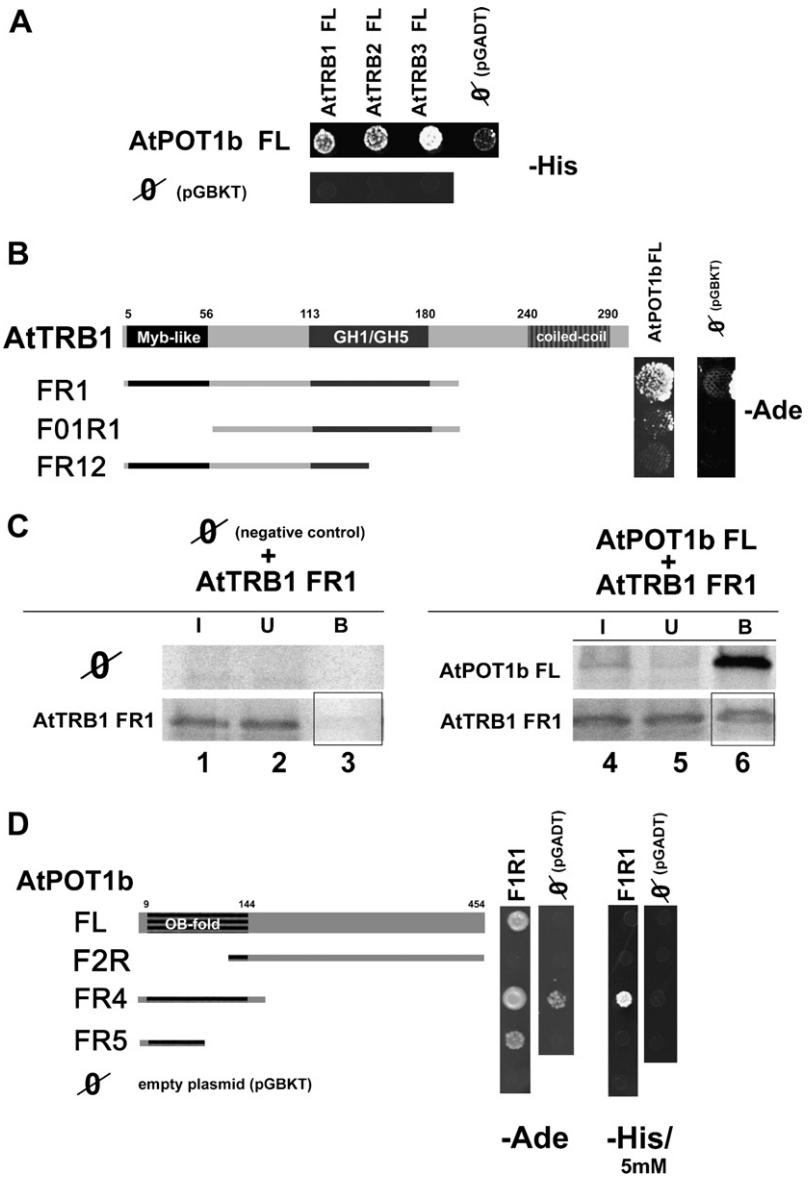

Fig. 2. Histone GH1/GH5 globular domain of AtTRB1 binds to the N-terminus of the AtPOT1b protein. (A) Full-length AtPOT1b FL interacts with AtTRB1 FL, AtTRB2 FL and AtTRB3 FL in two-hybrid assay when scored for growth on -His plates (for Y2H details see Fig. 1A). (B) Yeast two-hybrid cells containing FR1 (aa 1–201), F01R1 (aa 58–201), FR12 (aa 1–159) fragments are combined with AtPOT1b FL and tested on -Ade plates for protein–protein interactions. Only fragments containing the GH1/GH5 histone globular domain interact with the AtPOT1b protein. (C) In the co-immunoprecipitation assay, the TNT expressed AtTRB1 FR1 fragment (lanes 1–6) was mixed with full-length AtPOT1b FL protein (lanes 4–6) and incubated with anti-myc antibody (same conditions as in Fig. 1B). In the control experiment, the FR1 fragment was incubated with antibody and beads in the absence of the partner protein (lanes 1–3). (D) The PJ69-4a cells containing AtTRB1 fragment F1R1 (aa 101–201) were cotransformed with full-length (FL) and/or following fragments F2R (aa 135–454), FR4 (aa 1–150), FR5 (aa 1–90) of AtPOT1b. Transformants containing FL, FR4 and FR5 fragments grow on -Ade plate (first column), however, a weak self-activation can be seen with FR4 fragment on a control plate (second column). When these cells were grown on -His plates with increasing concentrations of 3-AT the addition of 3-AT to 5 mM concentration abolishes the self-activation of FR4 (fourth column) while keeping its specific interaction with the F1R1 fragment of AtTRB1 (third column). These results suggest that the AtTRB1-AtPOT1b interaction is mediated by the binding of the GH1/GH5 domain of the AtTRB protein to the N-terminus (bearing the OB-fold domain) of the AtPOT1b protein.

GH1/GH5 histone globular domain supported the growth of PJ69-4 diploid strain on -Ade plates (Fig. 1A, top panel), suggesting that the interactions are not mediated by the coiled-coil region. Instead, interactions between all three AtTRB proteins and fragments containing the GH1/GH5 histone globular domain were observed, in particular AtTRB1 FR1 (1–201), AtTRB1 F01R1 (58–201) and AtTRB1 F1R1 (101–201). Fragments containing truncated or completely deleted GH1/GH5, as in the AtTRB1 FR2 (1–106), AtTRB1 F01R12 (58–159) and AtTRB1 FR12 (1–159) constructs, lost the interaction with AtTRB1, as well as with the other AtTRB proteins. Thus, the shortest AtTRB1 fragment displaying the interaction with AtTRB proteins is F1R1 (101–201), which contains a GH1/GH5 domain and short flanking regions (Fig. 1A, middle panel).

The PJ69-4 cells containing the F1R1 construct were also grown on -His plates with increasing concentrations of 3-amino-1,2,3-triazol (3-AT) to compare binding affinities to

different AtTRB proteins (data not shown). At 2 mM 3-AT only the interactions of F1R1 with AtTRB2 and AtTRB3 were detected (Fig. 1A, bottom panel). To verify these results we used another two-hybrid strain (MaV203 strain has His3-reporter gene under a less tightly controlled promoter). When the full-length AtTRB1 or its FR1 fragment (covering both myb-like and GH1/GH5 domains) was used in the His-reporter assay, interactions with all three AtTRB proteins were positive up to 5 mM 3-AT. A further increase of 3-AT to 20 mM resulted in a loss of interaction with AtTRB1, while keeping interactions with AtTRB2 and 3 (Supplementary Fig. S1). Altogether, these data suggest that heterotypic complexes of AtTRB1 are more stable than homotypic ones.

To test the above Y2H results by an independent approach, co-immunoprecipitation (CoIP) assays were performed with the above AtTRB1 fragments. In particular, interactions were assayed between F1R1 and the three AtTRB proteins. Fig. 1B shows that the myc-tagged AtTRB2 and AtTRB3 proteins are able to pull-down the F1R1 fragment while the full-length AtTRB1 is not. These results confirm a low affinity of the GH1/GH5 domain of AtTRB1 to full-length AtTRB1 (insufficient to provide a positive result in CoIP) and a higher affinity to both AtTRB2 and AtTRB3.

3.2. AtTRB1 interaction with AtPOT1b

The protein AtPOT1b is thought important for "chromosome capping" in *A. thaliana* and interactions previously detected with AtTRB1 may be of functional significance [5,6]. Fig. 2A shows that the interaction of AtPOT1b is not limited to AtTRB1, but also occurs with AtTRB2 and AtTRB3 proteins (Fig. 2A).

For mapping the interaction between the AtTRB1 and AtPOT1b the same AtTRB1 fragments in PJ69-4a cells (see Fig. 1A) were crossed with PJ69-4α cells containing full-length AtPOT1b. Only the diploid cells with AtTRB1 fragments containing the GH1/GH5 domain grow on -Ade plates (Fig. 2B and D; data not shown). These results suggest a role of the GH1/GH5 domain in binding to AtPOT1b.

CoIP assays were performed using the FR1 fragment of AtTRB1 and the full-length AtPOT1b. The FR1 fragment co-precipitated with the myc-tagged AtPOT1b protein (Fig. 2C). This positive result confirms the above findings obtained by Y2H.

In the case of AtPOT1b the following fragments were generated and cloned into pGBKT7: POT1b F2R (135–454), POT1b FR4 (1–150) and POT1b FR5 (1–90). The PJ69-4a cells containing AtTRB1 fragment F1R1 were cotransformed with

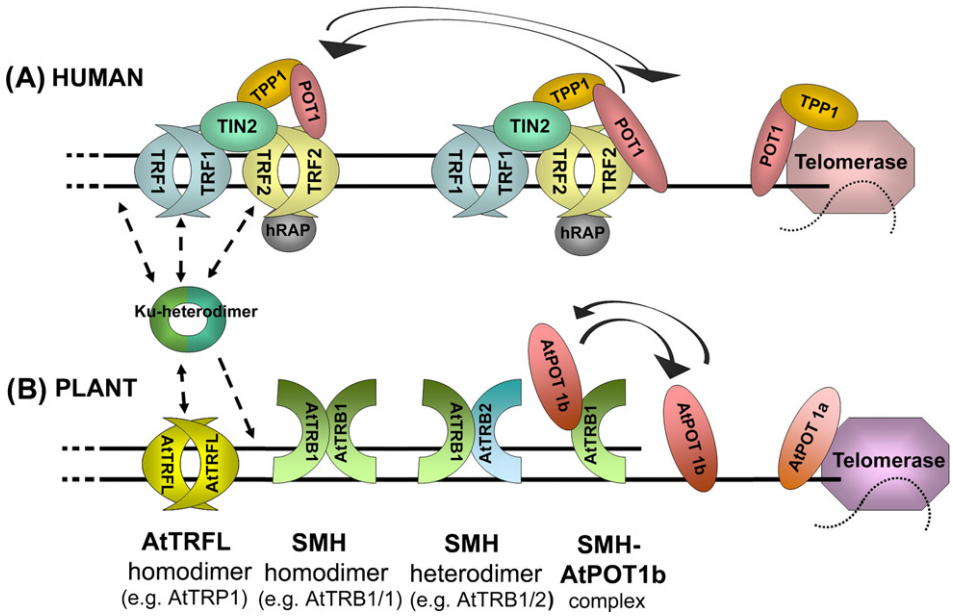

Fig. 3. Schematic depiction of the principal telomere components and their interactions in humans and plants. In humans (A), the complex of ubiquitously present telomere-associated proteins, termed as shelterin [1], consists of two components that can bind telomeric dsDNA (TRF1, TRF2), and recruit the shelterin components TIN2, TPP1 and Rap1. The sixth partner in shelterin is the single-stranded TTAGGG repeat-binding protein, POT1. In addition to its binding to the G-strand of telomeric DNA, it can associate with telomeres also through its interaction with TPP1. Transitions between these states are illustrated with arrows. Examples of functionally important interactions (with Ku-proteins and telomerase) are also shown. In plants (B), a number of TRF-like proteins, exemplified here by AtTRP1, have been identified which are able to form homodimers and bind telomeric dsDNA with their C-terminal telobox Myb-like domain [11,12]. Analogous to TRF2, AtTRP1 is able to interact with AtKu70 [5], providing thus (in similarity to other organisms) association of Ku-heterodimer with telomeres via protein–protein interaction, in addition to its possible direct DNA-binding. Besides the TRF-like proteins, plant possess the SMH family of proteins which are characterised by the N-terminal myb-like domain, a central GH1/GH5 histone globular domain and a C-terminal coiled-coil domain [15]. These proteins form both homomeric and heteromeric complexes among each other using their central GH1/GH5 domain. This domain can also bind DNA in a sequence-non-specific manner (not shown), the interaction possibly important to avoid protein aggregation or telomere chromatin folding [23]. In addition, SMH proteins can interact (using the same GH1/GH5 domain) with AtPOT1b [5], one of the POT1-like proteins in *Arabidopsis thaliana*, which participates in telomere end-protection [6]. It is noteworthy that AtPOT1b uses the same domain (N-terminal OB-fold) for interaction with both telomeric ssDNA, and AtTRB proteins. Transitions of AtPOT1b between its DNA- and SMH-associated state (arrows) may be important for AtPOT1b recruitment to telomeres and for its protective function. The other AtPOT1 paralog, AtPOT1a, possibly functions in telomerase regulation and recruitment [7,8,22]. The presence of two functionally divergent POT1-like proteins in *Arabidopsis* is similar to the situation in mice [24]. Only linear telomere conformation is shown and nucleosomes are not depicted for simplicity.

full-length (FL) and/or fragments of AtPOT1b. Only transformants containing FL, FR4 and FR5 fragments grew on -Ade plates (Fig. 2D), however, a weak self-activation can be seen with fragment FR4 on the control plate. When these cells were grown on -His plates with increasing concentrations of 3-AT the addition of 3-AT to 5 mM concentration abolished the self-activation of FR4 whilst keeping its specific interaction with the F1R1 fragment of AtTRB1 (Fig. 2D, right panel). These results suggest that the AtTRB1-AtPOT1b interaction is mediated by the binding of GH1/GH5 domain of the AtTRB protein to the N-terminus (bearing the OB-fold domain) of the AtPOT1b protein.

4. Discussion

Our results confirm previously published interactions between AtTRB proteins [16] and interactions between AtTRB1 and AtPOT1b [5]. They also provide a detailed map of those interactions. Interactions between AtPOT1b and other members of the Smh family (AtTRB2 and 3) are newly reported here. The function of AtPOT1b in chromosome protection and genome stability [6], highlights the importance of its interactions. AtTRB proteins, the only interaction partners of AtPOT1b identified so far, are representatives of the plant-specific Smh family of telomere-binding proteins. They have an N-terminal myb-like domain (instead of a usual C-terminal position in TRF-like proteins), and a central GH1/GH5 domain. The results of the assays show that AtTRB1 uses the central GH1/GH5 histone globular domain for interaction with AtTRB proteins and AtPOT1b. The GH1 and GH5 sub-domains are members of the 'winged helix' class of DNA-binding domains, although in contrast to other members of the family, they contain a distinct, additional cluster of positively charged amino acids. These residues form a second DNA-binding surface on the opposite side of the protein to the primary DNA-binding site [19]. Besides the ability to bind DNA, the GH5 domain is able to self-associate [20], which mediates AtTRB1 self-interaction and interactions with AtTRB2, AtTRB3 and AtPOT1b. Possibly, the weak interactions of the GH1/GH5 histone globular domain in AtTRB1 are of a similar nature to GH5 hydrophobic protein–protein interactions described previously [20]. The GH1/GH5 histone globular domain can also bind DNA in a sequence-non-specific manner, while their N-terminal Myb-like domain [16] provides the sequence-specific binding of AtTRB to telomeres (Mozgova et al., submitted for publication).

The use of the same domain for interacting with different proteins may be of functional importance. It is not only AtTRB1 which uses the same region to interact with all AtTRB proteins and AtPOT1b, but this is also observed for the N-terminus of AtPOT1b, which bears the OB-fold domain. This domain is thought to be involved in binding to telomere DNA and interacting with AtTRB proteins. These overlapping functions may be part of a regulatory mechanism, similar to that provided by binding properties of the components of the mammalian shelterin complex (Fig. 3). In the latter complex, there is a dynamic balance between POT1 bound directly to the telomere (to telomeric DNA) and via protein–protein interactions [21]. In plant shelterin, differences in expression levels of the proteins (see Supplementary figure S2) may also participate in modulation of telomere metabolism in a tissue- and developmental stage-specific manner. The observed differential tendency of AtTRB1 to form homomeric and heteromeric complexes with AtTRB proteins, plus the ability of AtPOT1b to form complexes with all three tested AtTRB proteins and the presence of two functionally divergent AtPOT1 proteins in *A. thaliana* [6–8,22] suggest that plant shelterins are highly complex and carry features not found in animal and fungal shelterin.

Acknowledgements: We thank Lumír Krejčí for suggestions regarding the two-hybrid techniques and Andrew Leitch (Queen Mary University, London) for critical reading of the manuscript. This work was supported by the Grant Agency of the Czech Republic (projects 521/05/0055 and 521/08P452), Czech Ministry of Education (LC06004) and the institutional support (MSM0021622415 and AVOZ50040507).

Appendix A. Supplementary data

Supplementary data associated with this article can be found, in the online version, at doi:10.1016/j.febslet.2008.03.034.

References

[1] de Lange, T. (2005) Shelterin: the protein complex that shapes and safeguards human telomeres. Genes Dev. 19, 2100–2110.
[2] Fajkus, J., Fulneckova, J., Hulanova, M., Berkova, K., Riha, K. and Matyasek, R. (1998) Plant cells express telomerase activity upon transfer to callus culture, without extensively changing telomere lengths. Mol. Gen. Genet. 260, 470–474.
[3] Riha, K., Fajkus, J., Siroky, J. and Vyskot, B. (1998) Developmental control of telomere lengths and telomerase activity in plants. Plant Cell 10, 1691–1698.
[4] Kuchar, M. (2006) Plant telomere-binding proteins. Biol Plantarum 50, 1–7.
[5] Kuchar, M. and Fajkus, J. (2004) Interactions of putative telomere-binding proteins in *Arabidopsis thaliana*: identification of functional TRF2 homolog in plants. FEBS Lett. 578, 311–315.
[6] Shakirov, E.V., Surovtseva, Y.V., Osbun, N. and Shippen, D.E. (2005) The Arabidopsis Pot1 and Pot2 proteins function in telomere length homeostasis and chromosome end protection. Mol. Cell. Biol. 25, 7725–7733.
[7] Rossignol, P., Collier, S., Bush, M., Shaw, P. and Doonan, J.H. (2007) Arabidopsis POT1A interacts with TERT-V(I8), an N-terminal splicing variant of telomerase. J. Cell. Sci. 120, 3678–3687.
[8] Surovtseva, Y.V., Shakirov, E.V., Vespa, L., Osbun, N., Song, X. and Shippen, D.E. (2007) Arabidopsis POT1 associates with the telomerase RNP and is required for telomere maintenance. EMBO J. 26, 3653–3661.
[9] Baumann, P., Podell, E. and Cech, T.R. (2002) Human Pot1 (protection of telomeres) protein: cytolocalization, gene structure, and alternative splicing. Mol. Cell Biol. 22, 8079–8087.
[10] Hwang, M.G. and Cho, M.H. (2007) *Arabidopsis thaliana* telomeric DNA-binding protein 1 is required for telomere length homeostasis and its Myb-extension domain stabilizes plant telomeric DNA binding. Nucleic Acids Res. 35, 1333–1342.
[11] Hwang, M.G., Chung, I.K., Kang, B.G. and Cho, M.H. (2001) Sequence-specific binding property of *Arabidopsis thaliana* telomeric DNA binding protein 1 (AtTBP1). FEBS Lett. 503, 35–40.
[12] Bilaud, T., Koering, C.E., Binet-Brasselet, E., Ancelin, K., Pollice, A., Gasser, S.M. and Gilson, E. (1996) The telobox, a Myb-related telomeric DNA binding motif found in proteins from yeast, plants and human. Nucleic Acids Res. 24, 1294–1303.
[13] Bundock, P., van Attikum, H. and Hooykaas, P. (2002) Increased telomere length and hypersensitivity to DNA damaging agents in an Arabidopsis KU70 mutant. Nucleic Acids Res. 30, 3395–3400.
[14] Riha, K., Watson, J.M., Parkey, J. and Shippen, D.E. (2002) Telomere length deregulation and enhanced sensitivity to geno-

toxic stress in Arabidopsis mutants deficient in Ku70. EMBO J. 21, 2819–2826.
[15] Marian, C.O. et al. (2003) The maize Single myb histone 1 gene, Smh1, belongs to a novel gene family and encodes a protein that binds telomere DNA repeats in vitro. Plant Physiol. 133, 1336–1350.
[16] Schrumpfova, P., Kuchar, M., Mikova, G., Skrisovska, L., Kubicarova, T. and Fajkus, J. (2004) Characterization of two *Arabidopsis thaliana* myb-like proteins showing affinity to telomeric DNA sequence. Genome 47, 316–324.
[17] James, P., Halladay, J. and Craig, E.A. (1996) Genomic libraries and a host strain designed for highly efficient two-hybrid selection in yeast. Genetics 144, 1425–1436.
[18] Lupas, A., Van Dyke, M. and Stock, J. (1991) Predicting coiled coils from protein sequences. Science 252, 1162–1164.
[19] Ramakrishnan, V. (1997) Histone structure and the organization of the nucleosome. Annu. Rev. Biophys. Biomol. Struct. 26, 83–112.
[20] Maman, J.D., Yager, T.D. and Allan, J. (1994) Self-association of the globular domain of histone H5. Biochemistry 33, 1300–1310.
[21] Liu, D., Safari, A., O'Connor, M.S., Chan, D.W., Laegeler, A., Qin, J. and Songyang, Z. (2004) PTOP interacts with POT1 and regulates its localization to telomeres. Nat. Cell Biol. 6, 673–680.
[22] Rotkova, G., Sykorova, E. and Fajkus, J. (2008) Protect and regulate: recent findings on plant POT1-like proteins. Biol. Plantarum. 52.
[23] Mozgova, I, Prochazkova Schrumpfova, P., Hofr, C. and Fajkus, J. (2008) Functional characterization of domains in AtTRB1, a putative telomere-binding protein in *Arabidopsis thaliana*. Phytochemistry 69.
[24] Hockemeyer, D., Daniels, J.P., Takai, H. and de Lange, T. (2006) Recent expansion of the telomeric complex in rodents: two distinct POT1 proteins protect mouse telomeres. Cell 126, 63–77.

Supporting Information

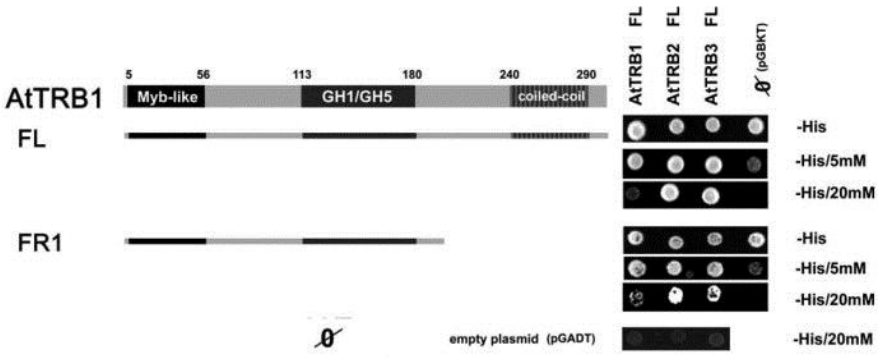

Supplementary Figure S1. AtTRB1 forms preferentially heterodimers with AtTRB2 and 3. Yeast two-hybrid strain MaV203 (with His3-reporter gene under less tightly controlled promoter) was cotransformed with either full-length AtTRB1 or FR1 fragment and with either of AtTRB FL constructs (for further details see Fig. 1). Drop test was performed with -His plates containing 5 mM and/or 20 mM 3-AT. At the 20 mM 3-AT concentration only AtTRB2 and AtTRB3 transformants grew suggesting that heterotypic complexes of AtTRB1 are more stable than homotypic ones.

A. SMH

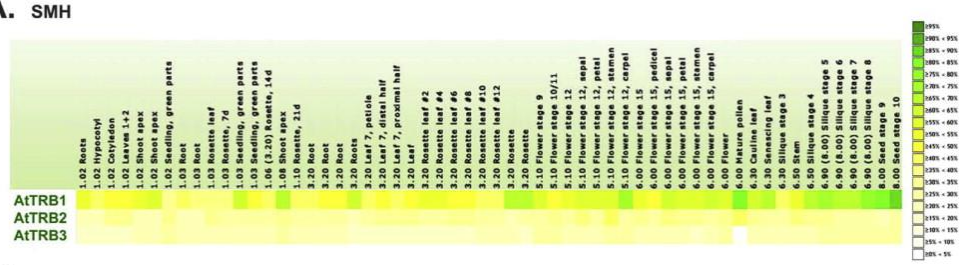

B. AtPOT1b

	Flowers	Stems	Rosette leaves	Cauline leaves	Roots	Callus
AtPOT1b	++	+	+	+	+++	+++

Supplementary Figure S2. Gene expression in various organs of A. thaliana. A. Gene expression of AtTRB1, 2 and 3 proteins (=SMH). Original data from chip expression database AtGenExpress were graphically transformed in Arabidopsis Gene Family Profiler (http://agfp.ueb.cas.cz) and modified for this article. B. Gene expression data for AtPOT1b protein are not available in any of general chip database. A schematic table of AtPOT1b expression is based on RT-PCR data published in [6].

Supplement D

Mozgová, I., **Schrumpfová, P.P.**, Hofr, C., Fajkus, J., **2008**. Functional characterization of domains in AtTRB1, a putative telomere-binding protein in Arabidopsis thaliana. Phytochemistry 69, 1814–1819

P.P.S. participated in the experiments design, evaluation of data and the ms editing

This journal did not provide open access, hence the article is not freely available.

Supplement E

Hofr, C., Sultesová, P., Zimmermann, M., Mozgová, I., **Schrumpfová, P.P.**, Wimmerová, M., Fajkus, J., **2009**. Single-Myb-histone proteins from Arabidopsis thaliana: a quantitative study of telomere-binding specificity and kinetics. Biochem. J. 419, 221–228

P.P.S. was involved in the experimental part (protein cloning, expression and purification)

BJ www.biochemj.org

BJ Plant

Biochem. J. (2009) **419**, 221–228 (Printed in Great Britain) doi:10.1042/BJ20082195

online data

Single-Myb-histone proteins from *Arabidopsis thaliana*: a quantitative study of telomere-binding specificity and kinetics

Ctirad HOFR*[1], Pavla ŠULTESOVÁ*, Michal ZIMMERMANN*, Iva MOZGOVÁ*, Petra PROCHÁZKOVÁ SCHRUMPFOVÁ*, Michaela WIMMEROVÁ† and Jiří FAJKUS*‡[1]

*Department of Functional Genomics and Proteomics, Institute of Experimental Biology, Faculty of Science, Masaryk University, CZ-62500 Brno, Czech Republic, †National Centre for Biomolecular Research and Department of Biochemistry, Faculty of Science, Masaryk University, CZ-61137 Brno, Czech Republic, and ‡Laboratory of DNA–Molecular Complexes, Institute of Biophysics, Czech Academy of Sciences, CZ-61265 Brno, Czech Republic

Proteins that bind telomeric DNA modulate the structure of chromosome ends and control telomere function and maintenance. It has been shown that AtTRB (*Arabidopsis thaliana* telomere-repeat-binding factor) proteins from the SMH (single-Myb-histone) family selectively bind double-stranded telomeric DNA and interact with the telomeric protein AtPOT1b (*A. thaliana* protection of telomeres 1b), which is involved in telomere capping. In the present study, we performed the first quantitative DNA-binding study of this plant-specific family of proteins. Interactions of full-length proteins AtTRB1 and AtTRB3 with telomeric DNA were analysed by electrophoretic mobility-shift assay, fluorescence anisotropy and surface plasmon resonance to reveal their binding stoichiometry and kinetics. Kinetic analyses at different salt conditions enabled us to estimate the electrostatic component of binding and explain different affinities of the two proteins to telomeric DNA. On the basis of available data, a putative model explaining the binding stoichiometry and the protein arrangement on telomeric DNA is presented.

Key words: *Arabidopsis thaliana*, fluorescence anisotropy, kinetics, single-Myb-histone protein (SMH protein), surface plasmon resonance, telomere protein–DNA interaction.

INTRODUCTION

Telomeres are nucleoprotein complexes consisting of repetitive DNA sequences, general chromatin proteins and telomere-specific proteins. Tandem repeats of telomeric DNA are short T- and G-rich sequences, such as d(GGGTTA) in humans and d(GGGTTTA) in the majority of plants.

Telomeres form protective capping structures at the ends of chromosomes [1]. These structures are essential for cell viability as they prevent chromosomes from unwanted end-to-end joining and recognition of chromosome tips as unrepaired double-strand breaks by the repair system of the cell. Changes in telomere structure and function induce chromosomal abnormalities and are directly connected with human aging and cancer [2].

Telomeres are usually maintained by telomerase, a ribonucleoprotein enzyme that adds telomeric repeats to the 3′-overhang of the G-rich DNA strand. The action of telomerase is regulated by its expression and by numerous proteins that control telomerase access to telomeres and organize telomeres into specific capping structures, such as telomeric loops that were observed in a number of organisms, including humans and plants [3,4].

Three DNA-binding proteins have been found to be responsible for specific recognition and direct interactions with the telomeric repeat sequence in humans. Two of them, TRF1 and TRF2 (where TRF is telomeric repeat-binding factor), described as negative regulators of telomere length [5], show substantial structural similarity and bind double-stranded telomeric DNA. The third protein, POT1 (protection of telomeres 1), binds the G-rich strand of telomeric DNA, participates in chromosome capping and is able to control telomere extension by telomerase, both positively and negatively [6,7]. The human TRFs and their homologues in other organisms possess a well conserved DNA-binding structural motif similar to the c-Myb-family of transcriptional activators [8]. The Myb domain of TRFs is C-terminally positioned and consists of three helices connected in a helix–turn–helix manner. The third helix contains a conserved amino acid sequence called a 'telobox', which has been shown to be important for recognition of telomeric double-stranded DNA [8].

Numerous TRF-like proteins have been identified in plants (reviewed in [9]), and, in a few cases, the influence of these proteins on telomere length homoeostasis has been demonstrated [10,11]. Interestingly, besides the TRF-like proteins, a plant-specific family of other telobox proteins has been described [12]. This group of proteins, termed the SMH (single-Myb-histone) family, is characterized by a triple-domain structure consisting of an N-terminal Myb domain, central globular histone H1/5 domain, and a C-terminal coiled-coil domain. In *Arabidopsis thaliana* (At), five SMH proteins were identified (AtTRB1–AtTRB5, where TRB is telomere-repeat-binding factor) [12], and three of them have been characterized [13,14]. These proteins show not only specific interactions with telomeric DNA, but also a number of protein–protein interactions functionally related to telomeres. In addition to their ability to form homodimers (similarly to TRFs), they can also form heterodimers and both homo- and heterotypic multimers [13–15] via their H1/5 histone domain. They also interact (using the same H1/5 domain) with one of the POT1 proteins in *A. thaliana*, AtPOT1b [15,16], which participates in telomere capping [17].

The emerging complexity of interactions of AtTRBs urges more detailed and quantitative studies of their DNA–protein and protein–protein interactions to reveal principles of their regulatory role. So far, only structural data for the Myb DNA-binding

Abbreviations used: At, *Arabidopsis thaliana*; EMSA, electrophoretic mobility-shift assay; FA, fluorescence anisotropy; LB, Luria–Bertani; POT1, protection of telomeres 1; RedX, Rhodamine Red-X; RT, reverse transcription; SMH, single-Myb-histone; SPR, surface plasmon resonance; TRB, telomere-repeat-binding factor; TRF, telomeric repeat-binding factor.

[1] Correspondence may be addressed to either of these authors (email hofr@sci.muni.cz or fajkus@sci.muni.cz).

domain are available [18]. Similarly, kinetic studies are limited to the interaction of a Myb-domain-bearing fragment with a short telomeric DNA oligonucleotide (13 bp) [18], and a non-equilibrium technique was used to describe binding kinetics of TRFs in rice [19]. In order to describe binding interactions more thoroughly, associations of the full-length proteins with telomeric DNA need to be evaluated.

The equilibrium binding kinetics of the full-length proteins can be studied by quantitative biophysical approaches. The binding of proteins to fluorescently labelled DNA may be monitored by FA (fluorescence anisotropy). This method gives well-resolved binding isotherms at different buffer conditions and therefore reliable kinetic and energetic parameters of binding. If the solution contains only free DNA molecules, FA is relatively low, owing to the fast rotational rearrangement of DNA molecules. After the binding of protein to DNA, a bulky slower-rotating protein–DNA complex is formed and the anisotropy is increased. Thus the anisotropy change of fluorescently labelled DNA duplexes, after each addition of protein into solution, describes the extent of protein–DNA binding [20,21].

In the present paper, we report a detailed study to reveal stoichiometry and kinetics of AtTRB1 and AtTRB3 binding to telomeric DNA. Proteins AtTRB1 and AtTRB3 have been chosen for these functional assays because they showed the highest structural stability within the AtTRB family of proteins. Interactions of full-length proteins with telomeric DNA are analysed by a combination of EMSA (electrophoretic mobility-shift assay) and quantitative biophysical methods employing FA and SPR (surface plasmon resonance). Kinetic analyses at different salt conditions enable us to estimate the electrostatic component of binding and explain different affinities of the two AtTRBs to telomeric and non-telomeric DNA. The kinetic measurements also contribute to the estimation of the length of double-stranded DNA for proper protein binding. On the basis of these data, a speculative model for binding stoichiometry and protein arrangement on telomeric DNA is presented.

EXPERIMENTAL

Cloning, expression and purification of AtTRB1 and AtTRB3

The cDNA sequence of AtTRB1 (locus At1g49950) was obtained by RT (reverse transcription)–PCR from total RNA as described previously [16]. AtTRB1 has been cloned into pET15b vector (Novagen) and expressed as a His-tagged fusion protein in *Escherichia coli* C41(DE3) cells [14]. The cells were grown on LB (Luria–Bertani) medium with ampicillin (100 μg/ml) at 37 °C overnight. The next day, cells were diluted 20-fold into ZYM 5052 complex autoinducing medium containing ampicilin [22]. The cells were incubated at 37 °C for 5 h. Then the temperature was set to 20 °C, and the incubation continued overnight.

The cDNA sequence of AtTRB3 (locus At3g49850) was obtained by RT–PCR from total RNA as described previously [13]. AtTRB3 has been cloned into pET30a(+) vector (Novagen) and expressed as a His-tagged fusion protein in *E. coli* BL21(DE3)pLysS cells. The cells were grown on LB medium with kanamycin (50 μg/ml) at 37 °C for 4 h. At a D_{600} of 0.6, the overexpression of AtTRB3 was induced by the addition of IPTG (isopropyl β-D-thiogalactoside) to a concentration of 1 mM. After lowering the incubation temperature to 25 °C, the growth continued for an additional 3 h.

The following extraction and purification steps were the same for both recombinant proteins. After harvesting by centrifugation at 8000 ***g*** for 8 min, the pellet was dissolved in buffer containing 50 mM sodium phosphate (pH 8.0) with 300 mM NaCl and 10 mM imidazole and was sonicated for 5 min. The sonicated cell extract was cleared by centrifugation at 14 000 rev./min for 1 h at 4 °C using a Beckman JA 14 rotor and subsequent filtration (0.45 μm filter). Affinity purification was performed on a column filled with a TALON® metal-affinity resin (BD Biosciences). Protein was eluted at 80 mM imidazole. The eluent was loaded on to a heparin HiTrap™ column (GE Healthcare). A concentration gradient of NaCl from 0.4 to 1 M NaCl was used for protein elution. The fractions containing pure protein were concentrated, and buffer-exchanged usually into 50 mM sodium phosphate (pH 7.5) with 100 mM NaCl by ultrafitration (Amicon 10K, Millipore) or by extensive dialysis. A typical yield was 1 mg of purified protein per litre of bacterial culture. The concentration of purified protein was determined using the Bradford assay [23].

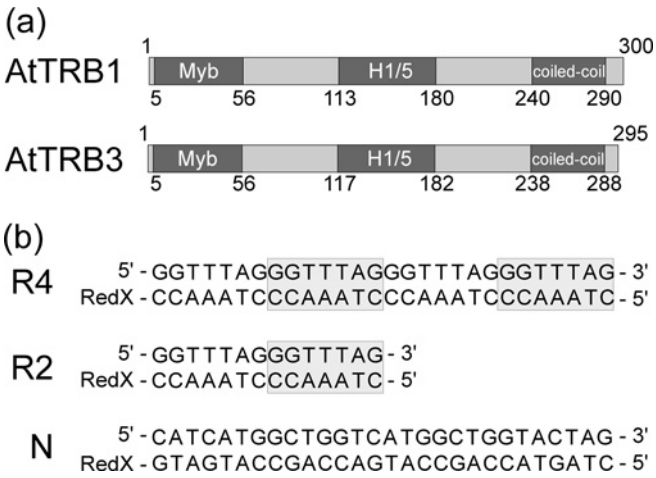

Figure 1 Proteins and oligonucleotide duplexes used for binding studies

(**a**) Organization of the AtTRB1 and AtTRB3 polypeptide chains. The localization of the Myb domain, histone-like H1/5 domain and coiled-coil domain is shown together with numbers denoting their positions in the sequence. (**b**) Base sequence of telomeric oligonucleotide duplex R4 and R2 along with non-telomeric duplex N. RedX denotes fluorescent label Rhodamine RedX. The nucleotides of putative Myb-domain-binding sites are shaded grey [18].

DNA substrates

Oligodeoxynucleotides were synthesized and HPLC-purified by Core Laboratory at Masaryk University. One of the strands in the duplexes was synthesized with the 3′-end C_6 aminoalkyl linker and labelled with RedX (Rhodamine Red-X) (Molecular Probes) using the protocol provided by the manufacturer. The duplexes comprising four and two telomeric repeats were denoted as R4 and R2 respectively. The DNA duplex with non-telomeric sequence was denoted as N. The molar absorption coefficients of the single strands were estimated with the employment of phosphate assay [24]. Molar absorption coefficients were 281 000 (RedX-labelled strand in R4), 278 000 (complementary strand in R4), 148 000 (RedX-labelled strand in R2), 140 000 (complementary strand in R2), 284 000 (RedX-labelled strand in N) and 265 000 $M^{-1} \cdot cm^{-1}$ (complementary strand in R2) for DNA oligonucleotides shown in Figure 1.

EMSA

Protein–DNA-binding reactions were performed in 10 μl volumes containing the same amount of labelled DNA duplex (30 pmol) and various concentrations of protein (0–180 pmol) in 50 mM sodium phosphate (pH 7.0) with 200 mM NaCl.

Reaction mixtures were incubated for 10 min at 25 °C. Protein–DNA complexes were resolved on horizontal 7.5 % (w/v) acrylamide/0.3 % bisacrylamide gels, as described in [25]. The electrophoresis proceeded at 1.5 V/cm for 30 min and for an additional 90 min at 3 V/cm. Gels were analysed with a LAS 3000 imaging system (Fujifilm). After the fluorescence imaging, Coomassie Blue staining of the gel was performed to reveal protein-containing bands in the gel.

Fluorescence anisotropy

Florescence anisotropy was measured on a FluoroMax-4 spectrofluorimeter (Horiba) with an L-format set up under control of an Origin-based FluorEssence software (version 2.1.6). Excitation and emission wavelengths were 572 and 591 nm respectively, with the same excitation and emission bandpath, 8 nm. The integration time was 3s. For each anisotropy value, five measurements were averaged. The titration experiments were carried out in a 10 mm × 4 mm quartz-glass cuvette with a magnetic bar stirrer. All measurements were conducted at 25 °C in 50 mM sodium phosphate buffer (pH 7.5) containing 100 mM NaCl if not stated otherwise. To 1500 μl of DNA solution (20 nM) in the buffer, protein solution was added stepwise. The decrease in DNA concentration during the titration was taken into account in the analysis of the data. A control titration of protein to RedX solution (without DNA) has been performed to confirm that there was no interaction between RedX and protein.

Dissociation constants of protein binding were evaluated by fitting of dilution-corrected binding isotherms using programs SigmaPlot 8 (Systat Software) and DynaFit3 (version 3.28) [26]. Analysis of the binding of protein to DNA duplexes was performed with the assumption of a non-co-operative binding mode. The association constants were calculated as reciprocal values of dissociation constants ($K_a = 1/K_d$). The association constants provided the free energies of association.

Electrostatic component of binding

In order to determine the contribution of electrostatic interactions upon binding of DNA with protein, the equilibrium binding constant was measured at different concentrations of NaCl (see Figure 4 and Table 2). The electrostatic component of binding originates from the formation of ion pairs between the cationic amino acid residues of the protein and the negatively charged DNA. The number of ion pairs formed upon protein–DNA binding and corresponding electrostatic contribution to overall binding affinity (K_a) could be derived from the dependence of the binding constant on salt concentration according to the eqn (1):

$$\log K_a = \log K_a^{nel} - Z\varphi \cdot \log [NaCl] \quad (1)$$

where Z is the number of DNA phosphates that interact with the protein, φ is the number of Na^+ cations per phosphate released upon protein binding. For B–DNA duplexes of 24 bp and shorter, the value for φ is approx. 0.64 [27]. The right-hand side of the equation divides overall binding affinity into the non-electrostatic part described by K_a^{nel} and a salt-dependent electrostatic part [28,29]. When the linear dependence of $\log K_a$ is extrapolated to the salt concentration of 1 M, the electrostatic term in eqn (1) can be removed: $\log K_a = \log K_a^{nel}$, i.e. the binding affinity is given only by non-electrostatic interactions. Similarly to the binding affinity, the overall binding energy defined as $\Delta G_a = -2.3RT \cdot \log K_a$ could be divided into electrostatic and non-electrostatic terms $\Delta G_a = \Delta G_a^{nel} + \Delta G_a^{el}$. The electrostatic term ΔG_a^{el} disappears when the salt concentration approaches 1 M and the overall energy of binding is given only by the non-electrostatic term, $\Delta G_a = \Delta G_a^{nel} = -2.3RT \cdot \log K_a^{nel}$.

Surface plasmon resonance

Sensorgrams were recorded on a Biacore 3000 instrument (GE Healthcare) using CM5 chips. More details are available in the Supplementary Online Data at http://www.BiochemJ.org/bj/419/bj4190221add.htm.

RESULTS

Stoichiometry of protein–DNA complexes

In order to estimate the binding ratio of AtTRBs and DNA, oligonucleotide substrates containing two or one putative binding sites were designed. The telomeric duplex R4 covers the length of four plant telomeric repeats and comprises two putative Myb-domain-binding sites. The shorter duplex, double-stranded DNA fragment R2, consists of two telomeric repeats and contains one Myb-domain-binding site. For comparative purposes, oligonucleotide duplex N, as a representative of non-telomeric DNA, was used in the present study (Figure 1).

Both AtTRB1 and AtTRB3 bind telomeric DNA with the stoichiometry of one protein monomer per one telomeric repeat

The binding stoichiometry was analysed by EMSA with samples containing a variable protein/DNA ratio. Figure 2 shows fluorescently visualized bands indicating the mobility of free and protein-bound DNA duplexes in non-denaturating acrylamide gels.

Increasing the concentration of protein shifted the free labelled DNA duplex to a new position corresponding to a protein–DNA complex. The band corresponding to the free duplex R4 disappeared when the AtTRB1/R4 ratio was 4:1 (Figure 2a). Similarly, the complete binding of AtTRB3 to substrate R4 was observed at the same protein/DNA ratio (Figure 2b). Both AtTRB1 and AtTRB3 bind telomeric DNA with the stoichiometry of one protein monomer per one telomeric repeat.

In order to characterize interaction stoichiometry of AtTRBs with telomeric DNA further, proteins were allowed to interact with the shorter substrate R2 bearing two telomeric repetitions (Figure 2c). The results of EMSA with R2 demonstrate that a 2-fold decrease in the length of DNA reduces the protein/DNA binding ratio proportionally. These results confirmed that the stoichiometry of binding is one monomer of AtTRB1 or AtTRB3 per one telomeric repeat. If we consider binding of protein in dimeric form, as was shown in our recent study [14], then two protein dimers bind one R4 substrate (four telomeric repeats) or, in other words, one dimer of AtTRB binds the fragment R2 (two telomeric repeats). On the basis of these data, we could rephrase our initial statement regarding stoichiometry to the following form: one dimer of AtTRB binds the region of two telomeric repeats.

AtTRB1 shows the same binding stoichiometry for telomeric and non-telomeric DNA sequences, whereas AtTRB3 exhibits different binding capacities for telomeric and non-telomeric DNA sequences

The effect of DNA sequence on binding ability of AtTRB1 and AtTRB3 was analysed by comparing the protein/DNA ratio needed for complete saturation of telomeric R4 and non-telomeric N substrate. In this respect, AtTRB1 behaves similarly in both cases; the binding stoichiometry of AtTRB1 remained the same, as demonstrated in Figure 2(a).

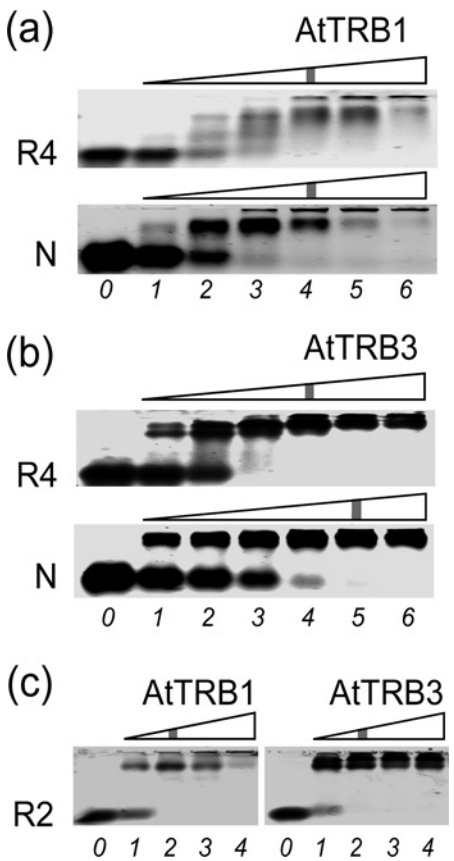

Figure 2 Non-denaturing EMSA

(**a**) AtTRB1 binding to fluorescently labelled oligonucleotide R4 with telomeric sequence and oligonucleotide N with non-telomeric sequence. (**b**) AtTRB3 binding to DNA oligonucleotides R4 and N. (**c**) AtTRB1 or AtTRB3 binding to oligonucleotide R2 with the sequence of two telomeric repetitions. The DNA oligonucleotides and AtTRBs were incubated with increasing amounts of protein. The numbers under electrophoretic lanes denote the stoichiometric protein/DNA ratio. The protein/DNA ratio corresponding to binding saturation is indicated with a grey line.

In contrast, AtTRB3 exhibits a markedly stronger dependence of the binding ability on DNA sequence that was manifested by a shift in ratio needed for saturation of the non-telomeric substrate N. The protein/DNA ratio was shifted to the higher values ($> 5:1$) in the case of duplex N than was the ratio for the telomeric duplex R4 (Figure 2b).

The difference in DNA-sequence-dependent saturation might be a result of different binding kinetics of AtTRB1 and AtTRB3. To assess this possibility, direct kinetic measurements were performed using FA.

Binding kinetics

The binding affinity of AtTRB variants to double-stranded DNA was analysed further by FA measurements. In these measurements, protein aliquots were added to the solution of labelled DNA duplex, and an increase of FA was observed. The equilibrium dissociation constants (K_d) obtained by analyses of anisotropy curves for binding are listed in Table 1.

AtTRB1 and AtTRB3 bind telomeric DNA with high affinity and specificity

The binding affinity of AtTRB1 to telomeric DNA is significantly higher in comparison with the binding to non-telomeric DNA. The titration curves obtained for AtTRB1 binding to DNA substrates

Table 1 Dissociation and association constants for binding of AtTRB1 and AtTRB3 to DNA

Values are means ± S.E.M. for three independent experiments in 50 mM sodium phosphate (pH 7.5) and 100 mM NaCl measured at 25 °C.

	R4		N		R2	
Protein	K_d (nM)	K_a (10^{-6} M^{-1})	K_d (nM)	K_a (10^{-6} M^{-1})	K_d (nM)	K_a (10^{-6} M^{-1})
AtTRB1	90 ± 20	11.0	1200 ± 300	0.83	210 ± 30	4.8
AtTRB3	400 ± 60	2.5	2900 ± 300	0.35	800 ± 100	1.3

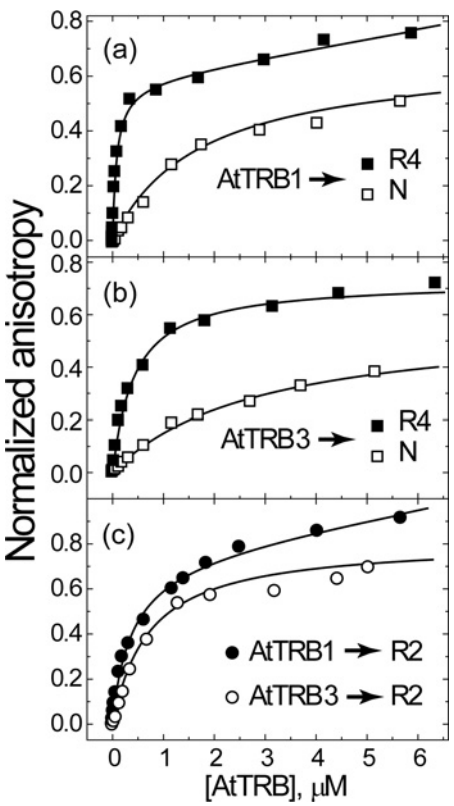

Figure 3 Binding of AtTRB1 and AtTRB3 to DNA duplexes

(**a**) FA measurements of binding of AtTRB1 to telomeric duplex R4 or non-telomeric duplex N. The binding at 20 nM DNA occurred in buffer containing 50 mM sodium phosphate (pH 7.5) and 100 mM NaCl. (**b**) FA measurements of binding of AtTRB3 to R4 or N duplex. Binding conditions were the same as in (**a**). (**c**) Binding isotherms of AtTRB1 and AtTRB3 with telomeric duplex R2 measured by FA. Binding conditions were the same as in (**a**).

R4 and N are shown in Figure 3(a). As expected, AtTRB1 shows significantly higher binding affinity to telomeric R4 than to the non-telomeric N DNA substrate. This can be clearly seen from the steeper rise of the curve corresponding to binding telomeric DNA. The evaluation of binding curves revealed K_d values of 90 and 1200 nM for R4 and N substrate respectively (Table 1). Comparison of dissociation constants thus demonstrates more than 13-fold higher affinity and binding specificity of AtTRB1 to DNA bearing telomeric sequences.

The binding affinity of AtTRB3 to telomeric sequence is higher in comparison with the binding to non-telomeric sequence, but the difference is less pronounced than in case of AtTRB1. AtTRB3 was allowed to bind either the telomeric substrate R4 or the non-telomeric duplex N (Figure 3b). The K_d values for the binding of AtTRB3 to R4 and N were 400 and 2900 nM respectively.

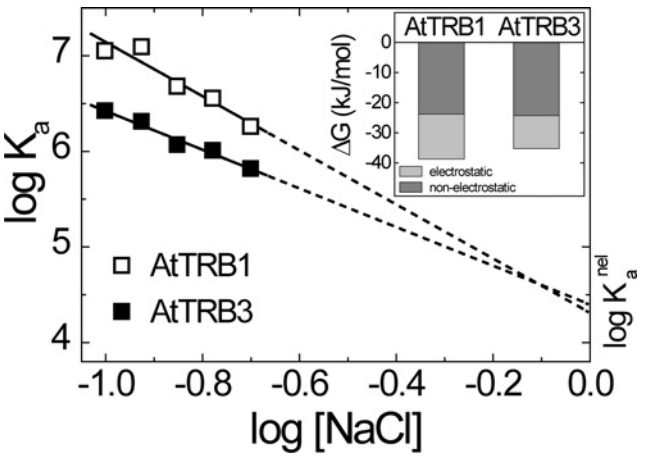

Figure 4 Dependence of the association constants for binding of AtTRB1 and AtTRB3 to substrate R4 on NaCl concentration

The inset shows the electrostatic and non-electrostatic components of the free energy of association of AtTRB1 or AtTRB3 with substrate R4.

AtTRB3 shows more than 7-fold higher affinity to telomeric DNA duplex than to non-telomeric DNA.

The absolute value of the dissociation constant was verified by SPR

In order to confirm the absolute values of binding constants obtained using FA, a reverse-order experiment was performed using SPR. In this experiment, AtTRB3 was immobilized on the chip surface, and duplex R4 was allowed to bind. The reverse arrangement of the SPR experiment changes interaction stoichiometry (one DNA duplex interacts with one immobilized protein, whereas four protein monomers bind one DNA duplex during FA measurements). This had been considered when the equilibrium binding constant was evaluated. The output of the non-linear fitting of SPR curves for different concentrations of DNA produces a K_d of 1700 nM, which agrees with the value determined previously with a factor of 2 at a similar salt concentration (see the Supplementary Online Data).

AtTRB1 and AtTRB3 show reduced binding affinity to R2 when compared with binding affinity to R4

When the length of DNA duplex is shortened from four to two telomeric repeats, the binding affinity decreases to the level of binding affinity recorded for the non-telomeric DNA. Even though there is one putative binding site present on the duplex R2, the binding affinity of AtTRB1 is quite low and is characterized by a K_d similar to that obtained for binding to duplex N. The shortening of telomeric DNA substrate has a similar effect on binding affinity of AtTRB3 (Table 1). The length reduction of telomeric DNA substrate thus results in a substantial fall in the binding affinity of both AtTRB1 and AtTRB3.

Electrostatic contribution to binding affinity

The binding of AtTRB1 or AtTRB3 to duplex R4 containing two putative binding sites induces the formation of four or three ion pairs respectively. Binding of both proteins to the substrate R4 was measured at different concentrations of NaCl. The change of binding parameters is set out in the double-log-plot of the association constants against salt concentration (Figure 4 and Table 2). From the slope, the parameter Z was calculated. Z denotes the number of newly formed ionic bonds between protein and DNA. This number is 4 (after rounding) for binding of AtTRB1, and 3 for AtTRB3. Thus approx. four ion pairs are formed upon binding of AtTRB1 and approx. three ion pairs upon binding of AtTRB3 to the telomeric DNA.

Table 2 Salt-concentration-dependence of association constants for binding of AtTRB1 and AtTRB3 to R4

Values are means ± S.E.M.

Protein	[NaCl] (mM)	log K_a	δlog K_a/δlog [NaCl]	log K_a^{nel}	Z
AtTRB1	100	7.04	2.8 ± 0.2	4.31 ± 0.2	4.4
	119	7.08			
	141	6.67			
	167	6.54			
	200	6.25			
AtTRB3	100	6.41	2.0 ± 0.1	4.4 ± 0.1	3.2
	119	6.31			
	141	6.06			
	167	6.00			
	200	5.81			

The binding energy is provided mainly by a non-electrostatic component in the case of both AtTRBs

Further evaluation of the salt-dependent binding constant was performed to obtain the non-electrostatic contribution to the binding affinity. The electrostatic and non-electrostatic components of the binding energy for AtTRB1 or AtTRB3 to R4 are shown in the inset of Figure 4. It is notable that the non-electrostatic components of binding energy ΔG_a^{nel} for the two proteins are identical within error range with magnitudes of 25 kJ · mol^{-1} for both AtTRB1 and AtTRB3. If this value is compared with the values of the overall binding energy 40 kJ · mol^{-1} for AtTRB1 and 37 kJ · mol^{-1} for AtTRB3, it can be concluded that the non-electrostatic interactions contribute to the total energy of binding by approx. 60 % for AtTRB1 and by approx. 70 % for AtTRB3. Hence, it is apparent that the major part of the binding energy originates from the non-electrostatic interactions.

The greater electrostatic component is responsible for a more favourable overall binding energy of AtTRB1 compared with AtTRB3

Further inspection of calculated energetic data allowed us to identify the main reason for different binding affinities between these similar proteins. It is demonstrated that the kinetics of protein–DNA interactions are different because of the electrostatic term of the binding energy (inset in Figure 4). In other words, the difference in the total binding energy for AtTRB1 and AtTRB3 is entirely given by the change in the electrostatic component of binding.

DISCUSSION

Kinetics and stoichiometry of binding

The present study shows that binding of AtTRB1 and AtTRB3 with the telomeric DNA proceeds with the stoichiometry of one protein monomer per one telomeric repeat. A higher protein/DNA ratio was observed only in case of AtTRB3 binding to non-telomeric DNA (Figure 2b). The shift in the ratio can be explained by the observed lower affinity of AtTRB3 for non-telomeric DNA. The decrease in binding affinity with the change from telomeric to non-telomeric sequence was confirmed also by our kinetic measurements (Table 1). All recently characterized AtTRBs form tightly bound homo- and hetero-dimers and multimers [14,15]. Relatively strong mutual interactions of AtTRBs were also

verified independently using SPR (results not shown) and their dimerization ability was demonstrated by gel chromatography (see the Supplementary Online Data). Therefore the feasibility of protein dimerization and stoichiometric data of the present study support the assumption that AtTRBs bind to DNA in dimeric form. In this respect, the AtTRBs behave similarly to human TRF1 and TRF2 [30–32], with the exception that TRFs do not form heterodimers.

Surprisingly, the affinity of AtTRB1 to telomeric substrate R4 is 4-fold higher than that of AtTRB3, although AtTRB1 and AtTRB3 are relatively similar in their primary sequences.

Interestingly, it has been found that K_d values observed in the present study for AtTRB1 and AtTRB3 correspond very well to K_d values obtained for the DNA-binding domain of human TRF1 and TRF2 when interacting with telomeric DNA [33]. Moreover, similarly to AtTRB1 and AtTRB3, human TRF1 binds telomeric DNA with a 4-fold higher affinity than that of TRF2.

In order to explain potential reasons for the different binding manner of AtTRB1 and AtTRB3, we compared our findings with available equilibrium kinetic data for the binding of the Myb domain. The K_d obtained for the binding of the Myb domain alone to telomeric DNA from NMR studies was in the range of 1 μM [18]. If we compare this value measured at physiological salt concentration with the values for the binding of full-length proteins measured in the present study at a corresponding NaCl concentration, the magnitude of K_d for AtTRB3 is slightly lower at 0.9 μM (see Table 1), and the K_d for AtTRB1 is significantly lower (0.2 μM). Both full-length proteins showed higher binding capacities than that reported for a Myb domain alone. Since the Myb domain sequence is highly conserved between AtTRB1 and AtTRB3, the higher binding affinity of AtTRB1 should originate from another part of the protein. The domain that may contribute to the tuning of binding affinity of AtTRBs to DNA is the H1/5 domain [13], as supported by our recent findings [14]. The conservation of the H1/5 domain between AtTRB1 and AtTRB3 is lower than that of the Myb domain and differs in a way that might allow the corresponding protein region to adopt a structure with a different net charge on the surface. The surface net charge is important for a long-range non-specific electrostatic attraction among proteins and DNA, whereas non-electrostatic interactions that are important for specific recognition of a DNA sequence comprise hydrogen bonds between outer groups of DNA and polar residues of the protein [18].

Electrostatic component of binding

Proteins controlling and regulating nucleic acid structure and function usually show both sequence-non-specific binding to DNA and a higher-affinity binding of their specific physiological DNA target. In general, protein–DNA binding takes place in two steps. In the first step, a non-specific, mainly electrostatic, binding to the phosphate backbone occurs; in the second step, the protein explores the DNA surface for specific non-electrostatic interactions such as hydrogen bonds [34].

Different contributions of electrostatic and non-electrostatic interactions to binding were observed for different classes of DNA-binding proteins. For example, telomere-binding protein α from *Oxytricha nova* induces the formation of two ion pairs upon binding to DNA, and the electrostatic contribution to the free energy of binding is approx. 15 % [25]. On the other hand, proteins containing a strongly positively charged scissor-grip motif for DNA recognition induce the formation of six ion pairs with the electrostatic contribution to the total free energy of binding being 45 % [29].

The different contribution of electrostatic attraction for binding of AtTRB1 and AtTRB3 was observed. We estimated the number of four and three ion pairs upon AtTRB1 or AtTRB3 binding to R4 and the corresponding electrostatic contribution to the total free energy of binding at 40 and 30 % respectively. This correlates well with data available for electrostatic interactions of other DNA-binding proteins. The DNA-binding event of AtTRBs is driven mainly by non-electrostatic interactions. On the whole, our results show that AtTRBs bind telomeric DNA primarily in a sequence-specific manner that is essential for the recognition of binding sites within telomeric DNA.

Kinetic data contribute to understanding of nucleoprotein complex arrangement

Analyses of our kinetic data together with available structural data may be also used to elucidate the arrangement of nucleoprotein complexes of AtTRBs with telomeric DNA.

In general, one might suppose that the same binding preferences to telomeric DNA are given primarily by the occurrence of the recognition sequence in DNA. For this reason, one would also expect the same binding kinetics for the telomeric DNA with one or two putative binding sites under the consideration of a non-co-operative independent binding. As follows from the previous assumptions, the duplex R2, containing one binding site, should have reached the saturation of binding sites faster (K_d would be lower) when compared with that for duplex R4, with two binding sites. However, our data show the opposite. The binding affinity of both examined proteins to duplex R2 is lower (K_d is shifted to higher values) than in the case of binding to R4. Our quantitative kinetics results confirmed a previously reported decrease in binding affinity of AtTRBs with the shortening of telomeric DNA substrate [13]. Moreover, the lower affinity to DNA containing only one putative binding site might be an indication of an insufficient space for the binding of an active protein. Importantly, it has been shown that the minimum length of DNA for Myb domain binding is approx. 13 bp [18]. If AtTRBs interacted with the DNA exclusively through the Myb domain and binding sites were positioned suitably within the sequence, the length of R2 duplex (14 bp) should have been sufficient for proper binding without a change in binding affinity. Since a significant fall in binding affinity was observed, the kinetics data suggest that there is also another domain taking part in the interaction. As a result, the binding affinity of AtTRBs to the 14 bp long and 28 bp long DNA duplex differs substantially. In our recent results, the H1/5 domain promotes interaction with DNA [14]. Presumably, the short length might prevent the H1/5 domain from properly interacting with the DNA. Hence, the constrained binding without H1/5 domain might be the main reason for the reduction of the overall binding affinity to substrate R2.

Although the picture of a molecular mechanism controlling telomerase activity is far from complete, it is important to consider how the protein-binding events measured in the present study relate to structural arrangements and subsequent interactions essential for the biology of telomeres. If we take into account the kinetic data and the dimerization ability of AtTRBs, a speculative protein arrangement on telomeric DNA could be considered (Figure 5).

The model of binding arrangement considers that the protein monomers form a dimer that binds two adjacent binding sites simultaneously. This type of interaction mode is quite common in the sequence-specific binding of proteins that take part in regulatory mechanisms [35]. This model, where two recognition sites on DNA are bound by one protein dimer, might explain well the fall of binding activity when the DNA substrate is

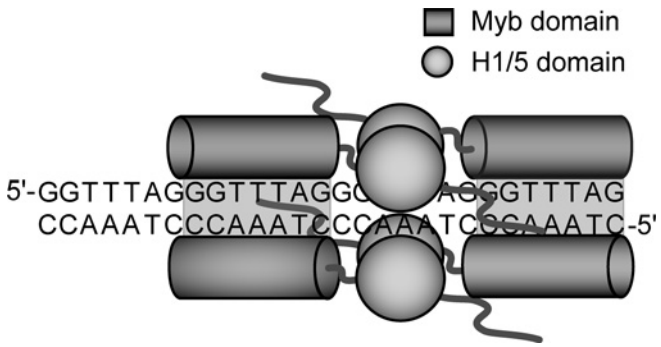

Figure 5 Speculative model of interaction of AtTRBs with telomeric DNA

Both homo- and hetero-dimers of AtTRB may participate in the interaction with telomeric DNA.

shortened from 28 to 14 bp as was observed for binding to the R4 and R2 duplex respectively. The introduced model is supported by stoichiometric and kinetic data presented here and it is also in accordance with our previous study demonstrating weaker binding to DNA containing fewer telomeric repeats [13]. The binding arrangement shown in Figure 5 also takes into consideration the multimerization ability of the H1/5 domain that could promote the arrangement of protein monomers in the DNA region between the binding sites. Moreover, the formation of homo- and hetero-multimers of SMH proteins and their ability to interact with other proteins (e.g. AtPOT1b [15,16]) contribute to a network of protein interactions that could be employed in the organization of telomere to form highly ordered chromatin structures, such as t-loops, in a similar way to human TRFs [31,32].

Thus, on the basis of results of the present study and the data available, we suggest that interactions of the two AtTRBs with telomeric DNA occur simultaneously with two binding sites. Therefore the minimal length of duplex DNA required for the proper binding of full-length AtTRB1 and AtTRB3 should harbour at least two putative binding sites that are bound by two dimers of AtTRBs. Consequently, SMH proteins are able to distinguish between short (< 10 bp) telomere-like sequences that are dispersed throughout the genome, e.g. in promoter regions [36], and longer tracts of telomere repeats occurring in telomeres.

There is still a considerable lack of general knowledge of intracellular arrangement, molecular crowding effects, association mechanisms and kinetics of protein–DNA-binding events in a living cell. Nevertheless, we can draw a speculative view of the *in vivo* consequences of our *in vitro* data, if we consider that the behaviour of a protein would not be markedly changed in the cellular environment. The access of AtTRBs to their telomeric target sites is restricted in both spatial and temporal ways by chromatin structure: the telomeric heterochromatin structure provides low accessibility upon its tight condensation, and thus the binding of specific proteins to DNA may occur preferentially in a short time slot between DNA replication and chromatin condensation [37].

AtTRBs might be first recruited by a weak non-specific binding to multiple chromosome regions. Then, once the specific target sites become accessible, highly specific binding occurs. On the other hand, the AtTRB molecules which are bound only by a highly dynamic non-specific interaction (in non-telomeric regions) can be easily displaced by other proteins binding with a higher affinity. Thus AtTRBs at non-telomeric sites do not impede other functional DNA–protein interactions.

In this way, non-specific binding could serve as a tool for increasing the local concentration of the proteins on DNA [34]. Accumulation of SMH proteins on DNA via non-specific electrostatic interactions may be important for their immediate availability for functional and specific binding to their telomere target sites.

Although further details of the binding interactions of proteins and their biological significance have yet to be determined, these results demonstrate the advantage of the approach employed in the present study by using a complete protein for *in vitro* studies rather than the commonly used Myb-domain-bearing fragment. Our data imply that AtTRB1 and AtTRB3 are telomere-specific proteins that bind telomeric DNA with distinct kinetics given by differences in their electrostatic interactions with DNA. To our knowledge, this is the first quantitative study of the plant-specific SMH family of proteins. The present paper demonstrates that the detailed quantification of protein–DNA interactions may provide new insights into the structural dynamics of telomeres.

ACKNOWLEDGEMENTS

We are grateful to M. Chester for the critical reading of the manuscript.

FUNDING

This work was supported by the Grant Agency of the Czech Republic [grant numbers 521/08/P452 and 204/08/H054], the Czech Ministry of Education [grant number LC06004], the Grant Agency of the Czech Academy of Sciences [grant number IAA500040801] and the institutional support [grant numbers MSM0021622415, MSM0021622413, AV0Z50040702 and AV0Z50040507].

REFERENCES

1 Zakian, V. A. (1995) Telomeres: beginning to understand the end. Science **270**, 1601–1607
2 Smogorzewska, A. and de Lange, T. (2004) Regulation of telomerase by telomeric proteins. Annu. Rev. Biochem. **73**, 177–208
3 Griffith, J. D., Comeau, L., Rosenfield, S., Stansel, R. M., Bianchi, A., Moss, H. and de Lange, T. (1999) Mammalian telomeres end in a large duplex loop. Cell **97**, 503–514
4 Cesare, A. J., Quinney, N., Willcox, S., Subramanian, D. and Griffith, J. D. (2003) Telomere looping in *P. sativum* (common garden pea). Plant J. **36**, 271–279
5 Smogorzewska, A., van Steensel, B., Bianchi, A., Oelmann, S., Schaefer, M. R., Schnapp, G. and de Lange, T. (2000) Control of human telomere length by TRF1 and TRF2. Mol. Cell. Biol. **20**, 1659–1668
6 Baumann, P. and Cech, T. R. (2001) Pot1, the putative telomere end-binding protein in fission yeast and humans. Science **292**, 1171–1175
7 Hockemeyer, D., Sfeir, A. J., Shay, J. W., Wright, W. E. and de Lange, T. (2005) POT1 protects telomeres from a transient DNA damage response and determines how human chromosomes end. EMBO J. **24**, 2667–2678
8 Bilaud, T., Koering, C. E., Binet-Brasselet, E., Ancelin, K., Pollice, A., Gasser, S. M. and Gilson, E. (1996) The telobox, a Myb-related telomeric DNA binding motif found in proteins from yeast, plants and human. Nucleic Acids Res. **24**, 1294–1303
9 Kuchar, M. (2006) Plant telomere-binding proteins. Biol. Plant. **50**, 1–7
10 Yang, S. W., Kim, S. K. and Kim, W. T. (2004) Perturbation of NgTRF1 expression induces apoptosis-like cell death in tobacco BY-2 cells and implicates NgTRF1 in the control of telomere length and stability. Plant Cell **16**, 3370–3385
11 Hwang, M. G. and Cho, M. H. (2007) *Arabidopsis thaliana* telomeric DNA-binding protein 1 is required for telomere length homeostasis and its Myb-extension domain stabilizes plant telomeric DNA binding. Nucleic Acids Res. **35**, 1333–1342
12 Marian, C. O., Bordoli, S. J., Goltz, M., Santarella, R. A., Jackson, L. P., Danilevskaya, O., Beckstette, M., Meeley, R. and Bass, H. W. (2003) The maize single myb histone 1 gene, *Smh1*, belongs to a novel gene family and encodes a protein that binds telomere DNA repeats *in vitro*. Plant Physiol. **133**, 1336–1350
13 Schrumpfova, P., Kuchar, M., Mikova, G., Skrisovska, L., Kubicarova, T. and Fajkus, J. (2004) Characterization of two *Arabidopsis thaliana* myb-like proteins showing affinity to telomeric DNA sequence. Genome **47**, 316–324
14 Mozgova, I., Prochazkova Schrumpfova, P., Hofr, C. and Fajkus, J. (2008) Functional characterisation of domains in AtTRB1, a putative telomere-binding protein in *Arabidopsis thaliana*. Phytochemistry **69**, 1814–1819

15 Prochazkova Schrumpfova, P., Kuchar, M., Palecek, J. and Fajkus, J. (2008) Mapping of interaction domains of putative telomere-binding proteins AtTRB1 and AtPOT1b from *Arabidopsis thaliana*. FEBS Lett. **582**, 1400–1406
16 Kuchar, M. and Fajkus, J. (2004) Interactions of putative telomere-binding proteins in *Arabidopsis thaliana*: identification of functional TRF2 homolog in plants. FEBS Lett. **578**, 311–315
17 Shakirov, E. V., Surovtseva, Y. V., Osbun, N. and Shippen, D. E. (2005) The *Arabidopsis* Pot1 and Pot2 proteins function in telomere length homeostasis and chromosome end protection. Mol. Cell. Biol. **25**, 7725–7733
18 Sue, S. C., Hsiao, H. H., Chung, B. C., Cheng, Y. H., Hsueh, K. L., Chen, C. M., Ho, C. H. and Huang, T. H. (2006) Solution structure of the *Arabidopsis thaliana* telomeric repeat-binding protein DNA binding domain: a new fold with an additional C-terminal helix. J. Mol. Biol. **356**, 72–85
19 Byun, M. Y., Hong, J. P. and Kim, W. T. (2008) Identification and characterization of three telomere repeat-binding factors in rice. Biochem. Biophys. Res. Commun. **372**, 85–90
20 Heyduk, T. and Lee, J. C. (1990) Application of fluorescence energy transfer and polarization to monitor *Escherichia coli* cAMP receptor protein and *lac* promoter interaction. Proc. Natl. Acad. Sci. U.S.A. **87**, 1744–1748
21 LeTilly, V. and Royer, C. A. (1993) Fluorescence anisotropy assays implicate protein-protein interactions in regulating trp repressor DNA binding. Biochemistry **32**, 7753–7758
22 Studier, F. W. (2005) Protein production by auto-induction in high density shaking cultures. Protein Expression Purif. **41**, 207–234
23 Bradford, M. M. (1976) A rapid and sensitive method for the quantitation of microgram quantities of protein utilizing the principle of protein-dye binding. Anal. Biochem. **72**, 248–254
24 Murphy, J. H. and Trapane, T. L. (1996) Concentration and extinction coefficient determination for oligonucleotides and analogs using a general phosphate analysis. Anal. Biochem. **240**, 273–282
25 Buczek, P. and Horvath, M. P. (2006) Thermodynamic characterization of binding *Oxytricha nova* single strand telomere DNA with the α protein N-terminal domain. J. Mol. Biol. **359**, 1217–1234
26 Kuzmic, P. (1996) Program DYNAFIT for the analysis of enzyme kinetic data: application to HIV proteinase. Anal. Biochem. **237**, 260–273
27 Olmsted, M. C., Bond, J. P., Anderson, C. F. and Record, Jr, M. T. (1995) Grand canonical Monte Carlo molecular and thermodynamic predictions of ion effects on binding of an oligocation (L8+) to the center of DNA oligomers. Biophys. J. **68**, 634–647
28 Record, Jr, M. T., Zhang, W. and Anderson, C. F. (1998) Analysis of effects of salts and uncharged solutes on protein and nucleic acid equilibria and processes: a practical guide to recognizing and interpreting polyelectrolyte effects, Hofmeister effects, and osmotic effects of salts. Adv. Protein Chem. **51**, 281–353
29 Dragan, A. I., Liu, Y., Makeyeva, E. N. and Privalov, P. L. (2004) DNA-binding domain of GCN4 induces bending of both the ATF/CREB and AP-1 binding sites of DNA. Nucleic Acids Res. **32**, 5192–5197
30 Bianchi, A., Smith, S., Chong, L., Elias, P. and de Lange, T. (1997) TRF1 is a dimer and bends telomeric DNA. EMBO J. **16**, 1785–1794
31 Fairall, L., Chapman, L., Moss, H., de Lange, T. and Rhodes, D. (2001) Structure of the TRFH dimerization domain of the human telomeric proteins TRF1 and TRF2. Mol. Cell **8**, 351–361
32 Khan, S. J., Yanez, G., Seldeen, K., Wang, H., Lindsay, S. M. and Fletcher, T. M. (2007) Interactions of TRF2 with model telomeric ends. Biochem. Biophys. Res. Commun. **363**, 44–50
33 Hanaoka, S., Nagadoi, A. and Nishimura, Y. (2005) Comparison between TRF2 and TRF1 of their telomeric DNA-bound structures and DNA-binding activities. Protein Sci. **14**, 119–130
34 Revzin, A. (1990) The Biology of Nonspecific DNA–Protein Interactions, CRC Press, Boca Raton
35 von Hippel, P. H. (2007) From "simple" DNA–protein interactions to the macromolecular machines of gene expression. Annu. Rev. Biophys. Biomol. Struct. **36**, 79–105
36 Regad, F., Lebas, M. and Lescure, B. (1994) Interstitial telomeric repeats within the *Arabidopsis thaliana* genome. J. Mol. Biol. **239**, 163–169
37 Fajkus, J. and Trifonov, E. N. (2001) Columnar packing of telomeric nucleosomes. Biochem. Biophys. Res. Commun. **280**, 961–963

Received 7 November 2008/18 December 2008; accepted 22 December 2008
Published as BJ Immediate Publication 22 December 2008, doi:10.1042/BJ20082195

Biochem. J. (2009) **419**, 221–228 (Printed in Great Britain) doi:10.1042/BJ20082195

online data

SUPPLEMENTARY ONLINE DATA

Single-Myb-histone proteins from *Arabidopsis thaliana*: a quantitative study of telomere-binding specificity and kinetics

Ctirad HOFR*[1], Pavla ŠULTESOVÁ*, Michal ZIMMERMANN*, Iva MOZGOVÁ*, Petra PROCHÁZKOVÁ SCHRUMPFOVÁ*, Michaela WIMMEROVÁ† and Jiří FAJKUS*‡[1]

*Department of Functional Genomics and Proteomics, Institute of Experimental Biology, Faculty of Science, Masaryk University, CZ-62500 Brno, Czech Republic, †National Centre for Biomolecular Research and Department of Biochemistry, Faculty of Science, Masaryk University, CZ-61137 Brno, Czech Republic, and ‡Laboratory of DNA–Molecular Complexes, Institute of Biophysics, Czech Academy of Sciences, CZ-61265 Brno, Czech Republic

EXPERIMENTAL

Gel-filtration chromatography

The molecular masses of the protein in monomeric and dimeric forms were estimated by size-exclusion gel-filtration chromatography through a Superdex 200 10/30 GL column (GE Healthcare), using a gel-filtration standard (Bio-Rad Laboratories) in a buffer containing 50 mM sodium phosphate (pH 7.5) and 300 mM NaCl. The molecular masses of proteins were estimated from a linear fit to the log M_r against elution volume plot generated with the protein standards. Supplementary Figure S1 shows the chromatograms.

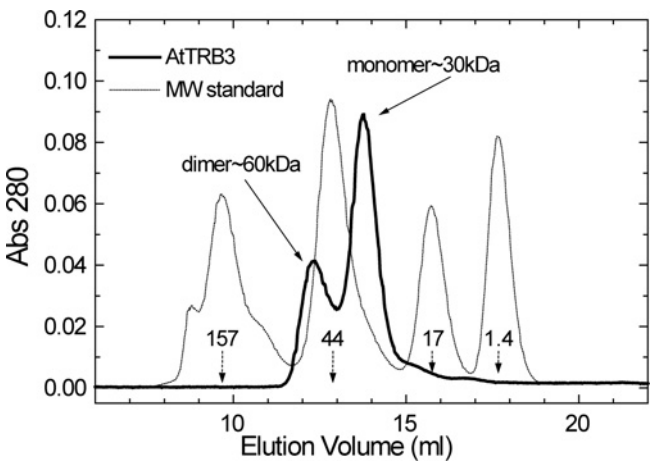

Figure S1 Size-exclusion chromatograms of protein AtTRB3 (continuous line) and molecular-mass standard (broken line)

Abs, absorbance; MW standard, molecular-mass standard. The numbers next to the arrows indicate determined molecular-mass values of monomeric and dimeric protein forms.

Surface plasmon resonance

All SPR experiments were performed with a Biacore 3000 instrument (GE Healthcare) at 25 °C using TBST (Tris-buffered saline with Tween 20: 10 mM Tris/HCl, pH 7.5, 150 mM NaCl, containing 0.005 % Tween 20) and a flow rate of 5 μl/min. AtTRB3 was immobilized on the research-grade CM5 sensor chip in a buffer containing 10 mM Hepes, 150 mM NaCl (pH 7.5) and 0.005 % Tween 20. Sensorgrams were run in the automatic subtraction mode using FC (flowcell) 1 as an unmodified reference. Data were collected for FC 2, FC 3 and FC 4, which contained various amounts of AtTRB3. Injections of DNA were made using the 'quickinject' injection mode, going from lowest to highest concentration samples, with a 5 min contact time and a 1200 s dissociation phase in all cases. Regeneration was achieved using several (two to five) 1 min pulses of 50 mM NaOH. All sensorgrams were obtained at 25 °C. Data were analysed by equilibrium analysis in addition to the kinetic analysis. The equilibrium response was plotted against the concentration of DNA and fitted to:

$$R = K_a[\mathrm{DNA}]R_{max}(K_a[\mathrm{DNA}] + 1)$$

where R is the equilibrium response at a specific concentration of DNA substrate, R_{max} is the response at saturation of the DNA substrate on the chip, K_a is the equilibrium association constant, which is the reciprocal of the dissociation constant K_d ($K_a = 1/K_d$). When assuming a non-co-operative binding model, the apparent K_d from SPR experiments should be divided by 4 to resemble different binding stoichiometry of FA and SPR experiments. The output of the non-linear fitting of SPR curves for different concentrations of DNA produces a K_d of 6.8 μM, which, divided by 4, gives 1.7 μM. This value agrees well with the value of K_d determined from FA measurements considering different buffer conditions. Supplementary Figure S2 shows the sensorgrams and the response curve.

Purification of AtTRBs

AtTRB1 and AtTRB3 were expressed in soluble forms in cytoplasm of *E. coli*. The purification strategy consisted of two affinity steps. A capture step by IMAC (immobilized metal-ion-affinity chromatography) was followed by a purification step using HAC (heparin-affinity chromatography). To confirm final purity, collected fractions were separated by SDS/PAGE (0.1 % SDS, 10 % acrylamide). Supplementary Figure S3 shows the gel-purified proteins.

[1] Correspondence may be addressed to either of these authors (email hofr@sci.muni.cz or fajkus@sci.muni.cz).

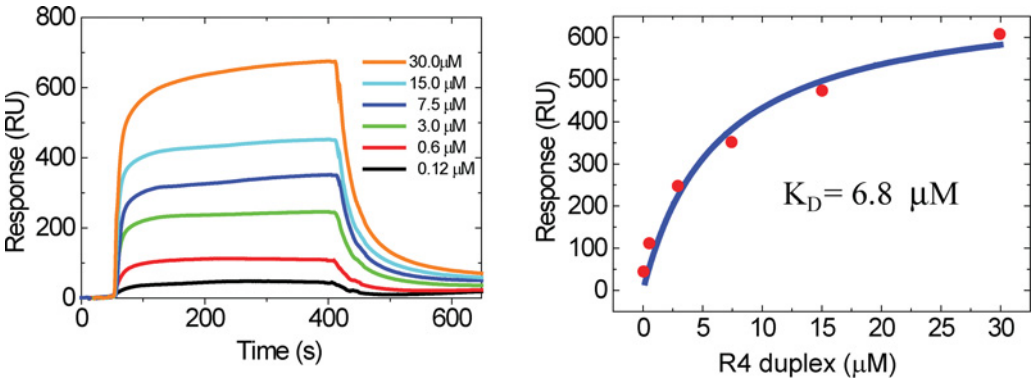

Figure S2 Binding of telomeric duplex R4 to immobilized AtTRB3

Response signals from the saturated region of the sensorgram have been used to calculate equilibrium dissociation constant K_d. RU, response units.

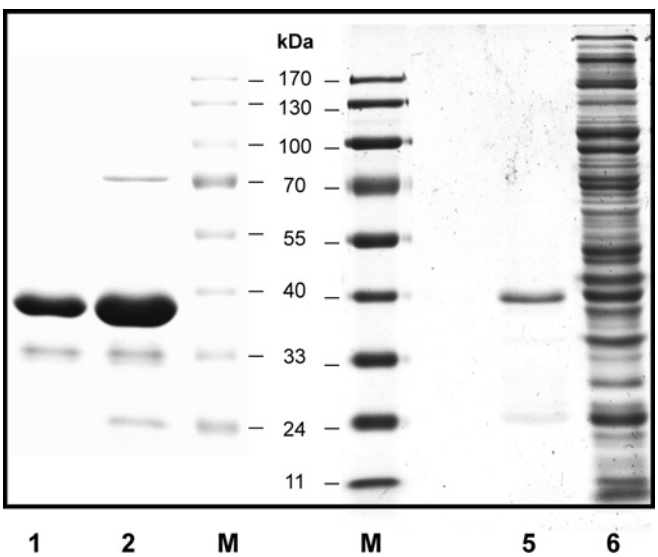

Figure S3 Analysis of purification steps using SDS/PAGE

Lane 1, collected fractions containing AtTRB3 after IMAC (immobilized metal-ion-affinity chromatography) and subsequent HAC (heparin-affinity chromatography) (10 μg); lane 2, collected fractions containing AtTRB3 after IMAC (15 μg); lanes M, molecular-mass markers (sizes are indicated in kDa); lane 5, collected fractions containing AtTRB1 after IMAC and subsequent HAC (3 μg); lane 6, clarified cytoplasmic extract with expressed AtTRB1 (35 μg). The proteins were stained with Coomassie Brilliant Blue.

Received 7 November 2008/18 December 2008; accepted 22 December 2008
Published as BJ Immediate Publication 22 December 2008, doi:10.1042/BJ20082195

Supplement F

Peška, V., **Schrumpfová, P.P.,** Fajkus, J., **2011**. Using the telobox to search for plant telomere binding proteins. Curr. Protein Pept. Sci. 12, 75–83

P.P.S. participated in the ms writing and editing

This journal did not provide open access, hence the article is not freely available.

Supplement G

Schrumpfová, P.P.*, Fojtová, M., Mokroš, P., Grasser, K.D., Fajkus, J., **2011**. Role of HMGB proteins in chromatin dynamics and telomere maintenance in Arabidopsis thaliana. Curr. Protein Pept. Sci. 12, 105–111

P.P.S. was significantly involved in the experimental, data evaluation, and in the ms writing and editing

Supplement H

Schrumpfová, P.P.*, Vychodilová, I., Dvořáčková, M., Majerská, J., Dokládal, L., Schořová, S., Fajkus, J., **2014.** Telomere repeat binding proteins are functional components of Arabidopsis telomeres and interact with telomerase. Plant J. Cell Mol. Biol. 77, 770–781.

P.P.S. participated in the design of experiments, significantly involved in the experimental part, data evaluation, and in the ms writing and editing

the plant journal

SEB Society for Experimental Biology

The Plant Journal (2014) **77,** 770–781 doi: 10.1111/tpj.12428

Telomere repeat binding proteins are functional components of Arabidopsis telomeres and interact with telomerase

Petra Procházková Schrumpfová[1,2,*], Ivona Vychodilová[1,2], Martina Dvořáčková[1,3], Jana Majerská[1,†], Ladislav Dokládal[1,3], Šárka Schořová[1,2] and Jiří Fajkus[1,2,3,*]

[1]*Mendel Centre for Plant Genomics and Proteomics, Central European Institute of Technology, Masaryk University, Kamenice 5, Brno, CZ 62500, Czech Republic,*

[2]*Functional Genomics and Proteomics, CEITEC National Centre for Biomolecular Research, Faculty of Science, Masaryk University, Kamenice 5, Brno, CZ 62500, Czech Republic, and*

[3]*Institute of Biophysics, Academy of Sciences of the Czech Republic, v.v.i, Královopolská 135, Brno, CZ 61265, Czech Republic*

Received 11 October 2013; revised 6 December 2013; accepted 23 December 2013; published online 8 January 2014.

*For correspondence (e-mails fajkus@sci.muni.cz or schpetra@centrum.cz).

[†]Present address: Swiss Institute for Experimental Cancer Research, Ecole Polytechnique Fédérale de Lausanne, Station 19, 1015, Lausanne, Switzerland.

SUMMARY

Although telomere-binding proteins constitute an essential part of telomeres, *in vivo* data indicating the existence of a structure similar to mammalian shelterin complex in plants are limited. Partial characterization of a number of candidate proteins has not identified true components of plant shelterin or elucidated their functional mechanisms. Telomere repeat binding (TRB) proteins from *Arabidopsis thaliana* bind plant telomeric repeats through a Myb domain of the telobox type *in vitro*, and have been shown to interact with POT1b (Protection of telomeres 1). Here we demonstrate co-localization of TRB1 protein with telomeres *in situ* using fluorescence microscopy, as well as *in vivo* interaction using chromatin immunoprecipitation. Classification of the TRB1 protein as a component of plant telomeres is further confirmed by the observation of shortening of telomeres in knockout mutants of the *trb1* gene. Moreover, TRB proteins physically interact with plant telomerase catalytic subunits. These findings integrate TRB proteins into the telomeric interactome of *A. thaliana*.

Keywords: telomerase, telomere, telomere repeat binding (TRB), *Arabidopsis thaliana*, telomere protein interaction, plant shelterin.

INTRODUCTION

Telomeres, nucleoprotein structures that form and protect the ends of chromosomes, have been the subject of intense studies for about three decades, starting with a description of the telomere DNA component (Blackburn and Gall, 1978) and the most common system of telomere maintenance by the ribonucleoprotein complex of telomerase (Greider and Blackburn, 1985, 1989). Proteins essential for telomere functions have been described in detail in yeasts and vertebrates. Among protein components of telomeres, the most important is indisputably telomerase itself, but other proteins are necessary to perform other functions of telomeres, such as inhibiting the DNA damage response at telomeres (de Lange, 2009), recruiting telomerase to chromosome ends (Nandakumar *et al.*, 2012), or facilitating telomere replication (Sfeir *et al.*, 2009). Current evidence suggests that these components assemble into two distinct complexes known as shelterin (de Lange, 2005) and CST (composed of CTC1/STN1/TEN1 proteins) complexes (Surovtseva *et al.*, 2009).

Human shelterin consists of six core components: telomeric repeat-binding factor 1 (TRF1), telomeric repeat-binding factor 2 (TRF2), represor/activator protein 1 (RAP1), TRF1-interacting protein (TIN2), TINT1/PIP1/PTOP1 (TPP1), protection of telomeres 1 (POT1). TRF1 and TRF2 anchor the complex to double-stranded telomeric DNA using a specific Myb-like motif termed a telobox (Bilaud *et al.*, 1996), and recruit two other shelterin components, RAP1 and TIN2, to the telomeres. TIN2 further interacts with TPP1 protein, which binds the final shelterin component, POT1. POT1 also binds the G–rich strand of telomeric DNA from either the single-stranded G–overhang or displacement loop (D–loop). In this way, shelterin may bridge the double- and single-stranded parts of telomeric DNA.

The CST complex, consisting of three components (Cdc13, Stn1 and Ten1), was originally described in yeast (Gao *et al.*, 2007) as a telomere-specific replication protein A-like complex that protects single-stranded chromosome termini and regulates telomere replication. Subsequent studies have shown that a CST-like complex also exists in plants and humans and contributes to telomere protection and replication (Surovtseva *et al.*, 2009; Price *et al.*, 2010). According to recent studies, both complexes participate in telomere capping, telomerase regulation and 3′ overhang formation (Giraud-Panis *et al.*, 2010; Pinto *et al.*, 2011; Chen *et al.*, 2012; Wu *et al.*, 2012).

In contrast to the CST complex, no functional and structural equivalent of shelterin has been found in plants. Although many putative shelterin-like protein components have been found in plants (Peska *et al.*, 2011), including those bearing a telobox Myb-like domain at their C–terminus (Hwang *et al.*, 2001, 2005; Karamysheva *et al.*, 2004) or N–terminus (Marian *et al.*, 2003; Schrumpfova *et al.*, 2004), as well as POT1 homologues (Baumann *et al.*, 2002; Kuchar and Fajkus, 2004; Shakirov *et al.*, 2005; Tani and Murata, 2005; Peska *et al.*, 2008), none of these have been shown to specifically associate with telomeres *in situ* or *in vivo*.

Molecular components responsible for reversible telomerase regulation in plant cells (Fajkus *et al.*, 1998; Riha *et al.*, 1998) are an attractive target for possible biomedical applications of telomere biology, and are sought primarily at the levels of protein components of plant telomeres, and regulation of the basic telomerase subunits TERT (telomerase reverse transcriptase) and TER (telomerase RNA).

In this study, we investigated the interactions and roles of Single myb histone (Smh) proteins at plant telomeres. Five members of the Smh family are encoded by the *A. thaliana* genome (TRB1–5). These proteins are specific to plants, and consist of an N–terminal Myb-like domain of the telobox type, which is responsible for specific recognition of double/single-stranded telomeric DNA (Schrumpfova *et al.*, 2004; Hofr *et al.*, 2009), a central histone-like domain, which is involved in non-specific DNA–protein interactions and mediates protein–protein interactions, including formation of homo- and heteromeric complexes of TRB proteins (Mozgova *et al.*, 2008), and a C–terminal coiled-coil domain to which no specific function has yet been attributed. We previously reported that TRB proteins interact via their histone-like domain with POT1b, an *A. thaliana* homologue of the G–overhang binding protein POT1 (Kuchar and Fajkus, 2004; Schrumpfova *et al.*, 2008; Rotkova *et al.*, 2009). In addition, POT1b also associates with an alternative telomerase nucleoprotein complex in Arabidopsis (Surovtseva *et al.*, 2007; Cifuentes-Rojas *et al.*, 2012). We have previously shown that TRB1 is localized in the nucleus and nucleolus *in vivo* and shows highly dynamic association with chromatin (Dvorackova *et al.*, 2010). Together, these findings indicate that TRB proteins are promising candidates for plant shelterin-like components.

Here we demonstrate that TRB proteins act as components of a plant telomere-protection complex. Microscopic and chromatin immunoprecipitation techniques showed co-localization of TRB1 with telomeric tracts *in vivo* and physical interaction of TRB proteins with the N–terminal part of the catalytic subunit of telomerase. In addition, loss of TRB1 protein leads to telomere shortening.

RESULTS

TRB1 co-localizes with telomeres

Although a possible association of GFP–TRB1 (*35Spro:GFP-TRB1*) with the telomere was suggested previously (Dvorackova *et al.*, 2010), whether the nuclear speckles are directly associated with telomeres remained to be determined.

Here, we took advantage of the well-established protocol of *Nicotiana benthamiana* leaf infiltration and the fact that *N. benthamiana* has longer telomeres that are easier to visualize compared to Arabidopsis.

As shown in Figure 1(c), the localization of transiently transformed TRB1 in *N. benthamiana* leaf is similar to that observed in Arabidopsis cell cultures, as was shown by Dvorackova *et al.* (2010), labelling the whole nucleus, with strong nucleolar signal and relatively strong nuclear speckles. Nuclei from transformed leaves were isolated and used for telomere peptide nucleic acid FISH. Fluorescence from GFP–TRB1 remained very bright during the isolation procedure; however, a gentle denaturation step was necessary during the FISH protocol to preserve the integrity of the GFP signal. These FISH results showed that telomeres co-localize or associate with TRB1 speckles in 59% and 31% of cases, respectively, with 90% association overall (Figure 1 and Table S1). Telomeric signals sometimes appeared as double dots connected to the TRB1 foci (Figure 1d, images 1, 2 and 3), but in other cases co-localize directly with TRB1 (Figure 1d, images 4 and 5). These results provide *in situ* evidence of telomere occupancy by TRB1.

TRB1 is associated with telomeric sequence *in vivo*

The observed co-localization of TRB1 with telomeric tracts, together with our previous detailed analyses of TRB1 binding to telomeric DNA *in vitro* (Schrumpfova *et al.*, 2004; Hofr *et al.*, 2009), suggest the possibility that TRB1 protein directly recognizes telomeric repeats and belongs to the core components that shelter telomeres. We used a chromatin immunoprecipitation assay to isolate DNA sequences associated with TRB1 protein. As source material, we used formaldehyde cross-linked seedlings of Arabidopsis plants stably transformed with a TRB1–GFP construct driven by the native promoter (*TRB1pro:TRB1-GFP*) (Dvorackova *et al.*, 2010). Despite using the native

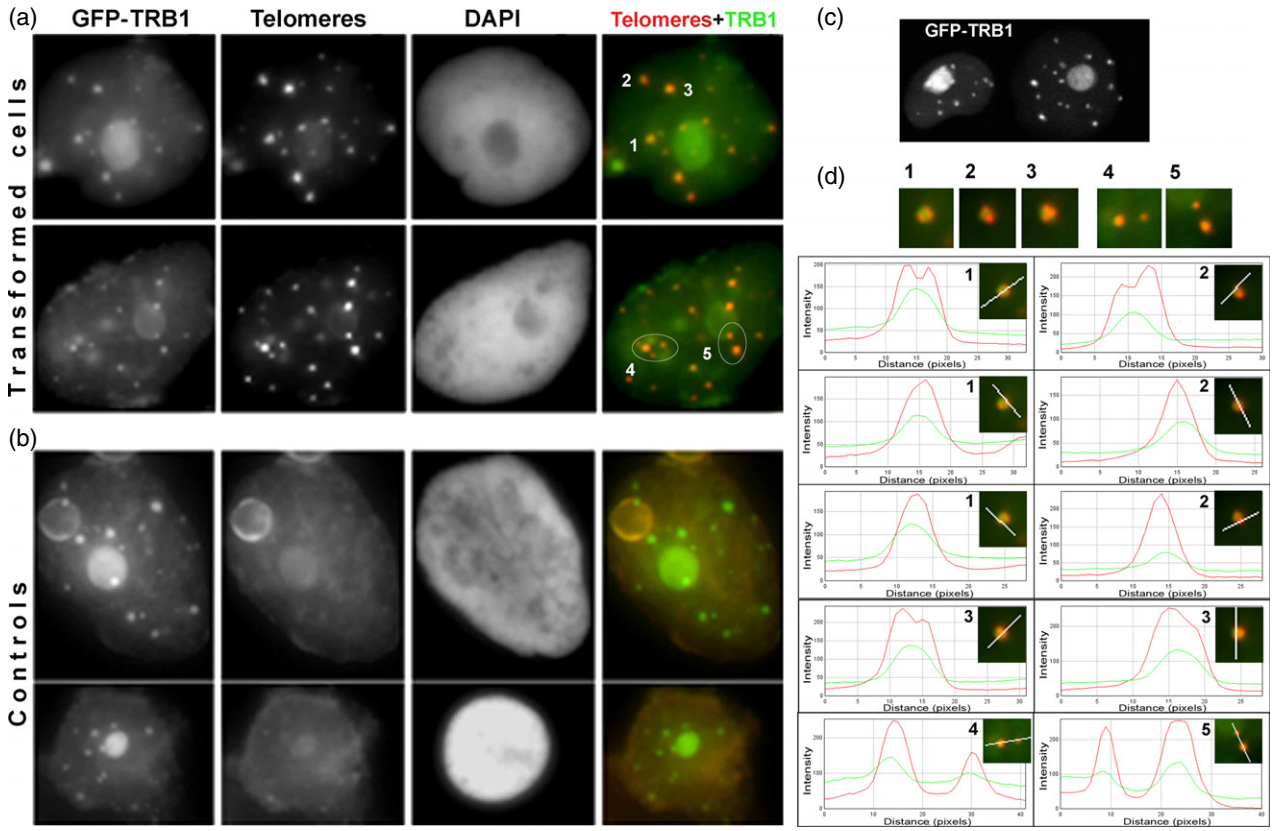

Figure 1. Co-localization of TRB protein with telomeric probe.
Nuclei isolated from *N. benthamiana* were transformed with *35Spro:GFP-TRB1* construct and hybridized with telomeric peptide nucleic acid (PNA) Cy3-labelled probe.
(a) Co-localization between GFP–TRB1 nuclear speckles (green) and telomeric PNA probe (red) is detectable in most of the foci.
(b) Control experiment without telomeric probe showing very little background present in the red channel.
(c) Confocal image of GFP–TRB1 expression in an *N. benthamiana* leaf without any further sample processing.
(d) Details of co-localizing speckles; ImageJ (http://rsbweb.nih.gov/ij/) was used to create intensity plots for red and green channels.

promoter, enhanced levels of TRB1–GFP protein were observed (see below). TRB1–GFP protein was immunoprecipitated from purified nuclei using GFP-Trap A matrix, which contains a single variable antibody domain that recognizes GFP. Non-specific binding of TRB1-GFP to the GFP-Trap A matrix was excluded by precise detection of GFP in all fractions (input, bound, unbound, wash, elution). We have shown that TRB1, but not TRB1-GFP is washed out (Figure S1). DNA co-purifying with TRB1–GFP was dot-blotted onto nylon membranes, and visualized by hybridization with radioactively labelled telomeric probe. Figure 2 shows that TRB1 protein is indeed associated with telomeric sequence *in vivo*, as telomeric sequence was repeatedly detected in TRB1–GFP but not wild-type samples. To demonstrate that the observed enrichment is indeed due to sequence-specific association and not due to the high copy number of the telomeric DNA, we hybridized DNA co-purified with TRB–GFP with a centromeric probe. As our previous results (Dvorackova *et al.*, 2010) showed localization of TRB1 protein in the nucleus and nucleolus, another candidate sequence investigated for association with TRB1 was ribosomal DNA (rDNA). Only negligible enrichment of the centromeric or 18S rDNA probe, in contrast to significant enrichment of the telomeric probe, was observed when comparing each wild-type to TRB–GFP sample (Figure S2).

Analysis of TRB1 expression in trb1 mutant, wild-type and *TRB1pro:TRB1-GFP*-transformed plants

To examine the role of TRB1 *in planta*, we analysed T–DNA insertion line SALK_025147 (ecotype Col–0). Three parallel wild-type (wild-type) and homozygous *trb1* (*trb1–/–*) lines (A, B and C) were derived from three independent heterozygous plants (see Figure 4a). The homozygosity of each parallel wild-type and *trb1* mutant plant line was determined by PCR (Figure 3b). The T–DNA insertion is located in the second intron (Figure 3a), and the absence of *trb1* transcript was confirmed by RT–PCR (Figure 3c).

TRB proteins consist of three domains: Myb-like, histone-like and a coiled-coil domain (Figure 3a). As no antibody recognizing either TRB proteins or the plant Myb

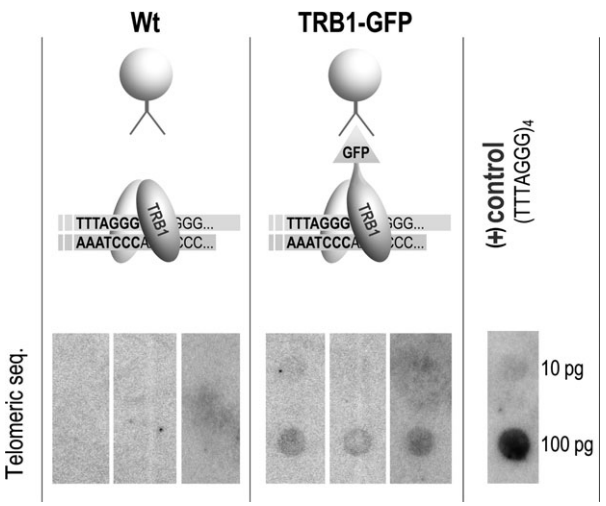

Figure 2. TRB1 proteins are associated with telomeric sequence *in vivo*.
DNA cross-linked with TRB1 protein was isolated by ChIP analysis using GFP-Trap A matrix from wild-type (Wt) and *TRB1pro:TRB1-GFP* plants. Hybridization of isolated DNA with radioactively labelled telomeric oligonucleotide $(CCCTAAA)_4$ in three biologically and technically replicated experiments confirmed the hypothesis that TRB1 protein is associated with telomeric sequence *in vivo*. As a control, telomeric oligonucleotide $(TTTAGGG)_4$ was dot-blotted on the same membrane and visualized together with immunoprecipitated DNA.

domain of the telobox type is commercially available, we developed specific mouse monoclonal antibodies in our laboratory. Two of them were used in this study: 1.2 (specific to TRB1) and 5.2 (specific for the conservative part of the Myb domain; this also recognizes other TRB proteins). The location of antibody recognition sites within the structure of TRB1 as determined by ELISA (Figure S3) is shown in Figure 3(a). Although the conservative part of the telobox Myb domain is also present in Arabidopsis TRF-like family (TRFL) proteins (Karamysheva *et al.*, 2004), these proteins are not recognized by the 1.2 or 5.2 antibodies. The anti-TRB 1.2 or 5.2 antibodies were unable to detect *in vitro* expressed TRFL2 or 9 or TRP1 (telomeric repeat binding protein 1) from the TRFL family (Figure S4, constructs kindly provided by D.E. Shippen, Department of Biochemistry,Texas A&M University,TX, USA).

Antibody 1.2 was used to detect native TRB1 protein in Arabidopsis plant protein extracts. The natural level of TRB1 protein was clearly observed on Western blots of wild-type plants (Figure 3d), but no TRB1 protein was observed for extracts from *trb1* mutant plants (Figure 3d). In addition, plant lines stably transformed with TRB1–GFP construct under the control of native promoter showed a distinct abundance of TRB1–GFP protein compared to the native TRB1 protein. Various expression levels of native TRB1 protein and TRB1–GFP were also apparent after immunolocalization *in vivo* (Figure 3e), in which TRB1 protein is visualized using either anti-TRB1 1.2 antibody or anti-GFP antibody.

We tested both antibodies by indirect immunofluorescence on *trb1* mutant and GFP–TRB1-expressing plants. These experiments showed evenly distributed nuclear and nucleolar signals for both 1.2 and 5.2 antibodies. Antibody 1.2 did not detect any signal in *trb1–/–* plants, but antibody 5.2 recognizes some epitopes in *trb1–/–* (Figure S5). However, the generated antibodies do not appear to be of sufficient quality for more demanding immunolocalization or ChIP experiments (as concluded from further testing).

Telomere shortening in *trb1* null mutant plants

Derivation of independent wild-type and *trb1–/–* plant lines from three heterozygous progeny (Figure 4a) provided reliable material for phenotypic studies of the *trb1* null mutation effect. All six homozygous plant lines were propagated for five generations.

Obvious shortening of telomeres was observed by terminal restriction fragment (TRF) analysis in all three *trb1* mutant lines analysed in the fifth generation compared to their segregated wild-type siblings. Hybridization with a radioactively labelled telomeric probe (Figure 4b) revealed truncation of telomeric tracts in *trb1* lines by approximately 10–20% (Figure 4c). The graph represents evaluation in the three biological replicates. Observations in earlier generations of *trb1* lines (Figure S6) show mild but progressive shortening that continues through the generations. Despite clear and reproducible telomere shortening in *trb1*, no significant morphological differences were observed in rosette diameter, leaf number, flowering and seed set when analysing soil-grown wild-type and *trb1–/–*plants.

TRB proteins interact with telomerase *in planta*

Our previous finding that TRB1 protein interacts with POT1b and evidence presented here showing that TRB1 co-localizes with telomeric repeats and is involved in regulation of telomere maintenance suggest its possible association with telomerase (Kuchar and Fajkus, 2004; Schrumpfova *et al.*, 2008). We therefore tested the possibility of direct interaction between TRB1 and TERT, as well as the influence of TRB1 on telomerase activity *in vitro*.

As TERT is a high-molecular-weight protein (approximately 130 kDa), we used TERT fragments containing N–terminal domains associated with distinct telomeric functions (Sykorova and Fajkus, 2009) to detect a possible direct interaction between TERT and TRB proteins (Figure 5a). We tested their ability to interact using a GAL4 based yeast two-hybrid system, in which interactions take place inside the nucleus. As shown in Figure 5(b), strong interaction between TRB1 and the TERT 1-271 fragment was observed on histidine-deficient plates. This interaction was confirmed under stringent adenine selection. Clear interactions between TRB3 and TERT 1-271 and a weak interaction between TRB2 and TERT 1-271 were also observed under histidine selection. Further testing TRB1

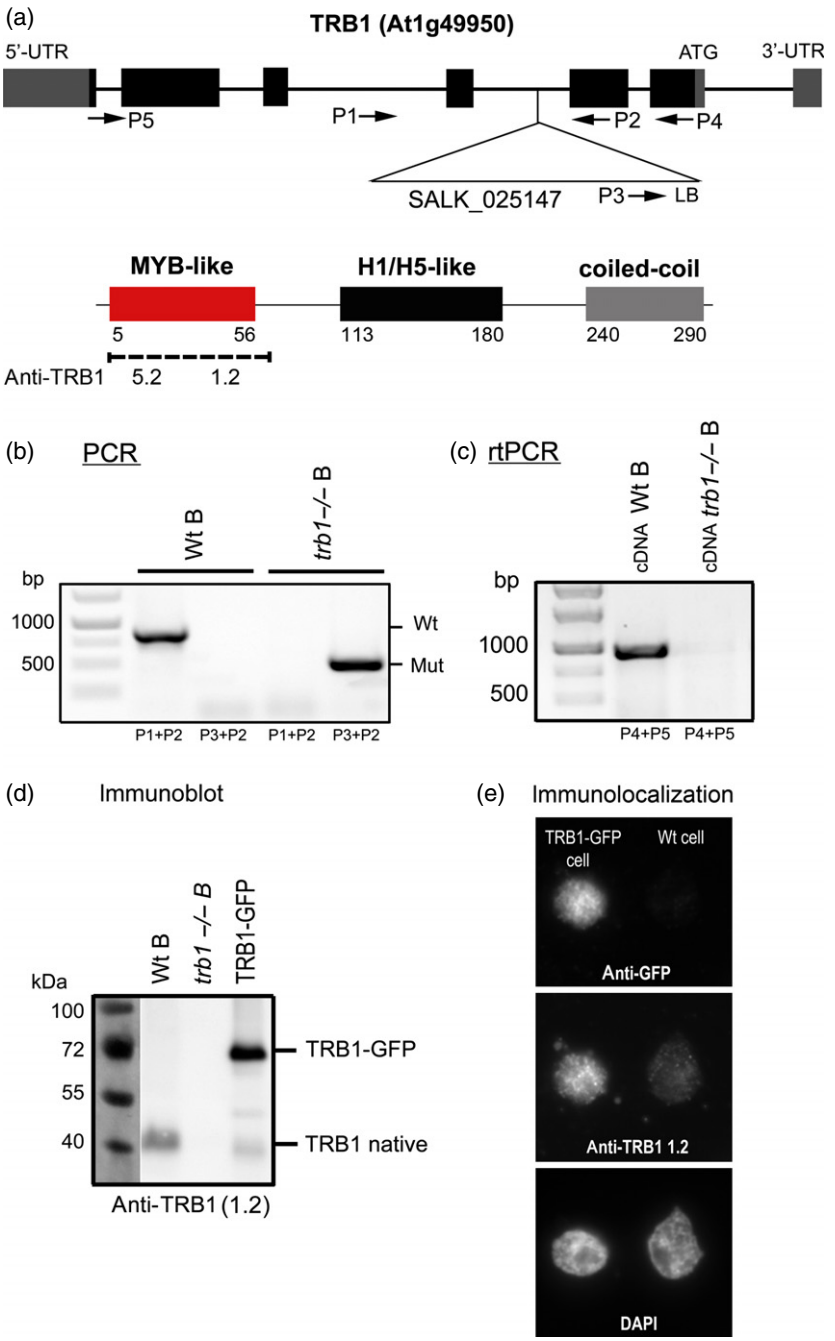

Figure 3. Expression analysis of TRB1 protein in mutant (*trb1*–/–), wild-type (Wt) and transformed *TRB1pro:TRB1-GFP* plants.

(a) Schematic illustration of specific primers and T–DNA insertion location within the *trb1* gene. The domain location and antibody recognition sites for two specific antibodies developed in our laboratory are shown below.

(b) Three individual plant lines (A, B and C) were derived from heterozygous progenitors (as shown in Figure 4a). Example of PCR analysis of genomic DNA isolated from Wt plants (primers P3 + P2) and mutant (*trb1*–/–) plants (primers P1 + P2) of line B.

(c) RT–PCR of RNA isolated from Wt and mutant (*trb1*–/–) plants of line B using primers P4 + P5.

(d) Immunodetection by Western blot analysis of TRB1 protein in Wt and mutant (*trb1*–/–) plants of line B and *TRB1pro:TRB1-GFP* plant nuclear extracts using specific antibody recognizing the Myb-like domain of TRB1 (anti-TRB1 1.2). The level of native TRB1 protein is lower compared to the TRB1–GFP fusion protein construct expressed under the control of the native promoter.

(e) Immunolocalization of TRB1 protein using anti-GFP and anti-TRB1 antibody. The level of native TRB1 protein in the wild-type is very low. The selected plant line does not show GFP labelling in all cells, so some nuclei contain a wild-type level of TRB1 and others show higher expression due to TRB1–GFP. Thus the intensity of signal may be clearly measured as Wt and over-expressing nuclei are present together on one slide and may be clearly distinguished using specific anti-TRB1 protein antibody 1.2 and anti-GFP antibody.

and TRB2 with a longer fragment of TERT (amino acids 1-582) confirmed these interactions.

To test whether the interactions observed in a yeast-two hybrid system are reproducible in the plant cell, we used a bimolecular fluorescence complementation assay (BiFC). Arabidopsis protoplasts were transfected with plasmids encoding nYFP-tagged TRB constructs and cYFP-tagged TERT fragments, and a clear intra-nuclear interaction was observed (Figure 5c and Figure S7). The TERT fragments used in BiFC (TERT 1-271 and TERT 229-582) overlap with the fragments tested in the yeast two-hybrid system.

The interaction was further verified by co-immunoprecipitation experiments in which proteins were expressed in rabbit reticulocyte lysate from the same vectors used in yeast two-hybrid system. As shown in Figure S8, clear interactions between TRB1 and all three TERT fragments (1-271, 229-582 and 1-582) were observed. Obvious interactions were also detected between TRB3 and TERT 1-271 or TERT 229-582, but only weak interactions were observed between TRB2 and TERT fragments. The generally weaker interactions of TRB2 or TRB3 proteins with TERT fragments in comparison to the corresponding interactions of TRB1

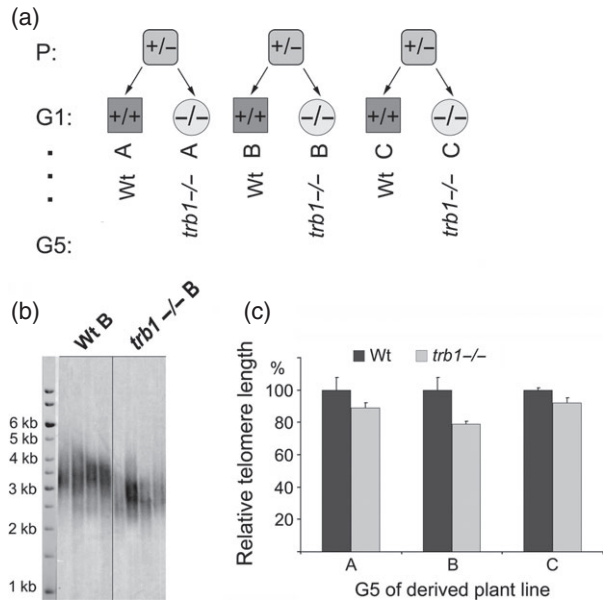

Figure 4. The telomeres are shortened in all three individually derived *trb1–/–* mutant plant lines.
(a) Derivation of three independent plant lines (A, B, C) that were propagated for five generations (G5).
(b) Terminal restriction fragment analysis, showing telomere shortening in the *trb1–/–* mutant line compared with the wild-type control in the fifth generation.
(c) Difference in mutant *trb1–/–* and wild-type telomere lengths in three independent plant lines. Error bars represent standard deviation.

were due to lower expression of TRB2 and TRB3 proteins in rabbit reticulocyte lysate.

To determine whether interaction between TRB proteins and TERT directly influences telomerase activity, we used a telomere repeat amplification protocol (TRAP). In extracts from *trb1–/–* plants, no changes in telomerase activity or processivity were observed. Correspondingly, no variations in telomerase activity were detected in transformed plants (*TRB1pro:TRB1-GFP*) expressing higher levels of protein (Figure S9). This observation is in agreement with our previous experiments in which *Escherichia coli*-expressed and purified TRB2 and TRB3 proteins were added to the TRAP assay (Schrumpfova *et al.*, 2004).

DISCUSSION

The composition of plant shelterin-like complex has long remained elusive due to the high number of candidate proteins with apparently redundant functions (Peska *et al.*, 2011). These obstacles and lack of convincing evidence raised doubts over the existence of such a complex, and its functions have been mostly attributed to the previously described CST complex, which is conserved throughout eukaryotes (Nelson and Shippen, 2012b). However, absence of evidence is not evidence of absence. Our present data suggest the existence of a telomere protein complex that includes plant-specific Smh proteins (termed TRB proteins in Arabidopsis). These proteins interact directly with the catalytic subunit of telomerase: TRB1 protein co-localizes with telomeres, specifically binds telomeric DNA *in vitro* and *in vivo*, and TRB1 loss results in telomere shortening. Moreover, TRB proteins also interact with POT1b, a POT1-like orthologue in *A. thaliana* (Kuchar and Fajkus, 2004; Schrumpfova *et al.*, 2008).

In previous studies, we considered in detail the localization of TRB1 protein, showing that, similar to TRB2 and TRB3, this is a nuclear factor with markedly increased nucleolar labelling and speckles present in the nucleus, especially in Arabidopsis cell cultures transiently transformed with GFP–TRB1 (Dvorackova *et al.*, 2010). We have previously speculated on the telomeric association of GFP–TRB1 speckles, but the low expression of GFP–TRB1 in stably transformed Arabidopsis plants/cultures and the short size of Arabidopsis telomeres impeded its direct demonstration (Dvorackova *et al.*, 2010). In this study, we used a plant system with longer telomeres and sufficient expression of TRB1–GFP protein, and clearly showed that TRB1 co-localizes with telomeres in plant leaves. Close linkage between TRB1 protein and the telomere was further supported by the finding that plant telomeric sequence may be isolated directly from plant seedlings together with TRB1–GFP using the anti-GFP immunoprecipitation system. Specific anti-TRB1 antibodies were also developed and successfully used for detection of TRB1 alone or all TRB proteins in the whole-protein extract by Western blot or ELISA procedures. Using these antibodies, clear nuclear and nucleolar localization of TRB1 protein was demonstrated. Although TRB1 protein need not associate exclusively with telomeres *in vivo*, the preferential association of TRB1 with the telomeric tracts as described here is in agreement with previous observations using independent approaches (Mozgova *et al.*, 2008; Hofr *et al.*, 2009; Dvorackova *et al.*, 2010). The obvious association of TRB1 with the nucleolus, which contains sub-telomeric clusters of rDNA, may be due to the fact that nucleoli associate with telomeres and telomerase at the cellular level: telomerase assembly occurs in nucleoli in a number of model organisms including plants (Lo *et al.*, 2006; Brown and Shaw, 2008; Kannan *et al.*, 2008), and nucleolus-associated telomere clustering and pairing precede meiotic chromosome synapsis in *Arabidopsis thaliana* (Armstrong *et al.*, 2001).

The key finding of this work is that TRB proteins interact with the N–terminal part of TERT. This part contains the telomerase-specific motifs TEN (telomerase essential N–terminal domain) and TRBD (N–terminal RNA-binding domain). The most conserved motif, the T–motif, with a high-affinity binding site for the TER subunit, is included in the TRBD domain (Lai *et al.*, 2001). Several distinct functions have been proposed for the TEN domain: e.g. as an

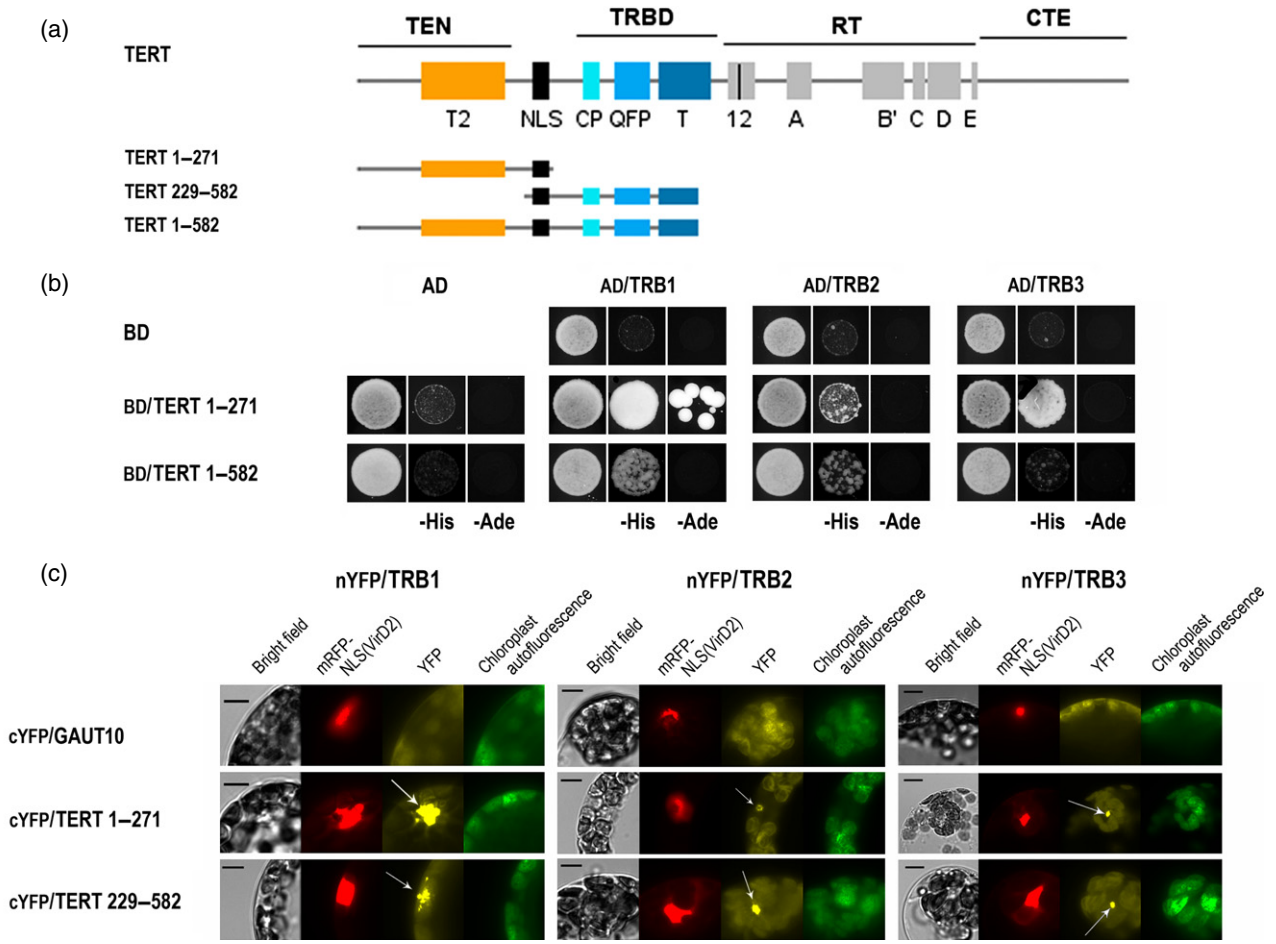

Figure 5. TRB proteins interact with plant telomerase (TERT).
(a) Schematic depiction of the catalytic subunit of telomerase (TERT) showing evolutionarily conserved motifs. N-terminal fragments containing the telomerase-specific motifs TEN (telomerase essential N–terminal domain) and TRBD (N–terminal RNA-binding domain) were used in protein–protein interaction analysis (amino acid numbering is shown).
(b) Yeast two-hybrid system was used to assess interaction of TRB proteins with N–terminal TERT fragments. Two sets of plasmids carrying the indicated segments of TERT fused to either the GAL4 DNA-binding domain (BD) or the GAL4 activation domain (AD) were constructed and introduced into yeast strain PJ69–4a carrying reporter genes *His3* and *Ade2*. Although weak interactions often fail to rescue growth under stringent adenine selection, plausible TRB–TERT interactions were observed on histidine-deficient plates. Co-transformation with an empty vector (AD/BD/vector) served as a negative control.
(c) Bimolecular fluorescence complementation confirmed the interaction of TRB proteins with TERT fragments. Arabidopsis leaf protoplasts were co-transfected with 10 μg each of plasmids encoding nEYFP-tagged TRB clones, cEYFP-tagged TERT fragments or Gaut10 (as negative control) and mRFP-VirD2NLS (to label cell nuclei and to determine transfection efficiency). The cells were imaged by epifluorescence microscopy after overnight incubation. Clear nuclear interactions of TRB proteins with TERT fragments are observed on the protoplast images: YFP fluorescence (yellow), mRFP fluorescence (red), chloroplast autofluorescence (green pseudocolor); chloroplast autofluorescence is also visible in the YFP channel (indicated by arrows). Scale bars = 7 μm.

anchor during template translocation (Lue, 2005; Wyatt *et al.*, 2007; Sealey *et al.*, 2010), involvement in positioning the 3′ end of a telomeric DNA primer in the active site during nucleotide addition (Jurczyluk *et al.*, 2011), putative mitochondrial localization (Santos *et al.*, 2004), and, last but not least, involvement in protein–protein interactions (Sealey *et al.*, 2011). Hence, the positioning of the region involved in interaction between TERT and TRB proteins in the N–terminal part of telomerase is not surprising. Identification of TRB proteins as the interaction partner of TERT is also supported by the observation that TRB1 protein is present in a group of proteins that were co-purified with the N–terminal part of TERT using tandem affinity purification (P.P.S., J.M., L.D., E.S and J.F., unpublished results).

The observation of TRB/telomerase interaction, together with the previously detected interaction between TRB and POT1b (Kuchar and Fajkus, 2004; Schrumpfova *et al.*, 2008), suggest that TRB proteins are part of the telomeric interactome of *A. thaliana.* Interaction of POT1b protein with the TRB1 protein is mediated by the central TRB histone-like domain (Schrumpfova *et al.*, 2008), but it is not yet clear how the interaction between telomerase and TRB is mediated. Determination of whether it occurs through the same histone-like domain or the N–terminal Myb domain or C–terminal coiled-coil domain would help to

determine mutual exclusion or co-existence of TERT and POT1b association with TRB proteins.

Importantly, POT1b is also an interaction partner of TER2, an alternative telomerase RNA subunit in Arabidopsis (Cifuentes-Rojas *et al.*, 2011, 2012). Together with TERT, dyskerin and Ku, these components form telomerase ribonucleoprotein complex that may participate in telomerase regulation, the DNA damage response and telomere protection, but do not substantially contribute to telomere maintenance (Cifuentes-Rojas *et al.*, 2011, 2012). Therefore, the observation that TRB1 interacts with TERT but its loss or increased expression does not change telomerase activity is not surprising. More importantly, interaction of TRB1 with TERT, together with its affinity for telomeric DNA, indicates a possible role of TRB1 in telomerase recruitment to telomeres. This also explains the observed absence of any direct effect of TRB1 on telomerase activity in the TRAP assay, as this *in vitro* assay uses a non-telomeric template oligonucleotide that is not recognized by the Myb-like domain of TRB1 (Mozgova *et al.*, 2008).

However, POT proteins are not the only putative single-stranded DNA telomere-binding proteins in Arabidopsis, as several other proteins have been identified, e.g. STEP1 (Kwon and Chung, 2004), WHY1 (Yoo *et al.*, 2007a) or CST complex components (Price *et al.*, 2010). Similarly, in addition to the TRB family of proteins, there are also other candidate double-stranded DNA telomere-binding proteins in Arabidopsis, such as TRFL family proteins (Karamysheva *et al.*, 2004). Association of these proteins with telomeres appears not to be mutually exclusive. Presumably, dynamic changes in the composition of telomeric nucleoprotein complexes may reflect the different functional states of telomeres. Two types of plant chromosome ends have been proposed: those with G–overhangs and blunt-ended ones that are recognized by the KU70/80 dimer (Riha *et al.*, 2000; Gallego *et al.*, 2003; Kazda *et al.*, 2012; Nelson and Shippen, 2012a). Thus, the apparently redundant proteins may operate concurrently at telomeres with respect to cell cycle, developmental stage or type of chromosome ends. For example, localization of TRB1 is quite consistent but highly dynamic during interphase; moreover, the level of nuclear-associated TRB1 diminishes during mitotic entry, and it progressively re-associates with chromatin during anaphase/telophase (Dvorackova *et al.*, 2010). Interestingly, our BiFC assay also showed interaction of N–terminal fragments of TERT with TRP1, a member of the TRFL I family (Figure S10) (Hwang *et al.*, 2001; Karamysheva *et al.*, 2004). Importantly, TRP1 also interacts with KU70 (Kuchar and Fajkus, 2004), which is presumably involved in protection of blunt chromosome ends and may also therefore be an integral part of the plant telomere protection complex (Figure 6).

Although it is tempting to draw possible analogies between mammalian shelterin components and the TRB and POT1b proteins involved in a similar plant complex,

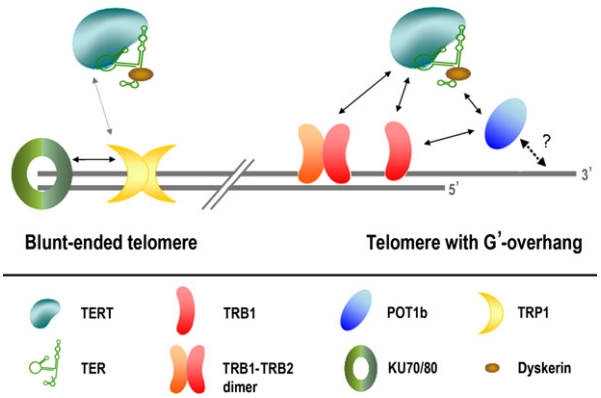

Figure 6. Schematic diagram of observed protein–protein interactions at telomeric ends.
Half the telomeric ends in *A. thaliana* are blunt-ended (Riha *et al.*, 2000; Kazda *et al.*, 2012). Here we show a simplified chart of interactions associated with telomeres. Solid arrows indicate protein–protein interactions that were verified in this study or in previous studies (Kuchar and Fajkus, 2004; Kannan *et al.*, 2008; Schrumpfova *et al.*, 2008; Cifuentes-Rojas *et al.*, 2012; Kazda *et al.*, 2012) using at least two independent approaches (i.e. BiFC, pull-down or yeast-two hybrid assay). The grey arrow indicates a TERT–TRP1 interaction observed only by BiFC. The dashed black arrow shows a presumed interaction between POT1b and telomere single-stranded DNA that has not yet been directly demonstrated. The interaction between POT1b and telomerase is specific for the TER2 isoform of TER, while the other interactions with the telomerase complex are dependent on the catalytic TERT subunit. The diagram suggests the existence of distinct telomerase recruitment pathways for blunt-ended telomeres and telomeres with a G–overhang.

an alternative interpretation of the function of TRB is possible when considering our data in connection with a recent description of mammalian HOT1 protein (Kappei *et al.*, 2013). This protein shows strikingly similar interactions and functions: it specifically binds double-stranded telomeric DNA repeats, localizes to a subset of telomeres (presumably those that are being elongated), and associates with active telomerase. Thus, HOT1 contributes to the association of telomerase with telomeres and to telomere length maintenance (Kappei *et al.*, 2013). Our findings suggest that TRB proteins may perform similar functions in plant telomeres, i.e. as direct telomere-binding proteins that act as positive regulators of telomere length.

EXPERIMENTAL PROCEDURES

Primers

The sequences of all primers and probes used in this study are provided in Table S2.

Plant material and construct generation

The *35Spro:GFP-TRB1* plants and construct have been described previously (Dvorackova *et al.*, 2010). The *TRBpro:TRB1-GFP* construct was prepared as follows: genomic DNA from *A. thaliana* Col–0 was isolated using a DNeasy plant mini kit (Qiagen, http://www.qiagen.com/), and used as a template for PCR to amplify the

TRB1 genomic sequence including the 5′ UTR. The 3′ UTR was amplified from BAC clone FJ10.16 (Arabidopsis Information Resource, http://www.arabidopsis.org/). We used 0.25 units of Hot Start Phusion polymerase (Finnzymes, http://www.thermoscientificbio.com/finnzymes/) with 0.2 mM dNTPs, 1× HF reaction buffer (Phusion Hot Start II high fidelity DNA polymerase; http://www.thermoscientificbio.com/), 3% dimethylsulfoxide and 0.5 μM of each primer (5′ UTRFw + TRB1 Rev or 3′ UTR Fw + 3′ UTR Rev). The conditions used were in accordance with the manufacturer's instructions (Finnzymes). PCR products were precipitated using poly(ethylene glycol), and cloned into a Gateway multi-site system (Invitrogen, http://www.lifetechnologies.com), together with the GFP tag (GFP in pDONR221, provided by Keke Yi, College of life Sciences, Zhejiang University, China). pKm43GW (Karimi *et al.*, 2005) was used as the destination vector. *A. thaliana* Col–0 was subsequently transformed by floral dipping (Clough and Bent, 1998), and transformants selected on MS medium containing 30 μg/ml kanamycin were scored for GFP expression.

PCR-based genotyping of plant lines

T–DNA insertion mutant plants of *trb1* (SALK_025147) in the Col–0 background were used. To distinguish between wild-type plants and those that were heterozygous or homozygous for the T–DNA insertion in the *trb1* gene, we isolated genomic DNA from leaves using NucleoSpin Plant II (Machery Nagel, http://www.mn-net.com/). The genomic DNA was used for PCR analysis with MyTaq DNA polymerase (Bioline, http://www.bioline.com). The conditions used were in accordance with the manufacturer's instructions. The primers used were specific for T–DNA (P3 + P2 primers) or the *TRB1* gene (P1 + P2 primers). Cycling conditions were 98°C for 1 min (initial denaturation), followed by 30 cycles of 94°C for 30 sec, 58°C for 45 sec and 72°C for 2 min, with a final extension at 72°C for 10 min.

Rt–pcr

Total RNA was extracted from approximately 50 mg of frozen plant tissue using an RNeasy plant mini kit (Qiagen), and RNA samples were treated with TURBO DNA-free (Applied Biosystems/Ambion, http://www.lifetechnologies.com TURBO DNA-free). The quality and quantity of RNA were determined by electrophoresis on 1% w/v agarose gels and by measurement of absorbance using an Implen nanophotometer (http://www.implen.de/). Reverse transcription was performed using random hexamers (Sigma-Aldrich, http://www.sigmaaldrich.com) with 1 μg RNA and Mu-MLV reverse transcriptase (New England Biolabs, https://www.neb.com/). The cDNA obtained was screened by PCR analysis for the presence of *trb1* transcripts using MyTaq DNA polymerase (Bioline) with primers P4 and P5. Thermal conditions were 95°C for 1 min (initial denaturation), followed by 30 cycles of 94°C for 45 sec, 55°C for 45 sec and 72°C for 2 min, with a final extension at 72°C for 10 min.

Nicotiana benthamiana transformation, nuclei isolation and FISH

Leaves of 5-week-old *N. benthamiana* plants were infiltrated with *Agrobacterium tumefaciens* containing *35Spro:GFP-TRB1* (vector pGWB6, strain LBA4404) (Dvorackova *et al.*, 2010), and *35Spro:p19* (Silhavy *et al.*, 2002) as described by Voinnet *et al.* (2003). The infiltration medium contained 10 mM MES (pH approximately 5.7) and 10 mM $MgCl_2$. After 3–4 days, leaf discs were checked under a fluorescence microscope, and protoplasts were prepared as described by Yoo *et al.* (2007b); the digestion medium contained also 0.25% Pectolyase Y23 (Duchefa, http://www.duchefa-biochemie.nl/) in addition to celullase and macerozyme and a 119 μm filter was used for filtration. Protoplasts in W5 buffer were collected by centrifugation at 50 ***g***, and resuspended in NIB (Nuclei Isolation Buffer; 10 mM MES, 0.2M Sucrose, 2.5 mM EDTA,10 mM NaCl, 10 mM KCl 2.5 mM DTT, 0.1 mM Spermine, 0.5 mM Spermidine) to extract nuclei as described by McKeown *et al.* (2008). Isolated nuclei were then fixed in 4% paraformaldehyde for 15 min, resuspended in wash buffer (50 mM Tris/Cl, pH 8.5, 5 mM $MgCl_2$, 20% glycerol), 4°C, spun down at 300g and stored in storage buffer (50 mM Tris/Cl, pH 8.5, 5 mM $MgCl_2$, 50% glycerol) at -20°C until use.

Then 20 μl of nuclei were spun on the Superfrost plus microscopic slide (http://www.menzel.de/) at 56 ***g***, and re-fixed in 4% paraformaldehyde in 1× PBS/0.05% Triton X-100 for 15 min. Slides were then treated with RNase (100 μg/ml) for 1 h at 37°C, and hybridized with telomeric Cy3-labelled peptide nucleic acid probe in 65% formamide/20% dextran sulfate/2× SSC at 37°C overnight. Post-hybridization washes were performed at 37°C using 2× SSC. Slides were counter-stained using 4,6–diamidino-2–phenylindole (1 μg/ml), and observed on a Zeiss (http://www.zeiss.cz/) Axioimager Z1 using an AHF filter set.

Immunolocalization

Arabidopsis seeds expressing *TRB1pro:TRB1-GFP* under the control of the native promoter and *trb1* seeds were bleach-sterilized for 10 min, washed in water and sown onto half-strength MS medium/1% agar plates. Seedlings grown under the constant light, at 22°C for 2 weeks, then chopped into small pieces. Protoplasts were prepared as described by Yoo *et al.* (2007b), and the nuclei and immunolocalization protocols were adapted from those described by McKeown *et al.* (2008). Slides were first blocked in a mixture of 2× block solution (Roche, http://www.roche.cz)/1× PBS/5% goat serum at room temperature for 30 min, then incubated with primary antibodies [mouse anti-TRB 1.2 or 5.2 or, anti-GFP (Abcam ab290, http://www.abcam.com/), all diluted 1:300] for 2 h at 37°C, and visualized using secondary antibodies A11001 and A21207 (Invitrogen) at 1:500 dilution.

Immunblot analysis

To determine the level of TRB1 protein in plants, we isolated nuclei as described by Bowler *et al.* (2004). The nuclei were lysed using SDS loading buffer (250 mM Tris/Cl, pH 6.8, 4% w/v SDS, 0.2% w/v bromophenol blue, 20% v/v glycerol, 200 mM β–mercaptoethanol), heated at 80°C for 10 min, and protein extracts were analysed by SDS–PAGE. Proteins were electrophoretically transferred to a nitrocellulose membrane at 360 mA for 1 hour in 192 mM glycine, 25 mM Tris, 0.5% SDS and 10% (v/v) methanol in a Bio-Rad Mini Trans-Blot cell. Ponceau S staining was performed to check the quality of the extracts and to ensure equal gel loading for immunodetection. Membranes were blocked with 5% non-fat dry milk in Tris-buffered saline/Tween, and probed using the monoclonal anti-TRB1 1.2 antibody and the secondary polyclonal horseradish peroxidase-conjugated rabbit anti-mouse immunoglobulins (DAKO, http://www.dako.com), both diluted 1:5000. Immunoreactive bands were visualized using LumiGLO reagent and peroxide (Cell Signaling Technology, http://www.cellsignal.com) on a Fujifilm LAS-3000 CCD system (http://www.fujifilm.com/).

Chromatin immunoprecipitation assay

The ChIP assay was performed as described by Bowler *et al.* (2004) with modifications. Chromatin extracts were prepared from seedlings treated with 1% formaldehyde. The chromatin from isolated nuclei was sheared to a mean length of 250–500 bp by soni-

cation using a Bioruptor (Diagenode, http://www.diagenode.com) and centrifuged (16 000 ***g***/5 min/4°C). The matrix GFP-Trap A (Chromtec, http://www.chromotek.com) was blocked against non-specific interaction using 200 mM ethanolamine, 1% BSA and the DNA sequences TR10–24–G and TR10–24–C (Table S2), which are not recognized by TRB proteins (Schrumpfova *et al.*, 2004). The pre-treated matrix was incubated with chromatin diluted with ChIP dilution buffer (16.7 mM Tris/Cl, pH 8,0, 1.2 mM EDTA, 167 mM NaCl, 0.1% Triton X–100, phenylmethanesulfonyl fluoride and protease inhibitors) at 4°C for 4 h, and subsequently washed with low-salt, high-salt, LiCl and 10 mM Tris (pH = 8,0), 1 mM EDTA (TE) buffers. In contrast to Bowler *et al.* (2004), the levels of detergents (Triton X–100, Nonidet P-40 and sodium deoxycholate) were reduced to 0.1%. The cross-linking was reversed using 0.2 M NaCl overnight, and was followed by treatment with proteinase K (Serva, http://www.serva.de) treatment, phenol/chlorophorm extraction and treatment with RNase A (Serva) as described by Bowler *et al.* (2004). ChIP assays were repeated using three biological replicates (plants grown at different times).

Dot-blot assay

DNA isolated using ChIP was diluted into 200 μl of 400 mM NaOH and 10 mM EDTA, and samples were denatured at 95°C for 10 min and cooled on ice. They were then spotted onto Hybond XL membrane (GE Healthcare, http://www3.gehealthcare.com) and subjected to hybridization with sequence-specific probe TR–4C (Table S2). The probe was hybridized in 250 M sodium phosphate, pH 7.5, 7% SDS and 16 mM EDTA overnight at 55°C, and washed with 0.2× SSC + 0.1% SDS. The signal was evaluated using MultiGauge software (Fujifilm). All experiments were performed using three independent biological replicates. Re-hybridization with centromeric and 18S rDNA probes was performed as described previously (Mozgova *et al.*, 2010).

TRAP assay

Protein extracts from 2-week-old seedlings were prepared as described by Fitzgerald *et al.* (1996). These extracts were subjected to the TRAP assay as described by Fajkus *et al.* (1998). TS21 was used as the substrate primer for extension by telomerase, and TEL-PR was used as the reverse primer in the subsequent PCR.

TRF analysis

TRF analysis was performed as described previously (Ruckova *et al.*, 2008) using 500 ng genomic DNA isolated from 5–7-week-old rosette leaves using NucleoSpin Plant II (Machery Nagel). Southern hybridization was performed using the end-labelled telomere-specific probe TR–4C (Table S2). Telomeric signals were visualized using an FLA7000 imager (Fujifilm), and a grey-scale intensity profile was generated using MultiGauge software (Fujifilm). Evaluation of fragment lengths was performed using a Gene Ruler 1 kb DNA ladder (Fermentas, http://www.thermoscientific bio.com/fermentas/) as the standard. Mean telomere lengths were calculated as described by Grant *et al.* (2001).

Yeast two-hybrid analysis

Yeast two-hybrid experiments were performed using the Matchmaker™ GAL4-based two-hybrid system (Clontech, http://www.clontech.com/). cDNA sequences encoding TERT N – terminal fragments comprising amino acids 1-271 and 1-582 were subcloned from pDONR/Zeo entry clones (Zachova *et al.*, 2013) into the Gateway-compatible destination vector pGBKT7-DEST (bait vector). The pGBKT7-DEST destination vector that was used in this study was created by Horak *et al.* (2008) who introduced the Gateway conversion cassette into the original Matchmaker system vector pGBKT7 (Clontech). The pGADT7 prey vectors (Clontech) carrying *TRB1*, *TRB2* and *TRB3* have been described previously (Schrumpfova *et al.*, 2008). Each bait/prey combination was co-transformed into *Saccharomyces cerevisiae* PJ69–4a, and colonies were inoculated into YPD medium and cultivated overnight. Successful co-transformation was confirmed on SD medium lacking Leu and Trp, and positive interactions were selected on SD medium lacking Leu, Trp and His or SD medium lacking Leu, Trp and Ade. Co-transformation with an empty vector served as a negative control for auto-activation. Each test was performed three times using two replicates at a time. In addition, the protein expression levels were verified by immunoblotting.

Bimolecular fluorescence complementation

For PCR amplification of sequences encoding the tested proteins, and to generate restriction site overhangs, Phusion HF DNA polymerase (Finnzymes) was used. The conditions used were in accordance with the manufacturer's instructions. The primers used were F–TRB1/2/3_BstBI, R–TRB1/2/3_SmaI, F–TERT_KpnI, R–RID1+BamHI, F–F2N_KpnI and R–F2N+BamHI, and plasmids encoding the tested proteins were used as templates. The amplified DNA fragments were gel-purified, digested with *Bst*BI/*Sma*I or *Kpn*I/*Bam*HI (New England Biolabs), and ligated into vectors pSAT1-nEYFP and pSAT1-cEYFP. As a negative control, we used an AtGaut10-cEYFP construct. To quantify transformation efficiency and to label cell nuclei, we co-transfected a plasmid expressing mRFP fused to the nuclear localization signal of the VirD2 protein of *A. tumefaciens* (mRFP-VirD2NLS; Citovsky *et al.*, 2006). The vectors and the mRFP-VirD2NLS and AtGaut10-cEYFP constructs were kindly provided by Stanton Gelvin (Department of Biological Sciences, Purdue University, IN, USA). *Arabidopsis thaliana* leaf protoplasts were prepared and transfected as described by Wu *et al.* (2009). DNA (10 μg of each construct) was introduced into 1×10^5 protoplasts. Transfected protoplasts were incubated in the light at room temperature overnight, and then observed for fluorescence using a Zeiss AxioImager Z1 epifluorescence microscope equipped with filters for YFP (Alexa Fluor 488), RFP (Texas Red) and CY5 (chloroplast autofluorescence).

In vitro translation and co-immunoprecipitation

Proteins were expressed from the same constructs as used in the yeast two-hybrid system with a haemagglutinin tag (pGADT7; TRB1, 2 and 3 proteins) or a Myc tag (pGBKT7; TERT fragments) using a TNT quick coupled transcription/translation system (Promega, https://www.promega.com) in 50 μl reaction volumes according to the manufacturer's instructions. The TRB proteins were radioactively labelled using ^{35}S-Met. The co-immunoprecipitation procedure was performed as described by Schrumpfova *et al.* (2011). Input, unbound and bound fractions were separated by 12% SDS–PAGE, and analysed using an FLA7000 imager (Fujifilm).

Accession numbers

Sequence data have been deposited in the Arabidopsis Genome Initiative or GenBank/EMBL databases under the following accession numbers: At1g49950 (TRB1), At5g67580 (TRB2, formerly TBP3), At3g49850 (TRB3, formerly TBP2,), At5g16850.1 (TERT), At2g20810 (Gaut10) and At5g59430 (TRP1).

ACKNOWLEDGEMENTS

We would thank to Dorothy E. Shippen (Department of Biochemistry,Texas A&M University,TX, USA) for donation of TRFL contructs, Stanton B. Gelvin (Department of Biological Sciences, purdue University, IN, USA) for donation of mRFP-VirD2NLS and AtGaut10-cEYFP constructs and his help with initial analysis of BiFC experiments, and Iva Mozgova (Department of Plant Biology and Forest Genetics, Swedish University of Agricultural Sciences, SW) for discussion and support. The research was supported by the Czech Science Foundation (13-06943S), by project CEITEC (CZ.1.05/1.1.00/02.0068) of the European Regional Development Fund, and project CZ1.07/2.3.00/30.0009 co-financed from European Social Fund and the state budget of the Czech Republic.

SUPPORTING INFORMATION

Additional Supporting Information may be found in the online version of this article.

Figure S1. Detection of TRB1–GFP protein by specific anti-TRB1 1.2 antibody in ChIP fractions.

Figure S2. Telomeric sequence is highly enriched compared to centromeric DNA or 18S rDNA.

Figure S3. Location of antibody recognition sites within the structure of TRB1 protein.

Figure S4. Anti-TRB 1.2 and 5.2 antibodies were unable to detect proteins from TRFL family.

Figure S5. Anti-TRB1 1.2 does not detect any signal on *trb1−/−* plants, but 5.2 recognizes some epitopes in *trb1−/−*mutant plant lines.

Figure S6. Telomere shortening in *trb1−/−*plants is progressive.

Figure S7. Whole images of protoplasts (whose segments are shown in Figure 5C) obtained by bimolecular fluorescence complementation.

Figure S8. TRB1, 2 and 3 proteins are able to pull-down TERT fragments.

Figure S9. Telomerase activity or processivity *in vitro* is not changed in response to TRB1 status.

Figure S10. TRP1 protein interacts with plant telomerase (TERT).

Table S1. Quantification of TRB1 foci co-localized/associated with telomeric foci.

Table S2. Sequences of all primers and probes used in this study.

REFERENCES

Armstrong, S.J., Franklin, F.C. and Jones, G.H. (2001) Nucleolus-associated telomere clustering and pairing precede meiotic chromosome synapsis in *Arabidopsis thaliana*. *J. Cell Sci.* **114**, 4207–4217.

Baumann, P., Podell, E. and Cech, T.R. (2002) Human Pot1 (Protection of telomeres) protein: cytolocalization, gene structure, and alternative splicing. *Mol. Cell. Biol.* **22**, 8079–8087.

Bilaud, T., Koering, C.E., Binet-Brasselet, E., Ancelin, K., Pollice, A., Gasser, S.M. and Gilson, E. (1996) The telobox, a Myb-related telomeric DNA binding motif found in proteins from yeast, plants and human. *Nucleic Acids Res.* **24**, 1294–1303.

Blackburn, E.H. and Gall, J.G. (1978) Tandemly repeated sequence at termini of extrachromosomal ribosomal RNA genes in *Tetrahymena*. *J. Mol. Biol.* **120**, 33–53.

Bowler, C., Benvenuto, G., Laflamme, P., Molino, D., Probst, A.V., Tariq, M. and Paszkowski, J. (2004) Chromatin techniques for plant cells. *Plant J.* **39**, 776–789.

Brown, J.W. and Shaw, P.J. (2008) The role of the plant nucleolus in pre-mRNA processing. *Curr. Top. Microbiol. Immunol.* **326**, 291–311.

Chen, L.Y., Redon, S. and Lingner, J. (2012) The human CST complex is a terminator of telomerase activity. *Nature*, **488**, 540–544.

Cifuentes-Rojas, C., Kannan, K., Tseng, L. and Shippen, D.E. (2011) Two RNA subunits and POT1a are components of Arabidopsis telomerase. *Proc. Natl Acad. Sci. USA* **108**, 73–78.

Cifuentes-Rojas, C., Nelson, A.D.L., Boltz, K.A., Kannan, K., She, X.T. and Shippen, D.E. (2012) An alternative telomerase RNA in Arabidopsis modulates enzyme activity in response to DNA damage. *Genes Dev.* **26**, 2512–2523.

Citovsky, V., Lee, L.Y., Vyas, S., Glick, E., Chen, M.H., Vainstein, A., Gafni, Y., Gelvin, S.B. and Tzfira, T. (2006) Subcellular localization of interacting proteins by bimolecular fluorescence complementation *in planta*. *J. Mol. Biol.* **362**, 1120–1131.

Clough, S.J. and Bent, A.F. (1998) Floral dip: a simplified method for *Agrobacterium*-mediated transformation of *Arabidopsis thaliana*. *Plant J.* **16**, 735–743.

Dvorackova, M., Rossignol, P., Shaw, P.J., Koroleva, O.A., Doonan, J.H. and Fajkus, J. (2010) AtTRB1, a telomeric DNA-binding protein from Arabidopsis, is concentrated in the nucleolus and shows highly dynamic association with chromatin. *Plant J.* **61**, 637–649.

Fajkus, J., Fulneckova, J., Hulanova, M., Berkova, K., Riha, K. and Matyasek, R. (1998) Plant cells express telomerase activity upon transfer to callus culture, without extensively changing telomere lengths. *Mol. Gen. Genet.* **260**, 470–474.

Fitzgerald, M.S., McKnight, T.D. and Shippen, D.E. (1996) Characterization and developmental patterns of telomerase expression in plants. *Proc. Natl Acad. Sci. USA* **93**, 14422–14427.

Gallego, M.E., Bleuyard, J.Y., Daoudal-Cotterell, S., Jallut, N. and White, C.I. (2003) Ku80 plays a role in non-homologous recombination but is not required for T-DNA integration in Arabidopsis. *Plant J.* **35**, 557–565.

Gao, H., Cervantes, R.B., Mandell, E.K., Otero, J.H. and Lundblad, V. (2007) RPA-like proteins mediate yeast telomere function. *Nat. Struct. Mol. Biol.* **14**, 208–214.

Giraud-Panis, M.J., Teixeira, M.T., Geli, V. and Gilson, E. (2010) CST meets shelterin to keep telomeres in check. *Mol. Cell* **39**, 665–676.

Grant, J.D., Broccoli, D., Muquit, M., Manion, F.J., Tisdall, J. and Ochs, M.F. (2001) Telometric: a tool providing simplified, reproducible measurements of telomeric DNA from constant field agarose gels. *Biotechniques*, **31**(1314–1316), 1318.

Greider, C.W. and Blackburn, E.H. (1985) Identification of a specific telomere terminal transferase activity in *Tetrahymena* extracts. *Cell*, **43**, 405–413.

Greider, C.W. and Blackburn, E.H. (1989) A telomeric sequence in the RNA of *Tetrahymena* telomerase required for telomere repeat synthesis. *Nature*, **337**, 331–337.

Hofr, C., Sultesova, P., Zimmermann, M., Mozgova, I., Schrumpfova, P.P., Wimmerova, M. and Fajkus, J. (2009) Single-Myb-histone proteins from *Arabidopsis thaliana*: a quantitative study of telomere-binding specificity and kinetics. *Biochem. J.* **419**, 221–228.

Horak, J., Grefen, C., Berendzen, K.W., Hahn, A., Stierhof, Y.D., Stadelhofer, B., Stahl, M., Koncz, C. and Harter, K. (2008) The *Arabidopsis thaliana* response regulator ARR22 is a putative AHP phospho-histidine phosphatase expressed in the chalaza of developing seeds. *BMC Plant Biol.* **8**, 77.

Hwang, M.G., Chung, I.K., Kang, B.G. and Cho, M.H. (2001) Sequence-specific binding property of *Arabidopsis thaliana* telomeric DNA binding protein 1 (AtTBP1). *FEBS Lett.* **503**, 35–40.

Hwang, M.G., Kim, K., Lee, W.K. and Cho, M.H. (2005) AtTBP2 and AtTRP2 in Arabidopsis encode proteins that bind plant telomeric DNA and induce DNA bending *in vitro*. *Mol. Genet. Genomics* **273**, 66–75.

Jurczyluk, J., Nouwens, A.S., Holien, J.K., Adams, T.E., Lovrecz, G.O., Parker, M.W., Cohen, S.B. and Bryan, T.M. (2011) Direct involvement of the TEN domain at the active site of human telomerase. *Nucleic Acids Res.* **39**, 1774–1788.

Kannan, K., Nelson, A.D. and Shippen, D.E. (2008) Dyskerin is a component of the Arabidopsis telomerase RNP required for telomere maintenance. *Mol. Cell. Biol.* **28**, 2332–2341.

Kappei, D., Butter, F., Benda, C. *et al.* (2013) HOT1 is a mammalian direct telomere repeat-binding protein contributing to telomerase recruitment. *EMBO J.* **32**, 1681–1701.

Karamysheva, Z.N., Surovtseva, Y.V., Vespa, L., Shakirov, E.V. and Shippen, D.E. (2004) A C–terminal Myb extension domain defines a novel family of double-strand telomeric DNA-binding proteins in Arabidopsis. *J. Biol. Chem.* **279**, 47799–47807.

Karimi, M., De Meyer, B. and Hilson, P. (2005) Modular cloning in plant cells. *Trends Plant Sci.* **10**, 103–105.

Kazda, A., Zellinger, B., Rossler, M., Derboven, E., Kusenda, B. and Riha, K. (2012) Chromosome end protection by blunt-ended telomeres. *Genes Dev.* **26**, 1703–1713.

Kuchar, M. and Fajkus, J. (2004) Interactions of putative telomere-binding proteins in *Arabidopsis thaliana*: identification of functional TRF2 homolog in plants. *FEBS Lett.* **578**, 311–315.

Kwon, C. and Chung, I.K. (2004) Interaction of an Arabidopsis RNA-binding protein with plant single-stranded telomeric DNA modulates telomerase activity. *J. Biol. Chem.* **279**, 12812–12818.

Lai, C.K., Mitchell, J.R. and Collins, K. (2001) RNA binding domain of telomerase reverse transcriptase. *Mol. Cell. Biol.* **21**, 990–1000.

de Lange, T. (2005) Shelterin: the protein complex that shapes and safeguards human telomeres. *Genes Dev.* **19**, 2100–2110.

de Lange, T. (2009) How telomeres solve the end-protection problem. *Science*, **326**, 948–952.

Lo, S.J., Lee, C.C. and Lai, H.J. (2006) The nucleolus: reviewing oldies to have new understandings. *Cell Res.* **16**, 530–538.

Lue, N.F. (2005) A physical and functional constituent of telomerase anchor site. *J. Biol. Chem.* **280**, 26586–26591.

Marian, C.O., Bordoli, S.J., Goltz, M., Santarella, R.A., Jackson, L.P., Danilevskaya, O., Beckstette, M., Meeley, R. and Bass, H.W. (2003) The maize *Single myb histone 1* gene, *Smh1*, belongs to a novel gene family and encodes a protein that binds telomere DNA repeats *in vitro*. *Plant Physiol.* **133**, 1336–1350.

McKeown, P., Pendle, A.F. and Shaw, P.J. (2008) Preparation of Arabidopsis nuclei and nucleoli. *Methods Mol. Biol.* **463**, 67–75.

Mozgova, I., Schrumpfova, P.P., Hofr, C. and Fajkus, J. (2008) Functional characterization of domains in AtTRB1, a putative telomere-binding protein in *Arabidopsis thaliana*. *Phytochemistry*, **69**, 1814–1819.

Mozgova, I., Mokros, P. and Fajkus, J. (2010) Dysfunction of chromatin assembly factor 1 induces shortening of telomeres and loss of 45S rDNA in *Arabidopsis thaliana*. *Plant Cell*, **22**, 2768–2780.

Nandakumar, J., Bell, C.F., Weidenfeld, I., Zaug, A.J., Leinwand, L.A. and Cech, T.R. (2012) The TEL patch of telomere protein TPP1 mediates telomerase recruitment and processivity. *Nature*, **492**, 285–289.

Nelson, A.D. and Shippen, D.E. (2012a) Blunt-ended telomeres: an alternative ending to the replication and end protection stories. *Genes Dev.* **26**, 1648–1652.

Nelson, A.D. and Shippen, D.E. (2012b) Surprises from the chromosome front: lessons from Arabidopsis on telomeres and telomerase. *Cold Spring Harb. Symp. Quant. Biol.* **77**, 7–15.

Peska, V., Sykorova, E. and Fajkus, J. (2008) Two faces of Solanaceae telomeres: a comparison between *Nicotiana* and *Cestrum* telomeres and telomere-binding proteins. *Cytogenet. Genome Res.* **122**, 380–387.

Peska, V., Schrumpfova, P.P. and Fajkus, J. (2011) Using the telobox to search for plant telomere binding proteins. *Curr. Protein Peptide Sci.* **12**, 75–83.

Pinto, A.R., Li, H., Nicholls, C. and Liu, J.P. (2011) Telomere protein complexes and interactions with telomerase in telomere maintenance. *Front. Biosci.* **16**, 187–207.

Price, C.M., Boltz, K.A., Chaiken, M.F., Stewart, J.A., Beilstein, M.A. and Shippen, D.E. (2010) Evolution of CST function in telomere maintenance. *Cell Cycle* **9**, 3157–3165.

Riha, K., Fajkus, J., Siroky, J. and Vyskot, B. (1998) Developmental control of telomere lengths and telomerase activity in plants. *Plant Cell*, **10**, 1691–1698.

Riha, K., McKnight, T.D., Fajkus, J., Vyskot, B. and Shippen, D.E. (2000) Analysis of the G–overhang structures on plant telomeres: evidence for two distinct telomere architectures. *Plant J.* **23**, 633–641.

Rotkova, G., Sykorova, E. and Fajkus, J. (2009) Protect and regulate: recent findings on plant POT1-like proteins. *Biol. Plant.* **53**, 1–4.

Ruckova, E., Friml, J., Prochazkova Schrumpfova, P. and Fajkus, J. (2008) Role of alternative telomere lengthening unmasked in telomerase knockout mutant plants. *Plant Mol. Biol.* **66**, 637–646.

Santos, J.H., Meyer, J.N., Skorvaga, M., Annab, L.A. and Van Houten, B. (2004) Mitochondrial hTERT exacerbates free-radical-mediated mtDNA damage. *Aging Cell*, **3**, 399–411.

Schrumpfova, P., Kuchar, M., Mikova, G., Skrisovska, L., Kubicarova, T. and Fajkus, J. (2004) Characterization of two *Arabidopsis thaliana* Myb-like proteins showing affinity to telomeric DNA sequence. *Genome*, **47**, 316–324.

Schrumpfova, P.P., Kuchar, M., Palecek, J. and Fajkus, J. (2008) Mapping of interaction domains of putative telomere-binding proteins AtTRB1 and AtPOT1b from *Arabidopsis thaliana*. *FEBS Lett.* **582**, 1400–1406.

Schrumpfova, P.P., Fojtova, M., Mokros, P., Grasser, K.D. and Fajkus, J. (2011) Role of HMGB proteins in chromatin dynamics and telomere maintenance in *Arabidopsis thaliana*. *Curr. Protein Peptide Sci.* **12**, 105–111.

Sealey, D.C., Zheng, L., Taboski, M.A., Cruickshank, J., Ikura, M. and Harrington, L.A. (2010) The N–terminus of hTERT contains a DNA-binding domain and is required for telomerase activity and cellular immortalization. *Nucleic Acids Res.* **38**, 2019–2035.

Sealey, D.C., Kostic, A.D., LeBel, C., Pryde, F. and Harrington, L. (2011) The TPR-containing domain within Est1 homologs exhibits species-specific roles in telomerase interaction and telomere length homeostasis. *BMC Mol. Biol.* **12**, 45.

Sfeir, A., Kosiyatrakul, S.T., Hockemeyer, D., MacRae, S.L., Karlseder, J., Schildkraut, C.L. and de Lange, T. (2009) Mammalian telomeres resemble fragile sites and require TRF1 for efficient replication. *Cell*, **138**, 90–103.

Shakirov, E.V., Surovtseva, Y.V., Osbun, N. and Shippen, D.E. (2005) The Arabidopsis Pot1 and Pot2 proteins function in telomere length homeostasis and chromosome end protection. *Mol. Cell. Biol.* **25**, 7725–7733.

Silhavy, D., Molnar, A., Lucioli, A., Szittya, G., Hornyik, C., Tavazza, M. and Burgyan, J. (2002) A viral protein suppresses RNA silencing and binds silencing-generated, 21- to 25-nucleotide double-stranded RNAs. *EMBO J.* **21**, 3070–3080.

Surovtseva, Y.V., Churikov, D., Boltz, K.A., Song, X.Y., Lamb, J.C., Warrington, R., Leehy, K., Heacock, M., Price, C.M. and Shippen, D.E. (2009) Conserved telomere maintenance component 1 interacts with STN1 and maintains chromosome ends in higher eukaryotes. *Mol. Cell* **36**, 207–218.

Surovtseva, Y. V., Shakirov, E. V., Vespa, L., Osbun, N., Song, X. and Shippen, D. E. (2007) Arabidopsis POT1 associates with the telomerase RNP and is required for telomere maintenance. *EMBO J.* **26**, 3653–3661.

Sykorova, E. and Fajkus, J. (2009) Structure–function relationships in telomerase genes. *Biol. Cell* **101**, 375–392.

Tani, A. and Murata, M. (2005) Alternative splicing of Pot1 (Protection of telomere)-like genes in *Arabidopsis thaliana*. *Genes Genet. Syst.* **80**, 41–48.

Voinnet, O., Rivas, S., Mestre, P. and Baulcombe, D. (2003) An enhanced transient expression system in plants based on suppression of gene silencing by the p19 protein of tomato bushy stunt virus. *Plant J.* **33**, 949–956.

Wu, F.H., Shen, S.C., Lee, L.Y., Lee, S.H., Chan, M.T. and Lin, C.S. (2009) Tape-*Arabidopsis* sandwich – a simpler *Arabidopsis* protoplast isolation method. *Plant Methods*, **5**, 16.

Wu, P., Takai, H. and de Lange, T. (2012) Telomeric 3′ overhangs derive from resection by Exo1 and Apollo and fill-in by POT1b-associated CST. *Cell*, **150**, 39–52.

Wyatt, H.D., Lobb, D.A. and Beattie, T.L. (2007) Characterization of physical and functional anchor site interactions in human telomerase. *Mol. Cell. Biol.* **27**, 3226–3240.

Yoo, H.H., Kwon, C., Lee, M.M. and Chung, I.K. (2007a) Single-stranded DNA binding factor AtWHY1 modulates telomere length homeostasis in Arabidopsis. *Plant J.* **49**, 442–451.

Yoo, S.D., Cho, Y.H. and Sheen, J. (2007b) Arabidopsis mesophyll protoplasts: a versatile cell system for transient gene expression analysis. *Nat. Protoc.* **2**, 1565–1572.

Zachova, D., Fojtova, M., Dvorackova, M., Mozgova, I., Lermontova, I., Peska, V., Schubert, I., Fajkus, J. and Sykorova, E. (2013) Structure–function relationships during transgenic telomerase expression in Arabidopsis. *Physiol. Plant.* **149**, 114–126.

Supporting Figures and Tables

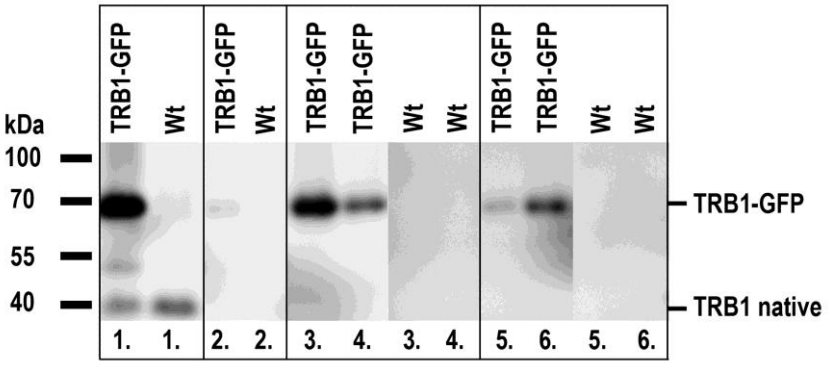

Figure S1
Detection of TRB1-GFP protein by specific anti-TRB1 1.2 antibody in ChIP fractions
20 µl of each ChIP fraction or 5 µl of GFP-TRAP_A Matrix were separated with SDS-PAGE, transferred to nitrocellulose membrane using standard wet western blot protocol and visualised with specific anti-TRB1 1.2 antibody (1:5 000) and secondary antibody anti-mouse HRP (DAKO) (1:10 000) 1. Input (chromatin after sonication); 2. Unbound (unbound chromatin that was previously diluted with ChIP buffer); 3. Matrix after chromatin binding before wash procedure; 4. Matrix after chromatin binding after whole wash procedure; 5. Matrix after elution; 6. Elution.

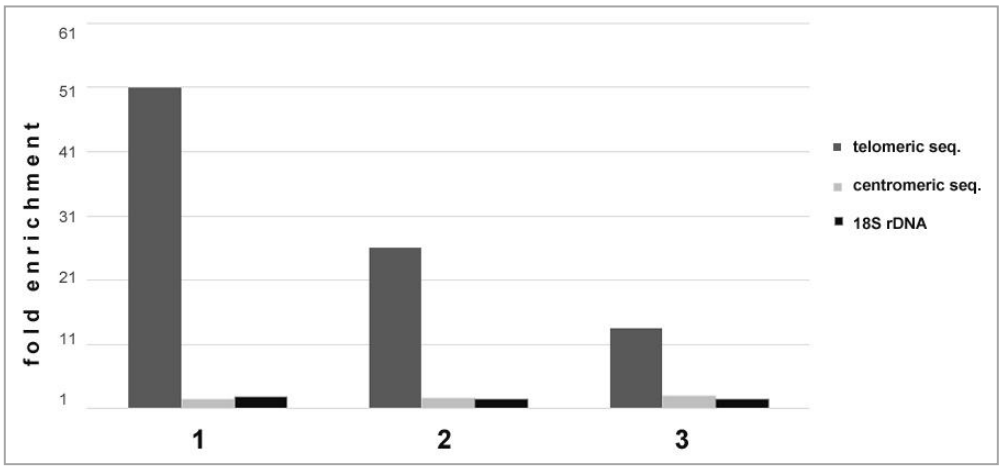

Figure S2
Telomeric sequence is highly enriched compared to the centromeric DNA or 18S rDNA
DNA cross-linked with TRB1 protein was isolated by ChIP analysis using GFP-TRAP_A matrix from Wt and *TRB1pro:TRB1-GFP* plants. Subsequent hybridisation of isolated TRB1-associated DNA with radioactively labelled telomeric, centromeric 18S rDNA probes in three biologically and technically replicated experiments has shown marked enrichment of telomeric DNA contrasting with only negligible enrichment of the centromeric DNA or 18S rDNA. The relative difference of the probed DNA co-precipitated with TRB1-GFP compared to the Wt was measured in each replicate (1, 2, 3; enrichment was related to Wt=1) using Multi Gauge software.

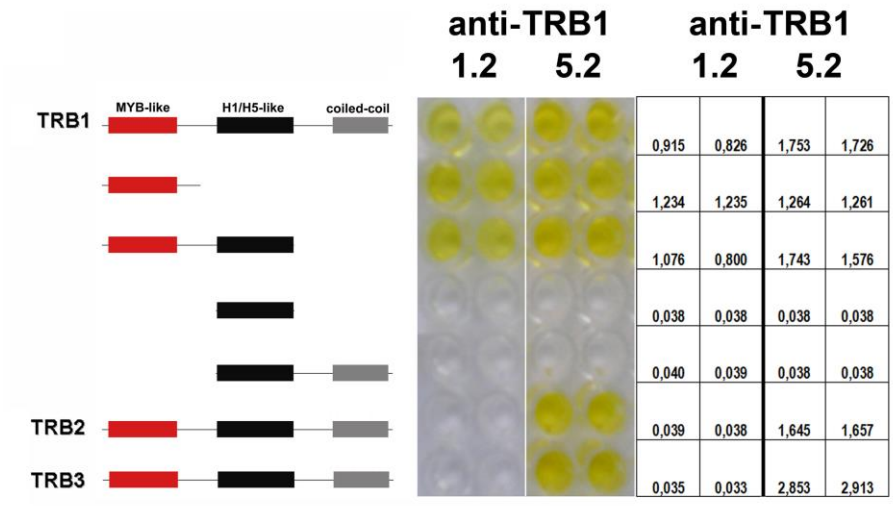

Figure S3

Location of antibody recognition sites within the structure of TRB1 protein with ELISA

Construction of vectors and protein expression/purification protocols of TRB1 - 3 proteins or TRB1 domains were previously described in (Schrumpfova, Kuchar et al. 2004, Mozgova, Schrumpfova et al. 2008). Purified proteins as antigens were coated onto a 96-well microtiter plate (Nunc MaxiSorp) with 500 ng / well of antigen. As primary antibody, we used supernatants of tested monoclonal hybridomes anti-TRB 1.2 and 5.2 (1:200). Colouring intensity of secondary antibody anti-mouse HRP (DAKO) (1:10 000) visualised with TMB (Test line) was measured as absorbance at 450 nm after 30min. Values of measured absorbance are listed in the table.

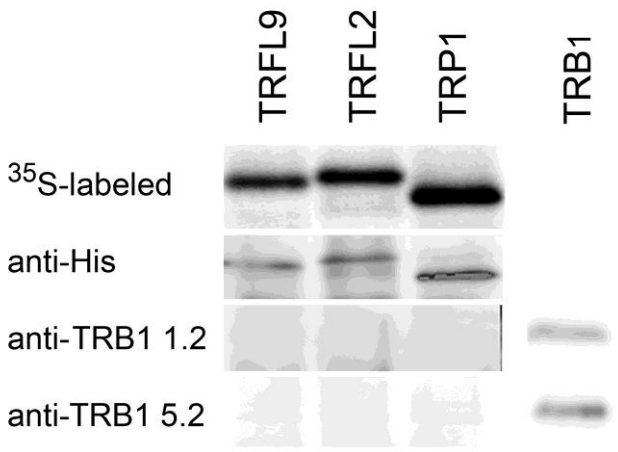

Figure S4

Anti-TRB 1.2 and 5.2 antibodies were unable to detect proteins from TRFL family

Genes coding for TRFL2, TRFL9 and TRP1 proteins were cloned into pET28 vector (Karamysheva, Surovtseva et al. 2004). Radioactively labeled proteins were synthesized by *in vitro* transcription and translation using rabbit reticulocyte system (Promega), separated with SDS-PAGE and transferred to nitrocellulose membrane (as described in (Schrumpfova, Kuchar et al. 2008)). Proteins were visualised using autoradiographic analysis with Typhoon FLA7000 (GE Healthcare) (^{35}S-labeled) or probed with the monoclonal antibodies (anti-His (Sigma); anti-TRB1 1.2; anti-TRB1 5.2 (1:5 000)). As a second antibody, polyclonal anti-mouse rabbit HRP (DAKO) was used. Both antibodies were diluted 1:5 000. Immunoreactive bands were visualised with LumiGLO Reagent and Peroxide (Cell Signaling Technology) a Fujifilm LAS-3000 CCD system. Extracts from isolated nuclei used in ChIP experiment were used as positive control (see Figure 3D).

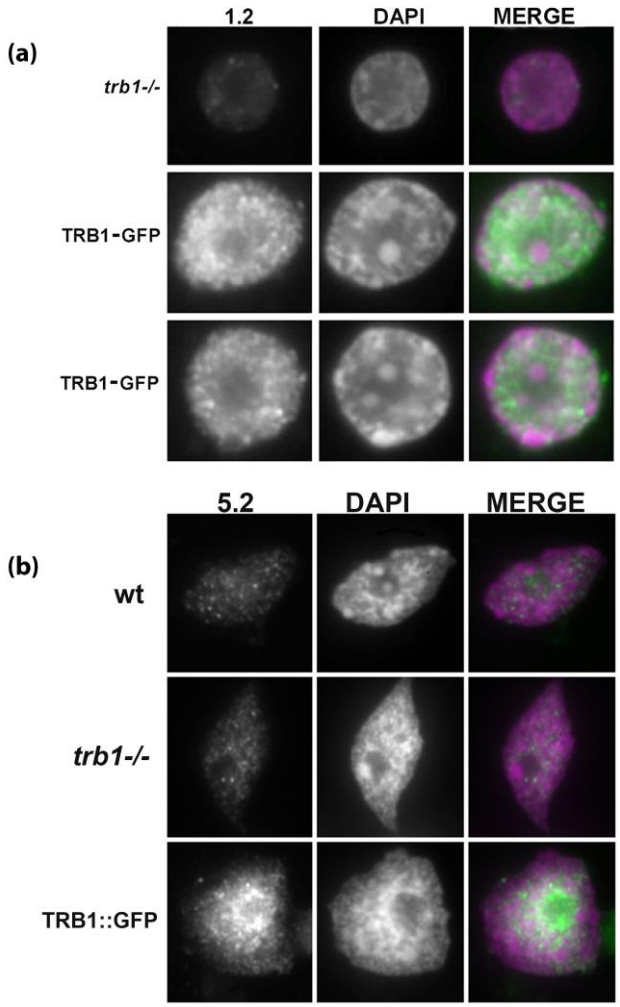

Figure S5

Anti-TRB1 1.2 does not detect any signal on *trb1-/-* plants, while 5.2 recognises some epitopes also in *trb1-/-* mutant plant lines

Antibodies 1.2 and 5.2. (green) were tested on isolated nuclei from *trb1-/-* and *TRB1pro:TRB1-GFP* plants (TRB1-GFP). Nuclei are counterstained with DAPI (magenta).

(a) 1.2 is specific to TRB1 protein since it recognises epitopes in the sample from TRB1-GFP plants, but not in *trb1-/-*.

(b) 5.2 antibody recognises also other members of the SMH protein family, thus producing a detectable signal in *trb1-/-* nuclei.

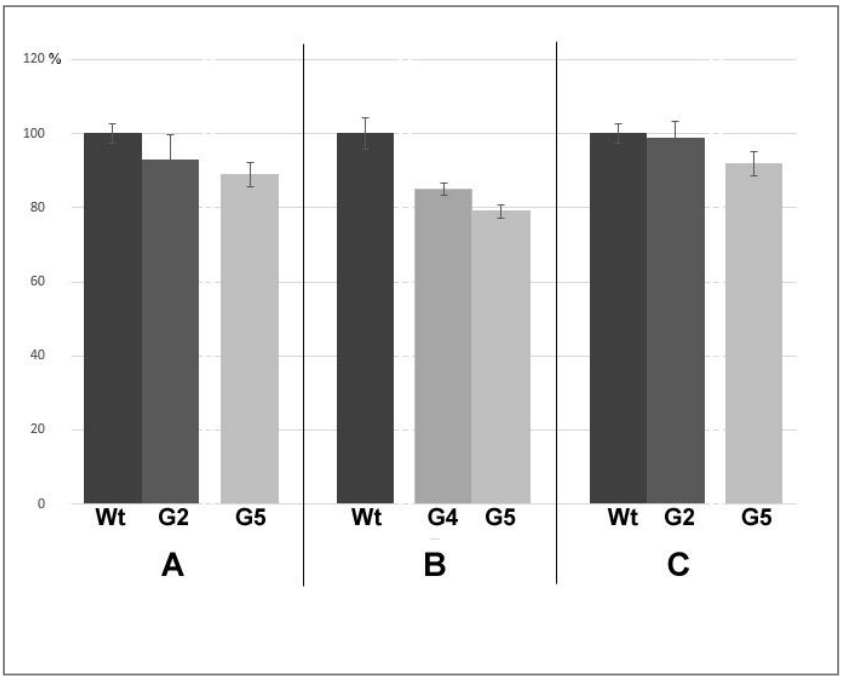

Figure S6

Telomere shortening in *trb1-/-* plants is moderately progressive.

Terminal restriction fragment analyses of *trb1-/-* plant lines A, B and C were performed in their 5th generation (G5) and in earlier generations (G2 or G4). Results are expressed relatively to the Wt control (Wt).

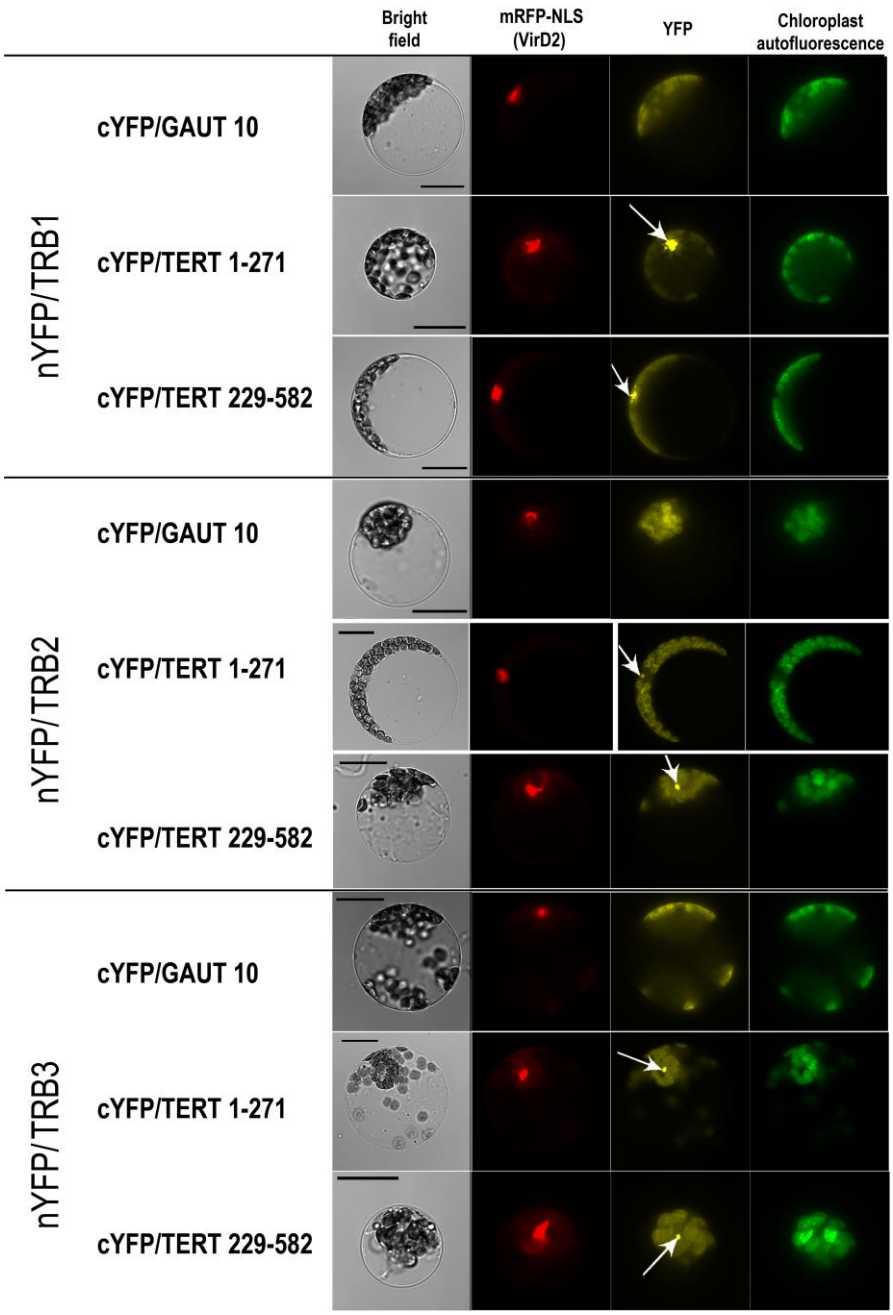

Figure S7

Whole images of protoplasts (whose segments are shown in Figure 5C) obtained by bimolecular fluorescence complementation.

Interactions of TRB proteins with TERT fragments are depicted with the arrows. Plasmids encoding nEYFP-tagged TRB clones, cEYFP-tagged TERT fragments or Gaut10 (as negative control), and mRFP-VirD2NLS (to mark cell nuclei and to determine transfection efficiency). [YFP fluorescence (yellow), mRFP fluorescence (red), and chloroplasts (green pseudocolor); chloroplast autofluorescence also visible in the YFP chanell]. Bar = 20 μm.

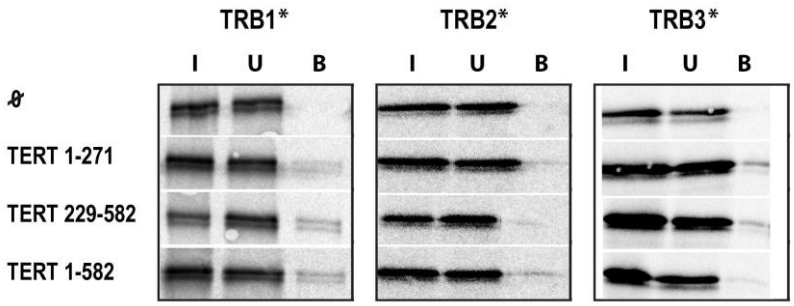

Figure S8
TRB1, 2 and 3 proteins are able to pull-down TERT fragments
The TNT expressed TRB1, 2 and 3 (35S-labelled*) were mixed with fragments of TERT (myc-tag) and incubated with anti-myc antibody. In the control experiment, the TRB proteins were incubated with myc-antibody and beads in the absence of partner protein. Input (I), unbound (U), and bound (B) fractions were collected and run in SDS–12% PAGE gels. Interactions of TRB2 and 3 proteins with TERT fragments appear to be relatively weaker than interaction between TRB1 and TERT fragments. Together, these results support yeast two-hybrid or bimolecular fluorescence complementation experiments.

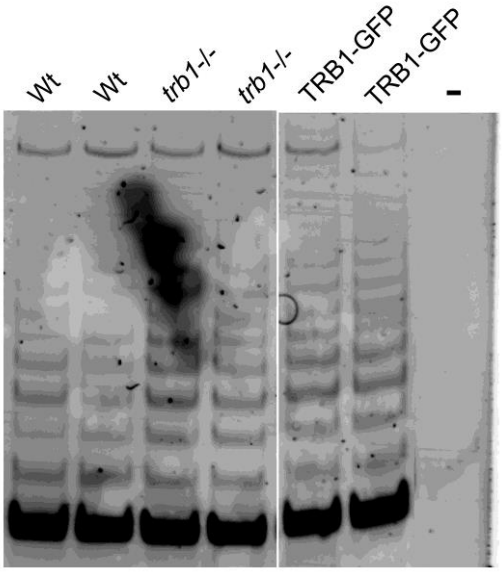

Figure S9
Telomerase activity or processivity *in vitro* is not changed in response to TRB1 status.
Ladder of telomeric repeats produced in TRAP assay (telomere repeat amplification protocol) has shown no differences in the *trb1* mutant or TRB1-GFP plant lines compared to wild-type lines. In negative control (-), no protein extract was used

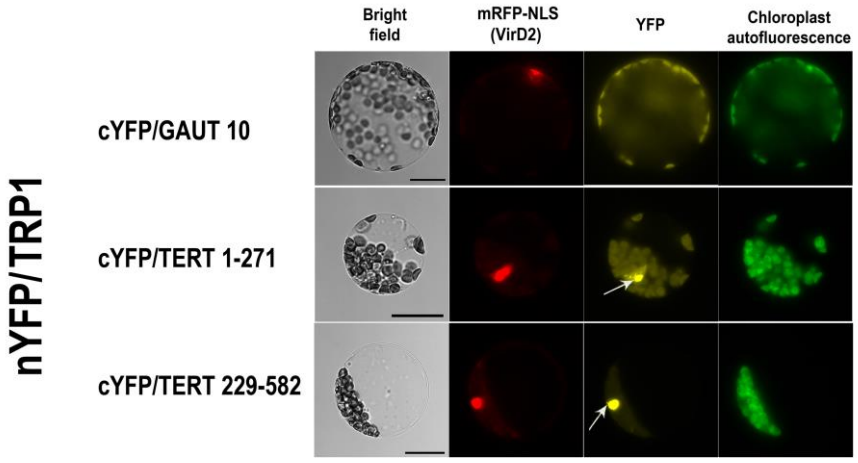

Figure S10
TRP1 protein interacts with plant telomerase (TERT)
Bimolecular fluorescence complementation has shown interaction of TRP1 protein with TERT fragments. *Arabidopsis* leaf protoplasts were transfected with 10 μg of each of plasmids encoding nEYFP-tagged TRP1 clones, cEYFP-tagged TERT fragments or Gaut10 (as negative control), and mRFP-VirD2NLS (to mark cell nuclei and to determine transfection efficiency). The cells were imaged by epifluorescence microscopy after overnight incubation. Protoplast image [YFP fluorescence (yellow), mRFP fluorescence (red), and chloroplasts (green pseudocolor); chloroplast autofluorescence also visible in the YFP chanell] we can observe clear nuclear interactions of TRP1 proteins with TERT fragments depicted with the arrows. Bar = 20 μm.

Table S1
Quantification of TRB1 foci co-localised/associated with telomeric foci
Isolated nuclei from leaves transformed with GFP-TRB1 were used for telomere PNA FISH. Number of fluorescence foci of GFP-TRB1 signal co-localised with telomeric signal is numbered in this Table. These FISH results showed that TRB1 speckles and telomere signals are associated (31%) or co-localised (59%) cases

IMAGE number	Telomeric foci	TRB1 foci	Colocalised telomeic foci	Associated telomeric foci
1	26	36	8	16
2	27	28	22	5
3	28	20	18	2
4	22	25	16	4
5	26	28	17	9
6	12	39	4	6
7	28	21	16	12
8	18	10	5	5
9	32	24	24	8
Foci total	219	231	130	67
%			**59**	**31**

Table S2
The sequences of all primers and probes used in this study.

Name	Sequence (5 ′→ 3 ′)
P1	GAGAGGAGAAGATAAAGATGTCACC
P2	CGTTCTCCCTTCCTAAACAGG
P3	CAACACTCAACCCTATCTCGG
P4	AGTATTCATATGGGTGCTCCTAAGCAGA
P5	CGGGATCCTCAGGCACGGATCATCATT
TR10-24-G	AGTACCAGCCATGACCAGCCATGA
TR10-24-C	TCATGGCTGGTCATGGCTGGTACT
TR-4C	CTAAACCCTAAACCCTAAACCCTAAACC
TS21	GACAATCCGTCGAGCAGAGTT
TEL-PR	CCGAATTCAACCCTAAACCCTAAACCCTAAACCC
5´UTR Fw	GGGGACAACTTTGTATAGAAAAGTTGTCCACCCATTAGAGGGACGAGTATGG
TRB1 Rev	GGGGAC TGC TTT TTTGTACAA ACTTGCGGCACGGATCATCTGTCGAAT
3´UTR Fw	GGGGACAGCTTTCTTGTACAAAGTGGCCggtaatggaaagcgagagaagaag
3´UTR Rev	GGGGACAACTTTGTATAATAAAGTTGCTATTTTAGTATGTCA AATTTCGGATGA
F-TRB1_BstBI	CCTTCGAAATGGGTGCTCCTAAGCAGAAATG
F-TRB2_BstBI	CCTTCGAAATGGGTGCACCAAAGCAGAAG
F-TRB3_BstBI	CCTTCGAAATGGGAGCTCCAAAGCTGAAG
R-TRB1_SmaI	ATCCCGGGGGCACGGATCATCATTTTGCAG
R-TRB2_SmaI	ATCCCGGGCCAAGGATGATTACGGATCCTG
R-TRB3_SmaI	ATCCCGGGCCGAGTTTGGCTATGCATTCTATAC
F-TERT_KpnI	atggtaccATGCCGCGTAAACCTAGACATC
R-RID1+BamHI	GAGGATCCTTAGGGAGTTATACAAGGAGCATTAC
F-F2N_KpnI	taggtaccGGCGAGGATGTAGACCAACAT
R-F2N+BamHI	GAGGATCCCTACCAGCTCCTTTTCCGGTA

Supplement I

Schrumpfová, P.P., Vychodilová, I., Hapala, J., Schořová, Š., Dvořáček, V., Fajkus, J., **2016**. Telomere binding protein TRB1 is associated with promoters of translation machinery genes in vivo. Plant Mol.Biol. 90, 189–206.

P.P.S. participated in the design of experiments, significantly involved in the experimental part, data evaluation, and in the ms writing and editing

Plant Mol Biol (2016) 90:189–206
DOI 10.1007/s11103-015-0409-8

Telomere binding protein TRB1 is associated with promoters of translation machinery genes in vivo

Petra Procházková Schrumpfová[1,2] · Ivona Vychodilová[1,2] · Jan Hapala[1,2] · Šárka Schořová[1,2] · Vojtěch Dvořáček[1,3] · Jiří Fajkus[1,2,3]

Received: 29 July 2015 / Accepted: 16 November 2015 / Published online: 23 November 2015

Abstract Recently we characterised TRB1, a protein from a single-myb-histone family, as a structural and functional component of telomeres in *Arabidopsis thaliana*. TRB proteins, besides their ability to bind specifically to telomeric DNA using their N-terminally positioned myb-like domain of the same type as in human shelterin proteins TRF1 or TRF2, also possess a histone-like domain which is involved in protein–protein interactions e.g., with POT1b. Here we set out to investigate the genome-wide localization pattern of TRB1 to reveal its preferential sites of binding to chromatin in vivo and its potential functional roles in the genome-wide context. Our results demonstrate that TRB1 is preferentially associated with promoter regions of genes involved in ribosome biogenesis, in addition to its roles at telomeres. This preference coincides with the frequent occurrence of telobox motifs in the upstream regions of genes in this category, but it is not restricted to the presence of a telobox. We conclude that TRB1 shows a specific genome-wide distribution pattern which suggests its role in regulation of genes involved in biogenesis of the translational machinery, in addition to its preferential telomeric localization.

Keywords Telomere repeat binding (TRB) · ChIP-seq · *Arabidopsis thaliana* · Ribosome · snoRNA · Translation machinery

Electronic supplementary material The online version of this article (doi:10.1007/s11103-015-0409-8) contains supplementary material, which is available to authorized users.

✉ Jiří Fajkus
fajkus@sci.muni.cz

[1] Mendel Centre for Plant Genomics and Proteomics, CEITEC – Central European Institute of Technology, Masaryk University, Kamenice 5, 625 00 Brno, Czech Republic

[2] Laboratory of Functional Genomics and Proteomics, National Centre for Biomolecular Research, Faculty of Science, Masaryk University, Kamenice 5, 625 00 Brno, Czech Republic

[3] Institute of Biophysics, Academy of Sciences of the Czech Republic, v.v.i., Královopolská 135, 61265 Brno, Czech Republic

Introduction

Telomere binding proteins and their complexes, exemplified by the shelterin complex in vertebrates (de Lange 2005), perform essential functions at chromosome ends. Primarily, they inhibit DNA-damage responses at telomeres to protect them from being mis-recognized as unrepaired chromosome breaks, thus solving the so-called end-protection problem (Sfeir and de Lange 2012) of linear chromosomes. Other functions of telomere proteins include, for example, telomerase recruitment and coordination of telomere elongation by telomerase with lagging strand synthesis by DNA polymerase during telomere replication (thereby solving the end-replication problem) (Latrick and Cech 2010; Sfeir et al. 2009; Soudet et al. 2014). However, the functions attributed to telomere-binding proteins are presumably not the original functions of these proteins in earlier stages of evolution, which preceded the onset of linear chromosomes connected with the necessity to solve the end-replication problem (Fajkus et al. 2005; Louis and Vershinin 2005; Nosek and Tomaska 2003; Valach et al. 2011). Examples supporting this notion can be seen, for example, in DNA repair proteins which paradoxically are also implicated in the control of telomere organization and length although their

presence at telomeres apparently contradicts the end-protective telomere functions (Kazda et al. 2012; Weaver 1998).

One of the best known telomere-binding proteins in budding yeast, the repressor-activator protein 1 (RAP1), is also well known for its involvement in gene activation and repression and in DNA replication. Further studies have examined additional roles for RAP1 in heterochromatin boundary-element formation, creation of hotspots for meiotic recombination, and chromatin opening (reviewed in Morse 2000). The TTAGGG DNA repeat-binding proteins 1 and 2 (TRF1 and TRF2) bind to mammalian telomeres as part of the shelterin complex and are essential for maintaining chromosome end stability. While most of their binding sites identified in a chromatin immunoprecipitation sequencing (ChIP-seq) study corresponded to telomeric regions, these two proteins also localize to extratelomeric sites (Simonet et al. 2011) of which the vast majority contain interstitial telomeric sequences (ITSs). However, non-ITS sites were also identified which correspond to centromeric and pericentromeric satellite DNA, and these TRF-binding sites are often located in the proximity of genes or within introns. It was thus suggested that TRF1 and TRF2 may couple the functional state of telomeres to the long-range organization of chromosomes and gene regulation networks by binding to extratelomeric sequences (Simonet et al. 2011). Even the specific telomere-elongation tool, telomerase, is involved in a number of non-telomeric processes (reviewed in Majerska et al. 2011). These examples demonstrate that the function of telomere-localized proteins may not be exclusively telomere-associated and that telomere metabolism/protection may be mediated by proteins which play more general roles in the genome.

Understanding of the composition and function of telomere-binding protein complexes in plants lags behind that in animals and yeasts. Nevertheless, we have recently characterized a key candidate shelterin-like component belonging to the plant-specific single-myb-histone group of proteins termed TRB (Telomere repeat binding) (Schrumpfova et al. 2014). In addition to our earlier studies which demonstrated specific binding of proteins from this group to telomeric DNA in vitro (Schrumpfova et al. 2004) and characterized their DNA-protein and protein–protein interactions in detail (Hofr et al. 2009; Mozgova et al. 2008; Prochazkova Schrumpfova et al. 2008), our recent study revealed preferential co-localization of a member of this group, TRB1, with telomeres in situ and in vivo, telomere shortening in *trb1* knockout mutants, and moreover its physical interaction with the catalytic subunit of telomerase, TERT (Prochazkova Schrumpfova et al. 2014). These results, together with our previous findings of TRB1 interaction with POT1b protein, one of the paralogs of Protection Of Telomeres (POT1) protein (Kuchar and Fajkus 2004; Schrumpfova et al. 2008) and the data on interaction of POT1 proteins with telomerase (Cifuentes-Rojas et al. 2011; Rossignol et al. 2007), make this protein currently the best-established component of a putative plant shelterin complex.

In addition to the results demonstrating sequence-specific binding of TRB1 to telomeric DNA and corresponding telomere-specific functions, this protein is also capable of binding to chromatin through protein–protein interactions or sequence-non-specific interactions with DNA via its H1/H5-like domain (Mozgova et al. 2008). In vivo, the protein shows highly dynamic association with chromatin and preferential localization to the nucleus and the nucleolus during interphase (Dvorackova et al. 2010). TRB1 localization is cell cycle-regulated, as the level of nuclear-associated TRB1 diminishes during mitotic entry and it progressively re-associates with chromatin during anaphase/telophase. Using fluorescence recovery after photobleaching and fluorescence loss in photobleaching, we determined that TRB1 interaction with chromatin is regulated at two levels at least, one of which is coupled with cell-cycle progression with the other involving rapid exchange (Dvorackova et al. 2010). These results strongly suggest additional roles for TRB1 connected with chromatin function.

In this study, we thus set out to investigate the genome-wide localization pattern of TRB1 to examine its preferential sites of binding to DNA in vivo and its potential functional roles in the genome-wide context. Using ChIP followed by next generation sequencing (ChIP-seq), we show that TRB1 associates with promoter regions of certain genes in addition to binding long telomeric repeats. Classification of these genes using GO analysis revealed a strong link between TRB1 binding and promoters of translation machinery-related genes.

Materials and methods

Plant material and construct generation

The *TRBpro:GFP-TRB1* and *trb1−/−* plants and constructs were described previously (Schrumpfova et al. 2014). All the *A. thaliana* plants used in this study have a *Col0* background.

Chromatin immunoprecipitation assay

The ChIP assay was performed as described (Bowler et al. 2004) with modifications described in (Schrumpfova et al. 2014). Chromatin extracts were prepared from seedlings treated with 1 % formaldehyde. The chromatin from

isolated nuclei was sheared to an average length of 250–500 bp by sonication (Bioruptor, Diagenode) and centrifuged. Anti-TRB1 5.2 antibody (Schrumpfova et al. 2014) was bound to a Protein G agarose matrix (Pierce) for 3 h at 4 °C which was subsequently washed with ChIP dilution buffer (16.7 mM Tris–HCl, pH 8.0, 1.2 mM EDTA, 167 mM NaCl, 0.1 % Triton X-100, 0.1 mM PMSF and protease inhibitors). The experimental procedures for isolating TRB-GFP protein on GFP-TRAP_A (Chromtec) and native TRB1 protein on an Protein G agarose matrix (Pierce) with bound anti-TRB1 antibody were as described in (Schrumpfova et al. 2014). Both matrices were blocked against non-specific interaction with 200 mM ethanolamine, 1 % BSA and TR10-24-G and TR10-24-C (Schrumpfova et al. 2014), incubated with chromatin diluted with ChIP dilution buffer, and subsequently washed with low salt; high salt; LiCl; TE buffers as in Bowler (Bowler et al. 2004). The cross-linking was reversed by 0.2 M NaCl overnight followed by proteinase K (Serva) treatment, phenol/chlorophorm extraction, and RNase A (Serva) treatment.

ChIP-qPCR and RT-qPCR reactions

Primers used for ChIP-qPCR are described in Fig. 4 and are listed in Supplementary Table S1a. Three ul of ChIP DNA was added to the 20 ul reaction mix of FastStart SYBR Green Master (Roche) and the final concentration of each forward and reverse primer was 0.4 uM. Reactions were done in triplicate; the PCR cycle consisted of 5 min of initial denaturation at 95 °C followed by 40 cycles of 5 s at 95 °C, 20 s at 60 °C and 15 s at 72 °C. At least two biological replicates in two technical replicates were analysed. The relative copy number of each selected gene in Wt (−) or TRB-GFP (+) samples compared to that in the genomic input fraction was calculated by the $2^{-\Delta Ct}$ method (Pfaffl 2004).

Total RNA was isolated from *Arabidopsis* seedlings using the RNeasy Plant Mini Kit (Qiagen) followed by the DNaseI treatment (TURBO DNA-free, Applied Biosystems/Ambion) according to the manufacturers' instructions. The quality and quantity of RNA was checked by electrophoresis on 1 % (w/v) agarose gels and by absorbance measurement (NanoPhotometr IMPLEN). cDNA was prepared by reverse transcription of 1 µg of RNA using M-MuLV reverse transcriptase (NEB) and Random Nonamers (Sigma). Quantification of the transcripts of translation machinery related genes was related to the ubiquitin reference gene and was done using qPCR GreenMaster with UNG/lowROX (Jena Bioscience) by the Rotorgene6000 (Qiagen) machine. Four µl of 12× diluted cDNA was added to the 20 µl reaction mix; the final concentration of each forward and reverse primer was 0.3 µM (Supplementary Table S1b). Reactions were done in triplicates; the PCR program consisted of 5 min of initial denaturation at 95 °C followed by 40 cycles of 15 s at 95 °C, 20 s at 58 °C and 30 s at 72 °C. Analyses were performed for at least three biological replicates in three technical replicates. Transcript levels of chosen genes in the *trb1−/−* (Schrumpfova et al. 2014) were normalized to Ubq10 transcript and presented "relative transcript levels" were calculated as the fold increase/decrease relative to respective wild-type seedlings using ($2^{-\Delta\Delta Ct}$) method (Pfaffl 2004).

Library preparation and sequencing

Library preparation and sequencing was done by the European Molecular Biology Laboratory (EMBL) Genomics Core Facility, Heidelberg, Germany. Fifty microliters of immunoprecipitated DNA [0.2–6 ng DNA measured by Qubit dsDNA HS Assay Kit (Invitrogen)] was used for library preparation using NEBNext ChIP Seq Library Prep Master Mix (NEB), with Agencourt XP beads (Beckman) in the ratios described in the protocol with only one exception, dilution of the Adapter 1:17 in water. DNA fragments of 270–300 bp were selected on 2 % e-gels (Invitrogen). Subsequently, a PCR reaction (18 cycles) with indexed Primers 1–11 from the NEBNext Multiplex Oligo set (NEB) was performed.

The quality of the final libraries was checked on the Bioanalyzer (Agilent) and the quantity with the Qubit dsDNA HS Assay Kit (Invitrogen). The libraries were pooled equimolar and diluted to 10 pM (denaturation in NaOH) in Hyb Buffer 1 (HT1) from the TruSeq SR Cluster Kit v3-cBot-HS (Illumina). Libraries were sequenced (50 bp single-end reads) on an Illumina HiSeq 2500 using TruSeq SBS Kit v3-HS (Illumina) sequencing reagents.

Bioinformatic methods

Sequence logo construction

The sequence logo was created using a *k*-mer analysis. We counted all substrings of length *k* in two datasets, the 5′ UTR sequences and the 5′ UTR peak-covered regions only. We decided to use 8-mers sorted by their number of occurrence, and for fragment reconstruction used only those whose number was at least twice as high in peak regions as in the whole 5′ UTR dataset. The fragment was constructed by a modified version of the algorithm described in (Macas et al. 2010), and instead of extending the whole prefix and subsequently the whole suffix we extended both the prefix and the suffix alternately by one nucleotide. As fragments are composed of *k*-mers with diverse frequencies, every base of each fragment was

assigned a weight representing the frequency of its *k*-mer of origin. For better matching, some fragments were used as their reverse complements with preference for C-rich variants of DNA. Fragments were aligned with MUSCLE (Edgar 2004). The sequence logo (Schneider and Stephens 1990) was then generated from fragments with mean weight higher than 20. The y-axis displays position weights totalled from the aligned fragments.

Read mapping and filtration

We mapped the Illumina fastq reads onto the reference genome of *Arabidopsis thaliana* (A_thaliana_Jun_2009) with Bowtie2 (using the very-sensitive option) (Langmead and Salzberg 2012). Unmapped reads or reads with a low quality mapping score (<25) were removed. Biological replicates were merged into single files. The coverage of the mitochondrial DNA was negligible compared to the chromosomal DNA, while the chloroplast DNA was represented in the data more frequently. Therefore, we separated the reads from each dataset into three files, genomic, mitochondrial and chloroplast sequences, and peaks were called for all groups independently. However, we did not detect any peaks in mitochondria and chloroplasts. We used average profiles and heatmaps to illustrate the distribution of ChIP-seq reads along genes (±2000 bp). The pictures were produced by ngs.plot (Shen et al. 2014) with parameters –R genebody, –F protein_coding.

Peak calling

We called peaks in the data files using two programs, MACS v. 1.4.3 20131216 and PePr v. 1.0.2 (Zhang et al. 2008b, 2014). MACS is one of the most widely used programs for peak calling in sequencing data while PePr is a new peak-calling software which detected peaks visually more accurately in our data.

With MACS (parameters: effective genome size—g: 90000000, band width—bw 250, keeping all duplicate reads—keep-dup all, ChIP/control scaling ratio—ratio 1.215273 and 1.742786 for the first and second replicate, respectively) we obtained a set of peaks for each of the two replicates. The ChIP/control scaling ratios were calculated with NCIS (Liang and Keles 2012). We selected peaks with a false discovery rate (FDR) below 5 % from each replicate and calculated an intersection of these two sets. We produced another set of peaks with PePr (parameters: –peak-type = sharp) which accepts two replicates (both input and control files) and returns only peaks present in both of them. PePr peaks with too short (<30 bp) estimated fragment lengths in any of the two samples were removed (1879 peaks). Finally, we made an intersection (4995) of the PePr (24,219) and MACS (3690) peaks.

Peak analysis

We studied the relative amount of peaks in genomic regions with different functions. We downloaded annotated datasets provided by TAIR (ftp://ftp.arabidopsis.org/home/tair/Sequences/blast_datasets/TAIR10_blastsets/) that contain sequences separated with respect to their position within or outside of genes. We converted these FASTA files into genomic coordinate files (BED) and calculated intersections with the 4995 TRB1 genomic peaks.

Reference datasets

We examined intersections with 5′ UTR, 3′ UTR (variable length), upstream and downstream sequences (500 bp) and intergenic regions (variable length, trimmed by 1000 bp at both ends). In addition, we created a dataset of coding sequences derived from a coordinate file TAIR10_GFF3_genes.gff also provided by TAIR.

Coverage quantification

We calculated dataset coverage as the length of each reference dataset relative to the genome size. Overlapping base pairs of sequences of the same type (i.e. those on opposite strands) were counted once. In addition, for each dataset peak coverage was obtained as the total length of the dataset-peak intersection relative to the total size (bp) of the dataset. Finally, peak relative occurrence represents the number of peaks intersecting with any sequence of the particular dataset relative to the total size of the dataset (presented in Mb). In all cases, two elements intersect each other if they have at least 1 bp-overlap.

Quantification of telomeric, centromeric and 18SrDNA sequences

We analysed the unprocessed Illumina files for the occurrence of telomeric, centromeric and 18SrDNA sequences by counting the number of reads containing their respective sequence motifs, in particular AAACCCTAAACCC TAAACCCT for telomeres, TATGAGTCTTTGGCTTT GTGTCTT for centromeres, and CTAGAGCTAATACGT GCAACAAAC for 18SrDNA.

Telo-box occupation

We examined sequences from all reference datasets for the presence of a telobox (any of AAACCCTA, AACCCTAA, ACCCTAAA, TAAACCCT, TAGGGTTT, TTAGGGTT, TTTAGGGT and AGGGTTTA). Sequences containing one or more telo-boxes were included. Next, we counted

telo-boxes intersected by a TRB1 peak and calculated telo-box peak coverage as the ratio of these two numbers.

Gene ontology (GO) enrichment

We analysed the GO database using the program GoMiner (v. 2011-01) (Zeeberg et al. 2003, 2005). Only GO categories with a p value higher than 0.05 and categories with size 5–500 genes were arranged graphically in CIMminer software (http://discover.nci.nih.gov/cimminer/).

Data availability

The data have been deposited in NCBI's Gene Expression Omnibus (Edgar et al. 2002) and are accessible through GEO Series accession number GSE69431 (http://www.ncbi.nlm.nih.gov/geo/query/acc.cgi?acc=GSE69431).

Results

TRB1 is associated with telomeric sequences in vivo

Previously, we described the co-localization of TRB1 protein with telomeres in situ and showed that TRB1 can bind DNA containing telomeric sequences in vivo (Schrumpfova et al. 2014). Since TRB1 is capable of binding telomeric (via its myb-like domain) as well as non-telomeric DNA (via its histone-like domain) (Hofr et al. 2009; Mozgova et al. 2008; Schrumpfova et al. 2014), we pondered whether TRB1 is localized exclusively to telomeres or has also other binding sites in the genome in vivo. To address this question, we performed next-generation sequencing of DNA isolated by ChIP of native or GFP-tagged TRB1.

As source material, we used formaldehyde cross-linked *Arabidopsis* seedlings stably transformed with a construct driven by the native promoter TRB1pro:TRB1-GFP [TRB1-GFP (+)] (Dvorackova et al. 2010). Wild-type plants were used as negative controls [Wt (−)]. The experimental setup is depicted schematically in Fig. 1a for anti-GFP-TRB1. TRB1-GFP protein was immunoprecipitated from purified nuclei using a GFP-Trap A matrix which contains a single variable antibody domain that recognizes GFP, as described in (Schrumpfova et al. 2014). Furthermore, we performed another ChIP analysis using anti-TRB1 (5.2) antibody that specifically recognizes the conserved region of the myb domain of TRB proteins (Schrumpfova et al. 2014) (Fig. 1b). Native TRB1 protein was isolated from wild-type plants [TRB1 (+)] using Protein G magnetic beads. In the negative control, no antibody was used in a parallel ChIP [Wt (−)]. DNA recovered from ChIP underwent ultra-high-throughput Illumina sequencing.

For evaluation purposes, arrays of at least three perfect telomeric repeats [$(AAACCCT)_3$] were considered as "long telomeric repeats" and reads containing them were counted in each sequenced sample. The relative differences in the numbers of long telomeric repeats in TRB1-GFP (+) or TRB1 (+) samples were expressed relative to the relevant Wt (−) = 1 (Fig. 1c). Absolute values confirmed our previous results (Schrumpfova et al. 2014) and demonstrated that the observed enrichment of long telomeric sequences in these samples is not due to the high copy number of telomeric DNA in the *Arabidopsis* genome but due to sequence-specific association of TRB1 with telomeric sequences. No enrichment of other repetitive sequences examined—centromeric DNA or 18S rDNA—was found in the ChIP-seq data.

Association of TRB1 with euchromatin in vivo

To define the genomic regions that are associated with TRB1 protein, we mapped the ChIP-seq data onto the TAIR A_thaliana_Jun_2009 assembly (TAIR10 annotation) and visualised the data using Integrative Genomics Viewer (IGV). To limit falsely identified peaks in the data, we used two independent peak calling programs, MACS and PePr (for details see Methods). We examined peaks in all five chromosomes of *A. thaliana*. Only peaks detected by both programs in both ChIP approaches (anti-GFP-TRB1 and anti-TRB1) were used in subsequent analysis. This set contains 4995 peaks and here we term it *"TRB1 genomic peaks"*. No peaks were detected in mitochondrial or chloroplast DNA. However, mitochondrial DNA coverage was negligible compared to the nuclear DNA.

TRB1 genomic peaks are absent in centromeric regions or heterochromatic knobs localized on chromosomes 4 and 5, but appear associated with euchromatic genes in both variants of ChIP (Fig. 2a, b, and Fig. S1). As the TAIR9 assembly lacks clusters of repetitive sequences, long telomeric tracts or 45S rDNA repetitive sequences are not visible in the IGV viewer. Figure 2c shows the detailed enrichment of DNA regions in TRB1-GFP (+) and TRB1 (+) samples that were immunoprecipitated by ChIP and sequenced. It can be seen that only DNA regions in TRB1-GFP (+) or TRB1 (+) samples which were highly enriched with respect to the Wt (−) were considered as *TRB1 genomic peaks* (marked with an asterisk). The data have been deposited in NCBI's Gene Expression Omnibus (Edgar et al. 2002) and are accessible through GEO Series accession number GSE69431 (http://www.ncbi.nlm.nih.gov/geo/query/acc.cgi?acc=GSE69431).

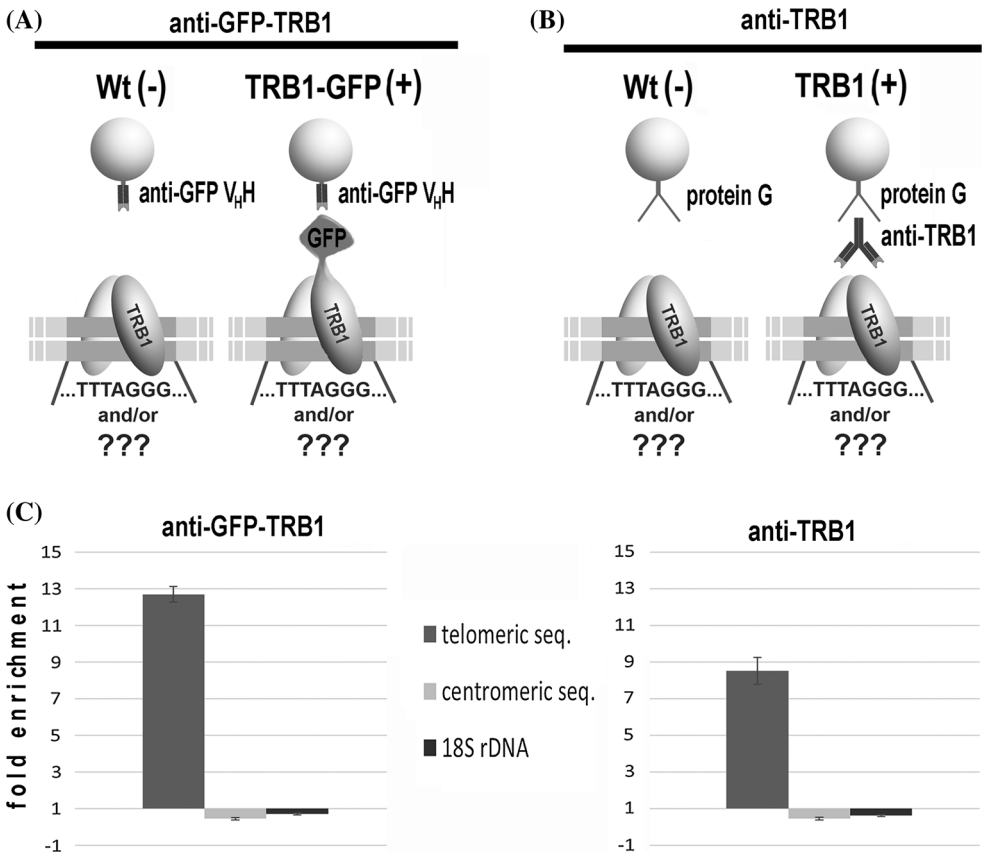

Fig. 1 Long telomeric tracts are tandem repeats preferentially targeted by TRB1 genome-wide. Schematic illustration of the two different approaches used in ChIP analysis: **a** first, TRB1 tagged with GFP was isolated using a GFP-Trap A matrix from crosslinked wild-type [Wt (−)] and *TRB1pro:TRB1-GFP* [TRB-GFP (+)] seedlings. **b** Second, native-TRB1 [TRB1 (+)] protein was isolated from crosslinked seedlings using anti-TRB1 antibody linked to a Protein G matrix; wild-type seedlings [Wt (−)] were used as a negative control. The associated DNA was subjected to next-generation sequencing (NGS) using the Illumina platform. Two biological replicates were analysed by both approaches. **c** Marked enrichment of long telomeric DNA repeats $(AAACCCT)_3$ compared to other repetitive sequences (centromeric or 18S rDNA) in ChIP-seq samples showing preferred association of TRB1 with telomeric sequence. The relative difference in the amount of the selected repetitive sequence was measured in each sequenced sample (biological replica) separately and enrichment was expressed relative to the relevant [Wt (−) = 1]

Analysis of TRB1 targets

To examine preferential targeting of TRB1 protein to specific *Arabidopsis* genome loci we visualized distribution of ChIP-seq reads along protein-coding genes genes. Clear enrichment of TRB1 was observed in the vicinity of transcription start sites (TSS) and transcription end sites (TES) using both purification approaches—anti-GFP-TRB1 and anti-TRB1 (Fig. 3).

For a more detailed resolution of TRB1 association with specific parts of genes, gene families and also non-protein coding genes we established various datasets covering specific parts of the *A. thaliana* genome according to TAIR10 blastsets (ftp://ftp.arabidopsis.org/home/tair/Sequences/blast_datasets/TAIR10_blastsets/). The major division of these datasets is into *Protein coding genes* and *Non-protein coding genes* (Fig. 4a, yellow boxes). The group of *Non-protein coding genes* includes rRNA, snoRNA, snRNA, tRNA, ncRNA, miRNA, other RNAs, pseudogenes and transposable element genes. In the vicinity of both *Protein coding* and *Non-protein coding gene* categories, datasets designated as *Upstream 500 bp* (from TSSs) or *Downstream 500 bp* (from TES) were classified. Moreover, four extra datasets close to the *Protein coding genes* sets were analysed: *5′ UTR*, *3′ UTR*, *Upstream translation start 500 bp*, and *Downstream translation stop 500 bp*. To clearly distinguish associations of all datasets that closely surround coding genes with which the TRB1 protein is associated, we designed a further dataset named *Intergenic* covering regions beginning more than 500 bp in front of the *Upstream 500 bp* or more than 500 bp behind the *Downstream 500 bp* datasets, i.e. 1000 bp distant from the transcription start or stop site of *Protein* or of *Non-protein coding genes*.

The relative coverage of the whole *A. thaliana* genome by each dataset (e.g., the dataset *Upstream 500 bp of*

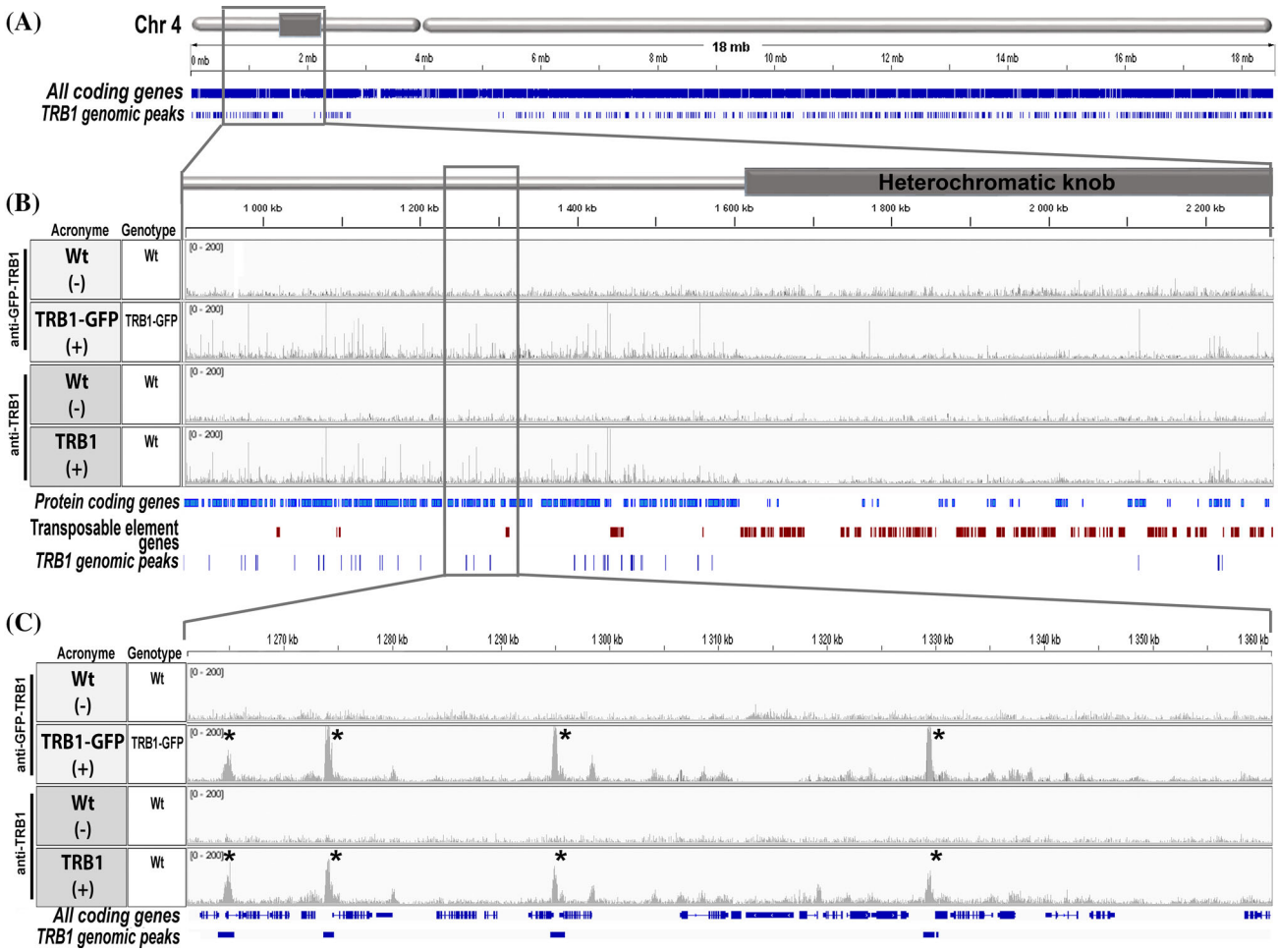

Fig. 2 TRB1 is preferentially associated with euchromatic regions. **a** IGV view of *All coding genes*, i.e. *Protein coding genes* and *Non-protein coding genes* (transposable element genes, rRNA, snoRNA, snRNA, tRNA, ncRNA, miRNA and pseudogenes) on chromosome 4. Regions where TRB1 binding was enriched are depicted as *TRB1 genomic peaks*. The absence of TRB1 association in the centromeric region and the heterochromatic knob (*grey box*) is visible. **b** IGV view of a 1.4 Mb region of the short arm of chromosome 4 (position 0.9–2.3 Mb) where the heterochromatin knob is located. Only *Protein coding genes* or "Transposable element genes" are depicted in separate lines below (modified from GBrowse). Significant enrichment of the TRB1-associated regions within euchromatin is visible not only as increasing peaks in IGV viewer [*boxes*: TRB1-GFP (+) and TRB1 (+)] but also in the line *TRB1 genomic peaks*. **c** The IGV view of a 620 kb region displays regions highly associated with TRB1 proteins used for further analyses (*asterisk*)

Protein coding genes covers 10.8 % of the whole genome) and the coverage of individual datasets by *TRB1 genomic peaks* obtained by combining both purification approaches (see above), is listed in Fig. 4b. It can be seen that in the vicinity of *Protein coding genes*, approximately 10 % of *Upstream* datasets (green boxes, 9.7–9.9 %) are covered by the TRB1 protein. This is approximately twice the value for TRB1 association with the entire *Protein coding genes* (yellow box, 3.9 %) or *Downstream* datasets (blue boxes, 4.8–6 %) although generally *Upstream* and *Downstream* datasets cover roughly the same proportion of the *A. thaliana* genome. The enrichment of TRB1 protein association with the *Upstream* in comparison to the *Downstream* genomic loci is obvious even in the *Non-protein coding genes* (3.7 % for *Upstream* compared to 0.8 % for *Non-protein coding genes* and 2.9 % for *Downstream* genomic loci). In contrast, the TRB1 protein is associated only with 1.5 % of the *Intergenic* sequences although these sequences cover almost 14 % of the genome. The preferential association of the TRB1 protein with sequences in *Upstream coding genes* is shown in the graph in Fig. 4c featuring the relative occurrence of *TRB1 genomic peaks* per sequence (dataset) length (displayed per Mb). The total bp size and the number of *TRB1 genomic peaks* in each dataset are listed in the Supplemental Table S2. The overall summary of sequences belonging to each dataset is given in the Supplemental Table S3.

Taken together, our results demonstrate that the TRB1 protein is preferentially associated in vivo with promoter regions of *coding genes* compared to gene bodies or *Downstream* genomic loci. Association of TRB1 with *Intergenic* sequences is very low. This detailed analysis

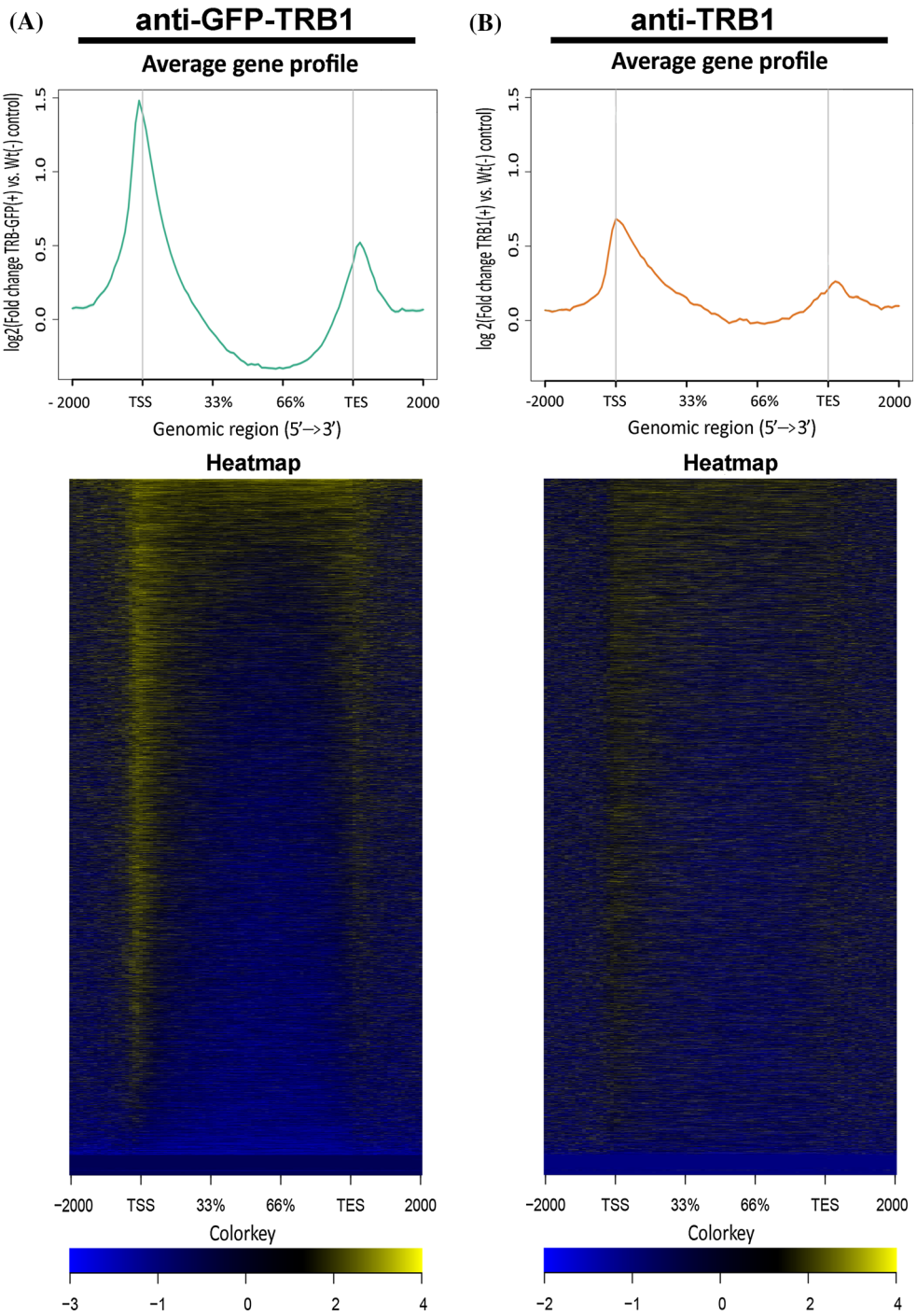

Fig. 3 TRB1 specifically associates with TSS and TES of genes. Distribution of ChIP-seq reads obtained using **a** immunoprecipitation of TRB1-GFP protein relative to negative control or **b** immunoprecipitation of native TRB1 protein relative to negative control, illustrated by average gene profiles (*upper panels*) and heatmaps (*lower panels*)

localizes extratelomeric TRB1-DNA association in euchromatin, especially in promoter regions.

Validation of TRB1 binding sites by ChIP-qPCR

To verify the TRB1 binding sites identified by ChIP-seq (Fig. 5a), we performed an independent ChIP experiment using the same seedlings as those used for the ChIP-seq analysis and purified DNA, and quantified the abundance of selected loci by qPCR. Preferential association of TRB1 protein with DNA regions that were identified as *TRB1 genomic peaks* was verified for several selected genomic loci (examples are shown in Fig. 5b). We confirmed by qPCR that all selected TRB1 binding sites are enriched in TRB1-GFP (+) samples with respect to the Wt (−) controls (examples of ribosomal protein L34, S5 and snoRNA

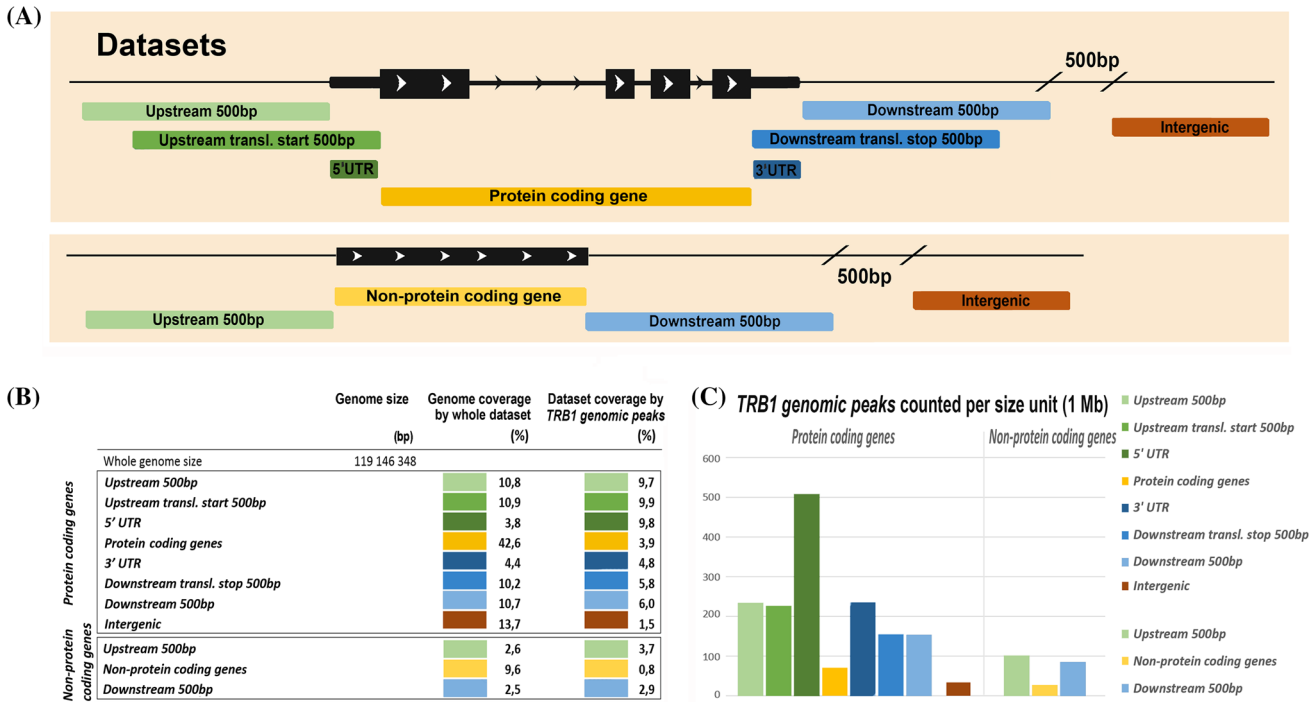

Fig. 4 Detailed analysis of TRB1-bound regions. **a** Schematic representation of the selected "datasets" (*coloured boxes*) used in detailed analysis of the DNA regions associated with TRB1 protein. These datasets were designed according to the TAIR10 annotation. The group of *Non-protein coding genes* contains genes depicted in TAIR10 as rRNA, snoRNA, snRNA, tRNA, ncRNA, miRNA, pseudogenes, transposable element genes and other RNAs. The *Intergenic* dataset is a collection of regions located at least 1000 bp from the transcription start or stop site (*Upstream* or *Downstream 500 bp*) of the *Protein coding genes* or of the *Non-protein coding genes* to avoid interference with other datasets. **b** An overview shows the percentage representation of each analysed dataset within the *A. thaliana* genome: "Genome coverage by whole dataset". "Dataset coverage by *TRB1 genomic peaks*" represents a portion of the dataset overlapping with the TRB1-enriched regions. **c** The number of the *TRB1 genomic peaks* counted per size unit (1 Mb) of each dataset

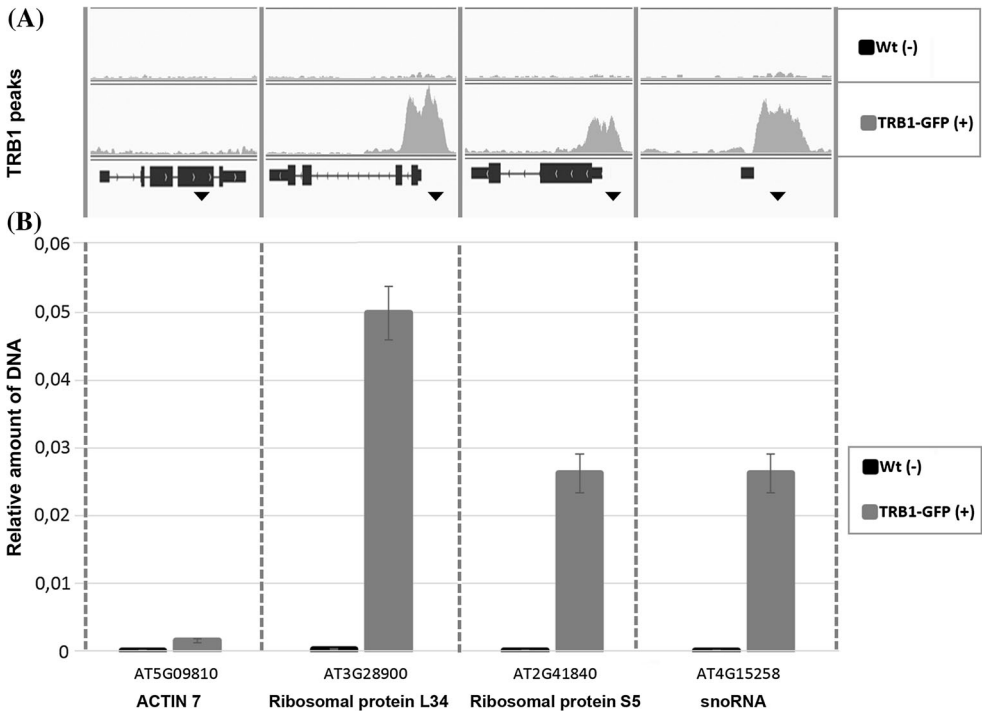

Fig. 5 Confirmation of the TRB1 protein binding sites by qPCR. Two ribosomal protein coding genes and one snoRNA coding region identified among *TRB1 genomic peaks*, with ACTIN 7 as negative control, were chosen for quantitative-PCR (qPCR) verification of regions enriched in ChIP-seq and defined as *TRB1 genomic peaks*. **a** IGV view of the *TRB1 genomic peaks* in Wt (−) or TRB-GFP (+) ChIP-seq samples where PCR amplicons are depicted by triangles below the simplified gene models. **b** Y-axis values represent the abundance of the DNA recovered from each locus related to the input DNA. Mean ± SD of three technical replicates are shown

are shown). In contrast, a site that was not included in the list of *TRB1 genomic peaks* (ACTIN 7) did not show any significant difference between TRB1-GFP (+) and Wt (−) control.

The telomeric repeat is the most conserved motif associated with TRB1

To determine the most frequent motif associated with TRB1 protein, we selected the dataset with the highest relative occurrence of *TRB1 genomic peaks* per 1 Mb, i.e. the *5′ UTR* dataset, and extracted regions associated with the TRB1 protein for further analysis. As promoter regions could be biased for some motifs, the TRB1-binding motif was reconstructed as a sequence logo from 8-mers twice as abundant in the TRB1-associated regions as in the whole *5′ UTR* dataset (see Table S4a, b). The sequence logo shows that the telomeric repeat is highly represented in the sequences recognised by the TRB1 protein (Fig. 6a). If the plant telomeric repeat unit (CCCTAAA) and its circular permutations are removed (Fig. 6b), a related motif (i.e. sequences enriched for CCTA) is still clearly overrepresented (Fig. 6c).

TRB1 is bound to short telomeric sequences in promoters

Binding of TRB proteins to the telomeric DNA sequences was initially shown in vitro (Schrumpfova et al. 2004) and binding of TRB proteins expressed in *E. coli* to the synthetic telomeric oligo was described in detail (Hofr et al. 2009; Mozgova et al. 2008; Schrumpfova et al. 2004). The present study confirmed recent observation by hybridisation with a radioactively labelled telomeric probe which showed that the DNA immunoprecipitated with TRB1 protein is enriched for long telomeric sequences (Schrumpfova et al. 2014).

The *Arabidopsis* genome contains short interspersed segments of the telomeric sequence both in terminal and interstitial positions, as well as the long telomeric repeats. These short interstitial telomere motifs, termed telo-boxes, exhibit a non-random distribution. They were described in the promoters of genes coding for translation elongation factor *EF1α* (Liboz et al. 1990), promoters of many ribosomal protein coding genes (Tremousaygue et al. 1999), and promoters of genes involved in the biogenesis of the translation machinery (Gaspin et al. 2010). The occurrence of telo-box motifs in the TRB1-associated regions from the above mentioned datasets was examined. The motifs analysed, AAACCCTA, AACCCTAA or ACCCTAAA (and their reverse complements), represent the most frequent permutations of the shortest telo-box motifs, as described in (Gaspin et al. 2010). Only telo-boxes directly covered by a *TRB1 genomic peak* were counted. Almost 28 % of telobox-sequences located in the 5′-UTR region of the *Protein coding genes* are covered by TRB1 peaks (Fig. 7 and Table S5). The total number of telo-boxes from each dataset and the number of *TRB1 genomic peaks* that

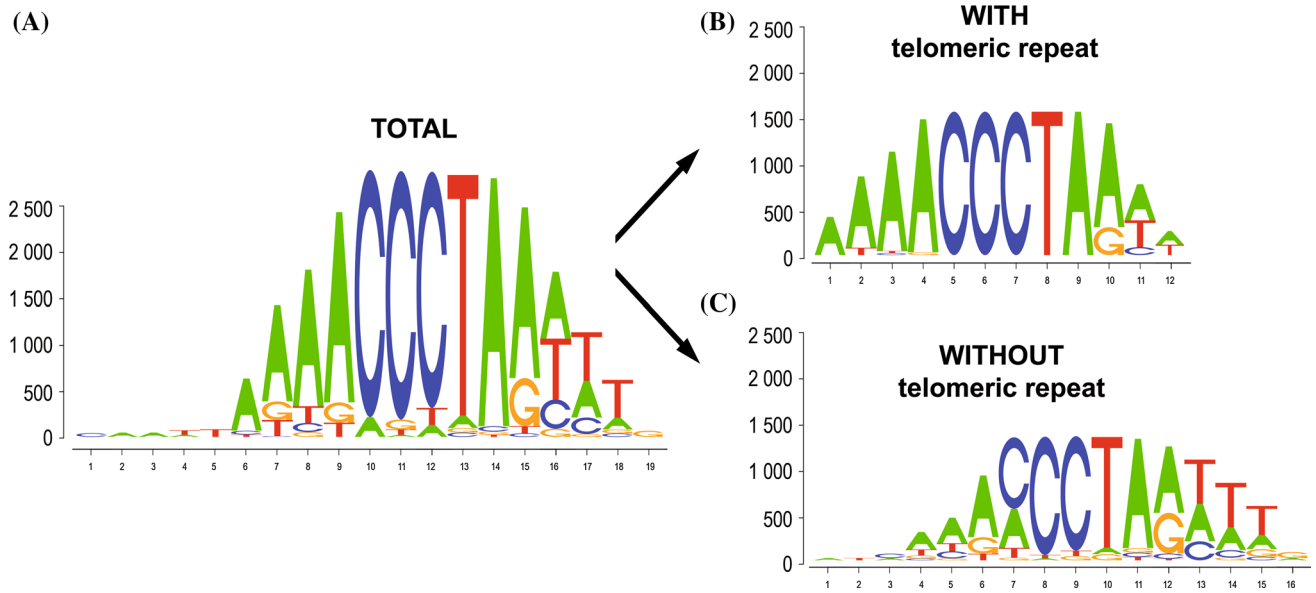

Fig. 6 The most conserved DNA motif associated with the TRB1 protein. Sequence logos were constructed from the most frequent 8-mers. **a** The total logo was created from the most frequent 8-mers present in the 5′ UTR regions and covered by the *TRB1 genomic peaks*. **b** Only 8-mers containing any permutation of at least one plant telomeric repeat were used for sequence logo construction *with telomeric repeat*. **c** The rest of the 8-mers, e.g. without any permutation of the plant telomeric repeat, were used for sequence logo construction *without telomeric repeat*

overlap these telo-boxes are listed in the supplementary Table S6. In general, it is evident that the TRB1 protein is associated at least twice as frequently with telo-box sequences in the *Upstream* datasets (22–28 %; green boxes) in comparison with the *Downstream* datasets (10–15 %; blue boxes) or with the low number (4 %) of *Interstitial* sequences.

The number of telo-box genes with which the TRB1 protein is associated is presumably underestimated here, because the two independent immunoprecipitation approaches and the very stringent detection and refinement of the *TRB1 genomic peaks* by two independent programs limits false positives to a minimum, while also discarding many true peaks. Therefore, although TRB1 is visibly associated with e.g., all three promoters of *eEF1 alpha-1, -2* and *-3* telo-box-containing genes (At1g07940, At1g07930 and At1g07920) (Figure S2), a *TRB1 genomic peak* was reported only in the *eEF1-alpha 1* gene (At1G07940). Our strict policy of selection of *TRB1 genomic peaks* is also visible in the Supplementary Figure S3, where the genes coding for ribosomal proteins RPS15B, RPS15C, RPS15D (At5g09490, At5g09500, At5g09510) are shown.

TRB1 protein is associated with genes related to ribosome biogenesis

As most of the TRB1-associated loci are located in gene promoter regions, we wanted to know whether these genes are related in their function, biological processes, or subcellular localization of their products. We selected genes with TRB1-enrichment in their upstream region (*Upstream 500 bp* dataset) and thus both the categories *Protein coding* and also *Non-protein coding genes* are included in this summary. The Arabidopsis Genome Initiative numbers (AGI numbers) of these genes were compared to the set of AGI numbers of all genes in the *Upstream 500 bp* datasets using Gene Ontology miner (GOMiner) (Zeeberg et al. 2003, 2005). The table of GO subcategories GO:0005575 Cellular component and GO:0008150 Biological process arranged graphically by Clustered Image Maps miner (CIMminer) demonstrates a statistically significant enrichment of these GO subcategories ($p \leq 0.05$) (Fig. 8). The total output of GOMiner and also of CIMminer with all genes and detailed description (e.g. name, gene type, function) is shown in Supplementary Table S7.

As is clearly visible in Fig. 7, protein coding genes with whose promoters the TRB1 protein is associated are enriched in GO:0005575 Cellular component in categories like GO:0005730 nucleolus/GO:0031981 nuclear lumen/GO:0005654 nucleoplasm/GO:0016604 nuclear body, etc. (GO categories highlighted in light orange). Also, terms associated with small and large ribosomal subunit (GO:0005732 small nucleolar ribonucleoprotein complex/GO:0015934 large ribosomal subunit/GO:0022626 cytosolic ribosome) (dark orange) are highly represented.

In the category GO:0008150 Biological process, many genes coding for ribosomal proteins were statistically enriched in subcategories GO:0071843 cellular component biogenesis at cellular level/GO:0042254 ribosome biogenesis/GO:0022613 ribonucleoprotein complex biogenesis (highlighted in dark orange). Names and functions of individual genes are visible in Supplementary Table S7, list "CIM with genes". Also, a significant number of intergenic snoRNA genes are bound by TRB1 protein in their

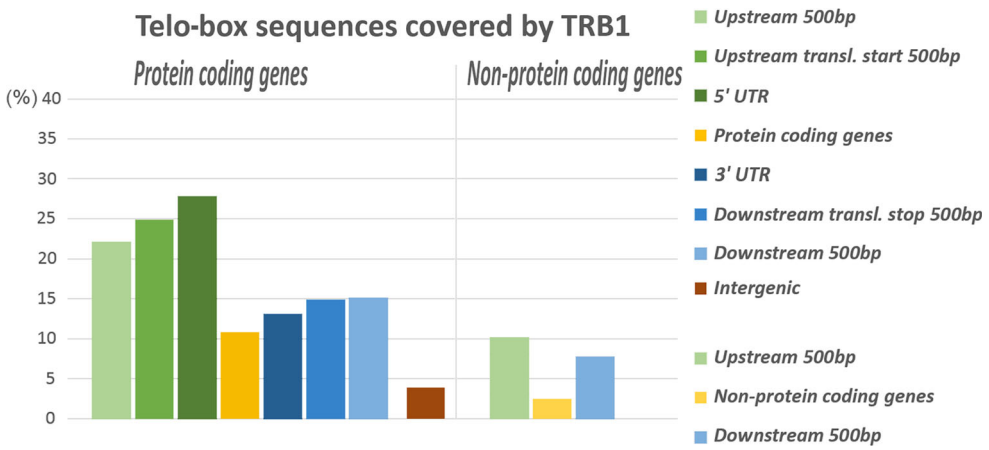

Fig. 7 The TRB1 protein preferentially occupies telo-box sequences. Sequences with at least one permutation of the telomeric repeat were extracted from each dataset. The chart shows the proportion of the sequences containing a telo-box motif that are covered by a *TRB1 genomic peak*. The clear preference of the TRB1 protein for telo-box sequences is especially apparent in the *5′-UTR* dataset in which almost 28 % of the telo-box sequences located in the 5′-UTR are recognized by the TRB1 protein

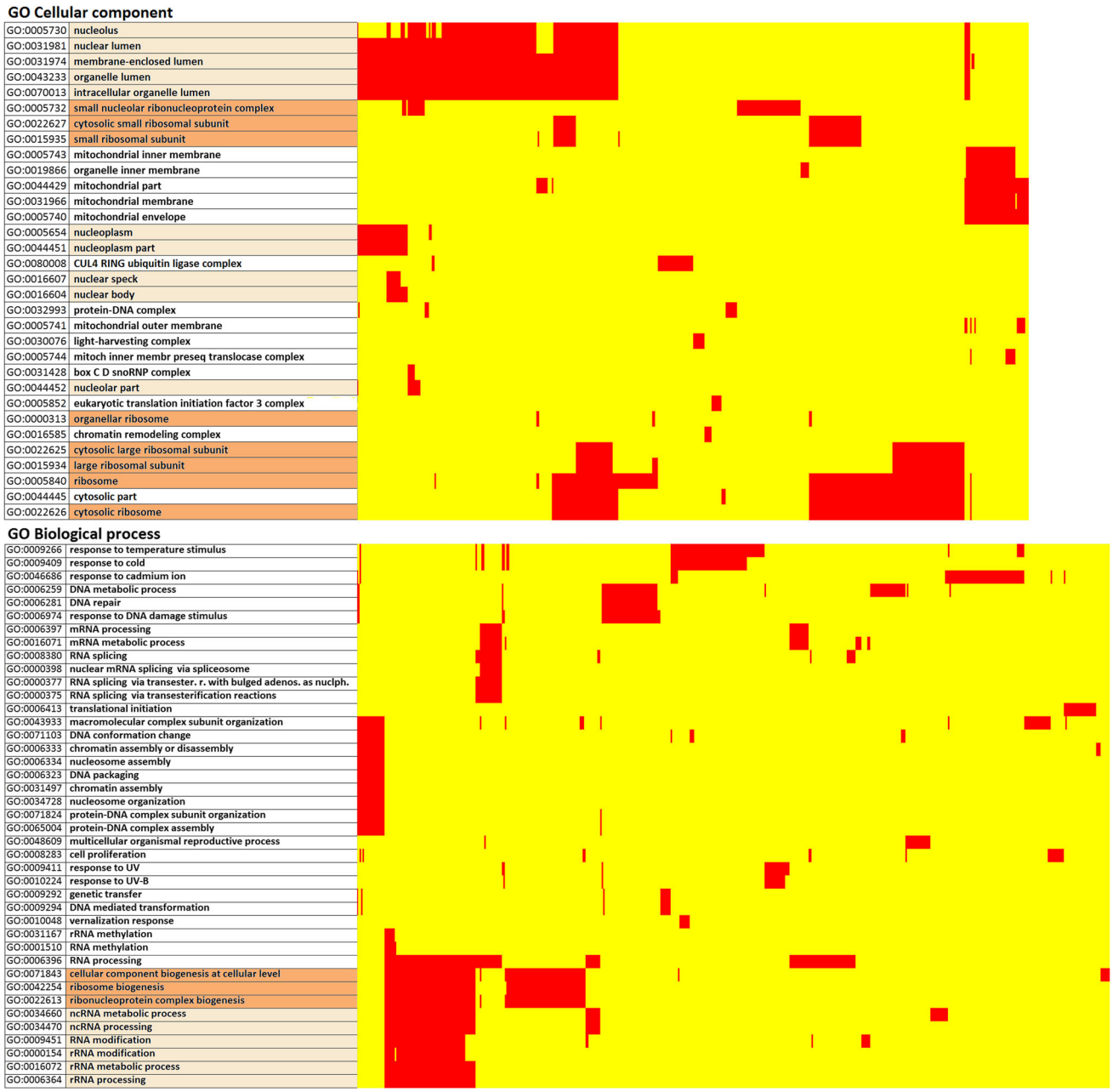

Fig. 8 Schematic view of Gene Ontology (GO) classification of categories significantly enriched in TRB1 protein. *All coding genes* (*Protein coding genes* together with *Non-protein coding genes*) that contain a *TRB1 genomic peak* in their 500 bp Upstream proximity (datasets: *Upstream 500 bp*) were analysed by the GOMiner software. The set of genes in which TRB1 protein is enriched in their 500 bp-upstream region was compared to the set of all coding genes from *A. thaliana*. General tables of the GO subcategories "GO:0005575 Cellular components" and "GO:0008150 Biological processes" were arranged graphically by CIMminer. The horizontal axes represent significantly enriched GO subcategories ($p \leq 0.05$) and the vertical axes represent individual genes, in clusters. Genes that contain a *TRB1 genomic peak* within 500 bp from the transcription start site and are significantly enriched in the GO subcategories are highlighted as *red boxes*. For a detailed description of individual genes, see Supplementary Table S7

Upstream 500 bp region and are included in the CIMminer Table. These snoRNA genes are highly enriched in categories such as e.g., GO:0034660 ncRNA metabolic process/GO:0000154 rRNA modification/GO:0006364 rRNA processing, etc.

Discussion

After recent findings, the previously-established concept that the shelterin proteins are located exclusively on the chromosome ends, the telomeres, has been superseded.

Emerging evidence indicates that the shelterin components also possess non-telomeric functions such as transcriptional regulation (Martinez et al. 2010; Zhang et al. 2008a), DNA repair (Bradshaw et al. 2005), NF-κB activation (Teo et al. 2010), Epstein-Barr virus replication (Deng et al. 2002), or regulation of mitochondrial oxidative phosphorylation (Chen et al. 2012). Some of these non-telomeric functions could be explained, at least partially, by their binding to ITSs (Bosco and de Lange 2012; Krutilina et al. 2003; Mignon-Ravix et al. 2002; Simonet et al. 2011) or even to unrelated DNA sequences which remain to be identified in future studies.

Association of TRB1 with telomeric sequences

Besides the terminally located long telomeric repeats, the *A. thaliana* genome contains two long interstitial telomeric tracts that consist of degenerate telomeric repeats with islands of perfect plant telomeric sequences (Uchida et al. 2002). In a previous study we speculated on the telomeric association of GFP–TRB1 speckles in *A. thaliana* (Dvorackova et al. 2010), and using a plant system with longer telomeres, *N. benthamiana*, we showed clear in situ co-localization of TRB1-GFP with telomeres in leaves (Schrumpfova et al. 2014). However, localization of TRB1 in many speckles in *A. thaliana* nuclei, together with the fact that the TAIR9 assembly, used as the reference genome, lacks not only telomeres but also interstitial telomeric regions, did not allow us to determine whether the TRB1-associated telomeric tracts are terminally or interstitially located. In the current study we describe a significant enrichment of perfect long plant telomeric repeats associated with the TRB1 protein using ChIP-seq.

TRB1 specific binding to telomeric sequence

Many different telomere-binding proteins possess a single myb-related DNA-binding domain with Helix-Turn-Helix (HTH) organization (reviewed in Peska et al. 2011). In the case of human TRF1 and TRF2, the X-ray crystal structures of complexes with telomeric DNA show that they recognize the same AACCCTA binding site by means of homeodomains, as does the yeast telomeric protein Rap1p; TRF dimers specifically recognize two of the three G-C base pairs in the major groove that characterize telomeric repeats (Court et al. 2005; Hanaoka et al. 2005; Nishikawa et al. 2001). Our search for a sequence-specific motif recognized by TRB1 revealed that the telo-box sequence is highly abundant in promoter regions, and moreover the core of this sequence (CCTA) containing two G-C base pairs is still present if we focus only on sequences without the complete telo-box motif. Thus we conclude that potential TRB1-binding motifs are associated with short interstitial telomere sequences as well as with long telomeric tracts, and furthermore the TRB1 protein binds to the core segment of telomeric repeats (CCTA) through its myb-domain in the same manner as human TRF proteins.

Preferential association of TRB1 with promoter regions

The landscape of the *A. thaliana* epigenome can be classified into four main chromatin states (Roudier et al. 2011) which have been further subdivided in a recent more detailed study, providing a total of nine chromatin states (Sequeira-Mendes et al. 2014). Only a small proportion of the TRB1 protein is associated with two heterochromatin states, mostly located in the centromeric regions or knobs on the short arm of chromosome 4 or the long arm of chromosome 5. In contrast, most of the TRB1 protein shows a preferential euchromatic localization, especially with sequences in the *Upstream* regions, mostly 5′ UTR regions. Association of TRB1 protein with entire gene bodies or intergenic regions is markedly lower. A similar distribution of the TRB1 protein preferring DNA *Upstream* from TSSs was observed in both *Protein coding* and *Non-protein coding genes*. The partial increase in TRB1 association with the genomic loci behind the transcription stop, *Downstream*, may be due to the fact that neighbouring downstream genes transcribed in the same direction are frequent at a distance of 100–700 bp (Alexandrov et al. 2006), and thus an overlap of the genomic regions located *Upstream* from TSSs or *Downstream* from the transcriptional stop may result in unspecific enrichment in one of these datasets. However, association of TRB1 with the upstream regions is markedly higher.

In accordance with the localization of TRB1 in euchromatin, we found that the overlap between the list of the chromosome 4 genes associated with marks of silent euchromatin (H3K9me3) and Polycomb-regulated chromatin (H3K27me3) (Turck et al. 2007) and the genes with a TRB1 genomic peak in their 500 bp upstream vicinity (*Upstream 500 bp* of *Protein* and *Non-protein coding genes* datasets) is considerably higher (20 and 9 %, respectively) than the overlap between the genes associated with the heterochromatin mark H3K9me2 and the genes with a TRB1 genomic peak in proximity to their 500 bp upstream region (0.3 %) (Turck et al. 2007).

TRB1 target genes are connected with ribosome biogenesis

The distribution of short interspersed telomeric repeats or telo-boxes within the *Arabidopsis* genome is not uniform and their frequency is higher within 5′ flanking regions (Gaspin et al. 2010). In this study we show that telo-boxes

located *Upstream* from TSSs are more likely to be associated with the TRB1 protein than those located *Downstream* from the transcription stop region or even in entire *Protein coding* or *Non-protein coding* gene bodies or within the *Intergenic* range. The occurrence of telo-boxes is enriched in promoter regions of genes participating in translation, e.g. genes coding for ribosomal proteins, translation elongation factors (EF1 α), eukaryotic initiation factors (eIFs), and small nucleolar RNAs (snoRNAs), or in the promoters of genes involved in rRNA processing (Gaspin et al. 2010; Liboz et al. 1990; Tremousaygue et al. 1999). The majority of telo-boxes of plant translation-related genes are located within a narrow window located between −50 and +50 relative to the TSS (Gaspin et al. 2010). Telo-boxes are not able, by themselves, to activate gene expression in transgenic plants but act in synergy with other cis-acting elements like site II motifs or TEF boxes that show conservative topological association with telo-boxes in *Arabidopsis* and *O. sativa* (Gaspin et al. 2010; Manevski et al. 2000; Tremousaygue et al. 2003). In agreement with this observation, we found that TRB1 shows a statistically significant enrichment in *500 bp Upstream* regions of the genes connected in GO with terms describing small and large subunit of the ribosome, nucleolus, or rRNA modification.

Since many snoRNA genes that are involved in the processing of rRNA are transcribed in clusters or are located in introns (Brown et al. 2008), the total number of snoRNA genes with TRB1-binding sites in their promoter is underestimated because the distal snoRNA gene in a transcribed cluster may be farther than 500 bp away from the transcription start site and, consequently, is not included in our analysis. Another similar case is intronic snoRNA genes, which are indistinguishable from the protein coding genes. For details, see supplementary Figure S4 (snoRNA clusters) which displays the IGV view of snoRNA clusters significantly associated with TRB1 protein in their shared promoter. We proved that only the snoRNAs category is associated with the TRB1 protein in its *500 bp Upstream* proximity (Fig. 9a). Other categories from the *Non-protein coding* dataset e.g., *rRNA, snRNA, tRNA, ncRNA, miRNA, other RNA, pseudogenes* and *transposable element* do not exhibit increased association with TRB1. We found that more than 80 % of intergenic orphan snoRNA genes (not transcribed in clusters) or intergenic snoRNAs with a telo-box in proximity to their their *500 bp Upstream* are covered by *TRB1 genomic peaks* (Fig. 9b, c).

Our analysis of 192 ribosomal protein coding genes, used for a transcription level study (Savada and Bonham-Smith 2014), revealed that almost 85 % of them contain a telo-box in proximity to their *500 bp Upstream translation start* and 65 % of these telo-box sequences are covered by *TRB1 genomic peaks*. At least nine of ten promoters of the most frequently transcribed ribosomal genes in *A. thaliana* seedlings (Savada and Bonham-Smith 2014) are recognised by the TRB1 protein. By contrast, promoters of the ribosomal protein-coding genes (which are transcribed at the lowest level in *A. thaliana* seedlings (Savada and Bonham-Smith 2014)) showed either lower or a zero level of TRB1 binding.

Analogous estimation of eIFs with telo-boxes which are associated with the TRB1 protein was derived from a list of eIFs (https://www.arabidopsis.org/browse/genefamily/eIF.jsp). Almost 60 % of eIFs contain a telo-box sequence in proximity to their *500 bp Upstream translation start* and 50 % of these telo-box sequences are covered by *TRB1 genomic peaks*.

The pattern of TRB1 association with chromatin suggests its role as a transcription factor

In humans, some core shelterin subunits are documented to modulate gene expression outside of telomeres; for example, TRF2 interacts with the repressor element 1-silencing transcription factor (REST), a repressor of genes devoted to neuronal functions (Zhang et al. 2008a). Another example is mammalian RAP1 which is known to play a role in repression of subtelomeric genes, and more than 70 % of its binding sites are found at intragenic positions or in the vicinity of gene-coding chromatin (Martinez et al. 2010).

Strong nucleolar localization of the TRB1 protein, besides weaker nuclear and cytoplasmic localization, has been already shown (Dvorackova et al. 2010). Genes coding for 45S ribosomal RNA (rDNA) which organize nucleoli are close neighbours of telomeres in chromosomes of many eukaryotes including *Arabidopsis*, and also show a number of functional associations (Dvorackova et al. 2015; Fransz et al. 2002). A proteomic analysis has revealed that a significant portion of the nucleolar protein pool consists of ribosomal proteins (RPSs or RPLs), RNA modifying factors (snRNA or snoRNA binding), and proteins participating in translation (EF1s, eIFs) (Brown et al. 2005; Pendle et al. 2005). The majority of non-ribosomal nucleolar proteins occur in the nucleolus only transiently, since many of these factors fluctuate between the nucleus and nucleolus (Dundr et al. 1997; Snaar et al. 2000; Sprague and McNally 2005), and similar behaviour was observed for the TRB1 protein (Dvorackova et al. 2010) that is largely dispersed at prophase, coinciding with nucleolar disassembly, and re-localized in early anaphase after cytokinesis.

TRB1 association was detected in the promoters of the *H2AX A* and *H2AX B* genes, which also contain telo-box sequences in their promoter region. Phosphorylated products of these genes are involved in response to DNA double

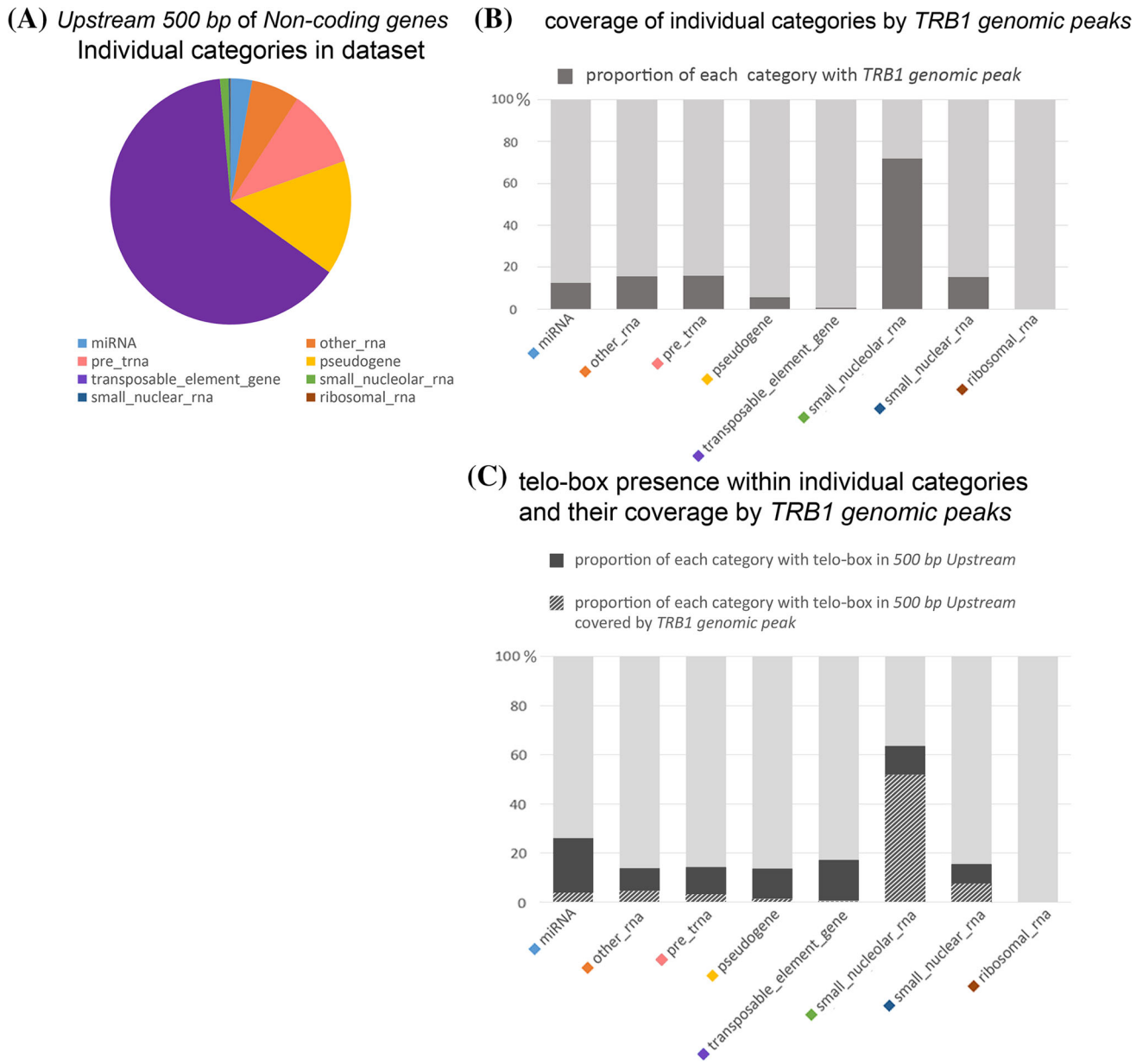

Fig. 9 Analysis of individual categories of the *Upstream 500 bp* of *Non-protein coding genes* dataset. The group of *Non-protein coding genes* includes *rRNA, snoRNA, snRNA, tRNA, ncRNA, miRNA, other RNA, pseudogenes* and *transposable element* genes categories. **a** The pie chart shows the proportional representation of individual categories. The most represented categories *transposable elements*, *pseudogenes, pre-tRNA, other RNA* cover nearly 64, 15, 10, and 6.5 %, respectively of the *Non-coding genes* dataset. By contrast, categories *miRNA, snoRNA, snRNA, rRNA* occupy only 2.9, 1.2, 0.2, and 0.1 %, respectively. **b** *Dark grey* represents the proportion of the genes in each category where any *TRB1 genomic peak* interferes with the genomic region located in region 500 bp upstream from the transcription start site of the relevant non-protein coding gene. **c** The *dark grey* part represents the proportion of the genes in each category that harbour at least one telo-box in their 500 bp upstream region. The hatched part represents the subset of the telobox-containing genes that are covered by *TRB1 genomic peaks*

strand breaks. All these connections indicate the importance to examine possible involvement of the TRB1 protein in regulation of transcription.

Whole-genome duplication events in *Arabidopsis* phylogeny often resulted in increased number of genes of the same family (Mandakova and Lysak 2008; Nelson et al. 2014). TRB1 protein belongs to the single-myb-histone family with five members (Marian et al. 2003; Schrumpfova et al. 2004, 2014). Although these proteins slightly differ in binding properties (Hofr et al. 2009; Schrumpfova et al. 2004, 2014) their partial functional redundancy in vivo cannot be excluded. Therefore, no observation of significant

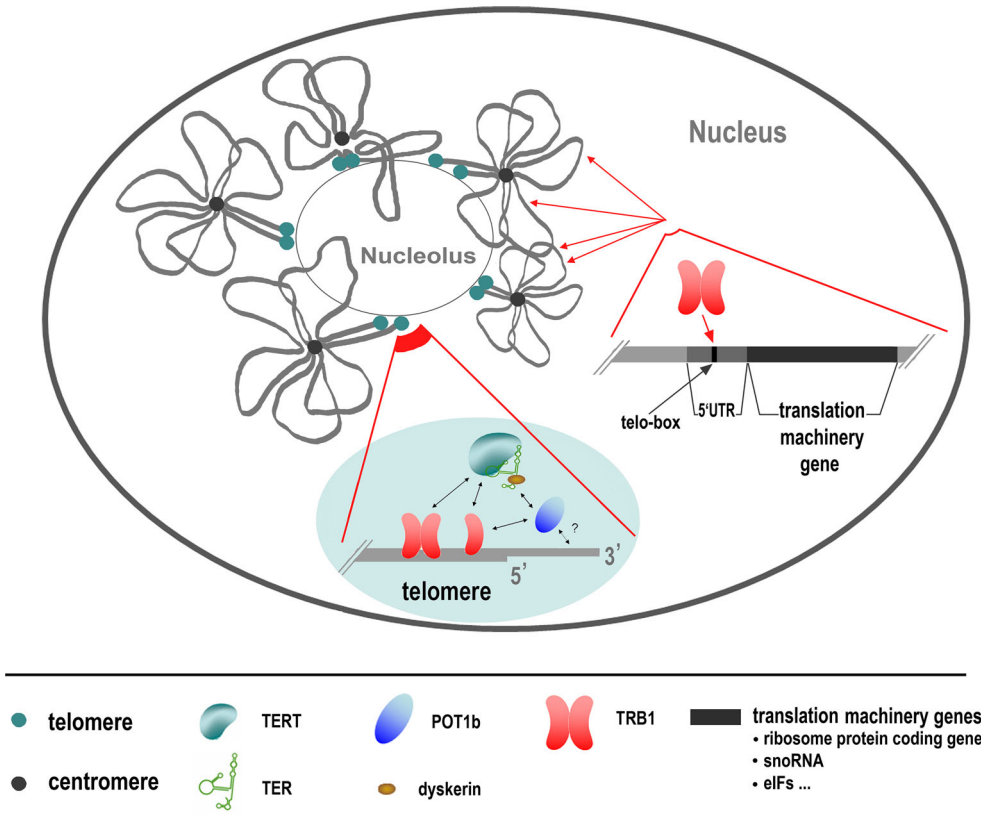

Fig. 10 Concluding overview of telomeric and non-telomeric locations and roles of TRB1 protein. TRB1 protein from *A. thaliana*, whose myb-domain shows high sequence similarity to the human TRF1 or TRF2 myb-domains, acts as a component of plant telomere-protection complex. TRB1 is co-localised with telomeric tracts in vivo, interacts with POT1b protein, telomerase reverse transcriptase (TERT) subunit and the loss of TRB1 protein leads to evident telomere shortening (Kuchar and Fajkus 2004; Schrumpfova et al. 2008, 2014). Furthermore, our present finding demonstrated association of TRB1 also to the 5′ flanking region of protein- or non-protein coding regions related to the translation machinery genes e.g.: ribosomal protein coding genes, snoRNA genes, and genes coding for eEF-1 and eIFs, correlated with a higher frequency of short telomere-like sequences (telo-boxes) in their promoters. Physical association of telomeres to nucleoli (depicted in the upper part) may hypothetically correspond to functional relevance of TRB1 for coordinated regulation of translation machinery genes

changes in transcript levels of chosen genes in *trb1−/−* mutant plants (Fig. S5) is not surprising and points to the need for using multiple *trb* mutants in further analyses.

In conclusion, this report demonstrates that the TRB1 protein from *A. thaliana*, whose N-terminal myb-domain shows high sequence homology with the human TRF1 or TRF2 C-terminal myb-domain, is associated in vivo with a subset of interstitial sites in the *Arabidopsis* genome besides its major location at telomeres (Schrumpfova et al. 2014). Our finding of an association of TRB1 with the 5′ flanking region of protein or non-protein coding regions, especially with sequences located upstream of the transcription start site of the ribosomal protein coding genes, snoRNA genes, and genes coding for elongation factors (eEF-1) and eukaryotic initiation factors (eIFs), correlated with a higher frequency of short telomere-like sequences (telo-boxes) in their promoters, together with its cell-cycle regulated localization (Dvorackova et al. 2010), suggest that the TRB1 protein may be functional also as a transcription factor (see concluding overview in Fig. 10). In this feature, TRB1 resembles other analogous shelterin proteins from diverse organisms which, besides their telomeric localization and functions, can bind to non-telomeric regions and have extra-telomeric functions in gene regulation networks.

Acknowledgments We thank Vladimir Benes from the European Molecular Biology Laboratory (EMBL), Genomics Core Facility, Heidelberg, Germany, for valuable comments and recommendations on our ChIP procedure. We also thank Ronald Hancock, Hôtel-Dieu de Québec for critical reading of the manuscript. Access to computing and storage facilities owned by parties and projects contributing to the National Grid Infrastructure MetaCentrum, provided under the programme "Projects of Large Infrastructure for Research, Development, and Innovations" (LM2010005), is greatly appreciated. This research was supported by the Czech Science Foundation (13-06943S) and by project CEITEC (CZ.1.05/1.1.00/02.0068) of the European Regional Development Fund.

References

Alexandrov NN, Troukhan ME, Brover VV, Tatarinova T, Flavell RB, Feldmann KA (2006) Features of Arabidopsis genes and genome discovered using full-length cDNAs. Plant Mol Biol 60:69–85. doi:10.1007/s11103-005-2564-9

Bosco N, de Lange T (2012) A TRF1-controlled common fragile site containing interstitial telomeric sequences. Chromosoma 121:465–474. doi:10.1007/s00412-012-0377-6

Bowler C, Benvenuto G, Laflamme P, Molino D, Probst AV, Tariq M, Paszkowski J (2004) Chromatin techniques for plant cells. Plant J 39:776–789. doi:10.1111/j.1365-313X.2004.02169.x

Bradshaw PS, Stavropoulos DJ, Meyn MS (2005) Human telomeric protein TRF2 associates with genomic double-strand breaks as an early response to DNA damage. Nat Genet 37:193–197. doi:10.1038/ng1506

Brown JW, Shaw PJ, Shaw P, Marshall DF (2005) Arabidopsis nucleolar protein database (AtNoPDB). Nucleic Acids Res 33:D633–D636

Brown JW, Marshall DF, Echeverria M (2008) Intronic noncoding RNAs and splicing. Trends Plant Sci 13:335–342. doi:10.1016/j.tplants.2008.04.010

Chen LY et al (2012) Mitochondrial localization of telomeric protein TIN2 links telomere regulation to metabolic control. Mol Cell 47:839–850. doi:10.1016/j.molcel.2012.07.002

Cifuentes-Rojas C, Kannan K, Tseng L, Shippen DE (2011) Two RNA subunits and POT1a are components of Arabidopsis telomerase. Proc Natl Acad Sci USA 108:73–78. doi:10.1073/pnas.1013021107

Court R, Chapman L, Fairall L, Rhodes D (2005) How the human telomeric proteins TRF1 and TRF2 recognize telomeric DNA: a view from high-resolution crystal structures. EMBO Rep 6:39–45. doi:10.1038/sj.embor.7400314

de Lange T (2005) Shelterin: the protein complex that shapes and safeguards human telomeres. Genes Dev 19:2100–2110. doi:10.1101/Gad.1346005

Deng Z, Lezina L, Chen CJ, Shtivelband S, So W, Lieberman PM (2002) Telomeric proteins regulate episomal maintenance of Epstein-Barr virus origin of plasmid replication. Mol Cell 9:493–503

Dundr M, Meier UT, Lewis N, Rekosh D, Hammarskjold ML, Olson MO (1997) A class of nonribosomal nucleolar components is located in chromosome periphery and in nucleolus-derived foci during anaphase and telophase. Chromosoma 105:407–417

Dvorackova M, Rossignol P, Shaw PJ, Koroleva OA, Doonan JH, Fajkus J (2010) AtTRB1, a telomeric DNA-binding protein from Arabidopsis, is concentrated in the nucleolus and shows highly dynamic association with chromatin. Plant J 61:637–649. doi:10.1111/j.1365-313X.2009.04094.x

Dvorackova M, Fojtova M, Fajkus J (2015) Chromatin dynamics of plant telomeres and ribosomal genes. Plant J. doi:10.1111/tpj.12822

Edgar RC (2004) MUSCLE: multiple sequence alignment with high accuracy and high throughput. Nucleic Acids Res 32:1792–1797. doi:10.1093/nar/gkh340

Edgar R, Domrachev M, Lash AE (2002) Gene expression omnibus: NCBI gene expression and hybridization array data repository. Nucleic Acids Res 30:207–210. doi:10.1093/Nar/30.1.207

Fajkus J, Sykorova E, Leitch AR (2005) Telomeres in evolution and evolution of telomeres. Chromosome Res 13:469–479. doi:10.1007/s10577-005-0997-2

Fransz P, De Jong JH, Lysak M, Castiglione MR, Schubert I (2002) Interphase chromosomes in Arabidopsis are organized as well defined chromocenters from which euchromatin loops emanate. Proc Natl Acad Sci USA 99:14584–14589. doi:10.1073/pnas.212325299

Gaspin C, Rami JF, Lescure B (2010) Distribution of short interstitial telomere motifs in two plant genomes: putative origin and function. BMC Plant Biol 10:283. doi:10.1186/1471-2229-10-283

Hanaoka S, Nagadoi A, Nishimura Y (2005) Comparison between TRF2 and TRF1 of their telomeric DNA-bound structures and DNA-binding activities. Protein Sci 14:119–130. doi:10.1110/ps.04983705

Hofr C, Sultesova P, Zimmermann M, Mozgova I, Schrumpfova PP, Wimmerova M, Fajkus J (2009) Single-Myb-histone proteins from *Arabidopsis thaliana*: a quantitative study of telomere-binding specificity and kinetics. Biochem J 419:221–228. doi:10.1042/BJ20082195

Kazda A, Zellinger B, Rossler M, Derboven E, Kusenda B, Riha K (2012) Chromosome end protection by blunt-ended telomeres. Genes Dev 26:1703–1713. doi:10.1101/gad.194944.112

Krutilina RI et al (2003) Protection of internal (TTAGGG)n repeats in Chinese hamster cells by telomeric protein TRF1. Oncogene 22:6690–6698. doi:10.1038/sj.onc.1206745

Kuchar M, Fajkus J (2004) Interactions of putative telomere-binding proteins in *Arabidopsis thaliana*: identification of functional TRF2 homolog in plants. FEBS Lett 578:311–315. doi:10.1016/j.febslet.2004.11.021

Langmead B, Salzberg SL (2012) Fast gapped-read alignment with Bowtie 2. Nat Methods 9:357–359. doi:10.1038/nmeth.1923

Latrick CM, Cech TR (2010) POT1-TPP1 enhances telomerase processivity by slowing primer dissociation and aiding translocation. EMBO J 29:924–933. doi:10.1038/emboj.2009.409

Liang K, Keles S (2012) Normalization of ChIP-seq data with control. BMC Bioinformatics 13:199. doi:10.1186/1471-2105-13-199

Liboz T, Bardet C, Le Van Thai A, Axelos M, Lescure B (1990) The four members of the gene family encoding the *Arabidopsis thaliana* translation elongation factor EF-1 alpha are actively transcribed. Plant Mol Biol 14:107–110

Louis EJ, Vershinin AV (2005) Chromosome ends: different sequences may provide conserved functions. BioEssays 27:685–697. doi:10.1002/Bies.20259

Macas J, Neumann P, Novak P, Jiang J (2010) Global sequence characterization of rice centromeric satellite based on oligomer frequency analysis in large-scale sequencing data. Bioinformatics 26:2101–2108. doi:10.1093/bioinformatics/btq343

Majerska J, Sykorova E, Fajkus J (2011) Non-telomeric activities of telomerase. Mol BioSyst 7:1013–1023. doi:10.1039/c0mb00268b

Mandakova T, Lysak MA (2008) Chromosomal phylogeny and karyotype evolution in x = 7 crucifer species (Brassicaceae). Plant Cell 20:2559–2570. doi:10.1105/tpc.108.062166

Manevski A, Bertoni G, Bardet C, Tremousaygue D, Lescure B (2000) In synergy with various cis-acting elements, plant insterstitial telomere motifs regulate gene expression in Arabidopsis root meristems. FEBS Lett 483:43–46

Marian CO et al (2003) The maize Single myb histone 1 gene, Smh1, belongs to a novel gene family and encodes a protein that binds telomere DNA repeats in vitro. Plant Physiol 133:1336–1350. doi:10.1104/pp.103.026856

Martinez P et al (2010) Mammalian Rap1 controls telomere function and gene expression through binding to telomeric and extratelomeric sites. Nat Cell Biol 12:768–780. doi:10.1038/ncb2081

Mignon-Ravix C, Depetris D, Delobel B, Croquette MF, Mattei MG (2002) A human interstitial telomere associates in vivo with specific TRF2 and TIN2 proteins. Eur J Hum Genet 10:107–112. doi:10.1038/sj.ejhg.5200775

Morse RH (2000) RAP, RAP, open up! New wrinkles for RAP1 in yeast. Trends Genet 16:51–53. doi:10.1016/S0168-9525(99)01936-8

Mozgova I, Schrumpfova PP, Hofr C, Fajkus J (2008) Functional characterization of domains in AtTRB1, a putative telomere-binding protein in *Arabidopsis thaliana*. Phytochemistry 69:1814–1819. doi:10.1016/j.phytochem.2008.04.001

Nelson AD, Forsythe ES, Gan X, Tsiantis M, Beilstein MA (2014) Extending the model of Arabidopsis telomere length and composition across Brassicaceae. Chromosome Res 22:153–166. doi:10.1007/s10577-014-9423-y

Nishikawa T, Okamura H, Nagadoi A, Konig P, Rhodes D, Nishimura Y (2001) Solution structure of a telomeric DNA complex of human TRF1. Structure 9:1237–1251

Nosek J, Tomaska L (2003) Mitochondrial genome diversity: evolution of the molecular architecture and replication strategy. Curr Genet 44:73–84. doi:10.1007/s00294-003-0426-z

Pendle AF et al (2005) Proteomic analysis of the Arabidopsis nucleolus suggests novel nucleolar functions. Mol Biol Cell 16:260–269

Peska V, Schrumpfova PP, Fajkus J (2011) Using the telobox to search for plant telomere binding proteins. Curr Protein Pept Sci 12:75–83

Pfaffl MW (2004) Quantification strategies in real-time PCR. International University Line (IUL), La Jolla

Rossignol P, Collier S, Bush M, Shaw P, Doonan JH (2007) Arabidopsis POT1A interacts with TERT-V(I8), an N-terminal splicing variant of telomerase. J Cell Sci 120:3678–3687

Roudier F et al (2011) Integrative epigenomic mapping defines four main chromatin states in Arabidopsis. EMBO J 30:1928–1938. doi:10.1038/emboj.2011.103

Savada RP, Bonham-Smith PC (2014) Differential transcript accumulation and subcellular localization of Arabidopsis ribosomal proteins. Plant Sci 223:134–145. doi:10.1016/j.plantsci.2014.03.011

Schneider TD, Stephens RM (1990) Sequence logos: a new way to display consensus sequences. Nucleic Acids Res 18:6097–6100

Schrumpfova P, Kuchar M, Mikova G, Skrisovska L, Kubicarova T, Fajkus J (2004) Characterization of two *Arabidopsis thaliana* myb-like proteins showing affinity to telomeric DNA sequence. Genome 47:316–324. doi:10.1139/g03-136

Schrumpfova PP, Kuchar M, Palecek J, Fajkus J (2008) Mapping of interaction domains of putative telomere-binding proteins AtTRB1 and AtPOT1b from *Arabidopsis thaliana*. FEBS Lett 582:1400–1406. doi:10.1016/j.febslet.2008.03.034

Schrumpfova PP, Vychodilova I, Dvorackova M, Majerska J, Dokladal L, Schorova S, Fajkus J (2014) Telomere repeat binding proteins are functional components of Arabidopsis telomeres and interact with telomerase. Plant J 77:770–781. doi:10.1111/Tpj.12428

Sequeira-Mendes J et al (2014) The functional topography of the Arabidopsis genome is organized in a reduced number of linear motifs of chromatin states. Plant Cell 26:2351–2366. doi:10.1105/tpc.114.124578

Sfeir A, de Lange T (2012) Removal of shelterin reveals the telomere end-protection problem. Science 336:593–597. doi:10.1126/science.1218498

Sfeir A, Kosiyatrakul ST, Hockemeyer D, MacRae SL, Karlseder J, Schildkraut CL, de Lange T (2009) Mammalian telomeres resemble fragile sites and require TRF1 for efficient replication. Cell 138:90–103. doi:10.1016/j.cell.2009.06.021

Shen L, Shao N, Liu X, Nestler E (2014) ngs.plot: quick mining and visualization of next-generation sequencing data by integrating genomic databases. BMC Genom 15:284. doi:10.1186/1471-2164-15-284

Simonet T et al (2011) The human TTAGGG repeat factors 1 and 2 bind to a subset of interstitial telomeric sequences and satellite repeats. Cell Res 21:1028–1038. doi:10.1038/cr.2011.40

Snaar S, Wiesmeijer K, Jochemsen AG, Tanke HJ, Dirks RW (2000) Mutational analysis of fibrillarin and its mobility in living human cells. J Cell Biol 151:653–662

Soudet J, Jolivet P, Teixeira MT (2014) Elucidation of the DNA end-replication problem in Saccharomyces cerevisiae. Mol Cell 53:954–964. doi:10.1016/j.molcel.2014.02.030

Sprague BL, McNally JG (2005) FRAP analysis of binding: proper and fitting. Trends Cell Biol 15:84–91

Teo H et al (2010) Telomere-independent Rap1 is an IKK adaptor and regulates NF-kappaB-dependent gene expression. Nat Cell Biol 12:758–767. doi:10.1038/ncb2080

Tremousaygue D, Manevski A, Bardet C, Lescure N, Lescure B (1999) Plant interstitial telomere motifs participate in the control of gene expression in root meristems. Plant J 20:553–561

Tremousaygue D, Garnier L, Bardet C, Dabos P, Herve C, Lescure B (2003) Internal telomeric repeats and 'TCP domain' protein-binding sites co-operate to regulate gene expression in *Arabidopsis thaliana* cycling cells. Plant J 33:957–966

Turck F et al (2007) Arabidopsis TFL2/LHP1 specifically associates with genes marked by trimethylation of histone H3 lysine 27. PLoS Genet 3:e86. doi:10.1371/journal.pgen.0030086

Uchida W, Matsunaga S, Sugiyama R, Kawano S (2002) Interstitial telomere-like repeats in the *Arabidopsis thaliana* genome. Genes Genet Syst 77:63–67

Valach M et al (2011) Evolution of linear chromosomes and multipartite genomes in yeast mitochondria. Nucleic Acids Res 39:4202–4219. doi:10.1093/nar/gkq1345

Weaver DT (1998) Telomeres: moonlighting by DNA repair proteins. Curr Biol 8:R492–R494

Zeeberg BR et al (2003) GoMiner: a resource for biological interpretation of genomic and proteomic data. Genome Biol 4:R28

Zeeberg BR et al (2005) High-throughput GoMiner, an 'industrial-strength' integrative gene ontology tool for interpretation of multiple-microarray experiments, with application to studies of Common Variable Immune Deficiency (CVID). BMC Bioinform 6:168. doi:10.1186/1471-2105-6-168

Zhang P, Pazin MJ, Schwartz CM, Becker KG, Wersto RP, Dilley CM, Mattson MP (2008a) Nontelomeric TRF2-REST interaction modulates neuronal gene silencing and fate of tumor and stem cells. Curr Biol 18:1489–1494. doi:10.1016/j.cub.2008.08.048

Zhang Y et al (2008b) Model-based analysis of ChIP-seq (MACS). Genome Biol 9:R137. doi:10.1186/gb-2008-9-9-r137

Zhang Y, Lin YH, Johnson TD, Rozek LS, Sartor MA (2014) PePr: a peak-calling prioritization pipeline to identify consistent or differential peaks from replicated ChIP-seq data. Bioinformatics 30:2568–2575. doi:10.1093/bioinformatics/btu372

Plant Molecular Biology

Telomere Binding Protein TRB1 is Associated with Promoters of Translation Machinery Genes *in vivo*

Petra Procházková Schrumpfová[1,2], Ivona Vychodilová[1,2], Jan Hapala[1,2], Šárka Schořová[1,2], Vojtěch Dvořáček and Jiří Fajkus[1,2,3§]

[1] Mendel Centre for Plant Genomics and Proteomics, CEITEC – Central European Institute of Technology, Masaryk University, Kamenice 5, CZ-625 00 Brno, Czech Republic; [2] Laboratory of Functional Genomics and Proteomics, National Centre for Biomolecular Research, Faculty of Science, Masaryk University, Kamenice 5, CZ-625 00 Brno, Czech Republic; [3] Institute of Biophysics, Academy of Sciences of the Czech Republic, v.v.i., Královopolská 135, CZ-61265 Brno, Czech Republic

Coresponding author:

e-mail: fajkus@sci.muni.cz

tel: +420 549 49 4003

fax: +420 549 492 654

Supplementary Figures and Tables

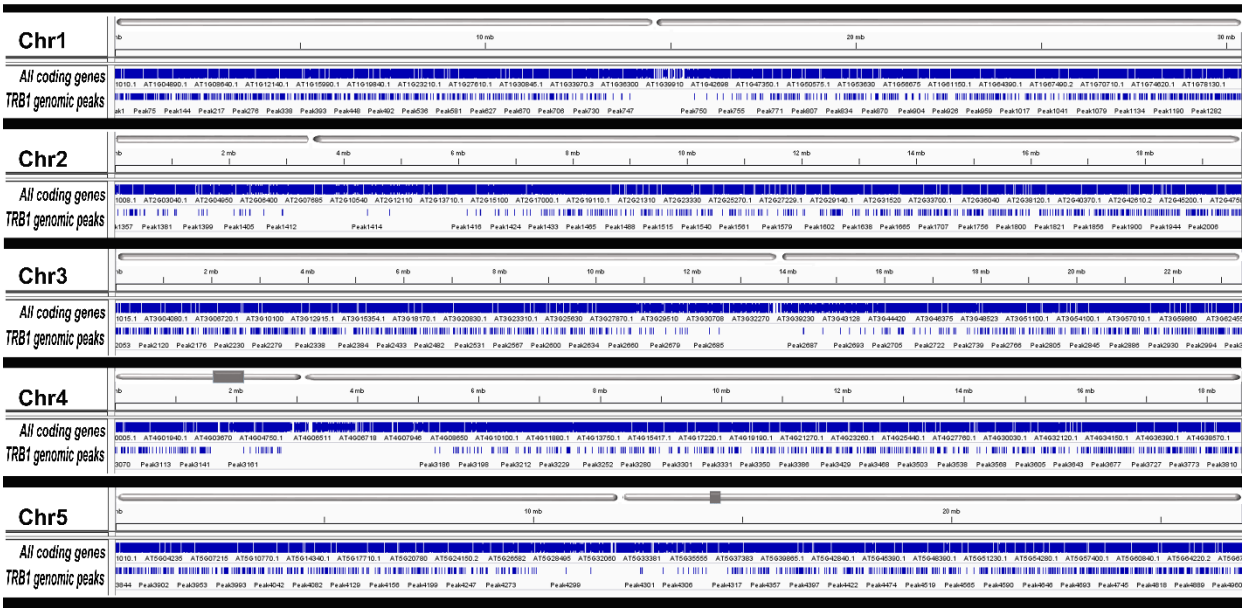

Figure S1- Overview of all *TRB1 genomic peaks* in each chromosome

The IGV view of all five chromosomes from *A. thaliana* visualizes the preference of the TRB1 protein binding outside of heterochromatic regions (centromeres and heterochromatin knobs). The *All coding genes* category represents both *Protein coding genes* and *Non-protein coding genes*. *TRB1 genomic peaks* represents TRB1-enriched regions. The heterochromatin knobs on chromosome 4 and 5 are indicated by grey boxes.

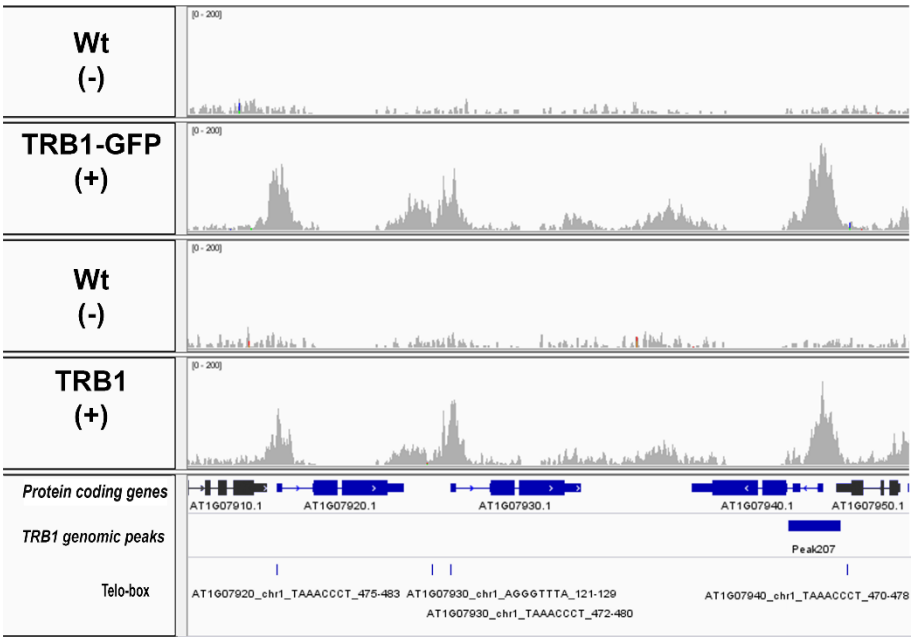

Figure S2 - TRB1 association with the EF1-alpha genes

Three *EF1-alpha 1*, *2* and *3* genes that contain telo-box sequence in *Upstream 500 bp* distance (At1g07940, At1g07930 and At1g07920) are visualised with IGV viewer. Telo-box sequences are highlighted in separate rows. Although the pattern of TRB1 occupancy would visually suggest that TRB1 is occupying regions around TSSs of all three loci, only one (*EF1-alpha 1* gene (At1G07940)) has been detected as a *TRB1 genomic peak* under our stringent threshold criteria. So the number of the TRB1 associated regions should be actually higher.

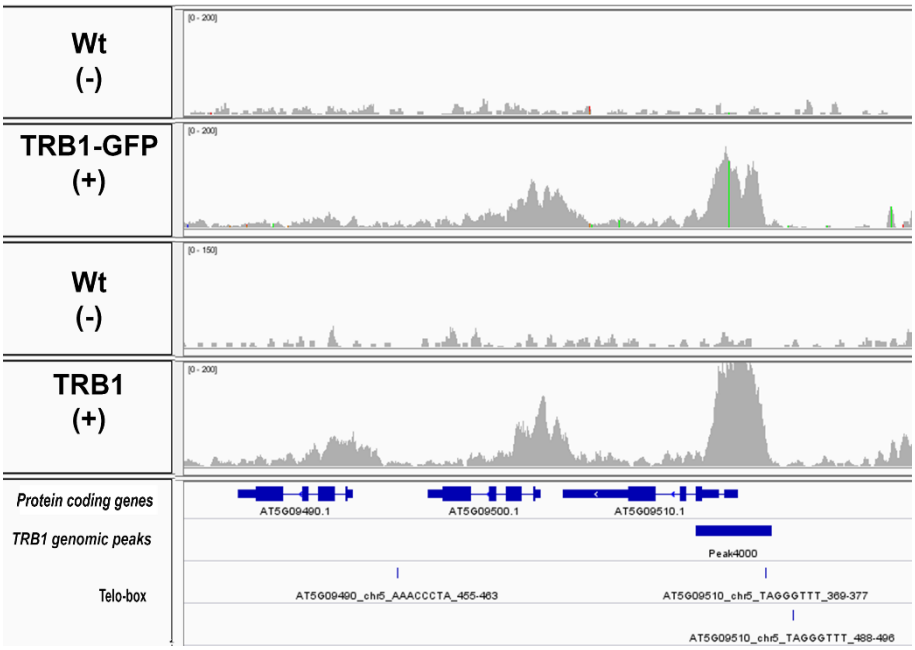

Figure S3 – TRB1 association with genes coding for ribosomal proteins

Three genes coding for ribosomal proteins RPS15B, RPS15C, RPS15D (At5g09490, At5g09500, At5g09510) are visualised with IGV viewer. Telo-box sequences are highlighted in separate rows. Although the pattern of TRB1 occupancy would visually suggest that TRB1 is occupying regions around TSSs of all three loci, only one (RPS15D gene (At5g09510)) has been detected as *TRB1 genomic peak* under our stringent threshold criteria. So the number of the TRB1 associated regions should be actually higher.

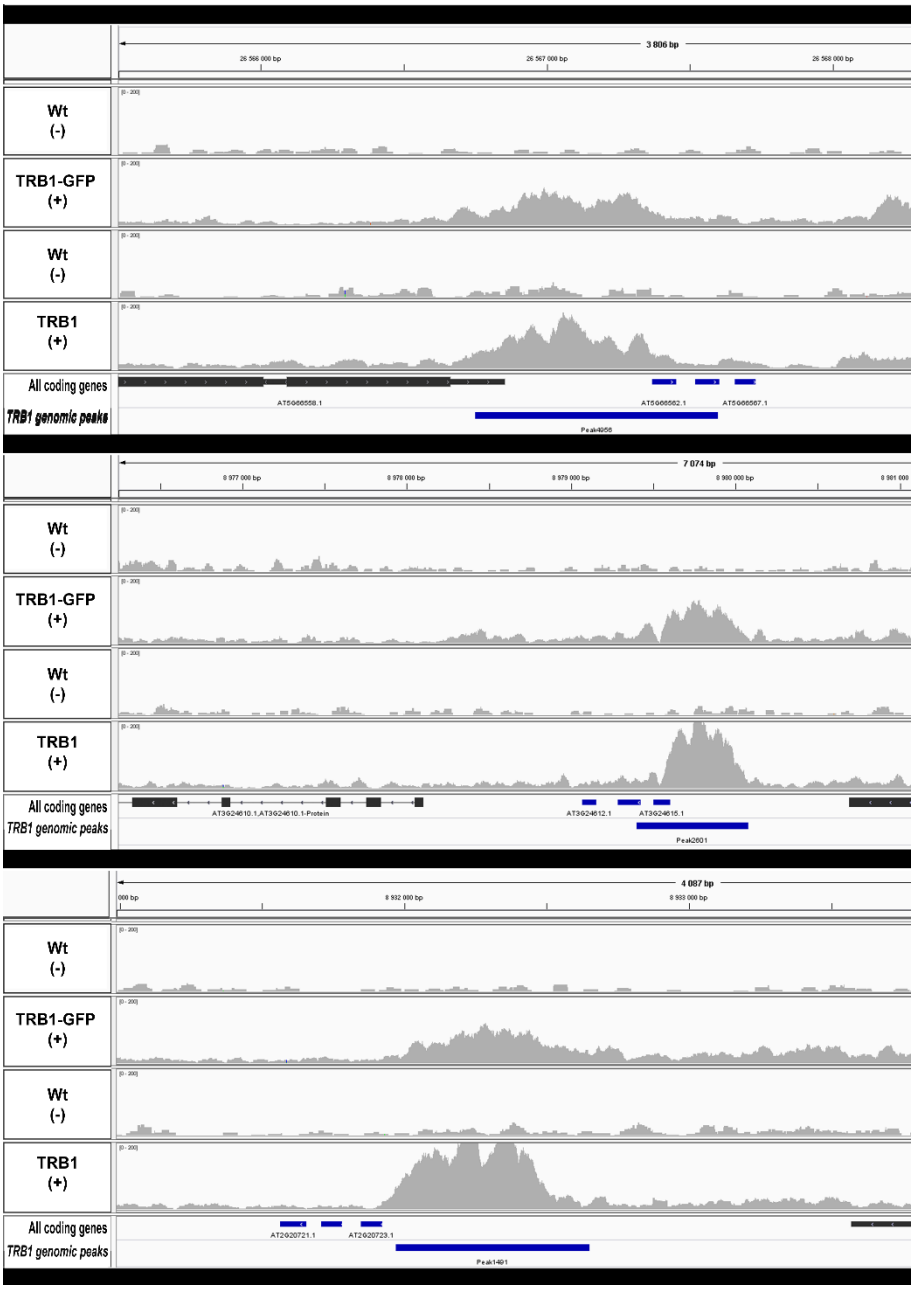

Figure S4 – Schematic view of the snoRNA clusters

An IGV view of three examples of association of the TRB1 protein with promoter sequences of the snoRNA genes that are clustered into one transcript (blue boxes). *TRB1 genomic peaks* are highlighted.

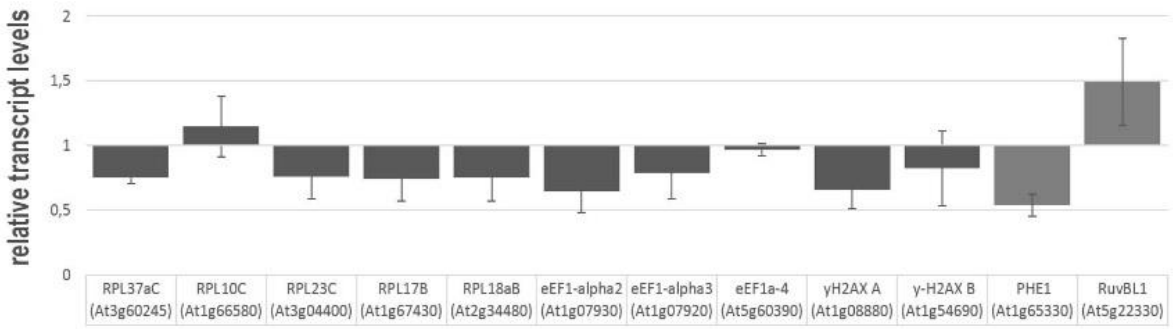

Figure S5 – Effect of TRB1 on transcription of selected TRB1-associated genes

Several genes with promoters visibly associated with TRB1 protein, coding for proteins of large or small ribosome subunits, and genes coding for eEFs and H2AX proteins were chosen for analysis of transcript levels in *trb1-/-* plants and compared to the respective wt control. For comparison, genes coding for Pheres (PHE) and RuvB-like AAA ATPase 1 (RuvBL1), lacking association with TRB1 protein (light grey), were also analysed. Y-axis values represent relative transcript levels (Wt=1).

Table S1 - List of primers used in the qChIP-qPCR and RT-PCR analysis.

List of primers used for ChIP-qPCR described in (a) Figure 4 and (b) Figure S5

A	**Actin 7 (AT5G09810)**	Forward	GGAAACATCGTTCTCAGTGGT
		Reverse	CTTGATCTTCATGCTGCTAGGT
	Ribosomal protein L34 (AT3G28900)	Forward	AGGTGATCTCTTGAGCCCTAG
		Reverse	AAAGATAAAAAACACTACAATCAATCTGAG
	Ribosomal protein S5 (AT2G41840)	Forward	AGGCCTTGTTGGGTTTGT
		Reverse	TTGTTCTGATTAACGTGTGACATTAG
	snoRNA (AT4G15258)	Forward	CGAAACCTTATAAATACACAGACACAG
		Reverse	TTGGGCCGAGAACCTAAAATAG
B	**RPL37aC (at3g60245)**	Forward	AGGTTGGAATCGTCGGCAAA
		Reverse	TCACTCCGTACTTGCCACAG
	RPL10C (at1g66580)	Forward	ACCGTGCTGAGTACACGAAG
		Reverse	TCATTCTTATTCGCTAGTGGCTGA
	RPL23C (at3g04400)	Forward	GCCACTGTGAACTGTGCTGA
		Reverse	CAACACACGCTGATGGCAAA
	RPL17B (at1g67430)	Forward	GTACTCGCAAGAACCCGACA
		Reverse	TGGTAGCTTCCTGATTGCGT
	RPL18aB (at2g34480)	Forward	GGACAGATGCTCGCCATCAA
		Reverse	CATCTGCTCAACAGCTCCGT
	eEF1-alpha 2 (at1g07930)	Forward	GTCTGTTGAGATGCACCACG
		Reverse	CCCTCTCTTAAGATCCTTCACGG
	eEF1-alpha 3 (at1g07920)	Forward	GCTGCTAACTTCACCTCCCA
		Reverse	TCTCCTTACCAGAACGCCTG
	eEF1a-4 (at5g60390)	Forward	ACAAGCGTGTCATCGAGAGG
		Reverse	TCACGCTCGGCCTTAAGTTT
	γH2AX A (at1g08880)	Forward	ATGAGTACAGGCGCAGGAAG
		Reverse	CTAGCGATTCTTCCGACGGG
	γH2AX B (at1g54690)	Forward	ACAACTAAAGGTGGCAGAGGA
		Reverse	TCGGCGTATTTACCGGCTTTA
	eEF1-alpha 3 (at1g07920)	Forward	GCTGCTAACTTCACCTCCCA
		Reverse	TCTCCTTACCAGAACGCCTG
	eEF1a-4 (at5g60390)	Forward	ACAAGCGTGTCATCGAGAGG
		Reverse	TCACGCTCGGCCTTAAGTTT
	γH2AX A (at1g08880)	Forward	ATGAGTACAGGCGCAGGAAG
		Reverse	CTAGCGATTCTTCCGACGGG
	γH2AX B (at1g54690)	Forward	ACAACTAAAGGTGGCAGAGGA
		Reverse	TCGGCGTATTTACCGGCTTTA
	PHE (At1g65330)	Forward	GATCGCCAAAGAAACAGAACG
		Reverse	ATCTCAACCCTACGAATAACACC
	RuvBL1 (At5g22330)	Forward	CGGATTGCTACTCACACCCA
		Reverse	GCTGCCTCTCTAGCCTCAAG
	UBQ10 (At4g05320)	Forward	AACGGGAAAGACGATTAC
		Reverse	ACAAGATGAAGGGTGGAC

Table S2 – Computation of the TRB1 protein coverage dataset per size unit of 1 Mb

The size of each dataset analysed in this study (bp) is listed in the column "whole dataset size". Overlapping base pairs were counted once. The proportional representation of these numbers is shown in Figure 3b as "Genome coverage by whole dataset". The section "Number of *TRB1 genomic peaks* in dataset" represents the absolute number of DNA sequences from each dataset that were covered at least partly by one (or more) *TRB1 genomic peak*. The "*TRB1 genomic peaks* per size unit of 1 Mb" column is illustrated graphically in the Figure 3c and represents the frequency of *TRB1 genomic peaks* per one megabase of each dataset.

Table S2: Computation of the TRB1 protein coverage dataset per size unit of 1 Mb

			Whole dataset size (bp)	Number of *TRB1 genomic peaks* in dataset	*TRB1 genomic Peaks* per size unit of 1 Mb
	Whole genome size (bp)	119146348			
Protein coding genes	***Upstream 500bp***		12 897 461	3 008	**233**
	Upstream transl. start 500bp		13 006 712	2 941	**226**
	5' UTR		4 529 898	2 301	**508**
	Protein coding genes		51 137 472	3 637	**71**
	3' UTR		5 294 049	1 241	**234**
	Downstream transl. stop 500bp		12 226 923	1 886	**154**
	Downstream 500bp		12 797 523	1 960	**153**
	Intergenic		16 270 943	543	**33**
Non-protein coding genes	***Upstream 500bp***		2 977 811	302	**101**
	Non-protein coding genes		11 098 033	302	**27**
	Downstream 500bp		2 941 489	249	**85**

Table S3 - Overall summary of sequences belonging to each dataset

(In separate Supplementary .xls file)

A table of DNA sequences in each dataset that are significantly covered with the TRB1 protein (*TRB1 genomic peaks*).

Table S4 - List of 8-mers and List of fragments used in the logo construction

(In separate Supplementary .xls file)

(A) A list of every unique substring of the length *k* (8) in the dataset *5'UTR covered by TRB1 genomic peaks.* The proportion of purple 8-mers is twice as high in the dataset *5'UTR covered by TRB1 genomic peaks* as in the *whole 5'UTR* dataset. Only these purple 8-mers were used for fragment construction of the *total* sequence logo (Fig. 5a). The green boxes highlight 8-mers with a permutation of at least one plant telomeric repeat and used for partial sequence logo construction *with telomeric repeat* (see Fig. 5b). The rest of the purple 8-mers do not contain any telomeric repeat and were used for partial sequence logo construction *without telomeric repeat* (Fig. 5c).

(B) Here are listed fragments constructed from 8-mers separately for each sequence logo (*total, with telomeric repeat, without telomeric repeat* (Fig. 5)). Fragments in their forward or reverse complementary version (orange) were aligned by MUSCLE. The mean weight of each fragment or the relative weight for each base in the fragment is included.

Table S5 - Table of Telo-box sequences in each dataset

The number of all sequences in the datasets which contain at least one telo-box are listed in the column "All telo-box containing sequences". The column "Telo-box covered by *TRB1 genomic peaks*" lists the number of sequences where at least one telo-box is preferentially recognized by the TRB1 protein and thus termed a *TRB1 genomic peak*. The last column corresponds to the graphical illustration in Figure 6 where the percentages of all sequences from each dataset covered by *TRB1 genomic peak* are shown.

Table S5- Table of Telo-box sequences in each dataset

		All telo-box containg seq.	Telo-box covered by *TRB1 genomic peaks*	Percentages of telo-boxes covered by TRB1 (%)
Protein coding genes	***Upstream 500bp***	4832	1065	**22,0**
	Upstream transl. start 500bp	5637	1401	**24,9**
	5' UTR	2452	682	**27,8**
	Protein coding genes	7370	796	**10,8**
	3' UTR	790	103	**13,0**
	Downstream transl. stop 500bp	2494	371	**14,9**
	Downstream 500bp	3519	531	**15,1**
	Intergenic	2188	85	**3,9**
Non-protein coding genes	***Upstream 500bp***	1024	104	**10,2**
	Non-protein coding genes	1183	29	**2,5**
	Downstream 500bp	748	58	**7,8**

Table S6 - List of telo-box sequences belonging to each dataset

(In separate Supplementary .xls file)

Genomic coordinates of all telo-boxes and telo-boxes with *TRB1 genomic peaks*.

Table S7- Detailed reports from GOMiner and CIMminer

(In separate Supplementary .xls file)

Two main GO categories, GO:0008150 Biological process and GO:0005575 Cellular component, were individually analyzed in GOMiner and CIMminer. The list "CIM" contains GO subcategories of these GO categories which are statistically enriched ($p \leq 0.05$). For this table, only GO subcategories (listed in horizontal rows) containing 5−500 members were selected. Separate genes are listed vertically (AGI gene codes), so this table corresponds to Figure 7 in the main text.

The list "CIM with genes" contains highly enriched GO subcategories ($p \leq 0.05$), ordered vertically, and selected genes where AGI gene codes are presented with detailed description of the gene names and function in rows.

The list "Total vs. Total Report" contains a comparison of *All coding genes* from *A. thaliana* (Total file; *Protein coding genes* together with *Non-protein coding genes*) together with the set of genes where the TRB1 protein is enriched in the region 500 bp upstream from the transcription start site ("Changed" file). All coding genes involved in each GO subcategory are listed and marked whether they were enriched in the region 500 bp upstream from the transcription start site or not ("no change/changed"). GO subcategories are ordered according to the number of members.

The list "Gene Category Report" contains a detailed analysis of individual genes involved in each GO subcategory. GO subcategories are ordered according to the p-value so the GO subcategories where the amount of genes associated with TRB1 protein in their *Upstream 500 bp* proximity is highest are listed in the upper part of the Table.

The list "Category Summary Report" summarizes the results for all GO subcategories (Gene Category Report). GO subcategories are ordered by p-value.

Supplement J

Schrumpfová, P.P.*, Schořová, Š., Fajkus, J., **2016**. Telomere- and Telomerase-Associated Proteins and Their Functions in the Plant Cell. Front. Plant Sci. 7:851

P.P.S. wrote the ms and was significantly involved the ms editing

frontiers in Plant Science

REVIEW
published: 28 June 2016
doi: 10.3389/fpls.2016.00851

Telomere- and Telomerase-Associated Proteins and Their Functions in the Plant Cell

Petra Procházková Schrumpfová[1,2], Šárka Schořová[2] and Jiří Fajkus[1,2,3]*

[1] *Mendel Centre for Plant Genomics and Proteomics, Central European Institute of Technology, Masaryk University, Brno, Czech Republic,* [2] *Laboratory of Functional Genomics and Proteomics, National Centre for Biomolecular Research, Faculty of Science, Masaryk University, Brno, Czech Republic,* [3] *Institute of Biophysics, Academy of Sciences of the Czech Republic, v.v.i., Brno, Czech Republic*

Telomeres, as physical ends of linear chromosomes, are targets of a number of specific proteins, including primarily telomerase reverse transcriptase. Access of proteins to the telomere may be affected by a number of diverse factors, e.g., protein interaction partners, local DNA or chromatin structures, subcellular localization/trafficking, or simply protein modification. Knowledge of composition of the functional nucleoprotein complex of plant telomeres is only fragmentary. Moreover, the plant telomeric repeat binding proteins that were characterized recently appear to also be involved in non-telomeric processes, e.g., ribosome biogenesis. This interesting finding was not totally unexpected since non-telomeric functions of yeast or animal telomeric proteins, as well as of telomerase subunits, have been reported for almost a decade. Here we summarize known facts about the architecture of plant telomeres and compare them with the well-described composition of telomeres in other organisms.

Keywords: telomere, telomerase, telomeric proteins, shelterin, telomeric repeat binding (TRB), plant

OPEN ACCESS

Edited by:
Anne-Catherine Schmit, Institut de Biologie Moléculaire des Plantes, CNRS UPR2357, France

Reviewed by:
Takashi Murata, National Institute for Basic Biology, Japan
Franziska Katharina Turck, Max Planck Society, Germany

****Correspondence:***
Petra Procházková Schrumpfová
schpetra@centrum.cz

Specialty section:
This article was submitted to Plant Cell Biology, a section of the journal Frontiers in Plant Science

Received: *12 November 2015*
Accepted: *31 May 2016*
Published: *28 June 2016*

Citation:
Procházková Schrumpfová P, Schořová Š and Fajkus J (2016) Telomere- and Telomerase-Associated Proteins and Their Functions in the Plant Cell. Front. Plant Sci. 7:851. doi: 10.3389/fpls.2016.00851

TELOMERES AS NUCLEOPROTEIN STRUCTURES

Telomeres are nucleoprotein structures at the ends of eukaryotic chromosomes that protect linear chromosomes against damage by endogenous nucleases and erroneous recognition as unrepaired chromosomal breaks. It is now known that telomeric structures are formed by telomeric DNA, histone octamers, and a number of proteins that bind telomeric DNA, either directly or indirectly, and together, form the protein telomere cap (Fajkus and Trifonov, 2001; de Lange, 2005; Bianchi and Shore, 2008; Sfeir, 2012). The telomeric cap proteins of diverse organisms are less conserved than one might expect. Even within a single taxonomic class, such as mammals, telomeric proteins display less conservation than other chromosomal proteins (Linger and Price, 2009). On the other hand, in many plant families, whole-genome duplication events have occurred, resulting in a multitude of genomic changes, such as deletions of large fragments of chromosomes, silencing of duplicate genes, and recombining of homologous chromosomal segments, as was shown, e.g., in crucifer species (Mandakova and Lysak, 2008). Polyploidy can result in increased numbers of genes of the same family (Taylor and Raes, 2004; He and Zhang, 2005; Freeling, 2009), which may show sub-functionalization, neo-functionalization, and partial or full redundancy and complicates assignment of an actual and specific function for individual proteins *in vivo*. Gene duplications and losses in plant phylogeny can be traced also in telomere associated protein families

(e.g., in *Arabidopsis thaliana*: single myb histone (SMH) family, TRF-like (TRFL) family, or Pot1-like family) (Nelson et al., 2014; Beilstein et al., 2015).

In land plants, the telomere is mostly composed of *Arabidopsis*-type TTTAGGG repeats (Richards and Ausubel, 1988; **Figure 1A**). Known exceptions are species in the order Asparagales, starting from divergence of the Iridaceae family, which shares the human-type telomeric repeat (TTAGGG; probably caused by a mutation that altered the RNA template subunit of telomerase ∼80 Mya; Adams et al., 2001; Weiss and Scherthan, 2002; Sykorova et al., 2003). The human-type telomere is also shared by species of the Allioideae subfamily, except for the *Allium* genus (Sykorova et al., 2006), where novel telomeric sequence (CTCGGTTATGGG) was recently described (Fajkus et al., 2016). An unusual telomeric motif (TTTTTTAGGG) was found in the family Solanaceae, in *Cestrum elegans* and related species (Peska et al., 2015). Also some of the species from the carnivorous genus *Genlisea* display, instead normal *Arabidopsis*-type of telomere, two intermingled sequence variants (TTCAGG and TTTCAGG; Tran et al., 2015).

Moreover, across the Plantae kingdom, outside of land plants but including red algae, green algae, and Glaucophytes (Koonin, 2010), telomere types also vary (**Figure 1B**). For example, in algae, in addition to the *Arabidopsis*-type of telomeric repeat, the *Chlamydomonas*-type (TTTTAGGG), human-type (TTAGGG), and a novel TTTTAGG repeat have been described (Fulnecková et al., 2013; Fulnečková et al., 2015).

The length of plant telomeric DNA at a single chromosomal arm can be as small as 500 base pairs (bp) in *Physcomitrella patens* (Shakirov et al., 2010; Fojtova et al., 2015), as long as 160 kb in *Nicotiana tabacum* (Fajkus et al., 1995), or 200 kb in *Nicotiana sylvestris* (Kovarik et al., 1996). Besides the remarkable variation in telomere lengths among diverse plant genera or orders, telomere lengths can also vary at the level of the species or ecotypes: e.g., *Arabidopsis* telomeres range from 1.5 to 9 kb, depending on the ecotype. Also in the long-living organism *Betula pendula*, telomeres in different genotypes varied from a minimum length of 5.9–9.6 kb to a maximum length of 15.3–22.8 kb (Shakirov and Shippen, 2004; Maillet et al., 2006; Aronen and Ryynanen, 2014).

Since telomeric DNA serves as a landing pad for a set of proteins, the total length or composition of telomeric tracts could markedly affect the number or selection of telomere-associated proteins and subsequently influence telomere packaging, structural transitions, or launch various biochemical pathways (see below).

NUCLEAR LOCALIZATION AND DYNAMICS OF TELOMERES

In some species during interphase, telomeres, and centromeres could be located at opposite sides of the nucleus, at the nuclear periphery, in limited regions or clusters; this is known as the Rabl organization (Rabl, 1885; for review, see Cowan et al., 2001). The Rabl organization (Wen et al., 2012) was observed in wheat, rye, barley, and oats. Other plant species, such as maize (*Zea mays*) and sorghum (*Sorghum bicolor*), despite having fairly large genomes, are not known to exhibit the Rabl configuration (Dong and Jiang, 1998). A recent study among *Brachypodium* species revealed a positive correlation between Rabl configuration and an increase in DNA content (resulting from replication) and a negative influence of increasing nuclear elongation (Idziak et al., 2015). A rosette-like organization of chromosomes in interphase nuclei was observed in *Arabidopsis*: telomeres show persistent clustering at the nucleolus while centromeres do not cluster (Armstrong et al., 2001; Tiang et al., 2012). Moreover, during early meiotic prophase, at the leptotene–zygotene transition, telomeres of most plant species cluster to form a bouquet (Bass et al., 1997; Martinez-Perez et al., 1999; Cowan et al., 2002; Corredor and Naranjo, 2007; Higgins et al., 2012; Phillips et al., 2012). *Arabidopsis* belongs to a small group of species that do not form telomeric bouquets (Armstrong et al., 2001).

Chromatin attachment to the inner nuclear membrane in plants, as well as in other species, is mediated by a well conserved multi-protein complex gathered around SUN (Sad1-UNC-84 homology)-KASH (Klarsicht, ANC-1, and Syne homology) proteins [respectively AtSUN-AtSINE (SUN domain-interacting NE proteins) in *A. thaliana*; Starr et al., 2001; Zhou et al., 2014; Tamura et al., 2015]. In fission and budding yeasts, interactions during meiosis between telomeres and the nuclear envelope, via interactions between SUN domain proteins and telomere-binding proteins, was described: in *Saccharomyces cerevisiae* SUN-domain protein yMps3 (monopolar spindle protein 3) is needed for yKu80-mediated telomeric chromatin anchoring (Schober et al., 2009), while in *Schizosaccharomyces pombe*, interactions between telomeric protein pRap1 (repressor activator protein 1) and pSUN proteins are mediated by pBqt1 and pBqt2 (telomere bouquet protein 1 and 2; Chikashige et al., 2006). The tethering of human telomeres to the nuclear matrix was proposed to depend on an isoform of telomere repeat binding factor 1 (TRF1) interacting partner (hTIN2), named hTIN2L (Kaminker et al., 2009), or an A-type lamin (Ottaviani et al., 2008; for review, see Giraud-Panis et al., 2013). Various homologs of SUN domain proteins were identified in *Arabidopsis* or in maize. In *Arabidopsis*, they are also localized to the inner nuclear membrane in somatic cells (Graumann et al., 2010; Tamura et al., 2015), however, homologs of Bqt proteins or TIN2 proteins have not been found in plants and their sequences are poorly conserved.

Telomeres are processed by a telomere-specific machinery that includes telomerase and its regulatory units, as well as nucleases, as exemplified by the exonuclease 1 (AtEXO1) ortholog in *Arabidopsis* (Kazda et al., 2012; Derboven et al., 2014). In plants, as well as in most of other kingdoms, replication of chromosomal ends results in single-stranded 3′ DNA protrusions (G-overhangs) after degradation of the last RNA primer at the 5′ terminus of a nascent strand. In *Silene latifolia* or *A. thaliana*, relatively short (20–30 nucleotides) G-overhangs were detected. Moreover, half of the Silene and *Arabidopsis* telomeres showed no overhangs or overhangs less than 12 nucleotides in length (Riha et al., 2000; Kazda et al., 2012). These G-overhangs are also thought to be required for chromosome end protection by forming secondary DNA structures such as

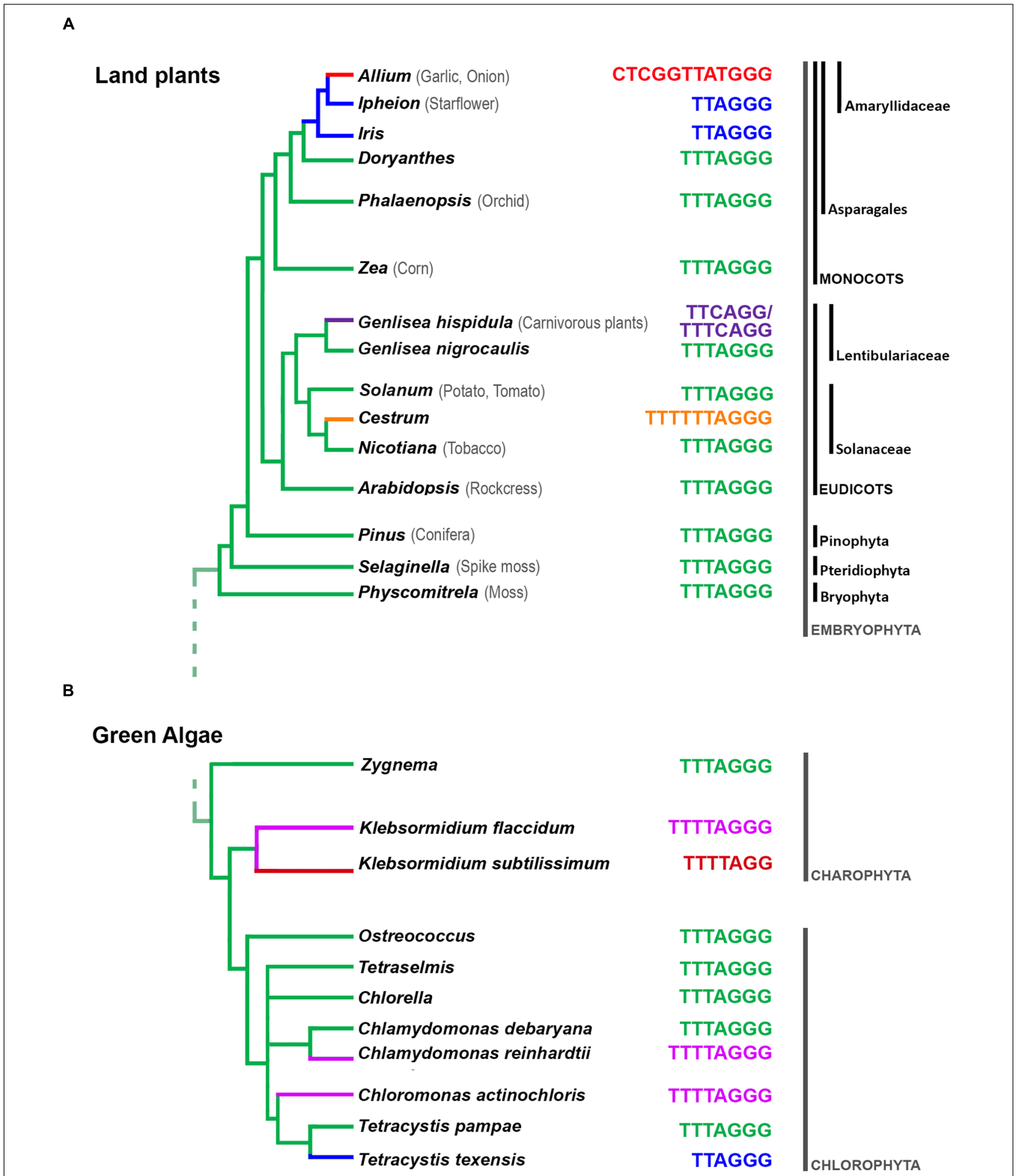

FIGURE 1 | Summary of current knowledge on telomere DNA diversity in land plants (A) and green algae (B). The prevalent plant telomeric sequence motif TTTAGGG was first described in *A. thaliana* (Richards and Ausubel, 1988). Divergent telomeric sequences have been observed in Asparagales (Sykorova et al., 2003), in *Cestrum* spp. (Peska et al., 2015), in *Genlisea* (Tran et al., 2015), or in *Allium* (Fajkus et al., 2016). While *Arabidopsis*-type telomeric sequence is dominant in "green lineages" of algae Chlorophyta and Streptophyta, this ancestral motif was replaced several times with a novel motifs (reviewed in Fulnečková et al., 2015). (The relationships between families and genera are adapted from the schematic phylogenetic tree presented in Fulnečková et al., 2015 and Fajkus et al., 2016.)

t-loops (reviewed in Tomaska et al., 2009). Although formation of t-loop structures was demonstrated among plants only in the garden pea (*Pisum sativum*; Cesare et al., 2003), it is believed that excision from a t-loop in *Arabidopsis* may result in t-circle formation and in telomere rapid deletion (Watson and Shippen, 2007). In tobacco cell culture, knockdown of one of three human hnRNP homologs, named NgGTBP1 (G-strand specific single-stranded telomere-binding protein 1), led to frequent formation of extrachromosomal t-circles, inhibition of single-stranded invasion into double-stranded telomeric DNA and the loss of protection of telomeres against inter-telomeric recombination (Lee and Kim, 2010, 2013).

As well as in humans, mouse, or *Caenorhabditis* (Uringa et al., 2011; Vannier et al., 2012), the regulator of telomere elongation helicase 1 (AtRTEL1) plays a putative role in *Arabidopsis* in the destabilization of DNA loop structures such as t-loops or d-loops (Recker et al., 2014). However, a substantial portion of telomeres in *Arabidopsis* does not apparently undergo nucleolytic resection, and 3′ ends produced by leading-strand replication remain blunt-ended (Riha et al., 2000). It is believed that blunt-ends in *Arabidopsis* are specifically recognized and protected by the AtKu70/80 heterodimer although *in situ* localization of Ku to telomeres remains elusive (Kazda et al., 2012).

PROTEINS ASSOCIATED WITH TELOMERIC DNA

Telomere-associated proteins can regulate lengths of telomere tracts by modulating access of telomerase or affecting conventional DNA replication machinery. In mammals, telomeric DNA associates with a six-protein complex called shelterin. The specific telomeric dsDNA binding is mediated by TRF1 and TRF2 (Broccoli et al., 1997; Court et al., 2005), through their Myb-like domain with an LKDKWRT amino acid motif that is also conserved in other telobox binding proteins, not only in mammals but also in plants (Bilaud et al., 1996; Feldbrugge et al., 1997). A bridge between proteins directly associated with DNA—TRF1, TRF2, and ssDNA binding protein Pot1 (Protection of telomeres 1)—is mediated by TIN2 and the oligosaccharide/oligonucleotide binding (OB)-fold domain of TPP1 (TINT1, PTOP, PIP1) protein (for review see Schmidt and Cech, 2015; Lazzerini-Denchi and Sfeir, 2016). Moreover, protein Rap1, the last component of shelterin, interacts with TRF2 (Arat and Griffith, 2012) and modulates its recruitment to telomeric DNA (Janouskova et al., 2015). A schematic model of mammalian telomere-associated proteins (**Figure 2A**) and a proposed model of the telomeric complex in *A. thaliana* (**Figure 2B**) summarizes recent knowledge in mammalian and plant telomere biology and provides a clear comparison of conserved structures at chromosome termini. In addition, a general overview of telomere-associated proteins that have been described in plants is given in **Table 1**. Detailed description of telomeric and putative telomeric dsDNA and ssDNA binding proteins from *A. thaliana* is shown in **Table 2**.

Telomeric dsDNA-Associated Proteins

Myb-like Proteins

In plants, telomeric dsDNA sequence binding proteins with a Myb-like domain of a telobox (short telomeric motif) type can be classified into three main groups: (i) with a Myb-like domain at the N-terminus (SMH family), (ii) with a Myb-like domain at the C-terminus (TRFL family), and (iii) with a Myb-like domain at the C-terminus (AID family; reviewed in Peska et al., 2011; Du et al., 2013).

The first group of proteins, with a Myb-like domain at the N-terminus, also contains a central histone-like domain with homology to the H1 globular domain found in the linker histones H1/H5, and is therefore called the SMH family (Marian et al., 2003; Schrumpfova et al., 2004). Proteins with an SMH motif are plant-specific but are well conserved throughout the plant kingdom (e.g., eudicots, monocots, moss, or red algae; Du et al., 2013). In *A. thaliana*, there are five members of the SMH family, named telomere repeat binding (AtTRB) proteins (Marian et al., 2003; Schrumpfova et al., 2004). AtTRB1 protein specifically binds plant telomeric repeats through a Myb-like domain *in vitro* (Mozgova et al., 2008), co-localizes with telomeres *in situ*, and physically interacts with AtTERT (**Figure 2B**). Moreover shortening of telomeres was observed in *attrb1* knockout mutants (Schrumpfova et al., 2014). Also other members of this family, AtTRB2 and AtTRB3 (previously named AtTBP3 and AtTBP2, respectively; Schrumpfova et al., 2004), bind telomeric dsDNA as well as telomeric ssDNA *in vitro* as homo- or heteromultimers (Schrumpfova et al., 2004; Mozgova et al., 2008; Hofr et al., 2009; Lee W.K. et al., 2012; Yun et al., 2014). In *Arabidopsis*, AtTRB1 protein physically interacts via its histone-like domain with AtPot1b (Schrumpfova et al., 2008), an *A. thaliana* homolog of the G-overhang binding protein Pot1, and a component of an alternative telomerase holoenzyme complex (Tani and Murata, 2005; He et al., 2006; Surovtseva et al., 2007). Also other members of SMH family proteins in land plants show telomeric dsDNA binding capability: e.g., *Oryza sativa* OsTRBFs (Byun et al., 2008) or *Z. mays* ZmSMHs (Marian et al., 2003). In addition, proteins with Myb-like domain of a telobox type in plants, adopt distinct non-telomeric functions, e.g., PcMYB1 from *Petroselinum crispum* acts only as a transcription factor (Feldbrugge et al., 1997). Recently it was shown that AtTRB1 from *A. thaliana* was not only telomere- and telomerase-binding but was also associated, *in vivo*, with promoters, mostly with a *telo* box motif of translation machinery genes (**Figure 3**; Schrumpfova et al., 2016). The AtTRB1 association with *telo* box motif was then proven by Zhou et al. (2016). Moreover AtTRB proteins seem to have a new role as chromatin modulators: AtTRB1 competes with LIKE HETEROCHROMATIN PROTEIN 1 (AtLHP1) to maintain downregulation of polycomb group (PcG) target genes (Zhou et al., 2016) and protein AtTRB2 directly interacts with histone deacetylases, HDT4 and HDA6, *in vitro* and *in vivo* (Lee and Cho, 2016). Deacetylase activity of HDT4 (Lee and Cho, 2016) and HDA6 (To et al., 2011) against H3K27ac, could be important for subsequent methylations of H3K27me3, that is among others target also for AtLHP1.

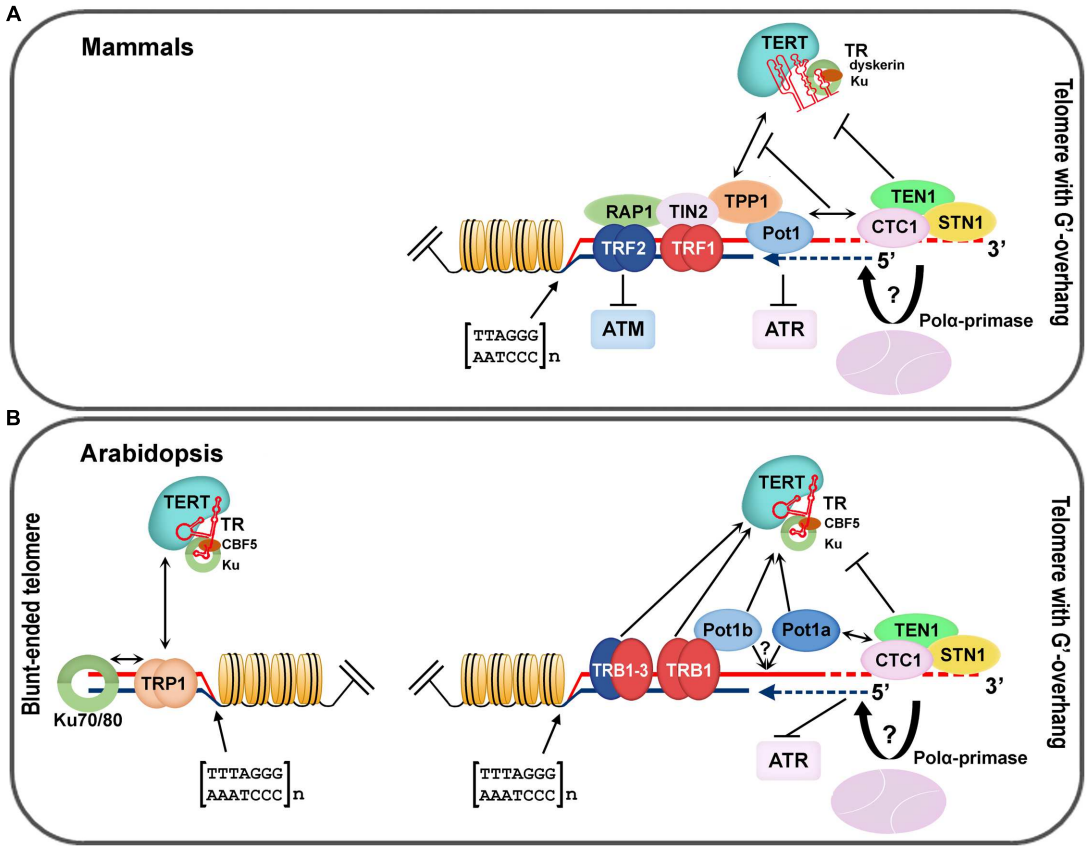

FIGURE 2 | Nucleoprotein complexes associated with mammalian and *A. thaliana* telomeres. (A) Mammalian shelterin proteins (TRF1/2, Rap1, TIN2, TPP, and Pot1) modulate access to the telomerase complex and the ATR/ATM dependent DNA damage response pathway. The CST complex (CTC1–STN1–TEN1) affects telomerase and DNA polymerase α recruitment to the chromosomal termini, and thus coordinates G-overhang extension by telomerase with fill-in synthesis of the complementary C-strand (blue dashed line; figure adopted from Chen and Lingner, 2013). **(B)** *Arabidopsis* TRB1, 2 and 3 interact with the telomeric sequence due to the same Myb-like binding domain as mammalian TRF1/2 (Marian et al., 2003; Kuchar and Fajkus, 2004; Schrumpfova et al., 2004). TRB proteins interact with TERT and Pot1b and when localized at chromosomal ends they are eligible to function as components of the plant shelterin complex, mainly at telomeres with a G-overhang (Schrumpfova et al., 2008, 2014). An evolutionary conserved CST complex is suggested to coordinate the unique requirements for efficient replication of telomeric DNA in plants as well as in other organisms (Derboven et al., 2014). Blunt-ended telomeres are specifically recognized and protected by the KU70/80 heterodimer that directly interacts with TRP1, and by extension, with TERT (Kuchar and Fajkus, 2004; Kazda et al., 2012; Schrumpfova et al., 2014).

Taken together, two lines of evidence classify the AtTRB proteins as novel epigenetic regulators that potentially impact transcription status of thousands of genes: (i) association of AtTRB1 with *telo* box DNA motif (Schrumpfova et al., 2016; Zhou et al., 2016) that is linked with PcG protein pathway (Deng et al., 2013; Wang et al., 2016; Zhou et al., 2016), (ii) involvement of AtTRB proteins in control of H3K27 epigenetic modifications (Lee and Cho, 2016; Zhou et al., 2016), that are also connected with PcG chromatin remodelers.

The second group of proteins, with a Myb-like domain at the C-terminus, is also named TRFL. However a TRFL Myb-like domain alone is not sufficient for telomere binding and requires a more extended domain—Myb-extension (Myb-ext)—for telomeric dsDNA interactions *in vitro* (Karamysheva et al., 2004; Ko et al., 2008). Consequently, two families of TRFL can be distinguished: TRFL family 1 with a Myb-ext, whose protein members bind telomeric dsDNA *in vitro*, and TRFL family 2 without a Myb-ext, whose protein members do not bind telomeric dsDNA specifically *in vitro* and they are usually not considered as telomeric proteins (Karamysheva et al., 2004). The first identification of a TRFL family protein from *O. sativa*—telomere-binding protein 1 (OsRTBP1; Yu et al., 2000) was soon followed by numerous other TRFL members: e.g., *Nicotiana glutinosa* (NgTRF1; Yang et al., 2003), *Solanum lycopersicum* (LeTBP1; Moriguchi et al., 2006), *A. thaliana* (AtTBP1, AtTRP1, AtTRFL2-10; Chen et al., 2001; Hwang et al., 2001; Karamysheva et al., 2004), *Cestrum parqui* (CpTBP; Peska et al., 2011). Even though *O. sativa* or *N. glutinosa* mutants for TRFL members exhibited markedly longer telomeres (Yang et al., 2004; Hong et al., 2007), in *A. thaliana*, a knockout of AtTRP1, member of TRFL family 1 with a Myb-ext, did not change telomere length significantly (Chen et al., 2005). Even multiple knock-out plant, deficient for all six proteins from TRFL family 1 in *A. thaliana* (AtTBP1, AtTRP1, AtTRFL1, AtTRFL2, AtTRFL4, and AtTRF9) did not exhibit changes in telomere length, or phenotypes

TABLE 1 | A general overview of telomere/telomerase associated proteins described in plants.

		A. thaliana	*O. sativa*	*Z. mays*	*N. glutinosa/ N. tabacum/ N. sylvestris*	*H. vulgare*	*S. lycopersicum/ S. tuberosum*	*C. parqui*	*P. crispum*
Telomeric dsDNA-associated proteins									
Myb-like proteins	Myb-like domain at the N-terminus (SMH family)	AtTRB1-3 (Schrumpfova et al., 2004)	OsTRBF1-3 (Byun et al., 2008; He et al., 2013)	ZmSMHs (Marian et al., 2003)					PcMYB1 (Feldbrugge et al., 1997)
	Myb-like domain at the C-terminus (TRFL-family)	AtTBP1 (Hwang et al., 2001) AtTRP1 (Chen et al., 2001) AtTRFL2-10 (Karamysheva et al., 2004)	OsRTBP1 (Yu et al., 2000)	ZmIBP1 (Lugert and Werr, 1994) ZmIBP2 (Moore, 2009)	NgTRF1 (Yang et al., 2003)		LeTBP1 (Moriguchi et al., 2006)	CpTBP1 (Peska et al., 2011)	PcBPF-1 (da Costa e Silva et al., 1993)
	Myb-like domain at the C-terminus (AID family)		OsAlD1 (Zhu et al., 2004; He et al., 2013)	ZmTacs1 (Marian and Bass, 2005)					
CST complex		AtStn1 (Song et al., 2008) AtTEN1 (Leehy et al., 2013) AtCTC1 (Surovtseva et al., 2009)							
Telomeric ssDNA-associated proteins									
OB-fold	Pot-like	AtPot1a-c (Kuchar and Fajkus, 2004; Tani and Murata, 2005; Rossignol et al., 2007)		ZmPot1a (Shakirov et al., 2009b) ZmPot1b (Shakirov et al., 2009b)		HvPot1 (Shakirov et al., 2009b)	StPot1 (Shakirov et al., 2009b)	CpPot1 (Peska et al., 2008)	
Non-OB fold	WHY	AtWhy1 (Yoo et al., 2007)				HvWhy1 (Grabowski et al., 2008)			
	RRM-motif	AtSTEP1 (Kwon and Chung, 2004)	Os08g0492100 (He et al., 2013) Os08g0320100 (He et al., 2013)		NtGTBP1-3 (Hirata et al., 2004; Lee and Kim, 2010)				
Telomerase associated									
TERT subunit		AtTERT (Fajkus et al., 1996)	OsTERT (Oguchi et al., 2004)	ZmTERT (Sykorova et al., 2009)	NtTERT, NsTERT (Sykorova et al., 2012)				
TERT/TR associated proteins	Myb-like domain at the N-terminus (SMH family)	AtTRB1-3 (Schrumpfova et al., 2014)							
	Myb-like domain at the C-terminus (TRFL family)	AtTRP1 (Schrumpfova et al., 2014)							
	Dyskerin-like	AtCBF5 (Lermontova et al., 2007)							
	Pot-like	AtPot1a (Rossignol et al., 2007)							
	RRM-motif	AtRRM (Lee L.Y. et al., 2012)							
	ARM-motif	AtARM (Lee L.Y. et al., 2012)							
	RNA-binding	AtG2p (Dokládal et al., 2015)							
	Metallothionein-like	AtMT2A (Dokládal et al., 2015)							

(Continued)

TABLE 1 | Continued

	A. thaliana	*O. sativa*	*Z. mays*	*N. glutinosa/ N. tabacum/ N. sylvestris*	*H. vulgare*	*S. lycopersicum/ S. tuberosum*	*C. parqui*	*P. crispum*
DNA processing and repair-associated proteins at telomerases								
Helicase	AtRTEL1 (Recker et al., 2014)							
Exonuclease	EXO1 (Kazda et al., 2012)							
Ku	AtKu70/80 (Bundock et al., 2002; Riha et al., 2002)	OsKu70 (Hong et al., 2010)						
PI3 kinase	AtATM (Amiard et al., 2011) AtATR (Amiard et al., 2011)							
MRN Complex	AtRad50 (Gallego and White, 2001) AtMre11 (Bundock and Hooykaas, 2002) AtNbs1 (Najdekrova and Siroky, 2012)							
Ku-independent EJ pathway	AtRad1 (Vannier et al., 2009) AtERCC1 (Vannier et al., 2009) AtXRCC1 (Amiard et al., 2014)							
Backup-NHEJ KU-independent pathway	AtPARP1, 2 (Boltz et al., 2014)							

Proteins that were proven as telomeric DNA- or telomerase-associated proteins are listed above. Their homologues involved in non-telomeric processes, while their associations with telomeres or telomerase have not been observed, are shown in green.

Single Myb Histone family (SMH); TRF-like (TRFL-family); Anther Indehiscence family (AID-family); Cdc13/CTC1-Stn1-Ten1 (CST); Oligonucleotide/Oligosaccharide Binding fold (OB-fold); proteins without Oligonucleotide/Oligosaccharide Binding fold (non-OB-fold); Protection of telomeres – like (Pot-like); Whirly (WHY); RNA Recognition Motifs (RRM-motif); Telomerase Reverse Transcriptase (TERT); Telomerase RNA template (TR); Armadillo/β-catenin-like Repeat-containing protein (ARM); Phosphoinositide 3-kinase (PI3 kinase); Mre11/Rad50/Nbs1 (MRN); End-joining (EJ); Non-homologous end-joining (NHEJ).

Arabidopsis thaliana (At): Telomeric Repeat Binding 1-3 (AtTRB1-3); Telomere Binding Protein 1 (AtTBP1); Telomere Repeat binding Factor 1 (AtTRF1); TRF-like 2-10 (AtTRFL2-10); Suppressor of cdc thirteen homolog (AtStn1); Telomeric pathways in association with Stn1(AtTen); Conserved telomere maintenance component 1 (AtCTC1); Protection of telomeres 1a, b, c (AtPot1a, b, c); Whirly 1 (AtWhy1); Single-stranded Telomere-binding Protein 1 (AtSTEP1); Telomerase Reverse Transcriptase (AtTERT); Cajal Bodies Factor 5 (AtCBF5); RNA Recognition Motifs (AtRRM); Armadillo/β-catenin-like Repeat-containing protein (AtARM); Gene 2 (AtG2p); Metallothionein-like 2A (AtMT2A); Regulator of Telomere Elongation Helicase 1 (AtRTEL1); Exonuclease 1 (AtEXO1); Ataxia telangiectasia mutated kinase (AtARM); ATM- and RAD3-related kinases (AtATR); DNA repair protein 50 (AtRad50); Meiotic recombination 11 (AtMre11); DNA repair protein 1 (AtRad1); Excision repair cross-complementation 1 (AtERCC1); X-ray repair cross-complementing 1 (XRCC1); Nijmegen breakage syndrome 1 (AtNbs1); Poly(ADP-Ribose) polymerase 1, 2 (AtPARP1, 2).

Oriza sativa (Os): Telomere Repeat Binding Factor 1 (OsTRBF1); Rice Telomere Binding Protein 1 (RTBP1); Anther Indehiscence 1 (OsAID1); Telomerase Reverse Transcriptase (OsTERT).

Zea mays (Zm): Single Myb Histone (ZmSMHs); Initiator-binding protein 1 (ZmIBP1); Initiator-binding protein 2 (ZmIBP2); Terminal acidic SANT 1 (ZmTacs1); Protection of telomeres 1a, b (ZmPot1a, b); Telomerase Reverse Transcriptase (ZmTERT).

Nicotiana glutinosa/tabacum/sylvestris (Ng/Nt/Ns): Telomere Repeat binding Factor 1 (NgTRF1); Telomeric ssDNA binding protein 1-3 (NtGTBP1-3); Telomerase Reverse Transcriptase (Ng/NtTERT).

Hordeum vulgare (Hv): Protection of telomeres 1(HvPot1); Whirly 1 (HvWhy1).

Solanum lycopersium/tuberosum (Le/St): Telomere Binding Protein1 (LeTBP1); Protection of telomeres 1 (StPot1).

Cestrum parqui (Cp): Telomere Binding Protein1 (CpTBP1); Protection of telomeres 1 (CpPot1).

Petroselinum crispum (Pc): Myb-like protein 1 (PcMYB1); Box P-binding Factor 1 (PcBPF-1).

TABLE 2 | Telomeric and putative telomeric dsDNA- and ssDNA-binding proteins from *Arabidopsis thaliana*.

		Protein abbreviation	Accession number	Schematic Depiction of Conserved Domains	Telomeric-Sequence-Binding *in vitro*	Localization on Telomeres *in situ*	Telomere length regulation	Reference
Telomeric dsDNA-associated proteins								
Myb-like proteins	Myb-like domain at the N-terminus (SMH family)	AtTRB1	At1g49950	Myb H1/5 CCD	(+)	(+)	(+)	Schrumpfova et al., 2004: Schrumpfova et al., 2014
		AtTRB2	At5g67580		(+)	(+/−)		Schrumpfova et al., 2004; Dvorácková et al., 2010
		AtTRB3	At3g49850		(+)	(+/−)	(+/−)	Schrumpfova et al., 2004; Dvorácková et al., 2010; Zhou et al., 2016
	Myb-like domain at the C-terminus (TRFL-family I)	AtTBP1	At5g13820	Myb -ext	(+)		(−)	Hwang et al., 2001; Fulcher and Riha, 2016
		AtTRP1	At5g59430		(+)		(−)	Chen et al., 2001; Fulcher and Riha, 2016
		AtTRFL1	At3g46590		(+)		(−)	Karamysheva et al., 2004; Hwang et al., 2005; Fulcher and Riha, 2016
		AtTRFL2	At1g07540		(+)		(−)	Karamysheva et al., 2004; Fulcher and Riha, 2016
		AtTRFL4	At3g53790		(+)		(−)	Karamysheva et al., 2004; Fulcher and Riha, 2016
		AtTRFL9	At3g12560		(+)		(−)	Karamysheva et al., 2004; Hwang et al., 2005; Fulcher and Riha, 2016
	Myb-like domain at the terminus (TRFL-family II)	AtTRFL3	At1g17460	Myb	(−)			Karamysheva et al., 2004
		AtTRFL5	At1g15720		(−)			Karamysheva et al., 2004
		AtTRFL6	At1g72650		(−)			Karamysheva et al., 2004
		AtTRFL7	At1g06910		(−)			Karamysheva et al., 2004
		AtTRFL8	At2g37025		(−)			Karamysheva et al., 2004
		AtTRFL10	At5g03780		(−)			Karamysheva et al., 2004
CST complex		AtStn1	At1g07130	OB		(+)	(+)	Song et al., 2008
		AtTen1	At1g56260			(+/−)	(+)	Leehy et al., 2013
		AtCTC1	At4g09680	OB OB OB		(+)	(+)	Surovtseva et al., 2009
Telomeric ssDNA-associated proteins								
OB-fold	Pot-like	AtPot1a	At2g05210	OB OB	(+/−)		(+)	Kuchar and Fajkus, 2004; Tani and Murata, 2005; Shakirov et al., 2005, 2009b; Surovtseva et al., 2007
		AtPot1b	At5g06310		(+/−)		(+)	Kuchar and Fajkus, 2004; Tani and Murata, 2005; Shakirov et al., 2005, 2009b
		AtPot1c	At2g04395	OB			(+)	Rossignol et al., 2007; Nelson, 2012
Non-OB fold	WHY	AtWhy1	At1g14410	Whirly	(+)		(+)	Yoo et al., 2007
	RRM-motif	AtSTEP1	At4g24770	RB RB	(+)			Kwon and Chung, 2004

Symbol (+) indicates published evidence of protein binding to telomeric sequence "Telomeric-sequence Binding in vitro," protein "Localization on Telomeres in situ", or that protein regulates telomere length in plants "Telomere Length Regulation." Symbol (+/−) means that only indirect evidence or ambiguous results exist. Symbol (−) indicates that protein does not specifically interact with telomeric DNA "Telomeric-sequence Binding in vitro," protein is not localized on telomeres "Localization on Telomeres in situ", or that protein does not regulate telomere length in plants "Telomere Length Regulation." Myb-like domain (Myb); Myb-extension (-ext); Histone-like domain (Hl/5); Coiled Coil Domain (CCD); Oligonucleotide/Oligosaccharide-Binding Fold domain (OB); Whirly domain (Whirly); RNA-binding domain (RB); A. thaliana (At); Telomeric Repeat Binding (AtTRB); TRF-like family (TRFL family); Suppressor of cdc thirteen homolog (AtStn1); Conserved telomere maintenance component 1 (AtCTC1); (CTC1-Stn1-Ten1) complex (CST); RNA recognition motifs (RRM); Protection of telomeres 1a, b, c (AtPot1 a,b,c); Whirly 1 (Why1); Single-stranded telomere-binding protein 1 (STEP1)

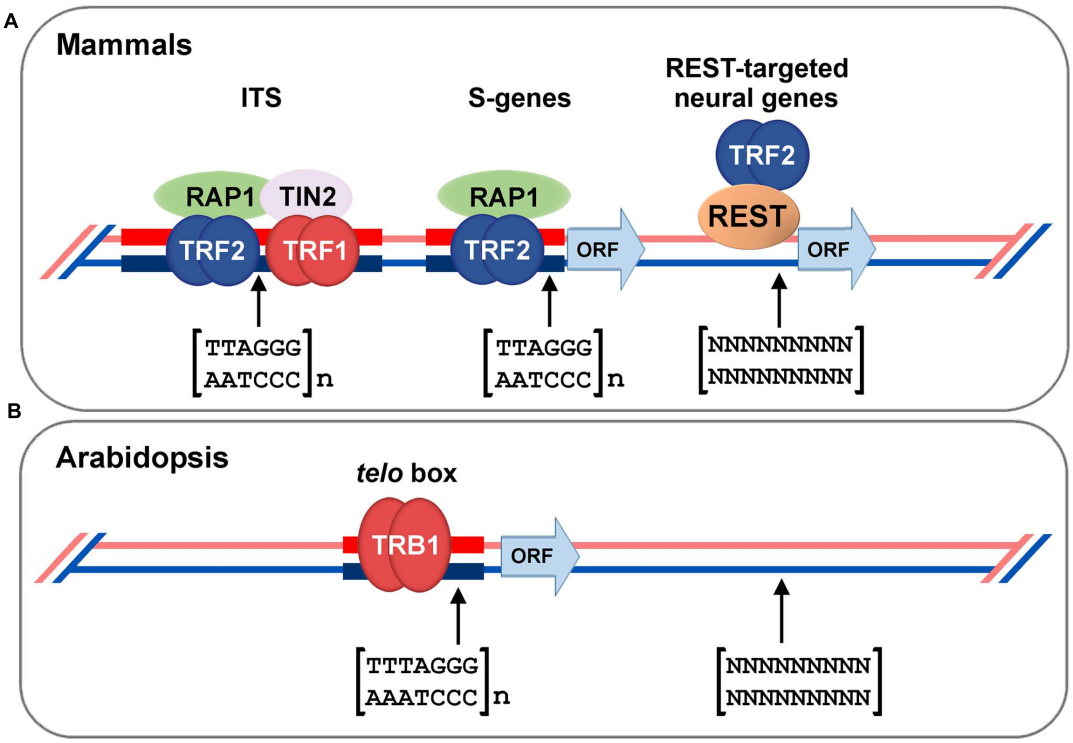

FIGURE 3 | Association of shelterin proteins with extra-telomeric sequences. (A) Mammalian telomere-binding proteins TRF1/2, TIN2, or Rap1 associate not only with terminally localized telomeric repeats but also with interstitial telomeric sequences (ITS) and satellite repeats (Krutilina et al., 2001; Mignon-Ravix et al., 2002; Simonet et al., 2011; Yang et al., 2011). Mouse Rap1, together with TRF2, acts as a gene transcription regulator, including subtelomeric-gene (S-gene) silencing, and also binds to non-coding genomic regions enriched with TTAGGG repeats (Martinez et al., 2010). Moreover, TRF2 regulates neuronal genes by interaction of TRF2 with repressor element 1-silencing transcription factor (REST; Zhang et al., 2008). **(B)** *Arabidopsis* TRB1 protein was found not only as a component of the telomeric interactome (Schrumpfova et al., 2014), but also as a factor associated with 5′ flanking regions (mostly comprising the *telo* box) of translation machinery genes (Schrumpfova et al., 2016; Zhou et al., 2016).

associated with telomere dysfunction (Fulcher and Riha, 2016). Thus, although the AtTRFL proteins from *A. thaliana* specifically bind telomeric DNA *in vitro* and an interaction between AtTRP1 and AtKu70 was observed, suggesting a putative telomere function (**Figure 2B**; Kuchar and Fajkus, 2004), no functional evidence exists for their role at telomeres. Another member of this family—ZmIBP2 (initiator-binding protein) protein—binds not only telomeric repeats (Moore, 2009), but was originally identified as a promoter binding ligand (Lugert and Werr, 1994). Moreover, some members of this Myb-like family were identified exclusively based on their ability to bind promoter regions of certain genes: ZmIBP1 (Lugert and Werr, 1994), PcBPF-1 (box P-binding factor) from *P. crispum* (da Costa e Silva et al., 1993) or CrBPF from *Catharanthus roseus* (van der Fits et al., 2000).

The third group with a Myb-like domain at the C-terminus (AID family) contains only a few members. The AID family is named according to anther indehiscence 1 (AID) protein from *O. sativa*—OsAID1 (Zhu et al., 2004). OsAID1 was initially identified as being involved in anther development. Another member of this family—ZmTacs1 (terminal acidic SANT) from *Z. mays*—may function in chromatin remodeling within the meristem (Marian and Bass, 2005).

In an affinity pull-down technique, 80 proteins from *O. sativa* were identified for their ability to bind to a telomeric repeat (He et al., 2013). Among them, two of three previously reported proteins from the SMH family–OsTRBF1 and OsTRBF2 (Byun et al., 2008), and one protein with a Myb-domain at the C-terminus (AID family)—OsAID1 (Zhu et al., 2004; Du et al., 2013) were demonstrated, while no member with a Myb-domain at the C-terminus of the TRFL family could be found. From other ribonucleoproteins or RNA-binding proteins with putative telomere association, two homologs of *N. tabacum* telomeric ssDNA binding protein NtGTBP1 (Os08g0492100 and Os08g0320100), with RNA recognition motifs (RRM; see below; Lee and Kim, 2010), were also identified.

Telomere-binding proteins in budding yeast (yRap1) or in mammals (TRF1, TRF2, Rap1, and TIN2) are associated with extra-telomeric sequences and thus participate in additional roles, e.g., gene activation and repression, DNA replication, heterochromatin boundary-element formation, creation of hotspots for meiotic recombination and chromatin opening (**Figure 3A**; Morse, 2000; Smogorzewska et al., 2000; Krutilina et al., 2001; Zhang et al., 2008; Martinez et al., 2010; Simonet et al., 2011; Yang et al., 2011; Maï et al., 2014; Ye et al., 2014).

CST Complex

An evolutionary conserved trimeric protein complex named CST (Cdc13/CTC1–Stn1–Ten1) is, similarly to Myb-like proteins, involved in several stages of telomere end formation. In yeast, these OB-fold proteins are required for recruitment of telomerase and DNA polymerase α to the chromosomal termini, and thus coordinate G-overhang extension by telomerase with the fill-in synthesis of the complementary C-strand (Qi and Zakian, 2000; Grossi et al., 2004; Giraud-Panis et al., 2010; Wellinger and Zakian, 2012). In mammals, CST is primarily involved in the rescue of stalled replication forks at the telomere and elsewhere in the genome, and limits telomerase action at individual telomeres to approximately one binding and extension event per cell cycle (**Figure 2A**; Chen et al., 2012; Stewart et al., 2012; Chen and Lingner, 2013; Kasbek et al., 2013).

In *A. thaliana*, a mutation in any CST subunits leads to severe morphological defects and is accompanied by a decrease in telomere length, single-strand G-overhang elongation, mostly subtelomere–subtelomere chromosomal fusions and the appearance of extra-chromosomal telomeric circles. Plants lacking Suppressor of cdc thirteen homolog (AtStn1) or Conserved telomere maintenance component 1 (AtCTC1) exhibit no change in telomerase activity whereas telomerase activity was elevated in *atten1* mutants (Song et al., 2008; Surovtseva et al., 2009; Leehy et al., 2013). Although circumstantial evidence indicates that CST in plants is needed for telomere integrity, clear evidence is absent that would show any direct physical interaction of any component of the CST complex with plant telomeric DNA. As *Arabidopsis* AtCTC1 interacts with the catalytic subunit of DNA polymerase α (ICU2) *in vitro* (Price et al., 2010) and *atstn1* mutant phenotypes can be partially phenocopied by impairment of DNA polymerase α, it was recently suggested that seemingly specific function(s) of CST in telomere protection may rather represent unique requirements for efficient replication of telomeric DNA (**Figure 2B**; Derboven et al., 2014). It seems that the CST complex controls access of telomerase, end-joining recombination and the ATR-dependent (ATM and Rad3-related) DNA damage response pathway at the chromosomal ends in wild-type plants (Boltz et al., 2012; Leehy et al., 2013; Amiard et al., 2014).

Telomeric ssDNA-Associated Proteins

Proteins with OB-fold

The telomeric G-rich overhang is evolutionarily conserved and is a substrate for ssDNA binding proteins. The majority of ssDNA binding proteins bind through OB motifs (OB-fold) and are required for both chromosomal end protection and regulation of telomere length, e.g., telomere-binding protein subunit alpha/beta (TEBPαβ) from *Oxytricha nova* (telomere end binding protein; Price and Cech, 1987), Cell division cycle 13 (Cdc13p) from *S. cerevisiae* (Garvik et al., 1995) and Pot1, are present in diverse organisms including human, mouse, chicken, or *S. pombe* (**Figure 2A**; Baumann and Cech, 2001; Lei et al., 2002; Wei and Price, 2004; Wu et al., 2006). In *A. thaliana*, three Pot-like proteins have been named AtPot1a, AtPot1b, AtPot1c (Kuchar and Fajkus, 2004; Rossignol et al., 2007; previously also named as AtPOT1-1, AtPOT1-2 (Tani and Murata, 2005) or AtPot1, AtPot2 (Shakirov et al., 2005; see Rotkova et al., 2009 for an overview). However, descriptions of their functions and binding properties are not unanimously agreed. While a very weak, but specific affinity of AtPot1a and AtPot1b for plant telomeric ssDNA was originally described (Shakirov et al., 2005), later these authors could not demonstrate AtPot1a and AtPot1b binding to telomeric ssDNA *in vitro* (Shakirov et al., 2009a,b). Nevertheless, stable telomeric ssDNA binding was observed for two full-length plant Pot1 proteins: OlPot1 from the green alga *Ostreococcus lucimarinus* as well as for ZmPot1b from *Z. mays* (Shakirov et al., 2009b). Although Pot1 proteins from plant species as diverse as *Hordeum vulgare* (HvPot1; barley), *Populus trichocarpa* (poplar), *Helianthus argophyllus* (sunflower), *Selaginella moellendorffii* (spikemoss), *Gossypium hirsutum* (cotton), *Pinus taeda* (pine), *Solanum tuberosum* (StPot1; potato), *Asparagus officinalis* and *Z. mays* (ZmPot1a) failed to bind telomeric DNA when expressed in a rabbit reticulocyte lysate expression system *in vitro* and subjected to an electrophoretic mobility shift assay (Shakirov et al., 2009b), binding of plant Pot1 proteins to telomeric DNA under native conditions cannot be excluded. Plants expressing AtPot1a truncated by an N-terminal OB-fold, showed progressive loss of telomeric DNA. In contrast, telomere length was unperturbed in plants expressing analogously trimmed AtPot1b, although overexpression of C-terminally truncated AtPot1b resulted in telomere shortening (Shakirov et al., 2005).

AtPot1a binds AtStn1 and AtCTC1 proteins (**Figure 2B**; Renfrew et al., 2014), associates with an N-terminally spliced variant of AtTERT (AtTERT-V(I8)) (Rossignol et al., 2007), TER1, one of the RNA subunits of *Arabidopsis* telomerase, and is required for maintenance of telomere length *in vivo* (Surovtseva et al., 2007). AtPot1b directly interacts with Myb-like proteins AtTRB1-3 from the SMH family (Schrumpfova et al., 2008), and associates with TER2 and TER2s, putative alternative RNA subunits of telomerase that negatively regulate the function of active telomerase particles (TER1-AtTERT; Cifuentes-Rojas et al., 2012). Nevertheless, AtPot1b does not seem to substantially contribute to telomere maintenance (Cifuentes-Rojas et al., 2012). Pot1-like proteins were also identified in plants with unusual telomeres (e.g., CpPot1 protein in *C. parqui*; Peska et al., 2008).

Non-OB-fold Telomeric ssDNA Binding Proteins

The transcriptional activator protein Whirly 1 (Why1), from a small protein family found mainly in land plants (Desveaux et al., 2000, 2002; Krause et al., 2005), was also identified in a fraction of telomere-binding proteins in *A. thaliana*, and an *atwhy1* knockout mutant appeared to have shorter telomeres (Yoo et al., 2007). While proteins from *A. thaliana* (AtWhy1; Yoo et al., 2007) and from *H. vulgare* (HvWhy1; Grabowski et al., 2008) were found to bind plant telomeric repeat sequences *in vitro*, diverse organelle localization of other Why family members from *O. sativa*, *A. thaliana*, *S. tuberosum* (Krause et al., 2005; Schwacke et al., 2007) and proposed binding to ssDNA of melted promoter regions (Desveaux et al., 2002), rather indicate a role

in communication between plastid and nuclear genes encoding photosynthetic proteins (Foyer et al., 2014; Comadira et al., 2015).

A truncated derivative of chloroplast RNA-binding protein (AtCP31) with RRMs from *A. thaliana*, named AtSTEP1 (single-stranded telomere-binding protein 1), localizes exclusively to the nucleus, specifically binding single-stranded G-rich plant telomeric DNA sequences and inhibiting telomerase-mediated telomere extension (Kwon and Chung, 2004).

A protein identified by gel mobility shift assay that specifically binds the G-strand of telomeric ssDNA from *N. tabacum* (NtGTBP1) also contains a tandem pair of RRMs (Hirata et al., 2004). NtGTBP1 is not only associated with telomeric sequences, as well as two additional GTBP paralogs (NtGTBP2 and NtGTBP3), but also inhibits telomeric strand invasion *in vitro* and leaves of knockdown tobacco plants contained longer telomeres with frequent formation of extrachromosomal t-circles (Lee and Kim, 2010). These observations correspond to a previously detected protein from tobacco nuclei that binds G-rich telomeric strands and reduces accessibility to telomerase or terminal transferase (Fulneckova and Fajkus, 2000).

In addition to the above described proteins, various telomeric ssDNA binding proteins have also been reported in nuclear extracts from *Glycine max*, *A. thaliana*, *O. sativa*, or *Vigna radiata* (Zentgraf, 1995; Kim et al., 1998; Lee et al., 2000; Kwon et al., 2004). However, precise characterization of these proteins, identified by gel mobility shift assay, is mostly missing.

DNA Repair Proteins and Telomeres

Ku in plants, as well as in other eukaryotes, is a highly conserved complex, consisting of two polypeptides (Ku70 and Ku80; Mimori et al., 1981). Due to its high affinity for DNA ends, Ku has a generally conserved role across species in protecting DNA from nucleolytic degradation. Ku is important for several cellular mechanisms: the DNA double-stranded break (DSB) repair pathway by the Ku-dependent non-homologous end-joining (NHEJ) pathway, the DNA damage response machinery, or protection of telomere ends from being recognized as DSBs, thereby preventing their recombination and degradation (reviewed in Fell and Schild-Poulter, 2015). Human Ku directly interacts not only with the shelterin proteins hTRF1, hTRF2, and hRap1, but also with telomerase subunits hTERT and hTR (RNA template; reviewed in Fell and Schild-Poulter, 2015). In contrast to a massive loss of telomeric DNA that was observed in human cells (Wang et al., 2009), mutations in Ku70 and Ku80 in the dicotyledonous *A. thaliana*, as well as in the monocotyledonous *O. sativa*, resulted in longer telomeres, suggesting their conserved role in the negative regulation of plant telomerase (Bundock et al., 2002; Riha et al., 2002; Gallego et al., 2003; Hong et al., 2010). On the other hand, severe developmental defects were observed in *O. sativa osku70* knockout mutants, but a similar mutation in *A. thaliana atku70* showed no effect on plant development (Bundock et al., 2002; Hong et al., 2010). In *S. latifolia* and *A. thaliana*, Ku contributes to the integrity of blunt-ended telomeres by protecting them from nucleolytic resection (Kazda et al., 2012). AtKu specifically interacts with AtTRP1 protein (see above; **Figure 2B**; Kuchar and Fajkus, 2004) and also assembles with TER2 and $TER2_S$ into alternative telomerase complexes that cannot sustain telomere repeats on chromosomal ends (Cifuentes-Rojas et al., 2012).

The mammalian shelterin complex is involved in the repression of the primary signal transducers of DNA breakage, two phosphatidylinositol-3-kinase-like (PI3K) protein kinases: ataxia telangiectasia mutated (ATM) and ATM- and RAD3-related (ATR) kinases. Mice TRF2 acts mainly to protect telomeres against ATM activation (Celli and de Lange, 2005) and POT1 is principally involved in repression of the ATR pathway (Denchi and de Lange, 2007; Guo et al., 2007). Short telomeres in telomerase-deficient plants activate both the AtATM and AtATR, whereas absence of members of the CST complex initiates only AtATR-dependent, but not AtATM-dependent DNA damage response (Amiard et al., 2011; Boltz et al., 2012). In mammals as well as in other organisms, DSBs activate ATM kinase in a manner dependent on the meiotic recombination 11 (Mre11), DNA repair protein 50 (Rad50), and Nijmegen breakage syndrome 1 (Nbs1) named MRN complex. The MRN complex has been found to associate with telomeres and contributes to their maintenance (reviewed in Lamarche et al., 2010). *A. thaliana* AtRad50 mutant plant cells show a progressive shortening of telomeric DNA (Gallego and White, 2001), while in AtMre11 mutant plants, telomere lengthening was observed (Bundock and Hooykaas, 2002). Contrary to these observations, the absence of the third MRN subunit, AtNbs1, does not affect the length of telomeres (Najdekrova and Siroky, 2012).

A. thaliana plants mutated in XPF (xeroderma pigmentosum group F-complementing) and ERCC1 (excision repair cross-complementation group 1) orthologs that form a structure-specific endonuclease essential for nucleotide excision repair (known as AtRad1 and AtERCC1), develop normally and show wild-type telomere length. However, in the absence of telomerase, mutations in either of these genes induce a significantly earlier onset of chromosomal instability, thus indicating a protective role of AtERCC1/AtRad1 against a 3′ G-strand overhang invasion of interstitial telomeric repeats (Vannier et al., 2009). In addition to the Ku proteins that are involved in Ku-dependent NHEJ, an alternative Ku-independent NHEJ pathway was described (reviewed in Decottignies, 2013). Members of the poly(ADP-ribose) polymerase family play a role not only in the base excision repair pathway and the backup-NHEJ KU-independent pathway (Decottignies, 2013) but were also studied in the context of telomere maintenance, association with shelterin proteins or modulation of telomerase activity (Smith et al., 1998; Cook et al., 2002; Beneke et al., 2008). However, analysis of *Arabidopsis* orthologs AtPARP1/AtPARP2 (poly(ADP-Ribose) polymerase) has revealed that, unlike in humans, AtPARPs play a minor role in telomere biology (Boltz et al., 2014). It was proposed that DSB repair pathways in *A. thaliana* are hierarchically organized and the Ku-dependent NHEJ restricts access and action of other DSB repair processes (Charbonnel et al., 2010, 2011). Furthermore the end-joining recombination proteins (AtKU80, AtXRCC1, AtRad1) restrict telomerase activity at deprotected telomeres (Amiard et al., 2014). It was found recently that structure-specific endonucleases AtMUS81 (MMS and UV-sensitive protein 81) and AtSEND1 (single-strand DNA endonuclease 1), which presumably act to repair potentially toxic

structures produced by DNA replication and recombination, are essential for telomere stability in *Arabidopsis*. Combined absence of these endonucleases results in increased occurrence of histone γ-H2AX foci in S-phase and in loss of telomeric DNA (Olivier et al., 2016).

PLANT TELOMERASE

Telomere length in plants and various other organisms is maintained by telomerase, a specialized reverse transcriptase which, in addition to its catalytic subunit (TERT), carries its own RNA template (TR) and elongates telomeric tracts at the chromosomal terminus (Blackburn and Gall, 1978; Fajkus et al., 1996).

TERT subunits consist of an N-terminal portion with telomerase-specific motifs important for binding the telomerase RNA subunit, catalytic domains with the telomerase reverse transcriptase (RT) motifs essential for enzyme activity, and the C-terminal extension, which is highly conserved among plants as well as vertebrates (Sykorova and Fajkus, 2009). Although most eukaryotes harbor only a single TERT gene, in the allotetraploid *N. tabacum* there are three NtTERT gene variants inherited from its diploid progenitor species *N. sylvestris* and *Nicotiana tomentosiformis*. All three NtTERT gene variants are transcribed.

Alternative splicing provides a major source of protein diversity within a given organism. Alternatively spliced variants of TERT transcripts with out-of-frame and/or in-frame mutations were identified not only in humans, mouse, chicken, or *Xenopus* (reviewed in Hrdlickova et al., 2006), but also in many plant species, e.g., *A. thaliana*, *Z. mays* (ZmTERT), *O. sativa* (OsTERT), *Iris tectorum*, and tobacco [with human-type (TTAGGG) telomere motif; reviewed in Sykorova and Fajkus, 2009; Sykorova et al., 2012]. Isoforms generated by alternative splicing may show changes or loss of specific function(s) or subcellular localization of the respective product, or could be functionally important, as was suggested for the *A. thaliana* variant AtTERT V(I8) that exclusively interacts with AtPot1a (Rossignol et al., 2007).

It has been proposed that human telomerase is subjected to posttranslational regulation such as phosphorylation (Kang et al., 1999). Putative phosphorylation sites were detected in the OsTERT sequences from *O. sativa* (Oguchi et al., 2004) or *N. tabacum* BY-2 cells (Yang et al., 2002) but not in AtTERT from *A. thaliana* (Oguchi et al., 2004).

Telomerase-Associated Proteins

Rich protein interactomes of yeast, mammalian or *Ciliate* TERT have been described, including the Ku heterodimer (Chai et al., 2002), HSP90 (heat-shock protein of 90 kDa; Holt et al., 1999; Grandin and Charbonneau, 2001), ATPases pontin and reptin (Venteicher et al., 2008), TEP1 (telomere protein 1; Harrington et al., 1997), and many others, in a broad study (Fu and Collins, 2007) and reviewed in a constantly updated telomerase database (Podlevsky et al., 2008).

In AtTERT, a mitochondrial targeting signal, multiple nuclear localization signals or a nuclear export signal have been reported (Zachova et al., 2013). As AtTERT protein and its domains localize mainly within the nucleus and the nucleolus (Zachova et al., 2013), it can be assumed that most interacting protein partners relevant to telomeric functions will be found among nuclear or nucleolar proteins.

In plants, a limited number of proteins that directly interact with TERT have been described. It was demonstrated by various direct methods that AtTRB proteins, a group of plant homologs of human TRF proteins with a Myb-domain at the N-terminus (see above), physically interact with N-terminal domains of AtTERT (**Figure 2B**; Schrumpfova et al., 2014). A mediated interaction between AtTRP1 protein that belongs to the TRFL family, and AtTERT, was also observed (Schrumpfova et al., 2014). Moreover, the N-terminal part of AtTERT exclusively interacts with AtPot1a but not AtPot1b (Rossignol et al., 2007). Also various proteins with an RRM-motif (AtRRM), an ARM-motif (armadillo/β-catenin-like repeat-containing protein; AtARM), metallothionein-like (AtMT2A), or RNA-binding (AtG2p) motifs were found as AtTERT interacting partners in *A. thaliana* (Lee L.Y. et al., 2012; Dokládal et al., 2015).

Indirect regulation of TERT by various proteins or hormones was further described in plants. In tobacco cell culture, phytohormones such as auxin or abscisic acid regulate phosphorylation of telomerase protein, which is required for the generation of a functional telomerase complex (Tamura et al., 1999; Yang et al., 2002). In *A. thaliana*, reduced endogenous concentrations of auxin in telomerase activator 1 (AtTAC1) mutant plants blocks the ability of this zinc-finger protein to induce AtTERT. However, AtTAC1 does not directly bind the AtTERT promoter (Ren et al., 2004, 2007). A minimal promoter region for AtTERT was proposed using a set of T-insertion mutant lines in the protein-coding region of the *AtTERT* gene or in lines with insertions at the 5′ end of *AtTERT* (Fojtova et al., 2011). Moreover T-DNA insertions in the region upstream of the ATG start of *AtTERT* also led to the activation of putative regulatory elements (Fojtova et al., 2011).

In vertebrates, only one TR per organism was described. The folding of the TR molecule offers interaction sites for various associating cofactors such as dyskerin, Ku, nucleolar protein 10 (NOP10), H/ACA ribonucleoprotein complex subunit 1 (GAR1), or subunit 2 (NHP2; Ting et al., 2005; for review, see Kiss et al., 2010). A single TR was also described among Brassicaceae family plants. However, in *A. thaliana*, two TRs were detected—TER1 and TER2, and the latter may be alternately spliced to a TER2s form (Beilstein et al., 2012). The *Arabidopsis* homolog of human dyskerin, named AtCBF5 (alias AtNAP57), is located within nucleoli and Cajal bodies (Lermontova et al., 2007), associates with active telomerase, and weakly with AtPOT1a, but not AtTERT or AtKu70 (Kannan et al., 2008).

Telomerase-Independent Processes in Plant Telomere Dynamics

Compared to the human model, knowledge of individual protein contributions to the maintenance of telomere length/

accessibility/folding in plants or telomerase biogenesis/regulation is still very limited. The process of telomere maintenance is complicated by the fact that besides the widespread system of telomere maintenance by telomerase (Fajkus et al., 1996; Heller et al., 1996) in plants as well as in other organisms, in the absence of telomerase, telomeres can be elongated by recombination-dependent and telomerase-independent alternative telomere lengthening (ALT) mechanisms (Fajkus et al., 2005). Moreover, in plants, the ALT events appear to participate in early plant development (Ruckova et al., 2008). It was shown that AtKu70 deficiency facilitates engagement of ALT lengthening in *A. thaliana* (Zellinger et al., 2007) and that ALT was suppressed in the absence of ATM protein (Vespa et al., 2007).

Telomeric DNA of higher eukaryotes, including plants, is associated not only with specific proteins, but also with histone complexes that form nucleosomes (**Figure 2**; reviewed in Dvořáčková et al., 2015). In various organisms, as well as in plants, telomeric nucleosomes display an unusually short periodicity (157 bp in length), usually 20–40 bp shorter than bulk nucleosomes of the corresponding organism (Fajkus et al., 1995; Fajkus and Trifonov, 2001; reviewed in Pisano et al., 2008). Moreover, the plant telomeric repeat (CCCTAAA) is a natural target for plant-specific asymmetric methylation (Cokus et al., 2008) that was shown to be mediated by an siRNA pathway (Vrbsky et al., 2010). Analysis of telomeres in *A. thaliana* (Vrbsky et al., 2010) and *N. tabacum* (Majerova et al., 2011) has demonstrated that telomeric histones were associated with both heterochromatin- and euchromatin-specific marks. Recent data strongly support the involvement of various epigenetic mechanisms (DNA methylation, posttranslational modifications of histones, nucleosome assembly or levels of telomere-repeat containing RNA) in maintenance of telomere stability (reviewed in Dvořáčková et al., 2015) thus demonstrating complexity of telomere regulation.

CONCLUSION

The need for protection of chromosomal termini remains conserved across most species. Nevertheless, an extraordinary plasticity of mechanisms protecting telomeres has been described among various organisms (reviewed in Giraud-Panis et al., 2013). While individual capping proteins can differ greatly, common features such as homologous binding domains, structures, or interacting partners exist between seemingly different capping systems. Plant systems show certain distinct features of telomere maintenance, including the reversible regulation of telomerase in somatic cells and the absence of developmental telomere shortening (Fajkus et al., 1998; Riha et al., 1998). These distinctions promote further efforts to elucidate plant telomere interactomes. Only recently the first complexes of telomere-binding proteins were demonstrated and meanwhile it seems that the plant telomere-maintenance system shares similarities with that described in mammals. For example, in *A. thaliana*, one of the most studied plant model systems: (i) the core plant telomeric dsDNA binding proteins (AtTRBs, AtTRP, etc.) contain similar Myb-domains which are also present in human TRF1 or TRF2 proteins; (ii) homologs of human telomeric ssDNA binding hPot1 (AtPOT1a-c) were described; (iii) cross-species conserved CST complexes (AtCTC1/AtTen1/AtStn1) retain its function in plants. The similarities between plant and mammalian telomeric DNA-associated proteins apply also to their roles in regulation of gene expression, which are independent of their roles in telomere capping (Lee and Cho, 2016; Schrumpfova et al., 2016; Zhou et al., 2016), as was previously described in their mammalian counterparts (reviewed in Maï et al., 2014; Ye et al., 2014). Elucidation of the composition of the plant version of shelterin and molecular dissection of its components and their roles will be important in the near future to assess the conservation and mechanisms of end-protection and end-replication processes in yeasts, plants and animals.

AUTHOR CONTRIBUTIONS

PPS contributed substantially to the writing of the manuscript, tables and drawing the figures; ŠS participated in preparation of tables; JF edited the manuscript. All authors read and approved the manuscript for publication.

FUNDING

This research was supported by the Czech Science Foundation (13-06943S and 16-01137S) and by the Ministry of Education, Youth and Sports of the Czech Republic under the project CEITEC 2020 (LQ1601).

REFERENCES

Adams, S. P., Hartman, T. P., Lim, K. Y., Chase, M. W., Bennett, M. D., Leitch, I. J., et al. (2001). Loss and recovery of *Arabidopsis*-type telomere repeat sequences 5′-(TTTAGGG)(n)-3′ in the evolution of a major radiation of flowering plants. *Proc. Biol. Sci.* 268, 1541–1546. doi: 10.1098/rspb.2001.1726

Amiard, S., Depeiges, A., Allain, E., White, C. I., and Gallego, M. E. (2011). *Arabidopsis* ATM and ATR kinases prevent propagation of genome damage caused by telomere dysfunction. *Plant Cell* 23, 4254–4265. doi: 10.1105/tpc.111.092387

Amiard, S., Olivier, M., Allain, E., Choi, K., Smith-Unna, R., Henderson, I. R., et al. (2014). Telomere stability and development of ctc1 mutants are rescued by inhibition of EJ recombination pathways in a telomerase-dependent manner. *Nucleic Acids Res.* 42, 11979–11991. doi: 10.1093/nar/gku897

Arat, N. O., and Griffith, J. D. (2012). Human Rap1 interacts directly with telomeric DNA and regulates TRF2 localization at the telomere. *J. Biol. Chem.* 287, 41583–41594. doi: 10.1074/jbc.M112.415984

Armstrong, S. J., Franklin, F. C., and Jones, G. H. (2001). Nucleolus-associated telomere clustering and pairing precede meiotic chromosome synapsis in *Arabidopsis thaliana*. *J. Cell Sci.* 114, 4207–4217.

Aronen, T., and Ryynanen, L. (2014). Silver birch telomeres shorten in tissue culture. *Tree Genet. Genomes* 10, 67–74. doi: 10.1007/s11295-013-0662-4

Bass, H. W., Marshall, W. F., Sedat, J. W., Agard, D. A., and Cande, W. Z. (1997). Telomeres cluster de novo before the initiation of synapsis: a three-dimensional spatial analysis of telomere positions before and during meiotic prophase. *J. Cell Biol.* 137, 5–18. doi: 10.1083/jcb.137.1.5

Baumann, P., and Cech, T. R. (2001). Pot1, the putative telomere end-binding protein in fission yeast and humans. *Science* 292, 1171–1175. doi: 10.1126/science.1060036

Beilstein, M. A., Brinegar, A. E., and Shippen, D. E. (2012). Evolution of the *Arabidopsis* telomerase RNA. *Front. Genet.* 3:188. doi: 10.3389/fgene.2012.00188

Beilstein, M. A., Renfrew, K. B., Song, X., Shakirov, E. V., Zanis, M. J., and Shippen, D. E. (2015). Evolution of the telomere-associated protein POT1a in *Arabidopsis thaliana* is characterized by positive selection to reinforce protein-protein interaction. *Mol. Biol. Evol.* 32, 1329–1341. doi: 10.1093/molbev/msv025

Beneke, S., Cohausz, O., Malanga, M., Boukamp, P., Althaus, F., and Burkle, A. (2008). Rapid regulation of telomere length is mediated by poly(ADP-ribose) polymerase-1. *Nucleic Acids Res.* 36, 6309–6317. doi: 10.1093/nar/gkn615

Bianchi, A., and Shore, D. (2008). How telomerase reaches its end: mechanism of telomerase regulation by the telomeric complex. *Mol. Cell.* 31, 153–165. doi: 10.1016/j.molcel.2008.06.013

Bilaud, T., Koering, C. E., Binet-Brasselet, E., Ancelin, K., Pollice, A., Gasser, S. M., et al. (1996). The telobox, a Myb-related telomeric DNA binding motif found in proteins from yeast, plants and human. *Nucleic Acids Res.* 24, 1294–1303. doi: 10.1093/nar/24.7.1294

Blackburn, E. H., and Gall, J. G. (1978). A tandemly repeated sequence at the termini of the extrachromosomal ribosomal RNA genes in *Tetrahymena*. *J. Mol. Biol.* 120, 33–53.

Boltz, K. A., Jasti, M., Townley, J. M., and Shippen, D. E. (2014). Analysis of poly(ADP-Ribose) polymerases in *Arabidopsis* telomere biology. *PLoS ONE* 9:e88872. doi: 10.1371/journal.pone.0088872

Boltz, K. A., Leehy, K., Song, X., Nelson, A. D., and Shippen, D. E. (2012). ATR cooperates with CTC1 and STN1 to maintain telomeres and genome integrity in *Arabidopsis*. *Mol. Biol. Cell* 23, 1558–1568. doi: 10.1091/mbc.E11-12-1002

Broccoli, D., Smogorzewska, A., Chong, L., and de Lange, T. (1997). Human telomeres contain two distinct Myb-related proteins, TRF1 and TRF2. *Nat. Genet.* 17, 231–235. doi: 10.1038/ng1097-231

Bundock, P., and Hooykaas, P. (2002). Severe developmental defects, hypersensitivity to DNA-damaging agents, and lengthened telomeres in *Arabidopsis* MRE11 mutants. *Plant Cell* 14, 2451–2462. doi: 10.1105/tpc.005959

Bundock, P., van Attikum, H., and Hooykaas, P. (2002). Increased telomere length and hypersensitivity to DNA damaging agents in an *Arabidopsis* KU70 mutant. *Nucleic Acids Res.* 30, 3395–3400. doi: 10.1093/nar/gkf445

Byun, M. Y., Hong, J. P., and Kim, W. T. (2008). Identification and characterization of three telomere repeat-binding factors in rice. *Biochem. Biophys. Res. Commun.* 372, 85–90. doi: 10.1016/j.bbrc.2008.04.181

Celli, G. B., and de Lange, T. (2005). DNA processing is not required for ATM-mediated telomere damage response after TRF2 deletion. *Nat. Cell Biol.* 7, 712–718. doi: 10.1038/ncb1275

Cesare, A. J., Quinney, N., Willcox, S., Subramanian, D., and Griffith, J. D. (2003). Telomere looping in *P. sativum* (common garden pea). *Plant J.* 36, 271–279. doi: 10.1046/j.1365-313X.2003.01882.x

Chai, W., Ford, L. P., Lenertz, L., Wright, W. E., and Shay, J. W. (2002). Human Ku70/80 associates physically with telomerase through interaction with hTERT. *J. Biol. Chem.* 277, 47242–47247. doi: 10.1074/jbc.M208542200

Charbonnel, C., Allain, E., Gallego, M. E., and White, C. I. (2011). Kinetic analysis of DNA double-strand break repair pathways in *Arabidopsis*. *DNA Repair (Amst.)* 10, 611–619. doi: 10.1016/j.dnarep.2011.04.002

Charbonnel, C., Gallego, M. E., and White, C. I. (2010). Xrcc1-dependent and Ku-dependent DNA double-strand break repair kinetics in *Arabidopsis* plants. *Plant J.* 64, 280–290. doi: 10.1111/j.1365-313X.2010.04331.x

Chen, C. M., Wang, C. T., and Ho, C. H. (2001). A plant gene encoding a Myb-like protein that binds telomeric GGTTTAG repeats in vitro. *J. Biol. Chem.* 276, 16511–16519. doi: 10.1074/jbc.M009659200

Chen, C. M., Wang, C. T., Kao, Y. H., Chang, G. D., Ho, C. H., Lee, F. M., et al. (2005). Functional redundancy of the duplex telomeric DNA-binding proteins in *Arabidopsis*. *Bot. Bull. Acad. Sin.* 46, 315–324.

Chen, L. Y., and Lingner, J. (2013). CST for the grand finale of telomere replication. *Nucleus* 4, 277–282. doi: 10.4161/nucl.25701

Chen, L. Y., Redon, S., and Lingner, J. (2012). The human CST complex is a terminator of telomerase activity. *Nature* 488, 540–544. doi: 10.1038/nature11269

Chikashige, Y., Tsutsumi, C., Yamane, M., Okamasa, K., Haraguchi, T., and Hiraoka, Y. (2006). Meiotic proteins bqt1 and bqt2 tether telomeres to form the bouquet arrangement of chromosomes. *Cell* 125, 59–69. doi: 10.1016/j.cell.2006.01.048

Cifuentes-Rojas, C., Nelson, A. D., Boltz, K. A., Kannan, K., She, X., and Shippen, D. E. (2012). An alternative telomerase RNA in *Arabidopsis* modulates enzyme activity in response to DNA damage. *Genes Dev.* 26, 2512–2523. doi: 10.1101/gad.202960.112

Cokus, S. J., Feng, S., Zhang, X., Chen, Z., Merriman, B., Haudenschild, C. D., et al. (2008). Shotgun bisulphite sequencing of the *Arabidopsis* genome reveals DNA methylation patterning. *Nature* 452, 215–219. doi: 10.1038/nature06745

Comadira, G., Rasool, B., Kaprinska, B., Garcia, B. M., Morris, J., Verrall, S. R., et al. (2015). WHIRLY1 functions in the control of responses to nitrogen deficiency but not aphid infestation in barley. *Plant Physiol.* 168, 1140–1151. doi: 10.1104/pp.15.00580

Cook, B. D., Dynek, J. N., Chang, W., Shostak, G., and Smith, S. (2002). Role for the related poly(ADP-Ribose) polymerases tankyrase 1 and 2 at human telomeres. *Mol. Cell. Biol.* 22, 332–342. doi: 10.1128/MCB.22.1.332-342.2002

Corredor, E., and Naranjo, T. (2007). Effect of colchicine and telocentric chromosome conformation on centromere and telomere dynamics at meiotic prophase I in wheat-rye additions. *Chromosome Res.* 15, 231–245. doi: 10.1007/s10577-006-1117-7

Court, R., Chapman, L., Fairall, L., and Rhodes, D. (2005). How the human telomeric proteins TRF1 and TRF2 recognize telomeric DNA: a view from high-resolution crystal structures. *EMBO Rep.* 6, 39–45. doi: 10.1038/sj.embor.7400314

Cowan, C. R., Carlton, P. M., and Cande, W. Z. (2001). The polar arrangement of telomeres in interphase and meiosis. Rabl organization and the bouquet. *Plant Physiol.* 125, 532–538.

Cowan, C. R., Carlton, P. M., and Cande, W. Z. (2002). Reorganization and polarization of the meiotic bouquet-stage cell can be uncoupled from telomere clustering. *J. Cell Sci.* 115, 3757–3766. doi: 10.1242/jcs.00054

da Costa e Silva, O., Klein, L., Schmelzer, E., Trezzini, G. F., and Hahlbrock, K. (1993). BPF-1, a pathogen-induced DNA-binding protein involved in the plant defense response. *Plant J.* 4, 125–135.

de Lange, T. (2005). Shelterin: the protein complex that shapes and safeguards human telomeres. *Genes Dev.* 19, 2100–2110. doi: 10.1101/gad.1346005

Decottignies, A. (2013). Alternative end-joining mechanisms: a historical perspective. *Front. Genet.* 4:48. doi: 10.3389/fgene.2013.00048

Denchi, E. L., and de Lange, T. (2007). Protection of telomeres through independent control of ATM and ATR by TRF2 and POT1. *Nature* 448, 1068–1071. doi: 10.1038/nature06065

Deng, W., Buzas, D. M., Ying, H., Robertson, M., Taylor, J., Peacock, W. J., et al. (2013). *Arabidopsis* Polycomb Repressive Complex 2 binding sites contain putative GAGA factor binding motifs within coding regions of genes. *BMC Genomics* 14:593. doi: 10.1186/1471-2164-14-593

Derboven, E., Ekker, H., Kusenda, B., Bulankova, P., and Riha, K. (2014). Role of STN1 and DNA polymerase alpha in telomere stability and genome-wide replication in *Arabidopsis*. *PLoS Genet.* 10:e1004682. doi: 10.1371/journal.pgen.1004682

Desveaux, D., Allard, J., Brisson, N., and Sygusch, J. (2002). A new family of plant transcription factors displays a novel ssDNA-binding surface. *Nat. Struct. Biol.* 9, 512–517. doi: 10.1038/nsb814

Desveaux, D., Despres, C., Joyeux, A., Subramaniam, R., and Brisson, N. (2000). PBF-2 is a novel single-stranded DNA binding factor implicated in PR-10a gene activation in potato. *Plant Cell* 12, 1477–1489. doi: 10.1105/tpc.12.8.1477

Dokládal, L., Honys, D., Rana, R., Lee, L.-Y., Gelvin, S., and Sýkorová, E. (2015). cDNA library screening identifies protein interactors potentially involved in non-telomeric roles of *Arabidopsis* telomerase. *Front. Plant Sci.* 6:985. doi: 10.3389/fpls.2015.00985

Dong, F., and Jiang, J. (1998). Non-Rabl patterns of centromere and telomere distribution in the interphase nuclei of plant cells. *Chromosome Res.* 6, 551–558. doi: 10.1023/A:1009280425125

Du, H., Wang, Y. B., Xie, Y., Liang, Z., Jiang, S. J., Zhang, S. S., et al. (2013). Genome-wide identification and evolutionary and expression analyses of MYB-related genes in land plants. *DNA Res.* 20, 437–448. doi: 10.1093/dnares/dst021

Dvořáčková, M., Fojtova, M., and Fajkus, J. (2015). Chromatin dynamics of plant telomeres and ribosomal genes. *Plant J.* 83, 18–37. doi: 10.1111/tpj.12822

Dvorácková, M., Rossignol, P., Shaw, P. J., Koroleva, O. A., Doonan, J. H., and Fajkus, J. (2010). AtTRB1, a telomeric DNA-binding protein from *Arabidopsis*, is concentrated in the nucleolus and shows highly dynamic association with chromatin. *Plant J.* 61, 637–649. doi: 10.1111/j.1365-313X.2009.04094.x

Fajkus, J., Fulneckova, J., Hulanova, M., Berkova, K., Riha, K., and Matyasek, R. (1998). Plant cells express telomerase activity upon transfer to callus culture, without extensively changing telomere lengths. *Mol. Gen. Genet.* 260, 470–474. doi: 10.1007/s004380050918

Fajkus, J., Kovarik, A., and Kralovics, R. (1996). Telomerase activity in plant cells. *FEBS Lett.* 391, 307–309. doi: 10.1016/0014-5793(96)00757-0

Fajkus, J., Kovarik, A., Kralovics, R., and Bezdek, M. (1995). Organization of telomeric and subtelomeric chromatin in the higher plant *Nicotiana tabacum*. *Mol. Gen. Genet.* 247, 633–638. doi: 10.1007/BF00290355

Fajkus, J., Sykorova, E., and Leitch, A. R. (2005). Telomeres in evolution and evolution of telomeres. *Chromosome Res.* 13, 469–479. doi: 10.1007/s10577-005-0997-2

Fajkus, J., and Trifonov, E. N. (2001). Columnar packing of telomeric nucleosomes. *Biochem. Biophys. Res. Commun.* 280, 961–963. doi: 10.1006/bbrc.2000.4208

Fajkus, P., Peska, V., Sitova, Z., Fulnecková, J., Dvorackova, M., Gogela, R., et al. (2016). *Allium* telomeres unmasked: the unusual telomeric sequence (CTCGGTTATGGG)n is synthesized by telomerase. *Plant J.* 85, 337–347. doi: 10.1111/tpj.13115

Feldbrugge, M., Sprenger, M., Hahlbrock, K., and Weisshaar, B. (1997). PcMYB1, a novel plant protein containing a DNA-binding domain with one MYB repeat, interacts in vivo with a light-regulatory promoter unit. *Plant J.* 11, 1079–1093. doi: 10.1046/j.1365-313X.1997.11051079.x

Fell, V. L., and Schild-Poulter, C. (2015). The Ku heterodimer: function in DNA repair and beyond. *Mutat. Res. Rev. Mutat. Res.* 763, 15–29. doi: 10.1016/j.mrrev.2014.06.002

Fojtova, M., Peska, V., Dobsakova, Z., Mozgova, I., Fajkus, J., and Sykorova, E. (2011). Molecular analysis of T-DNA insertion mutants identified putative regulatory elements in the AtTERT gene. *J. Exp. Bot.* 62, 5531–5545. doi: 10.1093/jxb/err235

Fojtova, M., Sykorova, E., Najdekrova, L., Polanska, P., Zachova, D., Vagnerova, R., et al. (2015). Telomere dynamics in the lower plant *Physcomitrella patens*. *Plant Mol. Biol.* 87, 591–601. doi: 10.1007/s11103-015-0299-9

Foyer, C. H., Karpinska, B., and Krupinska, K. (2014). The functions of WHIRLY1 and REDOX-RESPONSIVE TRANSCRIPTION FACTOR 1 in cross tolerance responses in plants: a hypothesis. *Philos. Trans. R. Soc. Lond. B Biol. Sci.* 369:20130226. doi: 10.1098/rstb.2013.0226

Freeling, M. (2009). Bias in plant gene content following different sorts of duplication: tandem, whole-genome, segmental, or by transposition. *Annu. Rev. Plant Biol.* 60, 433–453. doi: 10.1146/annurev.arplant.043008.092122

Fu, D., and Collins, K. (2007). Purification of human telomerase complexes identifies factors involved in telomerase biogenesis and telomere length regulation. *Mol. Cell* 28, 773–785. doi: 10.1016/j.molcel.2007.09.023

Fulcher, N., and Riha, K. (2016). Using centromere mediated genome elimination to elucidate the funcional redudancy of candidate telomere binding proteins in *Arabidopsis thaliana*. *Front. Genet.* 6:349. doi: 10.3389/fgene.2015.00349

Fulneckova, J., and Fajkus, J. (2000). Inhibition of plant telomerase by telomere-binding proteins from nuclei of telomerase-negative tissues. *FEBS Lett.* 467, 305–310. doi: 10.1016/S0014-5793(00)01178-9

Fulnecková, J., Sevcíková, T., Fajkus, J., Lukesová, A., Lukes, M., Vlcek, C., et al. (2013). A broad phylogenetic survey unveils the diversity and evolution of telomeres in eukaryotes. *Genome Biol. Evol.* 5, 468–483. doi: 10.1093/gbe/evt019

Fulnečková, J., Ševčikova, T., Lukešová, A., and Sýkorová, E. (2015). Transtitions between the *Arabidopsis*-type and the human-type telomere sequence in green algae (clade Caudivolvoxa, Chlamydomonadales). *Chromosoma*. doi: 10.1007/s00412-015-0557-2 [Epub ahead of print].

Gallego, M. E., Jalut, N., and White, C. I. (2003). Telomerase dependence of telomere lengthening in Ku80 mutant *Arabidopsis*. *Plant Cell* 15, 782–789. doi: 10.1105/tpc.008623

Gallego, M. E., and White, C. I. (2001). RAD50 function is essential for telomere maintenance in *Arabidopsis*. *Proc. Natl. Acad. Sci. U.S.A.* 98, 1711–1716. doi: 10.1073/pnas.98.4.1711

Garvik, B., Carson, M., and Hartwell, L. (1995). Single-stranded DNA arising at telomeres in cdc13 mutants may constitute a specific signal for the RAD9 checkpoint. *Mol. Cell. Biol.* 15, 6128–6613. doi: 10.1128/MCB.15.11.6128

Giraud-Panis, M. J., Pisano, S., Benarroch-Popivker, D., Pei, B., Le, Du, M. H., et al. (2013). One identity or more for telomeres? *Front. Oncol.* 3:48. doi: 10.3389/fonc.2013.00048

Giraud-Panis, M. J., Teixeira, M. T., Geli, V., and Gilson, E. (2010). CST meets shelterin to keep telomeres in check. *Mol. Cell.* 39, 665–676. doi: 10.1016/j.molcel.2010.08.024

Grabowski, E., Miao, Y., Mulisch, M., and Krupinska, K. (2008). Single-stranded DNA-binding protein Whirly1 in barley leaves is located in plastids and the nucleus of the same cell. *Plant Physiol.* 147, 1800–1804. doi: 10.1104/pp.108.122796

Grandin, N., and Charbonneau, M. (2001). Hsp90 levels affect telomere length in yeast. *Mol. Genet. Genom.* 265, 126–134. doi: 10.1007/s004380000398

Graumann, K., Runions, J., and Evans, D. E. (2010). Characterization of SUN-domain proteins at the higher plant nuclear envelope. *Plant J.* 61, 134–144. doi: 10.1111/j.1365-313X.2009.04038.x

Grossi, S., Puglisi, A., Dmitriev, P. V., Lopes, M., and Shore, D. (2004). Pol12, the B subunit of DNA polymerase alpha, functions in both telomere capping and length regulation. *Genes Dev.* 18, 992–1006. doi: 10.1101/gad.300004

Guo, X., Deng, Y., Lin, Y., Cosme-Blanco, W., Chan, S., He, H., et al. (2007). Dysfunctional telomeres activate an ATM-ATR-dependent DNA damage response to suppress tumorigenesis. *EMBO J.* 26, 4709–4719.

Harrington, L., McPhail, T., Mar, V., Zhou, W., Oulton, R., Bass, M. B., et al. (1997). A mammalian telomerase-associated protein. *Science* 275, 973–977. doi: 10.1126/science.275.5302.973

He, H., Multani, A. S., Cosme-Blanco, W., Tahara, H., Ma, J., Pathak, S., et al. (2006). POT1b protects telomeres from end-to-end chromosomal fusions and aberrant homologous recombination. *EMBO J.* 25, 5180–5190. doi: 10.1038/sj.emboj.7601294

He, Q., Chen, L., Xu, Y., and Yu, W. (2013). Identification of centromeric and telomeric DNA-binding proteins in rice. *Proteomics* 13, 826–832. doi: 10.1002/pmic.201100416

He, X. L., and Zhang, J. Z. (2005). Gene complexity and gene duplicability. *Curr. Biol.* 15, 1016–1021. doi: 10.1016/j.cub.2005.04.035

Heller, K., Kilian, A., Piatyszek, M. A., and Kleinhofs, A. (1996). Telomerase activity in plant extracts. *Mol. Gen. Genet.* 252, 342–345. doi: 10.1007/BF02173780

Higgins, J. D., Perry, R. M., Barakate, A., Ramsay, L., Waugh, R., Halpin, C., et al. (2012). Spatiotemporal asymmetry of the meiotic program underlies the predominantly distal distribution of meiotic crossovers in barley. *Plant Cell* 24, 4096–4109. doi: 10.1105/tpc.112.102483

Hirata, Y., Suzuki, C., and Sakai, S. (2004). Characterization and gene cloning of telomere-binding protein from tobacco BY-2 cells. *Plant Physiol. Biochem.* 42, 7–14. doi: 10.1016/j.plaphy.2003.10.002

Hofr, C., Sultesova, P., Zimmermann, M., Mozgova, I., Prochazkova Schrumpfova, P., Wimmerova, M., et al. (2009). Single-Myb-histone proteins from *Arabidopsis thaliana*: a quantitative study of telomere-binding specificity and kinetics. *Biochem. J.* 419, 221–228. doi: 10.1042/BJ20082195 , 222 p following 228.

Holt, S. E., Aisner, D. L., Baur, J., Tesmer, V. M., Dy, M., Ouellette, M., et al. (1999). Functional requirement of p23 and Hsp90 in telomerase complexes. *Genes Dev.* 13, 817–826. doi: 10.1101/gad.13.7.817

Hong, J. P., Byun, M. Y., An, K., Yang, S. J., An, G., and Kim, W. T. (2010). OsKu70 is associated with developmental growth and genome stability in rice. *Plant Physiol.* 152, 374–387. doi: 10.1104/pp.109.150391

Hong, J. P., Byun, M. Y., Koo, D. H., An, K., Bang, J. W., Chung, I. K., et al. (2007). Suppression of RICE TELOMERE BINDING PROTEIN 1 results in severe and gradual developmental defects accompanied by genome instability in rice. *Plant Cell* 19, 1770–1781. doi: 10.1105/tpc.107.051953

Hrdlickova, R., Nehyba, J., Liss, A. S., and Bose, H. R. Jr. (2006). Mechanism of telomerase activation by v-Rel and its contribution to transformation. *J. Virol.* 80, 281–295. doi: 10.1128/JVI.80.1.281-295.2006

Hwang, M. G., Chung, I. K., Kang, B. G., and Cho, M. H. (2001). Sequence-specific binding property of *Arabidopsis thaliana* telomeric DNA binding protein 1 (AtTBP1). *FEBS Lett.* 503, 35–40. doi: 10.1016/S0014-5793(01)02685-0

Hwang, M. G., Kim, K., Lee, W. K., and Cho, M. H. (2005). AtTBP2 and AtTRP2 in *Arabidopsis* encode proteins that bind plant telomeric DNA and induce DNA bending in vitro. *Mol. Gen. Genom.* 273, 66–75. doi: 10.1007/s00438-004-1096-3

Idziak, D., Robaszkiewicz, E., and Hasterok, R. (2015). Spatial distribution of centromeres and telomeres at interphase varies among *Brachypodium* species. *J. Exp. Bot.* 66, 6623–6634. doi: 10.1093/jxb/erv369

Janouskova, E., Necasova, I., Pavlouskova, J., Zimmermann, M., Hluchy, M., Marini, V., et al. (2015). Human Rap1 modulates TRF2 attraction to telomeric DNA. *Nucleic Acids Res.* 43, 2691–2700. doi: 10.1093/nar/gkv097

Kaminker, P. G., Kim, S. H., Desprez, P. Y., and Campisi, J. (2009). A novel form of the telomere-associated protein TIN2 localizes to the nuclear matrix. *Cell Cycle* 8, 931–939. doi: 10.4161/cc.8.6.7941

Kang, S. S., Kwon, T., Kwon, D. Y., and Do, S. I. (1999). Akt protein kinase enhances human telomerase activity through phosphorylation of telomerase reverse transcriptase subunit. *J. Biol. Chem.* 274, 13085–13090. doi: 10.1074/jbc.274.19.13085

Kannan, K., Nelson, A. D., and Shippen, D. E. (2008). Dyskerin is a component of the *Arabidopsis* telomerase RNP required for telomere maintenance. *Mol. Cell. Biol.* 28, 2332–2341. doi: 10.1128/MCB.01490-07

Karamysheva, Z. N., Surovtseva, Y. V., Vespa, L., Shakirov, E. V., and Shippen, D. E. (2004). A C-terminal Myb extension domain defines a novel family of double-strand telomeric DNA-binding proteins in *Arabidopsis*. *J. Biol. Chem.* 279, 47799–47807. doi: 10.1074/jbc.M407938200

Kasbek, C., Wang, F., and Price, C. M. (2013). Human TEN1 maintains telomere integrity and functions in genome-wide replication restart. *J. Biol. Chem.* 288, 30139–30150. doi: 10.1074/jbc.M113.493478

Kazda, A., Zellinger, B., Rossler, M., Derboven, E., Kusenda, B., and Riha, K. (2012). Chromosome end protection by blunt-ended telomeres. *Genes Dev.* 26, 1703–1713. doi: 10.1101/gad.194944.112

Kim, J. H., Kim, W. T., and Chung, I. K. (1998). Rice proteins that bind single-stranded G-rich telomere DNA. *Plant Mol. Biol.* 36, 661–672. doi: 10.1023/A:1005994719175

Kiss, T., Fayet-Lebaron, E., and Jady, B. E. (2010). Box H/ACA small ribonucleoproteins. *Mol. Cell.* 37, 597–606. doi: 10.1016/j.molcel.2010.01.032

Ko, S., Jun, S. H., Bae, H., Byun, J. S., Han, W., Park, H., et al. (2008). Structure of the DNA-binding domain of NgTRF1 reveals unique features of plant telomere-binding proteins. *Nucleic Acids Res.* 36, 2739–2755. doi: 10.1093/nar/gkn030

Koonin, E. V. (2010). Preview. The incredible expanding ancestor of eukaryotes. *Cell* 140, 606–608. doi: 10.1016/j.cell.2010.02.022

Kovarik, A., Fajkus, J., Koukalova, B., and Bezdek, M. (1996). Species-specific evolution of telomeric and rDNA repeats in the tobacco composite genome. *Theor. Appl. Genet.* 92, 1108–1111. doi: 10.1007/BF00224057

Krause, K., Kilbienski, I., Mulisch, M., Rodiger, A., Schafer, A., and Krupinska, K. (2005). DNA-binding proteins of the Whirly family in *Arabidopsis thaliana* are targeted to the organelles. *FEBS Lett.* 579, 3707–3712. doi: 10.1016/j.febslet.2005.05.059

Krutilina, R. I., Oei, S., Buchlow, G., Yau, P. M., Zalensky, A. O., Zalenskaya, I. A., et al. (2001). A negative regulator of telomere-length protein trf1 is associated with interstitial (TTAGGG)n blocks in immortal Chinese hamster ovary cells. *Biochem. Biophys. Res. Commun.* 280, 471–475. doi: 10.1006/bbrc.2000.4143

Kuchar, M., and Fajkus, J. (2004). Interactions of putative telomere-binding proteins in *Arabidopsis thaliana*: identification of functional TRF2 homolog in plants. *FEBS Lett.* 578, 311–315. doi: 10.1016/j.febslet.2004.11.021

Kwon, C., and Chung, I. K. (2004). Interaction of an *Arabidopsis* RNA-binding protein with plant single-stranded telomeric DNA modulates telomerase activity. *J. Biol. Chem.* 279, 12812–12818. doi: 10.1074/jbc.M312011200

Kwon, C., Kwon, K., Chung, I. K., Kim, S. Y., Cho, M. H., and Kang, B. G. (2004). Characterization of single stranded telomeric DNA-binding proteins in cultured soybean (*Glycine max*) cells. *Mol. Cells* 17, 503–508.

Lamarche, B. J., Orazio, N. I., and Weitzman, M. D. (2010). The MRN complex in double-strand break repair and telomere maintenance. *FEBS Lett.* 584, 3682–3695. doi: 10.1016/j.febslet.2010.07.029

Lazzerini-Denchi, E., and Sfeir, A., (2016). Stop pulling my strings – what telomeres taught us about the DNA damage response. *Nat. Rev. Mol. Cell. Biol.* 17, 364–378. doi: 10.1038/nrm.2016.43

Lee, J. H., Kim, J. H., Kim, W. T., Kang, B. G., and Chung, I. K. (2000). Characterization and developmental expression of single-stranded telomeric DNA-binding proteins from mung bean (*Vigna radiata*). *Plant Mol. Biol.* 42, 547–557. doi: 10.1023/A:1006373917321

Lee, L. Y., Wu, F. H., Hsu, C. T., Shen, S. C., Yeh, H. Y., Liao, D. C., et al. (2012). Screening a cDNA library for protein-protein interactions directly in planta. *Plant Cell* 24, 1746–1759. doi: 10.1105/tpc.112.097998

Lee, W. K., and Cho, M. H. (2016). Telomere-binding protein regulates the chromosome ends through the interaction with histone deacetylases in *Arabidopsis thaliana*. *Nucl. Acids Res.* 44, 4610–4624. doi: 10.1093/nar/gkw067

Lee, W. K., Yun, J. H., Lee, W., and Cho, M. H. (2012). DNA-binding domain of AtTRB2 reveals unique features of a single Myb histone protein family that binds to both *Arabidopsis*- and human-type telomeric DNA sequences. *Mol. Plant* 5, 1406–1408. doi: 10.1093/mp/sss063

Lee, Y. W., and Kim, W. T. (2010). Tobacco GTBP1, a homolog of human heterogeneous nuclear ribonucleoprotein, protects telomeres from aberrant homologous recombination. *Plant Cell* 22, 2781–2795. doi: 10.1105/tpc.110.076778

Lee, Y. W., and Kim, W. T. (2013). Telomerase-dependent 3′ G-strand overhang maintenance facilitates GTBP1-mediated telomere protection from misplaced homologous recombination. *Plant Cell* 25, 1329–1342. doi: 10.1105/tpc.112.107573

Leehy, K. A., Lee, J. R., Song, X., Renfrew, K. B., and Shippen, D. E. (2013). MERISTEM DISORGANIZATION1 encodes TEN1, an essential telomere protein that modulates telomerase processivity in *Arabidopsis*. *Plant Cell* 25, 1343–1354. doi: 10.1105/tpc.112.107425

Lei, M., Baumann, P., and Cech, T. R. (2002). Cooperative binding of single-stranded telomeric DNA by the Pot1 protein of *Schizosaccharomyces* pombe. *Biochemistry* 41, 14560–14568. doi: 10.1021/bi026674z

Lermontova, I., Schubert, V., Bornke, F., Macas, J., and Schubert, I. (2007). *Arabidopsis* CBF5 interacts with the H/ACA snoRNP assembly factor NAF1. *Plant Mol. Biol.* 65, 615–626. doi: 10.1007/s11103-007-9226-z

Linger, B. R., and Price, C. M. (2009). Conservation of telomere protein complexes: shuffling through evolution. *Crit. Rev. Biochem. Mol. Biol.* 44, 434–446. doi: 10.3109/10409230903307329

Lugert, T., and Werr, W. (1994). A novel DNA-binding domain in the Shrunken initiator-binding protein (IBP1). *Plant Mol. Biol.* 25, 493–506. doi: 10.1007/BF00043877

Maï, M. E., Wagner, K. D., Michiels, J. F., Ambrosetti, D., Borderie, A., Destree, S., et al. (2014). The telomeric protein TRF2 regulates Angiogenesis by binding and activating the PDGFRβ promoter. *Cell Rep.* 9, 1047–1060. doi: 10.1016/j.celrep.2014.09.038

Maillet, G., White, C. I., and Gallego, M. E. (2006). Telomere-length regulation in inter-ecotype crosses of *Arabidopsis*. *Plant Mol. Biol.* 62, 859–866. doi: 10.1007/s11103-006-9061-7

Majerova, E., Fojtova, M., Mozgova, I., Bittova, M., and Fajkus, J. (2011). Hypomethylating drugs efficiently decrease cytosine methylation in telomeric DNA and activate telomerase without affecting telomere lengths in tobacco cells. *Plant Mol. Biol.* 77, 371–380. doi: 10.1007/s11103-011-9816-7

Mandakova, T., and Lysak, M. A. (2008). Chromosomal phylogeny and karyotype evolution in x = 7 crucifer species (Brassicaceae). *Plant Cell* 20, 2559–2570. doi: 10.1105/tpc.108.062166

Marian, C. O., and Bass, H. W. (2005). The terminal acidic SANT 1 (Tacs1) gene of maize is expressed in tissues containing meristems and encodes an acidic SANT

domain similar to some chromatin-remodeling complex proteins. *Biochim. Biophys. Acta* 1727, 81–86. doi: 10.1016/j.bbaexp.2004.12.010

Marian, C. O., Bordoli, S. J., Goltz, M., Santarella, R. A., Jackson, L. P., Danilevskaya, O., et al. (2003). The maize single myb histone 1 gene, Smh1, belongs to a novel gene family and encodes a protein that binds telomere DNA repeats in vitro. *Plant Physiol.* 133, 1336–1350.

Martinez, P., Thanasoula, M., Carlos, A. R., Gomez-Lopez, G., Tejera, A. M., Schoeftner, S., et al. (2010). Mammalian Rap1 controls telomere function and gene expression through binding to telomeric and extratelomeric sites. *Nat. Cell Biol.* 12, 768–780. doi: 10.1038/ncb2081

Martinez-Perez, E., Shaw, P., Reader, S., Aragon-Alcaide, L., Miller, T., and Moore, G. (1999). Homologous chromosome pairing in wheat. *J. Cell Sci.* 112, 1761–1769.

Mignon-Ravix, C., Depetris, D., Delobel, B., Croquette, M. F., and Mattei, M. G. (2002). A human interstitial telomere associates in vivo with specific TRF2 and TIN2 proteins. *Eur. J. Hum. Genet.* 10, 107–112. doi: 10.1038/sj.ejhg.5200775

Mimori, T., Akizuki, M., Yamagata, H., Inada, S., Yoshida, S., and Homma, M. (1981). Characterization of a high molecular weight acidic nuclear protein recognized by autoantibodies in sera from patients with polymyositis-scleroderma overlap. *J. Clin. Invest.* 68, 611–620. doi: 10.1172/JCI110295

Moore, J. (2009). *Investigating the DNA Binding Properties of the Initiator Binding Protein 2 (IBP2) in Maize (Zea Mays)*. Master thesis, Florida State University, Tallahassee.

Moriguchi, R., Kanahama, K., and Kanayama, Y. (2006). Characterization and expression analysis of the tomato telomere-binding protein LeTBP1. *Plant Sci.* 171, 166–174. doi: 10.1016/j.plantsci.2006.03.010

Morse, R. H. (2000). RAP, RAP, open up! New wrinkles for RAP1 in yeast. *Trends Genet.* 16, 51–53.

Mozgova, I., Schrumpfova, P. P., Hofr, C., and Fajkus, J. (2008). Functional characterization of domains in AtTRB1, a putative telomere-binding protein in *Arabidopsis thaliana*. *Phytochemistry* 69, 1814–1819. doi: 10.1016/j.phytochem.2008.04.001

Najdekrova, L., and Siroky, J. (2012). NBS1 plays a synergistic role with telomerase in the maintenance of telomeres in *Arabidopsis thaliana*. *BMC Plant Biol.* 12:167. doi: 10.1186/1471-2229-12-167

Nelson, A. D. J. (2012). *Telomerase regulation in Arabidopsis thaliana*. Ph.D. thesis, A&M University, Texas.

Nelson, A. D. J., Forsythe, E. S., Gan, X., Tsiantis, M., and Beilstein, M. A. (2014). Extending the model of *Arabidopsis* telomere length and composition across Brassicaceae. *Chromosome Res.* 22, 153–166. doi: 10.1007/s10577-014-9423-y

Oguchi, K., Tamura, K., and Takahashi, H. (2004). Characterization of *Oryza sativa* telomerase reverse transcriptase and possible role of its phosphorylation in the control of telomerase activity. *Gene* 342, 57–66. doi: 10.1016/j.gene.2004.07.011

Olivier, M., Da Ines, O., Amiard, S., Serra, H., Goubely, C., White, C., et al. (2016)). The structure-specific endonucleases MUS81 and SEND1 ere essential for telomere stability in *Arabidopsis*. *Plant Cell* 28, 74–86. doi: 10.1105/tpc.15.00898

Ottaviani, A., Gilson, E., and Magdinier, F. (2008). Telomeric position effect: from the yeast paradigm to human pathologies? *Biochimie* 90, 93–107. doi: 10.1016/j.biochi.2007.07.022

Peska, V., Fajkus, P., Fojtova, M., Dvorackova, M., Hapala, J., Dvoracek, V., et al. (2015). Characterisation of an unusual telomere motif (TTTTTTAGGG)n in the plant Cestrum elegans (Solanaceae), a species with a large genome. *Plant J.* 82, 644–654. doi: 10.1111/tpj.12839

Peska, V., Schrumpfova, P. P., and Fajkus, J. (2011). Using the telobox to search for plant telomere binding proteins. *Curr. Protein Pept. Sci.* 12, 75–83. doi: 10.2174/138920311795684968

Peska, V., Sykorova, E., and Fajkus, J. (2008). Two faces of Solanaceae telomeres: a comparison between *Nicotiana* and *Cestrum* telomeres and telomere-binding proteins. *Cytogenet. Genome. Res.* 122, 380–387. doi: 10.1159/000167826

Phillips, D., Nibau, C., Wnetrzak, J., and Jenkins, G. (2012). High resolution analysis of meiotic chromosome structure and behaviour in barley (*Hordeum vulgare* L.). *PLoS ONE* 7:e39539. doi: 10.1371/journal.pone.0039539

Pisano, S., Galati, A., and Cacchione, S. (2008). Telomeric nucleosomes: forgotten players at chromosome ends. *Cell Mol. Life. Sci.* 65, 3553–3563. doi: 10.1007/s00018-008-8307-8

Podlevsky, J. D., Bley, C. J., Omana, R. V., Qi, X., and Chen, J. J. (2008). The telomerase database. *Nucleic Acids Res.* 36, D339–D343. doi: 10.1093/nar/gkm700

Price, C. M., Boltz, K. A., Chaiken, M. F., Stewart, J. A., Beilstein, M. A., and Shippen, D. E. (2010). Evolution of CST function in telomere maintenance. *Cell Cycle* 9, 3157–3165. doi: 10.4161/cc.9.16.12547

Price, C. M., and Cech, T. R. (1987). Telomeric DNA-protein interactions of *Oxytricha* macronuclear DNA. *Genes Dev.* 1, 783–793. doi: 10.1101/gad.1.8.783

Qi, H., and Zakian, V. A. (2000). The *Saccharomyces* telomere-binding protein Cdc13p interacts with both the catalytic subunit of DNA polymerase alpha and the telomerase-associated est1 protein. *Genes Dev.* 14, 1777–1788.

Rabl, C. (1885). Uber Zelltheilung. *Morphologisches Jahrbuch* 10, 214–330.

Recker, J., Knoll, A., and Puchta, H. (2014). The *Arabidopsis thaliana* homolog of the helicase RTEL1 plays multiple roles in preserving genome stability. *Plant Cell* 26, 4889–4902. doi: 10.1105/tpc.114.132472

Ren, S., Johnston, J. S., Shippen, D. E., and McKnight, T. D. (2004). TELOMERASE ACTIVATOR1 induces telomerase activity and potentiates responses to auxin in *Arabidopsis*. *Plant Cell* 16, 2910–2922. doi: 10.1105/tpc.104.025072

Ren, S., Mandadi, K. K., Boedeker, A. L., Rathore, K. S., and McKnight, T. D. (2007). Regulation of telomerase in *Arabidopsis* by BT2, an apparent target of TELOMERASE ACTIVATOR1. *Plant Cell* 19, 23–31. doi: 10.1105/tpc.106.044321

Renfrew, K. B., Song, X., Lee, J. R., Arora, A., and Shippen, D. E. (2014). POT1a and components of CST engage telomerase and regulate its activity in *Arabidopsis*. *PLoS Genet.* 10:e1004738. doi: 10.1371/journal.pgen.1004738

Richards, E. J., and Ausubel, F. M. (1988). Isolation of a higher eukaryotic telomere from *Arabidopsis thaliana*. *Cell* 53, 127–136. doi: 10.1016/0092-8674(88)90494-1

Riha, K., Fajkus, J., Siroky, J., and Vyskot, B. (1998). Developmental control of telomere lengths and telomerase activity in plants. *Plant Cell* 10, 1691–1698. doi: 10.2307/3870766

Riha, K., McKnight, T. D., Fajkus, J., Vyskot, B., and Shippen, D. E. (2000). Analysis of the G-overhang structures on plant telomeres: evidence for two distinct telomere architectures. *Plant J.* 23, 633–641. doi: 10.1046/j.1365-313x.2000.00831.x

Riha, K., Watson, J. M., Parkey, J., and Shippen, D. E. (2002). Telomere length deregulation and enhanced sensitivity to genotoxic stress in *Arabidopsis* mutants deficient in Ku70. *EMBO J.* 21, 2819–2826. doi: 10.1093/emboj/21.11.2819

Rossignol, P., Collier, S., Bush, M., Shaw, P., and Doonan, J. H. (2007). *Arabidopsis* POT1A interacts with TERT-V(I8), an N-terminal splicing variant of telomerase. *J. Cell Sci.* 120, 3678–3687. doi: 10.1242/jcs.004119

Rotkova, G., Sykorova, E., and Fajkus, J. (2009). Protect and regulate: Recent findings on plant POT1-like proteins. *Biol. Plant.* 53, 1–4. doi: 10.1007/s10535-009-0001-7

Ruckova, E., Friml, J., Prochazkova Schrumpfova, P., and Fajkus, J. (2008). Role of alternative telomere lengthening unmasked in telomerase knock-out mutant plants. *Plant Mol. Biol.* 66, 637–646. doi: 10.1007/s11103-008-9295-7

Schmidt, J. C., and Cech, T. R. (2015). Human telomerase: biogenesis, trafficking, recruitment, and activation. *Genes Dev.* 29, 1095–1105. doi: 10.1101/gad.263863.115

Schober, H., Ferreira, H., Kalck, V., Gehlen, L. R., and Gasser, S. M. (2009). Yeast telomerase and the SUN domain protein Mps3 anchor telomeres and repress subtelomeric recombination. *Genes Dev.* 23, 928–938. doi: 10.1101/gad.1787509

Schrumpfova, P., Kuchar, M., Mikova, G., Skrisovska, L., Kubicarova, T., and Fajkus, J. (2004). Characterization of two *Arabidopsis thaliana* myb-like proteins showing affinity to telomeric DNA sequence. *Genome* 47, 316–324. doi: 10.1139/g03-136

Schrumpfova, P. P., Kuchar, M., Palecek, J., and Fajkus, J. (2008). Mapping of interaction domains of putative telomere-binding proteins AtTRB1 and AtPOT1b from *Arabidopsis thaliana*. *FEBS Lett.* 582, 1400–1406. doi: 10.1016/j.febslet.2008.03.034

Schrumpfova, P. P., Vychodilova, I., Dvorackova, M., Majerska, J., Dokladal, L., Schorova, S., et al. (2014). Telomere repeat binding proteins are functional components of *Arabidopsis* telomeres and interact with telomerase. *Plant J.* 77, 770–781. doi: 10.1111/tpj.12428

Schrumpfova, P. P., Vychodilova, I., Hapala, J., Schorova, S., Dvoracek, V., and Fajkus, J. (2016). Telomere binding protein TRB1 is associated with promoters of translation machinery genes in vivo. *Plant. Mol. Biol.* 90, 189–206. doi: 10.1007/s11103-015-0409-8

Schwacke, R., Fischer, K., Ketelsen, B., Krupinska, K., and Krause, K. (2007). Comparative survey of plastid and mitochondrial targeting properties of transcription factors in *Arabidopsis* and rice. *Mol. Genet. Genom.* 277, 631–646. doi: 10.1007/s00438-007-0214-4

Sfeir, A. (2012). Telomeres at a glance. *J. Cell Sci.* 125, 4173–4178. doi: 10.1242/jcs.106831

Shakirov, E. V., McKnight, T. D., and Shippen, D. E. (2009a). POT1-independent single-strand telomeric DNA binding activities in Brassicaceae. *Plant J.* 58, 1004–1015. doi: 10.1111/j.1365-313X.2009.03837.x

Shakirov, E. V., Perroud, P. F., Nelson, A. D., Cannell, M. E., Quatrano, R. S., and Shippen, D. E. (2010). Protection of telomeres 1 is required for telomere integrity in the moss *Physcomitrella patens*. *Plant Cell* 22, 1838–1848. doi: 10.1105/tpc.110.075846

Shakirov, E. V., Song, X., Joseph, J. A., and Shippen, D. E. (2009b). POT1 proteins in green algae and land plants: DNA-binding properties and evidence of co-evolution with telomeric DNA. *Nucleic Acids Res.* 37, 7455–7467. doi: 10.1093/nar/gkp785

Shakirov, E. V., and Shippen, D. E. (2004). Length regulation and dynamics of individual telomere tracts in wild-type *Arabidopsis*. *Plant Cell* 16, 1959–1967. doi: 10.1105/tpc.104.023093

Shakirov, E. V., Surovtseva, Y. V., Osbun, N., and Shippen, D. E. (2005). The *Arabidopsis* Pot1 and Pot2 proteins function in telomere length homeostasis and chromosome end protection. *Mol. Cell. Biol.* 25, 7725–7733. doi: 10.1128/MCB.25.17.7725-7733.2005

Simonet, T., Zaragosi, L. E., Philippe, C., Lebrigand, K., Schouteden, C., Augereau, A., et al. (2011). The human TTAGGG repeat factors 1 and 2 bind to a subset of interstitial telomeric sequences and satellite repeats. *Cell Res.* 21, 1028–1038. doi: 10.1038/cr.2011.40

Smith, S., Giriat, I., Schmitt, A., and de Lange, T. (1998). Tankyrase, a poly(ADP-ribose) polymerase at human telomeres. *Science* 282, 1484–1487. doi: 10.1126/science.282.5393.1484

Smogorzewska, A., van Steensel, B., Bianchi, A., Oelmann, S., Schaefer, M. R., Schnapp, G., et al. (2000). Control of human telomere length by TRF1 and TRF2. *Mol. Cell. Biol.* 20, 1659–1668. doi: 10.1128/MCB.20.5.1659-1668.2000

Song, X., Leehy, K., Warrington, R. T., Lamb, J. C., Surovtseva, Y. V., and Shippen, D. E. (2008). STN1 protects chromosome ends in *Arabidopsis thaliana*. *Proc. Natl. Acad. Sci. U.S.A.* 105, 19815–19820. doi: 10.1073/pnas.0807867105

Starr, D. A., Hermann, G. J., Malone, C. J., Fixsen, W., Priess, J. R., Horvitz, H. R., et al. (2001). unc-83 encodes a novel component of the nuclear envelope and is essential for proper nuclear migration. *Development* 128, 5039–5050.

Stewart, J. A., Wang, F., Chaiken, M. F., Kasbek, C., Chastain, P. D. II, Wright, W. E., et al. (2012). Human CST promotes telomere duplex replication and general replication restart after fork stalling. *EMBO J.* 31, 3537–3549. doi: 10.1038/emboj.2012.215

Surovtseva, Y. V., Churikov, D., Boltz, K. A., Song, X., Lamb, J. C., Warrington, R., et al. (2009). Conserved telomere maintenance component 1 interacts with STN1 and maintains chromosome ends in higher eukaryotes. *Mol. Cell.* 36, 207–218. doi: 10.1016/j.molcel.2009.09.017

Surovtseva, Y. V., Shakirov, E. V., Vespa, L., Osbun, N., Song, X., and Shippen, D. E. (2007). *Arabidopsis* POT1 associates with the telomerase RNP and is required for telomere maintenance. *EMBO J.* 26, 3653–3661. doi: 10.1038/sj.emboj.7601792

Sykorova, E., and Fajkus, J. (2009). Structure-function relationships in telomerase genes. *Biol. Cell* 101, 375–392. doi: 10.1042/BC20080205.

Sykorova, E., Fulneckova, J., Mokros, P., Fajkus, J., Fojtova, M., and Peska, V. (2012). Three TERT genes in *Nicotiana tabacum*. *Chromosome Res.* 20, 381–394. doi: 10.1007/s10577-012-9282-3

Sykorova, E., Leitch, A. R., and Fajkus, J. (2006). Asparagales telomerases which synthesize the human type of telomeres. *Plant Mol. Biol.* 60, 633–646. doi: 10.1007/s11103-005-5091-9

Sykorova, E., Lim, K. Y., Kunicka, Z., Chase, M. W., Bennett, M. D., Fajkus, J., et al. (2003). Telomere variability in the monocotyledonous plant order Asparagales. *Proc. Biol. Sci.* 270, 1893–1904. doi: 10.1098/rspb.2003.2446

Tamura, K., Goto, C., and Hara-Nishimura, I. (2015). Recent advances in understanding plant nuclear envelope proteins involved in nuclear morphology. *J. Exp. Bot.* 66, 1641–1647. doi: 10.1093/jxb/erv036

Tamura, K., Liu, H., and Takahashi, H. (1999). Auxin induction of cell cycle regulated activity of tobacco telomerase. *J. Biol. Chem.* 274, 20997–21002. doi: 10.1074/jbc.274.30.20997

Tani, A., and Murata, M. (2005). Alternative splicing of Pot1 (Protection of telomere)-like genes in *Arabidopsis thaliana*. *Genes Genet. Syst.* 80, 41–48. doi: 10.1266/ggs.80.41

Taylor, J. S., and Raes, J. (2004). Duplication and divergence: the evolution of new genes and old ideas. *Annu. Rev. Genet.* 38, 615–643. doi: 10.1146/annurev.genet.38.072902.092831

Tiang, C. L., He, Y., and Pawlowski, W. P. (2012). Chromosome organization and dynamics during interphase, mitosis, and meiosis in plants. *Plant Physiol.* 158, 26–34. doi: 10.1104/pp.111.187161

Ting, N. S., Yu, Y., Pohorelic, B., Lees-Miller, S. P., and Beattie, T. L. (2005). Human Ku70/80 interacts directly with hTR, the RNA component of human telomerase. *Nucleic Acids Res.* 33, 2090–2098. doi: 10.1093/nar/gki342

To, T. K., Kim, J. M., Matsui, A., Kurihara, Y., Morosawa, T., Ishida, J., et al. (2011). *Arabidopsis* HDA6 regulates locus-directed heterochromatin silencing in cooperation with MET1. *PLoS Genet.* 7:e1002055. doi: 10.1371/journal.pgen.1002055

Tomaska, L., Nosek, J., Kramara, J., and Griffith, J. D. (2009). Telomeric circles: universal players in telomere maintenance? *Nat. Struct. Mol. Biol.* 16, 1010–1015. doi: 10.1038/nsmb.1660

Tran, D. T., Cao, H. X., Jovtchev, G., Neumann, P., Novak, P., Fojtova, M., et al. (2015). Centromere and telomere sequence alterations reflect the rapid genome evolution within the carnivorous plant genus *Genlisea*. *Plant J.* 84, 1087–1099. doi: 10.1111/tpj.13058

Uringa, E. J., Youds, J. L., Lisaingo, K., Lansdorp, P. M., and Boulton, S. J. (2011). RTEL1: an essential helicase for telomere maintenance and the regulation of homologous recombination. *Nucleic Acids Res.* 39, 1647–1655. doi: 10.1093/nar/gkq1045

van der Fits, L., Zhang, H., Menke, F. L., Deneka, M., and Memelink, J. (2000). A *Catharanthus roseus* BPF-1 homologue interacts with an elicitor-responsive region of the secondary metabolite biosynthetic gene Str and is induced by elicitor via a JA-independent signal transduction pathway. *Plant Mol. Biol.* 44, 675–685. doi: 10.1023/A:1026526522555

Vannier, J. B., Depeiges, A., White, C., and Gallego, M. E. (2009). ERCC1/XPF protects short telomeres from homologous recombination in *Arabidopsis thaliana*. *PLoS Genet.* 5:e1000380. doi: 10.1371/journal.pgen.1000380

Vannier, J. B., Pavicic-Kaltenbrunner, V., Petalcorin, M. I., Ding, H., and Boulton, S. J. (2012). RTEL1 dismantles T loops and counteracts telomeric G4-DNA to maintain telomere integrity. *Cell* 149, 795–806. doi: 10.1016/j.cell.2012.03.030

Venteicher, A. S., Meng, Z., Mason, P. J., Veenstra, T. D., and Artandi, S. E. (2008). Identification of ATPases pontin and reptin as telomerase components essential for holoenzyme assembly. *Cell* 132, 945–957. doi: 10.1016/j.cell.2008.01.019

Vespa, L., Warrington, R. T., Mokros, P., Siroky, J., and Shippen, D. E. (2007). ATM regulates the length of individual telomere tracts in *Arabidopsis*. *Proc. Natl. Acad. Sci. U.S.A.* 104, 18145–18150. doi: 10.1073/pnas.0704466104

Vrbsky, J., Akimcheva, S., Watson, J. M., Turner, T. L., Daxinger, L., Vyskot, B., et al. (2010). siRNA-mediated methylation of *Arabidopsis* telomeres. *PLoS Genet.* 6:e1000986. doi: 10.1371/journal.pgen.1000986

Wang, H., Liu, C., Cheng, J., Liu, J., Zhang, L., He, C., et al. (2016). *Arabidopsis* flower and embryo developmental genes are repressed in seedlings by different combinations of polycomb group proteins in association with distinct sets of cis-regulatory elements. *PLoS Genet.* 12:e1005771. doi: 10.1371/journal.pgen.1005771

Wang, Y., Ghosh, G., and Hendrickson, E. A. (2009). Ku86 represses lethal telomere deletion events in human somatic cells. *Proc. Natl. Acad. Sci. U.S.A.* 106, 12430–12435. doi: 10.1073/pnas.0903362106

Watson, J. M., and Shippen, D. E. (2007). Telomere rapid deletion regulates telomere length in *Arabidopsis thaliana*. *Mol. Cell. Biol.* 27, 1706–1715. doi: 10.1128/MCB.02059-06

Wei, C., and Price, C. M. (2004). Cell cycle localization, dimerization, and binding domain architecture of the telomere protein cPot1. *Mol. Cell. Biol.* 24, 2091–2102. doi: 10.1128/MCB.24.5.2091-2102.2004

Weiss, H., and Scherthan, H. (2002). Aloe spp. - plants with vertebrate-like telomeric sequences. *Chromosome Res.* 10, 155–164. doi: 10.1023/A:1014905319557

Wellinger, R. J., and Zakian, V. A. (2012). Everything you ever wanted to know about *Saccharomyces cerevisiae* telomeres: beginning to end. *Genetics* 191, 1073–1105. doi: 10.1534/genetics.111.137851

Wen, R., Moore, G., and Shaw, P. J. (2012). Centromeres cluster de novo at the beginning of meiosis in *Brachypodium distachyon*. *PLoS ONE* 7:e44681. doi: 10.1371/journal.pone.0044681

Wu, L., Multani, A. S., He, H., Cosme-Blanco, W., Deng, Y., Deng, J. M., et al. (2006). Pot1 deficiency initiates DNA damage checkpoint activation and aberrant homologous recombination at telomeres. *Cell* 126, 49–62. doi: 10.1016/j.cell.2006.05.037

Yang, D., Xiong, Y., Kim, H., He, Q., Li, Y., Chen, R., et al. (2011). Human telomeric proteins occupy selective interstitial sites. *Cell Res.* 21, 1013–1027. doi: 10.1038/cr.2011.39

Yang, S. W., Jin, E., Chung, I. K., and Kim, W. T. (2002). Cell cycle-dependent regulation of telomerase activity by auxin, abscisic acid and protein phosphorylation in tobacco BY-2 suspension culture cells. *Plant J.* 29, 617–626. doi: 10.1046/j.0960-7412.2001.01244.x

Yang, S. W., Kim, D. H., Lee, J. J., Chun, Y. J., Lee, J. H., Kim, Y. J., et al. (2003). Expression of the telomeric repeat binding factor gene NgTRF1 is closely coordinated with the cell division program in tobacco BY-2 suspension culture cells. *J. Biol. Chem.* 278, 21395–21407. doi: 10.1074/jbc.M209973200

Yang, S. W., Kim, S. K., and Kim, W. T. (2004). Perturbation of NgTRF1 expression induces apoptosis-like cell death in tobacco BY-2 cells and implicates NgTRF1 in the control of telomere length and stability. *Plant Cell* 16, 3370–3385. doi: 10.1105/tpc.104.026278

Ye, J., Renault, V. M., Jamet, K., and Gilson, E. (2014). Transcriptional outcome of telomere signalling. *Nat. Rev. Genet.* 15, 491–503. doi: 10.1038/nrg3743

Yoo, H. H., Kwon, C., Lee, M. M., and Chung, I. K. (2007). Single-stranded DNA binding factor AtWHY1 modulates telomere length homeostasis in *Arabidopsis*. *Plant J.* 49, 442–451. doi: 10.1111/j.1365-313X.2006.02974.x

Yu, E. Y., Kim, S. E., Kim, J. H., Ko, J. H., Cho, M. H., and Chung, I. K. (2000). Sequence-specific DNA recognition by the Myb-like domain of plant telomeric protein RTBP1. *J. Biol. Chem.* 275, 24208–24214. doi: 10.1074/jbc.M003250200

Yun, J. H., Lee, W. K., Kim, H., Kim, E., Cheong, C., Cho, M. H., et al. (2014). Solution structure of telomere binding domain of AtTRB2 derived from *Arabidopsis thaliana*. *Biochem. Biophys. Res. Commun.* 452, 436–442. doi: 10.1016/j.bbrc.2014.08.095

Zachova, D., Fojtova, M., Dvorackova, M., Mozgova, I., Lermontova, I., Peska, V., et al. (2013). Structure-function relationships during transgenic telomerase expression in *Arabidopsis*. *Physiol. Plant.* 149, 114–126. doi: 10.1111/ppl.12021

Zellinger, B., Akimcheva, S., Puizina, J., Schirato, M., and Riha, K. (2007). Ku suppresses formation of telomeric circles and alternative telomere lengthening in *Arabidopsis*. *Mol. Cell.* 27, 163–169. doi: 10.1016/j.molcel.2007.05.025

Zentgraf, U. (1995). Telomere-binding proteins of *Arabidopsis thaliana*. *Plant Mol. Biol.* 27, 467–475. doi: 10.1007/BF00019314

Zhang, P., Pazin, M. J., Schwartz, C. M., Becker, K. G., Wersto, R. P., Dilley, C. M., et al. (2008). Nontelomeric TRF2-REST interaction modulates neuronal gene silencing and fate of tumor and stem cells. *Curr. Biol.* 18, 1489–1494. doi: 10.1016/j.cub.2008.08.048

Zhou, X., Graumann, K., Wirthmueller, L., Jones, J. D., and Meier, I. (2014). Identification of unique SUN-interacting nuclear envelope proteins with diverse functions in plants. *J. Cell Biol.* 205, 677–692. doi: 10.1083/jcb.201401138

Zhou, Y., Hartwig, B., James, G. V., Schneeberger, K., and Turck, F. (2016). Complementary activities of TELOMERE REPEAT BINDING proteins and polycomb group complexes in transcriptional regulation of target genes. *Plant Cell* 28, 87–101. doi: 10.1105/tpc.15.00787

Zhu, Q. H., Ramm, K., Shivakkumar, R., Dennis, E. S., and Upadhyaya, N. M. (2004). The ANTHER INDEHISCENCE1 gene encoding a single MYB domain protein is involved in anther development in rice. *Plant Physiol.* 135, 1514–1525. doi: 10.1104/pp.104.041459

Conflict of Interest Statement: The authors declare that the research was conducted in the absence of any commercial or financial relationships that could be construed as a potential conflict of interest.

The handling Editor declared a current collaboration as co-Topic Editor in a Frontiers Research Topic with one of the authors, JF, and states that the process nevertheless met the standards of a fair and objective review. This was also confirmed by the Specialty Chief Editor of section Plant Cell Biology, Simon Gilroy.

Supplement K

Schrumpfová, P.P., Majerská, J., Dokládal, L., Schořová, Š., Stejskal, K., Obořil, M., Honys, D., Kozáková, L., Polanská, P.S., Sýkorová, E., **2017**. Tandem affinity purification of AtTERT reveals putative interaction partners of plant telomerase in vivo. Protoplasma 254, 1547–1562

P.P.S. participated in the design of experiments, was significantly involved in the experimental part, data evaluation and participated in the ms writing

Supplement L

Schrumpfová, P.P., Majerská, J., Dokládal, L., Schořová, Š., Stejskal, K., Obořil, M., Honys, D., Kozáková, L., Polanská, P.S., Sýkorová, E., **2018**. Correction to: Tandem affinity purification of AtTERT reveals putative interaction partners of plant telomerase in vivo. Protoplasma 255, 715

In the published online version, P.P. Schrumpfová was not recognized as the first co-author, and the affiliations were mixed up. Corrections were made to both the first co-authorship and the affiliation section.

Protoplasma (2018) 255:715
https://doi.org/10.1007/s00709-018-1224-2

CORRECTION

Correction to: Tandem affinity purification of AtTERT reveals putative interaction partners of plant telomerase in vivo

Jana Majerská[1,2,3] · Petra Procházková Schrumpfová[2] · Ladislav Dokládal[1] · Šárka Schořová[2] · Karel Stejskal[2] · Michal Obořil[2] · David Honys[4] · Lucie Kozáková[2] · Pavla Sováková Polanská[2] · Eva Sýkorová[1]

Published online: 14 February 2018

Correction to: Protoplasma (2017) 254:1547–1562
https://doi.org/10.1007/s00709-016-1042-3

In the published online version, the affiliations were mixed up. Corrected affiliation section is shown below. Also, the update has also been reflected in the author group section above.

Jana Majerská and Petra Procházková Schrumpfová are both co-authors

The online version of the original article can be found at https://doi.org/10.1007/s00709-016-1042-3

✉ Eva Sýkorová
evin@ibp.cz

[1] Institute of Biophysics, Academy of Sciences of the Czech Republic, v.v.i, Královopolská 135, CZ-61265 Brno, Czech Republic

[2] Central European Institute of Technology and Faculty of Science, Masaryk University, Kotlářská 2, CZ-61137 Brno, Czech Republic

[3] Present address: Swiss Institute for Experimental Cancer Research (ISREC), School of Life Sciences, École Polytechnique Fédérale de Lausanne (EPFL), 1015 Lausanne, Switzerland

[4] Institute of Experimental Botany, Academy of Sciences of the Czech Republic v.v.i, Rozvojová 263, CZ-16502 Prague, Czech Republic

Supplement M

Schrumpfová, P.P., Fojtová, M., Fajkus, J., **2019**. Telomeres in Plants and Humans: Not So Different, Not So Similar. Cells 8

P.P.S. was significantly involved in the ms writing and editing

cells

MDPI

Review

Telomeres in Plants and Humans: Not So Different, Not So Similar

Petra Procházková Schrumpfová [1], Miloslava Fojtová [1,2,3] and Jiří Fajkus [1,2,3,*]

[1] Laboratory of Functional Genomics and Proteomics, National Centre for Biomolecular Research, Faculty of Science, Masaryk University, CZ-61137 Brno, Czech Republic; petra.proch.schrumpfova@gmail.com (P.P.S.); miloslava.fojtova@gmail.com (M.F.)

[2] Mendel Centre for Plant Genomics and Proteomics, CEITEC, Masaryk University, CZ-62500 Brno, Czech Republic

[3] Institute of Biophysics of the Czech Academy of Sciences, CZ-61265 Brno, Czech Republic

* Correspondence: tttaggg@gmail.com; Tel.: +420-5494-94003

Received: 17 December 2018; Accepted: 7 January 2019; Published: 16 January 2019

Abstract: Parallel research on multiple model organisms shows that while some principles of telomere biology are conserved among all eukaryotic kingdoms, we also find some deviations that reflect different evolutionary paths and life strategies, which may have diversified after the establishment of telomerase as a primary mechanism for telomere maintenance. Much more than animals, plants have to cope with environmental stressors, including genotoxic factors, due to their sessile lifestyle. This is, in principle, made possible by an increased capacity and efficiency of the molecular systems ensuring maintenance of genome stability, as well as a higher tolerance to genome instability. Furthermore, plant ontogenesis differs from that of animals in which tissue differentiation and telomerase silencing occur during early embryonic development, and the "telomere clock" in somatic cells may act as a preventive measure against carcinogenesis. This does not happen in plants, where growth and ontogenesis occur through the serial division of apical meristems consisting of a small group of stem cells that generate a linear series of cells, which differentiate into an array of cell types that make a shoot and root. Flowers, as generative plant organs, initiate from the shoot apical meristem in mature plants which is incompatible with the human-like developmental telomere shortening. In this review, we discuss differences between human and plant telomere biology and the implications for aging, genome stability, and cell and organism survival. In particular, we provide a comprehensive comparative overview of telomere proteins acting in humans and in *Arabidopsis thaliana* model plant, and discuss distinct epigenetic features of telomeric chromatin in these species.

Keywords: telomere; telomerase; human; *Arabidopsis*; aging; chromatin; epigenetics; review

1. Introduction

Telomere biology, whose foundations were laid out in maize and *Drosophila* at the end of the 1930s and which developed at the molecular level in the 1980s, has flourished enourmously in the last 30 years. This interest in telomere biology follows from the generally attractive links between telomere functions, cell aging mechanisms, and the genesis of severe diseases in humans. Research in recent decades has elucidated the principles of protection of the ends of linear eukaryotic chromosomes from progressive shortening due to the incomplete replication (end-replication problem) [1] and from their erroneous recognition as unrepaired chromosome breaks (end-protection problem) [2–4]. In addition to these basic functions, other potential roles of telomeres have been suggested, such as a trap for reactive oxygen species [5,6]. Telomeres are composed of non-coding repetitive tandem repeats of $(TTAGGG)_n$ in humans and the other vertebrates, and $(TTTAGGG)_n$ in most plants. During human

aging, telomeres in most somatic cells are shortened at each cell division and it is generally assumed that when telomeres reach a critical length, cells enter a senescent state and cell division ceases [7,8]. However, most human individuals do not reach this critical telomere length brink during their life course [8,9], e.g., the mean leukocyte telomere length (LTL) in newborns is 9.5 kb [10] whereas a length of ~5 kb was defined as the 'telomeric brink', which denotes a high risk of imminent death, but only 0.78% of people younger than 90 years display an LTL $\leq$ 5 kb [9]. So it is obvious, that the link between shortened telomeres and human longevity is more complex than mere reaching the critical telomere length. For instance, age-dependent telomere shortening might alter gene expression in sub-telomeric regions (telomere position effect, TPE) or double strand DNA breaks in telomeres might be inefficiently repaired and initiate cell senescence [11,12]. Furthermore, it has been suggested that even a single critically short telomere in a cell can induce cellular senescence, which potentially contributes to organismal senescence [13,14]. In humans, five short telomeres were reported to predict the onset of cell senescence [15].

Although the principles of protection and replication of telomeres are conserved and point to common evolutionary roots of eukaryotes, their implications for cell and organism survival, senescence, and aging are not shared among kingdoms. In particular, plants show specific features of their growth and development, which lead to confusion of terms like lifespan or aging as commonly used and understood in animals. First, a plant's body plan is not fully established during embryogenesis and all tissues and organs are formed from proliferating meristem cells throughout the adult life. Second, plant growth is modular. Individual modules of the body (branches, flowers, leaves) are dispensable for survival, and their functions can be replaced by tissues newly differentiated from indefinitely proliferating meristems. This results in the enormous developmental plasticity of plants. Moreover, the vegetative meristems can give rise to a new organism, which will be a somatic clone, genetically indistinguishable from the parental organism. Since these general aspects distinguishing plant from animal development and aging have been well-reviewed [16], we will focus here on a more detailed view of peculiarities of plant telomere biology, including its latest developments.

2. Telomerase Core Components

The requirement to finish the incomplete replication of chromosome ends is common for all organisms with linear chromosomes. In eukaryotes, this requirement is commonly solved by a specific nucleoprotein enzyme complex called telomerase, which is considered as an ancestral telomere maintenance system that solves the end-replication problem of linear chromosomes. In humans, telomerase activity is detected in all early developmental stages from oocytes through to blastocyst stage embryos, and increases progressively with advancing embryo stage. Telomerase reaches its highest level in morula and blastocyst stage embryos and then decreases in the inner cell mass stage. In human fetuses—when the embryonic period and organogenesis are finished—telomerase is expressed in tissue-specific stem cells. However, just after birth, telomerase activity in somatic cells is downregulated with the exception of dividing cells (e.g., proliferating cells, T-lymphocytes) [17,18] (Figure 1A).

As seen in mammals, telomeres in plants are maintained by telomerase [19]. Active telomerase is detected in organs and tissues containing highly dividing meristem cells such as seedlings, root tips, young and middle-age leaves, flowers, and floral buds [20,21]. In terminally differentiated tissues (stems, mature leaves), telomerase activity is suppressed (Figure 1B). In some groups of organisms (in particular insects), telomerase has been lost and replaced by telomere-specific retrotransposons (in *Drosophila*) or tandem arrays of satellite repeats elongated by a gene conversion mechanism (reviewed in References [22,23]). Based on a long-term systematic search, no telomerase-independent exception has been found among vertebrates or land plants despite the variability of telomere DNA observed in land plants [24–27]. Besides the telomerase-based mechanism of telomere elongation, alternative lengthening of telomeres (ALT), which is based on homologous recombination (HR)

and may become active upon the loss of telomerase was described in humans as well as in plants (see below).

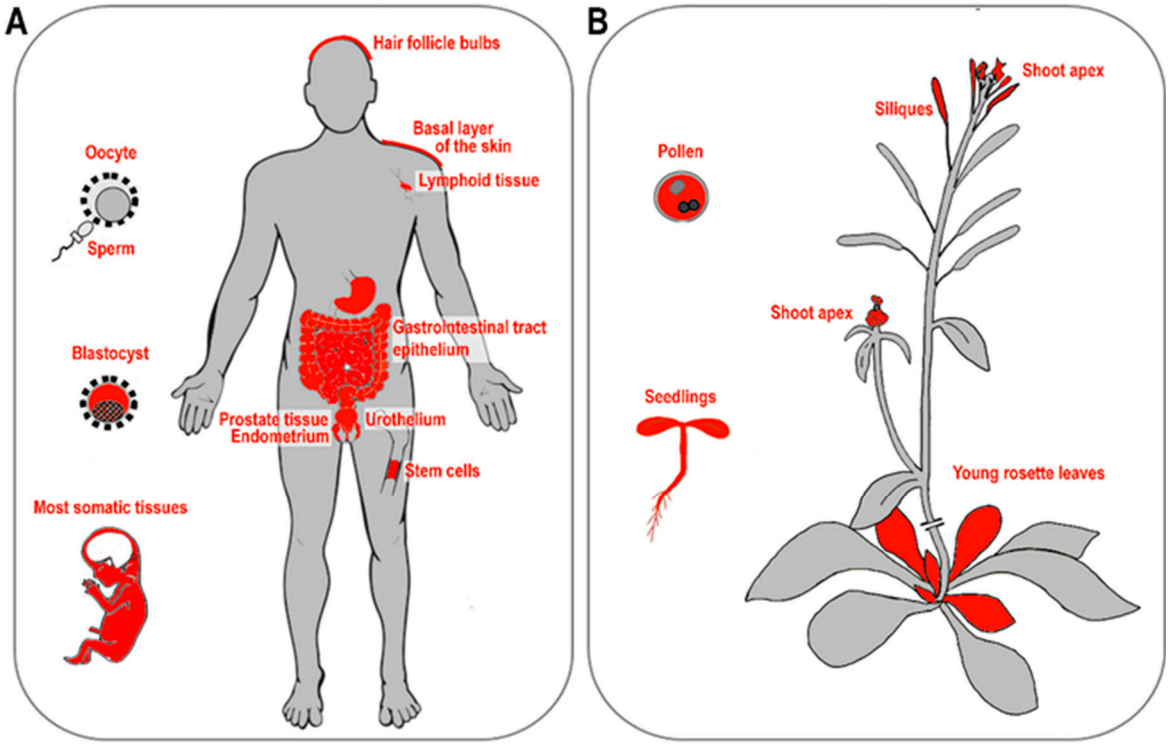

Figure 1. Telomerase activity in human and plant tissues. (**A**) During human embryonic development, high telomerase activity is detected in the blastocyst, but not in mature spermatozoa or oocytes. Highly active telomerase is detected in 16 to 20-week-old human fetuses in most somatic tissues with the exception of brain tissue [18,28]. In adults, low telomerase activity is detected in hair follicule bulbs [29], basal cells of crypt and villi or muconasal basal cells of the gastrointestinal tract, basal keratinocytes of the skin [30], lymphocytes, blood bone marrow, and stem cells [31–33], and urothelium [34]. High telomerase activity is detected in prostate tissues and endometrium [30,35]. (**B**) High telomerase activity is detected in plant pollen, seedling, young rosette leaves, and silliques [21,36–39]. Likewise, both apical meristems—shoot and root—show high telomerase activity [36–38]. Figures adopted from human and *Arabidopsis* eFP browsers [40].

In yeasts, animals, and plants, telomerase consists of the telomerase reverse transcriptase (TERT) protein subunit providing the catalytic activity, and the telomerase RNA (TR) subunit whose short region provides a template for reverse transcription [41,42]. Besides these two core subunits, the telomerase complex comprises several other accessory proteins with diverse roles in telomerase assembly, trafficking, localization, recruitment to telomeres, or the processivity of telomere synthesis [43,44]. During movement of the maturing human telomerase complex through the nucleolus to Cajal bodies and to the telomeres, the TERT catalytical subunit is associated with e.g., HSP90, p23, or pontin. Assembly of human TR, as well as other box C/D or H/ACA small nucleolar RNAs (snoRNAs), is governed by conserved scaffold proteins: dyskerin, NHP2, NOP10, NAF1 in the nucleoplasm, where NAF1 is replaced by GAR1 before the hTR RNP complex reaches the nucleolus. Several orthologues of these conserved scaffold have been identified in plants, e.g., CBF5 (dyskerin), RuvBL1 (pontin), RuvBL2a (reptin), and NAF1. The nucleolar localization of these orthologues suggests potential conservation of the trafficking pathway during telomerase maturation ([45–47]; Schorova et al., submitted). Human and plant homologues of proteins associated either with the telomerase protein subunit TERT (Table 1) or the telomerase RNA subunit (Table 2) are listed below.

Table 1. Comparative overview of proteins associated with the telomerase catalytic subunit TERT.

Telomerase Calytic Subunit (TERT) Associated Proteins.					
Human TERT Associated Proteins	**Protein Function and Direct Interactions**	**References**	***Arabidopsis* TERT Associated Proteins**	**Protein Function and Direct Interactions**	**References**
TERT	**Catalytic subunit of telomerase**	**[48]**	**TERT**	**Catalytic subunit of telomerase**	**[49]**
POT1	Shelterin. Int.: telomeric ssDNA, TPP1 and CTC1.	[50–54]	**POT1a**	Shelterin-like. Int.: TERT, telomeric ssDNA, TER1, TRFL9, CBF5, RuvBL1, CTC1 and STN1.	[47,55–58]
TRF1	Shelterin. Int.: telomeric dsDNA, TIN2, TANK1, PINX1, and ATM.	[59–63]	**TRB1-3**	Shelterin-like. Int.: TERT, telomeric dsDNA, POT1b, RuvBL1 and RuvBL2a.	[64–71]
TRF2	Shelterin. Int.: telomeric dsDNA; TIN2, NBS1, RAD50, Apollo, Ku70, PARP1, XPF-ERCC1, BLM, FEN1, POLB, ORC, RTEL1, ATM and HP1.	[61,72–80]	**TRP1**	Possible non-telomeric functions of telomerase. Int.: TERT, telomere dsDNA in vitro, ARM, Ku70 and TRFL9.	[66,69,81–83]
			TRFL2	Possible non-telomeric functions of telomerase. Int.: TERT, telomere dsDNA in vitro and ARM.	[69,83]
			TRFL11	Associates with TERT.	[84]
KPNA1	Promotes nuclear import of the TERT.	[85]	**ImpA4**	Associates with TERT.	[84]
NCL	Involves nucleolar localization of TERT.	[86]	**NUC-L1**	Role in telomere maintenance and telomere clustering.	[87,88]
pontin	Telomerase assembly. Int.: TERT and dyskerin.	[89]	**RuvBL1**	Associates with TERT via TRBs, regulates telomerase activity.	[84,90]
reptin	Telomerase assembly. Int.: dyskerin.	[89]	**RuvBL2a**	Associates with TERT via TRBs, regulates telomerase activity.	[84]
ARMC6	Int.: TRF2, telomerase.	[69,91]	**ARM**	May reflect posible non-telomeric functions of telomerase. Int.: TERT, TRP1, TRFL2, TRFL9 and CHR19.	[69,92]
TPP1	Shelterin, mediates telomerase recruitment. Int.: TERT, POT1, TIN2, CTC1 and STN1.	[51–54,75]	**n.a.**		

Table 1. *Cont.*

PINX1	Potent telomerase inhibitor. Int.: TERT and TRF1.	[62]	**n.a.**		
HOT1	Int.: telomeric dsDNA, active telomerase.	[93]	**n.a.**		
Ku70/80	Int.: TERT, TR, TRF2 and RAP1.	[94,95]	**Ku70/80**	Role in telomere length regulation, may protect blunt-ended telomeres Int.: TRP1, TER2 and TER2s.	[82,96–101]
Hsp90	TERT assembly. Int.: TERT.	[102]	**Hsp90**	NP_194150.1	[103]
p23	TERT assembly. Int.: TERT.	[102]	**p23**	CAC16575, NP_683525	[104]
Purα	p.h. Unwinds dsDNA telomeric oligonucleotides.	[105]	**PURα1**	Associates with TERT.	[84]
SMARCAD1	p.h. SWI/SNF-like protein that presumably associates with telomeres.	[106,107]	**CHR19**	May reflect possible non-telomeric functions of telomerase. Int.: TERT, ARM, TRB1 and TRFL9.	[69]
PABPN1	Promotes poly(A)-dependent TR 3′ end maturation.	[108]	**RRM**	Associates with TERT.	[92,109]
MT2A	p.h. Int.: HOT1.	[110,111]	**MT2A**	Associates with TERT.	[84,109]
PA2G4	NP_006182.2	[112]	**G2p**	Associates with TERT.	[84,109]

The proteins depicted in grey are involved in telomere maintenance, however, their association with telomerase has not been described. The proteins in green are structural homologous to their human/plant counterparts, however, any involvement in telomere maintenance or association with telomerase has not been described so far. Direct interaction partners (Int.) of TERT-associated proteins are enumerated. Cases with not yet identified sequence homologues are denoted with n.a. ATP-dependent DNA helicase 2 subunit 1 and 2 (Ku70/80); Origin recognition complex (ORC); RuvB-like 2 (reptin); TIN2- and POT1-organizing protein (TPP1); TRF1-interacting nuclear protein 2 (TIN2); TRF1-interacting protein 1 (PINX1); 5′ exonuclease Apollo (Apollo); Armadillo repeat-containing protein 6 (ARMC6); Armadillo/β-catenin-like repeat-containing protein (ARM); Ataxia telangiectasia mutated kinase (ATM); Bloom syndrome protein (BLM); Centromere-binding factor (CBF5); Conserved telomere maintenance component 1 (CTC1); DNA polymerase beta (POLB); DNA repair protein RAD50 (RAD50); Double strand DNA (dsDNA); Excision repair cross-complementation 1 (ERCC1); Flap endonuclease 1 (FEN1); H/ACA ribonucleoprotein complex subunit DKC1 (dyskerin); Heterochromatin protein 1 (HP1); Homeobox telomere-binding protein 1 (HOT1); Hsp90 co-chaperone (p23); Chromatin remodeling 19 (CHR19); Importin-α5 (KPNA1); Importin subunit alpha-4 (ImpA4); Metallothionein-like 2A (MT2A); Nijmegen breakage syndrome protein 1 (NBS1); Nucleolin (NCL); Nucleolin like 1 (NUC-L1); Heat shock protein HSP 90 (Hsp90); Poly(ADP-ribose) polymerase 1 (PARP1); Polyadenylate-binding protein (PABPN1); Proliferation-associated 2G4 (PA2G4); Proliferation-associated protein (G2p); Protection of telomeres 1 (POT1); Protection of telomeres 1a, b (POT1a, b); Pur-alpha 1 (Purα1); Regulator of telomere elongation helicase 1 (RTEL1); RNA recognition motif (RRM); RuvB-like 1 (pontin); RuvB-like 1, 2a (RuvBL1, 2a); Single strand DNA (ssDNA); Suppressor of cdc thirteen homolog (STN1); SWI/SNF-related matrix-associated actin-dependent regulator of chromatin subfamily A containing DEAD/H box 1 (SMARCAD1); Tankyrase 1 (TANK1); Telomerase reverse transcriptase (TERT); Telomerase RNA (TR); Telomerase RNA subunit 1 (TER1); Telomere repeat-binding factor 1, 2, 3 (TRB1, 2, 3); Telomere repeat-binding protein 1 (TRP1); Telomeric repeat binding factor 1-like 2, 9, 11 (TRFL 2, 9, 11); Telomeric repeat-binding factor 1, 2 (TRF1, 2); Xeroderma pigmentosum group F (XPF1); putative homolog according to NCBI blastp (p.h.).

Table 2. Comparative overview of proteins associated with the RNA component of telomerase.

Telomerase RNA Associated Proteins					
Human TR Associated Proteins	**Protein Function and Direct Interactions**	**References**	***Arabidopsis* TR Associated Proteins**	**Protein Function and Direct Interactions**	**References**
TR	**RNA subunit of telomerase**	**[113]**	**TER1, TER2, TER2s**	**Putative RNA subunit of telomerase**	**[56,100]**
TERT	Catalytic subunit of telomerase	[48,114]	**TERT**	Catalytic subunit of telomerase	[100]
Dyskerin	H/ACA snoRNPs, associated with nucleolus. Int.: TR, GAR1, NHP2, NOP10 and TCAB1.	[44,115]	**CBF5**	H/ACA snoRNPs, Ath orthologue of Dyskerin, associated with nucleolus, subnuclear bodies and Cajal bodies, associated with telomerase RNP complex. Direct interaction with either of putative TERs not demonstrated. Int.: NAF1.	[45,57]
NOP10	H/ACA snoRNPs, associates with nucleolus. Int.: TR and dyskerin.	[44,116]	**NOP10**	H/ACA snoRNPs, Ath orthologue of NOP10, associates with nucleolus.	[45,46]
NHP2	H/ACA snoRNPs, associates with nucleolus. Int.: TR, dyskerin and TCAB1.	[117,118]	**NHP2**	H/ACA snoRNPs, Ath orthologue of NHP2, associates with nucleolus.	[45,46]
GAR1	H/ACA snoRNPs, associated with nucleolus. Int.: dyskerin and TCAB1.	[44,118]	**GAR1, 2**	H/ACA snoRNPs, Ath orthologues of GAR1, associate with nucleolus.	[45,46]
NAF1	H/ACA snoRNPs, nucleolar shuttle - NAF1 is substituted by GAR1 during maturation of telomerase. Int.: dyskerin.	[119]	**NAF1**	H/ACA snoRNPs, Ath orthologue of NAF1, associates with nucleolus and Cajal bodies. Int.: CBF5.	[45]
Ku70/80	Int.: TR, TERT, TRF2 and RAP1.	[95,120]	**Ku70/80**	Role in telomere length regulation, may protect blunt-ended telomeres Int.: TRP1, TER2 and TER2s.	[100]

Table 2. *Cont.*

pontin	Telomerase assembly. Int.: TERT and dyskerin.	[89]	**RuvBL1**	Associates with TERT via TRBs, regulates telomerase activity.	Schorova et al., submitted
reptin	Telomerase assembly. Int.: dyskerin.	[89]	**RuvBL2a**	Associates with TERT via TRBs, regulates telomerase activity.	Schorova et al., submitted
RHAU	RNA helicase, unwinds a G4-quadruplex in human telomerase RNA. Int.: TR.	[121]	**RHAU**	NP_850255.1, NP_175298.2, NP_680142.2, NP_178223.2	n.a.
PARN	Poly(A)-specific ribonuclease, 3′-end maturation of the TR. Int.: TR	[122]	**PARN**	Poly(A) degradation activity, essential gene first required during early development.	[123]
TCAB1	H/ACA snoRNPs, driving telomerase to Cajal bodies. Int.: TR, dyskerin, NHP2 and GAR1.	[124]	**TCAB1**	NP_193883.2	n.a.

The proteins in green are structural homologues to their human counterparts, however, any involvement in telomere maintenance or association with RNA component of telomerase has not been described so far. Direct interaction partners (Int.) of TR-associated proteins are enumerated. Cases when reference is not available are denoted n.a. H/ACA ribonucleoprotein complex subunit DKC1 (dyskerin); RuvB-like 2 (reptin); *Arabidopsis* (Ath); ATP-dependent DNA helicase 2 subunit 1 and 2 (Ku70/80); box H/ACA small nucleolar RNA-protein complexes (H/ACA snoRNPs); Centromere-binding factor (CBF5); Glycine arginine rich 1, 2 (GAR1, 2); Non-histone protein 2 (NHP2); Nuclear assembly factor 1 (NAF1); Nucleolar protein 10 (NOP10); Repressor-activator protein 1 (RAP1); RNA helicase (PARN); RNA helicase (RHAU); RuvB-like 1 (pontin); RuvB-like 1, 2a (RuvBL1, 2a); Telomerase Cajal body protein 1 (TCAB1); Telomerase reverse transcriptase (TERT); Telomere repeat-binding factors (TRBs); Telomere repeat-binding protein 1 (TRP1); Telomerase RNA subunit 1, 2, 2s (TER1, 2, 2s); Telomeric repeat-binding factor 2 (TRF2); Telomerase RNA (TR).

Considerable homology in TERT sequences and domain organization exists among organisms, and this homology has frequently been used to identify novel TERTs in genomic or transcriptomic data (reviewed in Reference [125]). Human TERT, as well as the plant TERTs, can be split into the N-terminal part, the central catalytic reverse transcriptase (RT) motifs, and the C-terminal extension (CTE) which is highly conserved among vertebrates as well as among plants. The N-terminal part comprises regions of both low and high similarity, e.g., the structural domains TEN (telomerase essential N-terminal domain) or TRBD (RNA-binding domain). Although most eukaryotes, including humans, harbor a single *TERT* gene, in the allotetraploid *Nicotiana tabacum* plant, three transcribed variants of the *TERT* gene were described, which were inherited from its diploid progenitor species [126].

Compared to the conserved structure of the TERT subunit, TRs show high sequence diversity among more distant organisms, as exemplified by the length differences of TRs in protozoa (159 nt in ciliate *Tetrahymena*, 2200 nt in *Plasmodium*), zebrafish (317 nt), mouse (397 nt), human (451 nt), and budding yeasts (1160 nt). Even within yeasts, the homology among TRs is rather low and their lengths range from 930 to more than 2000 nt [42,113,127–133]. Analogous variance of TR within the plant kingdom is still questionable, since only putative TRs have been predicted in *A. thaliana* so far [56].

However, several secondary structure motifs in TRs which are essential for telomerase activity are conserved in fungi and animals. Starting from the 5′-end of TR, these include a core-enclosing helix (CEH) formed by pairing the 5′-terminus of TR with the complementary internal TR region, a template boundary element (TBE)—a hairpin defining the end of the sequence recognized by TERT as a template, the template sequence itself, and a pseudoknot [133]. Except for the template sequence, none of these structural elements has been recognized in TER1 in *Arabidopsis thaliana*, which is the only reported candidate TR among plants so far [56]. With respect to the above-mentioned sequence diversity of plant telomere repeats, it will be interesting to learn whether and how these evolutionary changes are reflected by the corresponding TR subunits. For example, when assuming the phylogeny of Asparagales plants, telomeres switched first from *Arabidopsis*-like repeats $(TTTAGGG)_n$ to human-like repeats $(TTAGGG)_n$ in the divergence of the Iridaceae family, and this repeat survived all downstream speciation events until the divergence of the genus *Allium*, when the human-type repeat was replaced with the unusual $(CTCGGTTATGGG)_n$ repeat [24,134,135]. The molecular basis underlying these evolutionary switches in telomere DNA sequences should be sought primarily in the corresponding TRs. We can consider the following possible scenarios. (i) TR remained essentially the same across Asparagales phylogeny and the observed switches in telomere synthesis occurred either as a result of mutations in the template region of TR or in its vicinity, which could have changed the boundaries of the region used as a template, (ii) a different RNA molecule took over the TR function. Experiments are in progress in our laboratory to provide a clear answer to this question.

3. Telomere Chromatin Composition

While the end-replication problem of telomeres is most commonly solved by telomerase, the other essential function of telomeres—their end-protection role (i.e., to distinguish natural chromosome ends from DNA breaks, and to eliminate unwanted repair events at telomeres)—is performed by other proteins associated with telomeres. In humans, these include proteins directly binding telomere DNA either in its double strand part (TRF1, TRF2) or at the single strand overhang (POT1). The other proteins bind telomeres via protein-protein interactions with these proteins (RAP1, TIN2, TPP1), which together form a complex termed shelterin [136,137]. Shelterin components and their interaction partners can inhibit the DNA damage response [138–141]. In addition to the end-protective function, shelterin components also play other roles as, e.g., the recruitment of telomerase to telomeres, facilitating replication fork movement through telomeres, or formation of telomere loops (t-loops) [142–149]. In particular, t-loops exist as a "closed-state" telomere conformation both in mammalians and plants [146,150]. While t-loop is considered as a structure inaccessible to telomerase, it may provide a template for telomerase-independent ALT (see below).

The composition of shelterin-like complexes shows differences in individual components among vertebrates, while the overall functions remain conserved. Human proteins associated with double and single strand telomeric DNA, together with their plant orthologues, are listed in Tables 3 and 4, respectively.

In plants, knowledge of a shelterin-like complex is incomplete. The only proteins with confirmed in vivo telomere localization and function are members of the single-myb-histone family, telomere repeat binding (TRB) proteins, which have been characterised in *Arabidopsis thaliana* [66,82,151] and their orthologues were identified in other plants ([152]; Schorova et al., submitted). TRB proteins bind specifically telomeric double strand DNA through their myb-like domain of a telobox type [153,154], as well as the human core components of shelterin—TRF1 and TRF2 proteins. While the myb-like domain in TRF1 and TRF2 is localized at the C-terminus, that of TRB proteins occupies the N-terminus. Additionally, TRB proteins contain the centrally located histone-like domain (H1/5) involved in DNA sequence-unspecific DNA-protein interactions, multimerization, and interaction with POT1b (one of the plant POT1 paralogues) [65,151]. This plant-specific protein-domain organization has not been described in animals. TRB proteins bind telomeric DNA in vitro and in vivo, localize to the telomeres in vivo, interact directly with the telomerase TERT subunit, and the deregulation of telomeres was observed in mutant plants [66,68].

TRB proteins are not only components of the terminal complex associated with telomeres/telomerase, but they are also associated in vivo with promoters of translation machinery genes, which mostly contain a short telomeric sequence [67]. It seems that TRB proteins serve as epigenetic regulators that potentially affect the transcription status of thousands of genes by playing a role of recruiting subunits of multiple epigenetically active multi-protein complexes [68–71,155,156]. These findings are consistent with the observations from yeast or mammals where telomeric proteins (e.g., TRF1, TRF2, and RAP1) are able to localize outside telomeric regions and regulate the transcription of genes involved in metabolism, immunity, and differentiation [157–164].

Surprisingly, no functions in telomere maintenance were found in *Arabidopsis* orthologues of mammalian TRF proteins (TRFL proteins) where a myb-domain of the telobox type is located C-terminally as in human TRF1 and TRF2 [165]. However, a recent study revealed protein-protein interactions between TRFL2 and TRP1, members of the TRFL family, and TERT from *A. thaliana* [66,69]. Plant TRFL2 and TRP1 proteins interact with armadillo/β-catenin-like repeat-containing protein (ARM). ARM directly interacts with plant TERT [70] and might be involved in translation initiation or in regulation of recombination-related genes [69]. Moreover, ARM interacts with the chromatin remodeling protein CHR19 (Table 1). ARM, TRB1, POT1a, and CHR19 (but none of the TRFL proteins) were found among proteins that co-purified with *Arabidopsis* TERT using tandem affinity purification [84]. Association of TERT with proteins that are not essential for telomere maintenance may reflect possible non-telomeric functions of telomerase.

A dual function for telomerase, both telomeric and non-telomeric, is not unique to plants, as mammalian telomerase is involved not only in elongation of telomeres but also non-telomeric activities have been described, including involvement in regulating cellular processes such as apoptosis, proliferation, and cell cycle progression ([166]; reviewed in Reference [167]). Human telomerase and human ARM proteins play a role in the Wnt/APC/β-catenin signaling pathway [168]. A putative human homologue of ARM, ARMC6, interacts with the shelterin protein TRF2 and immuno-precipitates telomerase activity [69].

An additional telomere maintenance component is—somewhat paradoxically—Ku70/80 heterodimer, a DNA repair factor with a high affinity for DNA ends, that plays essential roles in the maintenance of genome integrity in both human and plants cells. In human cells, Ku70/80 heterodimer interacts with the RNA component of telomerase hTR [120] and with catalytic subunit hTERT [94]. In plants, Ku proteins, as well POT1b protein, are associated with TER2. This is a candidate plant TR that is not required for telomere maintenance in *A. thaliana* [56]. Ku70/80 is, however, important for protection of blunt-ended telomeres and for suppression of ALT (see below).

An integrative updated schematic view based on these and previous studies is depicted in Figure 2. It is obvious that the number of plant telomere-associated and telomerase-associated orthologues (where they exist) is larger in comparison to their mammalian counterparts. The phenomenon of the multiplication of genes of the same family is not surprising, since in many plant families, polyploidy (i.e., whole genome duplication) resulting in retention of multiple gene paralogues may lead to their sub-functionalization, neo-functionalization, or partial or full redundancy [169,170]. In association with the previously mentioned evolutionary divergence of plant telomere DNA repeats toward human-like repeats or unusual telomeric repeats, it will be of interest to learn whether pre-existing components of plant shelterin-like complexes have adapted to the change in DNA sequence (this will be particularly interesting in proteins directly recognizing DNA sequences, such as the TRB or POT1 proteins), or whether some other proteins have replaced their function.

Besides the shelterin complex in mammals and its emerging equivalents in plants, there is yet another complex termed CST (CTC1-STN1-TEN1), which is involved in telomere maintenance. This tripartite complex binds the 3′-overhang of the G-rich strand of telomeric DNA and its function in telomere maintenance is conserved in both mammals and plants, and a similar complex exists also in yeast (with Cdc13 instead of CTC1 subunit) [171]. Recently, the roles of individual components of the human CST complex in telomere maintenance were elucidated: while CTC1-STN1 limits telomerase action to prevent G-overhang over-extension, TEN1 is essential for CST function in C-strand fill-in synthesis due to its stabilizing effect on binding the whole CST complex to telomeres and DNA polymerase α engagement in telomere synthesis [172,173]. CST functions, at least in humans, are not limited only to telomeres. CST is also required to avoid replication problem at G-rich sites throughout the genome, likely resolving replication fork stalling [174].

In addition to the telomere-specific proteins, the major part of telomeres is assembled into the nucleosomal chromatin structure which shows a shorter nucleosome periodicity (spacing) than that in the other parts of the chromosomes of the same organism [175–179]. Since shorter telomeres in cultured human cells show a lower nucleosome density than that in cells with longer telomeres, a close relationship was hypothesized between histone density, heterochromatin protein associations, telomere length, and TPE [180]. Interestingly, this feature of telomeric chromatin is conserved at least in vertebrates and plants, and may reflect the specific columnar structure of telomeric chromatin with stacked nucleosomes and weak determination of nucleosome positions by telomeric DNA sequence [181].

Table 3. Comparative overview of proteins associated with telomeric double strand DNA (dsDNA).

Telomeric dsDNA Associated Proteins					
Human Telomeric dsDNA Associated Proteins	**Protein Function and Direct Interactions**	**References**	***Arabidopsis* Telomeric dsDNA Associated Proteins**	**Protein Function and Direct Interactions**	**References**
TRF1	Shelterin. Int.: telomeric dsDNA, TIN2, TANK1 and PINX1. Non-telomeric: binding to ITS and chromatin and satellite DNA and modulation of their chromatin structure. Control of a common fragile site containing ITS.	[59–62] [162,182]	**TRB1, 2, 3**	Shelterin-like. Int.: telomeric dsDNA, TERT, POT1b, RuvBL1 and RuvBL2a. Non-telomeric functions - a recruitment subunit of protein complexes involved in epigenetic regulations. Binding to ITSs.	[64–66]; Schorova et al., submitted [67–71]
TRF2	Shelterin. Int.: telomeric dsDNA; TIN2, RAP1, NBS1, RAD50, Apollo, Ku70, PARP1, XPF-ERCC1, BLM, FEN1, POLB, ORC, RTEL1 and ATM.	[61,72–80, 183–187]	**TRP1**	Possible non-telomeric functions of telomerase. Int.: telomere dsDNA in vitro, TERT, ARM, Ku70, TRFL1 and TRFL9.	[66,69,81–83]
	Non-telomeric function: transcriptional regulator. Binding to ITSs and satellite III.	[155,163]	**TRFL2**	Possible non-telomeric functions of telomerase. Int.: telomere dsDNA in vitro, TERT and ARM.	[69,83]
			TRFL9	Possible non-telomeric functions of telomerase. Int.: telomere dsDNA in vitro, TRP1 and POT1a.	[69,83]
			TBP1, TRFL1, TRFL4	Int.: telomere dsDNA in vitro.	[83,188]
HOT1	Int.: telomeric dsDNA, active telomerase.	[93]	**n.a.**		
Ku70/80	The way of association with telomeric dsDNA is not fully elucidated. Int.: TRF2, RAP1, TR and TERT.	[95]	**Ku70/80**	Role in telomere length regulation, may protect blunt-ended telomeres Int.: TRP1, TER2 and TER2s.	[82,96–99,101]

The proteins depicted in grey are involved in telomere maintenance, however, their association with telomeric dsDNA has not been fully proven yet. Direct interaction partners (Int.) interacting with telomeric dsDNA-associated proteins and concerning their telomeric functions are enumerated. No sequence homologue has been identified yet (n.a.). Double-strand DNA (dsDNA); 5′ exonuclease Apollo (Apollo); Armadillo/β-catenin-like repeat-containing protein (ARM); Ataxia telangiectasia mutated kinase (ATM); ATP-dependent DNA helicase 2 subunit 1 and 2 (Ku70/80); Bloom syndrome protein (BLM); DNA polymerase beta (POLB); DNA repair protein RAD50 (RAD50); Excision repair cross-complementation 1 (ERCC1); Flap endonuclease 1 (FEN1); Homeobox telomere-binding protein 1 (HOT1); Interstitial telomeric sequences (ITSs); Nijmegen breakage syndrome protein 1 (NBS1); Origin recognition complex (ORC); Poly(ADP-Ribose); polymerase 1 (PARP1); Protection of telomeres 1b (POT1b); Regulator of telomere elongation helicase 1 (RTEL1); Repressor-activator protein 1 (RAP1); Telomerase RNA (TR); RuvB-like 1, 2a (RuvBL1, 2a); Tankyrase 1 (TANK1); Telomerase reverse transcriptase (TERT); Telomerase RNA subunit 2, 2s (TER2, TER2s); Telomere binding protein 1 (TBP1); Telomere repeat-binding factor 1, 2, 3 (TRB1, 2, 3); Telomere repeat-binding protein 1 (TRP1); Telomeric repeat binding Factor 1-like 1, 2, 4, 9 (TRFL1, 2, 4, 9); Telomeric repeat-binding factor 1 (TRF1); Telomeric repeat-binding factor 2 (TRF2); TRF1-interacting nuclear protein 2 (TIN2); TRF1-interacting protein 1 (PINX1); Xeroderma pigmentosum group F (XPF1).

Table 4. Comparative overview of proteins associated with telomeric single strand (ssDNA).

Telomeric ssDNA Associated Proteins					
Human Telomeric ssDNA Associated Proteins	**Protein Function and Direct Interactions**	**References**	***Arabidopsis* Telomeric ssDNA Associated Proteins**	**Protein Function and Direct Interactions**	**References**
POT1	Shelterin. Int.: telomeric ssDNA, TPP1 and CTC1.	[50–54]	**POT1a**	Shelterin-like. Int.: TERT, telomeric ssDNA, TER1, TRFL9, CBF5, RuvBL1, CTC1 and STN1.	[47,55–58,69,105,189]
			POT1b	Shelterin-like. Int.: TRB1, TER2, TER2s.	[56,82,100]
			POT1c	POT1 paralogue of unknown function.	[47]
TERT	Catalytic subunit of telomerase.	[190]	**TERT**	Catalytic subunit of telomerase.	
STN1	CST complex subunit, prevents G-overhang overextension. Int.: CTC1, TEN1, TPP1 and POLA.	[54,172,191,192]	**STN1**	CST complex subunit, controls access of telomerase and DDR, together with POLA may be involved in C-strand synthesis. Int.: CTC1, TEN1 and POT1a. Non-telomeric function. Facilitates re-replication at non-telomeric loci.	[189,193–195]
TEN1	CST complex subunit, involves C-strand fill-in synthesis. Int.: STN1.	[172,192]	**TEN1**	CST complex subunit, controls access of telomerase and DDR, coordinating synthesis of the C-strand. Int.: STN1.	[194]
CTC1	CST complex subunit, prevents G-overhang overextension. Int.: telomeric ssDNA, STN1, TPP1 and POT1.	[54,192]	**CTC1**	CST complex subunit, controls access of the telomerase and DDR, coordinating synthesis of the C-strand. Int.: STN1, POT1a and POLA.	[171,189,196]
Purα	p.h. Unwinds dsDNA telomeric oligonucleotides.	[105]	**PURα1**	Associates with TERT.	[84]
n.a.			**Why1**	Regulates telomere-length homeostasis. Int.: telomeric ssDNA.	[197]
n.a.			**STEP1**	Truncated derivative of chloroplast RNA-binding protein, role in plant telomere biogenesis. Int.: telomeric ssDNA.	[198]

The proteins depicted in grey are involved in telomere maintenance, however, their association with telomeric ssDNA has not been fully proven yet. The proteins in green are structural homologues of their human/plant counterparts, however, any involvement in telomere maintenance or association with telomeric sequences has not been described so far. Direct interaction partners (Int.) interacting with telomeric ssDNA associated proteins are enumerated. Cases with not yet identified sequence homologues are denoted with n.a. Single strand DNA (ssDNA); Double-strand DNA (dsDNA); Cajal bodies factor 5 (CBF5); Conserved telomere maintenance component 1 (CTC1); CST complex (CTC1, STN1 and TEN1 subunits); DNA damage response (DDR); DNA polymerase alpha (POLA); Protection of telomeres 1 (POT1); Protection of telomeres 1a, b, c (POT1a, b, c); Pur-alpha 1 (Purα1); RuvB-like 1 (RuvBL1); Single-stranded telomere-binding protein 1 (STEP1); Suppressor of cdc thirteen homolog (STN1); Telomerase reverse transcriptase (TERT); Telomerase RNA subunit 1, 2, 2s (TER1, 2, 2s); Telomeric pathways in association with STN1 (TEN1); Telomeric repeat binding factor 1 -like 9 (TRFL9); TIN2- and POT1-organizing protein (TPP1); Whirly 1 (Why1); putative homolog according to NCBI blastp (p.h.).

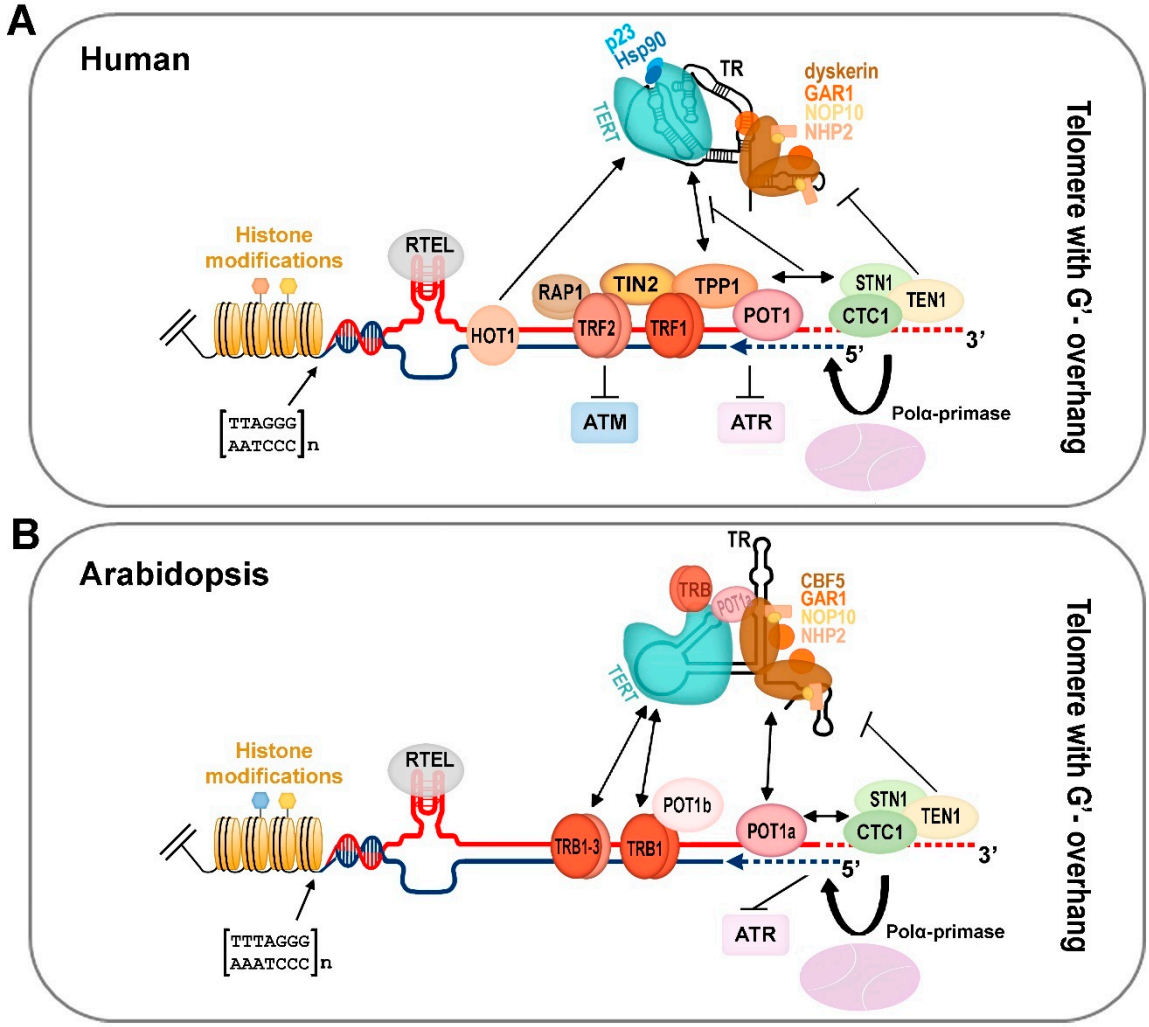

Figure 2. An integrative schematic view of the human and plant terminal telomeric complex. (**A**) Human active telomerase is associated with Hsp90 and p23 chaperones as well as with TR associated conserved scaffold proteins of box H/ACA small nucleolar RNAs (dyskerin, NHP2, NOP10, GAR1). Mammalian shelterin proteins (TRF1/2, RAP1, TIN2, TPP1, and POT1) modulate access to the telomerase complex and the ATR/ATM-dependent DNA damage response pathway. The CST complex (CTC1-STN1-TEN1) affects telomerase and DNA polymerase α recruitment to the chromosomal termini, and, thus, coordinates G-overhang extension by telomerase with fill-in synthesis of the complementary C-strand (blue dashed line). G-quadruplexes, D-loops, and t-loops during telomere replication are resolved by RTEL helicase. HOT1 directly binds double strand telomere repeats and associates with the active telomerase. Telomere nucleosomes show a shorter periodicity than that in the other parts of chromosomes. For human telomere histone modifications, see Figure 3. (**B**) *Arabidopsis* telomerase is associated with TRB proteins as well as with POT1a that interacts with the dyskerin orthologue CBF5. Plants possess all orthologue proteins of conserved scaffold box H/ACA of small nucleolar RNAs (CBF5, GAR1, NOP10, NHP2). Moreover, TRB proteins interact with the telomeric sequence due to the same myb-like binding domain as that in mammalian TRF1/2. TRB proteins interact with TERT and POT1b, and, when localized at chromosomal ends, they are eligible to function as components of the plant shelterin complex. An evolutionarily conserved CST complex is suggested to coordinate the unique requirements for efficient replication of telomeric DNA in plants as well as in other organisms. In addition, plant RTEL contributes to telomere homeostasis. For the sake of clarity, only the situation in telomere with 3′ overhang is depicted. For plant telomere histone modifications, see Figure 3.

4. Telomere Epigenetics

As chromatin structures, telomeres are natural targets for epigenetic modifications. At the DNA level, methylation at carbon 5 of cytosine represents the dominant mark in eukaryotic cells. Methylated cytosines (^{m}Cs) are generally enriched in heterochromatic regions of the genome and silenced promoters. Important differences in the sequence contexts, in which ^{m}Cs are located, exist between animals and plants. In mammalian cells, they are predominantly located in CG doublet motifs, with the symmetry of the sequence crucial for the maintenance of the methylation pattern during DNA replication (reviewed in Reference [199]). A fraction of ^{m}Cs in non-CG contexts was found in human embryonic cells. This fraction disappears after differentiation and is restored in induced pluripotent stem cells, which shows involvement of distinct methylation patterns in the regulation of gene expression [200]. Also in plants, cytosines in the CG motif are most frequently methylated, but ^{m}Cs are also commonly placed in non-CG sequences, symmetrical CHG triplets (H=C or A or T), or non-symmetrical CHH motifs (reviewed in Reference [201]). In telomeres, cytosines in non-symmetrical sequence contexts are present in the telomeric C-rich strand, i.e., in CCCTAA repeats in animals and CCCTAAA repeats in plants. Using shotgun bisulfite genomic sequencing, ^{m}Cs were detected in *A. thaliana* telomeric repeats with the inner cytosine most frequently methylated [202]. This pattern was confirmed by an independent approach, with high reliability at least in the proximal part of the telomere [203,204], and methylated telomeric cytosines were detected in cultured *Nicotiana tabacum* (tobacco) cells [205] and other plants [206]. Disruption of telomere homeostasis as a consequence of decreased genomic DNA methylation was observed in *A. thaliana* [203,207] but not in tobacco cells [205], which shows differences in the involvement of DNA methylation in regulation of telomere homeostasis between these model plants (for a more detailed review see Reference [208]).

Telomeres formed by mini-satellite repeats were traditionally considered as heterochromatic regions, and, thus, associated with heterochromatin-specific histone marks. Certain differences in histone modifications in heterochromatin have been described between animals and plants. In animals, constitutive heterochromatin is defined by the presence of H3K9me3 (trimethylation of lysine 9 of histone H3) (reviewed in Reference [209]) while in plants, this mark decorates silenced euchromatic genes, and constitutive heterochromatin is associated with H3K9me2 modification [210]. Facultative heterochromatin is enriched in H3K27me3 in cells of representatives of both kingdoms. In agreement with the hypothesis of the heterochromatic character of telomeres, the importance of heterochromatin-specific epigenetic marks for telomere maintenance and genome stability was demonstrated in numerous studies using human and mouse cells as models (reviewed in Reference [211]). On the other hand, data showing a low level of heterochromatin-specific modifications and an abundance of active marks on human telomeric histones have been presented [212–214], which shows certain dynamics of the human telomeric chromatin structure. Based on these and other reports, distinct differences exist in telomeric chromatin composition between the most important mammalian models, human and mouse cells, because H3K9me3 density and HP1 enrichment were significantly higher in mouse compared to humans [215,216]. Nevertheless, according to a study utilizing quantitative locus purification [217] the heterochromatic histone modification H4K20me3 is underrepresented at mouse telomeres even though it was previously detected by others at mouse [218,219] and also human [220] telomeres in analyses based on chromatin immuno-precipitation. Further research is necessary to draw final conclusions on the epigenetic nature of mammalian telomeres, especially considering other factors mentioned below.

Plant telomeric chromatin was shown to be associated with both heterochromatin-specific H3K9me2 and euchromatic H3K4me3 marks, with the latter less abundant [204,206,221]. Therefore, the plant telomeric chromatin exhibits a dual epigenetic character. Identification of the H3K27me3 modification, which is typical for facultative heterochromatin, in telomeric histones of *A. thaliana* [221,222] and *N. tabacum* [206] was rather surprising. However, it correlates with its presence at human telomeres [215], and with the recent observation that polycomb repressor complex 2-dependent

loading of H3K27me3 at human telomeres is essential for the proper establishment of H3K9me3 and H4K20me3 modifications [220]. Nevertheless, H3K27me3 was not detected at mouse telomeres [217]. Thus, although significantly fewer results are available on the epigenetics of telomeric chromatin in plants compared to mammals, interesting similarities as well as differences have already been described and hopefully others will be elucidated based on future studies using different model organisms, including plants with non-canonical telomere sequences [24,25,27,134].

When discussing telomeric chromatin, it is necessary to mention that analysis of epigenetic modifications may be complicated by the presence of non-terminally located telomeric repeats forming interstitial telomeric sequences (ITSs). ITSs are relatively abundant in subtelomeric, pericentromeric, and centromeric regions of most eukaryotic organisms and represent fragile parts of chromosomes, which are prone to rearrangements and recombinations. The detailed compositions of telomeres and ITSs are different. In contrast to telomeres consisting of long tracts of perfect telomeric repeats, ITSs are often degenerated and/or disrupted by non-telomeric sequences. However, ITSs may still contribute to the telomere-specific signal in epigenetic studies, mainly those based on hybridization of membrane-bound DNA. Frequently-used genome-wide sequencing analyses (ChIP-seq and bisulfite sequencing) do not completely solve this problem because telomeres, like other tandem repeats, are difficult to analyze, and even direct analysis of respective read counts (i.e., those comprising perfect telomeric repeats versus those formed by degenerated repeats and non-telomeric sequences) may be ambiguous due to the non-linearity of PCR amplification of repetitive sequences [223]. Both mammalian and plant telomeres are transcribed to long non-coding RNA called TERRA [204,224] and this transcriptional potency could reflect the relatively lower level of compactness of telomeric chromatin compared with heterochromatin. The apparent discrepancy between the association of heterochromatic marks with telomeric histones and the transcriptional activity of telomeres is weakened by the facts that a mechanistic relationship between TERRA transcription and loading of heterochromatic modifications to human telomeres has been described [220], and that in *Arabidopsis* a certain—maybe dominant—fraction of TERRA is transcribed from ITSs [204], which are purely heterochromatic [225].

At this stage of knowledge, it is difficult or even impossible to formulate any general conclusion on the epigenetic nature of telomeric chromatin (Figure 3). Without any doubt, the specific structure of telomeres is crucial for the maintenance of genome integrity. Telomeres are rigid enough to prevent repair and recombination at chromosome ends and to restrict telomere accessibility for telomerase, but open enough to be transcribed and, at least in a specific time window of the cell cycle, accessible to telomerase. Moreover, in disagreements about telomeric "heterochromatin" or "euchromatin", contribution of non-histone players, mainly shelterin proteins, to the telomeric chromatin compaction should be reflected (reviewed in Reference [226]). Why not admit, that telomeric chromatin is so specific that it does not fit into the existing criteria and that these should be widened? This suggestion is strengthened by the finding that other non-genic parts of the human genome, originally thought to be uniformly heterochromatic, are associated with different combinations of histone marks [213]. It is well possible that the epigenetic state of telomeres is more dynamic than previously thought and shows tissue-specific, cell-cycle specific, and developmental stage-specific changes. This would not only explain the diverse results of the above studies, but would be consistent with our current understanding of the epigenetics of other chromosome regions.

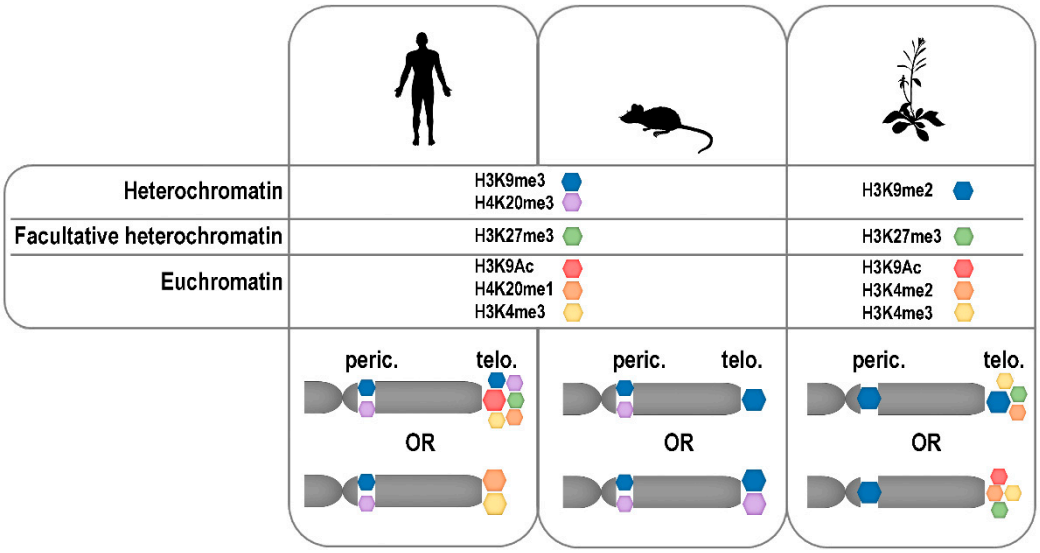

Figure 3. Modifications of mammalian and plant telomere (telo.) and pericentromere (peric.) histones. The relative enrichments of selected epigenetic modifications of telomeric and pericentromeric histones in human, mouse and *Arabidopsis* are schematically depicted according to data presented in References [204,212,213,215,217–222,225].

5. Telomere 3′-Overhangs, Blunt Ends, and Loops

Telomeres in vertebrates, in particular humans, possess 3′-overhangs at both chromosome ends. These overhangs are of different sizes on lagging versus leading strands [227]. In human telomeres a G-overhang is prevalent whose length varies from several tens to 280 nt [228–230]. Likewise, a 5′ C-rich overhang is present at the telomeres of human chromosomes, being far more prevalent in tumor cells using ALT (see below) [231]. This is not the case in *Arabidopsis thaliana*, *Silene latifolia*, and other angiosperm plants, which lack telomere overhangs or possess only short 1–3 nt overhangs at about half of their telomeres [232,233]. The telomere whose 3′- end is being synthesized in a given cell cycle by leading strand synthesis remains blunt-ended likely due to protection against end-processing by a specific exonuclease. This protection is dependent on the Ku70/80 heterodimer [233]. The role of the Ku complex in plant telomere protection was also suggested by our earlier studies, which indicated Ku as an interaction partner of AtTRP1, one of the TRF-like proteins in *A. thaliana* ([82]; see Reference [155] for a review). An analogous interaction between the shelterin components TRF2 and Ku70 was observed earlier in human cells [77]. Due to the asymmetry (non-equivalence) of plant telomeres, a different set of proteins may protect the telomere whose 3′-end serves as a template in "incomplete" lagging strand synthesis and can be elongated by telomerase. Protection of blunt-ended telomeres in *Arabidopsis* by the Ku70/80 complex seems paradoxical considering the presumed end-protective function of telomeres on one hand, and a key role of the Ku complex in non-homologous end-joining repair of double strand DNA breaks on the other hand. A possible solution of this enigma was suggested recently by a study which indicated different binding modes of the Ku complex to dsDNA breaks and to telomeres. Both functions were dissected using Ku mutants with impaired ability to translocate along DNA. While Ku sliding is not required for its association with plant telomeres, it is essential for its involvement in the non-homologous end joining pathway of DNA repair [101]. The presence of blunt-ended telomeres is, however, not common to all plants. For example, in the moss *Physcomitrella patens*, both telomeres of a chromosome possess overhangs and, correspondingly, lack of the Ku complex components shows no effect on telomere maintenance or end protection [234]. The Ku70/80 complex was also reported to be a negative regulator of telomerase function in *Arabidopsis* [99]. In addition to telomere elongation by telomerase,

an extension of telomere G-strand overhangs was observed in Ku mutants, which suggests a role of Ku70/80 in C-rich telomeric strand maintenance [235].

Besides telomerase, eukaryotic cells can also utilize a back-up mechanism of telomere maintenance—ALT—which is based on homologous recombination (HR) [236]. This telomerase-independent mechanism is activated in a number of human tumors, in human cells immortalized in culture, and also in normal somatic tissues [237]. In plants, the ALT mechanism is activated in mutants with telomerase dysfunction and possibly also during the earliest stages of normal plant development [238]. ALT relies on the formation of terminal telomeric loops (t-loops) [146], which parallels the first steps of HR. The eventual resolution of these t-loops and aberrant HR at telomeres generates not only telomeres of highly heterogeneous lengths but also extrachromosomal t-circles, which are the known hallmarks of ALT. In mutant plants that are deficient for components of the Ku70/80 complex, induction of t-circle formation was observed at telomeres but not at other regions rich in DNA repeats. Despite ongoing terminal deletions arising from excision of t-circles in mutant plants, the telomeres remain functional, which indicates an efficient telomere healing by telomerase [239].

Another interesting protein connecting telomeric loops and circles with DNA recombination and telomere replication is RTEL1. This was originally described in *Caenorhabditis elegans* as a functional homologue of the yeast Srs2 protein, which removes Rad51 from single strand DNA. Therefore, it prevents the homology search step of HR and helps to protect the cell from inappropriate HR (for review, see Reference [240]). Furthermore, in *C. elegans*, the RTEL1 helicase suppresses inappropriate recombination events by promoting disassembly of D-loop recombination intermediates, and the loss of its function results in increased genome instability [241]. In addition to its regulatory role in HR, RTEL1 acts in telomere maintenance in mammalian telomerase-positive cells [242]. This function was explained by the function of RTEL1 in opening t-loops, which blocked inappropriate excision of large telomere regions—the process known as telomere rapid deletion. To promote this t-loop unwinding, RTEL1 is recruited to telomeres in the S-phase by the telomeric protein TRF2 [186].

In addition to its role in t-loop stability, mouse RTEL1 can dissolve G4-DNA structures, which otherwise block replication fork progression and the extension of telomeres by telomerase [243]. Importantly, the role of RTEL1 in telomere dynamics was clearly confirmed by the finding that its mutation is causative for Hoyeraal-Hreidarsson syndrome, which is a severe form of dyskeratosis congenita, predisposing to bone-marrow failure and cancer. This disease is characterised by short telomeres and genome instability [244–246]. A recent report revealed that reversed replication forks occurring in telomeres of RTEL1-deficient cells is due to compromised telomere replication aberrantly recruiting telomerase, which prevents the restart of reversed replication forks at telomeres and leads to critically short telomeres [247]. In this context, telomerase paradoxically contributes to telomere shortening by stabilizing stalled replication forks at chromosome ends.

In addition, the *A. thaliana* RTEL1 homolog suppresses HR and is involved in processing DNA replication intermediates and interstrand and intrastrand DNA cross-links. Deficiency of the *Arabidopsis* RTEL1 triggers a SOG1-dependent replication checkpoint in response to DNA crosslinks [248]. Similarly to the situation in mammals, the *Arabidopsis* RTEL1 contributes to telomere homeostasis. The concurrent loss of RTEL1 and TERT accelerates telomere shortening, which results in a developmental arrest after four generations [249] compared to 10 generations in single-mutant *tert* plants [250]. This observation indicates a role of RTEL1 in ALT, which otherwise partially compensates for the loss of TERT [238]. In agreement with these results, it was recently demonstrated that RAD51-dependent homologous recombination participates in ALT in *A. thaliana* [251]. This is not surprising when considering the essential role of RAD51 in HR, and HR as a major molecular mechanism of ALT. However, the authors further showed that this role of RAD51 is dependent on RTEL1 helicase, which possibly functions in dissolution of the D-loop after telomere replication. In P. patens, RTEL1 has been found among genes, which are up-regulated after γ-irradiation. RTEL1 knockout resulted in a severe growth deficiency, which was independent of the presence

of bleomycin [252], and the authors hypothesized that this growth phenotype might be the result of telomere deficiency. Thus, the functions of RTEL1 seem widely conserved. In conclusion, the requirement for RTEL1 in multiple pathways to preserve plant genome stability can be explained by its putative role in the destabilization of DNA loop structures such as D-loops and t-loops, which aligns with previous studies in mammalian systems.

6. Cellular Aging and the Immortal DNA Strand Hypothesis

Cellular aging is characterized by progressive loss of physiological integrity that leads to impaired function and genomic instability and ultimately to a functional decline at the tissue and organ level. Telomere attrition during cell aging is classified as one of the several major hallmarks of aging—together with, e.g., genomic instability, epigenetic alterations, loss of proteostasis, mitochondrial dysfunction, cellular senescence, or altered intercellular communication [7]. In Metazoa, there is no universal pattern of telomere erosion [253], and, in some animals, the progressive telomere shortening with age has not been observed [254]. Nevertheless, telomere length is typically inversely correlated with lifespan, while telomerase expression co-evolved with body size [255]. A connection between cellular aging and replicative telomere shortening is widely accepted and experimentally validated in both humans and plants. Importantly, under normal conditions (in wild type plants) this type of cellular aging is prevented by telomerase activity in dividing cells [20,21,38]. The associations between telomere length and age-related disease and mortality in humans have been proven in several studies (reviewed in References [8,256,257]). However, telomere length of humans is not a determinant of aging but rather a marker able to explain life expectancy and disease risk.

In animals, the distribution of cellular age varies among tissues and cell compartments, including progenitor cell compartments, depending on the influx of stem cells and the dynamics of self-renewal and differentiation of progenitor cells. In particular, the mode of cell division of progenitor cells may be: (i) symmetric self-renewal, in which progenitor cell division results in two daughter progenitor cells (one generation older) remaining in the compartment, (ii) symmetric differentiation, resulting in two differentiated cells which leave the progenitor cell compartment, or (iii) asymmetric division resulting in one progenitor and one differentiated cell. Importantly, cellular age distributions between healthy and cancerous tissues may inform dynamic changes within the hierarchical tissue structure, i.e., an acquired increased self-renewal capacity in certain tumors [258]. In this connection, it is of interest to mention the hypothesis of the immortal DNA strand [259]. This hypothesis proposes that adult stem cells segregate their template and newly synthesized DNA strands non-randomly, preferentially retaining parental DNA strands in each division. This way, adult stem cells pass mutations resulting from replication errors onto non-stem cell daughter cells that differentiate and terminate division. Adult stem cells could thus reduce the accumulation of mutations and the associated deterioration of gene functions with each cell cycle. Moreover, this strategy would also slow down replicative telomere shortening. Thus, two major factors of cellular and organismal aging could be substantially limited if immortal DNA strand segregation operates in progenitor cells. Several studies have supported this hypothesis up to now. For example, using sequential pulses of halogenated thymidine analogues, high frequencies of segregation of older and younger template strands during proliferative expansion of mouse muscle stem cells was observed [260]. Template strand co-segregation was strongly associated with asymmetric cell divisions yielding daughters with divergent fates. Daughter cells inheriting the older templates retained a more immature phenotype, whereas daughters inheriting the newer templates acquired a more differentiated phenotype. It will be of interest to learn if the validity of this hypothesis is more general, and specifically to elucidate the molecular mechanism of non-random DNA segregation in asymmetric cell division. This principle may also be functional in meristem cell division and differentiation. While replicative telomere shortening is efficiently counteracted by telomerase in wild type plants (see above), reduction of accumulation of mutations would be extremely beneficial when considering e.g., trees sustaining their growth for centuries. Low telomere loss per plant generation has been

found in telomerase-deficient *Arabidopsis* mutants [250], which indicates a possible involvement of non-random DNA strand segregation in addition to ALT [238]. Unfortunately, the application of sequential pulse labeling in planta is technically too demanding, and any direct evidence for the immortal DNA strand hypothesis is, thus, missing in plants.

7. Concluding Remarks

Currently available data show remarkably conserved principles in telomere biology across eukaryotes, which is consistent with an association of telomere and telomerase emergence with the earliest steps of their evolution. At the same time, however, a number of specific features and exceptions cannot be ignored since they point to limitations of our wider understanding of these principles. Among a number of open questions to be answered, elucidation of the structure of telomeric chromatin (telochromatin), including its epigenetic and higher-order dynamics, with high spatial and temporal resolution is needed in various model systems. Furthermore, the biological relevance of non-canonical structures formed by telomeric DNA should be addressed mainly under in vivo conditions. Such studies are timely due to recent fast progress in adequate technical tools, including e.g., super-resolution and cryo-electron microscopy.

Studies of repair processes at telomeres and of telomerase regulation belong to the hot topics in this field, since this knowledge can clearly be applied to promote protection of genome stability. In this respect, plants are indispensable due to the natural telomerase-competent character of their cells which allows us to examine mechanisms of repression and activation of telomerase in association with proliferation, differentiation, and dedifferentiation of plant cells. This knowledge is essential for understanding carcinogenesis and is potentially applicable to tumor therapy and cell rejuvenation.

Author Contributions: P.P.S., M.F. and J.F. contributed to this paper with a literature review, drafting the paper, and approval of the final version.

Funding: This work was supported by the Czech Science Foundation (projects 16-01137S and 17-09644S), by the project SYMBIT, reg. number: CZ.02.1.01/0.0/0.0/15_003/0000477 financed by the ERDF, and by the Ministry of Education, Youth and Sports of the Czech Republic under the projects CEITEC 2020 (LQ1601) and INTER-COST (LTC17077).

Acknowledgments: We thank to Ladislav Dokládal and Ronald Hancock for reviewing and discussing the MS prior to submission.

Conflicts of Interest: The authors declare no conflict of interest.

References

1. Olovnikov, A.M. Principle of marginotomy in template synthesis of polynucleotides. *Dokl. Akad. Nauk. SSSR* **1971**, *201*, 1496–1499.
2. Muller, H.J. The remaking of chromosomes. *Collect. Net.* **1938**, *13*, 181–195.
3. McClintock, B. The fusion of broken chromosome ends of sister half-chromatids following chromatid breakage at meiotic anaphases. *Mo. Agric. Exp. Stn. Res. Bull.* **1938**, *290*, 1–48.
4. McClintock, B. The stability of broken ends of chromosomes in Zea mays. *Genetics* **1941**, *26*, 234–282.
5. Von Zglinicki, T. Oxidative stress shortens telomeres. *Trends Biochem. Sci.* **2002**, *27*, 339–344. [CrossRef]
6. Hoelzl, F.; Cornils, J.S.; Smith, S.; Moodley, Y.; Ruf, T. Telomere dynamics in free-living edible dormice (Glis glis): The impact of hibernation and food supply. *J. Exp. Biol.* **2016**, *219*, 2469–2474. [CrossRef]
7. Lopez-Otin, C.; Blasco, M.A.; Partridge, L.; Serrano, M.; Kroemer, G. The Hallmarks of Aging. *Cell* **2013**, *153*, 1194–1217. [CrossRef]
8. Simons, M.J.P. Questioning causal involvement of telomeres in aging. *Ageing Res. Rev.* **2015**, *24*, 191–196. [CrossRef]
9. Steenstrup, T.; Kark, J.D.; Verhulst, S.; Thinggaard, M.; Hjelmborg, J.V.B.; Dalgard, C.; Kyvik, K.O.; Christiansen, L.; Mangino, M.; Spector, T.D.; et al. Telomeres and the natural lifespan limit in humans. *Aging US* **2017**, *9*, 1130–1142. [CrossRef]

10. Factor-Litvak, P.; Susser, E.; Kezios, K.; McKeague, I.; Kark, J.D.; Hoffman, M.; Kimura, M.; Wapner, R.; Aviv, A. Leukocyte Telomere Length in Newborns: Implications for the Role of Telomeres in Human Disease. *Pediatrics* **2016**, *137*, e20153927. [CrossRef]
11. Robin, J.D.; Ludlow, A.T.; Batten, K.; Magdinier, F.; Stadler, G.; Wagner, K.R.; Shay, J.W.; Wright, W.E. Telomere position effect: Regulation of gene expression with progressive telomere shortening over long distances. *Genes Dev.* **2014**, *28*, 2464–2476. [CrossRef]
12. Victorelli, S.; Passos, J.F. Telomeres and Cell Senescence—Size Matters Not. *Ebiomedicine* **2017**, *21*, 14–20. [CrossRef]
13. Abdallah, P.; Luciano, P.; Runge, K.W.; Lisby, M.; Geli, V.; Gilson, E.; Teixeira, M.T. A two-step model for senescence triggered by a single critically short telomere. *Nat. Cell Biol.* **2009**, *11*, 988. [CrossRef]
14. Hemann, M.T.; Strong, M.A.; Hao, L.Y.; Greider, C.W. The shortest telomere, not average telomere length, is critical for cell viability and chromosome stability. *Cell* **2001**, *107*, 67–77. [CrossRef]
15. Kaul, Z.; Cesare, A.J.; Huschtscha, L.I.; Neumann, A.A.; Reddel, R.R. Five dysfunctional telomeres predict onset of senescence in human cells. *Embo Rep.* **2012**, *13*, 52–59. [CrossRef]
16. Watson, J.M.; Riha, K. Telomeres, aging, and plants: From weeds to Methuselah—A mini-review. *Gerontology* **2011**, *57*, 129–136. [CrossRef]
17. Barsov, E.V. Telomerase and primary T cells: Biology and immortalization for adoptive immunotherapy. *Immunotherapy* **2011**, *3*, 407–421. [CrossRef]
18. Shalaby, T.; Hiyama, E.; Grotzer, M.A. Telomere Maintenance as Therapeutic Target in Embryonal Tumours. *Anti-Cancer Agents Med. Chem.* **2010**, *10*, 196–212. [CrossRef]
19. Fajkus, J.; Kovarik, A.; Kralovics, R. Telomerase activity in plant cells. *Febs Lett.* **1996**, *391*, 307–309. [CrossRef]
20. Fajkus, J.; Fulneckova, J.; Hulanova, M.; Berkova, K.; Riha, K.; Matyasek, R. Plant cells express telomerase activity upon transfer to callus culture, without extensively changing telomere lengths. *Mol. Gen. Genet.* **1998**, *260*, 470–474. [CrossRef]
21. Fitzgerald, M.S.; McKnight, T.D.; Shippen, D.E. Characterization and developmental patterns of telomerase expression in plants. *Proc. Natl. Acad. Sci. USA* **1996**, *93*, 14422–14427. [CrossRef]
22. Fajkus, J.; Sykorova, E.; Leitch, A.R. Telomeres in evolution and evolution of telomeres. *Chromosome Res.* **2005**, *13*, 469–479. [CrossRef]
23. Louis, E.J. Are *Drosophila* telomeres an exception or the rule? *Genome Biol.* **2002**, *3*. [CrossRef]
24. Fajkus, P.; Peska, V.; Sitova, Z.; Fulneckova, J.; Dvorackova, M.; Gogela, R.; Sykorova, E.; Hapala, J.; Fajkus, J. Allium telomeres unmasked: The unusual telomeric sequence (CTCGGTTATGGG)(n) is synthesized by telomerase. *Plant J.* **2016**, *85*, 337–347. [CrossRef]
25. Peska, V.; Fajkus, P.; Fojtova, M.; Dvorackova, M.; Hapala, J.; Dvoracek, V.; Polanska, P.; Leitch, A.R.; Sykorova, E.; Fajkus, J. Characterisation of an unusual telomere motif $(TTTTTTAGGG)_n$ in the plant Cestrum *elegans* (Solanaceae), a species with a large genome. *Plant J.* **2015**, *82*, 644–654. [CrossRef]
26. Peska, V.; Sitova, Z.; Fajkus, P.; Fajkus, J. BAL31-NGS approach for identification of telomeres de novo in large genomes. *Methods* **2017**, *114*, 16–27. [CrossRef]
27. Tran, T.D.; Cao, H.X.; Jovtchev, G.; Neumann, P.; Novak, P.; Fojtova, M.; Vu, G.T.H.; Macas, J.; Fajkus, J.; Schubert, I.; et al. Centromere and telomere sequence alterations reflect the rapid genome evolution within the carnivorous plant genus Genlisea. *Plant J.* **2015**, *84*, 1087–1099. [CrossRef]
28. Wright, W.E.; Piatyszek, M.A.; Rainey, W.E.; Byrd, W.; Shay, J.W. Telomerase activity in human germline and embryonic tissues and cells. *Dev. Genet.* **1996**, *18*, 173–179. [CrossRef]
29. Ramirez, R.D.; Wright, W.E.; Shay, J.W.; Taylor, R.S. Telomerase activity concentrates in the mitotically active segments of human hair follicles. *J. Investig. Dermatol.* **1997**, *108*, 113–117. [CrossRef]
30. Hiyama, E.; Hiyama, K.; Yokoyama, T.; Shay, J.W. Immunohistochemical detection of telomerase (hTERT) protein in human cancer tissues and a subset of cells in normal tissues. *Neoplasia* **2001**, *3*, 17–26. [CrossRef]
31. Hiyama, E.; Hiyama, K. Telomere and telomerase in stem cells. *Br. J. Cancer* **2007**, *96*, 1020–1024. [CrossRef]
32. Hiyama, K.; Hirai, Y.; Kyoizumi, S.; Akiyama, M.; Hiyama, E.; Piatyszek, M.A.; Shay, J.W.; Ishioka, S.; Yamakido, M. Activation of Telomerase in Human-Lymphocytes and Hematopoietic Progenitor Cells. *J. Immunol.* **1995**, *155*, 3711–3715.
33. Yui, J.; Chiu, C.P.; Lansdorp, P.M. Telomerase activity in candidate stem cells from fetal liver and adult bone marrow. *Blood* **1998**, *91*, 3255–3262.

34. Ito, H.; Kyo, S.; Kanaya, T.; Takakura, M.; Inoue, M.; Namiki, M. Expression of human telomerase subunits and correlation with telomerase activity in urothelial cancer. *Clin. Cancer Res.* **1998**, *4*, 1603–1608.
35. Kyo, S.; Takakura, M.; Kohama, T.; Inoue, M. Telomerase activity in human endometrium. *Cancer Res.* **1997**, *57*, 610–614.
36. Jureckova, J.F.; Sykorova, E.; Hafidh, S.; Honys, D.; Fajkus, J.; Fojtova, M. Tissue-specific expression of telomerase reverse transcriptase gene variants in Nicotiana tabacum. *Planta* **2017**, *245*, 549–561. [CrossRef]
37. Ogrocka, A.; Sykorova, E.; Fajkus, J.; Fojtova, M. Developmental silencing of the AtTERT gene is associated with increased H3K27me3 loading and maintenance of its euchromatic environment. *J. Exp. Bot.* **2012**, *63*, 4233–4241. [CrossRef]
38. Riha, K.; Fajkus, J.; Siroky, J.; Vyskot, B. Developmental control of telomere lengths and telomerase activity in plants. *Plant Cell* **1998**, *10*, 1691–1698. [CrossRef]
39. Zachova, D.; Fojtova, M.; Dvorackova, M.; Mozgova, I.; Lermontova, I.; Peska, V.; Schubert, I.; Fajkus, J.; Sykorova, E. Structure-function relationships during transgenic telomerase expression in *Arabidopsis*. *Physiol. Plant.* **2013**, *149*, 114–126. [CrossRef]
40. Winter, D.; Vinegar, B.; Nahal, H.; Ammar, R.; Wilson, G.V.; Provart, N.J. An "Electronic Fluorescent Pictograph" Browser for Exploring and Analyzing Large-Scale Biological Data Sets. *PLoS ONE* **2007**, *2*. [CrossRef]
41. Greider, C.W.; Blackburn, E.H. Identification of a Specific Telomere Terminal Transferase-Activity in Tetrahymena Extracts. *Cell* **1985**, *43*, 405–413. [CrossRef]
42. Greider, C.W.; Blackburn, E.H. A Telomeric Sequence in the Rna of Tetrahymena Telomerase Required for Telomere Repeat Synthesis. *Nature* **1989**, *337*, 331–337. [CrossRef]
43. Chan, H.; Wang, Y.Q.; Feigon, J. Progress in Human and Tetrahymena Telomerase Structure Determination. *Annu. Rev. Biophys.* **2017**, *46*, 199–225. [CrossRef]
44. Nguyen, T.H.D.; Tam, J.; Wu, R.A.; Greber, B.J.; Toso, D.; Nogales, E.; Collins, K. Cryo-EM structure of substrate-bound human telomerase holoenzyme. *Nature* **2018**, *557*, 190. [CrossRef]
45. Lermontova, I.; Schubert, V.; Bornke, F.; Macas, J.; Schubert, I. *Arabidopsis* CBF5 interacts with the H/ACA snoRNP assembly factor NAF1. *Plant Mol. Biol.* **2007**, *65*, 615–626. [CrossRef]
46. Pendle, A.F.; Clark, G.P.; Boon, R.; Lewandowska, D.; Lam, Y.W.; Andersen, J.; Mann, M.; Lamond, A.I.; Brown, J.W.S.; Shaw, P.J. Proteomic analysis of the *Arabidopsis* nucleolus suggests novel nucleolar functions. *Mol. Biol. Cell* **2005**, *16*, 260–269. [CrossRef]
47. Rossignol, P.; Collier, S.; Bush, M.; Shaw, P.; Doonan, J.H. *Arabidopsis* POT1A interacts with TERT-V(18), an N-terminal splicing variant of telomerase. *J. Cell Sci.* **2007**, *120*, 3678–3687. [CrossRef]
48. Nakamura, T.M.; Morin, G.B.; Chapman, K.B.; Weinrich, S.L.; Andrews, W.H.; Lingner, J.; Harley, C.B.; Cech, T.R. Telomerase catalytic subunit homologs from fission yeast and human. *Science* **1997**, *277*, 955–959. [CrossRef]
49. Oguchi, K.; Liu, H.T.; Tamura, K.; Takahashi, H. Molecular cloning and characterization of AtTERT, a telomerase reverse transcriptase homolog in *Arabidopsis thaliana*. *Febs Lett.* **1999**, *457*, 465–469. [CrossRef]
50. Baumann, P.; Cech, T.R. Pot1, the putative telomere end-binding protein in fission yeast and humans. *Science* **2001**, *292*, 1171–1175. [CrossRef]
51. Houghtaling, B.R.; Cuttonaro, L.; Chang, W.; Smith, S. A dynamic molecular link between the telomere length regulator TRF1 and the chromosome end protector TRF2. *Curr. Biol.* **2004**, *14*, 1621–1631. [CrossRef]
52. Liu, D.; Safari, A.; O'Connor, M.S.; Chan, D.W.; Laegeler, A.; Qin, J.; Zhou, S.Y. PTOP interacts with POT1 and regulates its localization to telomeres. *Nat. Cell Biol.* **2004**, *6*, 673–680. [CrossRef]
53. Ye, J.Z.S.; Hockemeyer, D.; Krutchinsky, A.N.; Loayza, D.; Hooper, S.M.; Chait, B.T.; de Lange, T. POT1-interacting protein PIP1: A telomere length regulator that recruits POT1 to the TIN2/TRF1 complex. *Genes Dev.* **2004**, *18*, 1649–1654. [CrossRef]
54. Chen, L.Y.; Redon, S.; Lingner, J. The human CST complex is a terminator of telomerase activity. *Nature* **2012**, *488*, 540. [CrossRef]
55. Tani, A.; Murata, M. Alternative splicing of Pot1 (Protection of telomere)-like genes in *Arabidopsis thaliana*. *Genes Genet. Syst.* **2005**, *80*, 41–48. [CrossRef]
56. Cifuentes-Rojas, C.; Kannan, K.; Tseng, L.; Shippen, D.E. Two RNA subunits and POT1a are components of *Arabidopsis* telomerase. *Proc. Natl. Acad. Sci. USA* **2011**, *108*, 73–78. [CrossRef]

57. Kannan, K.; Nelson, A.D.L.; Shippen, D.E. Dyskerin is a component of the *Arabidopsis* telomerase RNP required for telomere maintenance. *Mol. Cell. Biol.* **2008**, *28*, 2332–2341. [CrossRef]
58. Arora, A.; Beilstein, M.A.; Shippen, D.E. Evolution of *Arabidopsis* protection of telomeres 1 alters nucleic acid recognition and telomerase regulation. *Nucleic Acids Res.* **2016**, *44*, 9821–9830. [CrossRef]
59. Van Steensel, B.; de Lange, T. Control of telomere length by the human telomeric protein TRF1. *Nature* **1997**, *385*, 740–743. [CrossRef]
60. Kim, S.H.; Kaminker, P.; Campisi, J. TIN2, a new regulator of telomere length in human cells. *Nat. Genet.* **1999**, *23*, 405–412. [CrossRef]
61. Ye, J.Z.S.; de Lange, T. TIN2 is a tankyrase 1 PARP modulator in the TRF1 telomere length control complex. *Nat. Genet.* **2004**, *36*, 618–623. [CrossRef]
62. Zhou, X.Z.; Lu, K.P. The Pin2/TRF1-interacting: Protein PinX1 is a potent telomerase inhibitor. *Cell* **2001**, *107*, 347–359. [CrossRef]
63. Wu, Y.; Xiao, S.; Zhu, X.D. MRE11-RAD50-NBS1 and ATM function as co-mediators of TRF1 in telomere length control. *Nat. Struct. Mol. Biol.* **2007**, *14*, 832–840. [CrossRef]
64. Schrumpfova, P.; Kuchar, M.; Mikova, G.; Skrisovska, L.; Kubicarova, T.; Fajkus, J. Characterization of two *Arabidopsis thaliana* myb-like proteins showing affinity to telomeric DNA sequence. *Genome* **2004**, *47*, 316–324. [CrossRef]
65. Schrumpfova, P.P.; Kuchar, M.; Palecek, J.; Fajkus, J. Mapping of interaction domains of putative telomere-binding proteins AtTRB1 and AtPOT1b from *Arabidopsis thaliana*. *Febs Lett.* **2008**, *582*, 1400–1406. [CrossRef]
66. Schrumpfova, P.P.; Vychodilova, I.; Dvorackova, M.; Majerska, J.; Dokladal, L.; Schorova, S.; Fajkus, J. Telomere repeat binding proteins are functional components of Arabidopsis telomeres and interact with telomerase. *Plant J.* **2014**, *77*, 770–781. [CrossRef]
67. Schrumpfova, P.P.; Vychodilova, I.; Hapala, J.; Schorova, S.; Dvoracek, V.; Fajkus, J. Telomere binding protein TRB1 is associated with promoters of translation machinery genes in vivo. *Plant Mol. Biol.* **2016**, *90*, 189–206. [CrossRef]
68. Zhou, Y.; Wang, Y.J.; Krause, K.; Yang, T.T.; Dongus, J.A.; Zhang, Y.J.; Turck, F. Telobox motifs recruit CLF/SWN-PRC2 for H3K27me3 deposition via TRB factors in Arabidopsis. *Nat. Genet.* **2018**, *50*, 638. [CrossRef]
69. Dokladal, L.; Benkova, E.; Honys, D.; Dupl'akova, N.; Lee, L.Y.; Gelvin, S.B.; Sykorova, E. An armadillo-domain protein participates in a telomerase interaction network. *Plant Mol. Biol.* **2018**, *97*, 407–420. [CrossRef]
70. Lee, W.K.; Cho, M.H. Telomere-binding protein regulates the chromosome ends through the interaction with histone deacetylases in *Arabidopsis thaliana*. *Nucleic Acids Res.* **2016**, *44*, 4610–4624. [CrossRef]
71. Tan, L.M.; Zhang, C.J.; Hou, X.M.; Shao, C.R.; Lu, Y.J.; Zhou, J.X.; Li, Y.Q.; Li, L.; Chen, S.; He, X.J. The PEAT protein complexes are required for histone deacetylation and heterochromatin silencing. *Embo J.* **2018**, *37*, e98770. [CrossRef] [PubMed]
72. Van Steensel, B.; Smogorzewska, A.; de Lange, T. TRF2 protects human telomeres from end-to-end fusions. *Cell* **1998**, *92*, 401–413. [CrossRef]
73. Kabir, S.; Sfeir, A.; de Lange, T. Taking apart Rap1 An adaptor protein with telomeric and non-telomeric functions. *Cell Cycle* **2010**, *9*, 4061–4067. [CrossRef] [PubMed]
74. Rai, R.; Hu, C.; Broton, C.; Chen, Y.; Lei, M.; Chang, S. NBS1 Phosphorylation Status Dictates Repair Choice of Dysfunctional Telomeres. *Mol. Cell* **2017**, *65*, 801. [CrossRef]
75. O'Connor, M.S.; Safari, A.; Liu, D.; Qin, J.; Zhou, S.Y. The human Rap1 protein complex and modulation of telomere length. *J. Biol. Chem.* **2004**, *279*, 28585–28591. [CrossRef] [PubMed]
76. Chen, Y.; Yang, Y.T.; van Overbeek, M.; Donigian, J.R.; Baciu, P.; de Lange, T.; Lei, M. A shared docking motif in TRF1 and TRF2 used for differential recruitment of telomeric proteins. *Science* **2008**, *319*, 1092–1096. [CrossRef] [PubMed]
77. Song, K.; Jung, D.; Jung, Y.; Lee, S.G.; Lee, I. Interaction of human Ku70 with TRF2. *Febs Lett.* **2000**, *481*, 81–85. [CrossRef]
78. Gomez, M.; Wu, J.; Schreiber, V.; Dunlap, J.; Dantzer, F.; Wang, Y.S.; Liu, Y. PARP1 is a TRF2-associated poly(ADP-ribose)polymerase and protects eroded telomere. *Mol. Biol. Cell* **2006**, *17*, 1686–1696. [CrossRef]

79. Dantzer, F.; Giraud-Panis, M.J.; Jaco, I.; Ame, J.C.; Schultz, I.; Blasco, M.; Koering, C.E.; Gilson, E.; Menissier-de Murcia, J.; de Murcia, G.; et al. Functional interaction between poly(ADP-ribose) polymerase 2 (PARP-2) and TRF2: PARP activity negatively regulates TRF2. *Mol. Cell. Biol.* **2004**, *24*, 1595–1607. [CrossRef]
80. Wu, Y.L.; Mitchell, T.R.H.; Zhu, X.D. Human XPF controls TRF2 and telomere length maintenance through distinctive mechanisms. *Mech. Ageing Dev.* **2008**, *129*, 602–610. [CrossRef]
81. Chen, C.M.; Wang, C.T.; Ho, C.H. A plant gene encoding a Myb-like protein that binds telomeric GGTTTAG repeats in vitro. *J. Biol. Chem.* **2001**, *276*, 16511–16519. [CrossRef]
82. Kuchar, M.; Fajkus, J. Interactions of putative telomere-binding proteins in *Arabidopsis thaliana*: Identification of functional TRF2 homolog in plants. *Febs Lett.* **2004**, *578*, 311–315. [CrossRef] [PubMed]
83. Karamysheva, Z.N.; Surovtseva, Y.V.; Vespa, L.; Shakirov, E.V.; Shippen, D.E. A C-terminal Myb extension domain defines a novel family of double-strand telomeric DNA-binding proteins in Arabidopsis. *J. Biol. Chem.* **2004**, *279*, 47799–47807. [CrossRef] [PubMed]
84. Majerska, J.; Schrumpfova, P.P.; Dokladal, L.; Schorova, S.; Stejskal, K.; Oboril, M.; Honys, D.; Kozakova, L.; Polanska, P.S.; Sykorova, E. Tandem affinity purification of AtTERT reveals putative interaction partners of plant telomerase in vivo. *Protoplasma* **2017**, *254*, 1547–1562. [CrossRef]
85. Jeong, S.A.; Kim, K.; Lee, J.H.; Cha, J.S.; Khadka, P.; Cho, H.S.; Chung, K. Akt-mediated phosphorylation increases the binding affinity of hTERT for importin alpha to promote nuclear translocation. *J. Cell Sci.* **2015**, *128*, 2287–2301. [CrossRef] [PubMed]
86. Khurts, S.; Masutomi, K.; Delgermaa, L.; Arai, K.; Oishi, N.; Mizuno, H.; Hayashi, N.; Hahn, W.C.; Murakami, S. Nucleolin interacts with telomerase. *J. Biol. Chem.* **2004**, *279*, 51508–51515. [CrossRef] [PubMed]
87. Pontvianne, F.; Abou-Ellail, M.; Douet, J.; Comella, P.; Matia, I.; Chandrasekhara, C.; DeBures, A.; Blevins, T.; Cooke, R.; Medina, F.J.; et al. Nucleolin Is Required for DNA Methylation State and the Expression of rRNA Gene Variants in *Arabidopsis thaliana*. *PLoS Genet.* **2010**, *6*, e1001225. [CrossRef]
88. Pontvianne, F.; Carpentier, M.C.; Durut, N.; Pavlistova, V.; Jaske, K.; Schorova, S.; Parrinello, H.; Rohmer, M.; Pikaard, C.S.; Fojtova, M.; et al. Identification of Nucleolus-Associated Chromatin Domains Reveals a Role for the Nucleolus in 3D Organization of the A. thaliana Genome. *Cell Rep.* **2016**, *16*, 1574–1587. [CrossRef]
89. Venteicher, A.S.; Meng, Z.J.; Mason, P.J.; Veenstra, T.D.; Artandi, S.E. Identification of ATPases pontin and reptin as telomerase components essential for holoenzyme assembly. *Cell* **2008**, *132*, 945–957. [CrossRef]
90. Holt, B.F.; Boyes, D.C.; Ellerstrom, M.; Siefers, N.; Wiig, A.; Kauffman, S.; Grant, M.R.; Dangl, J.L. An evolutionarily conserved mediator of plant disease resistance gene function is required for normal Arabidopsis development. *Dev. Cell* **2002**, *2*, 807–817. [CrossRef]
91. Giannone, R.J.; McDonald, H.W.; Hurst, G.B.; Shen, R.F.; Wang, Y.S.; Liu, Y. The Protein Network Surrounding the Human Telomere Repeat Binding Factors TRF1, TRF2, and POT1. *PLoS ONE* **2010**, *5*, e12407. [CrossRef] [PubMed]
92. Lee, L.Y.; Wu, F.H.; Hsu, C.T.; Shen, S.C.; Yeh, H.Y.; Liao, D.C.; Fang, M.J.; Liu, N.T.; Yen, Y.C.; Dokladal, L.; et al. Screening a cDNA Library for Protein-Protein Interactions Directly in Planta. *Plant Cell* **2012**, *24*, 1746–1759. [CrossRef] [PubMed]
93. Kappei, D.; Butter, F.; Benda, C.; Scheibe, M.; Draskovic, I.; Stevense, M.; Novo, C.L.; Basquin, C.; Araki, M.; Araki, K.; et al. HOT1 is a mammalian direct telomere repeat-binding protein contributing to telomerase recruitment. *Embo J.* **2013**, *32*, 1681–1701. [CrossRef] [PubMed]
94. Chai, W.H.; Ford, L.P.; Lenertz, L.; Wright, W.E.; Shay, J.W. Human Ku70/80 associates physically with telomerase through interaction with hTERT. *J. Biol. Chem.* **2002**, *277*, 47242–47247. [CrossRef]
95. Fell, V.L.; Schild-Poulter, C. The Ku heterodimer: Function in DNA repair and beyond. *Mutat. Res. Rev. Mutat. Res.* **2015**, *763*, 15–29. [CrossRef] [PubMed]
96. Bundock, P.; van Attikum, H.; Hooykaas, P. Increased telomere length and hypersensitivity to DNA damaging agents in an Arabidopsis KU70 mutant. *Nucleic Acids Res.* **2002**, *30*, 3395–3400. [CrossRef] [PubMed]
97. Riha, K.; Watson, J.M.; Parkey, J.; Shippen, D.E. Telomere length deregulation and enhanced sensitivity to genotoxic stress in Arabidopsis mutants deficient in Ku70. *Embo J.* **2002**, *21*, 2819–2826. [CrossRef]
98. West, C.E.; Waterworth, W.M.; Story, G.W.; Sunderland, P.A.; Jiang, Q.; Bray, C.M. Disruption of the Arabidopsis AtKu80 gene demonstrates an essential role for AtKu80 protein in efficient repair of DNA double-strand breaks in vivo. *Plant J.* **2002**, *31*, 517–528. [CrossRef]

99. Gallego, M.E.; Jalut, N.; White, C.I. Telomerase dependence of telomere lengthening in Ku80 mutant Arabidopsis. *Plant Cell* **2003**, *15*, 782–789. [CrossRef]
100. Cifuentes-Rojas, C.; Nelson, A.D.L.; Boltz, K.A.; Kannan, K.; She, X.T.; Shippen, D.E. An alternative telomerase RNA in Arabidopsis modulates enzyme activity in response to DNA damage. *Genes Dev.* **2012**, *26*, 2512–2523. [CrossRef]
101. Valuchova, S.; Fulnecek, J.; Prokop, Z.; Stolt-Bergner, P.; Janouskova, E.; Hofr, C.; Riha, K. Protection of Arabidopsis blunt-ended telomeres is mediated by a physical association with the Ku heterodimer. *Plant Cell* **2017**. [CrossRef] [PubMed]
102. Holt, S.E.; Aisner, D.L.; Baur, J.; Tesmer, V.M.; Dy, M.; Ouellette, M.; Trager, J.B.; Morin, G.B.; Toft, D.O.; Shay, J.W.; et al. Functional requirement of p23 and Hsp90 in telomerase complexes. *Genes Dev.* **1999**, *13*, 817–826. [CrossRef]
103. Chen, B.; Zhong, D.B.; Monteiro, A. Comparative genomics and evolution of the HSP90 family of genes across all kingdoms of organisms. *BMC Genom.* **2006**, *7*, 156.
104. Zhang, Z.M.; Sullivan, W.; Felts, S.J.; Prasad, B.D.; Toft, D.O.; Krishna, P. Characterization of plant p23-like proteins for their co-chaperone activities. *Cell Stress Chaperones* **2010**, *15*, 703–715. [CrossRef] [PubMed]
105. Wortman, M.J.; Johnson, E.M.; Bergemann, A.D. Mechanism of DNA binding and localized strand separation by Pur alpha and comparison with Pur family member, Pur beta. *Biochim. Biophys. Acta-Mol. Cell Res.* **2005**, *1743*, 64–78. [CrossRef] [PubMed]
106. Mermoud, J.E.; Rowbotham, S.P.; Varga-Weisz, P.D. Keeping chromatin quiet How nucleosome remodeling restores heterochromatin after replication. *Cell Cycle* **2011**, *10*, 4017–4025. [CrossRef]
107. Dona, M.; Scheid, O.M. DNA Damage Repair in the Context of Plant Chromatin. *Plant Physiol.* **2015**, *168*, 1206–1218. [CrossRef] [PubMed]
108. Nguyen, D.; St-Sauveur, V.G.; Bergeron, D.; Dupuis-Sandoval, F.; Scott, M.S.; Bachand, F. A Polyadenylation-Dependent 3′ End Maturation Pathway Is Required for the Synthesis of the Human Telomerase RNA. *Cell Rep.* **2015**, *13*, 2244–2257. [CrossRef] [PubMed]
109. Dokladal, L.; Honys, D.; Rana, R.; Lee, L.Y.; Gelvin, S.B.; Sykorova, E. cDNA Library Screening Identifies Protein Interactors Potentially Involved in Non-Telomeric Roles of Arabidopsis Telomerase. *Front. Plant Sci.* **2015**, *6*, 985. [CrossRef]
110. Ma, H.L.; Su, L.; Yue, H.W.; Yin, X.L.; Zhao, J.; Zhang, S.L.; Kung, H.F.; Xu, Z.G.; Miao, J.Y. HMBOX1 interacts with MT2A to regulate autophagy and apoptosis in vascular endothelial cells. *Sci. Rep.* **2015**, *5*, 15121. [CrossRef] [PubMed]
111. Feng, X.Y.; Luo, Z.H.; Jiang, S.; Li, F.; Han, X.; Hu, Y.; Wang, D.; Zhao, Y.; Ma, W.B.; Liu, D.; et al. The telomere-associated homeobox-containing protein TAH1/HMBOX1 participates in telomere maintenance in ALT cells. *J. Cell Sci.* **2013**, *126*, 3982–3989. [CrossRef] [PubMed]
112. Lamartine, J.; Seri, M.; Cinti, R.; Heitzmann, F.; Creaven, M.; Radomski, N.; Jost, E.; Lenoir, G.M.; Romeo, G.; Sylla, B.S. Molecular cloning and mapping of a human cDNA (PA2G4) that encodes a protein highly homologous to the mouse cell cycle protein p38-2G4. *Cytogenet. Cell Genet.* **1997**, *78*, 31–35. [CrossRef] [PubMed]
113. Feng, J.L.; Funk, W.D.; Wang, S.S.; Weinrich, S.L.; Avilion, A.A.; Chiu, C.P.; Adams, R.R.; Chang, E.; Allsopp, R.C.; Yu, J.H.; et al. The Rna Component of Human Telomerase. *Science* **1995**, *269*, 1236–1241. [CrossRef] [PubMed]
114. Cohen, S.B.; Graham, M.E.; Lovrecz, G.O.; Bache, N.; Robinson, P.J.; Reddel, R.R. Protein composition of catalytically active human telomerase from immortal cells. *Science* **2007**, *315*, 1850–1853. [CrossRef]
115. Heiss, N.S.; Knight, S.W.; Vulliamy, T.J.; Klauck, S.M.; Wiemann, S.; Mason, P.J.; Poustka, A.; Dokal, I. X-linked dyskeratosis congenita is caused by mutations in a highly conserved gene with putative nucleolar functions. *Nat. Genet.* **1998**, *19*, 32–38. [CrossRef]
116. Henras, A.; Henry, Y.; Bousquet-Antonelli, C.; Noaillac-Depeyre, J.; Gelugne, J.P.; Caizergues-Ferrer, M. Nhp2p and Nop10p are essential for the function of H/ACA snoRNPs. *Embo J.* **1998**, *17*, 7078–7090. [CrossRef]
117. Saito, H.; Fujiwara, T.; Shin, S.; Okui, K.; Nakamura, Y. Cloning and mapping of a human novel cDNA (NHP2L1) that encodes a protein highly homologous to yeast nuclear protein NHP2. *Cytogenet. Cell Genet.* **1996**, *72*, 191–193. [CrossRef] [PubMed]

118. Watkins, N.J.; Gottschalk, A.; Neubauer, G.; Kastner, B.; Fabrizio, P.; Mann, M.; Luhrmann, R. Cbf5p, a potential pseudouridine synthase, and Nhp2p, a putative RNA-binding protein, are present together with Gar1p in all H BOX/ACA-motif snoRNPs and constitute a common bipartite structure. *RNA* **1998**, *4*, 1549–1568. [CrossRef]
119. Fatica, A.; Dlakic, M.; Tollervey, D. Naf1p is a box H/ACA snoRNP assembly factor. *RNA* **2002**, *8*, 1502–1514.
120. Ting, N.S.Y.; Yu, Y.P.; Pohorelic, B.; Lees-Miller, S.P.; Beattie, T.L. Human Ku70/80 interacts directly with hTR, the RNA component of human telomerase. *Nucleic Acids Res.* **2005**, *33*, 2090–2098. [CrossRef]
121. Sexton, A.N.; Collins, K. The 5′ Guanosine Tracts of Human Telomerase RNA Are Recognized by the G-Quadruplex Binding Domain of the RNA Helicase DHX36 and Function To Increase RNA Accumulation. *Mol. Cell. Biol.* **2011**, *31*, 736–743. [CrossRef] [PubMed]
122. Moon, D.H.; Segal, M.; Boyraz, B.; Guinan, E.; Hofmann, I.; Cahan, P.; Tai, A.K.; Agarwal, S. Poly(A)-specific ribonuclease (PARN) mediates 3′-end maturation of the telomerase RNA component. *Nat. Genet.* **2015**, *47*, 1482. [CrossRef]
123. Chiba, Y.; Johnson, M.A.; Lidder, P.; Vogel, J.T.; van Erp, H.; Green, P.J. AtPARN is an essential poly(A) ribonuclease in *Arabidopsis*. *Gene* **2004**, *328*, 95–102. [CrossRef] [PubMed]
124. Venteicher, A.S.; Abreu, E.B.; Meng, Z.J.; McCann, K.E.; Terns, R.M.; Veenstra, T.D.; Terns, M.P.; Artandi, S.E. A Human Telomerase Holoenzyme Protein Required for Cajal Body Localization and Telomere Synthesis. *Science* **2009**, *323*, 644–648. [CrossRef] [PubMed]
125. Sykorova, E.; Fajkus, J. Structure-function relationships in telomerase genes. *Biol. Cell* **2009**, *101*, 375–392. [CrossRef]
126. Sykorova, E.; Fulneckova, J.; Mokros, P.; Fajkus, J.; Fojtova, M.; Peska, V. Three TERT genes in *Nicotiana tabacum*. *Chromosome Res.* **2012**, *20*, 381–394. [CrossRef] [PubMed]
127. Chakrabarti, K.; Pearson, M.; Grate, L.; Sterne-Weiler, T.; Deans, J.; Donohue, J.P.; Ares, M. Structural RNAs of known and unknown function identified in malaria parasites by comparative genomics and RNA analysis. *RNA* **2007**, *13*, 1923–1939. [CrossRef] [PubMed]
128. Webb, C.J.; Zakian, V.A. Identification and characterization of the Schizosaccharomyces pombe TER1 telomerase RNA. *Nat. Struct. Mol. Biol.* **2008**, *15*, 34–42. [CrossRef] [PubMed]
129. Leonardi, J.; Box, J.A.; Bunch, J.T.; Baumann, P. TER1, the RNA subunit of fission yeast telomerase. *Nat. Struct. Mol. Biol.* **2008**, *15*, 26–33. [CrossRef]
130. Xie, M.Y.; Mosig, A.; Qi, X.; Li, Y.; Stadler, P.F.; Chen, J.J.L. Structure and function of the smallest vertebrate telomerase RNA from teleost fish. *J. Biol. Chem.* **2008**, *283*, 2049–2059. [CrossRef]
131. Kachouri-Lafond, R.; Dujon, B.; Gilson, E.; Westhof, E.; Fairhead, C.; Teixeira, M.T. Large telomerase RNA, telomere length heterogeneity and escape from senescence in Candida glabrata. *Febs Lett.* **2009**, *583*, 3605–3610. [CrossRef]
132. Gunisova, S.; Elboher, E.; Nosek, J.; Gorkovoy, V.; Brown, Y.; Lucier, J.F.; Laterreur, N.; Wellinger, R.J.; Tzfati, Y.; Tomaska, L. Identification and comparative analysis of telomerase RNAs from Candida species reveal conservation of functional elements. *RNA-A Publ. RNA Soc.* **2009**, *15*, 546–559. [CrossRef]
133. Waldl, M.; Thiel, B.C.; Ochsenreiter, R.; Holzenleiter, A.; de Araujo Oliveira, J.V.; Walter, M.; Wolfinger, M.T.; Stadler, P.F. TERribly Difficult: Searching for Telomerase RNAs in Saccharomycetes. *Genes (Basel)* **2018**, *9*, 372. [CrossRef] [PubMed]
134. Sykorova, E.; Lim, K.Y.; Kunicka, Z.; Chase, M.W.; Bennett, M.D.; Fajkus, J.; Leitch, A.R. Telomere variability in the monocotyledonous plant order Asparagales. *Proc. R. Soc. B-Biol. Sci.* **2003**, *270*, 1893–1904. [CrossRef] [PubMed]
135. Sykorova, E.; Fajkus, J.; Meznikova, M.; Lim, K.Y.; Neplechova, K.; Blattner, F.R.; Chase, M.W.; Leitch, A.R. Minisatellite telomeres occur in the family Alliaceae but are lost in Allium. *Am. J. Bot.* **2006**, *93*, 814–823. [CrossRef] [PubMed]
136. De Lange, T. Shelterin: The protein complex that shapes and safeguards human telomeres. *Genes Dev.* **2005**, *19*, 2100–2110. [CrossRef]
137. De Lange, T. What I got wrong about shelterin. *J. Biol. Chem.* **2018**, *293*, 10453–10456. [CrossRef]
138. Palm, W.; de Lange, T. How Shelterin Protects Mammalian Telomeres. *Annu. Rev. Genet.* **2008**, *42*, 301–334. [CrossRef]
139. Sfeir, A.; de Lange, T. Removal of Shelterin Reveals the Telomere End-Protection Problem. *Science* **2012**, *336*, 593–597. [CrossRef]

140. Kibe, T.; Zimmermann, M.; de Lange, T. TPP1 Blocks an ATR-Mediated Resection Mechanism at Telomeres. *Mol. Cell* **2016**, *61*, 236–246. [CrossRef]
141. Zimmermann, M.; Lottersberger, F.; Buonomo, S.B.; Sfeir, A.; de Lange, T. 53BP1 Regulates DSB Repair Using Rif1 to Control 5 ' End Resection. *Science* **2013**, *339*, 700–704. [CrossRef] [PubMed]
142. Dalby, A.B.; Hofr, C.; Cech, T.R. Contributions of the TEL-patch Amino Acid Cluster on TPP1 to Telomeric DNA Synthesis by Human Telomerase. *J. Mol. Biol.* **2015**, *427*, 1291–1303. [CrossRef] [PubMed]
143. Latrick, C.M.; Cech, T.R. POT1-TPP1 enhances telomerase processivity by slowing primer dissociation and aiding translocation. *Embo J.* **2010**, *29*, 924–933. [CrossRef] [PubMed]
144. Nandakumar, J.; Bell, C.F.; Weidenfeld, I.; Zaug, A.J.; Leinwand, L.A.; Cech, T.R. The TEL patch of telomere protein TPP1 mediates telomerase recruitment and processivity. *Nature* **2012**, *492*, 285. [CrossRef] [PubMed]
145. Schmidt, J.C.; Cech, T.R. Human telomerase: Biogenesis, trafficking, recruitment, and activation. *Genes Dev.* **2015**, *29*, 1095–1105. [CrossRef] [PubMed]
146. Griffith, J.D.; Comeau, L.; Rosenfield, S.; Stansel, R.M.; Bianchi, A.; Moss, H.; de Lange, T. Mammalian telomeres end in a large duplex loop. *Cell* **1999**, *97*, 503–514. [CrossRef]
147. Stansel, R.M.; de Lange, T.; Griffith, J.D. T-loop assembly in vitro involves binding of TRF2 near the 3′ telomeric overhang. *Embo J.* **2001**, *20*, 5532–5540. [CrossRef]
148. Sfeir, A.; Kosiyatrakul, S.T.; Hockemeyer, D.; MacRae, S.L.; Karlseder, J.; Schildkraut, C.L.; de Lange, T. Mammalian Telomeres Resemble Fragile Sites and Require TRF1 for Efficient Replication. *Cell* **2009**, *138*, 90–103. [CrossRef]
149. Tong, A.S.; Stern, J.L.; Sfeir, A.; Kartawinata, M.; de Lange, T.; Zhu, X.D.; Bryan, T.M. ATM and ATR Signaling Regulate the Recruitment of Human Telomerase to Telomeres. *Cell Rep.* **2015**, *13*, 1633–1646. [CrossRef]
150. Cesare, A.J.; Quinney, N.; Willcox, S.; Subramanian, D.; Griffith, J.D. Telomere looping in P-sativum (common garden pea). *Plant J.* **2003**, *36*, 271–279. [CrossRef]
151. Mozgova, I.; Schrumpfova, P.P.; Hofr, C.; Fajkus, J. Functional characterization of domains in AtTRB1, a putative telomere-binding protein in *Arabidopsis thaliana*. *Phytochemistry* **2008**, *69*, 1814–1819. [CrossRef] [PubMed]
152. Marian, C.O.; Bordoli, S.J.; Goltz, M.; Santarella, R.A.; Jackson, L.P.; Danilevskaya, O.; Beckstette, M.; Meeley, R.; Bass, H.W. The maize Single myb histone 1 gene, Smh1, belongs to a novel gene family and encodes a protein that binds telomere DNA repeats in vitro. *Plant Physiol.* **2003**, *133*, 1336–1350. [CrossRef]
153. Bilaud, T.; Koering, C.E.; BinetBrasselet, E.; Ancelin, K.; Pollice, A.; Gasser, S.M.; Gilson, E. The telobox, a Myb-related telomeric DNA binding motif found in proteins from yeast, plants and human. *Nucleic Acids Res.* **1996**, *24*, 1294–1303. [CrossRef]
154. Peska, V.; Schrumpfova, P.P.; Fajkus, J. Using the Telobox to Search for Plant Telomere Binding Proteins. *Curr. Protein Pept. Sci.* **2011**, *12*, 75–83. [CrossRef] [PubMed]
155. Schrumpfova, P.P.; Schorova, S.; Fajkus, J. Telomere- and Telomerase-Associated Proteins and Their Functions in the Plant Cell. *Front. Plant Sci.* **2016**, *7*, 851.
156. Zhou, Y.; Hartwig, B.; James, G.V.; Schneeberger, K.; Turck, F. Complementary Activities of TELOMERE REPEAT BINDING Proteins and Polycomb Group Complexes in Transcriptional Regulation of Target Genes. *Plant Cell* **2016**, *28*, 87–101. [CrossRef]
157. El Mai, M.; Wagner, K.D.; Michiels, J.F.; Ambrosetti, D.; Borderie, A.; Destree, S.; Renault, V.; Djerbi, N.; Giraud-Panis, M.J.; Gilson, E.; et al. The Telomeric Protein TRF2 Regulates Angiogenesis by Binding and Activating the PDGFR beta Promoter. *Cell Rep.* **2014**, *9*, 1047–1060. [CrossRef]
158. Krutilina, R.I.; Oei, S.L.; Buchlow, G.; Yau, P.M.; Zalensky, A.O.; Zalenskaya, I.A.; Bradbury, E.M.; Tomilin, N.V. A negative regulator of telomere-length protein TRF1 is associated with interstitial (TTAGGG)n blocks in immortal Chinese hamster ovary cells. *Biochem. Biophys. Res. Commun.* **2001**, *280*, 471–475. [CrossRef]
159. Martinez, P.; Thanasoula, M.; Carlos, A.R.; Gomez-Lopez, G.; Tejera, A.M.; Schoeftner, S.; Dominguez, O.; Pisano, D.G.; Tarsounas, M.; Blasco, M.A. Mammalian Rap1 controls telomere function and gene expression through binding to telomeric and extratelomeric sites. *Nat. Cell Biol.* **2010**, *12*, 768. [CrossRef]
160. Morse, R.H. RAP, RAP, open up! New wrinkles for RAP1 in yeast. *Trends Genet.* **2000**, *16*, 51–53. [CrossRef]
161. Rizzo, A.; Iachettini, S.; Salvati, E.; Zizza, P.; Maresca, C.; D'Angelo, C.; Benarroch-Popivker, D.; Capolupo, A.; del Gaudio, F.; Cosconati, S.; et al. SIRT6 interacts with TRF2 and promotes its degradation in response to DNA damage. *Nucleic Acids Res.* **2017**, *45*, 1820–1834. [CrossRef]

162. Simonet, T.; Zaragosi, L.E.; Philippe, C.; Lebrigand, K.; Schouteden, C.; Augereau, A.; Bauwens, S.; Ye, J.; Santagostino, M.; Giulotto, E.; et al. The human TTAGGG repeat factors 1 and 2 bind to a subset of interstitial telomeric sequences and satellite repeats. *Cell Res.* **2011**, *21*, 1028–1038. [CrossRef]
163. Ye, J.; Renault, V.M.; Jamet, K.; Gilson, E. Transcriptional outcome of telomere signalling. *Nat. Rev. Genet.* **2014**, *15*, 491–503. [CrossRef] [PubMed]
164. Zhang, P.; Pazin, M.J.; Schwartz, C.M.; Becker, K.G.; Wersto, R.P.; Dilley, C.M.; Mattson, M.P. Nontelomeric TRF2-REST Interaction Modulates Neuronal Gene Silencing and Fate of Tumor and Stem Cells. *Curr. Biol.* **2008**, *18*, 1489–1494. [CrossRef] [PubMed]
165. Fulcher, N.; Riha, K. Using Centromere Mediated Genome Elimination to Elucidate the Functional Redundancy of Candidate Telomere Binding Proteins in *Arabidopsis thaliana*. *Front. Genet.* **2016**, *6*, 349. [CrossRef]
166. Perrault, S.D.; Hornsby, P.J.; Betts, D.H. Global gene expression response to telomerase in bovine adrenocortical cells. *Biochem. Biophys. Res. Commun.* **2005**, *335*, 925–936. [CrossRef]
167. Majerska, J.; Sykorova, E.; Fajkus, J. Non-telomeric activities of telomerase. *Mol. Biosyst.* **2011**, *7*, 1013–1023. [CrossRef] [PubMed]
168. Park, J.I.; Venteicher, A.S.; Hong, J.Y.; Choi, J.; Jun, S.; Shkreli, M.; Chang, W.; Meng, Z.J.; Cheung, P.; Ji, H.; et al. Telomerase modulates Wnt signalling by association with target gene chromatin. *Nature* **2009**, *460*, 66–U77. [CrossRef]
169. Freeling, M. Bias in Plant Gene Content Following Different Sorts of Duplication: Tandem, Whole-Genome, Segmental, or by Transposition. *Annu. Rev. Plant Biol.* **2009**, *60*, 433–453. [CrossRef]
170. Mandakova, T.; Lysak, M.A. Chromosomal Phylogeny and Karyotype Evolution in x=7 Crucifer Species (Brassicaceae). *Plant Cell* **2008**, *20*, 2559–2570. [CrossRef]
171. Price, C.M.; Boltz, K.A.; Chaiken, M.F.; Stewart, J.A.; Beilstein, M.A.; Shippen, D.E. Evolution of CST function in telomere maintenance. *Cell Cycle* **2010**, *9*, 3157–3165. [CrossRef] [PubMed]
172. Feng, X.Y.; Hsu, S.J.; Bhattacharjee, A.; Wang, Y.Y.; Diao, J.J.; Price, C.M. CTC1-STN1 terminates telomerase while STN1-TEN1 enables C-strand synthesis during telomere replication in colon cancer cells. *Nat. Commun.* **2018**, *9*, 2827. [CrossRef] [PubMed]
173. Feng, X.Y.; Hsu, S.J.; Kasbek, C.; Chaiken, M.; Price, C.M. CTC1-mediated C-strand fill-in is an essential step in telomere length maintenance. *Nucleic Acids Res.* **2017**, *45*, 4281–4293. [CrossRef] [PubMed]
174. Stewart, J.A.; Wang, F.; Chaiken, M.F.; Kasbek, C.; Chastain, P.D.; Wright, W.E.; Price, C.M. Human CST promotes telomere duplex replication and general replication restart after fork stalling. *Embo J.* **2012**, *31*, 3537–3549. [CrossRef] [PubMed]
175. Bedoyan, J.K.; Lejnine, S.; Makarov, V.L.; Langmore, J.P. Condensation of rat telomere-specific nucleosomal arrays containing unusually short DNA repeats and histone H1. *J. Biol. Chem.* **1996**, *271*, 18485–18493. [CrossRef] [PubMed]
176. Lejnine, S.; Makarov, V.L.; Langmore, J.P. Conserved Nucleoprotein Structure at the Ends of Vertebrate and Invertebrate Chromosomes. *Proc. Natl. Acad. Sci. USA* **1995**, *92*, 2393–2397. [CrossRef] [PubMed]
177. Makarov, V.L.; Lejnine, S.; Bedoyan, J.; Langmore, J.P. Nucleosomal Organization of Telomere-Specific Chromatin in Rat. *Cell* **1993**, *73*, 775–787. [CrossRef]
178. Tommerup, H.; Dousmanis, A.; Delange, T. Unusual Chromatin in Human Telomeres. *Mol. Cell. Biol.* **1994**, *14*, 5777–5785. [CrossRef] [PubMed]
179. Fajkus, J.; Kovarik, A.; Kralovics, R.; Bezdek, M. Organization of Telomeric and Subtelomeric Chromatin in the Higher-Plant *Nicotiana tabacum*. *Mol. Gen. Genet.* **1995**, *247*, 633–638. [CrossRef]
180. Dejardin, J.; Kingston, R.E. Purification of Proteins Associated with Specific Genomic Loci. *Cell* **2009**, *136*, 175–186. [CrossRef] [PubMed]
181. Fajkus, J.; Trifonov, E.N. Columnar packing of telomeric nucleosomes. *Biochem. Biophys. Res. Commun.* **2001**, *280*, 961–963. [CrossRef]
182. Bosco, N.; de Lange, T. A TRF1-controlled common fragile site containing interstitial telomeric sequences. *Chromosoma* **2012**, *121*, 465–474. [CrossRef] [PubMed]
183. Sun, H.; Karow, J.K.; Hickson, I.D.; Maizels, N. The Bloom's syndrome helicase unwinds G4 DNA. *J. Biol. Chem.* **1998**, *273*, 27587–27592. [CrossRef] [PubMed]

184. Muftuoglu, M.; Wong, H.K.; Imam, S.Z.; Wilson, D.M.; Bohr, V.A.; Opresko, P.L. Telomere repeat binding factor 2 interacts with base excision repair proteins and stimulates DNA synthesis by DNA polymerase beta. *Cancer Res.* **2006**, *66*, 113–124. [CrossRef] [PubMed]
185. Tatsumi, Y.; Ezura, K.; Yoshida, K.; Yugawa, T.; Narisawa-Saito, M.; Kiyono, T.; Ohta, S.; Obuse, C.; Fujita, M. Involvement of human ORC and TRF2 in pre-replication complex assembly at telomeres. *Genes Cells* **2008**, *13*, 1045–1059. [CrossRef] [PubMed]
186. Sarek, G.; Vannier, J.B.; Panier, S.; Petrini, J.H.J.; Boulton, S.J. TRF2 Recruits RTEL1 to Telomeres in S Phase to Promote T-Loop Unwinding. *Mol. Cell* **2015**, *57*, 622–635. [CrossRef]
187. Karlseder, J.; Hoke, K.; Mirzoeva, O.K.; Bakkenist, C.; Kastan, M.B.; Petrini, J.H.J.; de Lange, T. The telomeric protein TRF2 binds the ATM kinase and can inhibit the ATM-dependent DNA damage response. *PLoS Biol.* **2004**, *2*, 1150–1156. [CrossRef]
188. Hwang, M.G.; Chung, I.K.; Kang, B.G.; Cho, M.H. Sequence-specific binding property of *Arabidopsis thaliana* telomeric DNA binding protein 1 (AtTBP1). *Febs Lett.* **2001**, *503*, 35–40. [CrossRef]
189. Renfrew, K.B.; Song, X.Y.; Lee, J.R.; Arora, A.; Shippen, D.E. POT1a and Components of CST Engage Telomerase and Regulate Its Activity in *Arabidopsis*. *PLoS Genet.* **2014**, *10*, e1004738. [CrossRef]
190. Wyatt, H.D.M.; Tsang, A.R.; Lobb, D.A.; Beattie, T.L. Human Telomerase Reverse Transcriptase (hTERT) Q169 Is Essential for Telomerase Function In Vitro and In Vivo. *PLoS ONE* **2009**, *4*, e7176. [CrossRef]
191. Ganduri, S.; Lue, N.F. STN1-POLA2 interaction provides a basis for primase-pol alpha stimulation by human STN1. *Nucleic Acids Res.* **2017**, *45*, 9455–9466. [CrossRef] [PubMed]
192. Miyake, Y.; Nakamura, M.; Nabetani, A.; Shimamura, S.; Tamura, M.; Yonehara, S.; Saito, M.; Ishikawa, F. RPA-like Mammalian Ctc1-Stn1-Ten1 Complex Binds to Single-Stranded DNA and Protects Telomeres Independently of the Pot1 Pathway. *Mol. Cell* **2009**, *36*, 193–206. [CrossRef]
193. Derboven, E.; Ekker, H.; Kusenda, B.; Bulankova, P.; Riha, K. Role of STN1 and DNA Polymerase alpha in Telomere Stability and Genome-Wide Replication in *Arabidopsis*. *PLoS Genet.* **2014**, *10*, e1004682. [CrossRef] [PubMed]
194. Leehy, K.A.; Lee, J.R.; Song, X.Y.; Renfrew, K.B.; Shippen, D.E. MERISTEM DISORGANIZATION1 Encodes TEN1, an Essential Telomere Protein That Modulates Telomerase Processivity in *Arabidopsis*. *Plant Cell* **2013**, *25*, 1343–1354. [CrossRef]
195. Song, X.Y.; Leehy, K.; Warrington, R.T.; Lamb, J.C.; Surovtseva, Y.V.; Shippen, D.E. STN1 protects chromosome ends in *Arabidopsis thaliana*. *Proc. Natl. Acad. Sci. USA* **2008**, *105*, 19815–19820. [CrossRef]
196. Surovtseva, Y.V.; Churikov, D.; Boltz, K.A.; Song, X.Y.; Lamb, J.C.; Warrington, R.; Leehy, K.; Heacock, M.; Price, C.M.; Shippen, D.E. Conserved Telomere Maintenance Component 1 Interacts with STN1 and Maintains Chromosome Ends in Higher Eukaryotes. *Mol. Cell* **2009**, *36*, 207–218. [CrossRef] [PubMed]
197. Yoo, H.H.; Kwon, C.; Lee, M.M.; Chung, I.K. Single-stranded DNA binding factor AtWHY1 modulates telomere length homeostasis in *Arabidopsis*. *Plant J.* **2007**, *49*, 442–451. [CrossRef]
198. Kwon, C.; Chung, I.K. Interaction of an *Arabidopsis* RNA-binding protein with plant single-stranded telomeric DNA modulates telomerase activity. *J. Biol. Chem.* **2004**, *279*, 12812–12818. [CrossRef]
199. Li, E.; Zhang, Y. DNA Methylation in Mammals. *Cold Spring Harb. Perspect. Biol.* **2014**, *6*, a019133. [CrossRef]
200. Lister, R.; Pelizzola, M.; Dowen, R.H.; Hawkins, R.D.; Hon, G.; Tonti-Filippini, J.; Nery, J.R.; Lee, L.; Ye, Z.; Ngo, Q.M.; et al. Human DNA methylomes at base resolution show widespread epigenomic differences. *Nature* **2009**, *462*, 315–322. [CrossRef]
201. Zhang, X. The epigenetic landscape of plants. *Science* **2008**, *320*, 489–492. [CrossRef]
202. Cokus, S.J.; Feng, S.H.; Zhang, X.Y.; Chen, Z.G.; Merriman, B.; Haudenschild, C.D.; Pradhan, S.; Nelson, S.F.; Pellegrini, M.; Jacobsen, S.E. Shotgun bisulphite sequencing of the *Arabidopsis* genome reveals DNA methylation patterning. *Nature* **2008**, *452*, 215–219. [CrossRef] [PubMed]
203. Ogrocka, A.; Polanska, P.; Majerova, E.; Janeba, Z.; Fajkus, J.; Fojtova, M. Compromised telomere maintenance in hypomethylated *Arabidopsis thaliana* plants. *Nucleic Acids Res.* **2014**, *42*, 2919–2931. [CrossRef] [PubMed]
204. Vrbsky, J.; Akimcheva, S.; Watson, J.M.; Turner, T.L.; Daxinger, L.; Vyskot, B.; Aufsatz, W.; Riha, K. siRNA-Mediated Methylation of *Arabidopsis* Telomeres. *PLoS Genet.* **2010**, *6*, e1000986. [CrossRef] [PubMed]
205. Majerova, E.; Fojtova, M.; Mozgova, I.; Bittova, M.; Fajkus, J. Hypomethylating drugs efficiently decrease cytosine methylation in telomeric DNA and activate telomerase without affecting telomere lengths in tobacco cells. *Plant Mol. Biol.* **2011**, *77*, 371–380. [CrossRef] [PubMed]

206. Majerova, E.; Mandakova, T.; Vu, G.T.H.; Fajkus, J.; Lysak, M.A.; Fojtova, M. Chromatin features of plant telomeric sequences at terminal vs. internal positions. *Front. Plant Sci.* **2014**, *5*, 593. [CrossRef]
207. Xie, X.Y.; Shippen, D.E. DDM1 guards against telomere truncation in *Arabidopsis*. *Plant Cell Rep.* **2018**, *37*, 501–513. [CrossRef]
208. Fojtova, M.; Fajkus, J. Epigenetic Regulation of Telomere Maintenance. *Cytogenet. Genome Res.* **2014**, *143*, 125–135. [CrossRef]
209. Fransz, P.; ten Hoopen, R.; Tessadori, F. Composition and formation of heterochromatin in *Arabidopsis thaliana*. *Chromosome Res.* **2006**, *14*, 71–82. [CrossRef]
210. Roudier, F.; Ahmed, I.; Berard, C.; Sarazin, A.; Mary-Huard, T.; Cortijo, S.; Bouyer, D.; Caillieux, E.; Duvernois-Berthet, E.; Al-Shikhley, L.; et al. Integrative epigenomic mapping defines four main chromatin states in *Arabidopsis*. *Embo J.* **2011**, *30*, 1928–1938. [CrossRef] [PubMed]
211. Schoeftner, S.; Blasco, M.A. A 'higher order' of telomere regulation: Telomere heterochromatin and telomeric RNAs. *Embo J.* **2009**, *28*, 2323–2336. [CrossRef] [PubMed]
212. Cubiles, M.D.; Barroso, S.; Vaquero-Sedas, M.I.; Enguix, A.; Aguilera, A.; Vega-Palas, M.A. Epigenetic features of human telomeres. *Nucleic Acids Res.* **2018**, *46*, 2347–2355. [CrossRef] [PubMed]
213. Rosenfeld, J.A.; Wang, Z.B.; Schones, D.E.; Zhao, K.; DeSalle, R.; Zhang, M.Q. Determination of enriched histone modifications in non-genic portions of the human genome. *BMC Genom.* **2009**, *10*, 143. [CrossRef] [PubMed]
214. O'Sullivan, R.J.; Kubicek, S.; Schreiber, S.L.; Karlseder, J. Reduced histone biosynthesis and chromatin changes arising from a damage signal at telomeres. *Nat. Struct. Mol. Biol.* **2010**, *17*, 1218. [CrossRef] [PubMed]
215. Arnoult, N.; Van Beneden, A.; Decottignies, A. Telomere length regulates TERRA levels through increased trimethylation of telomeric H3K9 and HP1 alpha. *Nat. Struct. Mol. Biol.* **2012**, *19*, 948–956. [CrossRef] [PubMed]
216. Garcia-Cao, M.; O'Sullivan, R.; Peters, A.H.F.M.; Jenuwein, T.; Blasco, M.A. Epigenetic regulation of telomere length in mammalian cells by the Suv39h1 and Suv39h2 histone methyltransferases. *Nat. Genet.* **2004**, *36*, 94–99. [CrossRef]
217. Saksouk, N.; Barth, T.K.; Ziegler-Birling, C.; Olova, N.; Nowak, A.; Rey, E.; Mateos-Langerak, J.; Urbach, S.; Reik, W.; Torres-Padilla, M.E.; et al. Redundant Mechanisms to Form Silent Chromatin at Pericentromeric Regions Rely on BEND3 and DNA Methylation. *Mol. Cell* **2014**, *56*, 580–594. [CrossRef]
218. Benetti, R.; Gonzalo, S.; Jaco, I.; SChotta, G.; Klatt, P.; Jenuwein, T.; Blasco, M.A. Suv4-20h deficiency results in telomere elongation and derepression of telomere recombination. *J. Cell Biol.* **2007**, *178*, 925–936. [CrossRef]
219. Gonzalo, S.; Jaco, I.; Fraga, M.F.; Chen, T.P.; Li, E.; Esteller, M.; Blasco, M.A. DNA methyltransferases control telomere length and telomere recombination in mammalian cells. *Nat. Cell Biol.* **2006**, *8*, 416. [CrossRef]
220. Montero, J.J.; Lopez-Silanes, I.; Megias, D.; Fraga, M.F.; Castells-Garcia, A.; Blasco, M.A. TERRA recruitment of polycomb to telomeres is essential for histone trymethylation marks at telomeric heterochromatin. *Nat. Commun.* **2018**, *9*, 1548. [CrossRef]
221. Sovakova, P.P.; Magdolenova, A.; Konecna, K.; Rajecka, V.; Fajkus, J.; Fojtova, M. Telomere elongation upon transfer to callus culture reflects the reprogramming of telomere stability control in *Arabidopsis*. *Plant Mol. Biol.* **2018**, *98*, 81–99. [CrossRef]
222. Vaquero-Sedas, M.I.; Luo, C.Y.; Vega-Palas, M.A. Analysis of the epigenetic status of telomeres by using ChIP-seq data. *Nucleic Acids Res.* **2012**, *40*, e163. [CrossRef] [PubMed]
223. Bulut-Karslioglu, A.; Perrera, V.; Scaranaro, M.; de la Rosa-Velazquez, I.A.; van de Nobelen, S.; Shukeir, N.; Popow, J.; Gerle, B.; Opravil, S.; Pagani, M.; et al. A transcription factor-based mechanism for mouse heterochromatin formation. *Nat. Struct. Mol. Biol.* **2012**, *19*, 1023. [CrossRef] [PubMed]
224. Azzalin, C.M.; Reichenbach, P.; Khoriauli, L.; Giulotto, E.; Lingner, J. Telomeric repeat-containing RNA and RNA surveillance factors at mammalian chromosome ends. *Science* **2007**, *318*, 798–801. [CrossRef]
225. Vaquero-Sedas, M.I.; Gamez-Arjona, F.M.; Vega-Palas, M.A. *Arabidopsis thaliana* telomeres exhibit euchromatic features. *Nucleic Acids Res.* **2011**, *39*, 2007–2017. [CrossRef] [PubMed]
226. Tardat, M.; Dejardin, J. Telomere chromatin establishment and its maintenance during mammalian development. *Chromosoma* **2018**, *127*, 3–18. [CrossRef]
227. Chai, W.H.; Du, Q.; Shay, J.W.; Wright, W.E. Human telomeres have different overhang sizes at leading versus lagging strands. *Mol. Cell* **2006**, *21*, 427–435. [CrossRef]

228. Cimino-Reale, G.; Pascale, E.; Battiloro, E.; Starace, G.; Verna, R.; D'Ambrosio, E. The length of telomeric G-rich strand 3 '-overhang measured by oligonucleotide ligation assay. *Nucleic Acids Res.* **2001**, *29*, e35. [CrossRef]
229. Makarov, V.L.; Hirose, Y.; Langmore, J.P. Long G tails at both ends of human chromosomes suggest a C strand degradation mechanism for telomere shortening. *Cell* **1997**, *88*, 657–666. [CrossRef]
230. Wright, W.E.; Tesmer, V.M.; Huffman, K.E.; Levene, S.D.; Shay, J.W. Normal human chromosomes have long G-rich telomeric overhangs at one end. *Genes Dev.* **1997**, *11*, 2801–2809. [CrossRef]
231. Oganesian, L.; Karlseder, J. Mammalian 5′ C-Rich Telomeric Overhangs Are a Mark of Recombination-Dependent Telomere Maintenance. *Mol. Cell* **2011**, *42*, 224–236. [CrossRef]
232. Riha, K.; McKnight, T.D.; Fajkus, J.; Vyskot, B.; Shippen, D.E. Analysis of the G-overhang structures on plant telomeres: Evidence for two distinct telomere architectures. *Plant J.* **2000**, *23*, 633–641. [CrossRef]
233. Kazda, A.; Zellinger, B.; Rossler, M.; Derboven, E.; Kusenda, B.; Riha, K. Chromosome end protection by blunt-ended telomeres. *Genes Dev.* **2012**, *26*, 1703–1713. [CrossRef] [PubMed]
234. Fojtova, M.; Sykorova, E.; Najdekrova, L.; Polanska, P.; Zachova, D.; Vagnerova, R.; Angelis, K.J.; Fajkus, J. Telomere dynamics in the lower plant Physcomitrella patens. *Plant Mol. Biol.* **2015**, *87*, 591–601. [CrossRef]
235. Riha, K.; Shippen, D.E. Ku is required for telomeric C-rich strand maintenance but not for end-to-end chromosome fusions in *Arabidopsis*. *Proc. Natl. Acad. Sci. USA* **2003**, *100*, 611–615. [CrossRef]
236. Bryan, T.M.; Englezou, A.; DallaPozza, L.; Dunham, M.A.; Reddel, R.R. Evidence for an alternative mechanism for maintaining telomere length in human tumors and tumor-derived cell lines. *Nat. Med.* **1997**, *3*, 1271–1274. [CrossRef]
237. Neumann, A.A.; Watson, C.M.; Noble, J.R.; Pickett, H.A.; Tam, P.P.L.; Reddel, R.R. Alternative lengthening of telomeres in normal mammalian somatic cells. *Genes Dev.* **2013**, *27*, 18–23. [CrossRef] [PubMed]
238. Ruckova, E.; Friml, J.; Schrumpfova, P.P.; Fajkus, J. Role of alternative telomere lengthening unmasked in telomerase knock-out mutant plants. *Plant Mol. Biol.* **2008**, *66*, 637–646. [CrossRef]
239. Zellinger, B.; Akimcheva, S.; Puizina, J.; Schirato, M.; Riha, K. Ku suppresses formation of telomeric circles and alternative telomere lengthening in *Arabidopsis*. *Mol. Cell* **2007**, *27*, 163–169. [CrossRef] [PubMed]
240. Karpenshif, Y.; Bernstein, K.A. From yeast to mammals: Recent advances in genetic control of homologous recombination. *DNA Repair* **2012**, *11*, 781–788. [CrossRef]
241. Barber, L.J.; Youds, J.L.; Ward, J.D.; McIlwraith, M.J.; O'Neil, N.J.; Petalcorin, M.I.R.; Martin, J.S.; Collis, S.J.; Cantor, S.B.; Auclair, M.; et al. RTEL1 Maintains Genomic Stability by Suppressing Homologous Recombination. *Cell* **2008**, *135*, 261–271. [CrossRef]
242. Uringa, E.J.; Lisaingo, K.; Pickett, H.A.; Brind'Amour, J.; Rohde, J.H.; Zelensky, A.; Essers, J.; Lansdorp, P.M. RTEL1 contributes to DNA replication and repair and telomere maintenance. *Mol. Biol. Cell* **2012**, *23*, 2782–2792. [CrossRef] [PubMed]
243. Vannier, J.B.; Pavicic-Kaltenbrunner, V.; Petalcorin, M.I.R.; Ding, H.; Boulton, S.J. RTEL1 Dismantles T Loops and Counteracts Telomeric G4-DNA to Maintain Telomere Integrity. *Cell* **2012**, *149*, 795–806. [CrossRef] [PubMed]
244. Le Guen, T.; Jullien, L.; Schertzer, M.; Lefebvre, A.; Kermasson, L.; de Villartay, J.P.; Londono-Vallejo, A.; Revy, P. RTEL1 (regulator of telomere elongation helicase 1), a DNA helicase essential for genome stability. *Med. Sci.* **2013**, *29*, 1138–1144.
245. Vannier, J.B.; Sarek, G.; Boulton, S.J. RTEL1: Functions of a disease-associated helicase. *Trends Cell Biol.* **2014**, *24*, 416–425. [CrossRef] [PubMed]
246. Faure, G.; Revy, P.; Schertzer, M.; Londono-Vallejo, A.; Callebaut, I. The C-terminal extension of human RTEL1, mutated in Hoyeraal-Hreidarsson syndrome, contains Harmonin-N-like domains. *Proteins-Struct. Funct. Bioinform.* **2014**, *82*, 897–903. [CrossRef] [PubMed]
247. Margalef, P.; Kotsantis, P.; Borel, V.; Bellelli, R.; Panier, S.; Boulton, S.J. Stabilization of Reversed Replication Forks by Telomerase Drives Telomere Catastrophe. *Cell* **2018**, *172*, 439. [CrossRef]
248. Hu, Z.B.; Cools, T.; Kalhorzadeh, P.; Heyman, J.; De Veylder, L. Deficiency of the *Arabidopsis* Helicase RTEL1 Triggers a SOG1-Dependent Replication Checkpoint in Response to DNA Cross-Links. *Plant Cell* **2015**, *27*, 149–161. [CrossRef]
249. Recker, J.; Knoll, A.; Puchta, H. The *Arabidopsis thaliana* Homolog of the Helicase RTEL1 Plays Multiple Roles in Preserving Genome Stability. *Plant Cell* **2014**, *26*, 4889–4902. [CrossRef]

250. Riha, K.; McKnight, T.D.; Griffing, L.R.; Shippen, D.E. Living with genome instability: Plant responses to telomere dysfunction. *Science* **2001**, *291*, 1797–1800. [CrossRef]
251. Olivier, M.; Charbonnel, C.; Amiard, S.; White, C.I.; Gallego, M.E. RAD51 and RTEL1 compensate telomere loss in the absence of telomerase. *Nucleic Acids Res.* **2018**, *46*, 2432–2445. [CrossRef] [PubMed]
252. Kamisugi, Y.; Whitaker, J.W.; Cuming, A.C. The Transcriptional Response to DNA-Double-Strand Breaks in Physcomitrella patens. *PLoS ONE* **2016**, *11*, e0161204. [CrossRef] [PubMed]
253. Olsson, M.; Wapstra, E.; Friesen, C. Ectothermic telomeres: it's time they came in from the cold. *Philos. Trans. R. Soc. B-Biol. Sci.* **2018**, *373*, 20160449. [CrossRef] [PubMed]
254. Hoelzl, F.; Smith, S.; Cornils, J.S.; Aydinonat, D.; Bieber, C.; Ruf, T. Telomeres are elongated in older individuals in a hibernating rodent, the edible dormouse (Glis glis). *Sci. Rep.* **2016**, *6*, 36856. [CrossRef]
255. Gomes, N.M.V.; Ryder, O.A.; Houck, M.L.; Charter, S.J.; Walker, W.; Forsyth, N.R.; Austad, S.N.; Venditti, C.; Pagel, M.; Shay, J.W.; et al. Comparative biology of mammalian telomeres: Hypotheses on ancestral states and the roles of telomeres in longevity determination. *Aging Cell* **2011**, *10*, 761–768. [CrossRef] [PubMed]
256. Ahmed, W.; Lingner, J. Impact of oxidative stress on telomere biology. *Differentiation* **2018**, *99*, 21–27. [CrossRef] [PubMed]
257. Zhang, J.W.; Rane, G.; Dai, X.Y.; Shanmugam, M.K.; Arfuso, F.; Samy, R.P.; Lai, M.K.P.; Kappei, D.; Kumar, A.P.; Sethi, G. Ageing and the telomere connection: An intimate relationship with inflammation. *Ageing Res. Rev.* **2016**, *25*, 55–69. [CrossRef] [PubMed]
258. Bottcher, M.A.; Dingli, D.; Werner, B.; Traulsen, A. Replicative cellular age distributions in compartmentalized tissues. *J. R. Soc. Interface* **2018**, *15*, 20180272. [CrossRef]
259. Cairns, J. Mutation Selection and Natural-History of Cancer. *Nature* **1975**, *255*, 197–200. [CrossRef]
260. Conboy, M.J.; Karasov, A.O.; Rando, T.A. High incidence of non-random template strand segregation and asymmetric fate determination in dividing stem cells and their progeny. *PLoS Biol.* **2007**, *5*, 1120–1126.

Supplement N

Schořová, Š., Fajkus, J., Drábková, L.Z., Honys, D., **Schrumpfová, P.P.***, **2019**. The plant Pontin and Reptin homologues, RuvBL1 and RuvBL2a, colocalize with TERT and TRB proteins in vivo, and participate in telomerase biogenesis. Plant J. 98, 195–212

P.P.S. participated in the design of experiments, data evaluation and wrote the ms

the plant journal

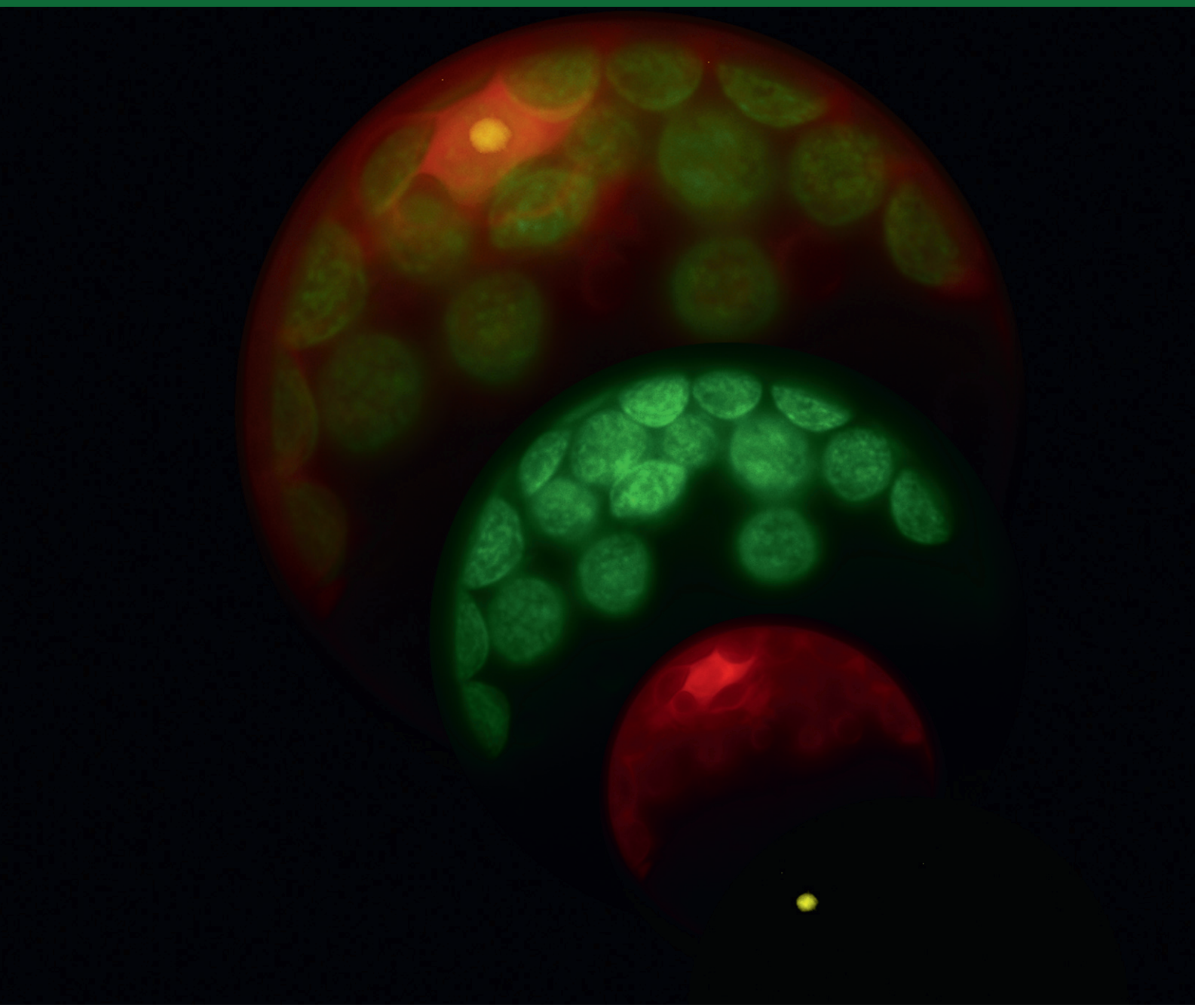

VOLUME 98 | NUMBER 2 | APRIL 2019
http://www.theplantjournal.com | ISSN 1365-313X
WILEY Blackwell

the plant journal

Editor-in-Chief

Lee Sweetlove
Department of Plant Sciences,
University of Oxford,
South Parks Road,
Oxford OX1 3RB, UK
Tel: +44 (0) 1865 275137
Email: lee.sweetlove@plants.ox.ac.uk

Research Interests:
Central metabolism; Metabolic flux; Metabolic modeling; Metabolic engineering; Metabolons and metabolite channelling

Previous Editors-in-Chief
Dianna Bowles (Founding EiC), 1990-2001
Harry Klee, 2002-2009
Christoph Benning, 2009-2017

Editorial Office

The Plant Journal Editorial Office,
Wiley Blackwell,
9600 Garsington Road, Oxford,
OX4 2DQ, UK
E-mail: tpj-general@wiley.com

Jim Ruddock *Managing Editor*
E-mail: tpj-editor@wiley.com

Lauren Dawson *Editorial Assistant*
E-mail: tpj-submissions@wiley.com,
tpj-manuscripts@wiley.com

Production Office

Rajalakshmi Sundararamanujam
Production Editor
E-mail: tpj@wiley.com

Senior Editors

Federica Brandizzi
Michigan State University, Plant Research Laboratory,
East Lansing, MI 48824, USA
Tel: (517) 353-7872; Fax: (517) 353-9168
Email: fb@msu.edu

Research Interests
Cell biology; Plant endomembranes; Endoplasmic reticulum stress; Fluorescent protein technology; Protein trafficking

Alisdair R. Fernie
Molecular Physiology,
Max-Planck Institute for Molecular Plant Physiology,
Golm 14476, Germany
Tel: +49 331 567 8211
Email: fernie@mpimp-golm.mpg.de

Research Interests
Carbohydrate metabolism; Metabolomics; Primary metabolism

Lyza Maron (Research highlights Editor)
Boyce Thompson Institute,
USDA/ARS Robert W. Holley Center for Agriculture & Health,
Ithaca, NY 14853, USA

Research Interests
Abiotic stress responses; Root biology; Natural variation; Gene expression regulation

Sheila McCormick (Consultant Editor)
Plant and Microbial Biology, 111 Koshland Hall, UC-Berkeley,
Berkeley, CA 94720, USA
Email: sheilamc@berkeley.edu

Research Interests
Pollen development; Plant gametes (sperm, egg, central cell); Pollen tube growth; Pollen-pistil interactions; Receptor kinase signaling (ligands); Genetics; Genomics

Editors

Asaph Aharoni
Weizmann Institute of Science, Department of Plant Sciences, P.O.B 26, Rehovot 76100, Israel
Tel: +972 8 934 3643; Fax: +972 8 934 4181
Email: asaph.aharoni@weizmann.ac.il

Research Interests
Fruit metabolism and ripening control, The plant surface (epidermis and the cuticle), Secondary metabolism, Functional genomics and metabolomics, Metabolic engineering, Metabolism – development interface

Jose Alonso
Department of Genetics,
North Carolina State University, 2548 Gardner Hall, Box 7614, Raleigh, North Carolina, 27695-7614, USA
Tel: +1 919 515-5729; Fax: +1 919 515-3355
Email: jmalonso@unity.ncsu.edu

Research Interests
Ethylene signaling and response pathway; Hormone interactions and signal integration; Arabidopsis functional genomics and tool development; Auxin biosynthesis; Post-transcriptional control of hormonal responses

Bonnie Bartel
Department of Biosciences, Rice University, 6100 Main Street, MS-140, Houston, Texas 77005, USA
Tel: +1 713 348 5602; Fax: +1 713 348 5154
Email:bartel@rice.edu

Research Interests
Cell biology; Peroxisome biology; Autophagy; Protein trafficking; Arabidopsis genetics

Jörg Bohlmann
Michael Smith Laboratories, University of British Columbia, 321-2185 East Mall, Vancouver V6T 1Z4
British Columbia, Canada
Tel: +1 604 822 0282; Fax: +1 604 822 2114
Email: bohlmann@interchange.ubc.ca

Research Interests
Secondary metabolism; Terpenoid synthases, cytochrome P450; Plant-herbivore interactions; Chemical ecology; Conifers, Poplar, Grapevine

Federica Brandizzi
Michigan State University,
Plant Research Laboratory, East Lansing, MI 48824, USA
Tel: +1517 353-7872; Fax: +1 517 353-9168
Email: fb@msu.edu

Research Interests
Cell biology; Protein trafficking; Plant endomembranes; Endoplasmic reticulum stress; Fluorescent protein technology

Jorge J. Casal
Faculty of Agronomy, University of Buenos Aires,
Av. San Martin 4453, 1417-Buenos Aires, Argentina
Tel: +5411 4524 8070/71; Fax: +5411 4514 8730
Email: casal@ifeva.edu.ar

Research Interests
Light signaling circuitry, its architecture and functional implications; Functional genomics, transcriptome patterns during plant development; Photomorphogenesis in crops

John Cushman
University of Nevada, Department of Biochemistry,
Mail Stop 330, 1664 N. Virginia St., Reno89557-0330, USA
Email: jcushman@unr.edu

Research Interests
Abiotic stress responses; Metabolic adaptation to stress; Crassulacean acid metabolism; Biosystem engineering

Brendan Davies
Centre for Plant Sciences, University of Leeds, Leeds LS2 9JT, UK
Tel: +44 113 343 3123; Fax: +44 113 343 3144
Email: b.h.davies@leeds.ac.uk

Research Interests
Plant development; Reproduction; Transcription factors; Nonsense-mediated mRNA decay

Katherine Denby
University of York, Department of Biology York, YO10 5DD, UK
Tel: +44 1904 328 670

Research Interests
Plant systems biology; Plant pathogen interaction; Functional genomics; Gene regulation; Gene regulatory networks; Crop breeding

Alisdair R. Fernie
Molecular Physiology, Max-Planck Institute for Molecular Plant Physiology,Golm 14476, Germany
Tel: +49 331 567 8211
Email:fernie@mpimp-golm.mpg.de

Research Interests
Carbohydrate metabolism; Metabolomics; Primary metabolism

Jaume Flexas
Universitat de les Illes Balears, Biologia, Carretera de Valldemossa Km 7.5, Palma de Mallorca, 07122, Spain
Tel: +34 971 172365; Fax: +34 971 173184
Email: jaume.flexas@uib.es

Research Interests
Photosynthesis; Ecophysiology; Abiotic stress; Mesophyll conductance; Drought

Crisanto Gutierrez
Centro de Biologia Molecular Severo Ochoa, Consejo Superior de Investigaciones Cientificas, Nicolas Cabrera 1, Cantoblanco, Madrid, 28049, Spain
Tel: +34 911964638; Fax: +34 911964420
Email: cgutierrez@cbm.uam.es

Research Interests
Cell cycle regulation, DNA replication/endoreplication, Chromatin/Gene expression, Retinoblastoma/E2F, Cell fate, cell differentiation – Meristems, cell proliferation in organs

Jose Gutierrez-Marcos
Life Sciences, University of Warwick, Coventry, CV4 7AL, UK
Tel: +44 247 6 57 5077
Email: j.f.gutierrez-marcos@warwick.ac.uk

Research Interests
Epigenetics; Seed development

Scott Jackson
Institute for Plant Breeding, Genetics and Genomics,
University of Georgia , 111 Riverbend Rd, Athens, Georgia, GA 30602, USA
Tel: +1 706.242.4021; Fax: +1 706-583-8120
Email: sjackson@uga.edu

Research Interests
Genomics; Cytogenetics; Evolutionary genomics; Legumes; Polyploidy

Kerstin Kaufmann
Humboldt-Universität zu Berlin, Chair for Plant Cell and Molecular Biology, Philippstr. 13, 10115 Berlin, Germany
Tel: +49(0)30209349740; Fax: +49(0)30209349741
Email: kerstin.kaufmann@hu-berlin.de

Research Interests
Gene regulatory networks; Flower development; Plant transcription factors; Epigenetics; Transcriptional regulation; Flowering

Tracy Lawson
University of Essex, School of Biological Siences,
Wivenhoe Park, Colchester, Essex CO4 3SQ, UK
Tel: +44 1206 873327; Fax: +44 1206 872552
Email: tlawson@essex.ac.uk

Research Interests
Plant physiology; Plant phenotyping; Conductance; Gas exchange; Water use efficiency

Olivier Loudet
INRA - IJPB, Route de Saint Cyr, 78000 Versailles, France
Email: olivier.loudet@versailles.inra.fr

Research Interests
Natural variation; Quantitative genetics; Abiotic stress tolerance; High-throughput phenotyping; Arabidopsis genetics

Jianxin Ma
Purdue University, 915 S. University St, West Lafayette, Indiana 47907, USA
Tel: 765-496-3662; Fax: 765-496-7255; Email: maj@purdue.edu

Research Interests
ROS; Comparative genomics; Genome evolution; Transposable elements; Soybean genetics; Crop domestication

Hiroshi Maeda
University of Wisconsin – Madison, Department of Botany,
430 Lincoln Drive , Madison, Wisconsin 53706, USA
Tel: +1 608-262-5833; Fax: +1 608-262-7509;
Email: maeda2@wisc.edu

Research Interests
Amino acid metabolism; Specialized metabolism; Interaction of metabolism and plant development and physiology

Ron Mittler
University of North Texas College of Arts and Sciences,
Department of Biological Sciences, College of Science,
1155 Union Circle #305220, Denton, Texas 76203-5017, USA
Tel: +1 940 293 7170; Fax: +1 940 565 3821
Email: ron.mittler@unt.edu

Research Interests
ROS; Abiotic stress; Gene expression; Systems biology; Cancer biology

Eiji Nambara
University of Toronto, Cell & Systems Biology, 25 Willcocks Street, Toronto, Ontario M5S 3B2, Canada
Email: eiji.nambara@utoronto.ca

Research Interests
Plant hormone; Biosynthesis; Catabolism; Abscisic acid; Seed; Stress response

Holger Puchta
Plant Molecular Biology and Biochemistry Karlsruhe Institute of Technology (KIT), Hertzstr. 16 Geb. 06.35, Karlsruhe D-76187, Germany
Tel: +49 721 608 8894; Fax: +49 721 608 4874
Email: holger.puchta@kit.edu

Research Interests
DNA repair; Meiotic recombination; DNA processing enzymes; Genome evolution; Gene technology

Dominique Roby
Laboratory of Plant Microorganism Interactions (LIPM),
UMR CNRS-INRA 2594/441, BP 52627, F-31326,
Castanet-Tolosan cedex, France
Tel: +33 05 61 28 55 11; Fax: +33 05 61 28 50 61
Email: dominique.roby@toulouse.inra.fr

Research Interests
Plant-microbe interactions; Genetic analyses of plant disease resistance pathways; Defence regulatory proteins; Programmed cell death and transcriptional regulators; Pathogen effector activities; Quantitative resistance to pathogens

Ian Small
University of Western Australia,
ARC Centre of Excellence in Plant Energy Biology, 35 Stirling Highway, Crawley, Perth, 6009 Western Australia
Tel: +61 (0)8 6488 4499; Fax: +61 (0)8 6488 4401
Email: iansmall@cyllene.uwa.edu.au

Research Interests
Organelle biogenesis; Gene expression in mitochondria and chloroplasts; Protein and RNA targeting; Post-transcriptional regulation of gene expression; Energy metabolism; Functional genomics, bioinformatics and systems biology

Edgar Spalding
Department of Botany, University of Wisconsin-Madison,
430 Lincoln Drive Madison WI 53706, USA
Tel: +1 608 265 5294
Email: spalding@wisc.edu

Research Interests
Ion transport and electrophysiology Growth; control by light and auxin
Phenotype platforms; computer vision-based

Dorothea Tholl
Department of Biological Sciences, Virginia Polytechnic Institute and State University,408 Latham Hall, Agquad Lane,Blacksburg, VA 24061, USA
Tel: +1 540 231 4567; Fax: +1 540 231 3347
Email: tholl@vt.edu

Research Interests
Isoprenoid biochemistry, Secondary metabolism, Chemical diversity, Plant volatiles, Plant chemical interactions, Root biology, Metabolic pathways, Evolution, Engineering

Michael F. Thomashow
Michigan State University, MSU-DOE Plant Research Laboratory, Plant Biology Building, 312 Wilson Rd,
East Lansing, MI 48824, USA
Tel: 1 517 355 2299; Fax: 1 517 353 9168
Email: thomash6@msu.edu

Research Interests
Abiotic stress; Biotic stress

Yves Van de Peer
Department of Plant Biotechnology and Genetics,
University of Gent, Technologiepark 927,
9052 Zwijnaarde, Belgium
Tel: +09 331 38 07; Fax: +09 331 38 09
Email: yves.vandepeer@ugent.be

Research Interests
Comparative genomics, systems biology, evolutionary analysis, genome evolution, gene and genome duplication

Saskia van Wees
Utrecht University, Biology, Padualaan 8, Utrecht, 3584 CH, Netherlands
Tel: +31-302536861; Fax: +31-302532837;
Email:s.vanwees@uu.nl

Research Interests
Plant-microbe interactions; Plant-insect interactions; Defenses to pathogens and insects; Gene expression profiling; Gene expression regulation; Hormonal regulation of plant immunity

Daoxin Xie
School of Life Sciences, Tsinghua University,
Beijing 100084, China
Email: daoxinlab@tsinghua.edu.cn

Research Interests
Hormone perception; Jasmonate signal transduction; Strigolactone signaling; Hormonal crosstalk

Bin Yu
Center for Plant Science Innovation, & School of Biological Sciences,
University of Nebraska, Lincoln,
1901 Vine St, Lincoln, NE, USA
Tel: 402-472-2125;
Email: byu3@unl.edu

Research Interests
Small RNA metabolism; Epigenetics; RNA silencing; Non-coding RNAs; Arabidopsis genetics

ISSN 1365-313X (online)

the plant journal

Subscription information

The Plant Journal is published semi-monthly (four volumes per annum), with two issues published each month. Subscription prices for 2019 are: Online only: US$7274 (The Americas), US$8488 (Rest of World), €4996 (Europe); £3936 (UK). Prices are exclusive of tax. Asia-Pacific GST, Canadian GST and European VAT will be applied at the appropriate rates. For more information on current tax rates, please go to www.wileyonlinelibrary.com/tax-vat. The price includes online access to the current and all online back files to January 1st 2015, where available. For other pricing options, including access information and terms and conditions, please visit www.wileyonlinelibrary.com/access.

Back issues

Single issues from current and prior year are available at the single issue price from cs-journals@wiley.com. Earlier issues may be obtained from the Periodicals Service Company, 11 Main Street, Germantown, NY 12526, USA. Tel: +1 518 537 4700, Fax: +1 518 537 5899, Email: psc@periodicals.com.

Publisher

The Plant Journal is published by John Wiley & Sons Ltd, 9600 Garsington Road, Oxford OX4 2DQ. Tel: +44 (0)1865 776868; Fax: +44 (0)1865 714591.

Journal Customer Services

For ordering information, claims and any enquiry concerning your journal subscription please go to www.wileycustomerhelp.com/ask or contact your nearest office:
Americas: Email: cs-journals@wiley.com; Tel: +1 781 388 8598 or 1 800 835 6770 (Toll free in the USA & Canada).
Europe, Middle East and Africa: E-mail: cs-journals@wiley.com; Tel: +44 (0) 1865 778315
Asia Pacific: E-mail: cs-journals@wiley.com; Tel: +65 6511 8000
Japan: For Japanese speaking support, e-mail: cs-japan@wiley.com
Visit our Online Customer Help available in 7 languages at www.wileycustomerhelp.com.

Despatch

THE PLANT JOURNAL, (ISSN 0960-7412), is published semi-monthly (four volumes per annum). US mailing agent: Mercury Media Processing, LLC 1850 Elizabeth Avenue, Suite #C, Rahway, NJ 07065, USA. Periodical postage paid at Rahway, NJ.
Postmaster: Send all address changes to THE PLANT JOURNAL, John Wiley & Sons Inc., C/O The Sheridan Press, PO Box 465, Hanover, PA 17331.

Online Open

OnlineOpen is available to authors of primary research articles who wish to make their article available to non-subscribers on publication, or whose funding agency requires grantees to archive the final version of their article. With OnlineOpen, the author, the author's funding agency, or the author's institution pays a fee to ensure that the article is made available to non-subscribers upon publication via Wiley Online Library, as well as deposited in the funding agency's preferred archive. For the full list of terms and conditions, see http://wileyonlinelibrary.com/onlineopen#OnlineOpen_Terms.

Any authors wishing to send their paper OnlineOpen will be required to complete the payment form available from our website at: https://authorservices.wiley.com/bauthor/onlineopen_order.asp.

Prior to acceptance there is no requirement to inform an Editorial Office that you intend to publish your paper OnlineOpen if you do not wish to. All OnlineOpen articles are treated in the same way as any other article. They go through the journal's standard peer-review process and will be accepted or rejected based on their own merit.

The Journal is indexed by Current Contents/Life Sciences, Science Citation Index, Index Medicus, MEDLINE and BIOBASE/Current Awareness in Biological Sciences.

Access to this journal is available free online within institutions in the developing world through the AGORA initiative with the FAO, the HINARI initiative with the WHO and the OARE initiative with UNEP. For information, visit www.aginternet.org, www.healthinternetwork.org, www.oarescience.org.

Published by John Wiley & Sons Ltd, in association with the Society for Experimental Biology. Information on this journal can be accessed at http://www.theplantjournal.com. This journal is available online at Wiley Online Library. Visit wileyonlinelibrary.com to search the articles and register for Table of Contents email alerts.

Wiley's Corporate Citizenship initiative seeks to address the environmental, social, economic, and ethical challenges faced in our business and which are important to our diverse stakeholder groups. We have made a long-term commitment to standardize and improve our efforts around the world to reduce our carbon footprint. Follow our progress at www.wiley.com/go/citizenship.

Editorial correspondence

Correspondence relating to editorial matters should be directed to *The Plant Journal* Editorial Office, John Wiley & Sons Ltd, 9600 Garsington Road, Oxford, OX4 2DQ, UK (E-mail: tpj-general@wiley.com).

the plant journal

CONTENTS OF VOL. 98, NO. 2, APRIL 2019

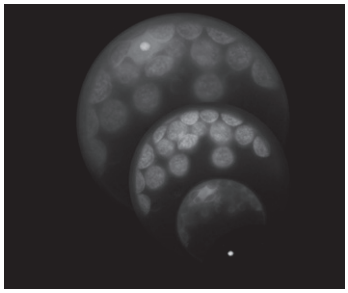

Front cover: The cover image shows an overlay and individual layers of *Arabidopsis thaliana* protoplast used for Bimolecular Fluorescence Complementation assay. In this case, interaction between AtCBF5 and AtTRB3 proteins was analysed. The biggest protoplast represents the final overlay of three layers, where the green one shows only chloroplasts, the red coloured protoplast symbolizes nuclear signal delivered by mRFP-VirD2NLS and finally, the yellow dot shows a specific interaction between selected proteins AtCBF5 and AtTRB3 localized in the nucleolus. For details, see article by Schořová *et al.* (pp.195–212).

the plant journal

SEB Society for Experimental Biology

The Plant Journal (2019) **98,** 193–194 doi: 10.1111/tpj.14328

RESEARCH HIGHLIGHT

The journey to the end of the chromosome: delivering active telomerase to telomeres in plants

Lee Sweetlove and Crisanto Gutierrez

Linked article: This is a Research Highlight about Šárka Schořová *et al.* To view this article visit https://doi.org/10.1111/tpj.14306.

Linear chromosomes offer many advantages over circular DNA for transcription and replication of large genomes, hence their prevalence in eukaryotes. But the linear arrangement of the DNA has a massive Achilles heel: the terminal ends, or telomeres, are unstable and prone to mutation. Moreover, DNA replication cannot proceed to the end of a linear DNA molecule because the synthesis of Okazaki fragments needs RNA primers to bind ahead of the lagging strand. Eukaryotes deal with both of these problems by adding repetitive DNA sequences to the telomeres that act as a disposable buffer, protecting terminal genes from being truncated during replication and from mutation. Because the telomere is shortened during each DNA replication, it is necessary to resynthesise telomere DNA using an enzyme, telomerase reverse transcriptase.

Our understanding of telomere biology is dominated by research into human telomeres. This is understandable due to the links between telomere biology and cellular mortality, ageing and a range of diseases including cancer. However, telomere biology in plants shows some specific differences to humans which may be crucial in our understanding of telomere biology in general. For example, telomerase activity in plant cells is well balanced with the cellular proliferation rate. The reversible regulation of telomerase activity is thought to be important in this context: its activity is turned off in differentiated tissues and turned on during cell periods of active cell replication, for example, during regeneration of plant tissues. Understanding the mechanism for this reversible regulation of telomerase activity could be beneficial in biomedical applications of telomere biology in humans.

But where to start? From protozoans and humans, it was known that telomerase was a ribonucleoprotein, carrying its own RNA molecules that are complementary to the telomere repeats and are used as a template for telomere elongation, catalysed by the reverse transcriptase activity of the enzyme. But, in addition, a number of accessory proteins are required to deliver functional telomerase to the telomeres, to regulate its activity and to protect the elongated telomere from DNA repair enzymes. These components assemble into two distinct complexes known as shelterin and CST. Functional homologues of the CST complex have been identified in plants, but the same is not true for the shelterin complex. In plants, not all of the homologues of the six core shelterin components exist, and only some of them seem to be associated with telomeres *in vivo*. The goal, therefore was to identify undiscovered telomerase accessory proteins in plants and to establish how active telomerase is formed and regulated.

Jiří Fajkus and his research group at Masaryk University, have been working on plant telomeres for over 20 years. A key member of his team in the hunt for plant telomerase-associated proteins has been Petra Procházková Schrumpfová, first as a Ph.D. student and then through several postdoc periods. Working in Arabidopsis, the group had already established that Telomere Repeat Binding proteins (TRB) were involved in recruitment of telomerase to the telomeres. These proteins are specific to plants and contain an N–terminal Myb-like domain which is responsible for specific recognition of telomeric DNA. Attention turned to the plant homologues of two human telomere associated proteins called Pontin and Reptin after they turned up in a pull-down of TERT, the catalytic subunit of Arabidopsis telomerase, in an experiment done in collaboration with Eva Sýkorová's group at the Institute of Biophysics in Brno.

The plant Pontin and Reptin homologues are encoded by *RuvBL1* and *RuvBL2a*, respectively. But despite the fact that RuvBL proteins were isolated from plant cells as TERT-associated, Jiří and his team were not able to prove a direct interaction between TERT and RuvBL as had already been described in mammals. Serendipity then intervened. During their characterisation of RuvBL interactions with TERT, they used several proteins as negative controls. Surprisingly, one of the supposed negative controls showed reproducibly positive interaction with RuvBL proteins. It was in this way that they discovered that TRB proteins interact with RuvBL. Knowing that TRB proteins directly interact with TERT they started to closely characterise the trimeric complex TERT-TRB-RuvBL and that is

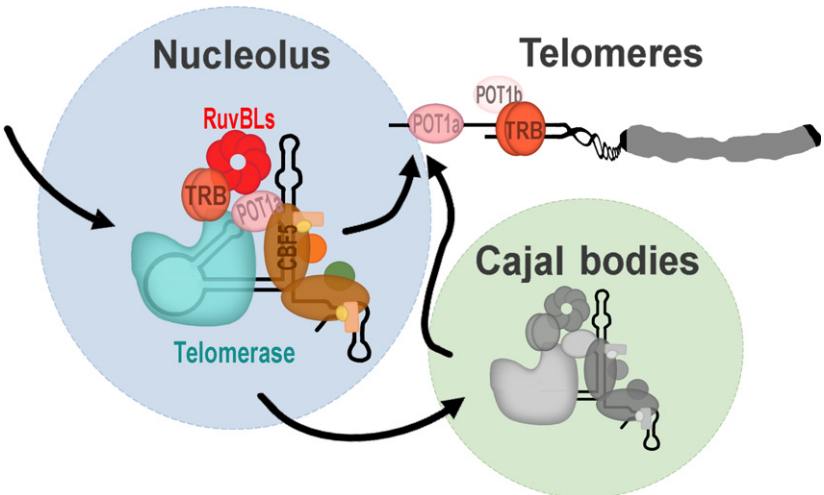

Figure 1. RuvBL1 and RuvBL2a, are orthologues of human Pontin and Reptin, respectively, in Arabidopsis.
Besides their mutual interactions, RuvBL1 associates with the catalytic subunit of telomerase (TERT) in the nucleolus *in vivo*. In contrast to mammals, interactions between TERT and RuvBL proteins in Arabidopsis are not direct but are mediated by one of the Telomere Repeat Binding (TRB) proteins. The plant orthologue of human dyskerin, named CBF5, is indirectly associated with TRB proteins but not with the RuvBL proteins in the plant nucleus/nucleolus, and interacts with the Protection of telomere 1 (POT1a) in the nucleolus or cytoplasmic foci.

the focus of the highlighted paper which is drawn from the MSc and PhD research of Šárka Schořová with Petra Procházková Schrumpfová and Jiří Fajkus as joint corresponding authors. The work also involved Lenka Záveská Drábková, a postdoc from David Honys's group at the Institute of Experimental Botany in Prague who did phylogenetic analysis of the RuvBL family in plants. That collaboration started late one afternoon during a short-term visit of Petra Procházková Schrumpfová to David Honys's lab that was focused on a completely different scientific topic. Such is the nature of science and scientists!

In this highlighted paper (Schořová *et al.*, 2019), a combination of BiFC, yeast-two hybrid and pull-down assays confirmed that there is no direct interaction between RuvBLs and TERT, but that the interaction is mediated by TRBs as an intermediary. It was also shown that RuvBL proteins form hetero- and homo-oligomers *in vivo*. Proof of the importance of RuvBL1/2 for telomerase biogenesis was provided by analysis of Arabidopsis knockout lines which had substantially reduced telomerase activity in flower buds (a rapidly proliferating tissue with high telomerase requirement). This crucial experiment turned out to be the hardest part of the research, with identification of knockout alleles a real struggle. Jiří and Petra say that they had to genotype hundreds of individual plants from several lines and were only able to identify a few heterozygous individuals of each gene with homozygous mutants being lethal.

Further protein interaction experiments identified another protein in the complex: CBF5, a homologue of mammalian dyskerin, a known telomerase-associated protein. Cell biological analyses were able to place all of these proteins in the nucleolus and some of them in Cajal bodies and, combined with previous studies, the authors were able to put together the most complete picture of the plant telomerase complex to date, as shown in Figure 1.

One of the most interesting facets of this picture is the similarities and divergence between plants and humans. On the one hand, identification of Reptin and Pontin in Arabidopsis and their conservation in humans, shows that the factors involved in telomerase biogenesis and function are evolutionary ancient. On the other, the interactions and mechanism of action of plant Reptin and Pontin is different than in human cells. The TERT subunit of Arabidopsis telomerase does not interact directly with Reptin and Pontin but through TRBs which in human cells are telomere-associated proteins but not TERT-accessory factors. This reveals that different mechanisms have evolved although using basically the same set of factors, a finding that would justify a similar study in other eukaryotic lineages to define the evolutionary history of complex formation between telomeric repeats, TERT, accessory factors and shelterin proteins.

One possible reason to explain the variety of mechanisms suggested by this study is the specific organization, and possibly the 3D structure, of TERT RNA (TER) molecules which may limit the ability of TERT to interact directly with them or require other bridging proteins, as it occurs in Arabidopsis. Differences in the subnuclear localization of telomeric sequences may be also important. For Jiří and his team, work will continue to unpick the regulation of synthesis of both basic subunits of telomerase, TER and TERT, their intracellular trafficking and assembly into the holoenzyme complex, together with a number of associated factors.

REFERENCE

Schořová, Š., Fajkus, J., Záveská Drábková, L., Honys, D. and Procházková Schrumpfová, P. (2019) The plant Pontin and Reptin homologues, RuvBL1 and RuvBL2a, colocalize with TERT and TRB proteins *in vivo*, and participate in telomerase biogenesis. *Plant J.* **98**, 195–212.

the plant journal

SEB Society for Experimental Biology

The Plant Journal (2019) **98,** 195–212 doi: 10.1111/tpj.14306

The plant Pontin and Reptin homologues, RuvBL1 and RuvBL2a, colocalize with TERT and TRB proteins *in vivo*, and participate in telomerase biogenesis

Šárka Schořová[1], Jiří Fajkus[1,2,3,*], Lenka Záveská Drábková[4], David Honys[4] and Petra Procházková Schrumpfová[1,*]

[1]*Laboratory of Functional Genomics and Proteomics, National Centre for Biomolecular Research, Faculty of Science, Masaryk University, Brno, Czech Republic,*

[2]*Mendel Centre for Plant Genomics and Proteomics, Central European Institute of Technology, Masaryk University, Brno, Czech Republic,*

[3]*Institute of Biophysics of the Czech Academy of Sciences, v.v.i., Brno, Czech Republic, and*

[4]*Laboratory of Pollen Biology, Institute of Experimental Botany of the Czech Academy of Sciences, v.v.i., Prague, Czech Republic*

Received 26 November 2018; revised 8 February 2019; accepted 26 February 2019; published online 4 March 2019.
*For correspondence (e-mails petra.proch.schrumpfova@gmail.com; fajkus@sci.muni.cz).

SUMMARY

Telomerase maturation and recruitment to telomeres is regulated by several telomerase- and telomere-associated proteins. Among a number of proteins, human Pontin and Reptin play critical roles in telomerase biogenesis. Here we characterized plant orthologues of Pontin and Reptin, RuvBL1 and RuvBL2a, respectively, and show association of *Arabidopsis thaliana* RuvBL1 (AtRuvBL1) with the catalytic subunit of telomerase (AtTERT) in the nucleolus *in vivo*. In contrast to mammals, interactions between AtTERT and AtRuvBL proteins in *A. thaliana* are not direct and they are rather mediated by one of the *Arabidopsis thaliana* Telomere Repeat Binding (AtTRB) proteins. We further show that plant orthologue of dyskerin, named AtCBF5, is indirectly associated with AtTRB proteins but not with the AtRuvBL proteins in the plant nucleus/nucleolus, and interacts with the Protection of telomere 1 (AtPOT1a) in the nucleolus or cytoplasmic foci. Our genome-wide phylogenetic analyses identify orthologues in RuvBL protein family within the plant kingdom. Dysfunction of *AtRuvBL* genes in heterozygous T-DNA insertion *A. thaliana* mutants results in reduced telomerase activity and indicate the involvement of AtRuvBL in plant telomerase biogenesis.

Keywords: telomerase assembly, Pontin, Reptin, AtTERT, AtTRB, AtRuvBL, AtPOT1a, nucleolus, *Arabidopsis*.

Linked article: This paper is the subject of a Research Highlight article. To view this Research Highlight article visit https://doi.org/10.1111/tpj.14328.

INTRODUCTION

Telomeres are nucleoprotein structures at the ends of eukaryotic chromosomes that protect linear chromosomes. Telomeric structures are formed by telomeric DNA, RNA, histones, and a number of other proteins that bind telomeric DNA, either directly or indirectly, together forming the protein telomere cap (Fajkus and Trifonov, 2001; de Lange, 2005; Schrumpfová *et al.*, 2016a). The core component of the telomere cap in mammals is a six-protein complex called shelterin. The specific telomeric double-stranded DNA binding of the shelterin is mediated by its TRF1 and TRF2 (Telomere Repeat Binding Factors 1 and 2) components through their Myb-like domain of a telobox type (Bilaud *et al.*, 1996; Peška *et al.*, 2011). In *Arabidopsis thaliana* Telomere Repeat Binding (AtTRB) proteins, that contain Myb-like domain of a telobox type and bind plant telomeric repeats *in vitro* (Schrumpfová *et al.*, 2004; Mozgová *et al.*, 2008), were found to colocalize with telomeres *in situ* and *in vivo* (Dvořáčková *et al.*, 2010; Schrumpfová *et al.*, 2014; Dreissig *et al.*, 2017), directly interacted with the telomerase reverse transcriptase (AtTERT) (Schrumpfová *et al.*, 2014) and physically interacted with AtPOT1b (Protection Of Telomeres 1) (Schrumpfová *et al.*, 2008). Moreover, shortening of telomeres was observed in *attrb* knockout mutants (Schrumpfová *et al.*, 2014, 2019; Zhou *et al.*, 2018).

Telomere- or telomerase-associated proteins can regulate lengths of telomere tracts by affecting the assembly of active telomerase complex or by modulation of the accessibility of telomeres to telomerase. The process of maturation and recruitment of human telomerase is partially understood (Schmidt and Cech, 2015; MacNeil *et al.*, 2016; Schmidt *et al.*, 2016). However, a similar description of telomerase assembly and recruitment to the telomeres in plants is still missing which would allow to distinguish between general and specific features of these processes.

Among a number of proteins, which were identified as associated with human telomerase, proteins named RuvBL (RuvB-like), that share limited sequence similarity to the bacterial RuvB helicase, were also identified. RuvBL proteins belong to the evolutionarily highly conserved AAA+ family (ATPase Associated with various cellular Activities) that are involved in ATP binding and hydrolysis (Matias *et al.*, 2006). Eukaryotic RuvBL1 (Pontin, TIP49a, Rvb1, TAP54α) and RuvBL2 (Reptin, TIP48, TIP49b, Rvb2, TAP54β) participate in many diverse cellular activities like chromatin remodeling (Jha *et al.*, 2008), transcriptional regulation (Ohdate *et al.*, 2003; Gallant, 2007), oncogenic transformation (Osaki *et al.*, 2013), epigenetic regulations (Gallant, 2007) or DNA-damage signaling (Rosenbaum *et al.*, 2013). RuvBL1 and RuvBL2 can also play a role in the assembly of box C/D or H/ACA of small nucleolar RNAs (snoRNAs) with specific proteins to form functional ribonucleoprotein particles (RNPs) (Watkins *et al.*, 2004; McKeegan *et al.*, 2007; Boulon *et al.*, 2008; Zhao *et al.*, 2008). Participation of RuvBL1 and RuvBL2 proteins in diverse cellular processes, as well as their association with specific interactors, can vary among cytoplasm, nucleus and nucleolus (Izumi *et al.*, 2012). RuvBL1 and also RuvBL2 monomers can assemble into different oligomeric forms, including hexameric structure with a central channel, or dodecamer composed of two hetero-hexameric rings with alternating RuvBL1 and RuvBL2 monomers (Torreira *et al.*, 2008; Niewiarowski *et al.*, 2010). RuvBL structure suggests that these proteins can act as scaffolding proteins, which explains their appearance in various cellular protein complexes (Matias *et al.*, 2006; Mao and Houry, 2017).

Mammalian RuvBL1 and RuvBL2, also termed as Pontin and Reptin, respectively, were found to play a critical role in telomerase biogenesis. Telomerase is a ribonucleoprotein enzyme complex composed of two core subunits: the catalytic telomerase reverse transcriptase (TERT) protein subunit and the telomerase RNA (TR) subunit (containing a box H/ACA motif). It performs the addition of telomeric DNA repeats onto the telomeres (Greider, 1996; Zhang *et al.*, 2011). Proper assembly of TERT with TR into a functional complex is a stepwise regulated process governed also by multiple associated proteins (Schmidt and Cech, 2015; MacNeil *et al.*, 2016). Human TR (hTR), as well as other box H/ACA snoRNPs, is associated with conserved scaffold proteins: dyskerin, NHP2, NOP10, NAF1 in the nucleoplasm, where NAF1 is replaced by GAR1 before the hTR RNP complex reaches the nucleolus. Association of hTR RNP with hTERT is proceeded in the nucleolus and the subsequent formation of catalytically active telomerase holoenzyme is localized into the Cajal bodies (CBs) (MacNeil *et al.*, 2016) that are evolutionary conserved mobile nuclear substructures involved in the RNA modification and the RNP assembly processes (Cioce and Lamond, 2005). Venteicher *et al.* (2008) demonstrated that hRuvBL1 (Pontin) and hRuvBL2 (Reptin) are interdependent proteins and are recruited to hTERT complexes through the association between hTERT and hRuvBL1. Additionally, they showed that both hRuvBL1 and hRuvBL2 directly interact with dyskerin and may help to assemble or remodel a nascent hTERT/hTR/dyskerin complex. The scaffold proteins, including dyskerin, together with hRuvBL1 and hRuvBL2, are required for a proper assembly of hTR RNP and are involved in the biogenesis of telomerase.

A homologue of human RuvBL1 from *A. thaliana* has been already described by Holt *et al.* (2002). They observed that plants with reduced *AtRuvBL1* (AT5G22330) mRNA levels had morphological defects and suggested that AtRuvBL1 was required in meristem development. Moreover, they observed that T-DNA insertion mutation in *AtRuvBL1* gene was lethal. In our laboratory, AtRuvBL1 protein and also one of two AtRuvBL2 homologues, named AtRuvBL2a (AT5G67630), were purified together with AtTERT using Tandem Affinity Purification (TAP) from *A. thaliana* suspension cultures (Majerská *et al.*, 2017).

In this study, we examined a mutual interaction of AtRuvBL1-AtRuvBL2a proteins and demonstrated that AtRuvBL proteins are associated with AtTERT in the nucleolus *in vivo*. However, in contrast to mammalian counterparts, interactions between AtTERT and AtRuvBL proteins are not direct and are likely to be mediated by one of the AtTRB proteins. We prove that AtTRB3 protein physically interacts with AtRuvBL1 and simultaneously with AtTERT. We further show that in plants, similarly to mammals, telomerase assembly is a dynamic process, as is supported by our observation that AtCBF5, a plant orthologue of dyskerin, is in the plant nucleus/nucleolus indirectly associated with three of AtTRB proteins, but not with the AtRuvBL proteins, and interacts with the AtPOT1a in the cytoplasmic or nucleolus foci. Heterozygous T-DNA insertion mutants in *AtRuvBL1* or *AtRuvBL2a* genes show reduced telomerase activity indicating the potential involvement of AtRuvBL proteins in telomerase assembly in *A. thaliana*. To identify new homologues of RuvBL protein family and elucidate their evolutionary relationships, we performed a survey of 83 plant species (80 angiosperms, one gymnosperm and two bryophytes).

RESULTS

AtRuvBL proteins form homomers or mutually interact

RuvBL1 and RuvBL2 proteins from mammals and yeast can co-exist in different monomeric or oligomeric complexes comprising dimers, trimers, hexamers or double-hexamers that can be composed as mixed multimers (Torreira *et al.*, 2008; Niewiarowski *et al.*, 2010; Queval *et al.*, 2014). Each RuvBL monomer contains three basic domains (DI, DII, DIII) (Figure 1a). Domain I (DI) together with domain III (DIII) represent the AAA+ core and are sufficient to form hexameric rings. In the AAA+ domain, the Walker A/B motifs are responsible for ATP binding and hydrolysis, while sensor I/II motifs sense whether the protein is bound to di- or triphosphates. Domain II (DII) corresponds to an insertion that is unique to RuvBL in comparison with other AAA+ family members (Silva-Martin *et al.*, 2016).

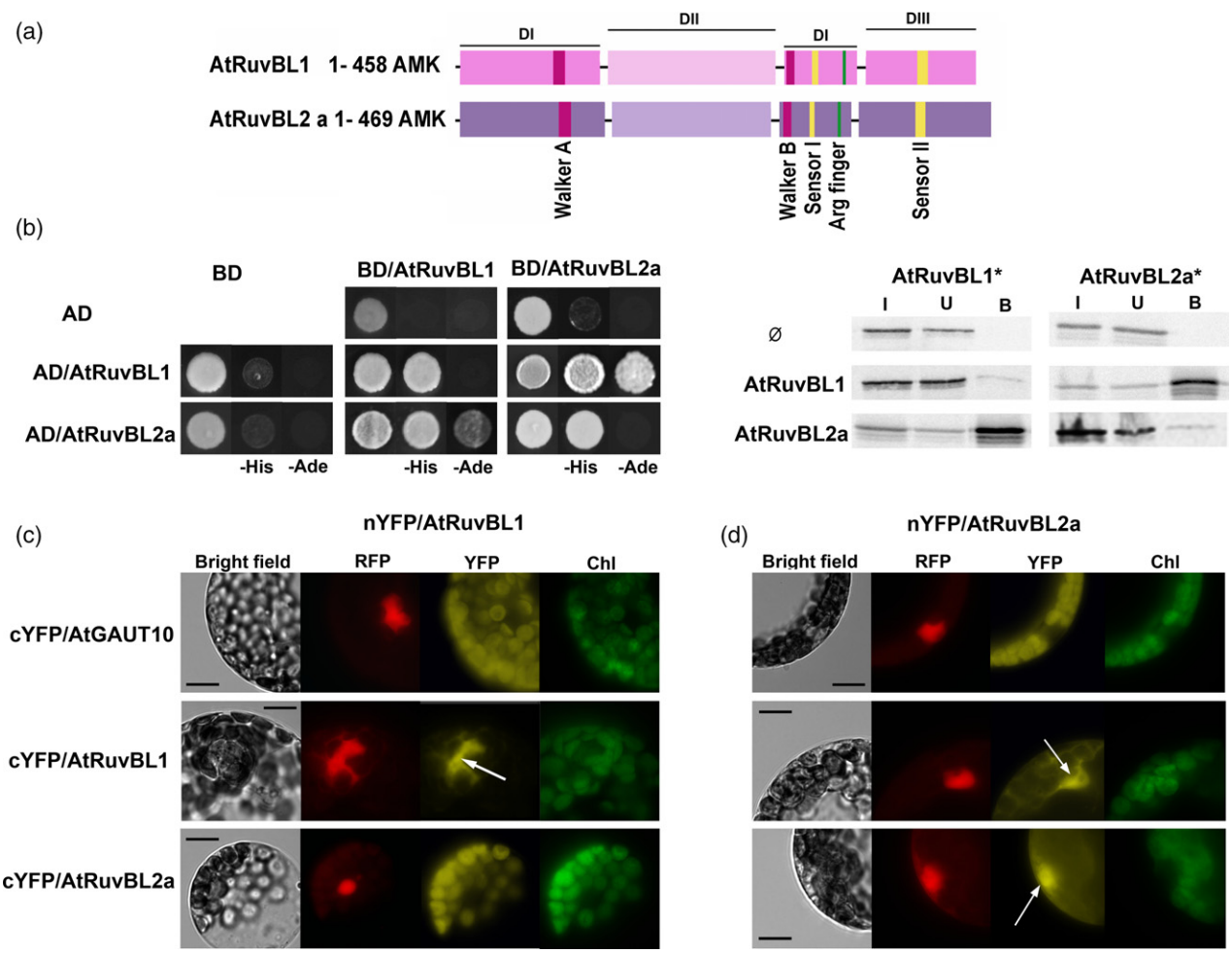

Figure 1. AtRuvBL proteins can form homo- or hetero-oligomers.
(a) Schematic representation of the conserved motifs of the RuvBL proteins from *Arabidopsis thaliana*. DI, DII, DIII, Domain I, II, III; Walker A/B, Walker motifs; Sensor I/II, sensors; Arg finger, arginine finger. AtRuvBL2a and AtRuvBL2b form closely related sequence pairs.
(b) Y2H system is used to assess homo- or heteromerization of AtRuvBL proteins. Two sets of plasmids carrying the indicated protein fused to either the GAL4 DNA-binding domain (BD) or the GAL4 activation domain (AD) are constructed and introduced into yeast strain PJ69-4a carrying reporter genes His3 and Ade2. Clear AtRuvBL1 and also AtRuvBL2a homomerization is detected on histidine-deficient plates. Mutual interaction between AtRuvBL1 and AtRuvBL2a is detected not only on histidine-deficient plates but also under stringent adenine selection. Co-transformation with an empty vector (AD, BD) serves as a negative control.
(c) Co-IP is performed with the TNT-RRL expressed AtRuvBL1* and AtRuvBL2a* (^{35}S-labelled*, prey) mixed with their protein counterparts AtRuvBL1 and AtRuvBL2a, fused with Myc-tag (anchor) and incubated with anti-Myc antibody. In the control experiment, the AtRuvBL* proteins are incubated with Myc-antibody and protein G-coupled magnetic beads in the absence of partner protein. Input (I), Unbound (U) and Bound (B) fractions are collected and run in 12% SDS-PAGE gels. Mutual AtRuvBL1 and AtRuvBL2a interactions appear to be stronger than entirely homo-interactions between AtRuvBL proteins.
(d) BiFC confirms homo- and also mutual heteromerization of AtRuvBL1 and AtRuvBL2a proteins. *A. thaliana* leaf protoplasts are co-transfected with 10 μg of each of the plasmids encoding nYFP-tagged or cYFP–tagged AtRuvBL1, AtRuvBL2a or AtGAUT10 clones (as negative control) and simultaneously with mRFP–VirD2NLS clone. Bright Field (left); RFP, mRFP–VirD2NLS (red fluorescent protein fused with nuclear localization signal) labels cell nuclei and determines transfection efficiency; YFP, yellow fluorescent protein signals indicate specific protein–protein interactions (PPI) also marked by white arrows; Chl, chloroplast autofluorescence is marked by green pseudocolor, chloroplast autofluorescence is also visible in the YFP channel. Scale bars = 10 μm.

To examine whether plant homologues of RuvBL proteins form homomers or mutual heteromers as their mammalian counterparts, or exist only as monomers, we performed several assays for protein–protein interactions (PPIs): yeast two-hybrid system (Y2H), co-immunoprecipitation (Co-IP) and bimolecular fluorescence complementation (BiFC).

First, we tested AtRuvBL1 and AtRuvBL2a homo-interactions. BiFC assay performed in *A. thaliana* leaf protoplasts, which enables direct visualization of protein interactions in living cells, demonstrated that AtRuvBL1 and AtRuvBL2a form homodimers or homomultimers *in vivo*. These results were confirmed using a GAL4 based Y2H assay, in which interactions took place inside the nucleus. We observed a clear homomeric interaction of AtRuvBL1 proteins as well as of AtRuvBL2a proteins in Y2H mating assay. The homomerization was further verified by Co-IP experiments in which proteins were expressed in the Coupled Transcription/Translation Rabbit Reticulocyte Lysate (TNT-RRL) System using the same vectors as in Y2H (Figure 1b, c).

Additionally, we expanded our BiFC study (Majerská *et al.*, 2017) and tested heteromerization of AtRuvBL1 and AtRuvBL2a not only in *Nicotiana tabacum* BY-2 protoplasts, but also in *A. thaliana* leaf protoplasts (Figure 1d). Analysis of subcellular localization of the AtRuvBL1-AtRuvBL2a interactions further showed that one reciprocal interaction of nYFP/AtRuvBL1 and cYFP/AtRuvBL2a was negative, and cYFP/AtRuvBL1 and nYFP/AtRuvBL2a showed nuclear, but not nucleolar localization, maybe due to the presence of a tag that may induce conformational changes of the AtRuvBL proteins (Cheung *et al.*, 2010). Using Y2H assay, we confirmed clear interaction not only on histidine-deficient (−His) plates but also under stringent adenine (−Ade) selection. Both Y2H and Co-IP experiments revealed that mutual AtRuvBL1−AtRuvBL2a interaction seemed stronger than pure homomerization of

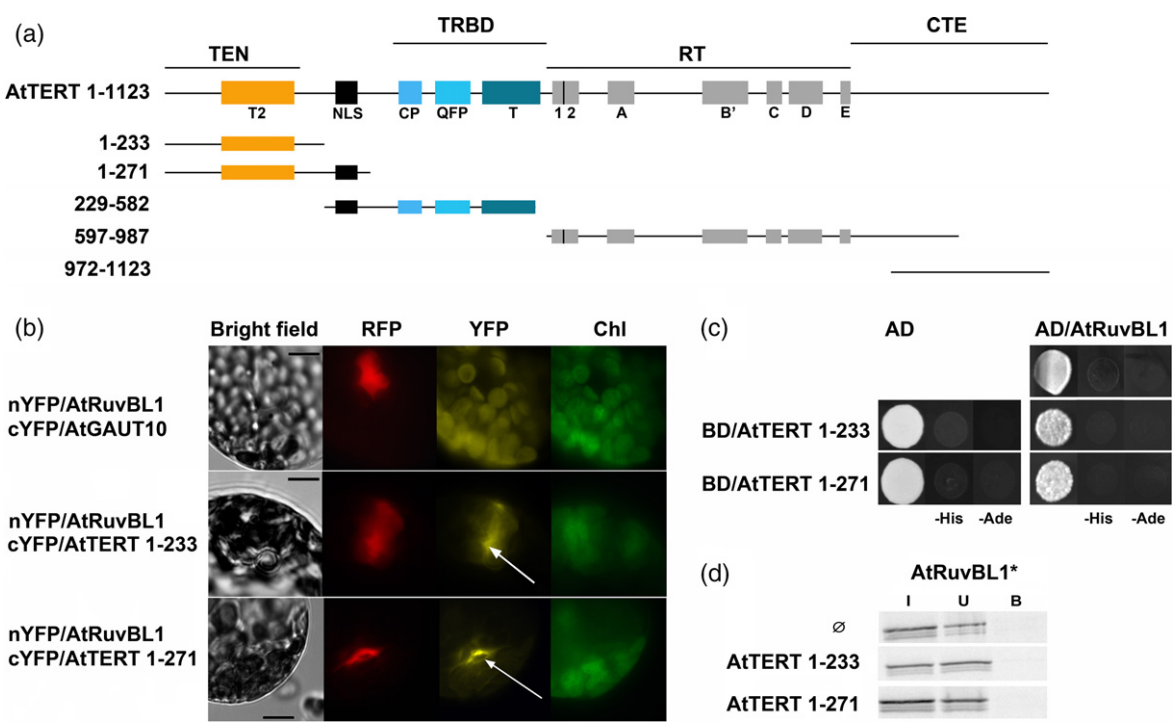

Figure 2. AtRuvBL1 interacts indirectly with N-terminal part of *Arabidopsis thaliana* catalytic subunit AtTERT. The analyses were performed as described in Figure 1.

(a) Schematic depiction of the plant catalytic subunit of telomerase (AtTERT) showing functional motifs. The regions of structural domains TEN (telomerase essential N-terminal domain), TRBD (RNA-binding domain), RT (reverse transcriptase domain) and CTE (C-terminal extension) are depicted above the conserved RT motifs (1, 2, A, B′, C, D and E), telomerase-specific motifs (T2, CP, QFP and T) and a NLS (nucleus localisation-like signal). All the depicted AtTERT fragments were used in protein–protein interaction analysis (amino acid numbering is shown). All AtTERT fragments were fused with activation domains (AD/BD or nYFP/cYFP) and used for further BiFC, Y2H and Co-IP analysis.

(b) BiFC in *A. thaliana* leaf protoplasts were used to detect the interaction between AtRuvBL1 and all AtTERT fragments from schematic depiction. Here we show PPI interaction (white arrows) of two N-terminal fragments of AtTERT (AtTERT 1−233 and AtTERT 1−271) and AtRuvBL1 located in the nucleolus. AtGAUT10, negative control; RFP, nucleus marker; YFP, detects PPI; Chl, Chloroplast autofluorescence. Scale bars = 10 μm.

(c) Y2H system fails to detect the interactions between AtRuvBL1 protein and N-terminal fragments of AtTERT (AtTERT 1−233 and AtTERT 1−271). BD, GAL4 DNA-binding domain; AD, GAL4 activation domain.

(d) Co-IP analysis does not detect interactions between AtTERT fragments and AtRuvBL1 protein which were demonstrated by BiFC. I, Input; U, Unbound; B, Bound fractions; asterisks*, ^{35}S-labelling.

AtRuvBL proteins. These results showed that RuvBL1 and RuvBL2a proteins from *A. thaliana* are able to form both homo- and heteromers, as well as their homologues in diverse organisms, although they preferably form heteromers.

AtRuvBL1 and AtTERT colocalize in the nucleus but contrary to mammalian homologues do not interact directly

Human RuvBL proteins are involved in the biogenesis and maturation of human telomerase complex. Human hRuvBL1 directly interacts with hTERT catalytic subunit. hRuvBL2 does not exhibit direct interaction with hTERT and seems to be recruited to an hTERT complex through bridging hRuvBL1 molecules (Venteicher *et al.*, 2008). To gain a deeper insight whether direct RuvBL-TERT interaction is conserved throughout the higher eukaryotes, we applied the above described Y2H, Co-IP and BiFC techniques. As TERT is a high-molecular-weight protein (approximately 130 kDa), we used the Gateway-compatible donor vectors carrying the AtTERT fragments that were described in Lee *et al.* (2012) and Zachová *et al.* (2013) (Figure 2a). We observed a clear nuclear interaction between AtRuvBL1 protein and AtTERT N-terminal fragments covering AtTERT domains localized in positions 1-233 and 1-271 in the *A. thaliana* leaf protoplasts using BiFC (Figure 2b). These results supported the observation from tobacco BY2 culture protoplasts where N-terminal fragments of AtTERT interact with AtRuvBL1 (Majerská *et al.*, 2017). As the central reverse transcriptase (RT) domain of hTERT is implicated in hRuvBL1 binding (Venteicher *et al.*, 2008), we expanded our interest to the other AtTERT fragments. However, no interactions were detected between AtRuvBL1 protein and AtTERT fragments localized in positions 229–582, 597–987 and 972–1123, therefore covering RT or C-terminal domains of AtTERT. Likewise, no interaction was observed between any of AtTERT fragments and AtRuvBL2a protein (Figure S1).

Notably, interactions of the N-terminal fragments between AtTERT domains and AtRuvBL1 were not confirmed in Y2H or Co-IP (Figure 2c, d). This discrepancy can be caused by the fact that the BiFC analysis detects the presence of proteins within the same macromolecular complex even in the absence of a direct contact between the proteins fused to the cYFP and nYFP fragments. The presence of proteins within the visualized macromolecular complex generally indicates that they participate in the same biological process (Kerppola, 2009). Our data show the interaction between AtRuvBL1 and AtTERT is localized in the nucleus and supports the suggestion of Majerská *et al.*, that AtRuvBL1-AtTERT interaction is mediated by an unknown partner and occurs in plant cells but not in RRL lysate or yeast system.

AtRuvBL proteins physically interact with AtTRB proteins

Previously, we have described that members of plant-specific group of AtTRB proteins physically interact with the N-terminal part of AtTERT and colocalized with telomeres *in situ* (Schrumpfová *et al.*, 2004, 2014; Mozgová *et al.*, 2008; Dreissig *et al.*, 2017; Zhou *et al.*, 2018). AtTRB1 interaction with double-stranded telomeric DNA is mediated by the Myb-like domain, while the H1/5 domain is involved in DNA sequence-non-specific DNA-protein interactions, interaction with AtPOT1b (Schrumpfová *et al.*, 2008) and in the multimerization of AtTRB1 (Mozgová *et al.*, 2008) (Figure 3a).

According to these findings, AtTRB proteins might be components of a putative shelterin-like complex in plants that modulates access of the telomerase to telomeres (Schrumpfová *et al.*, 2016a, 2019). Our BiFC analysis revealed the AtTRB3 protein interaction with both AtRuvBL1 and AtRuvBL2a proteins in the nucleus (Figure 3b). These interactions were confirmed by Y2H (Figure 3c) and also by Co-IP (Figure 3d), in which AtTRB3

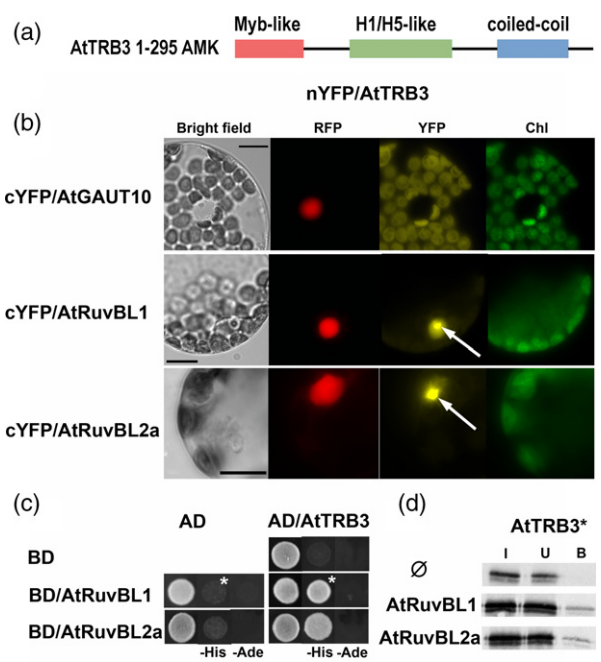

Figure 3. AtTRB3 proteins directly interact with AtRuvBL1 and AtRuvBL2a proteins. The methods are performed as is described in Figure 1.
(a) Schematic representation of the conserved motifs of the AtTRB3 protein from *Arabidopsis thaliana*. Myb-like, Telobox-containing Myb domain; H1/H5, histone-like domain; coiled-coil, C-terminal domain.
(b) BiFC shows interaction between AtTRB3 and both AtRuvBL proteins. PPIs marked by white arrows are localized in the nucleus. AtGAUT10, negative control; RFP, nucleus marker; YFP, detects PPI; Chl, Chloroplast autofluorescence. Scale bars = 10 μm.
(c) Y2H results show interactions between AtTRB3 and both AtRuvBL proteins on His- deficient plates. BD, GAL4 DNA-binding domain; AD, GAL4 activation domain; asterisks*, 5 mM 3-aminotriazol.
(d) Co-IP results confirm direct interactions between radioactively labelled AtTRB3 and Myc-tagged AtRuvBL proteins. I, Input; U, Unbound; B, Bound fractions; asterisks*, 35S-labelling.

protein was radioactively labelled by ^{35}S-methionine and mixed with its putative protein partners AtRuvBL1 or AtRuvBL2a fused with Myc-tag, and incubated with anti-Myc antibody. Clear nuclear interaction of AtTRB2 and AtRuvBL2a, but not of AtTRB2 with AtRuvBL1, was detected by BiFC and verified by Y2H and Co-IP. However, the nuclear interaction of AtTRB1 with AtRuvBL1 observed in BiFC seems to be indirect, as it was not proven by Y2H or Co-IP assays, but indicates that both proteins are present in the same macromolecular complex (Figure S2). Collectively, direct interactions of AtTRBs with AtTERT, as well as with AtRuvBL proteins, imply the role of AtTRB proteins as mediators of the interactions between AtRuvBL proteins and AtTERT telomerase subunit *in vivo*.

AtTRB3 protein mediates interaction between AtRuvBL1 and AtTERT

Our data, showing the indirect interaction between the N-terminal part of AtTERT and AtRuvBL1, suggested that this interaction could be mediated by AtTRB3 protein. We performed Co-IP assay with all three proteins of interest (Figure 4). Two prey proteins AtRuvBL1 and AtTRB3, were labelled with ^{35}S-methionine during the expression in TNT–RRL system. N-terminal fragment of AtTERT (AtTERT 1-271), fused with Myc-tag as an anchor, was expressed in TNT–RRL system in non-radioactive form ensuring a better resolution of the prey proteins in the 12% SDS-PAGE separation. Radioactively labelled AtTERT fragment was expressed in parallel tube to affirm the proper AtTERT 1-271 expression. The complex was captured with anti-Myc-antibody and protein G-coupled magnetic beads. Several negative controls were performed, where some of the monitored proteins were not present, to ensure specificity of the AtRuvBL1–AtTRB3–AtTERT complex. From these negative controls, it is evident that AtRuvBL1 protein neither directly interacts with the AtTERT 1–271 fragment nor is non-specifically bound to the magnetic beads. Conversely, the presence of AtTRB3 in immunoprecipitation mixture resulted in reproducible and significant increase of the AtRuvBL1 in the immunoprecipitated complex. So, it is evident that AtRuvBL1 is recruited to the AtTERT complex through an interaction with AtTRB3 protein, which mediates interaction of both proteins, AtTERT and AtRuvBL1.

Plant homologue of mammalian dyskerin AtCBF5 associates with AtTRB proteins in the plant nucleus

Mammalian protein dyskerin is a core component of mature and functional telomerase complex (He *et al.*, 2002; Schmidt and Cech, 2015; MacNeil *et al.*, 2016). Dyskerin binds the H/ACA box of small nuclear and nucleolar RNAs (sn- and sno-RNAs) and belongs to conserved scaffold proteins of human hTR (MacNeil *et al.*, 2016). Plant homologue AtCBF5 (also named AtNAP57) is localized within nucleoli and CBs (Lermontova *et al.*, 2007) and associates with enzymatically active telomerase RNP particles in an RNA-dependent manner (Kannan *et al.*, 2008).

Here we observed a clear indirect interaction of AtCBF5, fused with cYFP, with all three examined nYFP/AtTRB proteins using BiFC technique (Figure 5). As has already been discussed above, BiFC analysis can detect the presence of proteins within the same macromolecular complex even without a direct contact between the proteins fused with cYFP/nYFP (Kerppola, 2009). We assume that the interactions between AtCBF5 and AtTRBs are indirect because we

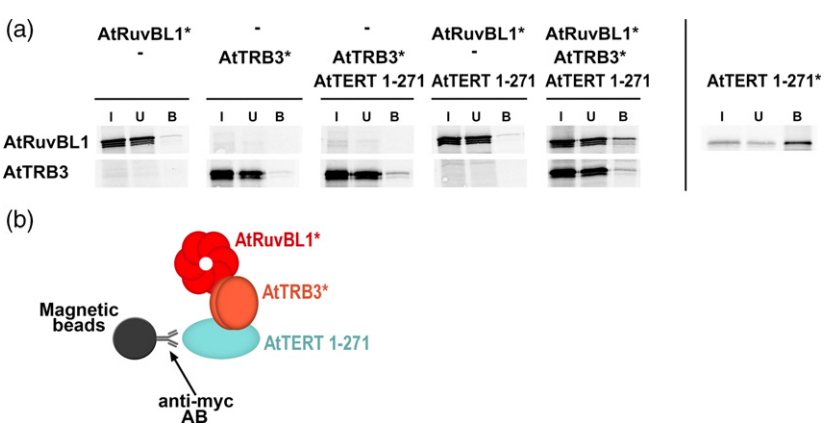

Figure 4. AtTRB3 protein is mediator of AtRuvBL1 and AtTERT interaction.
(a) Co-Immunoprecipitation of the three proteins of interest. Two proteins AtRuvBL1 and AtTRB3 are radioactively labelled by ^{35}S-methionine (marked with asterisks) during the expression in TNT-RRL lysate and subsequently incubated with non-radioactive Myc-tagged AtTERT 1–271 fragment and anti-Myc antibody. In the control experiments, the proteins are incubated with Myc-antibody and protein G-coupled magnetic beads in the absence of one or both partner proteins. Radioactively labeled AtTERT fragment is expressed in parallel tube as a control of the expression. From penult column it is evident that the presence of AtTRB3 results in significant increase of the AtRuvBL1 in the immunoprecipitated complex. I, Input; U, Unbound; B, Bound fractions were collected and run in 12% SDS-PAGE gels.
(b) Schematic depiction of the putative protein complex formed by proteins AtRuvBL1, AtTRB3 and AtTERT. AtRuvBL1 is depicted in its presumed hexameric form and AtTRB3 in its dimeric form.

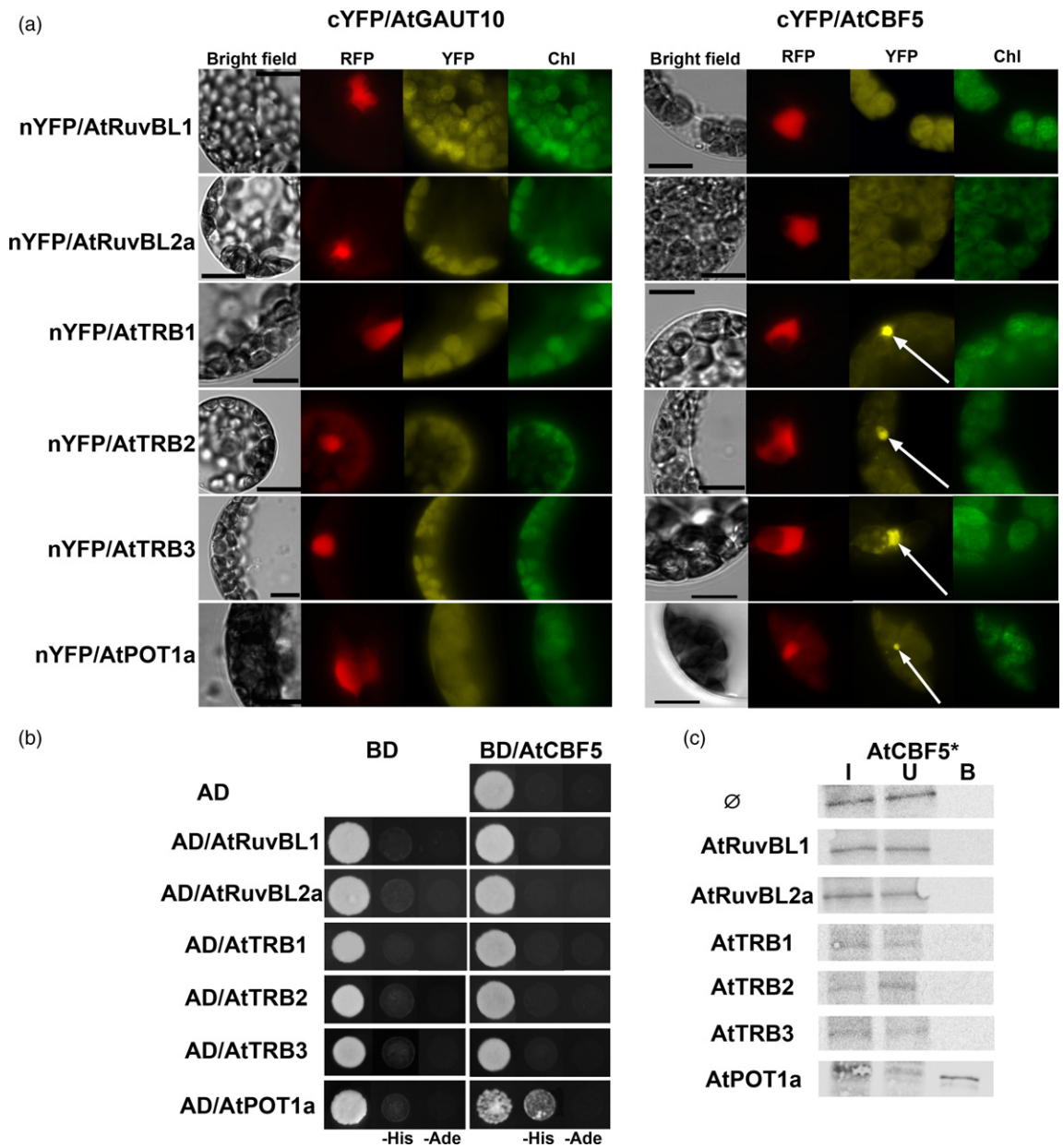

Figure 5. AtCBF5 associates with AtTRB proteins indirectly. The methods are done in the same manner as in Figure 1.
(a) BiFC assay shows indirect interaction between AtCBF5 and three proteins from AtTRB family (AtTRB1-3). AtCBF5 interacts also with AtPOT1a protein. PPIs are marked by white arrows. AtGAUT10, negative control; RFP, nucleus marker; YFP, detects PPI; Chl, Chloroplast autofluorescence. Scale bars represent 10 μm.
(b) Y2H assay analysis does not detect the interaction between AtCBF5 and AtTRB proteins which was found by BiFC. AtCBF5 protein interacts only with AtPOT1a on histidine deficient plate (-His). BD, GAL4 DNA-binding domain; AD, GAL4 activation domain.
(c) Co-IP analysis shows interaction only between AtCBF5 and AtPOT1a protein, fused with Myc-tag and incubated with Myc-antibody and protein G-coupled magnetic beads. I, Input; U, Unbound; B, Bound fractions; asterisks*, ^{35}S-labelling.

were not able to confirm the AtCBF5–AtTRBs interactions observed by BiFC in Y2H mating assay. Also Co-IP did not reveal any iteraction between proteins expressed in TNT–RRL system, fused with Myc-tag (AtRuvBL1, AtRuvBL2a, AtTRB1, AtTRB2 and AtTRB3) and with radioactively labelled AtCBF5 as a prey. Additionally, no interaction was detected between AtCBF5 and any of AtRuvBL proteins neither in BiFC nor in Y2H or Co-IP. As a positive control we used the interaction between AtCBF5 and AtPOT1a. Here we show that the AtCBF5 interacts with AtPOT1a not only in Y2H and Co-IP, as was shown in Kannan *et al.* (2008), but also in the plant nucleus using BiFC assay. In addition to the nucleolar localization of AtPOT1a–AtCBF5 interactions, we also observed this interaction in several

nuclear and cytoplasmic foci (Figure S3). Further, we observed a weak interaction between AtPOT1a–AtRuvBL1 proteins in Y2H and Co-IP assays but not in BiFC system (Figure S4). As a negative control in BiFC assay, we co-transfected protoplasts with cYFP/AtGAUT10. AtGAUT10 protein did not interact with any of the proteins of interest fused with nYFP: AtRuvBL1, AtRuvBL2a, AtTRB1, AtTRB2, AtTRB3 or AtPOT1a. Co-transformation with an empty vector (AD, BD) served as a negative control in Y2H experiments. In Co-IP experiment, the AtCBF5 proteins were incubated with Myc-antibody and protein G-coupled magnetic beads in the absence of partner protein as negative control. Together, we conclude that AtTRB proteins are associated in very close proximity with AtCBF5, the plant homologue of mammalian dyskerin, in the plant nucleus. However, at the same time, AtCBF5 is not localized in the nearby complex with the AtRuvBL proteins *in vivo*.

Association of AtRuvBLs, AtTRBs and AtTERT indicates the formation of their complex in the nucleolus

During the assembly of a fully functional complex of the human telomerase, the mature hTR gets recruited to the nucleolus where it binds the hTERT complex. Both of the core telomerase components, hTR and also hTERT, are previously processed by several proteins, including hRuvBL1 and hRuvBL2. It has already been published that in the interphase, the AtTRB proteins showed preferential localization to the nucleus and specially to the nucleolus (Dvořáčková *et al.*, 2010). In comparison with the mammalian nucleoli, plant nucleoli are larger, more frequently undergo fusions, and sometimes have a central clear region, often called the nucleolar vacuole, the size of which depends on nucleoli transcriptional activity (Shaw and Brown, 2012; Stepinski, 2014).

We analyzed the subcellular localizations of the interactions of our proteins of interest: AtTERT 1-271, AtRuvBL1, AtRuvBL2a, AtTRB3 and AtCBF5 fused with nYFP- or cYFP-tag in routinely performed BiFC experiments. The nucleoli were marked by control plasmid mRFP–AtFibrillarin 1 (Pih *et al.*, 2000). Figure 6 shows interactions between AtRuvBL1–AtTERT, AtTRB3–AtTERT, AtRuvBL1–AtTRB3 and AtRuvBL2a–AtTRB3, which occupy distinct areas within the plant nucleus that match to the plant nucleolus. The number of the PPIs foci localized exclusively in the nucleolus is listed in the Table S1. Similar patterns of nuclear or nucleolar PPI localization is visible also in Figure S5 where the whole nucleus was marked by mRFP–VirD2NLS. However, the AtCBF5–AtTRB3 interaction showed different localization pattern than the other examined PPIs. AtCBF5–AtTRB3 interaction seems to be localized in nucleoli and sometimes in additional nuclear bodies at the periphery or outside the nucleoli, which is consistent with localization of free AtCBF5 (Lermontova *et al.*, 2007). Together, our data indicate formation of AtRuvBLs–AtTRBs–AtTERT complex in the nucleolus.

Dysfunction of *AtRuvBL* genes reduces telomerase activity

In human cells, the hRuvBL1 and hRuvBL2 proteins associate with a significant population of hTERT molecules that do not yield high-level telomerase activity, measured by Telomere Repeat Amplification Protocol (TRAP). The depletion of hRuvBL1 and hRuvBL2 markedly impaired telomerase RNP accumulation and diminished human telomerase activity (Venteicher *et al.*, 2008). To assess whether mutations in *AtRuvBL* genes have any impact on telomerase activity in *A. thaliana*, we set to perform TRAP assay on telomerase extracts isolated from T-DNA insertion mutant lines. Extensive search of several T-DNA

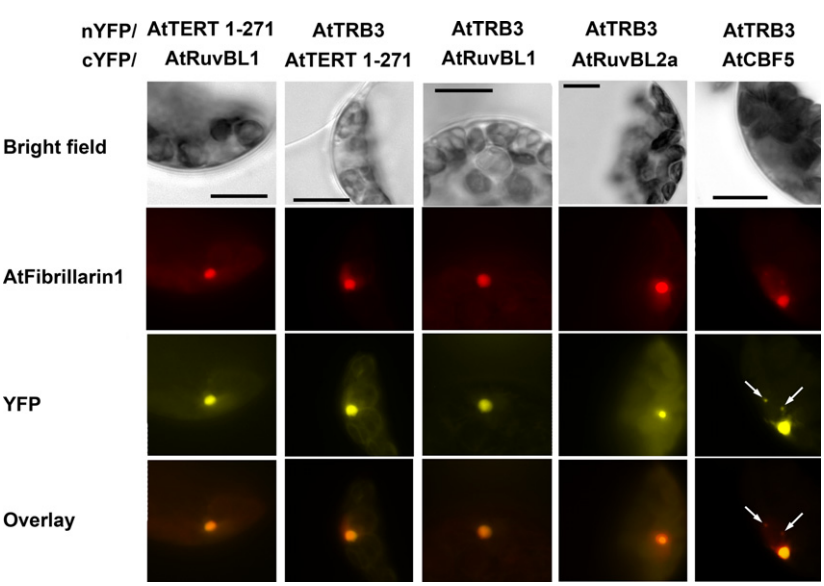

Figure 6. Association of AtRuvBLs, AtTRBs and AtTERT in the nucleolus in *A. thaliana* leaf protoplasts. Protoplasts are co-transfected with mRFP–AtFibrillarin 1 encoding RFP that labels nucleolus and simultaneously with each of the plasmids encoding nYFP-tagged or cYFP-tagged AtRuvBL1, AtRuvBL2a, AtTERT 1–271, AtTRB3 or AtCBF5 to determine PPI localization. AtRuvBL1–AtTERT, AtTRB3–AtTERT, AtRuvBL1–AtTRB3 or AtRuvBL2a–AtTRB3 interactions show nucleolar localization. Plant homologue of mammalian dyskerin, AtCBF5, is associated with AtTRB3 in the nucleolus and in additional nuclear bodies at the periphery of the nucleolus. RFP, marked nucleus; YFP, detects PPI; Scale bars = 10 μm.

insertion lines, which are available from several plant databases, revealed only two suitable plant lines with a limited number of heterozygous mutant plants but with no homozygous mutant plants: SAIL_397_C11 (*AtRuvBL1*) and GK-543F01 (*AtRuvBL2a*). In an additional seven tested T-DNA insertion plant lines we did not detect any viable mutant or heterozygous plants for *AtRuvBL1* or *AtRuvBL2a* genes (Table S2). Furthermore, genotypic ratios of offspring of individual heterozygous plants did not follow the expected Mendelian genotypic ratio. The observed ratio for *AtRuvBL1*$^{+/-}$ and for *AtRuvBL2a*$^{+/-}$ plants was (51:21:0) and (91:10:0), respectively, instead of (1:2:1) (Figure 7a) and the cause of this phenomenon will be further investigated.

Quantitative TRAP assay performed with telomerase extract isolated from flower buds of individual *AtRuvBL2a* heterozygous plants demonstrated that relative telomerase activity showed apparent reduction in comparison with telomerase extract from wild-type *A. thaliana* (Col-0$^{+/+}$) buds (Figure 7b). T-DNA insertion mutation in *AtRuvBL1* gene was lethal (Holt *et al.*, 2002) but we detected viable heterozygous *AtRuvBL1* plants. These plants showed a milder reduction of telomerase activity than *AtRuvBL2a*$^{+/-}$ plants, which supports the assumption that AtRuvBL1 protein is essential for meristem development (Holt *et al.*, 2002).

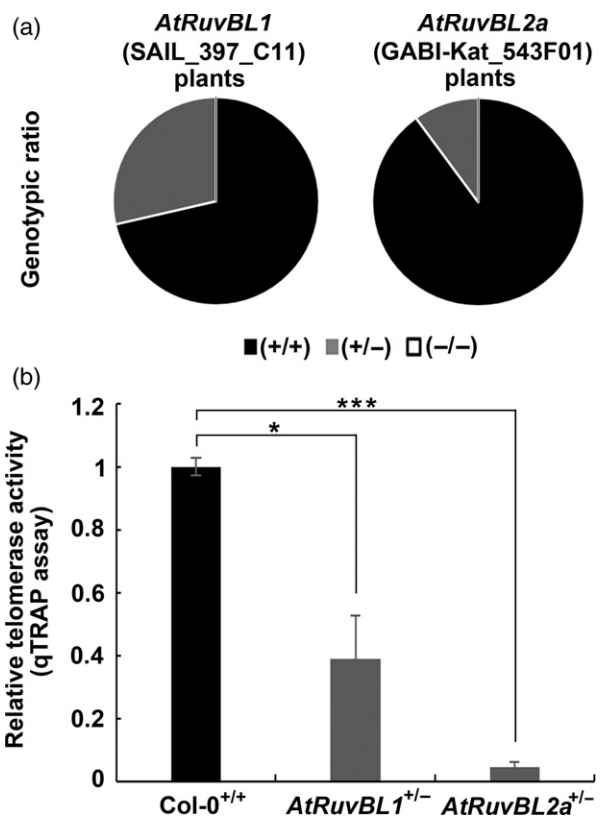

Figure 7. Reduction of relative telomerase activity in heterozygous *AtRuvBL* mutant plants.

(a) Genotypic ratio of the offspring of heterozygous *AtRuvBL1* and *AtRuvBL2a* T-DNA insertion mutant plants. Homozygous mutant plants in *AtRuvBL* genes are fully absent and even the number of heterozygous plants does not follow the Mendelian genotypic ratio.

(b) Samples isolated from *AtRuvBL1*$^{+/-}$ and *AtRuvBL2a*$^{+/-}$ buds are analyzed in three technical replicates by quantitative TRAP. Data are related to wild-type Col-0 sample (telomerase activity in Col-0 buds are arbitrarily chosen as 1). Relative telomerase activity is reduced in both *AtRuvBL1*$^{+/-}$ and especially in *AtRuvBL2a*$^{+/-}$ samples. $P < 0.05$ are considered as significant. Single asterisk denotes $0.01 < P < 0.05$. Three asterisks denote $0.01 < P < 0.001$.

Human RuvBL proteins are direct interactors of transcription factor MYC that is required for expressing many genes involved in cell-cycle transition events and proliferation (Wood *et al.*, 2000). hRuvBL2 regulates MYC-dependent transcription of *TERT* via targeting the hTERT promoter (Wood *et al.*, 2000; Li *et al.*, 2010; Flavin *et al.*, 2011; Zhao *et al.*, 2014). We analyzed the levels of *AtTERT* transcripts in *AtRuvBL1* and *AtRuvBL2a* heterozygous plants to detect whether the decrease of telomerase activity was caused by the negative regulation of AtTERT promoter i.e. the decrease of the abundance of *AtTERT* transcripts. We did not observe significant changes in transcripts of *AtTERT* gene in *AtRuvBL1* heterozygous mutant plants compared with the wild-type *A. thaliana*. Instead, we observed very slight, though significant, increase in *AtTERT* transcripts in *AtRuvBL2a* heterozygous mutant plant lines (Figure S6).

Due to the difficulties in maintaining the heterozygous *AtRuvBL* plant lines for several subsequent generations, we were not able to analyze the transgenerational effects of reduced telomerase activity on telomere lengths in plants heterozygous in *AtRuvBL1* and *AtRuvBL2a* genes. However, in the analyzed generation of *AtRuvBL1*$^{+/-}$ and *AtRuvBL2a*$^{+/-}$ plants that were descendants of heterozygous predecessors, we did not detect any significant changes in telomere lengths compared with the wild-type plants using Terminal Restriction Fragment analysis (TRF) (Figure S7).

Together, we conclude that the depletion of AtRuvBL1 and especially of AtRuvBL2a proteins reduces telomerase activity which suggests a conserved role of AtRuvBL proteins in maturation of functional telomerase complex across the mammals and also plants.

Identification and phylogenetic analysis of the RuvBL family in plants

RuvBL proteins, showing association with TERT in human cells, represent a group of proteins well conserved across all eukaryotic kingdoms, including Fungi, Animalia or Plantae.

Here, we present a genome-wide analysis of RuvBL proteins in 80 vascular plant species, one gymnosperm and two bryophytes, totally 83 taxa, that were analyzed for the presence of all three basic domains (DI, DII, DIII). The evolutionary relationships among the RuvBL proteins were

determined using maximum likelihood analyses based on multiple alignments producing a phylogenetic tree depicting the relationships among all currently accessible RuvBL sequences. The evolutionary hypotheses from these analyses were highly congruent. RuvBL protein family was divided in two distinct groups based on the similarity of sequences and branch length. Sequence similarity between RuvBL1 and RuvBL2 is generally low, about 35–40% while the sequence similarity within RuvBL subfamilies is about 80%. For instance, in *A. thaliana* AtRuvBL2a and AtRuvBL2b share 82% similarity. On the other hand, AtRuvBL1 with AtRuvBL2a or AtRuvBL1 with AtRuvBL2b share 37.5 and 38.8% similarity, respectively. However, only a subset of RuvBL1 was clearly separated (100% BS; blue branch in Figure 8). Surprisingly, based on BLAST search, RuvBL1 was found only in dicots and basal angiosperms (*Amborella trichopoda*) up to now, RuvBL2 was represented in both, dicots and monocots from angiosperms, but also in gymnosperms (*Picea sitchensis*) and bryophytes (*Physcomitrella patens* and *Marchantia polymorpha*). The number of the homologues varied from 1 to 8 (Data S1 and S2).

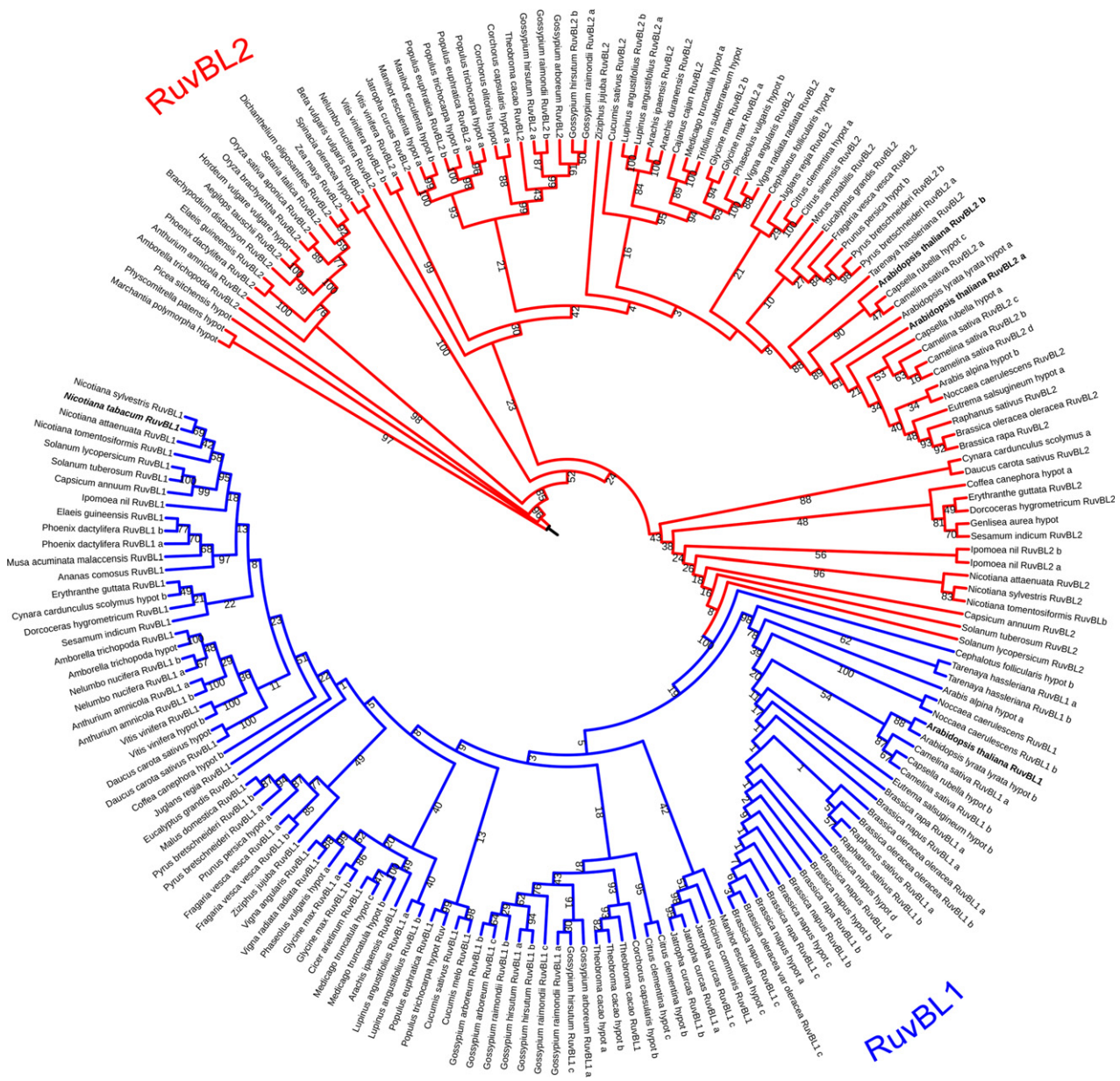

Figure 8. Phylogenetic analysis of the RuvBL family in plants.
Unrooted phylogenetic tree of 190 proteins sequences of RuvBL family with enumerated plant species. Numbers above branches means bootstrap support values. Orthologues from *Arabidopsis thaliana* and *Nicotiana tabacum* are in bold letters.

DISCUSSION

The formation of functional and enzymatically active telomerase, a multisubunit RNP complex, is a dynamic process governed by number of cofactors. In mammals, hRuvBL1 and hRuvBL2 proteins, Pontin and Reptin, respectively, are present in early steps of telomerase RNP biogenesis. We characterized plant homologues of RuvBL proteins: AtRuvBL1 and AtRuvBL2a, previously co-purified together with telomerase protein subunit AtTERT from *A. thaliana* suspension cultures (Majerská *et al.*, 2017). Here we show that AtRuvBL1 protein colocalizes with N-terminal part of AtTERT subunit of plant telomerase also *in vivo*. However, in contrast with the AtRuvBL mammalian counterparts, their interaction in plants seems to be indirect. Association of AtRuvBL proteins with AtTERT in the plant nucleolus appears to be bridged by telomeric AtTRB proteins. Requirement of AtRuvBL proteins for a proper telomerase assembly is endorsed by the fact that depletion of AtRuvBL1 and especially of AtRuvBL2a protein, reduces telomerase activity in plants heterozygous for *AtRuvBL1* or *AtRuvBL2a* genes. Moreover, AtTRB proteins are associated in the plant cell with a homologue of mammalian dyskerin, AtCBF5, that plays a role in telomerase RNP biogenesis and directly interacts with AtPOT1a protein. AtTRB proteins thus play a role of interaction hubs not only in telomere chromatin structure but also in telomerase biogenesis. AtRuvBL proteins are able to multimerize, which is analogous to the situation in mammalian cells, and our data show preference to form mutual heteromers. Detailed summary of protein–protein interactions between AtRuvBLs, AtTRBs, AtTERT fragments, AtPOT1s and AtCBF5 proteins, that have been detected using BiFC, Y2H or Co-IP assays in this and other relevant publications, are given in the Table 1.

Our detailed phylogeny proved that RuvBL proteins are evolutionarily conserved in land plants and implied plausible functional conservation of the RuvBL proteins. However, further biochemical validation of the possible conservation of mutual RuvBL–TRB interaction across the plant kingdom can be limited by the fact that the number of paralogues varies from 1 to 8 members in between RuvBL proteins. The multiplication of genes of the same family is not surprising as, in many plant families, the polyploidy (i.e. whole-genome duplication, WGD), resulting in retention of multiple gene paralogs may lead to their sub-functionalization, neo-functionalization or partial or full redundancy (Mandakova and Lysak, 2008; Freeling, 2009). These limitations might be deteriorated by the fact that the AtRuvBL proteins can be involved in a similar biochemical pathway but their interaction partners might slightly differ (this paper; Venteicher *et al.*, 2008).

RuvBL proteins are involved in various cellular processes

The exact function even of mammalian RuvBL proteins is still quite unknown as they interact with many molecular complexes with vastly different downstream effectors (Mao and Houry, 2017). Among others, hRuvBL2 was shown to regulate hTERT promoter likely through the regulation of MYC (c-myc), the transcription factor for *TERT* (Wood *et al.*, 2000; Li *et al.*, 2010; Flavin *et al.*, 2011; Zhao *et al.*, 2014). We observed no significant changes in transcripts of *AtTERT* gene in *AtRuvBL1* heterozygous mutant plants, however we detected a very slight increase in transcripts of *AtTERT* gene in *AtRuvBL2a* heterozygous plants. Although the transcript levels of *AtTERT* gene were slightly increased in *AtRuvBL2a* heterozygous plant lines, we observed a very significant reduction of telomerase activity

Table 1 A summary table of protein–protein interactions

	AtRuvBL1	AtRuvBL2	AtTRB1	AtTRB2	AtTRB3	AtTERT (1-233)	AtTERT (1-271)	AtTERT (1-582)	AtTERT (229-582)	AtTERT (597-987)	AtTERT (958-1123)	AtCBF5
AtRuvBL1	●●●$^{\alpha}$											
AtRuvBL2a	●●●$^{\alpha\eta}$	●●●$^{\alpha}$										
AtTRB1	●xx$^{\alpha}$	xxx$^{\alpha}$	-●●$^{\beta}$									
AtTRB2	xxx$^{\alpha}$	●●●$^{\alpha}$	-●●$^{\beta}$	–●–$^{\delta}$								
AtTRB3	●●●$^{\alpha}$	●●●$^{\alpha}$	-●●$^{\beta}$	–●–$^{\delta}$	–●–$^{\delta}$							
AtTERT (1-233)	●xx$^{\alpha\eta}$	xxx$^{\alpha}$	-x-$^{\omega}$	-x-$^{\omega}$	-x-$^{\omega}$	–x–$^{\eta}$						
AtTERT (1-271)	●xx$^{\alpha\eta}$	xxx$^{\alpha}$	●●●$^{\gamma}$	●●●$^{\gamma}$	●●●$^{\gamma}$	–x–$^{\eta}$	–●–$^{\eta}$					
AtTERT (1-582)	---	---	-●●$^{\gamma}$	-●●$^{\gamma}$	-●●$^{\gamma}$	–x–$^{\eta}$	–●–$^{\eta}$	–x–$^{\eta}$				
AtTERT (229-582)	xxx$^{\alpha}$	xxx$^{\alpha}$	●x●$^{\gamma\omega}$	●x●$^{\gamma\omega}$	●x●$^{\gamma\omega}$	–x–$^{\eta}$	–●–$^{\eta}$	–●–$^{\eta}$	–●–$^{\eta}$			
AtTERT (597-987)	xxx$^{\alpha}$	xxx$^{\alpha}$	-x-$^{\omega}$	-x-$^{\omega}$	-x-$^{\omega}$	–x–$^{\eta}$	–x–$^{\eta}$	–x–$^{\eta}$	–x–$^{\eta}$	–x–$^{\eta}$		
AtTERT (958-1123)	xxx$^{\alpha}$	xxx$^{\alpha}$	---	---	---	–x–$^{\omega}$	–x–$^{\omega}$	–x–$^{\omega}$	–x–$^{\omega}$	–x–$^{\omega}$	---	
AtCBF5	xxx$^{\alpha}$	xxx$^{\alpha}$	●xx$^{\alpha}$	●xx$^{\alpha}$	●xx$^{\alpha}$	---	---	---	---	---	---	---
AtPot1a	x●●$^{\omega}$	xxx$^{\omega}$	xx-$^{\omega}$	xx-$^{\omega}$	xx-$^{\omega}$	-●●$^{\zeta}$	●●●$^{\eta\zeta}$	–x–$^{\zeta}$	–x–$^{\zeta}$	–x–$^{\zeta}$	–x–$^{\zeta}$	●●●$^{\alpha\varepsilon}$
AtPot1b	xxx$^{\omega}$	xxx$^{\omega}$	-●●$^{\beta}$	-●-$^{\beta}$	-●-$^{\beta}$	–x–$^{\zeta}$	–x–$^{\zeta}$	---	---	---	---	xxx$^{\omega}$

●●●	BiFC, Y2H, Co-IP
●	INTERACTION
x	NO interaction
–	n.a. = not analysed
●	this publication
●	other relevant publications
α	this publication
β	Schrumpfova et al., 2008
γ	Schrumpfova et al., 2014
δ	Schrumpfova et al., 2004
ε	Kannan et al., 2008
ζ	Rossignol et al., 2007 (TERT fragments differ)
η	Majerská et al., 2017
ω	data not shown

Summary table shows all interactions between AtRuvBLs, AtTRBs, AtTERT fragments, AtPOT1s and AtCBF5 proteins that are detected using BiFC, Y2H or Co-IP assays.

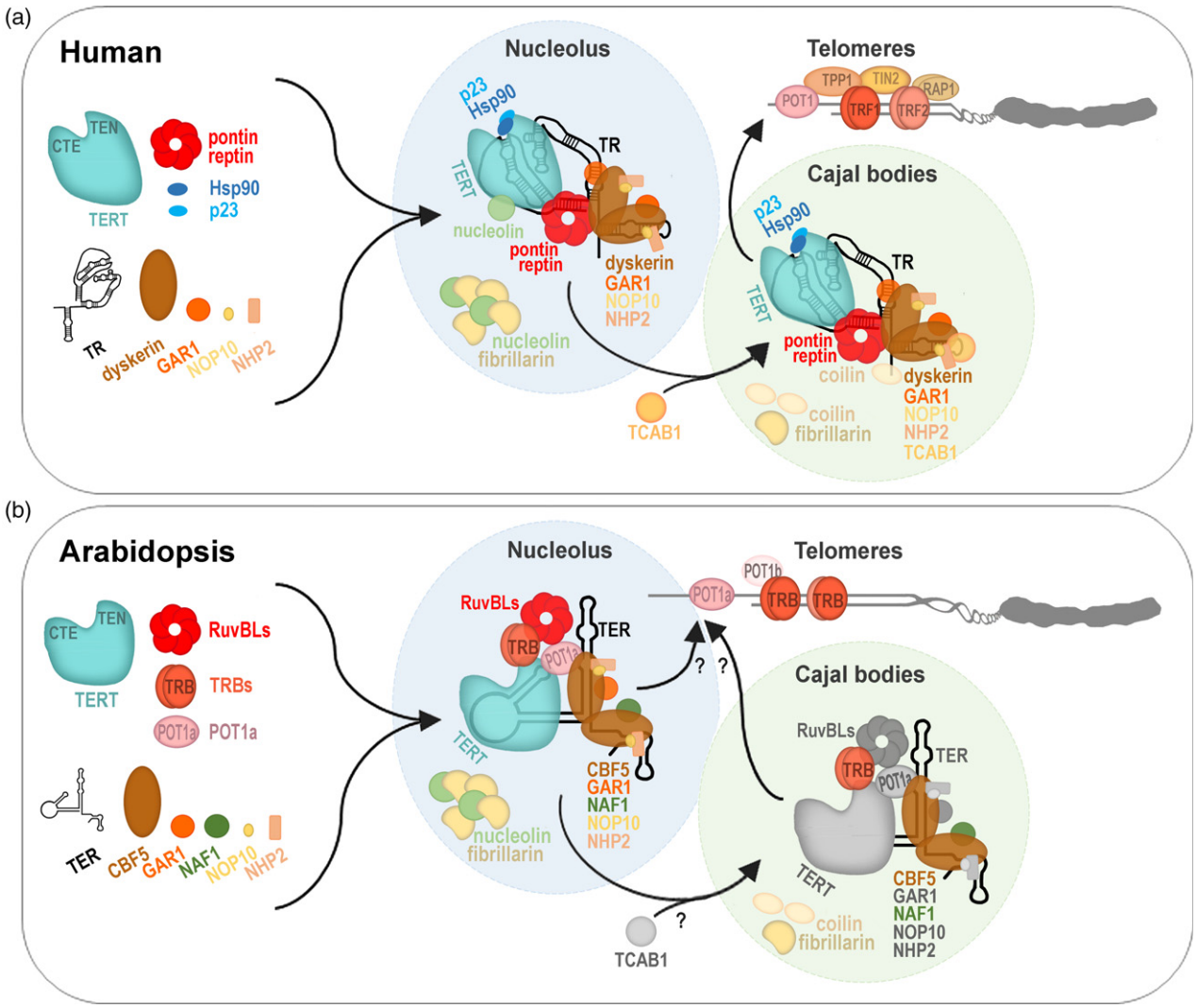

Figure 9. Comparative model of telomerase assembly in human and *Arabidopsis*.
(a) Human TR binds dyskerin, NHP2, NOP10, and GAR1 and human TERT associates with the chaperones Hsp90 and p23. The telomerase RNP is retained into the nucleoli through the interaction between TERT and nucleolin. Assembly of TR and TERT into catalytically active telomerase is aided by Pontin (hRuvBL1) and Reptin (hRuvBL2) AAA+ ATPases. Telomerase is recruited to Cajal bodies (CBs) by its interaction with TCAB1. The CBs will colocalize with telomeres, and telomerase is recruited to telomeres by the interaction with the shelterin component TPP1 (MacNeil *et al.*, 2016; Lim *et al.*, 2017).
(b) Arabidopsis CBF5, GAR1, NOP10, NHP2, but in contrast with human cells also NAF1, were localized into the plant nucleolus (Pendle *et al.*, 2005; Lermontova *et al.*, 2007). In the plant nucleolus, we observe colocalization of TERT with RuvBL AAA+ ATPases complex bridged by telomeric TRB proteins, as well as the interaction of telomeric protein POT1a with CBF5. *Arabidopsis* telomeres cluster at the periphery of the nucleolus which is mediated by the presence of nucleolin. Recruitment of the mature telomerase complex to telomeres with or without commitment of CBs in *Arabidopsis* needs further investigation. Proteins that were already proven as associated with CBs are highlighted in color in Cajal bodies. Proteins that have not yet been experimentally proven as CBs associated are marked with black and white.

in these plants. Telomerase activity was reduced also in *AtRuvBL1* heterozygous T-DNA insertion plant lines. To verify whether the regulation of telomerase activity was affected due to the compromised assembly of telomerase complex rather than due to regulation of transcript levels of *AtTERT* gene in AtRuvBL-dependent manner, however, needs further investigation.

The participation of RuvBL proteins in heterogeneous cellular process as well as their association with specific interactors can vary between cytoplasm, nucleus and nucleolus (Mao and Houry, 2017). It seems that, also in *A. thaliana*, the function of AtRuvBL proteins is not specific only to the telomerase assembly, as they were suggested as regulators of disease resistance (R) genes (Holt *et al.*, 2002). It has already been published that AtRuvBL1 is essential in meristem development (Holt *et al.*, 2002), the function consistent with its function in telomerase assembly observed in this work. Our extensive, but unsuccessful,

effort to receive homozygous mutant plants in several T-DNA insertion lines mutant in the *AtRuvBL1* and *AtRuvBL2a* genes also indicated the essentiality of AtRuvBL proteins in various cellular processes in plants. Furthermore, genotypic ratio of offspring of individual heterozygous plants does not follow the Mendelian genotypic ratio, indicating that both AtRuvBL proteins are essential regulators of plant development. Therefore, we suggest to investigate the function of AtRuvBLs in plant sporophyte or female gametophyte development in future studies.

Nucleolus localization of telomerase assembly complex

Telomere maintenance requires a proper assembly of the TERT and TR components of telomerase into RNP as well as a number of cofactors involved in maturation, stability and subcellular localization of telomerase. In mammals, the association of hTR RNP with hTERT proceeds in the nucleolus during the early S-phase (Lee *et al.*, 2014). Assembled and catalytically active telomerase RNP separates from the nucleoli and is transported to CBs during the S-phase for subsequent recruitment to telomeric chromatin and telomere extension (Figure 9a) (MacNeil *et al.*, 2016). Association of hTERT with human RuvBL proteins, Pontin and Reptin, peaks in S-phase, which may reflect cell-cycle regulation of total TERT and/or assembly of telomerase on telomeres (Venteicher *et al.*, 2008). RuvBL1 and RuvBL2a proteins, together with, for example, Fibrillarin 1 and many other proteins, were purified and identified in nucleoli isolated from *A. thaliana* cell culture protoplasts (Pendle *et al.*, 2005). Our data indicated that plant homologues of human Pontin and Reptin, the AtRuvBL proteins, are associated in the plant nucleolus with AtTERT, together with AtTRB proteins (Figure 9b). AtTRB proteins are highly dynamic and during the interphase, they are preferentially localized to the nucleolus or nuclear bodies of different size (Dvořáčková, 2010). AtTRBs behave as typical nucleolar resident proteins, being largely dispersed at prophase, coinciding with nucleolar disassembly. However, a small but detectable amount of the protein remains associated with the chromatin throughout mitosis (Azum-Gelade *et al.*, 1994; Dvořáčková *et al.*, 2010). Similarly, to the AtTRB proteins, also the N-terminal part of AtTERT was detected in the nucleoli in *A. thaliana* (Rossignol *et al.*, 2007; Zachová *et al.*, 2013).

In mammals, the telomerase RNP is retained in nucleoli through the interaction between hTERT and nucleolin in the dense fibrillar component (Khurts *et al.*, 2004; Lee *et al.*, 2014). In *A. thaliana*, null mutants for the nucleolar protein NUCLEOLIN 1 cause telomere shortening on all chromosome arms (Pontvianne *et al.*, 2016). Telomeres in *A. thaliana* do not form a Rabl conformation, as in some other species, but telomeres and their flanking regions strongly associated with the nucleolus in a rosette-like organization (Armstrong *et al.*, 2001; Fransz *et al.*, 2002; Roberts *et al.*, 2009; Pontvianne *et al.*, 2016; Schrumpfová *et al.*, 2016a). Our data indicated the presence of AtTERT–AtTRB–AtRuvBL complex in the nucleolus. Nucleolar localization of the AtTERT–AtTRB–AtRuvBL complex together with the close proximity of telomeres to the nucleolus, suggested the conservation of the recruitment of the maturating telomerase to the nucleolus during the telomerase assembly. Figure 9 shows a comparative model of the assembly and localization of telomerase in mammalian and plant cells.

Plausible conservation of the telomerase trafficking pathway

Cajal bodies are spherical suborganelles localized in the nucleoplasm either in the vicinity of the nucleolus and/or they are present free. The function of CBs is not completely understood, but they were implicated mainly in snRNAs synthesis and processing. CBs also contribute to the biogenesis of telomerase. In S-phase, CBs colocalize with telomeres and facilitate recruitment of the mature mammalian telomerase complex to the telomeres. Human dyskerin, hNHP2, hNOP10 and hGAR1, that displaces hNAF1 in the hTR RNP, belong to conserved scaffold proteins, which colocalize with CBs and are involved in hTR RNP assembly (MacNeil *et al.*, 2016). Expression of putative *AtGAR1*, *AtNOP10*, *AtNHP2* genes encoding protein components of the H/ACA box snoRNP complex correlate with that of *AtCBF5*, a plant homologue of dyskerin (Lermontova *et al.*, 2007). AtCBF5 directly interacts with AtNAF1 (Lermontova *et al.*, 2007) and has been identified as a component of the enzymatically active *A. thaliana* telomerase RNP (Kannan *et al.*, 2008). AtCBF5 localizes in nucleoli and sometimes in additional nuclear bodies at the periphery or outside the nucleoli, but AtCBF5 also colocalizes with TMG-capped snRNA, a marker for CBs (Lermontova *et al.*, 2007).

Here we show that plant dyskerin, AtCBF5, indirectly interacts with AtTRB proteins in the plant nucleolus or in other nuclear bodies. It has already been published that AtTRBs are located not only in the nucleolus but also in nuclear bodies of different size, some of which might be CBs (visualized by a marker protein Coilin) (Dvořáčková, 2010). Dvořáčková detected significant colocalization of AtTRB1 with Coilin present in the CBs adjacent to the nucleolus. However, no colocalization was detected between signals corresponding to the AtTRB1 and free CBs in the nucleoplasm. Presence of AtTRB1 protein entirely in the CBs adjacent to the nucleoli implies a potential conservation of the trafficking pathway during the telomerase maturation, which comprises movement of maturating telomerase complex through nucleolus to CBs and finally to the telomeres. Notably, not all the organisms (e.g. budding yeast and ciliates) rely on the CBs trafficking since telomerase RNAs from these species do not have H/ACA or CAB box motifs, and further studies

are needed to prove this hypothesis. We observe that interaction between AtCBF5 and AtPOT1a is localized mostly in the nucleolus but in few cases also in cytoplasmic foci. The cytoplasmic localization is not surprising as it has already been shown that plant AtPOT1a and AtPOT1b, as well as their human homologue hPot1, are localized in the nucleus, as well in the cytoplasm (Chen *et al.*, 2007; Rossignol *et al.*, 2007).

The assembly of hTR RNP to the telomerase holoenzyme is not fully elucidated and it is highly complex multistep process. Therefore, the absence of the interaction between AtCBF5 and AtRuvBLs in the plant nucleus in our experiments is also not surprising. For example, Machado-Pinilla *et al.* (2012) showed that dyskerin was sandwiched between two hSHQ1 domains in the first steps of the biogenesis of telomerase. C-terminal tail of hCBF5 was essential for hSHQ1 release mediated by hRuvBLs. However, a stable interaction with the tails is not a part of the process because hRuvBLs bind to hCBF5 in a pull-down assay, even in the absence of its tail. Assembly of functional AtTER RNP, as well as the assembly of mammalian hTR RNP, is certainly a multistep process that may include AtTER, AtCBF5, AtTRBs, AtRuvBLs, AtPOT1a and many other factors, whose presence/participation/mutual interactions will be the subjects of our future research. Dynamics and complexity of mutual interactions can be demonstrated by the fact that we detect the interacting complex of AtCBF5–AtPOT1a in the nucleolus or in the cytoplasmic and nuclear foci using BiFC assay, while AtCBF5–AtTRBs interactions are localized entirely to the nucleoli and additional nuclear bodies. Moreover, association of AtTRB3 with AtTERT and AtRuvBLs is entirely localized to the nucleolus.

Concluding remarks

Homologues of the mammalian Pontin and Reptin, named RuvBL proteins, as well as TRB proteins, might be involved in diverse processes in the plant cell. AtTRB proteins are not only components of terminal complex associated with telomeres and catalytic subunit of telomerase, AtTERT (Schrumpfová *et al.*, 2016a, 2019), but they also serve as epigenetic regulators that potentially impact the transcription status of thousands of genes as subunits of epigenetically active multiprotein complexes (Lee and Cho, 2016; Schrumpfová *et al.*, 2016b; Zhou *et al.*, 2016; Dokládal *et al.*, 2018; Tan *et al.*, 2018). AtRuvBL1 protein has been assumed as a regulator of R genes so far and is essential in meristem development (Holt *et al.*, 2002). Here we suggest involvement of AtRuvBL proteins in telomerase assembly pathway in *A. thaliana*. We detected new interactions of AtTRB proteins with AtRuvBL proteins, localized the AtTERT–AtTRB–AtRuvBL complex exclusively in the nucleolus and observed that heterozygous T-DNA insertion mutants in *AtRuvBL1* or *AtRuvBL2a* genes showed reduced telomerase activity. Further, our results showed interactions of AtCBF5, the plant orthologue of dyskerin, with AtTRB and AtPOT1, but not with the AtRuvBL proteins, which expanded our knowledge on the telomerase assembly process. Indispensability of the AtRuvBL proteins for the plant development was supported by our finding that homozygous *atruvbl1* and *atruvbl2a* mutant plants were not viable. Furthermore, we identified new homologues RuvBL proteins and analyzed their evolutionary relationships in plants. Altogether, our data show that the plant homologues of Pontin and Reptin, AtRuvBLs, and also AtTRB are involved in telomerase assembly and suggest conservation of telomerase trafficking pathway via the nucleolus to the telomeres in plants.

EXPERIMENTAL PROCEDURES

Searching transcriptomes and genomes for RuvBL homologues

RuvBL homologues were identified by BLASTP searches using *A. thaliana* proteins from the TAIR database (https://www.arabidopsis.org/) to query NCBI protein databases (http://www.ncbi.nlm.nih.gov/). The BLASTP searches used default parameters, adjusted to the lowest *E*-value. The duplicates from all searches were eliminated. We conducted an iterative search of the UniProt database (http://www.uniprot.org/) and the Phytozome version 11 database (https://phytozome.jgi.doe.gov) was next searched for proteins not found by BLASTP. We analyzed all sequences independently of their annotations, with no prior assumptions. Information summary of accession numbers for RuvBL are in Data S1 and S2.

Sequence alignment

Amino acid sequences were aligned using the Clustal Omega algorithm (Sievers *et al.*, 2011) in the Mobyle platform (Neron *et al.*, 2009), with homology detection by HMM-HMM comparisons (Soding, 2005). Protein isoforms with the same length were also used, because the differential expression patterns producing protein isoforms from various tissues suggested that isoforms could have different biological functions *in vivo* (Chen *et al.*, 2014).

Phylogenetic reconstruction

Maximum likelihood (ML) analyses of the matrices were performed in RAxML 8.2.4 (Stamatakis, 2014) to examine differences in optimality between alternative topologies. Using the Akaike information criterion as implemented in Modeltest 3.8 (Posada and Crandall, 1998), a GTR+I+Γ model was chosen as the best-fitting model, and 1000 replications were run for bootstrap values. The final data set for RuvBL contained 190 proteins of different species and length 576 bp. Phylogenetic trees were constructed and modified with iTOL v3.4 (Letunic and Bork, 2016).

Transgenic constructs

The Gateway-compatible donor and destination vectors carrying the AtTERT (AtTERT 1-233, 1-271, 229-582, 597-987, 958-1123) fragments were described in Zachová *et al.* (2013). The Gateway-compatible donor vectors carrying AtRuvBL1, AtRuvBL2a, AtPOT1a, AtPOT1b and AtGAUT10 were described in Majerská *et al.* (2017). The AtTRB1, 2 and 3 constructs have described previously (Schrumpfová *et al.*, 2014).

The cloned cDNA sequence of AtCBF5 (GC105080 from Arabidopsis Information Resource (http://www.arabidopsis.org/)) in pENTR223 was used as entry vector. For preparation of yeast two-hybrid (Y2H) and/or BiFC constructs, DNA fragments were introduced into the destination Gateway vectors pGBKT7-DEST, pGADT7-DEST (Horak *et al.*, 2008) and/or the pSAT5-DEST-c(175-end)EYFP−C1(B), pSAT4-DEST-n(174)EYFP−Cl (Lee *et al.*, 2012) using the LR recombinase reaction (Invitrogen, Carlsbad, CA, USA).

PCR-based genotyping of plant lines

Plants with annotated T-DNA insertion within *AtRuvBL1* gene (SAIL_397_C11, WiscDsLoxHs027_03G, WiscDsLoxHs117_06F, WiscDsLoxHs168_06D) and *AtRuvBL2a* gene (GK-543F01, SALK_071103, SALK_144539, SALK_144540, SAIL_500_C04) in the Col-0 background were used (Figure S8). To distinguish between wild-type plants and those that were heterozygous for the T-DNA insertion in the *AtRuvBL1* or *AtRuvBL2a* genes, we isolated genomic DNA from leaves by the standard protocol of Dellaporta *et al.* (1983). The genomic DNA was used for PCR analysis using MyTaq DNA polymerase (Bioline, http://www.bioline.com). The conditions used were in accordance with the manufacturer's instructions. The primers used were specific for T-DNA and *AtRuvBL1* or *AtRuvBL2a* genes (Table S3, Figure S9). Thermal conditions were 95°C for 1 min (initial denaturation), followed by 30 cycles of 95°C for 30 sec, 60°C for 30 sec and 72°C for 1 min 20 sec, with a final extension at 72°C for 10 min.

RT-PCR

Total RNA was extracted from approximately 100 mg of frozen young leaves using an RNeasy plant mini kit (Qiagen, Venlo, Netherlands) and RNA samples were treated with TURBO DNA-free (Applied Biosystems/Ambion, http://www.lifetechnologies.com TURBO DNA-free). The quality and quantity of RNA were determined by electrophoresis on 1% w/v agarose gels and by measurement of absorbance using NanoDrop™ 2000/2000c spectrophotometer (https://www.thermofisher.com/). Reverse transcription was performed using random nonamers (Sigma-Aldrich, http://www.sigmaaldrich.com) with 1 μg RNA and Mu-MLV RT (New England Biolabs, https://www.neb.com/). Quantification of transcript levels of the *AtRuvBL1*, *AtRuvBL2a* (Figure S10) and *AtTERT* genes (Fojtová *et al.*, 2011) was carried out by FastStart I SYBR Green Master (Roche, Basel, Switzerland), a Rotorgene 6000 cycler (Qiagen) and using the Ubiquitin-10 gene as suitable references for quantitative analyses in *A. thaliana.* A 2 μl aliquot of cDNA, from two biological replicates, were added to the 20 μl reaction mix; the final concentration of each forward and reverse primer (sequences are given in Table S3) was 0.25 μM. Three technical replicates were done for each reaction that was measured in triplicates; the PCR cycle consisted of 15 min of initial denaturation followed by 40 cycles of 15 sec at 95°C, 20 sec at 56°C and 30 sec at 72°C. SYBR Green I fluorescence was monitored consecutively after the extension step (Fojtová *et al.*, 2011) sequences of primers are given in Table S3. Statistical analysis was performed using unpaired Student's *t*-test.

Quantitative TRAP assay

Protein extracts from buds were prepared as described by Fitzgerald *et al.* (1996). qTRAP analysis was performed as described in Herbert *et al.* (2006) using FastStart SYBR Green Master (Roche) and TS21 and TEL-PR primers. Samples were analyzed in triplicate. A 1 μl aliquot of extract diluted to 50 ng μl^{-1} protein concentration was added to the 20 μl reaction mix. Ct values were determined using the Rotorgene 3000 (Qiagen) machine software, and relative telomerase activity was calculated by the ΔCt method (Pfaffl, 2004).

TRF analysis

TRF analysis was performed as described previously (Ruckova *et al.*, 2008) using 500 ng genomic DNA isolated from 5 to 7 weeks old rosette leaves using NucleoSpin Plant II (Machery Nagel). Hybridized samples (Hybond XL, GE Healthcare, Chicago, IL, USA) by Southern hybridization method were radioactively marked by random priming, in which the telomeric probe was prepared according to a modified protocol from Ijdo *et al.* (1991). Telomeric signals were visualized using an FLA7000 imager (Fujifilm, Tokyo, Japan). Evaluation of fragment lengths was performed using a Gene Ruler 1 kb DNA ladder (Fermentas, http://www.thermoscientificbio.com/fermentas/) as the standard. Mean telomere lengths were calculated as described by Grant *et al.* (2001).

Yeast two-hybrid assay

Yeast two-hybrid experiments were performed using the Matchmaker TM GAL4-based two-hybrid system (Clontech, Kyoto, Japan) as described in Schrumpfová *et al.* (2014). *AtRuvBL1* and *AtRuvBL2a* constructs from pDONR/221 entry clones were subcloned into the Gateway-compatible destination vector pGBKT7-DEST (bait vector) and pGADT7-DEST (prey vector). cDNA sequences encoding *AtTERT* fragments from pDONR/221 entry clones and *AtCBF5* from PENTR223 entry clone were subcloned into the Gateway-compatible destination vector pGBKT7-DEST (bait vector). *AtPOT1a* constructs were subcloned from pDONR/221 entry clones into the Gateway-compatible destination vector pGADT7-DEST (prey vector). The pGADT7 prey vectors (Clontech) carrying *AtTRB1-3* and *AtPOT1a* have been described previously (Schrumpfová *et al.*, 2008). Successful co-transformation of each bait/prey combination into *Saccharomyces cerevisiae* PJ69-4a was confirmed on SD plates lacking Leu and Trp, and positive interactions were selected on SD medium lacking Leu, Trp and His (with or without 3-aminotriazol (3-AT)) or SD medium lacking Leu, Trp and Ade. Co-transformation with an empty vector and homodimerization of the AtTRB1 protein served as negative and positive control, respectively (Schrumpfová *et al.*, 2014). Protein expression was verified by immunoblotting in equal amounts of protein extracts separated by SDS-PAGE (12%), blotted onto nitrocellulose membrane, and probed with mouse anti-Myc (1:1000; Sigma-Aldrich) and mouse anti-HA (1:1000) primary antibodies binding to specific protein epitope tags of AD- and BD-fusion proteins, followed by an anti-mouse HRP-conjugated secondary antibodies (1:8000; Sigma-Aldrich) for chemiluminescence detection.

In vitro translation and co-immunoprecipitation

Additionally, the Y2H constructs were employed for verification in assay as described in Schrumpfová *et al.* (2008). Briefly, radioactively (^{35}S-Met) labelled proteins with hemagglutinin tag (HA) (pGADT7, pGADT7-DEST), as well as non-radioactively labelled protein partners with a Myc-tag (pGBKT7, pGBKT7-DEST) were separately expressed in the TNT Quick Coupled Transcription/Translation System (TNT-RRL) (Promega, Fitchburg, WI, USA) in 50 μl of each reaction according to the manufacturer's instructions. The co-immunoprecipitation procedure was performed as described by Schrumpfová *et al.* (2008) with 1 μg anti-Myc-tag polyclonal antibody (Sigma-Aldrich, St. Louis, MO, USA) and incubated overnight at 4°C with 10 μl protein G magnetic particles (Dynabeads, Invitrogen-Dynal).

During the co-immunoprecipitation with three proteins of interest, two radioactively labeled proteins with HA-tag (AtRuvBL1, AtTRB3) and one non-radioactively labeled AtTERT 1-271 fragment with Myc-tag were expressed separately in TNT-RRL and incubated in the same manner as previous Co-IP together with protein G magnetic particles (Dynabeads, Invitrogen-Dynal) and 1 μg anti-Myc-tag polyclonal antibody (Sigma). Input, Unbound and Bound fractions were separated by 12% SDS-PAGE and analyzed by FLA7000 imager (Fujifilm).

Bimolecular fluorescence complementation

Arabidopsis thaliana leaf protoplasts were prepared and co-transfected with DNA (10 μg of each construct) as was described in Lee *et al.* (2012). The same entry vectors (pDONR/221, PENTR223), already used for *AtRuvBL1*, *AtRuvBL2a*, *AtTERT* fragments, *AtCBF5* and *AtPOT1a* Y2H constructs cloning (Majerská *et al.*, 2017) or entry vectors used for cloning *AtTRB1-3* (Schrumpfová *et al.*, 2008) were ligated into pSAT5-DEST-c(175-end)EYFP−C1(B), pSAT4-DEST-n(174)EYFP−CI vectors. As a negative control, we used the cYFP/AtGAUT10 construct. To control transformation efficiency and to label cell nuclei, we co-transfected a plasmid expressing mRFP fused to the nuclear localization signal of the VirD2 protein of *A. tumefaciens* (mRFP−VirD2NLS; Citovsky *et al.*, 2006). To label nucleolus we co-transfected a plasmid expressing mRFP fused to the to *AtFibrillarin 1* (Pih *et al.*, 2000). Transfected protoplasts were incubated in the light, at room temperature overnight, and then observed for fluorescence using a Zeiss AxioImager Z1 epifluorescence microscope equipped with filters for YFP (Alexa Fluor 488), RFP (Texas Red) and CY5 (chloroplast autofluorescence). The mRFP−VirD2NLS and AtGAUT10−cEYFP constructs for BiFC experiments were kindly provided by Prof. Stanton B. Gelvin (Purdue University, USA).

ACCESSION NUMBERS

AtRuvBL1 (AT5G22330); *AtRuvBL2a* (AT5G67630); *AtTERT* (AT5G16850); *AtTRB1* (AT1G49950); *AtTRB2,* formerly *TBP3* (AT5G67580); *AtTRB3*, formerly *TBP2* (AT3G49850); *AtCBF5* (AT3G57150); *AtPOT1a* (AT2G05210); *GAUT10* (AT2G20810); *AtFibrillarin 1* (AT5G52470).

ACKNOWLEDGEMENTS

This work was supported by the Czech Science Foundation (16-1137S), by the project SYMBIT, reg. number: CZ.02.1.01/0.0/0.0/15_003/0000477 financed by the ERDF, and by the Ministry of Education, Youth and Sports of the Czech Republic under the project CEITEC 2020 (LQ1601). We thank Inna Lermontova (IPK Gatersleben) for *AtCBF5* constructs. We further thank Eva Sýkorová and Vratislav Peška for providing us with the collection of *TERT* fragments and *Fibrillarin 1-RFP* vectors. We thank to Miloslava Fojtová for help with qTRAP assay. Jennifer McMahon is gratefully acknowledged for proofreading. The access to the computing and storage facilities owned by parties and projects contributing to the National Grid Infrastructure MetaCentrum provided under the program 'Projects of Large Infrastructure for Research, Development, and Innovations' (LM2010005) was highly appreciated, as was the access to the CERIT-SC computing and storage facilities provided under the program 'Center CERIT Scientific Cloud', part of the Operational Program Research and Development for Innovations, reg. no. CZ.1.05/3.2.00/08.0144. Core Facility Plant Sciences of CEITEC MU is acknowledged for the cultivation of experimental plants used in this paper.

CONFLICTS OF INTEREST

The authors declare no conflicts of interest.

AUTHORS' CONTRIBUTIONS

PPS designed the study, supervised the project and wrote the manuscript with support from SŠ, JF, LZD and DH.SŠ performed the experiments. LZD designed the phylogeny analysis. JF helped to supervise the project and wrote the manuscript. All authors discussed the results and contributed to the final manuscript.

SUPPORTING INFORMATION

Additional Supporting Information may be found in the online version of this article.

Figure S1. AtRuvBL1 does not interact with either the RT-domain or the C-terminus of AtTERT.

Figure S2. AtTRB2 proteins directly interact with AtRuvBL2a protein and AtTRB1 is associated with AtRuvBL1 in BiFC assay.

Figure S3. Nucleolar or cytoplasmic localization of AtPOT1a–AtCBF5 interactions.

Figure S4. Weak interaction between AtPOT1a and AtRuvBL1 proteins.

Figure S5. Association of AtRuvBLs, AtTRBs and AtTERT in the nucleolus in *A. thaliana* leaf protoplasts where the whole nucleus is marked.

Figure S6. Relative transcript levels of *AtTERT* gene in *AtRuvBL1* and *AtRuvBL2a* heterozygous mutant plants.

Figure S7. Terminal restriction fragment analysis.

Figure S8. Schematic illustration of specific primers and T-DNA insertion location within the *AtRuvBL1* and *AtRuvBL2a* genes.

Figure S9. Example of PCR analysis of genomic DNA isolated from wild-type (Wt) plants and heterozygous *AtRuvBL1* and *AtRuvBL2a* plants.

Figure S10. Relative *AtRuvBL1* and *AtRuvBL2a* transcript levels in heterozygous *AtRuvBL1* and *AtRuvBL2a* plants.

Table S1. The number of PPIs foci with exclusively nucleolar localization.

Table S2. List of T-DNA insertion lines.

Table S3. List of primers.

Data S1. List of the analyzed plant species sorted by phylogenetic system with number of homologues.

Data S2. List of the analyzed plant species for *AtRuvBL* homologues and their accession numbers.

REFERENCES

Armstrong, S.J., Franklin, F.C. and Jones, G.H. (2001) Nucleolus-associated telomere clustering and pairing precede meiotic chromosome synapsis in *Arabidopsis thaliana*. *J. Cell Sci.* **114**, 4207–4217.

Azum-Gelade, M.C., Noaillac-Depeyre, J., Caizergues-Ferrer, M. and Gas, N. (1994) Cell cycle redistribution of U3 snRNA and fibrillarin. Presence in the cytoplasmic nucleolus remnant and in the prenucleolar bodies at telophase. *J. Cell Sci.* **107** (Pt 2), 463–475.

Bilaud, T., Koering, C.E., Binet-Brasselet, E., Ancelin, K., Pollice, A., Gasser, S.M. and Gilson, E. (1996) The telobox, a Myb-related telomeric DNA binding motif found in proteins from yeast, plants and human. *Nucleic Acids Res.* **24**, 1294–1303.

Boulon, S., Marmier-Gourrier, N., Pradet-Balade, B. *et al.* (2008) The Hsp90 chaperone controls the biogenesis of L7Ae RNPs through conserved machinery. *J. Cell Biol.* **180**, 579–595.

Chen, L.Y., Liu, D. and Songyang, Z. (2007) Telomere maintenance through spatial control of telomeric proteins. *Mol. Cell. Biol.* **27**, 5898–5909.

Chen, Y., Zou, M. and Cao, Y. (2014) Transcriptome analysis of the Arabidopsis semi-in vivo pollen tube guidance system uncovers a distinct gene expression profile. *J. Plant Biol.* **57**, 93–105.

Cheung, K.L., Huen, J., Houry, W.A. and Ortega, J. (2010) Comparison of the multiple oligomeric structures observed for the Rvb1 and Rvb2 proteins. *Biochem. Cell Biol.* **88**, 77–88.

Cioce, M. and Lamond, A.I. (2005) Cajal bodies: a long history of discovery. *Annu. Rev. Cell Dev. Biol.* **21**, 105–131.

Citovsky, V., Lee, L.Y., Vyas, S., Glick, E., Chen, M.H., Vainstein, A., Gafni, Y., Gelvin, S.B. and Tzfira, T. (2006) Subcellular localization of interacting proteins by bimolecular fluorescence complementation in planta. *J. Mol. Biol.* **362**, 1120–1131.

Dellaporta, S.L., Wood, J. and Hicks, J.B. (1983) A Plant DNA minipreparation. *Version II. Plant. Mol. Biol. Rep.* **1**, 19–21.

Dokládal, L., Benková, E., Honys, D., Dupľáková, N., Lee, L.Y., Gelvin, S.B. and Sýkorová, E. (2018) An armadillo-domain protein participates in a telomerase interaction network. *Plant Mol. Biol.* **97**, 407–420.

Dreissig, S., Schiml, S., Schindele, P., Weiss, O., Rutten, T., Schubert, V., Gladilin, E., Mette, M.F., Puchta, H. and Houben, A. (2017) Live-cell CRISPR imaging in plants reveals dynamic telomere movements. *Plant J.* **91**, 565–573.

Dvořáčková, M. (2010) Analysis of Arabidopsis telomere-associated proteins *in vivo*. PhD thesis, Masaryk University, Brno.

Dvořáčková, M., Rossignol, P., Shaw, P.J., Koroleva, O.A., Doonan, J.H. and Fajkus, J. (2010) AtTRB1, a telomeric DNA-binding protein from Arabidopsis, is concentrated in the nucleolus and shows highly dynamic association with chromatin. *Plant J.* **61**, 637–649.

Fajkus, J. and Trifonov, E.N. (2001) Columnar packing of telomeric nucleosomes. *Biochem. Biophys. Res. Commun.* **280**, 961–963.

Fitzgerald, M.S., McKnight, T.D. and Shippen, D.E. (1996) Characterization and developmental patterns of telomerase expression in plants. *Proc. Natl Acad. Sci. USA*, **93**, 14422–14427.

Flavin, P., Redmond, A., McBryan, J. *et al.* (2011) RuvBl2 cooperates with Ets2 to transcriptionally regulate hTERT in colon cancer. *FEBS Lett.* **585**, 2537–2544.

Fojtová, M., Peška, V., Dobšáková, Z., Mozgová, I., Fajkus, J. and Sýkorová, E. (2011) Molecular analysis of T-DNA insertion mutants identified putative regulatory elements in the AtTERT gene. *J. Exp. Bot.* **62**, 5531–5545.

Fransz, P., De Jong, J.H., Lysák, M., Castiglione, M.R. and Schubert, I. (2002) Interphase chromosomes in Arabidopsis are organized as well defined chromocenters from which euchromatin loops emanate. *Proc. Natl Acad. Sci. USA*, **99**, 14584–14589.

Freeling, M. (2009) Bias in plant gene content following different sorts of duplication: tandem, whole-genome, segmental, or by transposition. *Annu. Rev. Plant Biol.* **60**, 433–453.

Gallant, P. (2007) Control of transcription by Pontin and Reptin. *Trends Cell Biol.* **17**, 187–192.

Grant, J.D., Broccoli, D., Muquit, M., Manion, F.J., Tisdall, J. and Ochs, M.F. (2001) Telometric: a tool providing simplified, reproducible measurements of telomeric DNA from constant field agarose gels. *Biotechniques*, **31**, 1314–1318.

Greider, C.W. (1996) Telomere length regulation. *Annu. Rev. Biochem.* **65**, 337–365.

He, J., Navarrete, S., Jasinski, M., Vulliamy, T., Dokal, I., Bessler, M. and Mason, P.J. (2002) Targeted disruption of Dkc1, the gene mutated in X-linked dyskeratosis congenita, causes embryonic lethality in mice. *Oncogene*, **21**, 7740–7744.

Herbert, B.S., Hochreiter, A.E., Wright, W.E. and Shay, J.W. (2006) Nonradioactive detection of telomerase activity using the telomeric repeat amplification protocol. *Nat. Protoc.* **1**, 1583–1590.

Holt, B.F., Boyes, D.C., Ellerström, M., Siefers, N., Wiig, A., Kauffman, S., Grant, M.R. and Dangl, J.L. (2002) An evolutionarily conserved mediator of plant disease resistance gene function is required for normal Arabidopsis development. *Dev. Cell*, **2**, 807–817.

Horak, J., Grefen, C., Berendzen, K.W., Hahn, A., Stierhof, Y.D., Stadelhofer, B., Stahl, M., Koncz, C. and Harter, K. (2008) The *Arabidopsis thaliana* response regulator ARR22 is a putative AHP phospho-histidine phosphatase expressed in the chalaza of developing seeds. *BMC Plant Biol.* **8**, 77.

Ijdo, J.W., Wells, R.A., Baldini, A. and Reeders, S.T. (1991) Improved telomere detection using a telomere repeat probe (TTAGGG)n generated by PCR. *Nucleic Acids Res.* **19**, 4780.

Izumi, N., Yamashita, A. and Ohno, S. (2012) Integrated regulation of PIKK-mediated stress responses by AAA+ proteins RUVBL1 and RUVBL2. *Nucleus*, **3**, 29–43.

Jha, S., Shibata, E. and Dutta, A. (2008) Human Rvb1/Tip49 is required for the histone acetyltransferase activity of Tip60/NuA4 and for the downregulation of phosphorylation on H2AX after DNA damage. *Mol. Cell. Biol.* **28**, 2690–2700.

Kannan, K., Nelson, A.D. and Shippen, D.E. (2008) Dyskerin is a component of the Arabidopsis telomerase RNP required for telomere maintenance. *Mol. Cell. Biol.* **28**, 2332–2341.

Kerppola, T.K. (2009) Visualization of molecular interactions using bimolecular fluorescence complementation analysis: characteristics of protein fragment complementation. *Chem. Soc. Rev.* **38**, 2876–2886.

Khurts, S., Masutomi, K., Delgermaa, L., Arai, K., Oishi, N., Mizuno, H., Hayashi, N., Hahn, W.C. and Murakami, S. (2004) Nucleolin interacts with telomerase. *J. Biol. Chem.* **279**, 51508–51515.

de Lange, T. (2005) Shelterin: the protein complex that shapes and safeguards human telomeres. *Genes Dev.* **19**, 2100–2110.

Lee, W.K. and Cho, M.H. (2016) Telomere-binding protein regulates the chromosome ends through the interaction with histone deacetylases in *Arabidopsis thaliana*. *Nucleic Acids Res.* **44**, 4610–4624.

Lee, L.Y., Wu, F.H., Hsu, C.T. *et al.* (2012) Screening a cDNA library for protein–protein interactions directly in planta. *Plant Cell*, **24**, 1746–1759.

Lee, J.H., Lee, Y.S., Jeong, S.A., Khadka, P., Roth, J. and Chung, I.K. (2014) Catalytically active telomerase holoenzyme is assembled in the dense fibrillar component of the nucleolus during S phase. *Histochem. Cell Biol.* **141**, 137–152.

Lermontova, I., Schubert, V., Bornke, F., Macas, J. and Schubert, I. (2007) Arabidopsis CBF5 interacts with the H/ACA snoRNP assembly factor NAF1. *Plant Mol. Biol.* **65**, 615–626.

Letunic, I. and Bork, P. (2016) Interactive tree of life (iTOL) v3: an online tool for the display and annotation of phylogenetic and other trees. *Nucleic Acids Res.* **44**, W242–W245.

Li, W., Zeng, J., Li, Q., Zhao, L., Liu, T., Bjorkholm, M., Jia, J. and Xu, D. (2010) Reptin is required for the transcription of telomerase reverse transcriptase and over-expressed in gastric cancer. *Mol. Cancer*, **9**, 132.

Lim, C.J., Zaug, A.J., Kim, H.J. and Cech, T.R. (2017) Reconstitution of human shelterin complexes reveals unexpected stoichiometry and dual pathways to enhance telomerase processivity. *Nat. Commun.* **8**, 1075.

Machado-Pinilla, R., Liger, D., Leulliot, N. and Meier, U.T. (2012) Mechanism of the AAA+ ATPases pontin and reptin in the biogenesis of H/ACA RNPs. *RNA*, **18**, 1833–1845.

MacNeil, D.E., Bensoussan, H.J. and Autexier, C. (2016) Telomerase regulation from beginning to the end. *Genes (Basel)*, **7**, 1–33.

Majerská, J., Schrumpfová, P.P., Dokládal, L., Schořová, S., Stejskal, K., Obořil, M., Honys, D., Kozáková, L., Polanská, P.S. and Sýkorová, E. (2017) Tandem affinity purification of AtTERT reveals putative interaction partners of plant telomerase in vivo. *Protoplasma*, **254**, 1547–1562.

Mandáková, T. and Lysák, M.A. (2008) Chromosomal phylogeny and karyotype evolution in x=7 crucifer species (Brassicaceae). *Plant Cell*, **20**, 2559–2570.

Mao, Y.Q. and Houry, W.A. (2017) The role of Pontin and Reptin in cellular physiology and cancer etiology. *Front. Mol. Biosci.* **4**, 58.

Matias, P.M., Gorynia, S., Donner, P. and Carrondo, M.A. (2006) Crystal structure of the human AAA+ protein RuvBL1. *J. Biol. Chem.* **281**, 38918–38929.

McKeegan, K.S., Debieux, C.M., Boulon, S., Bertrand, E. and Watkins, N.J. (2007) A dynamic scaffold of pre-snoRNP factors facilitates human box C/D snoRNP assembly. *Mol. Cell. Biol.* **27**, 6782–6793.

Mozgová, I., Schrumpfová, P.P., Hofr, C. and Fajkus, J. (2008) Functional characterization of domains in AtTRB1, a putative telomere-binding protein in *Arabidopsis thaliana*. *Phytochemistry*, **69**, 1814–1819.

Neron, B., Menager, H., Maufrais, C., Joly, N., Maupetit, J., Letort, S., Carrere, S., Tuffery, P. and Letondal, C. (2009) Mobyle: a new full web bioinformatics framework. *Bioinformatics*, **25**, 3005–3011.

Niewiarowski, A., Bradley, A.S., Gor, J., McKay, A.R., Perkins, S.J. and Tsaneva, I.R. (2010) Oligomeric assembly and interactions within the human RuvB-like RuvBL1 and RuvBL2 complexes. *Biochem. J.* **429**, 113–125.

Ohdate, H., Lim, C.R., Kokubo, T., Matsubara, K., Kimata, Y. and Kohno, K. (2003) Impairment of the DNA binding activity of the TATA-binding protein renders the transcriptional function of Rvb2p/Tih2p, the yeast RuvB-like protein, essential for cell growth. *J. Biol. Chem.* **278**, 14647–14656.

Osaki, H., Walf-Vorderwulbecke, V., Mangolini, M., Zhao, L., Horton, S.J., Morrone, G., Schuringa, J.J., de Boer, J. and Williams, O. (2013) The AAA+ ATPase RUVBL2 is a critical mediator of MLL-AF9 oncogenesis. *Leukemia*, **27**, 1461–1468.

Pendle, A.F., Clark, G.P., Boon, R., Lewandowska, D., Lam, Y.W., Andersen, J., Mann, M., Lamond, A.I., Brown, J.W. and Shaw, P.J. (2005) Proteomic analysis of the Arabidopsis nucleolus suggests novel nucleolar functions. *Mol. Biol. Cell*, **16**, 260–269.

Peška, V., Schrumpfová, P.P. and Fajkus, J. (2011) Using the telobox to search for plant telomere binding proteins. *Curr. Protein Pept. Sci.* **12**, 75–83.

Pfaffl, M.W. (2004) Quantification strategies in real-time PCR. In *A-Z of Quantitative PCR* (Bustin, S.A., ed). La Jolla, CA: International University Line, pp 87–112.

Pih, K.T., Yi, M.J., Liang, Y.S., Shin, B.J., Cho, M.J., Hwang, I. and Son, D. (2000) Molecular cloning and targeting of a fibrillarin homolog from Arabidopsis. *Plant Physiol.* **123**, 51–58.

Pontvianne, F., Carpentier, M.C., Durut, N. *et al.* (2016) Identification of nucleolus-associated chromatin domains reveals a role for the nucleolus in 3D organization of the *A. thaliana* genome. *Cell Rep.* **16**, 1574–1587.

Posada, D. and Crandall, K.A. (1998) MODELTEST: testing the model of DNA substitution. *Bioinformatics*, **14**, 817–818.

Queval, R., Papin, C., Dalvai, M., Bystricky, K. and Humbert, O. (2014) Reptin and Pontin oligomerization and activity are modulated through histone H3 N-terminal tail interaction. *J. Biol. Chem.* **289**, 33999–34012.

Roberts, N.Y., Osman, K. and Armstrong, S.J. (2009) Telomere distribution and dynamics in somatic and meiotic nuclei of *Arabidopsis thaliana*. *Cytogenet. Genome Res.* **124**, 193–201.

Rosenbaum, J., Baek, S.H., Dutta, A., Houry, W.A., Huber, O., Hupp, T.R. and Matias, P.M. (2013) The emergence of the conserved AAA+ ATPases Pontin and Reptin on the signaling landscape. *Sci. Signal.* **6**, mr1.

Rossignol, P., Collier, S., Bush, M., Shaw, P. and Doonan, J.H. (2007) Arabidopsis POT1A interacts with TERT-V(I8), an N-terminal splicing variant of telomerase. *J. Cell Sci.* **120**, 3678–3687.

Růčková, E., Friml, J., Procházková Schrumpfová, P. and Fajkus, J. (2008) Role of alternative telomere lengthening unmasked in telomerase knockout mutant plants. *Plant Mol. Biol.* **66**, 637–646.

Schmidt, J.C. and Cech, T.R. (2015) Human telomerase: biogenesis, trafficking, recruitment, and activation. *Genes Dev.* **29**, 1095–1105.

Schmidt, J.C., Zaug, A.J. and Cech, T.R. (2016) Live cell imaging reveals the dynamics of telomerase recruitment to telomeres. *Cell*, **166**, 1188–1197 e1189.

Schrumpfová, P., Kuchař, M., Miková, G., Skřišovská, L., Kubičárová, T. and Fajkus, J. (2004) Characterization of two *Arabidopsis thaliana* myb-like proteins showing affinity to telomeric DNA sequence. *Genome*, **47**, 316–324.

Schrumpfová, P.P., Kuchař, M., Paleček, J. and Fajkus, J. (2008) Mapping of interaction domains of putative telomere-binding proteins AtTRB1 and AtPOT1b from *Arabidopsis thaliana*. *FEBS Lett.* **582**, 1400–1406.

Schrumpfová, P.P., Vychodilová, I., Dvořáčková, M., Majerská, J., Dokládal, L., Schořová, S. and Fajkus, J. (2014) Telomere repeat binding proteins are functional components of Arabidopsis telomeres and interact with telomerase. *Plant J.* **77**, 770–781.

Schrumpfová, P., Schořová, S. and Fajkus, J. (2016a) Telomere- and telomerase-associated proteins and their functions in the plant cell. *Front. Plant Sci.* **7**, 851.

Schrumpfová, P.P., Vychodilová, I., Hapala, J., Schořová, S., Dvořáček, V. and Fajkus, J. (2016b) Telomere binding protein TRB1 is associated with promoters of translation machinery genes in vivo. *Plant Mol. Biol.* **90**, 189–206.

Schrumpfová, P.P., Fojtová, M. and Fajkus, J. (2019) Telomeres in plants and humans: not so different, not so similar. *Cells*, **8**, 1–31.

Shaw, P. and Brown, J. (2012) Nucleoli: composition, function, and dynamics. *Plant Physiol.* **158**, 44–51.

Sievers, F., Wilm, A., Dineen, D. *et al.* (2011) Fast, scalable generation of high-quality protein multiple sequence alignments using Clustal Omega. *Mol. Syst. Biol.* **7**, 539.

Silva-Martin, N., Dauden, M.I., Glatt, S., Hoffmann, N.A., Kastritis, P., Bork, P., Beck, M. and Muller, C.W. (2016) The combination of x-ray crystallography and cryo-electron microscopy provides insight into the overall architecture of the dodecameric Rvb1/Rvb2 complex. *PLoS One*, **11**, e0146457.

Soding, J. (2005) Protein homology detection by HMM-HMM comparison. *Bioinformatics*, **21**, 951–960.

Stamatakis, A. (2014) RAxML version 8: a tool for phylogenetic analysis and post-analysis of large phylogenies. *Bioinformatics*, **30**, 1312–1313.

Stepinski, D. (2014) Functional ultrastructure of the plant nucleolus. *Protoplasma*, **251**, 1285–1306.

Tan, L.M., Zhang, C.J., Hou, X.M., Shao, C.R., Lu, Y.J., Zhou, J.X., Li, Y.Q., Li, L., Chen, S. and He, X.J. (2018) The PEAT protein complexes are required for histone deacetylation and heterochromatin silencing. *EMBO J.* **37**, 1–21.

Torreira, E., Jha, S., Lopez-Blanco, J.R., Arias-Palomo, E., Chacon, P., Canas, C., Ayora, S., Dutta, A. and Llorca, O. (2008) Architecture of the pontin/reptin complex, essential in the assembly of several macromolecular complexes. *Structure*, **16**, 1511–1520.

Venteicher, A.S., Meng, Z., Mason, P.J., Veenstra, T.D. and Artandi, S.E. (2008) Identification of ATPases pontin and reptin as telomerase components essential for holoenzyme assembly. *Cell*, **132**, 945–957.

Watkins, N.J., Lemm, I., Ingelfinger, D., Schneider, C., Hossbach, M., Urlaub, H. and Luhrmann, R. (2004) Assembly and maturation of the U3 snoRNP in the nucleoplasm in a large dynamic multiprotein complex. *Mol. Cell*, **16**, 789–798.

Wood, M.A., McMahon, S.B. and Cole, M.D. (2000) An ATPase/helicase complex is an essential cofactor for oncogenic transformation by c-Myc. *Mol. Cell*, **5**, 321–330.

Zachová, D., Fojtová, M., Dvořáčková, M., Mozgová, I., Lermontova, I., Peška, V., Schubert, I., Fajkus, J. and Sýkorová, E. (2013) Structure-function relationships during transgenic telomerase expression in Arabidopsis. *Physiol. Plant.* **149**, 114–126.

Zhang, Q., Kim, N.K. and Feigon, J. (2011) Architecture of human telomerase RNA. *Proc. Natl Acad. Sci. USA*, **108**, 20325–20332.

Zhao, R., Kakihara, Y., Gribun, A. *et al.* (2008) Molecular chaperone Hsp90 stabilizes Pih1/Nop17 to maintain R2TP complex activity that regulates snoRNA accumulation. *J. Cell Biol.* **180**, 563–578.

Zhao, Y., Cheng, D., Wang, S. and Zhu, J. (2014) Dual roles of c-Myc in the regulation of hTERT gene. *Nucleic Acids Res.* **42**, 10385–10398.

Zhou, Y., Hartwig, B., James, G.V., Schneeberger, K. and Turck, F. (2016) Complementary activities of TELOMERE REPEAT BINDING proteins and polycomb group complexes in transcriptional regulation of target genes. *Plant Cell*, **28**, 87–101.

Zhou, Y., Wang, Y., Krause, K., Yang, T., Dongus, J.A., Zhang, Y. and Turck, F. (2018) Telobox motifs recruit CLF/SWN-PRC2 for H3K27me3 deposition via TRB factors in Arabidopsis. *Nat. Genet.* **50**, 638–644.

SUPPORTING INFORMATION

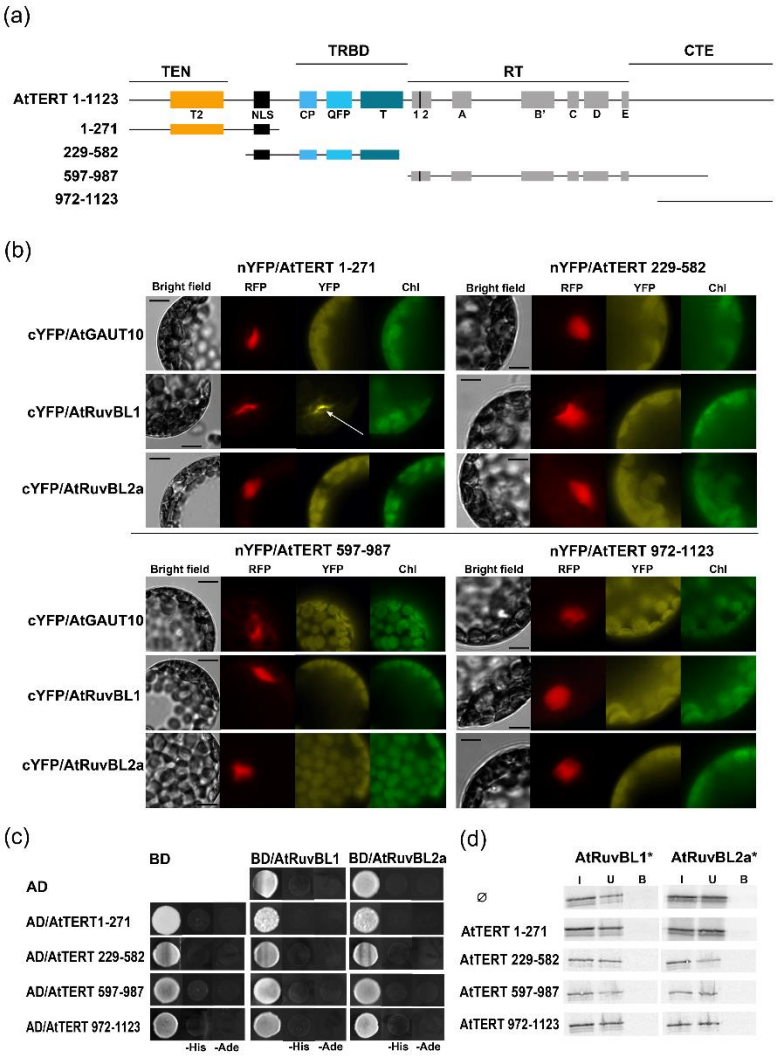

Figure S1. AtRuvBL1 Does Not Interact with either the RT-domain or the C-terminus of AtTERT. The analyses are performed as described in Figure 1.

(a) Schematic depiction of the catalytic subunit of plant telomerase - AtTERT.

(b) BiFC assay detects interaction between cYFP/AtRuvBL1 and the N-terminal part of AtTERT (nYFP/AtTERT 1-271). No interactions are detected between AtRuvBL1 protein and AtTERT fragments covering AtTERT domains localized in regions 229-582, 597-987 and 972-1123. No interactions are observed between any of AtTERT fragments and AtRuvBL2a protein in *A. thaliana* leaf protoplasts. PPIs are marked with white arrows. AtGAUT10, negative control; RFP, nucleus marker; YFP, detects PPI; Chl, Chloroplast autofluorescence. Scale bars = 10 µm.

(c) Y2H system results show no interaction between AD/AtRuvBL1 nor AD/AtRuvBL2a proteins and fragments of AtTERT fused with GAL4 DNA-binding domain (BD). Vectors with AD or BD without gene of interest are used as negative control.

(d) Co-IP analysis does not detect interaction between AtTERT fragments and AtRuvBL1 or AtRuvBL2a protein as is demonstrated by BiFC. I, Input; U, Unbound; B, Bound fractions; asterisks*, ^{35}S-labelling.

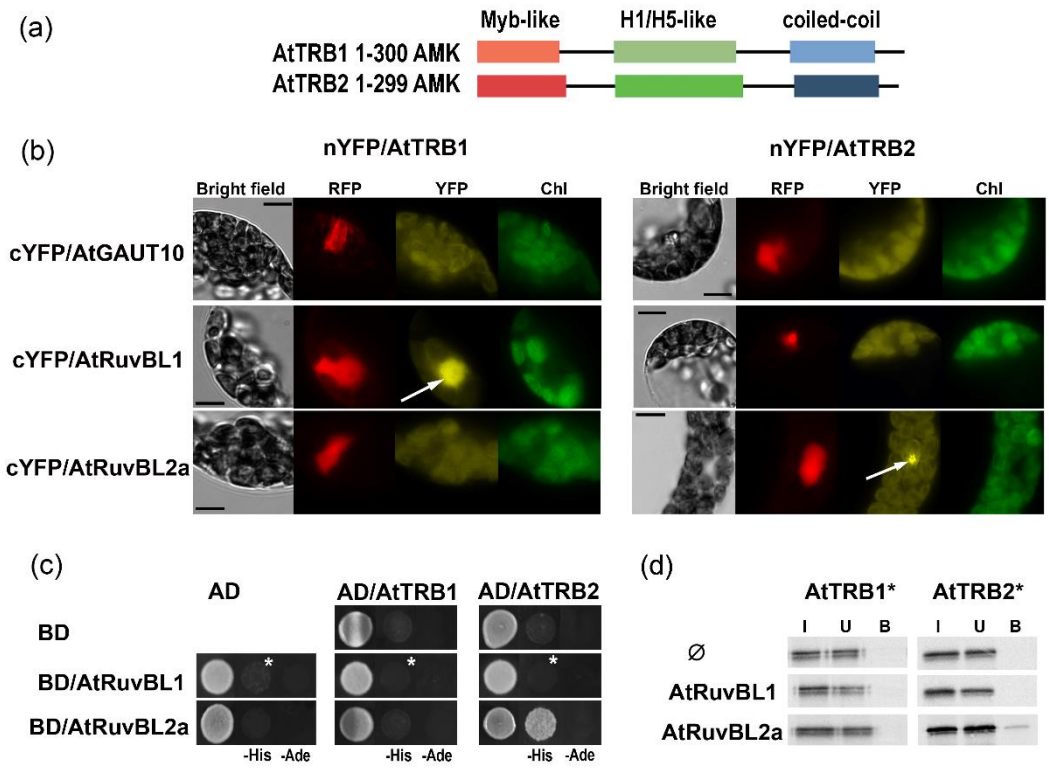

Figure S2. AtTRB2 Proteins Directly Interact with AtRuvBL2a Protein and AtTRB1 is Associated with AtRuvBL1 in BiFC Assay. The methods are performed as is described in Figure 1.

(a) Schematic representation of the conserved motifs of the AtTRB1 and AtTRB2 proteins from *A. thaliana*. Myb-like, Telobox-containing Myb domain; H1/H5, histone-like domain; coiled-coil, C-terminal domain.

(b) BiFC assay reveals interactions between nYFP/AtTRB1 and cYFP/AtRuvBL1 and between nYFP/AtTRB2 and cYFP/AtRuvBL2a. PPIs are marked with white arrows. AtGAUT10, negative control; RFP, Red Fluorescent Protein, positive control; YFP, Yellow Fluorescent Protein, PPI; Chl, Chloroplast autofluorescence, control. Scale bars = 10 µm.

(c) Y2H results confirm the interaction between AD/AtTRB2 and BD/AtRuvBL2 on His- deficient plates, but not the interaction between AD/AtTRB1 and BD/AtRuvBL1. BD, GAL4 DNA-binding domain; AD, GAL4 activation domain; asterisks*, 5mM 3-aminotriazol.

(d) Co-IP results confirm interactions between radioactively labelled AtTRB2 and Myc-tagged AtRuvBL2 protein. I, Input; U, Unbound; B, Bound fractions; asterisks*,35S-labelling.

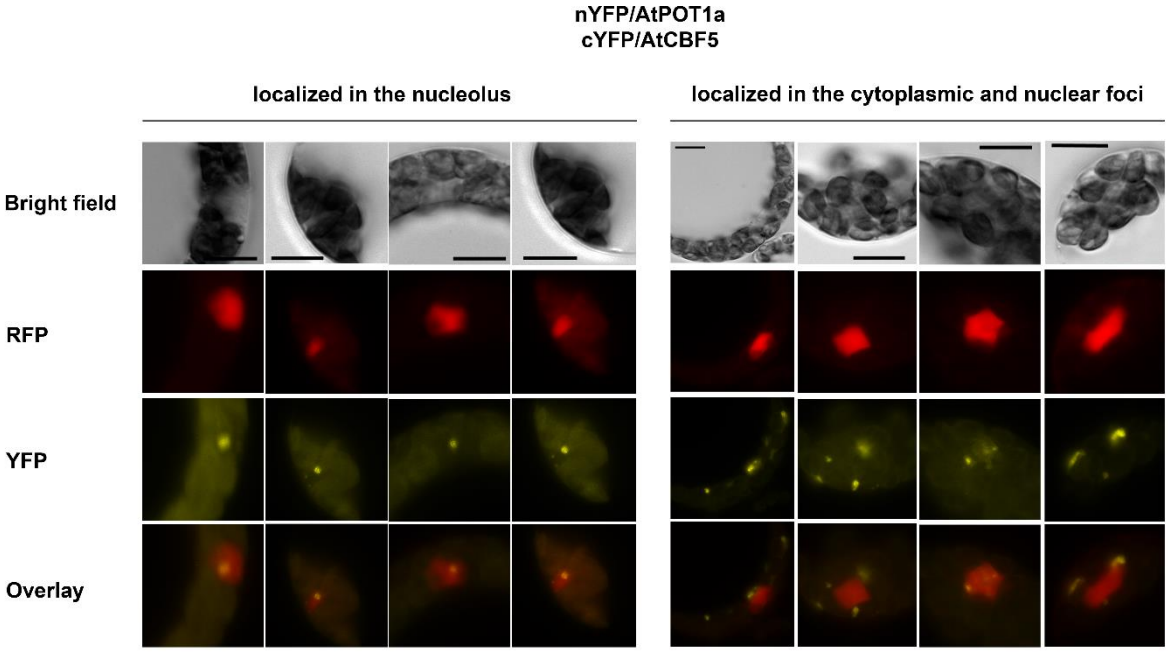

Figure S3. Nucleolar or Cytoplasmic Localization of AtPOT1a-AtCBF5 Interactions.

BiFC performed in *A. thaliana* leaf protoplasts show either clear nucleolar AtPOT1a-AtCBF5 foci or cytoplasmic and nuclear foci. The examples of AtPOT1a-AtCBF5 interactions localized in the nucleolus are given in the first four columns. The following four columns show AtPOT1a-AtCBF5 interactions localized in the cytoplasmic and nucleus foci. The whole nucleus was marked by mRFP-VirD2NLS.

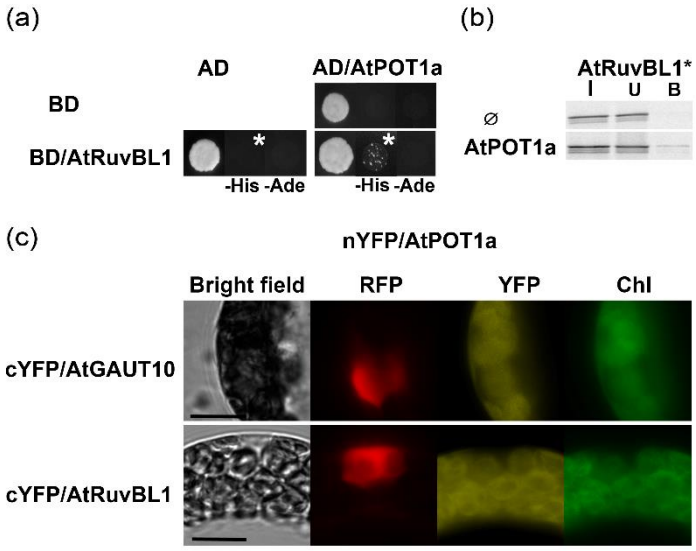

Figure S4. Weak Interaction Between AtPOT1a and AtRuvBL1 Proteins. The analyses are performed as is described in Figure 1.

(a) Y2H results show weak but reproducible interactions between AtPOT1a and AtRuvBL1 protein on His- deficient plates. BD, GAL4 DNA-binding domain; AD, GAL4 activation domain.

(b) Co-IP results confirm direct interactions between radioactively labelled AtRuvBL1 and Myc-tagged AtPOT1a protein. I, Input; U, Unbound; B, Bound fractions; asterisks*, 35S-labelling

(c) BiFC does not detect any interaction between AtPOT1a and AtRuvBL1 proteins. AtGAUT10, negative control; RFP, nucleus marker; YFP, detects PPI; Chl, Chloroplast autofluorescence. Scale bars = 10 µm

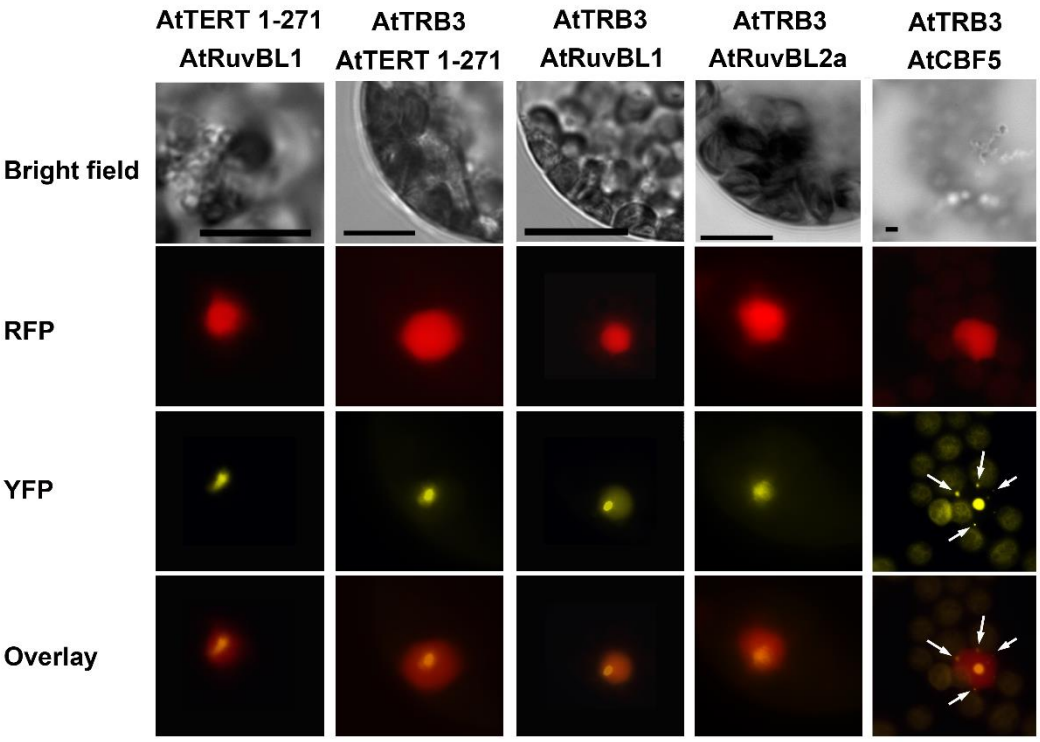

Figure S5. Association of AtRuvBLs, AtTRBs and AtTERT in the nucleolus in *A. thaliana* Leaf Protoplasts where the Whole Nucleus is Marked.

A. thaliana leaf protoplast are co-transfected with mRFP-VirD2NLS encoding RFP that labels the whole nucleus and simultaneously with each of the plasmids encoding nYFP-tagged or cYFP-tagged AtRuvBL1, AtRuvBL2a, AtTERT 1-271, AtTRB3 or AtCBF5 to determine PPI localization. AtRuvBL1-AtTERT, AtTRB3-AtTERT, AtRuvBL1-AtTRB3 or AtRuvBL2a-AtTRB3 interactions show nucleolar localization. Plant homologue of mammalian dyskerin, AtCBF5, is associated with AtTRB3 in nucleolus and in additional nuclear bodies at the periphery of nucleolus. RFP, marked nucleus; YFP, detects PPI; Scale bars = 10 µm.

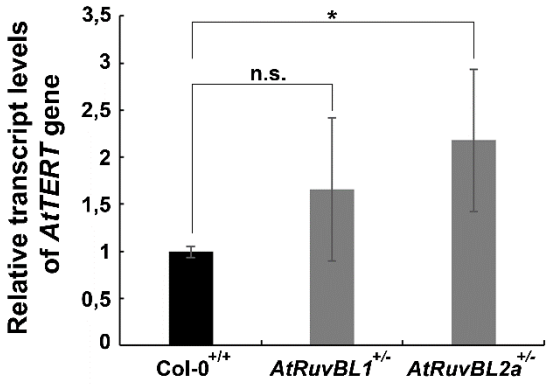

Figure S6. Relative Transcript Levels of *AtTERT* Gene in *AtRuvBL1* and *AtRuvBL2a* Heterozygous Mutant Plants.

No significant differences are detected in the transcript levels of *AtTERT* gene in the heterozygous mutant plants in *AtRuvBL1* gene. We detect a slight increase of transcripts of *AtTERT* gene in the plants heterozygous in *AtRuvBL2a* genes compared to the wild-type. Levels or *AtTERT* transcripts from WT Col-0 are arbitrarily set as 1. P values<0.05 are considered significant. Single star denotes 0.01<P<0.05.

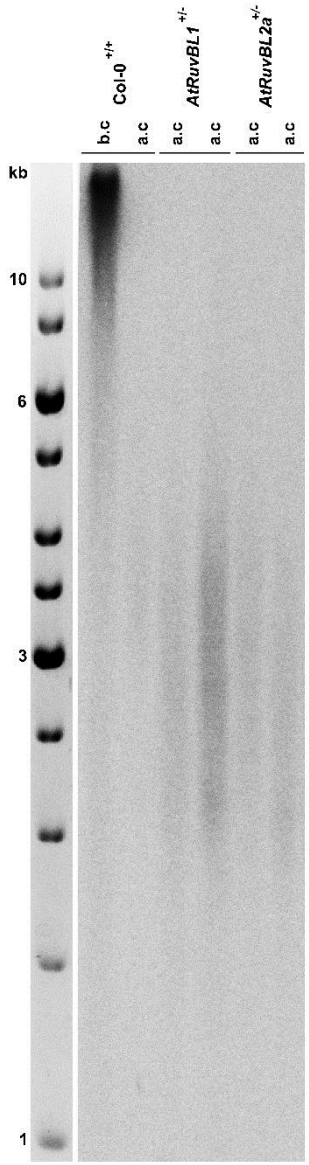

Figure S7. Terminal Restriction Fragment Analysis

TRF analysis does not reveal any changes in telomere lengths in the analyzed *AtRuvBL1+/-* and *AtRuvBL2a+/-* plants. Genomic DNA either before (b.c.) or after cleavage (a.c.) with MseI enzyme was hybridized with radioactively labeled telomeric probe.

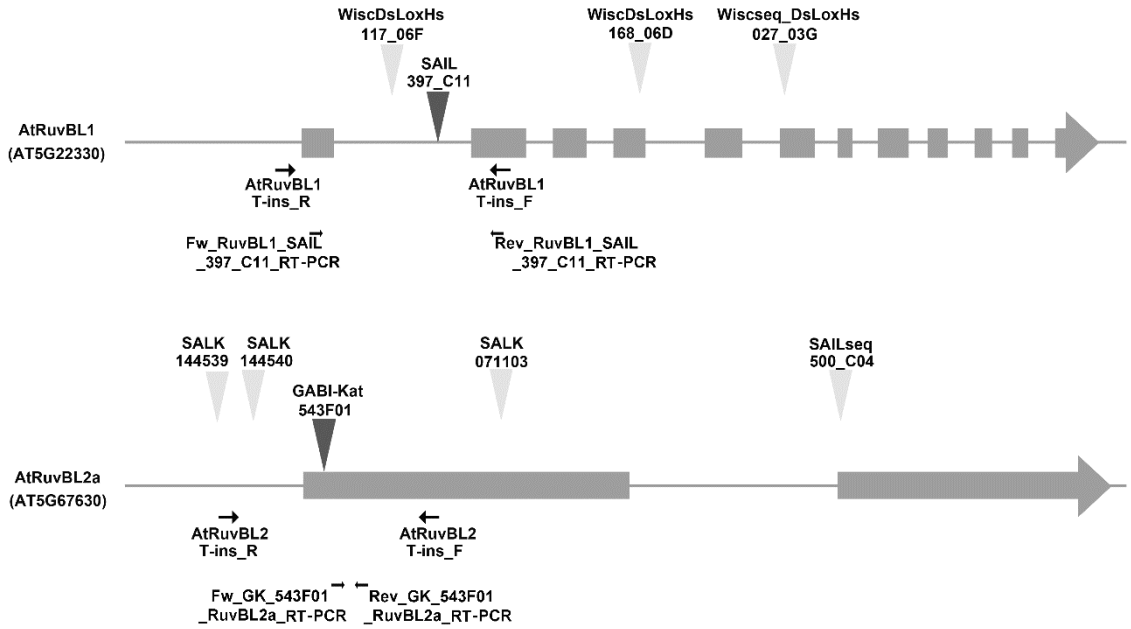

Figure S8. Schematic Illustration of Specific Primers and T-DNA Insertion Location within the *atruvbl1* and *atruvbl2a* Genes.

Schematic illustration of locations of various T-DNA insertion lines available from several plant databases (see also Table S2). T-insertion lines with limited number of heterozygous AtRuvBL1 and AtRuvBL2a plants are marked with dark grey triangles (SAIL_397_C11, GABI-Kat_543F01, respectively). The other T-insertion lines are marked by light triangles, since they did not provide either homozygotes or heterozygotes plants. Primers used for PCR analysis of genomic DNA (T-ins.) or analysis of relative transcript levels (RT-PCR) are marked by black arrows.

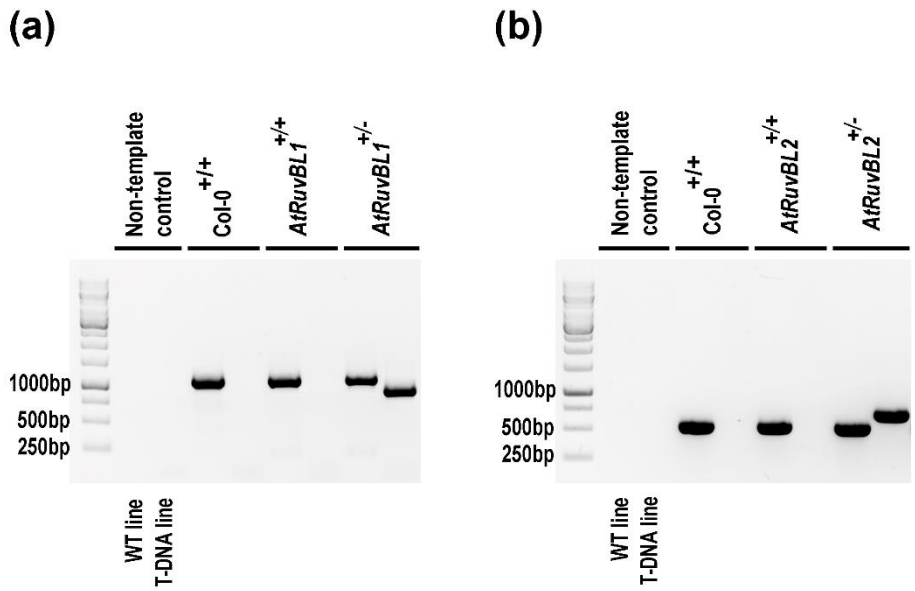

Figure S9. Example of PCR Analysis of Genomic DNA Isolated from wild-type (Wt) Plants and Heterozygous *AtRuvBL1* and *AtRuvBL2a* Plants.

We used PCR analysis to distinguish heterozygous *AtRuvBL1* and *AtRuvBL2a* plant lines from wild-type AtRuvBL1 and AtRuvBL2a plants. As positive control was used genomic DNA isolated from wild-type Col-0 plants.

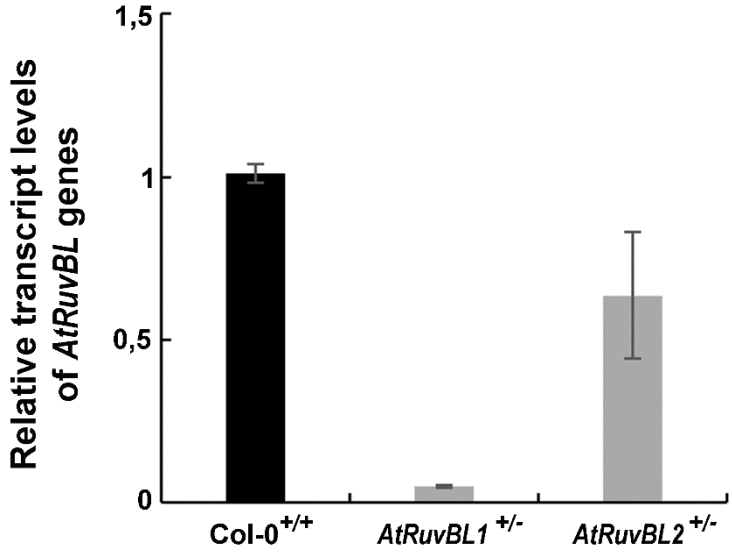

Figure S10. Relative *AtRuvBL1* and *AtRuvBL2a* Transcript Levels in Heterozygous *AtRuvBL1* and *AtRuvBL2a* Plants.

RT-PCR was used to detect transcript levels in the heterozygous *AtRuvBL1* and *AtRuvBL2a* plant lines. The transcript levels of *AtRuvBL1* and *AtRuvBL2a* genes were reduced compare to the wild-type Col-0 plants in both heterozygous *AtRuvBL1*and *AtRuvBL2a* plants, respectively. Levels or *AtRuvBL1* and *AtRuvBL2a* transcripts from wild-type Col-0 are arbitrarily set as 1.

Table S1. The Number of PPIs Foci with Exclusively Nucleolar Localization.

	Total *A. thaliana* protoplasts	**Exclusively nucleolar** localization	**Nuclear and at the same time nucleolar** localization
AtRuvBL1-AtTRB3	30	27	3
AtRuvBL2a-AtTRB3	30	28	2
AtTRB3-AtTERT	30	28	2
AtRuvBL1-AtTERT	30	19	11

To quantify the numbers of the PPIs between AtRuvBL1-AtTRB3, AtRuvBL2a-AtTRB3, AtTRB3-AtTERT and AtRuvBL1-AtTERT with exclusively nucleolar localization we performed at the same day several BiFC analysis. Total 30 *A. thaliana* protoplasts from each protein-protein combination, with positive PPIs, were analyzed for either exclusively nucleolar or nucleolar and at the same time nuclear localization of these PPIs interactions.

Table S2. List of T-insertion Lines

AtRuvBL1 **T-insertion lines**	***AtRuvBL2a*** **T-insertion lines**
Wiscseq_DsLoxHs027_03G	SALK_071103
WiscDsLoxHs117_06F	SALK_144539
WiscDsLoxHs168_06D	SALK_144540
SAIL_397_C11*	SAIL_500_C04
	GK - 543F01*

Accession numbers of T-insertion lines that are tested for the presence of mutation in the *AtRuvBL1 or AtRuvBL2a* genes. Lines marked with asterisks provided limited number of heterozygous mutant plants, that are analyzed.

Table S3. List of Primers

The name of primer	Sequence (5'→3')	Method
AtRuvBL1_F	AAAAAGCAGGCTACATGGAGAAAGTAAAGATTGAAGAA	Gateway cloning
AtRuvBL1_R	AGAAAGCTGGGTGCTATGAGATGTATTTTTCTTGTTGCC	Gateway cloning
AtRuvBL2a_F	AAAAAGCAGGCTACATGGCGGAACTAAAGCTATCA	Gateway cloning
AtRuvBL2a_R	AGAAAGCTGGGTCTCAGATCTGCATAGCATCTTG	Gateway cloning
attB1 adapter primer	GGGACAAGTTTGTACAAAAAAGCAGGCT	Gateway cloning
attB2 adapter primer	GGGGACCACTTTGTACAAGAAAGCTGGGT	Gateway cloning
AtRuvBL1_T-ins_F (SAIL_397_C11)	TTTTTGTTTCGCCCTTTTCTC	Genotyping
AtRuvBL1_T-ins_R (SAIL_397_C11)	AGAGATTCCAAGAGCCAAAGC	Genotyping
SAIL_T-ins_LB1	GCCTTTTCAGAAATGGATAAATAGCCTTGCTTCC	Genotyping
AtRuvBL2a-T-ins_F (GK-543F01)	ACAACTTGTTCGACCAAATGC	Genotyping
AtRuvBL2a-T-ins_R (GK-543F01)	TTTGATCCTAACACCAATCGC	Genotyping
GK-T-ins_8474_F	ATAATAACGCTGCGGACATCTACATTTT	Genotyping
R1_Wisc_027_03G.6_LP	CGGTTAATTCTTCAACTTGCG	Genotyping
R1_Wisc_027_03G.6_RP	TCAGTTTGTTCCAAAACCTGC	Genotyping
R1_Wisc_117_06F_LP	AAACCGCAAATAGCAACACAC	Genotyping
R1_Wisc_117_06F_RP	GCGTTGCAAACTCAATAAAGC	Genotyping
R1_Wisc_168_06D_LP	ATTTGCTGCATCCAGATCTTG	Genotyping
Wisc_T-ins	AACGTCCGCAATGTGTTATTAAGTTGTC	Genotyping
R1_Wisc_168_06D_RP	TAAAATTGGCAGCTGGATTTG	Genotyping
R2a_SAIL_500_C04.2_LP	CTTTTCGTAAAGCGATTGGTG	Genotyping
R2a_SAIL_500_C04.2_RP	ACGTCCGATCAATGTCAAAAG	Genotyping
R2a_SALK_071103.2_LP	CGGGTCGGGCTATTCTAATAG	Genotyping
R2a_SALK_071103.2_RP	ACAAGGATTGGTGACATTTCG	Genotyping
R2a_SALK_144539_LP	AATTGGGGATTGCAGAGAAAC	Genotyping
R2a_SALK_144539_RP	CTATTAGAATAGCCCGACCCG	Genotyping
R2a_SALK_144540_LP	AATTGGGGATTGCAGAGAAAC	Genotyping
R2a_SALK_144540_RP	CTATTAGAATAGCCCGACCCG	Genotyping
SALK_T-ins_LBb1.3	ATTTTGCCGATTTCGGAAC	Genotyping
TS21	GACAATCCGTCGAGCAGAGTT	qTRAP assay
TEL-PR	CCGAATTCAACCCTAAACCCTAAACCCTAAACCC	qTRAP assay
Fw_RuvBL1_SAIL_397_C11_RT-PCR	CAACGGATTGCTACTCACAC	RT-PCR
Rev_RuvBL1_SAIL_397_C11_RT-PCR	AAGAGCCAAAGCTGTTTTCC	RT-PCR
Fw_GK_543F01_RuvBL2a_RT-PCR	TATGGTCGGTCAAGTGAAGG	RT-PCR
Rev_GK_543F01_RuvBL2a_RT-PCR	GGGTTGACCCGCTATTAGAA	RT-PCR
Fw_AtTERT_ex1	CCGATGATCCCATTCACTACCGTAAACT	RT-PCR
Rev_AtTERT_ex1	TCTCTGTGACCACCAAGATGTTGGAGA	RT-PCR

Data S1. List of the Analyzed Plant Species Sorted by Phylogenetic System with Number of Homologues.

	Order	Family	Species	No.RuvBL homologues
BRYOPHYTES	Marchantiales	Marchantiaceae	*Marchantia polymorpha* ssp. *polymorpha*	**1**
	Funariales	Funariaceae	*Physcomitrella patens*	**1**
GYMNOSPERMS	Pinales	Pinaceae	*Picea sitchensis*	**1**
BASAL ANGIOSPERMS	Amborellales	Amborellaceae	*Amborella trichopoda*	**3**
MONOCOTS	Alismatales	Araceae	*Anthurium amnicola*	**3**
	Arecales	Arecaceae	*Elaeis guineensis*	**2**
			Phoenix dactylifera	**3**
	Zingiberales	Musaceae	*Musa acuminata* ssp. *malaccensis*	**1**
	Poales	Bromeliaceae	*Ananas comosus*	**1**
		Poaceae	*Aegilops tauschii*	**1**
			Brachypodium distachyon	**1**
			Dichanthelium oligosanthes	**1**
			Hordeum vulgare ssp. *vulgare*	**1**
			Oryza brachyantha	**1**
			Oryza sativa var. *japonica*	**1**
			Setaria italica	**1**
			Zea mays	**1**
DICOTS	Proteales	Nelumbonaceae	*Nelumbo nucifera*	**3**
	Vitales	Vitaceae	*Vitis vinifera*	**4**
	Fabales	Fabaceae	*Arachis duranensis*	**1**
			Arachis ipaensis	**2**
			Cajanus cajan	**1**
			Cicer arietinum	**1**
			Lupinus angustifolius	**4**
			Medicago truncatula	**3**
			Phaseolus vulgaris	**2**
			Trifolium subterraneum	**1**
			Vigna angularis	**2**
			Vigna radiata ssp. *radiata*	**2**
	Rosales	Moraceae	*Morus notabilis*	**1**
		Rhamnaceae	*Ziziphus jujuba*	**2**
		Rosaceae	*Fragaria vesca* ssp. *vesca*	**3**
			Malus domestica	**1**
			Prunus persica	**2**
			Pyrus x bretschneideri	**4**
	Fagales	Juglandaceae	*Juglans regia*	**2**
	Cucurbitales	Cucurbitaceae	*Cucumis melo*	**1**
			Cucumis sativus	**2**
	Oxalidales	Cephalotaceae	*Cephalotus follicularis*	**2**
	Malphigiales	Euphorbiaceae	*Jatropha curcas*	**4**

			Manihot esculenta	**3**
			Ricinus communis	**1**
		Salicaceae	*Populus euphratica*	**3**
			Populus trichocarpa	**3**
	Myrtales	Myrtaceae	*Eucalyptus grandis*	**2**
	Sapindales	Rutaceae	*Citrus clementina*	**3**
			Citrus sinensis	**1**
	Malvales	Malvaceae	*Corchorus capsularis*	**2**
			Corchorus olitorius	**1**
			Glycine max	**3**
			Gossypium arboreum	**4**
			Gossypium hirsutum	**5**
			Gossypium raimondii	**5**
			Theobroma cacao	**4**
		Cleomaceae	*Tarenaya hassleriana*	**3**
		Brassicaceae	*Arabidopsis lyrata* ssp. *lyrata*	**2**
			Arabidopsis thaliana	**3**
			Arabis alpina	**2**
			Brassica napus	**8**
			Brassica oleracea var. *oleracea*	**4**
			Brassica rapa	**4**
			Camelina sativa	**6**
			Capsella rubella	**3**
			Eutrema salsugineum	**2**
			Noccaea caerulescens	**3**
			Raphanus sativus	**3**
	Caryophyllales	Amaranthaceae	*Beta vulgaris* spp. *vulgaris*	**1**
	Gentianales	Rubiaceae	*Coffea canephora*	**2**
	Solanales	Convolvulaceae	*Ipomoea nil*	**3**
		Solanaceae	*Capsicum annuum*	**2**
			Nicotiana attaenuata	**2**
			Nicotiana sylvestris	**2**
			Nicotiana tabacum	**1**
			Nicotiana tomentosiformis	**2**
			Solanum lycopersicum	**2**
			Solanum tuberosum	**2**
			Spinacia oleracea	**1**
	Lamiales	Gesneriaceae	*Dorcoceras hygrometricum*	**2**
		Phrymaceae	*Erythranthe guttata*	**2**
		Lentibulariaceae	*Genlisea aurea*	**1**
		Pedaliaceae	*Sesamum indicum*	**2**
	Asterales	Asteraceae	*Cynara cardunculus* ssp. *scolymus*	**2**
	Apiales	Apiaceae	*Daucus carota* var. *sativus*	**3**

Data S2. List of the Analyzed Plant Species for RuvBL Homologues and Their Accession Numbers.

Species	**Codes**	**Acc. Nos.**
Aegilops tauschii	Aegilops tauschii RuvBL2	EMT28256.1
Amborella trichopoda	Amborella trichopoda hypot	ERN15972.1
	Amborella trichopoda RuvBL1	XP_006854505.2
	Amborella trichopoda RuvBL2	XP_006852153.1
Ananas comosus	Ananas comosus RuvBL1	OAY71163.1
Anthurium amnicola	Anthurium amnicola RuvBL1	JAT57168.1
	Anthurium amnicola RuvBL1	JAT60842.1
	Anthurium amnicola RuvBL2	JAT67104.1
Arabidopsis lyrata ssp. *lyrata*	Arabidopsis lyrata lyrata hypot a	XP_002864989.1
	Arabidopsis lyrata lyrata hypot b	XP_002874064.1
Arabidopsis thaliana	**Arabidopsis thaliana RuvBL1**	**NP_197625.1**
	Arabidopsis thaliana RuvBL2 a	**NP_201564.1**
	Arabidopsis thaliana RuvBL2 b	**NP_190552.1**
Arabis alpina	Arabis alpina hypot a	KFK23151.1
	Arabis alpina hypot b	KFK28446.1
Arachis duranensis	Arachis duranensis RuvBL2	XP_015972776.1
Arachis ipaensis	Arachis ipaensis RuvBL1	XP_016172459.1
	Arachis ipaensis RuvBL2	XP_016166745.1
Beta vulgaris ssp. *vulgaris*	Beta vulgaris vulgaris RuvBL2	XP_010679660.1
Brachypodium distachyon	Brachypodium distachyon RuvBL2	XP_003562823.1
Brassica napus	Brassica napus hypot a	CDX88801.1
	Brassica napus hypot b	CDX98571.1
	Brassica napus hypot c	CDY09131.1
	Brassica napus hypot d	CDY35680.1
	Brassica napus RuvBL1 a	XP_013667200.1
	Brassica napus RuvBL1 b	XP_013680083.1
	Brassica napus RuvBL1 c	XP_013715810.1
	Brassica napus RuvBL1 d	XP_013723522.1
Brassica oleracea var. *oleracea*	Brassica oleracea oleracea RuvBL1 a	XP_013612873.1
	Brassica oleracea oleracea RuvBL1 b	XP_013621188.1
	Brassica oleracea oleracea RuvBL1 c	XP_013625320.1
	Brassica oleracea oleracea RuvBL2	XP_013630404.1
Brassica rapa	Brassica rapa RuvBL2	XP_009150681.1
	Brassica rapa RuvBL1 a	XP_009120666.1
	Brassica rapa RuvBL1 b	XP_009126536.1
	Brassica rapa RuvBL1 c	XP_009131872.1
Cajanus cajan	Cajanus cajan RuvBL2	KYP76213.1
Camelina sativa	Camelina sativa RuvBL1	XP_010454496.1
	Camelina sativa RuvBL1	XP_019084763.1
	Camelina sativa RuvBL2	XP_010463807.1
	Camelina sativa RuvBL2	XP_010484449.1
	Camelina sativa RuvBL2 a	XP_010426510.1

	Camelina sativa RuvBL2 b	XP_010444617.1
Capsella rubella	Capsella rubella hypot a	XP_006282280.1
	Capsella rubella hypot b	XP_006287714.1
	Capsella rubella hypot c	XP_006292981.1
Capsicum annuum	Capsicum annuum RuvBL1	XP_016548155.1
	Capsicum annuum RuvBL2	XP_016570371.1
Cephalotus follicularis	Cephalotus follicularis hypot a	GAV57713.1
	Cephalotus follicularis hypot b	GAV85060.1
Cicer arietinum	Cicer arietinum RuvBL1	NP_001265936.1
Citrus clementina	Citrus clementina hypot a	XP_006426097.1
	Citrus clementina hypot b	XP_006430524.1
	Citrus clementina hypot c	XP_006430525.1
Citrus sinensis	Citrus sinensis RuvBL2	XP_006466461.1
Coffea canephora	Coffea canephora hypot a	CDP02620.1
	Coffea canephora hypot b	CDP07117.1
Corchorus capsularis	Corchorus capsularis hypot a	OMO56475.1
	Corchorus capsularis hypot b	OMO91824.1
Corchorus olitorius	Corchorus olitorius hypot	OMP01809.1
Cucumis melo	Cucumis melo RuvBL1	XP_008443365.1
Cucumis sativus	Cucumis sativus RuvBL2	XP_004143406.1
	Cucumis sativus RuvBL1	XP_004136684.1
Cynara cardunculus ssp. *scolymus*	Cynara cardunculus scolymus hypot a	KVI07257.1
	Cynara cardunculus scolymus hypot b	KVI09360.1
Daucus carota var. *sativus*	Daucus carota sativus hypot	KZN05222.1
	Daucus carota sativus RuvBL2	XP_017215222.1
	Daucus carota sativus RuvBL1	XP_017231242.1
Dichanthelium oligosanthes	Dichanthelium oligosanthes RuvBL2	OEL27319.1
Dorcoceras hygrometricum	Dorcoceras hygrometricum RuvBL1	KZV49640.1
	Dorcoceras hygrometricum RuvBL2	KZV33016.1
Elaeis guineensis	Elaeis guineensis RuvBL1	XP_010922426.1
	Elaeis guineensis RuvBL2	XP_010943144.1
Erythranthe guttata	Erythranthe guttata RuvBL1	XP_012836027.1
	Erythranthe guttata RuvBL2	XP_012854107.1
Eucalyptus grandis	Eucalyptus grandis RuvBL2	XP_010028079.1
	Eucalyptus grandis RuvBL1	XP_010031536.1
Eutrema salsugineum	Eutrema salsugineum hypot a	XP_006384768.1
	Eutrema salsugineum hypot b	XP_006400738.1
Fragaria vesca ssp. *vesca*	Fragaria vesca vesca RuvBL1	XP_004294694.1
	Fragaria vesca vesca RuvBL1	XP_011458673.1
	Fragaria vesca vesca RuvBL2	XP_004288244.1
Genlisea aurea	Genlisea aurea hypot	EPS69881.1
Glycine max	Glycine max RuvBL2 a	XP_014626670.1
	Glycine max RuvBL2 b	XP_014634945.1
	Glycine max RuvBL1	XP_006583068.1
Gossypium arboreum	Gossypium arboreum RuvBL1 a	XP_017603372.1
	Gossypium arboreum RuvBL1 b	XP_017608006.1
	Gossypium arboreum RuvBL1 c	XP_017608007.1

	Gossypium arboreum RuvBL2	XP_017638900.1
Gossypium hirsutum	Gossypium hirsutum RuvBL1 a	XP_016669038.1
	Gossypium hirsutum RuvBL1 b	XP_016669039.1
	Gossypium hirsutum RuvBL1 c	XP_016750696.1
	Gossypium hirsutum RuvBL2 a	XP_016697338.1
	Gossypium hirsutum RuvBL2 b	XP_016740101.1
Gossypium raimondii	Gossypium raimondii RuvBL1 a	XP_012447317.1
	Gossypium raimondii RuvBL1 b	XP_012485133.1
	Gossypium raimondii RuvBL1 c	XP_012485134.1
	Gossypium raimondii RuvBL2 a	XP_012470737.1
	Gossypium raimondii RuvBL2 b	XP_012491995.1
Hordeum vulgare ssp. *vulgare*	Hordeum vulgare vulgare hypot	BAK05068.1
Ipomoea nil	Ipomoea nil RuvBL1	XP_019167132.1
	Ipomoea nil RuvBL2 a	XP_019173339.1
	Ipomoea nil RuvBL2 b	XP_019182975.1
Jatropha curcas	Jatropha curcas RuvBL1 a	XP_012068093.1
	Jatropha curcas RuvBL1 b	XP_012068094.1
	Jatropha curcas RuvBL1 c	XP_012068095.1
	Jatropha curcas RuvBL2	XP_012079431.1
Juglans regia	Juglans regia RuvBL1	XP_018844889.1
	Juglans regia RuvBL2	XP_018817409.1
Lupinus angustifolius	Lupinus angustifolius RuvBL1 a	XP_019436439.1
	Lupinus angustifolius RuvBL1 b	XP_019454631.1
	Lupinus angustifolius RuvBL2 a	XP_019433128.1
	Lupinus angustifolius RuvBL2 b	XP_019449887.1
Malus domestica	Malus domestica RuvBL1	XP_008378810.1
Manihot esculenta	Manihot esculenta hypot a	OAY33600.1
	Manihot esculenta hypot b	OAY35617.1
	Manihot esculenta hypot c	OAY51378.1
Marchantia polymorpha ssp. *polymorpha*	Marchantia polymorpha hypot	OAE28740.1
Medicago truncatula	Medicago truncatula hypot a	XP_003600480.1
	Medicago truncatula hypot b	XP_003603117.1
	Medicago truncatula hypot c	XP_003618820.1
Morus notabilis	Morus notabilis RuvBL2	XP_010106923.1
Musa acuminata ssp. *malaccensis*	Musa acuminata malaccensis RuvBL1	XP_009397499.1
Nelumbo nucifera	Nelumbo nucifera RuvBL1	XP_010248994.1
	Nelumbo nucifera RuvBL1	XP_010250729.1
	Nelumbo nucifera RuvBL2	XP_010273117.1
Nicotiana attaenuata	Nicotiana attaenuata RuvBL1	XP_019255439.1
	Nicotiana attaenuata RuvBL2	XP_019251608.1
Nicotiana sylvestris	Nicotiana sylvestris RuvBL1	XP_009798172.1
	Nicotiana sylvestris RuvBL2	XP_009785904.1
Nicotiana tabacum	**Nicotiana tabacum RuvBL1**	**XP_016434317.1**
Nicotiana tomentosiformis	Nicotiana tomentosiformis RuvBL1	XP_009592138.1
	Nicotiana tomentosiformis RuvBL2	XP_009615360.1
Noccaea caerulescens	Noccaea caerulescens RuvBL1	JAU05222.1
	Noccaea caerulescens RuvBL1 b	JAU35471.1

	Noccaea caerulescens RuvBL2	JAU89129.1
Oryza brachyantha	Oryza brachyantha RuvBL2	XP_006657884.2
Oryza sativa var. *japonica*	Oryza sativa japonica RuvBL2	XP_015644421.1
Phaseolus vulgaris	Phaseolus vulgaris a	XP_007135667.1
	Phaseolus vulgaris b	XP_007146707.1
Phoenix dactylifera	Phoenix dactylifera RuvBL1	XP_008776327.1
	Phoenix dactylifera RuvBL1	XP_008788050.1
	Phoenix dactylifera RuvBL2	XP_008806201.1
Physcomitrella patens	Physcomitrella patens hypot	XP_001779312.1
Picea sitchensis	Picea sitchensis hypot	ABR17735.1
Populus euphratica	Populus euphratica RuvBL1	XP_011006555.1
	Populus euphratica RuvBL2 a	XP_011015752.1
	Populus euphratica RuvBL2 b	XP_011018846.1
Populus trichocarpa	Populus trichocarpa	XP_002323491.1
	Populus trichocarpa	XP_006381348.1
	Populus trichocarpa Ruv	XP_006384768.1
Prunus persica	Prunus persica a	XP_007205168.1
	Prunus persica b	XP_007223107.1
Pyrus x *bretschneideri*	Pyrus bretschneideri RuvBL1 a	XP_009374971.1
	Pyrus bretschneideri RuvBL1 b	XP_009377811.1
	Pyrus bretschneideri RuvBL2 a	XP_009362554.1
	Pyrus bretschneideri RuvBL2 b	XP_009379332.1
Raphanus sativus	Raphanus sativus RuvBL1 a	XP_018442937.1
	Raphanus sativus RuvBL1 b	XP_018471784.1
	Raphanus sativus RuvBL2	XP_018493256.1
Ricinus communis	Ricinus communis RuvBL1	XP_002523847.1
Sesamum indicum	Sesamum indicum RuvBL1	XP_011071718.1
	Sesamum indicum RuvBL2	XP_011073680.1
Setaria italica	Setaria italica RuvBL2	XP_004957042.1
Solanum lycopersicum	Solanum lycopersicum RuvBL1	XP_004241955.1
	Solanum lycopersicum RuvBL2	XP_004234506.1
Solanum tuberosum	Solanum tuberosum RuvBL1	XP_006365976.1
	Solanum tuberosum RuvBL2	XP_006343323.1
Spinacia oleracea	Spinacia oleracea hypot	KNA25984.1
Tarenaya hassleriana	Tarenaya hassleriana RuvBL1 a	XP_010520446.1
	Tarenaya hassleriana RuvBL1 b	XP_010535704.1
	Tarenaya hassleriana RuvBL2	XP_010536617.1
Theobroma cacao	Theobroma cacao hypot a	EOY33372.1
	Theobroma cacao hypot b	EOY33373.1
	Theobroma cacao RuvBL1	XP_017983833.1
	Theobroma cacao RuvBL2	XP_007047571.1
Trifolium subterraneum	Trifolium subterraneum	GAU13448.1
Vigna angularis	Vigna angularis RuvBL1	XP_017407371.1
	Vigna angularis RuvBL2	XP_017436661.1
Vigna radiata ssp. *radiata*	Vigna radiata radiata RuvBL1	XP_014515071.1
	Vigna radiata radiata RuvBL2	XP_014519124.1
Vitis vinifera	Vitis vinifera b	CBI16308.3

	Vitis vinifera RuvBL1	XP_002285127.1
	Vitis vinifera RuvBL2	CAN80826.1
	Vitis vinifera RuvBL2	XP_003635231.2
Zea mays	Zea mays RuvBL2	NP_001148563.1
Ziziphus jujuba	Ziziphus jujuba RuvBL1	XP_015895701.1
	Ziziphus jujuba RuvBL2	XP_015890340.1

Supplement O

Schrumpfová, P.P.* and Fajkus, J. **2020**. Composition and Function of Telomerase - a polymerase associated with the origin of eukaryotes. Review. Biomolecules, 10(10):1425

P.P.S. was significantly involved in the ms writing and editing

biomolecules

MDPI

Review

Composition and Function of Telomerase – a polymerase associated with the origin of eukaryotes

Petra Procházková Schrumpfová [1,2,*], Jiří Fajkus [1,2,3]

[1] Laboratory of Functional Genomics and Proteomics, National Centre for Biomolecular Research, Faculty of Science, Masaryk University, Kotlářská 2, CZ-61137, Brno, Czech Republic.
[2] Mendel Centre for Plant Genomics and Proteomics, Central European Institute of Technology, Masaryk University, Kamenice 5, CZ-62500, Brno, Czech Republic.
[3] The Czech Academy of Sciences, Institute of Biophysics, Královopolská 135, 612 65, Brno, Czech Republic.
petra.proch.schrumpfova@gmail.com (P.P.S), fajkus@sci.muni.cz (J.F)
* Correspondence: petra.proch.schrumpfova@gmail.com

Received: date; Accepted: date; Published: date

Abstract: Canonical DNA polymerases involved in replication of the genome are unable to fully replicate the physical ends of linear chromosomes, called telomeres. Chromosomal termini thus become shortened in each cell cycle. The maintenance of telomeres requires telomerase - a specific RNA-dependent DNA polymerase enzyme complex that carries its own RNA template and adds telomeric repeats to the ends of chromosomes using a reverse transcription mechanism. Both core subunits of telomerase - its catalytic telomerase reverse transcriptase (TERT) subunit and telomerase RNA (TR) component – were identified in quick succession in Tetrahymena more than 30 years ago. Since then both telomerase subunits have been described in various organisms including yeasts, mammals, birds, reptiles and fish. Despite the fact that telomerase activity in plants was described 25 years ago and the TERT subunit four years later, a genuine plant TR has only recently been identified by our group. In this review, we focus on the structure, composition and function of telomerases. In addition, we discuss the origin and phylogenetic divergence of this unique RNA-dependent DNA polymerase as a witness of early eukaryotic evolution. Specifically, we discuss the latest information regarding the recently discovered TR component in plants, its conservation and structural features.

Keywords: telomerase; evolution; telomerase RNA (TR); telomerase reverse transcriptase (TERT); plant TERT; plant TR.

1. Telomerase Activity

Telomerase reverse transcriptase is a specific nucleoprotein enzyme complex that solves the problem that conventional DNA replication machinery cannot - to fill the gap after removal of the RNA primer of a most distal Okazaki fragment at the 5′ - terminus of the lagging strand. This results in a loss of a small portion of chromosomal DNA. This phenomenon is called the end-replication problem (Figure 1), first defined by Olovnikov [1]. Moreover, the ends of eukaryotic chromosomes - telomeres - must be long enough to assemble a protective nucleoprotein "capping" structure that can distinguish a natural terminus from an unrepaired chromosomal break. Dysfunctional telomeres may trigger genome instability, cell cycle arrest, and – at least in humans- replicative cell senescence and apoptosis (reviewed in [2,3]).

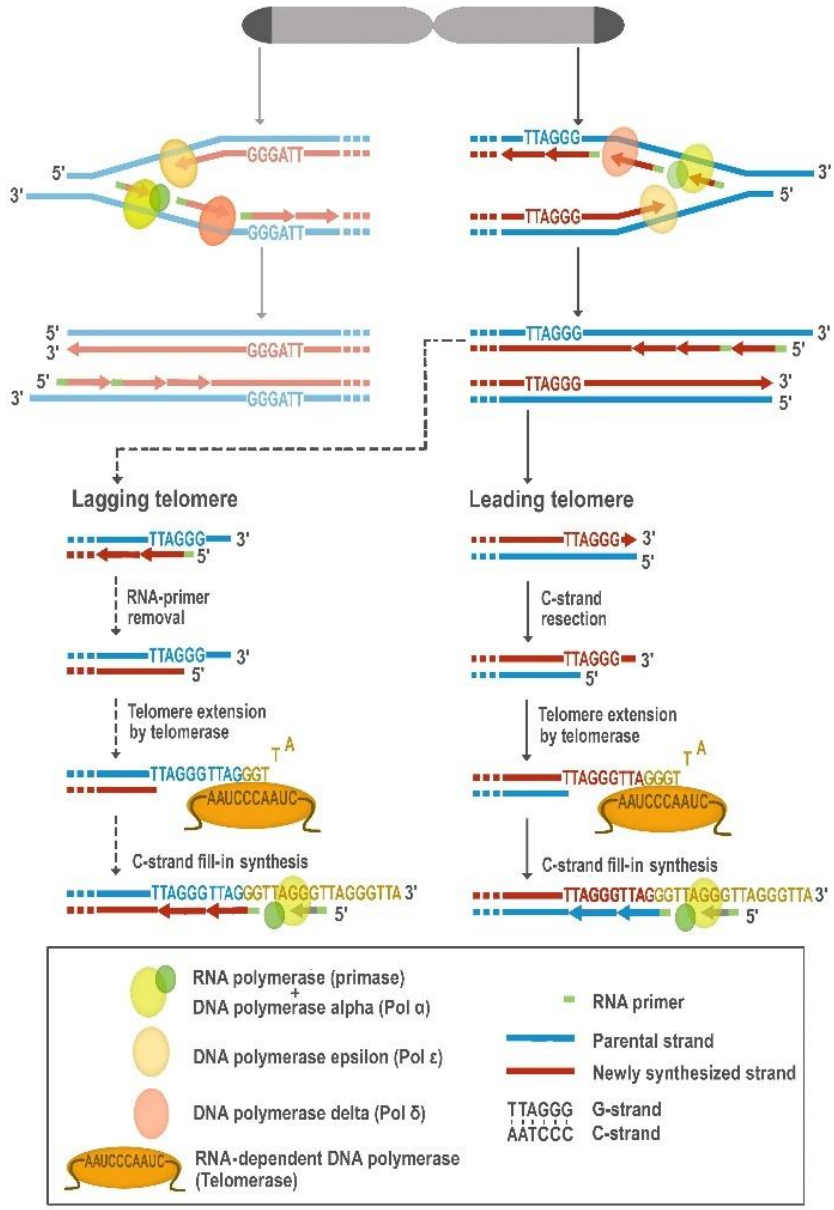

Figure 1. The replicating DNA in eukaryotes: DNA polymerases involved in replication. During semiconservative DNA replication, each strand serves as a template for DNA polymerases to synthesize a new complementary strand. A specialized RNA polymerase (primase), that is a part of DNA Pol α, synthesizes the RNA primer. A single RNA primer aids DNA replication on the leading strand and multiple primers initiate Okazaki fragment synthesis on the lagging strand. Further DNA synthesis is carried out by DNA Pol ε and DNA Pol δ (reviewed in [4]). The newly replicated telomere resulting from the lagging strand synthesis (Lagging telomere) retains the terminal RNA primer, which is subsequently removed. Attachment of the last RNA primer more proximally on the DNA strand, together with RNA-primer removal, creates an overhang on the G-rich strand. The initial product of the leading strand DNA synthesis (Leading telomere) is a blunt terminus whose C-strand is then resected by an exonuclease to create the mature G-rich overhang. In cells with an active RNA-dependent DNA polymerase (Telomerase), the G-rich overhangs originating from Lagging or Leading telomeres, can undergo elongation (reviewed in [5]). Telomerase carries its own RNA molecule, which is used as a template, and can anneal through the first few nucleotides of its template region to the distal-most nucleotides of the G-rich overhang of the telomere DNA, add a new telomere repeat (GGTTAG) sequence, translocate and then repeat the process. The complementary C-strand is then in-filled by DNA Pol α-primase [6].

In humans, telomerase activity is detected in all early developmental stages and increases progressively with advancing embryonic stages. After completion of organogenesis in the human fetus, telomerase is expressed only in proliferating tissue-specific stem cells (e.g., bone marrow progenitor cells and neural stem cells), while telomerase activity in somatic cells is downregulated (reviewed in [7]. However, a tendency to repress telomerase in mammalian somatic tissues was described only for mammalian species of weight greater than 1 kg; e.g., laboratory mice have a constitutive telomerase. It was proposed that in long-lived species, telomerase downregulation may have evolved to limit cell proliferation and reduce the risk of cancer. Correspondingly, ca. 90% of all human tumors display telomerase reactivation to achieve cellular immortality [8].

Telomerase, as a primary mechanism for telomere maintenance, is also conserved in plants. Analogous to mammals, telomerase activity is suppressed in terminally differentiated tissues, e.g., mature leaves or stems. Active telomerase is detected in organs and tissues such as seedlings, shoot and root tips, young and middle-age leaves, flowers, and floral buds with proliferating meristematic cells [7,9–13].

Telomerase carries, in addition to its protein catalytic subunit (telomerase reverse transcriptase; TERT), its own RNA templating subunit (telomerase RNA; TR) (reviewed in [14]). The expression of human TERT is strictly controlled at the transcript level and closely associated with telomerase activity, which suggests that hTERT is the primary determinant of enzyme activity [15]. In most human tissues, TR is ubiquitously expressed regardless of telomerase activity, and therefore, it has been considered by some authors as a non-limiting factor for telomerase activity [16]. However, telomerase activity in human T lymphocytes has been reported to relate to hTR levels but not hTERT protein levels [17,18].

In plants, contrary to most human cells, expression of the TR subunit, recently characterized by Fajkus et al. (2019) [19], follows a tissue-specific pattern similar to that which is typical for expression of TERT. In thale cress (*Arabidopsis thaliana*), the highest TERT mRNA levels were detected in flower buds, lower transcript levels were detected in seedlings and young leaves, and the lowest levels were observed in aged leaves [11]. Similarly, TR transcripts were most abundant in flower buds and 7-day-old seedlings. Markedly lower, yet detectable levels, were observed using RT-qPCR in 3-week-old seedlings and young leaves. Absolute levels of TR transcripts were 60-70 times higher than TERT mRNA levels [19]. Whole-mount *in situ* hybridization detected TR transcripts in primary root and lateral root apices of 3-week-old seedlings and in cultured cells, but in other tissue samples, using northern hybridization, no TR signal was found [20]. Levels of TR or TERT transcripts correlate strongly with telomerase activities observed in various plant tissues [7,11].

2. The Origin of Telomerase

The telomerase RNA-dependent DNA polymerase arose specifically within the eukaryotic lineage and was able to successfully solve the end-replication problem of linear chromosomes that leads to telomere shortening [21]. Telomeres are composed of short non-coding tandem repeat units, the length of which can significantly vary among diverse taxons. The lengths of telomere arrays can also vary at the level of the species or ecotypes (reviewed in [22,23]). The human-type $(TTAGGG)_n$ telomeric sequence is conserved across several eukaryotic 'supergroups' [24] including Amorphea supergroup with metazoan and fungal species (reviewed in [25,26]. At the same time, several exceptions are known across the Amorphea supergroup, e.g., in insects $(TTAGG)_n$ [27,28], in Nematodes $(TTAGGC)_n$ [29] or in several fungal genera, where very complex or irregular telomeric runs were described [26,30] (Figure 2). Additionally, telomeres of some insects are constituted with unusual telomeric motifs of even with telomeric repeats that consist of arrays of non-long-terminal-repeat (non-LTR) retrotransposons [31–33]. The *TERT* gene disappeared from the genomes of some insects with non-LTR retrotransposons, as in the vinegar fly (e.g. *Drosophila melanogaster*). In silkworm (*Bombyx mori)*, TERT is very weakly expressed in various tissues, telomerase activity is barely detectable and retrotransposition is required to maintain the length of chromosome ends [33–36].

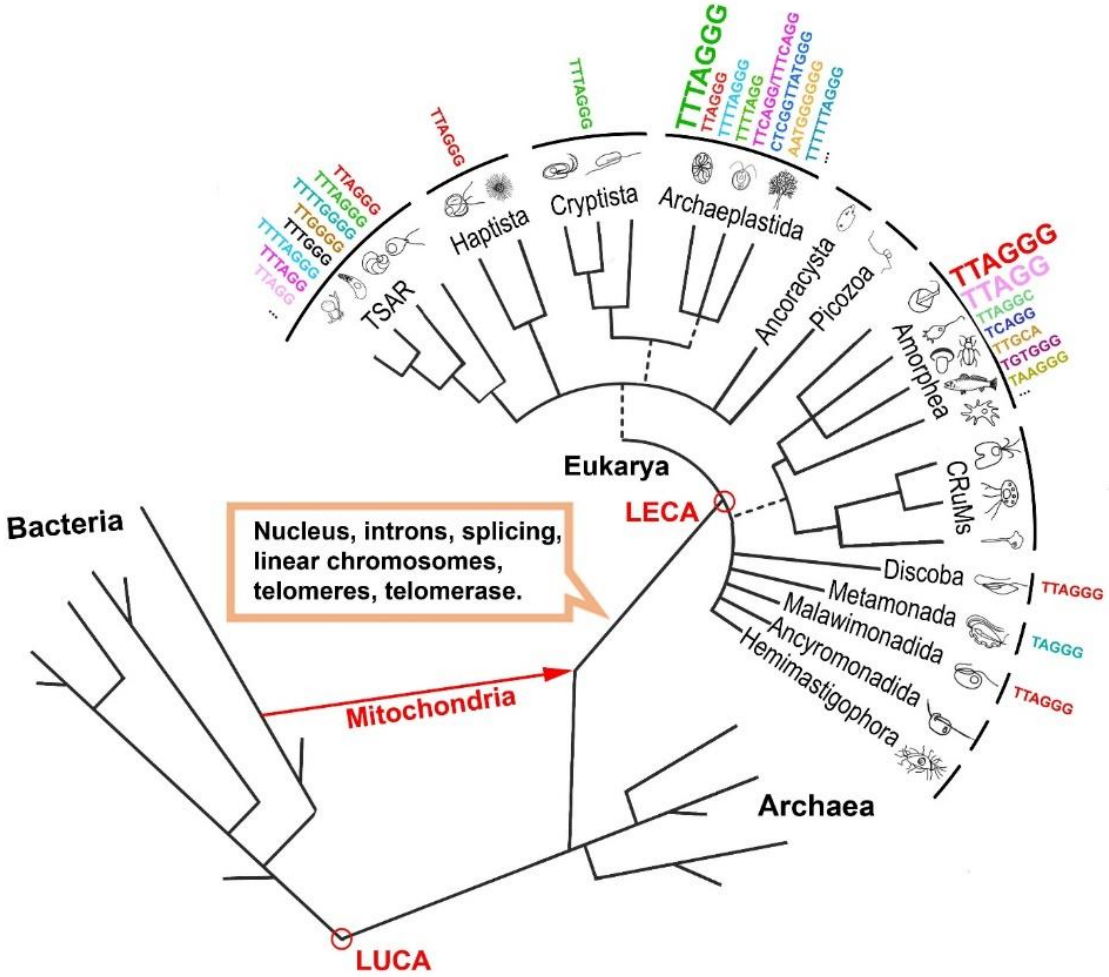

Figure 2. Telomeres and Telomerase in the Evolutionary Tree. A simplified phylogenetic tree is shown, where telomeres and telomerase evolved upon linearization of chromosomes by the insertion of Group II self-splicing introns [37]. In the Eukaryote branch, the groupings correspond to the current 'supergroups' according to the recent eukaryotic Tree of Life (eToL) [24]. Unresolved branching orders among lineages are shown as multifurcations. Broken lines reflect lesser uncertainties about the monophyly of certain groups. Examples of known telomeric repeat variants are listed next to respective supergroups (see also Table S1). The major known telomeric repeat variants in the supergroups are marked with a larger font [22,36,38] (see text for details). Last eukaryote common ancestor (LECA); last universal common ancestor (LUCA). The living species icons are partly adopted from Adl et al., 2012 [39].

In the Archaeplastida supergroup that includes the land plants, mosses, red algae and green algae, the telomere is mostly composed of $(TTTAGGG)_n$ repeats, first described in *A. thaliana* (Arabidopsis-type repeats [40]. Despite this, the human-type telomere repeat is shared by several plant taxa from the order Asparagales [41], including species of the Allioideae subfamily, except for the Allium genus [42], where a more complex telomeric sequence $(CTCGGTTATGGG)_n$ was described [43]. An unusual telomeric motif $(TTTTTTAGGG)_n$ was found in the genus *Cestrum* (Solanaceae) [44], and in some species from the carnivorous genus *Genlisea* (TTCAGG and TTTCAGG) [45]. Outside of land plants, repeats other than the Arabidopsis-type were characterized in some algae and glaucophyte species ($(AATGGGGGG)_n$, $(TTTTAGGG)_n$, $(TTTTAGG)_n$ etc.) [22,38,46]. Unlike insects, even the unusual plant telomeric sequences characterized so far are synthesized by telomerases using TRs with corresponding template regions [19,43,44,47].

Before the linear chromosomes of eukaryotes emerged, ~1 Gy ago, circular chromosomes had been successfully used for 2 Gy in eubacteria and archaea, and they still predominate in most bacterial forms [48]. In a concept elaborated by E. V. Koonin [37], the origin of linear chromosomes, telomeres and telomerase is associated with invasion of archaeal hosts by an alpha-proteobacterial progenitor that resulted in mitochondrial endosymbiosis and invasion of Group II self-splicing introns, the most ancient genetic entities **(Figure 2).** Group II introns were suggested as eukaryotic evolutionary ancestors of retrotransposons and spliceosomal introns. They consist of a catalytically active intron RNA and an intron-encoded reverse transcriptase (RT), which is related to non-LTR-retrotransposon RTs and assists splicing by stabilizing the catalytically active RNA structure (reviewed in [49]. Invasion of Group II introns resulted in the evolution of spliceosomal introns, compartmentalization of the majority of genetic information in the nucleus and linearization of chromosomes.At the same time, solution of the end-replication problem was hinted at by a mechanism pre-existing in a primordial pool of 'virus-like' genetic elements in the earliest stages of life's evolution [37]. It seems that incipient eukaryotes, due to the presence of Group II sequences, could have had stable linear chromosomes without the need for telomerase or telomere specific proteins [48].

The TERT component of telomerase is highly conserved, having a centrally positioned reverse transcriptase motif (RT domain) [50–52]. The presence of TERT was detected in early branching eukaryotes [53,54]. It was proposed that telomerase originated as an ancient reverse transcriptase (RT) that internalized a primitive template-bearing RNA during early eukaryotic evolution and later evolved into modern telomerase RNPs with various indispensable and stably TR-associated components [55,56]. In accordance with this notion, the TERT subunit has the ability to bind the RNA molecule that provides the template sequence for DNA synthesis (TR) and various non-telomeric sequences [57,58]. The conserved RT motifs between TERT and other RTs indicates that TERT protein is closely related to RTs from the group of Penelope-like Elements (PLEs) and non-long-terminal-repeat (non-LTR) retrotransposons [55]. PLEs have an RT that lacks endonuclease activity and it is plausible that ancient retrotransposons similar to these terminal PLEs might be the progenitors of TERT proteins [56].

Interestingly, besides the telomerase-dependent mechanism of telomere elongation, yeast, mammalian, as well as plant cells can use alternative mechanisms of lengthening of telomeres (ALT) based on homologous recombination (HR). ALT usually results in telomeres that are highly heterogeneous in length and sequence [59–61]. In plants, the ALT mechanism is activated in mutants with telomerase dysfunction and possibly also during the earliest stages of normal plant development [59–62].

It is suggested that the canonical telomeric repeats have been changed or lost independently several times during evolution [36,46] and telomerase may have even occasionally been lost [36]. It would be interesting to further investigate the occurrence of unusual telomeric motifs, the co-evolution of genes encoding core telomerase subunits (TERT and TR), and replacement of telomerase by telomerase independent ALT systems (probably the ancestral telomere maintenance tools) in cases where there is evolutionary loss of telomerase.

3. RNA subunit of Telomerase

The non-coding RNA serving as telomerase RNA (TR), also known as TER or TERC, contains the template region for addition of telomeric repeats. TR is highly divergent, compared to TERT, ranging in size from ~150 nucleotides (nt) in ciliates to over 3000-nt in yeasts [63]. TR has a number of conserved structural domains, consisting of the template/pseudoknot (t/PK) domain, template boundary element (TBE) and stem-loop region. In humans, the stem-loop region contains conserved structural domains: A conserved region 4/5 (CR4/5); the 3' H/ACA (H-box (consensus ANANNA); an ACA-box (ACA) domain; and a Cajal body box (CAB-box) motif (reviewed in [64,65]) (Figure 3a). Although the gene coding telomerase RNA had already been identified in *Tetrahymena* in 1989, and in humans in 1995 [14,66], it took another three decades for the first *bona fide* plant TR genes to be characterized, in 2019 [19]. Interestingly, the unusual length of the Allium telomere repeat unit (12-

nt) [43] was used to identify candidate TRs not only in *Allium* species but subsequently across the phylogeny of land plants with either canonical or unusual types of telomere repeats [19]. Previously characterized TER1 and TER2 in *A. thaliana* were shown not to act as telomerase RNAs [19,67] and the original paper describing them has been retracted [68,69].

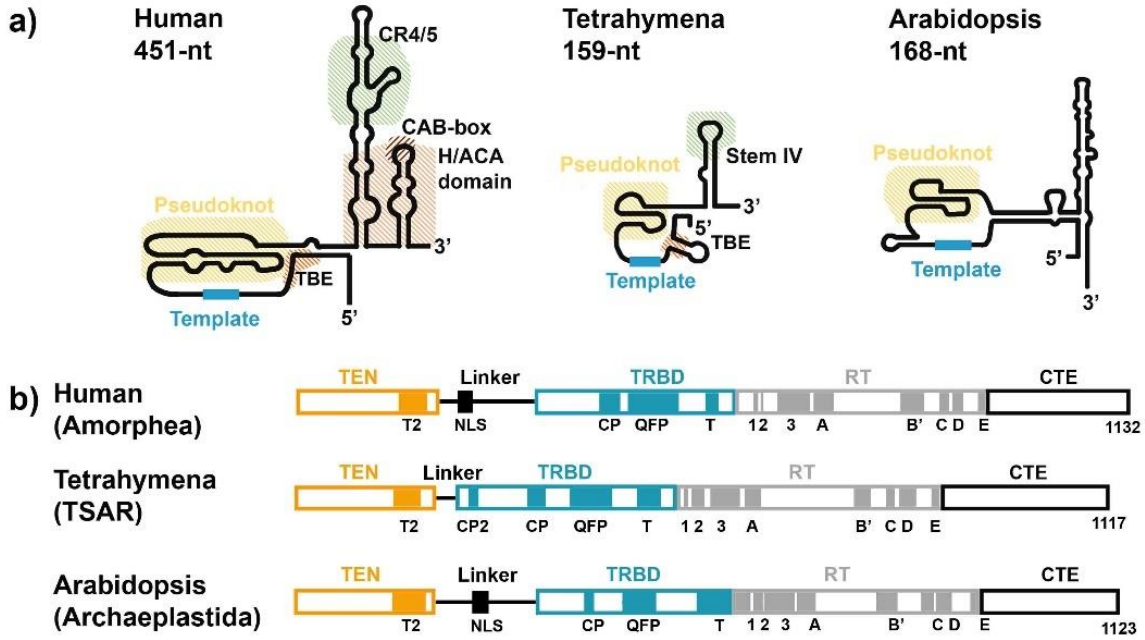

Figure 3. Conservation of functional domains of two core telomerase subunits – TERT and TR. **a)** Models of secondary structures of human, Tetrahymena and Arabidospis TRs suggest conservation of several structural motives including pseudoknot in the vicinity of the template (t/PK domain) and stem-loop regions [70,71]. In humans the stem-loop region contains the conserved 4/5 (CR4/5) region, the H (AnAnnA) and ACA-boxes (H/ACA) domains and the Cajal body box (CAB-box) motif that serve as binding sites for other protein components of the telomerase holoenzyme complex (dyskerin, NOP10, NHP2, and GAR1). In Tetrahymena the stem-loop 4 (SL4) is directly bound by p65 protein [72]. To date, particular interactors and their binding sites have not been demonstrated directly in Arabidopsis (see also Table 1). **b)** Domain arrangement of human (Animals), Tetrahymena (Ciliates) and Arabidopsis (Plants) TERTs. The supergroup for each species is given. N-terminus: telomerase essential N-terminal (TEN) domain and RNA-binding domain (TRBD domain) are separated by Linker that contains a nucleus localization-like signal (NLS). The central RT domain: catalytical part of the enzyme that contains seven evolutionary-conserved RT motifs (1, 2, A, B′, C, D and E motifs) and also telomerase specific 3 motif [73–75]. C-terminus: C-terminal extension (CTE) domain.

In mammals, telomerase RNA belongs to the family of small nucleolar (snoRNAs) and small Cajal body (scaRNAs) RNAs [76,77]. Both snoRNAs and scaRNAs are encoded in introns and transcribed by RNA polymerase II (RNA Pol II) along with their host structural genes [78–80]. The human TR primary transcript is synthesized by RNA Pol II, capped on its 5′ end with a monomethylguanosine (MMG) cap that is further methylated to N2, 2, 7 trimethylguanosine (TMG) cap [81–83], internally modified, and processed at its 3′ end to generate the mature, functional TR (reviewed in [65,84]. Several structural motifs and formation of the overall tertiary structure of TR are needed for a proper interaction with the TERT subunit (reviewed in [85]. Although TERT can bind to TR through the t/PK domain alone, additional binding with the CR4/5 domain is required [86,87].

Like many other polymerases, telomerase catalyzes nucleotide addition to the 3′ hydroxyl group of a primer, forming a product–template duplex. Accurate telomeric repeat synthesis depends on strict boundaries of a template region within TR, which functions as a STOP signal in the telomerase extension step (reviewed in [70]). In humans, to synthesize 6-nt telomeric repeats of the human-type telomeric motif, telomerase anneals five nucleotides of its 11-nt long template region with terminal nucleotides of the telomere DNA and extends it with 6-nts complementary to the rest of the template region [88].

Telomerase processivity requires repeated cycles of annealing, synthesis, translocation and re-annealing of substrate DNA–TR base-pairing [70]. Telomerase remains associated with substrate DNA even when DNA–RNA base-pairing is disrupted, however the exact mechanism was unknown [89–91]. Recently, details of processive telomerase catalysis were revealed using high-resolution optical tweezers. The authors demonstrated that a stable substrate DNA binding at an anchor site within telomerase facilitates the processive synthesis of telomeric repeats, which results in synthesizing multiple telomeric repeats before releasing them in a single step. The product DNA synthesized by telomerase can be recaptured by the anchor site or folded into G-quadruplex structures [92].

It remains controversial whether active telomerase enzyme in humans functions as a dimer (TR and TERT) or only as a monomer of each subunit [93–96]. In contrast to the human telomerase complex, the affinity-purified telomerase from *Tetrahymena* is monomeric [97]. The possible dimerization of telomerase was also suggested in plants. Dimerization, modulated by a conserved TRBD domain from *A. thaliana* TERT that is able to interact separately with the N-terminal fragments and itself, was observed using yeast two-hybrid analysis of interactions [98].

While the mechanism of the telomerase catalytic cycle may be similar among telomerases from different kingdoms, recent characterization of plant TRs across the whole land plant phylogeny revealed some features distinct from TRs described in mammals or fungi. First, plant TRs are transcribed with RNA Pol III [19], similarly to TRs in Ciliates, while mammalian or yeast TRs are RNA Pol II products [55]. The closer relationship between TR biogenesis in Ciliates (supergroup TSAR) and Plants (supergroup Archaeplastida) on the one hand, and fungi and animals (supergroup Amorphea) on the other hand, corresponds to current versions of the phylogenetic tree of eukaryotes, (which is supported by phylogenomic studies), and respective ancestral supergroups [24]. Plant TRs show relatively conserved structures of their RNA Pol III promoters (so called Type 3 RNA Pol III promoter [99] with a typical Upstream Sequence Element (USE) and TATA box. Further, TRs in land plants have a monophyletic origin [19]. This contradicts the previous paradigm, according to which, relatively conserved TERT subunits associate with very diverse - and unrelated – RNAs [57,58].

Interestingly, template regions of plant TRs are of relatively diverse lengths. They are mostly of the length corresponding to one and one half of the telomere repeat, which allows for substrate DNA annealing. The template regions may, however, also be shorter (e.g., in *A. thaliana* TR, whose template region is only 9-nt long) or longer - as long as two complete telomere repeat units, e.g., as in wild carrot (*Daucus carota*) [19]. However, it is important to note that the authentic, functional part of the template region may be shorter than the putative predicted template (the region complementary to the synthesized telomere repeat, e.g., *Cestrum elegans*), as it is delimited by secondary structural elements in TRs. Some other secondary structural motifs of TRs - e.g., the pseudoknot structure downstream of the template region - seem conserved among animal, plant and fungal TRs [55,64,71].

Whether a primary transcript of plant telomerase RNA is generated similarly as in Ciliates (synthesized by RNA Pol III, not spliced, leaving a 3′ polyuridine tail [64,100] or which motifs, domains or stems of TR are involved in TR-TERT interaction need to be clarified. Moreover, the functions of TR expand far beyond its templating function as it forms a flexible scaffold that functions in correct telomerase RNP assembly.

4. TERT Subunit of Telomerase

Most of the catalytic subunits of telomerase, TERTs, including the human and plant TERTs, can be classified into three major parts. At the N-terminus are positioned telomerase-specific motifs (N-terminal domain), reverse transcriptase motifs (RT domain) are positioned centrally, and at the C-terminus of the TERT protein are localized conserved motifs - these are more or less specific for particular groups of organisms (C-terminal extension, CTE) (Figure 3b).

The central RT domain is the catalytical part of the enzyme and contains seven evolutionarily-conserved RT motifs (1, 2, A, B′, C, D and E motifs). This domain is organized into two subdomains, the "fingers" involved in nucleotide binding and processivity, and the "palm" providing the polymerase catalytic residues and DNA primer grip [50,51,94,101].

There are two main domains recognized within the N-terminal part: the TEN domain (telomerase essential N-terminal, also known as the RNA interaction domain 1 (RID1)) [102,103] and the RNA-binding domain (TRBD) (reviewed in [75]. Moreover, a variable linker physically and functionally separates these two domains and has been shown to be biologically essential for the function of TERT (reviewed in [103]. The nucleus localization-like signal (NLS), placed between TEN and TRBD domains, is responsible for nuclear import of TERTs [104].

The TEN domain has both DNA-binding and nonspecific RNA-binding properties and may also stabilize short RNA–DNA duplexes during telomere extension: i.e., repeated cycles of telomerase annealing, synthesis, translocation, and re-annealing.

Despite poor sequence homology, the CTE-part is almost universally conserved, although several roundworm species appear to lack this structure entirely [102]. The crystal structure of the human CTE domain identified three highly conserved regions within the CTE-region [105]. It is proposed that CTE is involved in promoting telomerase processivity, in regulating telomerase localization and is involved in differential binding of DNA, but not in essential catalytic functions, as reviewed in [106].

It was proposed that TERT in metazoan ancestors possesses all three major parts and 11 canonical motifs: GQ, CP, QFP, T motifs within the N-terminal part, and 1, 2, A, B′, C, D and E motifs within the RT part. However, GQ and CP motifs might be missing in some beetles (e.g., *Tribolium castaneum*) [103] or unicellular relatives of metazoans (e.g., Trypanosoma sp.). Similarly, the plant TERTs possess three major parts, 11 canonical motifs and CTE-part [75].

Although the TERT protein is highly conserved, the gene structure differs among the group of organisms as they differ in exon/intron organization. In Ciliates, species with 1 exon (e.g., *Euplotes aediculatus*) to 19 exons (*Tetrahymena thermophila*) were identified [75]. Contrary to Ciliates, the TERT exon-intron structure is conserved across the Vertebrata. Mammalian TERT has 16 exons whereas TERTs in non-mammalian vertebrates have anywhere between 14 to 17 exons [50,103,107–109]. Among plants, TERT genes with 12 exons are highly conserved [75]. Although most eukaryotes, including humans, harbor a single TERT gene, in polyploid plant species, as in allotetraploid *Nicotiana tabacum* (tobacco), multiple TERT paralogs exist that are differentially regulated [10,110].

5. Telomerase Regulation

As described above, the primary determinant for telomerase enzyme activity in humans seems to be a strictly controlled transcription level of the TERT subunit [15] rather than expression of the TR subunit, which is ubiquitously expressed in almost all tissues regardless of telomerase activity [16].

Many studies have dissected the mammalian TERT promoter and identified cis-elements (E-boxes, GC motifs, ETS domain) bound by general transcription factors (TFs) such as c-MYC, NF-κB, STAT3, SP1 or ETS2 (Figure 4a) (reviewed in [101,111–113]). Moreover, these general TFs can be regulated by a number of other proteins; e.g., human RuvBL2 (reptin) regulates c-MYC-dependent transcription of TERT [114]. The core functional promoter essential for transcriptional activation of human TERT in cancer cells was suggested in the 181-bp [115] or 208-bp fragment [116] respectively, upstream of the transcription start site. In plants, the 336 bp long promoter region of the TERT promoter seems to be essential for successful complementation of telomerase and reversion of the

short telomere phenotype in *tert -/- A. thaliana* plants (Table 1a) [13,117]. Crhák et al. showed efficient and tissue-specific control of telomerase reconstitution. At the same time, the results have shown that the level of *AtTERT* transcript is not the sole determinant for the successful restoration of telomeric function of telomerase, which suggests posttranscriptional control of telomerase expression [117]. Moreover, restoration of telomerase activity, as evaluated in complemented plant extracts *in vitro*, not always correlated with the ability to restore telomere maintenance *in planta*.

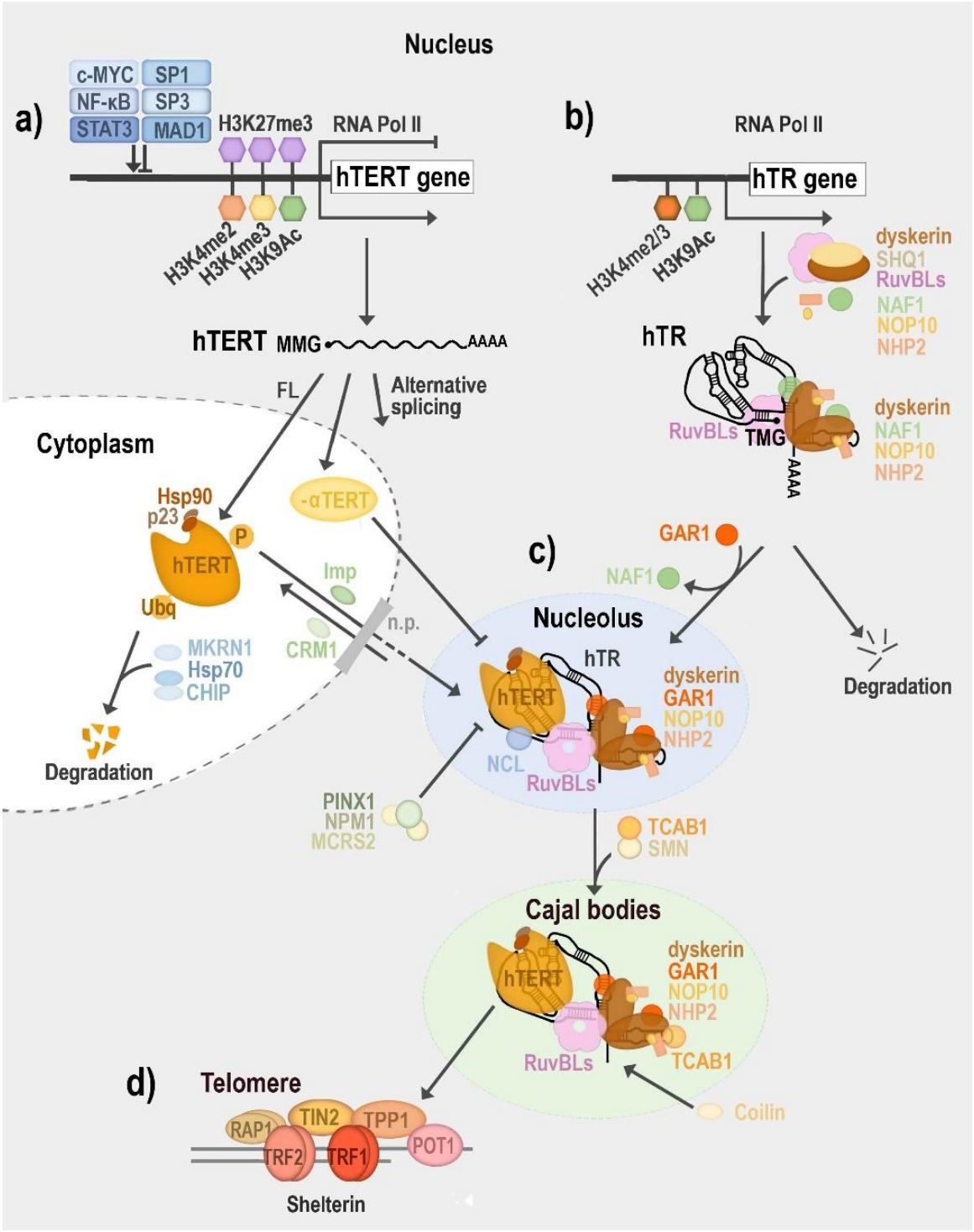

Figure 4. Regulation of human telomerase biogenesis.

a) Transcription of the human telomerase reverse transcriptase gene (*hTERT*) by RNA polymerase II (RNA Pol II) is regulated by several activators and repressors acting at the promoter level (e.g. c-MYC, Nuclear Factor κB (NF- κB), Signal Transducer and Activator of Transcription 3 (STAT3), Specificity Protein 1/3 (SP1/3), MAD1). Histone modification H3K27me3 often silences *hTERT*, however the mutated *hTERT* allele is marked by the active histone marks H3K4me2, H3K4me3 and H3K9ac. *hTERT* pre-mRNA with a 5′ mono-methylguanosine (MMG) cap and poly(A) 3′ tail, can be spliced into full-length (FL) or multiple alternative isoforms (Alternative splicing) that are catalytically inactive or even inhibit telomerase activity (e.g. minus alpha TERT (-α TERT) due to their competition for hTR with FL hTERT mRNA). Binding of heat shock protein 90 (Hsp90) with its co-chaperone (p23) in the cytoplasm enables hTERT phosphorylation (P). hTERT is further imported back to the nucleus by Importin α or β1 (Imp) *via* nuclear pores (n.p.), while export of hTERT may be mediated by the chromosome region maintenance 1 protein homolog (CRM1, also known as exportin-1). The ubiquitin (Ubq) -proteasomal degradation of TERT is driven by E3 ubiquitin-protein ligase makorin-1 (MKRN1), heat shock protein 70 (Hsp70) and carboxyl-terminus of Hsp70 Interacting Protein (CHIP).

b) Histone modifications H3K4me2/3 or H3K9Ac help to regulate read-through of the human telomerase RNA (hTR) gene by RNA Pol II in telomerase-positive cell lines. SHQ1 chaperone and RuvB-like proteins (RuvBLs) facilitate assembly of nascent RNA with RNA scaffold proteins (dyskerin, NOP10, NHP2, and NAF1). Mature TR is capped with a tri-methylguanosine (TMG) cap at the 5′ end, polyadenylated at the 3′ end and co-transcriptionally associated with scaffold proteins. The hTR variants with shorter or longer 3′ ends or associated with variant proteins may lead to degradation of hTR. NAF1 is replaced by GAR1 before the hTR ribonucleoprotein complex reaches the nucleolus.

c) RuvBLs (pontin and reptin) enable telomerase assembly and allow hTERT recruitment to the nucleolus to form a mature telomerase complex while bound by nucleolin (NCL). PIN2/TERF1—interacting telomerase inhibitor 1 (PINX1), together with nucleophosmin (NPM) and microspherule protein 2 (MCRS2), regulate hTERT availability in a cell cycle-dependent manner. Telomere Cajal body protein 1 (TCAB1, also known as WRAP53) recognizes the Cajal body box (CAB-box) of the hTR in the mature telomerase complex and recruits it to the Cajal bodies (CBs). In CBs, hTR interacts with local proteins such as coilin while survival motor neuron protein (SMN) binds hTERT.

d) In S-phase, the CBs colocalize with telomeres and facilitate the recruitment of the mature telomerase complex to the telomeres *via* interaction with TPP1 protein, which is one of the subunits of a protein complex localized at telomeres, termed as Shelterin. The presence of Shelterin proteins (telomeric-repeat binding factor 1/2 (TRF1/2), protection of telomeres protein 1 (POT1), TRF1-interacting nuclear factor 2 (TIN2), repressor/activator site binding protein (RAP1) and TPP1 helps distinguish chromosomal ends (telomeres) from DNA breaks. (For references see Text or Table 1.)

The wild-type promoter of the human TERT gene is often silenced by the repressive trimethylation of Lys27 in histone H3 (H3K27me3) modification. Consistent with this finding, the mutated human TERT allele is marked by the active histone marks H3K4me2, H3K4me3 and acetylated histone H3 Lys9 (H3K9ac) [118,119]. Analysis of the epigenetic states of the TERT gene in Arabidopsis telomerase-positive and telomerase-negative tissues revealed differential levels of H3K27me3, the mark of developmentally silenced heterochromatin regions in plants, whereas euchromatin-specific marks (H3K4me3 and H3K9Ac) were approximately at the same levels in all tissues [11]. The striking stability of the epigenetic status of the TERT promoter in Arabidopsis may reflect a unique attribute of plants – their totipotency – which is in accordance with the reversible and dynamic character of telomerase silencing [120].

Table 1. Human and Arabidopsis telomerase assembly - a comparative overview (a-d classification corresponds to Figure 4).

		Mammals (human)	Reference(s)	Plants (*Arabidopsis thaliana*)	Reference(s)
a) TERT	**Minimal promoter**	330 bp upstream of the translation start site to 228 bp downstream.	[115,116,121]	336 bp long promoter region of the translation start site with plausible regulatory intron 1.	[13,117]
	RNA Polymerase	RNA Pol II	[115]	RNA Pol II	[122]
	Histone modifications of promoter	Telomerase-negative tissues: H3K27me3; telomerase-positive tissues (mutated TERT allele): H3K4me2, H3K4me3 and H3K9ac.	[118,119,123]	Telomerase-negative tissues: H3K27me3, H3K4me3, H3K9Ac; telomerase-positive tissues: H3K4me3, H3K9Ac.	[11]
	TERT expression in organism	TERT expression is strictly controlled at the transcript level.	[15,124]	The dynamics of TERT transcripts correlates with telomerase activity observed in plant tissues.	[7,11]
	Number of exons	16 exons	[75,121]	12 exons	[75]
	Alternative splicing of mRNA	hTERT pre-mRNA can be spliced into at least 22 isoforms.	[125]	AtTERT pre-mRNA can be spliced into 3 isoforms.	[75]
	Post-translational modifications	Phosphorylation or ubiquitination.	[126,127]	No putative phosphorylation site in *A. thaliana* TERT (but predicted in rice or tabacum TERT).	[128,129]
	Import to the cell nucleus	Importin α promotes nuclear import of the TERT.	[130]	Importin subunit alpha-4 is associated with TERT.	[98]
	Protein domains	TEN, TRBD, RT, CTE.	[75,108]	TEN, TRBD, RT, CTE.	[75]
	Protein length	1132 aa	[108]	1123 aa	[131]
b) TR	**Histone modifications**	hTR expression in telomerase-positive cell lines is associated with H3K4me2/3, H3K9Ac and hyperacetylation of H4.	[132,133]	Not known yet.	
	RNA Polymerase	RNA Pol II	[66]	RNA Pol III	[19,20]
	Modifications	5′ end cap, internally modified, poly (A) tail	[83]	Not known yet.	
	Template region	11-nt long template region (synthesizes 6-nt telomeric repeats GGTTAG).	[66,88]	9-nt long template region (synthesizes 7-nt telomeric repeat GGTTAG).	[19]
	TR gene length	451-nt long transcript	[66]	268-nt long transcript	[19,20,71]
	TR expression in organism	In most tissues TR is ubiquitously expressed regardless of telomerase activity.	[16,17]	The dynamics of TR transcripts correlates with telomerase activity observed in plant tissues.	[7,11]
c) Nucleolus and CBs	**TR scaffold proteins**	Dyskerin, NOP10, NHP2, NAF1/GAR1.	[96] [84]	Not known yet. Dyskerin (CBF5), NOP10, NHP2, NAF1, and GAR1 are	[19,134–136]

				localized in the nucleolus. Telomerase activity can be immunoprecipitated with dyskerin (CBF5) in plants. Dyskerin associates with TRB proteins.	
	Nucleolin	NCL involves nucleolar localization of TERT.	[137]	NUC-L1 has a role in telomere maintenance and telomere clustering.	[138,139]
	RuvBLs	RuvBLs (pontin and reptin) interact with TERT and dyskerin.	[140]	Interactions between TERT and RuvBL proteins is mediated by TRB proteins.	[134]
	coilin	Interacts with TR.	[141,142]	Colocalizes with TRB1 in the CBs adjacent to the nucleolus.	[143]
d) Association with telomere		The TPP1 protein interacts with TERT and facilitates the recruitment of the mature telomerase complex to the telomeres.	[144]	The TRB proteins interact with TERT and may help to recruit telomerase to the plant telomeres.	[145]

Additionally, TERT transcripts in many animal species, including vertebrates, insects or nematodes, are alternatively spliced [75,103,146,147]. Specific patterns of TERT mRNA variants expressed in humans and rodents during development indicate that splicing events are not random and could have a physiological function (Figure 4a) [75,148–151]. Human TERT pre-mRNAs in early development can be spliced into 22 isoforms, while telomerase activity is associated only with the full-length hTERT (reviewed in [152]. Some of the alternate hTERT mRNA forms (e.g., the minus alpha-variant) may not only be catalytically inactive, but even show a dominant negative inhibition of telomerase activity [153]. Correspondingly, differential patterns of hTERT mRNA splicing were observed between normal (fetal human colon, FHC) and adenocarcinoma colon (HT-29) cells during their sodium butyrate-induced differentiation. The higher abundance of the minus alpha-variant of hTERT mRNA was observed in FHC cells, which may be involved in the more rapid loss of telomerase activity in these cells during differentiation [154]. Spliced variants may also have non-canonical roles, for example in cell proliferation [125,155]. Alternative splicing was also described in many plant species (e.g., A. thaliana, Oryza sativa (rice), Iris tectorum (roof iris)) (reviewed in [75]. Short isoforms of TERT protein originating from the alternate splicing events could be functionally important, as suggested for the A. thaliana variant AtTERT V(I8)) (TERT variant in intron 8). This isoform of AtTERT is able to bind Protection of telomeres protein 1a (AtPOT1a), (one of the Arabidopsis orthologues of the human or fission yeast single-stranded telomeric sequence binding protein POT1), more efficiently than full-length AtTERT [156,157].

It has been proposed that human telomerase is subjected to posttranslational regulation such as phosphorylation or ubiquitination [126,127], reviewed in [112]. Putative phosphorylation sites were identified in TERT amino acid sequences from O. sativa [128] or N. tabacum [129] but not in AtTERT from A. thaliana [128].

In plants, indirect regulation of telomerase by various proteins or hormones has also been described. In tobacco cell culture, phytohormones such as abscisic acid or auxin regulate phosphorylation of telomerase protein, which is required for the generation of a functional telomerase complex [129,158]. In A. thaliana, reduced endogenous concentrations of auxin in telomerase activator 1 (AtTAC1) mutant plants block the ability of this zinc-finger protein to induce AtTERT. However, AtTAC1 does not directly bind the AtTERT promoter [159,160]. Similar to humans, AtRuvBL2a protein may be involved in regulation of TERT transcription in plants because

in AtRuvBL2a heterozygous mutants, a moderate but significant increase in AtTERT transcripts was observed. Interestingly, telomerase activity in these plants was reduced to ca. 5% compared to WT plants [134].

The regulation of telomerase activity may also be driven by modulation of TR maturation. As described previously, biogenesis of the human TR involves a complex series of posttranscriptional modifications (Figure 4b, Table 1b) (reviewed in [84]. In humans, the set of TR transcripts with heterogenous 3′-ends may be trimmed by various exonucleases [161]. Similarly, various 5′ cap-binding complexes can be recruited to a mono- or tri-methylguanosine cap [82,162].

There is also evidence that in addition to its canonical role in telomere maintenance, both telomerase subunits - TERT and TR - can function independently of telomerase [163]. It was demonstrated that, e.g., the TR subunit was upregulated at very early stages of tumorigenesis, whereas telomerase activity was detected in end-stage tumors [164], and that the RNA component seems to be capable of DNA damage response (DDR regulation) [165]. The TERT subunit, independently of its action on telomeres, regulates the cell-cycle, inhibits apoptosis, regulates gene expression, modulates cell signaling (e.g., Wnt/β-catenin, NF-κB pathways) and DDR, or binds to and protects mitochondrial DNA (mtDNA) (reviewed in [85,163,166].

In plants, the armadillo/β-catenin-like repeat-containing protein (ARM) or Chromatin remodeling 19 (CHR19) proteins associated with TERT may reflect possible non-telomeric functions of telomerase [167]. ARM proteins play a role in the Wnt/β-catenin signaling pathway in humans [168], but non-telomeric functions of plant TERT or TR remain elusive.

6. Composition of Enzymatically Active Telomerase

The active human telomerase is composed not only of a core complex of TR encircled by TERT but is assembled as a functional complex in a stepwise regulated process governed by multiple stably- or transiently-associated proteins.

Human telomerase RNPs, as well as other box snoRNPs or scaRNPs, are associated with two conserved H/ACA boxes, (H box (consensus ANANNA) and the ACA box (ACA)) binding protein complexes: dyskerin, NOP10, NHP2 and NAF1 in the nucleoplasm, where NAF1 is replaced by GAR1 before the hTR RNP complex reaches the nucleolus (Figure 4c) (reviewed in [84,169]). Assembly of TR and TERT into catalytically active telomerase is aided by RUVBL1 (pontin) and RUVBL2 (reptin) AAA+ ATPases, due to their direct interaction with TERT and dyskerin [140]. In mammals, the telomerase RNP is retained in nucleoli through the interaction between TERT and nucleolin in the dense fibrillar component [137,170]. Telomerase activity is negatively regulated by the nucleolar protein PIN2/TERF1—interacting telomerase inhibitor 1 (PINX1) [171]. Nucleophosmin (NPM) and microspherule protein 2 (MCRS2) may be S phase specific co-effectors of PINX1, working against each other to modulate the human TERT pool (reviewed in [172]. Telomerase is then recruited to Cajal bodies (CBs). CBs are spherical sub-nuclear organelles that reside at the nucleolar periphery and are implicated in RNA-related metabolic processes. TCAB1 (also known as WDR79, WRAP53), bound to the CAB-box motif of TR, promotes the translocation to CBs [96]. CB-related proteins, such as coilin and survival motor neuron (SMN), interact with telomerase and may regulate the formation of an active telomerase complex [141,173–175]. The CBs colocalize with telomeres and facilitate the recruitment of the mature telomerase complex to the telomeres *via* the telomere-associated protein TPP1, a subunit of the Shelterin complex localized at telomeres (Figure 4d) [144,176].

A broad conservation of a dyskerin-TR association was proposed among diverse organisms, including plants. For example, telomerase activity and TR were immunoprecipitated with the anti-dyskerin antibody in onion *(Allium cepa)* (Table 1c) [19]. In *A. thaliana*, null mutants for the nucleolar protein NUCLEOLIN 1 caused telomere shortening on all chromosomal arms although a direct interaction between NUCLEOLIN 1 and TERT in Arabidopsis was not observed [138]. Similarly, we demonstrated that the plant RuvBL1 and RuvBL2a proteins interacted with TERT only indirectly in the nucleolus *in vivo*. In contrast to mammals, interactions between TERT and RuvBL proteins in *A. thaliana* were not direct but rather they were mediated by one of the Telomere Repeat Binding (TRB) proteins [134,177]. It was also shown that in *A. thaliana,* dyskerin directly interacted with NAF1. Plant

dyskerin was localized not only in nucleoli, but was also detected in CBs [136]. The main abundant signature protein of CBs in plants, as well as in mammals, is coilin (reviewed in [178]). Dvořáčková detected significant colocalization of TRB1 with coilin present in the CBs adjacent to the nucleolus (Dvořáčková- thesis). TRB proteins, which are the only proteins with confirmed *in vivo* plant telomere localization and function [145,179–181], may help to recruit telomerase to telomeres as they directly interact with TERT (Table 1d) [145]. Moreover, TRB proteins associate with the dyskerin orthologue CBF5 in the nucleolus, and they directly interact with POT1b (one of the plant paralogues of the Shelterin POT1 subunit). For a recent list of proteins associated with human and plant telomerase or with telomeric sequences see Procházková Schrumpfová 2019 [7].

Thus, while telomerase-interacting proteins (reviewed in [172] show relatively extensive conservation, individual interactions remain to be elucidated and carefully classified into direct and indirect ones. Due to the recently described differences in TR biogenesis pathways between plants and Ciliates on one hand, and mammals and yeasts on the other hand, orthologs of known TR interactors in human (dyskerin, NOP10, NHP2, NAF1 or GAR1), as well as e.g., orthologues of the La-family protein (p65) from Ciliates, or Sm proteins from yeasts (reviewed in [64] should also be examined in plants. Ideally, a new independent screen and subsequent analyses should identify plant TR direct interactors *de novo*.

7. Conclusions

Here we have provided an updated overview on telomerase – its origin, biogenesis, regulation and function. Despite the extensive conservation of telomerase as a tool to overcome the end-replication problem of linear eukaryotic chromosomes, subsequent evolution of this ancient molecular machine resulted in alternative solutions for particular aspects of its biogenesis and composition, as exemplified by the recent description of telomerase RNAs or telomerase interacting proteins in land plants. Further investigation of telomerase diversity across the width of eukaryotic phylogeny is needed for a deeper understanding of truly fundamental principles of telomere and telomerase regulation, and potential application of this knowledge in medicine, plant breeding or protection of biodiversity.

Supplementary Materials: The following are available online at www.mdpi.com/xxx/s1, Table S1: Telomere repeats in representative species.

Author Contributions: P.P.S. contributed to this paper with a literature review, drafting the paper, drawing the figures and creating the tables. J.F. contributed with a literature review and manuscript editing. Both authors approved the final version.

Funding: This work was supported by the Czech Science Foundation (project 20-01331X), and the institutional support by the Ministry of Education, Youth and Sports of the Czech Republic [project CEITEC 2020 (LQ1601)] and European Regional Development Fund [project SYMBIT, reg. no.CZ.02.1.01/0.0/0.0/15_003/0000477].

Acknowledgments: We thank to Lucie Bozděchová for discussing the MS prior to submission.

Conflicts of Interest: The authors declare no conflict of interest

References

1. Olovnikov, A.M. [Principle of marginotomy in template synthesis of polynucleotides]. *Dokl. Akad. Nauk SSSR* **1971**, *201*, 1496–1499.
2. Greider, C.W. Telomeres and senescence: The history, the experiment, the future. *Current Biology* **1998**, *8*, R178–R181, doi:10.1016/S0960-9822(98)70105-8.
3. Aubert, G.; Lansdorp, P.M. Telomeres and Aging. *Physiological Reviews* **2008**, *88*, 557–579, doi:10.1152/physrev.00026.2007.
4. Leman, A.; Noguchi, E. The Replication Fork: Understanding the Eukaryotic Replication Machinery and the Challenges to Genome Duplication. *Genes* **2013**, *4*, 1–32, doi:10.3390/genes4010001.

5. Gilson, E.; Géli, V. How telomeres are replicated. *Nat Rev Mol Cell Biol* **2007**, *8*, 825–838, doi:10.1038/nrm2259.
6. Diede, S.J.; Gottschling, D.E. Telomerase-Mediated Telomere Addition In Vivo Requires DNA Primase and DNA Polymerases α and δ. *Cell* **1999**, *99*, 723–733, doi:10.1016/S0092-8674(00)81670-0.
7. Procházková Schrumpfová, P.; Fojtová, M.; Fajkus, J. Telomeres in Plants and Humans: Not So Different, Not So Similar. *Cells* **2019**, *8*, 58, doi:10.3390/cells8010058.
8. Shay, J.W.; Wright, W.E. Senescence and immortalization: role of telomeres and telomerase. *Carcinogenesis* **2005**, *26*, 867–874, doi:10.1093/carcin/bgh296.
9. Fajkus, J.; Kovařík, A.; Královics, R. Telomerase activity in plant cells. *FEBS Letters* **1996**, *391*, 307–309, doi:10.1016/0014-5793(96)00757-0.
10. Jurečková, J.F.; Sýkorová, E.; Hafidh, S.; Honys, D.; Fajkus, J.; Fojtová, M. Tissue-specific expression of telomerase reverse transcriptase gene variants in Nicotiana tabacum. *Planta* **2017**, *245*, 549–561, doi:10.1007/s00425-016-2624-1.
11. Ogrocká, A.; Sýkorová, E.; Fajkus, J.; Fojtová, M. Developmental silencing of the AtTERT gene is associated with increased H3K27me3 loading and maintenance of its euchromatic environment. *Journal of Experimental Botany* **2012**, *63*, 4233–4241, doi:10.1093/jxb/ers107.
12. Riha, K.; Fajkus, J.; Siroky, J.; Vyskot, B. Developmental Control of Telomere Lengths and Telomerase Activity in Plants. *Plant Cell* **1998**, *10*, 1691–1698, doi:10.1105/tpc.10.10.1691.
13. Zachová, D.; Fojtová, M.; Dvořáčková, M.; Mozgová, I.; Lermontova, I.; Peška, V.; Schubert, I.; Fajkus, J.; Sýkorová, E. Structure-function relationships during transgenic telomerase expression in *Arabidopsis*. *Physiol Plantarum* **2013**, *149*, 114–126, doi:10.1111/ppl.12021.
14. Shay, J.W.; Wright, W.E. Telomeres and telomerase: three decades of progress. *Nat Rev Genet* **2019**, *20*, 299–309, doi:10.1038/s41576-019-0099-1.
15. Cong, Y.-S.; Wright, W.E.; Shay, J.W. Human Telomerase and Its Regulation. *MMBR* **2002**, *66*, 407–425, doi:10.1128/MMBR.66.3.407-425.2002.
16. Avilion A; Piatyszek M; Gupta J; Shay J; Bacchetti S; Greider C Human Telomerase RNA and Telomerase Activity in Immortal Cell Lines and Tumor Tissues. *Cancer Research* **1996**, *1996*, 645–650.
17. Liu, K.; Hodes, R.J.; Weng, N. Cutting Edge: Telomerase Activation in Human T Lymphocytes Does Not Require Increase in Telomerase Reverse Transcriptase (hTERT) Protein But Is Associated with hTERT Phosphorylation and Nuclear Translocation. *J Immunol* **2001**, *166*, 4826–4830, doi:10.4049/jimmunol.166.8.4826.
18. Weng, N.; Levine, B.L.; June, C.H.; Hodes, R.J. Regulation of telomerase RNA template expression in human T lymphocyte development and activation. *J. Immunol.* **1997**, *158*, 3215–3220.
19. Fajkus, P.; Peška, V.; Závodník, M.; Fojtová, M.; Fulnečková, J.; Dobias, Š.; Kilar, A.; Dvořáčková, M.; Zachová, D.; Nečasová, I.; et al. Telomerase RNAs in land plants. *Nucleic Acids Research* **2019**, *47*, 9842–9856, doi:10.1093/nar/gkz695.
20. Wu, J.; Okada, T.; Fukushima, T.; Tsudzuki, T.; Sugiura, M.; Yukawa, Y. A novel hypoxic stress-responsive long non-coding RNA transcribed by RNA polymerase III in Arabidopsis. *RNA Biology* **2012**, *9*, 302–313, doi:10.4161/rna.19101.
21. Greider, C.W.; Blackburn, E.H. The telomere terminal transferase of Tetrahymena is a ribonucleoprotein enzyme with two kinds of primer specificity. *Cell* **1987**, *51*, 887–898, doi:10.1016/0092-8674(87)90576-9.
22. Procházková Schrumpfová, P.; Schořová, Š.; Fajkus, J. Telomere- and Telomerase-Associated Proteins and Their Functions in the Plant Cell. *Front. Plant Sci.* **2016**, *7*, doi:10.3389/fpls.2016.00851.
23. Kim, S.; Parrinello, S.; Kim, J.; Campisi, J. Mus musculus and Mus spretus homologues of the human telomere-associated protein TIN2. *Genomics* **2003**, *81*, 422–432, doi:10.1016/S0888-7543(02)00033-2.
24. Burki, F.; Roger, A.J.; Brown, M.W.; Simpson, A.G.B. The New Tree of Eukaryotes. *Trends in Ecology & Evolution* **2020**, *35*, 43–55, doi:10.1016/j.tree.2019.08.008.
25. Aksenova, A.Y.; Mirkin, S.M. At the Beginning of the End and in the Middle of the Beginning: Structure and Maintenance of Telomeric DNA Repeats and Interstitial Telomeric Sequences. *Genes* **2019**, *10*, 118, doi:10.3390/genes10020118.
26. Sepsiova, R.; Necasova, I.; Willcox, S.; Prochazkova, K.; Gorilak, P.; Nosek, J.; Hofr, C.; Griffith, J.D.; Tomaska, L. Evolution of Telomeres in Schizosaccharomyces pombe and Its Possible Relationship to the Diversification of Telomere Binding Proteins. *PLoS ONE* **2016**, *11*, e0154225, doi:10.1371/journal.pone.0154225.

27. Kuznetsova, V.; Grozeva, S.; Gokhman, V. Telomere structure in insects: A review. *J Zool Syst Evol Res* **2020**, *58*, 127–158, doi:10.1111/jzs.12332.
28. Vítková, M.; Král, J.; Traut, W.; Zrzavý, J.; Marec, F. The evolutionary origin of insect telomeric repeats, (TTAGG) N. *Chromosome Res* **2005**, *13*, 145–156, doi:10.1007/s10577-005-7721-0.
29. Wicky, C.; Villeneuve, A.M.; Lauper, N.; Codourey, L.; Tobler, H.; Muller, F. Telomeric repeats (TTAGGC)n are sufficient for chromosome capping function in Caenorhabditis elegans. *Proceedings of the National Academy of Sciences* **1996**, *93*, 8983–8988, doi:10.1073/pnas.93.17.8983.
30. Červenák, F.; Juríková, K.; Sepšiová, R.; Neboháčová, M.; Nosek, J.; Tomáška, L. Double-stranded telomeric DNA binding proteins: Diversity matters. *Cell Cycle* **2017**, *16*, 1568–1577, doi:10.1080/15384101.2017.1356511.
31. Fujiwara, H.; Osanai, M.; Matsumoto, T.; Kojima, K.K. Telomere-specific non-LTR retrotransposons and telomere maintenance in the silkworm, Bombyx mori. *Chromosome Res* **2005**, *13*, 455–467, doi:10.1007/s10577-005-0990-9.
32. Casacuberta, E. Drosophila: Retrotransposons Making up Telomeres. *Viruses* **2017**, *9*, 192, doi:10.3390/v9070192.
33. Servant, G.; Deininger, P.L. Insertion of Retrotransposons at Chromosome Ends: Adaptive Response to Chromosome Maintenance. *Front. Genet.* **2016**, *6*, doi:10.3389/fgene.2015.00358.
34. Sasaki, T.; Fujiwara, H. Detection and distribution patterns of telomerase activity in insects: Telomerase activity in insects. *European Journal of Biochemistry* **2000**, *267*, 3025–3031, doi:10.1046/j.1432-1033.2000.01323.x.
35. Takahashi, H.; Okazaki, S.; Fujiwara, H. A New Family of Site-Specific Retrotransposons, SART1, Is Inserted into Telomeric Repeats of the Silkworm, Bombyx Mori. *Nucleic Acids Research* **1997**, *25*, 1578–1584, doi:10.1093/nar/25.8.1578.
36. Mason, J.M.; Randall, T.A.; Capkova Frydrychova, R. Telomerase lost? *Chromosoma* **2016**, *125*, 65–73, doi:10.1007/s00412-015-0528-7.
37. Koonin, E.V. [No title found]. *Biol Direct* **2006**, *1*, 22, doi:10.1186/1745-6150-1-22.
38. Fulnečková, J.; Ševčíková, T.; Fajkus, J.; Lukešová, A.; Lukeš, M.; Vlček, Č.; Lang, B.F.; Kim, E.; Eliáš, M.; Sýkorová, E. A Broad Phylogenetic Survey Unveils the Diversity and Evolution of Telomeres in Eukaryotes. *Genome Biology and Evolution* **2013**, *5*, 468–483, doi:10.1093/gbe/evt019.
39. Adl, S.M.; Simpson, A.G.B.; Lane, C.E.; Lukeš, J.; Bass, D.; Bowser, S.S.; Brown, M.W.; Burki, F.; Dunthorn, M.; Hampl, V.; et al. The Revised Classification of Eukaryotes. *J. Eukaryot. Microbiol.* **2012**, *59*, 429–514, doi:10.1111/j.1550-7408.2012.00644.x.
40. Richards, E.J.; Ausubel, F.M. Isolation of a higher eukaryotic telomere from Arabidopsis thaliana. *Cell* **1988**, *53*, 127–136, doi:10.1016/0092-8674(88)90494-1.
41. Sýkorová, E.; Lim, K.Y.; Kunická, Z.; Chase, M.W.; Bennett, M.D.; Fajkus, J.; Leitch, A.R. Telomere variability in the monocotyledonous plant order Asparagales. *Proc. R. Soc. Lond. B* **2003**, *270*, 1893–1904, doi:10.1098/rspb.2003.2446.
42. Sýkorová, E.; Leitch, A.R.; Fajkus, J. Asparagales Telomerases which Synthesize the Human Type of Telomeres. *Plant Mol Biol* **2006**, *60*, 633–646, doi:10.1007/s11103-005-5091-9.
43. Fajkus, P.; Peška, V.; Sitová, Z.; Fulnečková, J.; Dvořáčková, M.; Gogela, R.; Sýkorová, E.; Hapala, J.; Fajkus, J. *Allium* telomeres unmasked: the unusual telomeric sequence (CTCGGTTATGGG) $_n$ is synthesized by telomerase. *Plant J* **2016**, *85*, 337–347, doi:10.1111/tpj.13115.
44. Peška, V.; Fajkus, P.; Fojtová, M.; Dvořáčková, M.; Hapala, J.; Dvořáček, V.; Polanská, P.; Leitch, A.R.; Sýkorová, E.; Fajkus, J. Characterisation of an unusual telomere motif (TTTTTTAGGG) $_n$ in the plant *Cestrum elegans* (Solanaceae), a species with a large genome. *Plant J* **2015**, *82*, 644–654, doi:10.1111/tpj.12839.
45. Tran, T.D.; Cao, H.X.; Jovtchev, G.; Neumann, P.; Novák, P.; Fojtová, M.; Vu, G.T.H.; Macas, J.; Fajkus, J.; Schubert, I.; et al. Centromere and telomere sequence alterations reflect the rapid genome evolution within the carnivorous plant genus *Genlisea*. *Plant J* **2015**, *84*, 1087–1099, doi:10.1111/tpj.13058.
46. Fulnečková, J.; Ševčíková, T.; Lukešová, A.; Sýkorová, E. Transitions between the Arabidopsis-type and the human-type telomere sequence in green algae (clade Caudivolvoxa, Chlamydomonadales). *Chromosoma* **2016**, *125*, 437–451, doi:10.1007/s00412-015-0557-2.
47. Peska, V.; Garcia, S. Origin, Diversity, and Evolution of Telomere Sequences in Plants. *Front. Plant Sci.* **2020**, *11*, 117, doi:10.3389/fpls.2020.00117.
48. de Lange, T. A loopy view of telomere evolution. *Front. Genet.* **2015**, *6*, doi:10.3389/fgene.2015.00321.

49. Lambowitz, A.M.; Zimmerly, S. Group II Introns: Mobile Ribozymes that Invade DNA. *Cold Spring Harbor Perspectives in Biology* **2011**, *3*, a003616–a003616, doi:10.1101/cshperspect.a003616.
50. Nakamura, T.M. Telomerase Catalytic Subunit Homologs from Fission Yeast and Human. *Science* **1997**, *277*, 955–959, doi:10.1126/science.277.5328.955.
51. Lingner, J. Reverse Transcriptase Motifs in the Catalytic Subunit of Telomerase. *Science* **1997**, *276*, 561–567, doi:10.1126/science.276.5312.561.
52. Boeke, J.D. The Unusual Phylogenetic Distribution of Retrotransposons: A Hypothesis. *Genome Research* **2003**, *13*, 1975–1983, doi:10.1101/gr.1392003.
53. Dreesen, O. Telomere structure and shortening in telomerase-deficient Trypanosoma brucei. *Nucleic Acids Research* **2005**, *33*, 4536–4543, doi:10.1093/nar/gki769.
54. Giardini, M.A.; Lira, C.B.B.; Conte, F.F.; Camillo, L.R.; de Siqueira Neto, J.L.; Ramos, C.H.I.; Cano, M.I.N. The putative telomerase reverse transcriptase component of Leishmania amazonensis: gene cloning and characterization. *Parasitol Res* **2006**, *98*, 447–454, doi:10.1007/s00436-005-0036-4.
55. Podlevsky, J.D.; Chen, J.J.-L. Evolutionary perspectives of telomerase RNA structure and function. *RNA Biology* **2016**, *13*, 720–732, doi:10.1080/15476286.2016.1205768.
56. Abhishek Dey; Kausik Chakrabarti Current Perspectives of Telomerase Structure and Function in Eukaryotes with Emerging Views on Telomerase in Human Parasites. *IJMS* **2018**, *19*, 333, doi:10.3390/ijms19020333.
57. Fragnet, L.; Blasco, M.A.; Klapper, W.; Rasschaert, D. The RNA Subunit of Telomerase Is Encoded by Marek's Disease Virus. *JVI* **2003**, *77*, 5985–5996, doi:10.1128/JVI.77.10.5985-5996.2003.
58. Trapp-Fragnet, L.; Marie-Egyptienne, D.; Fakhoury, J.; Rasschaert, D.; Autexier, C. The human telomerase catalytic subunit and viral telomerase RNA reconstitute a functional telomerase complex in a cell-free system, but not in human cells. *Cellular and Molecular Biology Letters* **2012**, *17*, doi:10.2478/s11658-012-0031-6.
59. Bryan, T.M.; Englezou, A.; Gupta, J.; Bacchetti, S.; Reddel, R.R. Telomere elongation in immortal human cells without detectable telomerase activity. *EMBO J.* **1995**, *14*, 4240–4248.
60. Dunham, M.A.; Neumann, A.A.; Fasching, C.L.; Reddel, R.R. Telomere maintenance by recombination in human cells. *Nat Genet* **2000**, *26*, 447–450, doi:10.1038/82586.
61. Lundblad, V.; Blackburn, E.H. An alternative pathway for yeast telomere maintenance rescues est1− senescence. *Cell* **1993**, *73*, 347–360, doi:10.1016/0092-8674(93)90234-H.
62. Růčková, E.; Friml, J.; Procházková Schrumpfová, P.; Fajkus, J. Role of alternative telomere lengthening unmasked in telomerase knock-out mutant plants. *Plant Mol Biol* **2008**, *66*, 637–646, doi:10.1007/s11103-008-9295-7.
63. Kachouri-Lafond, R.; Dujon, B.; Gilson, E.; Westhof, E.; Fairhead, C.; Teixeira, M.T. Large telomerase RNA, telomere length heterogeneity and escape from senescence in *Candida glabrata*. *FEBS Letters* **2009**, *583*, 3605–3610, doi:10.1016/j.febslet.2009.10.034.
64. Egan, E.D.; Collins, K. Biogenesis of telomerase ribonucleoproteins. *RNA* **2012**, *18*, 1747–1759, doi:10.1261/rna.034629.112.
65. Collins, K. The biogenesis and regulation of telomerase holoenzymes. *Nat Rev Mol Cell Biol* **2006**, *7*, 484–494, doi:10.1038/nrm1961.
66. Feng, J.; Funk, W.; Wang, S.; Weinrich, S.; Avilion, A.; Chiu, C.; Adams, R.; Chang, E.; Allsopp, R.; Yu, J.; et al. The RNA component of human telomerase. *Science* **1995**, *269*, 1236–1241, doi:10.1126/science.7544491.
67. Dew-Budd, K.; Cheung, J.; Palos, K.; Forsythe, E.S.; Beilstein, M.A. Evolutionary and biochemical analyses reveal conservation of the Brassicaceae telomerase ribonucleoprotein complex. *PLoS ONE* **2020**, *15*, e0222687, doi:10.1371/journal.pone.0222687.
68. Cifuentes-Rojas, C.; Kannan, K.; Tseng, L.; Shippen, D.E. Two RNA subunits and POT1a are components of Arabidopsis telomerase. *Proc Natl Acad Sci USA* **2011**, *108*, 73–78, doi:10.1073/pnas.1013021107.
69. Retraction for Cifuentes-Rojas et al., Two RNA subunits and POT1a are components of Arabidopsis telomerase. *Proc Natl Acad Sci USA* **2019**, *116*, 24908–24908, doi:10.1073/pnas.1918863116.
70. Wu, R.A.; Upton, H.E.; Vogan, J.M.; Collins, K. Telomerase Mechanism of Telomere Synthesis. *Annu. Rev. Biochem.* **2017**, *86*, 439–460, doi:10.1146/annurev-biochem-061516-045019.
71. Song, J.; Logeswaran, D.; Castillo-González, C.; Li, Y.; Bose, S.; Aklilu, B.B.; Ma, Z.; Polkhovskiy, A.; Chen, J.J.-L.; Shippen, D.E. The conserved structure of plant telomerase RNA provides the missing link for an

673 evolutionary pathway from ciliates to humans. *Proc Natl Acad Sci USA* **2019**, *116*, 24542–24550,
674 doi:10.1073/pnas.1915312116.
675 72. Jiang, J.; Chan, H.; Cash, D.D.; Miracco, E.J.; Ogorzalek Loo, R.R.; Upton, H.E.; Cascio, D.; O'Brien Johnson,
676 R.; Collins, K.; Loo, J.A.; et al. Structure of Tetrahymena telomerase reveals previously unknown subunits,
677 functions, and interactions. *Science* **2015**, *350*, aab4070–aab4070, doi:10.1126/science.aab4070.
678 73. Xie, M.; Podlevsky, J.D.; Qi, X.; Bley, C.J.; Chen, J.J.-L. A novel motif in telomerase reverse transcriptase
679 regulates telomere repeat addition rate and processivity. *Nucleic Acids Research* **2010**, *38*, 1982–1996,
680 doi:10.1093/nar/gkp1198.
681 74. Chan, H.; Wang, Y.; Feigon, J. Progress in Human and *Tetrahymena* Telomerase Structure Determination.
682 *Annu. Rev. Biophys.* **2017**, *46*, 199–225, doi:10.1146/annurev-biophys-062215-011140.
683 75. Sýkorová, E.; Fajkus, J. Structure-function relationships in telomerase genes. *Biology of the Cell* **2009**, *101*,
684 375–406, doi:10.1042/BC20080205.
685 76. Lukowiak, A.A.; Narayanan, A.; Li, Z.H.; Terns, R.M.; Terns, M.P. The snoRNA domain of vertebrate
686 telomerase RNA functions to localize the RNA within the nucleus. *RNA* **2001**, *7*, 1833–1844.
687 77. Zhu, Y.; Tomlinson, R.L.; Lukowiak, A.A.; Terns, R.M.; Terns, M.P. Telomerase RNA Accumulates in Cajal
688 Bodies in Human Cancer Cells. *MBoC* **2004**, *15*, 81–90, doi:10.1091/mbc.e03-07-0525.
689 78. Blasco, M.; Funk, W.; Villeponteau, B.; Greider, C. Functional characterization and developmental
690 regulation of mouse telomerase RNA. *Science* **1995**, *269*, 1267–1270, doi:10.1126/science.7544492.
691 79. Kiss, T.; Filipowicz, W. Exonucleolytic processing of small nucleolar RNAs from pre-mRNA introns. *Genes*
692 *& Development* **1995**, *9*, 1411–1424, doi:10.1101/gad.9.11.1411.
693 80. Kiss, T.; Fayet-Lebaron, E.; Jády, B.E. Box H/ACA Small Ribonucleoproteins. *Molecular Cell* **2010**, *37*, 597–
694 606, doi:10.1016/j.molcel.2010.01.032.
695 81. Galloway, A.; Cowling, V.H. mRNA cap regulation in mammalian cell function and fate. *Biochimica et*
696 *Biophysica Acta (BBA) - Gene Regulatory Mechanisms* **2019**, *1862*, 270–279, doi:10.1016/j.bbagrm.2018.09.011.
697 82. Chen, L.; Roake, C.M.; Galati, A.; Bavasso, F.; Micheli, E.; Saggio, I.; Schoeftner, S.; Cacchione, S.; Gatti, M.;
698 Artandi, S.E.; et al. Loss of Human TGS1 Hypermethylase Promotes Increased Telomerase RNA and
699 Telomere Elongation. *Cell Reports* **2020**, *30*, 1358-1372.e5, doi:10.1016/j.celrep.2020.01.004.
700 83. Jády, B.E.; Bertrand, E.; Kiss, T. Human telomerase RNA and box H/ACA scaRNAs share a common Cajal
701 body–specific localization signal. *Journal of Cell Biology* **2004**, *164*, 647–652, doi:10.1083/jcb.200310138.
702 84. MacNeil, D.; Bensoussan, H.; Autexier, C. Telomerase Regulation from Beginning to the End. *Genes* **2016**,
703 *7*, 64, doi:10.3390/genes7090064.
704 85. Rubtsova, M.; Dontsova, O. Human Telomerase RNA: Telomerase Component or More? *Biomolecules* **2020**,
705 *10*, 873, doi:10.3390/biom10060873.
706 86. Robart, A.R.; Collins, K. Investigation of Human Telomerase Holoenzyme Assembly, Activity, and
707 Processivity Using Disease-linked Subunit Variants. *J. Biol. Chem.* **2010**, *285*, 4375–4386,
708 doi:10.1074/jbc.M109.088575.
709 87. Huang, J.; Brown, A.F.; Wu, J.; Xue, J.; Bley, C.J.; Rand, D.P.; Wu, L.; Zhang, R.; Chen, J.J.-L.; Lei, M.
710 Structural basis for protein-RNA recognition in telomerase. *Nat Struct Mol Biol* **2014**, *21*, 507–512,
711 doi:10.1038/nsmb.2819.
712 88. Chen, Y.; Podlevsky, J.D.; Logeswaran, D.; Chen, J.J. A single nucleotide incorporation step limits human
713 telomerase repeat addition activity. *EMBO J* **2018**, *37*, doi:10.15252/embj.201797953.
714 89. Collins, K.; Greider, C.W. Tetrahymena telomerase catalyzes nucleolytic cleavage and nonprocessive
715 elongation. *Genes & Development* **1993**, *7*, 1364–1376, doi:10.1101/gad.7.7b.1364.
716 90. Lue, N.F. A Physical and Functional Constituent of Telomerase Anchor Site. *J. Biol. Chem.* **2005**, *280*, 26586–
717 26591, doi:10.1074/jbc.M503028200.
718 91. Akiyama, B.M.; Parks, J.W.; Stone, M.D. The telomerase essential N-terminal domain promotes DNA
719 synthesis by stabilizing short RNA-DNA hybrids. *Nucleic Acids Research* **2015**, *43*, 5537–5549,
720 doi:10.1093/nar/gkv406.
721 92. Patrick, E.M.; Slivka, J.D.; Payne, B.; Comstock, M.J.; Schmidt, J.C. Observation of processive telomerase
722 catalysis using high-resolution optical tweezers. *Nat Chem Biol* **2020**, *16*, 801–809, doi:10.1038/s41589-020-
723 0478-0.
724 93. Moriarty, T.J.; Marie-Egyptienne, D.T.; Autexier, C. Functional Organization of Repeat Addition
725 Processivity and DNA Synthesis Determinants in the Human Telomerase Multimer. *MCB* **2004**, *24*, 3720–
726 3733, doi:10.1128/MCB.24.9.3720-3733.2004.

94. Sauerwald, A.; Sandin, S.; Cristofari, G.; Scheres, S.H.W.; Lingner, J.; Rhodes, D. Structure of active dimeric human telomerase. *Nat Struct Mol Biol* **2013**, *20*, 454–460, doi:10.1038/nsmb.2530.
95. Sandin, S.; Rhodes, D. Telomerase structure. *Current Opinion in Structural Biology* **2014**, *25*, 104–110, doi:10.1016/j.sbi.2014.02.003.
96. Nguyen, T.H.D.; Tam, J.; Wu, R.A.; Greber, B.J.; Toso, D.; Nogales, E.; Collins, K. Cryo-EM structure of substrate-bound human telomerase holoenzyme. *Nature* **2018**, *557*, 190–195, doi:10.1038/s41586-018-0062-x.
97. Jiang, J.; Miracco, E.J.; Hong, K.; Eckert, B.; Chan, H.; Cash, D.D.; Min, B.; Zhou, Z.H.; Collins, K.; Feigon, J. The architecture of Tetrahymena telomerase holoenzyme. *Nature* **2013**, *496*, 187–192, doi:10.1038/nature12062.
98. Majerská, J.; Procházková Schrumpfová, P.; Dokládal, L.; Schořová, Š.; Stejskal, K.; Obořil, M.; Honys, D.; Kozáková, L.; Polanská, P.S.; Sýkorová, E. Tandem affinity purification of AtTERT reveals putative interaction partners of plant telomerase in vivo. *Protoplasma* **2017**, *254*, 1547–1562, doi:10.1007/s00709-016-1042-3.
99. Dergai, O.; Hernandez, N. How to Recruit the Correct RNA Polymerase? Lessons from snRNA Genes. *Trends in Genetics* **2019**, *35*, 457–469, doi:10.1016/j.tig.2019.04.001.
100. Cunningham, D.D.; Collins, K. Biological and Biochemical Functions of RNA in the Tetrahymena Telomerase Holoenzyme. *MCB* **2005**, *25*, 4442–4454, doi:10.1128/MCB.25.11.4442-4454.2005.
101. Roake, C.M.; Artandi, S.E. Regulation of human telomerase in homeostasis and disease. *Nat Rev Mol Cell Biol* **2020**, *21*, 384–397, doi:10.1038/s41580-020-0234-z.
102. Malik, H.S.; Burke, W.D.; Eickbush, T.H. Putative telomerase catalytic subunits from Giardia lamblia and Caenorhabditis elegans. *Gene* **2000**, *251*, 101–108, doi:10.1016/S0378-1119(00)00207-9.
103. Lai, A.G.; Pouchkina-Stantcheva, N.; Di Donfrancesco, A.; Kildisiute, G.; Sahu, S.; Aboobaker, A.A. The protein subunit of telomerase displays patterns of dynamic evolution and conservation across different metazoan taxa. *BMC Evol Biol* **2017**, *17*, 107, doi:10.1186/s12862-017-0949-4.
104. Chung, J.; Khadka, P.; Chung, I.K. Nuclear import of hTERT requires a bipartite nuclear localization signal and Akt-mediated phosphorylation. *Journal of Cell Science* **2012**, *125*, 2684–2697, doi:10.1242/jcs.099267.
105. Hoffman, H.; Rice, C.; Skordalakes, E. Structural Analysis Reveals the Deleterious Effects of Telomerase Mutations in Bone Marrow Failure Syndromes. *J. Biol. Chem.* **2017**, *292*, 4593–4601, doi:10.1074/jbc.M116.771204.
106. Autexier, C.; Lue, N.F. The Structure and Function of Telomerase Reverse Transcriptase. *Annu. Rev. Biochem.* **2006**, *75*, 493–517, doi:10.1146/annurev.biochem.75.103004.142412.
107. Kilian, A.; Bowtell, D.D.L.; Abud, H.E.; Hime, G.R.; Venter, D.J.; Keese, P.K.; Duncan, E.L.; Reddel, R.R.; Jefferson, R.A. Isolation of a Candidate Human Telomerase Catalytic Subunit Gene, Which Reveals Complex Splicing Patterns in Different Cell Types. *Human Molecular Genetics* **1997**, *6*, 2011–2019, doi:10.1093/hmg/6.12.2011.
108. Harrington, L.; Zhou, W.; McPhail, T.; Oulton, R.; Yeung, D.S.K.; Mar, V.; Bass, M.B.; Robinson, M.O. Human telomerase contains evolutionarily conserved catalytic and structural subunits. *Genes & Development* **1997**, *11*, 3109–3115, doi:10.1101/gad.11.23.3109.
109. Meyerson, M.; Counter, C.M.; Eaton, E.N.; Ellisen, L.W.; Steiner, P.; Caddle, S.D.; Ziaugra, L.; Beijersbergen, R.L.; Davidoff, M.J.; Liu, Q.; et al. hEST2, the Putative Human Telomerase Catalytic Subunit Gene, Is Up-Regulated in Tumor Cells and during Immortalization. *Cell* **1997**, *90*, 785–795, doi:10.1016/S0092-8674(00)80538-3.
110. Sýkorová, E.; Fulnečková, J.; Mokroš, P.; Fajkus, J.; Fojtová, M.; Peška, V. Three TERT genes in Nicotiana tabacum. *Chromosome Res* **2012**, *20*, 381–394, doi:10.1007/s10577-012-9282-3.
111. Khattar, E.; Tergaonkar, V. Transcriptional Regulation of Telomerase Reverse Transcriptase (TERT) by MYC. *Front. Cell Dev. Biol.* **2017**, *5*, doi:10.3389/fcell.2017.00001.
112. Jie, M.-M.; Chang, X.; Zeng, S.; Liu, C.; Liao, G.-B.; Wu, Y.-R.; Liu, C.-H.; Hu, C.-J.; Yang, S.-M.; Li, X.-Z. Diverse regulatory manners of human telomerase reverse transcriptase. *Cell Commun Signal* **2019**, *17*, 63, doi:10.1186/s12964-019-0372-0.
113. Ramlee, M.; Wang, J.; Toh, W.; Li, S. Transcription Regulation of the Human Telomerase Reverse Transcriptase (hTERT) Gene. *Genes* **2016**, *7*, 50, doi:10.3390/genes7080050.
114. Flavin, P.; Redmond, A.; McBryan, J.; Cocchiglia, S.; Tibbitts, P.; Fahy-Browne, P.; Kay, E.; Treumann, A.; Perrem, K.; McIlroy, M.; et al. RuvBl2 cooperates with Ets2 to transcriptionally regulate hTERT in colon cancer. *FEBS Letters* **2011**, *585*, 2537–2544, doi:10.1016/j.febslet.2011.07.005.

115. Takakura M; Kyo S; Kanaya T; Hirano H; Takeda J; Yutsudo M; Inoue M Cloning of Human Telomerase Catalytic Subunit (hTERT) Gene Promoter and Identification of Proximal Core Promoter Sequences Essential for Transcriptional Activation in Immortalized and Cancer Cells. *Cancer Research* **1999**, *59*.
116. Horikawa I; Cable PL; Afshari C; Barrett Cloning and Characterization of the Promoter Region of Human Telomerase Reverse Transcriptase Gene. *Cancer Research* **1999**, *59*.
117. Crhák, T.; Zachová, D.; Fojtová, M.; Sýkorová, E. The region upstream of the telomerase reverse transcriptase gene is essential for in planta telomerase complementation. *Plant Science* **2019**, *281*, 41–51, doi:10.1016/j.plantsci.2019.01.001.
118. Stern, J.L.; Theodorescu, D.; Vogelstein, B.; Papadopoulos, N.; Cech, T.R. Mutation of the *TERT* promoter, switch to active chromatin, and monoallelic *TERT* expression in multiple cancers. *Genes Dev.* **2015**, *29*, 2219–2224, doi:10.1101/gad.269498.115.
119. Akıncılar, S.C.; Khattar, E.; Boon, P.L.S.; Unal, B.; Fullwood, M.J.; Tergaonkar, V. Long-Range Chromatin Interactions Drive Mutant TERT Promoter Activation. *Cancer Discovery* **2016**, *6*, 1276–1291, doi:10.1158/2159-8290.CD-16-0177.
120. Fajkus, J.; Fulnečková, J.; Hulánová, M.; Berková, K.; Říha, K.; Matyášek, R. Plant cells express telomerase activity upon transfer to callus culture, without extensively changing telomere lengths. *Mol Gen Genet* **1998**, *260*, 470–474, doi:10.1007/s004380050918.
121. Cong, Y.; Wen, J.; Bacchetti, S. The human telomerase catalytic subunit hTERT: organization of the gene and characterization of the promoter. *Human Molecular Genetics* **1999**, *8*, 137–142, doi:10.1093/hmg/8.1.137.
122. Antosz, W.; Pfab, A.; Ehrnsberger, H.F.; Holzinger, P.; Köllen, K.; Mortensen, S.A.; Bruckmann, A.; Schubert, T.; Längst, G.; Griesenbeck, J.; et al. The Composition of the Arabidopsis RNA Polymerase II Transcript Elongation Complex Reveals the Interplay between Elongation and mRNA Processing Factors. *Plant Cell* **2017**, *29*, 854–870, doi:10.1105/tpc.16.00735.
123. Stern, J.L.; Paucek, R.D.; Huang, F.W.; Ghandi, M.; Nwumeh, R.; Costello, J.C.; Cech, T.R. Allele-Specific DNA Methylation and Its Interplay with Repressive Histone Marks at Promoter-Mutant TERT Genes. *Cell Reports* **2017**, *21*, 3700–3707, doi:10.1016/j.celrep.2017.12.001.
124. Bodnar, A.G. Extension of Life-Span by Introduction of Telomerase into Normal Human Cells. *Science* **1998**, *279*, 349–352, doi:10.1126/science.279.5349.349.
125. Hrdlickova, R.; Nehyba, J.; Bose, H.R. Alternatively Spliced Telomerase Reverse Transcriptase Variants Lacking Telomerase Activity Stimulate Cell Proliferation. *Molecular and Cellular Biology* **2012**, *32*, 4283–4296, doi:10.1128/MCB.00550-12.
126. Kang, S.S.; Kwon, T.; Kwon, D.Y.; Do, S.I. Akt Protein Kinase Enhances Human Telomerase Activity through Phosphorylation of Telomerase Reverse Transcriptase Subunit. *J. Biol. Chem.* **1999**, *274*, 13085–13090, doi:10.1074/jbc.274.19.13085.
127. Kim, J.H. Ubiquitin ligase MKRN1 modulates telomere length homeostasis through a proteolysis of hTERT. *Genes & Development* **2005**, *19*, 776–781, doi:10.1101/gad.1289405.
128. Oguchi, K.; Tamura, K.; Takahashi, H. Characterization of Oryza sativa telomerase reverse transcriptase and possible role of its phosphorylation in the control of telomerase activity. *Gene* **2004**, *342*, 57–66, doi:10.1016/j.gene.2004.07.011.
129. Yang, S.W.; Jin, E.; Chung, I.K.; Kim, W.T. Cell cycle-dependent regulation of telomerase activity by auxin, abscisic acid and protein phosphorylation in tobacco BY-2 suspension culture cells. *The Plant Journal* **2002**, *29*, 617–626, doi:10.1046/j.0960-7412.2001.01244.x.
130. Jeong, S.A.; Kim, K.; Lee, J.H.; Cha, J.S.; Khadka, P.; Cho, H.-S.; Chung, I.K. Akt-mediated phosphorylation increases the binding affinity of hTERT for importin to promote nuclear translocation. *Journal of Cell Science* **2015**, *128*, 2287–2301, doi:10.1242/jcs.166132.
131. Fitzgerald, M.S.; Riha, K.; Gao, F.; Ren, S.; McKnight, T.D.; Shippen, D.E. Disruption of the telomerase catalytic subunit gene from Arabidopsis inactivates telomerase and leads to a slow loss of telomeric DNA. *Proceedings of the National Academy of Sciences* **1999**, *96*, 14813–14818, doi:10.1073/pnas.96.26.14813.
132. Atkinson, S.P.; Hoare, S.F.; Glasspool, R.M.; Keith, W.N. Lack of Telomerase Gene Expression in Alternative Lengthening of Telomere Cells Is Associated with Chromatin Remodeling of the *hTR* and *hTERT* Gene Promoters. *Cancer Res* **2005**, *65*, 7585–7590, doi:10.1158/0008-5472.CAN-05-1715.
133. Cairney, C.J.; Hoare, S.F.; Daidone, M.-G.; Zaffaroni, N.; Keith, W.N. High level of telomerase RNA gene expression is associated with chromatin modification, the ALT phenotype and poor prognosis in liposarcoma. *Br J Cancer* **2008**, *98*, 1467–1474, doi:10.1038/sj.bjc.6604328.

134. Schořová, Š.; Fajkus, J.; Záveská Drábková, L.; Honys, D.; Procházková Schrumpfová, P. The plant Pontin and Reptin homologues, Ruv BL 1 and Ruv BL 2a, colocalize with TERT and TRB proteins *in vivo* , and participate in telomerase biogenesis. *Plant J* **2019**, *98*, 195–212, doi:10.1111/tpj.14306.
135. Pendle, A.F.; Clark, G.P.; Boon, R.; Lewandowska, D.; Lam, Y.W.; Andersen, J.; Mann, M.; Lamond, A.I.; Brown, J.W.S.; Shaw, P.J. Proteomic Analysis of the *Arabidopsis* Nucleolus Suggests Novel Nucleolar Functions. *MBoC* **2005**, *16*, 260–269, doi:10.1091/mbc.e04-09-0791.
136. Lermontova, I.; Schubert, V.; Börnke, F.; Macas, J.; Schubert, I. Arabidopsis CBF5 interacts with the H/ACA snoRNP assembly factor NAF1. *Plant Mol Biol* **2007**, *65*, 615–626, doi:10.1007/s11103-007-9226-z.
137. Khurts, S.; Masutomi, K.; Delgermaa, L.; Arai, K.; Oishi, N.; Mizuno, H.; Hayashi, N.; Hahn, W.C.; Murakami, S. Nucleolin Interacts with Telomerase. *J. Biol. Chem.* **2004**, *279*, 51508–51515, doi:10.1074/jbc.M407643200.
138. Pontvianne, F.; Carpentier, M.-C.; Durut, N.; Pavlištová, V.; Jaške, K.; Schořová, Š.; Parrinello, H.; Rohmer, M.; Pikaard, C.S.; Fojtová, M.; et al. Identification of Nucleolus-Associated Chromatin Domains Reveals a Role for the Nucleolus in 3D Organization of the A. thaliana Genome. *Cell Reports* **2016**, *16*, 1574–1587, doi:10.1016/j.celrep.2016.07.016.
139. Pontvianne, F.; Abou-Ellail, M.; Douet, J.; Comella, P.; Matia, I.; Chandrasekhara, C.; DeBures, A.; Blevins, T.; Cooke, R.; Medina, F.J.; et al. Nucleolin Is Required for DNA Methylation State and the Expression of rRNA Gene Variants in Arabidopsis thaliana. *PLoS Genet* **2010**, *6*, e1001225, doi:10.1371/journal.pgen.1001225.
140. Venteicher, A.S.; Meng, Z.; Mason, P.J.; Veenstra, T.D.; Artandi, S.E. Identification of ATPases Pontin and Reptin as Telomerase Components Essential for Holoenzyme Assembly. *Cell* **2008**, *132*, 945–957, doi:10.1016/j.cell.2008.01.019.
141. Poole, A.R.; Hebert, M.D. SMN and coilin negatively regulate dyskerin association with telomerase RNA. *Biology Open* **2016**, *5*, 726–735, doi:10.1242/bio.018804.
142. Hebert, M.D.; Shpargel, K.B.; Ospina, J.K.; Tucker, K.E.; Matera, A.G. Coilin Methylation Regulates Nuclear Body Formation. *Developmental Cell* **2002**, *3*, 329–337, doi:10.1016/S1534-5807(02)00222-8.
143. Dvorackova, M. Analysis of Arabidopsis telomere-associated proteins in vivo. Ph.D. thesis, Masaryk University, Brno, Czech Republic, **2010**.
144. Zhong, F.L.; Batista, L.F.Z.; Freund, A.; Pech, M.F.; Venteicher, A.S.; Artandi, S.E. TPP1 OB-Fold Domain Controls Telomere Maintenance by Recruiting Telomerase to Chromosome Ends. *Cell* **2012**, *150*, 481–494, doi:10.1016/j.cell.2012.07.012.
145. Procházková Schrumpfová, P.; Vychodilová, I.; Dvořáčková, M.; Majerská, J.; Dokládal, L.; Schořová, Š.; Fajkus, J. Telomere repeat binding proteins are functional components of Arabidopsis telomeres and interact with telomerase. *Plant J* **2014**, *77*, 770–781, doi:10.1111/tpj.12428.
146. Ulaner G; Hu JF; Vu T; Giudice L; Hoffman A Telomerase Activity in Human Development Is Regulated by Human Telomerase Reverse Transcriptase (hTERT) Transcription and by Alternate Splicing of hTERT Transcripts. **1998**, *58*.
147. Nehyba, J.; Hrdlickova, R.; Bose, H.R. The Regulation of Telomerase by Alternative Splicing of TERT. In *Reviews on Selected Topics of Telomere Biology*; Li, B., Ed.; InTech, **2012** ISBN 978-953-51-0849-8.
148. Ulaner G; Hu JF; Vu TH; Giudice LC; Hoffman AR Tissue-specific alternate splicing of human telomerase reverse transcriptase (hTERT) influences telomere lengths during human development. *IJC* **2001**, *91*, 644–649.
149. Brenner, C.A.; Wolny, Y.M.; Adler, R.R.; Cohen, J. Alternative splicing of the telomerase catalytic subunit in human oocytes and embryos. *MHR: Basic science of reproductive medicine* **1999**, *5*, 845–850, doi:10.1093/molehr/5.9.845.
150. Kaneko, R.; Esumi, S.; Yagi, T.; Hirabayashi, T. Predominant Expression of rTERTb, an Inactive TERT Variant, in the Adult Rat Brain. *PPL* **2006**, *13*, 59–65, doi:10.2174/092986606774502108.
151. Ludlow, A.T.; Slusher, A.L.; Sayed, M.E. Insights into Telomerase/hTERT Alternative Splicing Regulation Using Bioinformatics and Network Analysis in Cancer. *Cancers* **2019**, *11*, 666, doi:10.3390/cancers11050666.
152. Wong, M.S.; Wright, W.E.; Shay, J.W. Alternative splicing regulation of telomerase: a new paradigm? *Trends in Genetics* **2014**, *30*, 430–438, doi:10.1016/j.tig.2014.07.006.
153. Colgin, L.M.; Wilkinso, C.; Englezou, A.; Kilian, A.; Robinson, M.O.; Reddel, R.R. The hTERTα Splice Variant is a Dominant Negative Inhibitor of Telomerase Activity. *Neoplasia* **2000**, *2*, 426–432, doi:10.1038/sj.neo.7900112.

154. Kunická, Z.; Mucha, I.; Fajkus, J. Telomerase activity in head and neck cancer. *Anticancer Res.* **2008**, *28*, 3125–3129.
155. Listerman, I.; Sun, J.; Gazzaniga, F.S.; Lukas, J.L.; Blackburn, E.H. The Major Reverse Transcriptase-Incompetent Splice Variant of the Human Telomerase Protein Inhibits Telomerase Activity but Protects from Apoptosis. *Cancer Research* **2013**, *73*, 2817–2828, doi:10.1158/0008-5472.CAN-12-3082.
156. Rossignol, P.; Collier, S.; Bush, M.; Shaw, P.; Doonan, J.H. Arabidopsis POT1A interacts with TERT-V(I8), an N-terminal splicing variant of telomerase. *Journal of Cell Science* **2007**, *120*, 3678–3687, doi:10.1242/jcs.004119.
157. Rotková G; Sýkorová E; Fajkus J Protect and regulate: recent findings on plant POT1-like proteins. *BIOLOGIA PLANTARUM* **2009**, *53*, 1–4.
158. Tamura, K.; Liu, H.; Takahashi, H. Auxin Induction of Cell Cycle Regulated Activity of Tobacco Telomerase. *J. Biol. Chem.* **1999**, *274*, 20997–21002, doi:10.1074/jbc.274.30.20997.
159. Ren, S.; Johnston, J.S.; Shippen, D.E.; McKnight, T.D. TELOMERASE ACTIVATOR1 Induces Telomerase Activity and Potentiates Responses to Auxin in Arabidopsis. *Plant Cell* **2004**, *16*, 2910–2922, doi:10.1105/tpc.104.025072.
160. Ren, S.; Mandadi, K.K.; Boedeker, A.L.; Rathore, K.S.; McKnight, T.D. Regulation of Telomerase in *Arabidopsis* by *BT2*, an Apparent Target of TELOMERASE ACTIVATOR1. *Plant Cell* **2007**, *19*, 23–31, doi:10.1105/tpc.106.044321.
161. Nguyen, D.; Grenier St-Sauveur, V.; Bergeron, D.; Dupuis-Sandoval, F.; Scott, M.S.; Bachand, F. A Polyadenylation-Dependent 3′ End Maturation Pathway Is Required for the Synthesis of the Human Telomerase RNA. *Cell Reports* **2015**, *13*, 2244–2257, doi:10.1016/j.celrep.2015.11.003.
162. Tseng, C.-K.; Wang, H.-F.; Burns, A.M.; Schroeder, M.R.; Gaspari, M.; Baumann, P. Human Telomerase RNA Processing and Quality Control. *Cell Reports* **2015**, *13*, 2232–2243, doi:10.1016/j.celrep.2015.10.075.
163. Majerská, J.; Sýkorová, E.; Fajkus, J. Non-telomeric activities of telomerase. *Mol. BioSyst.* **2011**, *7*, 1013, doi:10.1039/c0mb00268b.
164. Blasco, M.A.; Rizen, M.; Greider, C.W.; Hanahan, D. Differential regulation of telomerase activity and telomerase RNA during multi-stage tumorigenesis. *Nat Genet* **1996**, *12*, 200–204, doi:10.1038/ng0296-200.
165. Kedde, M.; le Sage, C.; Duursma, A.; Zlotorynski, E.; van Leeuwen, B.; Nijkamp, W.; Beijersbergen, R.; Agami, R. Telomerase-independent Regulation of ATR by Human Telomerase RNA. *J. Biol. Chem.* **2006**, *281*, 40503–40514, doi:10.1074/jbc.M607676200.
166. Ségal-Bendirdjian, E.; Geli, V. Non-canonical Roles of Telomerase: Unraveling the Imbroglio. *Front. Cell Dev. Biol.* **2019**, *7*, 332, doi:10.3389/fcell.2019.00332.
167. Dokládal, L.; Benková, E.; Honys, D.; Dupľáková, N.; Lee, L.-Y.; Gelvin, S.B.; Sýkorová, E. An armadillo-domain protein participates in a telomerase interaction network. *Plant Mol Biol* **2018**, *97*, 407–420, doi:10.1007/s11103-018-0747-4.
168. Park, J.-I.; Venteicher, A.S.; Hong, J.Y.; Choi, J.; Jun, S.; Shkreli, M.; Chang, W.; Meng, Z.; Cheung, P.; Ji, H.; et al. Telomerase modulates Wnt signalling by association with target gene chromatin. *Nature* **2009**, *460*, 66–72, doi:10.1038/nature08137.
169. Yu, Y.-T.; Meier, U.T. RNA-guided isomerization of uridine to pseudouridine—pseudouridylation. *RNA Biology* **2014**, *11*, 1483–1494, doi:10.4161/15476286.2014.972855.
170. Lee, J.H.; Lee, Y.S.; Jeong, S.A.; Khadka, P.; Roth, J.; Chung, I.K. Catalytically active telomerase holoenzyme is assembled in the dense fibrillar component of the nucleolus during S phase. *Histochem Cell Biol* **2014**, *141*, 137–152, doi:10.1007/s00418-013-1166-x.
171. Cheung, D.H.-C.; Ho, S.-T.; Lau, K.-F.; Jin, R.; Wang, Y.-N.; Kung, H.-F.; Huang, J.-J.; Shaw, P.-C. Nucleophosmin Interacts with PIN2/TERF1-interacting Telomerase Inhibitor 1 (PinX1) and Attenuates the PinX1 Inhibition on Telomerase Activity. *Sci Rep* **2017**, *7*, 43650, doi:10.1038/srep43650.
172. Nguyen, K.T.T.T.; Wong, J.M.Y. Telomerase Biogenesis and Activities from the Perspective of Its Direct Interacting Partners. *Cancers* **2020**, *12*, 1679, doi:10.3390/cancers12061679.
173. Broome, H.J.; Carrero, Z.I.; Douglas, H.E.; Hebert, M.D. Phosphorylation regulates coilin activity and RNA association. *Biology Open* **2013**, *2*, 407–415, doi:10.1242/bio.20133863.
174. Broome, H.J.; Hebert, M.D. Coilin Displays Differential Affinity for Specific RNAs In Vivo and Is Linked to Telomerase RNA Biogenesis. *Journal of Molecular Biology* **2013**, *425*, 713–724, doi:10.1016/j.jmb.2012.12.014.

175. Mahmoudi, S.; Henriksson, S.; Weibrecht, I.; Smith, S.; Söderberg, O.; Strömblad, S.; Wiman, K.G.; Farnebo, M. WRAP53 Is Essential for Cajal Body Formation and for Targeting the Survival of Motor Neuron Complex to Cajal Bodies. *PLoS Biol* **2010**, *8*, e1000521, doi:10.1371/journal.pbio.1000521.
176. Venteicher, A.S.; Abreu, E.B.; Meng, Z.; McCann, K.E.; Terns, R.M.; Veenstra, T.D.; Terns, M.P.; Artandi, S.E. A Human Telomerase Holoenzyme Protein Required for Cajal Body Localization and Telomere Synthesis. *Science* **2009**, *323*, 644–648, doi:10.1126/science.1165357.
177. Sweetlove, L.; Gutierrez, C. The journey to the end of the chromosome: delivering active telomerase to telomeres in plants. *Plant J* **2019**, *98*, 193–194, doi:10.1111/tpj.14328.
178. Love, A.J.; Yu, C.; Petukhova, N.V.; Kalinina, N.O.; Chen, J.; Taliansky, M.E. Cajal bodies and their role in plant stress and disease responses. *RNA Biology* **2017**, *14*, 779–790, doi:10.1080/15476286.2016.1243650.
179. Schrumpfová, P.; Kuchař, M.; Miková, G.; Skří□ovská, L.; Kubičárová, T.; Fajkus, J. Characterization of two *Arabidopsis thaliana* myb-like proteins showing affinity to telomeric DNA sequence. *Genome* **2004**, *47*, 316–324, doi:10.1139/g03-136.
180. Mozgová, I.; Procházková Schrumpfová, P.; Hofr, C.; Fajkus, J. Functional characterization of domains in AtTRB1, a putative telomere-binding protein in Arabidopsis thaliana. *Phytochemistry* **2008**, *69*, 1814–1819, doi:10.1016/j.phytochem.2008.04.001.
181. Peska, V.; Procházková Schrumpfová, P.; Fajkus, J. Using the Telobox to Search for Plant Telomere Binding Proteins. *CPPS* **2011**, *12*, 75–83, doi:10.2174/138920311795684968.

Table S1. Telomere repeats in representative species.

Telomere repeat	Representative species	Reference
TSAR		
TTAGGG	*Ectocarpus siliculosus* (Stramenopiles)	[1] and references herein
TTTAGGG	*Phytophthora infestans* (Oomycetes)	[1] and references herein
TTTTGGGG	*Euplotes aediculatus* (Ciliata)	[1] and references herein
TTGGGG	*Tetrahymena* (Ciliata)	[1] and references herein
TTTGGG	*Chilodonella uncinata* (Ciliata)	[1] and references herein
TTTTAGGG	*Theileria annulata* (Apicomplexa)	[1] and references herein
TTTAGG	*Cryptosporidium parvum Iowa II* (Apicomplexa)	[1] and references herein
TTAGG	*Aurantiochytrium limacinum* (Stramenopiles)	[1] and references herein
Haptista		
TTAGGG	*Emiliania huxleyi* (Haptophyta)	[1] and references herein
Cryptista		
TTTAGGG	*Guillardia theta* (Cryptophyceae)	[1] and references herein
Archaeplastida		
TTTAGGG	*Arabidopsis thaliana* (Brassicaceae)	[2]
TTAGGG	*Asparagus officinalis* (Asparagales)	[3]
TTTTAGGG	*Chlamydomonas reinhardtii* (Chlorophyceae)	[4]
TTTTAGG	*Klebsormidium subtilissimum* (Charophyta*)*	[1]
TTCAGG/TTTCAGG	*Genlisea hispidula* (Lentibulariaceae)	[5]
CTCGGTTATGGG	*Allium cepa* (Amaryllidaceae)	[6]
AATGGGGGG	*Cyanidioschyzon merolae* (Rhodophyta)	[7,8]
TTTTTTAGGG	*Cestrum elegans* (Solanaceae)	[9]

Amorphea		
TTAGGG	*Homo sapiens* (Animalia)	[10]
TTAGG	*Bombyx mori* (Insects)	[11]
TTAGGC	*Ascaris lumbricoides* (Nematodes)	[12]
TCAGG	*Tribolium castaneu*m (Anthropoda)	[13]
TTGCA	*Parascaris univalens* (Nematoda)	[1] and references herein
TGTGGG	*Bdelloidea* (Rotifera)	[1] and references herein
TAAGGG	*Polysphodylium pallidum* (Amoebozoa)	[1] and references herein
Discoba		
TTAGGG	*Andalucia godoyi* (Jakobida)	[1] and references herein
Metamonada		
TAGGG	*Giardia lamblia* (Fornicata)	[1] and references herein
Malawimonadida		
TTAGGG	*Malawimonas californiana* (Malawimonadida)	[1] and references herein

1. Fulnečková, J.; Ševčíková, T.; Fajkus, J.; Lukešová, A.; Lukeš, M.; Vlček, Č.; Lang, B.F.; Kim, E.; Eliáš, M.; Sýkorová, E. A Broad Phylogenetic Survey Unveils the Diversity and Evolution of Telomeres in Eukaryotes. *Genome Biology and Evolution* **2013**, *5*, 468–483, doi:10.1093/gbe/evt019.
2. Richards, E.J.; Ausubel, F.M. Isolation of a higher eukaryotic telomere from Arabidopsis thaliana. *Cell* **1988**, *53*, 127–136, doi:10.1016/0092-8674(88)90494-1.
3. Sýkorová, E.; Lim, K.Y.; Kunická, Z.; Chase, M.W.; Bennett, M.D.; Fajkus, J.; Leitch, A.R. Telomere variability in the monocotyledonous plant order Asparagales. *Proc. R. Soc. Lond. B* **2003**, *270*, 1893–1904, doi:10.1098/rspb.2003.2446.
4. Petracek, M.E.; Lefebvre, P.A.; Silflow, C.D.; Berman, J. Chlamydomonas telomere sequences are A+T-rich but contain three consecutive G-C base pairs. *Proceedings of the National Academy of Sciences* **1990**, *87*, 8222–8226, doi:10.1073/pnas.87.21.8222.

5. Tran, T.D.; Cao, H.X.; Jovtchev, G.; Neumann, P.; Novák, P.; Fojtová, M.; Vu, G.T.H.; Macas, J.; Fajkus, J.; Schubert, I.; et al. Centromere and telomere sequence alterations reflect the rapid genome evolution within the carnivorous plant genus *Genlisea*. *Plant J* **2015**, *84*, 1087–1099, doi:10.1111/tpj.13058.
6. Fajkus, P.; Peška, V.; Sitová, Z.; Fulnečková, J.; Dvořáčková, M.; Gogela, R.; Sýkorová, E.; Hapala, J.; Fajkus, J. *Allium* telomeres unmasked: the unusual telomeric sequence (CTCGGTTATGGG) $_n$ is synthesized by telomerase. *Plant J* **2016**, *85*, 337–347, doi:10.1111/tpj.13115.
7. Fulnečková, J.; Hasíková, T.; Fajkus, J.; Lukešová, A.; Eliáš, M.; Sýkorová, E. Dynamic Evolution of Telomeric Sequences in the Green Algal Order Chlamydomonadales. *Genome Biology and Evolution* **2012**, *4*, 248–264, doi:10.1093/gbe/evs007.
8. Matsuzaki, M.; Misumi, O.; Shin-i, T.; Maruyama, S.; Takahara, M.; Miyagishima, S.; Mori, T.; Nishida, K.; Yagisawa, F.; Nishida, K.; et al. Genome sequence of the ultrasmall unicellular red alga Cyanidioschyzon merolae 10D. *Nature* **2004**, *428*, 653–657, doi:10.1038/nature02398.
9. Peška, V.; Fajkus, P.; Fojtová, M.; Dvořáčková, M.; Hapala, J.; Dvořáček, V.; Polanská, P.; Leitch, A.R.; Sýkorová, E.; Fajkus, J. Characterisation of an unusual telomere motif (TTTTTTAGGG) $_n$ in the plant *Cestrum elegans* (Solanaceae), a species with a large genome. *Plant J* **2015**, *82*, 644–654, doi:10.1111/tpj.12839.
10. Moyzis, Robert K The Human Telomere. **1991**, *265*, 48–57.
11. Sahara, K.; Marec, F.; Traut, W. TTAGG Telomeric Repeats in Chromosomes of Some Insects and Other Arthropods. *Chromosome Research* **1999**, *7*, 449–460, doi:10.1023/A:1009297729547.
12. Müller, F.; Wicky, C.; Spicher, A.; Tobler, H. New telomere formation after developmentally regulated chromosomal breakage during the process of chromatin diminution in ascaris lumbricoides. *Cell* **1991**, *67*, 815–822, doi:10.1016/0092-8674(91)90076-B.
13. Mravinac, B.; Meštrović, N.; Čavrak, V.V.; Plohl, M. TCAGG, an alternative telomeric sequence in insects. *Chromosoma* **2011**, *120*, 367–376, doi:10.1007/s00412-011-0317-x.

Supplement P

Pecinka A, **Schrumpfová, P.P.**, Fischer L., Dvořák Tomaštíková E., and Mozgová I., **2022**. The Czech Plant Nucleus Workshop 2021. Biologia Plantarum, 66: 39-45

P.P.S. was significantly involved in the ms writing and editing

biologia plantarum
an international journal for experimental botany

BIOLOGIA PLANTARUM (2022) 66: 39-45 DOI: 10.32615/bp.2022.003

CONFERENCE REPORT

The Czech Plant Nucleus Workshop 2021

A. PECINKA[1,*], P. PROCHÁZKOVÁ SCHRUMPFOVÁ[2,3], L. FISCHER[4], E. DVOŘÁK TOMAŠTÍKOVÁ[1], and I. MOZGOVÁ[5,6]

[1] *Institute of Experimental Botany of the Czech Academy of Sciences, Centre of the Region Haná for Biotechnological and Agricultural Research, CZ-77900 Olomouc, Czech Republic*
[2] *Laboratory of Functional Genomics and Proteomics, National Centre for Biomolecular Research, Faculty of Science, Masaryk University, CZ-61137, Brno, Czech Republic*
[3] *Mendel Centre for Plant Genomics and Proteomics, Central European Institute of Technology, Masaryk University, CZ-62500, Brno, Czech Republic*
[4] *Department of Experimental Plant Biology, Charles University, Faculty of Science, CZ-12844, Prague, Czech Republic*
[5] *Biology Centre, Czech Acad Sci, Institute of Plant Molecular Biology, CZ-37005, České Budějovice, Czech Republic*
[6] *University of South Bohemia, Faculty of Science, CZ-37005 České Budějovice, Czech Republic*

[*]Corresponding author: E-mail: pecinka@ueb.cas.cz

Abstract

The Czech Plant Nucleus Workshop 2021 (CPNW2021) took place during mid-September 2021 in Olomouc, Czech Republic. About 80 researchers and students working in the field of plant nuclear and chromosome biology in the Czech Republic gathered together to present and discuss their current research. The meeting revealed many plant models that are used to study plant genomes and their organization, and also a great diversity of topics including epigenetic regulation of gene expression, genome stability, telomere biology, or sex chromosomes. CPNW2021 provided a broad platform for establishing new research contacts and collaborations. Here, we summarize the main research directions and findings presented at the CPNW2021 meeting.

Keywords: chromatin, chromosome, DNA damage repair, DNA methylation, environmental responses, nucleus, sex- and B-chromosomes.

Introduction

The cell nucleus is a fascinating organelle. It contains chromosomes that periodically condense in preparation for cell divisions in proliferating cells, separate sister chromatids into daughter nuclei, and de-condense for the interphase during which the chromosomes replicate and the whole cycle repeats. Chromosomal DNA serves as a basic template for transcription, which is orchestrated at many levels by complex regulatory machinery and takes place in specific nuclear compartments. In parallel to all these functions, the cell nucleus is under constant surveillance for the mitigation of DNA lesions.

Academic institutions within the Czech Republic have a very long and fruitful history of plant cell nuclei and chromosome research. To share the latest achievements in the field and to provide a platform for establishing new collaborations, we organized a community-focused meeting

Received 14 December 2021, *accepted* 8 February 2022.
Acknowledgements: We thank all participants at the CPNW2021 for their contributions, sharing unpublished data, and exciting and fruitful discussions during the meeting. We thank T. Mozga for extensive help during the meeting organization and M. Kovačik for developing and maintaining the CPNW2021 website. We acknowledge the financial support for the meeting from commercial and public sponsors.
Conflict of interest: The authors declare that they have no conflict of interest.

"The Czech Plant Nucleus Workshop 2021" (CPNW2021). The meeting took place at Fort Science, an interactive science centre of Palacký University in Olomouc on 14th and 15th September 2021 and was attended by more than 80 participants from the majority of national plant research institutions. This included the Institute of Experimental Botany of the Czech Academy of Sciences (IEB), Biology Centre of the Czech Academy of Sciences (BC), Institute of Biophysics of the Czech Academy of Sciences (IBP), the Central European Institute of Technology (CEITEC), Charles University (CUNI), Masaryk University (MUNI), and Palacký University (UP).

Nuclear biology research benefits from the technological advancements

The keynote opening lecture was presented by Prof. J. Doležel (IEB), who gave a historical overview of the progress in nuclear and chromosome research and emphasized that many of the fundamental findings were based on a combination of excellent research ideas and the use of the new technologies. Several examples of new approaches were presented at the meeting. P. Cápal (IEB) used advanced environmental scanning electron microscopy (A-ESEM), which allows observing samples in high resolution in their native state, with the aim to investigate the surface structure of barley mitotic chromosomes. This revealed a topologically complex surface with numerous protrusions and regularly spaced inter-chromatid bridges. A complex study of the higher-order 3D structure of both metaphase and interphase chromosomes was presented by H. Šimková (IEB). By a combination of Hi-C and chromosome painting techniques, she demonstrated that sister chromatids of barley metaphase chromosomes have a helical structure, where one turn contains 20 - 38 Mbp chromatin-packed DNA, depending on the position on the chromosome arm (Kubalová *et al.* 2021a). Microscopy is a classical technique to study cell nuclei and chromosomes. However, understanding their 3D organization using classical microscopic techniques is hampered by the diffraction limit. E. Hřibová (IEB) and M. Franek (CEITEC/MUNI) introduced super-resolution microscopy techniques including structural illumination microscopy (SIM), stimulated emission depletion (STED) microscopy, and direct stochastic optical reconstruction microscopy (dSTORM), and discussed challenges in the selection of fluorochromes and preparation of the plant samples (Kubalová *et al.* 2021b).

Chromatin regulates plant development and environmental responses

Very high developmental plasticity represents a unique and integral component of plant environmental responses. Well-controlled dynamics of chromatin structure that ensures stable but responsive gene expression is therefore of utmost importance in orchestrating developmental and environmental cues. Among the crucial developmental and cell identity modulators in plants as well as animals are the Polycomb Repressive Complexes 1 and 2 (PRC1 and PRC2) that establish two key repressive histone post-translational modifications H2Aub and H3K27me3, respectively (Bieluszewski *et al.* 2021). A. Sharaf and V. Mallika (BC) presented the identification of the components of PRC2 complexes in the basal eukaryotes (Sharaf *et al.* 2021) and algae of the green lineage. M.G. Trejo Arellano (BC) presented an evolutionary study of H3K27me3 distribution in unicellular and multicellular eukaryotes. Several contributions also tackled the recently emerging view of PRC2 involvement in environmental sensing and response in plants (Shen *et al.* 2021, Kim *et al.* 2021). I. Mozgová and M. Zhou presented recent findings on the role of PRC2 in ambient light response and photoautotrophic growth in *Arabidopsis* and T. Konečný (BC) showed enhanced heterochromatin formation in PRC2 mutant plants during de-etiolation. Using *Physcomitrium patens*, K. Sobotková (BC) demonstrated that the function of PRC2 in fine-tuning primary metabolism during photoautotrophic growth might be evolutionarily conserved.

Long non-coding RNAs (lncRNAs) are emerging as important players in chromatin modulation. For instance, the introduction of H3K27me3 by PRC2 in the FLC locus is aided by a lncRNA called COLDAIR (Xu and Chong 2018), and lncRNA APOLO has been implemented in PRC2-associated repressive chromatin looping at the PINOID locus, that encodes a major regulator of polar auxin transport (Ariel *et al.* 2014). J. Hajný (IEB) introduced a newly identified lncRNA that is expressed in the root protophloem and regulates the transcription of a xylem-expressed leucine-rich receptor-like kinase. This gene in turn controls the relationship between longitudinal anticlinal divisions in the endodermis and the stele area. The presented findings uncover an intriguing mechanism of cell division plane specification by long-distance coordination of lncRNA production and associated target gene expression. A.J. Wiese (IEB) demonstrated that upon heat stress, two bZIP transcription factors, bZIP18 and bZIP52, undergo dephosphorylation and relocate into the nucleus. Here, bZIP18 and bZIP52 regulate the transcription of several common genes, including lncRNA genes that are elevated in response to heat treatment (Wiese *et al.* 2021). These results demonstrate that phosphorylation can mediate extra-nuclear sequestration of transcription factors that orchestrate heat stress response, and perhaps suggest a more general mechanism of stress response attenuation under optimal conditions but rapid transcriptional response upon exposure to adverse environmental conditions.

Vernalization is a key trait regulating flowering time in plants relative to the winter or extended period of cold conditions. Among the well-described mechanisms is the vernalization response in *Brassicaceae* governed by PRC2, whereby the flowering inhibitor locus *FLC* is subjected to H3K27me3-mediated stable repression upon extended periods of cold (Xu and Chong 2018). Interestingly, the mechanism of vernalization response differs in monocot grasses including crops, where the release of transcriptional repression of the flowering

MADS-box activator *VERNALIZATION 1* (*VRN1*) is required for the induction of flowering. Analysis of over 100 hexaploid bread wheat cultivars by B. Strejčková (IEB) revealed several known as well as new vernalization insensitive *VRN1* alleles, supporting earlier evidence that *VRN1* is the major breeding locus in cereals (Strejčková *et al*. 2021). J. Šafář (IEB) showed that genetic and epigenetic regulation of VRN1, including a putative role of the recently identified bread wheat PRC2 components (Strejčková *et al*. 2020), remains unknown. Therefore, future plans towards the development of modifier and reporter VRN1 lines were presented.

Cereal grains are complex structures harbouring diploid embryo, triploid endosperm, and diploid seed coats of maternal origin. Cereal grain development starts with fertilization and consists of several phases including syncytium, cellularization, maturation, and desiccation (Nowicka *et al*. 2021). A. Pečinka (IEB) presented a transcriptomic meta-analysis of the embryo, endosperm, and seed maternal tissues from developing barley grains (Kovacik *et al*. 2020). This atlas of barley seed expression provides ample marker genes, indicates local and temporal specificity of biological pathways, and points to the dynamic role of epigenetic pathways.

DNA methylation - the guardian of the heterochromatic genome fraction

Methylation of cytosines is an important epigenetic mark used by plant cells to label chromatin for distinct functions. It is mostly present in the transcriptionally inactive chromatin where it occurs together with specific histone marks. *De novo* DNA methylation of native loci is driven by small RNAs (sRNAs) (Zhang *et al.* 2018). L. Fischer (CUNI) showed that the potential of sRNAs to induce DNA methylation depends not only on the level of sRNAs but also on their origin and likely also on the epigenetic state of the target locus (Čermák *et al*. 2020). Analysis of the dynamics of the initial phases of DNA methylation, using an experimental system for inducible production of sRNAs in a homogeneously responding tobacco BY-2 cell line, demonstrated that *de novo* cytosine methylation can occur already 12 h after the exposure to sRNAs (Přibylová *et al*. 2019). Furthermore, A. Přibylová (CUNI) showed that changing the chromatin state by *de novo* DNA methylation could affect the activity of the CRISPR/Cas9 editing tool and the subsequent repair of double-strand DNA breaks.

The analysis of epigenetic marks including DNA methylation is challenging in the repetitive genomic regions. Mapping DNA methylation in repeats is problematic when averaging cell populations or analyzing clusters of repeats in single-cell analysis. This problem can be overcome by analyzing individual DNA/chromatin fibres by an optimized method introduced by A. Kilar (CEITEC/MUNI). This DNA fibre extension technique combines immunofluorescence and fluorescence *in-situ* hybridization signals detected using super-resolution microscopy followed by the quantitative evaluation of DNA methylation levels using an image analysis approach (Franek *et al*. 2021).

Chromosome organization and regulation in large and polyploid genomes

Large grass genomes are generally thought to display the Rabl chromosome organization with centromeres and telomeres clustered at opposite nuclei poles (Rabl 1885). A. Doležalová (IEB) investigated the relationship between DNA replication, chromosome organization, and genome size in *Poaceae*. While there was a Rabl genome organization in *Brachypodium distachyon*, *Hordeum vulgare,* and *Triticum aestivum*, the non-Rabl organization was found in *Oryza sativa* and *Zea mays*. Prevailing replication of telomeric sequences was observed in the early and middle S phase, in contrast to centromeric sequences which underwent replication during the middle and late S phase (Němečková *et al*. 2020). Using FISH against major repetitive DNA sequences on isolated embryos and endosperm barley nuclei, A. Nowicka (IEB) showed striking differences in chromosome organization. While embryo nuclei showed typical Rabl configuration at all times, endosperm nuclei progressively lost Rabl organization in age and nuclear DNA content-dependent manner.

D. Kopecký (IEB) provided an overview of the research questions connected to interspecific hybridization and polyploidy with a particular focus on the allopolyploid genome evolution and stability and the phenomenon of genome dominance (Glombik *et al*. 2020). J. Majka (IEB) further corroborated this topic on the examples of *Allium roylei* × *Allium cepa* and *Festuca pratensis* × *Lolium multiflorum* hybrids and suggested that the shifts in genome composition towards one parent could be due to uneven behaviour of parental chromosomes during meiosis in these hybrids. There is a continuous debate on the effects of hybridization and polyploidization on gene transcription. M. Glombik (IEB) showed that in allopolyploids of *Festuca pratensis* × *Lolium multiflorum*, the overall transcript profile is much closer to that of *Lolium* parent, suggesting it as a transcriptionally dominant genome, presumably *via trans*-acting regulatory factors (Glombik *et al*. 2021). K. Perničková (IEB) analyzed the 3D nuclear positioning of a pair of rye chromosomes introgressed to the hexaploid wheat genome. She reported an occasional lack of contact between telomeres of the additional chromosomes and nuclear envelope, which could be responsible for the observed less efficient chromosome pairing in meiosis and transmission into subsequent generations (Perničková *et al*. 2019).

Unravelling the mysteries of plant sex- and B-chromosomes

R. Hobza (IBP) showed that separated sexes evolved independently and repeatedly in about 5 % of plant species. In many species, dioecy has evolved recently, so

these plants provide an excellent model for studying the early stages of sex chromosome divergence, which later in evolution leads to gradual sex chromosome degeneration (Hobza *et al*. 2018). Z. Kubát (IBP) showed that some TEs proliferate preferentially either in the male or in the female germline which can be connected with specific circumstances affecting TE management and activity in male and female plants and during gametophyte formation (Jesionek *et al*. 2021). The process of evolutionary diversification of sex chromosomes is also connected with specific chromatin modifications of both histones and cytosines in *Silene latifolia* as demonstrated by M. Hubinský (IBP) (Rodríguez Lorenzo *et al*. 2020). In addition to the pivotal role of *S. latifolia* in studying plant sex chromosome evolution, V. Hudzieczek (IBP) with colleagues aims to establish the genus *Silene* as a common model to study also other aspects of plant ecology, evolution, and development. For this purpose, they established a set of methods for *S. latifolia*, including *Agrobacterium*-mediated gene delivery, genome editing by TALENs and CRISPR/Cas9 or gene silencing *via* RNAi.
Certain genomes contain specific supernumerary chromosomes that carry a generally low number of protein-coding genes but often harbour molecular toolkits for their preferential inheritance. J. Bartoš (IEB) introduced plant B chromosomes and presented maize and *Sorghum* as promising models to study molecular mechanisms of non-disjunction, preferential fertilization, and chromosome elimination (Blavet *et al.* 2021, Karafiátová *et al*. 2021).

Plant nuclei functions and chromatin organization during DNA damage repair

DNA is constantly exposed to a variety of genotoxic factors that may alter its chemical and/or physical structure and result in DNA lesions. DNA damage response (DDR) is therefore a key mechanism contributing to genome stability. DDR is a very complex process, ultimately leading to DNA damage repair or cell death. After DNA damage is sensed, the local chromatin environment must be reorganized and histones are displaced. In accordance, FASCIATA1 (FAS1), a subunit of the H3-H4 histone chaperone complex CHROMATIN ASSEMBLY FACTOR 1 (CAF1), is important for genome stability and DNA damage repair (Kolářová *et al*. 2021). In her talk, M. Nešpor Dadejová (CEITEC/MUNI) introduced a newly developed *in vivo* method employing laser microirradiation-induced DNA damage. Using the PCNA1-GFP marker line (Yokoyama *et al*. 2016), this technique allows observing immediate relocation of PCNA1 during DNA damage response in wild type cells.

The Structural Maintenance of Chromosomes (SMC) complexes are key components of higher-order chromatin structure. The SMC5/6 complex is involved in homologous recombination, replication fork stability, and DNA damage repair and its basic structure is evolutionarily conserved (Díaz and Pecinka 2018). J. Paleček (MUNI) presented a detailed architectural analysis of the SMC5/6 complex in humans and yeast (Adamus *et al*. 2020), highlighted this SMC complex as the most ancestral in eukaryotes, and showed various models of its possible DNA processing activity. His laboratory identified the SMC5/6 complex subunits in the moss *Physcomitrium patens* and is planning to reveal the SMC5/6 complex architecture in plants. M. Holá (IEB) presented functional characterization of SMC5/6 in *P. patens*. Sensitivity assays revealed a critical role of SMC5/6 in double-strand-break (DSB) repair and proposed that the circularization of SMC5/6 complex by the kleisin subunit NSE4 is indispensable for the *P. patens* SMC5/6 function (Holá *et al*. 2021).

DNA-protein crosslinks (DPC) represent a specific type of DNA damage, caused by the covalent trapping of virtually any protein to DNA (Stingele and Jentsch 2015). E. Dvořák Tomaštíková (IEB) presented a forward-directed genetic screen that aimed to identify factors involved in the repair of zebularine-induced DPCs in *Arabidopsis* (Procházková *et al*. 2022). Besides several unknown factors undergoing characterization, the SMC5/6 complex was identified as an important DPC repair factor, representing a new DPC repair pathway.

Maintaining genome stability over generations is a key issue for all living organisms. F. Yang (IEB) explained how SMC5/6 complex functions contribute to normal male meiosis in *Arabidopsis* (Yang *et al*. 2021). Loss-of-function mutants in SMC5/6 subunits generate unreduced microspores. The diploid pollen leads to an unbalanced maternal and paternal genome dosage in endosperm, which is responsible for a frequent seed abortion but in about 10 - 15 % of seeds leads to the production of triploid offspring. Thus, SMC5/6 has an important role in the maintenance of gametophytic ploidy in *Arabidopsis*.

Maintenance of the chromosome ends

Telomeres consist predominantly of non-coding repetitive tandem repeats and protect the ends of linear eukaryotic chromosomes from progressive shortening and erroneous recognition as unrepaired chromosome breaks. A rosette-like organization of chromosomes, where telomeres show persistent clustering at the nucleolus in interphase nuclei while centromeres associate with nuclear envelope was observed in *A. thaliana* (Fransz *et al*. 2002). M. Kubová (CEITEC/MUNI) showed that the rosette-like configuration is not a universal model for interphase genome organization in *Brassicaceae*. In species with large-genome (≥ 1 Gb), centromeres and telomeres adopt either the Rabl-like configuration or a dispersed distribution in the nuclear interior, with telomeres being only rarely anchored to the nucleolus (Shan *et al*. 2021).

Telomeric repeats across the *Eukaryotes* typically follow the formula $(T_xA_yG_z)_n$ (Schrumpfová and Fajkus 2020). In plants, telomeres are mostly composed of the *Arabidopsis*-type $TTTAGGG_n$ repeats (Richards and Ausubel 1988). However, recent studies revealed significant variability in telomere sequences in lower and also higher plants (Peska and Garcia 2020). Moreover, telomeric or telomeric-like repeats are found also at multiple intra-chromosomal regions (Uchida *et al.* 2002, Majerová *et al*. 2014). This

phenomenon observed in many plant families is most likely caused by genome rearrangements during evolution. Interestingly, larger genomes in gymnosperm species than in angiosperms were previously reported to be associated with a larger proportion of repetitive sequences (Novák *et al*. 2020). A wide survey in gymnosperms, namely in the *Cycadaceae* family by R. Vozárová (IBP), has shown that canonical *Arabidopsis*-type telomeric repeats are located predominantly at chromosome ends, while pericentromeric blocks comprise other telomeric variants. Telomeric repeats are a natural target of epigenetic regulation and are traditionally considered heterochromatic regions. Recent studies show that telomeres in *A. thaliana* possess both euchromatic (H3.3, H3K4me3) and heterochromatic (H3K9me2, H3K27me1, H3K27me3) marks (Procházková Schrumpfová *et al*. 2019). Histone H3 deposition is maintained by histone chaperone proteins. A. Machelová (CEITEC/MUNI) focused on H3 chaperones and showed that HISTONE CELL CYCLE REGULATOR (HIRA) and ANTI-SILENCING FUNCTION 1 (ASF1) are required for telomere maintenance in *A. thaliana*, as their simultaneous depletion causes a lethal phenotype.

TELOMERE REPEAT BINDING (TRB) family represents a rare example of proteins with confirmed *in vivo* telomere localization in plants (Schrumpfová *et al*. 2014). These proteins bind telomeric DNA through the MYB-like domain and they possess plant-specific protein-domain organization (Peska *et al*. 2011). Conserved features of TRB proteins in *P. patens* and *A. thaliana* were discussed by A. Kusová (MUNI). Apart from binding telomeric sequences, TRB proteins directly interact with the protein catalytic subunit of telomerase (Schrumpfová *et al*. 2014). Telomerase adds telomeric repeats to the ends of chromosomes and consists of telomerase RNA (TR) and Telomerase reverse transcriptase (TERT) subunits. In humans, the expression of TERT is strictly controlled at the transcript level, but TR is ubiquitously expressed. Interestingly, the expression of the TR subunit follows a tissue-specific pattern similar to that of TERT expression in plants, and the plant *TR* gene is transcribed by RNA Polymerase III (Pol III), but not by Pol II, as in mammals or yeasts (Fajkus *et al*. 2019). All these features as well as the evolution of both subunits of telomerase were presented by P. Procházková Schrumpfová (SCI, MUNI) (Schrumpfová and Fajkus 2020; Fajkus *et al*. 2021). K. Konečná (IBP, CEITEC, MUNI) presented characterization of the Armadillo (ARM) repeat type plant-specific protein found as an interactor with TERT (Dokládal *et al*. 2018). The results suggested that ARM cellular activity is independent of the telomerase canonical function and implied the involvement of ARM protein in response to a drug, biotic, and abiotic stimuli.

Summarizing remarks

The CPNW2021 showed a remarkable diversity of the topics broadly linked to plant nuclear and chromosome biology that were studied in the Czech Republic. Particularly prominent were the topics of 3D genome organization, chromatin modifications, epigenetic regulation of gene expression, sex chromosomes, and genome stability. A variety of plant model species was also introduced (only selected species are listed here) *Arabidopsis thaliana*, *Silene latifolia*, *Nicotiana tabacum*, *Allium* sp., temperate cereals (*Triticum aestivum*, *Hordeum vulgare*), *Zea mays,* or *Physcomitrium patens*. This provided unique opportunities to discuss research questions and to establish new research connections. At the end of the meeting, the young researchers (under 35 years) were awarded in several categories. The awards for the best poster presentations were given to K. Kaduchová (IEB) and M.G. Trejo Arellano (BC). M. Glombik (IEB) and A. Přibylová (CUNI) were awarded for the best Ph.D. student talks and Mingxi Zhou (BC) for the best post-doc talk. Finally, it was announced that the next CPNW meeting will be held in 2023 in Brno.

References

Adamus, M., Lelkes, E., Potesil, D., Ganji, S.R., Kolesar, P., Zabrady, K., Zdrahal, Z., Palecek, J.J.: Molecular insights into the architecture of the human SMC5/6 complex. - J. mol. Biol. **432**: 3820-3837, 2020.

Ariel, F., Jegu, T., Latrasse, D., Romero-Barrios, N., Christ, A., Benhamed, M., Crespi, M.: Noncoding transcription by alternative RNA polymerases dynamically regulates an auxin-driven chromatin loop. - Mol. Cells **55**: 383-396, 2014.

Bieluszewski, T., Xiao, J., Yang, Y., Wagner, D.: PRC2 activity, recruitment, and silencing: a comparative perspective. - Trends Plant Sci. **26**: 1186-1198, 2021.

Blavet, N., Yang, H., Su, H.D., Solansky, P., Douglas, R.N., Karafiatova, M., Simkova, L., Zhang, J., Liu, Y., Hou, J., Shi, X.W., Chen, C., El-Walid, M., McCaw, M.E., Albert, P.S., Gao, Z., Zhao, C.Z., Ben-Zvi, G., Glick, L., Kol, G., Shi, J.H., Vrana, J., Simkova, H., Lamb, J.C., Newton, K., Dawe, R.K., Dolezel, J., Ji, T.M., Baruch, K., Cheng, J.L., Han, F.P., Birchler, J.A., Bartos, J.: Sequence of the supernumerary B chromosome of maize provides insight into its drive mechanism and evolution. - Proc. nat. Acad. Sci. USA **118**: e2104254118, 2021.

Čermák, V., Tyč, D., Přibylová, A., Fischer, L.: Unexpected variations in posttranscriptional gene silencing induced by differentially produced dsRNAs in tobacco cells. - Biochim. biophys. Acta - Gene Regul. Mech. **1863**: 194647, 2020.

Díaz, M., Pecinka, A.: Scaffolding for repair: understanding molecular functions of the SMC5/6 complex. - Genes (Basel) **9**: 36, 2018.

Dokládal, L., Benková, E., Honys, D., Dupľáková, N., Lee, L.-Y., Gelvin, S.B., Sýkorová, E.: An armadillo-domain protein participates in a telomerase interaction network. - Plant mol. Biol. **97**: 407-420, 2018.

Fajkus, P., Peška, V., Závodník, M., Fojtová, M., Fulnečková, J., Dobias, Š., Kilar, A., Dvořáčková, M., Zachová, D., Nečasová, I., Sims, J., Sýkorová, E., Fajkus, J.: Telomerase RNAs in land plants. - Nucl. Acids Res. **47**: 9842-9856, 2019.

Fajkus, P., Kilar, A., Nelson, A.D.L., Holá, M., Peška, V., Goffová, I., Fojtová, M., Zachová, D., Fulnečková, J., Fajkus, J.: Evolution of plant telomerase RNAs: farther to the past, deeper to the roots. - Nucl. Acids Res. **49**: 7680-7694, 2021.

Franek, M., Kilar, A., Fojtík, P., Olšinová, M., Benda, A., Rotrekl, V., Dvořáčková, M., Fajkus, J.: Super-resolution microscopy of chromatin fibers and quantitative DNA methylation analysis

of DNA fiber preparations. - J. Cell Sci. **134**: jcs258374, 2021.
Fransz, P., De Jong, J.H., Lysak, M., Castiglione, M.R., Schubert, I.: Interphase chromosomes in *Arabidopsis* are organized as well defined chromocenters from which euchromatin loops emanate. - Proc. nat. Acad. Sci. USA **99**: 14584-14589, 2002.
Glombik, M., Bačovský, V., Hobza, R., Kopecký, D.: Competition of parental genomes in plant hybrids. - Front. Plant Sci. **11**: 200, 2020.
Glombik, M., Copetti, D., Bartos, J., Stoces, S., Zwierzykowski, Z., Ruttink, T., Wendel, J.F., Duchoslav, M., Dolezel, J., Studer, B., Kopecky, D.: Reciprocal allopolyploid grasses (*Festuca* × *Lolium*) display stable patterns of genome dominance. - Plant J. **107**: 1166-1182, 2021.
Hobza, R., Hudzieczek, V., Kubat, Z., Cegan, R., Vyskot, B., Kejnovsky, E., Janousek, B.: Sex and the flower - developmental aspects of sex chromosome evolution. - Ann. Bot. **122**: 1085-1101, 2018.
Holá, M., Vágnerová, R., Angelis, K.J.:. Kleisin NSE4 of the SMC5/6 complex is necessary for DNA double strand break repair, but not for recovery from DNA damage in physcomitrella (*Physcomitrium patens*). - Plant mol. Biol. **107:** 355-364, 2021.
Jesionek, W., Bodláková, M., Kubát, Z., Čegan, R., Vyskot, B., Vrána, J., Šafář, J., Puterova, J., Hobza, R.: Fundamentally different repetitive element composition of sex chromosomes in *Rumex acetosa*. - Ann. Bot. **127**: 33-47, 2021.
Karafiátová, M., Bednářová, M., Said, M., Čížková, J., Holušová, K., Blavet, N., Bartoš, J.: The B chromosome of *Sorghum purpureosericeum* reveals the first pieces of its sequence. - J. exp. Bot. **72**: 1606-1616, 2021.
Kim, J., Bordiya, Y., Kathare, P.K., Zhao, B., Zong, W., Huq, E., Sung, S.: Phytochrome B triggers light-dependent chromatin remodelling through the PRC2-associated PHD finger protein VIL1. - Nat. Plants **7**: 1213-1219, 2021.
Kolářová, K., Nešpor Dadejová, M., Loja, T., Lochmanová, G., Sýkorová, E., Dvořáčková, M.: Disruption of NAP1 genes in *Arabidopsis thaliana* suppresses the *fas1* mutant phenotype, enhances genome stability and changes chromatin compaction. - Plant J. **106**: 56-73, 2021.
Kovacik, M., Nowicka, A., Pecinka, A.: Isolation of high purity tissues from developing barley seeds. - J. visualized Exp. **164**: e61681, 2020.
Kubalová, I., Câmara, A.S., Cápal, P., Beseda, T., Rouillard, J., Krause, G.M., Toegelová, H., Himmelbach, A., Stein, N., Houben, A., Doležel, J., Mascher, M., Šimková, H., Schubert, V.: Helical metaphase chromatid coiling is conserved. - bioRxiv: 2021.09.16.460607, 2021a.
Kubalová, I., Němečková, A., Weisshart, K., Hřibová, E., Schubert, V.: Comparing super-resolution microscopy techniques to analyze chromosomes. - Int. J. mol. Sci. **22**: 1903, 2021b.
Majerová, E., Mandáková, T., Vu, G.T.H., Fajkus, J., Lysak, M.A., Fojtová, M.: Chromatin features of plant telomeric sequences at terminal vs. internal positions. - Front. Plant Sci. **5**: 1-10, 2014.
Němečková, A., Koláčková, V., Vrána, J., Doležel, J., Hřibová, E.: DNA replication and chromosome positioning throughout the interphase in three-dimensional space of plant nuclei. - J. exp. Bot. **71**: 6262-6272, 2020.
Novák, P., Guignard, M.S., Neumann, P., Kelly, L.J., Mlinarec, J., Koblížková, A., Dodsworth, S., Kovařík, A., Pellicer, J., Wang, W., Macas, J., Leitch, I.J., Leitch, A.R.: Repeat-sequence turnover shifts fundamentally in species with large genomes. - Nat. Plants **6**: 1325-1329, 2020.
Nowicka, A., Kovacik, M., Tokarz, B., Vrána, J., Zhang, Y., Weigt, D., Doležel, J., Pecinka, A.: Dynamics of endoreduplication in developing barley seeds. - J. exp. Bot. **72**: 268-282, 2021.
Perničková, K., Koláčková, V., Lukaszewski, A.J., Fan, Ch., Vrána, J., Duchoslav, M., Jenkins, G., Phillips, D., Šamajová, O., Sedlářová, M., Šamaj, J., Doležel, J., Kopecký, D.: Instability of alien chromosome introgressions in wheat associated with improper positioning in the nucleus. - Int. J. mol. Sci. **20**: 1448, 2019.
Peska, V., Garcia, S.: Origin, diversity, and evolution of telomere sequences in plants. - Front. Plant Sci. **11**: 117, 2020.
Peska, V., Prochazkova Schrumpfova, P., Fajkus, J.:Using the Telobox to search for plant telomere binding proteins. - Curr. Protein Pept. Sci. **12**: 75-83, 2011.
Přibylová, A., Čermák, V., Tyč, D., Fischer, L.: Detailed insight into the dynamics of the initial phases of *de novo* RNA-directed DNA methylation in plant cells. - Epigenetics Chromatin **12**: 54, 2019.
Procházková, K., Finke, A., Dvořák Tomaštíková, E., Filo, J., Bente, H., Dvořák, P., Ovečka, M., Šamaj, J., Pecinka, A.:. Zebularine induces enzymatic DNA-protein crosslinks in 45S rDNA heterochromatin of *Arabidopsis* nuclei. - Nucl. Acids Res. **50**: 244-258, 2022.
Procházková Schrumpfová, P., Fojtová, M., Fajkus, J.: Telomeres in plants and humans: not so different, not so similar. - Cells **8**: 58, 2019.
Rabl, C.: Über Zelltheilung. - Morphologisches Jahrbuch **10**: 214–330, 1885.
Richards, E.J., Ausubel, F.M.: Isolation of a higher eukaryotic telomere from *Arabidopsis thaliana*. - Cell **53**: 127-136, 1988.
Rodríguez Lorenzo, J.L., Hubinský, M., Vyskot, B., Hobza, R.: Histone post-translational modifications in *Silene latifolia* X and Y chromosomes suggest a mammal-like dosage compensation system. - Plant Sci. **299**: 110528, 2020.
Schrumpfová, P.P., Fajkus, J.: Composition and function of Telomerase-A polymerase associated with the origin of Eukaryotes. - Biomolecules **10**: 1425, 2020.
Schrumpfová, P.P., Vychodilová, I., Dvořáčková, M., Majerská, J., Dokládal, L., Schořová, S., Fajkus, J.: Telomere repeat binding proteins are functional components of *Arabidopsis* telomeres and interact with telomerase. - Plant J. **77**: 770-781, 2014.
Shan, W., Kubová, M., Mandáková, T., Lysak, M.A.: Nuclear organization in crucifer genomes: nucleolus-associated telomere clustering is not a universal interphase configuration in *Brassicaceae*. - Plant J. **108**: 528-540, 2021.
Sharaf, A., Vijayanathan, M., Oborník, M., Mozgová, I.: Phylogenetic profiling suggests early origin of the core subunits of Polycomb Repressive Complex 2 (PRC2). - bioRxiv: 2021.07.16.452543, 2021.
Shen, Q., Lin, Y., Li, Y., Wang, G.: Dynamics of H3K27me3 modification on plant adaptation to environmental cues. - Plants (Basel) **10**: 1165, 2021.
Stingele, J., Jentsch, S.: DNA-protein crosslink repair. - Nat. Rev. mol. cell. Biol. **16**: 455-460, 2015.
Strejčková, B., Čegan, R., Pecinka, A., Milec, Z., Šafář, J.: Identification of polycomb repressive complex 1 and 2 core components in hexaploid bread wheat. - BMC Plant Biol. **20**: 175, 2020.
Strejčková, B., Milec, Z., Holušová, K., Cápal, P., Vojtková, T., Čegan, R., Šafář, J.: In-depth sequence analysis of bread wheat *VRN1* genes. - Int. J. mol. Sci. **22**: 12284, 2021.
Uchida, W., Matsunaga, S., Sugiyama, R., Kawano, S.: Interstitial telomere-like repeats in the *Arabidopsis thaliana* genome. - Genes Genet. Syst. **77**: 63-67, 2002.
Wiese, A.J., Steinbachová, L., Timofejeva, L., Čermák, V., Klodová, B., Ganji, R.S., Limones-Mendez, M., Bokvaj, P., Hafidh, S., Potěšil, D., Honys, D.: *Arabidopsis* bZIP18 and

bZIP52 accumulate in nuclei following heat stress where they regulate the expression of a similar set of genes. - Int. J. mol. Sci. **22**: 530, 2021.

Xu, S., Chong, K.: Remembering winter through vernalisation. - Nat. Plants **4**: 997-1009, 2018.

Yang, F., Fernández-Jiménez, N., Tučková, M., Vrána, J., Cápal, P., Díaz, M., Pradillo, M., Pecinka, A.: Defects in meiotic chromosome segregation lead to unreduced male gametes in *Arabidopsis* SMC5/6 complex mutants. - Plant Cell **33**: 3104-3119 2021.

Yokoyama, R., Hirakawa, T., Hayashi, S., Sakamoto, T., Matsunaga, S.: Dynamics of plant DNA replication based on PCNA visualization. - Nat. Publ. **6**: 29657, 2016.

Zhang, H., Lang, Z., Zhu, J.-K.: Dynamics and function of DNA methylation in plants. - Nat. Rev. Mol. Cell Biol. **19**: 489-506, 2018.

Supplement Q

Dvořák Tomaštíková E., Yang F., Mlynárová K., Hafid S., Schořová Š., Kusová A., Pernisová M., Přerovská M., Klodová B., Honys D., Fajkus J., Pecinka A., and **Schrumpfova P.P.*, 2023** RUVBL proteins are involved in plant gametophyte development, The Plant Journal 114, 325–337

P.P.S. participated in the design of experiments, data evaluation and wrote the ms

the plant journal

SEB SOCIETY FOR EXPERIMENTAL BIOLOGY

The Plant Journal (2023) **114,** 325–337 doi: 10.1111/tpj.16136

RUVBL proteins are involved in plant gametophyte development

Eva Dvořák Tomaštíková[1], Fen Yang[1,2], Kristína Mlynárová[3], Said Hafidh[4], Šárka Schořová[3], Alžbeta Kusová[3,5], Markéta Pernisová[3,5], Tereza Přerovská[3], Božena Klodová[4,6], David Honys[4,6], Jiří Fajkus[3,5,7], Ales Pecinka[1,2] and Petra Procházková Schrumpfová[3,5,*]

[1]*Centre of Plant Structural and Functional Genomics, Institute of Experimental Botany, Czech Academy of Sciences, Šlechtitelů 31, 77900 Olomouc, Czech Republic,*

[2]*Department of Cell Biology and Genetics, Faculty of Science, Palacký University, Šlechtitelů 27, 77900 Olomouc, Czech Republic,*

[3]*Laboratory of Functional Genomics and Proteomics, Faculty of Science, National Centre for Biomolecular Research, Masaryk University, Kamenice 5, CZ-62500 Brno, Czech Republic,*

[4]*Laboratory of Pollen Biology, Institute of Experimental Botany of the Czech Academy of Sciences, Rozvojová 263, CZ-165 02 Prague, Czech Republic,*

[5]*Mendel Centre for Plant Genomics and Proteomics, Central European Institute of Technology, Masaryk University, Kamenice 5, CZ-62500 Brno, Czech Republic,*

[6]*Department of Experimental Plant Biology, Faculty of Science, Charles University, Viničná 5, 128 00 Praha 2, Czech Republic, and*

[7]*Institute of Biophysics of the Czech Academy of Sciences, Královopolská 135, CZ-61265 Brno, Czech Republic*

Received 12 May 2022; revised 25 January 2023; accepted 1 February 2023; published online 8 February 2023.
*For correspondence (e-mail schpetra@sci.muni.cz).

SUMMARY

The proper development of male and female gametophytes is critical for successful sexual reproduction and requires a carefully regulated series of events orchestrated by a suite of various proteins. RUVBL1 and RUVBL2, plant orthologues of human Pontin and Reptin, respectively, belong to the evolutionarily highly conserved AAA$^+$ family linked to a wide range of cellular processes. Previously, we found that *RUVBL1* and *RUVBL2A* mutations are homozygous lethal in Arabidopsis. Here, we report that RUVBL1 and RUVBL2A play roles in reproductive development. We show that mutant plants produce embryo sacs with an abnormal structure or with various numbers of nuclei. Although pollen grains of heterozygous mutant plants exhibit reduced viability and reduced pollen tube growth *in vitro*, some of the *ruvbl* pollen tubes are capable of targeting ovules *in vivo*. Similarly, some *ruvbl* ovules retain the ability to attract wild-type pollen tubes but fail to develop further. The activity of the *RUVBL1* and *RUVBL2A* promoters was observed in the embryo sac, pollen grains, and tapetum cells and, for *RUVBL2A*, also in developing ovules. In summary, we show that the RUVBL proteins are essential for the proper development of both male and particularly female gametophytes in Arabidopsis.

INTRODUCTION

Successful plant sexual reproduction requires the formation of male and female gametophytes that contain male sperm cells and female egg cells. In angiosperms, microgametogenesis and megagametogenesis produce male and female gametophytes, respectively. During microgametogenesis, the meiosis of a microspore mother cell gives rise to a tetrad of haploid male spores (microspores). After being released from a tetrad, each microspore undergoes mitotic division (pollen mitosis I) to develop into a binucleate microspore containing a large vegetative cell and a small generative cell. The generative cell then migrates into the vegetative cell to form a unique cell-within-a-cell structure. The generative cell undergoes pollen mitosis II to produce two sperm cells enclosed in the vegetative cell (Hafidh & Honys, 2021). During female gametophyte development, typically three of the female spores generated by meiosis degenerate, and the remaining megaspore undergoes three rounds of mitotic divisions followed by cellularization. This results in eight nuclei within seven cells organized in a precise manner within the embryo sac. The mature embryo sac contains an egg cell flanked by two synergid cells at the

micropylar region, a homodiploid central cell in the middle region, and three antipodal cells in the chalazal region. The mature embryo sac develops within a specialized structure, the ovule, and is surrounded by diploid integuments of maternal origin (Drews & Yadegari, 2002; Kawashima & Berger, 2014).

Male and female gametogenesis are highly coordinated developmental processes. Many proteins regulate the various metabolic pathways or genetic and epigenetic processes that mediate the specification of cell identity (Hafidh & Honys, 2021; Sundaresan & Skinner, 2018). Defective female gametogenesis usually causes abnormal embryo sac development, presenting various arrest phenotypes, thus reducing the seed set (Yang, Fernández Jiménez, Majka, et al., 2021). Male gametophyte mutants in non-essential genes do not generally result in reduced seed sets because the abundance of pollen is not usually a limiting factor (Drews & Koltunow, 2011).

RUVB proteins belong to the evolutionarily highly conserved superfamily of AAA+ ATPases (i.e. ATPases associated with various cellular activities) (Neuwald et al., 1999). This class of ATPases contains conserved motifs for ATP-binding and hydrolysis, such as Walker boxes (Walker A and B) (Walker et al., 1982), Sensor residues (Sensor I and II), and Arg-fingers. AAA+ proteins use the hydrolysis of ATP to exert mechanical forces, and this is essential for their biological activity (Matias et al., 2006). Despite human RUVBL proteins sharing a high degree of homology with the bacterial RuvB helicase, the helicase activity of human RUVBL is surprisingly low (Matias et al., 2006).

Human RUVBL1 and RUVBL2 (also known as Pontin/Pontin 52/TIP49/TIP49a/INO80H/TIH1/Rvb1 and Reptin/Reptin 52/TIP48/TIP49b/INO80J/TIH2/Rvb2, respectively) are essential for many cellular activities and take part in various cellular complexes. Mammalian RUVBLs are members of chromatin remodeling complexes INOsitol auxotrophy 80 (INO80) and Swi2/Snf2-related (SWR1) (Jin et al., 2005; Willhoft & Wigley, 2020) or the Fanconi anemia core complex involved in DNA damage repair signaling (Rajendra et al., 2014). RUVBLs are important for the assembly of telomerase holoenzyme via interaction with telomerase catalytical subunit (TERT) (Venteicher et al., 2008) or assembly of the mammalian target of rapamycin complex (Kim et al., 2013; Shin et al., 2020). They are also involved in the biogenesis of small nucleolar ribonucleoproteins (Cloutier et al., 2017). In addition, RUVBLs were shown to be important transcriptional regulators, regulators of the cell cycle, and mitotic progressiondue to their interaction with MYC, E2F1, and other transcription factors. They are also involved in promoting mitotic spindle assembly (Mao & Houry, 2017). RUVBL1 assists actin-based cellular motility (mediate actin polymerization) (Taniuchi et al., 2014). These processes underline the central role of RUVBLs in promoting cell proliferation and survival.

The *Arabidopsis thaliana* (Arabidopsis) genome encodes one homolog of *RUVBL1* and two homologs of *RUVBL2*–*RUVBL2A* and *RUVBL2B*, where only *RUVBL1* and *RUVBL2A* appear to be functional (Brunkard et al., 2020; Julca et al., 2021). Importantly, RUVBL1 and RUVBL2A were suggested as essential for gametophyte development (Brunkard et al., 2020; Holt et al., 2002; Schořová et al., 2019).

Similar to their homologs in diverse organisms, Arabidopsis RUVBL1 and RUVBL2A can form both homo- and heteromers (Majerská et al., 2017; Schořová et al., 2019). Similarly, RUVBL proteins are not associated with just one cellular process but rather have roles in the regulation of various cellular mechanisms. We have previously described the association of RUVBL1 and RUVBL2A, but not RUVBL2B, with TERT from Arabidopsis (Majerská et al., 2017). Additionally, Arabidopsis RUVBL proteins contribute to the TOR signaling network by providing chaperone activity for the correct assembly of the TORC1 complex (Brunkard et al., 2020; Van Leene et al., 2019). Similarly, RUVBL1 and RUVBL2 are components of the plant chromatin remodeling complexes SWR1 and INO80, where they might have a regulatory role (Bieluszewski et al., 2015; Luo et al., 2020; Zander et al., 2019). RUVBL1 was suggested as a regulator of specific disease resistance (R) genes (Holt et al., 2002).

To shed light on the roles of RUVBL proteins during sexual reproduction, we analyzed the gametophyte development of *ruvbl* mutants. We performed reciprocal crosses and identified major problems in the development and fertilization of the female gametophyte. Microscopic analyses showed that *ruvbl1* and *ruvbl2a* failed to develop viable ovules. Moreover, RUVBL1 and RUVBL2A are involved in the development of viable pollen and pollen tube, although this role is less critical. These findings are in agreement with the reduced transmission of the mutant alleles also from the paternal side. Our observation revealed the essential role of RUVBL proteins in plant haploid stages in Arabidopsis because the RUVBL proteins are needed for the proper development of both the male and especially female gametophytes.

RESULTS

Mutations in RUVBL1 or RUVBL2A result in seed-setting defects

Our previous study showed that homozygous T-DNA insertion mutants of Arabidopsis *RUVBL1* and *RUVBL2A* are not viable and, from several T-DNA insertion lines, only *ruvbl1-1* and *ruvbl2a-1* alleles (Figure S1) showed heterozygous progeny. Their offspring genotypic ratios did not follow the expected Mendelian frequencies (Schořová et al., 2019).

To gain insight into the function of RUVBL1 and RUVBL2A in gametophyte and early sporophyte development,

we examined the seed production of the self-pollinated heterozygous *ruvbl1-1* and *ruvbl2a-1* mutant plants (hereafter *ruvbl1-1*/+ and *ruvbl2a-1*/+, respectively) using the fully elongated siliques of the main inflorescence stem. Our microscopic analyses revealed up to 41.7% (± 3.4%) and 51.1% (± 5.9%) aborted ovules in *ruvbl1-1*/+ and *ruvbl2a-1*/+ mutant siliques, respectively, whereas 0.5% (± 0.2%) of aborted ovules were observed in self-pollinated wild-type (WT) plants (Figure 1a,b). Next to the aborted ovules were seeds that appeared to have developed normally, and these were indistinguishable from those in WT plants. To validate our initial findings, we screened several additional available T-DNA insertional mutants and isolated more *RUVBL1* and *RUVBL2A* T-DNA insertional mutants *ruvbl1-6*+/− and *ruvbl2a-2*+/− (*ruvbl1-6*/+ and *ruvbl2a-2*/+; Figure S1). Microscopic analyses revealed up to 55.4% (± 5.6%) and 49.7% (± 5.2%) aborted ovules in *ruvbl1-6*/+ and *ruvbl2a-2*/+ mutant siliques (Figure S2a,b). This suggested that the absence of homozygous *ruvbl1* and *ruvbl2a* plants is not a result of embryo lethality, but might be the effect of almost complete lethality from the female gametophyte, which would correspond to 50% of aborted ovules according to Mendelian rules.

RUVBL genes are necessary for both male and female fertility

To assess the maternal and/or paternal effects on the frequency of aborted ovules, we performed reciprocal crosses between the *ruvbl1*/+ or *ruvbl2a*/+ and WT plants. We analyzed at least five fully elongated siliques of the main inflorescence stem from two to three plants for each combination specified in Figure 1. The percentages of aborted ovules in fully developed siliques of *ruvbl1-1*/+ and *ruvbl1-6*/+ mother plants pollinated by WT plants were 51.4% (± 2.3%) and 47.4% (± 2.3%), respectively. The percentages of aborted ovules of *ruvbl2a-1*/+ and *ruvbl2a-2*/+ mother plants pollinated by WT plants were 62.9% (± 6.7%) and 46.8% (± 3.1%), respectively. The control manual cross between two WT parents produced only 1.1% (± 0.4%) of such aborted ovules. Pollination of WT mother plant with *ruvbl1-1*/+ and *ruvbl1-6*/+ pollen resulted in 17.7% (± 10.6%) and 4.2% (± 4.5%) aborted ovules. Similarly, pollination of WT mother plant with *ruvbl2a-1*/+ and *ruvbl2a-2*/+ pollen resulted in 19.5% (± 1.4%) and 2.9% (± 3.4%), of aborted ovules, respectively (Figure 1c,d; Figure S2c,d). The number of the normally developed and aborted seeds was not affected by an error in plant handling during reciprocal crosses, as observable in Figure 1 (b,d).

Although reciprocal crosses between plants heterozygous for *RUVBL1* and *RUVBL2A* with WT revealed both male-related and female-related reduced fertility, female gametophyte development was more severely impaired by *RUVBL1* and *RUVBL2A* loss-of-function than male

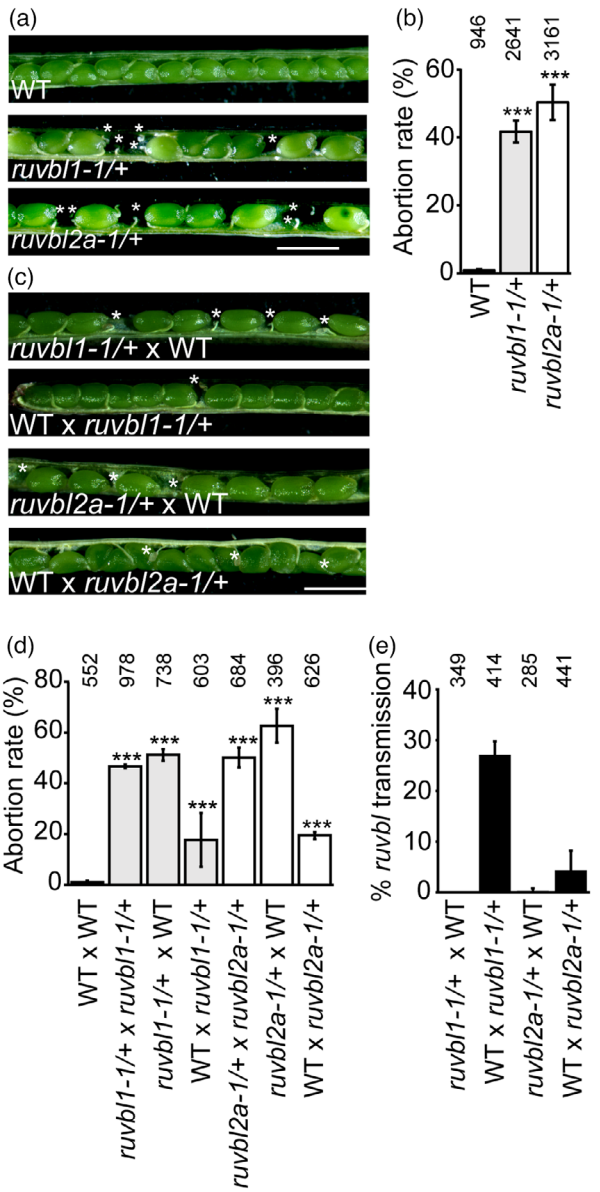

Figure 1. Analysis of seed setting in *RUVBL1* and *RUVBL2A* mutant plants and transmission ratio distortion in reciprocal crosses.
(a) Representative content of siliques in self-pollinated WT, *ruvbl1-1*/+, and *ruvbl2a-1*/+ plants. White asterisks indicate aborted ovules. Scale bar = 1 mm.
(b) Percentage of aborted ovules of self-fertilized WT and mutant plants. Numbers on top of bars correspond to the number of analyzed seeds. ***$P < 0.00001$ via Fisher's exact test (chi-squared). Error bars indicate the SD of the means of individually analyzed siliques.
(c) Representative content of siliques from reciprocal crosses between mutants and WT. The first genotype indicates the mother plants. Scale bar = 1 mm.
(d) Percentage of aborted ovules of manual reciprocal crosses between WT and mutant plants. Numbers on top of the bars correspond to the number of analyzed seeds. ***$P < 0.00001$ via Fisher's exact test (chi-squared). Error bars indicate the SD of the means of individual siliques analyzed.
(e) Transmission ratio distortion in reciprocal crosses between each of the *ruvbl1-1*/+ or *ruvbl2a-1*/+ and WT plants. Flowers were emasculated and fertilized manually with pollen. Numbers on top of the bars correspond to the number of analyzed plants. Error bars indicate the SD of the means of the individual analyzed siliques. WT, wild-type.

gametophyte development. The phenotypic analysis of seed abortion of self-pollinated or reciprocally crossed plants, described above, indicates the essential role of RUVBLs during the haploid gametophyte phase.

Reduced transmission of *ruvbl* mutant alleles

Our observation indicates that RUVBLs are required for the normal development of Arabidopsis gametophyte. To test whether male or female gametophytes are affected by dysfunctional RUVBL proteins, we analyzed the transmission efficiency of the *ruvbl1* and *ruvbl2a* mutant alleles through the female and the male gametophytes in the F1 progeny of the reciprocally crossed plants described above.

Assuming that RUVBLs are essential for the development of both micro- and megagametophytes, the expected number of heterozygous offspring would be 0%. Pollination of *ruvbl1-1*/+ or *ruvbl2a-1*/+ maternal plants with WT yielded 0% (0.0 ± 0.0%) or 0.3% (0.3 ± 0.6%), respectively, of heterozygous offspring. When pollen grains from either *ruvbl1-1*/+ or *ruvbl2a-1*/+ plants were used to pollinate WT mother plants, we identified 27.2% (± 2.8%) and 4.6% (± 3.9%), respectively, of heterozygous offspring (Figure 1e). This indicates that male gametophyte development is also affected by the *ruvbl1-1*/+ or *ruvbl2a-1*/+ mutations.

To investigate whether RUVBLs are also required for the development of other plant organs, we performed an extensive analysis of the heterozygous *RUVBL1* and *RUVBL2A* mutants using a semi-automated plant phenotyping system. However, the heterozygous plants for both genes did not reveal any significant differences concerning leaf morphology (shape, structure or diameter), growth dynamics, growth weight or shoot growth rate compared to WT Arabidopsis plants (Figure S3). This indicates that the *RUVBL1* and *RUBL2A* mutations used are recessive.

Our results suggest that the RUVBL1 and RUVBL2A proteins have a very important role in plant gametophyte development.

RUVBL1 and RUVBL2A are essential for ovule development

To examine the defects in female gametophyte development, we took a closer look at the development of the embryo sac in *ruvbl1-1*/+ and *ruvbl2a-1*/+ plants at stage 6 of female gametophyte development using confocal microscopy (Christensen et al., 1997). We observed a typical configuration in the WT embryo sac with one large central cell nucleus, one small egg cell nucleus, two synergid cell nuclei, and three antipodal cells. By contrast, *ruvbl1-1*/+ plants produced 63.2% (86/136) WT-like embryo sacs, 2.2% (3/136) with zero nuclei, 8.8% (12/136) with one nucleus, 14.7% (20/136) with two large nuclei, and 11.0% (15/136) with three or four nuclei. In *ruvbl2a-1*/+ plants, we found 53.3% (49/96) WT-like embryo sacs and 2.2% (2/92) with zero nuclei, 6.5% (6/92) with one nucleus, 26.1% (24/92) with two large nuclei, and 12.0% (11/92) with three or four nuclei (Figure 2). Similar numbers were obtained with differential interference contrast of cleared ovules (64.4% and 51.6% of WT-like embryo sacs) in *ruvbl1-1*/+ and *ruvbl2a-1*/+, respectively (Figure S4).

To test whether the *ruvbl* ovules with abnormal embryo sacs could still be viable to attract pollen tubes for fertilization, we pollinated *ruvbl1-1*/+ and *ruvbl2a-1*/+ pistils with WT pollen and monitored pollen tube attraction by aniline blue callose staining (Figure 3a,b) (Billey et al., 2021). Mutant ovules can be easily distinguished by callose accumulation in the embryo sac (Sun et al., 2004). In *ruvbl1-1*/+, 36.7% of the ovules failed to attract pollen tubes, and only 6% correctly received the pollen tube but failed to develop further (Figure 3c–f). In *ruvbl2a-1*/+, 47.1% of the ovules were not targeted by WT pollen tubes that failed to enter the micropyle, suggesting a more severe phenotype (Figure 3c–f).

The severe defects of the embryo sac with zero nuclei indicate either a failure to enter female meiosis or an abnormal female meiosis process that leads to megagametophyte nuclei degradation in *ruvbl1-1*/+ and *ruvbl2a-1*/+ plants. The severe defects of the embryo sacs from heterozygous plants indicate that there are also problems during mitosis. Interestingly, some of the *ruvbl* targeted ovules can still receive the WT pollen tube correctly, but then apparently fail to develop further.

RUVBL1 and RUVBL2A are required for pollen fertility

Microgametogenesis is a post-meiotic process that initially leads to the development of unicellular microspores and later tricellular mature pollen. In the mature Arabidopsis pollen grain, two sperm cells, enclosed within the vegetative cell, are assembled with the vegetative nucleus into the male germ unit.

To screen for the putative phenotypic defects, we used pollen grains and performed 4′,6-diamidino-2-phenylindole (DAPI) staining for the position and shape of vegetative and generative nuclei, as well as fluorescein diacetate (FDA) staining to distinguish intact and defective pollen grains. We restricted the phenotype screen to mature pollen because disorders, even in early developmental stages, are likely to be reflected at the mature pollen stage. We also paid special attention to structural disorders and nuclei organization (Reňák et al., 2012).

Pollen grains of *ruvbl1-1*/+ and *ruvbl2a-1*/+ plants showed standard phenotypes with no changes in the shape, size or cell wall structure compared to WT (Figure S5a; Table S1a). DAPI staining revealed that almost all mature pollen grains of WT, *ruvbl1-1*/+, and *ruvbl2a-1*/+ plants have a centrally positioned vegetative nucleus and two nearby located generative nuclei. The aberrant positioning of the nuclei and predominantly eccentric position

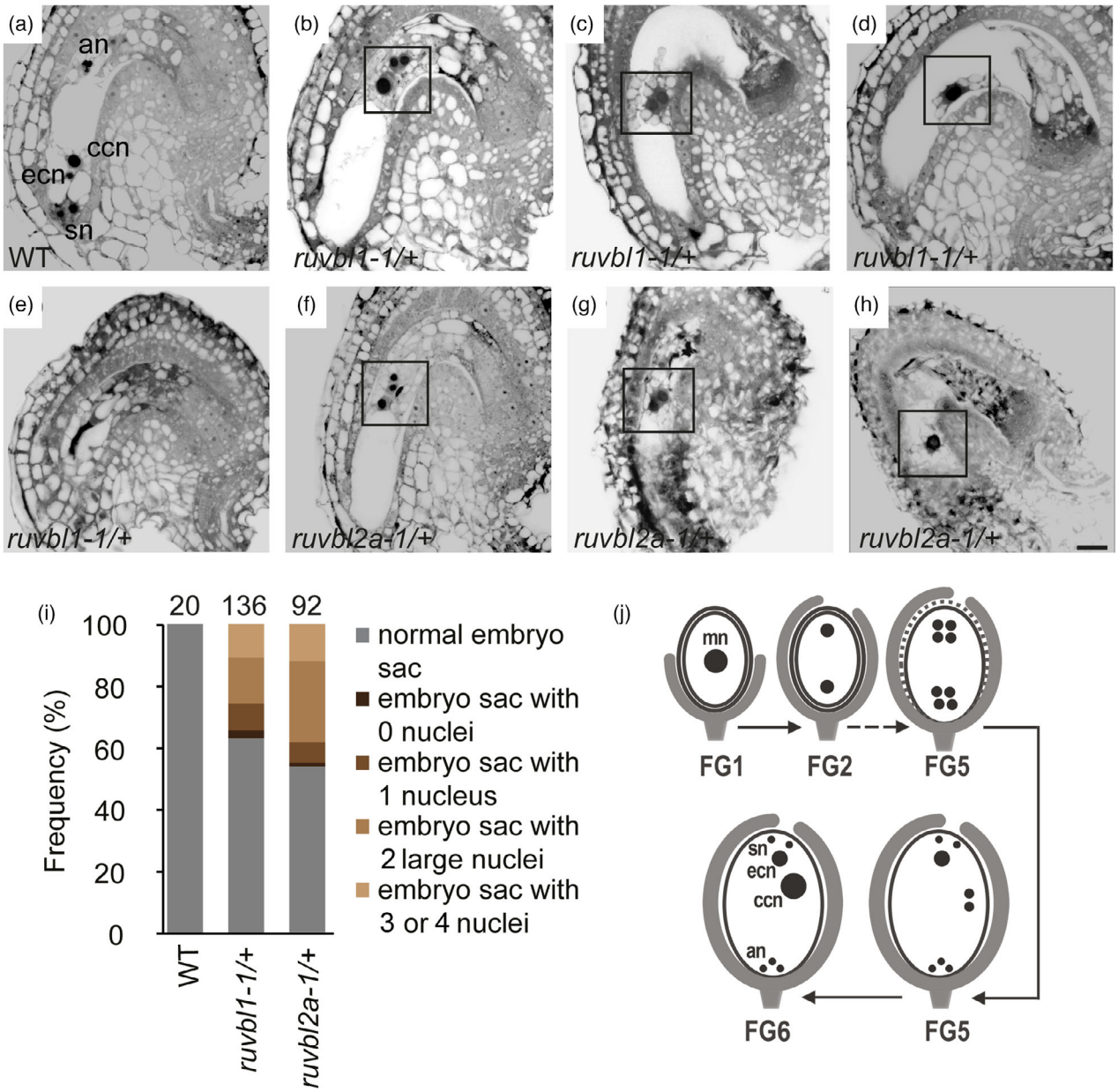

Figure 2. Confocal fluorescence micrographs of ovules from *ruvbl1-1*/+ and *ruvbl2a-1*/+ plants. Scale bar = 10 μm.
(a) Representative WT-like embryo sac with two synergid cell nuclei (sn), one egg cell nucleus (ecn), one central cell nucleus (ccn), and three antipodal cells (an).
(b–e) Examples of defective embryo sacs from *ruvbl1-1*/+ plants. Embryo sac with three nuclei (b, c). Embryo sac with one nucleus (d). Ovule with a degraded embryo sac (e). Black squares indicate aberrant ecn and ccn.
(f–h) Abnormal embryo sacs from *ruvbl2a-1*/+ plants. Embryo sac with three nuclei (f). Embryo sac with two large nuclei (g). Embryo sac with one nucleus (h). Black squares indicate aberrant ecn and ccn.
(i) Percentage of normal and abnormal ovules from analyzed genotypes. Ovules were analyzed from at least three different plants. Numbers on top of the bars correspond to the number of analyzed ovules.
(j) Schematic of female gametophyte stages (FG1–6) showing the sequence of syncytial mitotic divisions that lead to cellularization and formation of the embryo sac with fused central cell nucleus. an, antipodal cells; ccn, central cell nucleus; ecn, egg cell nucleus; mn, megaspore nucleus; sn, the synergid cell nucleus. WT, wild-type.

of individual sperm nuclei was found only in 1.9% (± 1.9%), 2.4% (± 1.5%) or 3.7% (± 1.7%) pollen grains from WT, *ruvbl1-1*/+, and *ruvbl2a-1*/+ plants, respectively. These data indicate that the position of nuclei in the mature pollen grains differs in *ruvbl2a-1*/+, but not in *ruvbl1-1*/+, compared to WT (Figure S5b; Table S1b). Analysis of intact pollen grains with FDA staining revealed significant reductions from 93.7% (± 2.8%) in WT to 56.8%

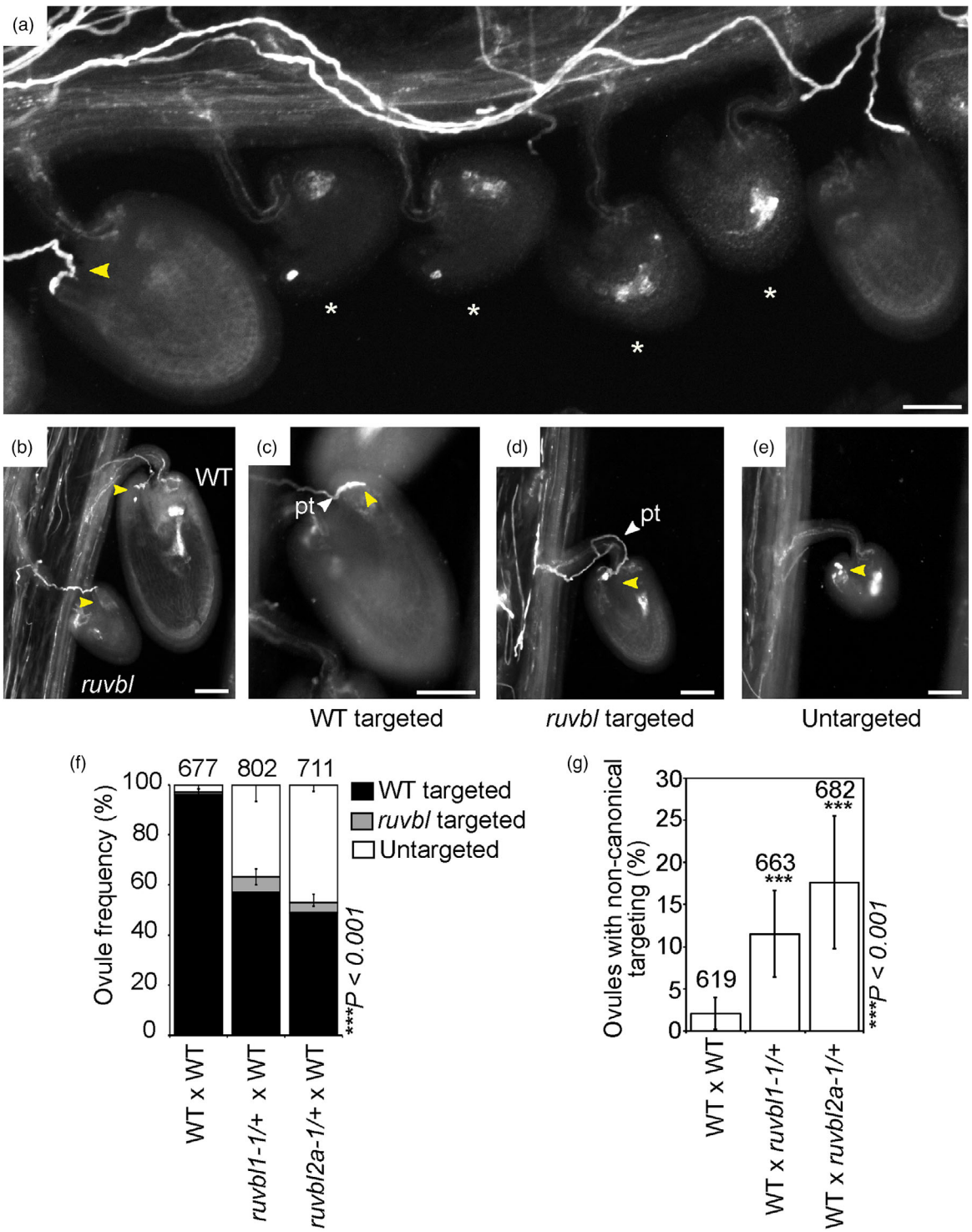

Figure 3. *ruvbl1* and *ruvbl2a* control ovule competence for pollen tube attraction.
(a) Surgically dissected pistil 24 h after pollination (hap) with wild-type pollen stained with aniline blue. Yellow arrows indicate the position of successful pollen tube entry and reception at the micropyle. Asterisks point out untargeted *ruvbl* ovules. Scale bar = 50 μm.
(b) Seed size differences of successfully targeted WT and *ruvbl* ovule 48 hap. Scale bar = 50 μm.
(c–e) Three phenotypic classes scored for panel (f). WT ovule, correct pollen tube attraction and reception (c); *ruvbl* ovule, correct pollen tube attraction and reception (d); *ruvbl* ovule, attraction (e). pt, pollen tube. Yellow arrows point to the micropyle pollen tube entry and reception site. Scale bars = 50 μm.
(f, g) Quantification of pollen tube ovule-targeting competence. Numbers on top of the bars correspond to the number of analyzed ovules. ***$P < 0.001$. Two-sided Student's *t*-test was used to calculate *P* values between the groups.

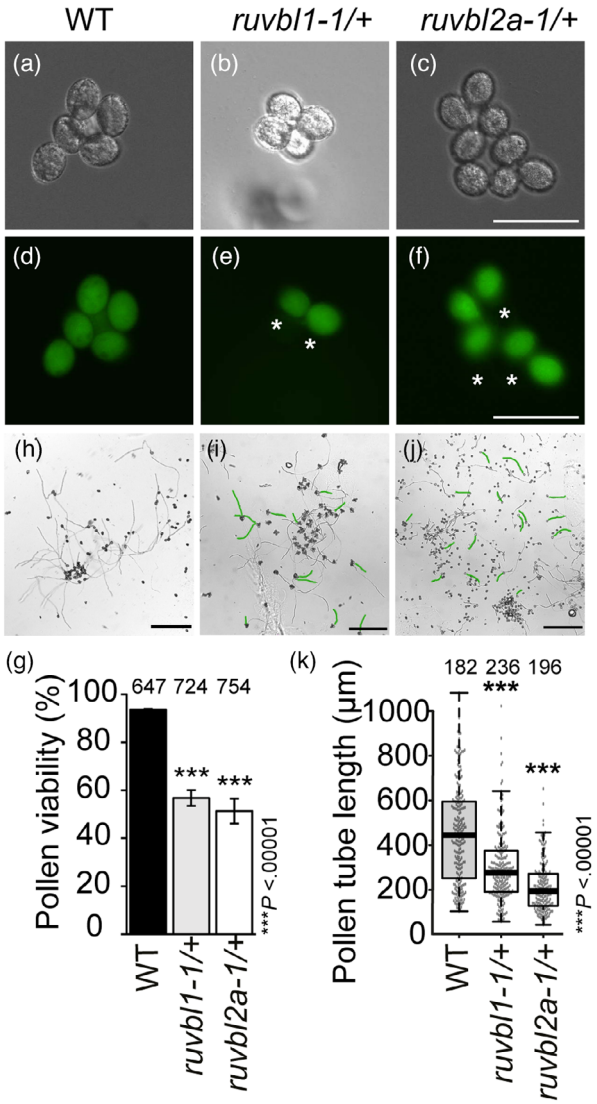

Figure 4. *ruvbl1-1*/+ and *ruvbl2a-1*/+ plants produce defective pollen grains.
(a–f) Fluorescein diacetate (FDA) epifluorescence micrographs of stained pollen grains. Asterisks mark defective pollen grains. Scale bars = 50 μm. The pollen in *ruvbl1-1*/+ remains attached to a tetrad due to homozygous *qrt1* mutation.
(g) The proportion of live pollen grains determined by FDA staining. Mean values from three independent experiments with three different plants are plotted. Statistical significance was calculated using Fisher's exact test. ***$P < 0.00001$.
(h–j) *In vitro* WT, *ruvbl1-1*/+, and *ruvbl2a-1*/+ pollen tube growth. Green lines indicate representative short pollen tubes in *ruvbl* mutants.
(k) Box-and-whisker plot showing the pollen tube length distribution of the WT, *ruvbl1-1*/+, and *ruvbl2a-1*/+. Middle bars are median values; boxes indicate the first to third interquartile ranges, whiskers indicate 1.5 of minimum and maximum interquartile, and dots outside interquartile boxes indicate outlier values. Numbers on top of the bars correspond to the total number of measured pollen tubes. WT, wild-type.

(± 12.4%) in *ruvbl1-1*/+ and 51.3% (± 10.2%) in *ruvbl2a-1*/+ (Figure 4a–g; Table S1c).

Our observations suggest that the paternally induced abortion ratio is partially caused by decreased viability of pollen grains in *ruvbl1*/+ and *ruvbl2a*/+ plants, but is accompaniedby only minor changes in mature pollen phenotypes relating to nucleus positioning in *ruvbl2a*/+ plants.

RUVBL1 and RUVBL2A are involved in pollen tube growth

To investigate whether *ruvbl* pollen can germinate and grow pollen tubes, we analyzed pollen tube growth *in vitro* for both heterozygous *ruvbl1-1*/+ and *ruvbl2a-1*/+ lines. *In vitro* germination assays showed a reduced germination rate of 54.1% in *ruvbl2a-1*/+ (n = 196) and 61.8% in *ruvbl1-1*/+ (n = 236), whereas the germination rate of WT was 75.8% (n = 182) (Table S2). Germinated pollen tubes from *ruvbl1-1*/+ and *ruvbl2a-1*/+ plants grew significantly shorter (447.4 μm in WT to 302.6 μm in *ruvbl1-1*/+ and 215.3 μm in *ruvbl2a-1*/+) relative to WT, suggesting an additional defect in pollen tube growth (Figure 4h–k).

We took advantage of the fact that the *ruvbl1-1*/+ SAIL T-DNA insertion line contains an *uidA* gene encoding *β-glucuronidase* under the control of pollen-specific LAT52 promoter (*proLAT52::GUS*) (Sessions et al., 2002). Histochemical GUS activity staining of tissues from *ruvbl1-1*/+ allowed us to specifically follow *ruvbl1* mutant pollen tube growth within the pistil. This staining revealed very limited and shorter *ruvbl1-1* pollen tube growth in the pistil, consistent with our *in vitro* observation (Figure S6a).

Because *ruvbl1-1*/+ and *ruvbl2a-1*/+ germinate poorly and grow significantly shorter pollen tubes, we considered whether pollen tubes from *ruvbl1-1*/+ and *ruvbl2a-1*/+ plants are sufficiently competent to target WT ovules for fertilization. To assess their competence, we pollinated WT pistils with *ruvbl1-1*/+ and *ruvbl2a-1*/+ pollen, followed by pollen tube callose staining with aniline blue (Billey et al., 2021). Twenty-four hours after pollination (24 hap), aniline blue staining revealed that both *ruvbl1-1* and *ruvbl2a-1* pollen tubes are partially capable of targeting WT ovules. In WT plants pollinated with *ruvbl1-1*/+ and *ruvbl2a*/+ pollen, we observed 11.5% (n = 663) and 17.6% (n = 682) of non-canonically targeted ovules, respectively. However, only 2% (n = 619) of aberrant, non-canonically targeted ovules were observed in control WT plants pollinated with WT pollen (Figure 3g; Figure S7). Additionally, we used the *proLAT52::GUS* marker of *ruvbl1-1* SAIL T-DNA line to observe *ruvbl1* mutant pollen targeting the WT ovules using the blue-dot GUS assay. We pollinated emasculated WT pistils with *ruvbl1-1*/+ pollen grains. As a control, we pollinated WT pistil with *proLAT52::GUS*/+ pollen. Blue-dot assays revealed that 11.67% (n = 411) of the WT ovules were targeted by *ruvbl1* pollen tubes, whereas 47.68% (n = 409) of the WT ovules were targeted by control *proLAT52::GUS* pollen tubes (Figure S6b,c).

Overall, our results show that *ruvbl1-1*/+ and *ruvbl2a-1*/+ lines have a reduced germination rate and defects in pollen tube growth. In addition, we observed that pollen

tubes from *ruvbl1-1*/+ and *ruvbl2a-1*/+ plants are partially capable of targeting WT ovules.

Tissue-specific expression of the RUVBL genes in Arabidopsis

To obtain further insight into the *RUVBL* expression pattern, we generated stable reporter lines where *RUVBL1* and *RUVBL2A* promoters were fused to the GUS. In 7-day-old seedlings, high activity of the *RUVBL2A* promoter was detected in the root apical meristems and at the positions of forming lateral roots (Figure S8). The activity of the *RUVBL1* promoter was found only in lateral root primordia. The activity of both promoters was not detected in other seedling tissues or in some other plant tissues (e.g. true leaves, stems, sepals, petals). Consistent with gametophytic lethality, we observed *RUVBL1* and *RUVBL2A* promoter activity in inflorescences in different stages of flower development (Alvarez-Buylla et al., 2010) (Figure 5a, f), which prompted us to analyze individual tissues. Activity of the *RUVBL1* and *RUVBL2A* promoters was observed in pollen as well as in the adjacent tapetum layer (Figure 5b–d,g–i). Furthermore, we detected *RUVBL2A* promoter activity in developing ovules and strong promoter activity of both *RUVBL1* and *RUVBL2A* genes in fertilized ovules, but not in ovule integuments (Figure 5e,j).

To consider the broader context of developmental processes and conditions in which RUVBL proteins might play a role, we compared our observations with global transcriptome data from various developmental stages and tissues from Arabidopsis (Julca et al., 2021) (Figure S9). These data supported our observation that *RUVBL1* and *RUVBL2A* genes are transcribed during pollen development in ovules and meristems. Taken together, the data relating to the expression of *RUVBL1* and *RUVBL2A* are consistent with the genetically determined role of RUVBL proteins during gametophyte development.

DISCUSSION

RUVBL proteins are highly conserved ATPases from the AAA+ superfamily (Neuwald et al., 1999). They are related to bacterial RUVB helicase, which participates in Holliday junction resolution (Putnam et al., 2001). Despite their importance in transcriptional regulation, chromatin remodeling, DNA damage signaling and repair, and their extensive characterization in animals and yeasts (Dauden et al., 2021), only limited information is available regarding their functions in plants.

The human genome encodes two homologs of RUVB proteins, RUVBL1 (Pontin) and RUVBL2 (Reptin), whereas the Arabidopsis genome contains three *RUVBL* genes. Arabidopsis RUVBL1 protein has a high sequence similarity (88%) to human RUVBL1/Pontin (Figure S10). Two RUVBL2 proteins in Arabidopsis, namely RUVBL2A and RUVBL2B, show high mutual sequence similarity (91%), suggesting that they are paralogs, and also a high similarity with human RUVBL2 (87 and 82%, respectively) (Figure S11). Although the overall sequence similarity between Arabidopsis RUVBL1 and RUVBL2A or RUVBL2B proteins is lower (63 or 60%, respectively), all three proteins share conserved Domains (DI, DII, and DIII) with several highly conserved motifs. Domain II (DII) is an insertion unique to RUVBL compared to other AAA+ family members (Silva-Martin et al., 2016). Walker A/B motifs are proposed to coordinate ATP binding and hydrolysis, sensor I/II motifs sense whether the protein is bound to di- or triphosphates, and the Arg finger allows the efficient hydrolysis of ATP (Matias et al., 2006) (Figure S12).

Phylogenetic studies showed that the *RUVBL1* gene diverged from an archaeal *RUVBL2* ancestor when eukaryotes evolved from archaea (Kurokawa et al., 1999; Schořová et al., 2019). This corresponds to our observation that plant RUVBL proteins are not functionally redundant because loss-of-function mutations in either *RUVBL1* or *RUVBL2A* lead to gametophyte lethality. Moreover, *RUVBL2B* is considered a pseudogene because *RUVBL2B* is not expressed and no phenotypes in a line carrying a T-DNA insertion in the *RUVBL2B* coding sequence were observed (Brunkard et al., 2020).

The present study aimed to investigate the involvement of RUVBL proteins in plant sporophyte and male/female gametophyte development. Our extensive semi-automated phenotyping analysis did not reveal any significant differences in *ruvbl1-1*/+ and *ruvbl2a-1*/+ T-DNA insertion mutant plants during the development of sporophytes (seedlings, roots, stem, leaves). However, future experiments with weak alleles of *ruvbl1* and *ruvbl2a* are needed to better understand the function of RUVBL1 and RUVBL2A in the sporophyte development of Arabidopsis.

Mammalian RUVBLs interact with many molecular complexes with vastly different downstream effectors, which is also true for their plant homologs. It was observed that Arabidopsis RUVBL proteins associate with the TERT subunit of telomerase via interaction with TELOMERE REPEAT BINDING (TRB) proteins that colocalize with

Figure 5. Detection of *RUVBL1* and *RUVBL2A* promoter activity by GUS histochemical staining.
(a, f) Inflorescence. Scale bars = 2 mm.
(b, g) Pollen grains from flower stage (from left) 9, 10/11, 12, 15/16. Scale bars = 10 μm.
(c, h) Anthers isolated from flower stages 10 (left) and 16 (right).
(d, i) Flowers at different stages of development; flower stages (from left) 8/9, 9, 10/11, 12, 14, 15/16. Scale bars = 500 μm.
(e, j) An unfertilized ovule from flower stages 9, 10/11, 11/12, 12, and 12. A fertilized ovule from floral stage 15 (bottom right corner). Scale bars = 50 μm.

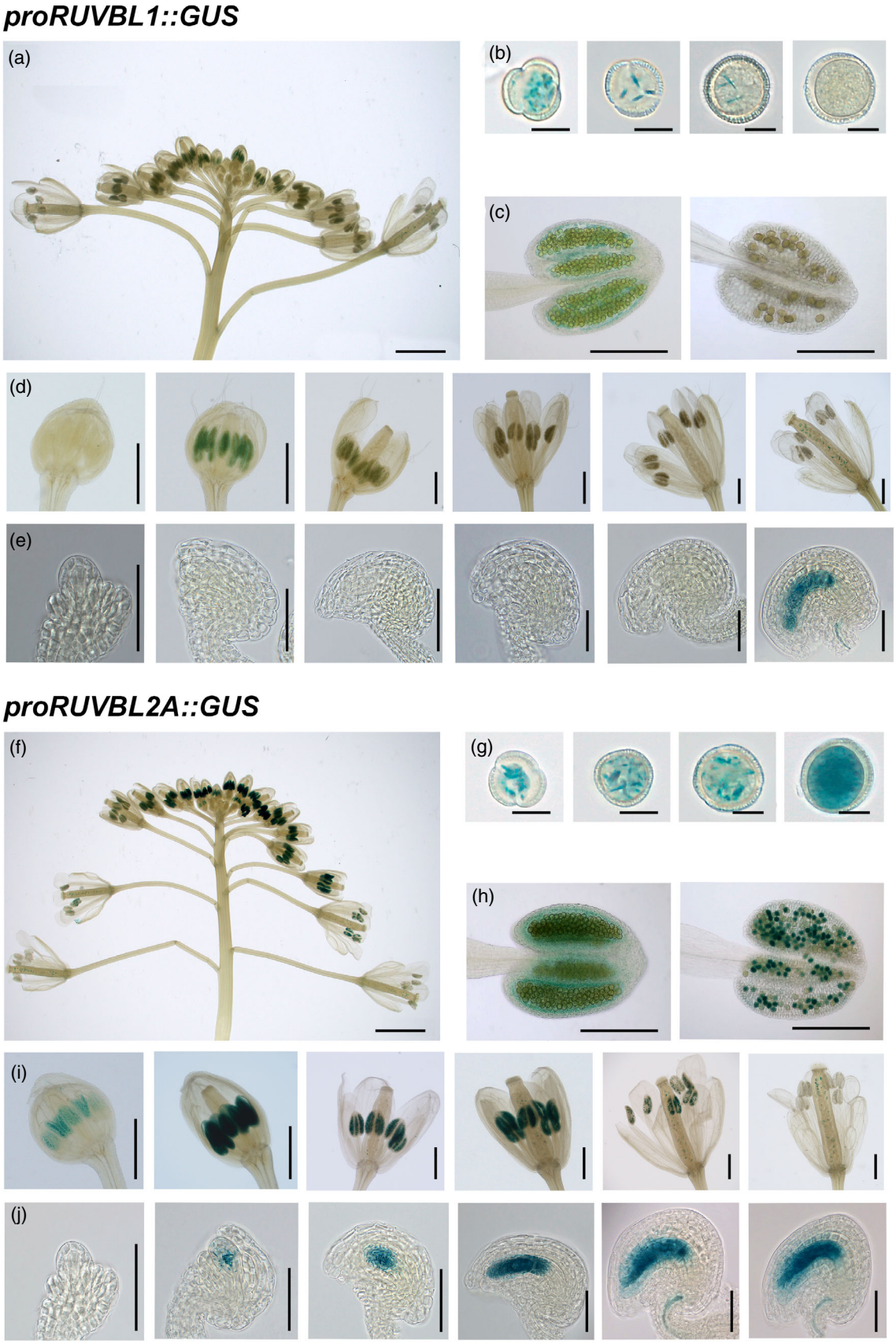

telomeric sequences *in situ* and *in vivo* (Dvořáčková et al., 2010; Mozgová et al., 2008; Schrumpfová et al., 2004; Schrumpfová et al., 2016). Telomere- and telomerase-related functions of RUVBL proteins (Schrumpfová & Fajkus, 2020) correspond well to the RUVBL expression pattern observed in the present study (Figure 4). RUVBL proteins interact with ACTIN-RELATED PROTEIN 4 (ARP4). ARP4, in addition to being a component of the SWR1 chromatin remodeling complex (Bieluszewski et al., 2015), also interacts directly with TERT (Fulnečková et al., 2021), thus representing another link between RUVBL and telomerase, in addition to that of RUVBL-TRB-TERT (Schořová et al., 2019). RUVBL1 was reported to be a regulator of disease resistance (R) genes (Holt et al., 2002). Arabidopsis RUVBL1 and RUVBL2A were also reported as members of the plant TOR signaling network, similar to that of yeast or mammals (Brunkard et al., 2020; Van Leene et al., 2019). However, further studies are needed to understand the full complexity of the involvement of RUVBL proteins in various signaling pathways.

We analyzed the transcription of *RUVBL1* and *RUVBL2A* using promoter-reporter lines and found high expression of both genes in both male and female reproductive structures and meristem tissues. We did not observe transcription in the root differentiation zone in seedlings, nor in cotyledons, true leaves, stems, sepals or petals. We detected *RUVBL1* and *RUVBL2A* promoter activity in fertilized ovules and for *RUVBL2A* also strong activity in developing ovulesbut not in ovule integuments. In male gametophytes, we observed that *RUVBL* promoters are active not just in pollen grains, but also in the adjacent tapetum. These observations are not surprising because tapetum cells form the innermost of the four anther somatic layers, surrounding the developing reproductive cells to provide materials for early pollen development, after which they undergo programmed cell death (Ischebeck, 2016). These data agree very well with the available transcriptomic data (Julca et al., 2021; Susaki et al., 2021). Recent analyses of female gametophyte cells using markers of cell fate to distinguish different cell types showed increased expression of both *RUVBL* genes in central and egg cells, but not in synergids (Susaki et al., 2021), which further supports our observations. The involvement of RUVBL proteins in the regulation of early developmental processes is consistent with high transcription of *RUVBL1* and *RUVBL2A*, but not *RUVBL2B*, detected in eggs, ovules, endosperm, pollen (Julca et al., 2021) and the tapeta (Figure 5; Figure S9).

The loss-of-function mutants of *ruvbl1-1* or *ruvbl2a-1* strongly impacted female gametogenesis producing an aberrant embryo sac. Similarly, male gametogenesis was compromised by reduced pollen germination and pollen tube guidance. Our results imply that the failure to transmit the *ruvbl* mutant allele through the female is most likely attributable to the presence of an aberrant embryo sac in *ruvbl1-1* and *ruvbl2a-1* ovules. This is further aggravated by the lack of *ruvbl* ovule competence to attract pollen tubes for fertilization, resulting in collapsed ovules in *ruvbl1-1*/+ and *ruvbl2a-1*/+ siliques. The genetic data correspond with the GUS signals in the reproductive tissues of the mutants, showing that the major problem arises from embryo sac development and microspores. These are the exact same tissues where we detected transcriptional activities of RUVBL1 and RUVBL2A using promoter GUS reporter lines (Figure 5).

In summary, the RUVBL1/2 complex has been implicated in many cellular and physiological processes, ranging from DNA repair, chromatin remodeling, small nucleolar ribonucleoprotein, telomerase assembly, TOR complex assembly, cell cycle, transcription regulation and others (Dauden et al., 2021; Mao & Houry, 2017). Here, we have uncovered a function of RUVBL proteins in gametophyte development in plants, and we have described the crucial dominant role of RUVBL proteins in megagametogenesis, as well as in microgametogenesis.

EXPERIMENTAL PROCEDURES

Plant material

Arabidopsis thaliana (L.) Heynh. ecotype Columbia (Col-0) was used as WT control. Previously described T-DNA insertion lines used in the present study were: *ruvbl1-1* (SAIL_397_C11), *ruvbl1-6* (SALK_133101), *ruvbl2a-1* (GK-543F01), and *ruvbl2a-2* (SALK_071103) in the Col-0 background were used. For genotyping of T-DNA mutants, genomic DNA was isolated from small leaves according to Edwards et al. (1991) and used for PCR analysis using DreamTaq polymerase (Thermo Fisher Scientific, Waltham, MA, USA) with primers listed in Schořová et al. (2019). The conditions used were in accordance with the manufacturer's instructions. For promoter-reporter constructs, regions 1000 bp upstream of the *RUVBL1* or *RUVBL2A* transcription start sites were PCR-amplified, cloned into *pDONR207*, and recombined into the binary Gateway vector *pKGWFS7.0* containing the *uidA* gene encoding GUS. The final plasmids were transformed into *Agrobacterium tumefaciens* strain GV3101 and then into Arabidopsis Col-0 using the floral dip method (Clough & Bent, 1998). T1 generation seeds were screened on 1/2 MS plates containing 50 μg ml^{-1} kanamycin (Duchefa, Haarlem, The Netherlands) and resistant plants were transferred to soil. T2 populations with approximately 75% resistant seedlings, indicating single locus T-DNA insertions, were considered for further analyses. Primers used for cloning are listed in Table S3.

Semi-automated phenotyping

Plants were grown in soil under a 12:12 h light/dark photocycle, with a light intensity of 120 μmol m^{-2} sec^{-1} white light and 4.5 μmol m^{-2} sec^{-1} far-red light at 21°C and 60% relative humidity. Twenty plants per line were used for phenotyping. Data acquisition and image analysis were performed using Photon Systems Instruments, spol. s r.o. (Drásov, Czech Republic). The relative leaf growth rate, roundness, compactness or growth weight were measured every third day.

Plant growth conditions

Plants were grown in soil for 16 h, with a light intensity of approximately 200 μmol m^{-2} sec^{-1} and 21°C during the day, and for 8 h at 19°C during the night, and 70% relative humidity. For seedling growth, seeds were surface-sterilized for 5 min in 70% ethanol and 5 min in 10% sodium hypochlorite, followed by three washes with sterile water. Sterilized seeds were kept in the dark at 4°C for 2 days for stratification and germinated on vertical plates with 1/2 MS medium (Duchefa) containing 0.05% MES, 0.8% agar at 22°C under a 16:8 h light/dark photocycle.

Genetic transmission through male and female gametes

To determine the gametophytic transmission of T-DNA, reciprocal test crosses were performed between the WT and each heterozygous mutant. Plants were emasculated approximately 48 h before pollination in crossing experiments. Harvested seeds from individual siliques were sown on 1/2 MS containing plates containing 50 μg ml^{-1} Phosphinothricin for *ruvbl1-1*/+ and 75 μg ml^{-1} sulfadiazine for *ruvbl2a-1*/+, DNA was extracted by the standard Edwards protocol (Edwards et al., 1991), and plants were genotyped as described in the section above on 'Plant material'.

GUS histochemical staining

GUS staining was performed as described in Nowicka et al. (2020) and Vladejić et al. (2023) with minor modifications. Briefly, 7-day-old seedlings of *proRUVBL1::GUS* and *proRUVBL2A::GUS* were stained in GUS staining buffer [0.1 M sodium phosphate buffer (pH 7.0), 0.05% Triton X-100, 0.1% X-Glc sodium salt (Duchefa)] containing 1 mM $K_3[Fe(CN)_6]$ and 1 mM $K_4[Fe(CN)_6]$ for 7 h, at 37°C. The inflorescences from 40-day-old plants were stained in GUS staining buffer containing 2 mM $K_3[Fe(CN)_6]$ and 2 mM $K_4[Fe(CN)_6]$ for 48 or 72 h for pollen or ovules stained in inflorescence, respectively, at 37°C. Subsequently, the samples were incubated overnight in 80% ethanol (v/v) at room temperature shaking at 50 rpm, as described previously (Malamy & Benfey, 1997). Ovules and pollen grains were extracted from inflorescences before microscopic analysis, which was performed using an AxioZoom.V16-Apotome2 microscope or AxioImager.Z2-ZEN in a bright field (Carl Zeiss GmbH, Jena, Germany).

Blue dot GUS assay

Young buds of WT-plants before anther dehiscence were emasculated and left to mature for 24 h until the stigma papillae fully developed. Pistils were then pollinated with *ruvbl1-1*/+ pollen or control WT pollen grains as described by Khouider et al. (2021) expressing the *proLAT52::GUS*. Pistils were collected at 24 hap. Fertilized pistils were dissected under a binocular dissection microscope (Leica Microsystems, Wetzlar, Germany) and strips of ovules attached to the septum were transferred to GUS staining solution [0.2 M Na_2HPO_4, 0.2 M NaH_2PO_4, 10 mM EDTA, 0.1% Triton X-100, 1 mM $K_3Fe(CN)_6$, 2 mM X-Gluc]. Samples were stained for 24 h. Stained tissues were cleared of chlorophyll by bleaching in an ethanol series of 90, 70, 50, and 30% (v/v) before imaging. Stained pistils were imaged with a stereomicroscope SteREO Discovery V8 (Carl Zeiss GmbH) equipped with an AxioCam HRc camera and Zeiss Axioimager Apotome2 using ZEN software.

Aniline blue callose staining

Aniline blue pollen tube stain was performed as described by Billey et al. (2021) and Liu and Meinke (1998).

FDA staining

FDA staining was performed as described by Li (2011) with modifications (Yang, Fernández Jiménez, Majka, et al., 2021; Yang, Fernández-Jiménez, Tučková, et al., 2021). Fluorescence was observed after 20 min of staining using an inverted microscope (IX 83; Olympus, Tokyo, Japan) at 543/620 nm excitation/emission wavelengths and the same region was photographed with differential interference contrast optics to determine the quantities of pollen grains.

DAPI staining buffer

For phenotype analysis, three fully open flowers in developmental stage 14 (Smyth et al., 1990) were collected. Fifty microlitres of DAPI was added to each sample as previously described in Reňák et al. (2012) and shaken briefly to release pollen grains from anthers. Pollen was observed using an inverted microscope Zeiss Axio Imager.Z1 in bright field and UV epifluorescence. The percentage of phenotypic defects was calculated from observations of at least 200 pollen grains in each sample.

Ovule clearing

Clearing of ovules was performed as described by Liu and Meinke (1998).

Confocal microscopy of ovules

The confocal observation of ovules was performed according to the method described by Christensen et al. (1997) with the modifications. Flowers at stage 13 were emasculated approximately 48 h before the ovules were examined. Sepals, petals, and stigmas were removed from the isolated flowers. Then, the remaining pistils were exposed in fixation buffer [4% glutaraldehyde and 12.5 mM cacodylate (pH 6.9)] for 2 h at room temperature. The initial 15 min of fixation was performed under in-house vacuum. Following fixation, the tissue was dehydrated using a graded ethanol series (20, 40, 60, 80, and 96% for 20 min each). Following dehydration, the tissue was cleared in a 2:1 mixture of benzyl benzoate:benzyl alcohol. Ovules were mounted in immersion oil under coverslips (25 × 4024 × 40 mm). The autofluorescence of ovules was observed using a confocal microscope (TCS SP8; Leica Microsystems) and HC PL PAO CS2 63×/1.4 OIL objective equipped with LAS-X software (Leica Microsystems) with 488 nm laser lines for excitation and 550 nm emission filters.

In vitro pollen tube growth

In vitro pollen tube growth was performed according to the protocol of Boavida and McCormick (2007). Approximately 300 μl of freshly prepared pollen tube growth medium [0.01% boric acid, 5 mM $CaCl_2$, 5 mM KCl, 1 mM $MgSO_4$, 10% sucrose, pH 7.5 (KOH), 1.5% Phytagel (Sigma-Aldrich, St Louis, MO, USA)] was directly poured onto a microscope slide to create a pollen tube germination pad. Mature pollen was deposited on the solid medium and slides incubated for 4 h in a humid chamber at 22°C in the dark. Pollen tube lengths were measured after 4 h of *in vitro* growth using the ZEN BLUE software (Carl Zeiss GmbH).

Multiple sequence alignment

Multiple sequence alignment was performed using CLUSTAL OMEGA (Madeira et al., 2019). This alignment was then edited using JALVIEW 2 (Waterhouse et al., 2009). Regions with conserved physicochemical properties (Conservation) were colored using JALVIEW 2 according

to the CLUSTAL X color scheme (Jeanmougin et al., 1998; Livingstone & Barton, 1993). Consensus prediction of the secondary structure (JNetPRED) of the first sequence in each alignment was performed using two independent prediction algorithms: the hidden Markov model and position-specific scoring matrices using JPRED (Drozdetskiy et al., 2015). The confidence of secondary structure prediction was estimated using JPRED (JNetCONF) (Cole et al., 2008).

ACCESSION NUMBERS

RUVBL1 (AT5G22330); *RUVBL2A* (AT5G67630); *RUVBL2B* (AT3G49830).

ACKNOWLEDGEMENTS

This work was supported by the Czech Science Foundation projects 21-15841S (PPS and MK), 20-01331X (AK and JF), 22-00871S (EDT, FY, and AP), and 22-29717S (SH). AP and FY also received funding from the Czech Academy of Sciences (Purkyně fellowship and PPPLZ, respectively). We acknowledge the core facility CELLIM supported by MEYS CR (LM2018129 Czech-BioImaging). The Plant Sciences Core Facility of CEITEC Masaryk University is acknowledged for its technical support. We acknowledge Leon Jenner for editing and proofreading the manuscript submitted for publication.

AUTHOR CONTRIBUTIONS

PPS and EDT designed the study, supervised the project and wrote the manuscript with support from AP, JF, and DH. EDT, FY, KM, SH, ŠS, AK, MP, and TP conducted experiments and analyzed data. BK analyzed the transcriptomic data.

CONFLICT OF INTEREST

The authors declare no conflict of interest.

SUPPORTING INFORMATION

Additional Supporting Information may be found in the online version of this article.

Table S1. Percentage of aberrant pollen grains determined in bright field (BF), 4′,6-diamidino-2-phenylindole (DAPI) and fluorescein diacetate (FDA) staining and pollen grain germination.

Table S2. Quantification of pollen tube germination determined by an *in vitro* test.

Table S3. List of the primers used in the present study.

Figure S1. Schematic illustration of T-DNA insertions within the *RUVBL1* and *RUVBL2A* genes.

Figure S2. Analysis of seed setting in the identified *RUVBL1* and *RUVBL2A* T-DNA insertional mutants and transmission ratio distortion in reciprocal crosses.

Figure S3. Phenotypic analysis of plants heterozygous for RUVBL1 and RUVBL2A mutations.

Figure S4. Differential interference contrast micrographs of cleared ovules from *ruvbl1-1*/+ and *ruvbl2a-1*/+ plants.

Figure S5. Phenotypic analysis of mature pollen grains.

Figure S6. *ruvbl1-1* pollen tubes lack the competence to target ovules for fertilization.

Figure S7. Phenotypic classes observed after pollination of WT ovules with mutant pollen.

Figure S8. Detection of *RUVBL1* and *RUVBL2A* promoter activity in seedlings by GUS histochemical staining.

Figure S9. Graphical summary of *RUVBL* mutations on plant viability.

Figure S10. Multiple sequence alignment of RUVBL1 from human and *A. thaliana*.

Figure S11. Multiple sequence alignment of RUVBL2 from human and *A. thaliana*.

Figure S12. Multiple sequence alignment of RUVBLs from *A. thaliana*.

OPEN RESEARCH BADGES

This article has earned Open Data and Open Materials badges. Data and materials are available.

REFERENCES

Alvarez-Buylla, E.R., Benítez, M., Corvera-Poiré, A., Chaos Cador, Á., de Folter, S., Gamboa de Buen, A. *et al.* (2010) Flower development. *The Arabidopsis Book*, **8**, e0127.

Bieluszewski, T., Galganski, L., Sura, W., Bieluszewska, A., Abram, M., Ludwikow, A. *et al.* (2015) AtEAF1 is a potential platform protein for Arabidopsis NuA4 acetyltransferase complex. *BMC Plant Biology*, **15**, 1–15.

Billey, E., Hafidh, S., Cruz-Gallardo, I., Litholdo, C.G., Jr., Jean, V., Carpentier, M.C. *et al.* (2021) LARP6C orchestrates posttranscriptional reprogramming of gene expression during hydration to promote pollen tube guidance. *Plant Cell*, **33**, 2637–2661.

Boavida, L.C. & McCormick, S. (2007) Temperature as a determinant factor for increased and reproducible in vitro pollen germination in *Arabidopsis thaliana*. *The Plant Journal*, **52**, 570–582.

Brunkard, J.O., Xu, M., Regina Scarpin, M., Chatterjee, S., Shemyakina, E.A., Goodman, H.M. *et al.* (2020) TOR dynamically regulates plant cell–cell transport. *Proceedings of the National Academy of Sciences of the United States of America*, **117**, 5049–5058.

Christensen, C.A., King, E.J., Jordan, J.R. & Drews, G.N. (1997) Megagametogenesis in Arabidopsis wild type and the gf mutant. *Sexual Plant Reproduction*, **10**, 49–64.

Clough, S.J. & Bent, a.F. (1998) Floral dip: a simplified method for agrobacterium-mediated transformation of *Arabidopsis thaliana*. *The Plant Journal*, **16**, 735–743.

Cloutier, P., Poitras, C., Durand, M., Hekmat, O., Fiola-Masson, É., Bouchard, A. *et al.* (2017) R2TP/Prefoldin-like component RUVBL1/RUVBL2 directly interacts with ZNHIT2 to regulate assembly of U5 small nuclear ribonucleoprotein. *Nature Communications*, **8**, 1–14.

Cole, C., Barber, J.D. & Barton, G.J. (2008) The Jpred 3 secondary structure prediction server. *Nucleic Acids Research*, **36**, 197–201.

Dauden, M.I., López-Perrote, A. & Llorca, O. (2021) RUVBL1–RUVBL2 AAA-ATPase: a versatile scaffold for multiple complexes and functions. *Current Opinion in Structural Biology*, **67**, 78–85.

Drews, G.N. & Koltunow, A.M.G. (2011) The female gametophyte. *The Arabidopsis Book*, **2011**, e0155.

Drews, G.N. & Yadegari, R. (2002) Development and function of the angiosperm female gametophyte. *Annual Review of Genetics*, **36**, 99–124.

Drozdetskiy, A., Cole, C., Procter, J. & Barton, G.J. (2015) JPred4: a protein secondary structure prediction server. *Nucleic Acids Research*, **43**, 389–394.

Dvořáčková, M., Rossignol, P., Shaw, P.J., Koroleva, O.A., Doonan, J.H. & Fajkus, J. (2010) AtTRB1, a telomeric DNA-binding protein from Arabidopsis, is concentrated in the nucleolus and shows highly dynamic association with chromatin. *The Plant Journal*, **61**, 637–649.

Edwards, K., Johnstone, C. & Thompson, C. (1991) A simple and rapid method for the preparation of plant genomic DNA for PCR analysis. *Nucleic Acids Research*, **19**, 1349.

Fulnečková, J., Dokládal, L., Kolářová, K., Nešpor Dadejová, M., Procházková, K., Gomelská, S. *et al.* (2021) Telomerase interaction partners-insight from plants. *International Journal of Molecular Sciences*, **23**, 368.

Hafidh, S. & Honys, D. (2021) Reproduction multitasking: the male gametophyte. *Annual Review of Plant Biology*, **72**, 581–614.

Holt, B.F., Boyes, D.C., Ellerström, M., Siefers, N., Wiig, A., Kauffman, S. *et al.* (2002) An evolutionarily conserved mediator of plant disease resistance gene function is required for normal Arabidopsis development. *Developmental Cell*, **2**, 807–817.

Ischebeck, T. (2016) Lipids in pollen — they are different. *Biochimica et Biophysica Acta (BBA) - Molecular and Cell Biology of Lipids*, **1861**, 1315–1328.

Jeanmougin, F., Thompson, J.D., Gouy, M., Higgins, D.G. & Gibson, T.J. (1998) Multiple sequence alignment with Clustal X. *Trends in Biochemical Sciences*, **23**, 403–405.

Jin, J., Cai, Y., Yao, T., Gottschalk, A.J., Florens, L., Swanson, S.K. *et al.* (2005) A mammalian chromatin remodeling complex with similarities to the yeast INO80 complex. *The Journal of Biological Chemistry*, **280**, 41207–41212.

Julca, I., Ferrari, C., Flores-Tornero, M., Proost, S., Lindner, A.C., Hackenberg, D. *et al.* (2021) Comparative transcriptomic analysis reveals conserved programmes underpinning organogenesis and reproduction in land plants. *Nature Plants*, **7**, 1143–1159.

Kawashima, T. & Berger, F. (2014) Epigenetic reprogramming in plant sexual reproduction. *Nature Reviews. Genetics*, **15**, 613–624.

Khouider, S., Borges, F., LeBlanc, C., Ungru, A., Schnittger, A., Martienssen, R. *et al.* (2021) Male fertility in Arabidopsis requires active DNA demethylation of genes that control pollen tube function. *Nature Communications*, **12**, 410.

Kim, S.G., Hoffman, G.R., Poulogiannis, G., Buel, G.R., Jang, Y.J., Lee, K.W. *et al.* (2013) Metabolic stress controls mTORC1 lysosomal localization and dimerization by regulating the TTT-RUVBL1/2 complex. *Molecular Cell*, **49**, 172–185.

Kurokawa, Y., Kanemaki, M., Making, Y. & Tamura, T.A. (1999) A notable example of an evolutionary conserved gene: studies on a putative DNA helicase TIP49. *DNA Sequence*, **10**, 37–42.

Li, X. (2011) Pollen fertility/viability assay using FDA staining. *Bio-Protocol*, **101**, e75. https://doi.org/10.21769/BioProtoc.75

Liu, C.M. & Meinke, D.W. (1998) The titan mutants of Arabidopsis are disrupted in mitosis and cell cycle control during seed development. *The Plant Journal*, **16**, 21–31.

Livingstone, C.D. & Barton, G.J. (1993) Protein sequence alignments: a strategy for the hierarchical analysis of residue conservation. *Computer Applications in the Biosciences*, **9**, 745–756.

Luo, Y.-X., Hou, X.-M., Zhang, C.-J. *et al.* (2020) A plant-specific SWR1 chromatin-remodeling complex couples histone H2A.Z deposition with nucleosome sliding. *The EMBO Journal*, **39**, e102008.

Madeira, F., Park, Y.M., Lee, J., Buso, N., Gur, T., Madhusoodanan, N. *et al.* (2019) The EMBL-EBI search and sequence analysis tools APIs in 2019. *Nucleic Acids Research*, **47**, 636–641.

Majerská, J., Schrumpfová, P.P., Dokládal, L., Schořová, Š., Stejskal, K., Oboril, M. *et al.* (2017) Tandem affinity purification of AtTERT reveals putative interaction partners of plant telomerase in vivo. *Protoplasma*, **254**, 1547–1562.

Malamy, J. & Benfey, P. (1997) Organization and cell differentiation in lateral roots of *Arabidopsis thaliana*. *Development*, **124**, 33–44.

Mao, Y.Q. & Houry, W.A. (2017) The role of pontin and reptin in cellular physiology and cancer etiology. *Frontiers in Molecular Biosciences*, **4**, 58.

Matias, P.M., Gorynia, S., Donner, P. & Carrondo, M.A. (2006) Crystal structure of the human AAA+ protein RuvBL1. *Journal of Biological Chemistry*, **281**, 38918–38929.

Mozgová, I., Schrumpfová, P.P., Hofr, C. & Fajkus, J. (2008) Functional characterization of domains in AtTRB1, a putative telomere-binding protein in Arabidopsis thaliana. *Phytochemistry*, **69**, 1814–1819.

Neuwald, A.F., Aravind, L., Spouge, J.L. & Koonin, E.V. (1999) AAA+: a class of chaperone-like ATPases associated with the assembly, operation, and disassembly of protein complexes. *Genome Research*, **9**(27), 43.

Nowicka, A., Tokarz, B., Zwyrtková, J., Dvořák Tomaštíková, E., Procházková, K., Ercan, U. *et al.* (2020) Comparative analysis of epigenetic inhibitors reveals different degrees of interference with transcriptional gene silencing and induction of DNA damage. *Plant Journal*, **102**, 68–84.

Putnam, C.D., Clancy, S.B., Tsuruta, H., Gonzalez, S., Wetmur, J.G. & Tainer, J.A. (2001) Structure and mechanism of the RuvB Holliday junction branch migration motor. *Journal of Molecular Biology*, **311**, 297–310.

Rajendra, E., Garaycoechea, J.I., Patel, K.J. & Passmore, L.A. (2014) Abundance of the Fanconi anaemia core complex is regulated by the RuvBL1 and RuvBL2 AAA+ ATPases. *Nucleic Acids Research*, **42**, 13736–13748.

Reňák, D., Dupl'áková, N. & Honys, D. (2012) Wide-scale screening of T-DNA lines for transcription factor genes affecting male gametophyte development in Arabidopsis. *Sexual Plant Reproduction*, **25**, 39–60.

Schořová, Š., Fajkus, J., Záveská Drábková, L., Honys, D. & Schrumpfová, P.P. (2019) The plant Pontin and Reptin homologues, RuvBL1 and RuvBL2a, colocalize with TERT and TRB proteins in vivo, and participate in telomerase biogenesis. *The Plant Journal*, **98**, 195–212.

Schrumpfová, P., Kuchař, M., Miková, G., Skřišovská, L., Kubičárová, T. & Fajkus, J. (2004) Characterization of two Arabidopsis thaliana myb-like proteins showing affinity to telomeric DNA sequence. *Genome*, **47**, 316–324.

Schrumpfová, P.P. & Fajkus, J. (2020) Composition and function of telomerase—a polymerase associated with the origin of eukaryotes. *Biomolecules*, **10**, 1425.

Schrumpfová, P.P., Vychodilová, I., Hapala, J., Schořová, Š., Dvořáček, V. & Fajkus, J. (2016) Telomere binding protein TRB1 is associated with promoters of translation machinery genes in vivo. *Plant Molecular Biology*, **90**, 189–206.

Sessions, A., Burke, E., Presting, G., Aux, G., McElver, J., Patton, D. *et al.* (2002) A high-throughput Arabidopsis reverse genetics system. *Plant Cell*, **14**, 2985–2994.

Shin, S.H., Lee, J.S., Zhang, J.M., Choi, S., Boskovic, Z.V., Zhao, R. *et al.* (2020) Synthetic lethality by targeting the RUVBL1/2-TTT complex in mTORC1-hyperactive cancer cells. *Science Advances*, **6**, 1–15.

Silva-Martin, N., Daudén, M.I., Glatt, S., Hoffmann, N.A., Kastritis, P., Bork, P. *et al.* (2016) The combination of X-ray crystallography and Cryo-electron microscopy provides insight into the overall architecture of the Dodecameric Rvb1/Rvb2 complex. *PLoS One*, **11**, e0146457.

Smyth, D.R., Bowman, J.L. & Meyerowitz, E.M. (1990) Early flower development in Arabidopsis. *Plant Cell*, **2**, 755–767.

Sun, K., Hunt, K. & Hauser, B.A. (2004) Ovule abortion in Arabidopsis triggered by stress. *Plant Physiology*, **135**, 2358–2367.

Sundaresan, V. & Skinner, D.J. (2018) Recent advances in understanding female gametophyte development. *F1000Res*, **7**, F1000 Faculty Rev-804.

Susaki, D., Suzuki, T., Maruyama, D., Ueda, M., Higashiyama, T. & Kurihara, D. (2021) Dynamics of the cell fate specifications during female gametophyte development in Arabidopsis. *PLoS Biology*, **19**, e3001123.

Taniuchi, K., Furihata, M., Iwasaki, S., Tanaka, K., Shimizu, T., Saito, M. *et al.* (2014) RUVBL1 directly binds actin filaments and induces formation of cell protrusions to promote pancreatic cancer cell invasion. *International Journal of Oncology*, **45**, 1945–1954.

Van Leene, J., Han, C., Gadeyne, A. *et al.* (2019) Capturing the phosphorylation and protein interaction landscape of the plant TOR kinase. *Nature Plants*, **5**, 316–327.

Venteicher, A.S., Meng, Z., Mason, P.J., Veenstra, T.D. & Artandi, S.E. (2008) Identification of ATPases pontin and reptin as telomerase components essential for holoenzyme assembly. *Cell*, **132**, 945–957.

Vladejić, J., Yang, F., Dvořák Tomaštíková, E., Doležel, J., Palecek, J.J. & Pecinka, A. (2023) Analysis of BRCT5 domain-containing proteins reveals a new component of DNA damage repair in Arabidopsis. *Frontiers in Plant Science*, 4923.

Walker, J.E., Saraste, M., Runswick, M.J. & Gay, N.J. (1982) Distantly related sequences in the alpha- and beta-subunits of ATP synthase, myosin, kinases and other ATP-requiring enzymes and a common nucleotide binding fold. *The EMBO Journal*, **1**, 945–951.

Waterhouse, A.M., Procter, J.B., Martin, D.M.A., Clamp, M. & Barton, G.J. (2009) Jalview version 2—a multiple sequence alignment editor and analysis workbench. *Bioinformatics*, **25**, 1189–1191.

Willhoft, O. & Wigley, D.B. (2020) INO80 and SWR1 complexes: the non-identical twins of chromatin remodelling. *Current Opinion in Structural Biology*, **61**, 50–58.

Yang, F., Fernández Jiménez, N., Majka, J., Pradillo, M. & Pecinka, A. (2021) Structural maintenance of chromosomes 5/6 complex is necessary for tetraploid genome stability in *Arabidopsis thaliana*. *Frontiers in Plant Science*, **12**, 2139.

Yang, F., Fernández-Jiménez, N., Tučková, M., Vrána, J., Cápal, P., Díaz, M. *et al.* (2021) Defects in meiotic chromosome segregation lead to unreduced male gametes in Arabidopsis SMC5/6 complex mutants. *Plant Cell*, **33**, 3104–3119.

Zander, M., Willige, B.C., He, Y., Nguyen, T.A., Langford, A.E., Nehring, R. *et al.* (2019) Epigenetic silencing of a multifunctional plant stress regulator. *eLife*, **8**, e47835.

Supplemental Figures:

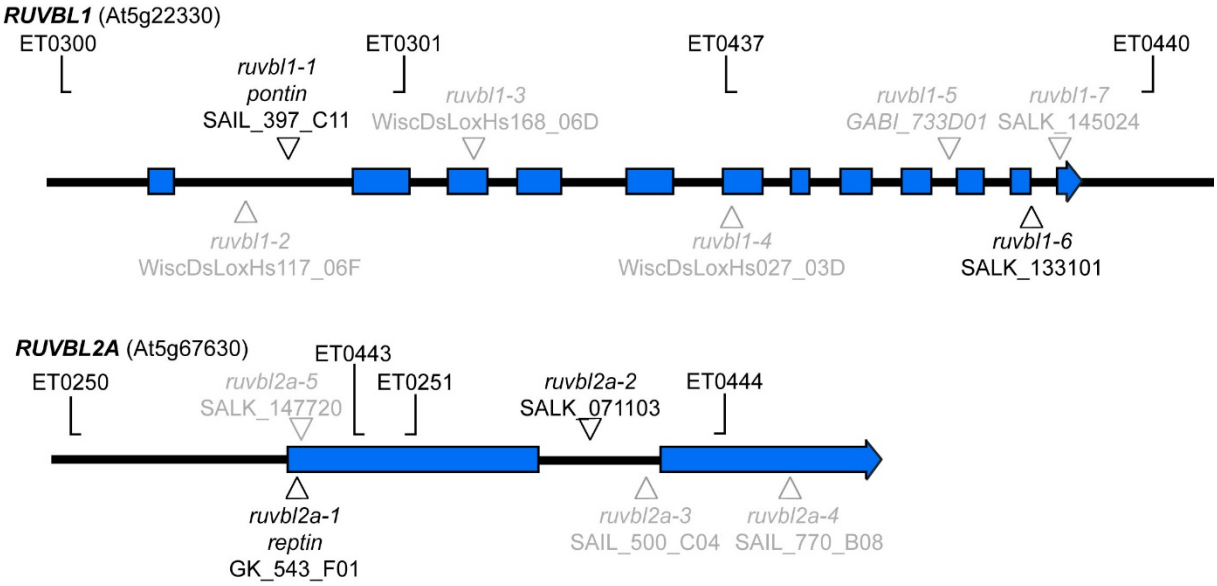

Figure S1. Schematic illustration of T-DNA insertions within the *RUVBL1* and *RUVBL2A* genes. Blue boxes indicate exons and black lines introns. Locations of various T-DNA insertions in the coding sequences of the *RUVBL1* and *RUVBL2A* genes available from several plant databases are marked with triangles. Dark grey triangles mark T-DNA insertion lines with a limited number of heterozygous progeny (*ruvbl1-1* (SAIL_397_C11), *ruvbl1-6* (SALK_133101), *ruvbl2a-1* (GABI-Kat_543F01), and *ruvbl2a-2* (SALK_071103)). Light grey triangles mark lines that did not provide any homozygote or heterozygote plants.

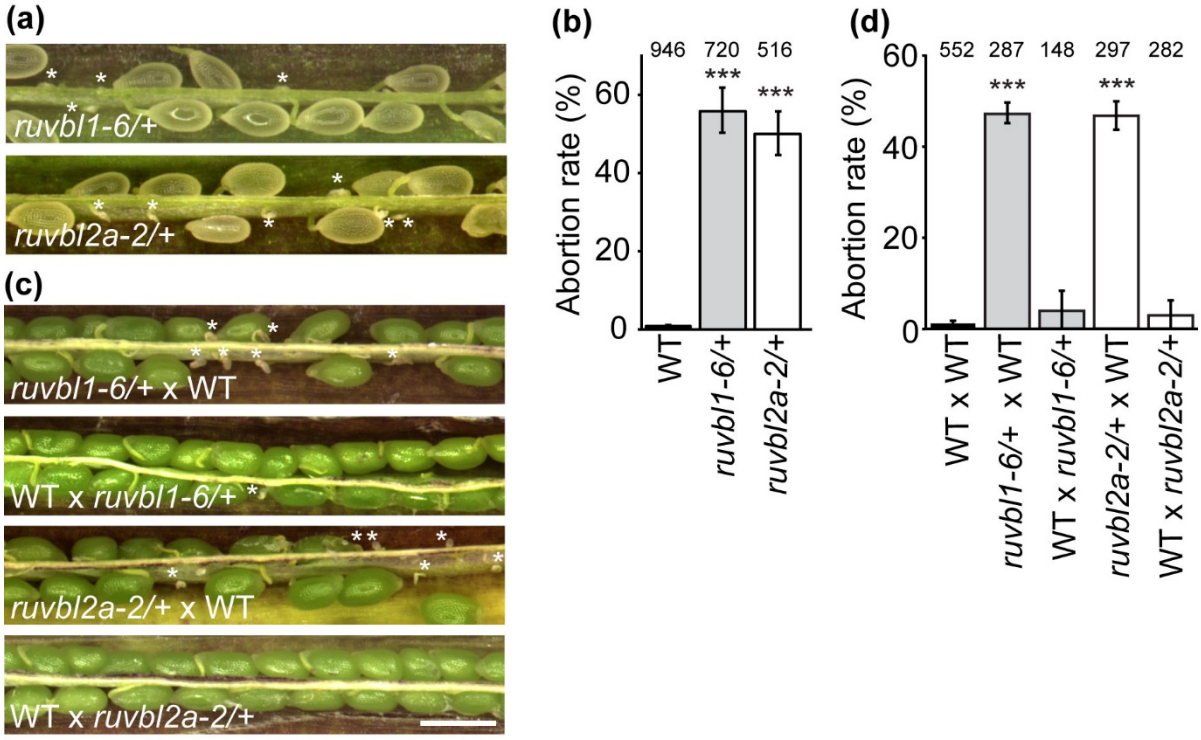

Figure S2. Analysis of seed setting in newly identified *RUVBL1* and *RUVBL2A* T-DNA insertional mutants and transmission ratio distortion in reciprocal crosses.
(a) Representative content of siliques in self-pollinated WT, *ruvbl1-6/+,* and *ruvbl2a-2/+* plants. The white asterisks indicate aborted ovules.
(b) Percentage of aborted ovules of self-fertilized WT and mutant plants. The numbers on top of the bars correspond to the number of seeds analyzed. ****P* < 0.00001 in Fisher´s exact test (X^2). Error bars indicate the standard deviation of individually analyzed siliques.
(c) Representative content of siliques from reciprocal crosses between mutants and WT. The first genotype indicates the mother plants. Scale bar, 1 mm.
(d) Percentage of aborted ovules of manual reciprocal crosses between WT and mutant plants. The numbers on top of the bars correspond to the number of analyzed seeds. ****P* < 0.00001 in X^2. Error bars indicate the standard deviation of the means of individual siliques analyzed.

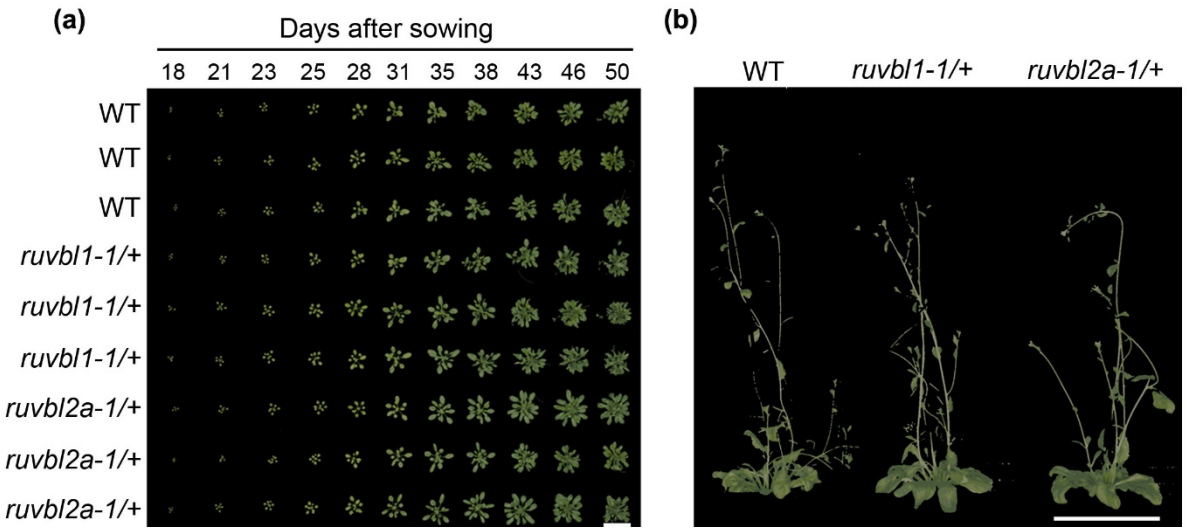

Figure S3. Phenotypic analysis of plants heterozygous for *RUVBL1* and *RUVBL2A* mutations. The WT and the PCR-validated *ruvbl1-1/+,* and *ruvbl2a-1/+* plants were analyzed using a semi-automated phenotyping pipeline (Photon System Instruments). (a), Top view imaging using RGB cameras. (b), Side view imaging using RGB cameras 50 days after sowing. Scale bars, 6.5 cm.

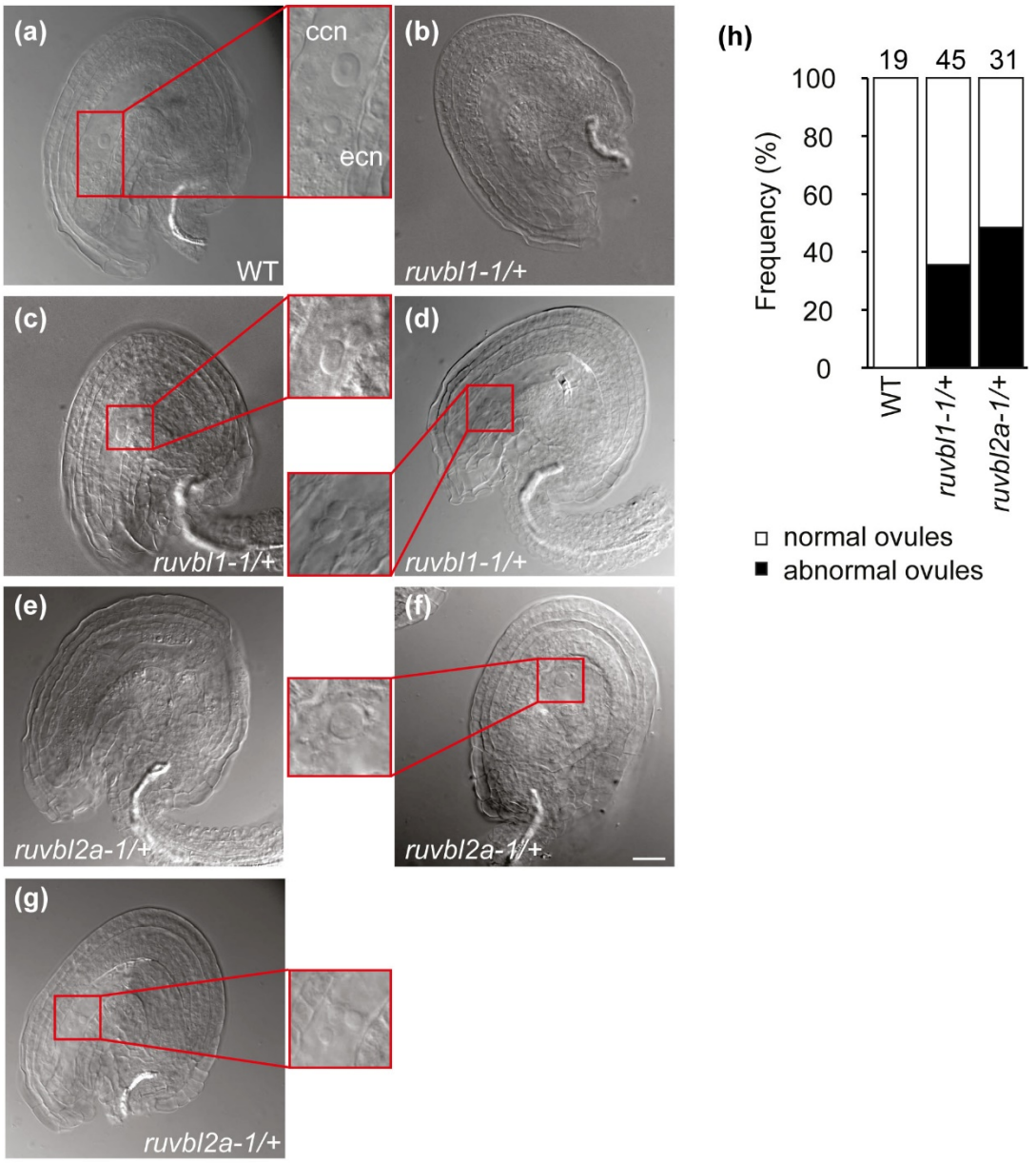

Figure S4. Differential interference contrast micrographs of cleared ovules from *ruvbl1-1/+* and *ruvbl2a-1/+* plants. Scale bar, 20 µm.
(a) Representative WT-like embryo sac with one egg cell nucleus (ecn) and one central cell nucleus (ccn).
(b-d) Examples of defective embryo sacs from *ruvbl1-1/+* plants. Ovule with a degraded embryo sac (b). Embryo sac with two large nuclei (c). Embryo sac with three nuclei (d).
(e-g) Abnormal embryo sacs from *ruvbl2a-1/+* plants. Ovule with a degraded embryo sac (e). Embryo sac with one nucleus (f). Embryo sac with three nuclei (g).
(h) Percentage of normal and abnormal ovules from analyzed genotypes. Ovules were analyzed from at least three independent plants. The numbers on top of the bars correspond to the number of analyzed ovules.

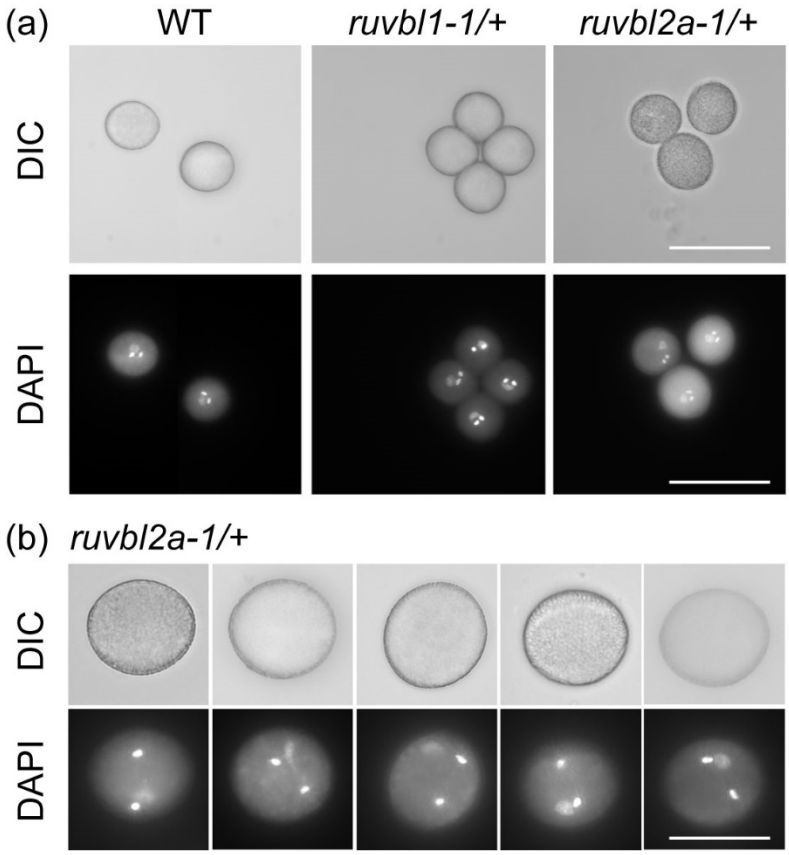

Figure S5. Phenotypic analysis of mature pollen grains.
(a) Bright field (DIC), and corresponding 4′,6-diamidino-2-phenylindole (DAPI) epifluorescence micrographs. Scale bars, 50 μm.
(b) Examples of *ruvbl2a-1*/+ pollen grains with aberrant positioning of the nuclei stained with DAPI. Scale bars, 20 μm.

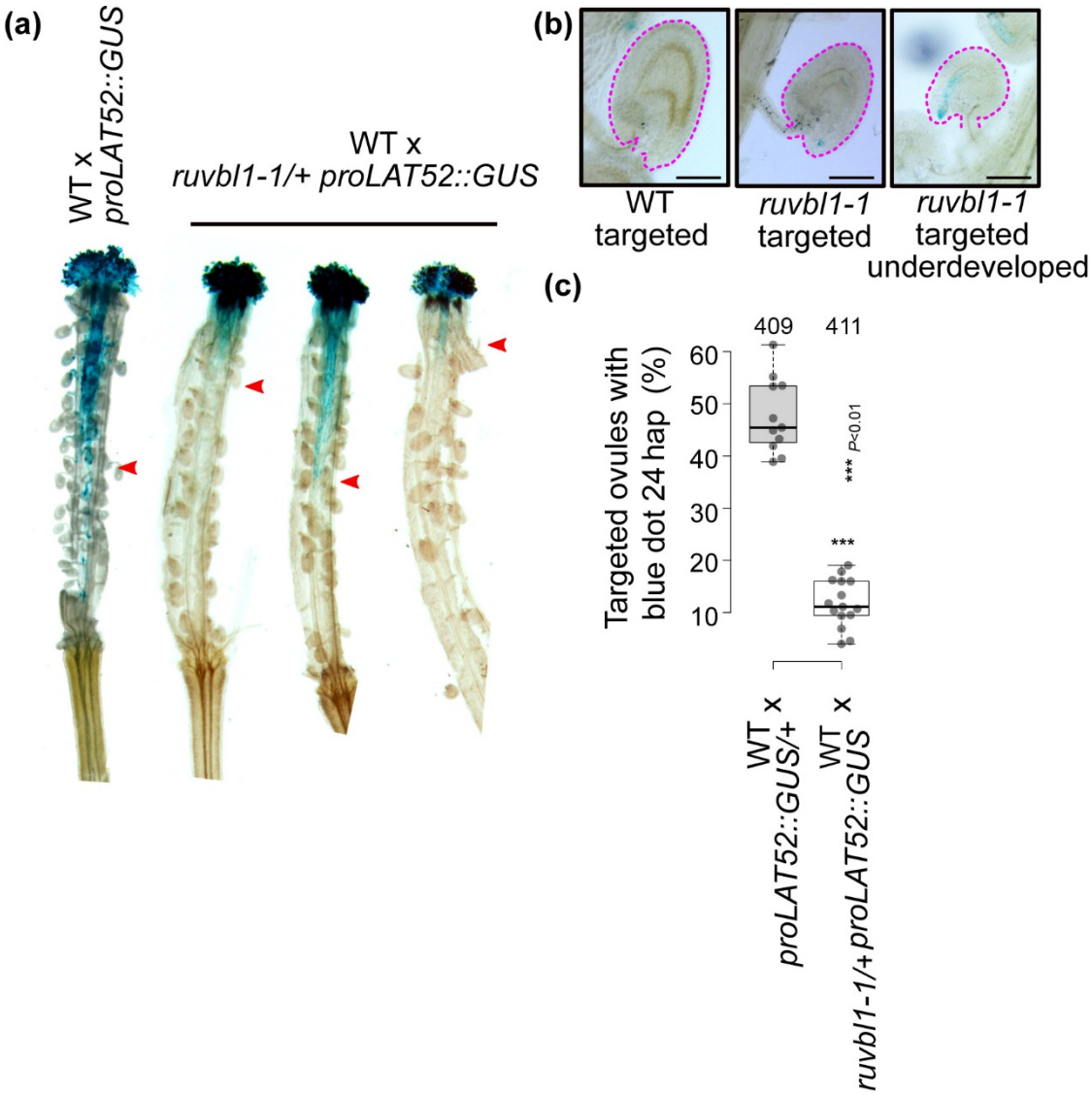

Figure S6. *ruvbl1-1* pollen tubes lack competence to target ovules for fertilization.
(a) *In vivo* pollen tube growth 24 hap of control WT expressing *proLAT52::GUS* and *ruvbl1-1*/+ containing *proLAT52::GUS* associated with the SAIL T-DNA allele. Red arrows mark the approximate pollen tube length detected within the pistil.
(b) Representative classes of WT ovules targeted with WT pollen tubes (no GUS stain) or with *ruvbl1-1* pollen tubes (with GUS blue dot). Scale bar, 50 µm.
(c) Quantification of the ovule classes from b. Statistics were performed with two-sided Student's t test.

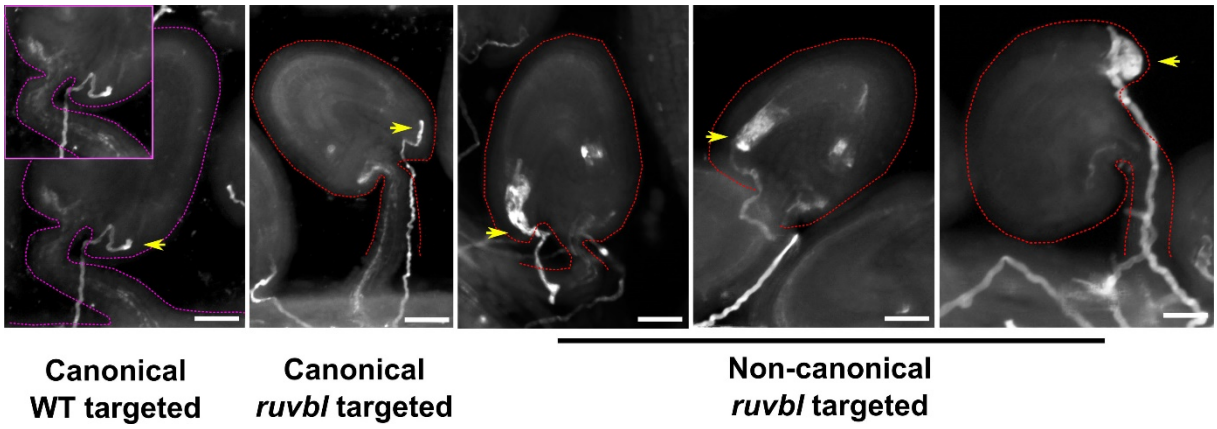

Figure S7. Phenotypic classes observed after pollination of WT ovules with mutant pollen. Scale bars, 20 µm.

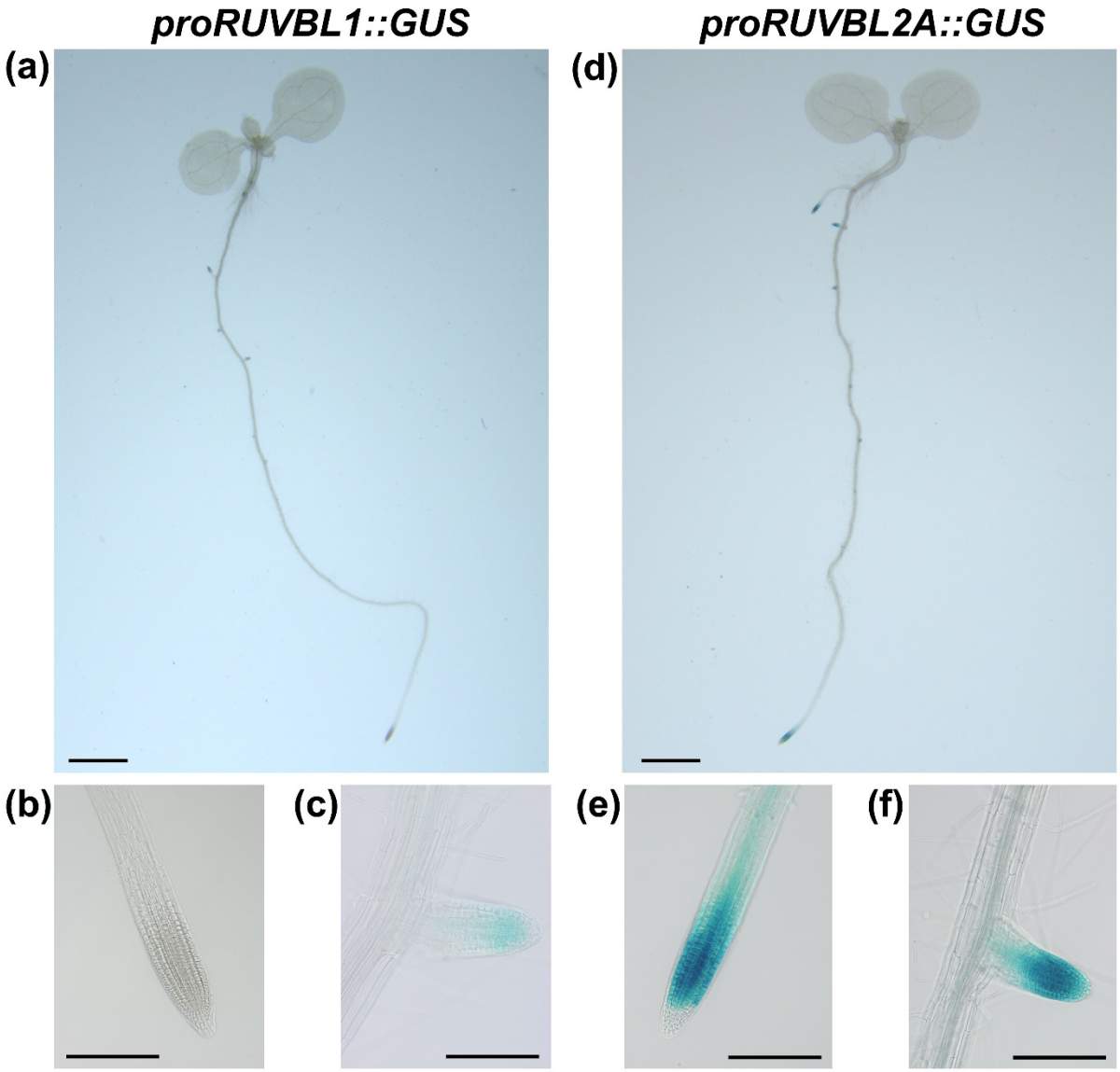

Figure S8. Detection of *RUVBL1* and *RUVBL2A* promoter activity in seedlings by GUS histochemical staining.
(a, d) 7 days old seedlings. Scale bars, 1 mm. (b, e) Primary roots. Scale bars, 200 μm. (c, f) Lateral roots. Scale bars, 100 μm.

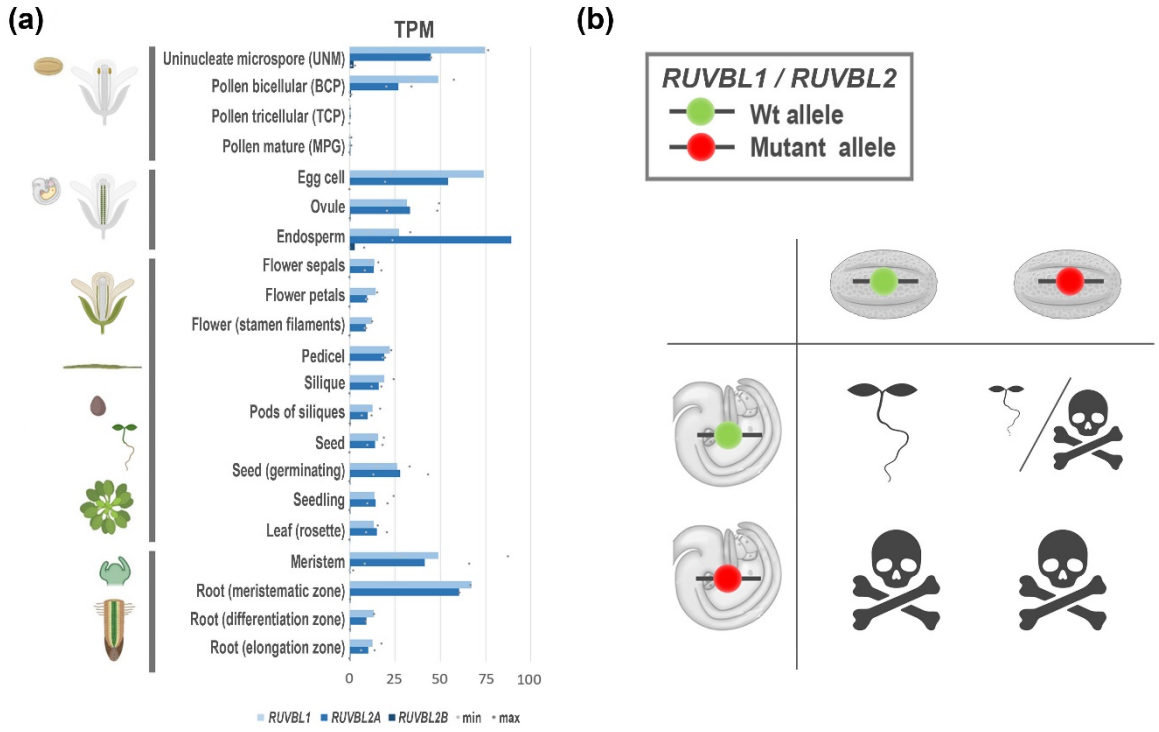

Figure S9. Graphical summary of *RUVBL* mutations on plant viability.
(a) The analysis of global transcriptome data from various developmental stages. Data were generated using the CoNekT Database and adapted (Julca et al., 2021). Pictograms were created with BioRender.com. TPM, transcript per million.
(b) Graphical summary of the role of RUVBL1 and RUVBL2A in securing the viability of male and female gametophytes. Heterozygous mutant plants produce 50% of gametes containing WT allele (green) and 50% containing mutant allele (red). All megagametes carrying mutant alleles die (50% lethality) and the remaining are mix of pollen carrying WT and mutant alleles. The frequency of the pollen with the mutant allele participating in fertilization is again very much reduced resulting in a low number of heterozygous offspring.

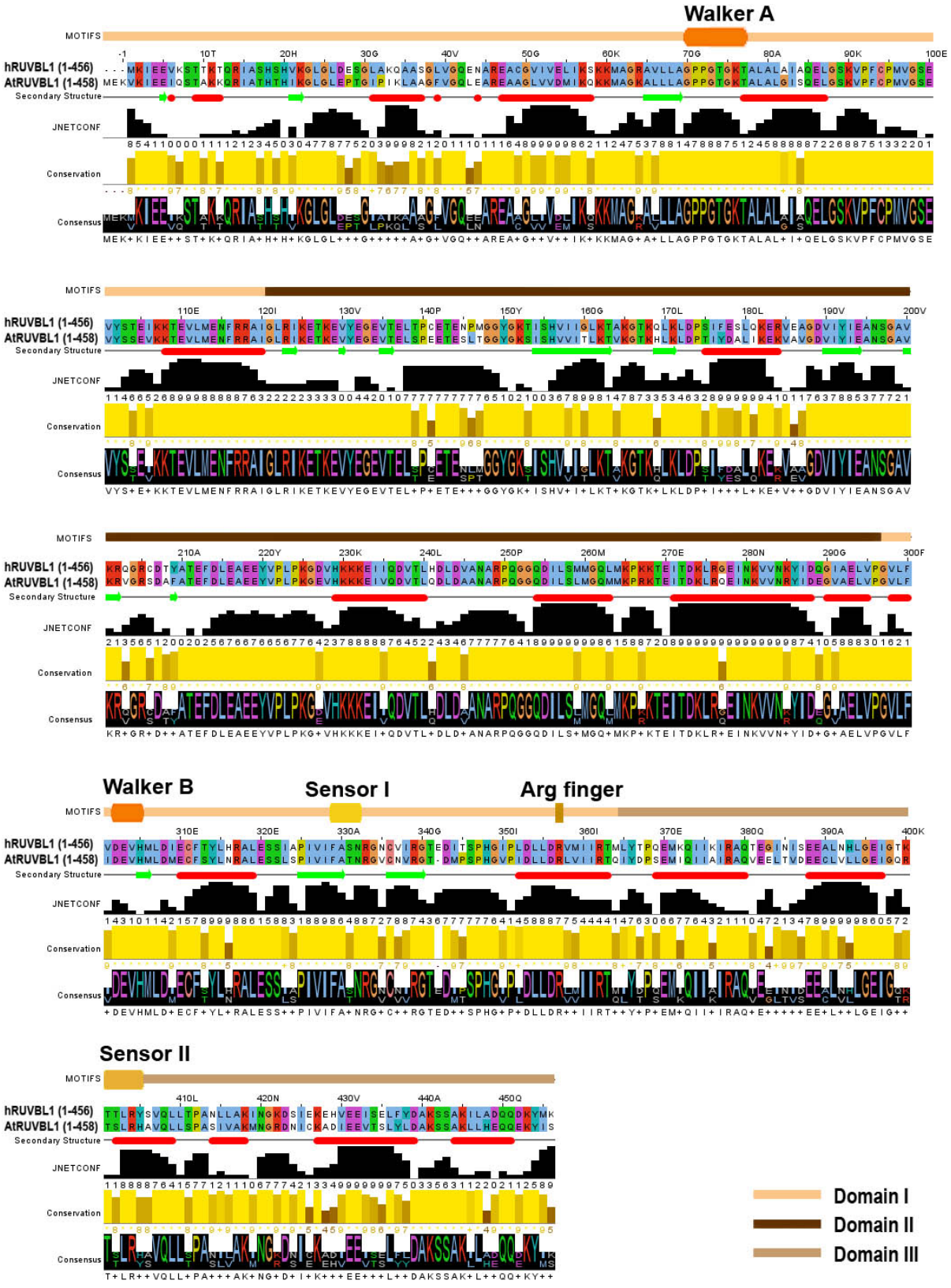

Figure S10. Multiple sequence alignment of RUVBL1 from human and *A. thaliana*. Regions with conserved physicochemical properties were coloured according to the Clustal X colour scheme (Jeanmougin *et al.*, 1998). Domains and highly conserved motifs (Motifs) were marked according to similarity with human RUVBL1 protein (Matias *et al.*, 2006; Gorynia *et al.*, 2011). The secondary structure (Secondary Structure) of the first sequence in the alignment was

predicted, helices are marked as red tubes, beta sheets are marked as dark green arrows. Confidence values for secondary structure prediction were estimated (JNetCONF) - high values indicate high confidence. Regions with high conserved physicochemical properties (Conservation) are marked in light yellow. The alignment consensus (Consensus) is given in the percentage of the modal residue per column and the sequence logo indicates the relative number of residues per column.

Figure S11. Multiple sequence alignment of RUVBL2 from human and *A. thaliana*. The analyses were performed as described in Figure S10.

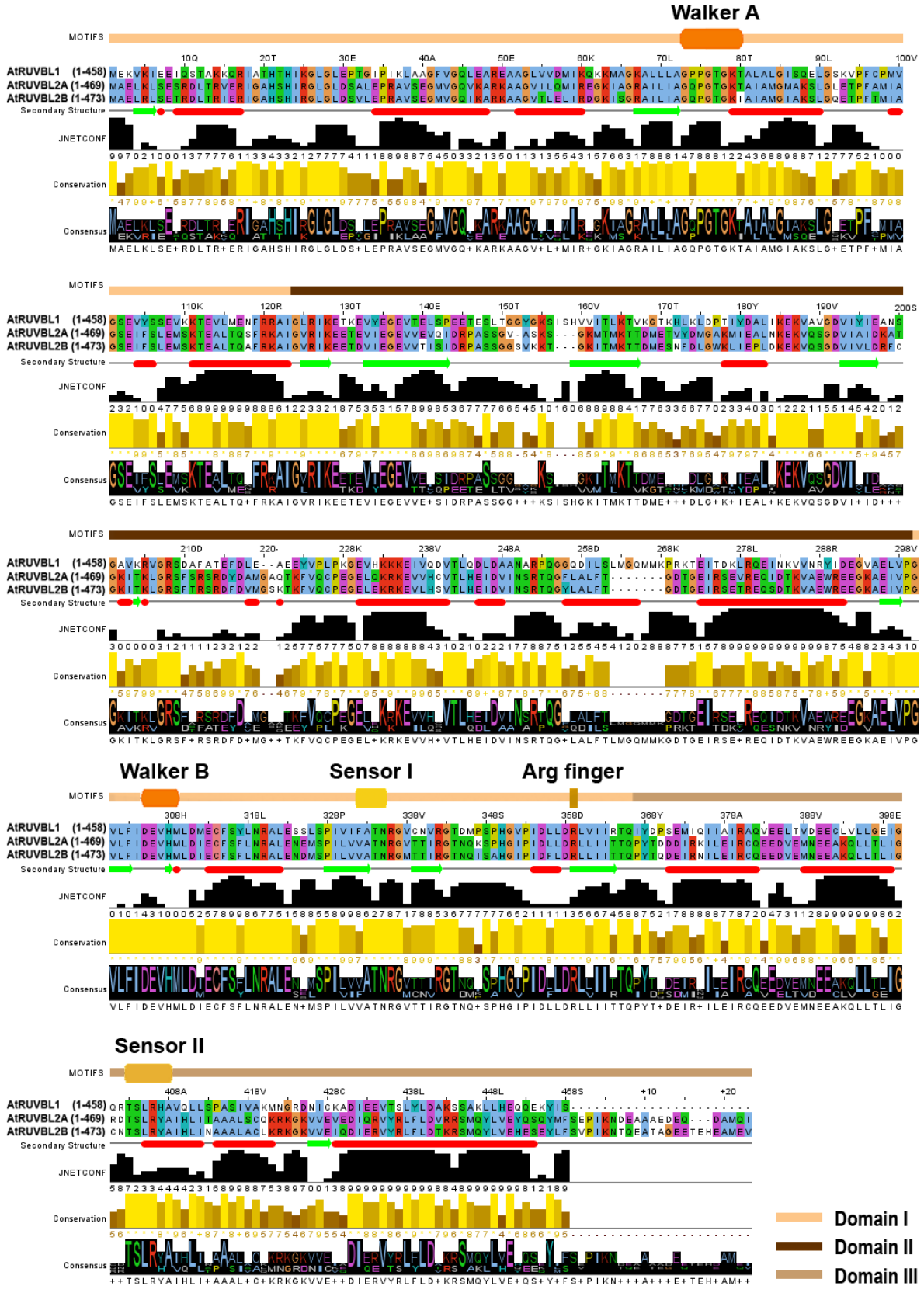

Figure S12. Multiple sequence alignment of RUVBLs from *A. thaliana*. The analyses were performed as described in Figure S10.

Gorynia, S., Bandeiras, T.M., Pinho, F.G., et al. (2011) Structural and functional insights into a dodecameric molecular machine – The RuvBL1/RuvBL2 complex. *J. Struct. Biol.*, **176**, 279–291.

Jeanmougin, F., Thompson, J.D., Gouy, M., Higgins, D.G. and Gibson, T.J. (1998) Multiple sequence alignment with Clustal X. *Trends Biochem. Sci.*, **23**, 403–405.

Julca, I., Ferrari, C., Flores-Tornero, M., et al. (2021) Comparative transcriptomic analysis reveals conserved programmes underpinning organogenesis and reproduction in land plants. Nat. Plants, 7, 1143–1159.

Matias, P.M., Gorynia, S., Donner, P. and Carrondo, M.A. (2006) Crystal Structure of the Human AAA+ Protein RuvBL1. *J. Biol. Chem.*, **281**, 38918–38929.

Supplement R

Kusova A., Steinbachova L., Přerovská T., Záveská Drábková L., Paleček J., Khan A., Rigóová G., Gadoiu Z., Jourdain C., Stricker T., Schubert D., Honys D., and **Schrumpfová P.P**.*, **2023**. Completing the TRB family: newly characterized members show ancient evolutionary origins and distinct localization, yet similar interactions Plant Molecular Biology 112:61–83.

P.P.S. participated in the design of experiments, data evaluation and wrote the ms

Plant Molecular Biology (2023) 112:61–83
https://doi.org/10.1007/s11103-023-01348-2

Completing the TRB family: newly characterized members show ancient evolutionary origins and distinct localization, yet similar interactions

Alžbeta Kusová[1,2] · Lenka Steinbachová[3] · Tereza Přerovská[1] · Lenka Záveská Drábková[3] · Jan Paleček[1,2] · Ahamed Khan[4] · Gabriela Rigóová[1] · Zuzana Gadiou[3] · Claire Jourdain[5] · Tino Stricker[5] · Daniel Schubert[5] · David Honys[3,6] · Petra Procházková Schrumpfová[1,2]

Received: 9 December 2022 / Accepted: 2 March 2023 / Published online: 28 April 2023

Abstract

Telomere repeat binding proteins (TRBs) belong to a family of proteins possessing a Myb-like domain which binds to telomeric repeats. Three members of this family (TRB1, TRB2, TRB3) from *Arabidopsis thaliana* have already been described as associated with terminal telomeric repeats (telomeres) or short interstitial telomeric repeats in gene promoters (*telo*-boxes). They are also known to interact with several protein complexes: telomerase, Polycomb repressive complex 2 (PRC2) E(z) subunits and the PEAT complex (PWOs-EPCRs-ARIDs-TRBs). Here we characterize two novel members of the TRB family (TRB4 and TRB5). Our wide phylogenetic analyses have shown that TRB proteins evolved in the plant kingdom after the transition to a terrestrial habitat in Streptophyta, and consequently TRBs diversified in seed plants. TRB4-5 share common TRB motifs while differing in several others and seem to have an earlier phylogenetic origin than TRB1-3. Their common Myb-like domains bind long arrays of telomeric repeats in vitro, and we have determined the minimal recognition motif of all TRBs as one *telo*-box. Our data indicate that despite the distinct localization patterns of TRB1-3 and TRB4-5 in situ, all members of TRB family mutually interact and also bind to telomerase/PRC2/PEAT complexes. Additionally, we have detected novel interactions between TRB4-5 and EMF2 and VRN2, which are Su(z)12 subunits of PRC2.

Key message

TRB proteins bind short/long telomeric repeats and attract telomerase, PRC2 or PEAT complexes. Here we show the unique features of novel members of TRB family that have earlier phylogenetic origin.

Keywords Telomere repeat binding · TRB · PRC2 · PEAT · TERT · Telomeric

Introduction

Telomere repeat binding proteins (TRBs) were originally characterized as proteins in *Arabidopsis thaliana* with a binding affinity to telomeric DNA sequences proportional to the number of telomeric repeats (Schrumpfová et al. 2004). They belong to the plant-specific Single myb histone 1 (SMH) family with an N-terminal Myb-like domain (Myb-like), a central histone-like (H1/5-like) domain, and a coiled-coil domain near the C-terminus (Marian et al. 2003). Three members of the TRB family (TRB1, TRB2 and TRB3) in *A. thaliana* exhibit self-interactions and mutual interactions in the yeast-two hybrid (Y2H) system (Kuchař and Fajkus 2004; Schrumpfová et al. 2004).

Alžbeta Kusová and Lenka Steinbachová shared co-first authorship.

Accession numbers TRB1 (AT1G49950); TRB2, formerly TBP3 (AT5G67580); TRB3, formerly TBP2 (AT3G49850); TRB4 AT1G17520; TRB5 AT1G72740; RUVBL1 (AT5G22330); RUVBL2A (AT5G67630); TERT (AT5G16850); POT1a (AT2G05210); POT1b (AT5G06310); Fibrillarin1 (AT5G52470); SRp34 (AT1G02840); EMF2 (AT5G51230); VRN2 (AT4G16845); CLF (AT2G23380); SWN (AT4G02020); PWO1 also named as PWWP1 (AT3G03140); PWO2 also named as PWWP2 (AT1G51745); PWO3 also named as PWWP3 (AT3G21295).

✉ Petra Procházková Schrumpfová
schpetra@sci.muni.cz

Extended author information available on the last page of the article

They bind plant telomeric repeats $(TTTAGGG)_n$ through the Myb-like domain (Mozgová et al. 2008), while the H1/5-like domain is responsible for dimerization with other TRB proteins (Schrumpfová et al. 2008).

TRB1-3 proteins are proposed to participate in telomerase biogenesis. They interact directly with the catalytic protein subunit of telomerase (TERT) (Schrumpfová et al. 2014) and mediate interactions between TERT and Recombination UV B-like (RUVBL) proteins (Schořová et al. 2019), homologs of the essential mammalian telomerase assembly components Pontin and Reptin (Venteicher et al. 2008). Nuclear and predominantly nucleolar localization of TRB1-3 interacting with TERT and RUVBLs, as well as with the plant ortholog of dyskerin, CBF5 (Lermontova et al. 2007), was observed using Bimolecular fluorescence complementation (BiFC) (Sweetlove and Gutierrez 2019). Moreover, the TRB1 protein interacts via its H1/5-like domain with Protection of telomeres 1 (POT1b) (Schrumpfová et al. 2008), an *A. thaliana* homolog of the G-overhang binding protein Pot1, a core component of mammalian telomere cap complex, Shelterin (Tani and Murata 2005; Surovtseva et al. 2007). Additionally, in situ co-localization of TRB1 with telomeric DNA repeats has been detected in plant cells (Schrumpfová et al. 2014; Dreissig et al. 2017).

Telomere shortening was observed in *trb1* mutants in the *A. thaliana* ecotype Columbia, with otherwise-stable telomere lengths (Shakirov and Shippen 2004; Schrumpfová et al. 2014). In contrast, telomere extension was detected in *trb2* knockout mutants of the *A. thaliana* ecotype Wassilewskija, which exhibits telomere length polymorphism in wild-type plants (Shakirov and Shippen 2004; Maillet et al. 2006; Lee and Cho 2016). Triple homozygous mutant plants, containing the alleles from Columbia (*trb1* and *trb3*) and from Wassilewskija (*trb2*), exhibit telomere shortening (Zhou et al. 2018).

In multicellular organisms, Polycomb repressive complex 1 (PRC1) and PRC2 repress target genes through histone modification and chromatin compaction. In *Drosophila melanogaster,* four core PRC2 subunits are present: the histone methyltransferase Enhancer of zeste [E(z)], Suppressor of zeste 12 [Su(z)12], Extra sex combs (Esc), and the histone-binding nucleosome remodelling factor 55 kDa (Nurf55). The E(z) homologs in *A. thaliana*, named CURLY LEAF (CLF) and SWINGER (SWN), are implicated in sporophyte development (reviewed in Mozgova and Hennig 2015). The PRC2 complex primarily methylates histone H3 on lysine 27 (H3K27me3), a mark of transcriptionally silent chromatin. TRB1–3 interact with the PRC2 proteins CLF and SWN (Zhou et al. 2018). We have shown that TRB1 proteins are not only associated with long arrays of telomeric repeats but also with interstitially located short telomeric sequences *telo*-box motifs, especially in the promoters of translation machinery genes (Schrumpfová et al. 2016). It was further shown that these *telo*-boxes are part of the cis-regulatory elements that may relate to PRC2 recruitment (Zhou et al. 2016, 2018).

Besides the PRC2 complex, TRB1-3 are components of the PEAT complex (PWOs-EPCRs-ARIDs-TRBs) mediating histone acetylation/deacetylation and heterochromatin condensation. They potentially regulate the RNA-directed DNA methylation (RdDM) pathway (Tan et al. 2018; Tsuzuki and Wierzbicki 2018). The involvement of TRB proteins in histone deacetylation supports the previous observation that TRB2 directly interacts with histone deacetylases (HDT4 and HDA6) (Lee and Cho 2016). Recently, it has also been proposed that histone 1 (H1) selectively prevents H3K27me3 accumulation at telomeres and large pericentromeric interstitial telomeric repeat (ITR) domains by restricting DNA accessibility to TRB proteins (Teano et al. 2020).

Here we show that the plant-specific TRB proteins can be recognized in lower plants, such as Streptophytic algae, as well as in higher plants. In seed plants, TRB proteins are divided into three main lineages. We speculate that due to whole genome duplication (WGD) in *A. thaliana*, three ancestral TRB proteins have multiplied to the current five TRB members. We characterize new members of TRB family in *A. thaliana* (TRB4 and TRB5) and demonstrate that all members of the TRB family can bind long arrays of telomeric repeats with high specificity. We defined the minimal recognition motif for all TRBs as one *telo*-box. Even though TRB4 and TRB5 share very high sequence and structural homology with TRB1, TRB2 and TRB3, they differ in terms of the surface of their Myb-domains and their cellular localization. We provide evidence that TRB4-5 mutually interact with other members of the TRB family and physically interact with TERT, POT1a/b, SWN/CLF, and PWO1-3. Novel interactions were also detected between TRB4-5 and EMF2/VRN2, which represent the Su(z)12 subunits of PRC2. Completing TRB family analysis permits further exploration of the biological roles of these important plant-specific proteins.

Materials and methods

Primers

The sequences of all primers and probes used in this study are provided in Supplemental Table 1.

Plant material

For transient assays, *Nicotiana benthamiana* plants were grown in soil in LD conditions up to 4 weeks and subsequently used for *Agrobacterium tumefaciens* infiltration.

Phylogenetic analyses

We combined two homology searches based on *A. thaliana* TRB1-5. First, we searched completely sequenced genomes using Phytozome v12 and second using BLASTP from available databases (NCBI) and publicly available sequences.

Protein sequences were aligned using the Clustal Omega (Sievers et al. 2011) algorithm in the Mobyle platform (Néron et al. 2009), with homology detection by HMM–HMM comparisons. We screened data after alignment in the BioEdit program (Hall 1999).

Maximum likelihood (ML) analyses of the matrices were performed in RAxML 8.2.4 (Stamatakis 2014) to examine differences in optimality between alternative topologies. 1000 replications were run for bootstrap values. Phylogenetic trees were constructed and modified with iTOL v3.4 (Letunic and Bork 2016). The MEME search was set to identify domains and conserved amino acid (aa) sequence motifs under these conditions: a maximum of 15 motifs for each protein with a wide sequence motif from 2 to 50 and a total number of sites from 2 to 600 MEME 4.11.2 (Bailey et al. 2009). The evolutionarily conserved aa residues were visualized using ConSurf 2016 (Ashkenazy et al. 2016).

Analysis of protein structures

The AlphaFold (Jumper et al 2021; Varadi et al 2022) and SwissModel (Waterhouse et al 2018) tools were used to generate in silico protein models. Structural models were compared as previously described (Palecek & Gruber 2015). All structures including electrostatic potential of their molecular surfaces were visualized using PyMOL Molecular Graphics System, Version 2.4.1, Schrödinger, LLC.

Cloning

For yeast two-hybrid assays (Y2H), most of the Y2H constructs in pGADT7-DEST or pGBKT7-DEST (Horák et al. 2008) were prepared previously: TERT constructs (RID1, TEN, Fw1N, Fw3_NLS, Fw3N and RT) were reported in Majerská et al. 2017, TRB1-3 were reported in Schrumpfová et al. 2014, RUVBL1 and RUVBL2A were reported in Schořová et al. 2019, POT1a and POT1b were reported in Majerská et al. 2017, $SWN_{\Delta}SET$ and $CLF_{\Delta}SET$ were reported in Chanvivattana et al. 2004 and Hohenstatt et al. 2018). PWO1 was reported in Hohenstatt et al. 2018, VRN2 and EMF2 were reported in Lindner et al. 2013. The coding sequences of PWO2 and the fragment of PWO3 were cloned in the pGBKT7 and pGADT7 vectors (Clontech), passing through pDONR221 (Invitrogen) as described in Hohenstatt et al. 2018.

For the TRB4 construct, the cloned cDNA sequence of *TRB4* (G60951 from Arabidopsis Biological Resource Center; ABRC, https://abrc.osu.edu/) in pENTR223 was used as the entry clone. Site-directed mutagenesis using the QuikChange XL Site-Directed Mutagenesis Kit (Agilent Technologies) was performed following the manufacturer's instructions to remove the mutation V122A in the protein encoded by pENTR223-TRB4 as described in Wiese et al. 2021. To generate an entry vector containing the cDNA sequence of the *TRB5* gene, the total RNA from 7-day-old *A. thaliana* Col-0 seedlings isolated by TRI reagent (Molecular Research Center) was used for cDNA preparation using M-MuLV Reverse Transcriptase (New England Biolabs). The cDNA sequence of *TRB5* was amplified using gene specific Gateway-compatible primers according to the manufacturer's instructions with primers specified in Supplemental Table 1, and the RT-PCR products were recombined into the Gateway donor vector pDONR207 (Invitrogen). DNA fragments were introduced into the destination Gateway vectors pGBKT7-GW, pGADT7-GW (Addgene) using the LR recombinase reaction (Invitrogen).

For BiFC experiments, the Multisite Gateway® system (Invitrogen) was used to create pBiFCt-2in1 constructs (Grefen and Blatt 2012). The genes encoding *TRB1-5* from *A. thaliana* Col-0 were PCR-amplified from the constructs used in the Y2H system described above by two-step PCR using primers specified in Supplemental Table 1 and Phusion™ High-Fidelity DNA Polymerase (Thermo Fisher Scientific) as described in Wiese et al. 2021. The amplicons with *TRB1,2,3,5* genes were cloned into Gateway pDONR221 entry vectors (Thermo Fisher Scientific) carrying either attP1-P4 or attP3-P2 recombination sites using the BP Clonase™ II enzyme mix (Thermo Fisher Scientific). To generate pDONR221 entry clones carrying the *TRB4* gene, the In-Fusion® Snap Assembly cloning kit (Takara Bio USA) was used, where PCR-generated TRB4 amplicons with one half of att-sites obtained in the first Phusion PCR step of the Gateway® cloning were fused with linearized PCR-generated pDONR221 backbone with appropriate attL sites by recognizing 15-base pairs (bp) overlaps at their ends according to the manufacturer's instructions. All entry clones were subsequently used in LR Clonase™ II Plus (Thermo Fisher Scientific) reactions to create pBiFCt-2in1-CC and pBiFCt-2in1-NN expression constructs harboring two protein coding regions C- or N-terminally fused to either the N- or C-terminal eYFP halves (e.g., TRB1-nYFP and TRB1-cYFP). After verification by Sanger sequencing (Macrogene), the constructs were used for transient expression in *N. benthamiana* leaves.

For transient expression of TRB1-5 fused with GFP in *N. benthamiana* leaf epidermal cells, the specific entry clones described above (TRB1-3, 5 in pDONR207 and TRB4 in pENTR223) were used in LR Clonase™ II (Thermo Fisher Scientific) reactions to create the pGWB6 (N-terminal GFP fusion under the 35S promoter) expression vectors

(Nakagawa et al. 2007). To label nucleolus or nucleoplasm, we co-transfected *N. benthamiana* leaf epidermal cells with constructs expressing Fibrillarin1-mRFP (Koroleva et al. 2009) or SRp34-mRFP (Lorković et al. 2004; Koroleva et al. 2009), respectively.

For protein expression in *Escherichia coli*, constructs in pDONR207 (for TRB1 and TRB5) or in pENTR223 (for TRB4) were used as donor vectors for LR Clonase™ reactions (Thermo Fisher Scientific), where genes coding proteins of interest (TRB1, 4 and 5) were transferred into the destination vector pHGWA (Busso et al. 2005).

Yeast two-hybrid assays

Y2H was performed using the Matchmaker TM GAL4-based two-hybrid system (Clontech) as described in Schrumpfová et al. 2014. Successful co-transformation of each bait/prey combination into *Saccharomyces cerevisiae* PJ69-4a was confirmed on SD plates lacking Leu and Trp, and interactions assessed on SD medium lacking Leu, Trp and His (with or without 1 mM or 3 mM 3-aminotriazol (3-AT)) or SD medium lacking Leu, Trp and Ade at 30 °C. Co-transformation with an empty vector and homodimerization of the TRB1 protein served as a negative and positive control, respectively (Schrumpfová et al. 2014). Each combination was co-transformed at least three times, and at least three independent drop tests were carried out. Protein expression was verified as described in Schořová et al. 2019.

In vitro translation and co-immunoprecipitation

Proteins were expressed from constructs similar to those used in the yeast two-hybrid system with a hemagglutinin tag (pGADT7-DEST; VRN2, EMF2 and POT1a proteins) or a myc-tag (pGBKT7-DEST; TRB proteins) using a TNT Quick Coupled Transcription/Translation system (Promega) in 50 µl reaction volumes according to the manufacturer's instructions. The VRN2, EMF2 or POT1a proteins were radioactively labelled using ^{35}S-Met. The co-immunoprecipitation procedure was performed as described by Schrumpfová et al. 2008. Input, Unbound and Bound fractions were separated by 10% SDS – PAGE, and analyzed using a FLA7000 imager (Fuji-film).

Transient heterologous expression

A. tumefaciens competent cells (strain GV3101) were transformed with selected expression clones and selected on YEB medium supplemented with gentamycin (50 µg/mL), rifampicin (50 µg/mL), and a vector-specific selection agent (pBiFCt-2in1: spectinomycin 100 µg/mL, pGWB6: kanamycin and hygromycin both 50 µg/mL, pROK2: kanamycin 50 µg/mL) at 28 °C for 48 h. Colonies were inoculated in the same media lacking agar and grown overnight at 28 °C. Bacterial cells of overnight cultures were pelleted by centrifugation (5 min at 1620 g), washed twice, re-suspended, and diluted to an OD_{600} of 0.5 with infiltration medium (10 mM MES pH 5.6, 10 mM $MgCl_2$ and 200 µM acetosyringone). A suspension of *Agrobacterium* cells carrying the p19 repressor plasmid was added in a 1:1 ratio with *Agrobacterium* suspensions harboring plasmids of interest to suppress gene silencing and enhance transient expression (Gehl et al. 2009). Mixed suspensions were incubated with moderate shaking for 1.5–2 h at room temperature and subsequently injected into the abaxial side of leaves of 4-week-old *N. benthamiana* plant. On the third day after infiltration, tobacco epidermal cells were microscopically analyzed. Microscopy images were acquired using the Zeiss LSM880 laser scanning microscope (Axio Observer Z1, inverted) with Definite Focus 2 (excitation 488 nm for GFP/YFP and 561 nm for mRFP). Images were processed using Fiji/ImageJ (Schindelin et al. 2012) and Adobe Photoshop CS6 (Adobe, San Jose, CA, USA) software.

Nuclei isolation and immunofluorescence

Isolation of nuclei was performed using 10-day-old seedlings as described in (McKeown et al. 2008). Nuclei were centrifuged for 20 min at 350 g and 4 °C, resuspended in 1 × PBS and spotted onto slides. Nuclei were briefly dried at 4 °C, then fixed in 4% paraformaldehyde in 1 × PBS, 0.5% Triton-X for 10 min. Nuclei were rinsed three times in 1 × PBS, blocked in 5% goat serum with 0.05% Tween-20 for 30 min at RT and incubated overnight with antibody anti-TRB 5.2 (Schrumpfová et al. 2014) diluted 1:300 in 5% BSA in 1 × PBS. Nuclei were washed three times for 5 min in 1 × PBS supplemented with 0,05% Tween-20 (PBST), then incubated 1 h with an anti-mouse Alexa 488 antibody, Invitrogen (1:750 dilution). Slides were washed three times for 5 min in 1 × PBST, then dehydrated in ethanol series as described in Kutashev et al. 2021. Coverslips were mounted in 4′,6-Diamidine-2′-phenylindole dihydrochloride (DAPI), 2 µg/mL in Vectashield and imaged using fluorescence using a Zeiss AxioImager Z1 epifluorescence microscope.

Expression of TRB1, 4 and 5 in *E. coli*

Proteins fused with His-tags were expressed in *E. coli* (BL21(DE3) RIPL) from the destination vector pHGWA. BL21(DE3) RIPL were grown in Luria–Bertani medium supplemented with ampicillin and chloramphenicol to final concentration 100 ug/ml and 12,5 ug/ml at 37 °C until OD_{600} reached 0.5. Cells were cultured for 4 h at 25 °C after the addition of IPTG to a final concentration of 0.5 mM. Cells were collected by centrifugation (8,000 g, 8 min, 4 °C). The cell pellet was dissolved in lysis buffer containing 50 mM

sodium phosphate (pH 8.0), 300 mM NaCl, 10 mM imidazole, 5 mM β-mercaptoethanol, and protease inhibitor cocktail cOmplete tablets EDTA-free (Roche). The cell suspension was sonicated on ice for 6 min of process time with 1 s pulse and 2 s pause (Misonix). Cell lysate supernatant was collected after centrifugation at 20,000 g, 4 °C for 1 h. Proteins were purified by immobilized-metal affinity chromatography using TALON® metal affinity resin (Clontech), where filtered supernatant (0.45 µm filter) was mixed with TALON® beads and incubated for 1 h. The proteins of interest were eluted with 100 mM imidazole in the same buffer. These proteins were then concentrated, and the buffer was exchanged for 50 mM sodium phosphate (pH 7.0), 300 mM NaCl by ultrafiltration (Amicon 3 K/30 K, Millipore). The concentration of purified proteins was determined using the Bradford assay. We evaluated protein purity using SDS–polyacrylamide gel electrophoresis, with gels stained by Bio-Safe Coomassie G250 (Bio-Rad). To ensure successful purification, the purified proteins were detected by specific monoclonal mouse anti-polyhistidine antibody as described previously (Schrumpfová et al. 2004) and by matrix-assisted laser desorption-ionization tandem mass spectrometry (MALDI-MS/MS) (CEITEC Proteomics Core Facility).

Electrophoretic mobility shift assay (EMSA)

DNA probes and competitors used are described in Supplemental Table 1. To reduce a non-specific DNA–protein binding, 10 pmol of purified TRB1, 4 or 5 were preincubated with 1, 10, or 100 pmol of a specific competitor (oligodeoxynucleotides of non-telomeric or competitor telomeric sequence in double-stranded form, as indicated in Results) for 20 min in EMSA buffer (10 mM Tris–HCl pH 8.0, 1 mM EDTA, 1 mM dithiothreitol, 50 mM NaCl, and 5% w/v glycerol). Probes were end-labelled using [γ-^{32}P]ATP and polynucleotide kinase (New England Biolabs), according to (Sambrook et al. 1989). A probe (1 pmol) was added to the reaction mixture on ice and incubated for 20 min before the mixture was loaded onto a 7.5% w/v non-denaturing polyacrylamide gel (AA:BIS = 37.5:1, 0.5 × TBE, 1.5 mm thick). Electrophoresis was at 15 °C for 3 h at 10 V/cm in a precooled buffer. Signals of labelled oligonucleotides were detected using a phosphorimager FLA-7000IP (Fujifilm).

Results

Sequence and structural divergences in the TRB family

Two decades ago, in silico analysis already predicted that the *A. thaliana* SMH family contains five TRB members (Marian et al. 2003). We used a combination of recent genome and transcriptome annotations (Lamesch et al. 2012; Cheng et al. 2017) and predicted sequence and structural similarity to characterize the TRB family members TRB4 and TRB5. These were each found to contain an N-terminal Myb-like domain, a central H1/5-like domain, and a C-terminal coiled-coil domain, similar to previously characterized family members TRB1-3 (Fig. 1A) (Marian et al. 2003; Schrumpfová et al. 2004; Mozgová et al. 2008).

We then performed a phylogenetic reconstruction of TRB proteins from the *Brassicaceae* family based on a matrix including 52 TRBs, with 357 aligned positions. The tree shows that in *A. thaliana*, as well as in other *Brassicaceae*, TRB4 and TRB5 are grouped in a monophyletic lineage that is distant from TRB1-3 (Fig. 1B, Supplemental Table 2).

The Myb-like domain is composed of a helix-turn-helix (HTH) motif (Ogata et al. 1992; Bilaud et al. 1996). Even though the domain composition of SMH proteins is unique to the plant lineage, the Myb-like domain shows high aa sequence conservation across the plant and animal kingdoms (Fig. 1C). Predicted three-dimensional (3D) models of *A. thaliana* TRB Myb-like structural features were overlaid with the X-ray diffraction-resolved crystal structure of human Telomeric repeat-binding factor 2 (hTRF2) (Fig. 1D) and it was found that the 3D structure of the Myb-like domain is well conserved in both plant and animal kingdoms. Interestingly, all TRBs show a slight difference in the composition of the second helix. However, the aa residues mediating the interaction between hTRF2 and the human telomeric repeat sequence (TTAGGG) are fully conserved in *A. thaliana* even though the plant telomeric sequence slightly differs (TTTAGGG) from the human one (Fig. 1C, D).

The central linker histone globular domain (H1/5-like domain) adopts a winged-helix fold including a HTH motif and a "wing" defined by two β-loops (Ramakrishnan et al. 1993). Using the SWISS-MODEL tool, the *Xenopus laevis* (Xl) H1 domain (XlH1.0) appeared to be the closest template to *A. thaliana* TRBs H1/5-like domain (Bednar et al. 2017). We compared the 3D structure of the histone globular domain from XlH1.0-B, obtained by cryo-electron microscopy (Cryo-EM) and X-ray crystallography (Bednar et al. 2017), with the AlphaFold protein structure predictions of the H1/5-like domain of *A. thaliana* TRBs (Varadi et al. 2022). Although the sequence conservation between the XlH1 domain and the H1/5-like domain of *A. thaliana* TRBs is lower than in the Myb-like domain, the 3D structure of the H1/5-like domain in TRBs is highly similar (Fig. 1C, D).

The C-terminal coiled-coil domains usually contain a repeated pattern of hydrophobic and charged aa residues, referred to as a heptad repeat (Lupas and Gruber 2005). This repeating pattern enables two helices to wrap/coil around each other. The conservation of hydrophobic residues (Alanine (A), Isoleucine (I), Valine (V), Phenylalanine (F) or Methionine (M)) and an acidic residue (Glutamic acid (E))

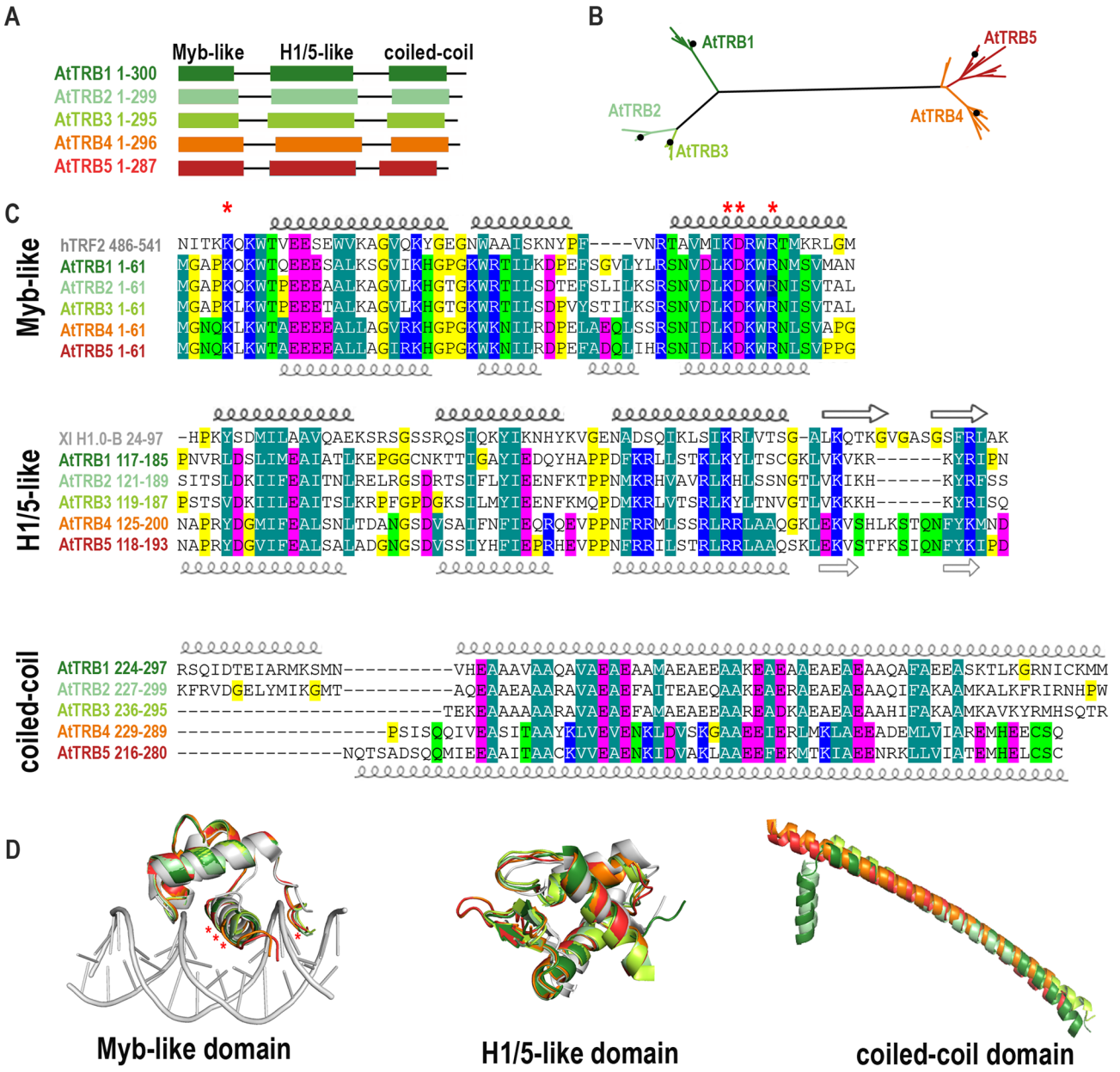

Fig. 1 Sequence and structural alignments of TRB family proteins. (**A**) Schematic representation of the conserved domains of TRBs from *A. thaliana*. *Myb-like*, Myb-like domain; *H1/5-like*, histone-like domain; *coiled-coil*, C-terminal domain. (**B**) Unrooted Maximum likelihood (ML) phylogenetic tree of *Brassicaceae* TRB proteins. The length of the branches are proportional, and the black dots indicate the position of TRB1-5 from *A. thaliana*. For a list of species, see Supplementary Table 2. (**C**) Multiple alignments of the Myb-like, H1/5-like and coiled-coil domains. The positions of α-helices or β-sheets of the uppermost or the lowermost sequence in each alignment are highlighted: *bold*, experimentally determined structures (cryo-EM or X-ray crystallography); *thin*, AlphaFold prediction. Human Telomeric repeat-binding factor 2 (hTRF2) and *Xenopus laevis* histone H1.0 (Xl H1.0-B) were used to show the most conserved amino acid (aa) residues. Amino acid shading indicates the following conserved amino acids: *dark green*, hydrophobic and aromatic; *light green*, polar; *blue*, basic; *magenta*, acidic; *yellow*, without side chain (glycine and proline). The aa of hTRF2 that mediate intermolecular contacts between telomeric DNA and hTRF2 are marked with an asterisk. (**D**) Structural models of Myb-like, H1/5-like and coiled-coil domains. AlphaFold protein structure predictions deposited in the EMBL database were used (Varadi et al. 2022). The three-dimensional model of the Myb-like domain fits best the hTRF2-DNA interaction structure (PDB: 1WOU) (Court et al. 2005). The structure of the histone-like domain is most similar to *X. laevis* histone H1 structure (PDB: 5NL0) (Bednar et al. 2017). The positions of the aa of hTRF2 that mediate intermolecular contacts between telomeric DNA and hTRF2 are marked with an asterisk

is obvious in all coiled-coil domains from *A. thaliana* TRBs. Only one long α-helix is predicted by AlphaFold in TRB4-5, while the coiled-coil domains from TRB1 and TRB2 seem to have an additional short α-helix (Fig. 1C, D). However, these predictions await experimental verification.

The most divergent of the three domains in TRBs (Myb-like, H1/5-like and coiled-coil) is the coiled-coil domain. Our alignments suggest that although TRB4 and TRB5 are distant from TRB1-3 members in terms of sequence, they are folded into similar three-dimensional structures, with only minor differences.

The evolution of TRBs within the plant lineage

We performed comprehensive phylogenetic analysis to investigate whether TRBs are conserved across lower and higher plants, and whether TRB4-5 form a distinct group to TRB1-3 in all species, as observed in the higher plant *A. thaliana*. We used a data set of 268 proteins and 599 aligned positions and found that TRB proteins first evolved in Streptophyta in *Klebsormidiophyceae*, although TRBs are missing in the other Streptophyte algae studied, including *Charophyceae* and *Zygnematophyceae*. In *Klebsormidium nites* only one TRB homolog was identified. Following the evolutionary tree, an increasing number of TRB homologues were found in Bryophyta and Tracheophyta. There are three homologues of TRB in mosses *Sphagnum fallax* and *Physcomitrium patens*, and these TRBs share very high sequence similarities. Contrastingly, there is only one homologue in the moss *Ceratodon purpureus*. Perhaps due to limited sequence information available for the genomes of hornworts or liverworts, TRB was not found in these lineages. In seed plants, which have undergone more rounds of whole genome duplication events (WGDs) than Bryophyta and Lycophyta (Clark and Donoghue 2018), predominantly three TRB proteins were recognized. Within *Brassicaceae*, which has undergone an additional recent round of WGD (Walden et al. 2020), five TRB homologs were revealed (Fig. 2A).

Next, the MEME search (Bailey et al. 2009) was used to identify the 15 most typical motifs in TRBs across the plant kingdom (Supplemental Fig. 1). For ease of presentation, a simplified tree was used with 83 representatives from 33 families and 26 orders, each family having only one member (Fig. 2B, Supplemental Table 3). TRB proteins were divided into three main lineages named TRB_A, TRB_B and TRB_C, into the latter of which the TRB_D sub-lineage is integrated. The lineage TRB_A includes Streptophyte algae, Bryophyta and Lycophyta and diverges from seed plant lineages TRB_B and TRB_C in terms of the length of introns, disordered parts of proteins or additional motifs. A clear diversification of TRBs into monocots and dicots was revealed in both TRB_B and TRB_C lineages. In seed plants, the TRB_B lineage seems to be less abundant than the TRB_C lineage.

Consistent with previous findings, the canonical N-terminal Myb-like (motif 1), a central H1/5-like (motifs 2, 4 and 7), and a C-terminal coiled-coil (motif 3) domains include the top conserved motifs present in all TRBs (Fig. 2B). Within the lineage TRB_A, a unique aa motif was detected in Bryophytes (motif 15; EEREH). Interestingly, the coiled-coil domains of the proteins from TRB_B lineage contain the specific motif 11 (EDTDS), but most of the proteins from the TRB_A and TRB_C lineage contain the motif 6 (DAEAA) instead. However, motif 6 is not present in the *A. thaliana* protein TRB5 that has diverged from TRB4. The *A. thaliana* proteins TRB4 and TRB5 (belonging to the TRB_B lineage) lack motif 8 (DDVKI) adjacent to the coiled-coil domain. In contrast, this motif is present within proteins of the TRB_C lineage, including *A. thaliana* TRB1-3 proteins.

The TRB_D sub-lineage is embedded within TRB_C lineage but supported by a high 99% bootstrap value. TRB2 and TRB3 from *A. thaliana* are nested within the TRB_D sub-lineage. This lineage lacks motif 5 (MSVMA), a motif adjacent to the Myb-like domain, which is present in the rest of the TRBs in the TRB_C lineage. Similarly to *Brassicaceae*, divergence to the TRB_D sub-lineage was detected within several other dicot families (e.g., *Rhamnaceae - Ziziphus jujuba, Cucurbitaceae - Cucumis sativus*, *Euphorbiaceae - Ricinus communis*, *Rutaceae - Citrus sinensis, Malvaceae - Glycine max, Cleomaceae - Tarenaya hassleriana*).

In general, TRBs were detected in lower and higher plants. TRBs in Streptophyte algae, Lycophyta and Bryophyta (grouped in TRB_A lineage) are more closely related to *A. thaliana* TRB4 and TRB5 proteins (TRB_B lineage) than to *A. thaliana* TRB1-3 (TRB_C lineage). Lineage TRB_B and TRB_C differ in several motifs accompanying the canonical H1/5-like or coiled-coil domains. The specificity of the sub-lineage TRB_D, embedded into TRB_C lineage, is highlighted by its lack of a specific motif 5 following the canonical Myb-like domain.

The TRB4-5 from dicots differ in solution accessible surface of the Myb-like domain

The N-terminal Myb-like domain is the most conspicuous structural unit in TRBs. In order to compare the structural characteristics of this, we further examined the sequence conservation and estimated evolutionary conservation of predicted 3D structures. The TRB groups (TRB_A, B, C, D), established in Fig. 2B, were subdivided into Lycophytes, Bryophytes, Monocots and Dicots. Consensus sequences of the Myb-like domain in each individual group are visualized in Fig. 3A.

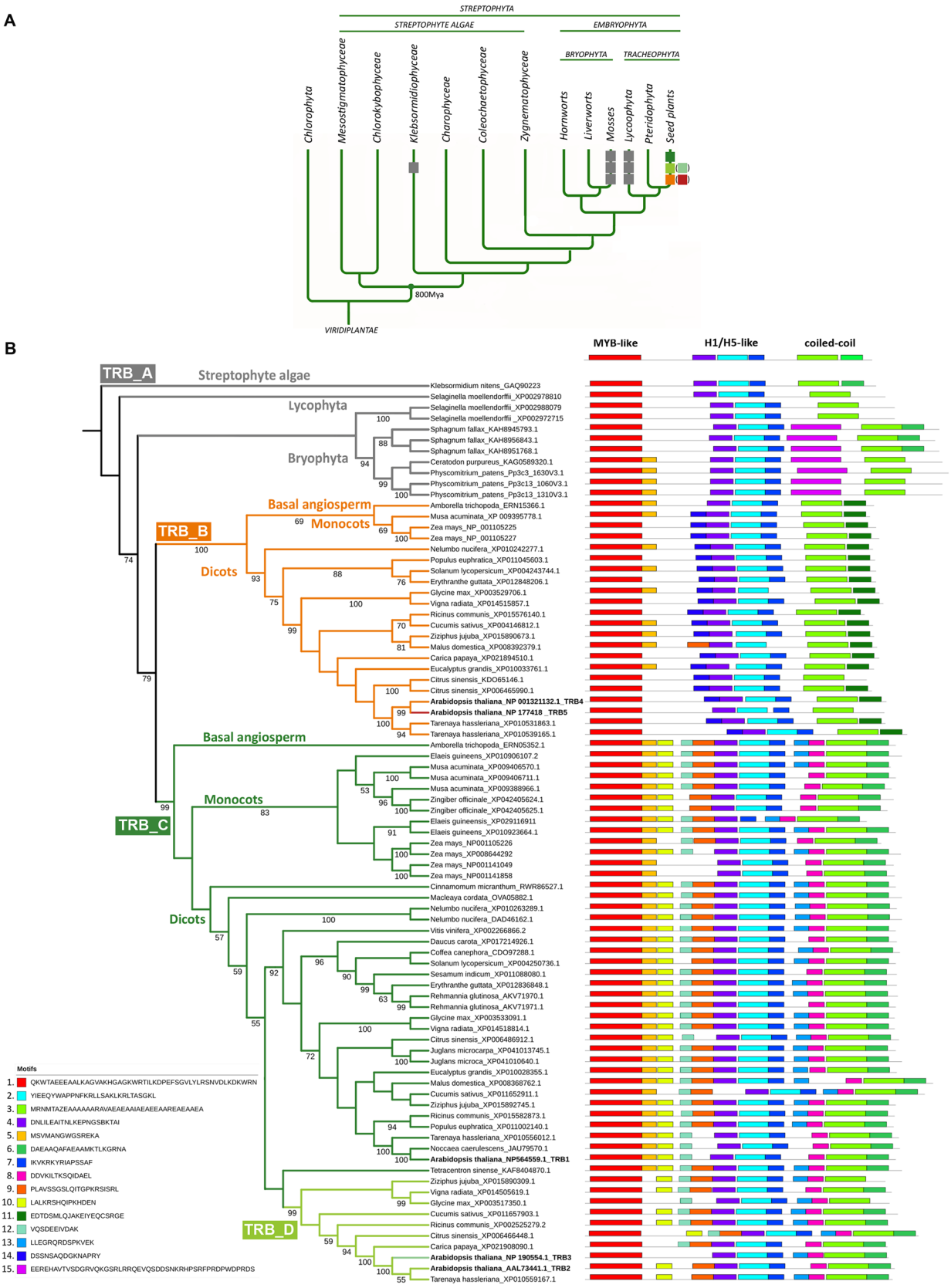
A
STREPTOPHYTA
STREPTOPHYTE ALGAE
EMBRYOPHYTA
BRYOPHYTA
TRACHEOPHYTA
Chlorophyta
Mesostigmatophyceae
Chlorokybophyceae
Klebsormidiophyceae
Charophyceae
Coleochaetophyceae
Zygnematophyceae
Hornworts
Liverworts
Mosses
Lycoophyta
Pteridophyta
Seed plants
800Mya
VIRIDIPLANTAE
B
MYB-like
H1/H5-like
coiled-coil
TRB_A
Streptophyte algae
Lycophyta
Bryophyta
TRB_B
Basal angiosperm
Monocots
Dicots
TRB_C
Basal angiosperm
Monocots
Dicots
TRB_D
Klebsormidium nitens_GAQ90223
Selaginella moellendorffii_XP002978810
Selaginella moellendorffii_XP002988079
Selaginella moellendorffii _XP002972715
Sphagnum fallax_KAH8945793.1
Sphagnum fallax_KAH8956843.1
Sphagnum fallax_KAH8951768.1
Ceratodon purpureus_KAG0589320.1
Physcomitrium_patens_Pp3c3_1630V3.1
Physcomitrium_patens_Pp3c13_1060V3.1
Physcomitrium_patens_Pp3c13_1310V3.1
Amborella trichopoda_ERN15366.1
Musa acuminata_XP 009395778.1
Zea mays_NP_001105225
Zea mays_NP_001105227
Nelumbo nucifera_XP010242277.1
Populus euphratica_XP011045603.1
Solanum lycopersicum_XP004243744.1
Erythranthe guttata_XP012848206.1
Glycine max_XP003529706.1
Vigna radiata_XP014515857.1
Ricinus communis_XP015576140.1
Cucumis sativus_XP004146812.1
Ziziphus jujuba_XP015890673.1
Malus domestica_XP008392379.1
Carica papaya_XP021894510.1
Eucalyptus grandis_XP010033761.1
Citrus sinensis_KDO65146.1
Citrus sinensis_XP006465990.1
Arabidopsis thaliana_NP 001321132.1_TRB4
Arabidopsis thaliana_NP 177418 _TRB5
Tarenaya hassleriana_XP010531863.1
Tarenaya hassleriana_XP010539165.1
Amborella trichopoda_ERN05352.1
Elaeis guineens_XP010906107.2
Musa acuminata_XP009406570.1
Musa acuminata_XP009406711.1
Musa acuminata_XP009388966.1
Zingiber officinale_XP042405624.1
Zingiber officinale_XP042405625.1
Elaeis guineensis_XP029116911
Elaeis guineens_XP010923664.1
Zea mays_NP001105226
Zea mays_XP008644292
Zea mays_NP001141049
Zea mays_NP001141858
Cinnamomum micranthum_RWR86527.1
Macleaya cordata_OVA05882.1
Nelumbo nucifera_XP010263289.1
Nelumbo nucifera_DAD46162.1
Vitis vinifera_XP002266866.2
Daucus carota_XP017214926.1
Coffea canephora_CDO97288.1
Solanum lycopersicum_XP004250736.1
Sesamum indicum_XP011088080.1
Erythranthe guttata_XP012836848.1
Rehmannia glutinosa_AKV71970.1
Rehmannia glutinosa_AKV71971.1
Glycine max_XP003533091.1
Vigna radiata_XP014518814.1
Citrus sinensis_XP006486912.1
Juglans microcarpa_XP041013745.1
Juglans microca_XP041010640.1
Eucalyptus grandis_XP010028355.1
Malus domestica_XP008368762.1
Cucumis sativus_XP011652911.1
Ziziphus jujuba_XP015892745.1
Ricinus communis_XP015582873.1
Populus euphratica_XP011002140.1
Tarenaya hassleriana_XP010556012.1
Noccaea caerulescens_JAU79570.1
Arabidopsis thaliana_NP564559.1_TRB1
Tetracentron sinense_KAF8404870.1
Ziziphus jujuba_XP015890309.1
Vigna radiata_XP014505619.1
Glycine max_XP003517350.1
Cucumis sativus_XP011657903.1
Ricinus communis_XP002525279.2
Citrus sinensis_XP006466448.1
Carica papaya_XP021908090.1
Arabidopsis thaliana_NP 190554.1_TRB3
Arabidopsis thaliana_AAL73441.1_TRB2
Tarenaya hassleriana_XP010559167.1
Motifs
1. QKWTAEEEAALKAGVAKHGAGKWRTILKDPEFSGVLYLRSNVDLKDKWRN
2. YIEEQYWAPPNFKRLLSAKLKRLTASGKL
3. MRNMTAZEAAAAAARAVAEAEAAIAEAEEAARREAEAAEA
4. DNLILEAITNLKEPNGSBKTAI
5. MSVMANGWGSREKA
6. DAEAAQAFAEAAMKTLKGRNA
7. IKVKRKYRIAPSSAF
8. DDVKILTKSQIDAEL
9. PLAVSSGSLQITGPKRSISRL
10. LALKRSHQIPKHDEN
11. EDTDSMLQJAKEIYEQCSRGE
12. VQSDEEIVDAK
13. LLEGRQRDSPKVEK
14. DSSNSAQDGKNAPRY
15. EEREHAVTVSDGRVQKGSRLRRQEVQSDDSNKRHPSRFPRDPWDPRDS

◂**Fig. 2** Phylogenetic analysis of TRB proteins. (**A**) Simplified evolution of the main Viridiplantae lineages with known TRB proteins. One TRB protein evolved initially in Streptophyta in *Klebsormidiophyceae*, then diversified to three similar homologues in Mosses and Lycophyta and several diverse homologues in seed plants, with five members in *A. thaliana* from *Brassicaceae*. The evolutionary tree was adopted from Rensing 2020 and Cheng et al. 2019. (**B**) ML phylogenetic tree of TRB proteins. Twenty-seven species were included in 83 sequences with 465 bp in the final data set. Only one species from the family was selected for the final analysis. The ML likelihood is -24,356.573420. The numbers below branches indicate bootstrap support values > 50%. Four major groups are shown in the phylogenetic tree: TRB_A for Streptophyte algae, Lycophyta and Bryophyta; TRB_B including AtTRB4 and AtTRB5 for Embryophyta; TRB_C for Embryophyta with AtTRB1 and the nested TRB_D encompassing AtTRB2 and AtTRB3. Motifs are ranked and ordered by the highest probability of occurrence. Fifteen most probable motifs are depicted. For sequence and sequence conservation information, see Supplementary Fig. 1. For a list of species, see Supplementary Table 3

The evolutionary dynamics of aa substitutions in *A. thaliana* TRB4, 1 and 2, representing Dicots from lineages TRB_B, C and D, respectively, were visualized using ConSurf 2016 (Ashkenazy et al. 2016). Visualization has shown a very strong conservation of the DNA-binding surface in all lineages (Supplemental Fig. 2), consistent with the above analysis (Figs. 1 and 2). In comparison, opposite solution-accessible surface was less conserved; in Dicots from the TRB_D lineage, conservation was lower than in Dicots from TRB_B and TRB_C lineages (Fig. 3B, Supplemental Fig. 2). Dicots in all three lineages exhibit a variant unstructured N-terminus of the MYB-domain which is conserved within the lineage. The aa at the N-terminal position 3 in Dicots from the TRB_B lineage, including TRB4-5 from *Arabidopsis*, show significantly conserved substitutions of Alanine (A) residues to the polar uncharged aa Asparagine (N) (Fig. 3, *Inverted triangle*). The unstructured C-terminal tail of the Myb-like domain in the TRB_B lineage (Fig. 3, *Triangle*, Supplemental Fig. 2A) shows less conservation than in TRB_C and TRB_D lineages, where these residues are part of the third helix.

Surface models showing the charge of the Myb-like domain were visualized using PyMol viewer (Fig. 3C, Supplemental Fig. 2C, F). In the TRB_B lineage, visualizations reveal a negatively charged aa (E/D) at position 14 (Fig. 3, *Rhombus*) flanking conserved EEE motif (Fig. 3, *Circle),* whereas proteins in the TRB_A and TRB_C lineages possess uncharged Alanine (A) at the position 14. Interestingly, the aa (positively charged aa K/R at position 17) proximal to the E/D motif, are replaced to uncharged (L) in Dicots from TRB_B lineage (Fig. 3C, *Trapezoid*).

These data indicate that the E/D motif at position 14 together with aa at position 17 are responsible for the additional areas of negative charge on the solution-accessible surface of the Myb-domain in Dicots from TRB_B lineage.

Even one telomeric unit is sufficient for TRB binding

Our previous findings revealed that the N-terminal Myb-like domains of TRB1-3 are responsible for specific recognition of long arrays of telomeric DNA (Schrumpfová et al. 2004; Mozgová et al. 2008). The DNA-binding preference for oligodeoxynucleotide (oligo) substrates was tested using the electrophoretic mobility shift assay (EMSA). Oligo sequences were designed to assess the effect of TRB4 and TRB5 binding to long arrays of telomeric sequences as well as to interstitially located *telo*-boxes (Fig. 4A, Supplemental Table 1). Either a tetramer of telomeric sequences or a *telo*-box sequence (1.2 telomeric units) flanked with non-telomeric DNA were used as the labelled probes. A non-telomeric oligonucleotide, added in 1, 20 and 100-fold excess, served as competitor DNA and vice versa. Parallel experiments with the TRB1 protein were used for comparison.

The results obtained from these experiments clearly show that TRB4 and TRB5 do indeed preferentially bind long arrays of telomeric sequences or *telo*-boxes positioned within a non-telomeric DNA sequence (Fig. 4B–D). TRBs bind to telomeric dsDNA in a similar mode as was described for TRB1-3, forming a high-molecular-weight complex which does not migrate into the gel (Schrumpfová et al. 2004; Mozgová et al. 2008). The binding of all three TRB proteins to the telomeric sequence is highly specific, as even a 100-fold higher concentration of non-telomeric competitor does not prevent the formation of protein-telomeric DNA complex.

Our data indicate that TRB4-5, as well as other TRBs, are capable of binding long arrays of telomeric sequences or short motifs with as little as one telomeric repeat. This is in contrast to human TRF1/TRF2, which bind two telomeric repeats as preformed dimers (Court et al. 2005) and also to previous predictions (Hofr et al. 2009). Having defined the TRB minimal recognition motif as one *telo*-box, the binding properties of TRBs are poised for further investigation.

Unlike other TRB family members, TRB5 is preferentially localized in the cytoplasm

To compare *Arabidopsis* TRB proteins further, we examined the subcellular localization of native TRB proteins in *Arabidopsis* cells, using a mouse monoclonal antibody developed in our laboratory specific for the conserved section of the Myb-like domain found in the TRB family. The anti-TRB 5.2 antibody recognizes all five members of TRB family (Schrumpfová et al. 2014). Nuclei isolated from 10-day-old seedlings were subjected to immunofluorescence using

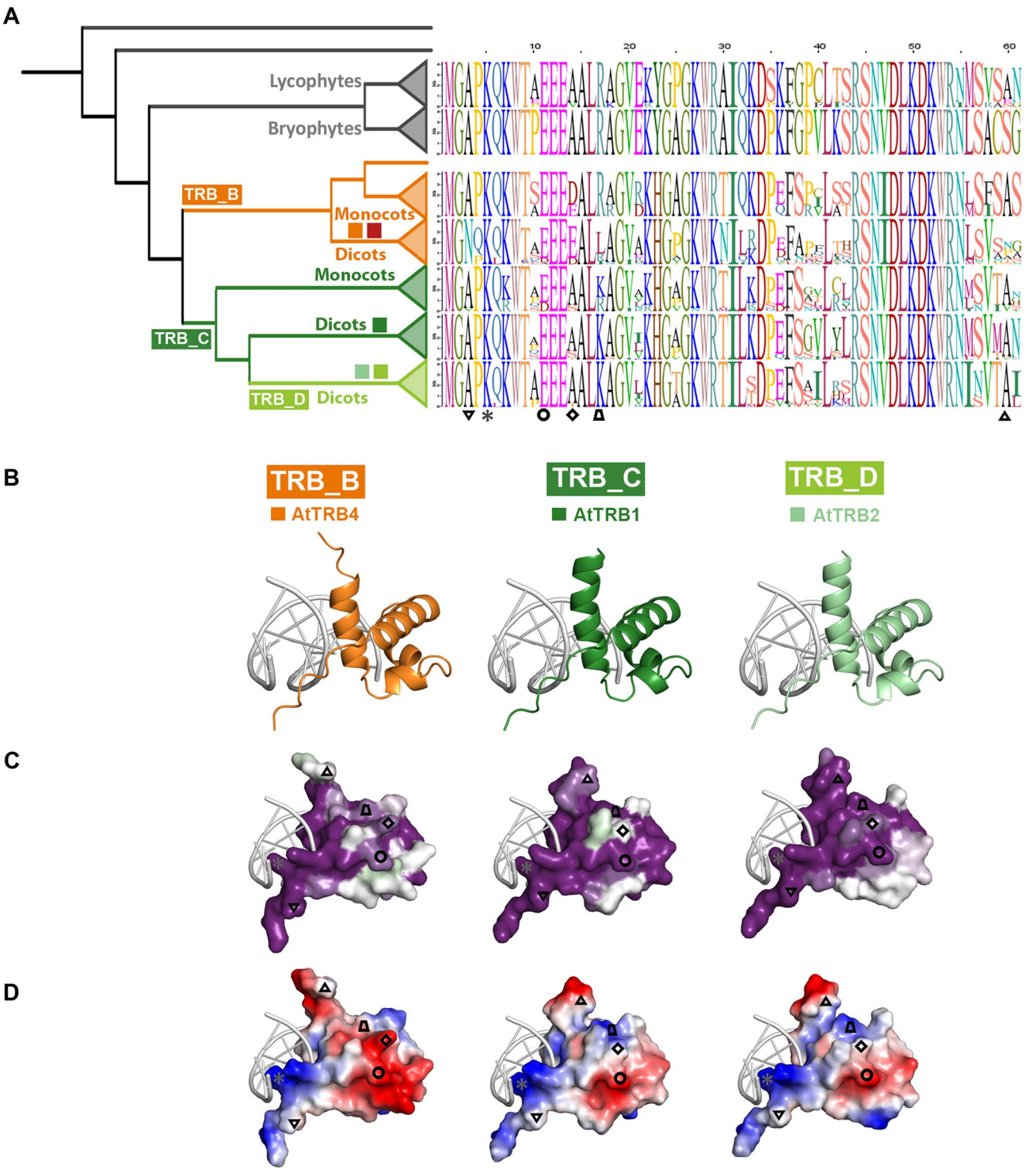

this anti-TRB antibody combined with DAPI staining. We observed a speckled distribution of TRBs in the nucleus and nucleolus (Fig. 5A).

As the anti-TRB 5.2 antibody does not distinguish the localization of individual proteins, we proceeded to the subcellular localization of individual members of TRB family using TRBs fused with green fluorescent protein (GFP). Confocal microscopy showed that TRB1-3 fused with GFP expressed from pGWB6 after transient *Agrobacterium*-mediated transformation in *N. benthamiana* leaf epidermal cells are localized mainly in nucleoli and nucleoplasmic fluorescence foci, as was described previously (Schrumpfová et al. 2014; Zhou et al. 2016). Interestingly, TRB4 is distributed not only in nucleoli and nucleoplasmic

◂**Fig. 3** Conserved features of MYB-like domain through TRB lineages. (**A**) Consensus sequences of Myb-like domain in each evolutionary lineage were visualised using sequence logos. *Colored squares*, represent TRB1-5 proteins from *A. thaliana*; *Inverted triangle*, the aa at position 3 (**B**) at N-terminus of TRBs that is replaced in Dicots from TRB_B lineage to N; *Asterisk*, the aa at position 5 (K) that mediates intermolecular contacts between telomeric DNA and N-terminus of all TRBs (Fig. 1C); *Circle*, the negatively charged aa (E/D) at position 11 conserved across all TRB lineages; *Rhombus*, the aa at position 14 replaced from uncharged (A/S) to negatively charged (E/D) in the whole TRB_B lineage; *Trapezoid*, the aa at position 17 that is in Dicots from TRB_B lineage partially replaced from positively charged (K/R) to hydrophobic (L); *Triangle*, the aa at position 60 that shows lower conservation in Dicots from TRB_B lineage than in other lineages. (**C**) The representative members of Dicots from TRB_B, TRB_C and TRB_D lineages, namely *A. thaliana* TRB4, TRB1 and TRB2, respectively, were analyzed. The three-dimensional model of the Myb-like domains from the site opposing the DNA-binding viewpoints are based on the hTRF2-DNA interaction model (PDB: 1WOU) (Court et al. 2005). The evolutionary dynamics of aa substitutions among aa residues within Myb-domain of these exemplified were visualized using ConSurf 2016 (Ashkenazy et al. 2016). The conservation of residues is presented in a scale, where the most conserved residues are shown in dark magenta and non-conserved residues as white. (**D**) Surface models showing the charge on the Myb-like domain are presented from the site opposing the DNA-binding viewpoint for each model. Residue charges are coded as red for negative, blue for positive, and white for neutral, visualised using PyMol, Version 2.4.1, Schrödinger, LLC

fluorescence foci of different sizes, but also throughout the nucleoplasm. Conversely, TRB5 fused with GFP is localized mainly in the cytoplasm with only minor localization in the nucleolus and nucleoplasm (Fig. 5B, Supplemental Figs. 3, 4).

Co-expression of GFP-TRBs with the nucleolar marker Fibrillarin1 or nucleoplasm marker Serine-arginine-rich proteins 34 (SRp34) fused with a monomeric red fluorescent protein (mRFP) after transient *Agrobacterium*-mediated transformation in *N. benthamiana* leaf epidermal cells verified the subnuclear localizations of the TRB4 and TRB5 described above. Using Fibrillarin-mRFP we clearly identified the stronger localization of GFP-TRB4 in the nucleolus, but the weak nucleolar localization of GFP-TRB5. The relative positioning of GFP-TRB and the nucleoplasm marker SRp34-mRFP also supports our observation that the GFP-TRB5 is preferentially localized in the cytoplasm (Fig. 5C).

TRB4-5 fused with GFP show a distinct localization in the plant cell compared to TRB1-3, proteins with a later evolutionary origin. In particular, GFP-TRB5 manifests strong cytoplasmic localization, suggesting a possible specific functional role or spatiotemporal regulation.

Dimerization of TRB proteins

To shed light on the conservation of mutual interactions between TRB proteins from *Arabidopsis*, we analyzed interactions between all members of TRB family. To date, self and mutual dimerization of TRB1-3 has been investigated by Y2H or by co-immunoprecipitation experiments (Co-IP) (Kuchař and Fajkus 2004; Schrumpfová et al. 2004, 2008; Mozgová et al. 2008), however knowledge of the precise subcellular localization of mutual TRB interactions is missing.

First, the interactions of TRB4 and TRB5 with other TRB family members were investigated using a GAL4 based Y2H assay. Mutual interactions between TRB family members from *Arabidopsis* appear to be conserved, as both TRB4 and TRB5, interact with all TRB family members. Moreover, TRB4-5 form self-dimers in a similar way to TRB1-3 (Fig. 6A).

Next, BiFC assays with equal protein levels were used to detect self- and mutual interactions of TRBs at the level of cellular compartments. The TRB coding sequences were introduced into 2in1 multiple expression cassettes within a single vector backbone with an internal marker for transformation and expression-mRFP1 (Grefen and Blatt 2012). TRBs were fused with an N- and/or C-terminal half of yellow fluorescent protein (nYFP, cYFP) as both N-terminal and C-terminal fusions. A list of all constructs is provided in Supplemental Table 4. Fluorescence was detected using confocal laser scanning microscopy after transient *Agrobacterium*-mediated transformation in *N. benthamiana* epidermal cells. Our observations show self- and mutual interactions of TRB1-4 in the nucleolus and/or in nucleoplasmic fluorescence foci that were of different numbers and sizes. Interestingly, the TRB5 homodimeric interaction was found to be clearly cytoplasmic with a reduced nuclear speckle size compared to other TRB interactions. Additionally, TRB1-3, but not TRB4, interact moderately with TRB5 in the nucleolus, as well as in more prominent nucleoplasmic fluorescence foci (Fig. 6B, Supplemental Figs. 5, 6).

Overall, our characterization of mutual TRB interactions revealed that all TRB members have the ability to form self-dimers and mutually interact. However, TRB5 homodimeric interactions are predominantly localized in the cytoplasm, which differs from TRB1-4 homodimeric interactions, which are nucleolar or localized in nucleoplasmic fluorescence foci.

Novel interaction partners of TRB proteins—PRC2 subunits EMF2 and VRN2

To further elucidate the conservation of protein interaction partners throughout the TRB family, we looked for interactions between TRB4 and TRB5 with TERT, RUVBLs, POT1b, PWO1-3, SWN, CLF interactors, which have already been described as interacting with TRB1-3 (Schrumpfová et al. 2008, 2014; Hohenstatt et al. 2018; Zhou et al. 2018; Tan et al. 2018; Schořová et al. 2019;

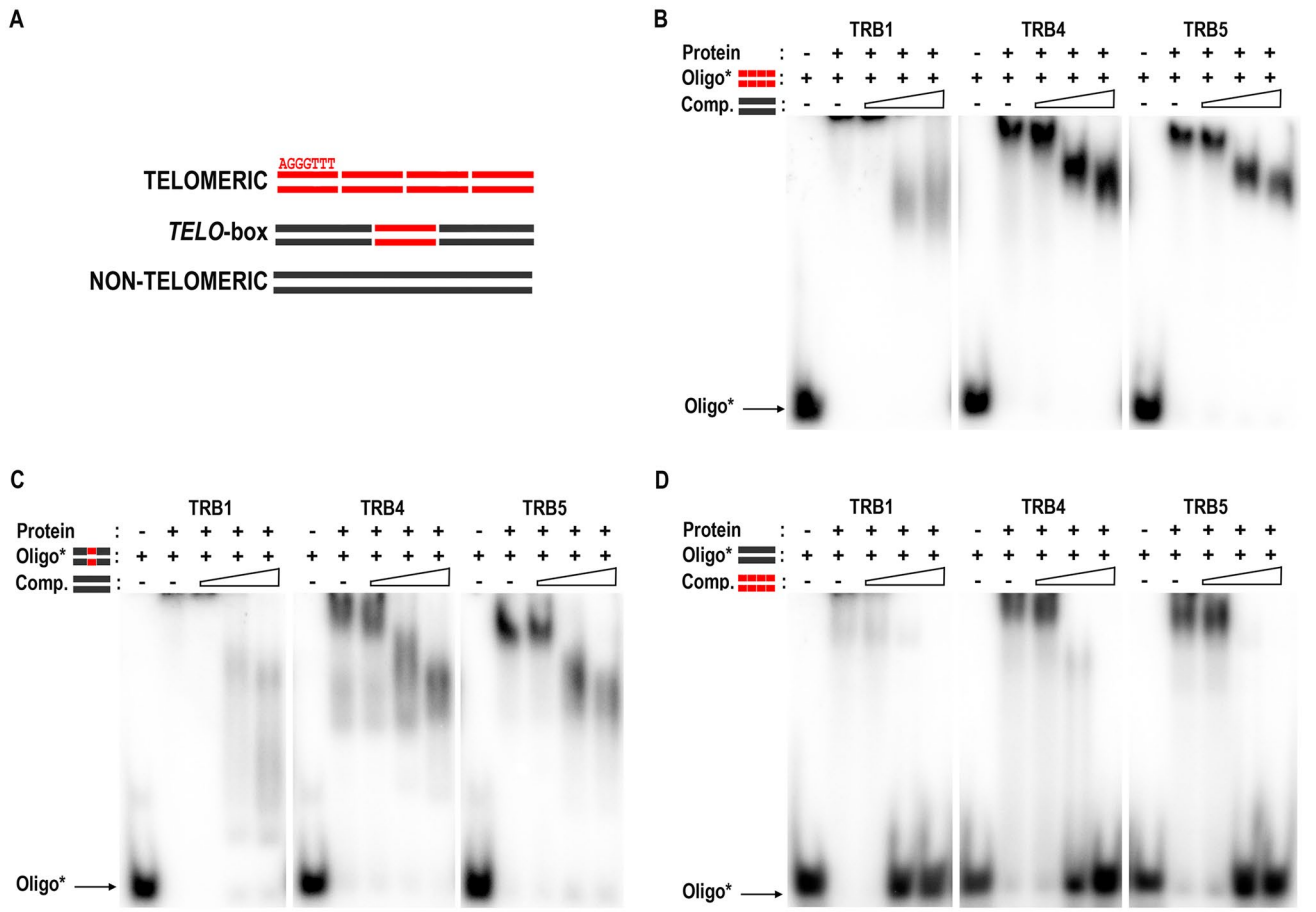

Fig. 4 EMSA of TRB1, TRB4 and TRB5 binding of radioactively-labelled oligonucleotides. (**A**) Schematic depiction of oligonucleotides employed. *Telomeric*, four repeats of plant telomeric DNA sequence; *telo-box*, 1.2 plant telomeric units flanked with non-telomeric DNA sequence; *non-telomeric*, oligonucleotide with non-telomeric DNA. (**B**) EMSA of TRB1, TRB4 and TRB5 proteins binding radioactively-labelled double-strand (ds) tetramers of telomeric sequence with unlabelled tetramers of non-telomeric oligonucleotides as competitor DNA. The concentration of unlabelled competitor increases from 1-, 20- to 100-fold the concentration of the labelled probe (as depicted by the triangle). Oligo*: protein ratio is 1:10. (**C**) EMSA of the same proteins with a radioactively-labelled ds *telo*-box oligonucleotides with unlabelled non-telomeric oligonucleotides as competitor DNA, performed as in B. (**D**) EMSA of the same proteins with a radioactively-labelled ds of non-telomeric oligonucleotides with unlabelled ds tetramers of telomeric sequence as competitor DNA, performed as in B

Mikulski et al. 2019). These interactions were investigated using a GAL4-based Y2H assay, and TRB interactions with newly identified protein interactors were verified by Co-IP.

Our results revealed that TRB4-5 interact with the N-terminal domains of TERT called telomerase essential N-terminal (TEN, 1 – 233 aa) and RNA interaction domain 1 (RID1, 1 – 271 aa) fragments, in a similar manner to that described for TRB1-3 (Schrumpfová et al. 2014). Interactions of TRBs with TERT seem to be mediated only via the N-terminal domain of TERT, as the centrally positioned Telomerase RNA-binding domain (TRBD) or reverse transcriptase domain (RT) domain do not show interactions (Supplemental Fig. 7). We also observed interactions of TRB4-5 with RUVBL1, RUVBL2A and POT1b in the same manner as was observed for TRB1-3. Moreover, Y2H experiments detected novel interactions between TRB4-5 with a second homolog of the human POT1 protein in *A. thaliana* - POT1a. These interactions were further confirmed by the Co-IP of these proteins (Fig. 7A, Supplemental Fig. 8A).

Furthermore, TRB4-5 interact with PWOs, members of the PEAT complex, as was already observed for TRB1-3 (Tan et al. 2018). A strong interaction was detected between TRB4-5 and PWO1 full-length (Supplemental Fig. 8B) or PWO1 N-terminal sections, including PROLINE-TRYPTOPHANE-TRYPTOPHANE-PROLINE (PWWP) domain (1–223 aa) (Fig. 7B). PWO2 and 3 interact with TRB4 via their N-terminal parts (1–216 and 1–204 aa, respectively). Similarly, we detected the interactions of the N-terminal parts of PWO1 and PWO3 with TRB5.

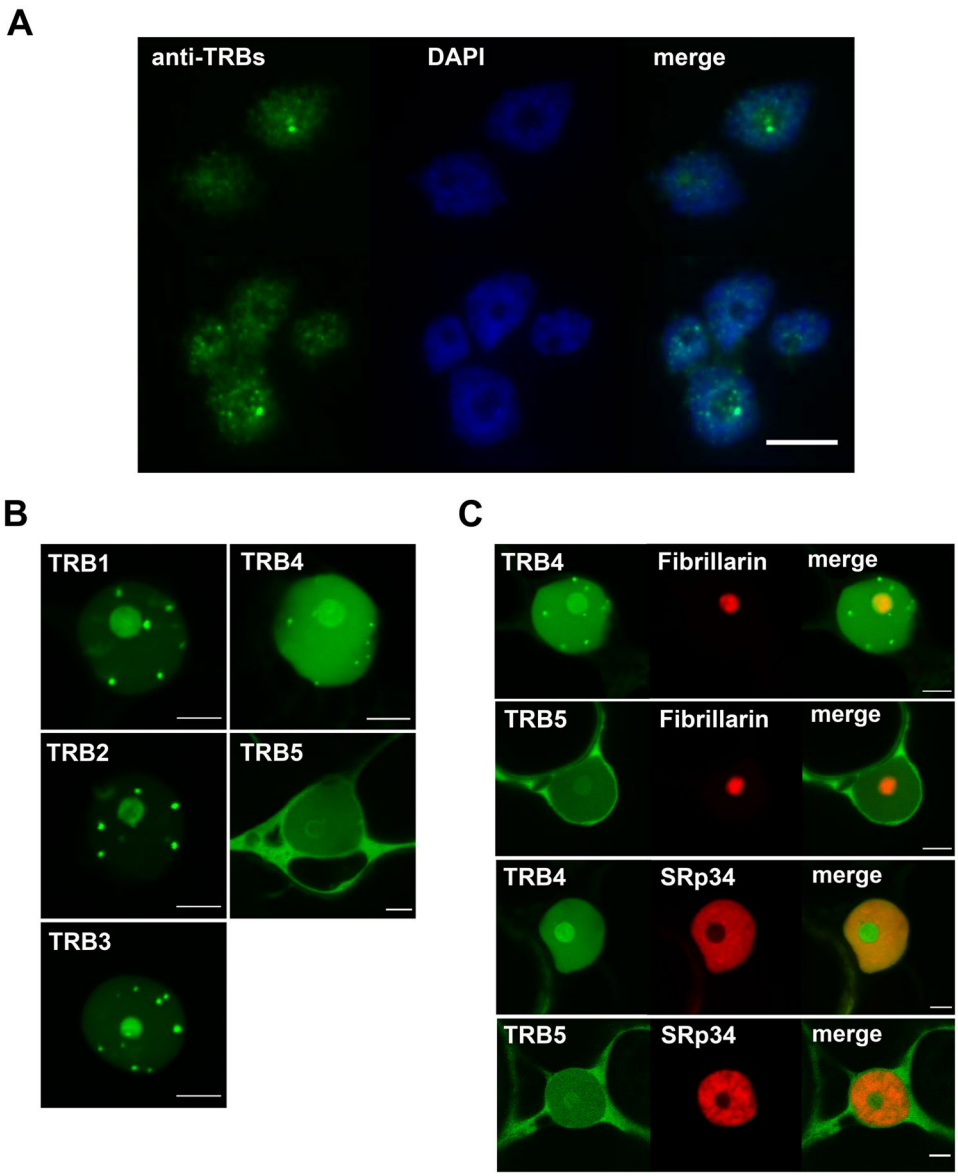

Fig. 5 Subcellular localization of native TRBs and GFP-TRB fusion proteins. (**a**) Isolated nuclei from *A. thaliana* seedlings were subjected to immunofluorescence using an anti-TRB antibody combined with DAPI staining. All five native members of the TRB family are visualized. Scale bar = 10 µm. (**b**) TRB1-5 were fused with GFP (N-terminal fusions), expressed in *N. benthamiana* leaf epidermal cells and observed by confocal microscopy. Single images of areas with nuclei are presented. Scale bars = 5 µm. (**c**) Co-localization of TRB4 and TRB5 (N-terminal GFP fusions) with a nucleolar marker (Fibrillarin-mRFP) and a nucleoplasm marker (SRp34-mRFP) was performed as described in B). Single images of areas with nuclei are presented. Scale bars = 5 µm

To identify TRB interactions with E(z) homologs, members of the PRC2 complex, we used SWN and CLF proteins without the SET [Su(var)3–9, E(z), Trx] domain that confers histone methyltransferase activity ($SWN_{\Delta}SET$ and $CLF_{\Delta}SET$) (Chanvivattana et al. 2004; Hohenstatt et al. 2018). The SET-domain does not seem to be involved in interactions of SWN and CLF with TRB4-5 as Y2H experiments identified interactions between TRB4-5 and $SWN_{\Delta}SET$ and $CLF_{\Delta}SET$ (Fig. 7C).

It was shown recently that the rice homologue of TRB, Telomere repeat-binding factor 2 (TRBF2), and rice Su(z)12 homologues of the PRC2 complex named EMBRYONIC FLOWER 2b (EMF2b) interact with each other (Xuan et al. 2022). We observed novel interactions, not only between *Arabidopsis* TRB4-5 and EMF2, but also between TRB4-5 and other Su(z)12 homologue VERNALIZATION 2 (VRN2). The observed interactions from Y2H system were verified by Co-IP (Fig. 7C).

This broad screen of TRB4-5 protein interaction partners suggests a role of TRBs in various protein complexes. TRBs might contribute to the recruitment of these complexes to telomeric DNA repeats (e.g., Telomerase complex to telomeres) (Fig. 8A) or to *telo*-boxes localized in the promoter regions of the various genes (e.g., PEAT complex or PRC2 subunits to *telo*-boxes) (Fig. 8C, D, F).

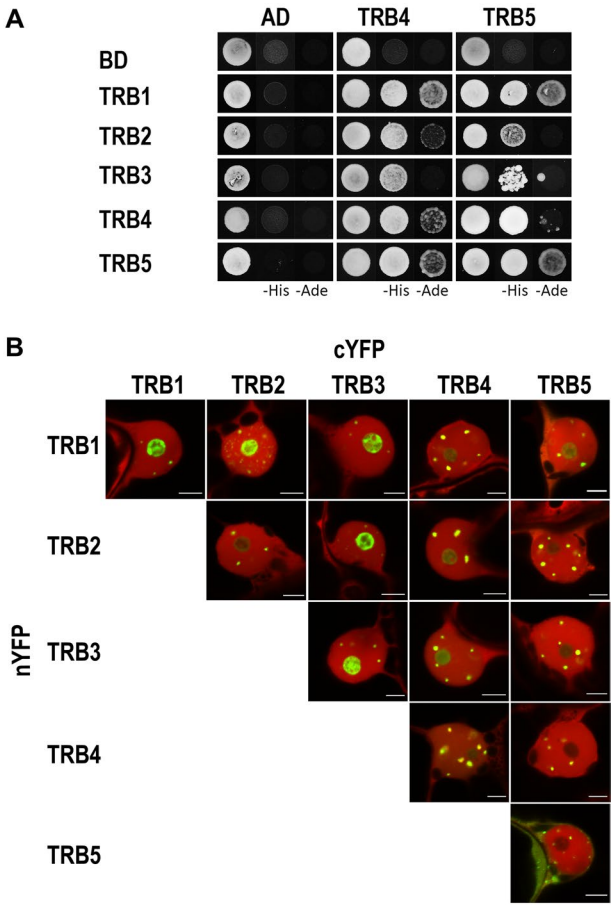

Fig. 6 Dimerization of TRB proteins. (**a**) The Y2H system was used to assess mutual protein–protein interactions of TRBs. Two sets of plasmids carrying the indicated protein fused to either the GAL4 DNA-binding domain (BD) or the GAL4 activation domain (AD) were constructed and introduced into yeast strain PJ69-4a carrying reporter genes His3 and Ade2. Interactions were detected on histidine-deficient SD medium (–His), or under stringent adenine-deficient SD medium (–Ade) selection. Co-transformation with an empty vector (AD, BD) served as a negative control. (**b**) Interactions of TRBs fused with nYFP or cYFP part were detected using the Bimolecular fluorescence complementation (BiFC) assay in *N. benthamiana* leaf epidermal cells. Shown here are single images of merged signals of reconstructed YFP (interaction of the tested proteins) and signals of mRFP (internal marker for transformation and expression) fluorescence detected by confocal microscopy. For separated fluorescent emissions, see Supplemental Fig. 5. Scale bars = 5 µm

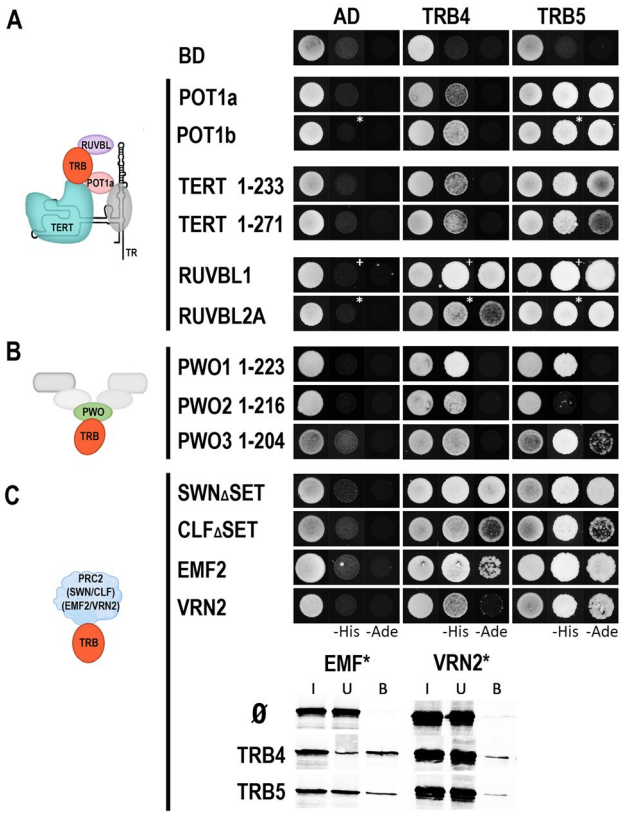

Fig. 7 Interaction of TRB4-5 with various partners. (**A**) The Y2H system was used to assess protein–protein interactions of TRB4-5 proteins with TERT fragments, RUVBLs and POT1a/b as in Fig. 6. Co-transformation with an empty vector (AD, BD) served as a negative control. *Asterisks*, 1 mM 3-aminotriazol (3-AT); *cross*, 3 mM 3-AT. (**B**) Interactions between N-terminal domain of PWO1-3 and TRB4-5 were detected as in A). Interactions with full length PWO1-2 proteins are in Supplementary Fig. 8B. (**C**) Novel interactions between TRB4-5 and EMF2/VRN2, as well as interactions with $SWN_{\Delta}SET/CLF_{\Delta}SET$ were tested using Y2H system as in A). Novel interactions were verified by Co-IP. The TNT expressed VRN2 and EMF2 (^{35}S-labelled*) were mixed with TRB4-5 (myc-tag) and incubated with anti-myc antibody. In the control experiment, the VRN2 and EMF2 proteins were incubated with anti-myc antibody and Protein G magnetic particles in the absence of partner protein. Input (I), unbound (U), and bound (B) fractions were collected and separated in SDS–10% PAGE gels

Discussion

Although the TRBs were originally characterized as being associated with long arrays of telomeric repeats (Schrumpfová et al. 2004, 2014; Mozgová et al. 2008; Dvořáčková et al. 2010; Dreissig et al. 2017) (Fig. 8A), recent observations indicate broad engagement of TRB proteins in various cellular pathways. The most important TRB functions (Fig. 8B–F) include interactions with the telomerase complex (Schrumpfová et al. 2014; Schořová et al. 2019), association with *telo*-boxes in the promoters mainly of translation machinery genes (Schrumpfová et al. 2016), recruitment of PRC2 and PEAT complexes to *telo*-boxes (Zhou et al. 2018; Tan et al. 2018; Tsuzuki and Wierzbicki 2018; Mikulski et al. 2019) or antagonisms between TRB1 and H1 at long interstitial telomeric DNA repeats (Teano et al. 2020).

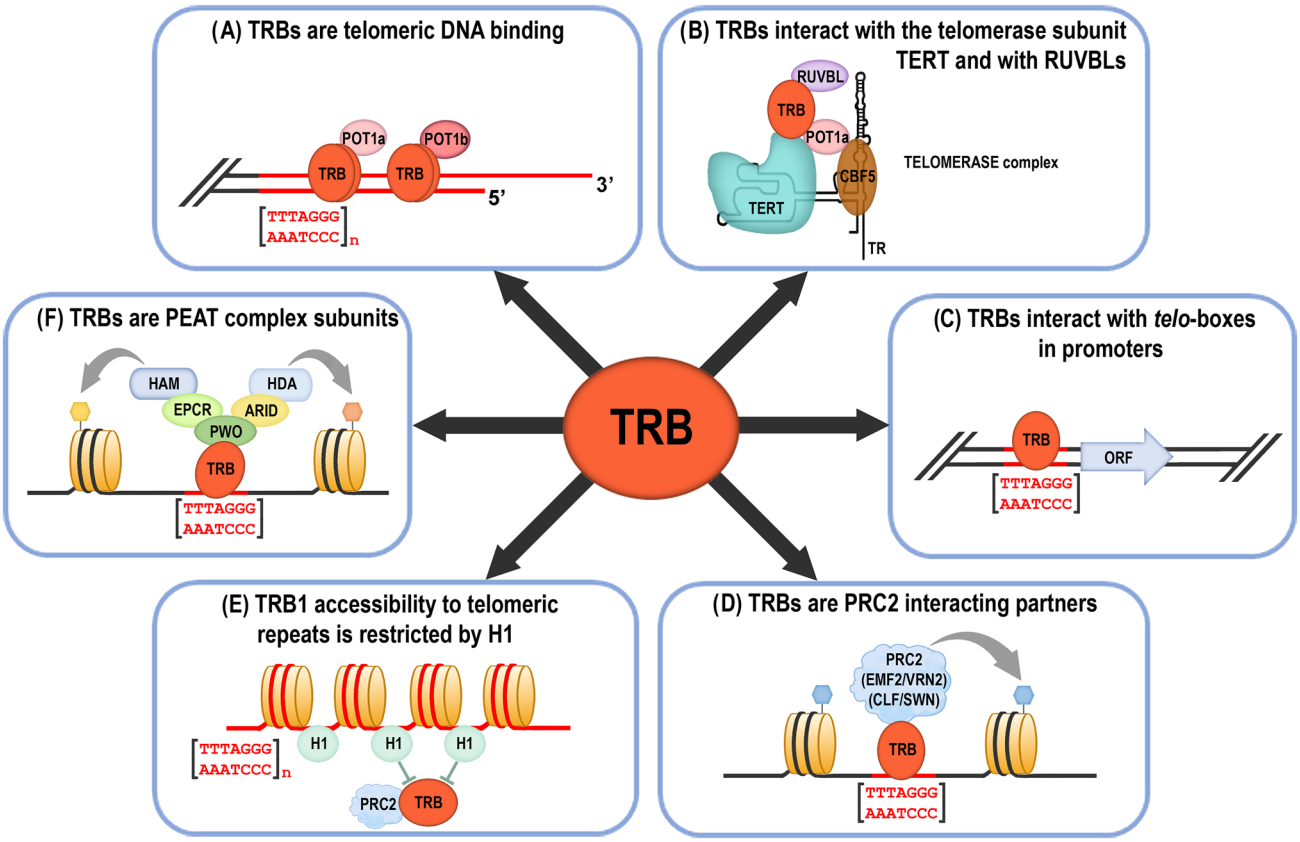

Fig. 8 Overview of the main Telomere repeat binding proteins (TRBs) functions. (**A**) TRBs are associated with the physical ends of chromosomes (telomeres) via their Myb-like domain (Schrumpfová et al. 2004, 2014; Mozgová et al. 2008; Dvořáčková et al. 2010; Dreissig et al. 2017). TRBs interact with *Arabidopsis* homologs of the G-overhang binding protein Protection of telomere 1a, b (POT1a, b) (Schrumpfová et al. 2008, this study). (**B**) TRBs mediate interactions of Recombination UV B – like (RUVBL) proteins with the catalytic subunit of telomerase (TERT), and participate in telomerase biogenesis (Schrumpfová et al. 2014; Schořová et al. 2019). TRBs are associated in the nucleus/nucleolus with POT1a (Schořová et al. 2019), and also with a plant orthologue of dyskerin, named CBF5 (Lermontova et al. 2007) that binds the RNA subunit of telomerase (TR) (Fajkus et al. 2019; Song et al. 2021). (**C**) TRBs are associated with short telomeric sequences (*telo*-boxes) in the promoters of various genes in vivo, mainly with translation machinery genes (Schrumpfová et al. 2016). ORF, Open reading frame. (**D**) *Telo*-box motifs recruit Polycomb repressive complexes (PRC2) via interactions of PRC2 subunits with TRB (Zhou et al. 2016, 2018, this study) CLF, CURLY LEAF; SWN, SWINGER; EMF2, EMBRYONIC FLOWER 2; VRN2, VERNALIZATION 2. (**E**) Histone H1 prevents the invasion of H3K27me3 and TRB1 over telomeres and long interstitial telomeric regions (Teano et al. 2020). (**F**) TRB proteins, as subunits of the PEAT (PWO-EPCR-ARID-TRB) complex, are involved in heterochromatin formation and gene repression, but also have a locus-specific activating role, possibly through the promotion of histone acetylation (Tan et al. 2018; Tsuzuki and Wierzbicki 2018; Mikulski et al. 2019)

TRB4-5 are evolutionarily closer to TRBs from lower plants

Our phylogeny indicates that TRB proteins with N-terminal Myb-domains are conserved in plants and probably arose in Streptophyte algae within the family *Klebsormidiophyceae*. This corresponds to the transition of plants to a terrestrial habitat 800 Mya ago (Cheng et al. 2019) (Fig. 2). However, other groups of Streptophyte algae do not have TRB proteins, favoring a birth and death model of gene evolution (Nei et al., 2005; Eirín- López et al., 2012) or total divergence (Pinho and Hey 2010), such as to the TRF-like (TRFL) genes with a C-terminal Myb-domain (Karamysheva et al. 2004; Hwang and Cho 2007; Fulcher and Riha 2016; Majerská et al. 2017).

Recurrent gene duplications over many generations have created orthologs and paralogs in the plant genome, giving rise to several new protein functions. In green algae, the majority of gene families contain only one gene (Clark and Donoghue 2018; Qiao et al. 2019), consistent with this, only one copy of the TRB protein was detected in Streptophyte algae. An increased number of TRB homologs were found in Embryophyta, which could be a result of WGD within these derived groups. In Mosses (taxon Bryophyta), the genome was duplicated in several independent events. Two WGD events in *Sphagnum* and *Physcomitrium* around 200

Mya and 120 Mya, respectively (Lang et al. 2018; Clark and Donoghue 2018), resulted in three almost identical TRB proteins clustered in the lineage TRB_A. The moss *Ceratodon* also underwent WGD, but unlike *Sphagnum* and *Physcomitrium*, the TRB duplication was not detected. No TRBs were found in hornworts and liverworts, but this may be due to the limited data available on these genomes.

Our results suggest diversification of the TRB gene family in seed plants which is linked with multiple subsequent or independent events of WGD. Lineage TRB_B seems to have evolved in the ancient past and is closely related to TRB_A in Bryophytes. The sub-lineage TRB_D is present in dicots in many families and embedded within the TRB_C lineage.

Within *Brassicaceae*, nested WGDs resulted in multiple TRB homologs. *A. thaliana* has five TRBs with closely related proteins TRB2-3 and TRB4-5. However, within Brassicales the situation differs. The genome of *Carica papaya* (*Caricaceae*) possesses only two TRB proteins, each belonging to one of the lineages TRB_B or TRB_C lineages. This observation is in agreement with an older paleoploidy event in the *Brassicaceae* lineage (β) that is not shared by *C. papaya* but is shared by all other analyzed *Brassicaceae* species (Dassanayake et al. 2011; Wang et al. 2011). As summarized by Rockinger et al. 2016, the ancestor of all *Caricaceae* underwent only a single WGD event, in comparison to the ancestor of *A. thaliana,* which underwent a more recent, additional round of WGD (α) (Bowers et al. 2003; Kagale et al. 2014). Similarly, in monocots, where several independent WGDs have occurred, an increased number of TRB proteins were found, e.g., six TRBs were detected in *Zea mays* (Fig. 2B).

The complexity of plant genomes is extremely high, and annotations of plant genomes are undergoing intensive improvement at present (Kress et al. 2022). Further revision and reinvestigation of the TRB evolutionary tree may help to elucidate species-specific TRB variants such as the one identified in *Malus domestica.*

Conserved structure of individual domains

Although TRB4-5 are grouped in a monophyletic lineage that is distant to TRB1-3 proteins, our assessment of predicted structural models implies that all TRB family members are folded into similar three-dimensional structures. The TRB Myb-like domain is very closely related to that of other telomere-binding proteins, including human TRF1 and TRF2 (Chong et al. 1995; van Steensel et al. 1998; Smogorzewska and de Lange 2004). TRF1 and TRF2 bind to DNA as preformed homodimers (Bianchi et al. 1997, 1999; Broccoli et al. 1997). It was suggested that in vitro the Myb-like binding domain of TRF1 binds to DNA essentially independently of the rest of the protein (König et al. 1998; Bianchi et al. 1999; Court et al. 2005). Specificity in DNA recognition of TRF1 and TRF2 is achieved by several direct contacts from aa side chains to the DNA, mainly via helix 3 and an extended N-terminal arm (Hanaoka et al. 2005; Court et al. 2005). Predicted models of the plant Myb-like domain (Fig. 1) show that the overall 3D structure is preserved in both plant and animal kingdoms, and that the surface mediating protein-DNA interactions are fully conserved. However, the surface side and extended N-terminal arm of the Myb-domain of proteins from the TRB_B family differ to those of the TRB_A or TRB_C families (Fig. 3).

Consistent with the conserved features of the Myb domain, our EMSA results showed the conserved ability of TRB4-5 proteins to bind telomeric sequences. Notably, not all proteins with Myb-like domains are able to bind telomeric repeats, as *Arabidopsis* proteins from the TRFL family, with this motif at the C-terminus, need an accessory Myb-extension domain for telomeric dsDNA interactions in vitro (Karamysheva et al. 2004; Ko et al. 2008). Moreover, unlike TRBs, only *Arabidopsis* plants deficient in one particular member (Hwang and Cho 2007), but not plants deficient for all six TRFL proteins with Myb-extension domain, exhibit changes in telomere length (Fulcher and Riha 2016). Our EMSA results showed the ability of TRB4-5 proteins to bind longer telomeric tracts as well as short *telo*-boxes, containing roughly one telomeric repeat flanked by non-telomeric sequence (Fig. 4). These observations suggest that TRB4-5 proteins may be associated with cis-regulatory elements in the promoter regions of *Arabidopsis* genes as was described for TRB1-3 (Zhou et al. 2016; Schrumpfová et al. 2016). The presence of only one telomeric repeat in the *telo*-box raises the question of whether TRB proteins operate on promoter regions as monomers/dimers or multimers. Based on our quantitative DNA-binding study, we propose that TRB1 and TRB3 bind long telomeric DNA arrays with the stoichiometry of one protein monomer per one telomeric repeat (Hofr et al. 2009), but the stoichiometry of TRBs in regulatory complexes associated with *telo*-boxes needs further elucidation.

The sequence-specific interaction between telomeric dsDNA and TRB1-3 is mediated predominantly by the Myb-like domain, although additional domains from TRBs can also contribute to non-specific DNA interactions (Schrumpfová et al. 2004; Mozgová et al. 2008; Hofr et al. 2009). The H1/5-like domains of TRB proteins belong to the same group as central globular domain of core H1 histones, the incorporation of which directly influences the physicochemical properties of the chromatin fiber and further modulates nucleosome distribution, chromatin compaction and contributes to the local variation in transcriptional activity by affecting the accessibility of transcription factors and RNA polymerases to chromatin (Fan and Roberts 2006; Zhou

et al. 2015; Hergeth and Schneider 2015; Bednar et al. 2017; Fyodorov et al. 2018). The H1/5-like domain of TRB mediates non-specific DNA interactions (Mozgová et al. 2008) as well as interactions with the other members of TRB family and also with the POT1b protein (Schrumpfová et al. 2008). The globular domain of H1 adopts a winged-helix fold with a "wing" defined by two β-sheets. 3D model predictions suggest only minor differences between TRB4-5 and TRB1-3 within the H1/5-like domain, as the loop between two antiparallel β-sheets in the H1/5-like domain of TRB4-5 is longer than in TRB1-3.

Coiled-coil domains are structural motifs that consist of two or more α-helical peptides that are wrapped around each other in a superhelical fashion that may mediate interactions between proteins (Lupas and Gruber 2005; Apostolovic et al. 2010). Only minor differences were predicted for the 3D structure of the coiled coil domain of TRB4-5 and TRB1-3. However, the motifs at the C-terminal sections of the coiled-coil domains in TRBs from TRB_B differ from those motifs at the C-terminal parts of TRB_C lineages, and clearly distinguish these two evolutionarily distinct groups.

TRB4-5 differ in subcellular localization from TRB1-3

In previous studies, it was shown that TRB1-3 are highly dynamic DNA-binding proteins with cell-cycle regulated localization. During interphase, GFP-fused TRB1-3 proteins are preferentially localized in the nucleus, with a strong nucleolar signal and relatively strong nuclear speckles of different sizes (Dvořáčková et al. 2010; Schrumpfová et al. 2014; Zhou et al. 2018). A similar pattern was observed in transiently or stably transformed *Arabidopsis* cells (Dvořáčková et al. 2010) or in tobacco epidermal cells (Schrumpfová et al. 2014) despite the fact that tobacco telomeres are dispersed throughout the nucleus (so-called non-Rabl chromosome configuration), while *Arabidopsis* telomeres are clustered around the nucleolus (rosette-like chromosome configuration) (Shan et al. 2021). Our results show that even native TRBs in isolated *Arabidopsis* nuclei can be detected with a specific antibody, and are localized in the speckles. Some of these speckles in the vicinity of the *Arabidopsis* nucleoli might be telomeric (Dvořáčková et al. 2010), or might be Cajal bodies (Dvořáčková 2010), as was demonstrated for speckles detected in tobacco nuclei.

Here we show that TRB4 and TRB5 fused to GFP have, in contrast to TRB1-3, a distinct subcellular localization pattern (Fig. 5B, C). In addition, unlike all other members of the TRB family, TRB5 is preferentially localized in the cytoplasm. It remains to be clarified whether it is sequestered there or plays a specific functional role.

Our Y2H or BiFC assays proved that TRB4-5 could form homo- and hetero-dimers, as observed in TRB1-3 (Kuchař and Fajkus 2004; Schrumpfová et al. 2004). In addition to dimers, TRB1-3 are capable of forming both homo- and heterotypic multimers via their H1/5-like domain (Schrumpfová et al. 2004; Mozgová et al. 2008; Hofr et al. 2009). Similar multimerization can also be assumed for TRB4 and TRB5, as we observed the formation of high molecular weight complexes for TRB4-5 in EMSAs, which did not migrate into the gel (Warren et al. 2003).

Despite distinct subcellular localization of GFP-TRB4 and GFP-TRB5, we observed mutual interactions between all TRB family members using BiFC, predominantly in the nuclear speckles (Fig. 6B). Only the TRB5 homodimeric interaction was found to be clearly cytoplasmic with nuclear speckles of decreased size compared to the size of speckles in the other homodimeric or mutual TRB interactions. Our BiFC assays showed that TRB1-3, but not TRB4, have the ability to drag TRB5 into the nucleolus, as TRB4 does not interact with TRB5 in the nucleolus. We can assume that TRB proteins form various heteromers in different subcellular compartments that might possess different functions related to distinct biochemical pathways.

Interconnection of TRBs with various protein complexes

Even though TRB4-5 show slightly distinct localization patterns compared to TRB1-3, it appears that all TRBs may interact with similar partners in vitro (Fig. 7). TRB4-5 proteins directly interact with the N-terminal domains of TERT as was also shown for TRB1-3 proteins (Schrumpfová et al. 2014). Additionally, TRB4-5 interact with both RUVBL1 and RUVBL2A proteins, which may imply that they may mediate interactions in the trimeric complex RUVBL-TRB-TERT as was proposed for TRB1-3 (Schořová et al. 2019). Telomerase might also be modulated by POT1 proteins: *A. thaliana* POT1a positively regulates telomerase activity, POT1b is proposed to negatively regulate telomerase and promote chromosome end protection (Beilstein et al. 2015). We observed not only the expected interaction between TRB4-5 and POT1b (Schrumpfová et al. 2008), but also revealed novel interactions of TRB proteins with POT1a. Altogether, we can assume that TRB4-5 are associated with the telomerase complex as was proved for TRB1-3.

In addition to telomeres (Schrumpfová et al. 2014), TRB1-3 regulate the PRC2 target genes (Zhou et al. 2016, 2018). Interestingly, H3K27me3 is present at telomeres of *Arabidopsis* (Adamusová et al. 2020; Vaquero-Sedas and Vega-Palas 2023). The observation that not only TRB1-3 (Zhou et al. 2018), but also TRB4-5, physically interact with homologs of E(z) subunit of PRC2 complex named CLF and SWN suggests that all TRBs can target PRC2 to Polycomb response elements (PREs) including *telo*-boxes (Deng et al. 2013; Zhou et al. 2016; Godwin and Farrona 2022). Moreover, the novel interaction between TRBs and Su(z)12

A. thaliana homologues EMF2 and VRN2 described here, tightly interconnects all TRBs with the core PRC2 components. These observations support the recently published observation that *O. sativa* single Myb transcription factor TRBF2 forms phase-separated droplets, which aggregate with PRC2 via rice OsCLF and OsEMF2 (Xuan et al. 2022).

In *Arabidopsis*, the PWO1 protein interacts with all three E(z) homologs, including CLF and SWN through its conserved N-terminal PWWP domain (Mikulski et al. 2019). Furthermore, PWO1-3 are associated with members of the PEAT complex, which was recently identified as being able to silence transposable elements (Tan et al. 2018). Our data suggest that the interaction between TRBs and PWOs is not restricted to only TRB1 and 2 (Tan et al. 2018), instead other TRB members, including TRB4-5, interact with N-terminal part of PWO1 and PWO3 from *A. thaliana,* containing PWWP domains. Additionally, the N-terminal part of PWO2 is recognized by *Arabidopsis* TRB4. Interestingly, in tobacco PWO1 tethers CLF to nuclear speckles (Hohenstatt et al. 2018; Mikulski et al. 2019) which have a similar distribution to speckles of TRB proteins.

Overall, we conclude that TRB proteins, including the newly characterized TRB4-5, are associated with several complexes, including telomerase, PRC2 or PEAT complexes. However, TRBs are unlikely to be permanently associated with all of these complexes (Tan et al. 2018; Schubert 2019), and we might speculate that TRB subunits are partially interchangeable within these complexes.

It should be noted that the number of identified interaction partners of TRBs in *Arabidopsis* may increase in the future, as these promiscuous proteins may play a role in various additional biochemical processes that are not yet elucidated. For example, the *A. thaliana TRB1* gene is responsive to several types of hormones, including jasmonate (JA) (Yanhui et al. 2006); TRB homologue from apple dynamically modulates JA-mediated accumulation of anthocyanin and proanthocyanidin (An et al. 2021); soybean TRB homologue was identified as candidate gene regulating total soluble sugar in soybean seeds (Xu et al. 2022).

Conclusion

Proteins from the TRB family are plant-specific and apparently first evolved in lower plants. We speculate, that due to WGDs one ancestral TRB was multiplied to the current five TRB members in *A. thaliana* increasing the potential of diversification of their particular functions. Further research is needed to confirm whether newly described TRB4-5 proteins specifically target to telomeric sequences located terminally (Schrumpfová et al. 2004, 2014; Mozgová et al. 2008; Dvořáčková et al. 2010; Dreissig et al. 2017) or interstitially (Schrumpfová et al. 2016) via their Myb-like domain like other members of this family TRB1-3. Additionally, the versatile interactions of all TRBs members with other proteins contribute to the multiple functions that they adopt in the cell nucleus, including participation in telomerase biogenesis (Schrumpfová et al. 2014; Schořová et al. 2019), recruitment of PRC2 or PEAT complexes (Zhou et al. 2016, 2018; Tan et al. 2018; Tsuzuki and Wierzbicki 2018; Mikulski et al. 2019) or competing with H1 for binding to interstitially localized telomeric sequences (Teano et al. 2020). The cytoplasmic localization of TRB5 and its implications deserve further investigation. As additional functions and interaction partners of TRBs are discovered, it can be expected that research in plants will lead to a better understanding of the mode of action of the different TRBs and also to the elucidation of novel functions.

Supplementary Information The online version contains supplementary material available at https://doi.org/10.1007/s11103-023-01348-2.

Acknowledgements This work was supported by the Czech Science Foundation projects 21-15841S (P.P.S., M.K., D.H.) and 20-01331X (A.K), and Czech Ministry of Education, Youth and Sports grant number LTAUSA18115 (L.S.). The Plant Sciences Core Facility of CEITEC Masaryk University is acknowledged for its technical support. We acknowledge the Imaging Facility of the Institute of Experimental Botany AS CR supported by the MEYS CR (LM2018129 Czech-BioImaging) and IEB AS CR.

We acknowledge Sara Farrona (Plant and AgriBiosciences Centre, National University Ireland, IR) for providing us with *SWN*, *CLF* and *EMF2* constructs. Moreover, we acknowledge Eva Sykorova (Institute of Biophysics of the Czech Academy of Sciences, Brno, Czech Republic) for providing us constructs with *POT1a-b* and *TERT* fragments and Ali Pendle (John Innes Centre, Norwich, United Kingdom) for the sub-nuclear localization markers. We also acknowledge Yvona Stražická and Michal Franek for the help with the immunofluorescence on *Arabidopsis* nuclei.

We acknowledge Leon Jenner and Iva Mozgová for proofreading and manuscript editing.

The access to the computing and storage facilities owned by parties and projects contributing to the National Grid Infrastructure MetaCentrum provided under the programme Projects of Large Infrastructure for Research, Development, and Innovations (LM2010005) was highly appreciated, as was the access to the CERIT-SC computing and storage facilities provided under the programme Center CERIT Scientific Cloud, part of the Operational Program Research and Development for Innovations, reg. no. CZ.1.05/3.2.00/08.0144.

Author contribution Petra Procházková Schrumpfová and David Honys designed the study, supervised the project. Petra Procházková Schrumpfová wrote the manuscript with support from David Honys, Jan Paleček, Daniel Schubert. Lenka Steinbachová, Zuzana Gadiou, Alžbeta Kusová, Tereza Přerovská, Claire Jourdain and Tino Stricker performed cloning, Lenka Steinbachová performed localization and BiFC, Alžbeta Kusová and Ahmed Khan performed Y2H, Tereza Přerovská performed EMSA, Gabriela Rigóová performed Co-IP, Jan Paleček analyzed 3D structures, Lenka Záveská Drábková performed evolution analysis. Petra Procházková Schrumpfová conducted experiments and analyzed data.

Funding Open access publishing supported by the National Technical Library in Prague.

Data availability All data generated or analysed during this study are included in this published article.

Declaration

Competing interest The authors report no competing interests.

References

Adamusová K, Khosravi S, Fujimoto S, Houben A, Matsunaga S, Fajkus J, Fojtová M (2020) Two combinatorial patterns of telomere histone marks in plants with canonical and non-canonical telomere repeats. Plant J 102:678–687. https://doi.org/10.1111/tpj.14653

An J-P, Xu R-R, Liu X, Zhang J-C, Wang X-F, You C-X, Hao Y-J (2021) Jasmonate induces biosynthesis of anthocyanin and proanthocyanidin in apple by mediating the JAZ1–TRB1–MYB9 complex. Plant J 106:1414–1430. https://doi.org/10.1111/tpj.15245

Apostolovic B, Danial M, Klok H-A (2010) Coiled coils: Attractive protein folding motifs for the fabrication of self-assembled, responsive and bioactive materials. Chem Soc Rev 39:3541–3575. https://doi.org/10.1039/B914339B

Ashkenazy H, Abadi S, Martz E, Chay O, Mayrose I, Pupko T, Ben-Tal N (2016) ConSurf 2016: an improved methodology to estimate and visualize evolutionary conservation in macromolecules. Nucleic Acids Res 44:W344–W350. https://doi.org/10.1093/nar/gkw408

Bailey TL, Boden M, Buske FA, Frith M, Grant CE, Clementi L, Ren J, Li WW, Noble WS (2009) MEME SUITE: Tools for motif discovery and searching. Nucleic Acids Res 37:W202-208. https://doi.org/10.1093/nar/gkp335

Bednar J, Garcia-Saez I, Boopathi R, Cutter AR, Papai G, Reymer A, Syed SH, Lone IN, Tonchev O, Crucifix C, Menoni H, Papin C, Skoufias DA, Kurumizaka H, Lavery R, Hamiche A, Hayes JJ, Schultz P, Angelov D, Petosa C, Dimitrov S (2017) Structure and dynamics of a 197 bp nucleosome in complex with linker histone H1. Mol Cell 66:384-397.e8. https://doi.org/10.1016/j.molcel.2017.04.012

Beilstein MA, Renfrew KB, Song X, Shakirov EV, Zanis MJ, Shippen DE (2015) Evolution of the telomere-associated protein POT1a in Arabidopsis thaliana Is characterized by positive selection to reinforce protein-protein interaction. Mol Biol Evol 32:1329–1341. https://doi.org/10.1093/molbev/msv025

Bianchi A, Smith S, Chong L, Elias P, de Lange T (1997) TRF1 is a dimer and bends telomeric DNA. EMBO J 16:1785–1794. https://doi.org/10.1093/emboj/16.7.1785

Bianchi A, Stansel RM, Fairall L, Griffith JD, Rhodes D, de Lange T (1999) TRF1 binds a bipartite telomeric site with extreme spatial flexibility. EMBO J 18:5735–5744. https://doi.org/10.1093/emboj/18.20.5735

Bilaud T, Koering CE, Binet-Brasselet E, Ancelin K, Pollice A, Gasser SM, Gilson E (1996) The telobox, a Myb-Related telomeric DNA binding motif found in proteins from yeast, plants and human. Nucleic Acids Res 24:1294–1303. https://doi.org/10.1093/nar/24.7.1294

Bowers JE, Chapman BA, Rong J, Paterson AH (2003) Unravelling angiosperm genome evolution by phylogenetic analysis of chromosomal duplication events. Nature 422:433–438. https://doi.org/10.1038/nature01521

Broccoli D, Smogorzewska A, Chong L, de Lange T (1997) Human telomeres contain two distinct Myb–related proteins, TRF1 and TRF2. Nat Genet 17:231–235. https://doi.org/10.1038/ng1097-231

Busso D, Delagoutte-Busso B, Moras D (2005) Construction of a set Gateway-based destination vectors for high-throughput cloning and expression screening in *Escherichia coli*. Anal Biochem 343:313–321. https://doi.org/10.1016/j.ab.2005.05.015

Chanvivattana Y, Bishopp A, Schubert D, Stock C, Moon Y-H, Sung ZR, Goodrich J (2004) Interaction of Polycomb-group proteins controlling flowering in *Arabidopsis*. Development 131:5263–5276. https://doi.org/10.1242/dev.01400

Cheng C-Y, Krishnakumar V, Chan AP, Thibaud-Nissen F, Schobel S, Town CD (2017) Araport11: a complete reannotation of the *Arabidopsis thaliana* reference genome. Plant J89:789–804. https://doi.org/10.1111/tpj.13415

Cheng S, Xian W, Fu Y, Marin B, Keller J, Wu T, Sun W, Li X, Xu Y, Zhang Y, Wittek S, Reder T, Günther G, Gontcharov A, Wang S, Li L, Liu X, Wang J, Yang H, Xu X, Delaux P-M, Melkonian B, Wong GK-S, Melkonian M (2019) Genomes of subaerial zygnematophyceae provide insights into land plant evolution. Cell 179:1057-1067.e14. https://doi.org/10.1016/j.cell.2019.10.019

Chong L, van Steensel B, Broccoli D, Erdjument-Bromage H, Hanish J, Tempst P, de Lange T (1995) A Human Telomeric Protein Science 270:1663–1667. https://doi.org/10.1126/science.270.5242.1663

Clark JW, Donoghue PCJ (2018) Whole-genome duplication and plant macroevolution. Trends Plant Sci 23:933–945. https://doi.org/10.1016/j.tplants.2018.07.006

Court R, Chapman L, Fairall L, Rhodes D (2005) How the human telomeric proteins TRF1 and TRF2 recognize telomeric DNA: A view from high-resolution crystal structures. EMBO Rep 6:39–45. https://doi.org/10.1038/sj.embor.7400314

Dassanayake M, Oh D-H, Haas JS, Hernandez A, Hong H, Ali S, Yun D-J, Bressan RA, Zhu J-K, Bohnert HJ, Cheeseman JM (2011) The genome of the extremophile crucifer *Thellungiella parvula*. Nat Genet 43:913–918. https://doi.org/10.1038/ng.889

Deng W, Buzas DM, Ying H, Robertson M, Taylor J, Peacock WJ, Dennis ES, Helliwell C (2013) *Arabidopsis* Polycomb Repressive Complex 2 binding sites contain putative GAGA factor binding motifs within coding regions of genes. BMC Genom 14:593. https://doi.org/10.1186/1471-2164-14-593

Dreissig S, Schiml S, Schindele P, Weiss O, Rutten T, Schubert V, Gladilin E, Mette MF, Puchta H, Houben A (2017) Live-cell CRISPR imaging in plants reveals dynamic telomere movements. Plant J 91:565–573. https://doi.org/10.1111/tpj.13601

Dvořáčková M (2010) Analysis of *Arabidopsis* telomere-associated proteins in vivo. Dissertation, Masaryk University, Faculty of Science

Dvořáčková M, Rossignol P, Shaw PJ, Koroleva OA, Doonan JH, Fajkus J (2010) AtTRB1, a telomeric DNA-binding protein from *Arabidopsis*, is concentrated in the nucleolus and shows highly dynamic association with chromatin. Plant J 61:637–649. https://doi.org/10.1111/j.1365-313X.2009.04094.x

Eirin-Lopez JM, Rebordinos L, Rooney AP and & Rozas J. (2012) The birth-and-death evolution of multigene families revisited. Genome Dyn 7:170–196. https://doi.org/10.1159/000337119.

Fan L, Roberts VA (2006) Complex of linker histone H5 with the nucleosome and its implications for chromatin packing. Proc Natl Acad Sci 103:8384–8389. https://doi.org/10.1073/pnas.0508951103

Fulcher N, Riha K (2016) Using Centromere Mediated Genome Elimination to Elucidate the Functional Redundancy of Candidate Telomere Binding Proteins in *Arabidopsis thaliana*. Front Genet 6:349. https://doi.org/10.3389/fgene.2015.00349

Fyodorov DV, Zhou B-R, Skoultchi AI, Bai Y (2018) Emerging roles of linker histones in regulating chromatin structure and function. Nat Rev Mol Cell Biol 19:192–206. https://doi.org/10.1038/nrm.2017.94

Gehl C, Waadt R, Kudla J, Mendel R-R, Hänsch R (2009) New GATEWAY vectors for high throughput analyses of protein-protein interactions by bimolecular fluorescence complementation. Mol Plant 2:1051–1058. https://doi.org/10.1093/mp/ssp040

Godwin J, Farrona S (2022) The importance of networking: Plant polycomb repressive complex 2 and its interactors. Epigenomes 6:8. https://doi.org/10.3390/epigenomes6010008

Grefen C, Blatt MR (2012) A 2in1 cloning system enables ratiometric bimolecular fluorescence complementation (rBiFC). Biotechniques 53:311–314. https://doi.org/10.2144/000113941

Hall TA (1999) BioEdit: a user-friendly biological sequence alignment editor and analysis program for Windows 95/98/NT. Nucleic Acids Symp Ser 41:95–98

Hanaoka S, Nagadoi A, Nishimura Y (2005) Comparison between TRF2 and TRF1 of their telomeric DNA-bound structures and DNA-binding activities. Protein Sci 14:119–130. https://doi.org/10.1110/ps.04983705

Hergeth SP, Schneider R (2015) The H1 linker histones: Multifunctional proteins beyond the nucleosomal core particle. EMBO Rep 16:1439–1453. https://doi.org/10.15252/embr.201540749

Hofr C, Sultesová P, Zimmermann M, Mozgová I, Procházková Schrumpfová P, Wimmerová M, Fajkus J (2009) Single-Myb-histone proteins from *Arabidopsis thaliana*: A quantitative study of telomere-binding specificity and kinetics. Biochem J 419:221–230. https://doi.org/10.1042/BJ20082195

Hohenstatt ML, Mikulski P, Komarynets O, Klose C, Kycia I, Jeltsch A, Farrona S, Schubert D (2018) PWWP-DOMAIN INTERACTOR OF POLYCOMBS1 interacts with polycomb-group proteins and histones and regulates *Arabidopsis* flowering and development. Plant Cell 30:117–133. https://doi.org/10.1105/tpc.17.00117

Horák J, Grefen C, Berendzen KW, Hahn A, Stierhof Y-D, Stadelhofer B, Stahl M, Koncz C, Harter K (2008) The *Arabidopsis thaliana* response regulator ARR22 is a putative AHP phospho-histidine phosphatase expressed in the chalaza of developing seeds. BMC Plant Biol 8:77. https://doi.org/10.1186/1471-2229-8-77

Hwang MG, Cho MH (2007) Arabidopsis thaliana telomeric DNA-binding protein 1 is required for telomere length homeostasis and its Myb-extension domain stabilizes plant telomeric DNA binding. Nucleic Acids Res 35:1333–1342. https://doi.org/10.1093/nar/gkm043

Jumper J, Evans R, Pritzel A, Green T, Figurnov M, Ronneberger O, Tunyasuvunakool K, Bates R, Zidek A, Potapenko A et al (2021) Highly accurate protein structure prediction with AlphaFold. Nature 596:583–589. https://doi.org/10.1038/s41586-021-03819-2

Kagale S, Robinson SJ, Nixon J, Xiao R, Huebert T, Condie J, Kessler D, Clarke WE, Edger PP, Links MG, Sharpe AG, Parkin IAP (2014) Polyploid Evolution of the Brassicaceae during the Cenozoic Era. Plant Cell 26:2777–2791. https://doi.org/10.1105/tpc.114.126391

Karamysheva ZN, Surovtseva YV, Vespa L, Shakirov EV, Shippen DE (2004) A C-terminal Myb extension domain defines a novel family of double-strand telomeric DNA-binding proteins in *Arabidopsis*. J Biol Chem 279:47799–47807. https://doi.org/10.1074/jbc.M407938200

Ko S, Jun S-H, Bae H, Byun J-S, Han W, Park H, Yang SW, Park S-Y, Jeon YH, Cheong C, Kim WT, Lee W, Cho H-S (2008) Structure of the DNA-binding domain of NgTRF1 reveals unique features of plant telomere-binding proteins. Nucleic Acids Res 36:2739–2755. https://doi.org/10.1093/nar/gkn030

König P, Fairall L, Rhodes D (1998) Sequence-specific DNA recognition by the Myb-like domain of the human telomere binding protein TRF1: A model for the protein-DNA complex. Nucleic Acids Res 26:1731–1740. https://doi.org/10.1093/nar/26.7.1731

Koroleva OA, Calder G, Pendle AF, Kim SH, Lewandowska D, Simpson CG, Jones IM, Brown JWS, Shaw PJ (2009) Dynamic behavior of *Arabidopsis* eIF4A-III, putative core protein of exon junction complex: Fast relocation to nucleolus and splicing speckles under hypoxia. Plant Cell 21:1592–1606. https://doi.org/10.1105/tpc.108.060434

Kress WJ, Soltis DE, Kersey PJ, Wegrzyn JL, Leebens-Mack JH, Gostel MR, Liu X, Soltis PS (2022) Green plant genomes: What we know in an era of rapidly expanding opportunities. Proc Natl Acad Sci 119:e2115640118. https://doi.org/10.1073/pnas.2115640118

Kuchař M, Fajkus J (2004) Interactions of putative telomere-binding proteins in *Arabidopsis thaliana*: identification of functional TRF2 homolog in plants. FEBS Lett 578:311–315. https://doi.org/10.1016/j.febslet.2004.11.021

Kutashev KO, Franek M, Diamanti K, Komorowski J, Olšinová M, Dvořáčková M (2021) Nucleolar rDNA folds into condensed foci with a specific combination of epigenetic marks. Plant J 105:1534–1548. https://doi.org/10.1111/tpj.15130

Lamesch P, Berardini TZ, Li D, Swarbreck D, Wilks C, Sasidharan R, Muller R, Dreher K, Alexander DL, Garcia-Hernandez M, Karthikeyan AS, Lee CH, Nelson WD, Ploetz L, Singh S, Wensel A, Huala E (2012) The *Arabidopsis* Information Resource (TAIR): Improved gene annotation and new tools. Nucleic Acids Res 40:D1202–D1210. https://doi.org/10.1093/nar/gkr1090

Lang D, Ullrich KK, Murat F, Fuchs J, Jenkins J, Haas FB, Piednoel M, Gundlach H, Van Bel M, Meyberg R, Vives C, Morata J, Symeonidi A, Hiss M, Muchero W, Kamisugi Y, Saleh O, Blanc G, Decker EL, van Gessel N, Grimwood J, Hayes RD, Graham SW, Gunter LE, McDaniel SF, Hoernstein SNW, Larsson A, Li F-W, Perroud P-F, Phillips J, Ranjan P, Rokshar DS, Rothfels CJ, Schneider L, Shu S, Stevenson DW, Thümmler F, Tillich M, Villarreal Aguilar JC, Widiez T, Wong GK-S, Wymore A, Zhang Y, Zimmer AD, Quatrano RS, Mayer KFX, Goodstein D, Casacuberta JM, Vandepoele K, Reski R, Cuming AC, Tuskan GA, Maumus F, Salse J, Schmutz J, Rensing SA (2018) The *Physcomitrella patens* chromosome-scale assembly reveals moss genome structure and evolution. Plant J 93:515–533. https://doi.org/10.1111/tpj.13801

Lee WK, Cho MH (2016) Telomere-binding protein regulates the chromosome ends through the interaction with histone deacetylases in *Arabidopsis thaliana*. Nucleic Acids Res 44:4610–4624. https://doi.org/10.1093/nar/gkw067

Lermontova I, Schubert V, Börnke F, Macas J, Schubert I (2007) *Arabidopsis* CBF5 interacts with the H/ACA snoRNP assembly factor NAF1. Plant Mol Biol 65:615–626. https://doi.org/10.1007/s11103-007-9226-z

Letunic I, Bork P (2016) Interactive tree of life (iTOL) v3: an online tool for the display and annotation of phylogenetic and other

trees. Nucleic Acids Res 44:W242–W245. https://doi.org/10.1093/nar/gkw290
Lindner M, Simonini S, Kooiker M, Gagliardini V, Somssich M, Hohenstatt M, Simon R, Grossniklaus U, Kater MM (2013) TAF13 interacts with PRC2 members and is essential for *Arabidopsis* seed development. Dev Biol 379:28–37. https://doi.org/10.1016/j.ydbio.2013.03.005
Lorković ZJ, Hilscher J, Barta A (2004) Use of fluorescent protein tags to study nuclear organization of the spliceosomal machinery in transiently transformed living plant cells. MBoC 15:3233–3243. https://doi.org/10.1091/mbc.e04-01-0055
Lupas AN, Gruber M (2005) The structure of α-helical coiled coils. Adv Protein Chem 70:37–38. https://doi.org/10.1016/S0065-3233(05)70003-6
Maillet G, White CI, Gallego ME (2006) Telomere-length regulation in inter-ecotype crosses of *Arabidopsis*. Plant Mol Biol 62:859–866. https://doi.org/10.1007/s11103-006-9061-7
Majerská J, Schrumpfová PP, Dokládal L, Schořová Š, Stejskal K, Obořil M, Honys D, Kozáková L, Polanská PS, Sýkorová E (2017) Tandem affinity purification of AtTERT reveals putative interaction partners of plant telomerase in vivo. Protoplasma 254:1547–1562. https://doi.org/10.1007/s00709-016-1042-3
Marian CO, Bordoli SJ, Goltz M, Santarella RA, Jackson LP, Danilevskaya O, Beckstette M, Meeley R, Bass HW (2003) The maize single myb histone 1 Gene, Smh1, belongs to a novel gene family and encodes a protein that binds telomere DNA repeats in vitro. Plant Physiol 133:1336–1350. https://doi.org/10.1104/pp.103.026856
McKeown P, Pendle AF, Shaw PJ (2008) Preparation of *Arabidopsis* nuclei and nucleoli. In: Hancock R (ed) The nucleus. Methods in molecular biology, vol 463. Humana Press, Totowa, NJ, pp 67–75. https://doi.org/10.1007/978-1-59745-406-3_5
Mikulski P, Hohenstatt ML, Farrona S, Smaczniak C, Stahl Y, Kalyanikrishna null, Kaufmann K, Angenent G, Schubert D, (2019) The chromatin-associated protein PWO1 interacts with plant nuclear lamin-like components to regulate nuclear size. Plant Cell 31:1141–1154. https://doi.org/10.1105/tpc.18.00663
Mozgova I, Hennig L (2015) The polycomb group protein regulatory network. Annu Rev Plant Biol 66:269–296. https://doi.org/10.1146/annurev-arplant-043014-115627
Mozgová I, Schrumpfová PP, Hofr C, Fajkus J (2008) Functional characterization of domains in AtTRB1, a putative telomere-binding protein in *Arabidopsis thaliana*. Phytochemistry 69:1814–1819. https://doi.org/10.1016/j.phytochem.2008.04.001
Nakagawa T, Kurose T, Hino T, Tanaka K, Kawamukai M, Niwa Y, Toyooka K, Matsuoka K, Jinbo T, Kimura T (2007) Development of series of gateway binary vectors, pGWBs, for realizing efficient construction of fusion genes for plant transformation. J Biosci Bioeng 104:34–41. https://doi.org/10.1263/jbb.104.34
Nei M, Rooney AP (2005) Concerted and birth-and-death evolution in multigene families. Annu Rev Genet 39:121–152. https://doi.org/10.1146/annurev.genet.39.073003.112240
Néron B, Ménager H, Maufrais C, Joly N, Maupetit J, Letort S, Carrere S, Tuffery P, Letondal C (2009) Mobyle: a new full web bioinformatics framework. Bioinformatics 25:3005–3011. https://doi.org/10.1093/bioinformatics/btp493
Ogata K, Hojo H, Aimoto S, Nakai T, Nakamura H, Sarai A, Ishii S, Nishimura Y (1992) Solution structure of a DNA-binding unit of Myb: a helix-turn-helix-related motif with conserved tryptophans forming a hydrophobic core. Proc Natl Acad Sci 89:6428–6432. https://doi.org/10.1073/pnas.89.14.6428
Palecek JJ, Gruber S (2015)Kite proteins: A superfamily of SMC/Kleisin partners conserved across bacteria, archaea, and eukaryotes. Structure 23:2183–2190. https://doi.org/10.1016/j.str.2015.10.004
Pinho C, Hey J (2010) Divergence with gene flow: Models and data. Annu Rev Ecol Evol Syst 41(1):215–230. https://doi.org/10.1146/annurev-ecolsys-102209-144644
Qiao X, Li Q, Yin H, Qi K, Li L, Wang R, Zhang S, Paterson AH (2019) Gene duplication and evolution in recurring polyploidization–diploidization cycles in plants. Genome Biol 20:38. https://doi.org/10.1186/s13059-019-1650-2
Ramakrishnan V, Finch JT, Graziano V, Lee PL, Sweet RM (1993) Crystal structure of globular domain of histone H5 and its implications for nucleosome binding. Nature 362:219–223. https://doi.org/10.1038/362219a0
Rockinger A, Sousa A, Carvalho FA, Renner SS (2016) Chromosome number reduction in the sister clade of *Carica papaya* with concomitant genome size doubling. Am J Bot 103:1082–1088. https://doi.org/10.3732/ajb.1600134
Sambrook J, Fritsch EF, Maniatis T (1989) Molecular Cloning: A Laboratory Manual, 2nd edn. Cold Spring Harbor, NY, Cold Spring Laboratory Press
Schindelin J, Arganda-Carreras I, Frise E, Kaynig V, Longair M, Pietzsch T, Preibisch S, Rueden C, Saalfeld S, Schmid B, Tinevez J-Y, White DJ, Hartenstein V, Eliceiri K, Tomancak P, Cardona A (2012) Fiji: an open-source platform for biological-image analysis. Nat Methods 9:676–682. https://doi.org/10.1038/nmeth.2019
Schořová Š, Fajkus J, Záveská Drábková L, Honys D, Schrumpfová PP (2019) The plant Pontin and Reptin homologues, RuvBL1 and RuvBL2a, colocalize with TERT and TRB proteins in vivo, and participate in telomerase biogenesis. Plant J 98:195–212. https://doi.org/10.1111/tpj.14306
Schrumpfová P, Kuchar M, Miková G, Skrísovská L, Kubicárová T, Fajkus J (2004) Characterization of two *Arabidopsis thaliana* myb-like proteins showing affinity to telomeric DNA sequence. Genome 47:316–324. https://doi.org/10.1139/g03-136
Schrumpfová P, Vychodilová I, Dvořáčková M, Majerská J, Dokládal L, Schořová Š, Fajkus J (2014) Telomere repeat binding proteins are functional components of *Arabidopsis* telomeres and interact with telomerase. Plant J 77:770–781. https://doi.org/10.1111/tpj.12428
Schrumpfová PP, Kuchař M, Paleček J, Fajkus J (2008) Mapping of interaction domains of putative telomere-binding proteins AtTRB1 and AtPOT1b from *Arabidopsis thaliana*. FEBS Lett 582:1400–1406. https://doi.org/10.1016/j.febslet.2008.03.034
Schrumpfová PP, Vychodilová I, Hapala J, Schořová Š, Dvořáček V, Fajkus J (2016) Telomere binding protein TRB1 is associated with promoters of translation machinery genes in vivo. Plant Mol Biol 90:189–206. https://doi.org/10.1007/s11103-015-0409-8
Schubert D (2019) Evolution of Polycomb-group function in the green lineage. F1000Res Faculty Rev-268. https://doi.org/10.12688/f1000research.16986.1
Shakirov EV, Shippen DE (2004) Length regulation and dynamics of individual telomere tracts in wild-type *Arabidopsis*. Plant Cell 16:1959–1967. https://doi.org/10.1105/tpc.104.023093
Shan W, Kubová M, Mandáková T, Lysak MA (2021) Nuclear organization in crucifer genomes: Nucleolus-associated telomere clustering is not a universal interphase configuration in Brassicaceae. Plant J 108:528–540. https://doi.org/10.1111/tpj.15459
Sievers F, Wilm A, Dineen D, Gibson TJ, Karplus K, Li W, Lopez R, McWilliam H, Remmert M, Söding J, Thompson JD, Higgins DG (2011) Fast, scalable generation of high-quality protein multiple sequence alignments using Clustal Omega. Mol Syst Biol 7:539. https://doi.org/10.1038/msb.2011.75
Smogorzewska A, de Lange T (2004) Regulation of Telomerase by Telomeric Proteins. Annu Rev Biochem 73:177–208. https://doi.org/10.1146/annurev.biochem.73.071403.160049
Stamatakis A (2014) RAxML version 8: A tool for phylogenetic analysis and post-analysis of large phylogenies. Bioinformatics 30:1312–1313. https://doi.org/10.1093/bioinformatics/btu033
Surovtseva YV, Shakirov EV, Vespa L, Osbun N, Song X, Shippen DE (2007) *Arabidopsis* POT1 associates with the telomerase RNP

and is required for telomere maintenance. EMBO J 26:3653–3661. https://doi.org/10.1038/sj.emboj.7601792
Sweetlove L, Gutierrez C (2019) The journey to the end of the chromosome: Delivering active telomerase to telomeres in plants. Plant J 98:193–194. https://doi.org/10.1111/tpj.14328
Tan L-M, Zhang C-J, Hou X-M, Shao C-R, Lu Y-J, Zhou J-X, Li Y-Q, Li L, Chen S, He X-J (2018) The PEAT protein complexes are required for histone deacetylation and heterochromatin silencing. EMBO J 37:e98770. https://doi.org/10.15252/embj.201798770
Tani A, Murata M (2005) Alternative splicing of Pot1 (Protection of telomere)-like genes in *Arabidopsis thaliana*. Genes Genet Syst 80:41–48. https://doi.org/10.1266/ggs.80.41
Teano G, Concia L, Carron L, Wolff L, Adamusová K, Fojtová M, Bourge M, Kramdi A, Colot V, Grossniklaus U, Bowler C, Baroux C, Carbone A, Probst AV, Schrumpfová PP, Fajkus J, Amiard S, Grob S, Bourbousse C, Barneche F (2020) Histone H1 protects telomeric repeats from H3K27me3 invasion in *Arabidopsis*. bioRxiv. https://doi.org/10.1101/2020.11.28.402172
Tsuzuki M, Wierzbicki AT (2018) Buried in PEAT—discovery of a new silencing complex with opposing activities. EMBO J 37:e100573. https://doi.org/10.15252/embj.2018100573
van Steensel B, Smogorzewska A, de Lange T (1998) TRF2 Protects Human Telomeres from End-to-End Fusions. Cell 92:401–413. https://doi.org/10.1016/S0092-8674(00)80932-0
Vaquero-Sedas and Vega-Palas (2023) Epigenetic nature of Arabidopsis thaliana telomeres. Plant Physiol 191:47–55. https://doi.org/10.1093/plphys/kiac471
Varadi M, Anyango S, Deshpande M, Nair S, Natassia C, Yordanova G, Yuan D, Stroe O, Wood G, Laydon A et al (2022) AlphaFold protein structure database: Massively expanding the structural coverage of protein-sequence space with high-accuracy models. Nucleic Acids Res 50:D439–D444. https://doi.org/10.1093/nar/gkab1061
Venteicher AS, Meng Z, Mason PJ, Veenstra TD, Artandi SE (2008) Identification of ATPases pontin and reptin as telomerase components essential for holoenzyme assembly. Cell 132:945–957. https://doi.org/10.1016/j.cell.2008.01.019
Walden N, German DA, Wolf EM, Kiefer M, Rigault P, Huang X-C, Kiefer C, Schmickl R, Franzke A, Neuffer B, Mummenhoff K, Koch MA (2020) Nested whole-genome duplications coincide with diversification and high morphological disparity in Brassicaceae. Nat Commun 11:3795. https://doi.org/10.1038/s41467-020-17605-7
Wang X, Wang H, Wang J, Sun R, Wu J, Liu S, Bai Y, Mun J-H, Bancroft I, Cheng F, Huang S, Li X, Hua W, Wang J, Wang X, Freeling M, Pires JC, Paterson AH, Chalhoub B, Wang B, Hayward A, Sharpe AG, Park B-S, Weisshaar B, Liu B, Li B, Liu B, Tong C, Song C, Duran C, Peng C, Geng C, Koh C, Lin C, Edwards D, Mu D, Shen D, Soumpourou E, Li F, Fraser F, Conant G, Lassalle G, King GJ, Bonnema G, Tang H, Wang H, Belcram H, Zhou H, Hirakawa H, Abe H, Guo H, Wang H, Jin H, Parkin IAP, Batley J, Kim J-S, Just J, Li J, Xu J, Deng J, Kim JA, Li J, Yu J, Meng J, Wang J, Min J, Poulain J, Wang J, Hatakeyama K, Wu K, Wang L, Fang L, Trick M, Links MG, Zhao M, Jin M, Ramchiary N, Drou N, Berkman PJ, Cai Q, Huang Q, Li R, Tabata S, Cheng S, Zhang S, Zhang S, Huang S, Sato S, Sun S, Kwon S-J, Choi S-R, Lee T-H, Fan W, Zhao X, Tan X, Xu X, Wang Y, Qiu Y, Yin Y, Li Y, Du Y, Liao Y, Lim Y, Narusaka Y, Wang Y, Wang Z, Li Z, Wang Z, Xiong Z, Zhang Z (2011) The genome of the mesopolyploid crop species *Brassica rapa*. Nat Genet 43:1035–1039. https://doi.org/10.1038/ng.919
Warren CM, Krzesinski PR, Greaser ML (2003) Vertical agarose gel electrophoresis and electroblotting of high-molecular-weight proteins. Electrophoresis 24:1695–1702. https://doi.org/10.1002/elps.200305392
Waterhouse A, Bertoni M, Bienert S, Studer G, Tauriello G, Gumienny R, Heer FT, de Beer TAP, Rempfer C, Bordoli L et al (2018) SWISS-MODEL: homology modelling of protein structures and complexes. Nucleic Acids Res 46:W296–W303. https://doi.org/10.1093/nar/gky427
Wiese AJ, Steinbachová L, Timofejeva L, Čermák V, Klodová B, Ganji RS, Limones-Mendez M, Bokvaj P, Hafidh S, Potěšil D, Honys D (2021) *Arabidopsis* bZIP18 and bZIP52 accumulate in nuclei following heat stress where they regulate the expression of a similar set of genes. Int J Mol Sci 22:530. https://doi.org/10.3390/ijms22020530
Xu W, Liu H, Li S, Zhang W, Wang Q, Zhang H, Liu X, Cui X, Chen X, Tang W, Li Y, Zhu Y, Chen H (2022) GWAS and identification of candidate genes associated with seed soluble sugar content in vegetable soybean. Agronomy 12:1470. https://doi.org/10.3390/agronomy12061470
Xuan H, Liu Y, Zhao J, Shi N, Li Y, Zhou Y, Pi L, Li S, Xu G, Yang H (2022) Phase-separated TRB-PRC2 aggregates contribute to Polycomb silencing in plants. bioRxiv. https://doi.org/10.1101/2022.03.27.485997
Yanhui C, Xiaoyuan Y, Kun H, Meihua L, Jigang L, Zhaofeng G, Zhiqiang L, Yunfei Z, Xiaoxiao W, Xiaoming Q, Yunping S, Li Z, Xiaohui D, Jingchu L, Xing-Wang D, Zhangliang C, Hongya G, Li-Jia Q (2006) The MYB transcription factor superfamily of *Arabidopsis*: Expression analysis and phylogenetic comparison with the rice MYB family. Plant Mol Biol 60:107–124. https://doi.org/10.1007/s11103-005-2910-y
Zhou B-R, Jiang J, Feng H, Ghirlando R, Xiao TS, Bai Y (2015) Structural mechanisms of nucleosome recognition by linker histones. Mol Cell 59:628–638. https://doi.org/10.1016/j.molcel.2015.06.025
Zhou Y, Hartwig B, James GV, Schneeberger K, Turck F (2016) Complementary Activities of TELOMERE REPEAT BINDING Proteins and Polycomb Group Complexes in Transcriptional Regulation of Target Genes. Plant Cell 28:87–101. https://doi.org/10.1105/tpc.15.00787
Zhou Y, Wang Y, Krause K, Yang T, Dongus JA, Zhang Y, Turck F (2018) Telobox motifs recruit CLF/SWN–PRC2 for H3K27me3 deposition via TRB factors in *Arabidopsis*. Nat Genet 50:638–644. https://doi.org/10.1038/s41588-018-0109-9

Authors and Affiliations

Alžbeta Kusová[1,2] · Lenka Steinbachová[3] · Tereza Přerovská[1] · Lenka Záveská Drábková[3] · Jan Paleček[1,2] · Ahamed Khan[4] · Gabriela Rigóová[1] · Zuzana Gadiou[3] · Claire Jourdain[5] · Tino Stricker[5] · Daniel Schubert[5] · David Honys[3,6] · Petra Procházková Schrumpfová[1,2]

[1] Laboratory of Functional Genomics and Proteomics, Faculty of Science, National Centre for Biomolecular Research, Masaryk University, Brno, Czech Republic

[2] Mendel Centre for Plant Genomics and Proteomics, Central European Institute of Technology, Masaryk University, Brno, Czech Republic

[3] Laboratory of Pollen Biology, Institute of Experimental Botany of the Czech Academy of Sciences, Prague, Czech Republic

[4] Institute of Plant Molecular Biology, Biology Centre of the Czech Academy of Sciences, České Budějovice, Czech Republic

[5] Institute of Biology, Freie Universität Berlin, 14195 Berlin, Germany

[6] Department of Experimental Plant Biology, Faculty of Science, Charles University, Prague, Czech Republic

Completing TRB family: newly characterized members show ancient evolutionary origins and distinct localization, yet similar interactions

Alžbeta Kusová[1,2+], Lenka Steinbachová[3+], Tereza Přerovská[1], Lenka Záveská Drábková[3], Jan Paleček[1,2], Ahamed Khan[4], Gabriela Rigóová[1], Zuzana Gadiou[3], Claire Jourdain[5], Tino Stricker[5], Daniel Schubert[5], David Honys[3,6], and Petra Procházková Schrumpfová[1,2*]

[1] Laboratory of Functional Genomics and Proteomics, National Centre for Biomolecular Research, Faculty of Science, Masaryk University, Brno, Czech Republic
[2] Mendel Centre for Plant Genomics and Proteomics, Central European Institute of Technology, Masaryk University, Brno, Czech Republic
[3] Laboratory of Pollen Biology, Institute of Experimental Botany of the Czech Academy of Sciences, Prague, Czech Republic
[4] Biology Centre of the Czech Academy of Sciences, Institute of Plant Molecular Biology, České Budějovice, Czech Republic
[5] Institute of Biology, Freie Universität, 14195 Berlin, Germany
[6] Department of Experimental Plant Biology, Faculty of Science, Charles University, Prague, Czech Republic

* Author for correspondence: schpetra@sci.muni.cz
+ Co-authors: Shared co-first authorship.

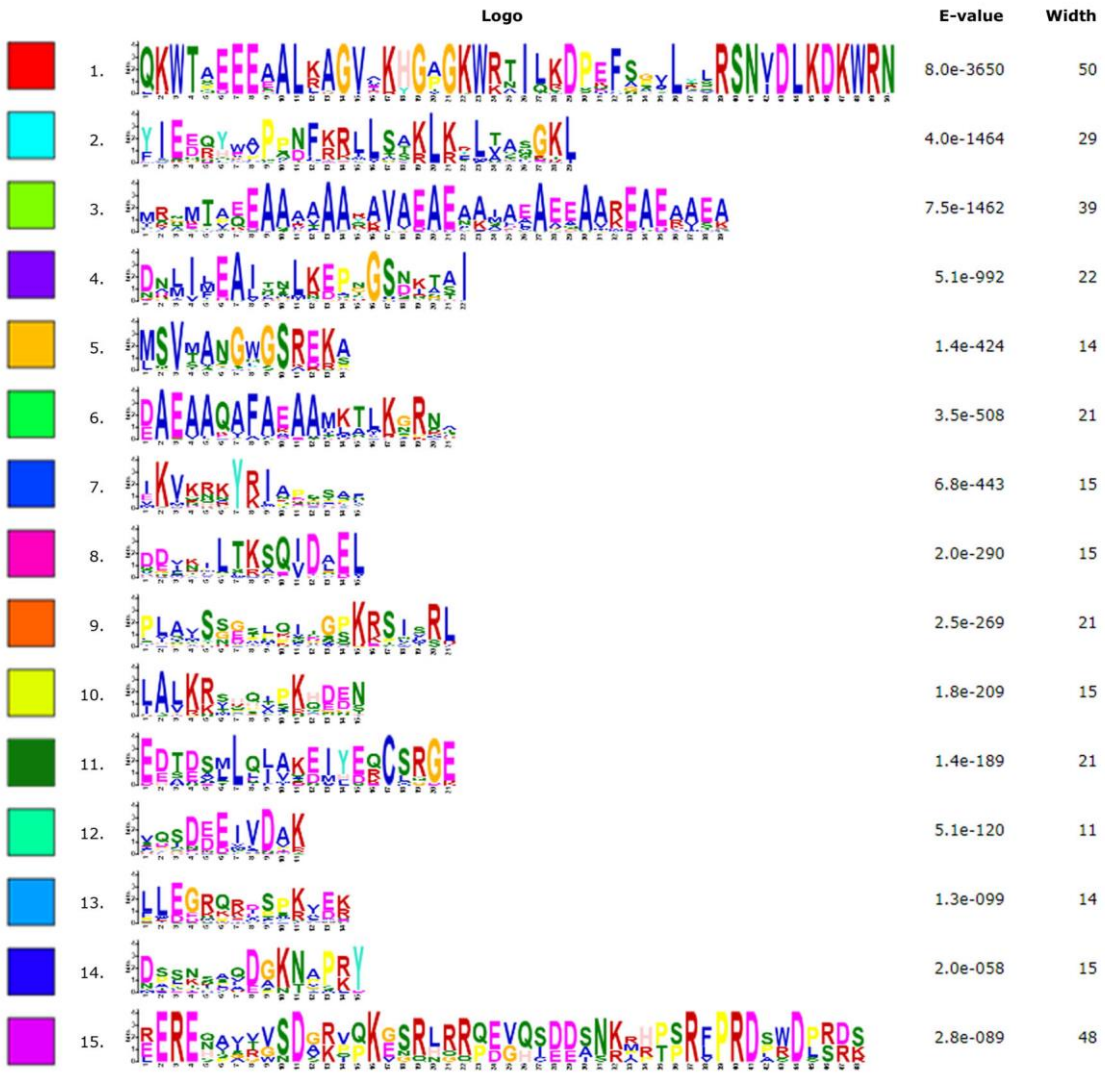

Supplemental Fig. 1 The 15 most conserved motifs in plant TRB protein motifs

Motifs are ranked and ordered by highest probability of occurrence. Motif 1 corresponds to the MYB-like domain. Motifs 2, 4 and 7 belong to the H1/H5-like domain. Motifs 3 and 6 or 3 and 11 create the coiled-coil domain.

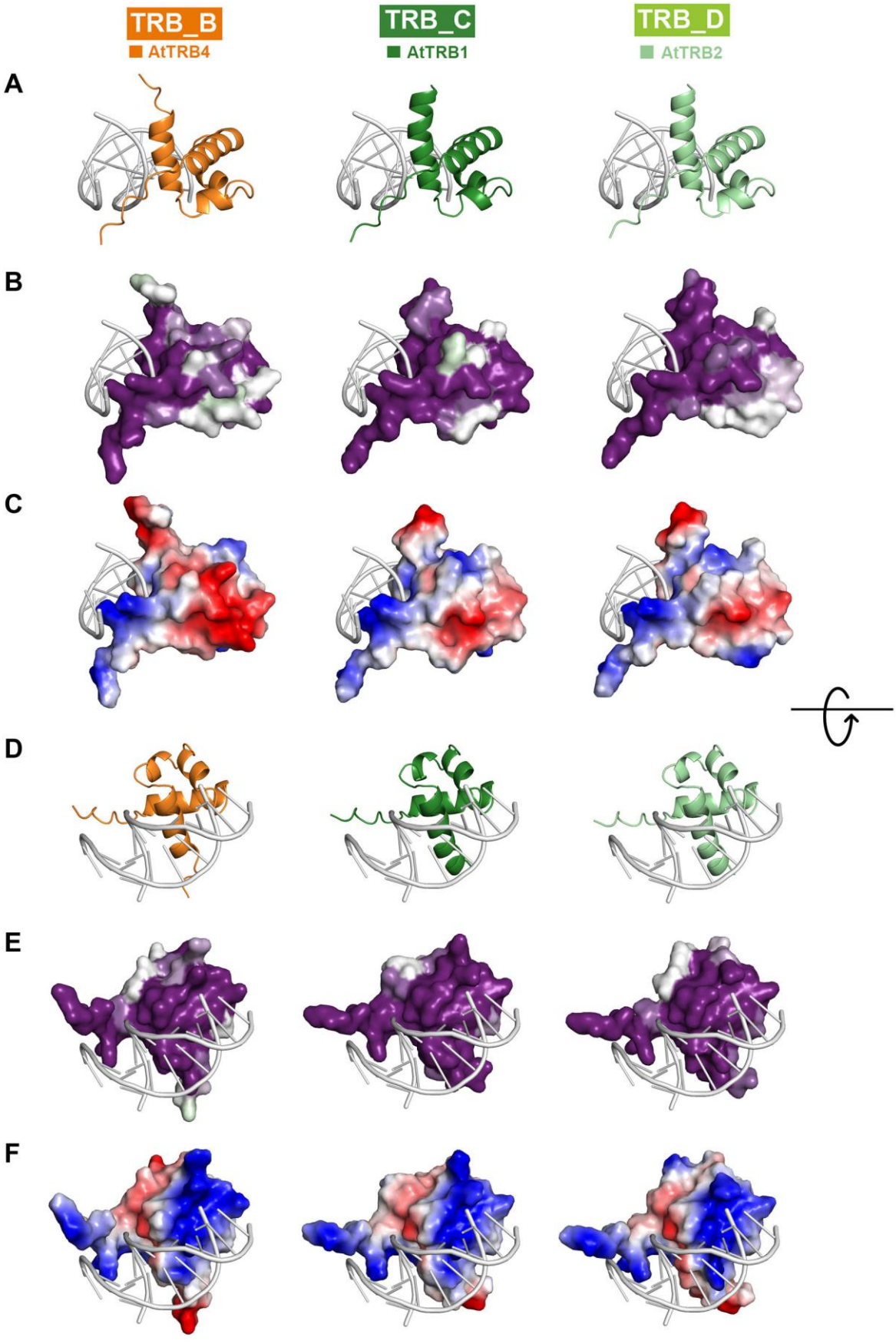
TRB_B
AtTRB4
TRB_C
AtTRB1
TRB_D
AtTRB2
A
B
C
D
E
F

Supplemental Fig. 2 Conserved residues and electrostatic charge visualization of the Myb-like domain in *Arabidopsis* members of Dicots from TRB_B, TRB_C and TRB_D lineages

The representative members of Dicots from TRB_B, TRB_C and TRB_D lineages, namely *A. thaliana* TRB4, TRB1 and TRB2, respectively, were analyzed. The three-dimensional model of the Myb-like domains from the site opposing the DNA-binding (A-C) and from the DNA binding (D-F) viewpoints are based on the hTRF2-DNA interaction model (PDB: 1WOU) (Court et al. 2005).

B) and E) The evolutionary dynamics of aa substitutions among aa residues were visualized in ConSurf 2016 (Ashkenazy et al., 2016). The conservation of residues is presented in a scale, where the most conserved residues are shown in dark magenta and non-conserved residues as white.

C) and F) Surface models showing the charge on the Myb-like domains. Residue charges are coded as red for acidic, blue for basic, and white for neutral, visualized using PyMol, Version 2.4.1, Schrödinger, LLC.

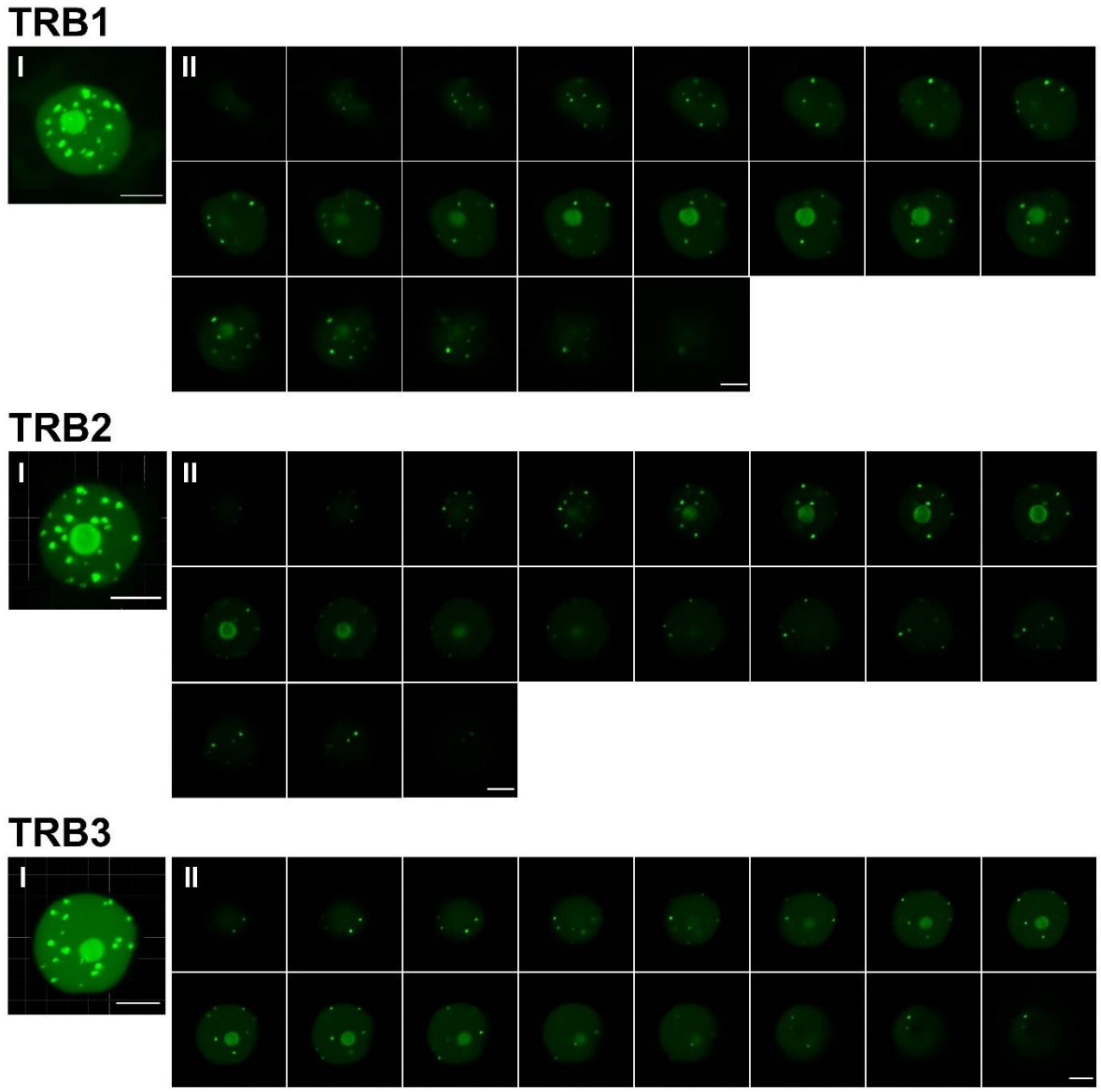

Supplemental Fig. 3 Maximum intensity projections and Z-stacks of TRB1-3 GFP-fusion proteins in nuclei of *N. benthamiana* leaf epidermal cells

TRB1-3 fused with GFP (N-terminal fusions), expressed in *N. benthamiana* leaf epidermal cells and observed by confocal microscopy. Figures represent Maximum Intensity projections (I) of entire Z-stack images of nuclei (II; TRB1 - 0,53 µm each; TRB2 and TRB3 – 0,47 µm each). Scale bars = 5 µm.

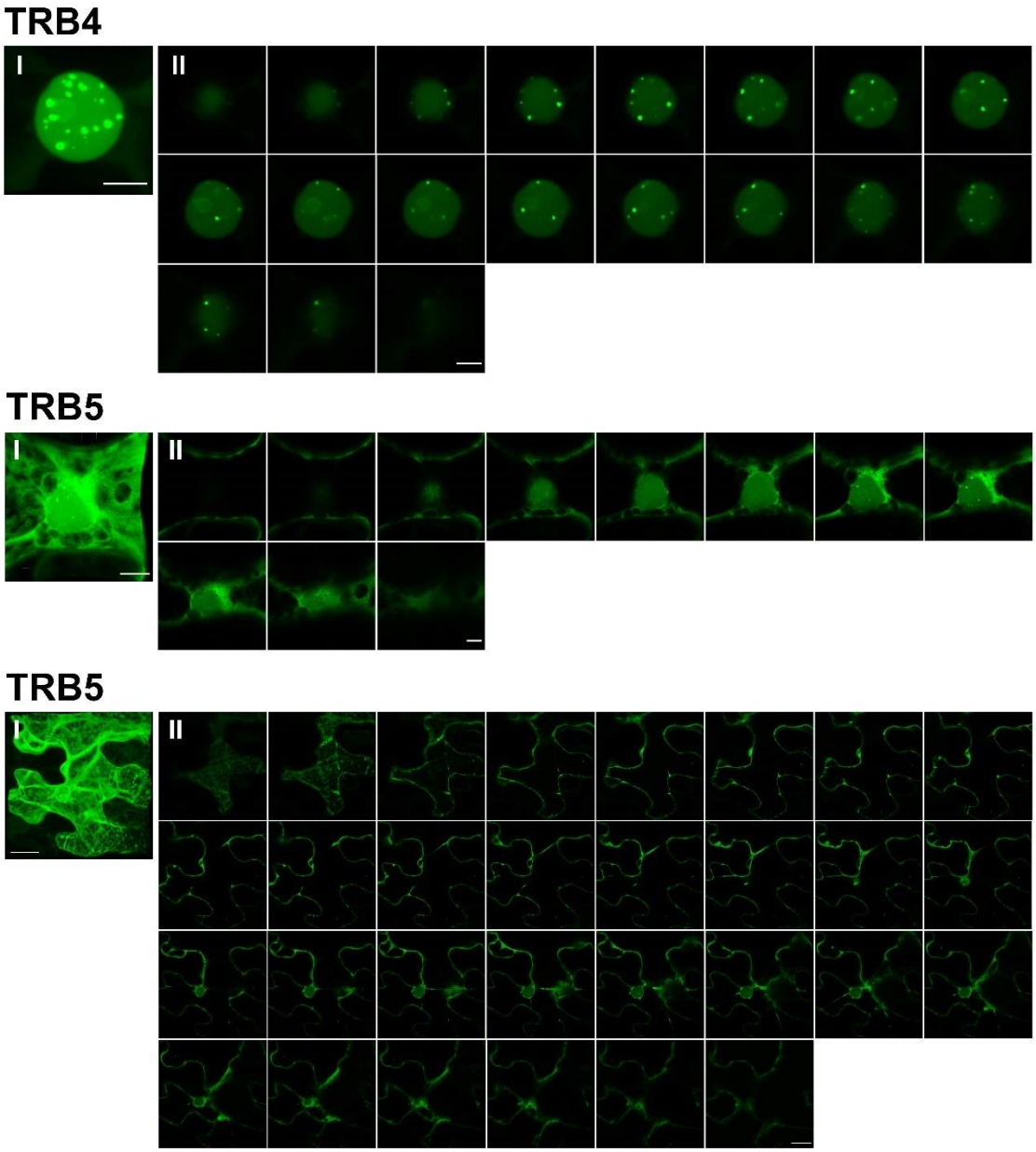

Supplemental Fig. 4 Maximum intensity projections and Z-stacks of TRB4-5 GFP-fusion proteins in *N. benthamiana* leaf epidermal cells

TRB4-5 fused with GFP (N-terminal fusions), expressed in *N. benthamiana* epidermal cells, and observed by confocal microscopy. Figures represent Maximum Intensity projections (I) of entire Z-stack images (II) of nuclei (TRB4 - 0,52 µm each; TRB5 - 0,82 µm each; scale bars = 5 µm) and whole epidermal cell (TRB5 - 0,78 µm each; scale bar = 20 µm).

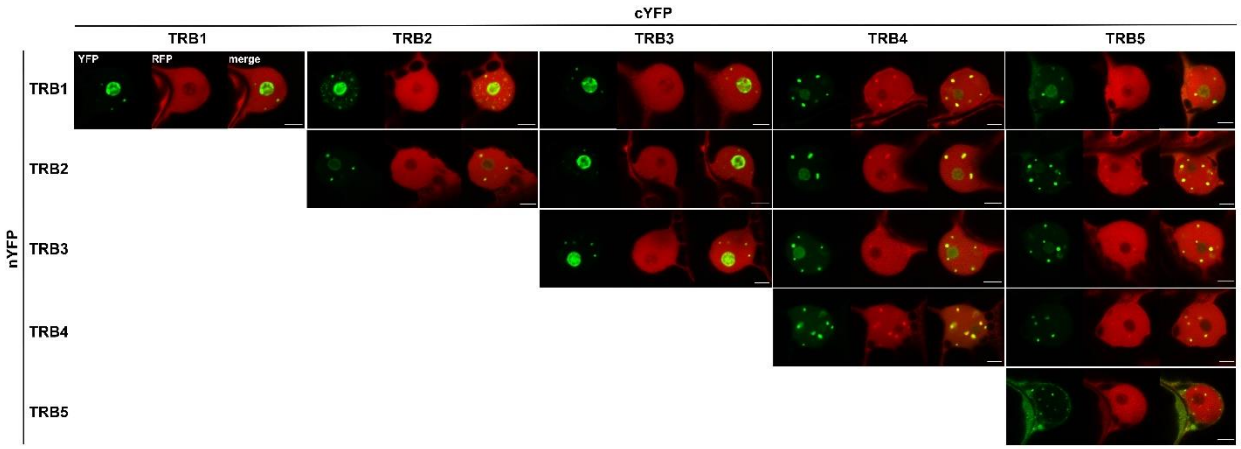

Supplemental Fig. 5 Mutual TRB interactions detected by BiFC in *N. benthamiana*

Protein-protein interactions of TRB proteins fused with nYFP or cYFP part were detected in *N. benthamiana* leaf epidermal cells by confocal microscopy. Shown here are single images of fluorescence signals from individual channels (*YFP*, Yellow fluorescence protein; *RFP*, red fluorescence protein – an internal marker for transformation and expression) and merged signals (*merge*, merged YFP and RFP channels). Scale bars = 5 µm.

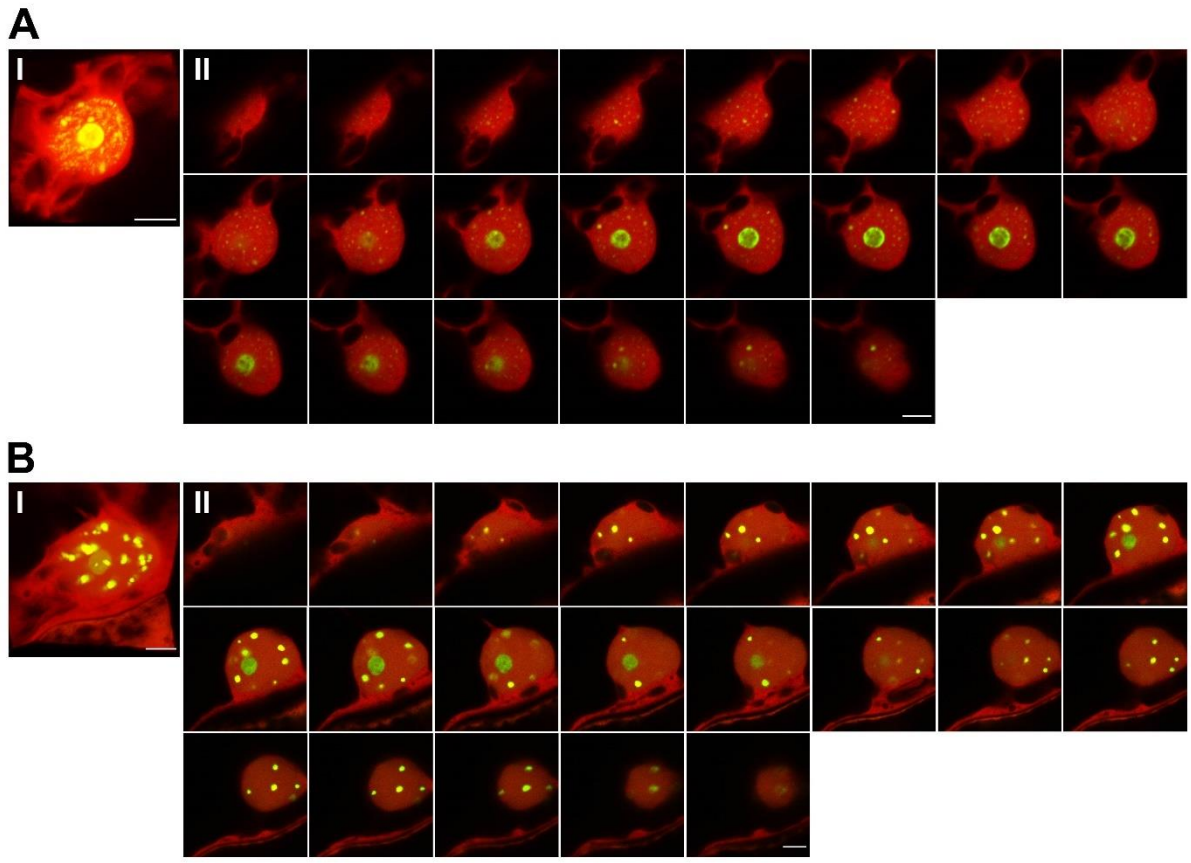

Supplemental Fig. 6 Maximum Intensity projections and Z-stacks of *N. benthamiana* epidermal cells nuclei presenting BiFC analyses

Maximum Intensity Projections (I) of entire Z-stack images (II) of nuclei of *N. benthamiana* leaf epidermal cells displaying BiFC interactions of TRB proteins. Shown here are merged images of YFP (interaction of the tested proteins) and mRFP (internal marker for transformation and expression) fluorescence detected by confocal microscopy. Scale bars = 5 µm.

A) Interaction of TRB1 and TRB2 proteins (nYFP-TRB1 + cYFP-TRB2 pBiFCt-2in1-NN construct). Optical sections 0,48 µm each.
B) Interaction of TRB1 and TRB4 proteins (nYFP TRB1 + cYFP TRB4 pBiFCt-2in1-NN construct). Optical sections 0,55 µm each.

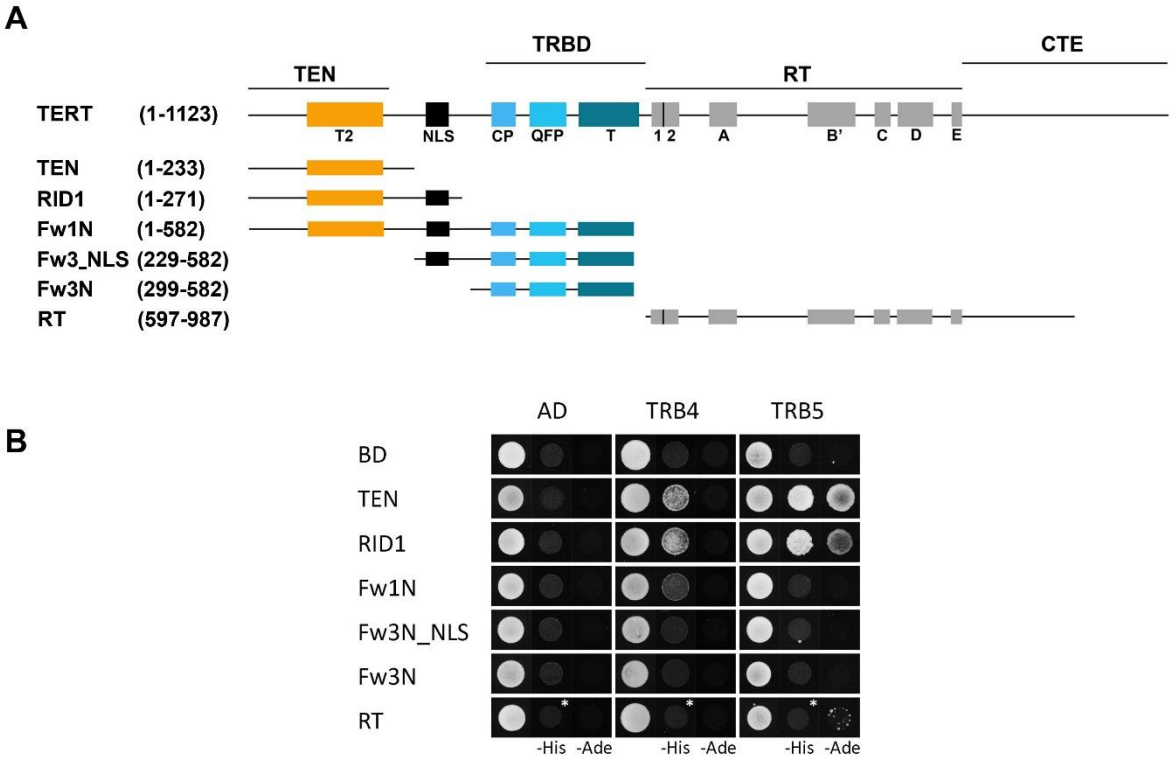

Supplemental Fig. 7 Interactions of TRB4-5 with TERT domains

A) Schematic depiction of the plant catalytic subunit of telomerase (TERT) showing functional motifs. The regions of structural domains TEN (telomerase essential N-terminal domain), TRBD (Telomerase RNA-binding domain), RT (reverse transcriptase domain) and CTE (C-terminal extension) are depicted above the conserved RT motifs (1, 2, A, B, C, D and E), telomerase-specific motifs (T2, CP, QFP and T) and a NLS (nucleus localization-like signal). All of the depicted TERT fragments were used for protein-protein interaction analysis (amino acid numbering is shown).

B) TERT fragments from Majerská et al. 2017 were fused with the GAL4 DNA-binding domain (BD). TRB4 and TRB5 were fused with the GAL4 activation domain (AD). Both constructs were introduced into yeast strain PJ69-4a carrying reporter genes His3 and Ade2. Interactions were detected on histidine-deficient SD medium (-His), or under stringent adenine-deficient SD medium (-Ade) selection. Co-transformation with an empty vector (AD, BD) served as a negative control. *Asterisks* *, 3 mM 3-aminotriazol.

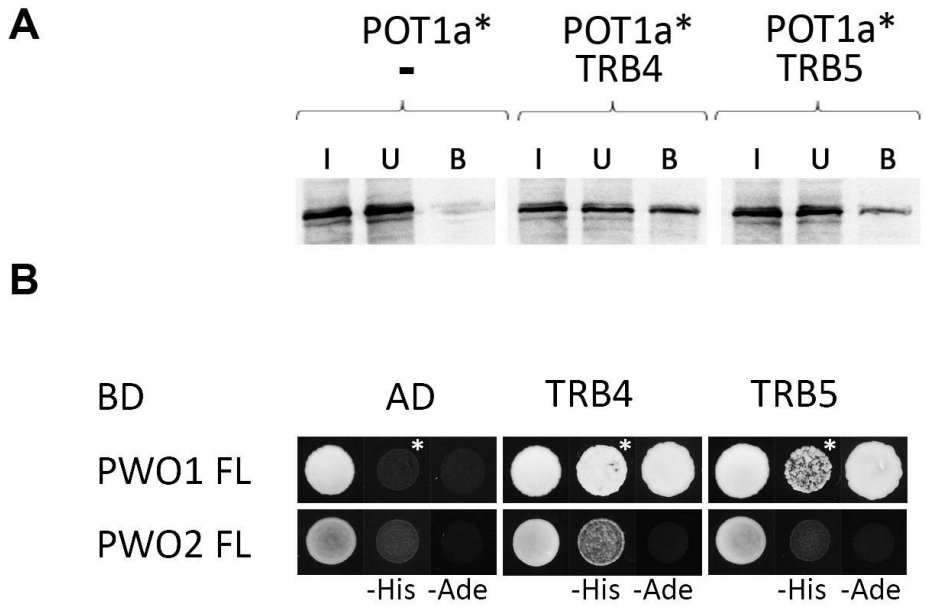

Supplemental Fig. 8 Protein-protein interactions of TRBs with various proteins

A) TNT expressed proteins, POT1a (^{35}S-labelled*) and TRB4/TRB5 (myc-tag), were mixed and incubated with an anti-myc antibody and Protein G magnetic particles. In the control experiment, the POT1a proteins were incubated with an anti-myc antibody and Protein G magnetic particles in the absence of partner protein. Input (I), unbound (U), and bound (B) fractions were collected and run in SDS–10% PAGE gels. *Asterisks* *, ^{35}S labelling.

B) Interactions of TRB4-5 were evaluated using the Y2H system. Interactions between TRB4-5 and full-length PWO1-2 were tested as in Fig. 7B. Interactions were detected on histidine-deficient SD medium (-His), or under stringent adenine-deficient SD medium (-Ade) selection. Co-transformation with an empty vector (AD, BD) served as a negative control. *Asterisks* *, 3 mM 3-aminotriazol.

Supplement S

Teano G., Concia L., Wolff L., Carron L., Biocanin I., Adamusová K., Fojtová M., Bourge M., Kramdi A., Colot V., Grossniklaus U., Bowler Ch., Baroux C., Carbone A., Probst A.V., **Schrumpfová P.P.,** Fajkus J., Amiard S., Grob S., Bourbousse C., and Barneche F. **2023**. Histone H1 protects telomeric repeats from H3K27me3 invasion in Arabidopsis. Cell Reports, 42(8):112894.

P.P.S. participated in the design of experiments and ms editing

Article

Cell Reports

Histone H1 protects telomeric repeats from H3K27me3 invasion in *Arabidopsis*

Graphical abstract

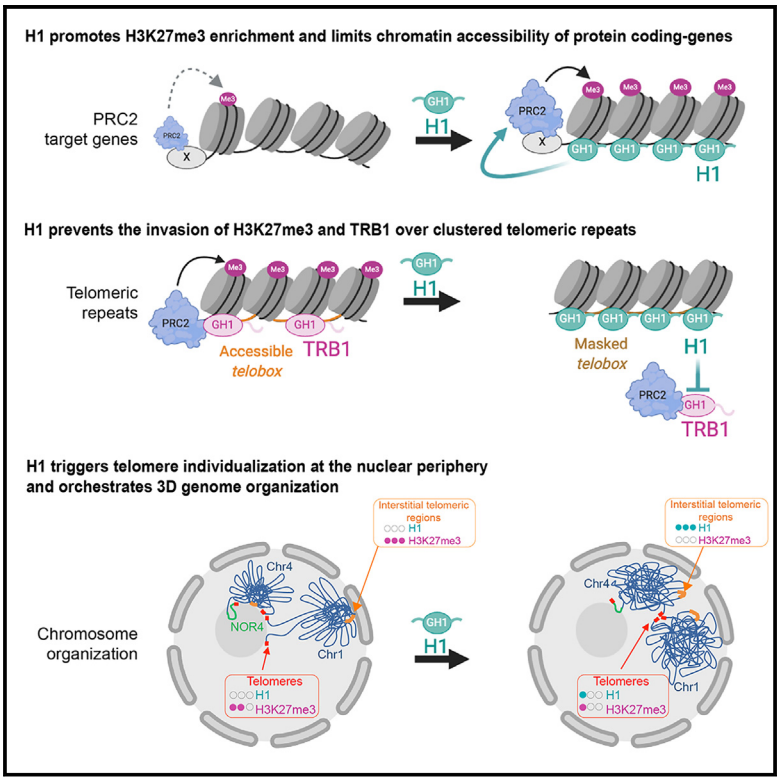

Highlights

- H1 promotes PRC2 activity at a majority of genes
- H1 limits PRC2 activity at telomeres and interstitial telomeric repeats (ITRs)
- H1 orchestrates the spatial organization of telomeres and ITRs
- PRC2 repression is achieved by restricting accessibility to TRB proteins

Authors

Gianluca Teano, Lorenzo Concia, Léa Wolff, ..., Stefan Grob, Clara Bourbousse, Fredy Barneche

Correspondence

barneche@bio.ens.psl.eu

In brief

Teano et al. report that linker histone H1 and a group of H1-related telomeric proteins interplay to selectively influence the *Polycomb* repressive landscape at telomeric repeats in *Arabidopsis*. These findings provide a mechanistic framework by which H1 affects the epigenome and nuclear organization in a sequence-specific manner.

Teano et al., 2023, Cell Reports *42*, 112894
August 29, 2023
https://doi.org/10.1016/j.celrep.2023.112894

CellPress

Cell Reports

CellPress
OPEN ACCESS

Article

Histone H1 protects telomeric repeats from H3K27me3 invasion in *Arabidopsis*

Gianluca Teano,[1,8,9] Lorenzo Concia,[1,9] Léa Wolff,[1] Léopold Carron,[2] Ivona Biocanin,[1,8] Kateřina Adamusová,[3,4] Miloslava Fojtová,[3,4] Michael Bourge,[5] Amira Kramdi,[1] Vincent Colot,[1] Ueli Grossniklaus,[6] Chris Bowler,[1] Célia Baroux,[6] Alessandra Carbone,[2] Aline V. Probst,[7] Petra Procházková Schrumpfová,[3,4] Jiří Fajkus,[3,4] Simon Amiard,[7] Stefan Grob,[6] Clara Bourbousse,[1] and Fredy Barneche[1,10,*]

[1]Institut de biologie de l'École normale supérieure (IBENS), École normale supérieure, CNRS, INSERM, Université PSL, Paris, France
[2]Sorbonne Université, CNRS, IBPS, UMR 7238, Laboratoire de Biologie Computationnelle et Quantitative (LCQB), 75005 Paris, France
[3]Mendel Centre for Plant Genomics and Proteomics, Central European Institute of Technology, Masaryk University, Brno, Czech Republic
[4]Laboratory of Functional Genomics and Proteomics, NCBR, Faculty of Science, Masaryk University, Brno, Czech Republic
[5]Cytometry Facility, Imagerie-Gif, Université Paris-Saclay, CEA, CNRS, Institute for Integrative Biology of the Cell (I2BC), 91198 Gif-sur-Yvette, France
[6]Department of Plant and Microbial Biology & Zurich-Basel Plant Science Center, University of Zurich, Zurich, Switzerland
[7]CNRS UMR6293, Université Clermont Auvergne, INSERM U1103, GReD, CRBC, Clermont-Ferrand, France
[8]Université Paris-Saclay, 91190 Orsay, France
[9]These authors contributed equally
[10]Lead contact
*Correspondence: barneche@bio.ens.psl.eu
https://doi.org/10.1016/j.celrep.2023.112894

SUMMARY

While the pivotal role of linker histone H1 in shaping nucleosome organization is well established, its functional interplays with chromatin factors along the epigenome are just starting to emerge. Here we show that, in *Arabidopsis*, as in mammals, H1 occupies Polycomb Repressive Complex 2 (PRC2) target genes where it favors chromatin condensation and H3K27me3 deposition. We further show that, contrasting with its conserved function in PRC2 activation at genes, H1 selectively prevents H3K27me3 accumulation at telomeres and large pericentromeric interstitial telomeric repeat (ITR) domains by restricting DNA accessibility to Telomere Repeat Binding (TRB) proteins, a group of H1-related Myb factors mediating PRC2 *cis* recruitment. This study provides a mechanistic framework by which H1 avoids the formation of gigantic H3K27me3-rich domains at telomeric sequences and contributes to safeguard nucleus architecture.

INTRODUCTION

Both local and higher-order chromatin architecture rely to a large extent on the regulation of nucleosome density and accessibility, in which linker histone H1 and *Polycomb* Repressive complexes 1 and 2 (PRC1/2) play distinct roles. H1 modulates nucleosome distribution by contacting the nucleosome dyad with its central globular (GH1) domain and by binding linker DNA at the nucleosome entry and exit sites with its disordered carboxy-terminal domain. This indirectly contributes to dampen transcriptional activity by affecting the accessibility of transcription factors and RNA polymerases to DNA but also through interactions with histone and DNA modifiers (reviewed elsewhere[1–3]).

Polycomb group activity is another determinant of chromatin organization that extensively regulates transcriptional activity, cell identity, and differentiation in metazoans,[4,5] plants,[6] and unicellular eukaryotes.[7] While H1 incorporation directly influences the physicochemical properties of the chromatin fiber, PRC1 and PRC2 display enzymatic activities mediating histone H2A Lysine monoubiquitination (H2Aub) and histone H3 lysine 27 trimethylation (H3K27me3), respectively.[4,5] In metazoans, chromatin of PRC target genes is highly compacted,[8–10] a feature thought to hinder transcription (reviewed in Schuettengruber et al. and Illingworth[5,11]). PRC2 can favor chromatin compaction either by promoting PRC1 recruitment or through its subunit Enhancer of Zeste Homolog 1 (Ezh1) in a mechanism not necessarily relying on the H3K27me3 mark itself.[12]

Mutual interplay between H1 and PRC2 activity first emerged *in vitro*. Human H1.2 preferentially binds to H3K27me3-containing nucleosomes[13] while, vice versa, human and mouse PRC2 complexes display substrate preferences for H1-enriched chromatin fragments. The latter activity is stimulated more on di-nucleosomes than on mono- or dispersed nucleosomes.[14,15] *In vivo*, recent studies unveiled that H1 is a critical regulator of H3K27me3 enrichment over hundreds of PRC2 target genes in mouse cells.[16,17] Chromosome conformation capture (Hi-C) analysis of hematopoietic cells,[16] germinal center B cells,[17] and embryonic stem cells[18] showed that H1 triggers distinct genome folding during differentiation in mammals. These major advances raise the question of the mechanisms enabling H1 sequence-specific interplays with PRC2 activity in chromatin regulation and their evolution in distinct eukaryotes.

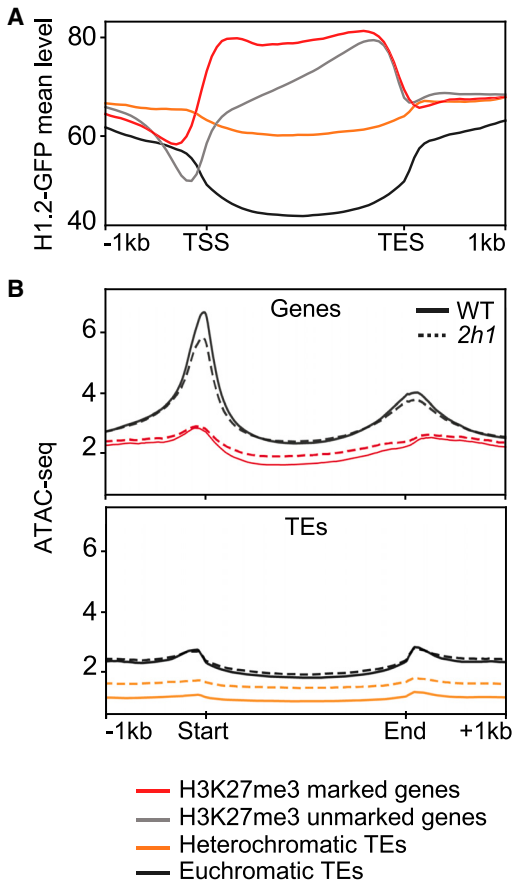

Figure 1. H1.2-GFP is enriched at PRC2-target genes where it contributes to restrain DNA accessibility

(A) H1.2-GFP mean read coverage at protein-coding genes and TEs.

(B) ATAC-seq analysis of chromatin accessibility of genes and TEs described in (A) in WT (plain lines) and *2h1* (dashed lines) nuclei. Chromatin accessibility is estimated as read coverage. TSS, transcription start site; TES, transcription end site. In (A) and (B), H3K27me3-marked genes (n = 7,542) are compared to all other annotated protein-coding genes. Heterochromatic versus euchromatic TEs were defined previously.[43] The plots represent the mean of three (H1.2-GFP) or two (ATAC-seq) independent biological replicates.

In *Arabidopsis thaliana*, two canonical linker histone variants, H1.1 and H1.2, represent the full H1 complement in most somatic cells.[19–21] These two linker histones, hereafter referred to as H1, are enriched over heterochromatic transposable elements (TEs) displaying high nucleosome occupancy; CG, CHG, and CHH methylation; as well as H3K9 dimethylation.[22,23] H1 also contributes to CG methylation-mediated gene silencing[24] and is less abundant over expressed genes.[22,23] As in mammals, *Arabidopsis* H1 incorporation is thought to dampen RNA Pol II transcription, an effect that also applies in plants to RNA polymerase Pol IV, which produces short interfering RNAs (siRNAs).[25] *Arabidopsis* H1 also restricts accessibility to DNA methyltransferases and demethylases, which mediates gene or TE silencing.[26–30] This process is counter-balanced by incorporation of the H2A.W histone variant, presumably competing with H1 for DNA binding through its extended C-terminal tail.[31]

Besides TE silencing, recent studies suggested that H1 dynamics may affect PRC2 activity during *Arabidopsis* development. The first piece of evidence is that H1 is largely absent from the vegetative cell nucleus of pollen grain and is degraded during spore mother cell (SMC) differentiation at the onset of heterochromatin loosening and H3K27me3 reduction.[26,32–34] Further evidence comes from the observation that *H1* loss-of-function mutant nuclei display a ~2-fold lower H3K27me3 chromatin abundance, while a few discrete H3K27me3 sub-nuclear foci of undetermined nature displayed increased H3K27me3 signals.[35] Hence, despite evidence that variations in H1 abundance mediate epigenome reprogramming during plant development, there is no information on how H1 interplays with PRC2 activity and on the consequences of this interaction on the chromatin landscape and topology in these organisms.

Here, we profiled H3K27me3 in *h1* mutant plants and found that, while a majority of genes expectedly lost H3K27me3, telomeres and pericentromeric interstitial telomeric repeat (ITR) regions or interstitial telomeric sequences (ITSs) were massively enriched in this mark. We identified that H1 prevents PRC2 activity at these loci by hindering the binding of Telomere Repeat Binding (TRB) proteins, a group of H1-related proteins with extra-telomeric function in PRC2 recruitment.[36,37] H1 safeguards telomeres and ITRs against excessive H3K27me3 deposition and preserves their topological organization. Collectively, our findings led us to propose a mechanism by which H1 orchestrates *Arabidopsis* chromosomal organization and contributes to the control of H3K27me3 homeostasis between structurally distinct genome domains.

RESULTS

H1 is abundant at H3K27me3-marked genes and reduces their chromatin accessibility

To assess the relationships between H1, PRC2 activity, and chromatin accessibility, we first compared the genomic distribution of H3K27me3 with that of H1.2, the most abundant canonical H1 variant in *Arabidopsis* seedlings.[22] To maximize specificity, we used a GFP-tagged version of H1.2 expressed under the control of its endogenous promoter.[22] In agreement with previous studies in several eukaryotes,[22,23,38,39] H1.2 covers most of the *Arabidopsis* genome without displaying clear peaks. However, a closer examination revealed that, as compared to genes and to TEs that are not enriched in H3K27me3,[40–42] H1 level was higher at coding genes marked by H3K27me3, especially toward their 5′ regions (Figures 1A and S1A–S1C).

Having found that H1 is enriched at PRC2 marked genes, we tested whether H1 also contributes to regulate chromatin accessibility using assay for transposase-accessible chromatin followed by sequencing (ATAC-seq) in nuclei of wild-type (WT) and *h1.1h1.2* double-mutant plants (hereby named *2h1* for short). As previously reported in WT plants,[44] H3K27me3-marked genes tend to display low chromatin accessibility as compared to non-marked genes, which are usually expressed and typically display a sharp ATAC peak at their transcription start sites (TSSs) corresponding to the nucleosome-free region (Figure 1B). In *2h1* nuclei, gene body regions of H3K27me3-marked loci displayed a significant increase in accessibility (Figures 1B and S1D).

Hence, H1 tends to abundantly occupy PRC2 target gene bodies where it has a minor but detectable contribution in restricting chromatin accessibility.

H1 promotes H3K27me3 enrichment at a majority of PRC2 target genes while protecting a few genes displaying specific sequence signatures

To determine at which loci H1 influences PRC2 activity, we profiled the H3K27me3 landscape in WT and *2h1* seedlings. To enable absolute quantifications despite the general reduction of H3K27me3 in the mutant nuclei, we employed chromatin immunoprecipitation sequencing (ChIP-seq) with reference exogenous genome (ChIP-Rx) by spiking in equal amounts of *Drosophila* chromatin to each sample.[45] Among the ~7,500 genes significantly marked by H3K27me3 in WT plants, more than 4,300 were hypomethylated in *2h1* plants (Figures 2A–2C and S2A–S2D; Table S1). Hence, general loss of H3K27me3 in *2h1* seedlings identified by immunoblotting and cytology[35] results from a general effect at a majority of PRC2-regulated genes. It is noteworthy that ~85% of the genes marked by H3K27me3 in WT plants were still significantly marked in *2h1* plants (Figure S2D). Hence, H1 is required for efficient H3K27me3 maintenance or spreading rather than for PRC2 seeding. Our RNA sequencing (RNA-seq) analysis showed that genes encoding PRC1/PRC2 subunits are not downregulated in *2h1* plants, excluding indirect effects resulting from less-abundant PRC2 (Table S2). Unexpectedly, we also found that ~500 genes were hyper-marked or displayed *de novo* marking in *2h1* plants (Figures 2A–2C and S2A–S2D; Table S1).

To determine whether the hypo/hyper/unaffected gene sets had different functional properties, we inspected their transcript levels. Hyper-marked genes correspond to the least expressed gene category in WT plants, whereas many hypo-marked genes are significantly more expressed than unaffected genes (Figure 2D). Functional categorization of hypo-marked genes notably identified an over-representation of genes involved in transcriptional regulation and meristem maintenance (Figure S2H). These classifications are consistent with former reports of PRC2 repressing these biological processes.[46] In contrast, a feature of the hyper-marked gene set is the presence of TE or TE-gene annotations (Figure S2I; Table S1). Hence, H1-mediated PRC2 activation[14–16] is most likely conserved in plants, but, in *Arabidopsis*, this property is contrasted by a heretofore-unsuspected negative effect at a minority of poorly expressed genes sometimes displaying TE features.

In vitro, PRC2 activity was proposed to be favored by local H1 abundance and/or at densely organized nucleosome arrays.[14] Instead, we found that hypo-marked genes tend to display lower H1 level, to be more accessible and expressed than other genes marked by H3K27me3 (Figures 2D–2F and S2E). We therefore tested nucleosome density using ChIP-seq profiling of histone H3, confirming that hypo-marked genes display lower nucleosome occupancy than other marked gene categories (Figure S2G). Collectively, analysis of the hypo-marked loci suggests that chromatin of the corresponding genes is not sufficiently nucleosome dense to favor PRC2 local activity when H1 is absent.

We further explored whether the specific influence of H1 on H3K27me3 enrichment at genes could rely on a sequence-dependent mechanism, especially at hyper-marked genes, since they do not incur H1-mediated PRC2 activation. In contrast to the promoter sequences of the hypo-marked genes in which no such motif is significantly over-represented, we identified three enriched motifs in the hyper-marked gene set (Figure S2J). A poly(A) motif is present in 84% of the gene promoters, and the AAACCCTA telomeric motif, referred to as *telobox*,[47,48] which serves as *Polycomb Response Elements* (*PREs*) in plants,[36,37] is found in 17% of them (Table S1). Based on these observations, we conclude that the capacity of H1 to counteract H3K27me3 enrichment at a small gene set presumably involves specific sequence features.

H1 contributes to define accessibility and expression of PRC2 target genes

To get insights into the functional consequences of H1 loss at genes where it either promotes or dampens H3K27me3 enrichment, we compared the chromatin accessibility and transcript levels of these gene sets in WT and *2h1* nuclei. ATAC-seq profiling showed that hypo-marked gene bodies were significantly more accessible in the mutant than in the WT line (Figures 2F and S2F), thereby correlating with reduced H3K27me3 levels. Accessibility of H3K27me3 hyper-marked genes was increased in *2h1* plants, still remaining at a very low level as compared to non-marked genes (Figures 2F and S2F). Conservation of this function in both hypo- and hyperH3K27me3 gene categories indicates that H1 incorporation reduces chromatin accessibility of *Arabidopsis* PRC2-target genes independently of its influence on H3K27me3 enrichment.

Confirming previous reports,[23,35] our RNA-seq analysis showed that *H1* loss of function triggers minor gene expression changes (Table S2). However, we identified a significant tendency for increased transcript levels of the H3K27me3 hypo- and hyper-marked genes set in the *2h1* line (Figure 2G). Taken together, these analyses showed that, at a majority of PRC2 target genes, H1 depletion triggers H3K27me3 loss associated with a moderate increase in DNA accessibility and expression.

H1 prevents H3K27me3 invasion over a specific family of heterochromatic repeats

Considering the observed H3K27me3 enrichment at a few TE-related genes in *2h1* plants, we extended our analysis to TEs, which typically lack H3K27me3 in *Arabidopsis*.[49,50] This revealed that 1,066 TEs are newly marked by H3K27me3 in *2h1* plants, most frequently over their entire length, thereby excluding *a priori* the possibility that H3K27me3 TE enrichment is due to spreading from neighboring genes (Figure 3A). We clustered H3K27me3-marked TEs into two groups, *TE cluster 1* and *TE cluster 2*, displaying high and low H3K27me3 enrichment, respectively (Figure 3A). While *TE cluster 2* (n = 850) is composed of a large variety of TE families, *TE cluster 1* (n = 216) mostly consists of *ATREP18* (189 elements) annotated in the TAIR10 genome as unassigned (Figure 3B). In total, *TE cluster 1* and *2* comprise 60% of all annotated *Arabidopsis ATREP18* elements, including many of the longest units (Figure S3A). A second distinguishing feature of *TE cluster 1* elements is their elevated H1 and H3 occupancy (Figures 3C and S3B–S3E). Accordingly, *TE cluster 1* and, more generally, *ATREP18* elements are strongly heterochromatic

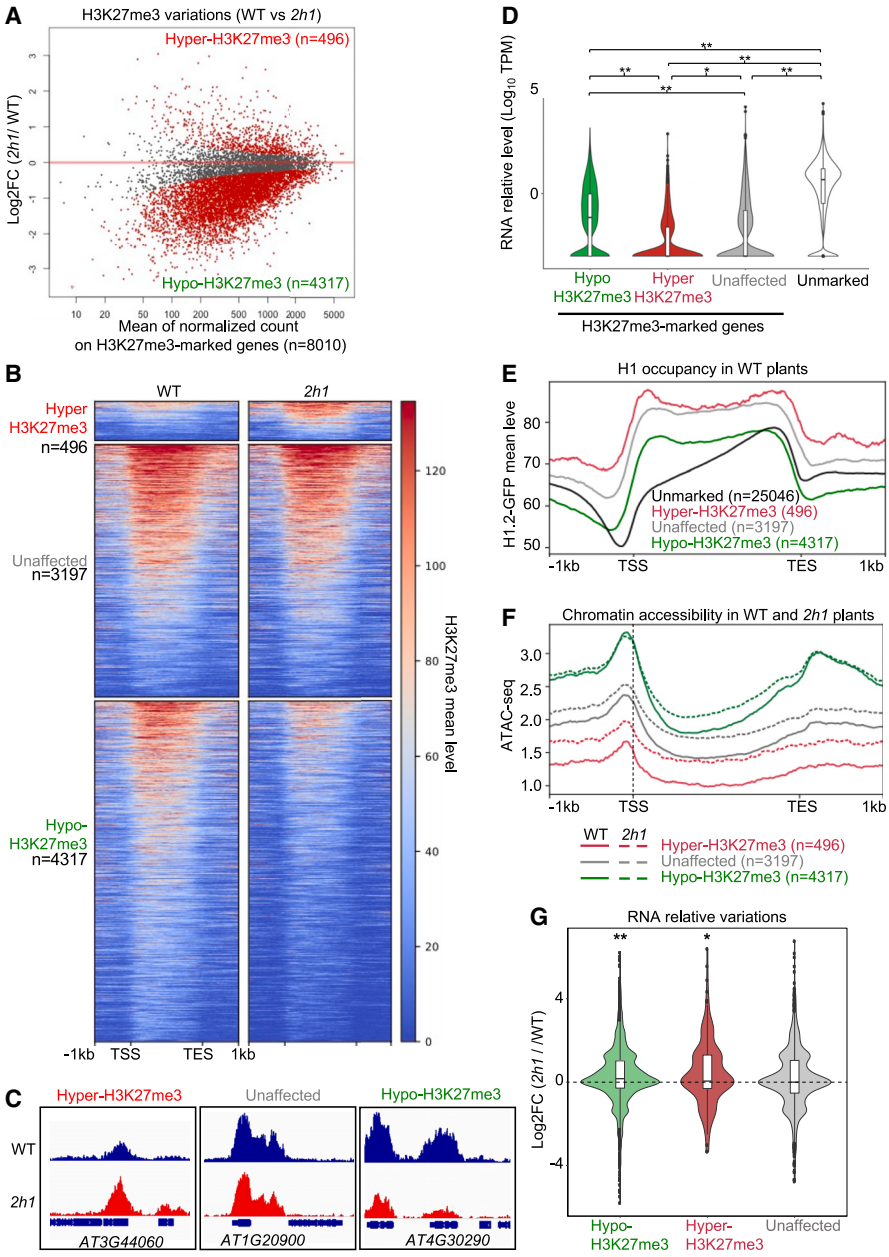

Figure 2. H1 influences H3K27me3 marking, chromatin accessibility, and expression of PRC2-target genes

(A) Identification of differentially marked genes using spike-in normalized DESeq2 ChIP-seq analysis identifies low H3K27me3 levels over a majority of the PRC2 target genes in *2h1* plants. All genes displaying an H3K27me3-enriched domain in WT or *2h1* plants (according to MACS2 peak detection; see STAR Methods) are individually shown as dots. Red dots, differentially marked genes (false discovery rate [FDR] <0.01).

(B) H3K27me3 profiles along all genes significantly marked in WT or *2h1* plants. Genes are grouped according to differential analysis in (A) and ranked within each group according to mean H3K27me3 levels.

(C) H3K27me3 profile of representative genes of the three sets identified in (A) exemplifying the general tendency of PRC2-target genes to keep a weak H3K27me3 domain in *2h1* plants.

(D) Transcript levels in WT seedlings. The values represent RNA-seq log10 transcripts per million (TPM) values. The embedded boxplots display the median, while lower and upper hinges correspond to the first and third quartiles. *$p < 10^{-9}$ and **$p < 10^{-15}$, Wilcoxon rank test.

(E) H1.2-GFP ChIP-seq profiling on the indicated gene sets (mean read coverage).

(F) ATAC-seq analysis of the indicated gene sets. ATAC-seq data are presented as in Figure 1B using mean read coverage.

(G) Transcript level variations between WT and *2h1* plants in the same three gene sets. The values represent mRNA $\log_2$ fold changes. The embedded boxplots display the median, while lower and upper hinges correspond to the first and third quartiles. *p < 5% and **p < 1%, Student's t test. ChIP-Rx, ATAC-seq, and RNA-seq data correspond to two biological replicates each, and H1.2-GFP ChIP-seq correspond to three biological replicates.

CellPress
OPEN ACCESS

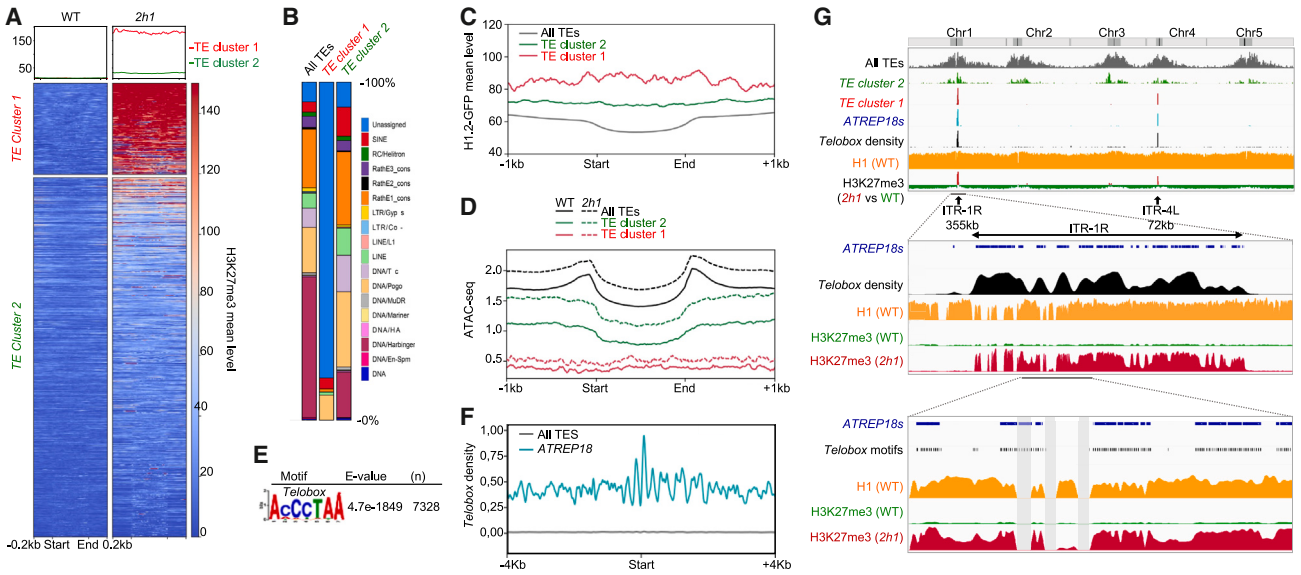

Figure 3. H1 hinders H3K27me3 enrichment at two pericentromeric ITR blocks spanning more than 420 kb

(A) Hyper-marked TEs were clustered into two groups according to H3K27me3 levels after spike-in normalization defining two TE clusters of 216 and 850 TEs, respectively. H3K27me3 profiles over all *TE cluster 1* and *2* elements are ranked in each group according to H3K27me3 mean spike-in normalized coverage.

(B) Relative TE superfamily composition of H3K27me3-enriched TEs. *TE cluster 1* comprises a strong over-representation of "unassigned" annotations mainly corresponding to *ATREP18* elements, while *TE cluster 2* elements correspond to a wide variety of TE super-families.

(C) *TE cluster 1* elements display high H1 occupancy. The plot represents H1.2-GFP mean read coverage over the indicated repertoire of TEs and repeats.

(D) Chromatin accessibility of *TE cluster 1* elements remains very low in *2h1* nuclei. ATAC-seq data are presented as in Figure 1B using mean read coverage.

(E) Motif enrichment search identified an over-representation of *telobox* motifs in *TE cluster 1* sequences. E values were calculated against all TE sequences.

(F) *ATREP18* repeats display outstanding density and a distinct pattern of *telobox* motifs as compared to the whole set of annotated TEs. The plot represents the density of perfect *telobox* sequence motifs in all *ATREP18s* as compared to all TEs within 50-bp bins.

(G) Chromosome distribution of H3K27me3 defects in *2h1* plants and their link to *ATREP18*, *TE cluster 1*, and *TE cluster 2* elements. The sharp peaks of *telobox* density in the pericentromeres of chromosome 1 and 4 correspond to ITR-1R and ITR-4L. Chromosome 1 pericentromeric region displays a sharp overlap between *2h1*-specific H3K27me3 enrichment and the *telobox*-rich ITR-1R. Bottom panel, shaded boxes correspond to blacklisted TAIR10 genome sequences (see STAR Methods). Complementary profiles over ITR-4L and other interspersed elements from *TE cluster 2* are shown in Figures S3L and S3M.

with elevated nucleosome occupancy, H3K9me2, cytosine methylation, and very low chromatin accessibility (Figures 3D and S3C–S3H and S3K). Taken together, these observations indicate that H1 prevents H3K27me3 accumulation over a set of H1-rich, heterochromatic, and highly compacted repeats, which contrasts with its positive influence on H3K27me3 marking over thousands of PRC2-target genes.

Noteworthy, while MNase-seq analyses[22,23] and our ATAC-seq data showed that heterochromatic TEs tend to be more accessible in *2h1* nuclei, the chromatin of *TE cluster 1* and *ATREP18* repeats remained very poorly accessible despite H1 loss (Figures 3D, S3C, and S3D). Hence, chromatin "inaccessibility" of *TE cluster 1* elements is either H1 independent or compensated by other mechanisms, possibly a local increase in PRC2 activity.

Repeats gaining H3K27me3 in *2h1* plants are parts of two large pericentromeric telomeric regions

Aiming at determining the features potentially leading to a selective role of H1 at *TE cluster 1* elements, we first envisaged that H1 could locally prevent conversion of the H3K27me1 heterochromatic mark into H3K27me3. However, analysis of public datasets[51] showed that, as compared to other TEs, H3K27me1 is not particularly abundant at *TE cluster 1* or at *ATREP18* elements, therefore ruling out this first hypothesis (Figure S3F). We then explored the possibility that H1 could favor H3K27me3 de-methylation. Examination of the H3K27me3 profile in loss-of-function plants for the three major histone H3K27me3 demethylases EARLY FLOWERING 6 (ELF6), RELATIVE OF ELF 6 (REF6), and JUMONJI 13 (JMJ13)[52] showed no H3K27me3 increase at *TE cluster 1* elements (Figure S3I) or at hyper-marked genes (Figure S3J). This led us to rule out the hypothesis that, in WT plants, H3K27me3 could be regulated at these loci though active erasure. Last, considering the tendency for cytosine methylation to be mutually exclusive with H3K27me3 deposition in *Arabidopsis*,[53–55] we envisioned that H3K27me3 enrichment at *TE cluster 1* may indirectly result from decreased DNA methylation induced by H1 loss. Examination of cytosine methylation patterns of *TE cluster 1* elements in *2h1* plants oppositely showed an increase in CG, CHG, and CHH methylation (Figure S3K). We did not ascertain whether methylated cytosines and H3K27me3-containing nucleosomes co-occur at individual *TE cluster 1* chromatin fragments, yet this observation ruled out that H1 indirectly hinders PRC2 activity at these loci by promoting cytosine methylation, a possibility that would have been supported if an opposite effect was observed.

Having not found evidence for indirect roles of H1 on H3K27me3 marking at *TE cluster 1*, we concluded that H1 hinders PRC2 recruitment or activity at these repeats, and this

despite a densely packed chromatin organization that theoretically constitutes an excellent substrate. As previously done for hyper-marked genes, we therefore tested whether *TE cluster 1* elements are distinguishable from other TEs by specific DNA motifs. MEME search identified a prominent sequence signature, the *telobox* motif (Figure 3E), which we had already identified in 17% of the hyper-marked genes (Figure S2J). As compared to all other TEs, *teloboxes* were found to be ~100-fold more densely represented in *ATREP18* elements as compared to all TEs (Figures 3E and 3F). With 7,328 *telobox* motifs, *TE cluster 1* contains ~53% of the whole TAIR10 *telobox* repertoire. Hence, if not considering proper telomeres that span 2 to 5 kb at the end of each chromosome,[56,57] *TE cluster 1* repeats display the majority of telomeric motifs of *Arabidopsis* genome and the strongest propensity to attract PRC2 activity upon H1 loss.

Remarkably, these two properties can be seen at a chromosome scale by contrasting the genome distribution of *telobox* density and of H3K27me3 differential marking, since about 95% of *TE cluster 1* elements cluster within two outstandingly *telobox*-rich regions situated in the pericentromeres of chromosomes 1 and 4 (Figures 3G and S3L). Given this characteristic, we consider these domains as two of the nine *Arabidopsis* genome loci proposed to constitute ITRs,[58,59] hereby referred to as ITR-1R and ITR-4L of ~355 kb and ~72 kb, respectively. In agreement with the description of ITRs in plants and vertebrates,[60,61] *ATREP18* elements that constitute most of these domains display a high density in *telobox* motifs frequently organized as small clusters (Figures 3G, S3L, S3N, and S3O). Further supporting their telomeric evolutionary origin, *ATREP18s* encode no open reading frame or other TE features, are mostly oriented on the same DNA strand, and are tandemly organized (nearly 90% of them being positioned within 1 kb of each other; Figures S3P–S3R), hence they do not constitute *stricto sensu* TEs. Ectopic H3K27me3 deposition was also found at several interspersed elements of *TE cluster 2* located in all pericentromeric regions outside these two ITR blocks (Figure S3M), but our main conclusion is that H1 abundantly occupies two large blocks of pericentromeric ITRs where it prevents H3K27me3 marking.

H1 influences telomere chromatin composition and sub-nuclear positioning

Considering that telomeres display hundreds of perfect *telobox* motifs, the question arose whether, similarly to ITRs, H1 also prevents H3K27me3 deposition at chromosome ends. Because the perfect continuum of terminal telomeric motifs is not suited for quantitative NGS analyses, ChIPs were analyzed through hybridization with radioactively labeled concatenated telomeric probes.[62] H3K27me3 ChIP dot blots led to the estimation that telomeres display an average ~4-fold more H3K27me3 enrichment in *2h1* as compared to WT plants, independently of detectable changes in nucleosome occupancy probed by anti-H3 ChIP dot blot (Figures 4A and S4A).

To assess whether H3K27me3 enrichment concerns a few telomeres or affects them all, we explored its occurrence in intact nuclei using H3K27me3 immunolabeling combined with telomere fluorescence *in situ* hybridization (DNA FISH). Consistent with our ChIP-blot analysis, most telomeric foci were enriched with H3K27me3 in *2h1* nuclei, with 2- to 4-telomere foci frequently presenting outstandingly strong H3K27me3 signals (Figures 4B and 4C). We could not ascertain whether some of these strong signals corresponded to cross-hybridizing pericentromeric ITRs, but their frequent positioning near to the nuclear periphery may point to the latter hypothesis. Indeed, in *2h1* nuclei, telomeric foci were frequently re-distributed toward the nucleus periphery, thereby contrasting with the telomere rosette model proposed by Fransz et al.,[63] first establishing that telomeres cluster around the nucleolus (Figure 4D). In addition, the number of telomere foci was reduced in the mutant nuclei (Figures 4B and 4C), indicating that H1 not only prevents accumulation of H3K27me3 at ITRs and at most telomeres but is also required for the sub-nuclear organization and proper individualization of these domains.

H1 promotes heterochromatin packing but attenuates ITR insulation and telomere-telomere contact frequency

To better understand the altered telomere cytogenetic patterns of *2h1* nuclei and to extend our analysis to ITR topology, we employed *in situ* Hi-C of dissected cotyledons, composed of 80% mesophyll cells, which enabled us to reach high resolution. In agreement with previous reports,[64–69] WT plants displayed frequent interactions within and between pericentromeric regions, which reflect packing of these domains within so-called chromocenters (Figures 5A, 5B, and S5E). Loosening of these heterochromatic structures in *2h1* mutant nuclei, formerly observed by microscopy,[23,35] was expectedly identified here as a more steep decay with distance[70] and lower long-range interaction frequency within pericentromeric regions (Figures 5A, 5B, and S5H–S5J). However, this tendency appears to be a general trend in the mutant nuclei since it was also observed for chromosome arms. As also seen in *crwn* and *condensin* mutants,[71] in a matrix of differential interaction frequency between WT and *2h1* nuclei these prominent defects are also visible as blue squares surrounding the centromeres, which are mirrored by increased interaction frequency between pericentromeric regions and their respective chromosome arms (i.e., red crosses along chromosome arms) (Figure 5C).

Having identified large-scale defects of chromosome organization in *2h1* mutant nuclei, we then focused on telomere-telomere interaction frequency. Because telomeres are not included in the TAIR10 reference genome, we used the most sub-telomeric 100-kb sequences of each chromosome end as a proxy to estimate telomere long-distance interactions, and these were controlled using an internal 100-kb region of each pericentromeric region as well as 100-kb regions randomly chosen in distal chromosomal arms. As previously noted, in WT plants, the telomere-proximal regions frequently interacted with each other through long-range interactions.[64–68] We further observed that ITR-1R and ITR-4L do not particularly associate with each other or with telomeres (Figure S5H). In *2h1* nuclei, with the exception of the regions adjacent to the nucleolar organizer regions (NORs) of chromosome 2 and 4 (SubNOR2 and SubNOR4), which displayed atypical patterns (detailed in Figures S5H–S5J), interaction frequencies between all sub-telomeric regions were increased (Figure 5D). Furthermore, ITR-1R and 4L also showed increased ITR-ITR and ITR-telomere

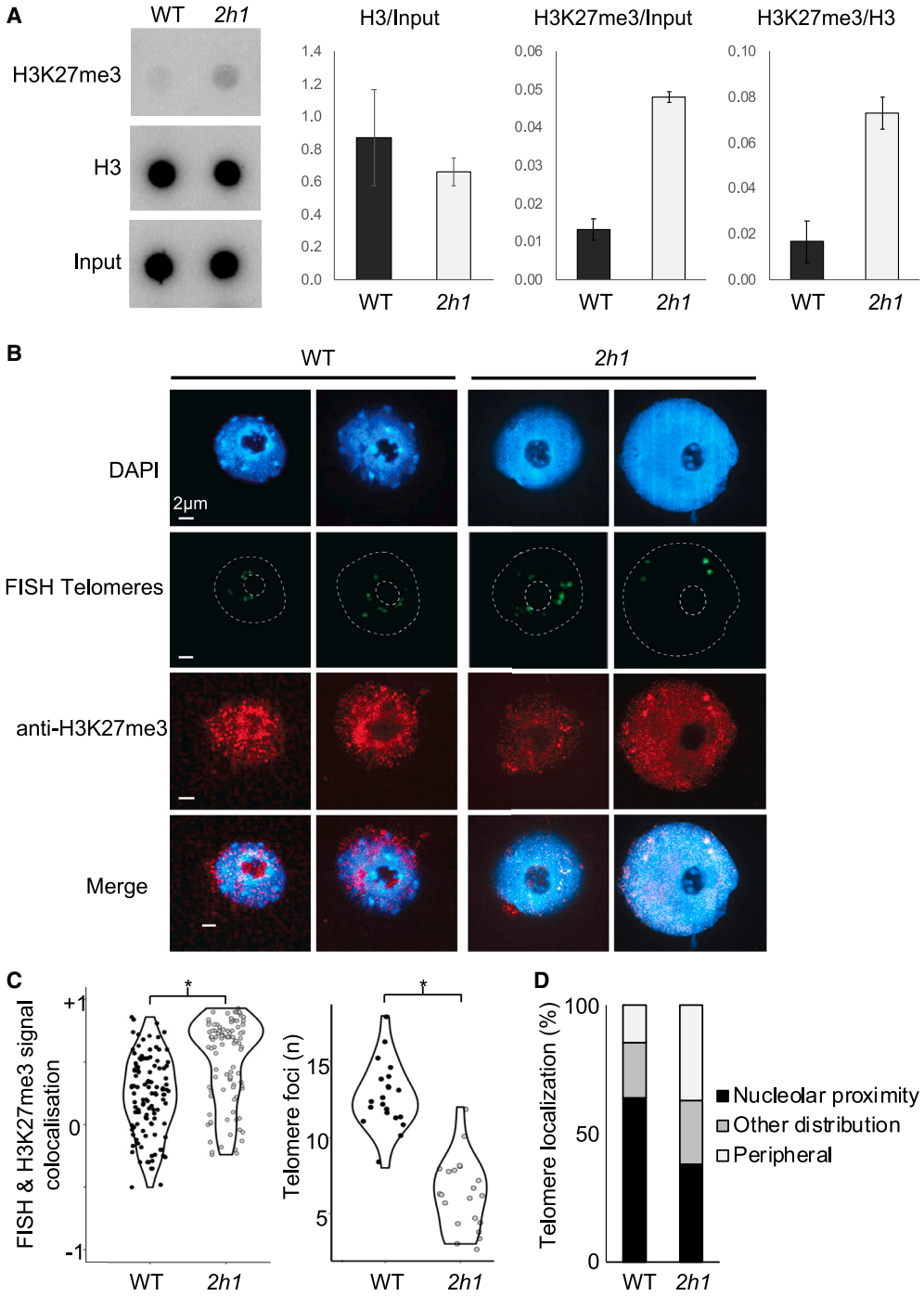

Figure 4. H1 influences both H3K27me3 enrichment and sub-nuclear organization of telomeres

(A) Increased H3K27me3 level at telomeres in *2h1* plants. H3 ChIP signal is used as a proxy of nucleosome occupancy. ChIPs were followed by dot-blot hybridization with a labeled telomeric probe. Data are the mean of two biologically and technically replicated experiments ±SE. A second biological replicate is shown in Figure S5.

(B) Most telomeric loci are enriched in H3K27me3 and re-distributed toward the nucleus periphery in *2h1* plants. Representative collapsed z stack projections of cotyledon nuclei subjected to H3K27me3 immunolabeling and telomere DNA FISH are shown. Blue, DAPI DNA counterstaining; green, telomere FISH signals; red, H3K27me3 immunolabeling.

(C) Quantification of sub-nuclear telomeric signal properties. *p < 1.6e−07, Wilcoxon signed-rank test.

(D) Quantification of nucleus classes displaying different patterns in telomere sub-nuclear localization. Number and position of telomeric foci were determined in two independent biological replicates (n > 20 each).

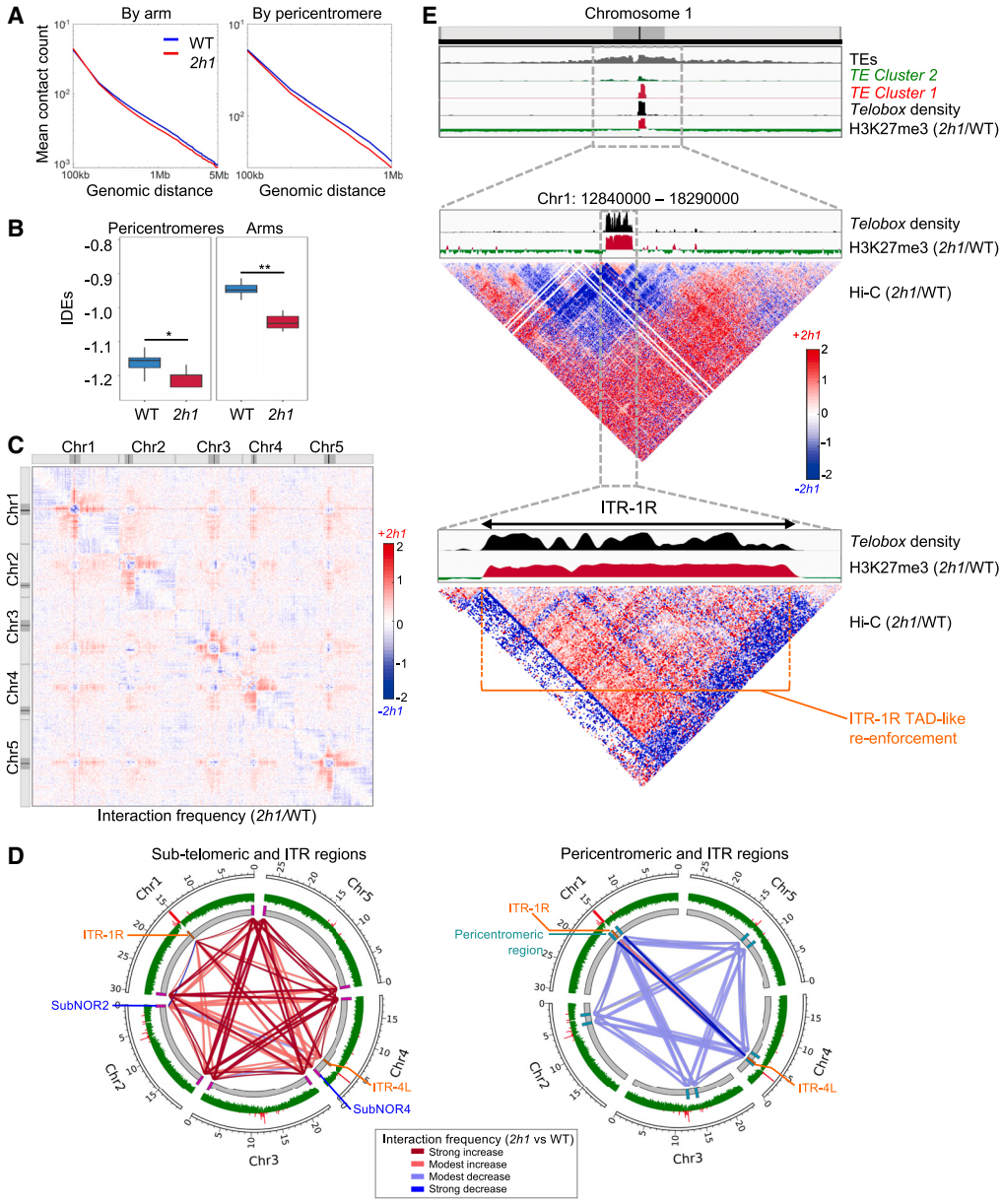

Figure 5. H3K27me3 accumulation at ITRs and at telomeres associates with ITR insulation and more frequent telomere-telomere interactions

(A) Mean contact count as a function of genomic distance for all chromosome arms at a 100-kb resolution.

(B) Distribution of interaction decay exponents (IDEs) determined at a 100-kb resolution for chromosome arms and pericentromeric regions of WT and *2h1* nuclei. Median IDE values of chromosome arms and pericentromeres were determined as −0.95/−1.16 in WT and −1.05/−1.2 in *2h1* nuclei, respectively. *p = 0.076 and **p = 0.001, pairwise Wilcoxon rank-sum test.

(C) Relative difference of interaction frequency between WT and *2h1* plants. The $\log_2$ values of observed/expected (O/E) interaction frequency along the five chromosomes in *2h1* versus WT are shown at a 100-kb resolution. Regions in red have more frequent contacts in *2h1* than in WT plants, while regions in blue have less. Pericentromeric regions are depicted in dark gray on the schematic chromosomes.

(D) H1 reduces the frequency of long-distance interactions between chromosome ends. Circos plots depict variations in inter-chromosomal interaction frequencies between telomere-proximal, pericentromeric, ITR-1R, and ITR-4L 100-kb domains. Yellow boxes, ITR regions. External green/red track, H3K27me3 variations in *2h1* versus WT plants (log2 ratio). Magenta boxes, telomere-proximal regions and SubNOR2 or SubNOR4.

(E) Reduced frequency of intra-pericentromeric O/E interactions in *2h1* mutant nuclei is contrasted by TAD re-enforcement of the H3K27me3-enriched ITR-1R 355 kb block. Top panel, location of ITR-1R in chromosome 1. Middle panel, magnification of the region surrounding chromosome 1 pericentromeres at a 10-kb resolution. Bottom panel, magnification of the pericentromere-embedded ITR-1R at a 2-kb resolution. Strong and modest increase correspond to $\log_2$FC > 1 and log2FC 0.35–1, respectively; modest and strong decrease correspond to log2FC −0.33 to −0.65 and log2FC < −0.65, respectively. Quantitative analyses are shown in the complementary Figures S4H–S4J. All Hi-C analyses combine three independent biological replicates.

interaction frequency (Figures 5D, S5G, and S5J). Consistent with a reduced number of telomere foci in intact *2h1* nuclei (Figure 4), this observation supports an organizational model in which telomeres tend to coalesce more frequently in the absence of H1.

Last, we examined chromosome topology at ITR loci. In WT plants, both of them formed large structures resembling topologically associating domains (TADs), which are themselves immersed within highly self-interacting pericentromeric regions. Interestingly, in *2h1* nuclei, intra-ITR interactions were strongly enhanced (i.e., TAD re-enforcement), while the surrounding pericentromeric environments expectedly showed an opposite trend linked to heterochromatin relaxation (Figures 5E and S5G). This observation was supported by comparing distal-to-local ratios (DLRs) of interaction frequency that showed clear local drops at each ITR in *2h1* nuclei, hence an increased tendency for interacting only with itself usually interpreted as increased domain compaction (Figure S5K).[72] Altogether, these observations show that, in contrast to its general role in heterochromatin packing, H1 dampens the local insulation of ITRs from their neighboring environment. Remarkably, the boundaries of these compaction defects in *2h1* nuclei sharply correspond with H3K27me3 enrichment (Figures 5E and S5K).

H1 antagonizes TRB-mediated PRC2 activity at ITRs

With the aim to determine the molecular mechanisms by which H1 selectively represses PRC2 activity at *telobox*-rich elements, and more particularly at ITRs, we envisioned that TRB proteins might have a prominent role (Figure 6A). The TRB1, TRB2, and TRB3 founding members of these plant-specific single-Myb-histone proteins constitute part of the telomere nucleoprotein structure required to maintain telomere length[73] (Figure 6B). Their Myb domain has strong affinity to the G-rich strand of *telobox* DNA motifs[73–75] and, combined with a coiled-coil domain that can associate with the CURLY-LEAF (CLF) and SWINGER (SWN) catalytic subunits of PRC2,[36,37] TRBs act as transcriptional regulators of protein-coding genes bearing a *telobox* motif.[76,77] Interestingly, despite their low protein sequence similarity to H1 (14% ± 2%; Figures S6A and S6B), TRBs display a typical GH1 domain.[19,78] Hence, we hypothesized that antagonistic chromatin incorporation of the GH1 domains of TRB and H1 proteins might modulate PRC2 recruitment at ITRs.

To test this model, we first compared H1 and TRB1 genomic distribution. Analysis of available TRB1 ChIP-seq data[76] showed that TRB1 peak summits expectedly correlate with the position of *telobox* motifs located in protein-coding genes. However, despite the presence of numerous *telobox* sequences, TRB1 poorly occupies *TE cluster 1* elements (Figures 6C and S6C). Reciprocally, H1 average occupancy is low at TRB1 peaks over the genome (Figures 6D and S6D). These observations hint at an antagonistic *cis* enrichment of H1 and TRB1 at chromatin. To better resolve these general patterns and link them to linker DNA positioning, we examined the profiles of H1, TRB1, *telobox* motifs, and nucleosome occupancy around well-positioned nucleosome (WPN) coordinates defined using MNase-seq.[28] As expected, H1.2-GFP distribution was enriched at DNA linker regions. Surprisingly, this was also the case for *telobox* motif distribution, which sharply coincided with regions serving as linker DNA. While TRB1 peaks appeared much broader, their summits were also more pronounced at regions corresponding to linker DNA coordinates (Figure 6E). Hence, if it exists, competitive binding between H1 and TRB proteins likely occurs at linker DNA.

These observations are all compatible with a mechanism by which high H1 occupancy at ITRs prevents TRB1 DNA binding. Vice versa, increased access to ITRs in *2h1* mutant plants would facilitate TRB1-mediated PRC2 recruitment. To functionally assess whether this model holds true, we first examined whether GFP-TRB1 accumulates at ITRs in *2h1* plants and then determined the H3K27me3 profile in mutant plants lacking both H1 and TRB1, TRB2, and TRB3. To undertake the first experiment, we crossed a *TRB1::GFP-TRB1* line[76,77] with *2h1* and revealed GFP-TRB1 genome association by ChIP-seq and ChIP telomere dot blot. Comparison of GFP-TRB1 chromatin association in WT and *2h1* plants showed a significantly increased association at *TE cluster 1*, ITR-1R and ITR-4L, and at telomeres (Figures 7A, S4B, S7A, and S7B), thereby providing evidence that H1 restricts TRB1 binding to these loci *in vivo*.

We then determined whether abolishing simultaneously the expression of linker H1 and TRB1, TRB2, and TRB3 proteins affects PRC2 activity at ITRs. To probe H3K27me3 profiles in *h1.1h1.2trb1trb2trb3* quintuple-mutant plants (hereinafter referred to as *htrbQ* for short), we crossed *2h1* double-mutant plants to *trb1(+/−)trb2trb3* triple mutant plants propagated as a heterozygous state to accommodate the seedling lethality induced by *TRB123* combined loss of function.[36,37] Homozygous *htrbQ* mutant seedlings exhibited an aggravated phenotype as compared to the *trb123* triple-mutant line (Figure 7B), a synergistic effect presumably reflecting a convergence of *H1* and *TRB123* functions in the regulation of common genes.[79] Despite the dwarf morphology of the quintuple-mutant line, we conducted a ChIP-Rx profiling of H3K27me3 in homozygous WT, *2h1*, *trb123*, and *htrbQ* seedlings, all segregating from a single crossed individual. As compared to the *2h1* co-segregant siblings, in the quintuple-mutant seedlings, H3K27me3 enrichment was almost completely abolished at ITR-1R and more generally at *TE cluster 1* elements (Figures 7C, 7D, S7B, and S7C). Taken together, these analyses demonstrate that H1 occupancy at ITRs antagonizes TRB protein recruitment, thereby constituting a mechanism preventing invasion of these large chromosome blocks by H3K27me3.

DISCUSSION

H1 has a dual impact on H3K27me3 deposition in *Arabidopsis*

We report that *Arabidopsis* H1 is highly enriched at PRC2 target genes, where it typically promotes H3K27me3 enrichment and diminishes chromatin accessibility. Contrasting with this general tendency, we also identified an opposite role of H1 in limiting H3K27me3 deposition at interstitial and terminal telomeres as well as at a few genes. This unveiled that, in plants, H1 has a differential effect on H3K27me3 levels over thousands of protein-coding genes on the one hand and over loci characterized by repeated telomeric motifs on the other hand.

Considering that PRC2 activation is favored at chromatin made of closely neighboring nucleosomes,[14] we postulate that

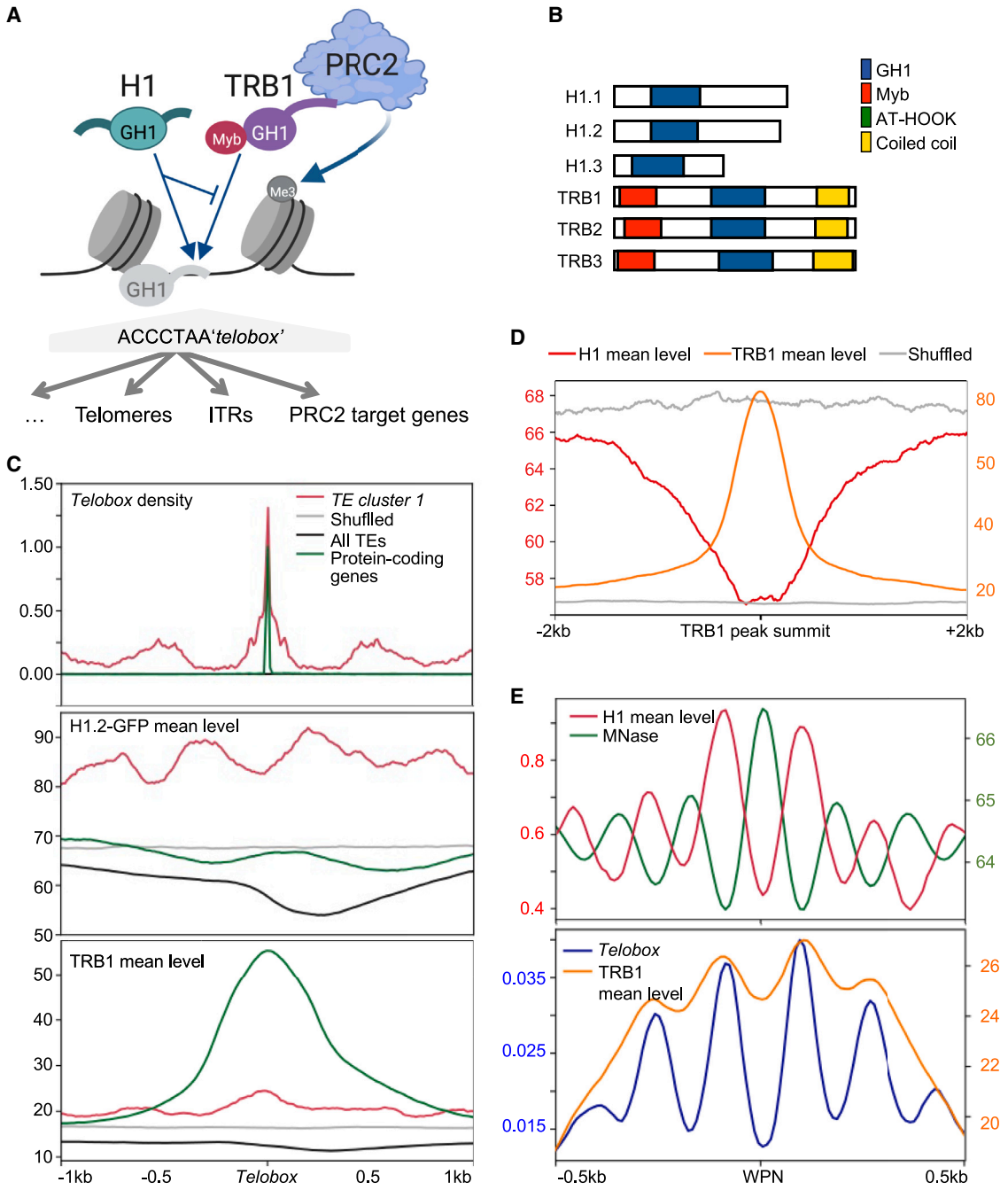

Figure 6. Antagonistic chromatin association of H1 and TRB1 over the genome

(A) Working model of H1/TRB1 antagonistic chromatin association at linker DNA-localized *telobox* motifs and its sequence-specific influence on PRC2 recruitment at distinct chromatin regions displaying telomeric repeats.

(B) TRB family members possess an amino-terminal single-Myb domain with sequence specificity for *telobox* motifs, a coiled-coil domain enabling their association with PRC2 subunits,[36,37] and a central GH1 domain that may trigger competitive binding with H1.

(C) H1 and TRB1 patterns are both influenced by *telobox* positioning, and they display an opposite trend at *TE cluster 1 telobox* motifs. The plots display TRB1 and H1 mean read coverage at all TAIR10 genome *telobox* motifs.

(D) H1 occupancy is reduced at genome loci corresponding to TRB1 peak summits.

(E) H1, TRB1, and *telobox* motifs all tend to associate with DNA linker regions. Genome-wide profiles of H1, TRB1, and *telobox* sequence motifs were plotted over the coordinates of all *Arabidopsis* WPNs defined by Lyons and Zilberman.[28] In (C) and (D), shuffled controls were produced with random permutations of genomic position of the regions of interest.

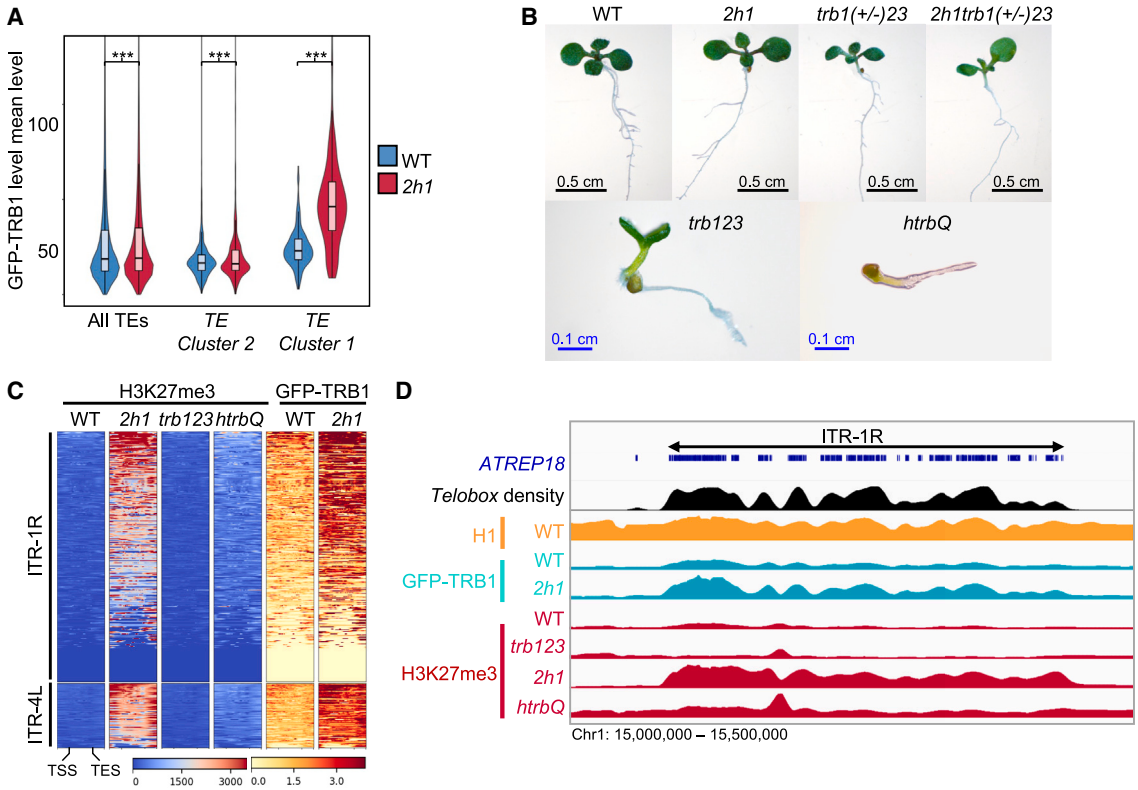

Figure 7. H1 antagonizes TRB1-mediated PRC2 activity at ITRs

(A) H1 restricts GFP-TRB1 protein association at *TE cluster 1* elements. The plots show GFP-TRB1 mean normalized coverage in WT and *2h1* seedlings at the indicated repeat categories. ***p <1.94e−05, Wilcoxon signed-rank test.

(B) Homozygous *h1.1h1.2trb1trb2trb3* (*htrbQ*) quintuple-mutant seedlings represented 25% of the segregating progeny and displayed strongly altered seedling phenotypes with deficient cotyledon development and slow root growth, indicating that morphogenesis is strongly affected upon combined *H1* and *TRB123* loss of function. WT, *2h1*, and *trb123* mutant lines have been selected as null F2 segregants from the same cross as the analyzed *htrbQ* plant line.

(C) H1 and TRB proteins are all required for H3K27me3 enrichment at ITR-1R and ITR-4L TEs. TAIR10 annotated repeats located within ITR-1R and ITR-4L coordinates were ranked similarly in all heatmaps. H3K27me3 levels were determined using spike-in normalized ChIP-seq analysis.

(D) Browser view showing that GFP-TRB1 and H3K27me3 enrichment at ITR-1R in *2h1* is lost in *htrbQ* mutant seedlings. Each ChIP series is shown as equally scaled profiles of the indicated genotypes. ChIP-seq and ChIP-Rx data represent the mean of two biological replicates each.

the repertoire of genes losing H3K27me3 upon H1 depletion are those where H1 is required to attain a compaction level enabling efficient PRC2 *cis* activity. Supporting this hypothesis, genes sensitive to H1 for efficient H3K27me3 marking tend to (1) display lower H1 and nucleosome occupancy, (2) be more accessible, and (3) be more expressed than genes unaffected by H1 depletion. In contrast, genes and TEs gaining H3K27me3 upon H1 loss tend to have an elevated nucleosome density and to be weakly accessible while exhibiting sequence signatures potentially triggering different mechanisms of PRC2 regulation, such as H1/TRB protein interplay. The large scale on which these antagonistic patterns are observed sheds light on the existence of prominent functional links between H1 and PRC2-based regulation, two main factors in the instruction of DNA accessibility.

Promoting H3K27me3 enrichment at genes: An evolutionarily conserved function of H1

We identified that H1 has a general role in H3K27me3 deposition at genes, yet most of the H3K27me3 peaks are still detectable in *2h1* plants. Hence, in agreement with the subtle phenotypes of *h1* mutant plants, H1 is likely not mandatory for the nucleation of PRC2 activity but rather for H3K27me3 maintenance or spreading in *Arabidopsis*. In term of chromatin function, H1 depletion results in a global increase in chromatin accessibility at gene bodies but its impact on expression was apparently more related to variations in H3K27me3 marking. Hence, consistent with the functional categories of the misregulated genes in *2h1* plants, part of the defects in gene expression resulting from H1 depletion might result from indirect consequences on PRC2 activity. The recent findings that depletion of H1 variants in mouse cells triggers widespread H3K27me3 loss and misregulation of PRC2-regulated genes, thereby phenocopying loss of EZH2,[16,17] suggest that favoring PRC2 activity is an evolutionarily conserved function of H1.

H1 hinders PRC2 activity at telomeric repeats by preventing local association of TRB proteins

We provide evidence that H1 antagonizes TRB-mediated PRC2 activity at telomeric repeats. Waiting for an assessment

of their relative affinity for *telobox* elements in a chromatin context, H1/TRB1 proteins' antagonistic association along the genome plausibly results from competitive DNA binding of their respective GH1 protein domains. First, chromatin incorporation of H1 and TRB1 is negatively correlated at a genome-wide scale. Second, analysis of nucleosome positioning showed that *telobox* motifs are preferentially situated in linker DNA where TRB1 association is also pronounced; so that competition with H1 can occur on linker DNA. Third, profiling of TRB1 chromatin association in *2h1* plants showed that TRB1 ectopically invades ITRs and other *telobox*-rich elements upon H1 loss. These observations reveal that, in WT plants, elevated H1 incorporation limits TRB1 enrichment and/or accessibility on these loci despite the presence of repeated *telobox* motifs for which the TRB1 Myb domain has strong affinity.[74,76]

H3K27me3 profiling in quintuple *2h1trb123* seedlings showed that H3K27me3 enrichment at ITRs in H1-depleted plants depends on TRB proteins, thereby demonstrating a functional framework in which repression of H3K27me3 deposition at telomeric repeats relies on H1 preventing local association of PRC2-associated TRB proteins. Future studies will determine whether other chromatin modifiers influencing H3K27me3 are implicated. The latter possibility cannot be discarded as, for example, the PRC1 subunit LIKE-HETEROCHROMATIN 1 (LHP1), acting as a chromatin reader of H3K27me3 in *Arabidopsis*,[80] prevents TRB1 enrichment at PRC2 target genes displaying *telobox* motifs.[77] The outstanding genome-wide pattern of *telobox* positioning in linker DNA also suggests a capacity of this sequence motif to influence chromatin organization, possibly by repelling nucleosomes.

H1 has a profound influence on the *Arabidopsis* 3D genome topology

Using Hi-C, we identified a reduced frequency of chromatin interactions within and among the pericentromeres in *2h1* nuclei. This is a typical feature of *Arabidopsis* mutants affecting chromocenter formation[64,65,67] or when chromocenters get disrupted in response to environmental stress.[68] These analyses refine the recent observation that chromocenter formation is impaired in *2h1* nuclei,[23,26,35] a defect that commonly reflects the spatial dispersion of pericentromeres within the nuclear space.[63] They also shed light on a complex picture in which ITR-1R and 4L embedded within the pericentromeres of chromosomes 1 and 4 escape the surrounding relaxation of heterochromatin induced by H1 depletion and organize themselves as TAD-like structures. In *2h1* nuclei, H3K27me3 invasion at ITRs might underlie the maintenance of compacted and poorly accessible chromatin, while neighboring heterochromatic regions tend to become more accessible. It is noteworthy that, in the absence of CTCF (CCCTC-binding factor) and of obvious related 3D structures, *Arabidopsis* is thought to lack proper TADs[81–83]; hence, H1 regulation of ITR insulation represents a new regulatory function of *Arabidopsis* genome topology.

We also report that H1 depletion leads to a reduction in the number of telomeric foci and of their proportion near the nucleolus. This suggested that *2h1* mutants are impaired in telomere spatial individualization, which is indeed supported in our Hi-C analyses by more frequent inter-chromosomal interactions between telomere-proximal regions. As the preferential positioning of telomeres around the nucleolus and centromeres near the nuclear periphery is an important organizing principle of *Arabidopsis* chromosome sub-nuclear positioning[63] and topology,[69] H1 therefore appears to be a crucial determinant of *Arabidopsis* nuclear organization.

Both PRC1 and PRC2 participate in defining *Arabidopsis* genome topology,[64,84] and H3K27me3 is favored among long-distance-interacting gene promoters.[66] This led to the proposal that, as in animals, this mark could contribute to shape chromosomal organization in *Arabidopsis*, possibly through the formation of *Polycomb* sub-nuclear bodies.[66,85] Here we mostly focused on large structural components of the genome, such as telomeres, pericentromeres, and ITR regions. In mammals, H1 depletion triggers not only higher-order changes in chromatin compartmentation[16,17] but also extensive topological changes of gene-rich and transcribed regions.[18] Future studies will determine to what extent the impact of H1 on the H3K27me3 landscape contributes to defining *Arabidopsis* genome topology.

H1 as a modulator of H3K27me3 epigenome homeostasis

In *Neurospora crassa*, artificial introduction of an $(TTAGGG)_{17}$ telomere repeats array at interstitial sites was shown to trigger the formation of a large H3K27me2/3-rich chromosome domain.[86] Followed by our study, this illustrates the intrinsic attractiveness of telomeric motifs for H3K27me3 deposition in multiple organisms. With several thousands of telomeric motifs altogether covering ~430 kb, ITRs represent at least twice the cumulated length of all telomeres in *Arabidopsis* diploid nuclei, thereby forming immense reservoirs of PRC2 targets. Our findings led us to hypothesize that H1-mediated repression of PRC2 activity at these scaffolding domains serves as a safeguard to avoid the formation of gigantic H3K27me3-rich blocks in both pericentromeric and telomeric regions, which not only can be detrimental for chromosome folding but could also be on a scale tethering PRC2 complexes away from protein-coding genes. In other terms, balancing PRC2 activity between protein-coding genes and telomeric repeats, H1 protein regulation may represent an important modulator of epigenome homeostasis during development.

Limitations of the study

Owing to their repetitive nature,[87–92] chromatin composition and organization of plant telomeres has long remained enigmatic.[93,94] Former studies indicated a dominance of H3K9me2 over H3K27me3 histone marks.[62,89,95] Using ChIP dot blot and *in situ* immunolocalization with telomeric probes, here we showed that H1 moderates the accumulation of H3K27me3 at telomeres by 2- to 4-fold, yet this effect could be indirect and not homogeneous. Hence, two limitations of our study are that we could not assess the precise distribution of HK27me3 enrichment along each telomere and whether H1 acts on PRC2 at telomeres in *cis*. In agreement with the mosaic chromatin status of telomeres in other organisms,[96] *Arabidopsis* telomeres are thought to be made of segments with distinct nucleosome repeat length (NRL) with average length of 150 bp,[97] a much

shorter size than the 189 bp estimated for H1-rich TEs.[23] Considering that H1 protects about 20 bp of DNA *in vitro*,[98] an NRL length of 150 bp is seemingly incompatible with H1 incorporation into telomere chromatin. For instance, H1 has been proposed to be under-represented at telomeres in plants[97,99] as it is in mammals.[93,100–102] This could explain the short NRL of *Arabidopsis* and human telomeres[97,103] that, long after being suspected,[104] have recently been re-constructed as an H1-free state columnar organization.[105] In conclusion, the existence of distinct chromatin states at *Arabidopsis* telomeres needs to be explored in more detail to establish whether the H1-mediated repression of PRC2 activity is a global property of telomeres or rather affects a few segments through H1 *cis* association.

STAR★METHODS

Detailed methods are provided in the online version of this paper and include the following:

- KEY RESOURCES TABLE
- RESOURCE AVAILABILITY
  - Lead contact
  - Materials availability
  - Data and code availability
- EXPERIMENTAL MODEL AND STUDY PARTICIPANT DETAILS
  - Arabidopsis thaliana
- METHOD DETAILS
  - Immuno-FISH
  - ATAC-seq
  - *In situ* Hi-C
  - RNA-seq
  - H1.2-GFP, GFP-TRB1 and H3 ChIP-seq experiments
  - H3K27me3 ChIP-Rx
  - H3K27me3 and H3 ChIP-blot analyses
  - Hi-C bioinformatics
  - ChIP-seq and ChIP-Rx bioinformatics
  - MNase-seq bioinformatics
  - ATAC-seq bioinformatics
  - DNA sequence analyses
  - Gene ontology analysis
  - Protein alignment
- QUANTIFICATION AND STATISTICAL ANALYSES

SUPPLEMENTAL INFORMATION

Supplemental information can be found online at https://doi.org/10.1016/j.celrep.2023.112894.

ACKNOWLEDGMENTS

The authors are grateful to Erwann Cailleux (IBENS, Paris, France) and David Latrasse (IPS2, Orsay, France) for technical guidance with ATAC-seq, Nicolas Valentin (I2BC, Gif, France) for assistance with FACS, Magali Charvin (IBENS, Paris, France) for technical assistance with the IBENS plant growth facility, Frédérique Perronet (IBPS, France) for providing *Drosophila* samples, and Kinga Rutowicz (University of Zurich, Switzerland) and Angélique Déléris (IBENS, Paris and I2BC, Gif-Sur-Yvette, France) for sharing unpublished results. This work benefitted from grants from the Agence Nationale de la Recherche projects (ANR-18-CE13-0004, ANR-17-CE12-0026-02) to F.B. Collaborative work between F.B. and C. Baroux was supported by a research grant from the Velux Foundation (Switzerland) and the Ricola Foundation (Switzerland). Collaborative work between F.B. and A.P. was supported by CNRS EPIPLANT Action (France). G.T. benefitted from a short-term fellowship of the COST Action CA16212 INDEPTH (EU) for training in Hi-C by S.G. in U.G.'s laboratory, which is supported by the University of Zurich (Switzerland) and the Switzerland National Science Foundation (project 31003A_179553). S.A. benefitted from a CAP20-25 Emergence research grant from Région Auvergne-Rhône-Alpes (France). Work in J.F.'s team was supported by the Czech Science Foundation (project 20-01331X) and Ministry of Education, Youth, and Sports of the Czech Republic, project INTER-COST (LTC20003).

AUTHOR CONTRIBUTIONS

G.T., L.W., I.B., and C. Bourbousse performed ChIP and ChIP-RX experiments. G.T. and L.W. performed ATAC-seq experiments. K.A. and M.F. performed telomere dot blots. I.B. performed phenotypic analyses. M.B. contributed to FACS nucleus sorting. S.A. performed cytological experiments. G.T. and S.G. generated the Hi-C datasets. A.K. and V.C. developed ATAC-seq bioinformatics tools. L. Concia, G.T., and C. Bourbousse performed RNA-seq, MNase-seq, ChIP-seq, and ATAC-seq bioinformatics analyses. L. Concia, L. Carron, and S.G. performed Hi-C bioinformatics. G.T., C. Bourbousse, L. Concia, and F.B. conceived the study. F.B., C. Bourbousse, A.C., C. Baroux, C. Bowler, A.C., S.A., A.P., U.G., P.P.S., J.F., and S.G. supervised research. F.B. wrote the manuscript and all authors edited the manuscript.

DECLARATION OF INTERESTS

The authors declare no competing interests.

INCLUSION AND DIVERSITY

We support inclusive, diverse, and equitable conduct of research.

Received: January 21, 2021
Revised: December 2, 2022
Accepted: July 13, 2023
Published: July 28, 2023

REFERENCES

1. Bednar, J., Hamiche, A., and Dimitrov, S. (2016). H1-nucleosome interactions and their functional implications. Biochim. Biophys. Acta *1859*, 436–443. https://doi.org/10.1016/j.bbagrm.2015.10.012.
2. Fyodorov, D.V., Zhou, B.-R., Skoultchi, A.I., and Bai, Y. (2018). Emerging roles of linker histones in regulating chromatin structure and function. Nat. Rev. Mol. Cell Biol. *19*, 192–206. https://doi.org/10.1038/nrm.2017.94.
3. Hergeth, S.P., and Schneider, R. (2015). The H1 linker histones: multifunctional proteins beyond the nucleosomal core particle. EMBO Rep. *16*, 1439–1453. https://doi.org/10.15252/embr.201540749.
4. Grossniklaus, U., and Paro, R. (2014). Transcriptional Silencing by Polycomb-Group Proteins. Cold Spring Harbor Perspect. Biol. *6*, 0193311–a19426. https://doi.org/10.1101/cshperspect.a019331.
5. Schuettengruber, B., Bourbon, H.M., Di Croce, L., and Cavalli, G. (2017). Genome Regulation by Polycomb and Trithorax: 70 Years and Counting. Cell *171*, 34–57. https://doi.org/10.1016/j.cell.2017.08.002.
6. Hugues, A., Jacobs, C.S., and Roudier, F. (2020). Mitotic Inheritance of PRC2-Mediated Silencing: Mechanistic Insights and Developmental Perspectives. Front. Plant Sci. *11*, 262–311. https://doi.org/10.3389/fpls.2020.00262.
7. Schubert, D. (2019). Evolution of Polycomb-Group Function in the Green Lineage. F1000Res *8*. https://doi.org/10.12688/f1000research.16986.1.

8. Francis, N.J., Kingston, R.E., and Woodcock, C.L. (2004). Chromatin compaction by a polycomb group protein complex. Science *306*, 1574–1577. https://doi.org/10.1126/science.1100576.

9. Shao, Z., Raible, F., Mollaaghababa, R., Guyon, J.R., Wu, C.T., Bender, W., and Kingston, R.E. (1999). Stabilization of Chromatin Structure by PRC1, a Polycomb Complex. Cell *98*, 37–46. https://doi.org/10.1016/S0092-8674(00)80604-2.

10. Shu, H., Wildhaber, T., Siretskiy, A., Gruissem, W., and Hennig, L. (2012). Distinct modes of DNA accessibility in plant chromatin. Nat. Commun. *3*, 1281. https://doi.org/10.1038/ncomms2259.

11. Illingworth, R.S. (2019). Chromatin Folding and Nuclear Architecture: PRC1 Function in 3D. https://doi.org/10.1016/j.gde.2019.06.006.

12. Margueron, R., Li, G., Sarma, K., Blais, A., Zavadil, J., Woodcock, C.L., Dynlacht, B.D., and Reinberg, D. (2008). Ezh1 and Ezh2 Maintain Repressive Chromatin through Different Mechanisms. Mol. Cell. *32*, 503–518. https://doi.org/10.1016/j.molcel.2008.11.004.

13. Kim, J.M., Kim, K., Punj, V., Liang, G., Ulmer, T.S., Lu, W., and An, W. (2015). Linker histone H1.2 establishes chromatin compaction and gene silencing through recognition of H3K27me3. Sci. Rep. *5*, 16714–16716. https://doi.org/10.1038/srep16714.

14. Yuan, W., Wu, T., Fu, H., Dai, C., Wu, H., Liu, N., Li, X., Xu, M., Zhang, Z., Niu, T., et al. (2012). Dense chromatin activates polycomb repressive complex 2 to regulate H3 lysine 27 methylation. Science *337*, 971–975. https://doi.org/10.1126/science.1225237.

15. Martin, C., Cao, R., and Zhang, Y. (2006). Substrate preferences of the EZH2 histone methyltransferase complex. J. Biol. Chem. *281*, 8365–8370. https://doi.org/10.1074/jbc.M513425200.

16. Willcockson, M.A., Healton, S.E., Weiss, C.N., Bartholdy, B.A., Botbol, Y., Mishra, L.N., Sidhwani, D.S., Wilson, T.J., Pinto, H.B., Maron, M.I., et al. (2021). H1 histones control the epigenetic landscape by local chromatin compaction. Nature *589*, 293–298. https://doi.org/10.1038/s41586-020-3032-z.

17. Yusufova, N., Kloetgen, A., Teater, M., Osunsade, A., Camarillo, J.M., Chin, C.R., Doane, A.S., Venters, B.J., Portillo-Ledesma, S., Conway, J., et al. (2021). Histone H1 loss drives lymphoma by disrupting 3D chromatin architecture. Nature *589*, 299–305. https://doi.org/10.1038/s41586-020-3017-y.

18. Geeven, G., Zhu, Y., Kim, B.J., Bartholdy, B.A., Yang, S.M., Macfarlan, T.S., Gifford, W.D., Pfaff, S.L., Verstegen, M.J.A.M., Pinto, H., et al. (2015). Local compartment changes and regulatory landscape alterations in histone H1-depleted cells. Genome Biol. *16*, 289. https://doi.org/10.1186/s13059-015-0857-0.

19. Kotliński, M., Knizewski, L., Muszewska, A., Rutowicz, K., Lirski, M., Schmidt, A., Baroux, C., Ginalski, K., and Jerzmanowski, A. (2017). Phylogeny-based systematization of arabidopsis proteins with histone H1 globular domain. Plant Physiol. *174*, 27–34. https://doi.org/10.1104/pp.16.00214.

20. Over, R.S., and Michaels, S.D. (2014). Open and closed: The roles of linker histones in plants and animals. Mol. Plant *7*, 481–491. https://doi.org/10.1093/mp/sst164.

21. Probst, A.V., Desvoyes, B., and Gutierrez, C. (2020). Similar yet critically different: the distribution, dynamics and function of histone variants. J. Exp. Bot. *71*, 5191–5204. https://doi.org/10.1093/jxb/eraa230.

22. Rutowicz, K., Puzio, M., Halibart-Puzio, J., Lirski, M., Kroteń, M.A., Kotliński, M., Kniżewski, Ł., Lange, B., Muszewska, A., Śniegowska-Świerk, K., et al. (2015). A Specialized Histone H1 Variant Is Required for Adaptive Responses to Complex Abiotic Stress and Related DNA Methylation in Arabidopsis. https://doi.org/10.1104/pp.15.00493.

23. Choi, J., Lyons, D.B., Kim, M.Y., Moore, J.D., and Zilberman, D. (2020). DNA Methylation and Histone H1 Jointly Repress Transposable Elements and Aberrant Intragenic Transcripts. Mol. Cell *63*, 310–311. https://doi.org/10.1016/j.molcel.2019.10.011.

24. Ichino, L., Boone, B.A., Strauskulage, L., Harris, C.J., Kaur, G., Gladstone, M.A., Tan, M., Feng, S., Jami-Alahmadi, Y., Duttke, S.H., et al. (2021). MBD5 and MBD6 couple DNA methylation to gene silencing through the J-domain protein SILENZIO. Science *372*, 1434–1439. https://doi.org/10.1126/science.abg6130.

25. Papareddy, R.K., Páldi, K., Paulraj, S., Kao, P., Lutzmayer, S., and Nodine, M.D. (2020). Chromatin regulates expression of small RNAs to help maintain transposon methylome homeostasis in Arabidopsis. Genome Biol. *21*, 251. https://doi.org/10.1186/s13059-020-02163-4.

26. He, S., Ye, C., Zhong, N., Yang, M., Yang, X., and Xiao, J. (2019). Natural depletion of H1 in sex cells causes DNA demethylation, heterochromatin decondensation and transposon activation. Elife *8*, 1–9. https://doi.org/10.7554/eLife.42530.001.

27. Liu, S., de Jonge, J., Trejo-Arellano, M.S., Santos-González, J., Köhler, C., and Hennig, L. (2021). Role of H1 and DNA methylation in selective regulation of transposable elements during heat stress. New Phytol. *229*, 2238–2250. https://doi.org/10.1111/nph.17018.

28. Lyons, D.B., and Zilberman, D. (2017). DDM1 and lsh remodelers allow methylation of DNA wrapped in nucleosomes. Elife *6*, 306744–e30720. https://doi.org/10.7554/eLife.30674.

29. Wollmann, H., Stroud, H., Yelagandula, R., Tarutani, Y., Jiang, D., Jing, L., Jamge, B., Takeuchi, H., Holec, S., Nie, X., et al. (2017). The histone H3 variant H3.3 regulates gene body DNA methylation in Arabidopsis thaliana. Genome Biol. *18*, 94–10. https://doi.org/10.1186/s13059-017-1221-3.

30. Zemach, A., Kim, M.Y., Hsieh, P.H., Coleman-Derr, D., Eshed-Williams, L., Thao, K., Harmer, S.L., and Zilberman, D. (2013). The Arabidopsis nucleosome remodeler DDM1 allows DNA methyltransferases to access H1-containing heterochromatin. Cell *153*, 193–205. https://doi.org/10.1016/j.cell.2013.02.033.

31. Bourguet, P., Picard, C.L., Yelagandula, R., Pélissier, T., Lorković, Z.J., Feng, S., Pouch-Pélissier, M.N., Schmücker, A., Jacobsen, S.E., Berger, F., and Mathieu, O. (2021). The histone variant H2A.W and linker histone H1 co-regulate heterochromatin accessibility and DNA methylation. Nat. Commun. *12*, 2683. https://doi.org/10.1038/s41467-021-22993-5.

32. Hsieh, P.H., He, S., Buttress, T., Gao, H., Couchman, M., Fischer, R.L., Zilberman, D., and Feng, X. (2016). Arabidopsis male sexual lineage exhibits more robust maintenance of CG methylation than somatic tissues. Proc. Natl. Acad. Sci. USA *113*, 15132–15137. https://doi.org/10.1073/pnas.1619074114.

33. She, W., Grimanelli, D., Rutowicz, K., Whitehead, M.W.J., Puzio, M., Kotliński, M., Jerzmanowski, A., and Baroux, C. (2013). Chromatin reprogramming during the somatic-to-reproductive cell fate transition in plants. Development (Camb.) *140*, 4008–4019. https://doi.org/10.1242/dev.095034.

34. She, W., and Baroux, C. (2015). Chromatin dynamics in pollen mother cells underpin a common scenario at the somatic-to-reproductive fate transition of both the male and female lineages in Arabidopsis. Front. Plant Sci. *6*, 294. https://doi.org/10.3389/fpls.2015.00294.

35. Rutowicz, K., Lirski, M., Mermaz, B., Teano, G., Schubert, J., Mestiri, I., Kroteń, M.A., Fabrice, T.N., Fritz, S., Grob, S., et al. (2019). Linker histones are fine-scale chromatin architects modulating developmental decisions in Arabidopsis. Genome Biol. *20*, 157. https://doi.org/10.1186/s13059-019-1767-3.

36. Xiao, J., Jin, R., Yu, X., Shen, M., Wagner, J.D., Pai, A., Song, C., Zhuang, M., Klasfeld, S., He, C., et al. (2017). Cis and trans determinants of epigenetic silencing by Polycomb repressive complex 2 in Arabidopsis. Nat. Genet. *49*, 1546–1552. https://doi.org/10.1038/ng.3937.

37. Zhou, Y., Wang, Y., Krause, K., Yang, T., Dongus, J.A., Zhang, Y., and Turck, F. (2018). Telobox motifs recruit CLF/SWN-PRC2 for H3K27me3 deposition via TRB factors in Arabidopsis. Nat. Genet. *50*, 638–644. https://doi.org/10.1038/s41588-018-0109-9.

38. Cao, K., Lailler, N., Zhang, Y., Kumar, A., Uppal, K., Liu, Z., Lee, E.K., Wu, H., Medrzycki, M., Pan, C., et al. (2013). High-Resolution Mapping of H1

Linker Histone Variants in Embryonic Stem Cells. PLoS Genet. *9*, e1003417. https://doi.org/10.1371/journal.pgen.1003417.

39. Izzo, A., Kamieniarz-Gdula, K., Ramírez, F., Noureen, N., Kind, J., Manke, T., van Steensel, B., and Schneider, R. (2013). The Genomic Landscape of the Somatic Linker Histone Subtypes H1.1 to H1.5 in Human Cells. Cell Rep. *3*, 2142–2154. https://doi.org/10.1016/j.celrep.2013.05.003.
40. Roudier, F., Ahmed, I., Bérard, C., Sarazin, A., Mary-Huard, T., Cortijo, S., Bouyer, D., Caillieux, E., Duvernois-Berthet, E., Al-Shikhley, L., et al. (2011). Integrative epigenomic mapping defines four main chromatin states in Arabidopsis. EMBO J. *30*, 1928–1938.
41. Sequeira-Mendes, J., Aragüez, I., Peiró, R., Mendez-Giraldez, R., Zhang, X., Jacobsen, S.E., Bastolla, U., and Gutierrez, C. (2014). The Functional Topography of the Arabidopsis Genome Is Organized in a Reduced Number of Linear Motifs of Chromatin States. Plant Cell *26*, 2351–2366. https://doi.org/10.1105/tpc.114.124578.
42. Wang, C., Liu, C., Roqueiro, D., Grimm, D., Schwab, R., Becker, C., Lanz, C., and Weigel, D. (2015). Genome-wide analysis of local chromatin packing in Arabidopsis thaliana. Genome Res. *25*, 246–256. https://doi.org/10.1101/gr.170332.113.
43. Bernatavichute, Y.V., Zhang, X., Cokus, S., Pellegrini, M., and Jacobsen, S.E. (2008). Genome-wide association of histone H3 lysine nine methylation with CHG DNA methylation in Arabidopsis thaliana. PLoS One *3*, e3156. https://doi.org/10.1371/journal.pone.0003156.
44. Lu, Z., Hofmeister, B.T., Vollmers, C., Dubois, R.M., Schmitz, R.J., and Schmitz, J. (2017). Combining ATAC-seq with nuclei sorting for discovery of cis-regulatory regions in plant genomes. Nucleic Acids Res. *45*, e41–e13. https://doi.org/10.1093/nar/gkw1179.
45. Nassrallah, A., Rougée, M., Bourbousse, C., Drevensek, S., Fonseca, S., Iniesto, E., Ait-Mohamed, O., Deton-Cabanillas, A.F., Zabulon, G., Ahmed, I., et al. (2018). DET1-mediated degradation of a SAGA-like deubiquitination module controls H2Bub homeostasis. Elife *7*, 1–29. https://doi.org/10.7554/eLife.37892.
46. de Lucas, M., Pu, L., Turco, G., Gaudinier, A., Morao, A.K., Harashima, H., Kim, D., Ron, M., Sugimoto, K., Roudier, F., and Brady, S.M. (2016). Transcriptional Regulation of Arabidopsis Polycomb Repressive Complex 2 Coordinates Cell-Type Proliferation and Differentiation. Plant Cell *28*, 2616–2631. https://doi.org/10.1105/tpc.15.00744.
47. Regad, F., Lebas, M., and Lescure, B. (1994). Interstitial Telomeric Repeats within the Arabidopsis thaliana Genome. J. Mol. Biol. *239*, 163–169. https://doi.org/10.1006/jmbi.1994.1360.
48. Tremousaygue, D., Manevski, A., Bardet, C., Lescure, N., and Lescure, B. (1999). Plant interstitial telomere motifs participate in the control of gene expression in root meristems. Plant J. *20*, 553–561. https://doi.org/10.1046/j.1365-313X.1999.00627.x.
49. Hisanaga, T., Romani, F., Wu, S., Kowar, T., Lintermann, R., Jamge, B., Montgomery, S.A., Axelsson, E., Dierschke, T., Bowman, J.L., et al. (2022). Transposons Repressed by H3K27me3 Were Co-opted as Cis-Regulatory Elements of H3K27me3 Controlled Protein Coding Genes during Evolution of Plants. https://doi.org/10.1101/2022.10.24.513474.
50. Déléris, A., Berger, F., and Duharcourt, S. (2021). Role of Polycomb in the control of transposable elements. Trends Genet. *37*, 882–889. https://doi.org/10.1016/j.tig.2021.06.003.
51. Ma, Z., Castillo-González, C., Wang, Z., Sun, D., Hu, X., Shen, X., Potok, M.E., and Zhang, X. (2018). Arabidopsis Serrate Coordinates Histone Methyltransferases ATXR5/6 and RNA Processing Factor RDR6 to Regulate Transposon Expression. Dev. Cell *45*, 769–784.e6. https://doi.org/10.1016/j.devcel.2018.05.023.
52. Yan, W., Chen, D., Smaczniak, C., Engelhorn, J., Liu, H., Yang, W., Graf, A., Carles, C.C., Zhou, D.X., and Kaufmann, K. (2018). Dynamic and spatial restriction of Polycomb activity by plant histone demethylases. Native Plants *4*, 681–689. https://doi.org/10.1038/s41477-018-0219-5.
53. Mathieu, O., Probst, A.V., and Paszkowski, J. (2005). Distinct regulation of histone H3 methylation at lysines 27 and 9 by CpG methylation in Arabidopsis. EMBO J. *24*, 2783–2791. https://doi.org/10.1038/sj.emboj.7600743.
54. Deleris, A., Stroud, H., Bernatavichute, Y., Johnson, E., Klein, G., Schubert, D., and Jacobsen, S.E. (2012). Loss of the DNA Methyltransferase MET1 Induces H3K9 Hypermethylation at PcG Target Genes and Redistribution of H3K27 Trimethylation to Transposons in Arabidopsis thaliana. PLoS Genet. *8*, e1003062. https://doi.org/10.1371/journal.pgen.1003062.
55. Weinhofer, I., Hehenberger, E., Roszak, P., Hennig, L., and Köhler, C. (2010). H3K27me3 Profiling of the Endosperm Implies Exclusion of Polycomb Group Protein Targeting by DNA Methylation. PLoS Genet. *6*, e1001152. https://doi.org/10.1371/journal.pgen.1001152.
56. Fitzgerald, M.S., Riha, K., Gao, F., Ren, S., McKnight, T.D., and Shippen, D.E. (1999). Disruption of the telomerase catalytic subunit gene from Arabidopsis inactivates telomerase and leads to a slow loss of telomeric DNA. Proc. Natl. Acad. Sci. USA *96*, 14813–14818. https://doi.org/10.1073/pnas.96.26.14813.
57. Richards, E.J., and Ausubel, F.M. (1988). Isolation of a higher eukaryotic telomere from Arabidopsis thaliana. Cell *53*, 127–136. https://doi.org/10.1016/0092-8674(88)90494-1.
58. Uchida, W., Matsunaga, S., Sugiyama, R., and Kawano, S. (2002). Interstitial telomere-like repeats in the Arabidopsis thaliana genome. Genes Genet. Syst. *77*, 63–67. https://doi.org/10.1266/ggs.77.63.
59. Vannier, J.B., Depeiges, A., White, C., and Gallego, M.E. (2009). ERCC1/XPF protects short telomeres from homologous recombination in Arabidopsis thaliana. PLoS Genet. *5*, 10003800–e1000411. https://doi.org/10.1371/journal.pgen.1000380.
60. Procházková Schrumpfová, P., Fojtová, M., and Fajkus, J. (2019). Telomeres in Plants and Humans: Not So Different, Not So Similar. Cells *8*, 58. https://doi.org/10.3390/cells8010058.
61. Aksenova, A.Y., and Mirkin, S.M. (2019). At the Beginning of the End and in the Middle of the Beginning: Structure and Maintenance of Telomeric DNA Repeats and Interstitial Telomeric Sequences. Genes *10*, 118. https://doi.org/10.3390/genes10020118.
62. Adamusová, K., Khosravi, S., Fujimoto, S., Houben, A., Matsunaga, S., Fajkus, J., and Fojtová, M. (2020). Two combinatorial patterns of telomere histone marks in plants with canonical and non-canonical telomere repeats. Plant J. *102*, 678–687. https://doi.org/10.1111/tpj.14653.
63. Fransz, P., de Jong, J.H., Lysak, M., Castiglione, M.R., and Schubert, I. (2002). Interphase chromosomes in Arabidopsis are organized as well defined chromocenters from which euchromatin loops emanate 10.1073/pnas.212325299. Proc. Natl. Acad. Sci. USA *99*, 14584–14589.
64. Feng, S., Cokus, S.J., Schubert, V., Zhai, J., Pellegrini, M., and Jacobsen, S.E. (2014). Genome-wide Hi-C analyses in wild-type and mutants reveal high-resolution chromatin interactions in Arabidopsis. Mol. Cell. *55*, 694–707. https://doi.org/10.1016/j.molcel.2014.07.008.
65. Grob, S., Schmid, M.W., and Grossniklaus, U. (2014). Hi-C analysis in Arabidopsis identifies the KNOT, a structure with similarities to the flamenco locus of Drosophila. Mol. Cell. *55*, 678–693. https://doi.org/10.1016/j.molcel.2014.07.009.
66. Liu, C., Wang, C., Wang, G., Becker, C., Zaidem, M., and Weigel, D. (2016). Genome-wide analysis of chromatin packing in Arabidopsis thaliana at single-gene resolution. Genome Res. *26*, 1057–1068. https://doi.org/10.1101/gr.204032.116.
67. Moissiard, G., Cokus, S.J., Cary, J., Feng, S., Billi, A.C., Stroud, H., Husmann, D., Zhan, Y., Lajoie, B.R., McCord, R.P., et al. (2012). MORC Family ATPases Required for Heterochromatin Condensation and Gene Silencing. Science *336*, 1448–1451. https://doi.org/10.1126/science.1221472.
68. Sun, L., Jing, Y., Liu, X., Li, Q., Xue, Z., Cheng, Z., Wang, D., He, H., and Qian, W. (2020). Heat stress-induced transposon activation correlates with 3D chromatin organization rearrangement in Arabidopsis. Nat. Commun. *11*, 1886. https://doi.org/10.1038/s41467-020-15809-5.

69. Di Stefano, M., Nützmann, H.W., Marti-Renom, M.A., and Jost, D. (2021). Polymer modelling unveils the roles of heterochromatin and nucleolar organizing regions in shaping 3D genome organization in Arabidopsis thaliana. Nucleic Acids Res. *49*, 1840–1858. https://doi.org/10.1093/nar/gkaa1275.

70. Sexton, T., Yaffe, E., Kenigsberg, E., Bantignies, F., Leblanc, B., Hoichman, M., Parrinello, H., Tanay, A., and Cavalli, G. (2012). Three-Dimensional Folding and Functional Organization Principles of the Drosophila Genome. Cell *148*, 458–472. https://doi.org/10.1016/j.cell.2012.01.010.

71. Sakamoto, T., Sakamoto, Y., Grob, S., Slane, D., Yamashita, T., Ito, N., Oko, Y., Sugiyama, T., Higaki, T., Hasezawa, S., et al. (2022). Two-step regulation of centromere distribution by condensin II and the nuclear envelope proteins. Native Plants *8*, 940–953. https://doi.org/10.1038/s41477-022-01200-3.

72. Heinz, S., Benner, C., Spann, N., Bertolino, E., Lin, Y.C., Laslo, P., Cheng, J.X., Murre, C., Singh, H., and Glass, C.K. (2010). Simple Combinations of Lineage-Determining Transcription Factors Prime cis-Regulatory Elements Required for Macrophage and B Cell Identities. Mol. Cell. *38*, 576–589. https://doi.org/10.1016/j.molcel.2010.05.004.

73. Schrumpfová, P.P., Vychodilová, I., Dvořáčková, M., Majerská, J., Dokládal, L., Schořová, S., and Fajkus, J. (2014). Telomere repeat binding proteins are functional components of Arabidopsis telomeres and interact with telomerase. Plant J. *77*, 770–781. https://doi.org/10.1111/tpj.12428.

74. Mozgová, I., Schrumpfová, P.P., Hofr, C., and Fajkus, J. (2008). Functional characterization of domains in AtTRB1, a putative telomere-binding protein in Arabidopsis thaliana. Phytochemistry *69*, 1814–1819. https://doi.org/10.1016/j.phytochem.2008.04.001.

75. Schrumpfová, P., Kuchař, M., Miková, G., Skrísovská, L., Kubicárová, T., and Fajkus, J. (2004). Characterization of two Arabidopsis thaliana myb-like proteins showing affinity to telomeric DNA sequence. Genome *47*, 316–324. https://doi.org/10.1139/g03-136.

76. Schrumpfová, P.P., Vychodilová, I., Hapala, J., Schořová, Š., Dvořáček, V., and Fajkus, J. (2016). Telomere binding protein TRB1 is associated with promoters of translation machinery genes in vivo. Plant Mol. Biol. *90*, 189–206. https://doi.org/10.1007/s11103-015-0409-8.

77. Zhou, Y., Hartwig, B., James, G.V., Schneeberger, K., and Turck, F. (2016). Complementary activities of TELOMERE REPEAT BINDING proteins and polycomb group complexes in transcriptional regulation of target genes. Plant Cell *28*, 87–101. https://doi.org/10.1105/tpc.15.00787.

78. Charbonnel, C., Rymarenko, O., Da Ines, O., Benyahya, F., White, C.I., Butter, F., and Amiard, S. (2018). The Linker Histone GH1-HMGA1 Is Involved in Telomere Stability and DNA Damage Repair. Plant Physiol. *177*, 311–327. https://doi.org/10.1104/pp.17.01789.

79. Pérez-Pérez, J.M., Candela, H., and Micol, J.L. (2009). Understanding synergy in genetic interactions. Trends Genet. *25*, 368–376. https://doi.org/10.1016/j.tig.2009.06.004.

80. Turck, F., Roudier, F., Farrona, S., Martin-Magniette, M.L., Guillaume, E., Buisine, N., Gagnot, S., Martienssen, R.A., Coupland, G., and Colot, V. (2007). Arabidopsis TFL2/LHP1 specifically associates with genes marked by trimethylation of histone H3 lysine 27. PLoS Genet. *3*, e86. https://doi.org/10.1371/journal.pgen.0030086.

81. Pontvianne, F., and Grob, S. (2020). Three-dimensional nuclear organization in Arabidopsis thaliana. J. Plant Res. *133*, 479–488. https://doi.org/10.1007/s10265-020-01185-0.

82. Santos, A.P., Gaudin, V., Mozgová, I., Pontvianne, F., Schubert, D., Tek, A.L., Dvořáčková, M., Liu, C., Fransz, P., Rosa, S., et al. (2020). Tiding-up the plant nuclear space: domains, function and dynamics. J. Exp. Bot., 1–19. https://doi.org/10.1093/jxb/eraa282.

83. Domb, K., Wang, N., Hummel, G., and Liu, C. (2022). Spatial Features and Functional Implications of Plant 3D Genome Organization. Annu. Rev. Plant Biol. *73*, 173–200. https://doi.org/10.1146/annurev-arplant-102720-022810.

84. Veluchamy, A., Jégu, T., Ariel, F., Latrasse, D., Mariappan, K.G., Kim, S.-K., Crespi, M., Hirt, H., Bergounioux, C., Raynaud, C., et al. (2016). LHP1 Regulates H3K27me3 Spreading and Shapes the Three-Dimensional Conformation of the Arabidopsis Genome. PLoS One *11*, 1–25. https://doi.org/10.1371/journal.pone.0158936.

85. Huang, Y., Sicar, S., Ramirez-Prado, J.S., Manza-Mianza, D., Antunez-Sanchez, J., Brik-Chaouche, R., Rodriguez-Granados, N.Y., An, J., Bergounioux, C., Mahfouz, M.M., et al. (2021). Polycomb-dependent differential chromatin compartmentalization determines gene coregulation in Arabidopsis. Genome Res. *31*, 1230–1244. https://doi.org/10.1101/gr.273771.120.

86. Jamieson, K., Mcnaught, K.J., Ormsby, T., Leggett, N.A., Honda, S., and Selker, E.U. (2018). Telomere repeats induce domains of H3K27 methylation in Neurospora. Elife *7*, e31216–e31218. https://doi.org/10.7554/eLife.31216.

87. Fojtová, M., and Fajkus, J. (2014). Epigenetic regulation of telomere maintenance. Cytogenet. Genome Res. *143*, 125–135. https://doi.org/10.1159/000360775.

88. Majerová, E., Mandáková, T., Vu, G.T.H., Fajkus, J., Lysak, M.A., and Fojtová, M. (2014). Chromatin features of plant telomeric sequences at terminal vs. internal positions. Front. Plant Sci. *5*, 1–10. https://doi.org/10.3389/fpls.2014.00593.

89. Vaquero-Sedas, M.I., Gámez-Arjona, F.M., and Vega-Palas, M.A. (2011). Arabidopsis thaliana telomeres exhibit euchromatic features. Nucleic Acids Res. *39*, 2007–2017. https://doi.org/10.1093/nar/gkq1119.

90. Vaquero-Sedas, M.I., Luo, C., and Vega-Palas, M.A. (2012). Analysis of the epigenetic status of telomeres by using ChIP-seq data. Nucleic Acids Res. *40*, e163. https://doi.org/10.1093/nar/gks730.

91. Vega-Vaquero, A., Bonora, G., Morselli, M., Vaquero-Sedas, M.I., Rubbi, L., Pellegrini, M., and Vega-Palas, M.A. (2016). Novel features of telomere biology revealed by the absence of telomeric DNA methylation. Genome Res. *26*, 1047–1056. https://doi.org/10.1101/gr.202465.115.

92. Vaquero-Sedas, M.I., and Vega-Palas, M.A. (2023). Epigenetic nature of Arabidopsis thaliana telomeres. Plant Physiol. *191*, 47–55. https://doi.org/10.1093/plphys/kiac471.

93. Achrem, M., Szućko, I., and Kalinka, A. (2020). The epigenetic regulation of centromeres and telomeres in plants and animals. Comp. Cytogenet. *14*, 265–311. https://doi.org/10.3897/CompCytogen.v14i2.51895.

94. Dvořáčková, M., Fojtová, M., and Fajkus, J. (2015). Chromatin dynamics of plant telomeres and ribosomal genes. Plant J. *83*, 18–37. https://doi.org/10.1111/tpj.12822.

95. Grafi, G., Ben-Meir, H., Avivi, Y., Moshe, M., Dahan, Y., and Zemach, A. (2007). Histone methylation controls telomerase-independent telomere lengthening in cells undergoing dedifferentiation. Dev. Biol. *306*, 838–846. https://doi.org/10.1016/j.ydbio.2007.03.023.

96. Farrell, C., Vaquero-Sedas, M.I., Cubiles, M.D., Thompson, M., Vega-Vaquero, A., Pellegrini, M., and Vega-Palas, M.A. (2022). A complex network of interactions governs DNA methylation at telomeric regions. Nucleic Acids Res. *50*, 1449–1464. https://doi.org/10.1093/nar/gkac012.

97. Ascenzi, R., and Gantt, J.S. (1999). Subnuclear distribution of the entire complement of linker histone variants in Arabidopsis thaliana. Chromosoma *108*, 345–355. https://doi.org/10.1007/s004120050386.

98. Simpson, R.T. (1978). Structure of the chromatosome, a chromatin particle containing 160 base pairs of DNA and all the histones. Biochemistry *17*, 5524–5531. https://doi.org/10.1021/bi00618a030.

99. Fajkus, J., Kovarík, A., Královics, R., and Bezděk, M. (1995). Organization of telomeric and subtelomeric chromatin in the higher plant Nicotiana tabacum. Mol. Gen. Genet. *247*, 633–638. https://doi.org/10.1007/BF00290355.

100. Déjardin, J., and Kingston, R.E. (2009). Purification of Proteins Associated with Specific Genomic Loci. Cell *136*, 175–186. https://doi.org/10.1016/j.cell.2008.11.045.

101. Galati, A., Micheli, E., and Cacchione, S. (2013). Chromatin Structure in Telomere Dynamics. Front. Oncol. *3*, 46. https://doi.org/10.3389/fonc.2013.00046.

102. Makarov, V.L., Lejnine, S., Bedoyan, J., and Langmore, J.P. (1993). Nucleosomal organization of telomere-specific chromatin in rat. Cell *73*, 775–787. https://doi.org/10.1016/0092-8674(93)90256-P.

103. Lejnine, S., Makarov, V.L., and Langmore, J.P. (1995). Conserved nucleoprotein structure at the ends of vertebrate and invertebrate chromosomes. Proc. Natl. Acad. Sci. USA *92*, 2393–2397. https://doi.org/10.1073/pnas.92.6.2393.

104. Fajkus, J., and Trifonov, E.N. (2001). Columnar packing of telomeric nucleosomes. Biochem. Biophys. Res. Commun. *280*, 961–963. https://doi.org/10.1006/bbrc.2000.4208.

105. Soman, A., Wong, S.Y., Korolev, N., Surya, W., Lattmann, S., Vogirala, V.K., Chen, Q., Berezhnoy, N.V., van Noort, J., Rhodes, D., and Nordenskiöld, L. (2022). Columnar structure of human telomeric chromatin. Nature *609*, 1048–1055. https://doi.org/10.1038/s41586-022-05236-5.

106. Fiorucci, A.-S., Bourbousse, C., Concia, L., Rougée, M., Deton-Cabanillas, A.-F., Zabulon, G., Layat, E., Latrasse, D., Kim, S.K., Chaumont, N., et al. (2019). Arabidopsis S2Lb links AtCOMPASS-like and SDG2 activity in H3K4me3 independently from histone H2B monoubiquitination. Genome Biol. *20*, 100. https://doi.org/10.1186/s13059-019-1705-4.

107. Samson, F., Brunaud, V., Balzergue, S., Dubreucq, B., Lepiniec, L., Pelletier, G., Caboche, M., and Lecharny, A. (2002). FLAGdb/FST: a database of mapped flanking insertion sites (FSTs) of Arabidopsis thaliana T-DNA transformants. Nucleic Acids Res. *30*, 94–97. https://doi.org/10.1093/nar/30.1.94.

108. Dobin, A., Davis, C.A., Schlesinger, F., Drenkow, J., Zaleski, C., Jha, S., Batut, P., Chaisson, M., and Gingeras, T.R. (2013). STAR: ultrafast universal RNA-seq aligner. Bioinformatics *29*, 15–21. https://doi.org/10.1093/bioinformatics/bts635.

109. Love, M.I., Huber, W., and Anders, S. (2014). Moderated estimation of fold change and dispersion for RNA-seq data with DESeq2. Genome Biol. *15*, 550. https://doi.org/10.1186/s13059-014-0550-8.

110. Anders, S., Pyl, P.T., and Huber, W. (2015). HTSeq—a Python framework to work with high-throughput sequencing data. Bioinformatics *31*, 166–169. https://doi.org/10.1093/bioinformatics/btu638.

111. Servant, N., Varoquaux, N., Lajoie, B.R., Viara, E., Chen, C.J., Vert, J.P., Heard, E., Dekker, J., and Barillot, E. (2015). HiC-Pro: An optimized and flexible pipeline for Hi-C data processing. Genome Biol. *16*, 259–311. https://doi.org/10.1186/s13059-015-0831-x.

112. Carron, L., Morlot, J.B., Matthys, V., Lesne, A., Mozziconacci, J., and Birol, I. (2019). Boost-HiC: Computational enhancement of long-range contacts in chromosomal contact maps. Bioinformatics *35*, 2724–2729. https://doi.org/10.1093/bioinformatics/bty1059.

113. Durand, N.C., Robinson, J.T., Shamim, M.S., Machol, I., Mesirov, J.P., Lander, E.S., and Aiden, E.L. (2016). Juicebox Provides a Visualization System for Hi-C Contact Maps with Unlimited Zoom. Cell Syst. *3*, 99–101. https://doi.org/10.1016/j.cels.2015.07.012.

114. Langmead, B., and Salzberg, S.L. (2012). Fast gapped-read alignment with Bowtie 2. Nat. Methods *9*, 357–359. https://doi.org/10.1038/nmeth.1923.

115. Zhang, Y., Liu, T., Meyer, C.A., Eeckhoute, J., Johnson, D.S., Bernstein, B.E., Nusbaum, C., Myers, R.M., Brown, M., Li, W., and Liu, X.S. (2008). Model-based Analysis of ChIP-Seq (MACS). Genome Biol. *9*, R137. https://doi.org/10.1186/gb-2008-9-9-r137.

116. Tarasov, A., Vilella, A.J., Cuppen, E., Nijman, I.J., and Prins, P. (2015). Sambamba: fast processing of NGS alignment formats. Bioinformatics *31*, 2032–2034. https://doi.org/10.1093/bioinformatics/btv098.

117. Quinlan, A.R., and Hall, I.M. (2010). BEDTools: a flexible suite of utilities for comparing genomic features. Bioinformatics *26*, 841–842. https://doi.org/10.1093/bioinformatics/btq033.

118. Thorvaldsdóttir, H., Robinson, J.T., and Mesirov, J.P. (2012). Integrative Genomics Viewer (IGV): high-performance genomics data visualization and exploration. Briefings Bioinf. *14*, 178–192. https://doi.org/10.1093/bib/bbs017.

119. Bailey, T.L., Johnson, J., Grant, C.E., and Noble, W.S. (2015). The MEME Suite. Nucleic Acids Res. *43*, W39–W49. https://doi.org/10.1093/nar/gkv416.

120. Supek, F., Bošnjak, M., Škunca, N., and Šmuc, T. (2011). REVIGO Summarizes and Visualizes Long Lists of Gene Ontology Terms. PLoS One *6*, e21800. https://doi.org/10.1371/journal.pone.0021800.

121. Notredame, C., Higgins, D.G., and Heringa, J. (2000). T-Coffee: A novel method for fast and accurate multiple sequence alignment. J. Mol. Biol. *302*, 205–217. https://doi.org/10.1006/jmbi.2000.4042.

122. IJdo, J.W., Wells, R.A., Baldini, A., and Reeders, S.T. (1991). Improved telomere detection using a telomere repeat probe (TTAGGG) n generated by PCR. Nucleic Acids Res. *19*, 4780. https://doi.org/10.1093/nar/19.17.4780.

123. Cournac, A., Marie-Nelly, H., Marbouty, M., Koszul, R., and Mozziconacci, J. (2012). Normalization of a chromosomal contact map. BMC Genom. *13*, 436. https://doi.org/10.1186/1471-2164-13-436.

124. Bolger, A.M., Lohse, M., and Usadel, B. (2014). Trimmomatic: a flexible trimmer for Illumina sequence data. Bioinformatics *30*, 2114–2120. https://doi.org/10.1093/bioinformatics/btu170.

125. Quadrana, L., Bortolini Silveira, A., Mayhew, G.F., LeBlanc, C., Martienssen, R.A., Jeddeloh, J.A., and Colot, V. (2016). The Arabidopsis thaliana mobilome and its impact at the species level. Elife *5*, e15716. https://doi.org/10.7554/eLife.15716.

126. Schep, A.N., Buenrostro, J.D., Denny, S.K., Schwartz, K., Sherlock, G., and Greenleaf, W.J. (2015). Structured nucleosome fingerprints enable high-resolution mapping of chromatin architecture within regulatory regions. Genome Res. *25*, 1757–1770. https://doi.org/10.1101/gr.192294.115.

127. Ramírez, F., Ryan, D.P., Grüning, B., Bhardwaj, V., Kilpert, F., Richter, A.S., Heyne, S., Dündar, F., and Manke, T. (2016). deepTools2: a next generation web server for deep-sequencing data analysis. Nucleic Acids Res. *44*, W160–W165. https://doi.org/10.1093/nar/gkw257.

128. Boyle, E.I., Weng, S., Gollub, J., Jin, H., Botstein, D., Cherry, J.M., and Sherlock, G. (2004). GO::TermFinder—open source software for accessing Gene Ontology information and finding significantly enriched Gene Ontology terms associated with a list of genes. Bioinformatics *20*, 3710–3715. https://doi.org/10.1093/bioinformatics/bth456.

STAR★METHODS

KEY RESOURCES TABLE

REAGENT or RESOURCE	SOURCE	IDENTIFIER
Antibodies		
Rabbit anti-H3K27me3	Merck	Cat# 07-449; RRID: AB_310624
Goat biotin anti Rabbit IgG	ThermoFisher	Cat# 65-6140; RRID: AB_2533969
Mouse anti-digoxigenin	Roche	Cat#11333062910; RRID: AB_514495
Rat anti-mouse FITC	Invitrogen	Cat# rmg101; RRID: AB_2556582
Mouse Cy3 anti-biotin antibody	Sigma	Cat# C5585; RRID: AB_258901
Anti-GFP	Thermo Fisher	Cat# A11122; RRID: AB_221569
Mouse Anti-H3	Abcam	Cat# Ab1791; RRID: AB_302613
Rabbit anti-H3K27me3	Diagenode	Cat# C15410069; RRID: AB_2814977
Chemicals, peptides, and recombinant proteins		
Percoll	Sigma-Aldrich	#P1644
Protein-A/G Dynabeads	Invitrogen	#10004D
Agencourt® AMPure® XP Beads	Beckman Coulter	#A63880
DpnII	New England Biolabs	#R0543T
DNA Polymerase I, Large (Klenow) Fragment	New England Biolabs	#M0210L
T4 ligase (HC)	Promega	#MI79A
Critical commercial assays		
Nextera DNA Library Prep Kit	Illumina	#FC-121-1030
MinElute® PCR Purification Kit	QIAGEN	#28004
RNeasy micro kit (Qiagen)	QIAGEN	#74004
KAPA LTP Library Preparation Kit	Roche	#KR0961
the Pierce™ BCA Protein Assay Kit	Thermo Scientific™	#23225
NEBNext® Ultra™ II DNA Library Prep Kit for Illumina®	New England Biolabs	#E7645
Deposited data		
ATAC-seq of WT and *2h1* plants	This study	GEO: GSE160408
H3K27me3 ChIP-Rx of Wt and *2h1* plants	This study	GEO: GSE160410
H1-2-GFP ChIP-seq of WT plants	This study	GEO: GSE160411
Hi-C in WT and *2h1* plants	This study	GEO: GSE160412
RNA-seq of WT and *2h1 plants*	This study	GEO: GSE160413
H3K4me3 ChIP-seq of WT plants	Fiorucci et al.,[106]	GEO: GSE124318
H2Bub ChIP-seq of WT plants	Nassrallah et al.,[45]	GEO: GSE112952
MNase-seq of WT and *2h1* plants	Lyons & Zilberman,[28]	GEO: GSE96994
WGBS of WT and *2h1* plants	Lyons & Zilberman.,[28]	GEO: GSE96994
H3K9me2 ChIP-seq of WT plants	Ma et al.,[51]	GEO: GSE111814
H3K27me1 ChIP-seq of WT plants	Ma et al.,[51]	GEO: GSE111814
TRB1 ChIP-seq of WT plants	Schrumpfová et al.,[76]	GEO: GSE69431
H3K27me3 ChIP-seq of WT and *ref. 6elf6jmj13* plants	Yan et al.,[52]	GEO: GSE106942
Experimental models: Organisms/strains		
Arabidopsis: Col 0	Arabidopsis Biological Resource Center	CS22625
h1.1h1.2	Rutowicz et al.,	N/A
TRB1::GFP-TRB1	Schrumpfová, P.P[73]	N/A
trb1	NASC	Salk_001540
trb2	FLAGdb/FST collection[107]	Flag_242F11
trb3	NASC	Salk_134641
trb1trb2trb3	This study	N/A

(*Continued on next page*)

Continued

REAGENT or RESOURCE	SOURCE	IDENTIFIER
Software and algorithms		
Trim Galore version: 0.6.4_dev Cutadapt version: 2.10	https://doi.org/10.5281/zenodo.5127898	N/A
STAR (version 2.7.3a)	Dobin et al.,[108]	N/A
DESeq2 package	Love et al.,[109]	N/A
HTSeq suite (version 0.11.3)	Anders et al.,[110]	N/A
R package dplyr	=https://CRAN.R-project.org/package=dplyr	N/A
Hi-C Pro pipeline	Servant et al.,[111]	N/A
Boost-HiC	Carron et al.,[112]	N/A
Juicebox toolsuite	Duran et al.,[113]	N/A
HOMER	Heinz et al.,[72]	N/A
Bowtie2v.2.3.2	Langmead at al.,[114]	N/A
MACS2	Zhang et al.,[115]	N/A
sambamba v0.6.8.	Tarasov et al.,[116]	N/A
bedtools v2.29.2	Qinlan et al.,[117]	N/A
Genomics Viewer (IGV) version 2.8.0	Thorvaldsdóttir et al.,[118]	N/A
ASAP ATAC-Seq data Analysis Pipeline	https://zenodo.org/record/1466008	N/A
MEME version 5.1.1	Bailey et al.,[119]	N/A
REVIGO	Supek et al.,[120]	N/A
T-Coffee	Notredame et al.,[121]	N/A

RESOURCE AVAILABILITY

Lead contact

Further information and requests for resources and reagents should be directed to and will be fulfilled by the lead contact, Fredy Barneche (barneche@bio.ens.psl.eu).

Materials availability

Arabidopsis transgenic and mutant lines generated in this study will be made available upon request.

Data and code availability

All data reported in this paper has been deposited at Gene Expression Omnibus (https://www.ncbi.nlm.nih.gov/geo/) public repository under the accession number GSE160414. This paper analyzes existing, publicly available datasets whose accession numbers are listed in the key resources table. All original code is available in this paper's supplemental information. Publicly available code used in this paper is listed in the key resources table. Any additional information required to reanalyze the data reported in this paper is available from the lead contact upon request.

EXPERIMENTAL MODEL AND STUDY PARTICIPANT DETAILS

Arabidopsis thaliana

Seeds were surface-sterilized, plated on half strength Murashige and Skoog (MS) medium with 0.9% agar and 0.5% sugar, and cultivated under long-day (16h/8h) at 23/19°C light/dark photoperiod (100 μmol m^{-2}.s−1) for 5 days unless otherwise stated. Cotyledons, when used, were manually dissected under a stereomicroscope. The *h1.1h1.2* (*2h1*) Arabidopsis mutant line and the transgenic *pH1.2::H1.2-GFP* line[22] were kindly provided by Dr. Kinga Rutowicz (University of Zurich, Switzerland). The *TRB1::GFP-TRB1* line described in.[76] The *2h1/TRB1::GFP-TRB1* transgenic line was obtained upon manual crossing of the *2h1* and *TRB1::GFP-TRB1* line described previously in.[76] The *trb123* triple mutant line was produced by crossing a *trb1trb2* double homozygous plant (derived from a cross between *trb1* (Salk_001540) and *trb2* (Flag_242F11) mutant alleles) with a double homozygous *trb2trb3* mutant plant (derived from a cross between *trb2* (Flag_242F11) with *trb3* (Salk_134641).

METHOD DETAILS

Immuno-FISH

After fixation in 4% paraformaldehyde in 1X PME, cotyledons of 7-day-old seedlings were chopped directly in 1% cellulase, 1% pectolyase, and 0.5% cytohelicase in 1X PME, and incubated 15 min. Nucleus suspensions were transferred to poly-Lysine-coated

slides. One volume of 1% lipsol in 1X PME was added to the mixture and spread on the slide. Then, 1 volume of 4% PFA in 1X PME was added and slides were dried. Immunodetection and FISH were conducted as described previously[78] using the following antibodies: rabbit H3K27me3 (#07–449 - Merck) diluted 1:200, Goat biotin anti Rabbit IgG (#65–6140 - ThermoFisher) 1:500, mouse anti-digoxigenin (#11333062910 -ROCHE) 1:125, rat anti-mouse FITC (#rmg101 - Invitrogen) at 1:500 at 1:100, mouse Cy3 anti-biotin antibody (#C5585 - Sigma) at 1:1000. Acquisitions were performed on a structured illumination (pseudo-confocal) imaging system (ApoTome AxioImager M2; Zeiss) and processed using a deconvolution module (regularized inverse filter algorithm). The colocalization was analyzed via the colocalization module of the ZEN software using the uncollapsed z stack files. To test for signal colocalization, the range of Pearson correlation coefficient of H3K27m3 vs. telomeric FISH signals were calculated with the colocalization module of the ZEN software using z stack files. Foci with coefficients superior to 0.5 were considered as being colocalized.

ATAC-seq

Nuclei were isolated from 200 cotyledons of 5-day-old seedlings and purified using a two-layer Percoll gradient at 3000 g before staining with 0.5 μM DAPI and sorting by FACS according to their ploidy levels using a MoFlo Astrios EQ Cell Sorter (Beckman Culture) in PuraFlow sheath fluid (Beckman Coulter) at 25 psi (pounds per square inch), with a 100-μmmicron nozzle. We performed sorting with ~43 kHz drop drive frequency, plates voltage of 4000–4500 V and an amplitude of 30–50 V. Sorting was performed in purity mode. For each sample, 20000 sorted 4C nuclei were collected separately in PBS buffer and centrifuged at 3,000 g at 4°C for 5 min. The nuclei were re-suspended in 20 μL of Tn5 transposase reaction buffer (Illumina). After tagmentation, DNA was purified using the MinElute PCR Purification Kit (Qiagen) and amplified with Nextera DNA Library Prep index oligonucleotides (Illumina). A size selection was performed with AMPure XP beads (Beckman Coulter) to collect library molecules longer than 150 bp. DNA libraries were sequenced by Beijing Genomics Institute (BGI Group, Hong-Kong) using the DNA Nanoballs (DNB) DNBseq in a 65 bp paired-end mode.

In situ Hi-C

Hi-C was performed as in Grob et al. (2014)[65] with downscaling using seedlings crosslinked in 10 mM potassium phosphate pH 7.0, 50 mM NaCl, 0.1 M sucrose with 4% (v/v) formaldehyde. Crosslinking was stopped by transferring seedlings to 30mL of 0.15 M glycine. After rinsing and dissection, 1000 cotyledons were flash-frozen in liquid nitrogen and ground using a Tissue Lyser (Qiagen). All sample were adjusted to 4 mL using NIB buffer (20 mM HEPES pH7.8, 0.25 M sucrose, 1 mM MgCl2, 0.5 mM KCl, 40% v/v glycerol, 1% Triton X-100) and homogenized on ice using a Dounce homogenizer. Nuclei were pelleted by centrifugation and resuspended in the DpnII digestion buffer (10 mM MgCl2, 1 mM DTT, 100 mM NaCl, 50 mM Bis-Tris-HCl, pH 6.0) before adding SDS to a final concentration of 0.5% (v/v). SDS was quenched by adding 2% Triton X-100. DpnII (200 u) was added to each sample for over-night digestion at 37°C dATP, dTTP, dGTP, biotinylated dCTP and 12 μL DNA Polymerase I (Large Klenow fragment) were added before incubation for 45 min at 37°C. A total of 50 unit of T4 DNA ligase along with 7 μL of 20 ng/μL of BSA (Biolabs) and 7 μL of 100 mM ATP were added to reach a final volume of 700μL. Samples were incubated for 4h at 16°C with constant shaking at 300rpm. After over-night reverse crosslinking at 65°C and protein digestion with 5 μL of 10 mg/μL proteinase K, DNA was extracted by phenol/chloroform purification and ethanol precipitation before resuspension in 100μL of 0.1X TE buffer. Biotin was removed from the unligated fragment using T4 DNA polymerase exonuclease activity. After biotin removal, the samples were purified using AMPure beads with a 1.6X ratio. DNA was fragmented using a Covaris M220 sonicator (peak power 75W, duty factor 20, cycles per burst 200, duration 150 s). Hi-C libraries were prepared using KAPA LTP Library Preparation Kit (Roche)[65] with 12 amplification cycles. PCR products were purified using AMPure beads (ratio 1.85X). Libraries were analyzed using a Qubit fluorometer (ThermoFisher) and a TAPE Station (Agilent) before sequencing in a 75 bp PE mode using a DNB-seq platform at the Beijing Genomics Institute (BGI Group; Honk Kong).

RNA-seq

Upon growth 5 days under long days conditions (16h light at 23°C, 8h dark at 19°C), seedlings were fixed in 100% cold acetone under vacuum for 10 min. Cotyledons from 100 plants were manually dissected and ground in 2 mL tubes using a Tissue Lyser (Qiagen) for 1 min 30 s at 30 Hz before RNA extraction using the RNeasy micro kit (Qiagen). RNA was sequenced using the DNBseq platform at the Beijing Genomics Institute (BGI Group) in a 100 bp paired-end mode. For raw data processing, sequencing adaptors were removed from raw reads with trim_galore! 0.6.4_dev Cutadapt version: 2.10. Reads were mapped onto TAIR10 genome using STAR version 2.7.3a[108] with the following parameters "–alignIntronMin 20 –alignIntronMax 100000 –outFilterMultimapNmax 20 –outMultimapperOrder Random –outFilterMismatchNmax 8 –outSAMtype BAM SortedByCoordinate –outSAMmultNmax 1 –alignMatesGapMax 100000". Gene raw counts were scored using the htseq-count tool from the HTSeq suite version 0.11.3[110] and analyzed with the DESeq2 package[109] to calculate Log2-fold change and to identify differentially expressed genes (p value <0.01). TPM (Transcripts per Million) were retrieved by dividing the counts over each gene by its length in kb and the resulting RPK was divided by the total read counts in the sample (in millions). Mean TPM values between two biological replicates were used for subsequent analyses. To draw metagene plots, genes were grouped into expressed or not and expressed genes split into four quantiles of expression with the function ntile() of the R package dplyr (=https://CRAN.R-project.org/package=dplyr).

H1.2-GFP, GFP-TRB1 and H3 ChIP-seq experiments

H1.2-GFP and parallel H3 profiling were conducted as in Fiorucci et al. (2019)[106] after sonicating chromatin to mono/di-nucleosome fragment sizes. WT Col-0 or *pH1.2::H1.2-GFP* seedlings were crosslinked for 15 min using 1% formaldehyde. After dissection, 400 cotyledons were ground in 2 mL tubes using a Tissue Lyser (Qiagen) for 2 × 1 min at 30 Hz. After resuspension in 100 μL Nuclei Lysis Buffer 0.1 %SDS, the samples were flash frozen in liquid nitrogen and chromatin was sheared using an S220 Focused-Ultrasonicator (Covaris) for 17 min at peak power 105 W, duty factor 5%, 200 cycles per burst, to get fragment sizes between 75 and 300 bp. Immunoprecipitation was performed on 150 μg of chromatin quantified using the Pierce BCA Protein Assay Kit (Thermo Fisher Scientific) with 60 μL of Protein-A/G Dynabeads and 3.5 μL of anti-GFP (Thermo Fisher #A11122) for H1.2-GFP and mock (WT) sample or anti-H3 (Abcam #Ab1791) for H3 IPs. Immunoprecipitated DNA was subjected to library preparation using the TruSeq ChIP Sample Preparation Kit (Illumina) and sequenced using a NextSeq 500 system or DNBSEQ-G400 in a single-end 50 bp mode (Genewiz, USA; Fasteris, Switzerland and DNBseq BGI, Hong-Kong).

H3K27me3 ChIP-Rx

ChIP-Rx of WT and *2h1* plants corresponding to Figures 1, 2, 3, 4, 5, and 6 and of WT, *2h1*, *trb123* and *htrbQ* plants corresponding to Figure 7 were performed using anti-H3K27me3 #07–449 (Millipore) and #C15410069 (Diagenode), respectively. Both ChIP-Rx series were conducted as in Nassrallah et al. (2018)[45] using two biological replicates of 8-day-old WT and 2h1 seedlings. For each biological replicate, two independent IPs were carried out using 120 μg of Arabidopsis chromatin mixed with 3% of Drosophila chromatin quantified using the Pierce BCA Protein Assay Kit (Thermo Fisher Scientific). DNA samples eluted and purified from the two technical replicates were pooled before library preparation (Illumina TruSeq ChIP) and sequencing (Illumina NextSeq 500, 1x50bp or DNBSEQ-G400, 1x50bp) of all input and IP samples by Fasteris (Geneva, Switzerland) and BGI (Hong-Kong), respectively.

H3K27me3 and H3 ChIP-blot analyses

Anti-H3K27me3 (Millipore, #07–449 antibody) and anti-H3 (Abcam #Ab1791 antibody) ChIPs were conducted using 2 g of tissue. Pellets of both inputs (20%) and immunoprecipitated DNA were resuspended in 40 μL of TE, pH 8.0 and analyzed through dot-blot hybridization using a radioactively labeled telomeric probe synthesized by non-template PCR.[62,122] ITRs contribution to the hybridization signal was minimized using high stringency hybridization as detailed in.[62]

Hi-C bioinformatics

Hi-C reads were mapped using the Hi-C Pro pipeline[111] with default pipeline parameters and merging data from three biological replicates at the end of the pipeline. Data were in visualized using the Juicebox toolsuite[113] and represented in Log10 scale after SCN normalization[123] with Boost-HiC[112] setting alpha parameter to 0.2. In Figure S4, we normalized the sequencing depth in each sample and scored the number of reads in each combination of genomic regions using HOMER.[72] Read counts were further normalized for the bin size and the median value between the three biological replicates was reported. Distal-to-Local [log2] Ratios (DLR) where implemented as described in HOMER[72] and adapted to define local interactions between a defined size window (k) and the two surrounding windows as distal regions at 10kb and 100kb for k = 2 to k = 150 bins and selected for each ITR a windows value corresponding of 3 ITR sizes (1050 kb for ITR-1R and 240 kb for ITR-4L).

ChIP-seq and ChIP-Rx bioinformatics

For H3K27me3 spike-in normalized ChIP-Rx, raw reads were pre-processed with Trimmomatic v0.36[124] to remove leftover Illumina sequencing adapters. 5′ and 3′ ends with a quality score below 5 (Phred+33) were trimmed and reads shorter than 20 bp after trimming were discarded (trimmomatic-0.36.jar SE -phred33 INPUT.fastq TRIMMED_OUTPUT.fastq ILLUMINACLIP:TruSeq3-SE.fa:2:30:10 LEADING:5 TRAILING:5 MINLEN:20). We aligned the trimmed reads against combined TAIR10 Arabidopsis thaliana and Drosophila melanogaster (dm6) genomes with Bowtie2v.2.3.2 using the ‘‘–very-sensitive’’ setting. Duplicated reads and reads mapping to regions with aberrant coverage or low sequence complexity defined in[125] were discarded with sambamba v0.6.8.[116] Peaks of H3K27me3 read density were called using MACS2[115] with the command ‘‘macs2 callpeak -f BAM –nomodel -q 0.01 -g 120e6 –bw 300 –verbose 3 –broad’’. Only peaks found in both biological replicates and overlapping for at least 10% were retained for further analyses. Annotation of genes and TEs overlapping with peaks of histone marks H3K27me3, H3K4me3, and H2Bub were identified using bedtools v2.29.2 intersect as for H3K27me3. We scored the number of H3K27me3 reads overlapping with marked genes using bedtools v2.29.2 multicov and analyzed them with the DESeq2 package[109] in the R statistical environment v3.6.2 to identify the genes enriched or depleted in H3K27me3 in *2h1* plants (p value <0.01). To account for differences in sequencing depth we used the function SizeFactors in DESeq2, applying a scaling factor calculated as in Nassrallah et al. (2018).[45] For GFP-TRB1, H1.2-GFP and H3 ChIP-seq datasets, raw reads were processed as for H3K27me3. We counted the reads over genes and TEs using bedtools v2.29.2 multicov and converted them in median counts per million, dividing the counts over each gene or TE by its length and by the total counts in the sample and multiplying by 106 to obtain CPMs (Counts per Million reads). Mean read coverage was used in Figure 1A, while the ratio between median value between biological replicates in IP and median value in Input was used for violin-plot analysis of H1.2-GFP in Figures S3B and S6C. To include nucleosomes in close proximity to gene TSS, an upstream region of 250 bp was also considered for the overlap (minimum 150 bp) for H3K27me3, TRB1 and H3K4me3 (datasets detailed in the key resources table). H3K27me3 TE cluster 1 and TE cluster 2 were identified using Deeptools plotHeatmap using the –kmeans

option set at 2. Tracks were visualized using Integrative Genomics Viewer (IGV) version 2.8.0.[118] Meta-gene plots and heatmaps were generated from depth-normalized read densities using Deeptools computeMatrix, plotHeatmap, and plotProfile. Violin-plots, histograms and box-plots were drawn using the package ggplot2 v3.2.1 (https://cran.r-project.org/web/packages/ggplot2/) in the R statistical environment. All scripts used will be made publicly available. Shuffled controls were produced with random permutations of genomic position of the regions if interest. The permutations were generated with bedtools v2.29.2 and the command "bedtools shuffle -chromFirst -seed 28776 -chrom".

MNase-seq bioinformatics

MNase read density[28] was obtained from NCBI GEO under the accession GSE96994. Genomic location of WPNs shared between WT and 2h1 plants were identified as overlapping WPN coordinates between the two genotypes calculated with bedtools v2.29.2 intersect.

ATAC-seq bioinformatics

Raw ATAC-seq data were treated using the custom-designed ASAP pipeline (ATAC-Seq data Analysis Pipeline; https://zenodo.org/record/1466008). Mapping was performed using Bowtie2 v.2.3.2[114] with parameters –very-sensitive -X 2000. Mapped reads with MAPQ<10, duplicate pairs, and reads mapping to the mitochondrial genome as well as regions with aberrant coverage of low sequence complexity defined in[125] were filtered out. Concordant read pairs were selected and shifted as previously described by 4 bp.[126] Peak calling was performed using MACS2[115] using broad mode and the following parameters: –nomodel –shift −50 –extsize 100. Heatmaps and metaplots were produced from depth-normalized read coverage (read per million) using the Deeptools suite.[127]

DNA sequence analyses

Motifs enriched in gene promoters (−500 bp to +250 bp after the TSS) and in annotated units of TE cluster 1 elements were identified using MEME version 5.1.1.[119] The following options were used for promoters: "-dna -mod anr -revcomp -nmotifs 10 -minw 5 -maxw 9" and for TEs: "-dna -mod anr -nmotifs 10 -minw 5 -maxw 9 -objfun de -neg Araport11_AllTEs.fasta -revcomp -markov_order 0 -maxsites 10000" where Araport11_AllTEs.fasta correspond to the fasta sequence of all TEs annotated in Araport11.

Telobox positioning was analyzed using the TAIR10 coordinates described in Zhou et al.[37] and obtained from ==+https://gbrowse.mpipz.mpg.de/cgi-bin/gbrowse/arabidopsis10_turck_public/?l=telobox;f=save+datafile. Telobox repeat numbers were scored over 10-bp non-overlapping bins, smoothed with a 50-bp sliding window and subsequently used to plot telobox density.

Gene ontology analysis

Gene ontology analysis of H3K27me3 differentially marked genes were retrieved using the GO-TermFinder software[128] via the Princeton GO-TermFinder interface (http://go.princeton.edu/cgi-bin/GOTermFinder). The REVIGO[120] platform was utilized to reduce the number of GO terms and redundant terms were further manually filtered. The Log10 p values of these unique GO terms were then plotted with pheatmap (https://CRAN.R-project.org/package=pheatmap) with no clustering.

Protein alignment

Protein sequences of H1.1, H1.2, H1.3, TRB1, TRB2 and TRB3 were aligned using T-Coffee[121] (http://tcoffee.crg.cat/apps/tcoffee/do:regular) with default parameters. Pairwise comparison for similarity and identity score were calculated using Ident and Sim tool (https://www.bioinformatics.org/sms2/ident_sim.html).

QUANTIFICATION AND STATISTICAL ANALYSES

Unless stated otherwise, statistical tests were performed with the R package rstatix_0.7.1 (=https://CRAN.R-project.org/package=rstatix) using the functions wilcox_test and wilcox_effsize. All pairwise comparisons between the read coverage in WT and 2h1 over a given set of gene or TEs were tested with Wilcoxon signed rank test for paired samples, using the wilcox_test function with the option "paired = TRUE". All other comparisons were tested with Wilcoxon rank-sum test for independent samples, setting the option "paired = FALSE".

Cell Reports, Volume *42*

Supplemental information

Histone H1 protects telomeric repeats from H3K27me3 invasion in *Arabidopsis*

Gianluca Teano, Lorenzo Concia, Léa Wolff, Léopold Carron, Ivona Biocanin, Kateřina Adamusová, Miloslava Fojtová, Michael Bourge, Amira Kramdi, Vincent Colot, Ueli Grossniklaus, Chris Bowler, Célia Baroux, Alessandra Carbone, Aline V. Probst, Petra Procházková Schrumpfová, Jiří Fajkus, Simon Amiard, Stefan Grob, Clara Bourbousse, and Fredy Barneche

Figure S1

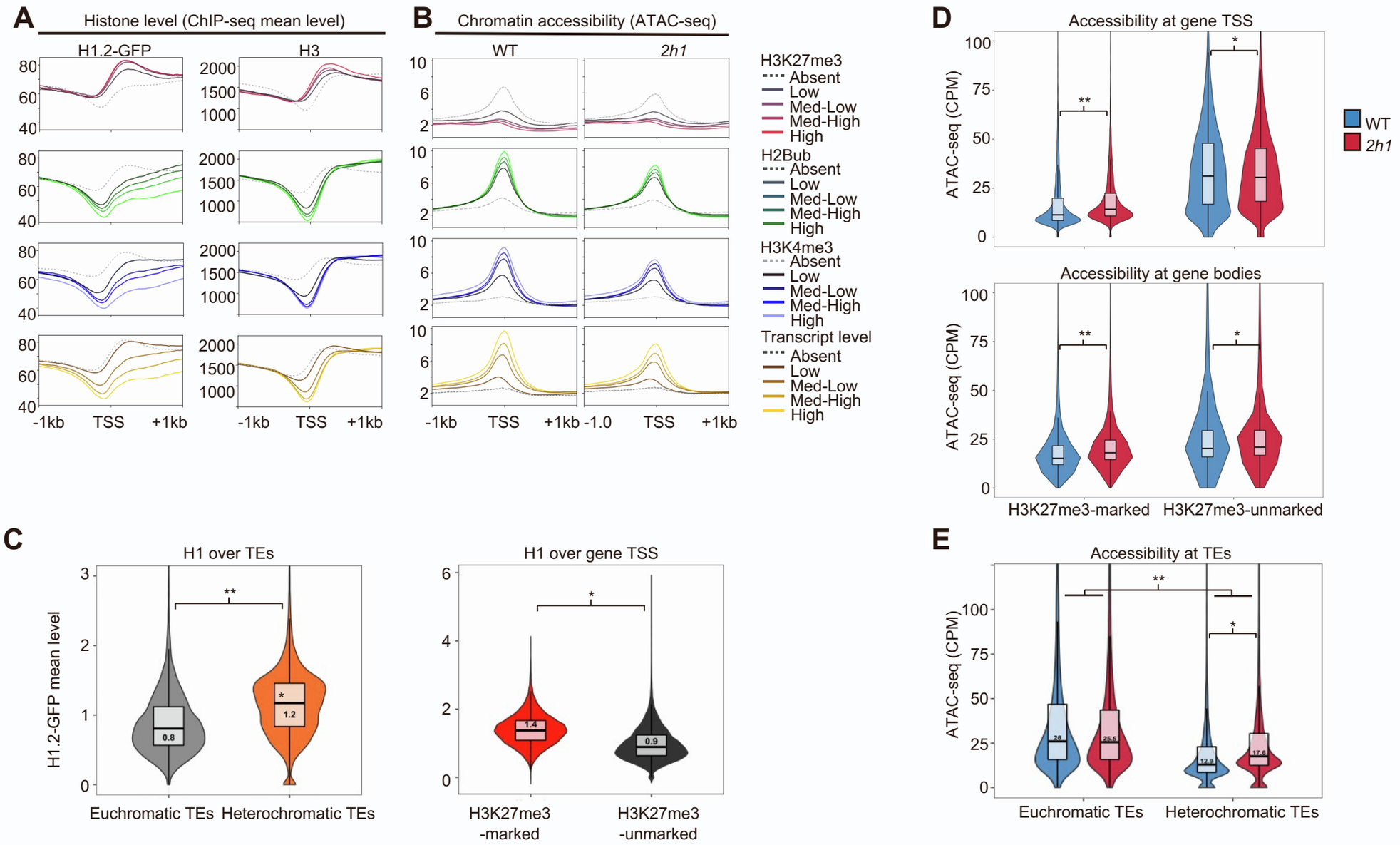

Figure S1: H1.2 is enriched at PRC2-target genes and at heterochromatic TEs where it contributes to modulate DNA accessibility, related to Figure 1.

(A) H1.2 distribution and its link to gene expression. H1.2-GFP and H3 levels over the TSS (+/- 250bp) of genes marked by different histone modifications characteristic of PRC2-based repression (H3K27me3; n=7542), of transcription initiation (H3K4me3; n=18735), transcription elongation (H2Bub; n=11357) or according to gene expression quartiles. Genes with no detectable reads in our RNA-seq analyses of WT plants were considered as not expressed genes (n=5894) as compared to other genes (n=22103). Data represent the merge of two biological replicates. All ChIPs have been generated in this study except H2Bub and H3K4me3. **(B)** DNA accessibility and its link to gene expression. Same analysis as in (A) for ATAC-seq. Normalized read coverage is used as a proxy of DNA accessibility in WT and *2h1* plants. **(C)** H1.2-GFP mean level at euchromatic and heterochromatic TEs (mean read coverage). Same analysis than in Figure S1A using TE annotation defined in Bernatavichute et al., (2008). For genes pValue < 10^{-16}; for TEs pValue <10^{-308} using a Wilcoxon rank sum test; effect size, moderate. **(D)** ATAC-seq read mean density (CPM) over the TSS (+/- 250bp) and full gene body of H3K27me3-marked genes (n=7542) compared to all other annotated protein-coding genes. * and ** indicate a pValue < 10^{-30} and < 10^{-100} using a Wilcoxon rank test, with small and large effects, respectively. **(E)** Same analysis than (B) for the whole annotations of the corresponding TE sets. * and ** indicate a pValue < 10^{-122} and < 10^{-308} , respectively, using a Wilcoxon rank test. ATAC-sea data correspond to the mean of two biological replicates.

Figure S2

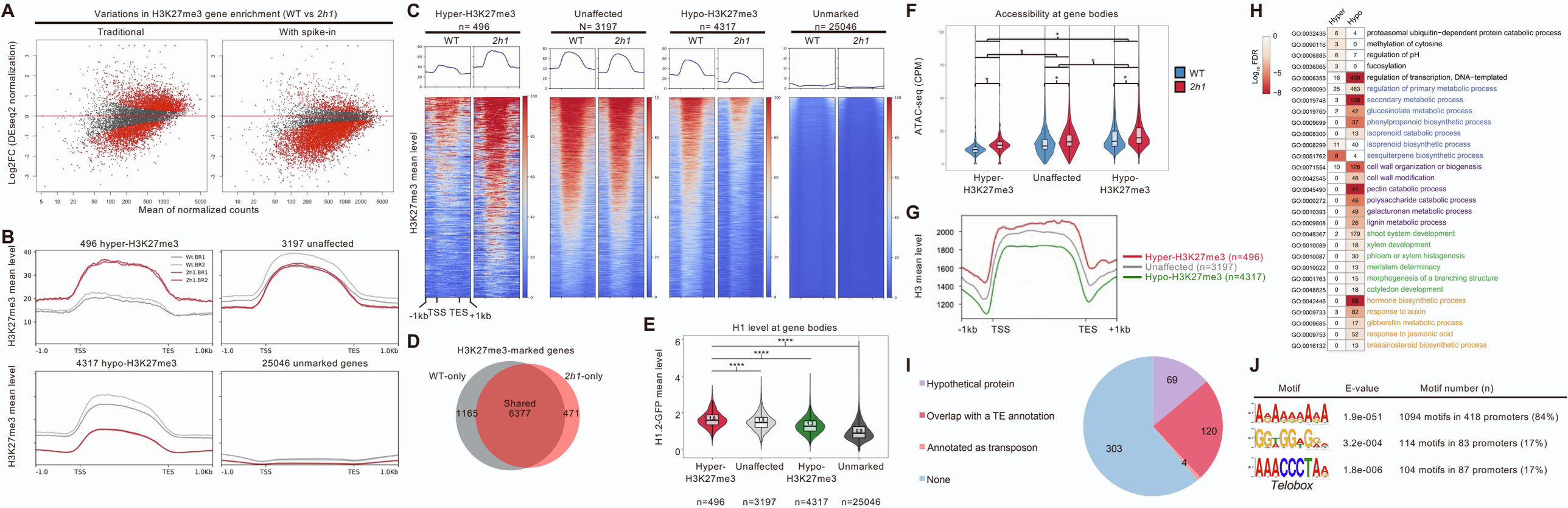

Figure S2: H1 influences H3K27me3 marking, chromatin accessibility and expression of PRC2-target genes, related to Figure 2.

(A) Comparison of the repertoire and chromatin properties of genes significantly marked by H3K27me3 in WT and *2h1* plants. MA-plots show DESeq2 results using either a spike-in normalization factor or DEseq2-based normalization. The plots were drawn using two biological replicates for each sample. **(B)** H3K27me3 levels at differentially marked genes (normalized mean read coverage). **(C)** Detailed analysis of data presented in Figure 2B. In each cluster genes were ranked according to mean H3K27me3 level. **(D)** Number of H3K27me3-marked genes in WT and *2h1* seedlings. Data correspond to two biological replicates. **(E)** H1.2-GFP level over the TSS (+/- 250bp) of the gene sets with differential H3K27me3 enrichment in *2h1* plants defined in Figure 2A. **** indicated a pValue <10e-11 using a Wilcoxon signed rank test on paired samples. **(F)** ATAC-seq mean read coverage (CPM) over the whole gene body of the corresponding gene sets. * indicated a pValue < 10e-70 using a Wilcoxon signed rank test on paired samples. **(G)** H3 level over the same gene sets than in (B). **(H)** Gene ontology analysis of the genes differentially marked in *2h1* plants. Association to a significantly over-represented gene function is denoted as a heatmap of false discovery rate (FDR). N=4317 hypo-marked genes; 496 hyper-marked genes. **(I)** Number of genes among the 496 hyper-marked genes that either overlap an annotated TE, are annotated as TEs, or are annotated as hypothetical proteins (Key resources table). **(J)** Sequence motifs over-represented in the promoters of the 496 H3K27me3 hyper-marked genes in *2h1* plants (E-value < 1e-220). E-values were calculated against random sequences. The two first motifs could not be matched to any previously known regulatory motif while the 3rd identified motif corresponds to the previously described *telobox* motif (AAACCCTA).

Figure S3

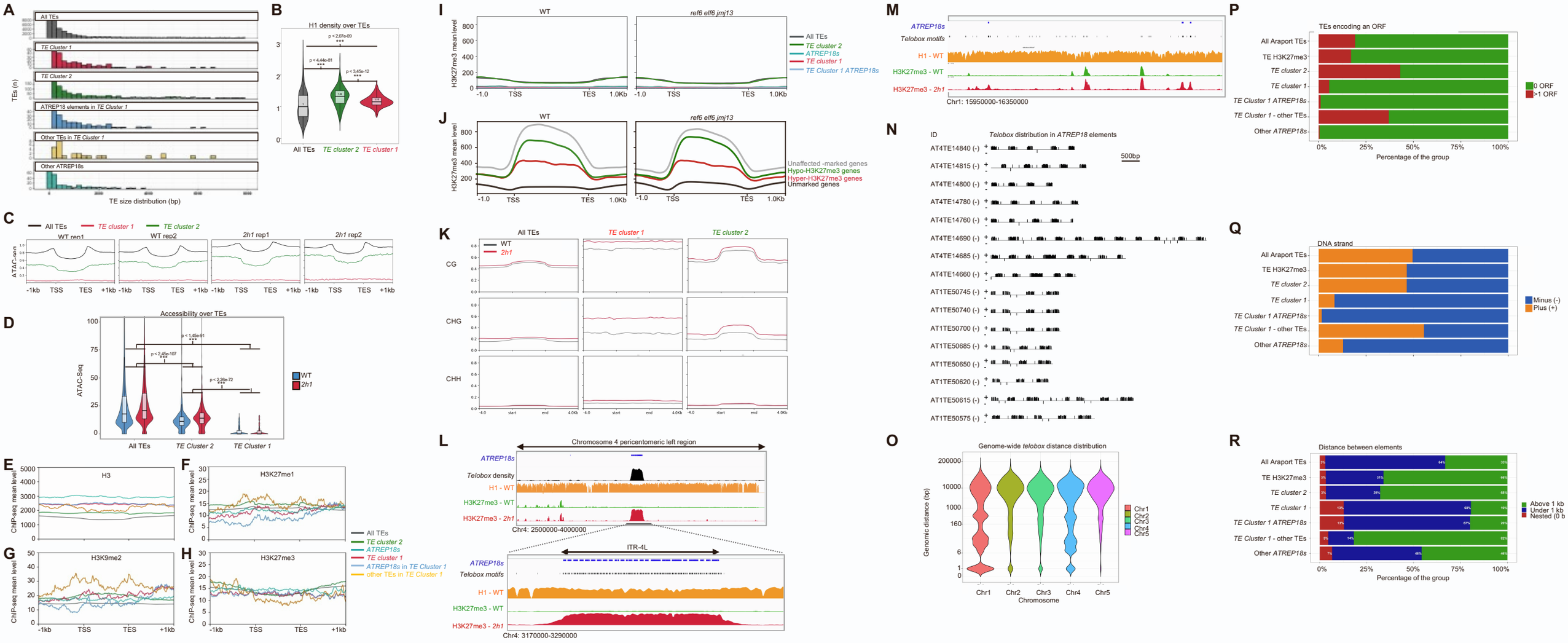

Figure S3: H1 hinders H3K27me3 enrichment at pericentromeric ITRs with specific chromatin and sequence signatures, related to Figure 3.

(A) Size distribution of TEs and TE-like repeats belonging to the repertoires defined in Figure 3A. **(B)** *TE Cluster 1* is enriched in H1.2-GFP as compared to other TEs (mean read coverage). P-values of differences between the medians assessed using a Wilcoxon rank-sum test are shown. **(C)** Independent biological replicate of ATAC-seq data completing Figure 3D. ATAC-seq mean read coverage of the indicated TE categories in WT and *2h1* nuclei. **(D)** ATAC-seq read coverage (CPM) over the whole annotated TE units of corresponding sets. P-values obtained using a Wilcoxon signed rank test on paired samples are given. **(E-H)** Profiling of H3, H3K9me2, H3K27me1 and H3K27me3 over indicated TE categories. (E) Histone H3 profiling indicates that *ATREP18s* and *TE Cluster1-ATREP18* elements display elevated nucleosome occupancy. This is consistent with the weak accessibility of these elements determined by ATAC-seq analyses. (F) H3K27me1 is not particularly enriched at *TE Cluster 1-2* nor at *ATREP18* elements as compared to other TEs. (G) H3K9me2 level is high at *TE Cluster 1* as compared to other TEs. (H) All TE types investigated in this study, including *ATREP18* elements, display low H3K27me3 levels in WT plants. H3K27me3 and H3 but not H3K27me1 and H3K9me2 ChIP-seq have been generated in this study. **(I)** H3K27me3 profiles of the indicated gene sets in WT and *ref6 elf6 jmj13* triple mutant plants impaired in H3K27me3 demethylation. **(J)** Same analysis than (I) for the indicated gene categories. **(K)** CG, CHG and CHH mean methylation at the indicated TE categories in WT and *2h1* mutant seedings. **(L)** Chromosome 4 distribution of *ATREP18* elements, *telobox* motif distribution and H3K27me3 profiles (normalized mean coverage). Top and bottom panels are as in Figure 3G. **(M)** Close-up view on interspersed H3K27me3-enriched repeats of *TE cluster 2*, exemplifying a physical correlation between H3K27me3 enrichment and *telobox*-rich domains in *2h1* pericentromeric regions. **(N)** Clustered patterns of *telobox* motif in *ATREP18* elements of *TE Cluster 1*. **(O)** Genomic distances between all perfect *telobox* motifs on each chromosome reflecting that ITR organizations in chromosome 1 and 4 constitute important differences as compared to other chromosomes in which interspersed *telobox* motifs are largely prevalent. Except at telomeres, chromosome 5 does not display adjacent *telobox* motifs. **(P)** Frequency of open reading regions (ORFs) identified in the indicated TE categories. *TE Cluster 1*, which contains many pericentromeric *ATREP18* elements, rarely encodes ORFs. In contrast, *TE Cluster 2* more frequently encodes ORFs as compared to the ensemble of all TEs. **(Q)** Strand distribution. *TE Cluster 1* consists mainly of *ATREP18* elements organized in a strand-specific manner. **(R)** Distribution of different groups of TEs in three classes of distances: nested (0 base pairs), closely located (under 1 kb) or distantly located (above 1 kb). Compared to the ensemble of all TEs, *TE Cluster 2* elements tend to be dispersed across the genome while, conversely, *TE Cluster 1* elements tend to be located in close proximity. This peculiar distribution is largely due to the overwhelming presence of *ATREP18* elements in *TE Cluster 1* elements in this group (189 out of 216, 87%).

Figure S4

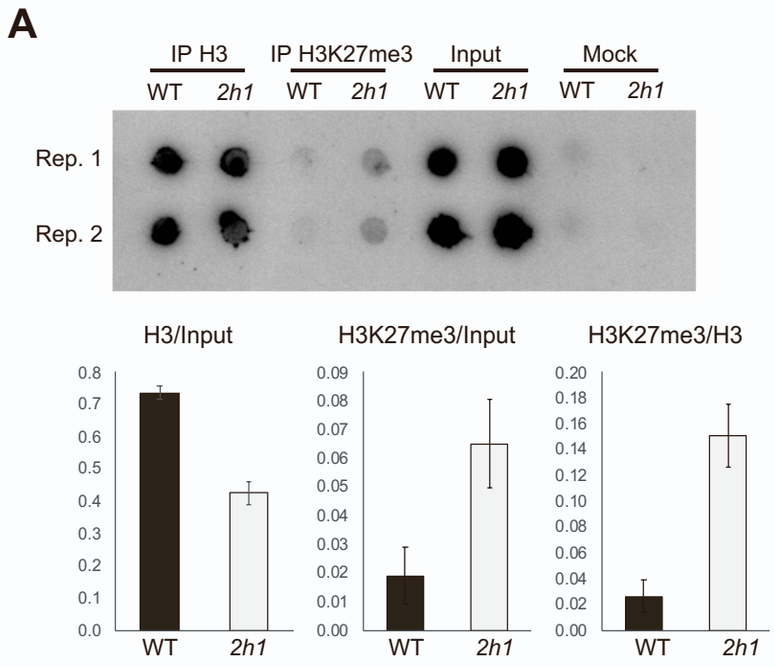

Figure S4: H1 influences H3K27me3 and TRB1 enrichment, related to Figure 4.

(A) Independent biological replicates of H3K27me3 and H3 ChIP DNA hybridization to telomeric probes completing Figure 4A. **(B)** GFP-TRB1 in enriched at telomeres in *2h1* nuclei as compared to WT. Anti-GFP ChIP-blotting was performed as in Figure, 4A and S4A using *TRB1::GFP-TRB1* and *2h1*/ *TRB1::GFP-TRB1* plants. The results of two independent biological replicates are shown in the upper panel, and corresponding signal quantification in the lower panel.

Figure S5

Figure S5: H3K27me3 accumulation at ITRs and at telomeres associates with ITR insulation and more frequent telomere-telomere interactions, related to Figure 5.

(A) Mapping results of Hi-C libraries and comparison with re-processed Hi-C datasets from Liu et al. (2016) and Wang et al. (2015). **(B)** Heatmap of similarity scores among WT and *2h1* mutant datasets calculated using Spearman rank correlation between each sample as 100 kb bins. **(C)** Comparison of intra-chromosomal reads over the total number of valid interactions among our samples and published DpnII-based Hi-C datasets from Liu et al. (2016) and Wang et al. (2015). Proportion of *cis* (intra-chromosomal) interactions among valid interactions is positively correlated with library quality for *in situ* Hi-C as in Sun et al. (2020). **(D)** Estimation of the Hi-C resolution achieved in this study. The curves show the Hi-C Spector score of chromosome 1 contact map down-sampled at 10% of contacts as in Carron et al. (2019). We computed 30 down-samples at a resolution of 2kb and computed Hi-C Spector score similarity, using an Eigen value of 10, against each Hi-C map with a resolution from 2kb to 150 kb. For each resolution, the maximum Hi-C Spector score of the 30 down-samplings is reported. This analysis was performed using the merge of three independent biological replicates. Public data sources are given in key resources table. **(E)** Hi-C interaction frequency heatmap showing normalized Log_{10} contact count at 100 kb resolution for all *Arabidopsis* chromosomes in WT (below the diagonal) and *2h1* (above the diagonal) nuclei. Lateral tracks depict the positions of centromeres (black) and pericentromeres (gray). **(F)** Relative differences of interaction frequency between WT and *2h1* nuclei for the ITR regions illustrated in (B). Log_2 ratios of normalized interaction frequencies of *2h1* vs WT nuclei are shown at a 10kb resolution. All Hi-C data were analyzed using the merge of three independent biological replicates. **(G)** Same analysis than (E) illustrating interaction frequencies between the chromosomal regions spanning 1 Mb around ITR-1R (Chr1:15086191-15441067) and ITR-4L (Chr4:3192760-3265098) at a 10 kb resolution. (**H-I)** Pericentromere-embedded ITR-1R and 4L frequently associate with other pericentromeric regions through inter-chromosomal contacts, but less frequently with all other tested chromosome domains except the *NOR2* region. Besides frequent long-range interactions with *NOR4*, the *NOR2*-adjacent Chr2L region also shows frequent interactions with several genome regions including ITR-4L and its neighboring pericentromeric regions on Chr4L. **(J)** Relative differences of interaction frequency between WT and *2h1* nuclei. With the exception of *NOR*-proximal Chr2L and Chr4L regions, telomere-telomere and telomere-ITR interactions tend to increase in the absence of H1. Similarly, interactions between ITR-1R and 4L are slightly more frequent in the mutant line. In contrast, interactions between ITRs and all pericentromeres tend to be reduced in the mutant line. The decrease in frequency of interaction is particularly marked between the *NOR*-adjacent regions and the pericentromeres of chromosome 2 and 4. Interaction frequencies are expressed as logarithm of the observed read pairs (H and I) or logarithm of their ratio (J) normalized for region size. The indicated values are the median of three biological replicates (H and I) and the ratio of the medians (J). In (H-J) we probed four groups of regions: 1) ITR-1R and 4L coordinates, 2) sub-telomeric regions defined as the 100 kb terminal chromosomal regions adjacent to the telomeres, 3) pericentromeric regions represented by 100-kb segments located at 1 Mb from centromeres, and 4) 100-kb chromosome arm regions located at 5 Mb from the telomere positions. The sub-telomeric regions of chromosome 2 and 4 left arms are separated from the telomeres by the *NOR2* and *NOR4*, and therefore referred to as subNOR2 and SubNOR4 respectively (blue label). Distal arm regions were used as control. **(K)** The upper panel displays log2 ratio of O/E interaction frequency (*2h1*/WT) around ITR-1R and ITR-4L regions. Middle panel, ΔDLR represents the variations in distal-to-Local [log2] ratios in *2h1 vs* WT (*2h1*/WT) (see Methods). Bottom panel, ratio of H3K27me3 mean levels between *2h1* and WT nuclei (*2h1*/WT). Data combine three independent biological replicates and are processed at a 10kb resolution.

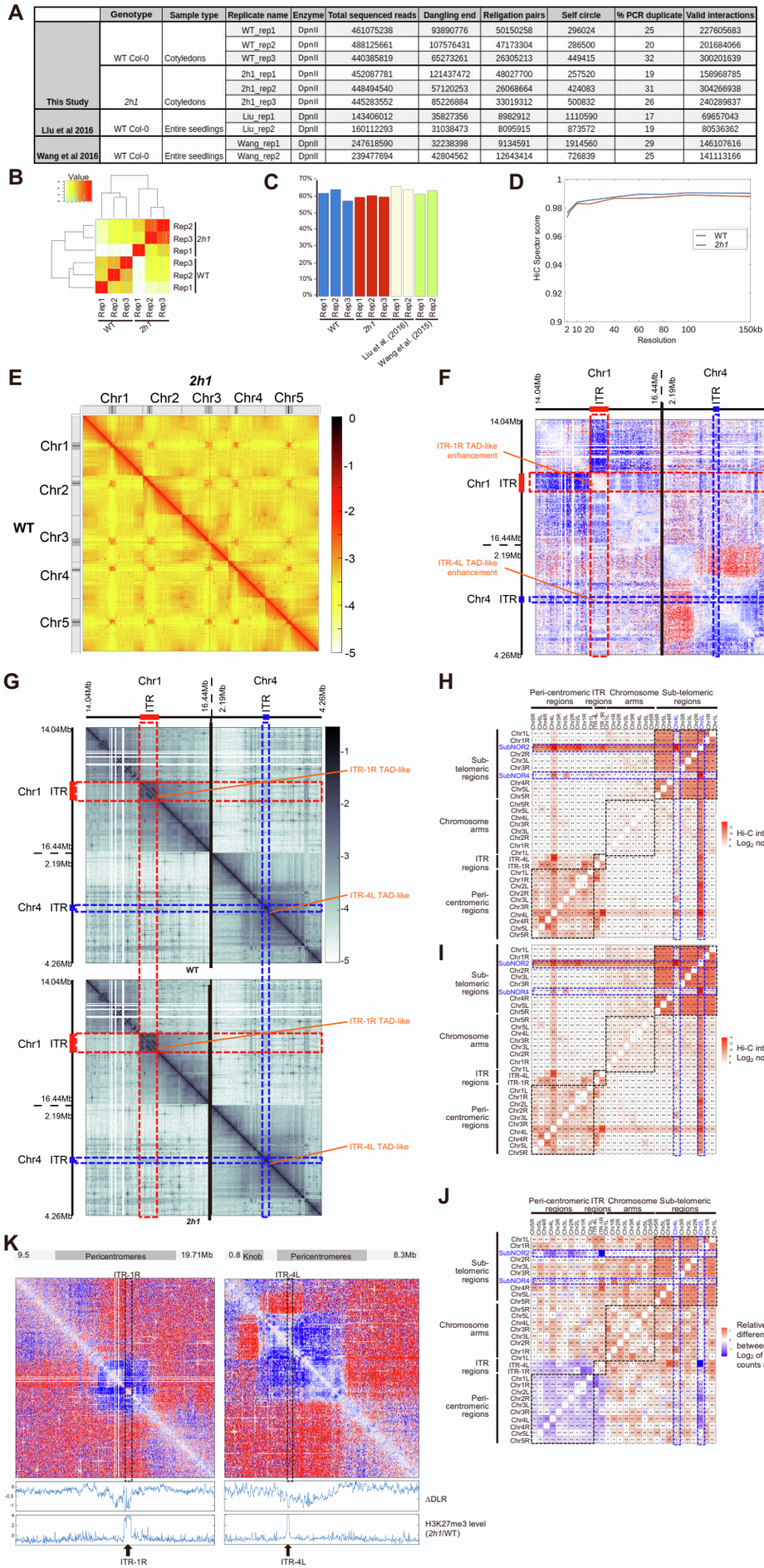

	Genotype	Sample type	Replicate name	Enzyme	Total sequenced reads	Dangling end	Religation pairs	Self circle	% PCR duplicate	Valid interactions
This Study	WT Col-0	Cotyledons	WT_rep1	DpnII	461075238	93890776	50150258	296024	25	227605683
			WT_rep2	DpnII	488125661	107576431	47173304	286500	20	201684066
			WT_rep3	DpnII	440385819	65273261	26305213	449415	32	300201639
	2h1	Cotyledons	2h1_rep1	DpnII	452087781	121437472	48027700	257520	19	158968785
			2h1_rep2	DpnII	448494540	57120253	26068664	424083	31	304266938
			2h1_rep3	DpnII	445283552	85226884	33019312	500832	26	240289837
Liu et al 2016	WT Col-0	Entire seedlings	Liu_rep1	DpnII	143406012	35827356	8982912	1110590	17	69657043
			Liu_rep2	DpnII	160112293	31038473	8095915	873572	19	80536362
Wang et al 2016	WT Col-0	Entire seedlings	Wang_rep1	DpnII	247618590	32238398	9134591	1914560	29	146107616
			Wang_rep2	DpnII	239477694	42804562	12643414	726839	25	141113166

Figure S6

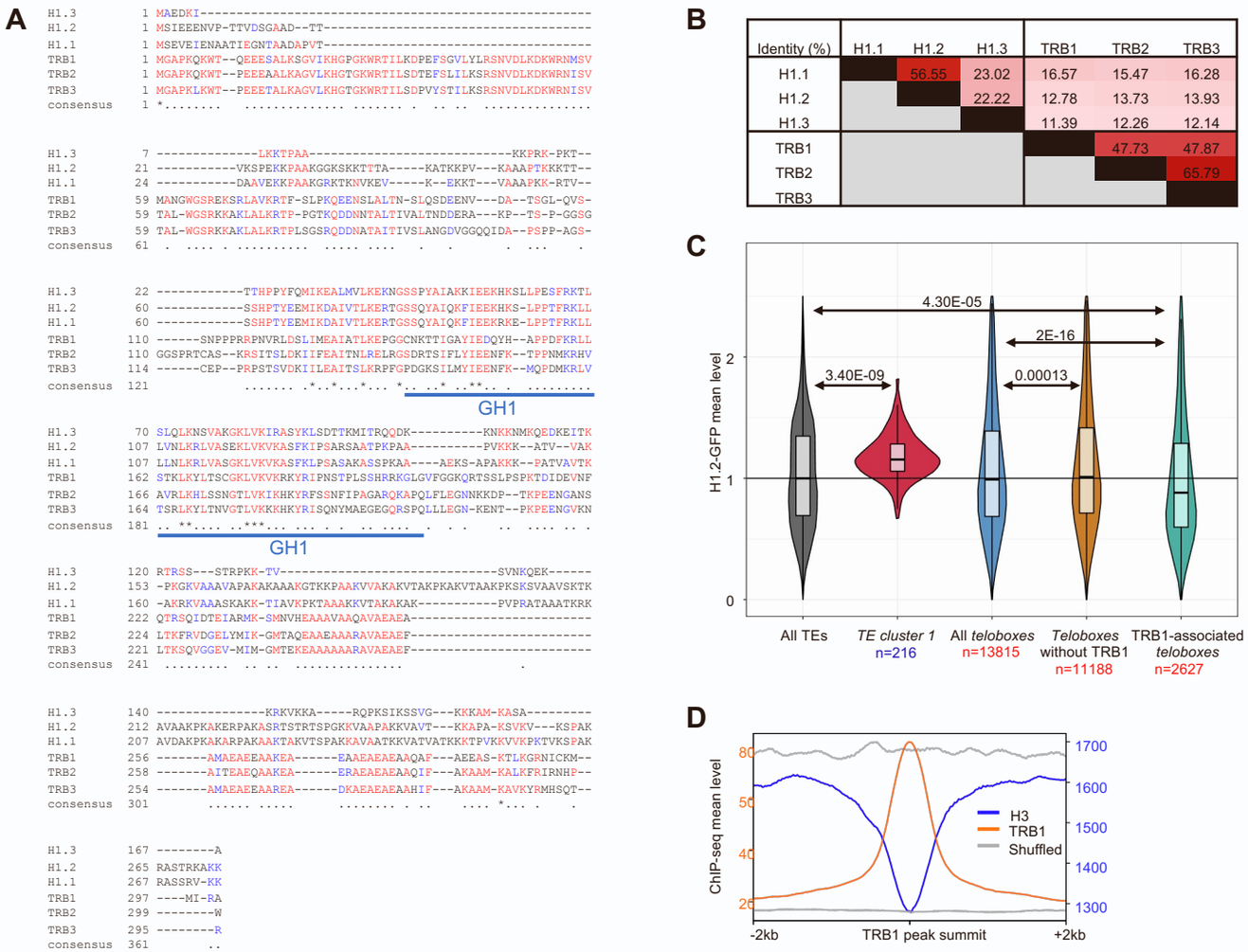

Figure S6: H1 and TRB1 share protein sequence features and prevalently associate to the genome in a mutually exclusive manner, related to Figure 6.

(A) ClustalW protein sequence alignment of TRB1, TRB2 and TRB3 proteins with the three H1 variants showing the relative conservation of a central globular H1 domain. **(B)** Amino-acids sequence identity between TRB1, TRB2 and TRB3 proteins and the three H1 variants. **(C)** *TE Cluster 1* displays elevated H1 level as compared to the ensemble of *Arabidopsis* TEs and to other *telobox*-containing regions. In agreement with the proposed mutually exclusive binding of H1 and TRB1 over *teloboxes*, the set of *teloboxes* matching a known TRB1 peak displays significantly less H1 occupancy than other *teloboxes* of the genome. P-values of differences between the medians assessed using a Wilcoxon rank-sum test are shown. **(D)** Figure 6D complementary data. H3 occupancy (mean read coverage) and randomly shuffled peaks are shown as control of data normalization. The shuffled control was produced with random permutations of genomic position of the regions of interest. TRB1 ChIP-seq data are from Schrumpfová et al. (2014).

Figure S7

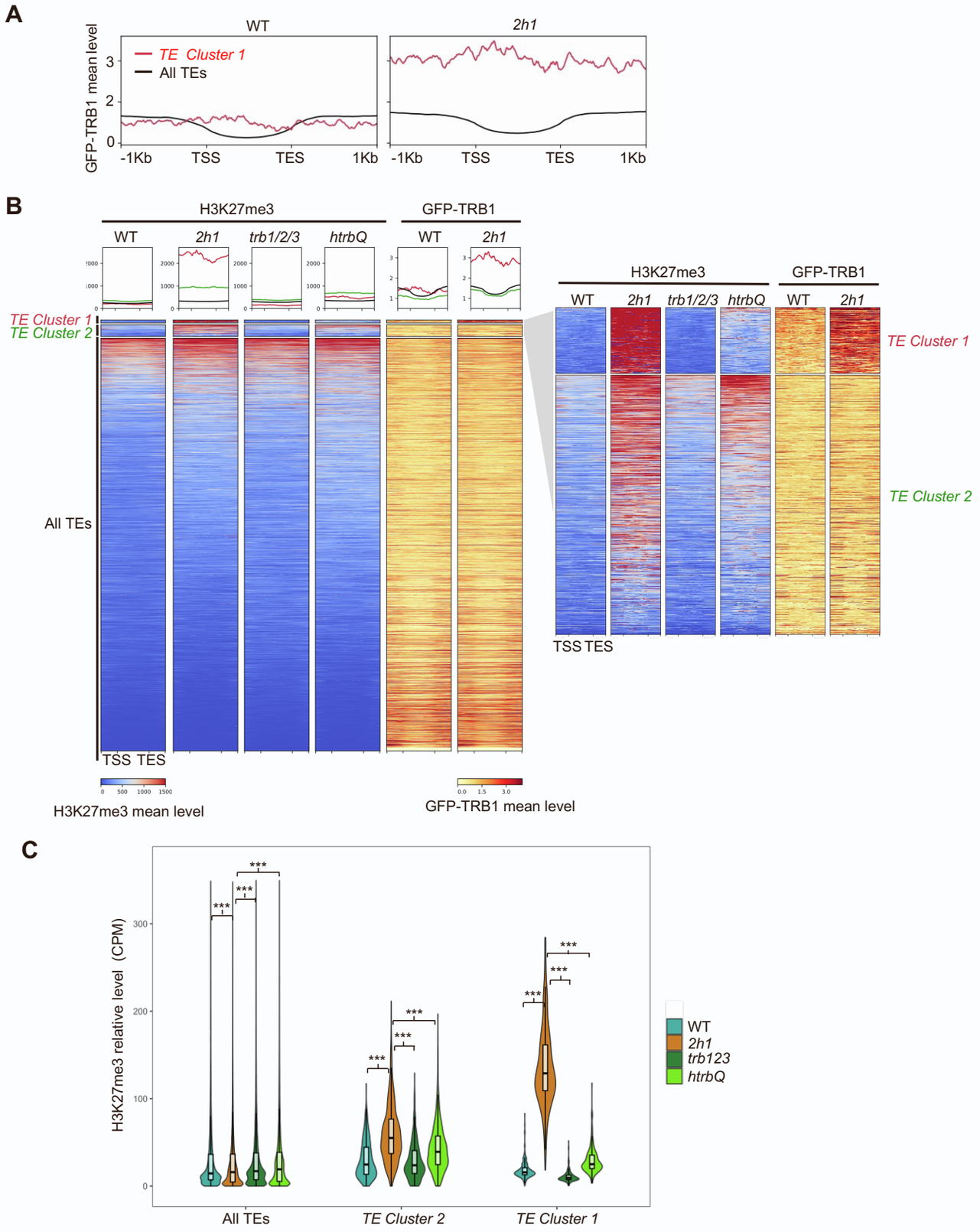

Figure S7: H1 prevents TRB1-mediated PRC2 activity at ITRs and at a few other repeats, related to Figure 7.

(A) GFP-TRB1 level at the indicated TE categories in WT and *2h1* nuclei (mean normalized coverage from two independent biological replicates). **(B)** H3K27me3 and GFP-TRB1 mean level of different TE categories in the indicated genotypes. In each heatmap, TEs were ranked from top to bottom according to H3K27me3 or GFP-TRB1 mean level after RPGC or spike-in based normalization, respectively. While GFP-TRB1 ChIP-seq were performed using parental lines, H3K27me3 ChIP-Rx was performed on WT, *2h1* and *trb123* mutant lines selected from null F2 segregants from the same cross than the analyzed *2h1trb1trb2trb3* (*htrbQ)* plant line. (**C)** Same analysis than (B) displaying H3K27me3 mean level over whole TE annotations. All data represent the mean of two independent biological replicates. ***, pValue < 1e-30 using a Wilcoxon rank sum test; effect size: small for All TEs comparisons, large or moderate for *TE Cluster 1* and *TE Cluster 2* comparisons.